

01 DS/MY.—5,000—24.9.45—SGPP Lahore.



**DELHI POLYTECHNIC**  
**LIBRARY**

**CLASS NO.** \_\_\_\_\_

**BOOK NO.** \_\_\_\_\_

**ACCESSION NO.** \_\_\_\_\_





**NATIONAL NUCLEAR ENERGY SERIES  
Manhattan Project Technical Section**

**Division IV — Plutonium Project Record  
Volume 14 B**

**THE TRANSURANIUM ELEMENTS**

**Research Papers**

**Part II: Papers 6.40 to 22.80**

## Contributing Authors of Part II

B. M. Abraham	J. J. Katz
D. P. Ames	C. W. Koch
H. H. Anderson	T. P. Kohman
L. B. Asprey	T. J. LaChapelle
W. C. Bentley	N. L. Lofgren
C. J. Borkowski	C. K. McLane
L. Brewer	L. B. Magnusson
L. Bromley	W. M. Manning
J. Chrisney	R. C. L. Mooney
J. A. Crawford	L. O. Morgan
B. B. Cunningham	P. R. O'Connor
R. Dandl	D. W. Osborne
N. R. Davidson	J. H. Parsons
H. W. Dodgen	I. Perlman
J. K. East	S. Peterson
L. Eyring	H. P. Robinson
P. Fields	G. K. Rollefson
P. Fineman	B. F. Scott
O. Flatau	G. T. Seaborg
A. E. Florin	J. Sedlet
S. Fried	I. Sheft
H. W. Fulbright	N. R. Sleight
A. Ghiorso	R. W. Stoughton
P. W. Gilles	M. H. Studier
J. W. Gollman	R. C. Thompson
R. Greenlee	S. G. Thompson
F. Hagemann	Q. Van Winkle
R. E. Hein	A. F. Voigt
J. C. Hindman	B. B. Weissbourd
H. H. Hopkins, Jr.	L. B. Werner
D. L. Hufford	E. F. Westrum, Jr.
E. K. Hyde	J. M. Wright
A. H. Jaffey	W. H. Zachariasen
R. A. James	

A complete list of contributing authors for Parts I and II, with affiliations, is given at the end of this volume.

# **THE TRANSURANIUM ELEMENTS**

## **Research Papers**

**Edited by**

**GLENN T. SEABORG**

**Department of Chemistry and Radiation Laboratory  
University of California, Berkeley**

**JOSEPH J. KATZ**

**Chemistry Division, Argonne National Laboratory**

**and**

**WINSTON M. MANNING**

**Chemistry Division, Argonne National Laboratory**

**Part II  
(Papers 6.40 to 22.80)**

**First Edition**

**New York - Toronto - London  
McGRAW-HILL BOOK COMPANY, INC.**

**1949**

**THE TRANSURANIUM ELEMENTS**  
**Research Papers**

Copyright, 1949, by the  
McGraw-Hill Book Company, Inc.

Printed in the United States of America

Copyright assigned, 1949, to the General Manager  
of the United States Atomic Energy Commission.  
All rights reserved. This book, or parts thereof,  
may not be reproduced in any form without per-  
mission of the Atomic Energy Commission.

Lithoprinted  
by  
Edwards Brothers, Incorporated  
Ann Arbor, Michigan

## CONTENTS

Paper		Page
6.40	The Thermodynamic Properties and Equilibria at High Temperatures of the Compounds of Plutonium . . . . .	861
	By L. Brewer, L. Bromley, P. W. Gilles, and N. L. Lofgren	
6.50	The Effect of Hydrochloric Acid Concentration on the Heat of Solution of Thorium Tetrachloride . . . . .	887
	By E. F. Westrum, Jr., and H. P. Robinson	
6.51	A Semi-microcalorimeter for Precise Thermochemical Measurements . . . . .	889
	By E. F. Westrum, Jr., and H. P. Robinson	
6.52	The Heat of Formation of Plutonium Trifluoride . . . .	908
	By E. F. Westrum, Jr., and L. Eyring	
6.53	The Heat of Formation of Plutonium Trichloride . . . .	914
	By E. F. Westrum, Jr., and H. P. Robinson	
6.54	The Dependence of the Heat of Solution of Plutonium Trichloride on the Concentration of Hydrochloric Acid . . . . .	922
	By H. P. Robinson and E. F. Westrum, Jr.	
6.55	The Heat of Formation of Plutonium Tribromide . . . .	926
	By E. F. Westrum, Jr.	
6.56	The Heat of Formation of Plutonium Oxychloride . . . .	930
	By E. F. Westrum, Jr., and H. P. Robinson	
6.57	The Preparation and Properties of Plutonium Oxides . . . . .	936
	By E. F. Westrum, Jr.	

6.60	Preparation of Plutonium Nitride . . . . .	945
	By B. M. Abraham, N. R. Davidson, and E. F. Westrum, Jr.	
6.80	The Composition of Plutonium Peroxide . . . . .	949
	By H. H. Hopkins, Jr.	
6.150	Determination of the Melting Points of Plutonium(III) Chloride and Plutonium(III) Bromide . . . . .	952
	By H. P. Robinson	
6.170	Studies of the Preparation and Properties of Plutonium Iodide and Plutonium Oxyiodide . . . . .	957
	By F. Hagemann, B. M. Abraham, N. R. Davidson, J. J. Katz, and I. Sheft	
6.220	Alkali Plutonium(IV) Nitrates . . . . .	964
	By H. H. Anderson	
14.1	Range of $\text{Np}^{237}$ Alpha Particles in Air . . . . .	968
	By T. J. LaChapelle	
14.2	The Radiations of $\text{Np}^{238}$ and the Half Life of $\text{Pu}^{238}$ . . .	978
	By A. H. Jaffey and L. B. Magnusson	
14.5	An Investigation of the Internal-conversion Line Spectrum of Neptunium 239 . . . . .	1011
	By H. W. Fulbright	
15.1	Chemistry of Neptunium. The Oxidation States of Neptunium in Aqueous Solution . . . . .	1032
	By J. C. Hindman, L. B. Magnusson, and T. J. LaChapelle	
15.2	Chemistry of Neptunium. Absorption Spectrum Studies of Aqueous Ions of Neptunium . . . . .	1039
	By J. C. Hindman, L. B. Magnusson, and T. J. LaChapelle	
15.3	Chemistry of Neptunium. Preparation and Properties of Neptunium(III) . . . . .	1050
	By L. B. Magnusson, T. J. LaChapelle, and J. C. Hindman	

15.4	Chemistry of Neptunium(V). Formal Oxidation Potentials of Neptunium Couples . . . . .	1059
	By L. B. Magnusson, J. C. Hindman, and T. J. LaChapelle	
15.5	The Basic Dry Chemistry of Neptunium . . . . .	1072
	By S. Fried and N. R. Davidson	
15.6	Chemistry of Neptunium. First Preparation and Solubilities of Some Neptunium Compounds in Aqueous Solutions . . . . .	1097
	By T. J. LaChapelle, L. B. Magnusson, and J. C. Hindman	
15.7	The Halides of Neptunium . . . . .	1111
	By L. Brewer, L. Bromley, P. W. Gilles, and N. L. Losgren	
15.9	A Tracer Study of the Valence States of Neptunium. .	1119
	By A. F. Voigt, N. R. Sleight, R. E. Hein, and J. M. Wright	
15.10	The Preparation and Decontamination of <sub>93</sub> Np <sup>239</sup> in Trace Concentrations. . . . .	1128
	By P. Fields	
15.11	Chemistry of Neptunium. Kinetics and Mechanisms of Aqueous Oxidation-Reduction Reactions of Neptunium . . . . .	1134
	By L. B. Magnusson, J. C. Hindman, and T. J. LaChapelle	
16.1	Techniques for the Preparation of Thin Films of Radioactive Material . . . . .	1149
	By D. L. Hufford and B. F. Scott	
16.2	An Improved Technique for Precise Alpha Radi- ometric Assay . . . . .	1185
	By E. F. Westrum, Jr.	
16.3	Back-scattering of Pu <sup>239</sup> Alpha Particles from Platinum . . . . .	1192
	By B. B. Cunningham, A. Ghiorso, and J. C. Hindman	

16.4	Note on Back-scattering of Pu <sup>239</sup> Alpha Particles from Platinum Sample Plates.....	1197
	By J. H. Parsons, O. Flatau, J. K. East, R. Dandl, and C. J. Borkowski	
16.6	Apparent Specific Activity of Uranium in a 2π- geometry Chamber.....	1198
	By B. B. Cunningham, A. Ghiorso, and A. H. Jaffey	
16.7	An Emanation Method for Radium Analysis .....	1206
	By P. Fineman, B. B. Weissbourd, H. H. Anderson, J. Sedlet, D. P. Ames, and T. P. Kohman	
16.8	A 48-channel Pulse-height Analyzer for Alpha-energy Measurements.....	1226
	By A. Ghiorso, A. H. Jaffey, H. P. Robinson, and B. B. Weissbourd	
16.55	Theoretical Calculations Concerning Back-scattering of Alpha Particles .....	1307
	By J. A. Crawford	
17.1	The Spectrum of Plutonium.....	1327
	By H. W. Dodgen, J. Chrisney, and G. K. Rollefson	
17.4	The Quantitative Micro Determination of Plutonium	1337
	By C. W. Koch	
19.1	The Tracer Chemistry of Americium and Curium in Aqueous Solutions .....	1339
	By S. G. Thompson, L. O. Morgan, R. A. James, and I. Perlman	
19.2	The First Isolation of Americium in the Form of Pure Compounds; Microgram-scale Observations on the Chemistry of Americium.....	1363
	By B. B. Cunningham	
19.3	Tracer Chemistry of Actinium .....	1371
	By C. K. McLane and S. Peterson	

19.4	Thermal Neutron Fission Properties of Ac <sup>227</sup> , Ra <sup>223</sup> , and Ra <sup>228</sup> . . . . .	1381
	By S. Peterson and A. Ghiorso	
19.5	Thermal Neutron Fission Properties of Ra <sup>228</sup> . . . . .	1383
	By D. Ames and A. Ghiorso	
19.6	Separation of Actinium from Rare Earths Using Ion-exchange Resin . . . . .	1385
	By C. K. McLane and S. Peterson	
19.7	Preparation of Radioactively Pure Ac <sup>228</sup> (MsTh <sub>2</sub> ) . . . . .	1388
	By C. K. McLane and S. Peterson	
19.8	Preparation of Carrier-free Ac <sup>228</sup> (MsTh <sub>2</sub> ) Tracer . . . . .	1391
	By S. Peterson	
19.9	Transmutation of Radium to Actinium (Ac <sup>227</sup> ) . . . . .	1393
	By S. Peterson	
19.10	Alpha Branching of Ac <sup>227</sup> . . . . .	1395
	By S. Peterson and A. Ghiorso	
19.11	Products of the Deuteron and Helium-ion Bombard- ments of Pa <sup>231</sup> . . . . .	1397
	By D. W. Osborne, R. C. Thompson, and Q. Van Winkle	
19.12	Half Life of Th <sup>227</sup> (Radioactinium) . . . . .	1424
	By S. Peterson and A. Ghiorso	
19.13	Nuclear Properties of U <sup>233</sup> : A New Fissionable Isotope of Uranium . . . . .	1426
	By G. T. Seaborg, J. W. Gofman, and R. W. Stoughton	
19.14	Production and Properties of U <sup>232</sup> and Pa <sup>232</sup> . . . . .	1427
	By J. W. Gofman and G. T. Seaborg	
19.15	Determination of the Half Life of U <sup>233</sup> . . . . .	1431
	By E. K. Hyde	

19.16	Determination of the Half Life of Ionium . . . . .	1435
	By E. K. Hyde	
19.17	A New Isotope of Protactinium: $\text{Pa}^{229}$ . . . . .	1439
	By E. K. Hyde, M. H. Studier, H. H. Hopkins, Jr., and A. Ghiorso	
20.1	Crystal Structure Studies of Oxides of Plutonium . . . . .	1442
	By R. C. L. Mooney and W. H. Zachariasen	
20.2	The Crystal Structure of Plutonium Nitride and Plutonium Carbide . . . . .	1448
	By W. H. Zachariasen	
20.3	The Crystal Structure of $\text{PuSi}_2$ . . . . .	1451
	By W. H. Zachariasen	
20.4	Crystal Structure Studies of Sulfides of Plutonium and Neptunium . . . . .	1454
	By W. H. Zachariasen	
20.5	X-ray Diffraction Studies of Fluorides of Plutonium and Neptunium; Chemical Identity and Crystal Structure . . . . .	1462
	By W. H. Zachariasen	
20.6	Crystal Structure Studies of Chlorides, Bromides, and Iodides of Plutonium and Neptunium . . . . .	1473
	By W. H. Zachariasen	
20.7	The Crystal Structure of Sodium Plutonyl and Sodium Neptunyl Acetates . . . . .	1486
	By W. H. Zachariasen	
20.8	The Crystal Structure of $\text{NpO}_2$ and $\text{NpO}$ . . . . .	1489
	By W. H. Zachariasen	
21.1	Electronic Structure of the Heaviest Elements . . . . .	1492
	By G. T. Seaborg	
22.1	The New Element Americium (Atomic Number 95) . . . . .	1525
	By G. T. Seaborg, R. A. James, and L. O. Morgan	

22.2	The New Element Curium (Atomic Number 96) . . . . .	1554
	By G. T. Seaborg, R. A. James, and A. Ghiorso	
22.3	The Neptunium ( $4n + 1$ ) Radioactive Family . . . . .	1572
	By G. T. Seaborg	
22.5	The Preparation and Isolation of Curium . . . . .	1586
	By L. B. Werner and I. Perlman	
22.7	Preparation and Radioactive Properties of Am <sup>242</sup> . . . .	1595
	By W. M. Manning and L. B. Asprey	
22.8	Products of Helium-ion and Deuteron Bombardment of U <sup>235</sup> and U <sup>238</sup> . . . . .	1604
	By R. A. James, A. E. Florin, H. H. Hopkins, Jr., and A. Ghiorso	
22.15	Products of the Deuteron and Helium-ion Bombard- ments of U <sup>233</sup> . . . . .	1622
	By E. K. Hyde, M. H. Studier, and A. Ghiorso	
22.16	The Bombardment of Np <sup>237</sup> with Deuterons and Helium Ions . . . . .	1634
	By R. A. James, S. G. Thompson, and H. H. Hopkins, Jr.	
22.26	Thermal Neutron Fission Properties of Np <sup>237</sup> . . . .	1639
	By A. Ghiorso, D. W. Osborne, and L. B. Magnusson	
22.29	High-sensitivity Apparatus for Fission Counting . . . .	1642
	By A. Ghiorso and W. C. Bentley	
22.30	The Bombardment of U <sup>233</sup> with 44-mev Helium Ions and the Formation of Pu <sup>234</sup> . . . . .	1651
	By I. Perlman, P. R. O'Connor, and L. O. Morgan	
22.50	A General Method for Determining Coincidence Corrections of Counting Instruments . . . . .	1655
	By T. P. Kohman	

22.60	The Specific Activity of Radium . . . . .	1675
	By T. P. Kohman, D. P. Ames, and J. Sedlet	
22.70	Rapid Radiometric Assay for Radium and Application to Uranium Ore Process Solutions . . . . .	1700
	By D. P. Ames, J. Sedlet, H. H. Anderson, and T. P. Kohman	
22.80	The Specific Alpha Radioactivity and Half Life of Plutonium Isotope of Mass 239 . . . . .	1717
	By E. F. Westrum, Jr., J. C. Hindman, and R. Greenlee	
	List of Contributing Authors . . . . .	1727

## Paper 6.40

# THE THERMODYNAMIC PROPERTIES AND EQUILIBRIA AT HIGH TEMPERATURES OF THE COMPOUNDS OF PLUTONIUM†

By L. Brewer, L. Bromley, P. W. Gilles,  
and N. L. Lofgren

### 1. THERMODYNAMIC TABLES

The usefulness of thermodynamic data as an aid in predicting what reactions may occur in any system is well recognized. This tool is especially valuable at high temperatures where most reactions are rapid. However, it is not only necessary to have thermodynamic data, but, if time is to be saved, it is also necessary to know the important species that are likely to exist in the system under consideration. In this paper the thermodynamic data of plutonium compounds are presented, and an attempt is made to indicate the species that are likely to be encountered in work with them at different conditions of pressure and temperature. A shorter but similar treatment of neptunium compounds is also available.<sup>50</sup>

This paper is rightly a part of a more comprehensive thermodynamic study of inorganic halides, which is found in the authors' Halide Report,<sup>12</sup> but because of the nature of the contents of this paper it is presented as a separate unit. The methods used in this report are the same as those used and discussed in some detail in the Halide Report. Further explanation of thermodynamic calculations can be found in another report<sup>38</sup> by the authors of this paper.

Table 1 gives values of the melting point, heat and entropy of fusion, vapor pressures, boiling point, and heat and entropy of vaporization. In Table 2 constants for the free-energy equation for vaporization are given. In Table 3 values of the free-energy function,  $(\Delta F - \Delta H_{298})/T$ ,

†Contribution from the Department of Chemistry, University of California, Berkeley.

at different temperatures, and the heat of formation,  $\Delta H_{298}$ , for the halides, oxides, carbides, nitrides, and silicides of plutonium are given. Contrary to what has been done in other papers,<sup>1-12</sup> values of the functions  $-(F - H_{298})/T$ ,  $H_T - H_{298}$ , and  $S_T - S_{298}$  are not included

Table 1 -- Melting Point, Fusion, and Vaporization Data for Plutonium Compounds<sup>†</sup>

Compound	Melting data			T <sub>p</sub> , temperature at which partial pressure is p atm, °K					
	T <sub>m</sub> , °K	ΔH <sub>m</sub> , kcal	ΔS <sub>m</sub> , e.u.	T <sub>10^-6</sub>	T <sub>10^-5</sub>	T <sub>10^-4</sub>	T <sub>10^-3</sub>	T <sub>10^-2</sub>	T <sub>1</sub>
PuF <sub>3</sub>	1680 ± 20	13	7.75	1380	1450	1560	1690	1870	2460
PuCl <sub>3</sub>	1033 ± 5	15.2	14.7	1000	1090	1195	1315	1480	2040
PuBr <sub>3</sub>	954	13.4	14.0	925	1000	1085	1190	1335	1785
PuI <sub>3</sub>	(1050)	(12.0)	(11.4)	(865)	(930)	(1000)	(1090)	(1225)	(1650)
PuO <sub>2</sub>					(2200)				
PuO				(1850)					

<sup>†</sup>Parentheses indicate estimates from corresponding uranium compounds.

Table 2 -- Constants<sup>†</sup> in Free Energy of Vaporization Equations of the Form  

$$\Delta F = \Delta H_v + 2.3 \Delta C_p T \log T + IT$$

Compound	Vaporization from solid			Vaporization from liquid			Heat and entropy of vaporization at b.p.	
	ΔH <sub>v</sub> , cal	ΔC <sub>p</sub> , e.u.	ΔI, e.u.	ΔH <sub>v</sub> , cal	ΔC <sub>p</sub> , e.u.	ΔI, e.u.	ΔH, kcal	ΔS, e.u.
PuF <sub>3</sub>	115,500	-14	-158.7	105,900	16	-167.8	66.6	27.1
PuCl <sub>3</sub>	84,340	-10	-125.1	71,220	-12	-126.3	46.74	22.9
PuBr <sub>3</sub>	(82,100)	(-12)	(-142.8)	72,500	-16	-160.1	44	24.9
PuI <sub>3</sub>	(69,400)	(-10)	(-120.3)	(59,500)	(-12)	(-124.8)	(39.7)	(24)

<sup>†</sup>Parentheses indicate estimates from corresponding uranium compounds.

because the corresponding values for the metal were not available, and it was easier to estimate directly the values of  $(\Delta F - \Delta H_{298})/T$  than to estimate heat capacities and to calculate the functions.<sup>12</sup> The values of the thermodynamic constants for formation of the ions are given in Table 4.

In so far as was possible, all data of thermodynamic significance available in the declassified literature on Feb. 1, 1949 have been considered in obtaining the values given in these tables. Where data were

not available or were considered to be too sketchy or inaccurate, estimates were made.

Such estimates were based largely upon data presented by the authors<sup>1,12</sup> of this paper for compounds of uranium and the rare-earth

Table 3—Values of the Free-energy Function ( $\Delta F - \Delta H_{298}/T$ )

Com- ound	Calories per °K				$\Delta H_{298}\dagger$ kcal
	298°K	500°K	1000°K	1500°K	
PuF <sub>3</sub>	60	59	59	58	-374
PuCl <sub>3</sub>	54	54	53	50(1)	-229.3
PuCl <sub>4</sub>	72	72	68(1)		-230
PuBr <sub>3</sub>	52	52	50(1)	48(1)	-199.0
PuI <sub>3</sub>	52	52	49	48(1)	-155
PuO <sub>2</sub>	43	42	41	41	-251
PuOT	21				
PuSi <sub>2</sub> †	-10				-211
PuC†	2				-25
PuN†	17				-95
PuOC†	38				-222.6
PuOBr†	33				-210
PuOIT	32				-195
Pu <sub>2</sub> S <sub>3</sub> †	72				-286

†The use of these values in the simple  $\Delta F = \Delta H - T\Delta S$  equation with  $\Delta C_p = 0$  will give correct  $\Delta F$  values at high temperatures even though room-temperature values may be off.

†All values are based upon gaseous standard states for fluorine, chlorine, bromine, iodine, sulfur (S<sub>2</sub>), nitrogen, and oxygen; solid graphite, plutonium, and silicon.

metals. It should therefore be noted that to maintain consistency, corresponding changes in plutonium values should be made if new data become available on the uranium system. The present revision of this paper is due to the April 1947 revision of the uranium report.<sup>1</sup>

All temperatures are expressed in degrees Kelvin. The references to the values in all the tables are given together under each compound.

Standard states are: gaseous fluorine, gaseous chlorine, gaseous bromine, gaseous iodine, gaseous nitrogen, gaseous diatomic sulfur, solid metals, solid graphite, and solid silicon. The units generally are kilocalories per mole for the energy terms and calories per degree per mole for the entropy and heat-capacity terms.

## 2. DESCRIPTION OF TABLES

The melting and boiling data in Table 1 are self-explanatory. For all vapor-pressure data in Table 1, experimental values, when avail-

able, were used to determine a free energy of vaporization equation using an estimated  $\Delta C_p$  of vaporization. This allowed more accurate extrapolation of the data to the boiling point. The equations used are given in Table 2. The vapor pressures given are the partial pressures of the gaseous species of the same composition as the solid or liquid, and as such are a measure of the free energy of vaporization. In many cases the compound vaporizes at a lower temperature than that given in the table because of decomposition or disproportionation. By reference to the figures it can be seen which method of vaporization is important.

Table 2 gives the constants for the free energy of vaporization equations

$$\Delta F = \Delta H_c - \Delta C_p T \ln T + IT$$

and

$$\log p = \frac{-\Delta F}{4.575T}$$

Constants are given for both the liquid and solid for most of the compounds. The heats and entropies of vaporization at the boiling point under 1 atm pressure are also given. In every case the free energy of vaporization refers to the simple vaporization from the solid or liquid standard state to the perfect-gas standard state at 1 atm pressure.

In Table 3 it will be noted that  $(\Delta F - \Delta H_{298})/T$  at 298°K is in reality  $-\Delta S$  for formation although the same relation does not hold at other temperatures. The reason for tabulating this function is that its variance with temperature is small; this allows accurate interpolation. It will be noted that

$$\frac{\partial(\Delta F - \Delta H_{298}/T)}{\partial(T)} = \frac{\Delta H_{298} - \Delta H}{T^2}$$

and hence at 298°K the rate of change of the function with temperature is zero, and, as long as  $\Delta H$  at other temperatures does not differ greatly from  $\Delta H_{298}$ , the function will change slowly with temperature. In the last column of the table are given the heats of formation,  $\Delta H_{298}$ , which can be used with the function  $(\Delta F - \Delta H_{298})/T$  to obtain  $\Delta F$  at any temperature. All heats of formation and other data are for gaseous fluorine, gaseous chlorine, gaseous bromine, gaseous iodine, gaseous oxygen, gaseous nitrogen, gaseous diatomic sulfur, solid metals, solid graphite, and solid silicon.

For the substances other than the halides and tetravalent oxide, no values for  $(\Delta F - \Delta H_{298})/T$  are given above 298°K. In such cases it is entirely satisfactory, for the most part, to assume that the  $\Delta H$  of formation is constant and equal to  $\Delta H_{298}$ , hence  $(\Delta F - \Delta H_{298})/T$  and also  $\Delta S$  are the same at any temperature. Since  $\Delta F = \Delta H - T\Delta S$ ,  $\Delta F$  is linear with temperature if  $\Delta H$  is constant. Since the values of  $\Delta H$  have been obtained from free energies derived from high-temperature chemistry for a number of substances in this class, it should be pointed out that they do not necessarily represent accurate or even good values of heat and entropy of formation at 298°K, but, when combined in the equation  $\Delta F = \Delta H - T\Delta S$ , they do give in the temperature range that is of most interest a value of  $\Delta F$  such that observed phenomena can be calculated.

The general procedure for the calculation of the heat and entropy of formation of a substance from high-temperature chemistry is to estimate from whatever data are given for any particular reaction some quantity, e.g., a pressure, partial pressure, or equilibrium constant, which is a measure of the free energy of the reaction at the temperature under consideration. From the tables of  $(\Delta F - \Delta H_{298})/T$  and  $\Delta H_{298}$ , free energies at this temperature may be calculated for the other substances involved in the reaction. Then from these free energies and the estimated free energy of reaction, the free energy of the compound under consideration may be calculated. This value together with an estimated entropy or  $(\Delta F - \Delta H_{298})/T$  will give a heat of formation according to the expression

$$\Delta H = \Delta F + T\Delta S$$

or

$$\frac{\Delta H_{298}}{T} = \frac{\Delta F}{T} - \frac{(\Delta F - \Delta H_{298})}{T}$$

An inescapable result of this method is that all values in the tables are inextricably connected and consequently a self-consistent table will not be maintained if newer and even better values are indiscriminately substituted in the table without making corresponding changes in the related values.

Values are given in Table 4 for the ions in 1M HCl and 1M  $HClO_4$ . The values for 1M  $HClO_4$  may be used as infinitely dilute values with little error. The calculations of the values are described in the references. These values for the aqueous ions are consistent with the thermodynamic data given for the solid compounds. Throughout this

paper  $\Delta H$ ,  $\Delta F$ , and  $\Delta S$  values for ionic species are partial molal quantities. Concentrations are in moles per kilogram of water. The  $\Delta F$  values are for all constituents at unit concentration, but with no corrections for activity coefficients, e.g., formal potentials.

It should be emphasized that neither the partial molal  $\Delta F$  values nor the  $E$  values given in the text are standard values corresponding

Table 4 — Thermodynamic Properties of the Aqueous Plutonium Ions†

	1M $HClO_4$			1M $HCl$	
	$\Delta \bar{H}_{298}$	$\Delta \bar{S}_{298}$	$\Delta \bar{F}_{298}$	$\Delta \bar{H}_{298}$	$\Delta \bar{F}_{298}$
$Pu + 3H^+ = Pu^{+3} + {}^1_2H_2$	-141.6	+3	-142.7	-141.9	-142.7
$Pu + 4H^+ = Pu^{+4} + 2H_2$	-128.6	-29	-120.1	-129.0	-120.6
$Pu + H^+ + 2H_2O = PuO_2^{+} + {}^1_2H_2$	-78	+54	-94	-78	-93
$Pu + 2H^+ + 2H_2O = PuO_2^{+2} + 3H_2$	-61.6	+38	-72.8	-62.2	-72.4

† $\Delta H$  and  $\Delta F$  values are in kilocalories per mole, and  $\Delta S$  values are in calories per degree. All values are partial molal values. All concentrations are expressed in moles per kilogram of water.

The  $\Delta \bar{S}$  and  $\Delta \bar{F}$  values are for the reacting species at unit concentration, but with no correction for activity coefficients. In other words,  $\Delta \bar{F}$  corresponds to a formal potential rather than to a molal potential.

to unity activities of the various species, but they are "formal" values corresponding to unit concentrations of the various species. Thus for



$$E = E_{\text{obs}} + 0.05914 \log m_{Pu^{+4}} / (m_{Pu^{+3}} m_{H^+})$$

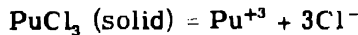
where  $E_{\text{obs}}$  is the observed potential for the cell composed of a hydrogen electrode in solution of  $m_{H^+}$  hydrogen-ion concentration against a  $Pu^{+3}$ - $Pu^{+4}$  electrode. The symbol  $m$  stands for concentration in moles per kilogram of water, and no activity-coefficient corrections of any sort have been made to the observed potentials. This is emphasized since other papers in this volume have used a so-called "formal" potential, which term is erroneously used since corrections are made for activity coefficients of some species and not for others.

### 3. DISCUSSION

After each formula are given the references to the data in Secs. 1 and 2 as well as a critical discussion of the chemistry of the compound. In the cases of the halides these discussions supplement the

figures in Sec. 4 of this paper, while in the cases of the oxyhalides, oxides, nitrides, and carbides these discussions are substitutes for figures.

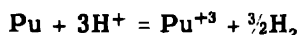
**3.1 Aqueous Ions.** (a)  $\text{Pu}^{+3}$ . Robinson and Westrum<sup>29,48</sup> have determined the heat of solution of  $\text{PuCl}_3$  in various concentrations of hydrochloric acid and have extrapolated their values to pure water. They have obtained for the reaction



$\Delta H_{298} = -31.9$  kcal. This value combined with the  $-39.943$  kcal from Rossini<sup>22</sup> for the heat of formation of  $\text{Cl}^-$ , and the heat of formation of  $\text{PuCl}_3$  (solid), gives, for the reaction at zero hydrochloric acid concentration,



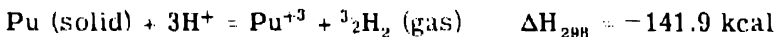
Applying the method used by Evans<sup>27</sup> we can calculate the entropy of  $\text{Pu}^{+3}$  from the entropy of  $\text{Gd}^{+3} = -32.5$  (reference 32) by correcting for different ionic radii, different masses, and different amounts of magnetic entropy. From graphs of ionic entropies for trivalent positive ions vs. ionic radii, it was found that the entropy changes about 82 units per angstrom. Zachariasen<sup>30</sup> gives 1.01 Å for the radius of  $\text{Pu}^{+3}$  and gives values for the radii  $\text{Ce}^{+3}$ ,  $\text{Pr}^{+3}$ ,  $\text{Nd}^{+3}$ , and  $\text{Sm}^{+3}$ . By comparison with the values given by Goldschmidt<sup>31</sup> for the same ions and for  $\text{Gd}^{+3}$ , we find that  $\text{Pu}^{+3}$  is larger than  $\text{Gd}^{+3}$  by 0.06 Å; this difference should make a contribution of 4.9 e.u. to the difference between the entropies of  $\text{Pu}^{+3}$  and  $\text{Gd}^{+3}$ . The magnetic entropy of gadolinium,  $R \ln 8 = 4.1$  e.u., should be subtracted, and the mass correction, 1.2, should be added, giving  $\sim 30.9$  without any contribution from the magnetic entropy of plutonium. Such a contribution would make the entropy less negative and so we have estimated  $-30$  for the entropy of  $\text{Pu}^{+3}$ . Combining this with the entropy of hydrogen<sup>33</sup> and an estimated entropy of plutonium of 13 e.u., we obtain  $\Delta S_{298}$  and subsequently, for the reaction at zero hydrochloric acid concentration,



$$\Delta H = -141.4 \text{ kcal} \quad \Delta S = 3.8 \text{ e.u.} \quad \Delta F = -142.5 \text{ kcal}$$

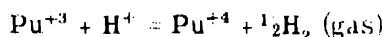
This corresponds to an  $E^\circ$  of 2.06 volts. These values may be used either for the infinitely dilute values or for the values in 1M  $\text{HClO}_4$  since the difference will be less than the uncertainties of these values.

The values for  $\text{Pu}^{+3}$  in 1M HCl may be obtained by using Robinson and Westrum's<sup>29,46</sup> partial molal  $\Delta H_{298} = -31.76$  kcal for  $\text{PuCl}_3$  (solid) dissolving in 0.1M HCl and  $-29.50$  for  $\text{PuCl}_3$  (solid) dissolving in 1.55 moles of HCl per kilogram of water to calculate  $\Delta H_{298} = -30.36$  kcal for  $\text{PuCl}_3$  (solid) dissolving in 1M HCl. This together with a value of  $L = 645$  cal for 1M HCl from Sturtevant<sup>40</sup> makes it possible to calculate for



in 1M HCl. As the best value that can be given for 1M HCl,  $\Delta F_{298} = -142.7$  kcal, the same as at infinite dilution, will be taken.

(b)  $\text{Pu}^{+4}$ . Evans<sup>27</sup> has determined the heat of oxidation of  $\text{Pu}^{+3}$  to  $\text{Pu}^{+4}$  by  $\text{Fe}^{+3}$  and  $\text{Cr}_2\text{O}_7^{2-}$ . Correcting her data to agree with recent determinations of the  $\text{Fe}^{+2}$ - $\text{Fe}^{+3}$  couple by Fontana,<sup>41</sup> the value  $\Delta H_{298} = 11.6$  kcal can be calculated for the  $\text{Pu}^{+3}$ - $\text{Pu}^{+4}$  couple in 0.5M  $\text{HClO}_4$ . However, Connick and McVey<sup>45</sup> have determined the potential of this couple in 1M  $\text{HClO}_4$  over a range of temperatures and have obtained  $\Delta H_{298} = 13.5$  kcal. The Connick and McVey value is considered more reliable. There should be no great difference between the value in 0.5M  $\text{HClO}_4$  and 1M  $\text{HClO}_4$ . For the reaction



we accept as the best value in 1M  $\text{HClO}_4$ ,

$$\Delta H_{298} = 13 \pm 1 \text{ kcal}$$

Connick and McVey<sup>45</sup> obtained  $-0.982$  volt as the formal potential, or actually observed value with no corrections, for the  $\text{Pu}^{+3}$ - $\text{Pu}^{+4}$  couple in 1M  $\text{HClO}_4$ , or  $\Delta F_{298} = 22.6$  kcal. This value together with the  $\Delta H$  of the couple yields  $\Delta H_{298} = -128.6$  kcal and  $\Delta F_{298} = -120.1$  kcal for the formation of  $\text{Pu}^{+4}$  in 1M  $\text{HClO}_4$  from the metal.

The  $\Delta F$  for the formation of  $\text{Pu}^{+4}$  in 1M HCl can be obtained from the  $\text{Pu}^{+3}$  value and the  $\text{Pu}^{+3}$ - $\text{Pu}^{+4}$  potential measurements in 1M HCl by Howland, Kraus, and Hindman,<sup>43</sup> by Kraus,<sup>25</sup> and by Hindman.<sup>34</sup> Connick and McVey<sup>45</sup> have recalculated these measurements to obtain  $-0.959$  volt for the formal potential in 1M HCl or the observed potential uncorrected for activity coefficients. This then corresponds to

$$\Delta F_{298} = 22.1 \pm 0.1 \text{ kcal}$$

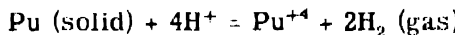
for



and therefore

$$\Delta F_{298} = -120.6 \text{ kcal}$$

for the formation of  $\text{Pu}^{+4}$  in 1M HCl from the metal according to the reaction



The  $\Delta H$  value in 1M HCl can be obtained by assuming the same  $\Delta S$  value for the  $\text{Pu}^{+3}$ - $\text{Pu}^{+4}$  couple as for the corresponding uranium couple or by assuming the same change in  $\Delta H$  in going from perchloric acid solutions to hydrochloric acid solutions as given in the case of uranium by Brewer, Bromley, Gilles, and Lofgren.<sup>1</sup> The two results agree closely. The average gives  $\Delta H_{298} = -129.0$  kcal for the formation of  $\text{Pu}^{+4}$  in 1M HCl.

(c)  $\text{PuO}_2^{++}$ . Correcting Evans's<sup>27</sup> determinations to agree with Fontana<sup>41</sup> as in the case of  $\text{Pu}^{+4}$ , we obtain for



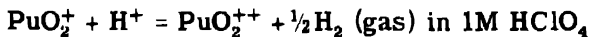
$\Delta H_{298} = 80 \pm 2$  kcal in 0.5M  $\text{HClO}_4$ , which will be also taken as the 1M  $\text{HClO}_4$  value. Connick and McVey<sup>45</sup> have combined the  $\text{Pu}^{+4}$ - $\text{PuO}_2^{++}$  potential measurements of Hindman<sup>34</sup> and of Kraus<sup>25</sup> with the equilibrium determinations of Kasha and Sheline<sup>42</sup> to obtain -1.042 volts as the formal potential for the  $\text{Pu}^{+4}$ - $\text{PuO}_2^{++}$  couple in 1M HCl. Connick and McVey<sup>45</sup> also give -1.023 volts for the couple in 1M  $\text{HClO}_4$ . Thus we obtain  $\Delta F_{298} = -72.4$  kcal for the formation of  $\text{PuO}_2^{++}$  from the metal in 1M HCl and  $\Delta F_{298} = -72.8$  for the formation in 1M  $\text{HClO}_4$ . The hydrochloric acid value would be expected to be more negative. The  $\text{Pu}^{+4}$ - $\text{PuO}_2^{++}$  potential in 1M  $\text{HClO}_4$  is probably not negative enough, but the differences are within the experimental error of the measurements.

The  $\Delta H$  given above for the  $\text{Pu}^{+3}$ - $\text{PuO}_2^{++}$  couple yields  $\Delta H_{298} = -61.6$  kcal for the formation of  $\text{PuO}_2^{++}$  from the metal in 1M  $\text{HClO}_4$ . To obtain the  $\Delta H$  value in 1M HCl, the same procedure will be used as was used for  $\text{Pu}^{+4}$  in 1M HCl. Assuming the same  $\Delta S$  as for the uranium system gives  $\Delta H = -62.7$  kcal. Assuming the same change from perchloric to hydrochloric acid solutions as in the case of uranyl ion,  $\Delta H = -61.7$  is obtained.  $\Delta H_{298} = -62.2$  kcal was taken as the partial heat of formation of  $\text{PuO}_2^{++}$  from the metal in 1M HCl.

(d)  $\text{PuO}_2^+$ . Kraus and Moore<sup>38</sup> report  $-0.930 \pm 0.015$  volt for the formal potential of the  $\text{PuO}_2^+ - \text{PuO}_2^{++}$  couple in about 0.1M  $\text{ClO}_4^-$ . We have taken this value as the 1M  $\text{HClO}_4$  value. The difference in entropies of  $\text{PuO}_2^+$  and  $\text{PuO}_2^{++}$  was estimated as 32 e.u. from graphs of ionic radius against entropy for monovalent and divalent ions. This gives

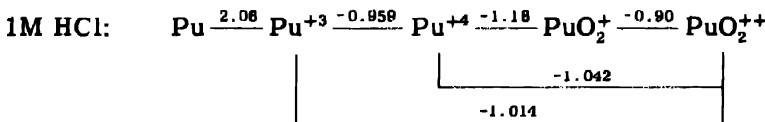
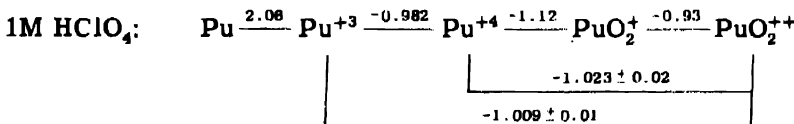
$$\Delta F_{298} = +21.4 \pm 0.4 \text{ kcal} \quad \Delta S_{298} = -16 \text{ e.u.} \quad \Delta H_{298} = +16.6 \pm 2 \text{ kcal}$$

for



Connick and McVey<sup>45</sup> give  $-0.912$  volt for the  $\text{PuO}_2^+ - \text{PuO}_2^{++}$  formal potential in 0.5M HCl. Using the uranium data to correct to 1M HCl,  $\Delta F_{298} = 20.8$  kcal is obtained. Using  $\Delta S_{298} = -16$  e.u.,  $\Delta H_{298} = 16.0$  kcal is obtained for the above reaction in 1M HCl.

(e) Summary of Heats and Free Energies of Ions. The accompanying diagrams summarize the aqueous formal potentials in volts.



The heats and free energies of formation of the ions from the metal are summarized in Table 4. The partial heats and free energies of formation of the ions from  $\text{Pu}^{+3}$  are given in kilocalories per mole as follows:

	1M $\text{HClO}_4$		1M HCl	
	$\Delta H_{298}$	$\Delta F_{298}$	$\Delta H_{298}$	$\Delta F_{298}$
$\text{Pu}^{+3} + \text{H}^+ = \text{Pu}^{+4} + \frac{1}{2}\text{H}_2 \text{ (gas)}$	$13.0 \pm 1$	$22.6 \pm 0.1$	$12.9 \pm 1$	$22.1 \pm 0.1$
$\text{Pu}^{+3} + 2\text{H}_2\text{O (liq)} = \text{PuO}_2^+ + 2\text{H}^+ + \frac{1}{2}\text{H}_2 \text{ (gas)}$	$63 \pm 3$	$48.5 \pm 1$	$64 \pm 3$	$49.5 \pm 1$
$\text{Pu}^{+3} + 2\text{H}_2\text{O (liq)} = \text{PuO}_2^{++} + \text{H}^+ + \frac{1}{2}\text{H}_2 \text{ (gas)}$	$80 \pm 2$	$69.9 \pm 1$	$80 \pm 2$	$70.3 \pm 1$

The presentation of the data in this manner has some advantages over Table 4 since these values do not depend upon the heat and free energy of solution of plutonium metal. Also, the uncertainties of the data are shown better here. However, either set of values will give the same results in calculations.

**3.2 Fluorides.**  $\text{PuF}_3$ . The vapor pressures, the boiling point, and heat and entropy of fusion have been recalculated from vapor pressure measurements of Phipps, Seifert, and Simpson.<sup>39</sup> These workers have plotted the logarithms of the vapor pressures against reciprocal temperatures and through the points have drawn two lines to represent solid and liquid vaporization. The intersection of these lines is at 1447°K. They have taken this temperature to be the melting point and from the slopes have calculated the heat and entropy of fusion to be 7.88 kcal and 5.47 e.u. An extrapolation of their equation gives a boiling point of 2310°K and a  $\Delta S$  of vaporization of 38 e.u. The values so obtained of the melting point, heat and entropy of fusion, and entropy of vaporization do not seem to be reasonable when compared with the corresponding values for other fluorides.

For this reason we have examined their data and find that their points could better be considered to lie on a curve instead of on two straight lines. This is to be expected if the  $\Delta C_p$  of vaporization is considered. A curve taking into account a  $\Delta C_p$  of sublimation of -14 e.u. would represent their data over their entire temperature range extremely well and would not indicate a melting point. Thus we have used their data to calculate a free energy of sublimation equation of the form

$$\Delta F = \Delta H_0 - 2.3(-14) T \log T + IT$$

from which the vapor pressures have been calculated up to  $10^{-4}$  atm. In accord with other fluorides, a melting point of 1680°K and a heat of fusion of 13 kcal have been estimated. These have been used with the solid vaporization equation to obtain a similar equation for the liquid, using  $\Delta C_p = -16$ , from which the remaining vapor pressures and the heat and entropy of vaporization at the normal boiling point have been calculated. The resulting entropy of vaporization has the reasonable value of 27 e.u.

$\text{PuF}_3$  forms black or purple hexagonal crystals of the  $\text{LaF}_3$  type with  $a_1 = 4.087$ ,  $a_3 = 7.240$ , and a density<sup>8,40</sup> of 9.32 g/cc.

Values for  $(\Delta F - \Delta H_{298})/T$  have been estimated from the values for  $\text{UF}_3$  calculated by the authors of this paper.<sup>1</sup> The heat of formation,  $\Delta H_{298}$ , was determined by Westrum and Eyring<sup>47</sup> from the heat of precipitation of  $\text{PuF}_3$ .

Calculations based on the values in the accompanying tables indicate that  $\text{PuF}_3$  vaporizes essentially undecomposed and that  $\text{PuF}_3$  (gas) is stable to above 4000°K at 1 atm (Fig. 1). At lower pressures it decomposes to gaseous metal and fluorine provided there are no important lower gaseous halides. At 1 atm total pressure, at the boiling

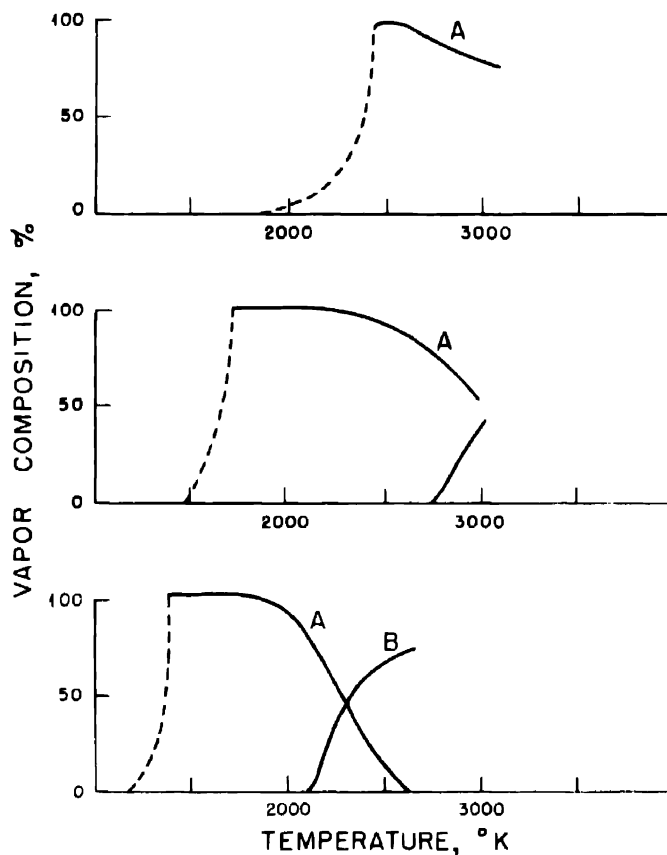


Fig. 1—Gaseous equilibrium over-all composition,  $\text{PuF}_3$ . Curve A,  $\text{PuF}_3$ ; curve B, monatomic fluorine. Pressures: top, 1 atm; center,  $10^{-3}$  atm; bottom,  $10^{-6}$  atm.

point of  $\text{PuF}_3$ ,  $\text{Pu}$  (gas) is barely noticeable owing to the slight disproportionation of the  $\text{PuF}_3$ .

**3.3 Chlorides.** (a)  $\text{PuCl}_3$ . Abraham, Brody, Davidson, Hagemann, Karle, Katz, and Wolf<sup>19</sup> studied the preparation and properties of  $\text{PuCl}_3$ . The melting point has been determined by Robinson.<sup>2</sup> The vapor pressures, boiling point, and heat and entropy of vaporization have been recalculated from the data of Erway, Gilpatrick,

Jasaitis, Johnson, Phipps, Sears, Seifert, and Simpson<sup>39</sup> by taking into account a  $\Delta C_p$  of vaporization of -12 and a  $\Delta C_p$  of sublimation of -10 e.u. This procedure gave a more reasonable entropy of vaporization at the boiling point than did an extrapolation of their equation. Their equation and the one chosen agree over the experimental range. The heat of fusion has been determined by the same workers from the slopes of vapor-pressure curves. The solid equation was obtained by using the heat of fusion and equating the vapor pressure of solid and liquid at the melting point. The vapor pressures used are somewhat lower than those of Weinstock<sup>3</sup> and may be in error because of impurities. This is evidenced by a lower melting point being obtained from the vapor-pressure curves than from a direct determination.  $\text{PuCl}_3$  forms green hexagonal  $\text{LaCl}_3$ -type crystals with  $a_1 = 7.380$ ,  $a_3 = 4.238$ , and a density of 5.70 g/cc.<sup>49</sup>

Values of the function  $(\Delta F - \Delta H_{298})/T$  have been estimated from those of the corresponding uranium compound.<sup>1</sup> Westrum and Robinson<sup>48, 29</sup> have obtained from the heats of solution of the metal and the chloride  $\Delta H = -229.3$  for the heat of formation of  $\text{PuCl}_3$  in kilocalories per mole.

Figure 2 indicates that  $\text{PuCl}_3$  vaporizes undecomposed, but that at higher temperatures and lower pressures it decomposes to gaseous monatomic elements if there are no stable intermediate lower chlorides.

(b)  $\text{PuCl}_4$ . There are no data that prove the existence of solid  $\text{PuCl}_4$ , and there are many data to indicate that it does not exist. Values of melting point, heat and entropy of fusion, vapor pressures, boiling point, and heat and entropy of vaporization can be taken the same as for uranium.<sup>1</sup> Values of the function  $(\Delta F - \Delta H_{298})/T$  have been estimated from the same source.

Calculations based upon these values indicate that the dissociation pressure of  $\text{Cl}_2$  over solid  $\text{PuCl}_4$  at room temperature is about  $10^7$  atm, which accounts for the fact that  $\text{PuCl}_4$  has not been found. Despite the nonexistence of solid  $\text{PuCl}_4$  there will be some  $\text{PuCl}_4$  in the gaseous phase. The maximum concentration of  $\text{PuCl}_4$  (gas) in a system of total composition  $\text{PuCl}_3$ , which will occur in the neighborhood of the boiling point of the trichloride, is about  $10^{-5}$  atm when the total pressure is 1 atm and the temperature is 2040°K. Much higher concentrations of  $\text{PuCl}_4$  (gas) can, of course, be obtained by increasing the halogen pressure, as by passing  $\text{Cl}_2$  over heated  $\text{PuCl}_3$ . For example, at 2000°K (where the vapor pressure of  $\text{PuCl}_3$  is about 0.1 atm), if the pressure of  $\text{Cl}_2$ , which equals approximately the pressure of  $\text{Cl}_1$ , is about 0.5 atm, the pressure of  $\text{PuCl}_4$  will be about  $2 \times 10^{-2}$  atm.

(c)  $\text{PuCl}_5$  and  $\text{PuCl}_6$ . There is no evidence for the existence of these substances in either the condensed or gaseous phase. They would be expected to be even more unstable than  $\text{PuCl}_4$  and to be of no importance under any conditions.

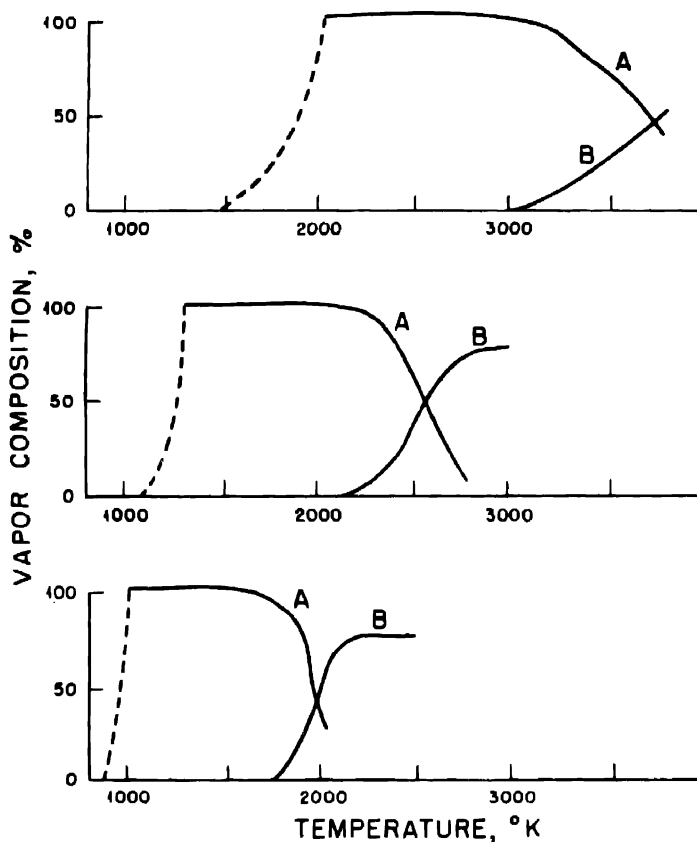


Fig. 2—Gaseous equilibrium over-all composition,  $\text{PuCl}_3$ . Curve A,  $\text{PuCl}_3$ ; curve B, monatomic chlorine. Pressures: top, 1 atm; center,  $10^{-3}$  atm; bottom,  $10^{-6}$  atm.

**3.4 Bromides.** (a)  $\text{PuBr}_3$ . Davidson, Hagemann, Hyde, Katz, and Sheft<sup>21</sup> studied the methods of preparation and properties of  $\text{PuBr}_3$ . The melting point has been determined by Robinson.<sup>2</sup> The heat of fusion has been determined by Phipps, Seifert, and Simpson<sup>39</sup> by the difference in slopes of vapor pressure curves for liquid and solid. The vapor pressures, boiling point, and heat and entropy of vaporization have been recalculated from the data of these workers by taking into account a  $\Delta C_p$  of vaporization of -16 and of sublimation of -12

e.u. The entropy of vaporization at the boiling point as determined by an extrapolation of their equation is far too large and is replaced by a more reasonable value when the extrapolation is made with the aid of an equation involving  $\Delta C_p$ . Zachariasen<sup>49</sup> reports that  $\text{PuBr}_3$  forms

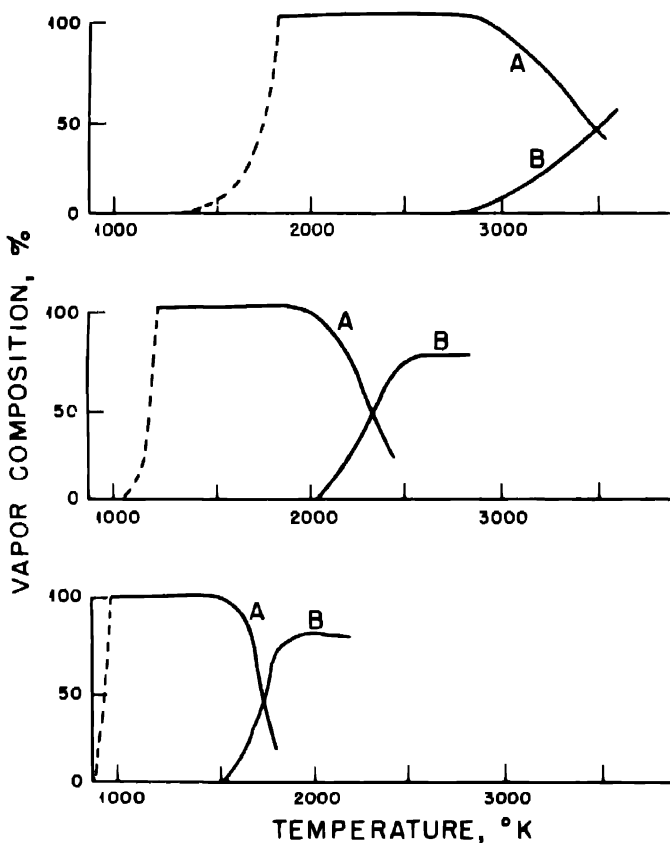


Fig. 3—Gaseous equilibrium over-all composition,  $\text{PuBr}_3$ . Curve A,  $\text{PuBr}_3$ ; curve B, monatomic bromine. Pressures: top, 1 atm; center,  $10^{-3}$  atm; bottom,  $10^{-6}$  atm.

green orthorhombic  $\text{NdBr}_3$ -type crystals with a density of 6.65 to 6.69 g/cc.

Values of the function  $(\Delta F - \Delta H_{298})/T$  have been estimated from corresponding values for uranium.<sup>1</sup> The heat of formation was obtained from the heats of solution of the metal and the salt in 6M HCl, i.e.,  $\Delta H = -30.9$  obtained by Westrum.<sup>29,26</sup> Westrum and Robinson<sup>48</sup> have recently recalculated their results to obtain  $\Delta H_{298} = -199.2$  kcal for the heat of formation of  $\text{PuBr}_3$ .

Figure 3 indicates that  $\text{PuBr}_3$  vaporizes undecomposed but that at higher temperatures and lower pressures decomposes to monatomic gaseous elements.

(b)  $\text{PuBr}_4$ . There are no indications that  $\text{PuBr}_4$  is stable in either a condensed or gaseous phase. Values of melting point, heat and entropy of fusion, vapor pressure, boiling point, and heat and entropy of vaporization have been taken the same as for the uranium system.<sup>1</sup> Values of the function  $(\Delta F - \Delta H_{298})/T$  have been estimated.

The calculated equilibrium decomposition pressure of  $\text{Br}_2$  over solid  $\text{PuBr}_4$  at room temperature is  $10^{18}$  atm. The  $\text{PuBr}_4$  stability and concentration even in the gaseous phase is expected to be quite small, although in the presence of halogen and solid trivalent halide in the neighborhood of its boiling point, appreciable quantities of gaseous tetravalent halide probably exist.

(c)  $\text{PuBr}_5$  and  $\text{PuBr}_6$ . These are expected to be even less stable than  $\text{PuBr}_4$  and to be of no importance.

3.5 Iodides. (a)  $\text{PuI}_3$ . Hagemann, Abraham, Davidson, Katz, and Sheft<sup>10</sup> have studied the preparation and properties of  $\text{PuI}_3$ . The melting point, heat and entropy of fusion, vapor pressures, boiling point, heat and entropy of vaporization, and values of the free-energy function  $(\Delta F - \Delta H_{298})/T$  have been estimated from the values<sup>1</sup> given for  $\text{UI}_3$  and from the values for some of the rare-earth iodides.<sup>12</sup> The heat of formation was estimated by taking the same difference between the heats of formation for  $\text{PuBr}_3$  and  $\text{PuI}_3$  as existed between the heats of formation for  $\text{UBr}_3$  and  $\text{UI}_3$ . This procedure is not completely reliable but can be expected to give fairly good values in this case. As an indication of the closeness of this approximation, we point to the difference of  $32.4 \pm 2$  kcal between the heats of formation of  $\text{UCl}_3$  and  $\text{UBr}_3$  (see reference 1) determined by the same worker and the difference of 30.3 between  $\text{PuCl}_3$  and  $\text{PuBr}_3$ .  $\text{PuI}_3$  forms a bright green orthorhombic  $\text{NdBr}_3$ -type crystal<sup>13</sup> with a density of 6.9 g/cc.

(b)  $\text{PuI}_4$ . See the discussion of  $\text{PuBr}_4$ . The calculated decomposition pressure of  $\text{I}_2$  at room temperature is  $10^{30}$  atm. It would be expected that the maximum concentration of  $\text{PuI}_4$  (gas) would be much less than that of  $\text{PuBr}_4$  (gas).

(c)  $\text{PuI}_5$  and  $\text{PuI}_6$ . These compounds would be expected to be much less stable than the corresponding bromine compounds.

3.6 Oxides. (a)  $\text{PuO}_3$ . According to estimated heats, no oxide above  $\text{PuO}_2$  would be expected to be stable.

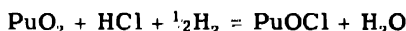
(b)  $\text{PuO}_2$ . Phipps, Seifert, and Simpson<sup>30</sup> have measured the quantity of plutonium that vaporizes in a vacuum from a sample originally  $\text{PuO}_2$ . They found that the pressure increases with the time until a steady state is obtained. They have attributed this change to a de-

composition of  $\text{PuO}_2$ . Thus from their data it is possible to give only a maximum vapor pressure of  $\text{PuO}_2$ . By comparing their results with the value for the vapor pressure<sup>1</sup> of  $\text{UO}_2$ , we have chosen a pressure of  $10^{-8}$  atm for  $\text{PuO}_2$  (gas) in equilibrium with  $\text{PuO}_2$  (solid) at 1800°K. From the free energy corresponding to this vapor pressure and an estimated entropy of vaporization of 30 e.u., the temperature at which the vapor pressure is equal to  $10^{-5}$  atm is calculated as 2200°K.

These workers also found in their curves a slight break at about 2000°K, which could be accounted for by a melting. However, this cannot be given definitely as the melting point of  $\text{PuO}_2$  since the solid species was probably not pure  $\text{PuO}_2$ .  $\text{PuO}_2$  forms yellow cubic  $\text{CaF}_2$ -type crystals with  $a = 5.386$  and a density of 11.44 g/cc as reported by Mooney and Zachariasen.<sup>37</sup>

Values of the function  $(\Delta F - \Delta H_{298})/T$  were estimated from the corresponding values in the uranium system.<sup>1</sup>

The heat of formation has been obtained by combining the values of  $(\Delta F - \Delta H_{298})/T$  with the data of Abraham and Davidson<sup>6</sup> on the reaction



These workers have measured the free-energy change for this reaction over the temperature range 723 to 915°K and have expressed their results in an equation of the form

$$\Delta F = -8.5 + 9.5T/1000 \text{ kcal}$$

Although they estimated corrections that should be applied to their values to account for the amount of hydrogen diffusing out through their quartz chamber, they have not used these corrections in summarizing their data. We have used their estimated corrections for this effect and have obtained a free-energy equation

$$\Delta F = -7.9 + 9.5T/1000 \text{ kcal}$$

instead of their

$$\Delta F = -8.5 + 9.5T/1000 \text{ kcal}$$

The values of the free energies of  $\text{PuOCl}$  from this report and of water and hydrochloric acid from Brewer<sup>15</sup> were combined with this equation to calculate the free energy of  $\text{PuO}_2$  at high temperatures. The heat of formation was then obtained from the free energy and the  $(\Delta F - \Delta H_{298})/T$  tables.  $\Delta H_{298} = -251$  kcal was obtained, which is in

excellent agreement with the  $U^{+4}$  and  $Pu^{+4}$  heats and the heat of formation of  $UO_2$ .

(c)  $Pu_2O_3$ . There are no data on the melting or vaporization. A constant entropy of formation of -63 e.u. has been assumed in accord with the entropies of formation of other metallic oxides as presented by Brewer.<sup>5</sup> A value of -387 kcal for the heat of formation of  $Pu_2O_3$  was obtained from a consideration of the difference in the heats of formation of  $\frac{1}{2}La_2O_3$  and  $LaCl_3$ , and the heat of formation of  $PuCl_3$ . The heat of formation used for  $\frac{1}{2}La_2O_3$  was -228 kcal from Bichowsky and Rossini<sup>14</sup> and for  $LaCl_3$  was -264 kcal from the Halide Report by the authors of this paper.<sup>12</sup>

The value so obtained indicates that if  $PuO$  is very stable, as is indicated by the measurements of Phipps, Seifert, and Simpson,<sup>39</sup> then  $Pu_2O_3$  will disproportionate to  $PuO$  and  $PuO_2$ . However, it appears that  $PuO_2$  may be reduced to a solid solution of  $PuO_2$  and  $Pu_2O_3$ . Mooney and Zachariasen<sup>37</sup> report a solid solution range around  $Pu_4O_7$ . Westrum<sup>6</sup> gives results on the reduction of  $PuO_2$  at high temperatures by potassium, sodium, carbon, barium, methane, tantalum, lithium, and calcium, but these are not too readily used for the calculation of thermodynamic quantities.

(d)  $PuO$ . There are no data for the melting of this compound. It forms black cubic sodium chloride-type crystals with  $a = 4.948$  and a density of 13.95 g/cc.<sup>37</sup> The entropy of formation has been assumed constant and has been estimated in comparison with data for other metallic oxides, which are summarized by Brewer.<sup>5</sup> The species volatilizing from the samples used by Phipps, Seifert, and Simpson<sup>39</sup> may be  $PuO$  (gas), but their results have not as yet been interpreted completely.

From the data given by these workers, a very rough phase diagram has been sketched which indicates that probably in their experiments with oxidized metal both  $PuO$  and  $Pu$  are vaporizing, while in the experiments with material originally  $PuO_2$ , both  $O_2$  and  $PuO$  are vaporizing. If this indication is correct, the composition would not change much and so the vapor pressure should approach a constant value at any temperature. This may be the explanation of their "steady state." From this diagram and also from a consideration of the vapor pressure of  $UO$  (see reference 1) a value for the vapor pressure of  $PuO$  was estimated.

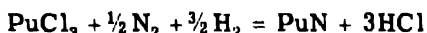
There are no data from which a good heat of formation may be calculated; however, an estimate may be made by considering some chemical evidence. From the fact that  $PuO$  is known to exist and  $Pu_2O_3$  is believed to disproportionate, the heat of formation must be more negative per equivalent than  $PuO_2$  and  $Pu_2O_3$ , in order to prevent disproportionation of the  $PuO$ . By considering these data we estimate

that the heat of formation of PuO lies between -130 and -140 kcal per mole. If PuO is actually as stable as this, we would predict that it might be possible to prepare the divalent halides by heating the trivalent halides with the metal.

**3.7 Carbide.** (a) PuC. The value of the entropy of formation was estimated from corresponding values of other diatomic carbides, which are considered by Brewer,<sup>5</sup> and was assumed constant with temperature. The heat of formation has not been measured; therefore only estimates can be made. PuC is reported by Zachariasen<sup>28,30</sup> to have the sodium chloride crystal structure with  $a = 4.910$  and a density of 13.99 g/cc. Considering the heat of formation<sup>1</sup> of UC we have estimated that the heat of formation of PuC is -25 kcal per mole.

**3.8 Nitride.** (a) PuN. The value for the entropy of formation was estimated from corresponding values for other metallic nitrides as summarized by Brewer<sup>5</sup> and was assumed constant with temperature. PuN is brown and has the cubic sodium chloride-type crystal structure with  $a = 4.895$  and a density of 14.22 g/cc, as reported by Zachariasen.<sup>28,40</sup>

There has been no determination of the heat of formation, and not much chemistry has been reported from which the heat can be calculated. Abraham, Davidson, and Westrum<sup>7</sup> report qualitative results on the reaction

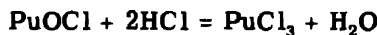


Estimates based upon their work indicate that the free energy of this reaction must be less than 73 kcal. This, when combined with the free energies of the other substances and the entropy of PuN, gives a heat of formation more negative than -49 kcal. The value of -95 kcal chosen from a consideration of the heats of formation of the other metallic nitrides and especially of UN (see reference 1) is consistent with the calculated value.

**3.9 Oxyhalides.** (a) PuOF. There is insufficient evidence for the calculation or estimation of thermodynamic constants. It has been found by Robinson<sup>2</sup> in some melting experiments and has been identified by Zachariasen.<sup>8,40</sup> It is black-metallic in color and has the cubic CuF<sub>2</sub> type of crystal structure with  $a = 5.70$  and a density of 9.76 g/cc. Estimates based upon the heats and entropies of formation of PuOC<sub>1</sub>, PuCl<sub>3</sub>, and PuF<sub>3</sub> indicate very roughly that the heat of formation of PuOF should be somewhat less negative than -270 kcal per mole and that the entropy of formation should be about -40 e.u.

(b) PuOCl. Abraham, Brody, Davidson, Hagemann, Karle, Katz, and Wolf<sup>19</sup> have studied the preparation and properties of PuOCl. There are no data on the melting point, heat and entropy of fusion,

vapor pressures, boiling point, or heat and entropy of vaporization. PuOCl is green or blue-green and has the tetragonal PbFCl-type crystal structure with  $a_1 = 4.004$ ,  $a_3 = 6.779$ , and a density of 8.81 g/cc.<sup>19</sup> The data of Sheft and Davidson<sup>23</sup> were used to obtain the values of the free-energy equation for the formation of PuOCl. These workers have measured the equilibrium pressures of the reaction



between the temperatures 814 and 969°K and have expressed their results in a free-energy equation

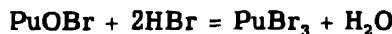
$$\Delta F = -20.8 + 30.9T/1000 \text{ kcal}$$

This equation, when combined with the  $\Delta H_{298}$  and  $(\Delta F_{1000} - \Delta F_{298})/T$  values of PuCl<sub>3</sub> from this paper and of hydrogen chloride and water vapor from Sec. I of the Halide Report by Brewer,<sup>15</sup> gave

$$\Delta F = -222.7 + 37.9T/1000 \text{ kcal}$$

for the formation of PuOCl around 1000°K. This is in excellent agreement with  $\Delta H_{298} = -222.8$  kcal, which was determined by Westrum and Robinson<sup>24,25</sup> for PuOCl from its heat of solution.

(c) PuOBr. Davidson, Hagemann, Hyde, Katz, and Sheft<sup>21</sup> have studied the preparation and properties of PuOBr. There are no data on the melting point, heat and entropy of fusion, vapor pressures, boiling point, or heat and entropy of vaporization. PuOBr is deep green and has the tetragonal PbFCl crystal structure with  $a_1 = 4.014$ ,  $a_3 = 7.556$ , and a density of 9.07 g/cc. Sheft and Davidson<sup>4</sup> have measured the equilibrium constants for the reaction



and have expressed their results as

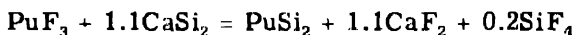
$$\Delta F = -22.8 + 33.2T/1000 \text{ kcal}$$

Their equation is used together with the  $\Delta H_{298}$  and  $(\Delta F_{1000} - \Delta F_{298})/T$  values of PuBr<sub>3</sub> from this paper and of hydrogen bromide and water vapor from Sec. I of the Halide Report by Brewer<sup>15</sup> to obtain  $\Delta F = -210 + 33T/1000$  kcal for the formation of PuOBr around 1000°K. By comparison with PuCl<sub>3</sub> and PuOCl one would estimate a  $\Delta H_{298}$  value

more negative by about 8 to 10 kcal and a  $(\Delta F_{1000} - \Delta H_{298})/T$  value somewhat more positive, but the values given in Table 3 should give  $\Delta F$  values of the right order of magnitude around 1000°K.

(d) PuOI. This compound has been prepared in the attempted preparations of PuI<sub>3</sub> and found to have a green color and the tetragonal PbFCl type of crystal structure with  $a_1 = 4.034$ ,  $a_3 = 9.151$ , and a density of 8.46 g/cc.<sup>49</sup> However, it has not been extensively studied, and therefore there are insufficient thermodynamic data to evaluate the heat and entropy of formation. However, estimates may be made based upon slight chemical evidence and the values of PuOBr and PuOCl. The entropy of formation of -32 e.u. is estimated for PuOI. From the paper reporting the preparation and properties of PuOI by Hagemann, Abraham, Davidson, Katz, and Sheft,<sup>10</sup> free-energy estimates have been made and combined with the above entropy to give a heat of formation more negative than -182 ( $\text{PuO}_2 = -254$ ) kcal per mole. On the basis of some other experiments, a value more negative than -167 ( $\text{PuO}_2 = -254$ ) was estimated. On the basis of the heats of formation for PuOBr, PuOCl, PuCl<sub>3</sub>, PuBr<sub>3</sub>, and PuI<sub>3</sub>, one can estimate a heat of formation for PuOI more negative than -195 kcal per mole, which is taken as a very rough value for  $\Delta H_{298}$ .

3.10 Silicide. (a) PuSi<sub>2</sub>. The work of Westrum,<sup>11</sup> who found that the silicide reaction



did not occur at 1573°K but did go at 1823°K, was used to calculate the free energy of the reaction, which was then used with the free energies of formation of the other substances to obtain a free energy of formation of PuSi<sub>2</sub>. The free energy and entropy of calcium fluoride were obtained from the Halide Report by the authors of this paper.<sup>12</sup> For silicon tetrafluoride the entropy of formation was calculated from the entropy of the compound as given by Kelley<sup>13</sup> and the entropies of the elements as given by Brewer;<sup>51</sup> the heat of formation was obtained from Bichowsky and Rossini.<sup>14</sup> For calcium silicide the entropy of formation was estimated from a consideration of the entropies of other compounds of calcium as tabulated by Brewer;<sup>5</sup> the heat of formation is from Bichowsky and Rossini.<sup>14</sup> The entropy of PuSi<sub>2</sub> was taken to be the same as for calcium silicide. The calculated free energy of PuSi<sub>2</sub> in the neighborhood of 1700°K is -228 kcal per mole, and this combined with the estimated entropy gives -211 kcal per mole as the very approximate heat of formation. PuSi<sub>2</sub> has a silvery metallic color and the tetragonal ThSi<sub>2</sub> crystal structure with  $a_1 = 3.97$ ,  $a_3 = 13.55$ , and  $d = 9.12$  g/cc as reported by Zachariasen.<sup>44</sup>

**3.11 Sulfides.** There is insufficient evidence to enable the calculation of the thermodynamic values for any of the plutonium sulfides. Abraham, Davidson, and Westrum<sup>16</sup> report the following observations. They heated  $\text{PuF}_3$  and calcium in a barium sulfide crucible (which was prepared by the authors of this paper<sup>17</sup>) and obtained a phase that has been thought to be  $\text{PuS}$ . It was golden bronze and was believed to have the cubic sodium chloride type of crystal structure. Using an apparatus similar to that used by the authors of this paper at Berkeley,<sup>18</sup> they passed hydrogen sulfide over  $\text{PuO}_2$  and obtained  $\text{Pu}_2\text{O}_2\text{S}$  and  $\text{Pu}_{3-x}\text{S}_4$ , both identified by Zachariasen.<sup>20</sup>  $\text{Pu}_2\text{O}_2\text{S}$  was slate black and had the hexagonal  $\text{La}_2\text{O}_3$  crystal structure with  $a_1 = 3.919$ ,  $a_3 = 6.755$ , and a density of 9.95 g/cc.  $\text{Pu}_2\text{S}_3$  was black with a purplish tinge and had the cubic  $\text{Ce}_3\text{S}_4$  type of crystal structure with  $a = 8.437$  and a density of 8.41 g/cc. In addition they obtained a product that was analyzed as nearly  $\text{Pu}_2\text{S}_3$  but was not isomorphous with the  $\text{Ce}_{3-x}\text{S}_4$  prepared in the graphite-hydrogen sulfide system. This system seems to be similar in all respects to the cerium-sulfur system since  $\text{Ce}_2\text{S}_3$  prepared with a slight amount of oxide impurity is also converted to a different noncubic crystal form, which may be the  $\text{Th}_2\text{S}_3$ -type crystal form.

An estimate of the heat of formation of  $\text{Pu}_2\text{S}_3$  can be made by taking the same difference between the heat of formation of  $\frac{1}{2}\text{Pu}_2\text{S}_3$  and  $\text{PuCl}_3$  as there is between  $\frac{1}{2}\text{Ce}_2\text{S}_3$  and  $\text{CeCl}_3$ . The heat of formation of  $\text{Ce}_2\text{S}_3$  is taken from Evans,<sup>36</sup> and the heat of formation of  $\text{CeCl}_3$  is taken from the Halide Report.<sup>12</sup> Such a procedure gives, as the heat of formation of  $\text{Pu}_2\text{S}_3$ , -240 kcal from rhombic sulfur and -286 kcal from  $\text{S}_2$  (gas). The value of  $(\Delta F - \Delta H_{298})/T$  has been taken the same as the entropy of formation per atom of sulfur of barium sulfide.<sup>18</sup>

#### 4. GRAPHS OF GASEOUS HALIDE EQUILIBRIA

The illustrations given here are for the purpose of indicating the important plutonium halide species for a given condition so that the thermodynamic constants given in Secs. 1 and 2 of this paper can be correctly used to calculate gaseous equilibria in plutonium systems.

Each illustration gives the percentages of each gaseous species in a system in which the total composition is fixed; for example, the  $\text{PuI}_3$  figure (Fig. 4) applies to a system in which the ratio of total I to Pu is always 3. The pressure is fixed at the value given, and the percentage of the total pressure due to any gaseous species is shown as a function of the temperature. Solid or liquid phases are not indicated but are usually evident from examination of Table 1 and the gaseous composition indicated in the figure.

Compositions intermediate between those given can usually be estimated by comparing the distribution of species from the figures nearest to the desired composition. By passing a large excess of halogen through the system, the species distribution can usually be estimated from an examination of the graph for the highest oxidation state.

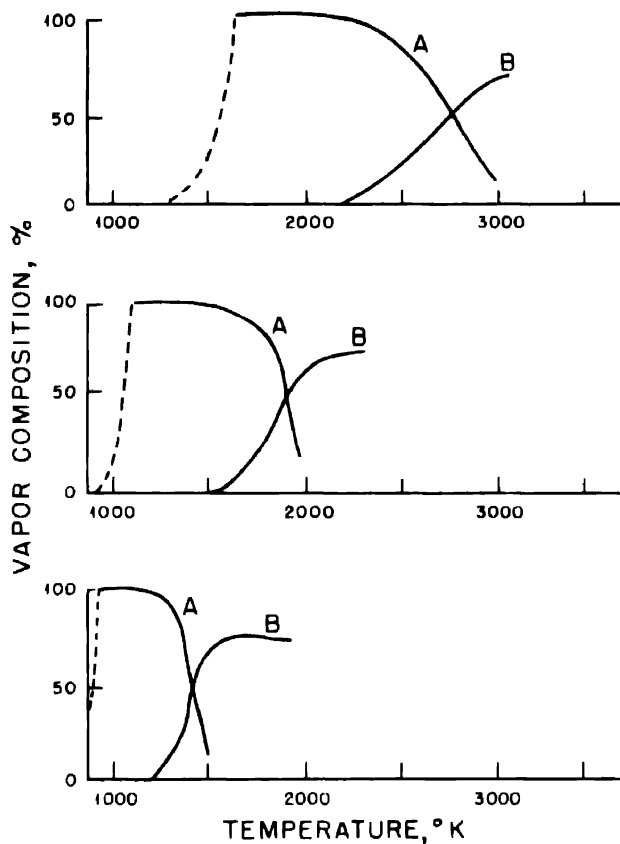


Fig. 4—Gaseous equilibrium over-all composition,  $\text{PuI}_3$ . Curve A,  $\text{PuI}_3$ ; curve B, monatomic iodine. Pressures: top, 1 atm; center,  $10^{-3}$  atm; bottom,  $10^{-6}$  atm.

Since no accurate data are available on the extent of solid or liquid solution formation, this formation was neglected in the calculations of these figures from the data of Tables 1 to 4. That is, all solids and liquids were assumed to be immiscible. In cases where the laws of solution are known, they may be used to calculate the system more precisely, and in cases where solution is known to occur but where

the law of solution is not known, Raoult's law may be assumed as a first approximation. In any event it is expected that the graphs would not be changed appreciably by more rigorous treatment. Certainly the form of the curves will remain unchanged. And, of course, since a large portion of each graph covers a range in which everything is gaseous, condensed solution laws are not significant. In the event that solid solutions do occur, then the thermodynamic calculations should not be based upon stoichiometric compounds but rather upon the ends of the solid solution range that is nearest the over-all composition if the latter is outside the solid solution limits. If the over-all composition is inside the solid solution limits, the midpoint of the range may be used for the calculations with sufficient accuracy.

Since the entropies are not known for any plutonium compounds, the entropies estimated in Table 3 may be in error by as much as 5 e.u., which means that most thermodynamic calculations may be in error by as much as a factor of 10. However, the entropies have in most cases been chosen to agree with experimental equilibrium data and therefore will accurately reproduce the experimental results.

### 5. SUMMARY

Values of the thermodynamic data for plutonium compounds have been given in four tables in Sec. 1. Table 1 gives melting, vapor pressure, and boiling data. Table 2 gives the constants for the free energy of vaporization equation together with heat and entropy of vaporization at the boiling point. Table 3 gives values of the free-energy function,  $(\Delta F - \Delta H_{298})/T$ , and  $\Delta H_{298}$ , the heat of formation. Table 4 gives the heat, free energy, and entropy of formation for the aqueous ions.

Section 3 contains a discussion of the high-temperature chemistry of the compounds considered. Section 4 presents five graphs to show the equilibrium concentrations of halogen or halide in plutonium and halogen systems at three different pressures, namely, 1,  $10^{-3}$ , and  $10^{-6}$  atm.

### REFERENCES

1. L. Brewer, L. A. Bromley, P. W. Gilles, and N. L. Lofgren, The thermodynamic properties and equilibria at high temperatures of uranium halides, oxides, nitrides, and carbides, Manhattan District Declassified Report MDDC-1543 (Apr. 1, 1947).
2. H. P. Robinson, Determination of the melting points of plutonium(III) chloride and plutonium(III) bromide, Paper 6.150, this volume.
3. B. Weinstock, Manhattan District Declassified Report MDDC-1345 (Aug. 16, 1944).
4. I. Sheft and N. R. Davidson, Equilibrium in the vapor-phase hydrolysis of plutonium tribromide, Paper 6.24, this volume.

5. L. Brewer, University of California Radiation Laboratory Report UCRL-104 (July 1948); L. Brewer, L. A. Bromley, P. W. Gilles, and N. L. Lofgren, Thermodynamic and physical properties of nitrides, carbides, sulfides, silicides, and phosphides, in National Nuclear Energy Series, Division IV, Volume 19 B, Paper 4 (Manhattan District Declassified Report MDDC-438-D).
6. E. F. Westrum, Jr., The preparation and properties of plutonium oxides, Paper 6.57, this volume (Metallurgical Project Report CC-3882).
7. B. M. Abraham, N. R. Davidson, and E. F. Westrum, Jr., Preparation of plutonium nitride, Paper 6.60, this volume.
8. W. H. Zachariasen, X-ray diffraction studies of fluorides of plutonium and neptunium; chemical identity and crystal structure, Paper 20.5, this volume (Argonne National Laboratory Report ANL-4072); Manhattan District Declassified Report MDDC-1151 (June 11, 1947).
9. B. M. Abraham and N. R. Davidson, Note on the high-temperature hydrolysis of plutonium oxychloride, Paper 6.10, this volume.
10. F. Hagemann, B. M. Abraham, N. R. Davidson, J. J. Katz, and I. Sheft, Studies of the preparation and properties of plutonium iodide and plutonium oxyiodide, Paper 6.170, this volume.
11. E. F. Westrum, Jr., Preparation and properties of plutonium silicides, Paper 6.5, this volume (Argonne National Laboratory Report ANL-4052).
12. L. Brewer, L. A. Bromley, P. W. Gilles, and N. L. Lofgren, The thermodynamic properties of the halides, in National Nuclear Energy Series, Division IV, Volume 19 B, Paper 6 (Manhattan District Declassified Report MDDC-438-F).
13. K. K. Kelley, U. S. Bur. Mines Bull. 434 (1941).
14. F. R. Bichowsky and F. D. Rossini, "The Thermochemistry of the Chemical Substances," Reinhold Publishing Corporation, New York, 1936.
15. L. Brewer, Manhattan District Declassified Report MDDC-438-E (July 13, 1945).
16. B. M. Abraham, N. R. Davidson, and E. F. Westrum, Jr., Preparation and properties of some plutonium sulfides and oxysulfides, Paper 6.18, this volume.
17. L. Brewer, L. A. Bromley, P. W. Gilles, and N. L. Lofgren, University of California Radiation Laboratory Report MB-LB-18-6.
18. L. Brewer, L. A. Bromley, P. W. Gilles, and N. L. Lofgren, University of California Radiation Laboratory Report MB-LB-18-5.
19. B. M. Abraham, B. B. Brody, N. R. Davidson, F. Hagemann, I. Karle, J. J. Katz, and M. J. Wolf, Preparation and properties of plutonium chlorides and oxychlorides, Paper 6.7, this volume.
20. W. H. Zachariasen, Crystal structure studies of sulfides of plutonium and neptunium, Paper 20.4, this volume (Argonne National Laboratory Report ANL-4071).
21. N. R. Davidson, F. Hagemann, E. K. Hyde, J. J. Katz, and I. Sheft, Preparation and properties of plutonium tribromide and oxybromide, Paper 6.8, this volume.
22. F. D. Rossini, J. Research Natl. Bur. Standards, 9: 679 (1932), RP 499.
23. I. Sheft and N. R. Davidson, Equilibrium in the vapor-phase hydrolysis of plutonium trichloride, Paper 6.25, this volume.
24. E. F. Westrum, Jr., and H. P. Robinson, The heat of formation of plutonium oxychloride, Paper 6.56, this volume (Metallurgical Project Report CC-3880).
25. K. A. Kraus, Manhattan District Declassified Report MDDC-814 (Mar. 19, 1947).
26. E. F. Westrum, Jr., The heat of formation of plutonium tribromide, Paper 6.55, this volume (Metallurgical Project Report CC-3879).
27. M. W. Evans, The heats and entropies of plutonium(III), plutonium(IV), and plutonium(VI) in 0.5M perchloric acid at 25°C, Paper 3.30, this volume (Manhattan District Declassified Report MDDC-1206).
28. W. H. Zachariasen, The crystal structure of plutonium nitride and plutonium carbide, Paper 20.2, this volume (Argonne National Laboratory Report ANL-4070).

29. E. F. Westrum, Jr., Atomic Energy Commission Declassified Document AECD-1903 (March 1948).
30. W. H. Zachariasen, Manhattan District Declassified Report MDDC-1572 (Nov. 17, 1947).
31. V. M. Goldschmidt, *Chem. Ber.*, 60: 1263 (1927).
32. L. V. Coulter and W. M. Latimer, *J. Am. Chem. Soc.*, 62: 2557 (1940).
33. W. M. Latimer, "Oxidation States of the Elements and Their Potentials in Aqueous Solutions," Prentice-Hall, Inc., New York, 1938.
34. J. C. Hindman, Ionic species of plutonium present in aqueous solution of different acids, Paper 4.4, this volume (Atomic Energy Commission Declassified Document AECD-1893).
35. K. A. Kraus, and G. E. Moore, Chemistry of plutonium(V). Potential of the plutonium (V)/(VI) couple. Ionic species of plutonium(V) in acidic solutions, Paper 4.19, this volume (Clinton Laboratories Report MonN-249).
36. M. W. Evans, Manhattan District Declassified Report MDDC-438-I (Aug. 13, 1945).
37. R. C. L. Mooney and W. H. Zachariasen, Manhattan District Declassified Report MDDC-1787 (July 1946).
38. L. Brewer, L. A. Bromley, P. W. Gilles, and N. L. Loegren, The use of the Halide Report and the thermodynamic properties of molybdenum and tungsten halides, Manhattan District Declassified Report MDDC-438-H (Sept. 1, 1945).
39. N. D. Erway, L. O. Gilpatrick, Z. V. Jasaitis, F. D. Johnson, T. E. Phipps, G. W. Sears, R. L. Seifert, and O. C. Simpson, Metallurgical Project Report CN-3223 (Sept. 26, 1945).
40. J. M. Sturtevant, *J. Am. Chem. Soc.*, 62: 3265 (1940); 64: 762 (1942).
41. B. J. Fontana, University of California Radiation Laboratory Report BC-66 (Apr. 1, 1947); Manhattan District Declassified Reports MDDC-542 (Oct. 18, 1946) and MDDC-1452 (Aug. 19, 1947).
42. M. Kasha and G. E. Sheline, Manhattan District Declassified Report MDDC-392 (Aug. 30, 1946).
43. J. J. Howland, Jr., J. C. Hindman, and K. A. Kraus, Potential measurements: the plutonium (III)/(IV) couple, Paper 3.3, this volume.
44. W. H. Zachariasen, The crystal structure of  $\text{PuSi}_2$ , Paper 20.3, this volume.
45. R. E. Connick and W. H. McVey, University of California Radiation Laboratory Report UCRL-70 (March 1948); M. Kasha, Manhattan District Declassified Report MDDC-904 (Aug. 30, 1946); L. Brewer, Atomic Energy Commission Documents AECD-1899 and AECD-1911 (February 1948).
46. H. P. Robinson and E. F. Westrum, Jr., The dependence of the heat of solution of plutonium trichloride on the concentration of hydrochloric acid, Paper 6.54, this volume (Metallurgical Project Report CC-3878).
47. E. F. Westrum, Jr., and L. Eyring, The heat of formation of plutonium trifluoride, Paper 6.52, this volume.
48. E. F. Westrum, Jr., and H. P. Robinson, The heat of formation of plutonium trichloride, Paper 6.53, this volume (Metallurgical Project Report CC-3872).
49. W. H. Zachariasen, in National Nuclear Energy Series, Division IV, Volume 14 A; Crystal structure studies of chlorides, bromides, and iodides of plutonium and neptunium, Paper 20.6, this volume (Argonne National Laboratory Report ANL-4073).
50. L. Brewer, L. A. Bromley, P. W. Gilles, and N. L. Loegren, The halides of neptunium, Paper 15.7, this volume (Manhattan District Declassified Document MDDC-1417).
51. L. Brewer, The properties of the elements, Manhattan District Declassified Report MDDC-1543 (Apr. 1, 1947).

## Paper 6.50

### THE EFFECT OF HYDROCHLORIC ACID CONCENTRATION ON THE HEAT OF SOLUTION OF THORIUM TETRACHLORIDE†

By E. F. Westrum, Jr., and H. P. Robinson

The need of checking certain calorimetric techniques<sup>1</sup> provided an opportunity to make heat-of-solution measurements on a very pure sample of anhydrous thorium tetrachloride, which was sublimed in a quartz tube in high vacuum to eliminate any oxychloride present. About 50 per cent of the material was sublimed, sealed off, and loaded

Table 1---The Heat of Solution of Thorium Tetrachloride in Hydrochloric Acid  
(Temperature, 25.0°C; molecular weight ThCl<sub>4</sub>, 373.95)

Molarity of HCl	Weight of acid, g (in vacuum)	Millimoles of ThCl <sub>4</sub> (in vacuum)	Heat evolved, cal	H solution, kcal/mole
1.000	192.25	0.7081 0.8827	40.66 50.68	57.43 57.41  57.42 ± 0.1
6.000	212.25	1.0258 1.2323	45.30 54.54	44.16 44.27  44.27 ± 0.1
9.000	217.25	1.4136 1.4256	49.39 49.74	34.94 34.89  34.93 ± 0.1

†Contribution from the Chemistry Division of the Metallurgical Laboratory, University of Chicago, now the Argonne National Laboratory.

Based on work reported in Metallurgical Laboratory Memorandum MUC-GTS-1808 (June 27, 1945).

into the sample bulbs within a dry box. The Analytical Section analyzed this material as 62.8 per cent thorium and 37.8 per cent chlorine† (theoretical 62.07 per cent Th, 37.93 per cent Cl). Although the analysis totals more than 100 per cent and therefore cannot be regarded as proof of the absence of oxychloride, it is estimated that the presence of as much as 2 per cent oxychloride would affect the heat of solution less than several tenths of a per cent.

As might be expected, the observed rate of change of the heat of solution with concentration of hydrochloric acid is considerably larger than that of a tripositive ion of similar radius.<sup>2</sup>

The value of Chauvenet<sup>3</sup> for the heat of formation of thorium tetrachloride is based on heats of solution of thorium in about 3.6M HCl and  $\text{ThCl}_4$  in water (-56.7 kcal per mole). Our data indicate that the neglect of the effect of the hydrochloric acid concentration in the combination of these thermochemical data makes his value of the heat of formation about 9 kcal too large. Similarly distorted values were obtained among many of the heats of formation of thorium compounds tabulated by Bichowsky and Rossini.<sup>4</sup> A redetermination of the heat of formation of thorium tetrachloride is considered very desirable.

#### REFERENCES

1. E. F. Westrum, Jr., and H. P. Robinson, A semi-microcalorimeter for precise thermochemical measurements, Paper 6.51, this volume (Metallurgical Project Report CC-3885).
2. W. Klemm, Z. anorg. Chem., 249: 23 (1942).
3. E. Chauvenet, Ann. chim. et phys., Series 8, 23: 425 (1911).
4. F. R. Bichowsky and F. D. Rossini, "The Thermochemistry of the Chemical Substances," p. 104, Reinhold Publishing Corporation, New York, 1936.

† Analysis by B. Holt, reported by R. W. Bane, Metallurgical Laboratory Memorandum MUC-JTW-530 (May 15, 1945).

Paper 6.51

A SEMI-MICROCALORIMETER FOR PRECISE  
THERMOCHEMICAL MEASUREMENTS†

By E. F. Westrum, Jr., and H. P. Robinson

The immediate need of reliable thermochemical data on plutonium compounds stimulated the construction of a semi-microcalorimeter capable of providing precise and accurate heats of reaction and solution and, thereby, heat of formation values on compounds of the heavy elements within  $\pm 0.3$  kcal, using samples of about 25 mg or less. The limited amounts of plutonium available for the studies and the correspondingly small thermal effects necessitated a choice between an intricate, sensitive thermometric system and a calorimetric system of small heat capacity. The health hazard in handling quantities of dry  $\alpha$ -active compounds and solutions and the necessity of decontaminating the calorimeter after measurements to ensure the validity of subsequent radiometric assays of solutions and to make modifications emphasized the desirability of rugged, simple construction, amenable to rather stringent cleaning procedures. Furthermore, the difficulty of immediate procurement of precision electrical instruments during wartime demanded relatively simple potentiometric, thermometric, and control circuits.

A small-scale calorimeter with high sensitivity of temperature determination and a heat capacity of about 200 cal was constructed. It incorporated several modifications and improvements but no fundamentally new principles as compared with a calorimeter previously described.<sup>1,2</sup> A few details of design and technique may prove helpful to workers in this field.

†Contribution from the Chemistry Division of the Metallurgical Laboratory, University of Chicago, now the Argonne National Laboratory..

Based on work reported in Metallurgical Laboratory Memorandum MUC-GTS-1808 (June 27, 1945), p. 6.

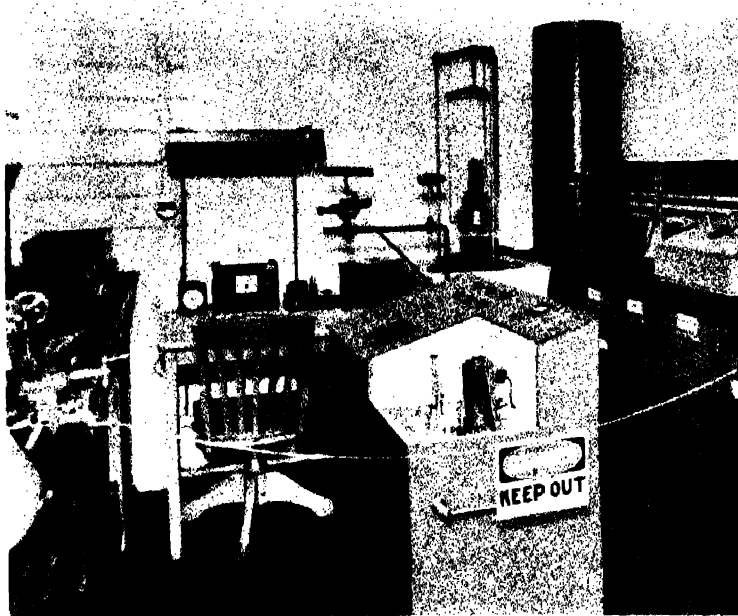


**Fig. 1a**—The calorimetric apparatus is shown assembled. The entire energy, thermometric, and thermostatic circuits as well as the storage cells and charging rectifier are contained in the main installation. The electric timers, communications receiver, impulse-selector circuit, and energy circuit galvanometer are on the desk and are connected by shielded cables. The cover of the thermostat and the galvanometer shield have been removed and placed to the right.

**Fig. 1b**—Schematic section through thermostat and calorimeter (the sensitive thermoregulator shown in Fig. 2 is not indicated in this sectional view).

A, stirring-head mechanism (detail in Fig. 5)

B, bakelite terminal block for leads

C, aluminum mounting panel for entire contents of the thermostat

D, 5-ply plywood foundation for panel

E, cylindrical pyrex jar, 12 in. in diameter and 22 in. deep

F, calorimeter submarine (detailed sectional view in Fig. 4)

G, dry sawdust insulation

H,  $\frac{1}{20}$ -hp electric induction motor

J, idler pulley stud—steel springs in V-grooved bakelite pulleys transmit rotation to calorimeter shaft

K, split rubber tubing providing vapor seal

L, auxiliary mercury thermoregulator

M, cold finger—cool tap water under a constant head is passed through a temperature-moderating interchanger to ensure balanced cooling irrespective of the ambient temperature

N, 250-watt knife heater

O, multiblade stirrer

P, baffle plate on stirring well

Q, valve for filling toluene coil

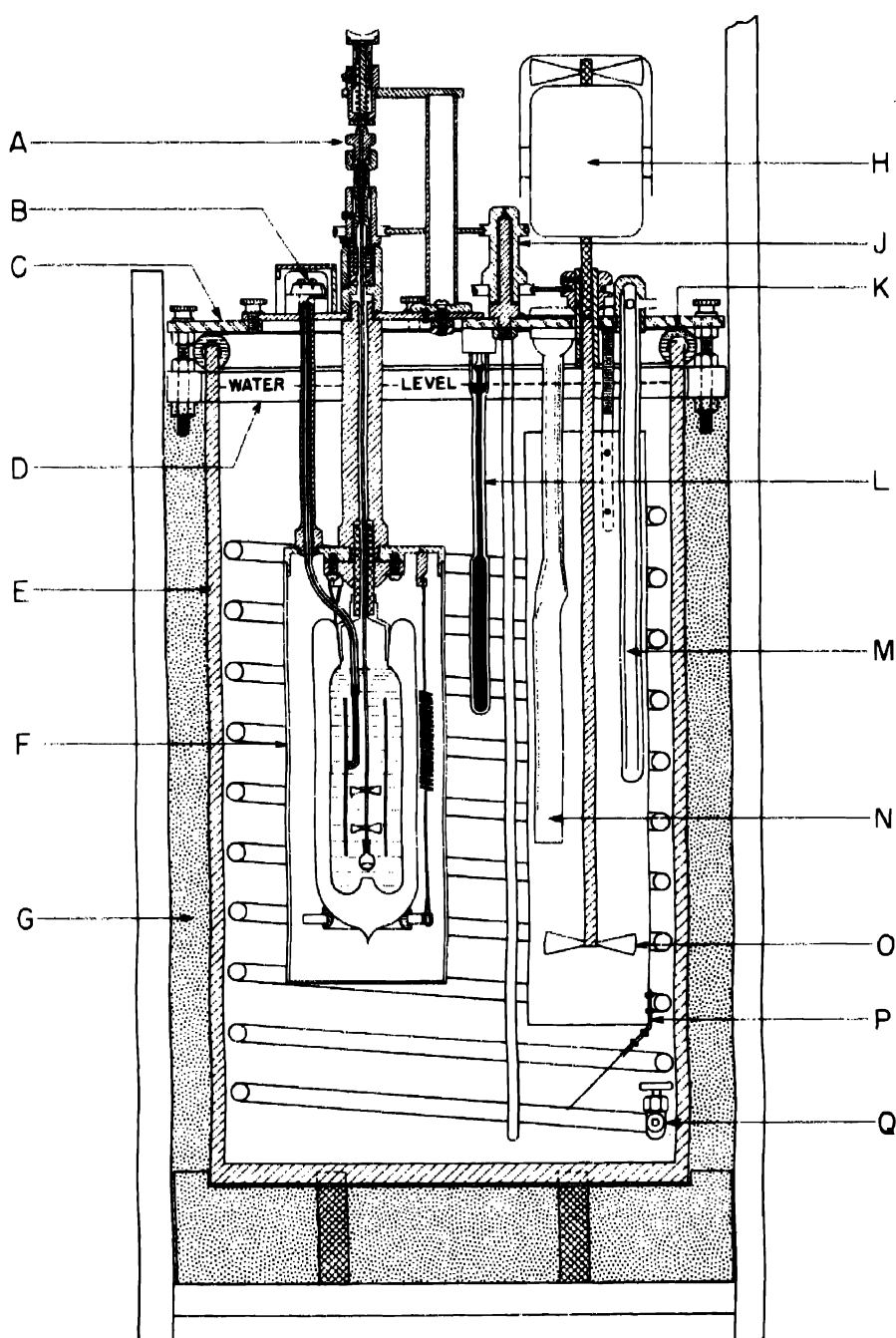


Fig. 1b—See facing page for legend.

The general arrangement of the thermostat and calorimeter is indicated in Fig. 1. The entire calorimetric unit, with the exception of the galvanometric systems, is enclosed in a wooden cabinet with bakelite panels to ensure greater temperature constancy for the circuits and to protect the experimental installation from dust and from damage by the routine daily scrubbing of the laboratory walls for health protection.

### 1. THE THERMOSTAT

Energy was supplied to the 40-liter water thermostat by means of a knife heater of extremely small lag. Since the ambient temperature was frequently greater than that of the calorimeter, a cold finger was provided through which cool water of moderated temperature was circulated under a constant head. Both the cold finger and the heater were located within the stirring well, with the blade of the heater so oriented as to prevent bulk rotation of the water column.

The average temperature of this thermostat is constant within  $0.001^{\circ}\text{C}$  for a period of several hours; over longer periods a variation of a few thousandths of a degree is noted. The fine detail of the temperature-time pattern was investigated with the low-lag calorimeter thermometer and found to be a symmetrical sinusoidal curve of about  $0.0006^{\circ}\text{C}$  amplitude and a period of 100 sec. The regulator did not show appreciable susceptibility to atmospheric-pressure changes.

1.1 Toluene Thermoregulator. The temperature of the bath was controlled by means of the expansion of toluene within a 10-meter helical coil of  $\frac{3}{8}$ -in.-diameter copper tubing. Electrical contact was provided by mercury in a glass capillary of the form shown in Fig. 2. The pyrex-glass capillary was permanently connected to the copper tubing by depositing a platinum film on the glass tube by thermal decomposition of a chloroplatinate solution,<sup>3</sup> reinforcing this film with an electrodeposition of copper, and soft-soldering it into the tinned copper tube. The needle B, which made electrical contact with the mercury, was of 0.5-mm tungsten, tapered at the tip to a sharp point by means of the thermally induced reaction with sodium nitrite. A bead of nonex glass fused 5 mm above the tip served to guide and center the needle. This needle was made to oscillate slightly by coupling it with the stirring motor; the vibration thus transmitted provided a more sensitive make-break action.

All the toluene used was treated with sodium plumbite and stored over mercury to eliminate the formation of crud at the mercury-toluene interface. Oxidation and fouling of the mercury-tungsten contact were prevented by a layer of toluene.

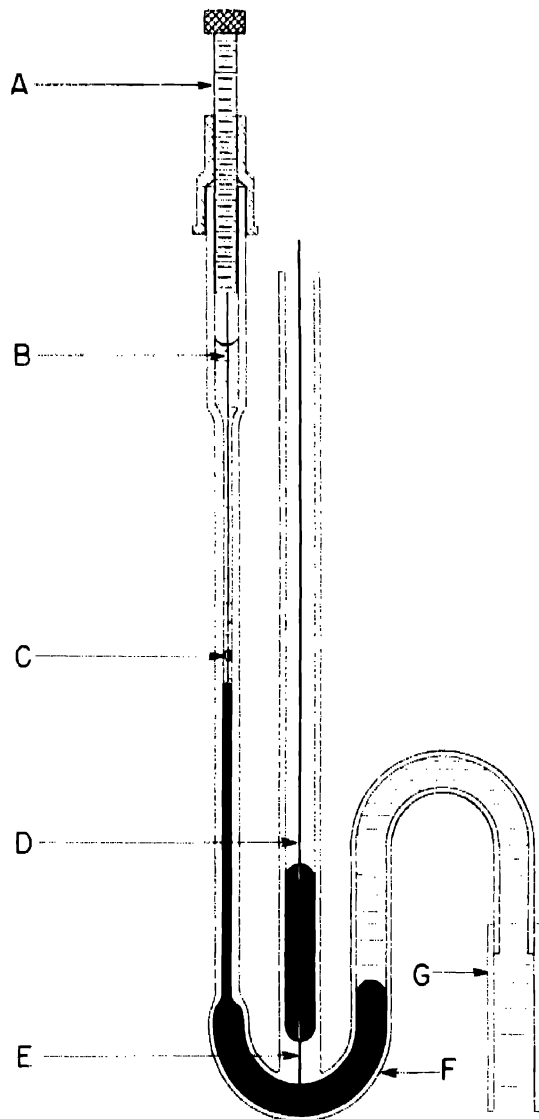


**Fig. 2—**Cross section of a thermoregulator. Solid section indicates mercury, dashed section indicates toluene.

A, adjusting screw with lock nut  
 B, tungsten electrode (about 15 mils diameter with pointed tip)  
 C, nonex glass bead fused to tungsten in center electrode

D, copper-wire electrode dipping into mercury  
 E, sealed-in tungsten-wire contact  
 F, mercury  
 G, copper tube

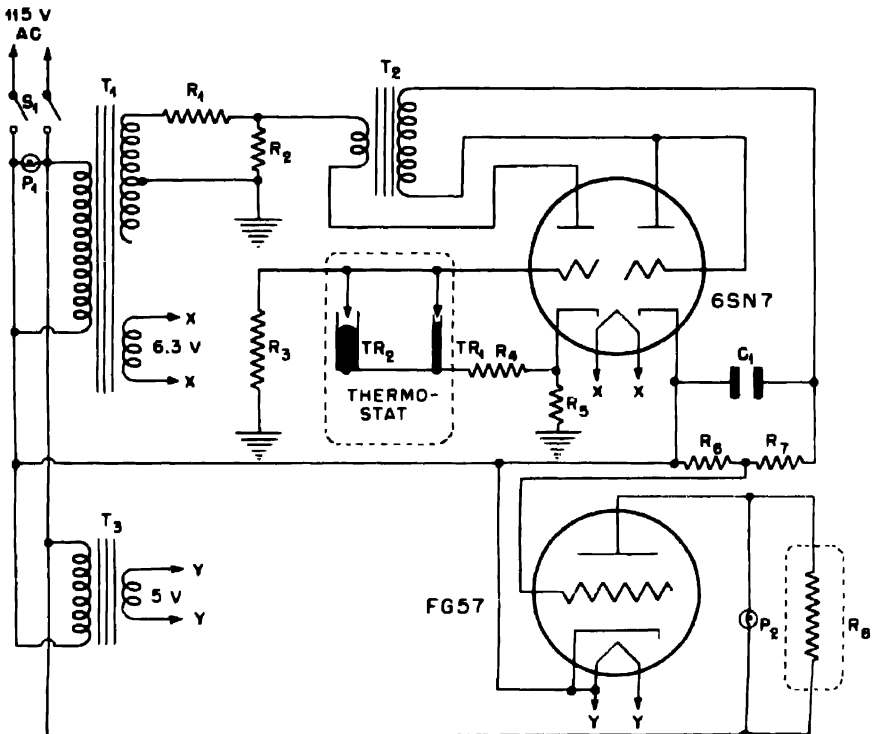


Fig. 3.—Thyatron energy-input circuit for thermostat.

C<sub>1</sub>, 0.1- $\mu$ f condenser  
 P<sub>1</sub>, 110-volt pilot light (green)  
 P<sub>2</sub>, 110-volt pilot light (red)  
 R<sub>1</sub>, 50,000 ohm 10-watt resistor  
 R<sub>2</sub>, 2,000 ohm 10-watt resistor  
 R<sub>3</sub>, 1-megohm resistor,  $\frac{1}{2}$  watt  
 R<sub>4</sub>, 0.1-megohm resistor,  $\frac{1}{2}$  watt  
 R<sub>5</sub>, 10,000-ohm 10-watt resistor  
 R<sub>6</sub>, 0.2-megohm resistor,  $\frac{1}{2}$  watt  
 R<sub>7</sub>, 1-megohm resistor,  $\frac{1}{2}$  watt

R<sub>8</sub>, 250-watt 115-volt knife heater (in thermostal)  
 S<sub>1</sub>, dpst switch  
 T<sub>1</sub>, Stancor transformer P-6289  
 T<sub>2</sub>, Thordarsen transformer T57A38  
 T<sub>3</sub>, Stancor transformer P-5000  
 TR<sub>1</sub>, sensitive thermoregulator (toluene)  
 TR<sub>2</sub>, protective auxiliary thermoregulator

**1.2 Electronic Relay.** An electronic relay activated by the expansion of the toluene-mercury regulator controlled the energy input into the thermostat. A diagram of the control circuit is shown in Fig. 3.

The operation of the circuit was as follows: Plate voltage to the first half of the 6SN7 was supplied by the high-voltage secondary of T<sub>1</sub> through the primary of T<sub>2</sub>. When the temperature of the bath was low the regulator contact of TR<sub>1</sub> was open, permitting the first grid of

the 6SN7 to have a bias voltage equal to the IR drop in  $R_5$ . This limited the plate current to a small value. When the temperature rose, the regulator made contact and removed the bias, permitting a large plate current to pass. The alternating component of this current, taken from the secondary of  $T_2$ , was rectified in the second half of the 6SN7. A portion of the rectified voltage developed across  $R_6 - R_7$  was applied to the grid of the FG57 thyratron as a negative bias, thus preventing it from firing. The plate of the FG57 was supplied from the 115-volt a-c line through the bath heater,  $R_8$ , so that when the thermoregulator contacts closed the heater current was cut off. A red pilot light,  $P_2$ , was connected across the heater to indicate when the latter was on.

To provide a safety cutoff in case the contacts of  $TR_1$  failed to close, a second thermoregulator,  $TR_2$ , was connected in parallel. This one was adjusted to close a tenth of a degree higher and was much less sensitive than the first. It was a commercial mercury unit completely sealed off from the atmosphere.

## 2. THE CALORIMETER

**2.1 Calorimetric Vessel.** A silvered and evacuated pyrex Dewar flask of about 200 ml capacity, provided with a ground standard-taper joint and an internal protuberance on the bottom to serve as an anvil on which to break the sample bulbs and facilitate circulation of the solution, served as the calorimetric vessel (Fig. 4). An attempt to use an evacuated silvered-glass stopper was unsuccessful on this scale because of the lag introduced by parts of comparatively high-heat capacity in such poor thermal contact as to reach equilibrium slowly. This type of stopper was unsatisfactory even when the Dewar flask and stopper were put directly into the bath. A stopper and supporting shaft of lucite also had appreciable lag. The arrangement finally used was a stopper with thin walls machined from lucite supported on a metal column in good thermal contact with the bath. This design proved to have negligible lag.

A cylindrical metal submarine surrounding the Dewar flask reduced the thermal-leakage modulus and provided additional protection. This can was sealed watertight with adhesive tape and was completely immersed in the thermostat.

The calorimeter fluid was stirred by two four-bladed platinum propellers about three-fourths the diameter of the stirring well provided by the thermometer cylinder.

The platinum propellers were shrunk-fit to the glass-tube stirring shaft, which also carried the very thin glass sample bulb at its lower extremity. A mechanism, shown in detail in Fig. 5, made possible the depression of the shaft by a predetermined amount in order to break

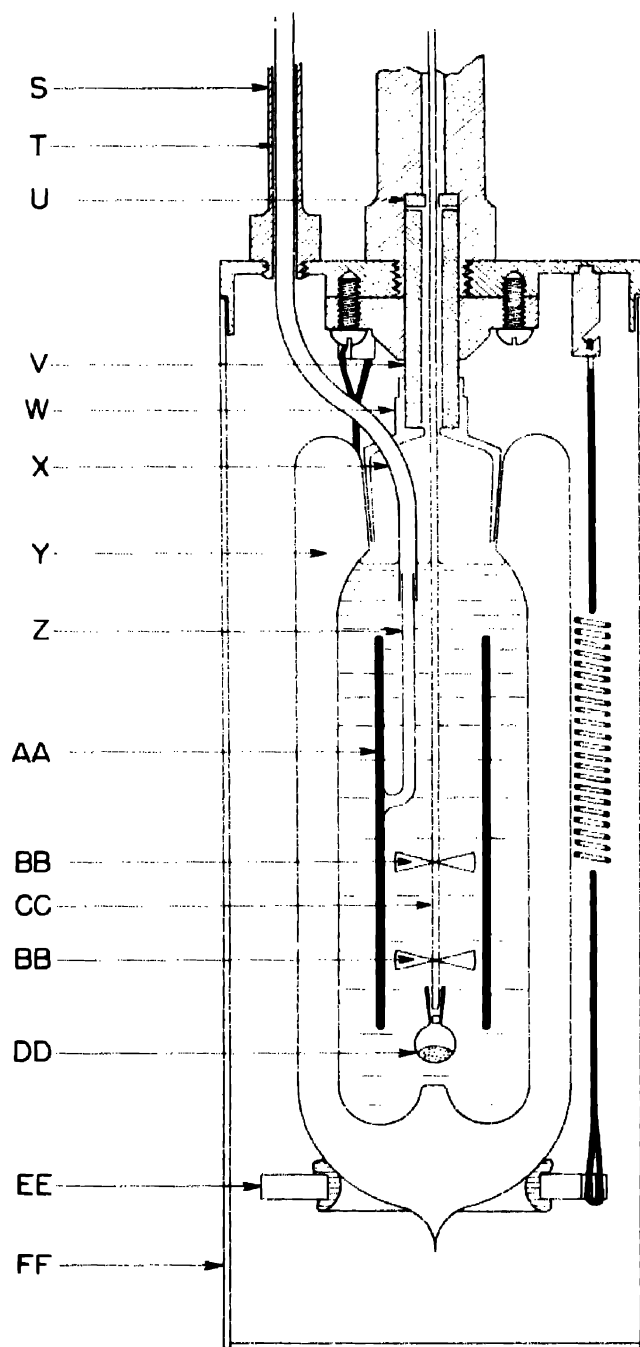


Fig. 4—See facing page for legend.

the sample bulb against the anvil without interfering with the rotation of the propellers. The constancy of the stirring speed was checked at frequent intervals with a revolution counter (200 to 250 rpm was found most satisfactory).

**2.2 Copper Resistance Thermometer.** A bifilar-wound copper resistance thermometer of negligible lag consisted of 33 ft of No. 40 double-silk-covered (dsc) annealed copper wire (49 ohms) provided with leads of No. 28 dsc manganin wire on the lower two thirds of an 8-mil platinum cylinder, 2.4 cm in diameter and 11.5 cm in length (AA, Fig. 4), which served not only to provide heat exchange and to integrate the temperature over a large region of the fluid but also as an effective stirring well. In the absence of the usual materials, a layer of lens paper and baked glyptal was used to insulate the lacquered coil from both the internal platinum cylinder and the 5-mil external jacket closely fitted over the windings. The outer jacket was welded to the inner cylinder with fine gold.

A simple bridge circuit (Fig. 6) containing essentially only a decade box, a high-sensitivity galvanometer, and some manganin resistors made possible a temperature sensitivity of  $0.00002^{\circ}\text{C}$ . The bridge, composed of bifilar-wound manganin resistors, was immersed in a 5-liter transformer oil bath within the cabinet adjacent to the thermostat. The steps of the decade box were accurately calibrated; the contact resistances were estimated to introduce errors less than the sensitivity of the thermometer.

---

Fig. 4—Cross-sectional detail of calorimeter.

- S, brass tube
- T, paraffin seal between glass and brass to insure thermal contact with thermostat. Paraffin was also used for this purpose within the glass tube around the leads
- U, bronze bearing on stirring shaft
- V, stainless-steel tube
- W, lucite stopper
- X, glass tube bearing energy and resistance thermometer leads
- Y, silvered and evacuated pyrex Dewar with 34/45 female joint and anvil on the bottom
- Z, platinum tube for leads (this was sealed to X with Apiezon W Wax)
- AA, double-walled platinum thermometer and heater cylinder and stirring well
- BB, two four-bladed platinum propellers with gold hubs, shrunk-fit to glass stirring shaft CC
- CC, glass-tube stirring shaft
- DD, fragile glass bulb containing sample to be dissolved
- EE, bakelite ring with rubber cushion supporting calorimeter
- FF, brass calorimeter submarine (all brass parts are nickel-plated to resist corrosion)

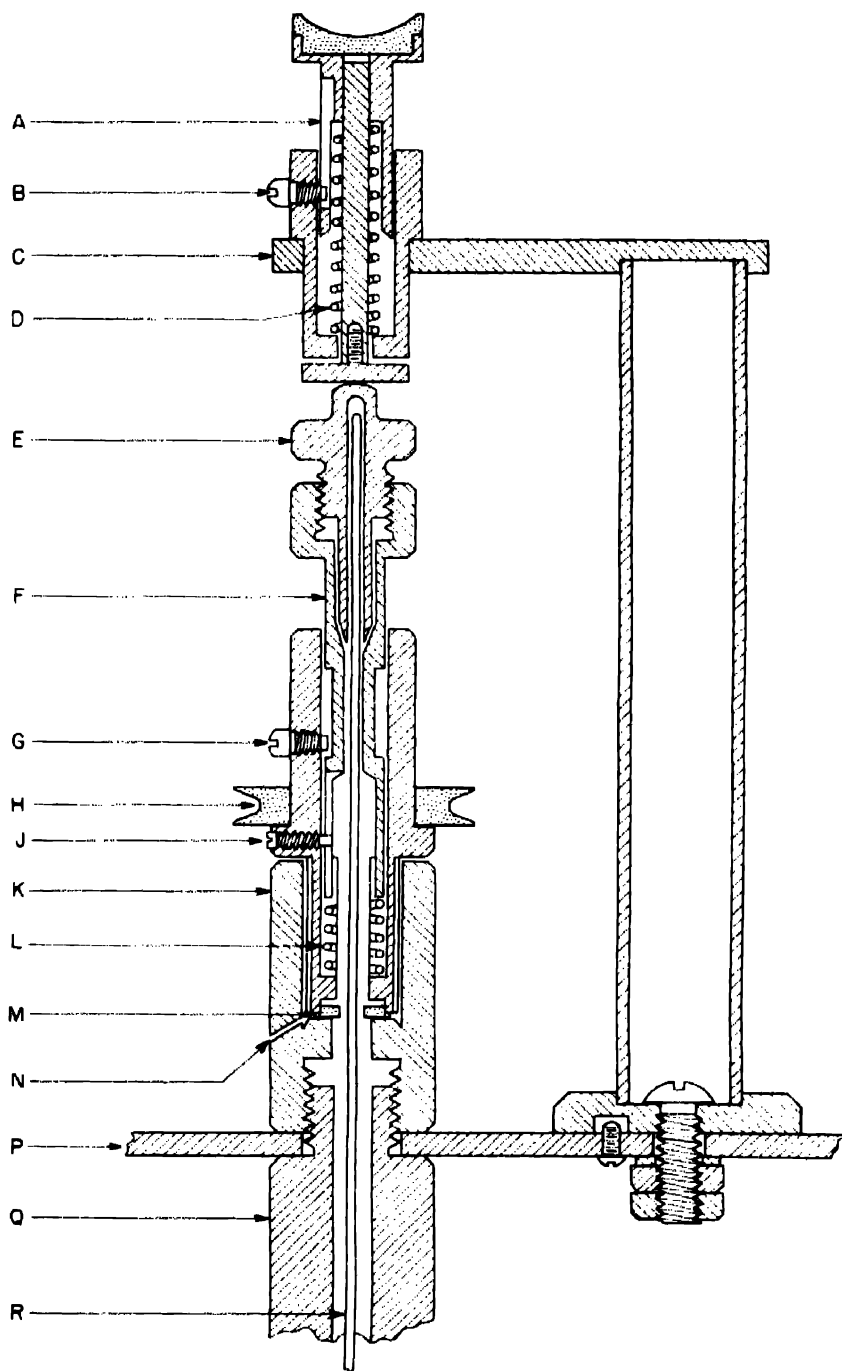


Fig. 5 -- See facing page for legend.

**2.3 Galvanometer Mounting.** A very simple vibration-free galvanometer mounting was provided by the device illustrated in Fig. 7. This mounting provided remarkable steadiness under extremely adverse circumstances, such as high space velocity of laboratory air, frequent pressure changes, and a vibrating building. It should prove of value in locations where, by virtue of temporary construction or heavy overhead ventilating equipment, the ceilings vibrate too much for a Julius-type suspension and where it is impracticable to provide a pillar independent of the building.

The mount consisted of the suspended massive lead base, the motion of which was damped by vanes in transformer oil. This was supported on an 800-lb column of dry sand contained in a wooden box mounted on a sheet of  $\frac{3}{4}$ -in. rubber on the laboratory floor; it was shielded from drafts and electrical fields by a sheet-metal cylinder provided with a celluloid observation port.

**2.4 Heater.** The heater consisted of 91.68 ohms of No. 34 silk-insulated manganin wire with single leads of No. 27 dsc copper wire extending from the platinum cylinder nearly to the top of the platinum tube. Leads of No. 24 dsc copper wire extended out of the solution to the binding posts. The very simple energy-input circuit (Fig. 8) permitted current to flow through a "ballast" resistor ( $R_{16}$ ) exactly balanced against the heater ( $R_{17}$ ). When energy was being put into the

---

Fig. 5.—Stirring-head mechanism. This assembly permits the momentary depression of the stirring shaft to break the fragile sample bulb without interference with the rotation of the shaft. Unless otherwise indicated, all parts are of brass, nickel-plated to prevent corrosion.

- A, manually depressed key for breaking sample bulb
- B, screw stop to limit motion and provide a locking catch on partial rotation of A
- C, arm and pillar supporting key; the entire unit can be rotated through 90 deg to permit removal of collet and pulley hub
- D, steel spring
- E, knurled collet for glass stirring shaft
- F, rotating unit carrying stirring shaft
- G, screw stop to limit vertical motion of unit F

- H, bakelite V-grooved pulley forced over splined section on pulley hub
- J, screw transmitting rotational motion of pulley from pulley hub to unit F
- K, upper bearing for pulley hub (steel shim is fitted over the pulley hub)
- L, steel spring to maintain unit F in neutral position
- M, fiber bearing
- N, oil channel
- P, disk for mounting calorimeter in thermostat or bracket
- Q, member connecting submarine with stirring head
- R, glass-tube stirring shaft

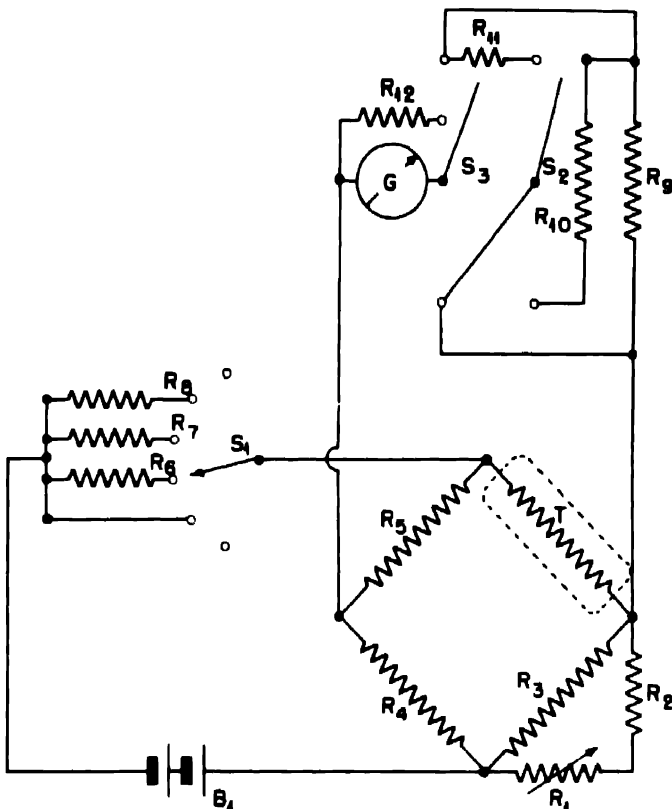


Fig. 6—Thermometric circuit for calorimeter.

B<sub>1</sub>, two lead storage cells  
 G, Leeds & Northrup high-sensitivity galvanometer (sensitivity 0.077  $\mu$ v per mm, C.D.R.X. 28 watts, resistance 21 ohms, period 8.8 sec.; galvanometer connected by means of two-conductor shielded cable and amphenol connectors)  
 R<sub>1</sub>, Leeds & Northrup 9,999-ohm four-decade precision resistance box  
 R<sub>2</sub>, 33,000-ohm manganin resistor  
 R<sub>3</sub>, 1,000-ohm manganin resistor  
 R<sub>4</sub>, 91.5-ohm manganin resistor  
 R<sub>5</sub>, 5-ohm manganin resistor (R<sub>2</sub>, R<sub>3</sub>, R<sub>4</sub>, and R<sub>5</sub> are all immersed in a large oil bath, the copper conductors to T are of No. 8 copper wire and are as short as possible)

R<sub>6</sub>, 35-ohm resistor  
 R<sub>7</sub>, 100-ohm resistor  
 R<sub>8</sub>, 300-ohm resistor  
 R<sub>9</sub>, 3,750-ohm manganin resistor  
 R<sub>10</sub>, 150-ohm manganin resistor  
 R<sub>11</sub>, 1,000-ohm manganin resistor  
 R<sub>12</sub>, 50-ohm copper galvanometer damping resistor  
 S<sub>1</sub>, six-position tap switch  
 S<sub>2</sub>, spdt copper knife switch  
 S<sub>3</sub>, spdt copper knife switch, with additional pole added as indicated  
 T, 49.0-ohm copper resistance thermometer (in calorimeter) noninductively wound with manganin leads.

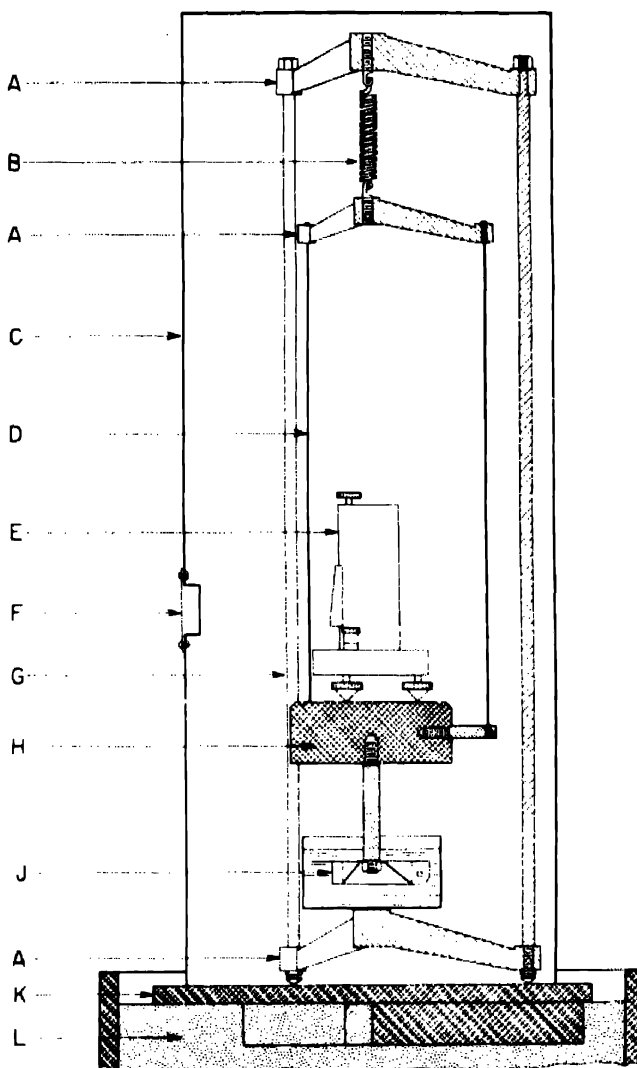


Fig. 7—Vibrationless galvanometer mounting.

- A, cast-iron triangular ring stand bases
- B, steel spring
- C, sheet-metal draft and electrical shield
- D, brass rods,  $\frac{1}{8}$  in. in diameter
- E, high-sensitivity galvanometer on kinematic mount
- F, observation port of transparent celluloid

- G, steel rods,  $\frac{1}{4}$  in. in diameter
- H, solid lead cylinder (about 35 lb)
- J, brass damping vanes in oil dashpot
- K, 5-ply, reinforced, circular wooden base
- L, about 800 lb of fine silica sand in a wooden box 22 in. square and 36 in. high

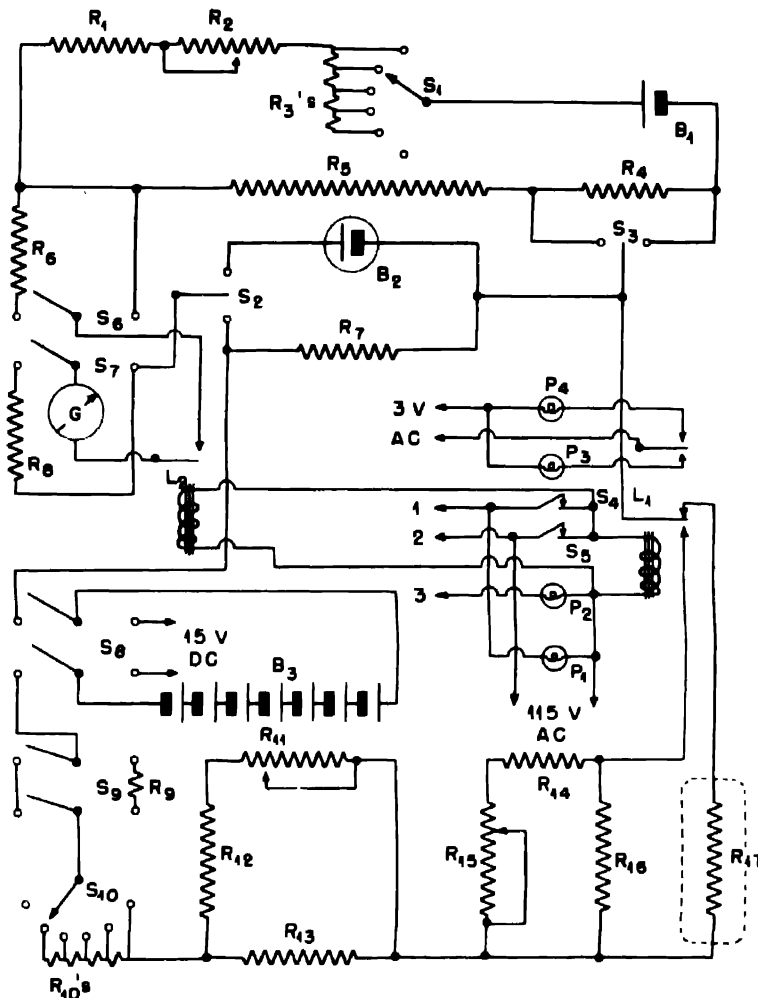


Fig. 8 — See facing page for legend.

calorimeter, the steady current was diverted through the heater by a relay electrically activated by time signals broadcast by the U. S. Bureau of Standards. The current was adjusted so that the IR drop across the standard resistor ( $R_7$ ) would be exactly that of the standard cell. The energy was calculated from the potential drop and the accurately known resistances of  $R_7$  and  $R_{17}$ . The resistances were calibrated in two laboratories against standards of approximately equal resistances.

**2.5 Impulse-selector Circuit.** Time signals received from the U. S. Bureau of Standards, Station WWV, consisted of 5 cycles of a 1,000-cycle tone repeated every second except the 59th second of each minute. Superimposed on these were a 440-cycle tone and a 4,000-

cycle tone. The transformer (Stancor A-3852) was tuned to 1,000 cycles by means of the condenser so that the 440- and 4,000-cycle tones were rejected to some extent.

The impulse selector (Fig. 9) operated as follows: The signal from the transformer was amplified in the first half of the first 6SN7 and applied to the other half, which was connected as a rectifier. A pulse was developed in the cathode circuit that was put to the first grid of the second 6SN7, closing relay  $L_2$  for 0.1 to 0.2 sec. This action was repeated every second and thus kept condenser  $C_5$  nearly discharged. On the 59th second no pulse was received, and  $C_5$  charged sufficiently in about 1.3 sec. to increase the plate current through  $L_1$  to a point where the latter closed. When the next pulse occurred,  $C_5$  was discharged and  $L_2$  opened, but if  $S_4$  was depressed in the meantime, the impulse relay controlling the energy input to the calorimeter was operated exactly on the second.

$R_{11}$  must be adjusted for the particular relay used so that it closed in about 1.3 sec. after a pulse. It was important for  $L_1$  to remain closed until  $L_2$  opened. When  $S_2$  was closed, the impulse relay could be operated on any signal.

---

Fig. 8—Calorimetric energy-input circuit. 1, 2, and 3 are cable connections with respective conductors on impulse-selector circuit. (see Fig. 9).

B<sub>1</sub>, lead storage cell  
 B<sub>2</sub>, Weston standard cell  
 B<sub>3</sub>, seven heavy-duty lead storage cells  
 G, galvanometer (sensitivity: 0.006 ma per millimeter)  
 L<sub>1</sub>, impulse ratchet-type sequence relay, advance-type 904A, 115 volts a-c, silver contacts  
 L<sub>2</sub>, spst relay, 115 volts a-c  
 P<sub>1</sub>, 120-volt pilot light (green)  
 P<sub>2</sub>, 120-volt pilot light (red)  
 P<sub>3</sub>, 6-volt pilot light (green)  
 P<sub>4</sub>, 6-volt pilot light (red)  
 R<sub>1</sub>, 8,300-ohm resistor  
 R<sub>2</sub>, 300-ohm potentiometer  
 R<sub>3</sub>, 285-ohm resistor  
 R<sub>4</sub>, 10-ohm resistor  
 R<sub>5</sub>, 10,000-ohm resistor  
 R<sub>6</sub>, 0.5-megohm manganin resistor  
 R<sub>7</sub>, 9.965-ohm standard resistor (IRC precision manganin, noninductively wound on ceramic core, immersed in oil bath)

R<sub>8</sub>, 50,000-ohm manganin resistor  
 R<sub>9</sub>, 5-ohm manganin resistor  
 R<sub>10</sub>, 1-ohm manganin resistor  
 R<sub>11</sub>, 12.5-ohm potentiometer  
 R<sub>12</sub>, 350-ohm resistor  
 R<sub>13</sub>, 42-ohm manganin resistor  
 R<sub>14</sub>, 1,000-ohm manganin resistor  
 R<sub>15</sub>, 125-ohm potentiometer  
 R<sub>16</sub>, 100.4-ohm manganin ballast resistor (immersed in oil bath)  
 R<sub>17</sub>, 91.68-ohm calorimeter heater of manganin wire noninductively wound with copper leads (in calorimeter)  
 S<sub>1</sub>, six-position tap switch  
 S<sub>2</sub>, spdt toggle switch  
 S<sub>3</sub>, spdt toggle switch  
 S<sub>4</sub>, push-button contact  
 S<sub>5</sub>, push-button contact  
 S<sub>6</sub>, spdt copper knife switch  
 S<sub>7</sub>, spdt copper knife switch  
 S<sub>8</sub>, dpst toggle switch (to rectifier for charging energy cells)  
 S<sub>9</sub>, dpdt toggle switch  
 S<sub>10</sub>, six-position tap switch

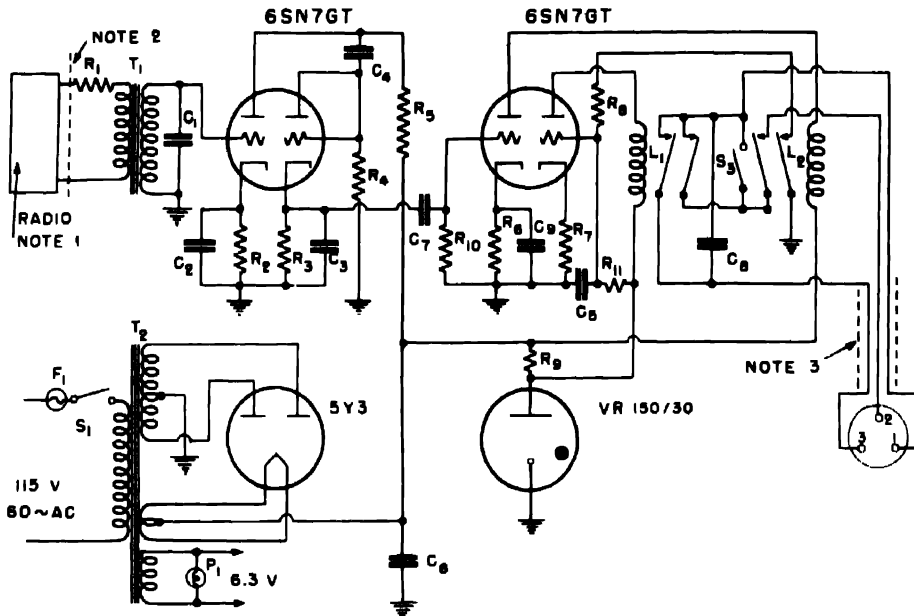


Fig. 9—Impulse-selector circuit for time signals.

$C_1$ , 0.0025 $\mu$ f condenser	$R_1$ , 10-megohm resistor
$C_2$ , 4- $\mu$ f condenser	$R_4$ , 0.1-ohm resistor
$C_3$ , 0.05- $\mu$ f condenser	$R_5$ , 25,000-ohm resistor
$C_4$ , 0.02- $\mu$ f condenser	$R_6$ , 4,400-ohm resistor
$C_5$ , 0.5- $\mu$ f condenser	$R_7$ , 2,000-ohm resistor
$C_6$ , 20- $\mu$ f condenser	$R_8$ , 50,000-ohm resistor
$C_7$ , 0.05- $\mu$ f condenser	$R_9$ , 4,000-ohm resistor
$C_8$ , 0.05- $\mu$ f condenser	$R_{10}$ , 15-megohm resistor
$C_9$ , 4- $\mu$ f condenser	$R_{11}$ , 20-megohm resistor (see text)
$F_1$ , 2 ampere fuse	$S_1$ , spdt switch
$L_1$ , 2,500-ohm dpst relays	$S_2$ , spdt switch
$L_2$ , 2,500-ohm dpst relays	$T_1$ , transformer (Stancor A-3852)
$R_1$ , 1,000-ohm resistor	$T_2$ , power transformer
$R_2$ , 750-ohm resistor	

Note 1, Hallicrafter's Echophone communications receiver EC-1.

Note 2, cable connection with communications receiver.

Note 3, shielded cable connection with relays, push buttons, etc., in calorimeter.

**2.6 Glass Sample Bulb.** The fragile glass sample bulbs are shown in Fig. 10. In order to be able to weigh the small samples of hygroscopic materials to  $\pm 10 \mu\text{g}$ , the following procedure was tested and adopted. In a very light glass beaker of about 1 ml capacity were placed a cleaned and dried bulb, a matched glass bead, and a globule of Apiezon W Wax weighing 2 or 3 mg. After a series of these units

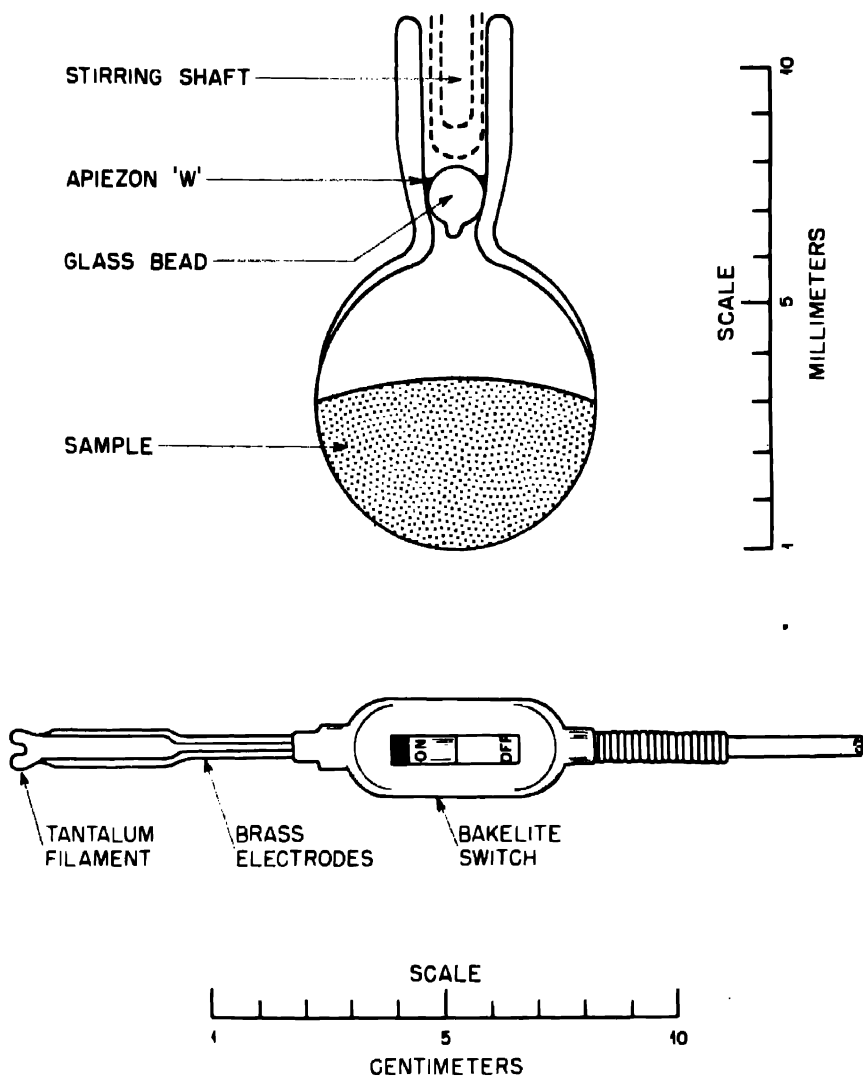


Fig. 10—Glass sample bulb and sealing unit.

were weighed, appropriate amounts of the hygroscopic samples were loaded into them by means of glass microfunnels, in a dry box with an anhydrous nitrogen atmosphere. The bead and globule of Apiezon W were put into place and the sealing was performed by warming the neck of the bulb with the sealing unit, also shown in Fig. 10. The melted wax formed an airtight fillet free from possible contact with the sample. The loaded units were then reweighed in the laboratory

atmosphere. Correction was made, where appropriate, for the change from air to nitrogen in the bulb.

A large number of previously weighed metallic samples, sealed and reweighed by the above procedure, demonstrated the reliability of the method to be within  $10 \mu\text{g}$ . The net thermal effect produced by the breaking of the bulb and the consequent liberation of the small volume of nitrogen was observed to be less than  $2 \times 10^{-5}$  and was, therefore, below the limit of detection and experimental error.

### 3. OPERATION AND CALIBRATION

The observed drift due to the thermometer and stirrer combined was  $0.00007^\circ\text{C}$  per minute, and the thermal leakage modulus was  $0.0009^\circ\text{C}$  per min. The thermostat temperature was set to give a conveniently small fore- and after-drift for the solution reaction, i.e., the calorimeter temperature was usually a few tenths of a degree above that of the bath. It can be argued, however, that for hydrochloric acid solutions of concentration as high as 6M there would be no tendency for distillation even for a temperature difference several times as great. The extremely rapid solution of the samples and the attainment of equilibrium resulted in total heat correction of about 0.3 per cent during the experimental period.

The amount of acid of given concentration in the Dewar vessel was accurately reproduced, by weighing, for each measurement. The heat capacity of the system was determined by electrical heating at two energy-input rates, one comparable with the rate of evolution of heat by the samples, and the other about half as great. The points representing the individual runs deviated from a smooth curve by less than 0.1 per cent for energy inputs varying in amount by a factor of 10. An electrical calibration was provided for each concentration of acid. These calibrations and the resistance of the heater were checked occasionally during the measurements of the heat of solution.

As an additional check on the precision and accuracy of the instrument, a "chemical" calibration was made using the heat of reaction of very pure, freshly cut crystals of magnesium metal in 1M HCl. Accurate measurements of this thermochemical quantity are given by Shomate and Huffman.<sup>4</sup> Duplicate runs under conditions and concentrations comparable to those used by the above investigators gave values of 111.24 and  $111.27 \pm 0.08$  kcal per mole for the heat of solution of magnesium compared to their mean value of  $111.322 \pm 0.041$  kcal per mole. All the values were similarly corrected for the vaporization of water by the evolved hydrogen.

Measurements of the heats of solution and formation of plutonium compounds are described in accompanying papers.

#### 4. SUMMARY

The construction, calibration, and operation of a calorimeter of about 200 cal heat capacity and a temperature sensitivity of  $0.00002^{\circ}\text{C}$  and auxiliary equipment have been described. The calorimeter was designed to measure heats of reaction and solution accurate to several tenths of a kilocalorie on about  $10^{-4}$  mole of plutonium and the plutonium compounds.

#### REFERENCES

1. K. S. Pitzer, J. Am. Chem. Soc., 59: 2365 (1937).
2. E. F. Westrum, Jr., Dissertation, Thermodynamics of the system  $\text{KHF}_2 = \text{KF} + \text{HF}$ , University of California, Berkeley, Calif. (1944).
3. J. Strong, "Procedures in Experimental Physics," p. 152, Prentice-Hall, Inc., New York, 1941.
4. C. H. Shomate and E. H. Huffman, J. Am. Chem. Soc., 65: 1625 (1943).

Paper 6.52

THE HEAT OF FORMATION OF PLUTONIUM TRIFLUORIDE†

By E. F. Westrum, Jr., and L. Eyring

Despite its insolubility in aqueous mediums, plutonium trifluoride lends itself to solution calorimetry at room temperature in that it separates from aqueous solution in crystallites of the anhydrous salt with average dimensions greater than 500 Å. X-ray diffraction analysis of the precipitate by Zachariasen provided evidence supporting this assertion.<sup>1</sup>

The following experimental procedure was adopted after consideration of available solubility data on plutonium trifluoride,<sup>2</sup> and several survey experiments were conducted to determine optimum conditions. A fraction of a millimole of plutonium(III) dissolved in about 170 g of 1.5M HCl was precipitated by the addition of several grams of relatively concentrated hydrofluoric acid, and the heat liberated in the process was determined calorimetrically. Subsequent measurements were made of the heat of mixing of the two acids and the possible complexing effect on the plutonium(III) remaining in solution. These data provide a measure of the heat of precipitation of plutonium trifluoride, which, when combined with other experimental thermochemical data, makes possible the calculation of the heat of formation of plutonium trifluoride.

1. EXPERIMENTAL METHOD AND DATA

The calorimeter of about 200 calories heat capacity provided with a copper resistance thermometer and a manganin heater as well as the method of electrical-energy calibration have already been described.<sup>3</sup> The instrument was used with only minor modifications. A separate motor was installed to provide constant stirring at 275 rpm.

†Contribution from the Department of Chemistry and the Radiation Laboratory, University of California, Berkeley.

The inner surface of the Dewar vessel, the stirring shaft, and the lead tube were coated with a thin film of paraffin to prevent attack by the hydrofluoric acid.

To facilitate the addition of the relatively concentrated hydrofluoric acid, the fragile glass sample bulb of the calorimeter was replaced by a somewhat larger cell of polystyrene (Fig. 1). No reaction of the

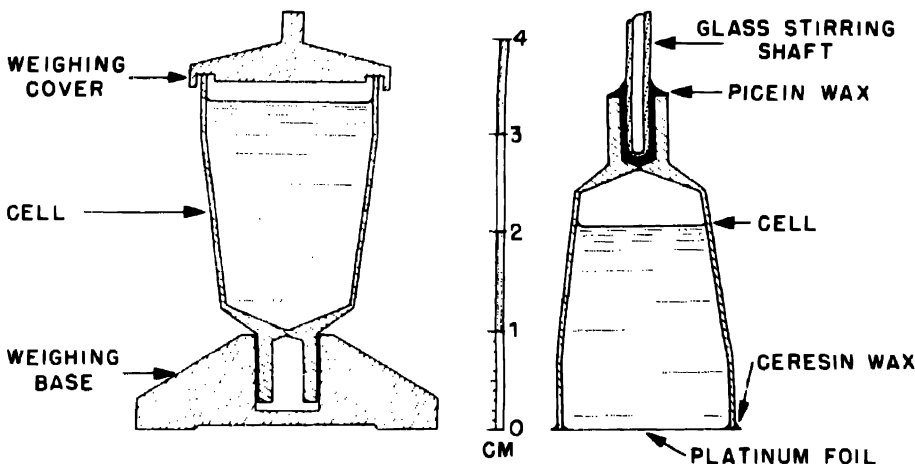


Fig. 1 — Polystyrene cell for weighing and admitting aqueous hydrofluoric acid to the calorimeter.

hydrofluoric acid was detected even after long contact with the polystyrene. This cell provided with a base and cover (Fig. 1) also served as a container in which to weigh the hydrofluoric acid and thus secure an exactly known quantity for the calorimetric measurements. The diluted c.p. hydrofluoric acid (standardized indirectly against mercuric oxide) was transferred from its ceresin bottle with a transfer pipet, the barrel and plunger of which were machined from polystyrene rod. After the acid-filled cell was weighed and the platinum foil was sealed in place with a mixture of paraffin and ceresin wax, the cell was attached to the stirring shaft with a small bead of picein or Apiezon W.

The solutions were mixed in the calorimeter by depressing the stirring shaft and thus rupturing the thin platinum foil against the "anvil" in the Dewar vessel. Electrical-energy calibrations of the heat capacity of the calorimetric system were made during the individual runs.

The solution in the calorimeter at the start of the run was 1.500M with respect to hydrogen chloride and contained a fraction of a milli-

mole of plutonium(III) per liter. The acid was standardized against mercuric oxide. Hydrogen (saturated with acid of identical concentration) was bubbled through the 1.5M acid continuously prior to the run to remove dissolved air and thus prevent possible oxidation of the plutonium. A plutonium(III) solution is stable for several days in

Table 1 — The Heat of Precipitation of  $\text{PuF}_3$ , at 25.0°C

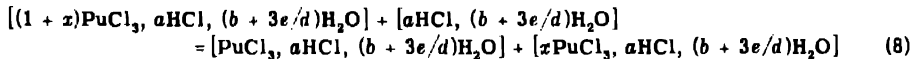
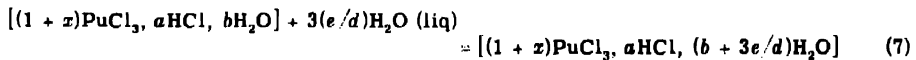
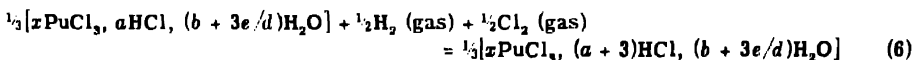
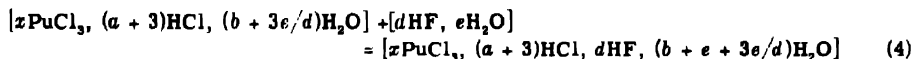
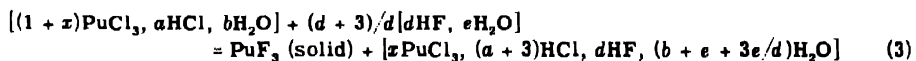
Legend	Run A	Run B	Uncertainty†
Amount of Pu(III) present initially in calorimeter (wt in vacuum confirmed by $\alpha$ radiometric assay), micromoles	386.65	511.42	$\pm 0.09$
Amount of Pu(III) in solution after precipitation of $\text{PuF}_3$ ( $\alpha$ radiometric assay), micromoles	9.61	8.05	$\pm 0.18$
Amount of $\text{PuF}_3$ precipitated (by difference), micromoles	357.04	503.37	$\pm 0.20$
Amount of HF in calorimeter (added as HF, 1.925 $\text{H}_2\text{O}$ ), millimoles	64.05	62.05	$\pm 0.00\ddagger$
Amount of 1.500M HCl (HCl, 35.97 $\text{H}_2\text{O}$ , in calorimeter in vacuum), g	172.33	172.56	$\pm 0.03$
Coefficients for Table 2:			
a	705.2	500.9	
b	25,368	18,017	
d	178.4	120.3	
e	339.6	331.6	
z	0.02692	0.01599	
Observed heat evolved, calories	21.57	22.10	$\pm 0.05$
Heat evolved on dilution of aqueous HF (reaction 4), calories	19.02	18.43	$\pm 0.09$
Heat of precipitation of $\text{PuF}_3$ , kcal/mole	-7.1	-7.3	$\pm 0.3$

†These values are conservative estimates of the maximum experimental error believed to be associated with the measured quantity. They are in general considerably larger than the average deviations where independent measurements provide such indications.

‡The uncertainty indicated here is a relative one; the error in the absolute amount of hydrofluoric acid present is about  $\pm 0.07$ .

hydrochloric acid thus treated. The plutonium trichloride, the preparation and purity of which has been described elsewhere,<sup>4</sup> was weighed in sealed bulbs and dissolved in a weighed quantity of the acid just prior to the run. After thorough mixing, aliquots of these solutions were withdrawn, and a confirmatory  $\alpha$  radiometric assay of the plutonium content was made by the weighing technique described in another paper.<sup>5</sup> The calorimetric measurements were made as

quickly as possible after the preparation of the solution to avoid the slow air oxidation of the plutonium(III). The thermal effect due to the mixing of the two acids appeared to be complete in about 25 sec; the somewhat slower evolution of heat from the precipitation of the plutonium trifluoride persisted for about 5 min before the effect on the drift was negligible. The experimental period was considered complete when the thermal drift had reached the calculated equilibrium value for the observed temperature.

Table 2 -- The Heat of Formation of  $\text{PuF}_3$ ,

$$\Delta H_9 = \Delta H_1 + \Delta H_2 + \Delta H_3 - \Delta H_4 + 3 \Delta H_5 - 3 \Delta H_6 - \Delta H_7 - \Delta H_8$$

The granular precipitate of  $\text{PuF}_3$  in the calorimeter after the run was observed to have the characteristic violet color of crystalline  $\text{PuF}_3$ . No evidence of higher oxidation states or of the presence of  $\text{PuF}_4$  was detected. In view of the rapidity of the process and the precautions taken such oxidation would not be expected to occur.

Immediately after the run aliquots by weight of the centrifuged supernatant solution from the calorimeter were diluted and plated by weight to determine the plutonium remaining in solution. No decrease in  $\alpha$  activity was noted in subsequent aliquots taken after intervals of several hours. The data from these determinations are summarized in Table 1. The atomic weight of the plutonium was taken as 239.07 and the molecular weight of  $\text{PuCl}_3$  as 345.44. The data are expressed in terms of a defined calorie equal to 4.1833 international joules.

Two determinations of the heat of mixing of the hydrofluoric acid and the hydrochloric acid solutions (reaction 4, Table 2) were made.

These runs were made with 172.56 g (in vacuum) of 1.508M aqueous HCl containing  $7.0 \pm 0.1$  micromoles of plutonium(III) to which was added 60.75 and 66.95 millimoles of HF (as HF, 1.925 H<sub>2</sub>O). The observed amounts of heat evolved were  $18.04 \pm 0.09$  and  $19.80 \pm 0.09$  cal, respectively. A somewhat less precise, and possibly less accurate, experimental arrangement was used for these two determinations.

## 2. THE HEAT OF FORMATION

The calculation of the heat of formation at 25°C can be summarized by the sequence of reactions indicated in Table 2.

The heat of formation of plutonium trichloride (reaction 1) and the heat of solution of this compound in 1.500M HCl (reaction 2) were evaluated from the data of Westrum and Robinson<sup>4,6</sup> as  $-230.0 \pm 0.3$  and  $-29.5 \pm 0.1$  kcal per mole, respectively. Reaction 3 corresponds to the precipitation reactions A and B (Table 1), reaction 4 to the supplementary heat of mixing experiments.

Graphical interpolation of values for the heat of reaction of reaction 5,<sup>7</sup> i.e., the formation of aqueous hydrofluoric acid (HF, 1.925 H<sub>2</sub>O), yields  $-75.15$  kcal per mole of HF at 25°C. No estimate of the reliability of this quantity is given; it is perhaps the major contribution to the uncertainty of the heat of formation of PuF<sub>3</sub>. The heat of reaction 6 is assumed to be uninfluenced by the very small concentration of plutonium ions and is evaluated from the data of Rossini<sup>7,8</sup> on the heat of formation of the infinitely dilute aqueous solution of hydrogen chloride,  $-40.02 \pm 0.04$  kcal per mole, and on the relative apparent molal heat content of the aqueous acid solutions. Neglecting the small concentration of plutonium ion, reaction 7 corresponds to the heat of solution of 5.78 moles of water in hydrochloric acid of concentration HCl, 35.97 H<sub>2</sub>O. The thermal effect of this process is estimated from the apparent molal heat content data of Rossini<sup>8</sup> to be  $-0.06$  kcal. Reaction 8 represents, essentially, the dilution of less than 3 per cent of the approximately 0.004M Pu(III) involved in precipitation reaction in 1.500M HCl with respect only to the concentration of the plutonium. The concentration of the acid and, therefore, the ionic strength of the solutions remain almost exactly constant. The heat of this reaction may therefore be assumed to be entirely negligible for the present calculation.

The heat of formation of crystalline plutonium trifluoride is then

$$\Delta H_{298.1^\circ K} = 230.0 - 29.5 - 7.2 - 3(75.15) - 3(-39.15) + 0.06 \\ = -374.6 \text{ kcal per mole}$$

### 3. SUMMARY

Measurement of the heat evolved by the precipitation of  $\text{PuF}_3$  from 1.5M aqueous hydrochloric acid upon addition of aqueous hydrofluoric acid and of the heat of mixing of the two acids yielded a value of  $-7.2 \pm 0.3$  kcal per mole for the heat of precipitation of  $\text{PuF}_3$  from the solution. Combination of this value with other thermochemical data results in a heat of formation of -375 kcal per mole for the crystalline  $\text{PuF}_3$  at 25°C.

### REFERENCES

1. W. H. Zachariasen and B. B. Cunningham, private communications.
2. P. R. O'Connor, private communication.
3. E. F. Westrum, Jr., and H. P. Robinson, A semi-microcalorimeter for precise thermochemical measurements, Paper 6.51, this volume (Metallurgical Project Report CC-3885).
4. H. P. Robinson and E. F. Westrum, Jr., The dependence of the heat of solution of plutonium trichloride on the concentration of hydrochloric acid, Paper 6.54, this volume (Metallurgical Project Report CC-3878).
5. E. F. Westrum, Jr., An improved technique for precise alpha radiometric assay, Paper 16.2, this volume (Metallurgical Project Report CN-3433).
6. E. F. Westrum, Jr., and H. P. Robinson, The heat of formation of plutonium trichloride, Paper 6.53, this volume (Metallurgical Project Report CC-3872).
7. Selected values of chemical thermodynamic properties, Natl. Bur. Standards U. S., Washington, Dec. 31, 1947.
8. F. D. Rossini, J. Research Natl. Bur. Standards, 9: 679 (1932).

## Paper 6.53

### THE HEAT OF FORMATION OF PLUTONIUM TRICHLORIDE†

By E. F. Westrum, Jr., and H. P. Robinson

The value of reliable thermochemical data for scientific and technical purposes does not need to be emphasized. Plutonium trichloride was selected as the first compound of a transuranium element to be investigated thermochemically. Other workers<sup>1</sup> have suggested a value of 260 to 270 kcal per mole for the heat of formation of  $\text{PuCl}_3$ , after failing to find evidence of reaction or evolution of heat in a mixture of  $\text{PuCl}_3$  and cerium. This estimate was based on the assumption that the heat of formation of  $\text{PuCl}_3$  is probably greater than that of  $\text{CeCl}_3$ .

This paper presents a description of the preparation of plutonium metal and the trichloride and the measurement of their heats of solution in hydrochloric acid, from which data the heat of formation is derived. Since very limited quantities of plutonium were available, it was necessary to operate on the semimicro scale both in the calorimetric measurements and in the chemical analyses.

#### 1. PREPARATION AND PURITY OF THE PLUTONIUM METAL SAMPLES

1.1 Plutonium Metal. This was prepared on the milligram scale by thermal high-vacuum reductions of plutonium halides prepared by the hydrohalogenation of plutonium(III) oxalate.<sup>2</sup> Samples from another laboratory were also used for some of the measurements.

†Contribution from the Chemistry Division of the Metallurgical Laboratory, University of Chicago, now the Argonne National Laboratory.

Based on work reported in Metallurgical Laboratory Memorandums MUC-GTS-1808 (June 27, 1945), p. 6, and MUC-GTS-1873 (July 28, 1945), and Metallurgical Project Report CS-3180 (July 24, 1945), p. 5.

**1.2 High-vacuum Valve.** To facilitate the micro-scale batch production of metal in high vacuum, the valve shown in Fig. 1 was developed and mounted in the line above the liquid-air trap. This valve had an aperture of nearly 3 cm, and it consisted of a pyrex glass plate

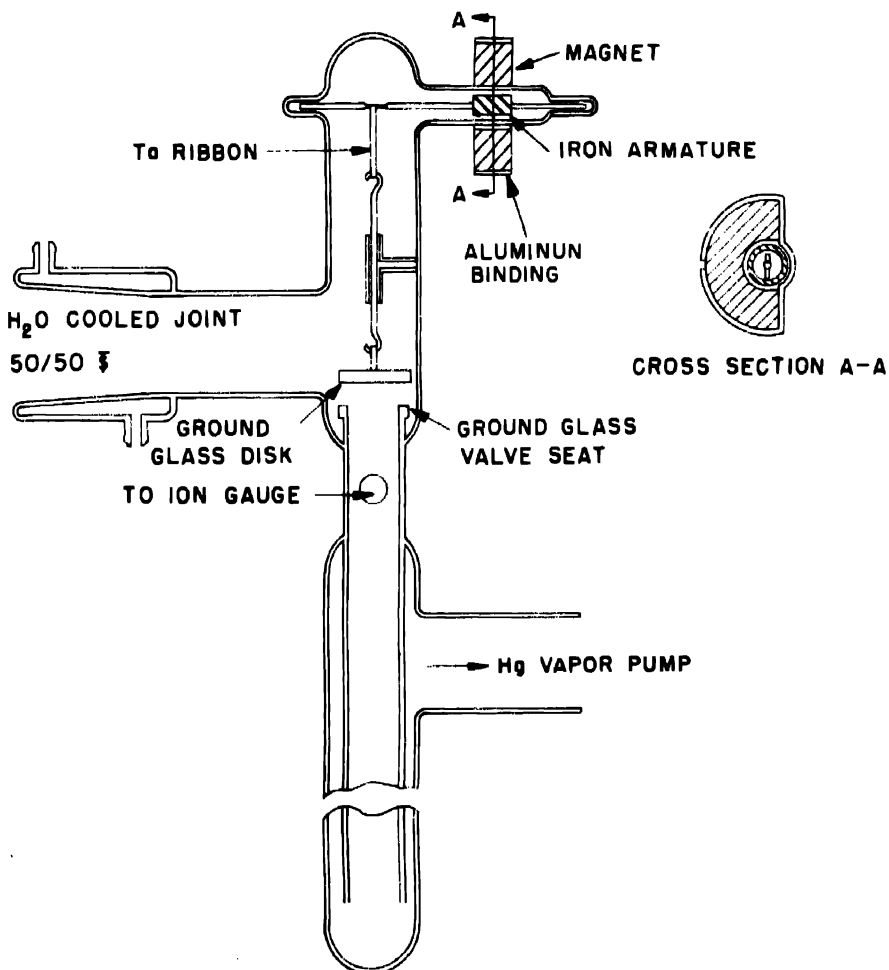


Fig. 1—Schematic cross-sectional diagram of glass high-vacuum valve.

and circular seat, both carefully ground to a plane surface. A windlass, operated magnetically from outside the glass line, permitted opening and closing the valve, which by virtue of its large aperture and the freedom from lubricants, packing, etc., could be flamed and was well suited to high-vacuum work in a glass system. It permitted

breaking the vacuum in the furnace bulb to atmospheric pressure, and allowed loading of the furnace without cooling the mercury diffusion pumps. With a pressure differential of 1 atm, a triple-stage mercury diffusion pump of about 60 liters per second capacity was able to maintain a vacuum of  $10^{-3}$  to  $10^{-4}$  mm Hg in the system. A small-diameter by-pass permitted reevacuation of the bulb with a separate mechanical pump.

Table 1

Element	Amount, ppm	Method
C	200 to 240	Microcombustion
N	20 to 30	Microcombustion
O	<200	Microcombustion
S	200 $\pm$ 50	Colorimetric
Fe	100	Colorimetric

1.3 Purity of the Plutonium Metal. Spectrochemical analyses of high sensitivity were obtained for all the plutonium metal samples employed in this study. These indicated the absence of more than a few parts per million of most cations.

Special microchemical analyses on certain samples gave the typical results shown in Table 1.

Still further evidence of the absence of significant amounts of plutonium compounds ( $\text{PuO}$ , etc.) was obtained by the precise comparison of the specific  $\alpha$  activities of these metal samples with those of samples prepared during an extensive investigation.<sup>3</sup>

To ensure a reproducible, well-defined standard state at 25°C, the globules of plutonium metal were treated so as to provide a stable material the uniformity of which could be established.

## 2. PREPARATION AND PURITY OF PLUTONIUM TRICHLORIDE

2.1 Preparation of Plutonium Trichloride. Plutonium(III) oxalate from the same stock used for the metal preparation was dehydrated in a platinum boat in a quartz reactor<sup>4</sup> by passing oxygen-free hydrogen over the  $\text{Pu}_2(\text{C}_2\text{O}_4)_3 \cdot x\text{H}_2\text{O}$  at a temperature which was gradually increased to about 150°C. Then anhydrous hydrogen chloride, purified by fractional distillation, and hydrogen (mole ratio of HCl to H<sub>2</sub> of about 1.5) were passed through the reactor at a rate of about 60 ml per minute while the temperature of the reactor was raised very gradually over a period of several hours to about 300°C. It was then raised slowly to 700°C and maintained there for 8 hr. After it had

been cooled to room temperature and had been evacuated, anhydrous nitrogen was admitted to the reactor, which was then sealed, removed from the preparation line, and opened in the dry box for the immediate loading of a quartz tube for sublimation in high vacuum at about 1000°C. The sublimate collected in emerald-green crystals approximately 0.3 mm in length. After the vacuum had been broken with purified anhydrous argon, the contents of the sealed-off sublimate section of the tube were loaded into the sample bulbs within a dry box. The identity of the material was established by the x-ray diffraction measurements of W. H. Zachariasen.

**2.2 Analysis of the Plutonium Trichloride.** Spectrochemical analysis indicated the essential absence of foreign cations.

Micro-scale ignition to  $\text{PuO}_2$  of samples of the preparation gave gravimetric confirmation of the composition of the  $\text{PuCl}_3$ . Platinum microcrucibles of the J. Lawrence Smith type, with well-fitted telescoping caps, made possible the loading of hygroscopic samples into the crucibles in the anhydrous nitrogen atmosphere of the dry box and weighing them in the laboratory atmosphere. Phosphorus pentoxide was weighed as a test material in preliminary experiments. Appropriate corrections for the nitrogen atmosphere and for reduction to vacuum were made. After they had been ignited to constant weight at temperatures higher than those to be used for the actual conversion, the crucibles were loaded with a few milligrams of  $\text{PuCl}_3$  in the dry box, weighed, opened, and placed on a platinum support which inclined the crucible at about 60 deg from the horizontal. A platinum baffle prevented contamination by foreign matter. The crucibles were then ignited to constant weight in a platinum wound microfurnace in air by gradually increasing the temperature to 850°C.

Two samples of  $\text{PuCl}_3$  from the above preparation showed losses in weight on ignition corresponding to 21.45 and  $21.50 \pm 0.3$  per cent (theoretical 21.52 per cent).

Confirmation of the plutonium content of the trichloride (and evidence of the completeness of dissolution) was obtained from precise  $\alpha$  radiometric assay of the solution in the calorimeter. These results, presented in detail in another paper,<sup>2</sup> show that the  $\alpha$  activity of the  $\text{Pu}^{239}$  from the trichloride preparation (assuming pure  $\text{PuCl}_3$ ) was  $70,730 \pm 60$  counts per minute per microgram; this may be compared with that of the metal used for these measurements ( $70,670 \pm 70$ ) and other larger specially prepared metal samples ( $70,660 \pm 70$ ).

### 3. CALORIMETRIC MEASUREMENTS

The calorimeter, circuits, and electrical and chemical calibration have been described elsewhere.<sup>5</sup> Electrical calibration of the heat

capacity of the system, with a weighed quantity of 6.0M HCl made at an energy input rate comparable to that of the solution reaction, showed consistency to better than 0.07 per cent.

Dissolved air was removed from the carefully standardized hydrochloric acid stock by a continuous slow stream of bubbles of purified hydrogen previously saturated with acid of identical concentration.

Table 2—Heat of Solution of Plutonium Metal in 6.000 M HCl at 25.00°C  
Weight of Acid (vacuum) = 212.25 g

Sample† particles	No. of	Plutonium			Analysis	Heat evolved, cal	Corrected‡ ΔH solution, kcal/mole
		Weight, vacuum, mg	content, radiometric	assay, %			
A	1	19.43	99.0 ± 0.3	1-2% Ca, 0.1% Na	Spec. pure.	11.231	(-138.5)§
B	2	30.38	100.0 ± 0.2		Spec. pure.	17.951	-141.57
C	3	47.29	100.0 ± 0.2		Spec. pure.	27.955	-141.63
D	2	44.24	100.1 ± 0.2		Cf. Table 1	26.155	-141.65
E	3	35.94	100.1 ± 0.2		Cf. Table 1	21.255	-141.70
(av.) - 141.64 ± 0.2							

†Samples A, B, and C were micro-scale reductions. Sample A was remelted on a tantalum filament in high vacuum at 1500°C. The surfaces of D and of E were mechanically cleaned with a glass-fiber brush.

‡Includes correction of ± 0.31 kcal per mole of Pu for vaporization of solvent by evolved hydrogen. It was assumed that the hydrogen gas was saturated with water vapor and hydrogen chloride on leaving the solution at the partial pressures given in the International Critical Tables, Vol. III, McGraw-Hill Book Company, Inc., New York, 1928.

§Preliminary run, rejected from average value because of impurities introduced from contamination of the laboratory distilled water supply.

The acid was standardized against mercuric oxide by J. W. Bane of the Analytical Section. It was weighed directly into the calorimeter. Approximately 1 hr later the sample bulb was broken. Within 30 sec at least 95 per cent of the total energy evolved by the reaction was already apparent in the temperature rise. An hour later the calorimeter was disassembled. Duplicate aliquots by weight of the solution were immediately taken. Another portion of the solution was put into a glass-stoppered cell, and the absorption spectrum in the region of interest was determined with a Beckman spectrophotometer to establish the ultimate oxidation state of the plutonium. None of the plutonium (within 1 per cent sensitivity) was detected in oxidation states

higher than 3. The solution in the spectrophotometer cell showed a gradual oxidation such that Pu(IV) could be detected in 12 hr, and after a week the pale blue-violet solution had perceptibly changed toward yellow-green, thereby indicating oxidation of the Pu(III) at a very slow rate.

Table 3—Heat of Solution of Plutonium Trichloride in 6.000 M HCl at 25.00°C

Weight of acid (vacuum) = 212.25 g

Sample	Weight, vacuum, mg	Plutonium content, radiometric assay, %	Heat evolved, cal	$\Delta H$ solution, kcal/mole
A	96.01	99.8 ± 0.3	6.754	-22.14
B	116.84	100.2 ± 0.3	7.51	-22.2
C	96.51	100.0 ± 0.3	6.188	-22.15
				-22.15 ± 0.1 (av.)

The energy produced by the radioactive  $\alpha$  disintegration of the plutonium provides no source of error on the scale of the present determinations. The energy of the liberated  $\alpha$  particles,  $2.8 \times 10^{-5}$  calories per minute per milligram, is absorbed by the calorimetric system whether the sample is solid or dissolved. The possibility of the production of a temperature gradient, caused by self-absorption of the  $\alpha$  particles within the solid sample, the surface of which is assumed to be at thermal equilibrium with the calorimeter, was considered and shown to cause an effect small compared to the experimental error.

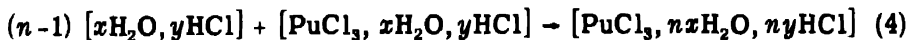
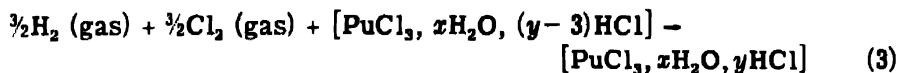
The heat-of-solution data are presented in Tables 2 and 3. The correction for the drift during the experimental period amounts to less than 1 per cent of the temperature rise because dissolution and the reattainment of thermal equilibrium were so rapid.

#### 4. THE HEAT OF FORMATION

These data are expressed in terms of a defined calorie equal to 4.1833 joules.<sup>6</sup> The atomic weight of the plutonium is taken as 239.07, and the molecular weight of  $\text{PuCl}_3$  is taken as 345.44.

Addition of the sequence of reactions:





Eq. 1 - Eq. 2 + Eq. 3 + Eq. 4 = Eq. 5 gives the desired formation reaction,



Reactions 1 and 2 correspond to the measured heats of solution with average values of  $x_1 = 58,000$ ,  $nx_2 = 32,000$ ,  $my_1 = x_1$ ,  $my_2 = x_2$  ( $m = 8.105$ ); consequently  $n = 0.56$ . For this value of  $n$ , the heat of reaction 4 is assumed to be zero since the salt is in high dilution in a medium of constant ionic strength.

The heat of reaction 3 is assumed to be uninfluenced by the very small concentration of plutonium(III) and is evaluated from the data of Rossini<sup>6,7</sup> on the heat of formation of the infinitely dilute aqueous solution of hydrogen chloride,

$$\Delta H_{298.1} = -40.023 \pm 0.040 \text{ kcal per mole}$$

and on the relative molal heat content of 6 molar (6.000 molar = HCl, 8.105 H<sub>2</sub>O).

The heat of formation of crystalline PuCl<sub>3</sub> is, therefore,

$$\Delta H_{298.1} = -141.6 + 22.15 - 3(36.84) = -230.0 \pm 0.3 \text{ kcal per mole}$$

Consideration of the precision of the measurements, of the accuracy of the calibration, and of the purity of the substances suggests the reliability of the probable error indicated.

## 5. SUMMARY

The heats of solution of plutonium metal and crystalline PuCl<sub>3</sub> were determined in 6M HCl at 25°C as  $-141.6 \pm 0.2$  kcal per mole and  $-22.15 \pm 0.1$  kcal per mole, respectively. The heat of formation of PuCl<sub>3</sub> from the elements was calculated to be  $-230.0 \pm 0.3$  kcal per mole at 25°C.

## REFERENCES

1. Reported by J. W. Kennedy and C. S. Smith, Los Alamos Report LAMS-101 (July 14, 1944).
2. E. F. Westrum, Jr., Metallurgical Project Reports CK-1586 (A-2251) (May 1944), p. 20, and CN-2495 (January 1945), p. 12; reported in J. Am. Chem. Soc., 70: 3543 (1948).
3. E. F. Westrum, Jr., J. C. Hindman, and R. Greenlee, The specific alpha radioactivity and half life of plutonium isotope of mass 239, Paper 22.80, this volume.
4. E. F. Westrum, Jr., and H. P. Robinson, The heat of formation of plutonium oxychloride, Paper 6.56, this volume (Metallurgical Project Report CC-3880).
5. E. F. Westrum, Jr., and H. P. Robinson, A semi-microcalorimeter for precise thermochemical measurements, Paper 6.51, this volume (Metallurgical Project Report CC-3885).
6. Selected values of chemical thermodynamic properties, Natl. Bur. Standards U. S., Washington, Dec. 31, 1947.
7. F. D. Rossini, J. Research Natl. Bur. Standards, 9: 679 (1932).

Paper 6.54

THE DEPENDENCE OF THE HEAT OF SOLUTION OF PLUTONIUM  
TRICHLORIDE ON THE CONCENTRATION OF  
HYDROCHLORIC ACID†

By H. P. Robinson and E. F. Westrum, Jr.

The heat of solution of  $\text{PuCl}_3$  in 1.5M HCl was measured as part of a sequence of reactions to determine the heat of formation of  $\text{PuF}_3$ . A value in more dilute acid was desirable to extrapolate the heat of solution to infinite dilution of the acid. Measurements were also made in more concentrated acid.

1. THE PREPARATION AND PURITY OF THE PLUTONIUM TRICHLORIDE

The method used for the preparation of these samples was similar to that previously described,<sup>1</sup> except that instead of the preparation being sublimed, the quartz reactor<sup>2</sup> was cooled from 700 to 100°C and evacuated. After it had cooled to room temperature, the high vacuum was broken with nitrogen dried over phosphorus pentoxide.

The preparation was identified and the crystallographic constants were determined by Dr. W. H. Zachariasen, using x-ray diffraction techniques. Spectrochemical analysis indicated the absence of foreign cations. Alpha radiometric assay on the solutions from the calorimeter compared with accurate standards prepared from plutonium metal globules<sup>4</sup> from the same stock indicated the percentage of plutonium in the trichloride to agree with the theoretical value within the experimental error ( $\pm 0.3$  per cent). Ignition of samples to the oxide gave a gravimetric confirmation of the composition ( $\pm 0.3$  per cent).

†Contribution from the Chemistry Division of the Metallurgical Laboratory, University of Chicago, now the Argonne National Laboratory.

Based on work reported in Metallurgical Laboratory Memorandums MUC-GTS-1998 (Oct. 4, 1945) and MUC-GTS-1999 (Oct. 5, 1945).

## 2. THE CALORIMETRIC MEASUREMENTS

The calorimeter, technique, and calibration have been described.<sup>5</sup> Hydrogen saturated with acid of identical concentration was bubbled through the acid stock continuously to remove dissolved oxygen prior to each of the determinations. R. W. Bane of the Analytical Section standardized the various concentrations of hydrochloric acid volumetrically against standard alkali or against mercuric oxide.

Table 1 — Heat of Solution of Plutonium Trichloride in Hydrochloric Acid at 25.00°C

Sample	Concentration of acid, molarity	Weight of acid (vacuum), g	Weight of PuCl <sub>3</sub> (vacuum), mg	Theoretical <sup>a</sup> plutonium by radiometric assay, %	Heat evolved, calories	ΔH(solution), kcal/mole
A	0.1000	192.26	67.16	100.0 ± 0.3	6.174	-31.76 ± 0.1
B	1.500	192.25	78.58	99.6 ± 0.3	6.694	-29.43
C		192.25	48.98	100.1 ± 0.3	4.192	-29.57
						-29.5 ± 0.1†
D‡	6.000	212.25	96.01	99.8 ± 0.3	6.154	-22.14
E‡		212.25	116.84	100.2 ± 0.3	7.51	-22.2
F‡		212.25	96.51	100.0 ± 0.3	6.188	-22.15
						-22.15 ± 0.1†
G	9.00	217.25	88.10		3.708	-14.54 ± 0.1
H	11.38	222.24	98.35	100.0 ± 0.3	2.8 - 2.9	-(9.8 - 10.2)

† Weighted average.

‡ See reference 1.

Solution of the finely divided crystalline trichloride takes place very rapidly (10 to 20 sec) if the hydrochloric acid concentration is 6M and below, is definitely slower in the 9M acid, and is apparently four or five times as slow in the 11.38M acid. Spectrophotometric measurements indicated the absence of oxidation states higher than +3 for the duration of the runs for all concentrations of acid. The rate of air oxidation of the solutions removed from the calorimeter was several times as rapid for the two highest acid concentrations as for the more dilute acids. The data are summarized in Table 1 in terms of a defined thermochemical calorie equal to 4.1833 international joules.

The single, unconfirmed value for the heat of solution in 11.38M acid is uncertain, at least to the extent indicated in Table 1, owing to

the presence of a hump of unknown origin in the temperature vs. time graph for the run. Three minutes after breaking the sample bulb the temperature rose to a maximum and smoothly decreased about  $0.001^{\circ}\text{C}$  over 8 min, then settled down to a normal afterdrift in agreement with the calculated value of less than  $10^{-6}$  degrees centigrade per minute. No evidence that this apparently unique effect could be attributed to some failure of the thermometric circuit was discerned.

### 3. DISCUSSION

As might be expected from an analogy with the large tripositive rare-earth ions and iron(III), plutonium(III) does not appear to form a chloride complex in appreciable concentration<sup>7</sup> below 4.4M HCl.

If the  $\Delta$  values (i.e., the slope of the heat of solution of a trichloride salt vs. hydrochloric acid concentration over the range of 0–2.6 moles per liter) are arranged against the ionic radius,<sup>8</sup> a linear relation is observed within the experimental error of the meager available data<sup>9</sup> on  $\text{GaCl}_3$ ,  $\text{InCl}_3$ ,  $\text{LaCl}_3$ , and  $\text{FeCl}_3$ . It is noted that by using the ionic radius of plutonium given by Zachariasen<sup>10</sup> appropriately adjusted to Goldschmidt's scale, the  $\Delta$  value for  $\text{PuCl}_3$  also falls on such a curve.

The three determinations of the heat of solution at 0.1M, 1.5M, and 8.0M HCl are linear when plotted against the molarity of the acid. The short extrapolation of the solutions about  $10^{-3}$ M with respect to plutonium gives  $\Delta H_{298.1} = -31.9$  kcal/mole for the reaction



Combining this value with heat of formation of the infinitely dilute aqueous solution of hydrogen chloride<sup>11,12</sup> and the heat of formation<sup>1</sup> of  $\text{PuCl}_3$  yields a value of  $\Delta H_{298} = -141.8$  kcal/mole for the reaction



The entropy of this reaction has been estimated<sup>13,14</sup>  $\Delta S_{298.1} = 3.8$  e.u. from which  $\Delta F_{298.1} = -142.9$  kcal/mole.

### 4. SUMMARY

The heat of solution (reaction) of  $\text{PuCl}_3$  has been measured at  $25^{\circ}\text{C}$  in hydrochloric acid of concentration 0.1M, 1.5M, 6M, 9M, and 11.4M. The heat of solution of  $\text{PuCl}_3$  in infinitely dilute hydrochloric acid has been found by extrapolation to be  $-31.9$  kcal/mole, and the heat of formation of Pu(III) ion has been calculated as  $-141.8$  kcal/mole.

## REFERENCES

1. Edgar F. Westrum, Jr., and H. P. Robinson, The heat of formation of plutonium trichloride, Paper 6.53, this volume (Metallurgical Project Report CC-3872).
2. Edgar F. Westrum, Jr., and H. P. Robinson, The heat of formation of plutonium oxychloride, Fig. 1, Paper 6.56, this volume (Metallurgical Project Report CC-3880).
3. E. F. Westrum, Jr., J. C. Hindman, and R. Greenlee, The specific alpha radioactivity and half life of plutonium isotope of mass 239, Paper 22.80, this volume.
4. Edgar F. Westrum, Jr., An improved technique for precise alpha radiometric assay, Paper 16.2, this volume (Metallurgical Project Report CN-3433).
5. Edgar F. Westrum, Jr. and H. P. Robinson, A semi-microcalorimeter for precise thermochemical measurements, Paper 6.51, this volume (Metallurgical Project Report CC-3885).
6. Edgar F. Westrum, Jr., An improved technique for precise alpha radiometric assay, Table 1, Paper 16.2, this volume.
7. J. C. Hindman, private communication.
8. V. M. Goldschmidt, Chem. Ber., 60: 1263 (1927).
9. W. Klemm, Z. anorg. Chem., 249: 23 (1942).
10. W. H. Zachariasen, Metallurgical Project Report CN-2526 (Jan. 2, 1945).
11. F. D. Rossini, J. Research Natl. Bur. Standards, 9: 679 (1932).
12. Selected values of chemical thermodynamic properties, Natl. Bur. Standards U. S., Washington, Dec. 31, 1947.
13. M. W. Evans, Metallurgical Project Report CN-3138 (Aug. 31, 1945).
14. L. Brewer, L. Bromley, P. W. Gilles, and N. L. Lofgren, Metallurgical Project Report CN-3378 (Dec. 1, 1945).

## THE HEAT OF FORMATION OF PLUTONIUM TRIBROMIDE†

By E. F. Westrum, Jr.

This paper presents measurements of the heat of solution of plutonium tribromide. These data, combined with our earlier measurements of the heat of solution of plutonium metal and other thermochemical data, permit the calculation of the heat of formation.

### 1. THE PREPARATION AND PURITY OF PuBr<sub>3</sub>

A portion of the stock of plutonium specially purified for the plutonium calorimetric work<sup>1</sup> was precipitated as Pu<sub>2</sub>(C<sub>2</sub>O<sub>4</sub>)<sub>3</sub>·xH<sub>2</sub>O and converted to PuBr<sub>3</sub> in a quartz reactor<sup>2</sup> with an equimolal mixture of oxygen-free anhydrous hydrogen and fractionally distilled hydrogen bromide prepared from hydrogen and bromine. The temperature of the reactor was gradually raised to 650°C, and the reactor was kept at this temperature for 4 hr. After the preparation was transferred to a 4-mm I.D. quartz tube in a dry box, it was distilled in a high vacuum at about 800°C. The quartz tube was sealed off after the vacuum was broken with anhydrous, oxygen-free argon; the tube was later opened in a dry box and immediately loaded into the sample bulbs, which were then sealed and weighed.

The identity and crystallographic constants of the preparation were established by W. H. Zachariasen. Ignition in air of two samples of PuBr<sub>3</sub> by the micro technique previously described<sup>1</sup> gave losses in weight of 43.37 and 43.29 ± 0.06 per cent compared to a theoretical loss of 43.39 per cent. The mean value of the analyses would correspond to about 0.2 per cent PuOBr if PuOBr is assumed to be the only

†Contribution from the Chemistry Division of the Metallurgical Laboratory, University of Chicago, now the Argonne National Laboratory.

Based on work reported in Metallurgical Project Report CS-3160 (July 24, 1945), p. 5, and Metallurgical Laboratory Memorandum MUC-GTS-1032 (Aug. 30, 1945).

impurity. Very sensitive spectrochemical analysis established the absence of other metals.

Alpha radiometric assay<sup>3</sup> of the final solutions in the calorimeter indicated the theoretical content of plutonium 239 within  $\pm 0.02$  per cent.

## 2. THE HEAT OF SOLUTION

Details of the calorimeter, the technique, and the calibration are described<sup>4</sup> in another paper of this volume.

The same 6M HCl stock used for calorimetric determinations on Pu and PuCl<sub>3</sub> was similarly saturated with hydrogen to remove dissolved air and to prevent oxidation of plutonium(III) in these measurements.

Table 1—The Heat of Solution of PuBr<sub>3</sub> in 6.000M HCl

Weight of hydrochloric acid (in vacuum), 212.25 g;  
temperature, 25.00°C; percentage of the theoretical  
plutonium content ( $\alpha$  radiometric analysis), 100.0  $\pm$  0.2 per cent

Sample	Weight of PuBr <sub>3</sub> , (vacuum), mg	Heat evolved, cal	$\Delta H$ solution, kcal/mole
A	120.33	7.752	-30.85
B	145.60	9.382	-30.85
$-30.85 \pm 0.1$ (av.)			

The dissolution of the PuCl<sub>3</sub> was more than 95 per cent complete in 20 sec. The data are given in Table 1. Spectrophotometric tracings of the absorption spectrum of the plutonium(III) solution from the calorimeter showed the absence of the tetrapositive and hexapositive oxidation states within the limit of detection of about 1 per cent. The  $\alpha$  radiometric assays of weighed aliquots of these solutions show the completeness of the dissolution.

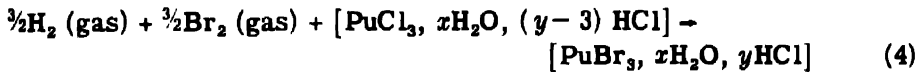
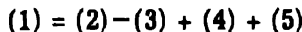
## 3. THE HEAT OF FORMATION

These data are expressed in terms of a defined calorie equal to 4.1840 absolute joules. The atomic weight of Pu<sup>239</sup> is taken as 239.07; the molecular weight of PuBr<sub>3</sub> is taken as 478.82.

The heat of formation of plutonium bromide,



is the resultant of the series of reactions, i.e.,



Reactions 2 and 3 correspond to measured heats of solution of plutonium<sup>1</sup> and plutonium tribromide with  $x_1 = 58,000 = my_1$ , and  $nx_2 = 35,000 = nmy_2$  ( $m = 8.105$ ); therefore,  $n = 0.60$ . The heat of the approximately twofold dilution of plutonium(III) bromide in 6M HCl (reaction 5) is taken as zero since the plutonium concentrations are less than  $3 \times 10^{-4}$ M. It is assumed that the heat of reaction 4 is not influenced by the vanishingly small concentration of plutonium and that the apparent heat of formation of hydrogen bromide is the same in an aqueous solution of hydrogen chloride as in an aqueous solution of hydrogen bromide of the same molality.

**3.1 PuBr<sub>3</sub>.** Graphical interpolation of values<sup>5</sup> for this heat of the reaction

$$\begin{aligned} \frac{1}{2}\text{H}_2 \text{ (gas)} + \frac{1}{2}\text{Br}_2 \text{ (liq)} + \left(\frac{y-3}{3}\right) [\text{HBr}, 8.1016\text{H}_2\text{O}] \\ = \frac{y}{3} [\text{HBr}, 8.105\text{H}_2\text{O}] \end{aligned}$$

gives

$$\Delta H_{298} = -27.41 - 1.72 = -25.69 \text{ kcal per mole}$$

To obtain the heat of formation of gaseous bromine, we correct for the heat of vaporization at 25°C, 7.34 kcal per mole, and obtain

$$\Delta H_{298} = -29.36 \text{ kcal per mole}$$

The heat of formation of plutonium tribromide from gaseous bromine and plutonium is

$$\Delta H_{298} = -141.6 + 30.85 - 3(29.36) = -198.8 \text{ kcal per mole}$$

The corresponding value using liquid bromine as the standard state is

$$\Delta H_{298} = -187.8 \text{ kcal per mole}$$

#### 4. SUMMARY

The preparation of  $\text{PuBr}_3$  has been described.

The heat of solution of  $\text{PuBr}_3$  has been measured in 6.0M HCl at 25.00°C and found to be  $-30.85 \pm 0.1$  kcal per mole. The heat of formation of  $\text{PuBr}_3(\text{c})$  from gaseous bromine and plutonium is calculated as -198.8 kcal per mole; the corresponding value using liquid bromine as the standard state is -187.8 kcal per mole.

#### ACKNOWLEDGMENT

The authors acknowledge with thanks the assistance of B. M. Abraham in the preparation of the compound.

#### REFERENCES

1. E. F. Westrum, Jr., and H. P. Robinson, The heat of formation of plutonium trichloride, Paper 6.53, this volume (Metallurgical Project Report CC-3872).
2. E. F. Westrum, Jr., and H. P. Robinson, The heat of formation of plutonium oxychloride, Paper 6.56, this volume (Metallurgical Project Report CC-3880).
3. E. F. Westrum, Jr., J. C. Hindman, and R. Greenlee, The specific alpha radioactivity and half life of plutonium isotope of mass 239, Paper 22.80, this volume.
4. E. F. Westrum, Jr., and H. P. Robinson, A semi-microcalorimeter for precise thermochemical measurements, Paper 6.51, this volume (Metallurgical Project Report CC-3885).
5. Selected values of chemical thermodynamic properties, Natl. Bur. Standards U.S., Washington, Dec. 31, 1947.

## Paper 6.56

### THE HEAT OF FORMATION OF PLUTONIUM OXYCHLORIDE†

By E. F. Westrum, Jr., and H. P. Robinson

Plutonium oxychloride has been prepared and its heat of solution in hydrochloric acid has been determined. These and other measurements permit calculation of an accurate value for its heat of formation.

#### 1. PREPARATION AND PURITY OF PLUTONIUM OXYCHLORIDE

Plutonium oxychloride was prepared from plutonium chloride by reaction with a stream of hydrogen, hydrogen chloride, and water vapor. The specially purified plutonium prepared for calorimetric purposes by the Recovery Group was reduced, precipitated as oxalate, and washed. The  $\text{Pu}_2(\text{C}_2\text{O}_4)_3 \cdot x\text{H}_2\text{O}$  was converted<sup>1</sup> to  $\text{PuCl}_3$ , in a quartz reactor (see Fig. 1) attached to a flow system and vacuum line, by passing oxygen-free hydrogen and fractionally distilled hydrogen chloride through the reactor. During the process the temperature was raised from 25 to 600°C over a period of 4 hr and maintained at the higher temperature for 12 hr. The reactor was then cooled to 150°C and evacuated to  $10^{-5}$  mm Hg pressure, the furnace was removed, and the sample was cooled to room temperature in purified argon. The preparation was made from oxalate via the trichloride because of the difficulty of hydrochlorinating  $\text{PuO}_2$ .

Hydrogen and hydrogen chloride were then passed into the system at such relative rates that upon saturation with water vapor and hydrogen chloride from the bubbler (see Fig. 1) containing concentrated

†Contribution from the Chemistry Division of the Metallurgical Laboratory, University of Chicago, now the Argonne National Laboratory.

Based on work reported in Metallurgical Project Report CS-3421 (Feb. 6, 1946) and Metallurgical Laboratory Memorandum MUC-GTS-2146 (Jan. 14, 1946), p. 3.

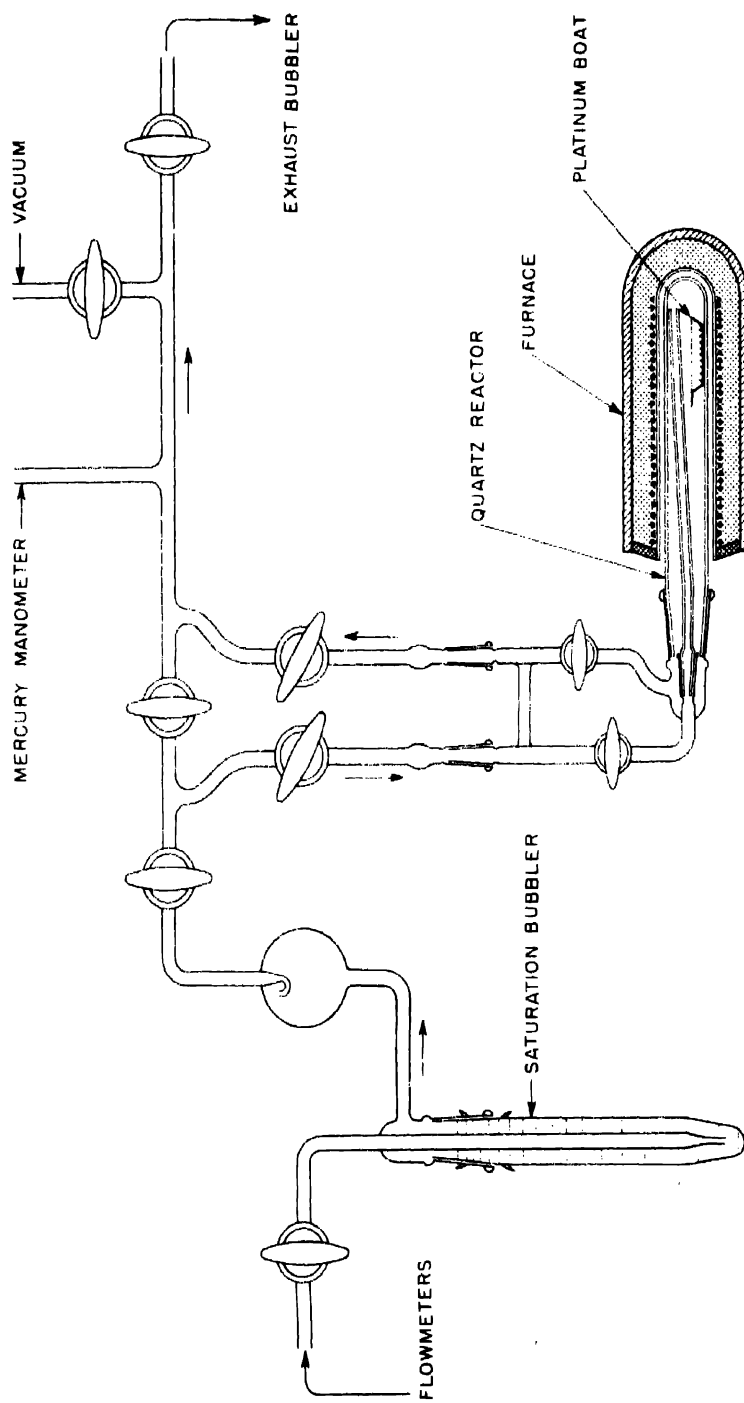


Fig. 1.—Reactor for the preparation of halides and oxyhalides of plutonium.

hydrochloric acid (11.8M), the composition of the hydrochloric acid remained constant. Under these conditions (suggested by the data of Sheft and Davidson<sup>2</sup> and modified empirically after further experimental study) the partial pressures of the H<sub>2</sub>O, HCl, and H<sub>2</sub> were 0.43 cm, 15.8 cm, and 74 cm, respectively. The total flow rate was about 110 cc per minute for a 400-mg batch. The temperature was raised gradually to 675°C and held at this value for 8 hr.

The PuOCl was a pale, bluish-green color nearly indistinguishable from that of PuCl<sub>3</sub>, of similar crystal size, and very porous. Zachariasen identified the phase as that of PuOCl by x-ray diffraction; he obtained no diffraction lines due to other phases, which indicated less than 10 per cent of a nonisomorphous crystalline impurity. He stated that the crystallite size was larger than 500 Å.

No metallic impurities were detected by spectrochemical analysis. Duplicate microgravimetric determinations of chloride as silver chloride made on the 8-mg scale indicated, respectively, 12.21 and  $12.19 \pm 0.1$  per cent chloride (theoretical, 12.21 per cent).

Alpha radiometric assay for plutonium (by the precise gravimetric method<sup>3</sup> developed by one of the authors) on the samples dissolved in the calorimeter runs A, B, and C yielded 82.24, 82.28, and  $82.26 \pm 0.07$  per cent, respectively (theoretical for PuOCl, 82.29 per cent plutonium).

Freshly prepared anhydrous PuOCl showed no increase ( $\pm 0.1$  per cent) in weight upon 2 hr exposure to the atmosphere at 25°C and a relative humidity of 34 per cent.

## 2. THE HEAT OF SOLUTION OF PuOCl

The calorimeter and its calibration and the technique used have been described.<sup>4</sup> Additional electrical energy calibrations of the heat capacity of the calorimeter made during these measurements were in excellent accord with previous values. Special care was used to saturate the acid with hydrogen and to remove traces of oxygen. The PuOCl samples dissolved very rapidly; 99 per cent of the temperature rise was observed in 25 sec after breaking the fragile sample bulb. The calorimetric data are presented in Table 1.

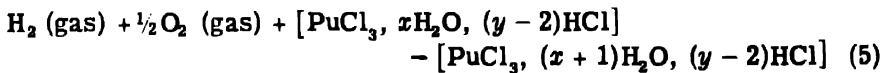
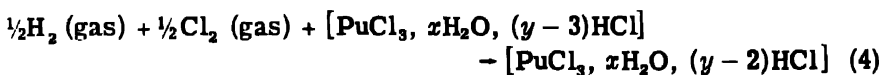
## 3. THE HEAT OF FORMATION

The appropriate atomic weight for the plutonium used in these measurements is 239.07, and the molecular weight of PuOCl is 290.53. These data are expressed in terms of a defined calorie equal to 4.1833 international joules.

The formation reaction of crystalline PuOCl from plutonium metal and gaseous chlorine and oxygen



is the resultant of the following reactions:



We have reported the heat of solution of plutonium metal in the same calorimeter<sup>1</sup> under conditions almost identical with those for

Table 1—The Heat of Solution of Plutonium Oxychloride in 6M HCl

Weight of acid, vacuum = 212.25 g; temperature = 25.00°C; percentage of theoretical plutonium content (radiometric assay<sup>3</sup> = 100.0 ± 0.2 per cent)

Run	Weight of PuOCl, vacuum, mg	Heat evolved, cal	ΔH solution, kcal/mole
A	100.96	8.398	-24.17
B	107.66	8.956	-24.17
C	108.32	9.008	-24.16
-24.17 ± 0.1 (av.)			

the heat of solution of PuOCl. The heat of dilution of plutonium(III) chloride in 6M HCl (with respect to the concentration of PuCl<sub>3</sub>, only) is taken as zero since the concentrations are so small and since the ionic strengths of the solutions are the same. It is further assumed that the heats of reactions 4 and 5 are the same in the absence of the approximately 0.0002M concentration of plutonium since the ionic strengths of the solutions compared are equal.

The heat of formation of the infinitely dilute aqueous solution<sup>6</sup> and the relative apparent molal heat content of 6 molar (= 6.844 molal) hydrogen chloride is used to evaluate reaction 4. The heat of formation of liquid water<sup>6</sup> at 25°C together with the apparent molal heat contents of the solutions provides the heat of reaction 5. Therefore at 298°K

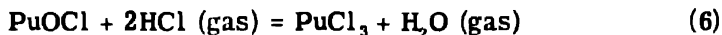
$$\Delta H_{(1)}^\circ = \Delta H_{(2)}^\circ - \Delta H_{(3)}^\circ + \Delta H_{(4)}^\circ + \Delta H_{(5)}^\circ$$

$$\Delta H_{298.1^\circ K}^\circ = -141.6 + 24.17 - 36.84 - 68.52 = -222.8 \text{ kcal per mole}$$

is the heat of formation of plutonium oxychloride from plutonium metal, oxygen, and chlorine gas.

#### 4. DISCUSSION

Sheft and Davidson<sup>2</sup> have studied the equilibrium pressures of the reaction



between temperatures of 814 and 969°K, and they have extrapolated a value of  $\Delta H_{298.1}^\circ = -22.2 \pm 0.7$  kcal per mole for reaction 6.

From our data on the heats of solution and the heats of formation of water and hydrogen chloride,<sup>6</sup> we estimate a value of  $\Delta H_{298}^\circ = -20.3 \pm 0.3$  for this reaction. The difference appears to be beyond their indicated experimental uncertainty. However, they clearly did not achieve complete equilibrium. Moreover, a straight line, the slope of which corresponds to our value of the  $\Delta H_{298}$  for reaction 6, can be drawn through their scattered experimental points (on a graph of  $\log K$  vs.  $1/T$ ) so that all the points which lie above the line are from experiments in which equilibrium was approached from the water-rich side, and, conversely, so that all the points which lie below the line are from experiments in which equilibrium was approached from the water-poor side.

Consequently it appears that the experimental data of Sheft and Davidson are entirely in accord with the values reported in this paper but that their treatment of the nonequilibrium data by the method of least squares and estimation of the experimental error on this basis may not be justified.

#### 5. SUMMARY

The heat of solution of plutonium oxychloride in 6M HCl at 25°C is  $-24.17 \pm 0.1$  kcal per mole. The heat of formation of PuOCl is  $-222.8 \pm 0.3$  kcal per mole. These data are correlated with other thermodynamic measurements.

#### REFERENCES

- E. F. Westrum, Jr., and H. P. Robinson, The heat of formation of plutonium trichloride, Paper 6.53, this volume (Metallurgical Project Report CC-3872).

2. I. Sheft and N. R. Davidson, Equilibrium in the vapor-phase hydrolysis of plutonium trichloride, Paper 6.25, this volume.
3. E. F. Westrum, Jr., An improved technique for precise alpha radiometric assay, Paper 16.2, this volume (Metallurgical Project Report CN-3433).
4. E. F. Westrum, Jr., and H. P. Robinson, A semi-microcalorimeter for precise thermochemical measurements, Paper 6.51, this volume (Metallurgical Project Report CC-3885).
5. E. F. Westrum, Jr., J. C. Hindman, and R. Greenlee, The specific alpha radioactivity and half life of plutonium isotope of mass 239, Paper 22.80, this volume.
6. Selected values of chemical thermodynamic properties, Natl. Bur. Standards U.S., Washington, Dec. 31, 1947.

## Paper 6.57

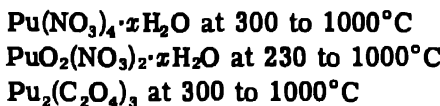
### THE PREPARATION AND PROPERTIES OF PLUTONIUM OXIDES<sup>†</sup>

By E. F. Westrum, Jr.

The chemistry of the plutonium oxides is important in evaluating the metal-oxygen systems of the heaviest elements. Consequently, methods of synthesis and observations of the properties and reactions of plutonium oxides are considered in this paper. The determination of the vapor pressure of plutonium oxide systems, and the crystal structure<sup>1</sup> are described in other reports. Plutonium hydroxides and peroxides are not included within the scope of this report, but they are considered elsewhere.

#### 1. PREPARATION OF PLUTONIUM DIOXIDE

The dioxide,  $\text{PuO}_2$ , is the most stable oxide of plutonium, and it is the final product of the ignition of most plutonium compounds in air. It is commonly prepared on the macro scale by igniting the following compounds in air at the temperature ranges indicated:



In addition to preparation by the above reactions, very reactive micro and milligram scale preparations are made from low-temperature air ignition of  $\text{Pu}(\text{OH})_4$  and  $\text{Pu}(\text{C}_2\text{O}_4)_2 \cdot x\text{H}_2\text{O}$ . The air ignition of

<sup>†</sup>Contribution from the Chemistry Division of the Metallurgical Laboratory, University of Chicago, now the Argonne National Laboratory.

Based on work reported in Metallurgical Project Reports CN-2159 (Oct. 1, 1944) and CN-2431 (Dec. 15, 1944). Summaries of this material are contained in Metallurgical Project Reports CK-2089 (Sept. 1, 1944) and CK-2240 (Oct. 1, 1944), and in Metallurgical Laboratory Memorandum MUC-GTS-858 (July 17, 1944).

$\text{PuF}_4$ ,  $\text{PuF}_3$ ,  $\text{PuCl}_3$ ,  $\text{PuBr}_3$ ,  $\text{PuOCl}$ ,  $\text{PuH}_3$ ,  $\text{PuS}$ ,  $\text{PuSi}_2$ , etc., also yields  $\text{PuO}_2$ . These reactions serve more for supplementary analytical purposes than for the preparation of the dioxide per se.

1.1 Preparation of  $\text{PuO}_2$  by Ignition of Plutonium(IV) Nitrate. The first preparation of a pure compound of plutonium (in fact, the first isolation of a weighable quantity of any synthesized isotope or element free of carrier material and other foreign matter) was that of "plutonous oxide" by Cunningham and Werner<sup>2</sup> on Aug. 18, 1942. This compound was prepared by ignition of "plutonous nitrate," and it was described as a yellow-brown solid, virtually insoluble in 6N  $\text{HNO}_3$  either at room temperature or at boiling temperature, but somewhat soluble in concentrated sulfuric acid. It was assumed to be  $\text{PuO}_2$ , and the specific activity of plutonium was determined on this basis. This formula was supported by the demonstration that "plutonous oxalate" contained two oxalates per plutonium atom<sup>3-7</sup> or that a plutonium(IV) state existed. The formula  $\text{PuO}_2$  was conclusively proved by the x-ray work of Zachariasen.<sup>8,9</sup>

$\text{PuO}_2$  is frequently prepared in this laboratory by the ignition of  $\text{Pu}(\text{NO}_3)_4 \cdot x\text{H}_2\text{O}$  in air. The aqueous plutonium stock is concentrated to 20 to 50 mg per milliliter by means of a hydroxide precipitation and subsequent solution in concentrated nitric acid. This solution is transferred to suitable platinum boats coated with a lucite film<sup>10</sup> to prevent adherence of the oxide to the platinum. The solution is then dried for several hours at room temperature in the boat in a vacuum desiccator with a small air leak. Meyer and Katz<sup>10</sup> state that concentrations of the nitrate greater than 50 mg per cubic centimeter are most likely to give a crystalline nitrate except in nitric acid concentrations approaching 70 per cent. The ignition is performed in air by slowly raising the temperature of the muffle furnace over the range 90 to 200°C, at which temperature dehydration occurs; then slowly to 300 to 400°C, where the lucite is charred; and finally to 800 to 850°C, where it is maintained for 30 min. The lucite coating burns away completely and frees the plutonium oxide from the boat so that it can later be removed quantitatively. At temperatures above 300°C the decomposition is nearly complete.<sup>11</sup> Constant weight is not achieved, however, below ignition temperatures of 800 to 1000°C.

A finely divided form of oxide such as that obtained by the ignition of nitrate at relatively low temperatures (275°C), or of  $\text{PuO}_2 \cdot x\text{H}_2\text{O}$  as described below, is suitable for the conversion of an oxide to a halide. The oxide ignited at 700 to 1300°C is very refractory, and it is dissolved with extreme difficulty in any aqueous reagents.

1.2 Preparation of  $\text{PuO}_2$  by Air-drying of  $\text{Pu}(\text{OH})_4$ . Plutonium hydroxide,  $\text{PuO}_2 \cdot x\text{H}_2\text{O}$ , precipitated from aqueous solution with am-

monium hydroxide and subsequently air-dried at 70°C, contains some  $\text{PuO}_2$  crystallites of about 30 Å in linear dimensions on the basis of x-ray diffraction data. This finely divided material is a useful starting material for the preparation of the halides of plutonium. In such experiments on a milligram scale the precipitation of the hydroxide may be conveniently performed in a centrifuge cone.<sup>12</sup> The gelatinous hydroxide in the tip of the cone contracts to a black pellet which may be readily transferred from the cone and, if desired, may then be ignited to higher temperatures in platinum. This method provides a small pellet that is handled conveniently in subsequent experiments.

**1.3 Preparation of  $\text{PuO}_2$  by Ignition of Plutonium(III) and (IV) Oxalate.** The hydrous oxalates of plutonium are convenient intermediates in the preparation of oxides on both the macro and the milligram scale in that the method produces divided reactive material for subsequent conversion to halides, etc. The  $\text{Pu}_2(\text{C}_2\text{O}_4)_3 \cdot x\text{H}_2\text{O}$  is useful because it is a compact precipitate readily washed and slurried, and it is nonadherent to the glass vessel; the  $\text{Pu}(\text{C}_2\text{O}_4)_2 \cdot x\text{H}_2\text{O}$  is more gelatinous and adherent and therefore more difficult to wash and transfer with high yield.

Both forms are conveniently air-dried and ignited to about 650°C without tending to adhere to the platinum boat. Plutonium(III) oxalate is also useful for ignition on a large scale because the evaporation of water from the insoluble oxalate is very rapid, and splattering is negligible in the early stages of the ignition.

**1.4 Properties and Reactions of  $\text{PuO}_2$ .** The highly ignited oxide is very refractory and will not dissolve readily in any of the common acids or alkalis but requires fusion with sodium carbonate or sodium pyrosulfate, or prolonged treatment with hydrobromic acid or concentrated sulfuric acid to get it into solution.

In summarizing the merits of the  $\text{PuO}_2$  prepared by the ignition of various intermediates it may be said that the nature and reactivity of the oxide and of halides prepared therefrom are to a certain extent dependent on the starting material. For example, ignition of crystalline  $\text{Pu}(\text{NO}_3)_3$  or of  $\text{PuO}_2(\text{NO}_3)_2$  yields a porous, fluffy, reactive  $\text{PuO}_2$ ;  $\text{Pu}(\text{OH})_4$  tends to give a glassy, dense, nonreactive  $\text{PuO}_2$ ; noncrystalline  $\text{Pu}(\text{NO}_3)_3$  gives a somewhat horny medium-dense product; and both oxalates produce porous, fine-grained, reactive products. The rate of decomposition and the final temperature also determine the ultimate state of the product.

## 2. PLUTONIUM SESQUIOXIDE

The phase  $\text{Pu}_2\text{O}_3\text{-Pu}_4\text{O}_7$ , has been characterized only by its x-ray pattern, which is a body-centered cubic lattice with 16 molecules<sup>13</sup>

per unit cell,  $a = 10.01 \text{ \AA}$ . It is therefore isomorphous with the rare-earth oxides from samarium through lutecium,  $\text{Sc}_2\text{O}_3$ ,  $\text{Mn}_2\text{O}_3$ ,  $\text{Y}_2\text{O}_3$ ,  $\text{Tl}_2\text{O}_3$ , etc. The observed structure is believed to be the abnormal form of a dimorphous crystal, the normal form of which is hexagonal and which is isomorphous with the oxides of the La-Ce-Pr-Nd group. The probable formula, based only on crystal chemical considerations, corresponds to an O/Pu ratio between 1.5 and 1.75.

**2.1 Attempts to Prepare  $\text{Pu}_2\text{O}_3$  by Controlled Decomposition<sup>14</sup> of  $\text{Pu}_2(\text{C}_2\text{O}_4)_3$ .** Three attempts have been made to prepare this phase. In one, anhydrous Pu(III) oxalate was heated to 300°C in a vacuum of  $10^{-5} \text{ mm Hg}$ . The accuracy of weighing and of oxygen analyses did not permit final decision as to whether the black powdery material obtained was  $\text{Pu}_2\text{O}_3$  or  $\text{PuO}_2$ . A second repetition of the experiment, in which a carbon dioxide atmosphere was used, gave no evidence of the presence of  $\text{Pu}_2(\text{CO}_3)_3$  or  $\text{Pu}_2\text{O}_3$ .  $\text{PuO}_2$  (identified by x-ray and gravimetric analyses) was formed above 300°C.

A similar result was obtained in a third experiment, in which an (oxygen-free) hydrogen atmosphere was used.

**2.2 Reduction of  $\text{PuO}_2$  with Atomic Hydrogen.** One of the phases produced by the treating of  $\text{PuO}_2$  with atomic hydrogen has been suggested to be  $\text{Pu}_2\text{O}_3$  by Zachariasen, who based his opinion on x-ray diffraction measurements.<sup>15</sup>

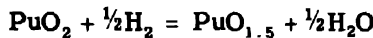
**2.3 The Decomposition of  $\text{PuO}_2$  on Tantalum in Vacuum.<sup>16</sup>** In separate experiments, two 10-mg cylindrical pellets of  $\text{PuO}_2$  (one yellow in color, prepared by air ignition of the nitrate; the other black in color, prepared by ignition of the hydrated oxide) were heated in high vacuum (about  $10^{-7} \text{ mm Hg}$ ), on an electrically heated tantalum ribbon.<sup>17</sup> Both samples acted similarly at high temperatures; the yellow oxide turned grayish at 1000°C. At a temperature estimated to be 1650 to 1800°C, the cylindrical pellet collapsed, and a molten metallic-appearing material extruded forth into the depression in the tantalum filament. The uncertainty in the initiating temperature for the reaction is a result of the fact that the oxide pellet was in poor thermal contact with the filament until it fused. The temperature range indicated is given by the apparent temperature of the pellet, taken with an optical pyrometer, and the true (i.e. corrected for emissivity) temperature of the hemispherical depression in the filament. The extruded material was identified as "Pu<sub>2</sub>O<sub>3</sub>-Pu<sub>4</sub>O<sub>7</sub>" by Zachariasen who used x-ray diffraction analysis. Although the tantalum filament had become somewhat embrittled, there was no evidence of localized reaction with it.

**2.4 Reduction of  $\text{PuO}_2$  on Iridium in Vacuum.** In an attempt to determine whether  $\text{PuO}_2$  is reduced to a lower oxide in a thermal de-

composition in which oxygen is evolved at a low pressure, or whether  $\text{PuO}_2$  is reduced by the filament (e.g., tantalum, with the formation of tantalum oxides volatile at these temperatures), an experiment was performed<sup>18</sup> in which a cylindrical pellet of about 5 mg of yellow  $\text{PuO}_2$  was placed in a triangular groove in an iridium plate (2 by 3 by 0.3 mm). Iridium oxides are sufficiently unstable that in the temperature ranges of the experiments, a vacuum is a better reducing agent for an oxide than is iridium. The iridium was supported by, and was in thermal contact with, a molybdenum ribbon heated by the passage of electrical current. The iridium and the molybdenum elements were well degassed before the oxide was placed on them. As the temperature was gradually raised to 1000°C in a vacuum of  $2 \times 10^{-6}$  mm Hg, the usual darkening in color of the oxide was observed. The original light yellow color was not restored to the pellet within 15 min of its being cooled to room temperature. No further changes in the oxide were observed on reheating until the temperature of the iridium plate had reached about 2100°C. Because of limited thermal contact between the iridium and the oxide the pellet was at a much lower temperature. The apparent temperature (uncorrected for the emissivity of the oxide) was observed to be 1520°C on the optical pyrometer. At this temperature the surface of the pellet assumed a silvery semimetallic luster similar to that of the previously described " $\text{Pu}_2\text{O}_3\text{-Pu}_4\text{O}_7$ ." This temperature (almost identically that of the  $\text{PuO}_2$  during the experiment on tantalum just referred to) was maintained for about 10 min, as had been done with the tantalum-mounted sample. Although in each experiment the true value of the temperature of the pellet is not known because of the unknown emissivity of the semimetallic surface of the lower oxide, the ultimate temperatures of the pellets used in the two experiments were very nearly the same. There was no indication of reaction with the supporting edges of the iridium. Dr. Zachariasen's analysis of the product revealed the presence of approximately 20 per cent " $\text{Pu}_2\text{O}_3\text{-Pu}_4\text{O}_7$ " and 80 per cent  $\text{PuO}_2$ , thus confirming the unchanged appearance of the interior of the pellet.

One significant difference between the behavior of the oxide pellets on tantalum and on iridium is that in the tantalum experiment the pellet appeared to collapse by melting and to spread somewhat on the filament, whereas in the iridium experiment no such melting was observed. The observed formation of " $\text{Pu}_2\text{O}_3\text{-Pu}_4\text{O}_7$ " on iridium seems to favor the thermal decomposition hypothesis inasmuch as a reduction by as noble a metal as iridium seems thermodynamically improbable at this temperature. With the thermal-decomposition hypoth-

esis, however, an outstanding difficulty is that a thermodynamic analysis of the free-energy changes for the reactions



by N. R. Davidson indicates that if the first reaction takes place at 1800°C with a low pressure of oxygen ( $10^{-5}$  mm Hg), then the second reaction should proceed readily at 1000 to 1500°C; such does not appear to be the case.

**2.5 Attempts<sup>18</sup> at Hydrogen Reduction of PuO<sub>2</sub>.** A 5-mg pellet of yellow PuO<sub>2</sub> was placed in the depression of a well-degassed electrically heated platinum ribbon. Anhydrous hydrogen was swept over the pellet at the rate of several hundred milliliters per minute for 1 hr while the pellet was maintained at 1200°C. A change in color to olive-green was observed, and a hole was formed in the platinum beneath the pellet. The hole increased in size with time. The pellet clung to one edge of the expanding hole and was displaced from its original position by nearly 2 mm. X-ray analysis by W. H. Zachariasen revealed the presence of only the PuO<sub>2</sub> phase in the pellet.

Since a mixture of PuOCl and PuO<sub>2</sub> results from heating PuCl<sub>3</sub>·6H<sub>2</sub>O in vacuum, it is apparent that Pu<sub>2</sub>O<sub>3</sub> readily reduces H<sub>2</sub>O with the formation of H<sub>2</sub> and PuO<sub>2</sub>.

### 3. PLUTONIUM MONOXIDE

**3.1 The Preparation of Plutonium Monoxide.** This substance has been identified on crystal-chemical considerations and on its formation from PuOCl and PuO<sub>2</sub>. Plutonium monoxide was first obtained in reductions of PuF<sub>3</sub> or PuF<sub>4</sub> with lithium or barium vapor on the micro scale in vacuum in systems that had not been thoroughly degassed.

The principal product of the reduction of a 5-mg sample of fairly pure PuOCl with barium vapor at 1250°C was PuO.<sup>19</sup> Subsequent reductions of purer PuOCl indicate that pure PuO is obtained on reduction with barium.<sup>20</sup> A single micro scale reduction of PuO<sub>2</sub> with barium metal was reported to have yielded PuO as a product.<sup>21</sup>

**3.2 Properties of PuO.** In massive form PuO appears as a semi-metallic substance with an almost metallic luster. It is more brittle and less malleable than the metal. The lattice constant of the cubic structure is  $a = 4.95$  Å. It seems probable that the binding in PuO has some metallic character.

The material is readily soluble in hydrochloric acid of higher concentration than 1M.

#### 4. ATTEMPTS TO PREPARE A HIGHER OXIDE OF PLUTONIUM

Unsuccessful searches for a volatile plutonium oxide analogous to the very volatile tetraoxides of osmium and ruthenium have been made. Early tracer-scale attempts to volatilize plutonium oxides from aqueous bromate, nitric acid, and perchloric acid solutions under conditions where ruthenium and osmium are volatilized were not successful.<sup>22</sup> Ozone solutions without a catalyst,<sup>22</sup> with ozone-ceric ion,<sup>23</sup> and with ozone-argentic ion<sup>24</sup> all failed to produce a volatile plutonium compound.

Plutonium did not readily volatilize from fused sodium peroxide at 500°C,<sup>25</sup> or from molten sodium peroxide in an oxygen atmosphere (to prevent its decomposition).<sup>26</sup>

Another tracer attempt (made by Voigt<sup>27</sup> at the Ames Laboratory) to oxidize plutonium to its highest valence with molten potassium chloride at 500 to 700°C and to collect any volatile plutonium tracer on a water-cooled cover gave negative results.

Experiments, made by Baldwin and Edwards at the Ames Laboratory,<sup>28</sup> in which dried ozone was passed over PuO<sub>2</sub> at 600 and 1000°C gave no indication of the formation of volatile oxides of plutonium.

Hydrated plutonium peroxide precipitated from solution has been shown by Howland<sup>29</sup> to be PuO<sub>4</sub>. $x$ H<sub>2</sub>O, containing tetrapositive plutonium and two peroxide groups per molecule.

PuO<sub>3</sub> was expected to be formed by controlled ignition of PuO<sub>2</sub>·(NO<sub>3</sub>)<sub>2</sub>· $x$ H<sub>2</sub>O but was not detected.<sup>30</sup> The nitrate decomposes to the dioxide at 275°C.

#### 5. SUMMARY

A description of methods and a discussion of techniques applicable to the synthesis and handling of plutonium dioxide on the micro scale is presented. Reductions of PuO<sub>2</sub> to Pu<sub>2</sub>O<sub>3</sub>-Pu<sub>4</sub>O<sub>7</sub> by means of atomic hydrogen, active metals, and graphite and by thermal decomposition in vacuum, and attempted reduction with hydrogen are described. Plutonium monoxide can be conveniently prepared by the thermal reduction of PuOCl with barium. Attempts to prepare an anhydrous oxide richer in oxygen than PuO<sub>2</sub> have been unsuccessful.

#### ACKNOWLEDGMENTS

Although the main function of this paper is to present the author's study of the lower oxides of plutonium, a second purpose is to trans-

mit some of the techniques of micro scale operations in the preparation and handling of the various oxides and, for completeness, to list the unsuccessful attempts to prepare a higher oxide. This information is obviously the result of the individual and combined efforts of many workers in this and other laboratories. An attempt to give appropriate credit is made in the bibliography references, but special mention should be made of the first preparation of  $PuO_2$  by Cunningham, Cefola, and Werner and of the guidance of H. L. Baumbach, B. B. Cunningham, N. R. Davidson, and R. E. Heath, who at various times were responsible for several phases of the work of the dry-chemistry groups, and to G. T. Seaborg, Section Chief, for his inspiring direction of the research program. The x-ray diffraction studies of W. H. Zachariasen were invaluable.

## REFERENCES

1. W. H. Zachariasen, Metallurgical Project Report CN-2069 (Sept. 28, 1944).
2. B. B. Cunningham, M. Cefola, and L. B. Werner, Metallurgical Project Report CN-261 (Sept. 15, 1942), p. 5.
3. B. B. Cunningham and L. B. Werner, Metallurgical Project Report CN-299 (Oct. 15, 1942), p. 1.
4. B. B. Cunningham and L. B. Werner, Metallurgical Project Report CN-419 (Jan. 15, 1943), p. 15.
5. B. B. Cunningham and L. B. Werner, Metallurgical Project Report CN-454 (Jan. 31, 1943), p. 1.
6. B. B. Cunningham and L. B. Werner, Metallurgical Project Report CN-467 (Feb. 15, 1943), p. 6.
7. B. B. Cunningham and L. B. Werner, Metallurgical Project Report CN-556 (Mar. 31, 1943), p. 1.
8. W. H. Zachariasen, Metallurgical Project Report CK-1096 (Nov. 27, 1943), p. 12.
9. W. H. Zachariasen and R. C. L. Mooney, Metallurgical Project Report CK-1119 (Dec. 8, 1943).
10. F. Meyer, and S. Katz, Metallurgical Project Report CK-1372 (A-2015) (Mar. 1, 1944), p. 17.
11. R. E. Heath and F. Meyer, unpublished work.
12. E. K. Hyde, N. R. Davidson, J. J. Katz, and M. J. Wolf, Metallurgical Project Report CK-1512 (A-2093) (Apr. 1, 1944), p. 5.
13. W. H. Zachariasen, Metallurgical Project Report CK-1518 (Apr. 5, 1944), p. 3.
14. C. S. Garner and I. B. Johns, reported by J. W. Kennedy and C. S. Smith in Los Alamos Report LAMS-112 (Oct. 6, 1944), p. 25.
15. W. H. Zachariasen, Metallurgical Project Report CK-1518 (Apr. 5, 1944), p. 3.
16. E. F. Westrum, Jr., Metallurgical Project Report CN-2159 (Oct. 1, 1944), p. 2.
17. E. F. Westrum, Jr., unpublished work.
18. E. F. Westrum, Jr., Metallurgical Project Report CN-2431 (Dec. 15, 1944), p. 22.
19. E. F. Westrum, Jr., Metallurgical Project Report CN-2159 (Oct. 1, 1944), p. 4.
20. E. F. Westrum, Jr., unpublished work.
21. A. Dirksen and S. Fried, Metallurgical Project Report CK-1372 (Mar. 1, 1944), p. 21.
22. S. G. English, reported by G. T. Seaborg, Metallurgical Project Report CC-169 (July 3, 1942), p. 10.

23. S. G. English, reported by G. T. Seaborg, Metallurgical Project Report CC-179 (July 11, 1942), p. 6.
24. S. G. English and R. A. James, reported in Metallurgical Project Report CN-239 (Aug. 15, 1942), p. 21.
25. J. E. Willard, reported in Metallurgical Project Report CN-250 (Aug. 31, 1942), p. 3.
26. C. S. Garner, reported in Metallurgical Project Report CN-261 (Sept. 15, 1942), p. 3.
27. A. F. Voigt, reported by F. H. Spedding in Metallurgical Project Report CN-266 (Sept. 14, 1942).
28. R. R. Baldwin and F. Edwards, Report A-1503 (July 1944), p. 23.
29. J. J. Howland, Metallurgical Project Report CK-1511 (Apr. 1, 1944).
30. Reported in Los Alamos Report LAMS-72.

## Paper 6.60

### PREPARATION OF PLUTONIUM NITRIDE†

By B. M. Abraham, N. R. Davidson, and E. F. Westrum, Jr.

A crystalline phase believed to be PuN was first identified by x-ray analysis in a sample obtained in an attempted atomic-hydrogen reduction<sup>6,7,8</sup> of PuF<sub>3</sub>. This identification was based on crystal-chemical considerations and was uncertain because of the presumably unfavorable conditions for the formation of a nitride. It was therefore of interest to attempt to prepare this compound by more reliable methods and establish its identity with certainty.

Early investigators of uranium chemistry found<sup>1</sup> that a uranium nitride believed to be U<sub>3</sub>N<sub>4</sub> could be prepared by the reaction of ammonia with uranium metal or UC<sub>14</sub>. Although these results are now known to be incorrect, these two methods have been applied to the problem of the preparation of PuN.

The preparation of PuN from plutonium metal and ammonia was carried out with a piece of metal weighing about 5 mg mounted in a depression in a platinum filament that could be heated electrically. The metal was heated to 1000°C, as measured with an optical pyrometer, for 5 min in the presence of anhydrous ammonia gas at 250 mm Hg. The ammonia had been dried by distillation from sodium metal. Progress of the reaction was observed through a microscope. A brown coating formed over the metal, not all of which reacted; some of the metal melted and wet the platinum filament. The brown material was characterized by x-ray analysis as a mixture of PuO<sub>2</sub> and the phase previously and tentatively identified as PuN. This result therefore made that identification certain.<sup>15</sup>

†Contribution from the Chemistry Division of the Metallurgical Laboratory, University of Chicago, now the Argonne National Laboratory.

Based on work partially reported in Metallurgical Project Report CN-2159 (Oct. 1, 1944).

In an attempt to prepare a higher nitride of plutonium at a lower temperature, plutonium metal powdered with hydrogen was used.<sup>9</sup> As in the previous experiment, the metal was supported on a platinum filament. The apparatus was modified, however, so that the product could be introduced into the x-ray capillary without removing it from the vacuum line. Figure 1 is a diagram of the apparatus; the circle in

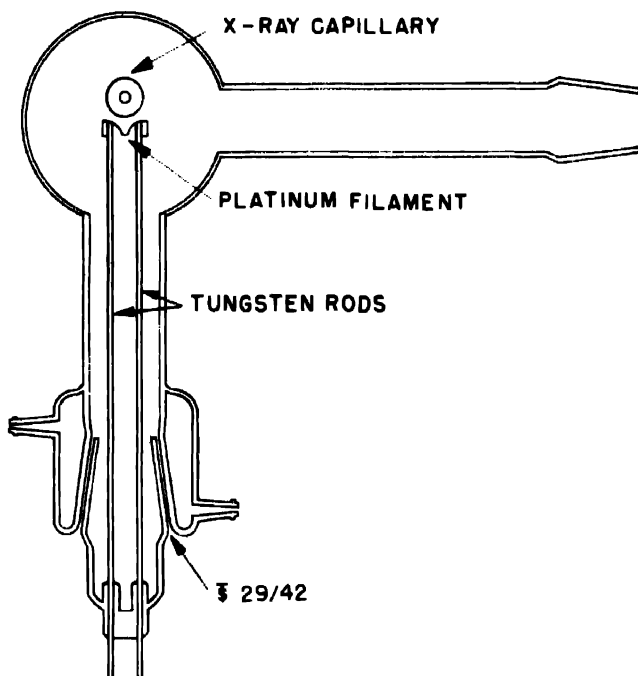


Fig. 1.—Diagram of apparatus used in the conversion of plutonium hydride to nitride.

the middle of the bulb represents the x-ray capillary, which is perpendicular to the plane of the paper. By rotating the furnaces through 90 deg around the horizontal joint the reaction products can be transferred from the filament to the capillary, which can then be sealed off the line. When hydrogen gas was admitted to the plutonium metal on the platinum filament at room temperature, there was a reaction to form plutonium hydride. The excess hydrogen was then pumped off. The powdered hydride was heated at 650°C for about 5 min in anhydrous ammonia at 250 mm Hg, then slowly cooled in the presence of ammonia. The product<sup>10</sup> consisted of a single phase, namely, PuN.

This result for plutonium is in striking contrast to the results of similar experiments<sup>2,3,4</sup> with uranium, which readily forms a series

of higher nitrides ranging in composition from  $\text{UN}_{1.33}$  to  $\text{UN}_{1.75}$ . The compound UN is obtained by heating the higher nitrides to 1300°C in vacuum whereas PuN was obtained at 650°C and lower in the presence of nitrogen at 60 mm Hg. The results of these experiments suggest that if a higher nitride of plutonium exists its decomposition pressure must be greater than 60 mm Hg at 650°C. Additional evidence as indicated below is furnished by the preparation of PuN from  $\text{PuCl}_3$  and ammonia.

PuN was prepared<sup>8</sup> by treating  $\text{PuCl}_3$  with a stream of ammonia at 900°C. About 5 mg of  $\text{PuCl}_3$  in a platinum microcrucible inside a quartz tube were heated in a slow stream of ammonia gas at atmospheric pressure. The flow rate was adjusted by immersion of the ammonia reservoir in a bath of frozen bromobenzene (m.p. -30.6°C). The ammonia had been dried by distillation from sodium metal. The temperature of the sample was slowly raised from 800 to 900°C over a period of 1 hr and maintained at 900°C for 15 min. The product of the reaction was a black solid that was insoluble in water but partially soluble in dilute hydrochloric acid. X-ray diffraction analysis<sup>9</sup> indicated that it contained approximately 35 per cent PuN, 50 per cent  $\text{PuO}_2$ , and 15 per cent  $\text{PuOCl}$ . It is possible that the water that formed the oxide and oxychloride came from the apparatus or from the  $\text{PuCl}_3$ .

Since the heats of formation of  $\text{CeCl}_3$  and  $\text{PuCl}_3$  have been measured as -261.5 and 234.1 kcal, respectively,<sup>11,14</sup> it is of interest to consider the thermodynamic characteristics of the cerium reaction, Eq. 2, and analogous to the plutonium reaction, Eq. 1:



The latter reaction is not recorded in the literature, but the heat of formation and entropy of formation of CeN are known.<sup>12</sup> The heats of formation and entropies of the gases are listed in references 11 and 13. It may be expected that the reaction to form PuN will be roughly similar in that the small amount of hydrogen chloride will have to be continuously removed, and the reaction will have a marked temperature coefficient.

Since reaction 1 does take place to some extent and since our calculations indicate that reaction 2 would take place only slowly as the resultant hydrogen chloride is swept out at a low partial pressure, it may be concluded that the heat of formation of PuN is not greater than about 30 kcal more positive and may very well be about equal to the -78 kcal per mole, which is the heat of formation of CeN.

## REFERENCES

1. "Gmelins Handbuch der anorganischen Chemie," S.N. 55, pp. 66 and 107, Verlag Chemie G.M.B.H., Berlin, 1936.
2. Battelle Memorial Institute, Metallurgical Project Report CT-956 (Sept. 10, 1943), p. 311.
3. Battelle Memorial Institute, Metallurgical Project Report CT-1009 (Oct. 10, 1943), p. 350.
4. A. S. Newton, R. Nottorf, and A. Daane, Metallurgical Project Report CC-1524 (Feb. 1, 1944), p. 16.
5. E. F. Westrum, Jr., and B. M. Abraham, Metallurgical Project Report CN-2159 (Oct. 1, 1944), p. 3.
6. W. H. Zachariasen, Metallurgical Project Report CK-1377 (Feb. 26, 1944), p. 3.
7. W. H. Zachariasen, Metallurgical Project Report CK-1530 (Mar. 30, 1944), p. 10.
8. W. H. Zachariasen, Metallurgical Project Report CN-2069 (Aug. 1, 1944), p. 23.
9. E. F. Westrum, Jr., unpublished results.
10. W. H. Zachariasen, personal communication.
11. F. R. Bichowsky and F. D. Rossini, "The Thermochemistry of the Chemical Substances," Reinhold Publishing Corporation, New York, 1936.
12. K. K. Kelley, Contributions to Data on Theoretical Metallurgy. VIII. Thermo-dynamic Properties of Metal Carbides and Nitrides, U.S. Bur. Mines Bull. 407, 1937.
13. K. K. Kelley, Contributions to Data on Theoretical Metallurgy. IX. The Entropies of Inorganic Substances, U.S. Bur. Mines Bull. 434, 1940.
14. E. F. Westrum, Jr., unpublished results.
15. W. H. Zachariasen, Metallurgical Project Report CN-2069 (Sept. 30, 1944), p. 36.

## Paper 6.80

### THE COMPOSITION OF PLUTONIUM PEROXIDE†

By H. H. Hopkins, Jr.

A determination of the composition of plutonium peroxide precipitated from nitric acid solution was regarded with interest from the standpoint of increasing the basic knowledge of plutonium chemistry. The method employed was to determine the peroxide oxygen content of exhaustively washed plutonium peroxide precipitates by an oxidation-reduction titration. From the data so obtained, and assuming existence of plutonium in the tetrapositive state, a formula could be calculated.

Experimental Procedure. Using the method of Howland,<sup>1</sup> samples containing 1 to 4 mg of plutonium were precipitated from 1.0N HNO<sub>3</sub> at room temperature with 10 per cent excess by weight of hydrogen peroxide. To remove as much of the hydrogen peroxide held in the precipitate as possible, the precipitate was washed twice with 0.1N H<sub>2</sub>SO<sub>4</sub>, once with water, twice with acetone, twice with alcohol, and once with 0.1N H<sub>2</sub>SO<sub>4</sub>, a volume of 150 microliters being employed for each wash. During the washings the slurry was chilled with ice water to prevent peroxide decomposition. Standard 0.5N Ce(NO<sub>3</sub>)<sub>4</sub> in 0.5N HNO<sub>3</sub> was then added to dissolve the peroxide by oxidation of both plutonium and peroxide oxygen atoms. When the reaction was complete, the solution was made 5M in NaNO<sub>3</sub> and 3M in NaC<sub>2</sub>H<sub>3</sub>O<sub>2</sub>, whereupon the plutonium(VI) precipitated as NaPuO<sub>2</sub>(C<sub>2</sub>H<sub>3</sub>O<sub>2</sub>)<sub>3</sub>. This precipitate was centrifuged off and washed once with 3M NaC<sub>2</sub>H<sub>3</sub>O<sub>2</sub>. The combined supernatant liquid and wash liquid, containing unreacted cerium (IV), was diluted to 2 ml, made 0.5M in H<sub>2</sub>SO<sub>4</sub>, and treated with excess ferrous ammonium sulfate. Erioglaucine indicator was

†Contribution from the Chemistry Division of the Metallurgical Laboratory, University of Chicago, now the Argonne National Laboratory.

Based on Metallurgical Project Report CN-1946 (Aug. 1, 1944), p. 21.

added at once, and the solution back-titrated with standard cerium(IV) solution.

Results. If the amount of plutonium precipitated as the peroxide and the net amount of oxidizing agent is known, the amount of oxidizing agent necessary to raise plutonium from the IV to the VI state can

Table 1—Calculation of the Empirical Formula of Plutonium(IV) Peroxide

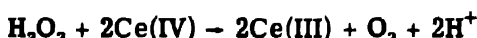
Expt. No.	Pu ptd. as peroxide, micromoles	Ce(IV) used to oxidize peroxide oxygens, microequivalents	Peroxide oxygen per mole of Pu, equivalents (x)	Anion radicals per mole of Pu, equivalents (4-x)
1	5.6	18.9	3.37	0.63
2	5.5	18.4	3.34	0.66
3†	11.3	34.7	3.07	0.94
4†	11.4	34.5	3.03	0.98
5‡	16.4	49.8	3.04	0.96
6‡	16.0	49.2	3.08	0.92
			3.15 (av.)	0.85 (av.)



†Precipitates washed with three portions of acetone and three of alcohol instead of twice with each.

‡Precipitates washed with five portions of acetone and five of alcohol instead of twice with each.

be subtracted, and the remainder is the amount of oxidizing agent used in oxidizing the peroxide oxygens. It is assumed that 2 equivalents of ceric ion are reduced for each peroxide oxygen pair present in the compound, in a manner analogous to that established for the oxidation of hydrogen peroxide, as shown by the equation



The above considerations show how the number of peroxide oxygen atoms per atom of plutonium can be determined, but they do not take into account the normal anions, e.g.,  $\text{NO}_3^-$  or  $\text{OH}^-$ , attached to the plutonium atom in plutonium peroxide. However, since at the time the present work was done it was generally accepted, and later was definitely proved by Werner,<sup>2</sup> that all the plutonium in the peroxide must be in the tetrapositive state, the empirical formula may be written in the form  $\text{Pu}^{+4}(\text{R}^-)_{4-x}(\text{O}^-)_x$ , where x represents the number of peroxide

oxygen atoms and  $(4 - x)$  represents the number of normal anion radicals per atom of plutonium. Obviously,  $x$  will be equal to the number of equivalents of cerium(IV) used in oxidizing the peroxide associated with 1 mole of plutonium. The empirical formula obtained on this basis is given in Table 1.

The average value obtained for this formula was  $\text{PuR}_{0.85}\text{O}_{3.15}$ . From this value, bearing in mind the experimental error, it is possible to assume a molecular formula of  $\text{Pu}_2\text{R}_2\text{O}_6$  with each molecule containing two nitrate or hydroxyl radicals (or one bivalent oxygen atom) and three peroxide oxygen pairs. However, there is no decisive reason for assuming that plutonium peroxide is precipitated as a compound of definite composition, and only the empirical formula can be proposed on the basis of the present data.

Summary. Using an oxidation-reduction titration method the number of peroxide oxygen atoms precipitated with one atom of plutonium was determined. Assuming the plutonium to be entirely in the tetra-positive state, an average empirical formula of  $\text{PuO}_{3.58}$  can be calculated from the data.

#### REFERENCES

1. J. J. Howland, Jr., Metallurgical Project Report CK-1511 (A-2092) (Apr. 1, 1944), pp. 9-10.
2. J. C. Kroner and L. Spector, Metallurgical Project Report CN-2213 (June 30, 1945).

## Paper 6.150

# DETERMINATION OF THE MELTING POINTS OF PLUTONIUM(III) CHLORIDE AND PLUTONIUM(III) BROMIDE†

By H. P. Robinson

### 1. INTRODUCTION

The melting points of plutonium trichloride and plutonium tribromide have been reported from Los Alamos<sup>1,2</sup> as being about 760°C and 685 ± 15°C, respectively. The melting points of these compounds as indicated from vapor-pressure measurements carried out in the Chicago laboratory<sup>3</sup> indicated that the values were 736 ± 10°C and 654 ± 9°C for the chloride and bromide, respectively. However, certain features of the pressure measurements indicated that the samples were impure, and therefore a redetermination of the melting points by an independent method seemed in order.

### 2. EXPERIMENTAL WORK

The melting points were determined indirectly by observing the temperature of a bath in which a sample was melted. The technique was similar to that commonly used in determining the melting points of organic compounds. A diagram of the apparatus is shown in Fig. 1. A molten salt bath consisting of a 15-mm quartz test tube about 25 cm long, half filled with fused lithium chloride-potassium chloride eutectic mixture (55 per cent KCl), was heated by means of a chromel ribbon wrapped spirally around the lower portion of the quartz tube. The current through the heater was controlled by means of a variac, which fed a low-voltage transformer connected to the chromel ribbon. The bath temperature could be measured by means of a chromel-

†Contribution from the Chemistry Division of the Metallurgical Laboratory, University of Chicago, now the Argonne National Laboratory.

Based on work reported in Metallurgical Project Report CN-2431 (Dec. 1, 1944).

alumel thermocouple encased in a 2-mm quartz tube extending into the fused salt. A simple potentiometer was used for the potential measurements, and the readings could be interpolated to an accuracy of about 2°C. The samples were contained in sealed quartz capillaries

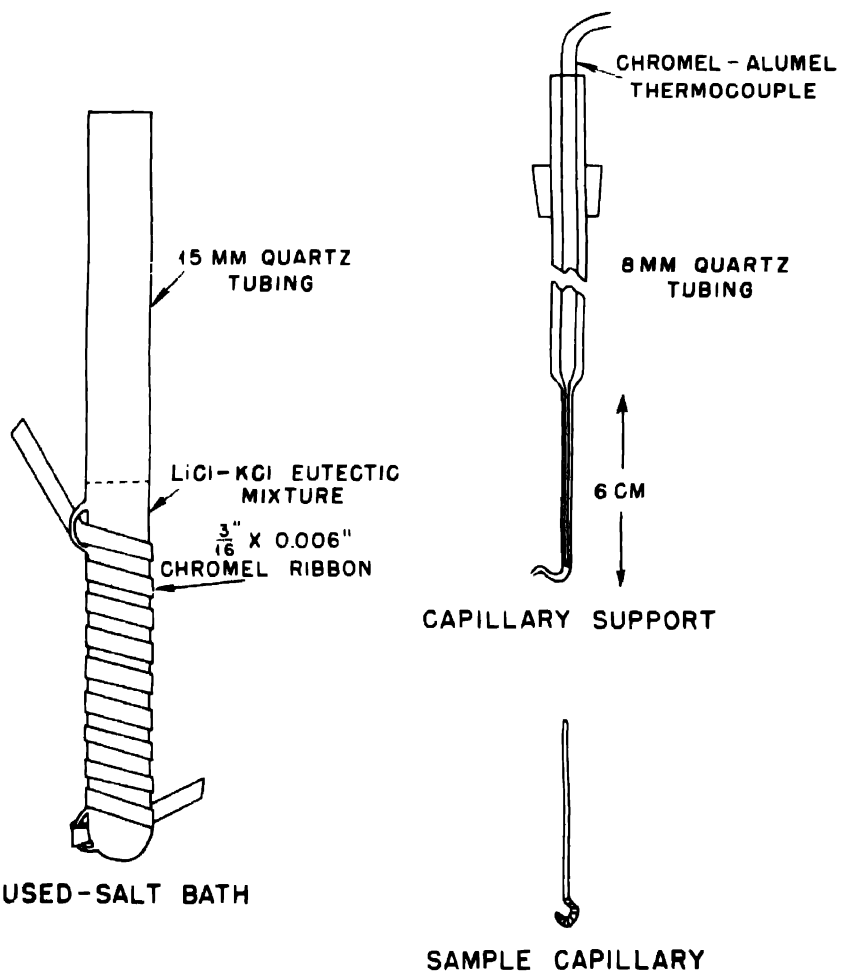


Fig. 1—Apparatus for melting-point determination.

that were hung in an inverted position on the hooked tip of the quartz enclosure for the thermocouple. The sample tube, being less dense than the bath, could be hung in an inverted position as illustrated. The melting behavior of the material in the quartz sample tube was observed through a microscope.

The melting point behavior of a sample of PuBr<sub>3</sub> prepared by the treatment of PuO<sub>2</sub>·xH<sub>2</sub>O with a sulfur- and bromine-vapor mixture<sup>4</sup> was first observed. This particular sample had been handled several times in a dry box before being used in this determination and could have contained some moisture. On being heated the PuBr<sub>3</sub> was first observed to shrink toward the center of the capillary at 645°C, and some slight melting was first observed at 650°C; the fluid formed was green in color. As the temperature was raised the melting progressed, until at 690°C one-half of the sample had melted, the color of the melt now having changed to amber. Progressive increases in temperature continued to cause more of the sample to melt, but even at 850°C not all the sample melted.

To purify the sample of PuBr<sub>3</sub>, about 1 mg was vacuum-distilled into a quartz capillary sample tube that had been connected by a ground-glass joint to a special vacuum distillation apparatus containing about 3 mg of the impure PuBr<sub>3</sub>. The distillation was continued about 15 min and yielded a solid mass of the compound with a thin cylindrical layer extending beyond into the cool end of the tube. This quartz sample capillary was sealed off, the hooked tip was made on the end, and it was then transferred to the salt bath. This thin layer had a sharp melting point at 681±3°C. Slight variations in the bath temperature caused by convection currents would alternately melt and freeze the pure layer of PuBr<sub>3</sub>. The melting of this larger mass of the compound was observed to take place over a range from 680 to 688°C, but later the material appeared to melt and freeze at 681±3°C. To test the reactivity toward quartz the sample was heated to 850°C for 5 min, after which the melting point was rechecked and found to be 681°C, indicating that for these experiments quartz is a suitable container for the bromide. At 850°C the liquid was amber in color. At the melting point the color was a deep green.

The melting behavior of a sample of PuCl<sub>3</sub> from the same preparation used in the vapor-pressure measurements was investigated as described for the bromide. The sample had been prepared by Karle<sup>5</sup> as sublimed chloride by the treatment of PuO<sub>2</sub>·xH<sub>2</sub>O with carbon tetrachloride vapor. It had been transferred in a dry box several times before being used for this experiment. With this material it was observed that melting started at 740°C and was substantially complete at 790°C. The green fluid was then cooled slowly, and crystallization did not set in until 620°C, when the entire sample suddenly congealed. From 36 mg of the crude material there was obtained about 18 mg of material purified by sublimation at 860°C in the quartz capillary attached to a vacuum apparatus. The purified PuCl<sub>3</sub> melted completely in the range 760 to 765°C, and when it was cooled crystallization began at 760°C.

An interesting comparison of the melting points of the trichlorides and bromides of uranium and plutonium with corresponding rare-earth elements is given in Table 1. The crystal lattice constants of these compounds are also included. They further confirm the resemblance of uranium(III) and plutonium(III) to the tripositive rare-earth halides.

Table 1 -- Comparison of Melting Points and Crystallographic Constants of Rare-earth and Heavy-metal Halides

Halide	M.p., °C	Reference	Lattice dimensions, Å		
			a <sub>1</sub>	a <sub>2</sub>	a <sub>3</sub>
Hexagonal form					
LaCl <sub>3</sub>	850	9	7.468 ± 0.003		4.366 ± 0.003
CeCl <sub>3</sub>	790–810	9	7.436 ± 0.004		4.304 ± 0.004
PrCl <sub>3</sub>	769–782	9	7.41 ± 0.01		4.25 ± 0.003
NdCl <sub>3</sub>	760	9	7.381 ± 0.004		4.231 ± 0.003
UCl <sub>3</sub>	842	8	7.428 ± 0.003		4.312 ± 0.003
PuCl <sub>3</sub>	760 ± 5	9	7.380 ± 0.001†		4.238 ± 0.001
LaBr <sub>3</sub>	783	9	7.951 ± 0.003		4.502 ± 0.003
CeBr <sub>3</sub>	732	9	7.936 ± 0.003		4.435 ± 0.003
PrBr <sub>3</sub>	693	9	7.92 ± 0.01†		4.38 ± 0.01
UBr <sub>3</sub>	755	7	7.926 ± 0.002		4.432 ± 0.002
Orthorhombic form					
NdBr <sub>3</sub>	681	9			
PuBr <sub>3</sub>	681	9	12.57 ± 0.05	4.11 ± 0.03	913 ± 0.04

†Reference 6.

### 3. SUMMARY

The melting points of PuCl<sub>3</sub> and PuBr<sub>3</sub> have been determined on samples purified by sublimation and have been found to be 760 ± 5°C and 681 ± 5°C, respectively.

### REFERENCES

1. C. S. Garner, Los Alamos Report LA-112 (July 24, 1944), p. 6.
2. B. A. Bluestein and C. S. Garner, Los Alamos Report LA-116 (July 28, 1944), p. 5.
3. T. E. Phipps, G. W. Sears, R. L. Seifert, and O. C. Simpson, The vapor pressure of plutonium halides, Paper 6.1a, this volume; T. E. Phipps, G. W. Sears, and O. C. Simpson, The volatility of plutonium dioxide, Paper 6.1b, this volume; N. D. Erway, L. O. Gilpatrick, Z. V. Jasaitis, F. D. Johnson, T. E. Phipps, G. W. Sears, R. L. Seifert, and O. C. Simpson, Metallurgical Project Report CN-3223 (Sept. 26, 1945).

## THE TRANSURANIUM ELEMENTS

4. E. K. Hyde, Metallurgical Project Report CN-2159 (Oct. 1, 1944), p. 9.
5. I. Karle, Metallurgical Project Report CK-1701 (June 1, 1944), p. 3.
6. W. H. Zachariasen, Crystal structure studies of chlorides, bromides, and iodides of plutonium and neptunium, Paper 20.6, this volume (Argonne National Laboratory Report ANL-4073); Metallurgical Project Report CN-2069 (August 1944), p. 18.
7. C. Thurmond, Metallurgical Project Report CC-2522 (Dec. 20, 1944).
8. C. A. Kraus, Report A-522 (Feb. 1, 1943); Report AM-251 (July 1, 1943).
9. D. M. Yost, Horace Russell, Jr., and C. S. Garner, "The Rare-earth Elements and Their Compounds," John Wiley & Sons, Inc., New York, 1947.

Paper 6.170

STUDIES OF THE PREPARATION AND PROPERTIES OF  
PLUTONIUM IODIDE AND PLUTONIUM OXYIODIDE†

By F. Hagemann, B. M. Abraham, N. R. Davidson,  
J. J. Katz, and I. Sheft

In order to prepare and characterize the plutonium iodides and oxyiodides, studies of the following proposed methods of synthesis of these compounds were carried out:

1. Reaction of plutonium metal with iodine or anhydrous hydrogen iodide.
2. Reactions of plutonium dioxide with anhydrous hydrogen iodide and with aluminum iodide, liquid or vapor.
3. Evaporation of a plutonium(III) iodide solution in a stream of hydrogen iodide.
4. Reaction of a plutonium dioxide - carbon mixture with hydrogen iodide.

Because of previous knowledge of the chemistry of the plutonium chlorides and bromides,<sup>1,2</sup> it was anticipated at the outset that the stable iodide and oxyiodide of plutonium would be  $\text{PuI}_3$  and  $\text{PuOI}$ , and that  $\text{PuI}_2$  would not be appreciably volatile below 750°C.

Reactions of Plutonium Metal with Iodide and Anhydrous Hydrogen Iodide. In the study of the reaction of plutonium metal with iodine, the iodine used was sublimed from a sample specially purified for us by Prof. V. W. Meloche. (The preparation of this sample is described by Arnold.<sup>3</sup>) It contained less than 7.5 ppm of chlorine or bromine.

The first reaction studied was the vapor phase iodination of a sample of metal contained in a quartz x-ray capillary.<sup>4</sup> The apparatus

†Contribution from the Chemistry Division of the Metallurgical Laboratory, University of Chicago, now the Argonne National Laboratory.

Based on work reported in Metallurgical Project Reports CK-1701 (June 1, 1944), CK-1763 (July 1, 1944), and CN-2159 (Oct. 1, 1944).

was similar to that used for the chlorination and bromination of metal.<sup>1,2</sup> With approximately 75  $\mu\text{g}$  of metal in the x-ray capillary, the apparatus was evacuated and some iodine was sublimed from a side arm into the 14-mm tubing to which the x-ray capillary was attached. This part of the apparatus was sealed off from the side arm and from the vacuum line. The capillary was heated to 400°C while the rest of the apparatus was maintained at 100°C, corresponding to a pressure of approximately 45 mm Hg for the iodine. After heating for 3 hr, the iodine was removed by cooling one side of the system in liquid nitrogen, and the capillary was sealed off. Zachariasen<sup>5,6</sup> identified the bright-green reaction product by x-ray analysis as the new compound, PuOI.

The sample was dissolved in dilute sulfuric acid and the iodine/plutonium ratio was determined by Dr. M. J. Wolf. The plutonium was determined by radiometric analysis, and the iodide was determined by conversion to iodine with iodate or dichromate as oxidizing agent, distillation of the iodine into 20 per cent KI solution, and titration of the iodine with standard thiosulfate.<sup>7</sup>

It was hoped that by working with a larger sample of plutonium the effect of traces of oxygen would be less, and it would be possible to prepare PuI<sub>3</sub>. In order to encourage more complete conversion the reaction was carried out in the liquid phase. About 500  $\mu\text{g}$  of metal was heated with excess iodine in a pyrex capillary bomb for 5 hr at a temperature of 200 to 300°C. (The boiling point of iodine is 189°C.) The bomb was opened and rapidly waxed to a vacuum apparatus, and the iodine sublimed away at 175°C in vacuum. The light-brown crystalline reaction product was only slightly soluble in water and dissolved slowly and incompletely in dilute sulfuric acid. The ratio of iodine to plutonium in the material soluble in 1N H<sub>2</sub>SO<sub>4</sub> was found to be 0.76. X-ray analysis by Zachariasen<sup>4</sup> indicated the material to be chiefly PuOI and a small amount of some other phase, possibly PuO<sub>2</sub>.

Several attempts were made to prepare PuI<sub>3</sub> by the reaction of plutonium metal in a platinum container with iodine. One hundred micrograms of metal in a well-degassed J. Lawrence Smith 1-ml platinum microcrucible contained in a quartz tube was treated with iodine vapor at 700°C. The dark-brown product was characterized by x-ray analysis as containing about 80 per cent PuOI and possibly some PuO<sub>2</sub>. About 300  $\mu\text{g}$  of plutonium metal was treated with liquid iodine in a sealed platinum capillary at 400°C. The experiment was performed with a platinum capillary approximately 20 cm long, 1 mm I.D., and 2 mm O.D., welded closed at one end and sealed to soft glass at the other end. After iodine had been distilled in, the platinum tube was crimped with a small vise and fused off the line. The light-green

reaction product turned brown when handled in a dry box. X-ray analysis<sup>8</sup> showed it to be at least 80 per cent PuOI.

All the dilute sulfuric acid solutions of PuOI were yellowish-green or green. Spectrophotometric examination<sup>8</sup> indicated that all the plutonium was present as plutonium(III).

In the only experiments on this scale in which PuI<sub>3</sub> was obtained, hydrogen iodide was used instead of iodine as the iodinating agent.<sup>9</sup> Anhydrous hydrogen iodide was obtained as described later in this report and purified further by vacuum distillation. A 75-μg sample of plutonium metal was treated with hydrogen iodide vapor (pressure, approximately 150 mm Hg) at 450°C in a quartz capillary. The bright-green product was identified by Zachariasen<sup>10</sup> by x-ray analysis as the new compound, PuI<sub>3</sub>, isomorphous with orthorhombic PuBr<sub>3</sub>. A second sample was similarly prepared from 500 μg of metal. The bright-green product was dissolved in dilute sulfuric acid and analyzed by Dr. M. J. Wolf. It contained 467 μg of plutonium and 588 μg of iodine, corresponding to an iodine/plutonium atom ratio of 2.37. When the sample was treated with the dilute sulfuric acid, it was observed that part of it dissolved rapidly and that some dissolved slowly with the evolution of a gas. This makes it probable that some unreacted metal was present, explaining why the iodine/plutonium atom ratio was less than 3.

The source of the oxygen in the various reactions of iodine with plutonium metal is not understood. Apparently there was some oxygen-bearing impurity in the iodine which was not removed by sublimation. For preparations on a larger scale, the difficulties due to oxygen-bearing impurities in the iodine would not be as important, and PuI<sub>3</sub> could be prepared by reaction of metal with either iodine or hydrogen iodide. In order to obtain complete reaction, powdering of the metal by hydride formation would be desirable.

Methods of synthesis of PuI<sub>3</sub> from PuO<sub>2</sub> or an aqueous solution of a plutonium salt were investigated since these starting materials are more accessible than plutonium metal. The action of hydrogen iodide on PuO<sub>2</sub> was investigated using a hydrogen-hydrogen iodide mixture (approximately 60 to 80 per cent hydrogen iodide) obtained by the reaction of hydrogen with iodine at 450°C using platinized asbestos as a catalyst. Purified hydrogen was passed over molten iodine at 150°C and then over the catalyst. The mixture was passed over a sample of PuO<sub>2</sub>·xH<sub>2</sub>O (3 to 10 mg of Pu) in a platinum crucible inside a quartz tube at 750°C. The treatment was continued for several hours. The black pellet of PuO<sub>2</sub>·xH<sub>2</sub>O had turned green and powdered. The powder was identified by x-ray analysis by Zachariasen<sup>11</sup> as PuOI.

A closely related possible mode of synthesis of  $\text{PuI}_3$  is the evaporation of an aqueous solution of  $\text{PuI}_3$  in a stream of hydrogen iodide at reduced pressures, and subsequent dehydration, in a stream of hydrogen iodide at temperatures up to 400°C, of the hydrated triiodide that crystallizes out of solution. Plutonium trichloride and plutonium tribromide have been successfully synthesized by analogous reactions.<sup>1,2</sup> In the case of the synthesis of some rare earth triiodides by this method, the addition of ammonium iodide to the solution and its subsequent sublimation at 400 to 600°C assists in the suppression of oxyiodide formation.<sup>12,13</sup>

To a plutonium(IV) chloride solution (3.6 mg of Pu in 50 microliters of 6M HCl) was added 15 mg of ammonium iodide to reduce the plutonium to the +3 state and provide excess ammonium iodide. The solution was contained in a pyrex tube, 10 mm O.D. and 15 cm long, closed at one end and provided at the other end with a ground joint by which it could be attached to the vacuum apparatus in a vertical position.

Hydrogen iodide condensed out of the hydrogen-hydrogen iodide mixture originating from the hydrogen iodide generator and was purified by fractional distillation. The condensed hydrogen iodide was maintained at a temperature of -78.4°C (vapor pressure approximately 60 mm Hg), and the vapor passed over the surface of the  $\text{PuCl}_3\text{-NH}_4\text{I}$  solution. The rate of flow of the hydrogen iodide was measured with a flowmeter using Apiezon oil as a manometric liquid, and the flow rate was controlled at approximately 1 cc/min by adjusting a stopcock leading through a liquid air trap to a vacuum pump assembly. The solution was taken to dryness in the hydrogen iodide stream at 50°C, and the solid residue was slowly heated to 350°C to sublime away the ammonium iodide. The green residue was characterized by x-ray analysis as  $\text{PuOI}$ .<sup>14</sup>

An attempt was made to synthesize  $\text{PuI}_3$  according to the reaction<sup>15</sup>



In this reaction it would be necessary to obtain the  $\text{PuI}_3$  as a sublimate in order to free it from the excess carbon. A plutonium(IV) oxalate precipitate (approximately 4 mg of Pu) was slurried with an equal weight of lamp black, oven-dried, pelleted, and placed in a platinum microcrucible. This was mounted in a system in which a slow stream of hydrogen iodide was passed over the crucible at 60 mm Hg pressure. The crucible was heated by induction to approximately 1000°C for 30 min and maintained at 1500°C for an equal period of time. The temperatures were estimated with an optical

pyrometer and are not very accurate. A small amount of a light-green sublimate collected in a water-cooled glass tube just above the crucible, but there was no other evidence of reaction and the sublimate that did form was not sufficient in quantity to be removed for x-ray analysis.

Several attempts were made to prepare  $\text{PuI}_3$  from  $\text{PuO}_2$  by the reaction



In one series of experiments,  $\text{PuO}_2 \cdot x\text{H}_2\text{O}$  (1 to 3 mg of Pu) in a quartz tube at 800°C was exposed for several hours to aluminum iodide vapor (approximately 10 mm Hg pressure) carried in a stream of hydrogen. There was no evidence of reaction.

Several 3-mg samples of  $\text{PuO}_2 \cdot x\text{H}_2\text{O}$  were sealed in quartz tubes with excess aluminum iodide, and the tubes heated to 450–500°C for 4 to 8 hr. The bombs were opened in vacuum and the aluminum iodide was distilled away at 150°C. The tubes were then heated to 800°C for an hour. In each case a green sublimate was observed just outside the furnace, but x-ray analysis showed no  $\text{PuI}_3$ , either in the sublimate or in the residue.<sup>16</sup>

The consistent failure of our attempts to convert  $\text{PuO}_2$ , or an aqueous plutonium solution, to  $\text{PuI}_3$  is in marked contrast to the ease with which  $\text{PuCl}_3$ , or  $\text{PuBr}_3$ , may be obtained from the same starting materials by a variety of reactions.<sup>1,2</sup> Other workers have experienced similar difficulties in preparing tripositive and tetrapositive iodides. The attempt of Fischer, Gewehr, and Wingchen<sup>17</sup> to prepare thorium iodide by the action of a hydrogen iodide stream on a thorium dioxide–carbon mixture failed, and they resorted to the action of hydrogen iodide on thorium metal for this preparation.

Jantsch and his coworkers have intensively investigated the preparation of the rare-earth triiodides. In their experience, the triiodides of lanthanum, praseodymium, and samarium can be prepared by treatment with a stream of anhydrous hydrogen iodide of high purity of a mixture in the molal ratio of 1 to 6 of the hexahydrated iodides with ammonium iodide at temperatures up to 600°C.<sup>18,12</sup> With samarium some oxyiodide is also formed.<sup>19</sup> This method of synthesis gives rise to basic salts when applied to gadolinium or the subsequent rare earths, which are less basic than the cerium earths and form more readily hydrolyzed salts. In these cases it is necessary to make the iodides by treatment of the anhydrous chlorides with hydrogen iodide.<sup>18,19</sup> This method suffers from the defect that any oxygen-bearing impurity in the gas stream will cause the formation of oxy-

iodide; in practice it is necessary to compromise between incomplete removal of the chloride by the hydrogen iodide and accumulation of oxide due to the prolonged treatment.<sup>13</sup>

Plutonium chloride and bromide are very similar to the corresponding neodymium salts in melting point and crystal structure. The difficulties encountered by us in the attempted "wet" syntheses of  $\text{PuI}_3$  suggest that for iodides plutonium is more like gadolinium. However, the possibility should not be excluded that by working with purer gases than used in the present work and altering the conditions of reaction somewhat, it will be found possible to prepare fairly pure  $\text{PuI}_3$  by a wet method so that  $\text{PuI}_3$  may then be considered analogous to neodymium or samarium.

**Summary.** Bright-green plutonium triiodide was prepared on the 50- and 500- $\mu\text{g}$  scale by treatment of plutonium metal with hydrogen iodide gas at 400°C. The reaction of 50- to 500- $\mu\text{g}$  quantities of plutonium metal with excess iodine in the liquid or vapor phase, in platinum or glass apparatus, gave rise to plutonium oxyiodide,  $\text{PuOI}$ , rather than the triiodide.

The oxyiodide was obtained when plutonium dioxide was treated with anhydrous hydrogen iodide at 750°C, or when a plutonium(III) iodide solution was evaporated to dryness in the presence of excess ammonium iodide in a stream of hydrogen iodide at reduced pressure. Attempts to make plutonium triiodide by treatment of the dioxide with aluminum iodide in the liquid or vapor phase or by treatment of a plutonium dioxide-carbon mixture with hydrogen iodide at elevated temperatures were not successful.

#### REFERENCES

1. B. M. Abraham, B. B. Brody, N. R. Davidson, F. Hagemann, I. Karle, J. J. Katz, and M. J. Wolf, Preparation and properties of plutonium chlorides and oxychlorides, Paper 6.7, this volume.
2. N. R. Davidson, F. Hagemann, E. K. Hyde, J. J. Katz, and I. Sheft, Preparation and properties of plutonium tribromide and oxybromide, Paper 6.8, this volume.
3. L. B. Arnold, Jr., Metallurgical Project Report CC-2757 (Jan. 1, 1945), p. 6.
4. F. Hagemann, Metallurgical Project Report CK-1701 (A-2430) (June 1, 1944), p. 8.
5. W. H. Zachariasen, Metallurgical Project Report CN-1733 (May 25, 1944), p. 3.
6. W. H. Zachariasen, Metallurgical Project Report CN-2069 (August 1944), p. 21.
7. M. J. Wolf, Metallurgical Project Report CK-1763 (A-2470) (July 1, 1944), pp. 10-11.
8. F. Hagemann, Metallurgical Project Report CK-1763 (A-2470) (July 1, 1944), p. 10.
9. *Ibid.*, p. 9.
10. W. H. Zachariasen, Metallurgical Project Report CN-2069 (August 1944), p. 19.
11. B. M. Abraham, N. R. Davidson, J. J. Katz, and I. Sheft, Metallurgical Project Report CN-2159 (Oct. 1, 1944), p. 10.
12. G. Jantsch and N. Skalla, *Z. anorg. Chem.*, 193: 391 (1930).
13. F. Bommer and E. Hohmann, *Z. anorg. Chem.*, 248: 370 (1941).

14. I. Sheft, Metallurgical Project Report CN-2159 (Oct. 1, 1944), p. 10.
15. I. Sheft and N. R. Davidson, Metallurgical Project Report CN-2159 (Oct. 1, 1944), p. 10.
16. F. Hagemann, Metallurgical Project Report CN-2159 (Oct. 1, 1944), p. 11.
17. W. Fischer, R. Gewehr, and H. Wingchen, Z. anorg. Chem., 242: 161 (1939).
18. G. Jantsch, H. Grubitsch, F. Hoffman, and H. Alber, Z. anorg. Chem., 185: 49 (1929).
19. G. Jantsch, N. Skalla, and H. Grubitsch, Z. anorg. Chem., 212: 65 (1933).

Paper 6.220

ALKALI PLUTONIUM(IV) NITRATES†

By H. H. Anderson

1. PREPARATIONS

For convenience in comparison the preparations have been summarized in Table 1.

Very slow mixing was used in the quinolinium preparation, with consequent formation of moderate-sized crystals. Slow horizontal

Table 1—Preparation of Complex Nitrates

RNO <sub>3</sub>	RNO <sub>3</sub> , mg	Pu(IV), mg	Ratio of R to Pu	Volume, ml	Free HNO <sub>3</sub> , molarity	Solubility of Pu, g/liter
C <sub>6</sub> H <sub>5</sub> NHNO <sub>3</sub>	80	5.6	18	0.175	3.7	0.50
CsNO <sub>3</sub>	9.5	5.6	2.1	0.122	6.5	3.4
RbNO <sub>3</sub>	11.2	8.4	2.2	0.220	12	4.6
TlNO <sub>3</sub>	12.5	4.2	3.7	0.100	12	26
KNO <sub>3</sub>	17.5	8.4	5	0.150	12	18 (at 1°C)
C <sub>5</sub> H <sub>5</sub> NHNO <sub>3</sub>	71	5.6	21	0.140	2.5	3 (est.)

rotation of the solution in a centrifuge cone tended to give relatively large crystals and to give equilibrium in solubility. Filtration by suction on a special sintered pyrex disk of 3 mm diameter separated the crystals from the mother liquor. A single wash of several drops of 95 per cent ethanol was used.

All preparations employed suction filtration on a disk and drying in a vacuum at room temperature. Solubilities are at approximately 28°C except for the potassium salt. Previous experience had shown

†Contribution from the Chemistry Division of the Metallurgical Laboratory, University of Chicago, now the Argonne National Laboratory.

that the cesium salt could not be washed in the usual preparative fashion with 50 per cent ethanol and then absolute methanol; a precipitate washed in this manner had a cesium/plutonium ratio of 2.6/1. In other words, plutonium nitrate was washed out of the double nitrate, leaving behind an excess of cesium nitrate.

Table 2—Analytical Data

	Plutonium		Alkali	
	Found, %	Calc., %	Found, %	Calc., %
$(C_6H_5NH)_2Pu(NO_3)_6$	27.2	27.4		
$Cs_2Pu(NO_3)_6$	26.8	27.26	31.0	30.3
$Rb_2Pu(NO_3)_6$	31.8	30.6		
$Tl_2Pu(NO_3)_6$	24.2	23.4		
$K_2Pu(NO_3)_6$	29.7†	34.7		
$(C_6H_5NH)_2Pu(NO_3)_6 \cdot 14H_2O\ddagger$	23.4	23.4		

†Contaminated by some free potassium nitrate. Probably 86 per cent  $K_2Pu(NO_3)_6$  and 14 per cent  $KNO_3$ .

‡Formula of hydrate based on percentage of plutonium only.

With rubidium plutonium nitrate this decomposition was severe since a sample washed freely with a mixture of methanol and concentrated nitric acid contained only 1.2 per cent plutonium. However, a fairly pure rubidium plutonium(IV) nitrate was prepared by slow mixing of solutions of the two nitrates, the mixing being accomplished by slow horizontal rotation for 20 min in a centrifuge cone to grow relatively large crystals. This was followed by filtration on a disk without any washing. Drying at room temperature at 0.3 mm Hg was followed by drying under a heat lamp for 20 min at about 125°C. There was slight decomposition with formation of some brown solid, but 98 to 99 per cent consisted of light-green crystals. Thus the percentage of plutonium in Table 2 is slightly high.

Thallous nitrate and plutonium nitrate gave very small crystals when agitated vigorously with a platinum stirring rod. Cooling in an ice-water bath did not help. A clear solution was finally seeded with about 1 µg of crude potassium plutonium(IV) nitrate crystals. Crystallization started at once. It was allowed to proceed for 3 hr with occasional horizontal rotation of the centrifuge cone. The crystals were filtered on a disk of sintered pyrex glass, washed with 1 drop of 95 per cent ethanol, and dried first in a vacuum at room temperature and then for 15 min at about 130°C.

Potassium plutonium(IV) nitrate was finally crystallized after considerable difficulty at about 1°C in an ice-water bath, followed by fil-

tration on a disk at 1°C without washing. Note that the solubility of this salt is at least 50 g of plutonium per liter at 28°C or even greater when dried in vacuum at 130°C. This preparation contained some free potassium nitrate, scavenged from the solution, as is shown by the analysis for plutonium in Table 2. The type  $\text{KPu}(\text{NO}_3)_5 \cdot 12\text{H}_2\text{O}$  is a possibility.

Pyridinium plutonium(IV) nitrate was prepared without any washing. After preliminary drying in a vacuum at room temperature the pale-green crystals were dried in platinum under a heat lamp. At about 110°C the crystals melted without decomposition. Recrystallization upon cooling is in keeping with the explanation that the compound was a hydrate and that the anhydrous salt was soluble in its water of hydration at 110°C. Table 2 gives the analysis for plutonium in the fused salt, which was in the form of light-green needles.

## 2. ANALYSES

Analyses for plutonium were carried out as described in a previous paper.<sup>1</sup> Cesium was estimated as cesium chloroplatinate, with allowance for the small plutonium content.

Table 2 lists the analytical results, which justify the formulas assigned to the series.

It should be remembered that 1 to 2 per cent decomposition in the rubidium sample upon drying undoubtedly raised the percentage of plutonium in the sample and that a value of 31.5 to 31.6 per cent plutonium might be closer.

Upon a numerical consideration of the values for the first four compounds, it may be concluded that: (1) The formulas assigned are probably correct. (2) Variation in the R/Pu ratio is not important in these four preparations, for they do not scavenge alkali nitrate as did the potassium analogue. (3) The double nitrates are not decomposed at 110 to 120°C, although at 130°C decomposition is great. (4) The agreement with the type formula is best with the quinolinium derivative and decreases as the size of R decreases. In other words, the quinolinium and cesium double nitrates are the most stable. Here stability and solubility are linked.

## 3. DISCUSSION OF RESULTS

In addition to the conclusions reached in the above paragraph, several others may be made.

Plutonium tetrannitrate is very soluble in 2M  $\text{HNO}_3$ , but the solubility is reduced by the presence of alkali ions. Plutonium tetrannitrate appears to be less soluble in concentrated nitric acid than in dilute acid.

The decomposition of certain double nitrates is consistent with several explanations. A dissociation may take place, such as



with removal of some plutonium in the dissociated form. Alternatively, the process could be an elution of plutonium nitrate from the  $\text{R}_2\text{Pu}(\text{NO}_3)_6$  crystals.

A high concentration of nitric acid is needed in the preparations. Probably plutonium exists as an entirely different species in very dilute nitric acid, perhaps even  $\text{Pu}^{+4}$ .

Now it is possible to explain the solution of  $\text{KPuF}_5$  in concentrated nitric acid: This process is a competition between  $\text{H}_2\text{Pu}(\text{NO}_3)_6$  and  $\text{KPuF}_5$  for the plutonium. As suggested previously,<sup>2</sup> the existence of an  $\text{HPuF}_5$  is unlikely. Therefore the solution in nitric acid could be expected.

#### 4. SUMMARY

Plutonium(IV) and certain alkali ions react in fairly concentrated nitric acid to give crystalline precipitates of the general formula  $\text{R}_2\text{Pu}(\text{NO}_3)_6$ .

In most cases the precipitates could not be washed, either because of excessive solubility or because of decomposition. Chemical analyses justified the following formulation: quinolinium plutonium(IV) hexanitrate,  $(\text{C}_9\text{H}_7\text{NH})_2\text{Pu}(\text{NO}_3)_6$ ; (di)cesium plutonium(IV) hexanitrate,  $\text{Cs}_2\text{Pu}(\text{NO}_3)_6$ ; rubidium plutonium(IV) hexanitrate,  $\text{Rb}_2\text{Pu}(\text{NO}_3)_6$ ; thallous plutonium(IV) hexanitrate,  $\text{Tl}_2\text{Pu}(\text{NO}_3)_6$ ; an impure potassium plutonium(IV) hexanitrate,  $\text{K}_2\text{Pu}(\text{NO}_3)_6$ ; a hydrated pyridinium plutonium(IV) hexanitrate,  $(\text{C}_5\text{H}_5\text{NH})_2\text{Pu}(\text{NO}_3)_6 \cdot 14\text{H}_2\text{O}$  approximately. The pyridinium salt melts at roughly 110°C and re-forms crystals upon cooling.

All the double nitrates were pale-green crystalline solids. Solubilities and details of preparations have been given. The existence of these double nitrates is consistent with the concept of a complex hexanitratoplutonium(IV) acid,  $\text{H}_2\text{Pu}(\text{NO}_3)_6$ , in 3M  $\text{HNO}_3$  or stronger.

#### REFERENCES

1. H. H. Anderson, Thallous and sodium plutonium(III) sulfates, Paper 6.19, this volume (Argonne National Laboratory Report ANL-4062).
2. H. H. Anderson, Alkali plutonium(IV) fluorides, Paper 6.9, this volume (Argonne National Laboratory Report ANL-4054).

## Paper 14.1

### RANGE OF Np<sup>237</sup> ALPHA PARTICLES IN AIR†

By T. J. LaChapelle

#### 1. INTRODUCTION

A study of the characteristic radiations of any radioactive nuclear species may include the determination of the range in absorbers in order to ascertain the exact nature of the radiation and to measure the energies associated with it. In the case of  $\alpha$ -emitting nuclei the range can be measured by interposing thin absorbers between the source and the ionization-sensitive space. Although mica, aluminum, and other materials can be used as absorbers, all ranges are usually converted to an adopted standard of dry air at 15°C and 760 mm Hg pressure.<sup>1</sup> If the mean range of a given  $\alpha$  particle is near that of another whose range is known accurately, a comparison of the extrapolated ranges of the two under identical conditions will give the unknown mean range.<sup>2</sup> The ranges of Np<sup>237</sup> and Pu<sup>239</sup> were compared in this way. When the value of the range in air thus obtained is used, the energy of the  $\alpha$  particle can be calculated from the known relation between these functions.<sup>3</sup>

The mean range of Np<sup>237</sup>  $\alpha$  particles was first reported as  $3.25 \pm 0.1$  cm of air<sup>4</sup> on the basis of low-geometry absorption in air at various pressures. Later the value 3.26 was found<sup>5</sup> by absorption with aluminum absorbers<sup>6</sup> in an ionization chamber of 5 to 10 per cent geometry. Both determinations were made on relatively thick samples of low activity which contained 10 per cent or more Pu<sup>239</sup> by  $\alpha$  count. The measurements described here have eliminated the errors due to thick samples and contamination by other  $\alpha$  radiation. This paper is

† Contribution from the Chemistry Division of the Metallurgical Laboratory, University of Chicago, now the Argonne National Laboratory.

Based on a revision of Metallurgical Project Report CN-2767 (Mar. 27, 1945) and other data.

a complete revision of an earlier interpretation of the data<sup>7</sup> and is based on the method of least squares.

## 2. EXPERIMENTAL TECHNIQUE

**2.1 Preparation of Neptunium Sample.** By repeated purifications<sup>8</sup> the contaminants were removed from several milligrams<sup>9</sup> of Np<sup>237</sup>. The source of the element was a batch originally mixed with several grams of Pu<sup>239</sup> produced in a graphite reactor at Clinton Laboratories. The plutonium was processed under such conditions<sup>10</sup> that a minimum of neptunium was lost. The separation procedure, which consisted of four oxidation-reduction cycles, removed plutonium as well as uranium from the neptunium, but introduced lanthanum as a carrier. Three oxidation-reduction cycles<sup>11</sup> involving potassium bromate as the oxidant, sulfur dioxide as the reductant, and hydrofluoric acid as the precipitant removed the lanthanum.

The 6.1 mg of neptunium so obtained was precipitated as neptunium(IV) hydroxide with ammonia, dissolved in nitric acid, and again precipitated as neptunium(V) hydroxide with ammonia. The hydroxide was washed four times with separate portions of water, and the last washing showed no traces of ammonium ion upon testing. Dissolution of the precipitate in dilute sulfuric acid was followed by a bromate-oxidation and precipitation as sodium neptunium(VI) dioxytriacetate. This salt was then dissolved in dilute sulfuric acid, the neptunium was reduced with sulfur dioxide, and neptunium(V) hydroxide was precipitated with ammonia. The hydroxide was dissolved in dilute sulfuric acid and oxidized with bromate, and sodium neptunium(VI) dioxytriacetate was again precipitated. The double acetate was dissolved in dilute nitric acid and treated with sulfur dioxide gas, and neptunium(V) hydroxide was precipitated with ammonia. The hydroxide was washed and dissolved in 1.0 ml of 0.5M H<sub>2</sub>SO<sub>4</sub> solution.

A 1.323-microliter aliquot of this solution was transferred to a drop of acid on a smooth, flat platinum disk. The disk diameter was 2.3 cm, and the thickness was 0.005 cm. The drop of acid was 20 microliters of 1M HNO<sub>3</sub> solution spread over the central area of the plate. Five microliters of 1M HF solution was added to precipitate the neptunium as fluoride. A fine platinum wire was used to stir the drop in order to prevent the settling of large aggregates of the fluoride. The solution was carefully evaporated by a combination of an infrared lamp and a hot plate. During this procedure the platinum disk rested on a brass ring. This ring heated only the rim of the platinum, so that at all times the periphery of the disk was at a higher temperature than the center. In this manner the sulfuric acid was kept from the edges of the plate during evaporation. After no more

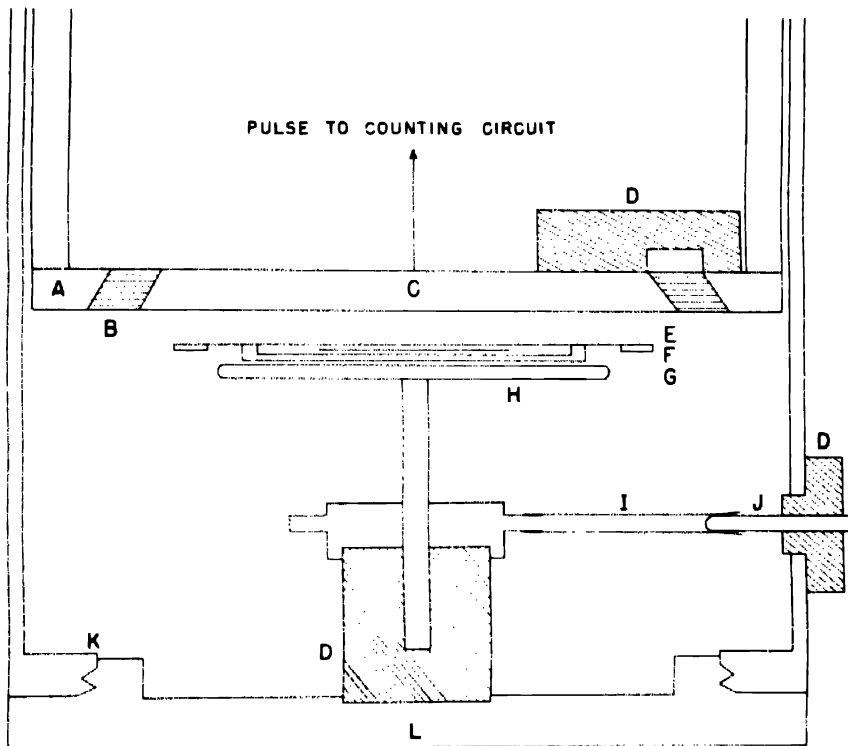
fumes of sulfur trioxide distilled from the sample, the neptunium film was again treated with hydrofluoric acid and dried. The plate was carefully passed over a bunsen-burner flame to remove all traces of combustible organic matter. The resulting disk had an even deposit of fluoride covering an area of about 2.5 sq cm. Examination under a 27-power binocular microscope showed no large aggregates of material. Radiometric assay of the plate gave  $3,704 \pm 6$  counts per minute in a parallel-plate geometry ionization chamber. On the basis of 790 counts per minute per microgram under the above conditions<sup>8</sup>  $4.69 \mu\text{g}$  of  $\text{Np}^{237}$  was present. If the assumption is made that a perfectly uniform dispersion of neptunium fluoride covers the area, the thickness would be 0.002 mg per square centimeter. The layer probably had an average value of about  $0.005 \pm 0.005$  mg per square centimeter.

**2.2 Determination of Range.** The range in mica of the  $\alpha$  particles from the  $\text{Np}^{237}$  plate was compared with that of the  $\alpha$  particles from  $\text{Pu}^{239}$ . These ranges were compared consecutively on the same parallel-plate ionization chamber<sup>12-15</sup> under identical conditions. The Cyclotron Specialties (California) type A linear amplifier and type B scale-of-eight counting circuit were used with the chamber. The temperature was about 25°C and the air pressure in the ionization chamber was atmospheric (about 730 mm). The variations of temperature and pressure during the entire measurement were negligible. The platinum disk plated with the  $\alpha$  emitter was placed on a small aluminum disk having a slightly raised edge. The dimensions of this disk were: 44 mm diameter, 1.0 mm thickness, and a rim 0.2 mm high and 3 mm wide. The purpose of the rim was to prevent the active samples from touching the mica absorber placed over it. The aluminum holder with the platinum plate centered on it rested on the bottom electrode of a parallel plate ( $2\pi$  geometry) ionization chamber. Over the sample were placed various mica absorbers. These absorbers were made by splitting sheets into various thicknesses with the aid of a sharp tungsten needle, examining each sheet under polarized light to detect nonuniformity, determining weight per unit area, and mounting the mica on narrow, flat brass rings of 60 mm diameter (see Fig. 1 for the geometrical arrangement of units in the ionization chamber).

The procedure followed was to count the  $\alpha$  activity with an absorber in place, remove the sample, and then determine the count due to the absorber alone. In this way the error due to possible contamination of the absorber could be eliminated.

The method was first employed with a  $\text{Pu}^{239}$  sample of negligible weight (on platinum), which had roughly the same number of disintegrations per minute as the  $\text{Np}^{237}$  sample. The determinations of

counts per minute were carried out for appropriate lengths of time so that the standard counting errors involved were less than 1 per cent in most cases. Absorbers 1, 4, 5, and 7 were used as standards since their surface densities had been checked many times in other



A GUARD RING	G ALUMINUM HOLDER
B PARAFFIN INSULATION	H HIGH VOLTAGE ELECTRODE
C COLLECTING ELECTRODE	I HIGH VOLTAGE WIPING CONTACT
D AMPHENOL INSULATOR	J HIGH VOLTAGE INLET
E MICA ABSORBER	K BREECH THREAD
F SAMPLE MOUNTED ON PLATINUM PLATE	L BOTTOM PLATE

Fig. 1 — Apparatus for range comparison.

experiments involving  $\alpha$ -range determinations.<sup>16</sup> Table 1 summarizes the data of the measurements involving the  $\text{Pu}^{239}$  sample.

A theoretical derivation of a linear relation between counting rate and absorber thickness has been made by A. H. Jaffey.<sup>18</sup> The following assumptions are made:

1. No range straggling.

**2. Stopping power of mica is independent of  $\alpha$ -particle energy.**  
 These assumptions are not strictly correct, but they do not introduce an important error.

Table 1—Mica-absorption Measurements on Pu<sup>239</sup> Alpha Particles

(1)	(2)	(3)	(4)	(5)	(6)	(7)	(8)
Absorber	D <sub>m</sub>	C <sub>M</sub>	$\pm \sigma_{C_M}$	w	C <sub>T</sub>	$(C_T - C_M)$	$\Delta C/\sigma_{C_M}$
1	$1.89 \pm 0.005$	2,980	27	0.137	3,001	+21	0.8
4	$2.84 \pm 0.005$	2,073	23	0.189	2,053	-20	0.9
5	$3.70 \pm 0.005$	1,203	17	0.346	1,195	-8	0.5
7	$4.15 \pm 0.005$	742	10	1.000	740	-2	0.2

0.6 (av. obtained)  
 0.798 (av. theoretical)

(1) Mica absorber.

(2) D<sub>m</sub> is the surface density of the mica absorber in milligrams per square centimeter and the estimated standard error of this value.

(3) C<sub>M</sub> stands for the counts per minute as measured for the sample with absorber in place, a correction having been made for any contamination of the absorber as well as for the counting loss (0.8 per cent per thousand counts per minute)<sup>16</sup> due to the resolving power of the electrical circuit.

(4)  $\pm \sigma_{C_M}$  refers to the standard error ( $\sigma$ ) of the value in the previous column based on a purely statistical variation of the counting rate. The relations between this criterion and three other commonly used criteria are to be found in standard texts;<sup>17</sup> the standard error is defined as the square root of the mean squared deviation and gives a 68.3 per cent probability of the error being less than this value.

(5) w is the weight given to a particular determination and is inversely proportional to the square of the value in column (4).

(6) C<sub>T</sub> is the theoretical counts per minute calculated from the equation for the straight line (see derivation for C below)

$$C_T = (4886 \pm 2) - (997.6 \pm 0.4)D_m \quad (1)$$

which is obtained by the method of least squares<sup>18</sup> from the data in columns 2, 3, and 5 of Table 1.

(7)  $\Delta C$  is the difference between the values of column (6) and column (3).

(8)  $\Delta C/\sigma_{C_M}$  shows the magnitude of the difference between theory and experiment in terms of the standard error for that measurement. The average of this magnitude should give  $0.798\sigma$  (the average error) when a large number of comparisons are made. The value obtained, 0.6, is in fair agreement with statistical theory, indicating that the data are internally consistent.

Let F = fraction of  $\alpha$  particles emitted which emerge from the absorber and are counted

R = range of  $\alpha$  in absorber material

r = residual range (reduced to the same units as R) which  $\alpha$  particle must have after passing out of absorber into ionization chamber before it can create a measurable pulse

$h$  = absorber thickness

$x$  = thickness of absorber equivalent to the absorption by the air between sample and mica

$H = x + h$

$L = R - r$  = path length in the absorber for  $\alpha$  particle which just barely does not count

$D$  = total disintegration rate

$C$  = counting rate

For an absorber  $h$  (see Fig. 2),

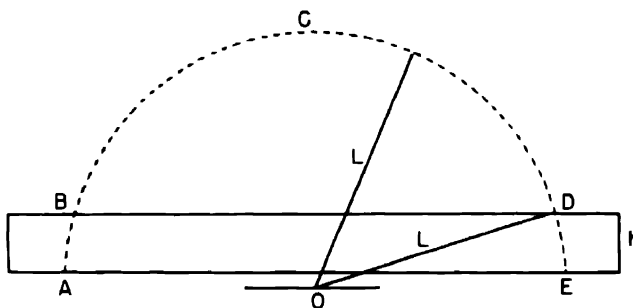


Fig. 2 — Solid angle subtended by circular aperture.

$$F = \frac{\text{solid angle of spherical segment BCD}}{4\pi} \quad (2)$$

$$\text{Solid angle of spherical segment BCD} = \frac{2\pi L^2 - 2\pi LH}{L^2}$$

$$= 2\pi \left(1 - \frac{H}{L}\right) \quad (3)$$

$$F = \frac{1}{2} \left(1 - \frac{H}{L}\right) \quad (4)$$

$$C = DF = \frac{D}{2} \left(1 - \frac{x+h}{R-r}\right)$$

$$C = \frac{D}{2} \left(\frac{R-r-x}{R-r}\right) - \frac{D}{2(R-r)} h \quad (5)$$

Obviously  $C$  (counting rate) is a linear function of  $h$  (absorber thickness).

$$\text{At } C = 0, \quad x + h = R - r \quad \text{or} \quad R = h + (x + r) \quad (6)$$

Since both  $x$  and  $r$  remain constant within the experimental conditions usually applied, the measurement of ranges by comparison to a standard then gives

$$R_1 - R_2 = h_1 - h_2 \quad (7)$$

The same  $\text{Pu}^{239}$  sample was counted through several new absorbers. Using the equation relating theoretical counts per minute and the surface density of the mica absorber, and substituting the observed activity for  $C_T$ , the densities of these absorbers were calculated and compared with measured densities. These results are shown in Table 2.

Table 2 --- Determination of New Absorber Densities

Absorber No.	$C_M$	$\pm \sigma_{C_M}$	$D'_M$ , rough value from weight per area	$D_M$ , calculated from equation	$\pm \sigma_{D_M}$ †
2	2,546	25	2.38	2.35	0.025
3	2,264	24	2.65	2.63	0.024
6	980	8	3.92	3.92	0.008
8	633	9	4.26	4.26	0.009
9	460†	5	4.43	4.43	0.005
				4.898	0.003

†By solving Eq. 1 for  $C_T = 0$ , the extrapolated end point for the range of  $\text{Pu}^{239}$  in mica under the experimental conditions is found to be  $4.898 \pm 0.003$  mg per square centimeter.

‡Based on reference 20.

Replacing the  $\text{Pu}^{239}$  sample with the  $\text{Np}^{237}$  specimen and determining the  $\alpha$  activity with various mica absorbers produced the results shown in Table 3.

Using Eq. 8 (footnote, Table 3), the surface density of mica required to reduce the  $\text{Np}^{237}$  count per minute to zero is

$$D = 4.260 \pm 0.007 \text{ mg per square centimeter} \quad (9)$$

The difference between the range of  $\text{Pu}^{239}$  and  $\text{Np}^{237}$  in mica is

$$(4.898 \pm 0.003) - (4.260 \pm 0.007) \\ = 0.638 \pm 0.008 \text{ mg per square centimeter of mica} \quad (10)$$

In order to convert the preceding data into range difference in air, the following value was experimentally determined by Ghiorso.<sup>16</sup>

Thickness of mica in milligrams per square centimeter equivalent to 1 cm of air for 4.7-mev particles = 1.40 0.03 (11)

The method used was to compare the extrapolated range of Np<sup>237</sup> with and without a mica absorber whose surface density was known. The measured activity was varied by changing the air pressure. The counts per minute were determined in a low-geometry arrangement

Table 3 — Mica Absorption Measurements on Np<sup>237</sup> Alpha Particles

(1) Absorber No.	(2) D <sub>m</sub>	(3) C <sub>M</sub>	(4) $\pm \sigma_{C_M}$	(5) w	(6) C <sub>T</sub>	(7) $(C_T - C_M)$	(8) $\Delta C/\sigma_{C_M}$
1	1.89	1,908	11	0.132	1,912	-4	0.4
2	2.35†	1,539	10	0.160	1,544	+2	0.2
3	2.63†	1,330	9	0.198	1,315	-15	1.7
4	2.84	1,133	9	0.198	1,146	+13	1.4
5	3.70	452	5	0.640	452	0	0.0
6	3.92†	274	4	1.000	275	+1	0.3
							0.7 (av. obtained)
							0.798 (av. theoretical)

Note: For explanation of columns see Table 1. Note, however, that in this table (2)† indicates a calculated value (see Table 2). In (6) the linear relation that best describes the data of columns (2), (3), and (5) is

$$C_T = (3436 \pm 4) - (806.5 \pm 0.9)D_m \quad (8)$$

so that the only  $\alpha$  particles involved were those coming off the sample plate in a small solid angle inclosing the perpendicular line. This procedure decreased the effect of back-scattered particles. The value obtained for the ratio agrees nicely with the value of 1.43 given in the literature<sup>22</sup> for 6-mev  $\alpha$  particles. This ratio is known to decrease with decrease in energy of the  $\alpha$  radiation.

Using Eq. 11, the difference in ranges is

$$\frac{0.638 \pm 0.008}{1.40 \pm 0.03} = 0.456 \pm 0.008 \text{ cm of air} \quad (12)$$

Since the mean range of Pu<sup>239</sup> has been found by measurement<sup>23,24</sup> to be  $3.68 \pm 0.02$  cm, by comparison with the known<sup>25</sup> mean range of Po<sup>210</sup>,  $3.842 \pm 0.006$  cm, the value for Np<sup>237</sup> is

$$(3.68 \pm 0.02) - (0.46 \pm 0.01) = 3.22 \pm 0.02 \text{ cm of dry air at } 15^\circ\text{C and 760 mm Hg} \quad (13)$$

This value corresponds<sup>26</sup> to an energy for the Np<sup>237</sup>  $\alpha$  particle of  $4.72 \pm 0.02$  mev.

Since the difference between the extrapolated and mean range changes but slowly as the alpha energy increases, a negligible error in the mean range determination arises when the extrapolated ranges compared are close together.<sup>2</sup>

The minimum purity of the neptunium sample with respect to plutonium was estimated by employing an absorber whose surface density lay between the  $\alpha$ -particle ranges of Pu<sup>239</sup> and Np<sup>237</sup>. Since the effect of straggling must be considered at the very end of the range curve, the absorber selected was greater than 0.15 mg per square centimeter beyond the theoretical value necessary to reduce the Np<sup>237</sup> count to zero. The experiment, carried out as part of the previously mentioned Np<sup>237</sup> run, indicated  $1.5 \pm 0.1$  counts per minute at 4.43 mg per square centimeter of mica. Using this point and the point at which the plutonium count was zero gave an extrapolated value of  $16 \pm 1$  counts per minute at zero absorber. Applying a geometry correction factor of 1.08 for the absorber arrangement gave a maximum of about 17 counts per minute of Pu<sup>239</sup> present in the original 3,704 total counts per minute. This is equivalent to a Pu<sup>239</sup> contamination of 0.46 per cent by  $\alpha$  activity and 0.0051 per cent by weight. A later measurement<sup>27</sup> of the impurity present in the sample by fission count in a beam of thermal neutrons verified this estimate. The error introduced in the Np<sup>237</sup> range by the presence of this amount of plutonium is well within the experimental error, and correction for it has therefore been omitted.

### 3. SUMMARY

The mean range of  $\alpha$  particles from Np<sup>237</sup> is  $3.22 \pm 0.02$  cm in dry air at 15°C and 760 mm Hg pressure when 3.68 cm is used for the comparative range of the Pu<sup>239</sup>  $\alpha$  particle. The corresponding energy of the neptunium radiation is  $4.72 \pm 0.02$  mev.

### REFERENCES

1. W. B. Lewis and C. E. Wynn-Williams, Proc. Roy. Soc., 136: 349 (1932).
2. M. S. Livingston and H. A. Bethe, Revs. Modern Phys., 9: 285 (1937).
3. M. G. Holloway and M. S. Livingston, Phys. Rev., 54: 18 (1938).
4. A. Ghiorso, Metallurgical Laboratory Memorandum MUC-GTS-501 (Mar. 2, 1944), p. 5.
5. A. H. Jaffey, Metallurgical Laboratory Memorandum MUC-GTS-677 (May 13, 1944), p. 6.

6. A. H. Jaffey, Metallurgical Project Report CC-3771 (Feb. 7, 1947), Sec. 6.2.2; also in National Nuclear Energy Series, Division IV, Volume 14A.
7. T. J. LaChapelle, Metallurgical Project Report CN-2767 (Mar. 27, 1945), p. 35.
8. L. B. Magnusson and T. J. LaChapelle, The first isolation of element 93 in pure compounds and a determination of the half life of  $\alpha$ Np<sup>237</sup>, Paper 1.7, this volume.
9. G. T. Seaborg, Science, 104: 384 (1946).
10. W. C. Beard, H. H. Hopkins, J. G. Malm, T. J. LaChapelle, J. J. Katz, and J. R. Gilbreath, Metallurgical Project Report CN-2688 (Feb. 27, 1945), p. 23.
11. L. B. Magnusson, J. C. Hindman, and T. J. LaChapelle, unpublished work.
12. A. H. Jaffey, T. P. Kohman, and J. A. Crawford, Metallurgical Project Report CC-1602 (March 1944), p. 2.
13. S. G. English, Metallurgical Project Report CL-1305 (Apr. 13, 1944), Chap. 11, p. 11.
14. Metallurgical project handbook, Metallurgical Project Report CL-897 (Nov. 24, 1944), Chap. 7B, Sec. 2.1.
15. A. H. Jaffey, Metallurgical Project Report CC-3771 (Feb. 7, 1947), Sec. 5.1; also in National Nuclear Energy Series, Division IV, Volume 14A.
16. A. Ghiorso, private communication, 1945.
17. A. G. Worthing and J. Geffner, "Treatment of Experimental Data," p. 157, John Wiley & Sons, Inc., New York, 1944.
18. Ibid, p. 243.
19. A. H. Jaffey, private communication, 1946.
20. Worthing and Geffner, op. cit., p. 250.
21. T. K. Sherwood and C. E. Reed, "Applied Mathematics in Chemical Engineering," p. 377, McGraw-Hill Book Company, Inc., New York, 1939.
22. Livingston, op. cit., p. 272.
23. O. Chamberlain, J. W. Gofman, E. Segrè, and A. C. Wahl, Los Alamos Report LA-9 (June 26, 1943).
24. E. Segrè, private communication, 1946.
25. Holloway, op. cit., p. 36.
26. Ibid., p. 31.
27. A. Ghiorso and T. J. LaChapelle, unreported data, 1945.

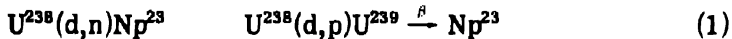
## Paper 14.2

### THE RADIATIONS OF $\text{Np}^{238}$ AND THE HALF LIFE OF $\text{Pu}^{238}\dagger$

By A. H. Jaffey and L. B. Magnusson

#### 1. INTRODUCTION

$\text{Np}^{238}$  was first reported<sup>2,3</sup> in 1942 when it was made by the reaction  $\text{U}^{238}(\text{d},2\text{n})\text{Np}^{238}$ . It was, however, mixed with a large amount of  $\text{Np}^{239}$  formed by the reactions



The radiations of  $\text{Np}^{238}$  could be partially determined from the gross absorption curve by subtracting a normalized  $\text{Np}^{239}$  curve, but the accuracy of the results was not known with any certainty owing to the difficulty of such analysis. However, a hard  $\beta$  ray (1.0 mev) and a hard  $\gamma$  ray (1.1 mev) were found. The half life was determined to be  $2.0 \pm 0.1$  days.

An attempt was made to make some  $\text{Np}^{238}$  free of  $\text{Np}^{239}$  by neutron bombardment of  $\text{Np}^{237}$ . A sample of  $\text{Np}^{237}$  (as the oxide) was irradiated in the "thimble" at the center of the Chicago heavy-water pile. It was found that large amounts of  $\text{Np}^{238}$  were formed (as later reported by Seaborg<sup>4,5</sup>), and that very little purification was required. One oxidation-reduction lanthanum fluoride purification cycle<sup>1</sup> was found to be sufficient. Absorption and coincidence measurements were made on the  $\text{Np}^{238}$  activity in order to characterize its radiations and to make a rough determination of the decay scheme. To determine the  $\text{Pu}^{238}$  half life, the growth of  $\alpha$  activity was measured, and an attempt was made to count the absolute disintegration rate of the  $\text{Np}^{238}$ .

<sup>†</sup>Contribution from the Chemistry Division of the Metallurgical Laboratory, University of Chicago, now the Argonne National Laboratory.

Work done by Arthur H. Jaffey and Lawrence B. Magnusson and report written by Arthur H. Jaffey. Preliminary results have been reported in Metallurgical Project Reports CN-2767 (March 1945) and CF-2914 (Apr. 24, 1945).

activity. With the practically pure Np<sup>238</sup> in the neutron-bombarded Np<sup>237</sup>, it was possible to measure the radiations more accurately, as described below.

The results of the measurements may be summarized in the tentative decay scheme shown in Fig. 1. Because of the lack of a magnetic spectrograph for analyzing the  $\beta$  and  $\gamma$  spectrum, this decay scheme can only be taken as tentative, although the results of the absorption measurements do make it seem rather plausible.

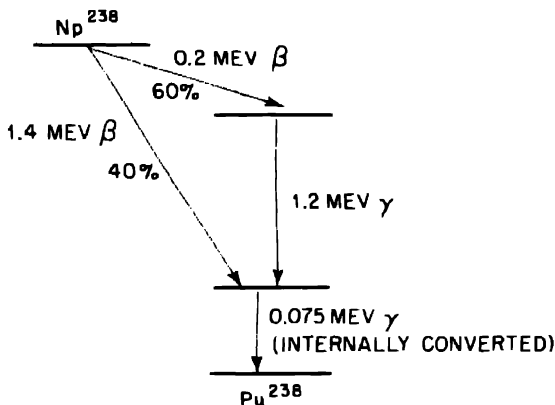


Fig. 1 — Decay scheme for Np<sup>238</sup>.

## 2. THE BETA RADIATIONS

It has been found that with the mica end-window Geiger-Mueller tube used in this laboratory,<sup>4,5,6</sup> an absorption curve does not start out with an initial straight-line slope (in a graph of log activity vs. absorber thickness) unless the sample is fairly close to the window and the absorbers are placed immediately below the window.<sup>7,8</sup> In order that a reasonably accurate straight-line extrapolation to zero absorber might be made, the Np<sup>238</sup> sample was placed as close as possible to the window, the limitation being the largest absorber used.

The samples were mounted on quartz to reduce back-scattering. Subsequent to the work described here, a detailed report on the magnitude of back-scattering was issued,<sup>9,10</sup> and it then became evident that the thick quartz used in the Np<sup>238</sup> experiments (essentially an "infinitely" thick back-scatterer) caused a relatively large amount of back-scattering.

Measurements have not yet been made with samples mounted on thin foils. The error due to uncertainties in the back-scattering cor-

rection constitutes one of the major sources of uncertainty in the  $\text{Pu}^{238}$  half-life evaluation.

Resolution-loss corrections were determined empirically by a split-sample technique, the method of least-squares calculation being that described by Kohman.<sup>11</sup>

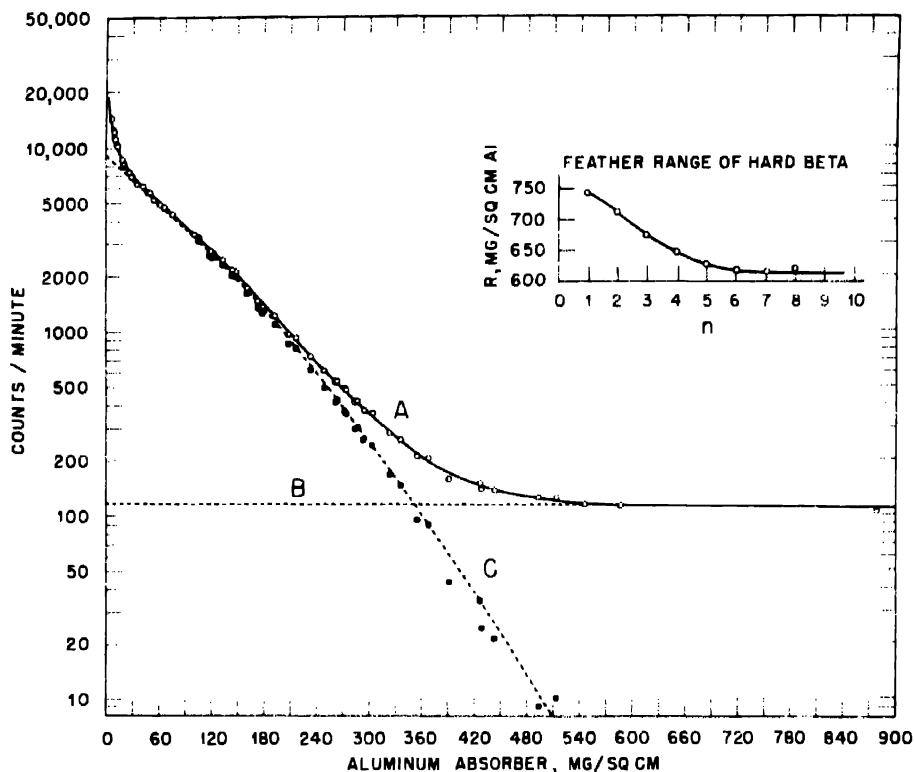


Fig. 2— $\text{Np}^{238}$   $\beta$  radiation. Absorption curve made on mica-window Geiger-Mueller tube (4.1 mg/sq cm window); sample on quartz, mounted 1.0 cm from window. A, complete absorption curve. B,  $\gamma$  ray. C, hard  $\beta$  ray.

Figure 2 shows an aluminum absorption curve for  $\text{Np}^{238}$ ; the values were taken with a standard mica-window counter,<sup>†</sup> the sample being mounted 1.0 cm from the window. An absorption curve of RaE was made under the same conditions, and the two curves were compared by Feather's method.<sup>12</sup>

<sup>†</sup>The circuit used involved a Neher-Harper quenching circuit and a scale-of-eight scaler made by the Cyclotron Specialties Co., Moraga, California.

Feather analysis of a number of curves gave an average value for the range of about 620 mg/sq cm of aluminum (the particular curve in Fig. 2 gave 613 mg/sq cm). From the revised range-energy relation<sup>13</sup>

$$E_{\max} = 1.85 R + 0.245 \quad (R > 0.3 \text{ g/sq cm}) \quad (2)$$

the value of  $E_{\max}$  is  $1.39 \pm 0.05$  mev.

The extrapolation to zero absorber (including air and window) shows this  $\beta$  ray to have a zero-absorber activity of 9,000 counts per minute. This value must be corrected for the x-ray count (see below), for back-scattering from the quartz, and for the electrons arising from conversion of the hard  $\gamma$  ray. As described in the appendix to this paper, the recalculated zero-absorber back-scattering correction on quartz is about 1.28. Corrected zero absorber count is then

$$\begin{array}{rcl} (\text{x ray}) & & (\text{electrons}) \\ \frac{(9,000 - 225)}{1.28} & - & 170 \\ & & = 6,660 \text{ counts/min} \end{array}$$

Figure 3 shows the beginning of the aluminum absorption curve in greater detail. In order to investigate the soft components more thoroughly, this part of the absorption curve was measured in a low-absorption Geiger-Mueller counter whose minimum absorption was 0.49 mg/sq cm.<sup>14</sup> It was inconvenient to attempt to determine resolution-loss corrections for the low-absorber counter, which was operated as a self-quenched Geiger-Mueller tube using argon and alcohol. Instead, the resolution-loss correction for a typical mica-window tube feeding into the same type of circuit was used. The correction amounted to about 0.5 per cent loss per 1,000 counts per minute.<sup>15</sup>

The "low-absorption" curve was normalized so that it matched the initial part of the absorption curve in Fig. 2 in the region in which they overlapped (5.4 to 29 mg/sq cm). The fit in the overlapping region was very good. The initial part of the absorption curve in Fig. 2 has therefore been replaced by the normalized low-absorption-counter curve and is shown in Fig. 3. The gamma and extrapolated hard  $\beta$  curves of Fig. 2 were subtracted to give the soft  $\beta$  components.

The analysis shows the following two components: (1) 12,000 zero-absorber (including air and window) counts of a 4.9 mg/sq cm aluminum half-thickness component; (2) approximately 25,000 zero-absorber counts of a 0.62 mg/sq cm aluminum half-thickness component.

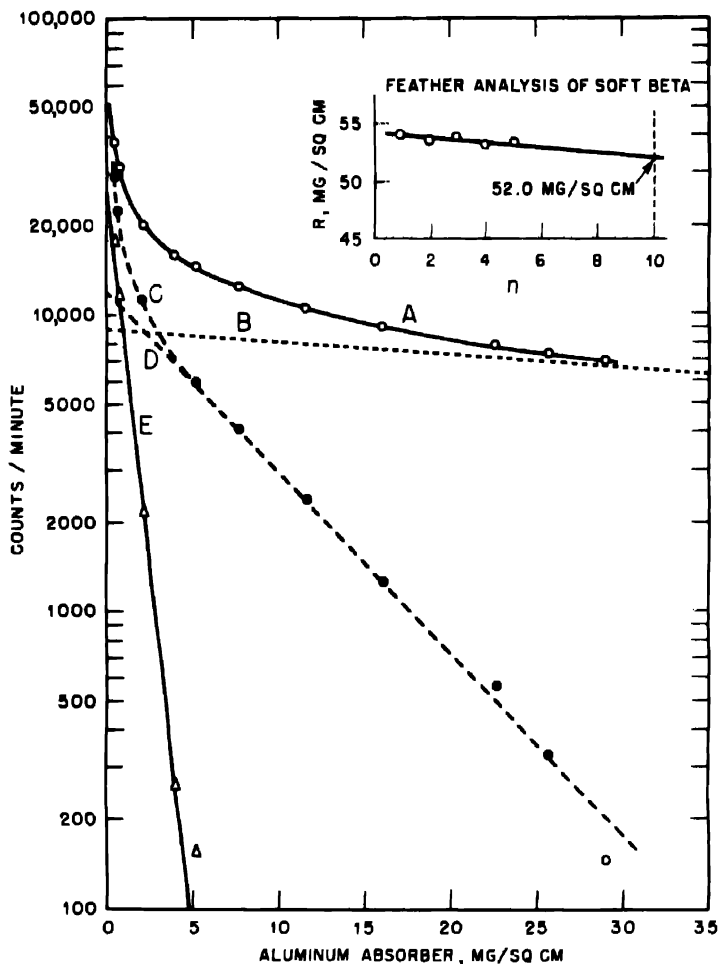


Fig. 3— $\text{Np}^{230}$  soft  $\beta$  rays. Sample on quartz, 1 cm from Geiger-Mueller tube window. A, normalized absorption curve determined in low-absorption counter. B, extrapolation of hard  $\beta$  curve ( $\gamma$  curve subtracted). C, residue curve after subtracting  $\gamma$  curve and curve B from curve A. D, extrapolation of straight part of curve C, half thickness = 4.9 mg/sq cm of aluminum. E, residue curve after subtracting curve D from curve C, half thickness = 0.62 mg/sq cm of aluminum.

The energy of the harder of the two components may be calculated in several ways. One method is to determine the range either by Feather's method<sup>12</sup> or by an empirical relation between initial half thickness (sample on first shelf) and range.<sup>16</sup> A Feather analysis gives a range of 52 mg/sq cm of aluminum. For this energy region the empirical ratio

$$\frac{\text{range}}{\text{initial half thickness}} = 10$$

Since  $T_{1/2} = 4.9 \text{ mg/sq cm}$ , the range is  $49 \text{ mg/sq cm}$ . From the revised range-energy relation<sup>13</sup> for low energies

$$E_{\max} = 1.92(R)^{0.725} \quad (0.02 \text{ g/sq cm} < R < 0.3 \text{ g/sq cm}) \quad (3)$$

the ranges  $52 \text{ mg/sq cm}$  and  $49 \text{ mg/sq cm}$  correspond to  $0.219$  and  $0.216 \text{ mev}$ , respectively.

An empirical correlation between initial half thickness and energy has been made by Sturm and Turkel,<sup>17</sup> giving the relation

$$E_{\max} = 8.30 T_{1/2}^{0.677} \quad (4)$$

This equation represents a least-squares fit for  $127 \beta$ -absorption curves. A degree of inaccuracy might be expected since the wide variety of experimental conditions under which the measurements were made resulted in a considerable scattering in the individual points. The initial half thickness is quite dependent on the relative positions of the sample, Geiger-Mueller tube, and absorbers, owing to scattering effects. From the value  $T_{1/2} = 0.0049 \text{ g/sq cm}$  of aluminum,  $E_{\max} = 0.226 \text{ mev}$ . The three methods seem to check fairly well, giving a value of  $0.22 \text{ mev}$ .

The zero-absorber count is corrected for "infinite" thickness back-scattering from quartz as described in the appendix. Since the x-ray and hard-conversion electrons have rather large half thicknesses (see below) they are primarily involved in the hard  $\beta$  absorption curve. No correction is necessary here. The zero-absorber count is then  $12,000/1.28 = 9,370$  counts per minute.

None of the above formulas have been checked for energies as low as that of the very soft component, but in the absence of better calibrations they will be used. Equation 4 gives  $0.055 \text{ mev}$ . Assuming the range is  $10 \times T_{1/2}$ , the value is  $6.2 \text{ mg/sq cm}$ . From the relation of Coryell and Glendenin,  $E_{\max} = 0.048 \text{ mev}$ . Using the range-energy data for homogeneous electrons<sup>18, 19, 20</sup> drawn in Coryell's  $\beta$  curve<sup>20</sup> as recommended by Coryell and Glendenin,<sup>13</sup>  $E_{\max} = 0.063 \text{ mev}$ . The energy may be assumed to lie between  $50$  and  $60 \text{ kev}$ .

The back-scattering correction has not been measured for such low energies, nor has it been measured for conversion electrons (which is the probable nature of the  $55\text{-kev}$  component). However, the recal-

culated value, 1.28 (appendix), is used to give  $25,000/1.28 = 19,500$  counts per minute at zero absorber.

### 3. GAMMA RADIATION

Figure 4 shows an absorption curve made with lead. The sample was mounted on the fourth shelf (5.0 cm from the window) and counted with a mica-window tube mounted in an upside-down position. The lead absorbers were placed just over the Geiger-Mueller tube window to minimize the effects of scattering. The Cyclotron Specialties Co. circuit was used with Neher-Harper quenching. Resolution corrections were determined by the split-pair technique.<sup>11</sup>

The half thickness was found to be 13.1 g/sq cm of lead. The energy was evaluated from the absorption coefficient-energy relation calculated by Heitler,<sup>21</sup> which was redrawn as a half thickness-energy relation by Coryell.<sup>20</sup> On this curve the 13.1 g/sq cm half thickness corresponds to 1.44 mev. It is quite evident that such a value for the  $\gamma$ -ray energy would not fit the decay scheme described above. There is, however, good reason to suspect that Heitler's relation may not be strictly applicable to the method of determining absorption curves described here. In calculating that portion of the absorption coefficient due to Compton scattering, Heitler assumed that a  $\gamma$  ray undergoing Compton scattering would be scattered out of the beam and would miss the detector. The  $\gamma$ -ray beam must be very sharply collimated<sup>22</sup> to fulfill this condition.

Since a large fraction of the Compton  $\gamma$  rays are scattered with a large forward component, the geometry used in this measurement allowed the counting of many of the Compton-scattered  $\gamma$  rays. This effect caused a slower dropping of measured activity with addition of absorbers than would occur in a collimated beam, resulting in a larger half thickness.

If it were possible to place a very large amount of lead between the sample and the Geiger-Mueller tube, the primary and secondary (Compton)  $\gamma$  rays would come to an equilibrium and the slope of the final part of the absorption curve would depend only upon the half thickness of the primary  $\gamma$  ray.<sup>23</sup> Because of limitations of sample activity, however, the sample was so close to the Geiger-Mueller tube as to make it difficult to use sufficient absorber to attain such equilibrium. Under the same conditions, absorption curves with aluminum and copper showed half thicknesses that were obviously much too high, giving energies well over 2 mev (from the half thickness-energy relation). For aluminum and copper larger amounts of absorber are necessary to attain primary-secondary equilibrium. Hence

absorption curves with these absorbers were even farther from equilibrium than was the lead absorption curve.

To check on the magnitude of this effect, experimental values of the half thicknesses of a number of fission products were compared with the spectrograph energies.<sup>24</sup>

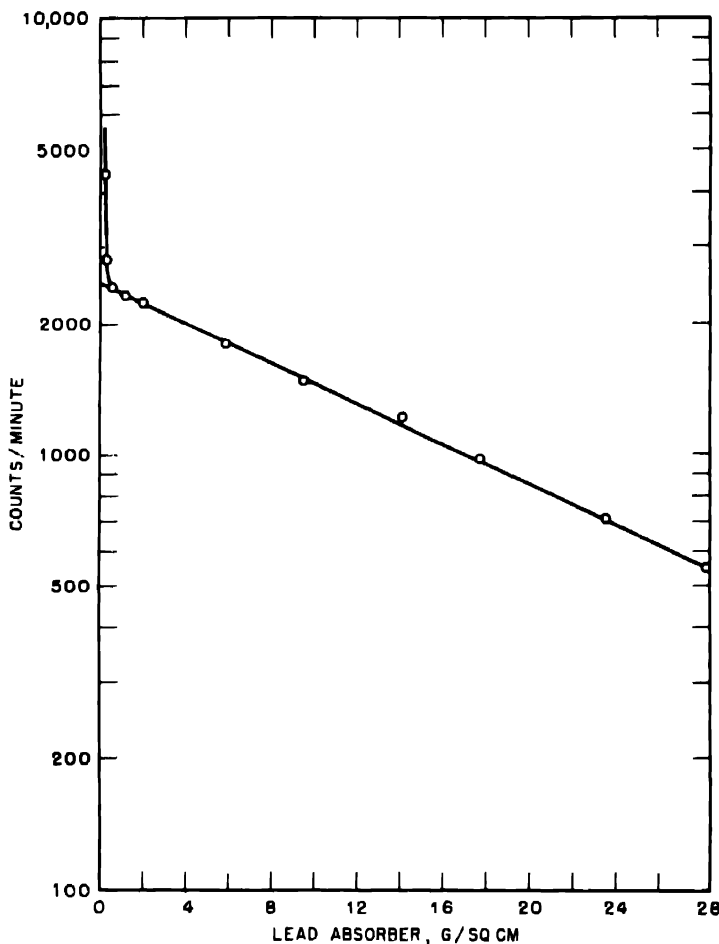


Fig. 4— $\text{Np}^{238}$   $\gamma$  ray. Sample on fourth shelf; absorbers placed just over window. Half thickness = 13.1 g/sq cm of lead.

The data are summarized in Table 1. Most of the  $\gamma$ -absorption curves taken in the Metallurgical and Clinton Laboratories and listed in this table were measured under conditions essentially the same as in the present experiment. The half thicknesses of all these absorp-

tion curves were translated into energy by means of Coryell's version of Heitler's curve.

The most interesting nuclear species,  $\text{La}^{140}$ , has a complicated  $\gamma$  spectrum. In order to make it possible to determine the magnitude of

Table 1—Energies of Some Fission Product Gamma Rays Determined by Both Spectrographic and Lead Absorption Methods

Isotope	Spectrograph energy, mev	Energy from lead absorption and Coryell's curve, mev
$\text{I}^{131}$	0.367	0.36
$\text{Zr}^{96}$	0.73	0.80
		0.88
$\text{La}^{140}$	0.335† (1.5%)	1.9 (83.9%)‡
	0.49† (6%)	0.36 (16.1%)‡
	0.85† (12%)	
	1.64† (75.5%)	0
	2.3† (5%)	

†These data are the average of the results of two slightly different spectrographic measurements.

‡These data are from the report by Metcalf et al.<sup>25</sup>

the discrepancy resulting from the Compton scattering, an "ideal" absorption curve for  $\text{La}^{140}$  was calculated in the following manner. The half thickness of each  $\gamma$  component found in the spectrograph measurement was determined from Coryell's curve. It was assumed that the counting efficiencies of each  $\gamma$  ray in the brass-shell counter lead-absorber system was proportional to the  $\gamma$  energy. This is known to be approximately true in the energy region considered.<sup>26</sup> The absorption curves were drawn and then added together. If the summary curve is carried out to 30 g/sq cm of lead (the maximum usually used in the absorption measurements), it may be very closely approximated by a straight line, the slope of which corresponds (on Coryell's curve) to 1.60 mev. Thus if Heitler's relation applied under these experimental conditions, the absorption curve would give an energy of 1.60 mev, whereas it actually gave 1.9 mev, a discrepancy of 0.3 mev.

There seems to be essentially no discrepancy at 0.36 mev, a 0.1-mev discrepancy at 0.7 mev and 0.3-mev discrepancy at 1.6 mev. It seems reasonable, therefore, to assume a discrepancy of between 0.2 and 0.25 mev for a  $\gamma$  ray whose nominal energy is 1.44 mev. It is assumed, therefore, that the energy of the  $\text{Np}^{238}$   $\gamma$  ray is 1.2 mev.

From Fig. 2 the zero-absorber  $\gamma$  count is 118 counts per minute. The corresponding soft  $\beta$  count (corrected for back-scattering) is

9,370 counts per minute. As will be shown later, the hard  $\gamma$  ray is 1.8 per cent converted. The ionization efficiency of the 1.2-mev  $\gamma$  ray is

$$\frac{118}{(9,370)(0.982)} = 0.0128 \text{ or } 1.3 \text{ per cent}$$

Ionization efficiency is defined as the ratio

$$\frac{\text{zero-absorber (extrapolated) counts due to the } \gamma \text{ ray}}{\text{zero-absorber (extrapolated) counts due to the } \beta \text{ ray}}$$

where the  $\beta$  ray is being emitted from the sample at the same rate as the  $\gamma$  ray.

Since the 118 counts per minute was evaluated by extrapolating the  $\gamma$  part of the aluminum absorption curve to zero absorber, the ionization probability of 1.3 per cent refers to the combined system of the brass-wall Geiger-Mueller tube window plus aluminum absorbers placed immediately in front of the tube window. The ionization probability is larger than that which would occur in the absence of the aluminum absorbers because of the counting of the Compton recoil electrons knocked out of the aluminum.

The value of 1.3 per cent holds, however, only when the amount of aluminum absorber exceeds the minimum required for equilibrium between the primary  $\gamma$  and the secondary (Compton) electrons as described by Rasetti.<sup>23</sup> This minimum value corresponds to the maximum range of the Compton electrons. An interesting example of this effect is found in the case of 35-day columbium, which has a very soft  $\beta$  ray (0.15 mev) and a hard  $\gamma$  ray (0.75 mev).<sup>24</sup> An aluminum absorption curve of 35-day columbium shows the typical decrease of  $\beta$  activity with the addition of absorbers, followed first by a small rise of activity (beyond the  $\beta$  range) up to a maximum value, and then a decrease, tapering into a straight-line  $\gamma$ -absorption curve.<sup>27</sup> The range of a 0.75-mev  $\beta$  ray is 280 mg/sq cm<sup>13</sup> whereas the tapering off into a constant slope occurs at about 275 mg/sq cm. This increase of counts due to a  $\gamma$  ray up to a maximum value is discussed by Rasetti; it is generally not observable in absorption curves determined in the standard manner because the effect, which is quite small, is usually hidden in the  $\beta$ -absorption curve. (Other examples of this effect are described by Meitner.<sup>28</sup>)

Since the energy of the hard  $\beta$  ray of Np<sup>238</sup> is greater than that of the hard  $\gamma$  ray, the absorption curve of the Compton electrons is buried in the  $\beta$ -absorption curve and hence is not observable. The effect is rather small at small absorber thicknesses and hence has little ef-

fect on the extrapolation of the  $\beta$  curves to zero absorber. Similarly, since the  $\gamma$  energy is less than the  $\beta$  energy, the  $\beta$ -range determination is not likely to have been appreciably affected.

#### 4. X RAYS

Figure 5 shows a lead absorption curve made with a standard mica-window argon-alcohol Geiger-Mueller tube with the sample mounted on the second shelf (19 mm from window). Immediately above the sample was placed a beryllium absorber, 1.9 g/sq cm in thickness, to stop the  $\beta$  rays with a minimum of Bremsstrahlung emission and a minimum of absorption of x rays. On subtracting the  $\gamma$  components, the residue shows a soft component of half thickness 9.9 mg/sq cm of lead. There is also a small residue of an even softer component, but not enough points were available to analyze it.

A half thickness of 9.9 mg/sq cm of lead corresponds to 12.8 or 22.3 kev,<sup>29</sup> since the half-thickness energy relation for lead is multi-valued in this region due to the lead L-absorption edges. The  $\gamma$  count of 212 counts per minute appears to be essentially equal to the activity of the 9.9 mg/sq cm x ray (210 counts per minute).

No evidence can be seen in the absorption curve for K x rays of plutonium, which should have energies between 100 and 124 kev<sup>31</sup> (lead half thicknesses of from 120 to 189 mg/sq cm), whereas the observed energy (12.8 or 22.3 kev) could correspond to the L x rays of plutonium, which range in energy from 14.1 to 21.4 kev.<sup>31</sup>

A more detailed picture of the x rays is obtained from the aluminum absorption curve (Fig. 6), which shows (after subtracting the  $\gamma$ -ray curve) two components of 130 and 32 mg/sq cm half thickness, corresponding to 17.5 and 10.4 kev, respectively.<sup>29</sup>

To check whether these radiations could correspond to the plutonium x rays, an ideal absorption curve was constructed for the plutonium L x rays. The energies of the more intense L lines were calculated by James by plotting the energies for elements 92 and below and extrapolating to element 94. The half thicknesses were taken from the absorption data of Compton and Allison. The relative intensities for the various lines were assumed to be the same as for uranium.<sup>30</sup> It is also assumed that the counting efficiencies for the various L components are the same. This is probably somewhat incorrect,<sup>32</sup> but is the simplest assumption to make.

Adding the absorption curves for the various components (14.3, 14.1, 18.2, 17.3, and 21.4 kev for the  $L\alpha_1$ ,  $L\alpha_2$ ,  $L\beta_1$ ,  $L\beta_2$ , and  $L\gamma_1$  components, respectively), the total absorption curve appeared as in

**Fig. 7.** This curve can be "analyzed" into two components, the exact analysis being somewhat arbitrary. Figure 7 shows two components, with half thicknesses of 118 and 41 mg/sq cm of aluminum,

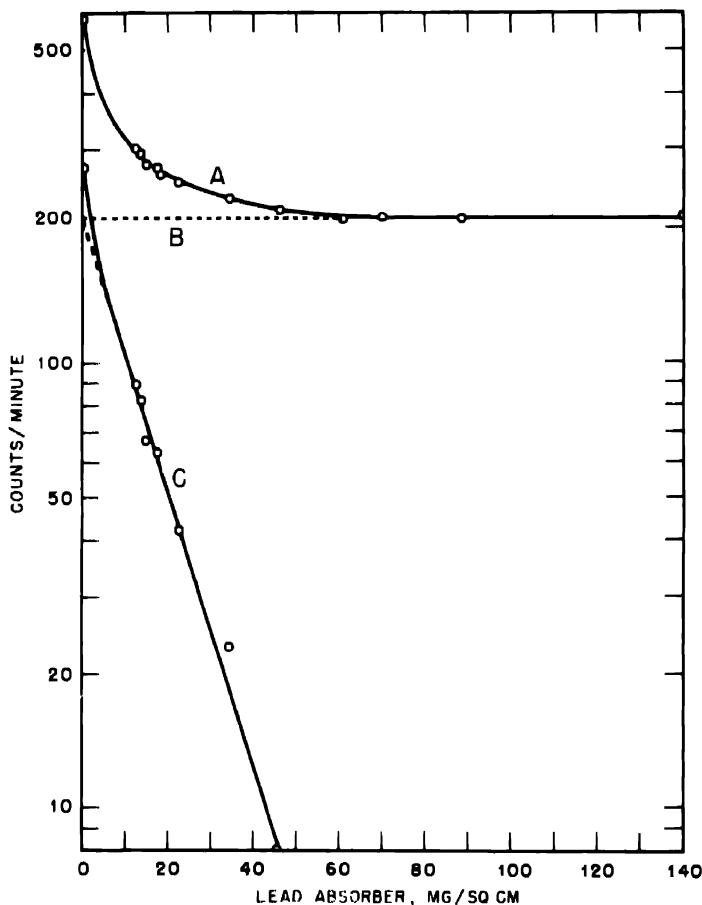


**Fig. 5—**X rays associated with Np<sup>238</sup> decay. Sample on quartz, 25 mm from mica window; 1.9 g/sq cm of beryllium over sample to remove  $\beta$  rays. A, lead-absorption curve. B, extrapolation of  $\gamma$  curve. C, x-ray curve (subtracting curve B from curve A); half thickness = 9.9 mg/sq cm of lead.

which correspond to 16.9 and 11.6 kev, respectively. It seems reasonable, therefore, to assume that the x rays found in this experiment were due to Pu<sup>239</sup>.

The x rays were also analyzed by lead and aluminum absorption measurements in which the  $\beta$  rays were bent out with a magnetic field

instead of being absorbed by beryllium. The energies measured were essentially the same as the measurements discussed above.

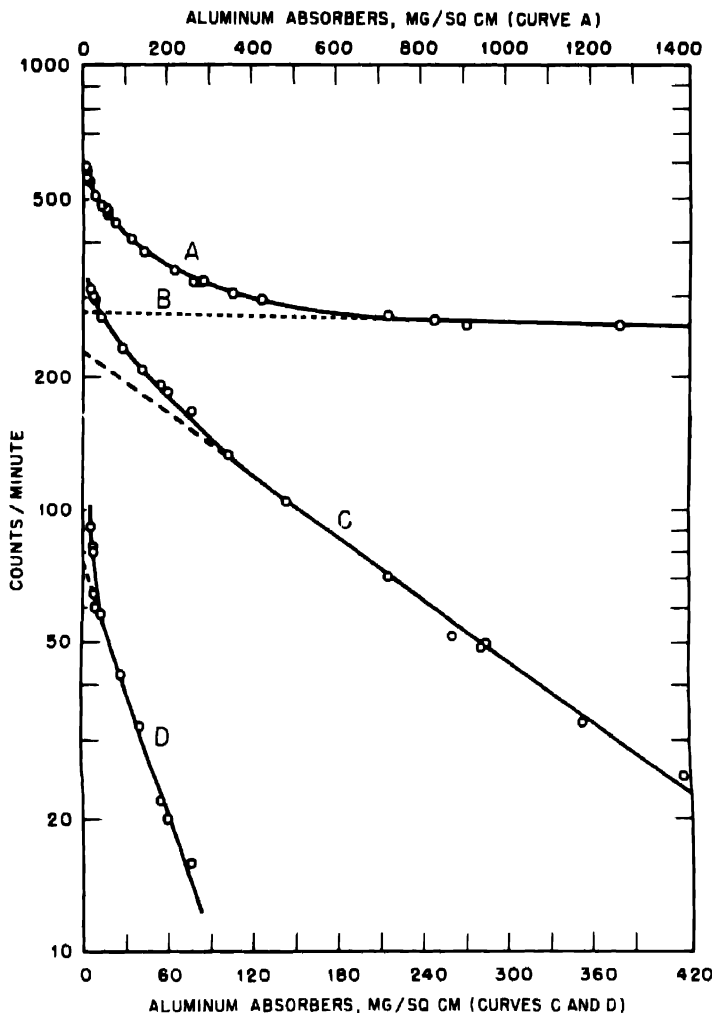


Fig. 6—X rays associated with  $\text{Np}^{238}$  decay. Sample on quartz, on second shelf (19 mm from window); 2.8 mg/sq cm window on Geiger-Mueller tube; 1.9 g/sq cm of beryllium over sample to remove  $\beta$  rays. A, aluminum absorption curve. B, extrapolation of  $\gamma$  curve. C, x-ray curve (after subtracting curve B from curve A), half thickness = 130 mg/sq cm of aluminum. D, softer x ray; half thickness = 32 mg/sq cm of aluminum.

As in the case of the lead absorption curve, there seems to be a small residue in the form of a very soft component for which the data are too scattered for accurate analysis. There is no evidence for

plutonium K x rays, which should have aluminum half thicknesses of from 4.07 to 4.63 g/sq cm.<sup>31</sup>

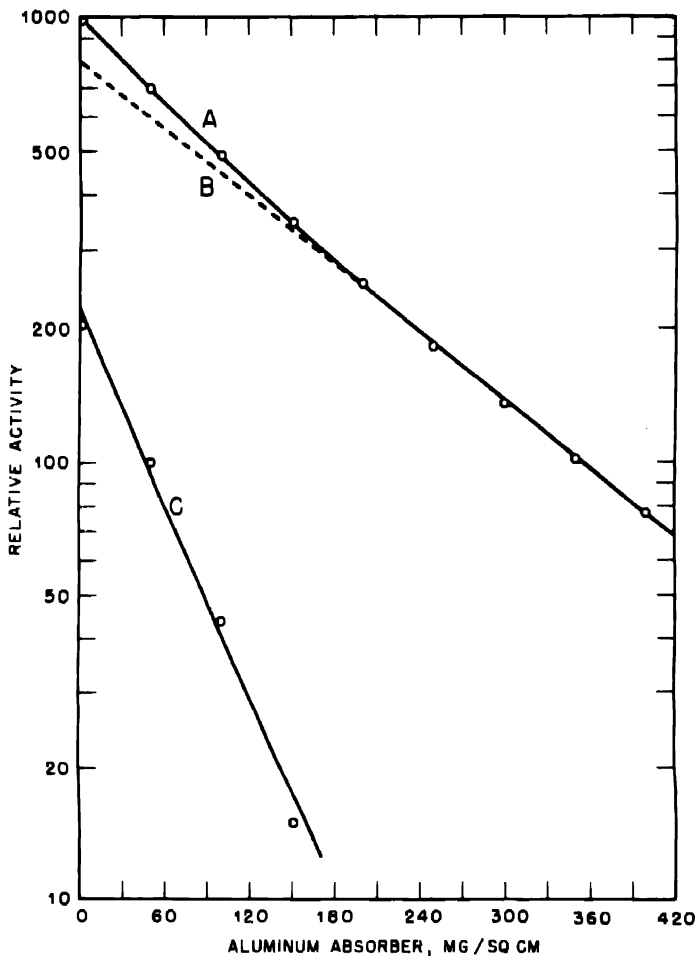


Fig. 7—Plutonium L x rays. A, theoretical curve constructed from absorption curves of most intense components of plutonium L spectrum, assuming counting efficiency of each component is the same. B, extrapolation of apparent hard component, half thickness = 118 mg/sq cm of aluminum. C, apparent soft component; half thickness = 41 mg/sq cm of aluminum.

The absorption curve shows that there are 302 counts per minute of the L x rays to 278 counts per minute of the  $\gamma$  ray. From the L x-ray energies and the absorption of beryllium for various energies<sup>29</sup> it can be shown that 1.9 g/sq cm of beryllium would cut the activity of the

*plutonium L x rays by 50 per cent (assuming the counting efficiencies of all the components to be the same). Thus, correcting for the beryllium absorption, the ratio of the L x-ray activity to  $\gamma$  activity is 604 to 278.*

From the decay scheme described above, the zero-absorber counts for hard  $\beta$  and soft  $\beta$  and the hard  $\gamma$  conversion factor, the following ratio is obtained (assuming complete L conversion of the soft  $\gamma$ )

$$\frac{\text{number of L x rays}}{\text{number of } \gamma \text{ rays}} = \frac{6,660 + 9,370}{(0.982)(9,370)} = 1.74 \quad (5)$$

From the previously calculated ionization efficiency of the Geiger-Mueller tube for this  $\gamma$  ray (1.3 per cent), it is evident that in the brass-wall argon-alcohol counter the average L x-ray ionization efficiency is

$$\frac{604}{278} \times 1.3\% = 2.8, \quad \frac{2.8}{1.74} = 1.6\%$$

Since the zero-absorber  $\gamma$  count is obtained by extrapolating the portion of the absorption curve beyond the range of the Compton electrons, the  $\gamma$ -ray efficiency applies to the same conditions as described above, i.e., the Geiger-Mueller tube window covered with sufficient aluminum absorber to provide saturation for the Compton electrons arising in the aluminum.

However, as pointed out by Meitner,<sup>28</sup> an absorber of low atomic number placed just over a  $\gamma$ -ray source can provide a fair number of Compton electrons, which enter the Geiger-Mueller tube. Since Compton scattering depends primarily upon the number of electrons per sq cm, beryllium is about as effective in this respect as aluminum (i.e., for a  $\gamma$  ray of about 1.2 mev). Some of the "x-ray counts," including the residual unidentified soft component, may be due to Compton electrons from  $\gamma$ -scattering in the beryllium absorber. If this were true the measured x-ray activity would be too large, and hence the x-ray efficiency would be less than 1.6 per cent. The effect, however, seems not to be very important, since coincidence measurements (discussed below) indicate the x-ray ionization efficiency to be higher than 1.6 per cent. The L x-ray efficiency is independent of the absorbers over the window, since the photoelectrons liberated in the absorption process have ranges less than the mica-window thickness.

### 5. COINCIDENCE MEASUREMENTS

Several coincidence measurements were carried out, using two standard mica-window Geiger-Mueller tubes and a coincidence circuit built by Bradley and Epstein.<sup>33</sup> As used in these measurements,

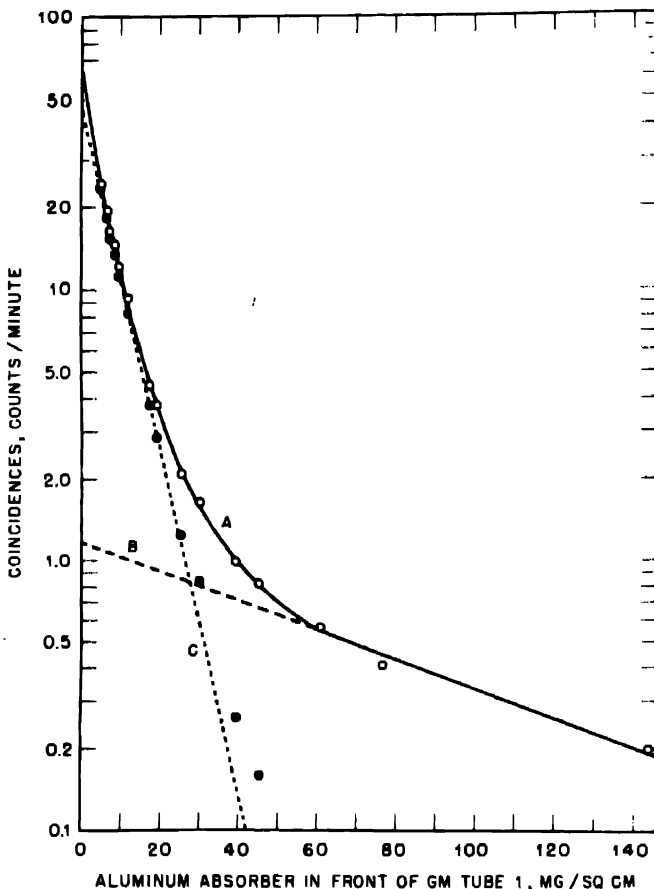


Fig. 8— $\text{Np}^{238}$   $\beta$ - $\gamma$  coincidences. Geiger-Mueller counter No. 2 covered with 1.267 g/sq cm of aluminum (only  $\gamma$  rays counted). Absorption curve determined with absorbers over Geiger-Mueller counter No. 1. A, complete curve. B, hard component coincident with  $\gamma$  ray, probably L  $\times$  ray, half thickness = 55 mg/sq cm. C, 0.2-mev  $\beta$  ray coincident with  $\gamma$  ray, half thickness = 5.0 mg/sq cm.

the circuit had a time constant (empirically determined),  $\tau = 1.0 \times 10^{-6}$  sec.

The first measurement involved an attempt to look for  $\beta$ - $\gamma$  coincidences. The two Geiger-Mueller tubes were placed with their axes

coinciding and mica windows facing each other. The sample (mounted on thin mica) was placed halfway between the two Geiger-Mueller tubes, with the face of the sample facing tube 1. Between the back of the sample and tube 2 was placed an aluminum absorber (1,267 mg/sq cm) that was sufficient to cut out the hard  $\beta$  rays and all the L x rays. The coincidence counting rate was corrected for chance coincidences<sup>34</sup> and for the cosmic-ray background. The coincidence rate was measured as a function of the absorber thickness in front of tube 1 as shown in Fig. 8.

The absorption curve was analyzed into two components (analysis described below in Eqs. 6 to 10). The half thickness of the major component is 5.0 mg/sq cm, in good agreement with the absorption curve in Fig. 3. This confirms the hypothesis shown in Fig. 1, namely, that the hard  $\gamma$  ray is in coincidence with the soft  $\beta$  ray.

The tail of the coincidence curve is apparently an L x ray coincident with the hard  $\gamma$  ray. To analyze the absorption curve the following assumptions were made about the decay scheme: (1) the hard  $\gamma$  ray is at most only slightly converted, and (2) the soft  $\gamma$  ray is completely converted.

This is made reasonable by the presence of the large number of very soft electrons and the apparent absence of any quantum radiation in the neighborhood of 75 kev.

Thus, according to these assumptions, each hard  $\gamma$  ray is coincident with a soft  $\beta$  ray ( $E_{\max} = 0.2$  mev), a very soft electron (which is completely cut out by the minimum absorber of mica window and air), and an L x ray. There may also be a few conversion electrons of about 1.1 mev energy coincident with the soft  $\beta$  ray and L x ray, but the measurement of Fig. 8 only measures the  $\gamma$ -ray coincidences.

Let  $A_{\beta\gamma}$  = measured coincidence rate, counts per minute

$A_\gamma$  = measured  $\gamma$ -counting rate in tube 2

$N$  = rate of a given event, e.g.,  $N_s$  = number of soft  $\beta$  rays emitted per min

$s$  = soft  $\beta$  ray

$h$  = hard  $\beta$  ray

$x_1$  = x ray coincident with soft  $\beta$  ray (and  $\gamma$  ray)

$x_2$  = x ray coincident with hard  $\beta$  ray

$c$  = internal conversion electrons of hard  $\gamma$  ray

$\gamma$  = hard  $\gamma$  ray

$f$  = internal conversion factor for the hard  $\gamma$  ray

$W$  = mg/sq cm of absorber over tube 1 (including window and air)

$E_i$  = Geiger-Mueller tube efficiency for particular radiation

$\lambda_i$  = mass-absorption coefficient for particular radiation

$G_i$  = geometry for particular radiation

$I_i$  = ionization efficiency for particular radiation (enough to cause count in Geiger-Mueller tube) (see Eq. 13)

It is assumed that the back-scattering effect was not important. At  $W = 0$  (zero-absorber extrapolation),

$$\begin{aligned} (A_{\beta\gamma})_{W=0} &= N_\gamma E_\gamma E_s (1 - E_x) + N_\gamma E_\gamma E_x (1 - E_s) + N_\gamma E_\gamma E_x E_s \\ &= N_\gamma E_\gamma (E_s + E_x - E_s E_x) \quad (6) \end{aligned}$$

since only one coincidence is registered if both an x ray and a soft  $\beta$  ray from the same disintegration ionize in tube 1. The first term represents  $\beta$ - $\gamma$  coincidences; the second term, x- $\gamma$  coincidences; and the third term, (x- $\beta$ ) - $\gamma$  coincidences.

For any  $W$  (for the region in which the  $\beta$  ray is absorbed exponentially)

$$A_{\beta\gamma} = N_\gamma E_\gamma [E_s e^{-\lambda_s W} + E_x e^{-\lambda_x W} - E_x E_s e^{-(\lambda_s + \lambda_x)W}] \quad (7)$$

Since  $\lambda_s \gg \lambda_x$ , for  $W$  large (i.e., at the tail of the curve)

$$_x(A_{\beta\gamma}) = N_\gamma E_\gamma E_x e^{-\lambda_x W} \quad (8)$$

Hence, extrapolation of the tail of the curve to zero absorber gives

$$_x(A_{\beta\gamma})_{W=0} = P_1 = N_\gamma E_\gamma E_x = 1.18 \text{ counts per minute} \quad (9)$$

From Eqs. 6 and 9

$$(A_{\beta\gamma})_{W=0} - P_1 = P_2 = N_\gamma E_\gamma [E_s - E_s E_x] = 47.5 \text{ counts per minute} \quad (10)$$

Dividing Eq. 9 by Eq. 10

$$\frac{P_1}{P_2} = \frac{E_x}{E_s (1 - E_x)} \quad (11)$$

Since  $E_s = 0.175$  (experimental measurement of geometry by use of a standard)

$$\frac{E_x}{E_s} = 0.0247 \quad (12)$$

$I_i$  is defined by the equation

$$G_i I_i = E_i \quad (13)$$

It is assumed that the geometries for x-ray counting and  $\beta$  counting are the same in the mica-window counter, and that  $I_s = 1$ . Hence,

$$\frac{E_x}{E_s} = I_x \quad (14)$$

and

$$I_x = 0.0247 \quad (12a)$$

From this measurement it would seem that the average ionization probability for plutonium L x rays is about 2.5 per cent. In the previous section this value was calculated as 1.6 per cent. However, it should be noted that if it were assumed that the soft  $\gamma$  rays were coincident only with the soft  $\beta$  rays and that the hard  $\beta$  rays decayed directly to the ground state, then the number of x rays assumed would be smaller, and the 1.6 per cent value would be corrected to 2.8 per cent. However, it would then be very difficult to explain the number of very soft electrons found in the low-absorber counter. It seems preferable to assume the decay scheme shown in Fig. 1 and to ascribe the difference between 1.6 per cent and 2.5 per cent to experimental error. This explanation seems plausible since another method of calculating  $I_x$  gives still another value.

In tube 2, assuming practically no absorption of the  $\gamma$  rays in 1,260 g/sq cm of aluminum

$$A_\gamma = N_\gamma E_\gamma \quad (15)$$

Dividing Eq. 9 by Eq. 15

$$\frac{P_1}{A_\gamma} = E_x = \frac{1.18}{344} = 0.00344 \quad (16)$$

From Eqs. 14 and 16 and the measured value of  $G_s$  (using a standard sample) of 17.5 per cent,

$$I_x = \frac{0.00344}{0.175} = 2.0 \text{ per cent} \quad (17)$$

The average of the three values for  $I_x$  (1.6, 2.5, and 2.0 per cent) is 2.0 per cent.

Another coincidence measurement was made in order to determine the internal conversion factor of the hard  $\gamma$  ray. The two mica-

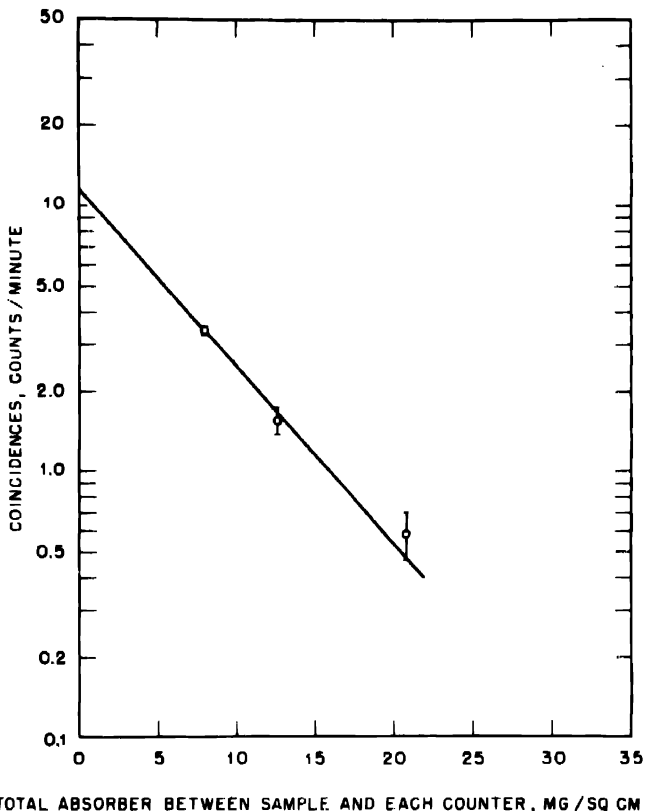


Fig. 9— $\text{Np}^{238}$   $\beta$ -e coincidences. Two Geiger-Mueller tubes with axes at right angles. Axes intersect at sample. Tubes symmetrical relative to sample. Absorbers placed over both tubes symmetrically. Half thickness = 4.5 mg/sq cm of aluminum.

window tubes were arranged with their axes at right angles but in the same plane. The sample was placed at the intersection of the two axes, facing both windows at an angle of 45 deg. The relation between the sample and each of the two tubes was completely symmetrical. Between the two tubes was placed a shield to prevent direct scattering of electrons from one tube to the other. The coincidence background due to multiple scattering was determined by using a RaE sample, which has no conversion electrons. The coincident rate was also corrected for cosmic-ray background.

An absorption curve was taken with equal absorbers in front of each tube. Figure 9 shows the coincidence rate as a function of absorber thickness.

The same notation is used as above, with the addition that  $(A_{\beta e})_{W=0}$  is the zero-absorber (extrapolated) coincidence rate. The coincidences result from three groups of disintegrations: those arising from  $fN_s$  events per minute giving double or triple coincidences between s, c, and x, those arising from  $(1-f)N_s$  events per minute giving rise to double or triple coincidences between s,  $\gamma$ , and x, and those arising from  $N_h$  events per minute giving rise to coincidences between h and x

$$(A_{\beta e})_{W=0} = 2fN_s [E_c E_x (1 - 2E_x) + E_x E_s (1 - 2E_s) + E_c E_s (1 - 2E_x) + 3E_x E_c E_s] + 2(1-f)N_s [E_\gamma E_x (1 - 2E_x) + E_x E_s (1 - 2E_\gamma) + E_\gamma E_s (1 - 2E_x) + 3E_x E_\gamma E_s] + 2N_h E_h E_x \quad (18)$$

The first three terms in each of the two brackets represent the double coincidences only, while the last term in each bracket represents the triple coincidences occurring when two ionizing "particles" enter one tube while one enters the other tube. The factor of 2 arises because either tube can record with equal efficiency any of the radiations.

$$(A_{\beta e})_{W=0} = P_3 = 2N_s [(E_x E_\gamma + E_x E_s + E_s E_\gamma - 3E_x E_\gamma E_s) + f(E_c E_x - E_x E_\gamma + E_c E_s - E_s E_\gamma - 3E_c E_x E_s + 3E_x E_\gamma E_s)] + 2N_h E_h E_x \quad (18a)$$

At zero absorber, the efficiencies of all the  $\beta$  rays may be considered approximately equal, and from the assumed decay scheme

$$N_h = N_{x_2}, \quad N_s = N_{x_1} = N_\gamma + N_c, \quad M = \frac{N_h}{N_s} = \frac{6,660}{9,370} = 0.711, \quad E_s = E_h = E_c \quad (19)$$

$$E_x = E_s I_x, \quad E_\gamma = E_s I_\gamma \quad (20)$$

From Eqs. 18a, 19, and 20

$$P_3 = 2N_s E_s^2 [(I_x I_\gamma + I_x + I_\gamma - 3E_s I_x I_\gamma + MI_x) + f(I_x - I_x I_\gamma + I_\gamma - 3E_s I_x + 3E_s I_x I_\gamma)] \quad (21)$$

$E_s$  was determined by first counting the sample in a counter whose geometry had been standardized with a geometry standard and then determining  $A_\beta$  in the coincidence set up. Both counts were corrected to zero absorber. The result was  $E_s = 0.0464$ . Using the value  $I_x = 0.02$  and  $I_y = 0.013$

$$P_3 = 2N_s E_s^2 (A + Bf) \quad (21a)$$

where  $A = 0.047$  and  $B = 1.004$ .

Now the total counts (extrapolated to zero absorber) in one of the Geiger-Mueller tubes is the sum of the counts due to each type of radiation

$$(A_\beta)_{W=0} = N_s E_s + N_{x_1} E_x + N_c E_c + N_h E_h + N_y E_y + N_{x_2} E_x \quad (22)$$

From Eqs. 19, 20, and 22

$$(A_\beta)_{W=0} = P_4 = N_s E_s (C_1 + C_2 f) \quad (23)$$

where  $C_1 = 1.74$  and  $C_2 = 0.98$ .

From Eqs. 21a and 23

$$f = \frac{2AE_s - C_1 \frac{P_3}{P_4}}{C_2 \frac{P_3}{P_4} - 2BE_s} \quad (24)$$

Using the observed values,  $P_3 = 11.5$  counts per minute and  $P_4 = 3,360$  counts per minute,  $f = 0.018$  or 1.8 per cent conversion. Because of the possibility of fairly large errors in the values of  $I_x$  and  $I_y$ , the value of  $f$  may be considerably in error.

## 6. THE DISINTEGRATION SCHEME OF Np<sup>238</sup>

Because most of the measurements have been made by absorption methods the results are not very accurate. It seems very likely, however, that Np<sup>238</sup> decays in the two following ways:

1. By a soft  $\beta$  ray of about 0.2 mev followed by a hard  $\gamma$  ray of about 1.2 mev, which is slightly converted. The hard  $\gamma$  ray is followed by a soft  $\gamma$  ray (about 75 kev), which is highly converted.
2. By a hard  $\beta$  ray (about 1.4 mev) which is followed by the same highly converted soft  $\gamma$  ray.

The energies of the  $\beta$  rays seem to be known with reasonable certainty, within 10 per cent for the hard  $\beta$  ray and 25 per cent for the

soft  $\beta$  ray. The effect of back-scattering on the slope of the soft  $\beta$  ray absorption curve<sup>7</sup> may have caused the measured value of the maximum energy of the soft  $\beta$  ray to be too low. The value of the energy of the hard  $\gamma$  ray is somewhat in doubt owing to the necessity for calibrating the apparatus for determining absorption curves. The identification of the radiation that passed unbent through a magnetic field and largely unabsorbed through beryllium as plutonium x rays seems quite reasonable in view of the similarity of the observed absorption curve to the ideal constructed curve.

The energy of the soft  $\gamma$  ray should be the sum of the conversion electron energies and the energies of the plutonium L-absorption edges. If an approximate value of 20 kev is used for the L binding energy, the soft  $\gamma$ -ray energy is about 75 kev.

The values of the internal conversion coefficients† measured in this experiment are considerably larger than would be expected if the  $\gamma$  rays were either dipole or quadripole radiation. The theoretical coefficient for a 1.2-mev line in element 94 is 0.003 for dipole radiation and 0.008 for quadripole,<sup>35</sup> whereas the measured value is 0.018. If this measurement is correct, the radiation may be partially magnetic-dipole (or multipole) since it has been shown that the conversion coefficient of magnetic dipole or magnetic multipole radiation is much higher than for the electrical case.<sup>36</sup> However, because of the crudeness of this measurement, the possibility of pure quadripole radiation is not excluded.

The fact that the number of very soft electrons is roughly equal to the total number of disintegration  $\beta$  rays and the fact that no evidence for a 75-kev  $\gamma$  ray was found indicates that the soft  $\gamma$  ray was very highly converted. According to Fisk's theoretical calculation,<sup>37</sup> the internal (L-shell) conversion coefficient for this energy at  $Z = 84$  is 0.5 for dipole radiation. It should not be a great deal different for  $Z = 94$ . In order to be as high as 0.9 or 1.0, the radiation would have to be partially magnetic-dipole or multipole.

If the conversion is not practically complete, the number of L x rays is less than the number of  $\beta$  rays, and the value of the x-ray-ionization efficiency in the argon-alcohol counter as calculated from the measurements will be greater than 2 per cent. This value is higher than the values calculated by Scott,<sup>32</sup> based upon the photoelectric absorption in argon, and still higher efficiencies would be even more difficult to explain.

†The internal conversion coefficient for a particular  $\gamma$  ray (often represented by  $\alpha$ ) is  $C/(C + \gamma)$ , where  $C$  = number of conversion electrons and  $\gamma$  = number of unconverted quanta.

The evaluation of the relative numbers of electrons of each type corresponding to a measured activity could not be made accurately, primarily because of the difficulties introduced by back-scattering from the quartz sample plates. As discussed in the appendix to this paper, the recalculation of the correction for soft  $\beta$  rays is based upon fragmentary data and unproved assumptions and may be considerably in error. In addition, since the corrections are rather large, errors in the experimental measurement of back-scattering would result in a considerable error in this experiment. However, using the corrected values, the soft  $\beta$  ray represents 60 per cent of the disintegrations and the hard  $\beta$  ray 40 per cent.

Table 2 — Relative Counting Rates of the Various Radiations at Zero Absorber

Radiation	Relative no. of counts
Soft $\beta$ rays	100
Hard $\beta$ rays	68
Soft conversion electron	208
Hard conversion electron	1.8
X rays†	2.7
Hard $\gamma$ rays‡	1.3

†This is taken from the aluminum absorption curve of the sample covered with beryllium. It corresponds to an x-ray-ionization efficiency of 1.6 per cent (provided the soft  $\gamma$  ray is coincident with both  $\beta$  rays and is completely converted).

‡Aluminum ( $> 500$  mg/sq cm) over the Geiger-Mueller tube window.

The zero-absorber (extrapolated) count (from an aluminum absorption curve), corrected for back-scattering, corresponds to the components given in Table 2. The number of soft conversion electrons seems to be too large by about 25 per cent. This difference may possibly be ascribed to experimental error because of the difficulties in extrapolating such a soft component to zero absorber and in correcting for back-scattering.

#### 7. THE HALF LIFE OF Np<sup>238</sup>

Figure 10 shows a decay curve for Np<sup>238</sup>. The counting rates have been corrected for resolution losses and background. The earliest

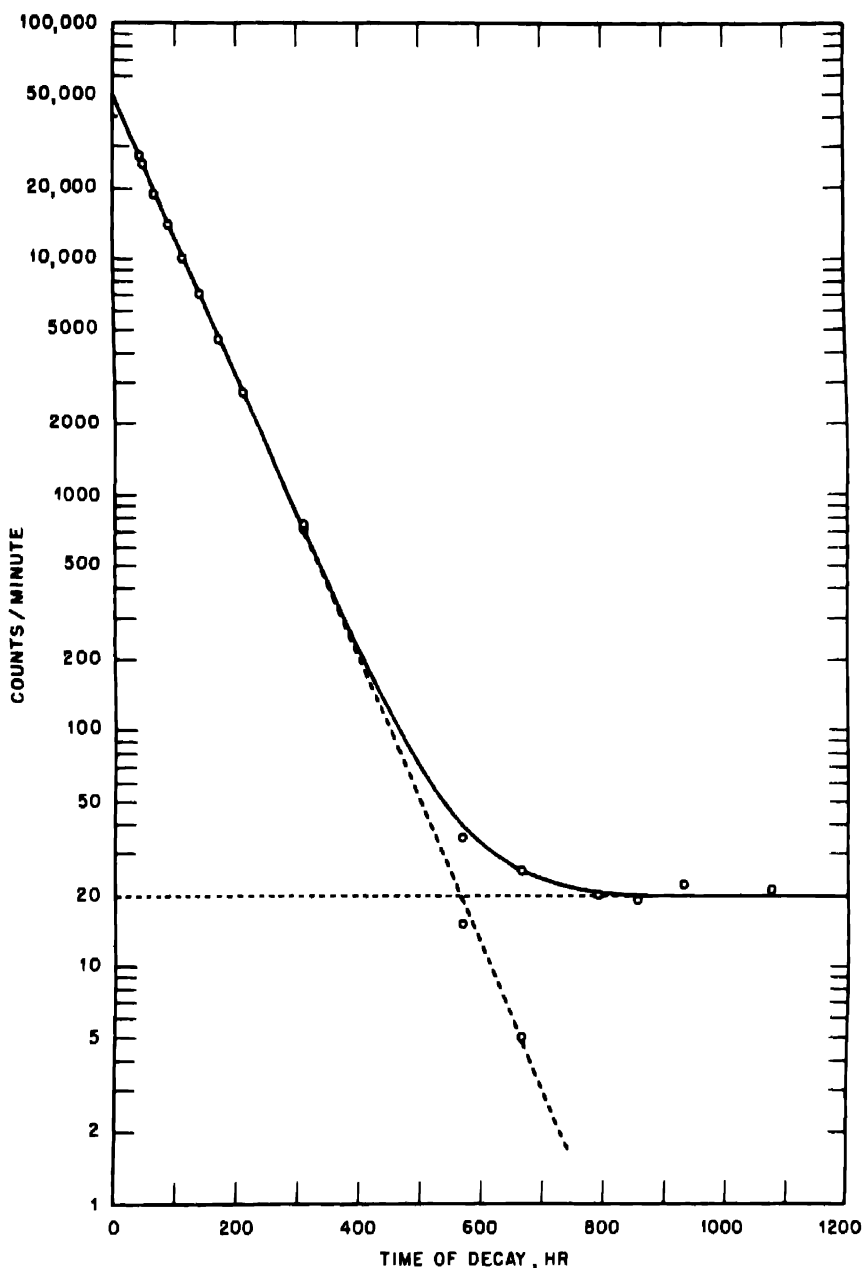


Fig. 10—Np<sup>234</sup> decay. Half life, 50.3 hr.

points were counted at a lower geometry (second shelf position) and corrected to first-shelf geometry by making several determinations of the ratio of first-shelf to second-shelf counting rates at later times. Averaging results from a number of samples, the half life appeared to be  $2.10 \pm 0.03$  days. This value has been used throughout the experiment.

#### 8. THE HALF LIFE OF Pu<sup>239</sup> FROM ABSOLUTE COUNTING RATES OF Np<sup>239</sup> AND Pu<sup>239</sup>

The measured quantities were (1) the  $\beta$  activity of samples measured at known (calibrated) geometries at known times after the bombardment, and (2) the growth of  $\alpha$  activity in larger samples (of known size ratio to the  $\beta$  samples).

The  $\beta$  activity was corrected for (1) extrapolation to zero absorber, (2) counts due to the  $\gamma$  rays,  $x$  rays, and the hard conversion electrons, (3) back-scattering, (4) geometry of  $\beta$  counter, and (5) decay since the end of the bombardment. These corrections yield the Np<sup>239</sup>  $\beta$  activity (disintegrations per minute) at the end of the bombardment.

The extrapolation to zero absorber was made by using the equation

$$\frac{A_w}{A_{w=0}} = \frac{12,000 e^{-0.693W/4.8} + 9,000 e^{-0.693W/68.5} + 118}{21,118} \quad (26)$$

where  $W$  = mica-window thickness + air absorption (mg/sq cm) and  $A$  =  $\beta$  activity. Counts due to the  $\gamma$  rays,  $x$  rays, and the hard conversion electrons were corrected for by means of the data in Table 2. It was not necessary to correct for the soft conversion electrons, since they were practically completely absorbed in the mica window and air above the sample. The back-scattering correction was based upon the use of the factor 1.28 derived in the appendix to this paper and used in Sec. 2.

The geometry was calibrated by the use of two secondary UX standards, No. 16 and No. 11, loaned by D. W. Engelkemeir. These were made of uranium oxide and had been calibrated against a practically weightless sample of UX<sub>1</sub>, precipitated from a known amount of old uranium and mounted on very thin mica to reduce back-scattering.<sup>8,38</sup> Using standard No. 16, the first-shelf geometry was determined to be 24.7 per cent; from No. 11, it was found to be 24.2 per cent, with an average of 24.5 per cent.

The growth of  $\alpha$  activity in several large samples of the bombarded  $\text{Np}^{237}$  was measured in a fast gas counter,<sup>39</sup> whose excellent discrimination against  $\beta$  radiation was required because of the large amount of  $\text{Np}^{238}$  present in each sample.

Let  $A_1 = \text{Np}^{237} \alpha$  activity

$A_2 = \text{Pu}^{238} \alpha$  activity formed since  $t = 0$  ( $t = 0$  at end of bombardment)

$(A_2)_{\infty} = A_2$  at  $t = \infty$

$A_3 = \text{Pu}^{238} \alpha$  activity formed during the bombardment

$A = \text{measured } \alpha \text{ activity}$

$A_{\infty} = A$  at  $t = \infty$

$\lambda = \text{decay constant of } \text{Np}^{238}$

$t = \text{time since the end of bombardment, then}$

$$A = A_1 + A_2 + A_3 = A_1 + A_3 + (A_2)_{\infty} (1 - e^{-\lambda t}) = A_{\infty} - (A_2)_{\infty} e^{-\lambda t} \quad (27)$$

$$(A_2)_{\infty} = \frac{A_{\infty} - A}{e^{-\lambda t}} \quad (27a)$$

Since  $A$ ,  $A_{\infty}$ , and  $t$  are measured,  $(A_2)_{\infty}$  can be determined from the growth curve.  $(A_2)_{\infty}$  represents the  $\text{Pu}^{238}$  grown from the decay of the  $\text{Np}^{238}$  present at the end of the bombardment.

The relative sizes of the samples used for  $\beta$  measurements and for the  $\text{Pu}^{238}$  growth measurements were determined by careful aliquoting. By use of the values of  $(A_2)_{\infty}$  calculated from equation (27a) and the value of  $A'_{38}$ , where  $A'_{38} = \text{measured disintegration rate of } \text{Np}^{238}$  at bombardment end, it is possible to calculate the half life of  $\text{Pu}^{238}$ .

$$Y = \frac{(\text{dis}/\text{min of } \text{Np}^{238})_{t=0}}{(\text{dis}/\text{min of } \text{Pu}^{238})_{t=\infty}} = \frac{\lambda_{38} N_{38}}{\lambda_{48} N_{48}} \quad (30)$$

where  $N_{48}$  = number of  $\text{Pu}^{238}$  atoms grown from the  $\text{Np}^{238}$  present at the end of the bombardment,  $\lambda_{38} = \lambda$  of  $\text{Np}^{238}$  and  $\lambda_{48} = \lambda$  of  $\text{Pu}^{238}$  and  $A'_{38}$  = numerator of  $Y$ .

The previously measured  $\text{Pu}^{238} \alpha$  activity,  $(A_2)_{\infty}$  of Eq. 27a, was corrected for the  $2\pi$  geometry and the 1.2%  $\alpha$  back-scattering by

dividing by 0.506.<sup>†</sup> The values for Y in two different determinations were  $1.36 \times 10^4$  and  $1.33 \times 10^4$ .

Since  $N_{38} = N_{48}$ ,

$$(T_{1/2})_{48} = Y(T_{1/2})_{38} = 2.82 \times 10^4 \text{ days} = 77 \text{ years} \quad (30a)$$

The half life of Pu<sup>238</sup> has been independently determined by two different methods. One involved the direct measurement<sup>41</sup> of the decay of Pu<sup>238</sup> formed by U<sup>238</sup>(d,2n)Np<sup>238</sup>  $\xrightarrow{\beta^-}$  Pu<sup>238</sup>. Correcting for the Pu<sup>238</sup> (half life = 2.7 years)<sup>42</sup> formed by U<sup>238</sup>(d,4n)Np<sup>238</sup>  $\xrightarrow{\beta^-}$  Pu<sup>238</sup>, and by U<sup>238</sup>(d,n)Np<sup>238</sup>, the half life of Pu<sup>238</sup> was measured as  $89 \pm 9$  years.

An alternate method was the measurement of the growth of Pu<sup>238</sup> from a known amount of Cm<sup>242</sup> (half life =  $5.0 \pm 0.5$  months).<sup>43</sup> This method gave a value of  $92 \pm 2$  years for the Pu<sup>238</sup> half life.<sup>42,44</sup> These experiments indicate that the Pu<sup>238</sup> half life is probably close to ninety years.

If either of these values is correct, then the experimental value for Y (Eq. 30) must be too small. It is most likely that the error would lie in the value of A'<sub>38</sub> because of the large number of corrections involved in determining the  $\beta$  disintegration rate. It is, of course, possible that the source of the discrepancy lies in an error in the determination of (A<sub>2</sub>) <sub>$\infty$</sub> , but this interpretation is less likely.

## APPENDIX

### BACK-SCATTERING CORRECTION AT ZERO ABSORBER

The only quantitative data for back-scattering from samples used in the standard mica-window Geiger-Mueller tube arrangement has been determined<sup>9,10</sup> by comparing the first-shelf count of a sample mounted on a very thin Zapon film to the count of the same sample with back-scattering material behind the film. These data may be used to correct for the back-scattering from a particular backing material. Because of the change of initial slope of an absorption

<sup>†</sup>It is assumed that the 4.0 per cent back-scattering on platinum applies to  $\alpha$  rays from Pu<sup>238</sup> as well as Pu<sup>239</sup>, for which the back-scattering was measured. The back-scattering on quartz is less than on platinum by the ratio 1.027, which is the value determined<sup>40</sup> for Am<sup>241</sup>, whose  $\alpha$  rays have approximately the same energy as those of Pu<sup>238</sup>.

curve resulting from the back-scattering, the same correction does not apply to the zero-absorber extrapolated count.

The back-scattered radiation is degraded, so that the window-and-air absorption is more important for it than for the primary radiation. As pointed out in the papers quoted,<sup>9,10</sup> this is probably the explanation for the apparently lower value for the back-scattering correction for a 0.20-mev  $\beta$  ray as compared to a 1.5-mev  $\beta$  ray. The degraded radiation from a 0.20-mev  $\beta$  ray is so soft as to be largely lost in the mica window, whereas the back-scattered  $\beta$  rays from a 1.5-mev  $\beta$  ray are still energetic enough to pass through the window with little absorption.

If the initial half thickness for the back-scattered radiation were known, however, it would be possible to calculate the zero-absorber back-scattering correction from the first-shelf back-scattering correction. There is evidence<sup>7</sup> that for a 1.2-mev  $\beta$  ray (RaE) back-scattered from infinitely thick aluminum, the half thickness of the scattered  $\beta$  ray is about one-half that of the primary. It is assumed that this same reduction in half thickness applies to mica and that it is independent of energy.

Since the window and air correction,  $W$ , was 4.0 mg/sq cm, the first-shelf count for the unscattered radiation is

$$A_p = A_0 e^{-\lambda_p W} \quad (46)$$

where  $A_0$  = zero-absorber count for the primary, and  $\lambda_p$  = mass absorption coefficient for the primary.

The first-shelf count for the back-scattered  $\beta$  rays is

$$A_B = A'_0 e^{-\lambda_B W} \quad (47)$$

where  $A'_0$  = zero-absorber count for the back-scattered radiation, and  $\lambda_B$  = mass absorption coefficient for scattered radiation. The values for  $(A_p + A'_0)/A_p$  are given by Engelkemeir.<sup>9,10</sup> What is required is the zero-absorber correction,  $(A_0 + A'_0)/A_0$ . From the assumption stated above,  $\lambda_B = 2\lambda_p$ , for all energies. Calculating  $\lambda_p$  from Eq. 4 and using the measured back-scattering corrections, the zero-absorber back-scattering corrections were calculated and are shown in Table 3. If the assumptions made are approximately right, the infinite thickness back-scattering on mica seems to be about 1.28, approximately independent of energy. For lower energies it seems preferable to

use this value for the zero-absorber back-scattering correction despite the tentativeness of the assumptions involved.

The same correction is used for quartz because of its chemical similarity to mica. For a given energy the back-scattering seems to vary smoothly and monotonically with atomic number, so that the

Table 3—Back-scattering Corrections on "Infinite Thickness"  
of Mica

Nuclear species	Maximum $\beta$ energy, mev	Measured $(A_p + A_B)/A_p$	Calculated $(A_0 + A'_0)/A_0$
35-day Cb	0.15	1.13	1.36
4.5-year Pm	0.20	1.13	1.26
RaE	1.17	1.26	1.27
55-day Sr	1.5	1.27	1.28

back-scattering from a solid composed of molecules should be a function of the amounts of each element present and the back-scattering from each element. White mica has the composition



Since aluminum and silicon are neighboring elements, for back-scattering calculations this composition may be approximated as  $\text{H}_4\text{K}_2\text{Si}_{12}\text{O}_{24}$ . This is sufficiently close in composition to silicon dioxide (quartz) since the larger back-scattering from the small fraction of potassium is sufficiently compensated for by the smaller back-scattering from hydrogen.

#### SUMMARY

The radiations and decay scheme of Np<sup>238</sup> were investigated by absorption methods and coincidence measurements. The suggested decay scheme includes two modes of decay: (1) 60 per cent through a 0.2-mev  $\beta$  ray, followed by a 1.2-mev  $\gamma$  ray (1.8 per cent converted), followed by a 75-kev  $\gamma$  ray almost completely converted in the L shell (2) 40 per cent through a 1.4-mev  $\beta$  ray, followed by the same 75-kev  $\gamma$  ray, also converted in the same fashion. X rays were found with absorption coefficients consistent with the assumption that they were Pu<sup>238</sup> L x rays. Assuming the decay scheme described, the counting efficiency of the Pu x rays (14 to 21 kev) averages around 2 per cent in an argon-alcohol mica-window Geiger-Mueller tube.

The  $\text{Np}^{238}$  half life was found to be  $2.10 \pm 0.03$  days. From the ratio of  $\text{Np}^{238}$  activity to the measured growth of  $\text{Pu}^{238}$   $\alpha$  activity, the  $\text{Pu}^{238}$  half life was found to be 77 years.

A back-scattering correction for the zero-absorber (extrapolated) count was evaluated from experimental back-scattering data. It is suggested that the fraction of zero-absorber infinite back-scattering of  $\beta$  rays from a particular substance is independent of the maximum  $\beta$  energy of the  $\beta$  emitter.

#### ACKNOWLEDGMENTS

We are very grateful to D. W. Engelkemeir for lending his absolute  $\beta$  standards and for his aid in the coincidence measurements. We are also indebted to D. W. Osborne for correcting the coincidence measurements calculations.

#### REFERENCES

1. L. B. Magnusson and T. J. LaChapelle, The first isolation of element 93 in pure compounds and a determination of the half life of  $_{93}\text{Np}^{237}$ , Paper 1.7, this volume.
2. G. T. Seaborg, A. C. Wahl, and J. W. Kennedy, Report A-136 (Mar. 20, 1942).
3. G. T. Seaborg, E. M. McMillan, J. W. Kennedy, and A. C. Wahl, A new element: radioactive element 94 from deuterons on uranium, *Phys. Rev.*, 69: 366 (1946); Paper 1.1a, this volume.
4. D. H. Copp and D. M. Greenberg, A mica-window Geiger counter tube for measuring soft radiations, *Rev. Sci. Instruments*, 14: 205-208 (1943).
5. A. H. Jaffey, T. P. Kohman, and J. A. Crawford, Metallurgical Laboratory Memorandum MUC-GTS-407 and Metallurgical Project Report CC-1602 (Jan. 1944); Manhattan District Declassified Document MDDC-388.
6. See National Nuclear Energy Series, Division IV, Volume 9, Part I.
7. T. B. Novey and N. Elliott, National Nuclear Energy Series, Division IV, Volume 9, Paper 3.
8. T. B. Novey, D. W. Engelkemeir, and P. W. Levy, National Nuclear Energy Series, Division IV, Volume 9, Paper 9.
9. D. W. Engelkemeir, Metallurgical Laboratory Memorandum MUC-NS-312 (Mar. 8, 1945).
10. D. W. Engelkemeir, J. A. Seiler, E. P. Steinberg, L. Winsberg, and T. B. Novey, National Nuclear Energy Series, Division IV, Volume 9, Paper 5.
11. T. P. Kohman, A general method for determining coincidence corrections of counting instruments, Paper 22.50, this volume (Metallurgical Project Report CP-3275); abstract in *Phys. Rev.*, 72: 181A (1947).
12. N. Feather, Further possibilities for the absorption method of investigating the primary beta particles from radioactive substances, *Proc. Cambridge Phil. Soc.*, 34: 599-611 (1938).
13. L. E. Glendenin and C. D. Coryell, National Nuclear Energy Series, Division IV, Volume 9, Paper 11; Argonne National Laboratory Memorandum ANL-NS-2.
14. N. Elliott, W. H. Sullivan, N. R. Sleight, E. M. Gladrow, S. Raynor, and M. S. Freedman, National Nuclear Energy Series, Division IV, Volume 9, Paper 8.

15. R. P. Metcalf and E. Hennessee, Metallurgical Project Report CP-2582 (February 1945).
16. D. W. Engelkemeir, private communication.
17. W. Sturm and S. Turkel, Metallurgical Project Report CP-2984 (Apr. 25, 1945).
18. B. F. Schonland, Proc. Roy. Soc. London, A108: 187 (1925).
19. J. S. Marshall and A. G. Ward, Can. J. Research, 15: 29 (1937).
20. G. T. Seaborg, S. G. English, V. C. Wilson, and C. D. Coryell, Metallurgical Project Report CL-440 (May 19 to July 16, 1943).
21. W. Heitler, "Quantum Theory of Radiation," Chap. V, Oxford University Press, New York, 1936.
22. J. M. Cork and R. W. Pidd, The absorption of gamma radiation in copper and lead, Phys. Rev., 66: 227-230 (1944); G. Goetzinger and L. Smith, Absorption of 2.8-mev gamma rays in lead, Phys. Rev., 67: 53L (1945).
23. F. Rasetti, "Elements of Nuclear Physics," pp. 95-96, Prentice-Hall, Inc., New York, 1936.
24. Nuclei formed in fission: Decay characteristics, fission yields, and chain relationship (Issued by the Plutonium Project), J. Am. Chem. Soc., 68: 2411-2442 (1946); Revs. Modern Phys., 18: 513-544 (1946).
25. R. Metcalf, W. Rubinson, J. A. Seiler, E. Steinberg, and L. Winsberg, Metallurgical Laboratory Memorandum MUC-NS-230 (N-1673) (Sept. 12, 1944).
26. W. C. Peacock, A study of the absolute efficiency of gamma-ray counters with application to nuclear spectroscopy, Ph. D. Thesis, Massachusetts Institute of Technology, 1944.
27. D. W. Engelkemeir, E. L. Brady, and E. P. Steinberg, National Nuclear Energy Series, Division IV, Volume 9, Paper 88.
28. L. Meitner, A simple method for the investigation of secondary electrons excited by gamma rays and the interference of these electrons with measurements of primary beta-ray spectra, Phys. Rev., 63: 73-76 (1943).
29. A. H. Compton and S. K. Allison, "X Rays in Theory and Experiment," D. Van Nostrand Company, Inc., New York, 1935.
30. A. H. Compton and S. K. Allison, ibid., p. 645.
31. R. A. James, Metallurgical Laboratory Memorandum MUC-GTS-1447 (Mar. 6, 1945).
32. B. F. Scott, Metallurgical Project Report CP-3501 (May 9, 1946).
33. W. Bradley and B. Epstein, Metallurgical Project Report CP-2725 (Oct. 23, 1944).
34. J. V. Dunworth, Application of the method of coincidence counting to experiments in nuclear physics, Rev. Sci. Instruments, 11: 167-180 (1940).
35. H. R. Hulme, N. F. Mott, F. Oppenheimer, and H. M. Taylor, The internal conversion coefficient for  $\gamma$  rays, Proc. Roy. Soc. London, A155: 315-330 (1936). (The values calculated are for Z = 84, but for hard gammas the coefficient is proportional to Z<sup>3</sup>.)
36. J. B. Fisk and H. M. Taylor, The internal conversion of  $\gamma$  rays, Proc. Roy. Soc. London, 146: 178-181 (1934).
37. J. B. Fisk, Calculation of internal conversion coefficients of  $\gamma$  rays, Proc. Roy. Soc. London, 143: 674-678 (1934).
38. T. B. Novey and P. W. Levy, Preparation of absolute  $\beta$  standards and application to the determination of neutron flux, Report N-1994 (CP-G) (Apr. 14, 1945).
39. A. H. Jaffey, Metallurgical Project Report CC-3771 (Feb. 7, 1947); also in National Nuclear Energy Series, Division IV, Volume 14A.
40. A. H. Jaffey, unpublished work.
41. A. H. Jaffey, Half life of Pu<sup>239</sup> by direct decay measurement, Paper 2.2, this volume (Argonne National Laboratory Report ANL-4020).

42. R. A. James, A. E. Florin, H. H. Hopkins, Jr., and A. Ghiorso, Products of helium-ion and deuteron bombardment of  $U^{235}$  and  $U^{238}$ , Paper 22.8, this volume.
43. G. T. Seaborg, R. A. James, and A. Ghiorso, The new element curium (atomic number 96), Paper 22.2, this volume.
44. R. A. James, private communication.
45. M. S. Freedman, in National Nuclear Energy Series, Division IV, Volume 9, Paper 7.
46. G. T. Seaborg, Science, 104: 379-386 (1946).

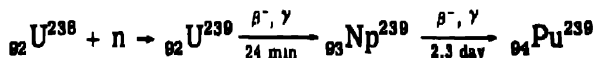
## Paper 14.5

# AN INVESTIGATION OF THE INTERNAL-CONVERSION LINE SPECTRUM OF NEPTUNIUM 239†

By H. W. Fulbright

### 1. INTRODUCTION

Element 93, now called neptunium, was discovered by McMillan<sup>1</sup> in 1939 and identified by McMillan and Abelson<sup>1</sup> in 1940. It was prepared by exposing uranium to slow neutrons. It decays by  $\beta$ -particle emission to form plutonium.



Several investigations of the radiation from  $\text{Np}^{239}$  have been made. In 1940, Helmholtz,<sup>2</sup> using a magnetic spectrograph, found four internal-conversion lines corresponding to the K- and L-level conversion (in plutonium atoms) of  $\gamma$  rays of energies 220 and 270 kev. In England Feather<sup>3</sup> made some absorption measurements which gave evidence that K and L x radiation of plutonium was emitted in the course of the decay of  $\text{Np}^{239}$ . In addition, he reported that the  $\beta$ -ray spectrum was complex and estimated that three  $\beta$  transitions were involved with energy limits of about 630, 400, and 140 kev. He reported about 0.6 photoelectron per disintegration. In 1943 Mitchell, Langer, and Brown,<sup>4</sup> using absorption and coincidence methods, found evidence for a 0.4-mev  $\gamma$  ray of low intensity. They found about 0.7 internal-conversion electron per disintegration.

†Contribution from the Department of Physics, Washington University, St. Louis.

This work was originally reported in Metallurgical Project Report CP-1727 (May 24, 1944). The present chapter is based on the original data, which have been studied carefully and reworked to yield a more satisfactory interpretation than that originally given.

This was the state of affairs in December 1943 when the work reported here was begun. The hope was that a study of the internal-conversion lines might lead to the establishment of an energy-level scheme for the  $\text{Pu}^{239}$  nucleus. Knowledge of such a scheme of levels might prove useful in studying the inelastic scattering of fast neutrons by plutonium. Because of the complexity of the spectrum, it turned out to be impossible to establish a definite energy-level diagram on the basis of the conversion-line work. A tentative energy-level scheme is proposed below, but a careful study of the continuous  $\beta$  spectrum is required to help establish the scheme completely. A magnetic  $\beta$ -ray spectrograph having a uniform field of large extent and using semicircular focusing and direct-photographic recording was built for use in this investigation. A magnetic-field regulator of a new type, which automatically kept the magnetic induction inside the spectrograph at a constant value, proved very useful.

A description of the spectrograph, experimental methods, and results is given in the following sections.

## 2. THE SPECTROGRAPH

The semicircular-focusing spectrograph with photographic recording has several advantages over other standard spectrometers when used to study conversion-line spectra.

1. No empirical energy calibration of the machine is required. Energies corresponding to the various lines can be calculated directly from the measured value of the magnetic induction  $B$ , the measured dimensions of the spectrograph, and the measured position of the line on the film.

2. The film records simultaneously electrons of a wide range of energies and provides a permanent record of the results.

3. The resolving power of the instrument can be made very great. However, this spectrograph has several disadvantages.

1. Accurate values for the absolute intensities of the various lines cannot be obtained because of the variation in sensitivity of the film with the energy of the incident electrons.

2. It is often difficult to prepare a line source with negligible self-absorption.

3. The difficulty of obtaining and maintaining a large uniform magnetic field must be overcome.

Only the first of these disadvantages proved serious.

A large electromagnet, which had previously been ordered by Prof. Jauncey and used by Baltzer<sup>5</sup> in an investigation of the radium E  $\beta$  spectrum, was already available in the laboratory. It was of the conventional "closed shell" type with 16-in.-diameter pole faces spaced

4 in. apart. It was mounted on two concrete pedestals so that the pole faces lay in vertical planes. This orientation had particular advantages that will be pointed out later. A preliminary survey of the field of the magnet showed that its core had considerable hysteresis so it was not possible to use the current through the field coils as a measure of the magnetic induction between the poles.

It was decided to construct a field controller that would hold the magnetic induction at a constant value. Several schemes were considered, including a rotating coil system with two coils on the same shaft, one in the magnetic gap of the spectrograph, the other in the field of a "standard" permanent magnet. The differences between the electromotive forces developed in the two coils could be amplified and used to regulate the field current of the magnet. This idea was discarded because of obvious mechanical difficulties arising from vibration and the use of slip rings and brushes. The Wynn-Williams controller<sup>6</sup> using a Grassot fluxmeter linked with the magnetic circuit was not employed because a somewhat more flexible apparatus suggested itself.

The scheme finally chosen is shown in Figs. 1 to 3. The sensitive element (Fig. 1) consists of two coils  $C_1$  and  $C_2$  mounted at the ends of a long galvanometer-type movement, which is supported at the top by a phosphor-bronze wire and held tight at the lower end by another similar wire. Connections to the coils are made through thin gold foils. The plane of the top coil lies in the direction of the spectrograph field; the plane of the bottom coil lies in the direction of a fixed standard magnetic field supplied by a well-aged permanent magnet. The vacuum chamber of the spectrograph has a reentrant wall to accommodate the top coil. A small direct current is passed through each coil in such a way that the torques exerted on the movement by the magnetic forces acting on  $C_1$  and  $C_2$  are in mutual opposition. For any ratio of currents in the two coils there is one and only one value of magnetic induction  $B$  for which the suspension is in equilibrium at its null position. Thus adjustment of the field current  $I$  so as to keep the suspension in equilibrium at its null position keeps the magnetic-field strength constant. This adjustment is accomplished by the use of an electronic amplifier controlled through a photocell by a beam of light reflected from a mirror mounted on the galvanometer movement.

The optical system is shown in Fig. 2. It consists of a light source, slit, lens, galvanometer mirror, and a double photocell. An image of the slit is focused midway across the double photocell when the galvanometer is in the null position. A deflection of the galvanometer swings the image of the slit to one side or the other and unbalances the currents flowing through the two halves of the photocell. Stops

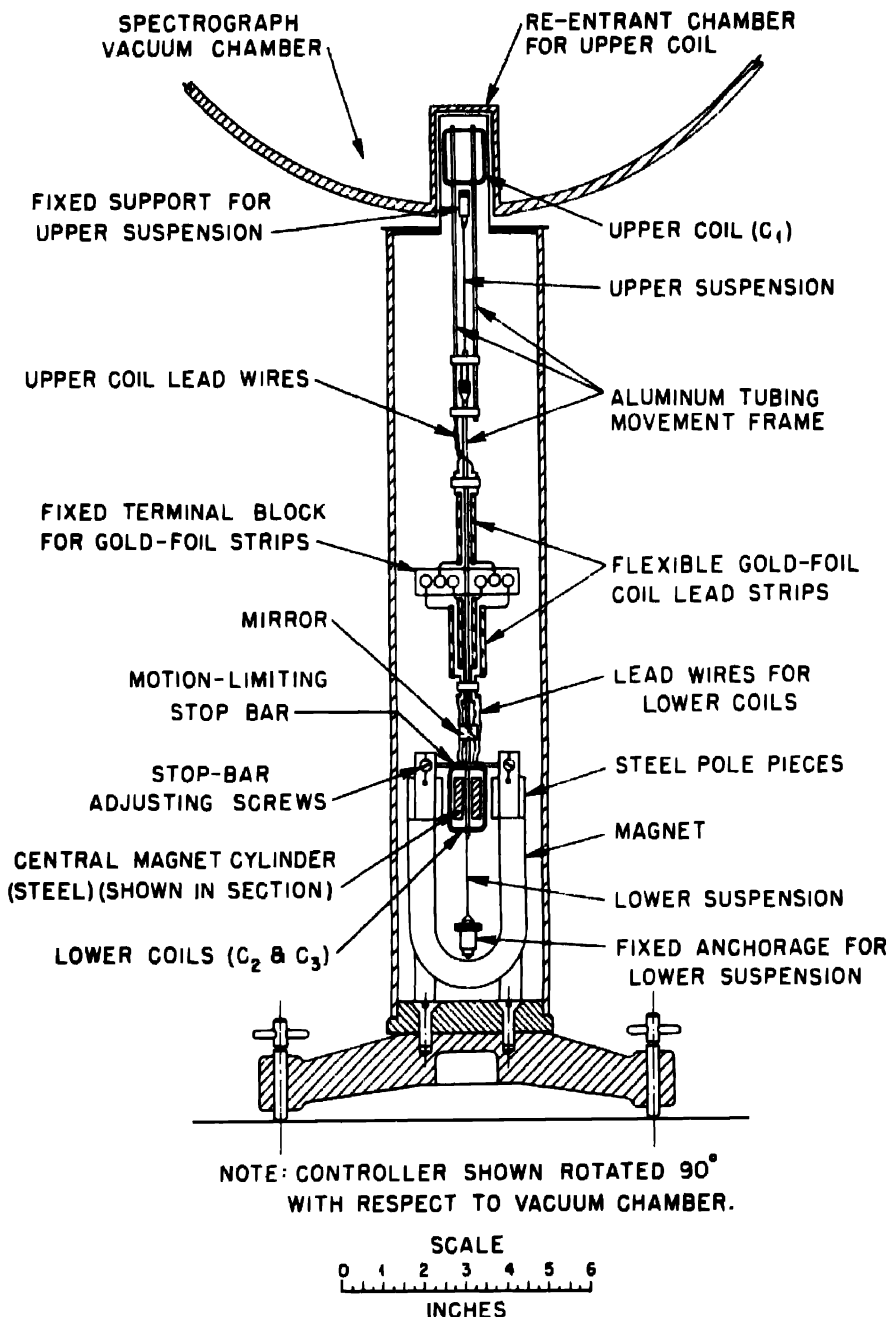


Fig. 1—Sensitive element of field controller.

are provided so that the movement cannot rotate far enough to swing the light spot entirely off either photocell. When the galvanometer is deflected, for example by a change in the d-c potential of the magnet power supply, the unbalanced current from the photocells, amplified many times, is impressed on the field current in the proper sense to

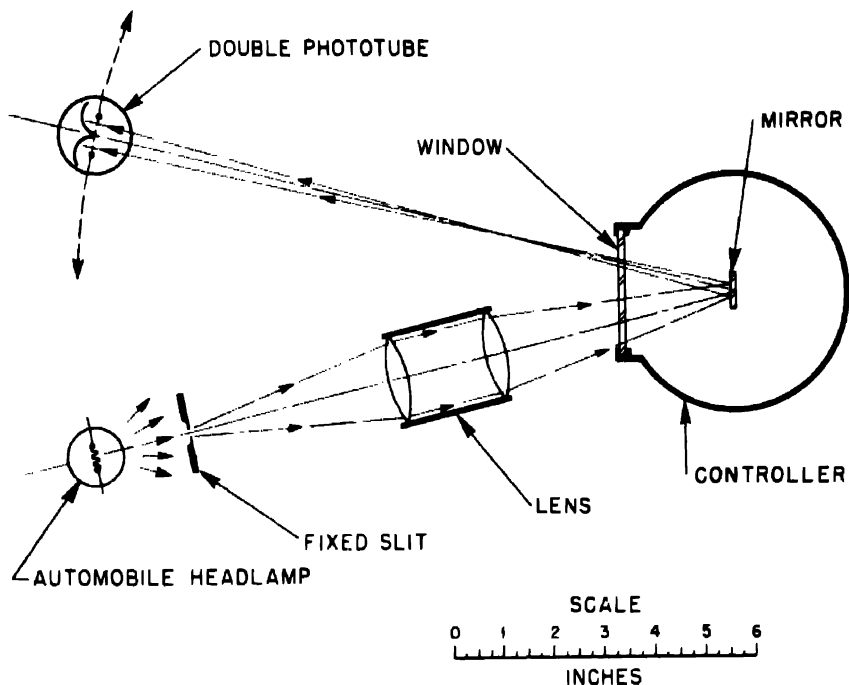


Fig. 2—Optical system for use with field controller.

restore the galvanometer to null position. If one of the field-current conditions is changing constantly (e.g., the battery voltage is fluctuating), the galvanometer hunts back and forth continuously around the null position. In actual operation changes in the circuit conditions are slow and are generally monotonic functions of time. Because of this and because of statistical variations in conditions, the controller hunts over only an extremely small hysteresis loop. For practical purposes it may be said that the controller does not hunt once equilibrium is established.

Because of the possibility that the hunting might break into a violent oscillation, a certain amount of degenerative coupling between the magnet field-current circuit and galvanometer movement was provided. A coil C<sub>3</sub> was wound along with C<sub>2</sub> on the lower end of the

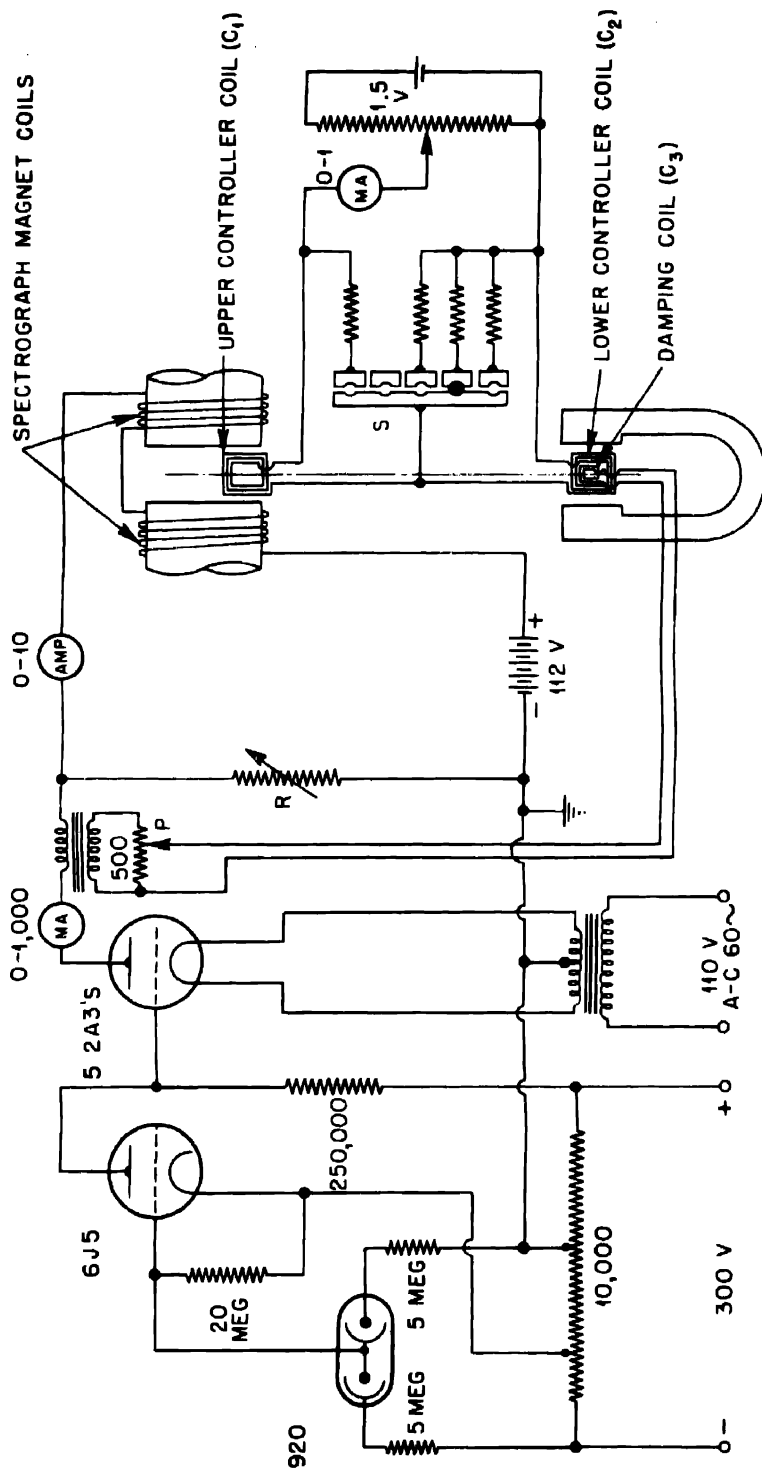


Fig. 3.—Schematic diagram for controller circuit.

movement so that damping currents could be applied to suppress mechanical oscillations. These currents were obtained from inductive coupling of  $C_3$  with the field-current circuit through a transformer (see Fig. 3). A potentiometer  $P$ , provided to alter the magnitude of the feedback, proved very useful. Disconnecting  $C_3$  when the controller is in operation leads to violent oscillations which disappear rather quickly when  $C_3$  is reconnected and the setting of  $P$  is advanced.

A schematic diagram of the controller circuits is shown in Fig. 3. The 2A3 current amplifier stage carries a fraction of the field current. The rest is carried by the heavy-duty laboratory-type resistor  $R$ . Four 2A3-type tubes are normally used, and these can handle 600 ma without running too hot. Normally, the resistor  $R$  is adjusted so that the tubes carry 100 to 200 ma, since the current through them usually increases with time as the battery potential falls. The storage cells used are permanent laboratory batteries in the battery room.

Current for coils  $C_1$  and  $C_2$  is supplied by a 1.5-volt dry cell. If the current through the coils is great enough (1 ma) operation is not affected by slight current variations, since the ratio of currents in  $C_1$  and  $C_2$  controls the field strength. This is an important point because it permits a simple unregulated source of current to be used in  $C_1$  and  $C_2$ .

**2.1 Operation.** The response of the controller to changes in operating conditions is fairly rapid, approximately 1 sec being required for complete readjustment of the field current to offset the effect of shorting out 10 per cent of the field coils. This rapid response is due to the fact that the torques operating on the movement are large compared with restoring torque of the suspension and the fact that the movement has a relatively small moment of rotational inertia.

Within the range of currents that can be passed by the 2A3 tubes the controller works very well. Many tests have been made to show its effectiveness. Shorting out of 25 to 50 per cent of the field winding leads to a change of less than 0.2 per cent in the field strength measured with a flip coil. Currents passed through auxiliary turns wrapped around the yoke of the magnet are normally unable to alter the steady-state value of  $B$  by a measurable amount.

The introduction of a thin razor blade into the top of the magnetic gap causes a visible change in the current flowing through the regulator tubes. This is an interesting effect since the reluctance of the gap as a whole is only slightly changed by the insertion of the blade and since the controller coil  $C_1$  is 14 in. away across the diameter of the poles.

The variation in the field current with the condition of the iron core is also striking. With a certain ratio of currents in  $C_1$  and  $C_2$ , a field

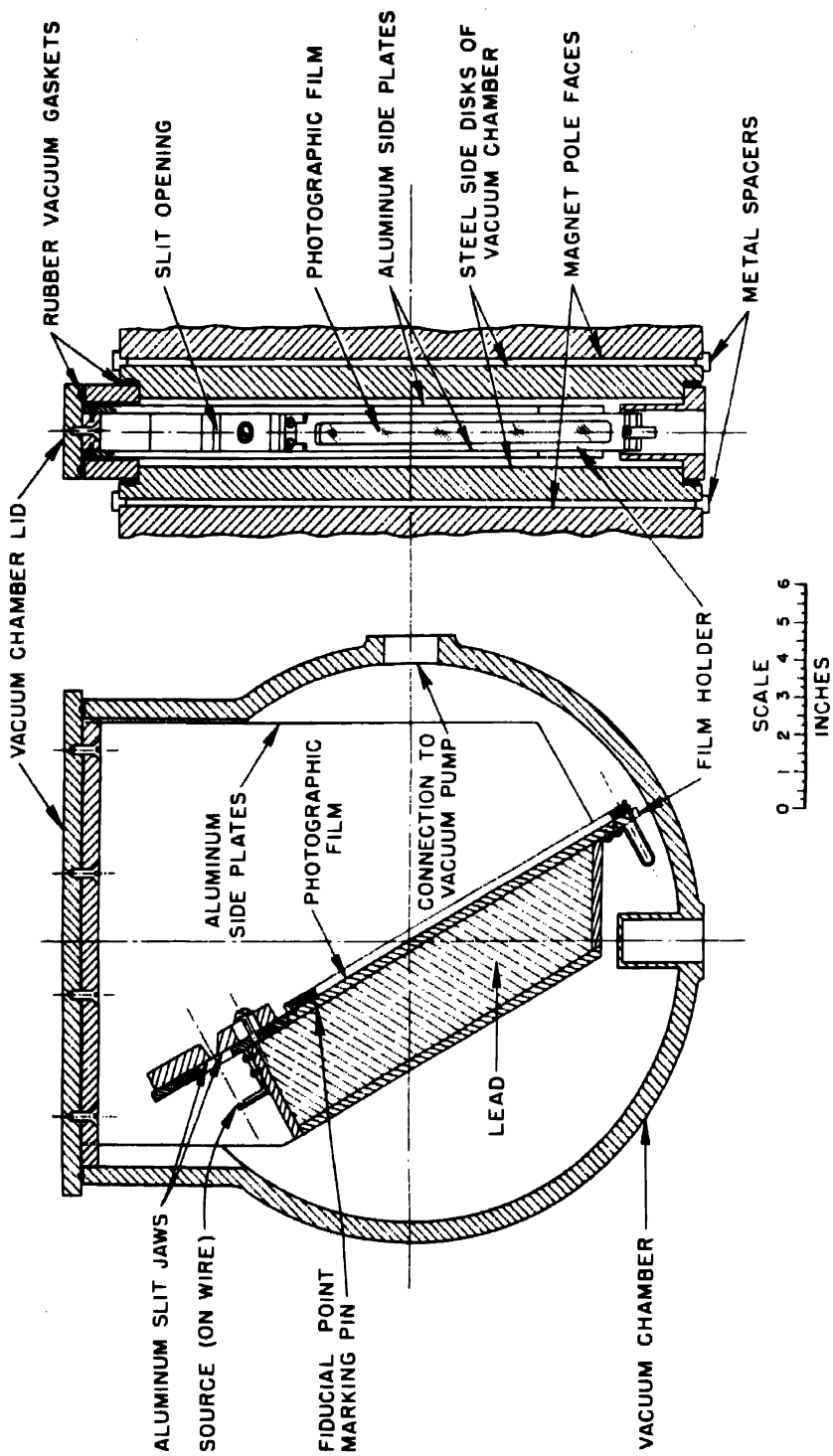


Fig. 4—Vacuum chamber and spectrograph unit for  $\beta$ -ray spectrum measurements.

strength was obtained corresponding to a field current of 0.40 amp. By adjustment of R (Fig. 3) the field current was deliberately raised to 1.5 amp and then lowered so that the controller was once more effective. The field strength was found to be unchanged as a net result of the violence done on the magnet, but the current had fallen to 0.37 amp. The current was then cut to zero and reapplied. This time the field was again found to have precisely the same strength, but the current had risen to 0.42 amp. This test shows clearly the value of the controller in overcoming hysteresis difficulties.

For spectrographic use (with film) the controller can be set to maintain  $B$  at any one of five values covering the energy range from 20 kev to 10 mev. To change  $B$  a plug is shifted from one position to another; this shift changes shunt resistances, thereby altering the ratio of currents in  $C_1$  and  $C_2$ . The "fixed" current through R is then adjusted so that the controller current is initially about 100 ma. Generally, these are the only changes required. It may be necessary to adjust the degeneration control P, although this is unusual since the setting of P is not critical over a wide range beyond the minimum position at which oscillation of the galvanometer movement ceases.

The controller has been used successfully in making exposures of more than 24 hr in length. The sharpness of the conversion lines obtained in these cases indicates that the average variations in the magnetic-field strength were less than 0.1 per cent.

**2.2 The Vacuum System.** The vacuum system consists of a round chamber supported between the poles of the magnet, a 3-in. oil-diffusion pump, a manifold, and a Cenco Megavac fore pump.

The vacuum chamber was made from a  $\frac{1}{2}$ -in. thick brass strip rolled into a ring. The various smaller brass bosses, etc. were silver-soldered together and then machined (see Fig. 4). Two 16-in. diameter by  $\frac{1}{8}$ -in. thick steel lids were placed in the ring and sealed to it with rubber gaskets. The plates pressed against brass spacer blocks which in turn pressed against the poles of the magnet, so that the lids were accurately parallel. The lids were carefully machined to have uniform thickness within 0.001 in. The top of the chamber had a  $1\frac{1}{2}$ - by 12-in. rectangular hole into which either spectrograph or spectrometer could be inserted. A smooth surface was provided so that  $\frac{1}{8}$  in.-diameter rubber gaskets set into grooves in the lids of the unit could easily seal the system. Atmospheric force is more than adequate to make the seal airtight. This makes film changing relatively easy.

The vertical position of the magnetic gap allowed for the simple quick-sealing feature of the chamber as well as for the new type field stabilizer. No disadvantage inherent in the magnet orientation has been found.

The entire vacuum system was metal and rubber except for the Western Electric manometer tube (D79510), which is sealed on with wax. An electronic emission-current control and ion-current amplifier were provided for the operation of this tube.

Valves were provided to permit the vacuum chamber to be "roughed down" with the fore pump after film changes were made; the oil pump could thus be kept hot all the time.

**2.3 The Spectrograph Unit.** The spectrograph unit is shown in Fig. 4. The electrons are kept from striking the steel cover plates of the chamber by two  $\frac{3}{16}$ -in. aluminum plates that also serve as supports for the rest of the unit. Preliminary experiments showed that the use of the aluminum channel walls was of advantage in reducing scattering and secondary effects, although a much wider channel would be available if the iron lids were left exposed. Heavy aluminum slit jaws are provided. In line-spectrum investigations samples are mounted on fibers or wires supported by thin aluminum brackets and held well away from metal surfaces (except at the ends, of course) to minimize back-scattering. For continuous spectrum work a light-weight film-source support would be required to reduce back-scattering. A section of one  $\frac{1}{16}$ -in. support plate is removable so that samples can be changed easily (see Fig. 4).

The film holder clamps the film securely. It slides into position in the spectrograph and is clipped there tightly. A small brass point in the holder makes a fiducial mark on the film.

### 3. FIELD MEASUREMENTS

The accuracy of the energy values obtained with the spectrograph depends upon the precision with which the magnetic induction  $B$  can be determined, since energy calculations depend only upon  $B\rho$  values, and since  $\rho$  (radius of curvature) can be determined with high precision.

A flip coil was wound in a helical groove machined in a hard rubber form. An integral number of turns was used. The diameter of the coil was about 3 in. and was measured to 0.001 in. Leads were brought out and twisted together to avoid stray linkage with the field.

The flip coil was mounted on the end of a rigid copper tube, which was mounted on bearings supported by the vacuum chamber so that the coil could swing from the center of the magnetic gap to a point where the stray magnetic field was substantially zero. All parts were of wood, brass, and other nonmagnetic material. The coil was connected to a ballistic galvanometer and swung out of the magnetic field to determine how fast the withdrawal must be to ensure a truly bal-

listic deflection. A wide latitude was found. Withdrawal times up to 1.5 sec gave the same deflection.

The standard solenoid used was carefully surveyed, and its constants were determined accurately by measurement of its geometry. A new secondary was wound beside the old to verify the number of turns in the old secondary coil. The current standard used was a Sensitive Research Instrument Corporation model C millivoltmeter with universal shunt. The accuracy of this meter is said to be better than 0.25 per cent.

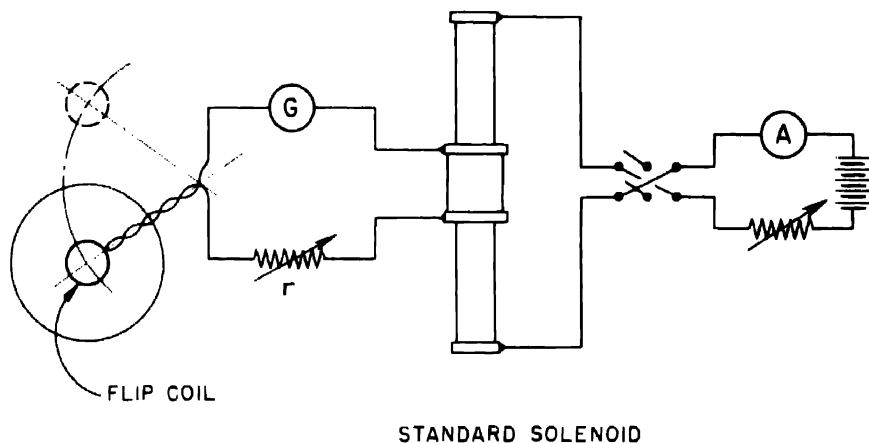


Fig. 5—Circuit for field-strength measurements.

The circuit used in making the field measurements is shown in Fig. 5. The resistor  $r$  was adjusted for each determination so that the galvanometer deflection was nearly full-scale. The experimental procedure consisted of duplicating, by reversal of the current in the primary of the standard solenoid, the ballistic deflections obtained by withdrawing the search coil from the center of the magnetic gap. The current required to duplicate the deflection was then used to calculate  $B$  by the usual method.

Swinging the search coil radially within the field caused small deflections of the ballistic galvanometer. From this the radial departure of the field strength from a constant value over the working part of the field was estimated to be less than 0.3 per cent.

#### 4. CALIBRATION MEASUREMENT OF RaB CONVERSION-LINE ENERGIES

Since the energies of the many RaB conversion lines have been established rather accurately by Ellis<sup>7</sup> and his coworkers, their val-

ues were used to check the accuracy of this calibration. A glass ampule containing 15 millicuries of radon gas was placed inside a special glass system and broken. The gas was then pumped into a small chamber by means of a Toeppler pump and the RaA plated onto a thin aluminum sample support maintained at a potential of -90 volts. Plating is possible under these conditions because the RaA is ionized when formed. The reactions are as follows:



Table 1 shows the result obtained from these measurements. The agreement is better than expected considering the limits of accuracy of our field measurements. Ellis estimates that his limits of error in absolute energy values are 0.2 per cent.

Table 1— $B\beta$  Values for Some RaB Lines

Ellis' values (RaB only)	Our values	Difference between two values, %
658	658	0
763	763	0
787	785	-0.25
1400	1400	0
1666	1666	0
1762	1766	+0.25
1925	1926	+0.05
2002	2003	+0.05

## 5. EXPERIMENTAL WORK ON Np<sup>239</sup>

The first two neptunium samples examined with the new  $\beta$ -ray spectrograph were supplied by Dr. G. T. Seaborg. These samples contained several milligrams of lanthanum fluoride carrier. Spectrograms made using these samples showed several conversion lines having sharp upper energy edges and broad smears on the lower energy side (see Figs. 6a and b). The smearing out was, of course, caused by the loss of energy of electrons passing through the relatively thick source. A proper measurement of the positions of these lines was impossible. Furthermore, lines of low intensity that might be present would tend to be lost in the large background of the continuous spectrum and the smeared-out lines of higher intensity. Moreover, two or more lines lying close to each other could not be distinguished from each other under these conditions.

An estimate of the upper energy limit of the  $\beta$  spectrum was made, and the electron energies corresponding to six lines were determined. The upper energy limit of the continuous  $\beta$  spectrum was set at about 0.70 mev. The six lines were found to correspond to the K, L, and M conversion of two  $\gamma$  rays emitted by the excited 94<sup>239</sup> nucleus following its formation. Values for the K, L, and M binding energies of plutonium were obtained by extrapolation of the experimental values for the heavy elements given in Compton and Allison.<sup>9</sup> The two  $\gamma$  rays were found by Helmholtz. Our values were 230 and 280 kev where his were 220 and 270 kev.

To get a rough check on the upper energy limit, a simple absorption measurement was made on the  $\beta$  spectrum using aluminum absorbers. Results indicate that the upper limit corresponds to 240 mg./sq. cm. The upper energy limit was then calculated by use of the Widdowson and Champion<sup>8</sup> equation for the range of  $\beta$  rays in absorbers

$$R = 0.536 E_m - 0.165$$

where R is the range in grams per square centimeter, and  $E_m$  = the maximum energy of  $\beta$  particles in million electron volts. The value 0.68 mev is found to be in good agreement with the spectrographic results of 0.70 mev.

#### 6. RESULTS OBTAINED USING ELECTROPLATED SAMPLES

Because of the difficulties encountered when crystalline sources were used, it was decided to try to prepare an essentially carrier-free electroplated source. Samples of uranyl nitrate were exposed to neutrons from the Washington University cyclotron for a period of about two days. A carrier-free sample of neptunium in solution was then prepared by a process making use of the discovery of McMillan and Abelson that neptunium if oxidized to a higher valence state does not precipitate as a fluoride along with the rare earths. A portion of the sample was then deposited electrolytically on a fine platinum wire, which was placed in the spectrograph.

The first film exposed with a carrier-free sample showed that a striking improvement had been achieved. The result is shown in Fig. 6c. The result obtained previously in the same energy range with a crystalline sample is shown in Fig. 6b. Several closely spaced lines that appear only as weak blurs in Fig. 6b are clearly resolved in Fig. 6c.

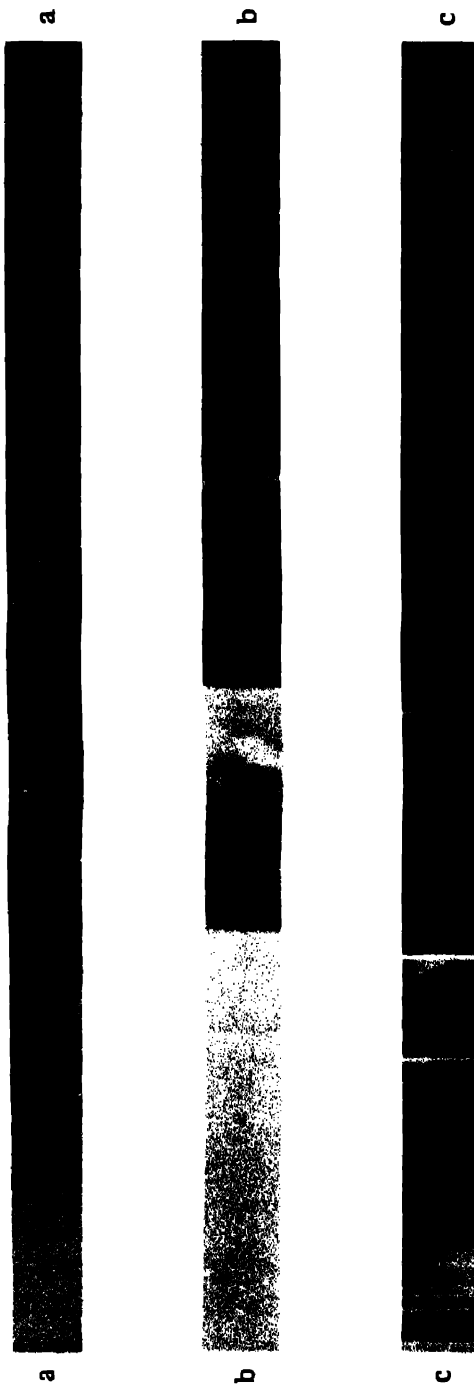


Fig. 6.— $\beta$ -ray spectrograms of  $\text{Np}^{239}$ . (a) First neptunium film; crystalline source. (b) Stronger neptunium; less carrier; crystalline source. (c) First film made with plated neptunium sample. All made with approximately the same field strength.

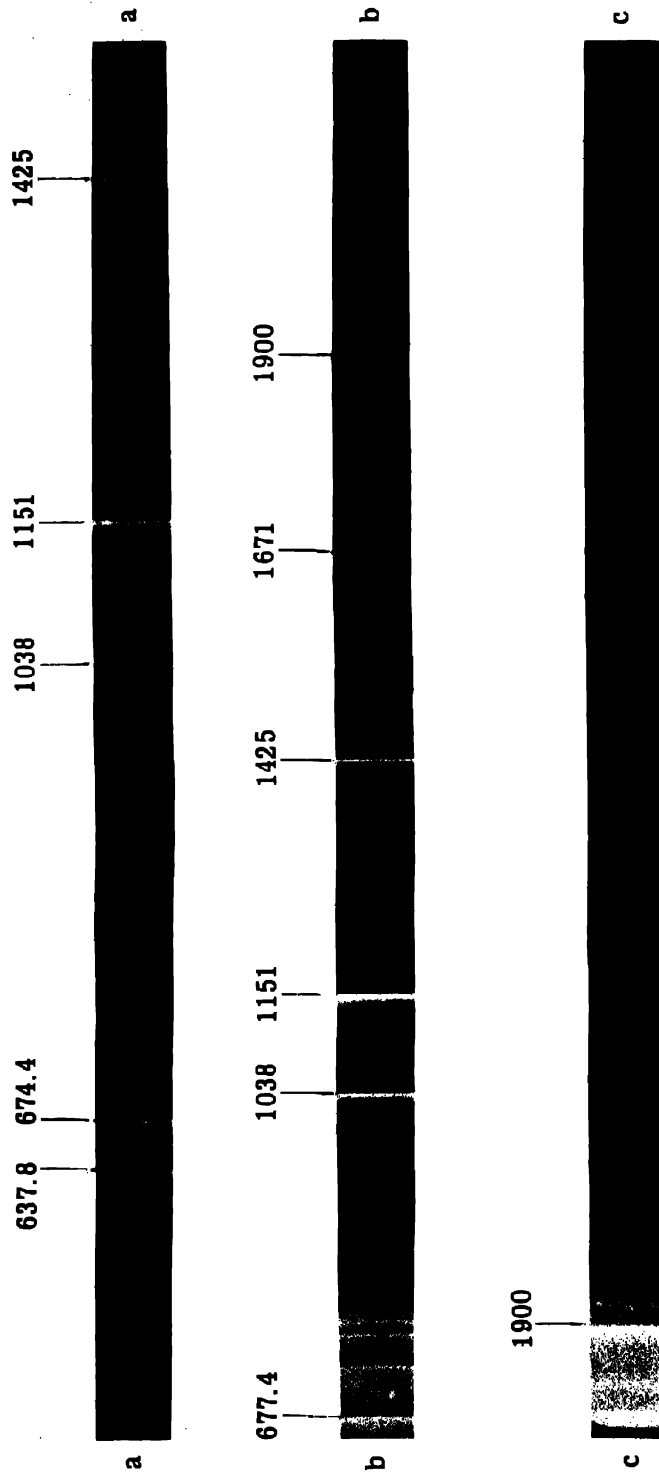


Fig. 7.— $\beta$ -ray spectrograms of  $\text{Np}^{2+}$ ; (a) low-energy range; (b) middle-energy range; (c) upper-energy range, limit of continuous spectrum.

## THE TRANSURANIUM ELEMENTS

Table 2—Neptunium 239 Conversion-line Spectrum

Line No.	Relative intensity, visual estimate	Measured $B\rho$ , gauss-cm	Corrected $B\rho$ , gauss-cm	Electron <sup>†</sup> energy, kev
1	1	492.19	496.9	21.28
2	1	505.81	510.7	22.45
3	1-1	547.14	552.2	26.15
4	2-m	554.18	559.3	26.82
5	3-n	596.93	602.4	30.98
6	6	632.15	637.8	34.61
7	2	673.2		38.42
8	7	677.4		38.89
9	1	711.9		42.80
10	2	715.4		43.20
11	2	718.8		43.59
12	2	725.7		44.40
13	5	731.9		45.13
14	1	752.0		47.54
15	1	761.6		48.70
16	5	766.5		49.30
17	5	782.3		51.27
18	5	789.9		52.22
19	3	814.8		55.40
20	2	823.8		56.57
21	1	845.9		59.49
22	3	863.1		61.79
23	3	870.0		62.73
24	2	893.5		65.97
25	1	901.1		67.03
26	3	1,006.1		82.40
27	3	1,011.6		83.24
28	8	1,037.8		87.29
29	2	1,115.2		99.68
30	1	1,122.8		100.93
31	2	1,140.7		103.9
32	10	1,151.1		105.6
33	9	1,425.2		155.1
34	3	1,581.2		186.1
35	1	1,664.8		203.3
36	7	1,671.0		204.6
37	1	1,675.2		205.5
38	3	1,751.8		221.8
39	1	1,773.2		226.4
40	6	1,900.3		254.3
41	2	1,976.2		271.4
42	1	1,996.2		276.0

<sup>†</sup>The physical constants used in the calculation of the electron energies are:

$$e = 4.8024 \times 10^{-10} \text{ e.s.u.}$$

$$m_0 = 9.1055 \times 10^{-28} \text{ g}$$

$$c = 2.9978 \times 10^{10} \text{ cm/sec}$$

The spectrum of Np<sup>239</sup> was examined in the energy range from 20 kev to about 6 mev using carrier-free samples. No darkening of the film was observed above about 0.70 mev, the limit found for the continuous spectrum. Altogether, 42 lines were found. These all appear on two films (Figs. 7a and b). The remarkable check with the results of Ellis on RaB was obtained at the magnetic field strength used in Fig. 7b, so the  $B\rho$  values found there are taken as standard. The  $B\rho$  values of the lines in film Fig. 7a are corrected upward so that thirteen lines in the overlapping portions of Figs. 7a and b have the best fit. The correction factor applied to the various lines showed a systematic variation with  $\rho$ , the radius of curvature, so that in general the correction factors used were different for different lines. They ranged from 1.0088 for line 8 to 1.0096 for lines 1 and 2. Table 2 gives a summary of the data on the 42 lines.†

Table 3 shows a summary of what now appear to be the best assignments of conversion lines to levels of conversion, along with the corresponding  $\gamma$ -ray energies. The 49.1-, 61.2-, 67.4-, 105.5-, 209.3-, 227.8-, and 277.4-kev  $\gamma$  rays seem well established. There is an element of speculation in the deduction that  $\gamma$  rays of energies 22.86 and 57.3 kev are also emitted, but even there the assignments are not unreasonable.

In preparing the data in Table 3 it was necessary to use values for the binding energy of electrons in the various electronic shells of the plutonium atom. These were not directly available from x-ray work, but were obtained by extrapolation of x-ray data given by Compton and Allison<sup>9</sup> and by Siegbahn.<sup>10</sup> To facilitate the extrapolation, Moseley diagrams were made for each level. The values finally chosen are given below in Table 4. The value of 122.2 kev for the K shell is somewhat higher than the 120.7-kev extrapolated value, but there was some fluctuation evident about the Moseley line in the cases of the points representing K binding energies of lighter elements; this value was therefore chosen for best agreement with the other conversion-line data when  $\gamma$ -ray energies were calculated.

Level Diagram. The energy-level diagram, Fig. 8, is based on the gamma-ray energies given in Table 3. It must be regarded as tentative. Careful work on the continuous spectrum will probably be required to find the correct diagram. The recent work of Släts<sup>11</sup> on the continuous  $\beta$  spectrum does not fit in with this level scheme because of the 1.179-mev  $\beta$ -ray limit that he found.

† In all, about fifteen spectrograms were made.  $B\rho$  values were reproducible within one part in fifteen hundred.

## THE TRANSURANIUM ELEMENTS

Table 3—Gamma-ray Energies

Line No.	Relative intensity, visual estimate	Level of conversion	Calculated $h\nu$ , kev†
1	1	N <sub>I</sub>	22.85
2	1	O <sub>I</sub>	22.86
			22.86 (av.)
3	1	L <sub>I</sub>	49.21
4	2-	L <sub>II</sub>	49.01
5	3-	L <sub>III</sub>	49.10
10	2	M <sub>I</sub>	49.15
11	2	M <sub>II</sub>	49.18
12†	2	M <sub>III</sub>	48.98
13†	5	M <sub>IV</sub>	49.10
14	1	N <sub>I</sub>	49.11
15	1	O <sub>I</sub>	49.11
			49.12 (av.)
6	6	L <sub>I</sub>	57.67
17	5	M <sub>I</sub>	57.22
18	5	M <sub>III</sub>	56.80
			57.34 (av.)
7	2	L <sub>I</sub>	61.48
8	7	L <sub>II</sub>	61.08
9	1	L <sub>III?</sub>	60.92
19	3	M <sub>I</sub>	61.35
20	2	M <sub>III</sub>	61.15
21	1	N <sub>I</sub>	61.06
			61.16 (av.)
12†	2	L <sub>I</sub>	67.40
13†	5	L <sub>II</sub>	67.32
16	5	L <sub>III</sub>	67.42
22	3	M <sub>I</sub>	67.74
23	3	M <sub>III</sub>	67.28
24	2	N <sub>I</sub>	67.54
25	1	O <sub>I</sub>	67.43
			67.45 (av.)
26	3	L <sub>I</sub>	105.46
27	3	L <sub>II</sub>	105.43
28	8	L <sub>III</sub>	105.41
29	2	M <sub>I</sub>	105.63
30	1	M <sub>III</sub>	105.51
31	2	N <sub>I</sub>	105.47
			105.48 (av.)

Table 3—(Continued)

Line No.	Relative intensity, visual estimate	Level of conversion	Calculated $h\nu$ , kev†
28	8	K	209.49
34	3	L <sub>I</sub>	209.16
35	1	M <sub>I</sub>	209.25
37	1	M <sub>V</sub>	209.26
			209.29 (av.)
32	10	K	227.80
36	7	L <sub>I</sub>	227.66
38	3	M <sub>I</sub>	227.75
39	1	N <sub>I</sub>	227.97
			227.80 (av.)
33	9	K	277.30
40	6	L <sub>I</sub>	277.36
41	2	M <sub>I</sub>	277.35
42	1	N <sub>I</sub>	277.57
			277.40 (av.)

†Each of these lines appears twice in the table. Because of a coincidence of energies, it is not possible to distinguish between the alternate assignments. It seems probable that many of the electrons forming line 13 are from the 67.45-kev  $\gamma$  ray converted in the L<sub>II</sub> shell.

†Fifth place digits given here are not significant.

Table 4—Assumed Electronic Binding Energies in Plutonium

Level	Energy, kev
K	122.20
L <sub>I</sub>	23.06
L <sub>II</sub>	22.19
L <sub>III</sub>	18.12
M <sub>I</sub>	5.95
M <sub>II</sub>	5.59
M <sub>III</sub>	4.58
M <sub>IV</sub>	3.97
M <sub>V</sub>	3.78
N <sub>I</sub>	1.57
O <sub>I</sub>	0.41

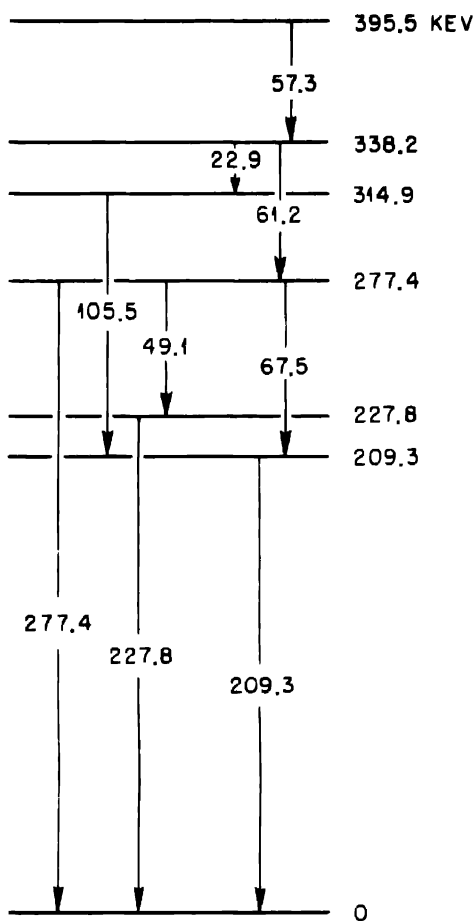


Fig. 8.—Tentative energy-level diagram for the  $_{94}\text{Pu}^{240}$  nucleus. The 314.9 level could equally well have been put at 232.2, since the 105.5  $\gamma$  ray may be emitted before the 22.9  $\gamma$  ray. The 227.8 level could equally well have been put at 49.1.

#### REFERENCES

1. E. McMillan, Phys. Rev., 55: 510 (1939); E. McMillan and P. H. Abelson, Phys. Rev., 57: 1185 (1940).
2. A. C. Helmholtz, private communication to G. T. Seaborg; G. T. Seaborg, Chem. Revs., 27: 1 (1940).
3. N. Feather, British Report CPB-83.
4. A. C. G. Mitchell, M. L. Langer, and L. J. Brown, Metallurgical Project Report CN-409 (Dec. 30, 1942).
5. O. Baltzer, Master's Thesis, Washington University, 1938.

6. C. E. Wynn-Williams, Proc. Roy. Soc. London, 145: 250 (1934).
7. C. D. Ellis, Proc. Roy. Soc. London, A143: 350 (1933).
8. G. T. Seaborg, S. G. English, V. C. Wilson, and C. D. Coryell, Metallurgical Project Report CL-440 (May 19 to July 16, 1942), p. 50.
9. A. H. Compton and S. K. Allison, "X Rays in Theory and Experiment," D. Van Nostrand Company, Inc., New York, 1935.
10. M. Siegbahn, "The Spectroscopy of X Rays," Oxford University Press, pp. 184-187, New York, 1925.
11. H. Siätis, Arkiv Mat. Astron. Fysik, 35A: 1-23 (1948).

## Paper 15.1

### CHEMISTRY OF NEPTUNIUM. THE OXIDATION STATES OF NEPTUNIUM IN AQUEOUS SOLUTION†

By J. C. Hindman, L. B. Magnusson, and T. J. LaChapelle

Up to the time of the present work, satisfactory identification of the oxidation states of neptunium stable in solution had not been obtained, although the first investigation at trace concentration by McMillan and Abelson,<sup>1</sup> the discoverers of element 93, had led these authors to the conclusion that there were tetrapositive and hexapositive states in solution in close analogy to uranium. The definite chemical evidence for the existence of at least one reduced and one oxidized state of the element led Seaborg and Wahl<sup>2</sup> to postulate the lower state as +3 or +4 and the upper state as +7 or less. Numerous experiments<sup>3-5</sup> at trace concentrations of neptunium were interpreted as evidence for the existence in solution of neptunium(III), although it appears that this interpretation was not correct since later experiments show that neptunium(III) could not exist under the described conditions. Duffield and Gofman<sup>6</sup> and Connick, King, and Beaufait,<sup>7</sup> as a result of numerous tracer experiments, proposed that there were three oxidation states of neptunium that were stable in solution. However, Magnusson<sup>8</sup> showed that these investigators had not obtained experimental evidence for more than two oxidation states. The first conclusive establishment of two oxidation states of neptunium was the preparation of microgram quantities of the solid compounds neptunium dioxide,  $\text{NpO}_2$  (see reference 9), and sodium neptunyl acetate,  $\text{NaNpO}_2(\text{OOCCH}_3)_3$ , (see reference 10).

It has been suggested that the elements 89 to 103 may be members of an actinide or thoride series in which progressive filling of the 5f

†Contribution from the Chemistry Division of the Metallurgical Laboratory, University of Chicago, now the Argonne National Laboratory.

Based on Metallurgical Project Report CN-2767 (Mar. 27, 1945).

shell occurs.<sup>11,17</sup> Consideration of neptunium as a member of this series led Seaborg to predict that neptunium would have a tripositive state intermediate in stability between the tripositive states of uranium and plutonium. As a member of this series neptunium might also exhibit the oxidation number +5. Trace-concentration experiments by Sleight, Hein, Wright, and Voigt<sup>13</sup> suggested the existence in solution of neptunium(V).

The recent isolation and purification of several milligrams of Np<sup>237</sup> in this laboratory made possible a more extensive and less tentative investigation of the chemistry of the element.

The initial objective of the work with pure neptunium was the identification of the oxidation states stable in solution. By analogy with uranium and plutonium it was expected that the various oxidation states of neptunium would possess highly characteristic absorption spectra in solution. One oxidation state of neptunium in solution was identified as a result of x-ray diffraction analysis by Zachariasen; the absorption spectrum characteristic of this state in solution was determined. Then, by stoichiometric addition of reducing agents, the oxidation numbers of other states as identified by their absorption spectra were obtained. A cross check was provided by stoichiometric addition of oxidizing agents to the lower oxidation state of neptunium. In this way it has been possible to demonstrate the existence of the tetra-, penta-, and hexapositive oxidation states of neptunium in solutions of perchloric, hydrochloric, and sulfuric acid. Watters<sup>14</sup> showed by polarographic studies that neptunium(III) could exist in aqueous solutions. More recently the authors<sup>15</sup> have prepared neptunium(III) in good yield and have described the properties of this state.

Experimental. The Np<sup>237</sup> used in this work was separated from Pu<sup>239</sup> by selective oxidation of the neptunium with bromate and precipitation of the plutonium with lanthanum fluoride. The pure Np<sup>237</sup> finally obtained contained less than 0.015 per cent Pu<sup>239</sup> by weight, as determined from the ratio of  $\alpha$  activities of the two isotopes and their known specific activities.

The first preparation for spectrophotometric examination was made by heating 1.16 mg of dry, olive-green neptunium hydroxide [later identified as neptunium(IV) hydroxide] in 52 microliters of 9.40M HClO<sub>4</sub>. After several hours of heating in a water bath, dilution with water produced a clear, pale-green solution, 1.0M in HClO<sub>4</sub>. The spectrum of this solution was marked by three sharp, strong absorption bands at 723, 964, and 984 m $\mu$ . Further details of this and other spectra are given in a subsequent paper.

An excess of argentic oxide was added to the green solution, which turned nearly colorless with a faint pink cast. The strong, sharp ab-

sorption bands associated with the initial spectrum had disappeared. A dark-brown "hydroxide" was thrown out of the solution by adding a slight excess of ammonia. The hydroxide was redissolved by warming in 10M HCl, and then diluted to 0.5 ml to give a yellow-green solution. The spectrum was very similar to that of the perchloric acid solution after the argentic oxidation. This was taken as evidence that the same oxidation state existed in both solutions.

An attempt to produce lower oxidation states was carried out by adding small aliquots of tin(II) to the oxidized neptunium chloride solution. It was found that addition of stannous chloride produced a steady increase in the extinction of the 984-m $\mu$  band until the amount of stannous chloride added was roughly equivalent to 0.5 mole per mole of neptunium. Further addition of stannous chloride produced only a slight reduction in peak height. A more precise duplication of this titration is illustrated in Fig. 1. An interesting phenomenon observed in the titration was the small growth of the 723-m $\mu$  peak observed in the original solution. The peak disappeared rather quickly.

A neptunium fluoride precipitate (tentatively identified as KNpF<sub>5</sub> or K<sub>2</sub>NpF<sub>6</sub>) was made from the above solution by saturating with sulfur dioxide and adding potassium fluoride to 1M and hydrofluoric acid to 4M. This green precipitate was fumed to dryness with sulfuric acid, yielding bright-green crystals. An absorption spectrum of the crystals dissolved in 0.5M H<sub>2</sub>SO<sub>4</sub> showed two prominent peaks at 727 and 971 m $\mu$ , analogous to the peaks at 723 and 964 m $\mu$  observed in the original neptunium solution in perchloric acid.

Oxidation of the neptunium sulfate solution was carried out by adding aliquots of 0.069M Ce(IV). A peak at 984 m $\mu$ , corresponding to the peak produced by reduction of an oxidized solution with tin(II), reached its maximum height when the mole ratio of adding cerium(IV) to neptunium was approximately 1. Further addition of cerium(IV) reduced the peak to zero optical density when 1 equivalent additional of Ce(IV) had been added (see Fig. 2). The spectrum of the latter solution was similar to that of the oxidized perchloric and hydrochloric acid solutions.

To determine the oxidation number of one of the oxidation states, a 6-microliter sample (10  $\mu$ g of neptunium) was removed from the ceric oxidized solution and precipitated in a capillary by making the solution 4M in Na<sup>+</sup> and 2M in CH<sub>3</sub>COO<sup>-</sup>. An x-ray diffraction pattern of the precipitate was found by Dr. Zachariasen to be identical with that of the salt he had previously identified<sup>10</sup> as sodium neptunyl acetate, NaNpO<sub>2</sub>(OOCCH<sub>3</sub>)<sub>3</sub>. On the basis of this evidence it was concluded that the highest oxidation state obtained was hexapositive. Data on the stoichiometric reduction of neptunium(VI) in 0.5M H<sub>2</sub>SO<sub>4</sub> by ferrous ion are given in Fig. 3.

Discussion. Differences in absorption spectra have led to the identification of three oxidation states of neptunium in aqueous solution. The lowest state obtained in this research is characterized by two strong, sharp absorption bands at 723 and 964 m $\mu$  in chloride or

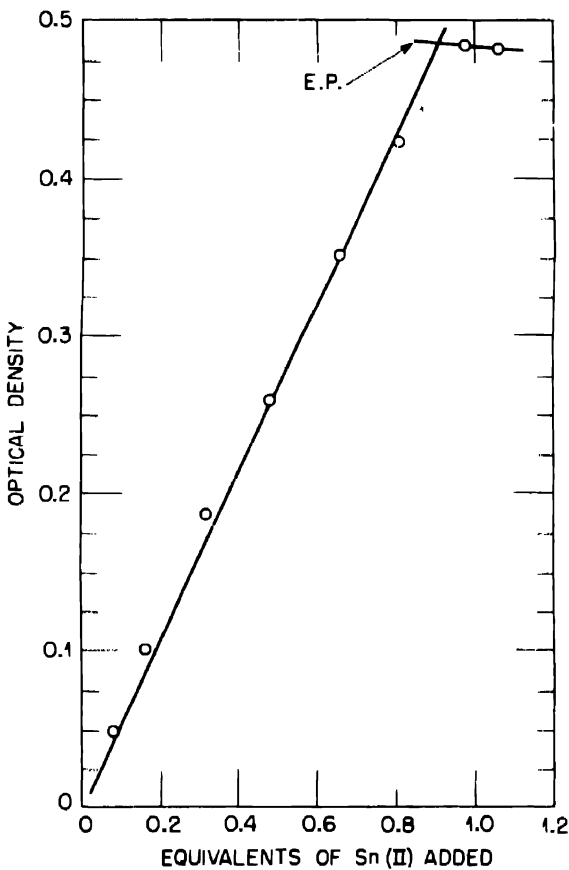


Fig. 1 — Titration of neptunium(VI) with tin(II).

perchlorate solution. These bands are shifted to 727 and 971 m $\mu$  in 0.5M H<sub>2</sub>SO<sub>4</sub> solution. The next higher oxidation state, which differs in oxidation number by 1 unit from both the lowest state and highest state obtained, as determined by stepwise spectrophotometric titration with oxidizing or reducing agents, has a spectrum characterized by a strong, sharp band at 984 m $\mu$  in perchlorate, chloride, or sulfate solutions. Isolation of the salt NaNpO<sub>2</sub>(OOCCH<sub>3</sub>)<sub>3</sub> from the solution of highest oxidation number has been used to identify this state as the

hexapositive state. On this basis the oxidation numbers of the other two states are +4 and +5. The spectrum of the hexapositive state has no marked bands in the visible region of the spectrum.

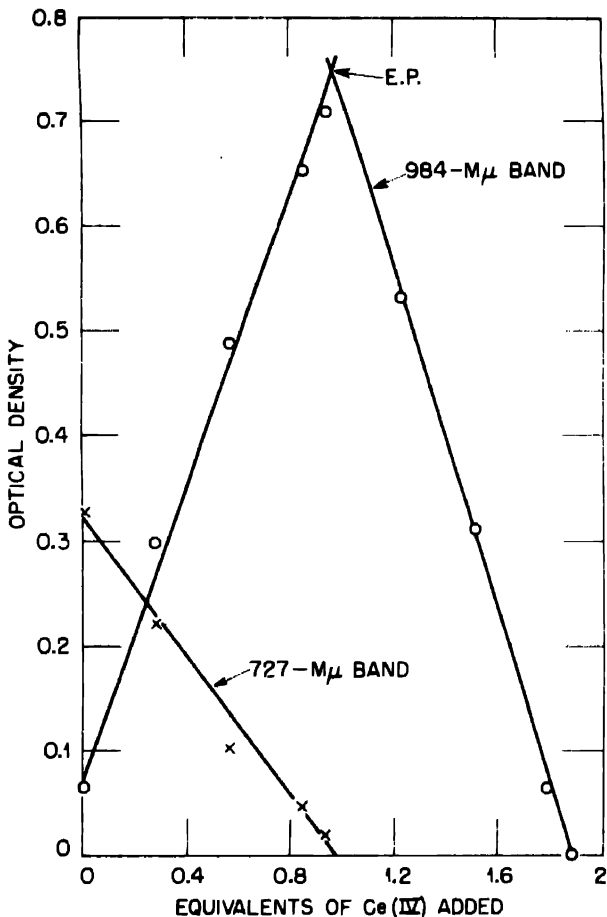


Fig. 2 — Titration of neptunium(IV) with cerium(IV).

Neptunium differs from both plutonium and uranium in that its pentapositive state is thermodynamically stable in 1.0M acid solution. This property is expected to prove very useful in the study and interpretation of the behavior and properties of the pentapositive ions of this series of elements.

The reduction of neptunium(VI) in hydrochloric acid with tin(II) is interesting. Potential measurements have shown that tin(II) is a sufficiently powerful reducing agent to potentially reduce neptunium(V)

or neptunium(VI) to the tetrapositive state. The reaction of tin(II) and neptunium(V) is apparently very slow, as the reduction appears to stop at the pentapositive state. It was noted, however, that during the titration there was a small amount of neptunium(IV) produced, which

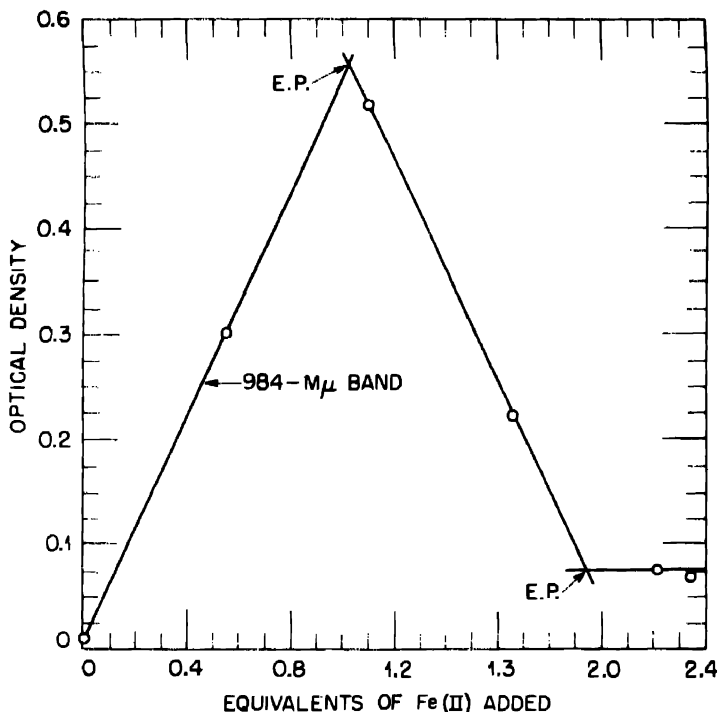
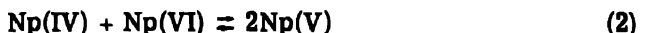


Fig. 3.—Titration of neptunium(VI) with iron(II).

disappeared rather quickly. This suggests that the reaction proceeds at least partially by the following steps:



It is also found that if iron is present in the solution, the reaction is catalyzed, and quantitative reduction of neptunium(V) to neptunium(IV) takes place.

Summary. Spectrophotometric titrations of neptunium solutions with oxidizing and reducing agents have been used, together with the

isolation of the salt  $\text{NaNpO}_2(\text{OOCCH}_3)_3$  from the solution of the highest oxidation state obtained, to establish the existence of the tetra-, penta-, and hexapositive states of neptunium. In contrast to both uranium and plutonium, the pentapositive state of neptunium has been found to be quite stable in acid solution.

## REFERENCES

1. E. McMillan and P. H. Abelson, *Phys. Rev.*, 57: 1185 (1940).
2. G. T. Seaborg and A. C. Wahl, Report A-135 (Mar. 19, 1942).
3. J. W. Gofman and R. E. Connick, Metallurgical Project Report CN-239 (Aug. 15, 1942).
4. R. B. Duffield, Metallurgical Project Report CN-250 (Aug. 31, 1943).
5. E. L. King, Metallurgical Project Report CN-1154 (Dec. 1, 1942).
6. R. B. Duffield and J. W. Gofman, Metallurgical Project Report CN-522 (Mar. 15, 1943).
7. R. E. Connick, E. L. King, and L. J. Beaufait, Metallurgical Project Reports CN-601 (Apr. 15, 1943), CN-654 (May 20, 1943), and CN-867 (Aug. 14, 1943).
8. L. B. Magnusson, Metallurgical Project Report CN-1764 (July 1, 1944).
9. T. J. LaChapelle and L. B. Magnusson, Metallurgical Project Report CN-1764 (July 1, 1944).
10. L. B. Magnusson and T. J. LaChapelle, Metallurgical Project Report CN-2088 (Sept. 1, 1944).
11. G. T. Seaborg, Metallurgical Laboratory Memorandum MUC-GTS-858 (July 1944).
12. S. Fried, A. E. Florin, and N. R. Davidson, Metallurgical Project Report CN-2689 (Feb. 27, 1945).
13. N. R. Sleight, R. E. Hein, J. M. Wright, and A. F. Voigt, Metallurgical Project Report CN-1979 (Oct. 10, 1944).
14. J. I. Watters, Metallurgical Laboratory Memorandum MUC-JIW-53 (Feb. 8, 1945).
15. L. B. Magnusson, T. J. LaChapelle, and J. C. Hindman, Chemistry of neptunium. Preparation and properties of neptunium(III), Paper 15.3, this volume; Metallurgical Project Report CN-3053 (June 28, 1945).
16. L. B. Magnusson, J. C. Hindman, and T. J. LaChapelle, Metallurgical Project Report CN-2767 (Mar. 27, 1945).
17. W. H. Zachariasen, Metallurgical Project Report CK-1518 (March 1944).

## Paper 15.2

### CHEMISTRY OF NEPTUNIUM. ABSORPTION SPECTRUM STUDIES OF AQUEOUS IONS OF NEPTUNIUM<sup>†</sup>

By J. C. Hindman, L. B. Magnusson, and T. J. LaChapelle

#### 1. INTRODUCTION

By analogy with uranium and plutonium, neptunium ions in aqueous solutions were expected to have characteristic absorption spectra. This has proved to be the case and the use of these characteristic spectra in determining the oxidation numbers of the +4, +5, and +6 states of the element has been described in a previous paper.<sup>1</sup> This paper gives further details of the absorption spectra of the ions of the various oxidation states of neptunium.

#### 2. EXPERIMENTAL PROCEDURE

The absorption-spectrum measurements were made with a Beckman quartz spectrophotometer. The instrument was operated, in general, at a slit width of 0.01 to 0.02 mm except as noted in the discussion. Readings were made at 2-m $\mu$  intervals in the spectral region from 350 to 600 m $\mu$ , at 2.5-m $\mu$  intervals in the region from 600 to 1000 m $\mu$ , and at 5-m $\mu$  intervals above 1000 m $\mu$  except in the vicinity of absorption bands where readings at 1-m $\mu$  intervals were made. In the case of very sharp absorption bands, the peak maximum was located by slowly rotating the wavelength drum and finding the point of maximum deflection of the galvanometer. Corex absorption cells of  $1.000 \pm 0.002$  cm and  $0.500 \pm 0.002$  cm were used with samples of 1.1 and 0.5 ml of solution, respectively. The adapters used have been described previously.<sup>2</sup>

<sup>†</sup>Contribution from the Chemistry Division of the Metallurgical Laboratory, University of Chicago, now the Argonne National Laboratory.

Based on Metallurgical Project Report CN-2767 (Mar. 27, 1945) and unpublished data.

The concentrations of the solutions used were from 0.002M to 0.01M. Details of the solution preparations can be briefly summarized.

2.1 Neptunium(III) in Hydrochloric Acid. This solution was prepared by reduction of a Np(IV) solution in 1.0M HCl at a mercury cathode. The reduction cell is described in a subsequent report.<sup>3</sup>

2.2 Neptunium(IV) in Perchloric Acid. Attempts to prepare pure Np(IV) solutions in perchloric acid were not successful since the hydroxide does not dissolve readily in this acid. This behavior is similar to that of U(IV) and Pu(IV) hydroxides and is explained by the fact that  $\text{ClO}_4^-$  has very little tendency to form complex ions. The spectrum of Np(IV) in 1.0M  $\text{HClO}_4$  was obtained from a solution that also contained appreciable concentrations of both Np(V) and Np(VI) prepared by heating the dried Np(IV) hydroxide with 9.5M  $\text{HClO}_4$ .

2.3 Neptunium(IV) in Hydrochloric Acid. Solutions of neptunium(IV) in 1M HCl and 8M HCl have been prepared by dissolving the washed neptunium(IV) hydroxide in concentrated hydrochloric acid and diluting.

2.4 Neptunium(IV) in Sulfuric Acid. Solutions of neptunium(IV) in 0.5M and 1.0M  $\text{H}_2\text{SO}_4$  have been prepared by (a) fuming the double fluoride of Np(IV),  $\text{KNpF}_5$ , with sulfuric acid to give crystals of neptunium(IV) sulfate, and (b) dissolving the washed neptunium(IV) hydroxide in concentrated sulfuric acid and diluting to volume.

2.5 Neptunium(V) in Perchloric Acid. The spectrum of neptunium(V) in 1M  $\text{HClO}_4$  has been observed in the solution of mixed oxidation states described above. A pure Np(V) solution in perchloric acid has also been made by dissolving the neptunium(V) hydroxide in acid of the desired concentration.

2.6 Neptunium(V) in Hydrochloric Acid. Solutions of neptunium(V) in 1M HCl have been prepared by (a) reduction of a Np(VI) solution in 1M HCl with stannous chloride and (b) reduction of a Np(VI) solution in hydrochloric or nitric acid with hydroxylamine hydrochloride, precipitation of the neptunium(V) hydroxide, dissolution of the washed hydroxide in acid, and dilution to volume.

2.7 Neptunium(V) in Nitric Acid. Neptunium(V) solutions in 1M  $\text{HNO}_3$  have been prepared by (a) oxidation of neptunium(IV) solutions by nitric acid in the cold, and (b) dissolution of neptunium(V) hydroxide in nitric acid and dilution to volume.

2.8 Neptunium(V) in Sulfuric Acid. Neptunium(V) solutions in 0.5 and 1M  $\text{H}_2\text{SO}_4$  have been prepared by (a) stoichiometric oxidation of Np(IV) with Ce(IV) and (b) dissolution of neptunium(V) hydroxide in sulfuric acid.

2.9 Neptunium(V) in Hydrogen Peroxide. A solution of neptuni-um(V) in 0.5M HNO<sub>3</sub> containing 1.5M H<sub>2</sub>O<sub>2</sub> was prepared by addition of hydrogen peroxide to a solution of Np(VI) in nitric acid. Reduction to Np(V) occurred. No precipitate was formed, which suggests that the neptunium peroxide prepared by LaChapelle<sup>4</sup> was the peroxide of neptunium(IV).

2.10 Neptunium(VI) in Perchloric Acid. A solution of neptuni-um(VI) in 1.0M HClO<sub>4</sub> was prepared by oxidation of a solution of mixed oxidation number with AgO.

2.11 Neptunium(VI) in Hydrochloric Acid. Solutions of neptuni-um(VI) in hydrochloric acid have been made by dissolution of the neptunium(VI) hydroxide in 1M HCl. Reduction of the Np(VI) by Cl<sup>-</sup> occurs even if dilute acid is added.

2.12 Neptunium(VI) in Sulfuric Acid. The spectrum of neptuni-um(VI) in a solution of 1.0M H<sub>2</sub>SO<sub>4</sub> prepared by stoichiometric oxida-tion with Ce(IV) was examined.

In addition to obtaining the spectra of the specific solutions men-tioned above, data were also obtained on the effect of slit width on the observed extinction of the sharp absorption bands and on the Beer's law behavior of certain of these bands. These data will be discussed later in the paper.

### 3. RESULTS AND DISCUSSION

In general, the spectra of the neptunium ions have characteristics which closely resemble those of the ions of the two neighboring ele-ments, uranium and plutonium. Neptunium(VI) in solution resembles U(VI) in that it does not exhibit any strong, sharp absorption bands in the visible region. There is an increasing absorption in the ultra-violet. Figure 1 illustrates the spectrum of neptunium(VI) in 1.0M HClO<sub>4</sub>. Addition of a complexing anion such as sulfuric acid increases the ultraviolet absorption. This suggests the formation of one or more complex ions between Np(VI) and sulfate, an observation in agreement with the fact that the transference behavior of neptuni-um(VI) shows an anion to be present in 1.0M H<sub>2</sub>SO<sub>4</sub> and with the more positive value of the Np (V)/(VI) potential in sulfuric acid solutions.<sup>5,6</sup> A satisfactory spectrum of Np(VI) in hydrochloric acid cannot be ob-tained since Cl<sup>-</sup> reduces Np(VI) to Np(V), and the liberated chlo-rine interferes with the spectral observations in the near ultraviolet region.

Figure 2 shows the neptunium(V) spectrum in 1.0M HCl. This spectrum is characterized by a very strong, sharp absorption band at 983 m $\mu$ . In addition there are several smaller bands present, the

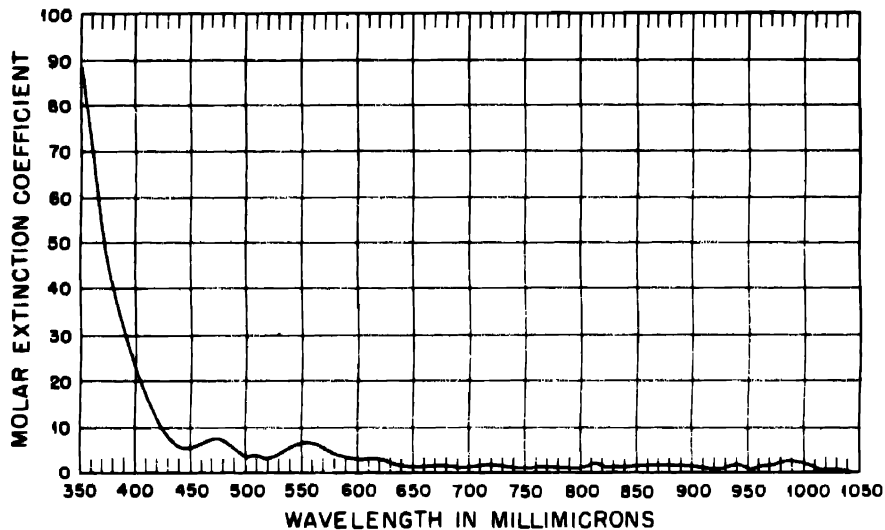


Fig. 1.—Absorption spectrum of Np(VI) in 1.0M  $\text{HClO}_4$ .

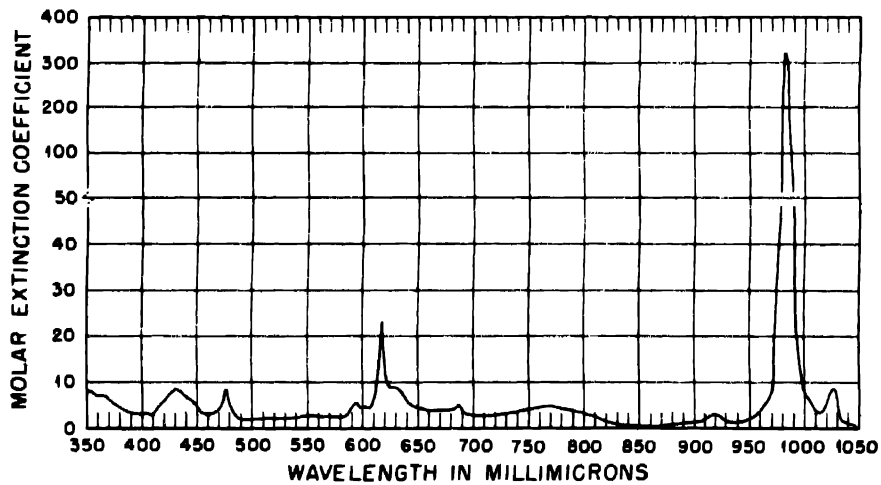


Fig. 2.—Absorption spectrum of Np(V) in 1.0M HCl.

most prominent of them being at  $617 \text{ m}\mu$ . The location and molar extinction coefficients of these bands are summarized in Table 1. There is a strong resemblance between the absorption spectrum of Np(V) and its isoelectronic analogue Pu(VI). The color of Np(V) in

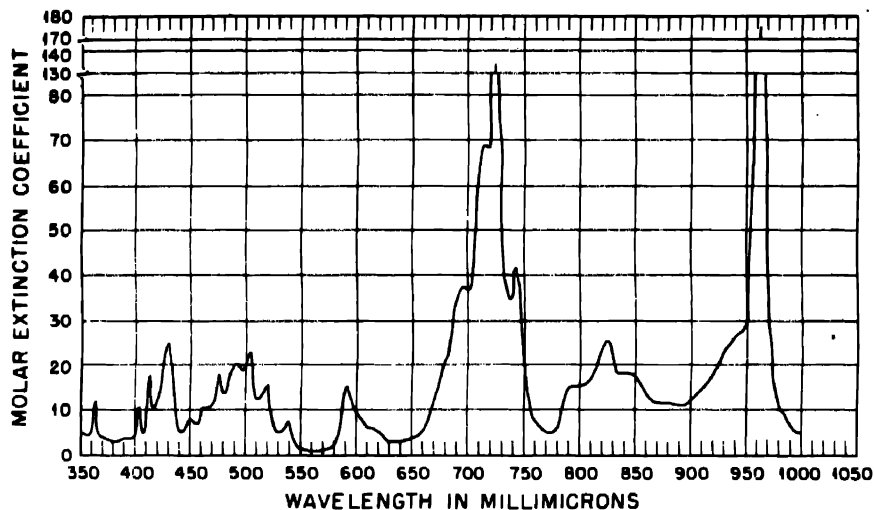


Fig. 3.—Absorption spectrum of Np(IV) in 1.0M HCl.

Table 1.—Neptunium(V) Absorption Bands in 1.0M HCl  
[0.0038M Np(V), 0.0127 mm slit width, 1.000  $\pm$  0.002 cm cell]

Absorption-band location, m $\mu$	Molar extinction coefficient	Absorption-band location, m $\mu$	Molar extinction coefficient
365	7	629	9.0
430	8.5	688	5.2
476	8.5	770, broad	5
594	5.5	717	2.8
602	4.5	983	3.25
618	23.5	1026	3.5

aqueous solution is blue-green. No spectral evidence for formation of complex ions of Np(V) exists. The spectrum appears the same in 1M  $\text{HClO}_4$ , 1M HCl, 1M  $\text{H}_2\text{SO}_4$ , 0.5M  $\text{HNO}_3$ —1.5M  $\text{H}_2\text{O}_2$ , and 1M  $\text{HNO}_3$ .

The neptunium(IV) spectrum is characterized by a number of sharp absorption bands, two intense bands being of particular interest. In perchloric and hydrochloric acid solutions these bands are located at 723 and 864 m $\mu$ . The neptunium(IV) spectrum in 1.0M HCl is illustrated in Fig. 3. A reconstruction of the neptunium(IV) spectrum in 1.0M  $\text{HClO}_4$  from the spectrum of a solution of mixed oxidation number indicates that within the experimental error the spectrum in the two acids is the same. This is reasonable in view of the low complex-

forming tendency of the perchlorate and chloride ions and leads to the conclusion that the neptunium(IV) spectrum in Fig. 3 is that of the uncomplexed ion. The Np(IV) spectrum in 8M HCl is considerably altered, and the absorption bands are decreased in intensity and broadened, indicating a complex ion is present in this solution. The location and molar extinction coefficients of the Np(IV) bands in 1.0M HCl are summarized in Table 2.

Figure 4 serves to illustrate the marked effect of sulfate on the Np(IV) spectrum. The bands have been considerably broadened and the intensity of absorption has been decreased. These changes have been accompanied by a shift of the peaks to the red, e.g., the 723-m $\mu$  peak shifts to 727 m $\mu$  and the 964-m $\mu$  peak to 971 m $\mu$ . The smaller peaks are similarly affected. The formation of a relatively stable complex ion of Np(IV) is suggested by these changes. The marked shifts of the neptunium (IV)/(V) potential from -0.74 volt in 1.0M HCl to -0.99 volt in 1.0M H<sub>2</sub>SO<sub>4</sub> is confirmatory evidence for the formation of a stable complex ion of neptunium(IV) and sulfate.<sup>6</sup>

The absorption spectrum of neptunium(III) in 1.0M HCl is illustrated in Fig. 5. More precise data on the band locations and extinction coefficients are given in a following paper.<sup>3</sup>

In general, the principal absorption bands of Np(IV) and Np(V) are similar in sharpness and extinction coefficients to the absorption bands of plutonium, particularly the principal 831-m $\mu$  band of Pu(VI). This resemblance suggested that these bands might be unsuitable for use in spectrophotometric analysis without careful standardization of the measurements since it has been shown that optical failure of the spectrophotometer leads to an apparent failure of the Pu(VI) absorption band at 831 m $\mu$  to obey Beer's law.<sup>7,8</sup> Observations showing the effect of slit width on the apparent optical densities of the principal bands are given in Fig. 6. Examination of these data shows that the deviation from linearity of the optical density, log I<sub>0</sub>/I, with slit width is most marked in the case of the 983-m $\mu$  Np(V) peak. In view of the Beer-Lambert relation

$$\log \frac{I_0}{I} = kcl$$

where I = percentage transmission

I<sub>0</sub> = 100 per cent transmission

k = constant

c = concentration of solution

l = cell length

Table 2—Neptunium(IV) Absorption Bands in 1.0M HCl  
 [0.00752M Np(IV), 0.0127 mm slit width, 1.000  $\pm$  0.002 cm cell]

Absorption-band location, m $\mu$	Molar extinction coefficient	Absorption-band location, m $\mu$	Molar extinction coefficient
363	10.3	539	7.4
403	7.9	590	14.0
412	15.0	617	8.1
429	24.2	723	126
430	6.8	742	40.0
463	10.5	795	16.7
476	17.4	820	26.3
492	20.1	844	18.6
503	22.3	965	160
519	14.9		

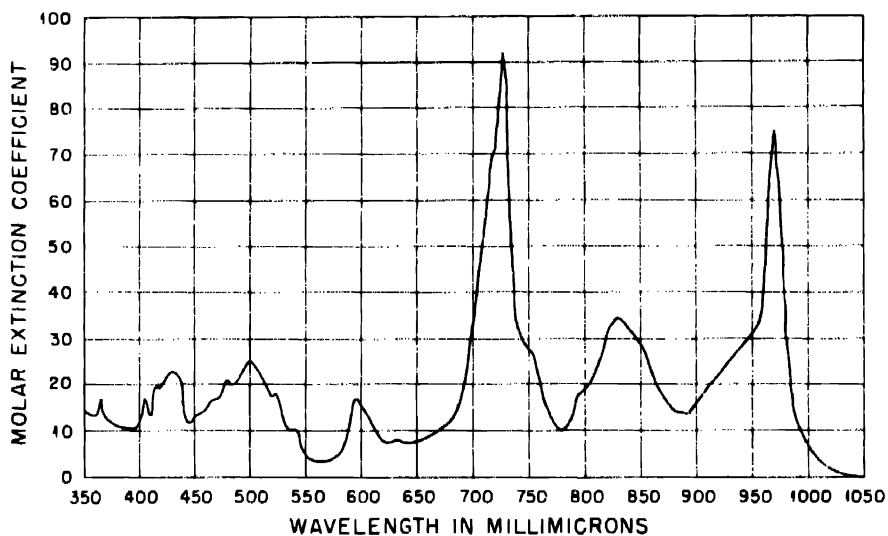
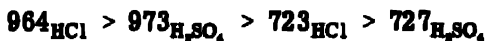


Fig. 4—Absorption spectrum of Np(IV) in 1.0M H<sub>2</sub>SO<sub>4</sub>.

this deviation would be expected to cause the apparent molar extinction coefficient to decrease with increasing concentration as in the case of the 831-m $\mu$  band of Pu(VI).

Measurements on solutions of Np(V) in sulfuric acid gave values of E<sub>683</sub> in agreement with the expected behavior (see Table 3). In the case of Np(IV) the magnitude of the effect is in the order



For a particular band width, the effect is greatest in that region in which the dispersion of the instrument is the least, i.e., in the longer

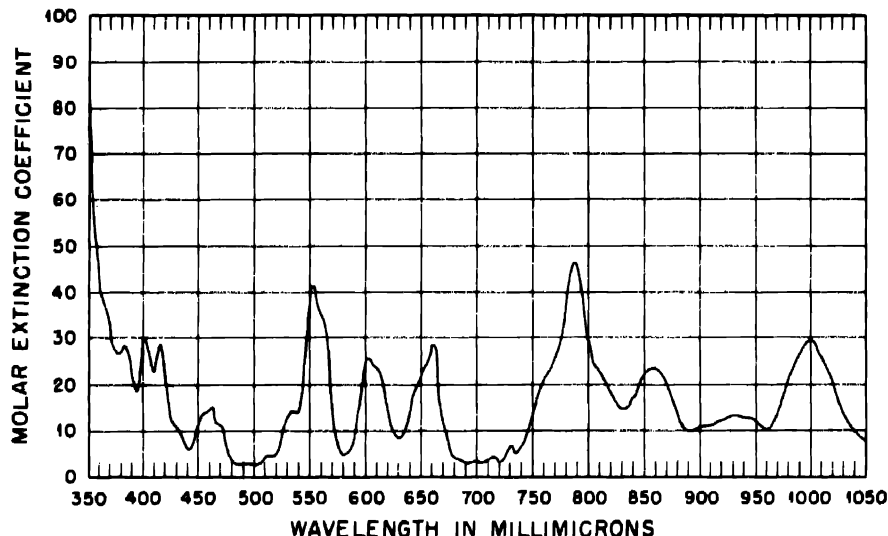


Fig. 5—Absorption spectrum of Np(III) in 1.0M HCl.

wavelength region (see Table 4). According to information given by Cary and Beckman,<sup>9</sup> aberrations in the instrument have the effect of widening the slits by about 0.02 mm in so far as spectral purity is concerned. Accepting their value for the spectral purity would mean that the Np(V) band at 983 is less than 2.5 mμ in width at the peak. Carniglia et al.<sup>8</sup> have suggested that the actual spectral purity may be less than that claimed by Cary and Beckman. Since the deviation for the Np(IV) chloride band at 964 mμ is less than for the 983-mμ Np(V) band, the width of the former absorption band would be nearer to the 2.5-mμ spectral band width. The deviation of the 723 Np(IV) chloride band from linearity would on this basis indicate a band width at the peak of not greater than 1.5 mμ. The broadening of the Np(IV) bands to a width greater than the spectral dispersion of the instrument in 0.5M H<sub>2</sub>SO<sub>4</sub> is shown by the fact that increasing slit width does not cause a dropping off in the peak optical density.

At the time the absorption spectra of plutonium were first observed with the Beckman quartz spectrophotometer,<sup>10</sup> the similarity between

the band characteristics for the ions of plutonium and those of the rare-earth ions was pointed out. The most striking similarity is in the type of bands observed, i.e., sharp bands, indicating protection

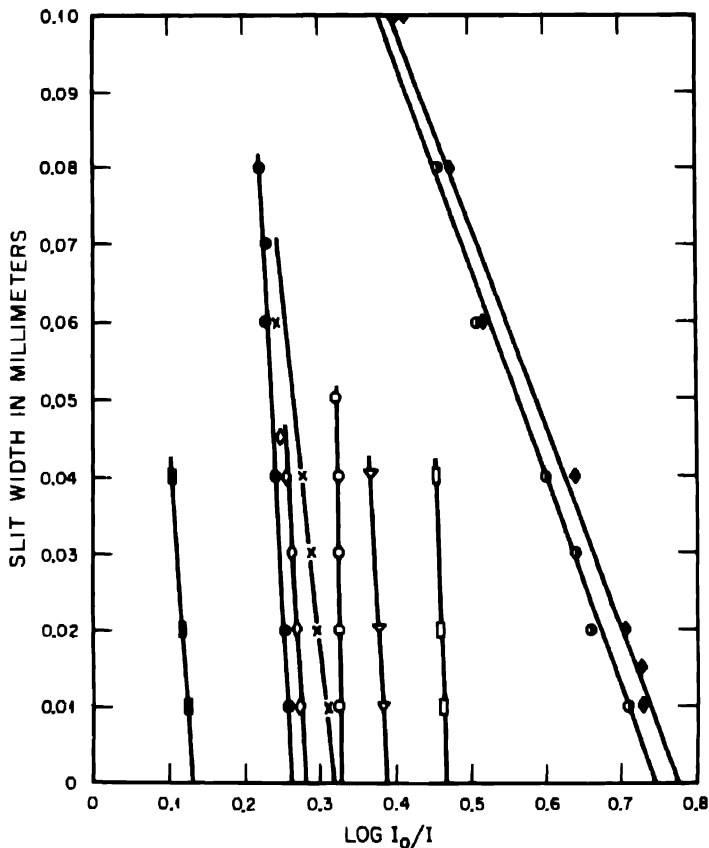


Fig. 6.—Effect of slit width on optical density of major Np(IV) and Np(V) absorption bands. ■, Np(V) sulfate 983-m $\mu$  peak; ●, Np(IV) sulfate 972-m $\mu$  peak; ◇, Np(IV) chloride 723-m $\mu$  peak; ×, Np(IV) chloride 964-m $\mu$  peak; ○, Np(IV) sulfate 727-m $\mu$  peak; ▽, Np(IV) sulfate 971-m $\mu$  peak; □, Np(IV) sulfate 727-m $\mu$  peak; ○, Np(V) sulfate 984-m $\mu$  peak; ♦, Np(V) chloride 984-m $\mu$  peak.

from perturbation by the fields of the surrounding atoms. It is interesting at this point to compare the band characteristics for those elements in the heavy-metal "rare-earth" series showing characteristic absorption spectra. Table 5 summarizes the general characteristics of the absorption bands of the tetrapositive ions in the series. Data on Nd(III) are included for comparison.

**Table 3 — Effect of Concentration on the Apparent Molar Extinction Coefficient of the 985-m $\mu$  Band of Np(V) in 1.0M H<sub>2</sub>SO<sub>4</sub> (Slit Width = 0.02 mm)**

Np(V), molarity	E <sub>985</sub>
0.00111	306
0.00421	280
0.00530	263
0.00676	231

**Table 4 — Effect of Concentration (Beer's Law Study) on the Apparent Molar Extinction Coefficient of the 727- and 971-m $\mu$  Bands of Np(IV) in 1.0M H<sub>2</sub>SO<sub>4</sub> (Slit Width = 0.02 mm)**

Np(IV), molarity	E <sub>727</sub>	E <sub>971</sub>
0.000512	94.0	82.0
0.00320	92.1	76.2
0.00516	89.9	73.6
0.00700	89.5	73.3
0.00991	89.5	73.3

**Table 5 — Comparison of Absorption-band Characteristics**

Ions	Band wavelength, m $\mu$	Half-intensity width, <sup>†</sup> m $\mu$	Molar extinction coefficient
U(IV) (1M HCl)	430	18	14.5
	550	20	18.5
	650	22	54
Np(IV) (1M HCl)	363	3	9.5
	723	20	126
	964	12	168
Pu(IV) (1M HCl)	426	10	27.5
	471	14	53
	656	41	36
Nd(III) (1M HNO <sub>3</sub> )	444	7	0.58
	578	14	1.80
	797	14	1.68

<sup>†</sup>Half-intensity width is defined as the band width at an extinction corresponding to one-half the molar extinction at the band peak.<sup>11</sup>

In the case of the rare earths it is now generally agreed that the transitions are forbidden (4f<sup>n</sup>) transitions where the values of the quantum numbers L and S change while the l's remain constant. The low intensity of absorption is due to the fact that the forbidden transitions are allowed only with low probability. Although the greater in-

tensity of absorption in the various sharp bands of the actinide series qualitatively suggests that the transitions are allowed with a somewhat greater probability than in the case of the rare-earth ions, the molar extinction coefficients observed are still  $10^4$  to  $10^5$  lower than for dipole radiation, and hence are still classified as due to forbidden transitions, probably  $5f^n$ .

The colors of the solutions of the ions of the various oxidation states are summarized in Table 6.

Table 6—The Colors of Aqueous Solutions of Approximately 0.005M Neptunium in 1.0M Acids

Ion	In $\text{HClO}_4$	In $\text{HCl}$	In $\text{H}_2\text{SO}_4$
Np(IV)	Pale yellow-green	Pale yellow-green	Pale yellow-green
Np(V)	Green-blue	Green-blue	Green-blue
Np(VI)	Pale pink		Dark yellow-green

#### 4. SUMMARY

The characteristics of the absorption spectra of the ions of neptunium of the +3, +4, +5, and +6 oxidation states in aqueous solution have been determined. Details of their spectra are given for solutions containing both complex-forming and noncomplex-forming anions.

#### REFERENCES

1. J. C. Hindman, L. B. Magnusson, and T. J. LaChapelle, Chemistry of neptunium. The oxidation states of neptunium in aqueous solution, Paper 15.1, this volume.
2. J. C. Hindman and D. P. Ames, unreported data.
3. L. B. Magnusson, T. J. LaChapelle, and J. C. Hindman, Chemistry of neptunium. Preparation and properties of neptunium(III), Paper 15.3, this volume.
4. T. J. LaChapelle, Metallurgical Project Report CN-2431 (Dec. 1, 1944).
5. C. K. McLane, J. S. Dixon, and J. C. Hindman, Complex ions of plutonium. Transference measurements, Paper 4.3, this volume.
6. L. B. Magnusson, J. C. Hindman, and T. J. LaChapelle, Chemistry of neptunium(V). Formal oxidation potentials of neptunium couples, Paper 15.4, this volume.
7. D. P. Ames, Metallurgical Project Report CK-1587 (A-2252) (May 1, 1944).
8. S. C. Carniglia, R. E. Connick, W. H. McVey, G. E. Sheline, and W. K. Wilmarth, Metallurgical Project Report CK-1945 (July 24, 1944).
9. H. H. Cary and A. O. Beckman, J. Optical Soc. Am., 31: 682 (1941).
10. J. C. Hindman, K. A. Kraus, and J. J. Howland, Metallurgical Project Report CK-1371 (Mar. 1, 1944).
11. T. R. Hogness, F. P. Zcheile, and A. E. Sidwell, Jr., J. Phys. Chem., 41: 379 (1937).

## Paper 15.3

# CHEMISTRY OF NEPTUNIUM. PREPARATION AND PROPERTIES OF NEPTUNIUM(III)†

By L. B. Magnusson, T. J. LaChapelle, and J. C. Hindman

### 1. INTRODUCTION

The oxidation states of neptunium in aqueous solution have been shown<sup>1,2</sup> to be +3, +4, +5, and +6. A preliminary attempt to prepare Np(III) by reduction of Np(IV) in 1.0M HCl at a platinum cathode was unsuccessful. This led to the conclusion that the potential for the Np (III)/(IV) couple was more positive than zero. It has been found, however, that the failure to obtain Np(III) may be attributed to the extremely rapid oxidation of Np(III) in the presence of air. Watters showed with the polarograph that Np(III) could be formed in solution; and, although the Np (III)/(IV) couple appeared to be irreversible at the dropping-mercury electrode, he estimated the formal potential of the couple in 0.25M H<sub>2</sub>SO<sub>4</sub> to be +0.1 volt. Further experiments by the authors revealed that Np(III) could be obtained in fair yield in hydrochloric acid by reduction of Np(IV) with a mercury-pool cathode, and that Np(III) is stable with respect to oxidation by hydrogen ion in 1M hydrochloric acid. This paper includes a description of a method for preparation of Np(III) in good yield in an oxygen-free atmosphere and the results of potential measurements on the Np (III)/(IV) couple.

### 2. EXPERIMENTAL PROCEDURE

Gross neptunium concentrations in these experiments were determined by radiometric assay. Assays of concentrations of the individ-

†Contribution from the Chemistry Division of the Metallurgical Laboratory, University of Chicago, now the Argonne National Laboratory.

Based on Metallurgical Project Report CN-3053 (June 1945).

ual oxidation states of neptunium were made spectrophotometrically using a Beckman spectrophotometer. All potential measurements were made at  $25 \pm 1^\circ\text{C}$  by using a Rubicon precision potentiometer and galvanometer of  $0.003 \mu\text{a}$  per millimeter sensitivity.

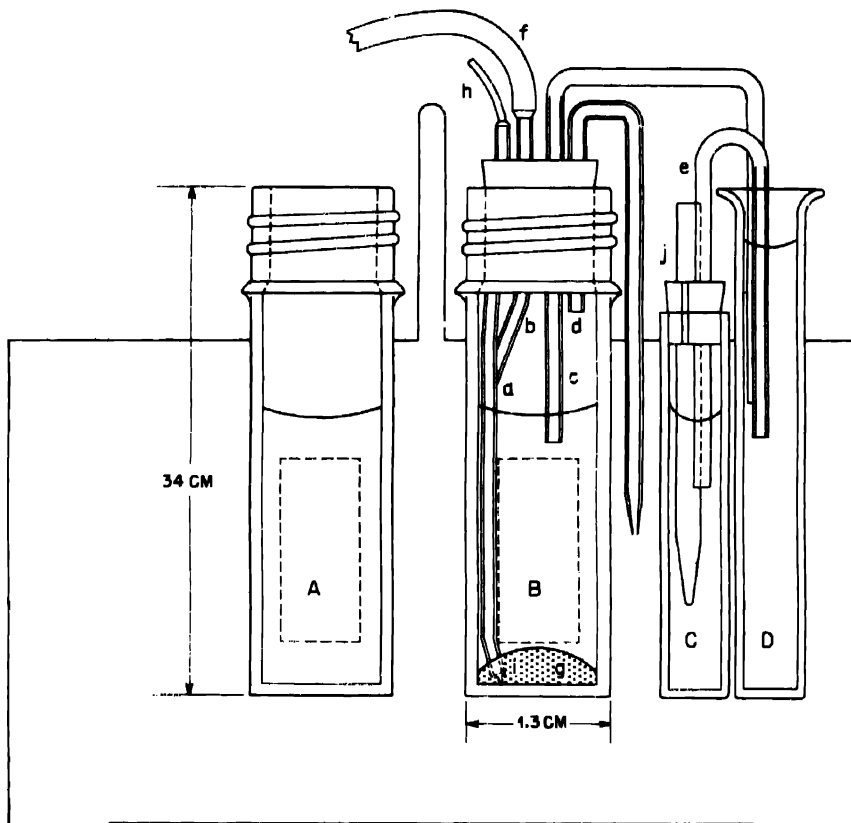


Fig. 1—Spectrophotometer electroreduction cell.

The micro-scale reduction cell employed for the preparation of Np(III) consisted of a 1-cm Corex spectrophotometer absorption cell with airtight connections (Fig. 1). The complete electrolytic apparatus was mounted in a Beckman spectrophotometer cell holder for convenient transfer to the spectrophotometer that was used for determining neptunium concentrations. Cells A and B are 1-cm absorption cells to which cylindrical, glass, threaded tops of 1 cm inside diameter were fastened with DeKhotinsky cement to prevent loss of solution by evaporation. Cell A, the spectrophotometer blank, contains dilute hydrochloric acid. Cell B is the neptunium-reduction cell,

which was closed by a small cork. Glass capillaries of 1 mm inside diameter are marked a, b, c, d, and e. Tube a is filled with mercury to make electrical contact with a copper-strand lead h and a platinum wire i in the tip, which in turn contacts the mercury-pool cathode g. Tube b is a nitrogen inlet, the tip of which (not shown) projects down into the solution. Tube f is a short section of flexible plastic tubing for connection to a nitrogen supply. Tube c is a saturated potassium chloride-agar bridge. Tube d is a vent, the tip of which extends below the solution level to prevent escape of the hydrogen-nitrogen blanket over the solution. All tubes in cell B were sealed into the cork with DeKhotinsky cement. Cell D contains saturated potassium chloride and is the central compartment for agar bridge connections. The potential of the neptunium solution in cell B was measured by inserting a saturated potassium chloride-agar bridge connected to an exterior calomel electrode (not shown) into cell D and making connection through the copper lead h. Cell C is the anode compartment containing dilute hydrochloric acid, and it is connected to D by the agar bridge e. The graphite anode j is a section of 2-mm soft pencil lead. A slit in the cork served as a chlorine vent. The spectrophotometer cell holder is shown in outline in Fig. 1. The approximate area of the slit apertures is indicated by the dashed rectangles in the absorption cells. A strip of ruled graph paper (not shown) attached to the back of cell B and above the slit aperture was calibrated to serve as a volume indicator.

A 1.5-ml volume of 0.00752M Np(IV) solution in 1.63M HCl was placed in cell B, and the cork was sealed with ceresin wax. Oxygen was removed by bubbling pure nitrogen saturated with water vapor through the solution for 10 min before the electrolysis. The solution was reduced by electrolyzing with a current density of approximately 8 ma/sq cm. An applied potential of 45 volts was required to maintain the current density. Nitrogen was continuously bubbled in to stir the solution and to assist in maintaining an oxygen-free atmosphere. The reduction was stopped periodically, and the nitrogen inlet and vent were disconnected and sealed with drops of rubber cement to permit insertion of the holder into the spectrophotometer. The extent of reduction was determined by observing the decrease in the 723-m $\mu$  absorption band of Np(IV). Since the electrical energy put into the cell was almost entirely converted by hydrogen evolution, the change in hydrochloric acid concentration was computed from the total number of coulombs that were passed through the cell. The solution was electrolyzed for a total of 1,278 ma-min, resulting in a reduction of the hydrochloric acid concentration to 0.96M (no volume change perceptible). The optical density of the 725-m $\mu$  band had been reduced

to 16 per cent of the value before electrolysis. The nitrogen inlet and vent were sealed, and the complete absorption spectrum of the solution was measured over the range of 350 to 1050 m $\mu$ . Over a period of 2 hr during the measurement of the absorption spectrum, the optical density at 723 m $\mu$  increased by only 1 per cent of the peak value.

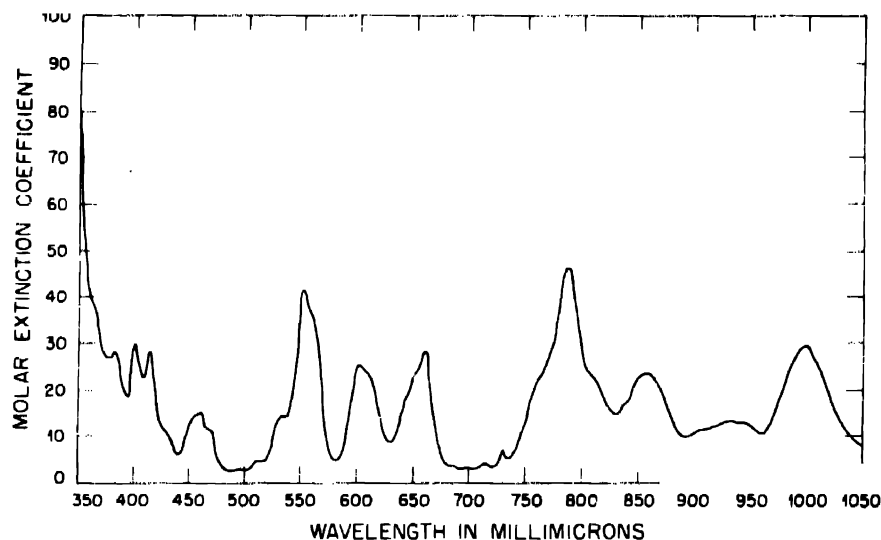


Fig. 2—Absorption spectrum of neptunium(III).

A few bubbles of air were blown through the solution, and the nitrogen inlet and vent were left open. Measurements of the 723-m $\mu$  absorption-band density and emf of the neptunium cell vs. a saturated calomel electrode were made and plotted against time. The 723-m $\mu$  absorption-band density was observed to increase steadily over a period of 5 hr to the maximum value of the pure Np(IV) solution that was observed before the electrolysis. The measured potentials were very stable and shifted slowly to less-positive values as the oxidation proceeded. At the completion of the experiment, radiometric assays showed the concentration of the neptunium to be the same as before the electrolysis.

### 3. CALCULATIONS AND RESULTS

The color of the Np(III) solution was pale purple, similar to that of U(III) and Pu(III). From a graph of the complete absorption spectrum measured immediately after the electrolysis, the amount of Np(IV) present in the solution was estimated by a series of approximations

from the measured optical densities over the range of 700 to 750 m $\mu$ . It was estimated that 87 per cent of the Np(IV) had been reduced to Np(III). The Np(III) absorption spectrum reproduced in Fig. 2 was obtained by subtracting the Np(IV) contribution at each wavelength of the measured spectrum. The principal absorption peaks and their molar extinction coefficients are listed in Table 1.

Table 1 — Principal Absorption Bands of Neptunium(III)

Wavelength, m $\mu$	Molar extinction coefficient	Wavelength, m $\mu$	Molar extinction coefficient
382	28.5	602	25.5
402	30.0	661	29.0
416	29.0	788	46.5
462	15.0	857	23.5
553	41.5	1,000	29.5

The optical density of the solution at the time of emf measurement was obtained by interpolation from the density-time graph. Concentrations of Np(III) and Np(IV) were obtained from the equation

$$\frac{D - E_{\text{III}} C}{E_{\text{IV}} - E_{\text{III}}} = C_{\text{IV}} \quad (1)$$

where  $C$  = total neptunium concentration

$D$  = measured density at 723 m $\mu$

$d_{\text{III}}$  = density of Np(III) at 723 m $\mu$

$d_{\text{IV}}$  = density of Np(IV) at 723 m $\mu$

$E_{\text{III}}$  = molar extinction coefficient of Np(III) at 723 m $\mu$

$E_{\text{IV}}$  = molar extinction coefficient of Np(IV) at 723 m $\mu$

$C_{\text{III}}$  = concentration of Np(III)

$C_{\text{IV}}$  = concentration of Np(IV)

$$C = C_{\text{III}} + C_{\text{IV}}$$

$$D = d_{\text{III}} + d_{\text{IV}}$$

$$d_{\text{III}} = E_{\text{III}} C_{\text{III}}$$

$$d_{\text{IV}} = E_{\text{IV}} C_{\text{IV}}$$

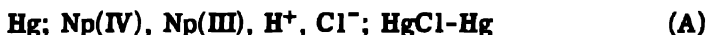
$$D = E_{\text{III}} C_{\text{III}} + E_{\text{IV}} C_{\text{IV}}$$

$$D = E_{\text{III}} (C - C_{\text{IV}}) + E_{\text{IV}} C_{\text{IV}}$$

$$D = E_{\text{III}} C + (E_{\text{IV}} - E_{\text{III}}) C_{\text{IV}}$$

The constants  $E_{\text{III}}$  and  $E_{\text{IV}}$  must be evaluated to solve the concentration equations. The measured optical density of the Np(IV) 723-m $\mu$  band has been found independently<sup>11</sup> to conform to Beer's law over

the range of concentrations of Np(IV) in this experiment; the molar extinction coefficient is equal to 126. A value for the molar extinction coefficient  $E_{\text{III}}$  of 4.2 was obtained by subtracting the estimated peak height at 723 m $\mu$  contributed by Np(IV) in a complete spectrum measured after reduction. Concentrations of Np(III) and Np(IV) at the times of emf measurement were calculated directly from the interpolated density at 723 m $\mu$  by using the expression for C and Eq. 1. The formal potential,  $E_f$ , of the Np (III)/(IV) couple was determined from the measured potential, E, of cell A and calculated concentrations by the use of Eq. 2.



$$E_f = -E_{\text{measured}} + E_{\text{Hg-HgCl}}^0 + 0.0591 \log \frac{[\text{Np(IV)}]}{[\text{Np(III)}]} \quad (2)$$

where  $E_{\text{Hg-HgCl}}^0 = -0.245$  volt (standard potential of saturated calomel electrode). The neptunium solution was found to be negative with respect to the calomel cell, and  $E_{\text{measured}}$  was taken as positive. In Table 2 are summarized the density and potential observations and calculations of concentrations and the formal potential.

The average formal potential for the Np (III)/(IV) couple obtained from these data is  $-0.137 \pm 0.001$  volt.

#### 4. DISCUSSION OF RESULTS

Although no direct titration was performed to determine the oxidation number of the neptunium reduced in the nitrogen apparatus, the constancy of the formal potential calculation based on a one-electron change over a seventyfold range of Np (IV)/(III) ratios is sufficient evidence that the reduced plutonium was in the tripositive state. This conclusion is in agreement with the polarographic results obtained by Watters.<sup>1</sup> It should also be noted that the constancy of the calculated formal potential is proof of the reversibility of the Np (III)/(IV) couple. This result differs from the polarographic behavior observed by Watters for a sulfate solution. No explanation for the difference in behavior can be given at present.

The oxidation potential of  $-0.137$  volt in 1M HCl obtained in this work is in satisfactory agreement with the value of  $+0.1$  volt estimated by Watters for 0.12M H<sub>2</sub>SO<sub>4</sub> solution. Preferential complexing of the tetrapositive ions by sulfate has been found by Heal<sup>3</sup> to shift the potential of the U (III)/(IV) couple  $+0.15$  volt in 0.5M H<sub>2</sub>SO<sub>4</sub> and by Ames and Hindman<sup>4</sup> to shift the potential of the Pu (III)/(IV) couple  $+0.08$  volt in 0.15M H<sub>2</sub>SO<sub>4</sub> relative to the potentials in noncomplexed solutions.

Table 2—Measurements of Oxidation Potential of Np (III)/(IV) Couple

Time, min	Density at 723 m $\mu$	Np(IV), M $\times 10^3$	Np(III), M $\times 10^3$	$\frac{\text{Np(IV)}}{\text{Np(III)}}$	$-\Delta E$	$E_{\text{meas.}}$ , volts	$E_f$ , volts
0	0.157	1.03	6.38	0.162	0.047	0.154	-0.138
1.4	0.158	1.04	6.37	0.163	0.047	0.154	-0.138
28.6	0.184	1.26	6.15	0.205	0.041	0.146	-0.140
29.3	0.185	1.27	6.14	0.207	0.040	0.145	-0.140
42.7	0.236	1.68	5.73	0.293	0.031	0.140	-0.136
43.5	0.239	1.71	5.70	0.300	0.031	0.140	-0.136
54.7	0.266	1.93	5.48	0.352	0.027	0.136	-0.136
55.8	0.270	1.96	5.45	0.359	0.026	0.135	-0.136
56.8	0.274	2.00	5.41	0.370	0.026	0.135	-0.136
68.8	0.314	2.32	5.09	0.456	0.020	0.129	-0.136
69.5	0.315	2.33	5.08	0.459	0.020	0.128	-0.137
75.2	0.332	2.47	4.94	0.500	0.018	0.126	-0.137
75.7	0.334	2.49	4.92	0.506	0.018	0.126	-0.136
81.1	0.357	2.68	4.73	0.567	0.015	0.123	-0.137
81.8	0.360	2.70	4.71	0.574	0.014	0.123	-0.136
88.0	0.384	2.90	4.51	0.643	0.011	0.121	-0.135
88.6	0.387	2.92	4.49	0.651	0.011	0.121	-0.135
100.4	0.436	3.33	4.08	0.817	0.005	0.115	-0.135
100.9	0.438	3.34	4.07	0.821	0.005	0.115	-0.135
114.7	0.484	3.72	3.69	1.01	0.000	0.108	-0.137
115.3	0.487	3.75	3.66	1.02	0.000	0.108	-0.136
127.1	0.543	4.21	3.20	1.31	0.007	0.102	-0.136
143.5	0.589	4.58	2.83	1.62	0.012	0.096	-0.137
143.9	0.590	4.59	2.82	1.63	0.013	0.096	-0.136
155.5	0.639	4.99	2.42	2.06	0.019	0.089	-0.137
155.9	0.640	5.00	2.41	2.07	0.019	0.089	-0.137
161.9	0.661	5.17	2.24	2.31	0.022	0.083	-0.140
162.5	0.666	5.21	2.20	2.36	0.022	0.083	-0.140
170.6	0.707	5.55	1.86	2.98	0.028	0.080	-0.137
178.1	0.740	5.82	1.59	3.66	0.033	0.075	-0.137
179.6	0.743	5.85	1.56	3.75	0.034	0.074	-0.137
191.3	0.778	6.13	1.28	4.79	0.040	0.067	-0.138
192.5	0.781	6.16	1.25	4.92	0.041	0.065	-0.138
192.9	0.782	6.17	1.24	4.98	0.041	0.064	-0.140
200.2	0.812	6.41	1.00	6.41	0.048	0.060	-0.137
200.6	0.813	6.43	0.98	6.56	0.048	0.060	-0.137
201.5	0.814	6.43	0.98	6.56	0.049	0.058	-0.138
203.0	0.816	6.45	0.95	6.79	0.049	0.056	-0.140
203.4	0.817	6.46	0.94	6.87	0.050	0.056	-0.139
204.5	0.818	6.46	0.94	6.87	0.050	0.055	-0.140
212.6	0.849	6.72	0.69	9.75	0.058	0.049	-0.138
212.9	0.850	6.73	0.68	9.80	0.059	0.049	-0.137
213.8	0.852	6.74	0.67	10.05	0.059	0.047	-0.139
214.1	0.853	6.75	0.66	10.20	0.060	0.047	-0.138
215.2	0.856	6.78	0.63	10.8	0.061	0.045	-0.139
215.6	0.858	6.79	0.62	10.9	0.061	0.045	-0.139

In view of the instability of Np(III), the earlier investigators<sup>5-7</sup> of neptunium when using trace concentrations of the Np<sup>239</sup> isotope probably never succeeded in forming the tripositive state in solution because sufficiently powerful reducing agents were not used.

The formal potentials in 1.0M HCl for the (III)/(IV) couples of uranium, neptunium, and plutonium measured under similar conditions are given in Table 3. The intermediate stability of the neptunium couple is in agreement with the theory that the tripositive ions increase in stability with increasing atomic number in this series as in the 4f series (see "actinide" hypothesis, reference 10).

Table 3—Formal Potentials of (III)/(IV) Couples in 1M HCl

Couple	$E_I$ , volts	Reference
$U(\text{III}) \rightleftharpoons U(\text{IV}) + e^-$	0.633	8
$\text{Np}(\text{III}) \rightleftharpoons \text{Np}(\text{IV}) + e^-$	-0.137	
$\text{Pu}(\text{III}) \rightleftharpoons \text{Pu}(\text{IV}) + e^-$	-0.965	9

## 5. SUMMARY

The formal potential of the Np (III)/(IV) couple was found to be -0.137 volt in 1.0M HCl. The Np(III) ion is intermediate in stability between U(III) and Pu(III) in aqueous solution. The couple behaved reversibly over a seventyfold change of ratio of concentration of Np(IV) to Np(III). Details of the absorption spectrum of the aqueous Np(III) ion are given.

## REFERENCES

1. J. I. Watters, Metallurgical Laboratory Memorandum MUC-JIW-53 (Feb. 8, 1945).
2. J. C. Hindman, L. B. Magnusson, and T. J. LaChapelle, Chemistry of neptunium. The oxidation state of neptunium in aqueous solution. Paper 15.1, this volume.
3. H. G. Heal, Canadian Report MC-95 (Oct. 20, 1944).
4. D. P. Ames and J. C. Hindman, unpublished data.
5. J. W. Gofman and R. E. Connick, Metallurgical Project Report CN-239 (Aug. 15, 1942).
6. R. B. Duffield, Metallurgical Project Report CN-250 (Aug. 31, 1942).
7. E. L. King, Metallurgical Project Report CN-1134 (Dec. 1, 1943).
8. J. J. Howland and L. B. Magnusson, Metallurgical Project Report CN-2888 (May 1945).

9. J. J. Howland, K. A. Kraus, and J. C. Hindman, Metallurgical Project Report CK-1371 (March 1944).
10. G. T. Seaborg, Metallurgical Laboratory Memorandum MUC-GTS-858 (July 1944); Electronic structure of the heaviest elements, Paper 21.1, this volume.
11. J. C. Hindman, L. B. Magnusson, and T. J. LaChapelle, Chemistry of neptunium. Absorption spectrum studies of aqueous ions of neptunium, Paper 15.2, this volume.

## Paper 15.4

### CHEMISTRY OF NEPTUNIUM(V). FORMAL OXIDATION POTENTIALS OF NEPTUNIUM COUPLES<sup>†</sup>

By L. B. Magnusson, J. C. Hindman, and T. J. LaChapelle

#### 1. INTRODUCTION

The determination of the formal potential of the neptunium (III)/(IV) couple in 1M HCl is reported in another paper of this series.<sup>1</sup>

The oxidation of the tetrapositive oxidation state to the pentapositive or hexapositive state is not an electrode-reversible process in the case of either uranium<sup>2</sup> or plutonium,<sup>3</sup> the irreversibility of the reaction being attributed to the process of gaining or losing oxygen by the metallic ion. The behavior of the neptunium (IV)/(V) couple in hydrochloric and sulfuric acid solutions has been studied. As a consequence of a similar irreversibility of the couple as found for uranium and plutonium, values for the formal potentials of the couple in 1M HCl were necessarily calculated from measurements of solutions containing Np(V), Np(IV), Fe(III), and Fe(II) in equilibrium. A formal potential for the neptunium (IV)/(V) couple in 1.0M H<sub>2</sub>SO<sub>4</sub> has been calculated from measurement of the disproportionation equilibrium of neptunium(V).

Neptunium(III) and neptunium(IV) are thought to be simple cations in acid solutions of non-complex-forming anions by analogy with the corresponding states of uranium and plutonium, which have been more extensively studied.<sup>4</sup> The unique ions of this group, in which the elements are in the pentapositive and hexapositive oxidation states, however, are not so well understood. The fact that hexapositive uranium, neptunium, and plutonium all form insoluble compounds of the types

<sup>†</sup>Contribution from the Chemistry Division of the Metallurgical Laboratory, University of Chicago, now the Argonne National Laboratory.

Based on Metallurgical Project Reports CN-2767 (Mar. 27, 1945) and CN-3053 (June 1945) and unpublished data.

$\text{NaXO}_2(\text{C}_2\text{H}_2\text{O}_3)_3$  is evidence for the existence of the ion  $\text{XO}_2^{++}$ . A large quantity of other evidence has been accumulated<sup>4</sup> to show that both plutonium and uranium have aqueous ions of the form  $\text{XO}_2^{++}$ . The ions of the pentapositive oxidation states of uranium and plutonium are unstable with respect to disproportionation into the tetrapositive and hexapositive states, so that considerable difficulty is attached to studying the pentapositive state in these elements.

Heal<sup>2</sup> and Harris and Kolthoff<sup>5</sup> have obtained polarographic evidence for a reversible uranium (V)/(VI) couple and the existence of the ion  $\text{UO}_2^+$ . Similarly, the plutonium(V)/(VI) couple has been found to behave fairly reversibly, and evidence has been presented for the existence of a  $\text{PuO}_2^+$  ion.<sup>6,7</sup> Neptunium(V) has been found to be quite stable and, hence, should be extremely useful in an extensive study designed to furnish more information about the properties of ions of the pentapositive state. Measurements of the hydrogen-ion dependency and of the formal potentials of the neptunium (V)/(VI) couple have been made.

## 2. THE NEPTUNIUM (IV)/(V) COUPLE

**2.1 The Neptunium (IV)/(V) Couple in 1M HCl.** (a) Experimental Work. Two separate measurements of the couple in 1M HCl solution were attempted, using a silver-silver chloride reference electrode and a bright-platinum electrode. The observed potentials drifted to less positive values, with no indication of approaching constancy. The first reading obtained on inserting the electrodes in the solution was used to estimate the formal potential. The concentration of the neptunium(IV) was determined spectrophotometrically, and the concentration of neptunium(V) by difference.

More satisfactory estimates of the potential of the couple were obtained from measurements in a system involving Np(IV), Np(V), Fe(II), and Fe(III) in oxidation-reduction equilibrium. A preliminary experiment showed that Np(V) was not reduced quantitatively by Fe(II) in 1.04M HCl. A titration of 2.0 ml of 0.0042M Np(VI) in 1.00M HCl was therefore made with a 1.00M Fe(II) solution in 1.00M HCl. The Fe(II) solution was prepared by dissolving a weighed quantity of iron in hydrochloric acid. The reduction was allowed to proceed to equilibrium after each addition of Fe(II). The reduction of Np(VI) to Np(V) was instantaneous, but for the 0.0042M Np(V) solution the reduction to Np(IV) took approximately 80 min to reach equilibrium after each addition of Fe(II). The titration was followed spectrophotometrically. The concentration of Np(IV) was calculated from the optical density of the 723-m $\mu$  band, and the concentration of the Np(V) by difference.

The height of this band for the completely reduced Np(IV) solution was obtained by adding stannous chloride after the completion of the Fe(II) titration.

In addition to the titration curve obtained above, two additional experiments were performed in the same manner. Potential readings were taken at two ratios of Np(IV) to Np(V) in each experiment.

Table 1 — Potential Measurements on the Neptunium (IV)/(V) Couple in 1.00M HCl, with 0.00423M Np at 25°C

Fraction Np as Np(IV)	[Np(V)]/[Np(IV)]	E (obs.), volts	E <sub>f</sub> , volts
0.1655	5.042	0.530	-0.734
0.3327	2.006	0.510	-0.737
0.5586	0.7902	0.487	-0.738
0.6913	0.4465	0.471	-0.732
0.9137	0.0944	0.440	-0.746
			-0.737 (av.)

Table 2 — Potential Measurements on Neptunium (IV)/(V) Couple in 1.00M HCl at 25°C

M <sub>Np</sub>	Fraction Np as Np(IV)	[Np(V)]/[Np(IV)]	E (obs.), volts	E <sub>f</sub> , volts
0.00366	0.8326	0.1674	0.453	-0.739
0.00366	0.9612	0.0388	0.423	-0.750
0.00274	0.5967	0.6759	0.491	-0.746
0.00274	0.8855	0.1293	0.430	-0.727
0.00396	0.8019	0.2470	0.474	-0.737
0.00396	0.9189	0.0883	0.436	-0.725
				-0.737 (av.)

(b) Results. The drifting emf showed clearly that the couple is not readily reversible at the platinum electrode. The estimated potential of the couple based on the initial observed emf of the two solutions was -0.68 and -0.72 volt, respectively.

From the titrations of Np(V) with Fe(II), a number of values of the couple potential have been obtained. The data are summarized in Tables 1 and 2. The average of the data gives  $-0.737 \pm 0.006$  volt for the neptunium (IV)/(V) couple in 1M HCl.

**2.2 The Neptunium (IV)/(V) Couple in 1M H<sub>2</sub>SO<sub>4</sub>.** (a) Experimental. Attempts were made to measure the oxidation potential in 1.0M H<sub>2</sub>SO<sub>4</sub> solutions containing various ratios of Np(IV) to Np(V), using a saturated potassium chloride-mercury-mercurous chloride reference

electrode. The emf of the cell was not steady upon insertion of the platinum electrode but drifted to lower values. After several hours of standing, the emf appeared to have reached a constant value. Stirring the solution however, resulted in erratic changes of the emf.

A limiting measurement on the potential of the neptunium (IV)/(V) couple in sulfuric acid was obtained in a solution containing Np(IV), Np(V), Fe(II), and Fe(III) ions in oxidation-reduction equilibrium. A slight excess of ferrous ion was added to a Np(V) sulfate solution, and the reduction was allowed to proceed to equilibrium. The potential of the cell relative to the saturated potassium chloride-mercurous chloride electrode was then measured, and the absorption spectrum was taken for the purpose of estimating any Np(V) remaining.

(b) Calculations and Results. The few attempts to measure the neptunium (IV)/(V) couple potential in sulfate solution have shown that the couple is not readily reversible at the platinum electrode. The measured potentials are unstable, and the formal potentials, calculated at different Np(V) to Np(IV) ratios, vary as much as 40 mv.

The potential of the couple in 1M H<sub>2</sub>SO<sub>4</sub> was delimited as follows: At a measured potential of 0.543 volt relative to the saturated calomel electrode in a solution containing ferrous, ferric, and neptunium ions, spectrophotometric examination showed no detectable Np(V) present. If the limit of detection of Np(V) is arbitrarily set at 1 per cent, the potential limit is set by the equation

$$E_f = -E + E_{Hg-HgCl}^0 + 0.059 \log 0.05 \quad (1)$$

Solution of equation 1 gives -0.91 volt as the most positive value possible for the formal potential of the couple.

A reliable value for the couple may be obtained from the disproportionation equilibrium<sup>8</sup> of Np(V) in 1.0M H<sub>2</sub>SO<sub>4</sub> and the formal potential of the neptunium (V)/(VI) couple (see Sec. 3).



$$K_{25} = \frac{[\text{Np(IV)}][\text{Np(VI)}]}{[\text{Np(V)}]} \quad (3)$$

$$K_{25} = 0.024 \quad (4)$$

The formal potential of the neptunium (V)/(VI) couple in 1.0M H<sub>2</sub>SO<sub>4</sub> is -1.082 volts, and the calculated value of the neptunium (IV)/(V) couple is -0.99 volt.

### 3. THE FORMAL POTENTIAL OF THE NEPTUNIUM (V)/(IV) COUPLE AND ITS DEPENDENCE ON HYDROGEN-ION CONCENTRATION

3.1 Experimental. The couple was measured in 1.0M HCl solution during the course of a stannous ion reduction of Np(VI). Cell A consisted of a bright-platinum-wire anode and a silver-silver chloride cathode



The neptunium was reduced by adding an aliquot of 0.05M SnCl<sub>2</sub> and measuring the potential after equilibrium was established, as judged by a constant optical density for the 984-m $\mu$  Np(V) absorption band. Reduction of Np(VI) by chloride caused a slow falling off of the measured potential, so the first reading obtained upon inserting the electrode was taken as most nearly representing the true potential.

Permanganate-ion titration of Np(V) provided various ratios of Np(VI) to Np(V) for the calculation of the potential of the couple in 1.0M H<sub>2</sub>SO<sub>4</sub>. The potential of the solution was determined in reference to a mercurous sulfate cathode with bright-platinum anode and a 1.0M H<sub>2</sub>SO<sub>4</sub> bridge, cell B.



The observed potentials were stable.

The hydrogen-ion dependency of the neptunium (V)/(VI) couple was measured in constant nitrate-ion concentration and varying hydrogen ion from 0.12M to 1.02M. From a 0.6M HNO<sub>3</sub> stock solution, 0.0093M in Np, 100-microliter portions were diluted to the constant volume of 0.5 ml with appropriate volumes of 5M HNO<sub>3</sub>, 1.12M NaNO<sub>3</sub>, and water to establish the desired range of hydrogen-ion compositions (see Table 3).

The cell used, cell C, was



Since a 20-mv variation in potential was found between the 0.12M and 1.02M hydrogen-ion solutions, an attempt was made to determine the relative junction-potential effects by comparing the potential difference between two saturated calomel electrodes. One calomel cell used was the asbestos-wick type, whereas the other, which was used in the neptunium cell, made connection to a middle compartment by a

saturated potassium nitrate bridge. The composition of the middle-compartment solution was changed from 0.1M H<sup>+</sup> to 1.0M H<sup>+</sup>, but a constant nitrate composition of 1.0M was maintained in a manner

Table 3—Hydrogen-ion Dependence of the Neptunium (V)/(VI) Couple

[Np(VI)]/[Np(V)]	[NO <sub>3</sub> ] moles/liter	H <sup>+</sup> , moles/liter	E (obs.), volts
0.96	1.02	1.02	0.892
0.96	1.02	0.62	0.900
0.96	1.02	0.42	0.904
0.96	1.02	0.22	0.910
0.96	1.02	0.12	0.912

analogous to the neptunium couple measurements. The make-up of cell D was



In Table 4 the measured potential of the saturated calomel half cell connected through the nitrate bridge is given for the two middle-compartment solutions.

Table 4—Relative Junction Potential of Saturated Potassium Nitrate Bridge

Solution	Potential, volts
1.0M HNO <sub>3</sub> , 1.0M NO <sub>3</sub> <sup>-</sup>	+0.0031
0.1M HNO <sub>3</sub> , 1.0M NO <sub>3</sub> <sup>-</sup>	-0.0072

**3.2 Calculations and Results.** The formal potential of the neptunium (V)/(VI) couple in 1.0M HCl was calculated in two ways from the data obtained. The results of the first method are given in Table 5. The ratios of Np(VI) to Np(V) for the emf equation were obtained directly from the density of the 983-m $\mu$  band of Np(V) and the volume of the solution according to the following:

$$\text{micromoles of Np(V)} = \frac{dV}{cE} \quad (5)$$

$$\text{micromoles of Np(VI)} = \text{total micromoles of Np} - \frac{dV}{cE} \quad (6)$$

where     $d$  = optical density of 983-m $\mu$  band  
            $E$  = molar extinction coefficient of 983-m $\mu$  band = 201  
            $V$  = volume of solution, microliters  
            $c$  = spectrophotometer cell length = 0.5 cm

The formal potential,  $E_f$ , was calculated from the equation

$$E_f = E_{Ag-AgCl} + 0.0591 \log a_{Cl^-} - E \text{ (meas.)} + 0.0591 \log \frac{[Np(VI)]}{[Np(V)]} \quad (7)$$

where  $E_{Ag-AgCl} = -0.222$  volt (standard potential of silver-silver chloride electrode)

$$a_{Cl^-} = 0.84 \text{ (mean activity of Cl}^- \text{ in 1M HCl)}$$

Although it is believed that the cell behaved reversibly in these measurements, two complicating factors reduced the precision of measurement: first, Np(VI) is slowly reduced by chloride in the presence of platinum, and second, the reduction of Np(VI) by Sn(II) is rather slow, so that attainment of equilibrium is somewhat uncertain.

The second method of utilizing the data gave more consistent results (see Table 6). The spectrophotometric densities were disregarded except for determination of equilibrium after each addition of stannous chloride solution. The amount of Np(VI) in the solution was obtained by subtraction according to the reaction equivalence



A few measurements of the molar extinction coefficient of the Np(V) 983-m $\mu$  band, at different concentrations of Np(V), have shown that the extinction coefficient varies with concentration; therefore, the potential calculations based on optical density are not reliable. The better agreement in the calculated values obtained by the second method places the formal potential for the neptunium (V)/(VI) couple in 1.0M HCl at  $-1.135 \pm 0.010$  volts.

Table 7 gives the spectrophotometrically determined concentrations of Np(V) and Np(VI), the observed potential,  $E$ , and the calculated formal potential,  $E_f$ , obtained in the potentiometric titration of Np(V) with 0.1N KMnO<sub>4</sub> in 1.0M H<sub>2</sub>SO<sub>4</sub>. The formal potential was calculated from the equation

$$E_f = -E - 0.673 + 0.059 \log \frac{[Np(VI)]}{[Np(V)]} \quad (9)$$

The term,  $-0.673$  volt, is believed to be a close approximation to the potential of the mercurous sulfate electrode referred to the standard

Table 5—Formal Oxidation Potential for the Neptunium (V)/(VI) Couple in  
1M HCl† (Total Np = 2.78 micromoles)

Np solution, microliters	$d_{405}$	Np(V), micromoles	Np(VI), micromoles	E (obs.), volts	$E_f$ , volts
500	0.189	0.94	1.84	0.912	-1.135
502	0.239	1.20	1.58	0.904	-1.137
503	0.292	1.47	1.31	0.900	-1.137
506	0.378	1.91	0.87	0.891	-1.151
509	0.450	2.29	0.49	0.875	-1.155

†Three additional readings were discarded because of uncertainty as to the volume of the solution.

Table 6—Formal Oxidation Potential for the Neptunium (V)/(VI)  
Couple in 1M HCl

SnCl <sub>2</sub> , micromoles	Np(V), micromoles	Np(VI), micromoles	E (obs.), volts	$E_f$ , volts
0	0.96	1.82	0.912	-1.135
0.076	1.11	1.67	0.904	-1.134
0.152	1.26	1.52	0.900	-1.135
0.303	1.57	1.21	0.891	-1.138
0.454	1.87	0.91	0.875	-1.134
0.606	2.17	0.61	0.863	-1.136
0.750	2.46	0.32	0.842	-1.135
0.91	2.78	0		

Table 7—Formal Oxidation Potential for the Neptunium (V)/(VI)  
Couple in 1.0M H<sub>2</sub>SO<sub>4</sub>†

Np(VI), molarity	Np(V), molarity	$-0.059 \log [Np(VI)/[Np(V)]$	E (obs.), volts	$E_f$ , volts
0.00084	0.00676	0.0536	0.356	-1.0826
0.00129	0.00558	0.0376	0.3665	-1.0771
0.00242	0.00474	0.0173	0.3867	-1.0770
0.00334	0.00379	0.0033	0.4060	-1.0823
0.00434	0.00256	-0.0136	0.4298	-1.0832
0.00546	0.00128	-0.0372	0.4478	-1.0836
0.00601	0.00065	-0.0571	0.4679	-1.0838
0.00628	0.00034	-0.075	0.487	-1.083

†The average potential for the neptunium (V)/(VI) couple in 1.0M H<sub>2</sub>SO<sub>4</sub> is -1.082 ± 0.002 volts.

hydrogen electrode in 1.0M H<sub>2</sub>SO<sub>4</sub>. The mean activity coefficients for sulfuric acid calculated by Harned and Hamer<sup>9</sup> cannot be used in evaluating the mercurous sulfate electrode potential at finite sulfuric acid concentrations because of incomplete dissociation. It is necessary, therefore, to make some reasonable guesses to obtain a value for the mercurous sulfate electrode potential. Since the dissociation constant<sup>10</sup> for HSO<sub>4</sub><sup>-</sup> = H<sup>+</sup> + SO<sub>4</sub><sup>2-</sup> is only about 0.01, the hydrogen-ion concentration in 1m H<sub>2</sub>SO<sub>4</sub> is very nearly 1m and the sulfate-ion concentration is about 0.01m. The ionic strength in 1m H<sub>2</sub>SO<sub>4</sub> should be, therefore, close to unity. The mean activity coefficient<sup>11</sup> of hydrogen ion in 1m HCl (ionic strength unity) is 0.84.

Hamer<sup>12</sup> observed the potential of the mercurous sulfate electrode referred to the hydrogen electrode to be 0.676 volt in 1m H<sub>2</sub>SO<sub>4</sub>. Neglecting the difference between the molal and molar scales and assuming that the activity coefficient of hydrogen ion is 0.84, it may be calculated that the mercurous sulfate electrode potential is -0.673 volt referred to the standard hydrogen electrode in 1.0M H<sub>2</sub>SO<sub>4</sub>.

The hydrogen-ion dependency of the neptunium (V)/(VI) couple potential is calculated for the nitrate solution from the emf of cell C by the equation

$$E_f = -E \text{ (meas.)} + E_{Hg-HgCl} + E_j + 0.059 \log \frac{[Np(VI)]}{[Np(V)]} + 0.059 \log [H^+]^x \quad (10)$$

As the experiment was carried out, E<sub>f</sub> or E (meas.) should remain constant unless the liquid-junction potential, E<sub>j</sub>, varies or the couple has a hydrogen-ion dependence. In the latter case, E<sub>f</sub> should become more negative by 120 or 240 mv for a tenfold increase in hydrogen ion concentration, depending on whether equation b or c represents the process



Examination of the data in Table 3 shows that the observed change of potential is small, 20 mv, and of the wrong sign to be explained by either process b or c. This result indicates that there may be a considerable liquid-junction effect in cell C. A simple explanation for this observed change in potential of cell C in going from 0.1M H<sup>+</sup> to 1.0M H<sup>+</sup> may be given on the basis of the high mobility of the hydrogen

ion as contrasted with the other ions involved at the junctions. Cell D serves to test this hypothesis.

The only variables in cell D were the hydrogen-ion and sodium-ion concentrations, the nitrate-ion concentration being held constant. Since the mobility of the sodium ion is approximately the same as that of the potassium ion, it may safely be assumed in this case that the variations in junction potential may be attributed, in the main, to the hydrogen ion. Since the right-hand electrode of the cell as written becomes more positive with increasing hydrogen-ion concentration, the saturated potassium nitrate bridge must be less effective in opposing hydrogen-ion diffusion than the saturated potassium chloride bridge. The potentials at the two bridge junctions due to hydrogen ion are in opposition so that the observed potential variation of about 10 mv is a minimum value for the actual variation of the junction potential between saturated potassium nitrate and 0.1M to 1.0M  $H^+$  (Table 4). The emf of cell C was observed (Table 3) to become smaller with increasing hydrogen-ion concentration, corresponding to the tendency of the potential of the calomel electrode connected through the nitrate bridge to become more positive. The observed variation of 20 mv is probably almost entirely due to change in the liquid-junction potential.

#### 4. DISCUSSION

No attempt has been made to apply corrections for liquid junctions in the derivations of formal potentials from emf measurements of cells including salt bridges. Only in the case of the measurements of the potentials involved in the determination of the hydrogen-ion dependency of the neptunium (V)/(VI) couple has an attempt been made to estimate the magnitude of the liquid junction. The measurements made in the latter case have been found to be consistent with the view that the change in potential observed with the change in hydrogen-ion concentration can be accounted for by a change in liquid-junction potential.

Since the neptunium (IV)/(V) couple is irreversible in both 1M HCl and 1M  $H_2SO_4$ , direct potentiometric measurements cannot be made. The irreversible behavior of the (IV)/(V) couples is exhibited by both uranium<sup>2</sup> and plutonium.<sup>13</sup> It is considered probable that the explanation of this behavior lies in the mechanism of oxygenation of the ions of the pentapositive state. X-ray diffraction studies indicate that the oxygens attached to the hexapositive "yl" ions of this series are bonded to the central metal atom by partially covalent forces. This is probably true in the case of the pentapositive ions as well since the (V)/(VI) couples are reversible. The irreversibility of the (IV)/(V)

couples would then be attributable to the very slow removal of these covalent-bonded oxygens at a noble-metal electrode. A similar behavior has been observed in the case of tungsten and molybdenum solutions. Whereas the (V)/(VI) couples are reversible or partially reversible for both these elements, the (VI)/(V) couples are irreversible in hydrochloric acid solutions.<sup>14,15</sup> In each case the (IV)/(V) couple becomes reversible when the metal forms covalent octocyanide-complex ions.<sup>16</sup>

The values of the formal potentials, -0.74 volt in 1M HCl and -0.99 volt in 1M  $H_2SO_4$ , are approximations, which are considered to be accurate to within about 0.01 volt. The shift in potential from -0.74 volt in chloride to -0.99 volt in sulfate is also consistent with the expected preferential complex formation of the  $Np^{+4}$  ion with respect to the oxygenated  $NpO_2^+$  ion.

The neptunium (V)/(VI) couple potential has been found to be -1.135 volts in 1M HCl, -1.14<sup>†</sup> volts in 1M  $HNO_3$ , and -1.082 volts in 1M  $H_2SO_4$ . Investigation of the hydrogen-ion behavior of the couple in nitrate solution has further revealed that the potential of the couple is independent of hydrogen-ion concentration between 0.1M  $H^+$  and 1M  $H^+$ . Several lines of evidence have led to the conclusion that the hexapositive ions of both uranium and plutonium are "yl" ions in acid solution<sup>4</sup> having the formula  $XO_2^{++}$ . Isolation of the salt  $NaNpO_2(C_2H_3O_2)_3$ , analogous to  $NaUO_2(C_2H_3O_2)_3$  and  $NaPuO_2(C_2H_3O_2)_3$ , has supplied partial evidence that a hexapositive ion of neptunium, of the formula  $NpO_2^{++}$ , also exists. In addition both the uranium (V)/(VI) and plutonium (V)/(VI) couples<sup>2,4</sup> are hydrogen-ion independent in the same range of acid concentrations as is the neptunium (V)/(VI) couple. This behavior is interpreted to mean that the pentapositive ions in moderately acid solution probably have the formula,  $XO_2^+$ .

The 50-mv difference in the potential of the neptunium (V)/(VI) couple in sulfuric acid from that in either nitric or hydrochloric acid, both of which probably complex the  $Np(V)$  or  $Np(VI)$  ions only slightly, can be interpreted as evidence for complex formation involving  $Np(VI)$  and sulfate ion. This view is supported by the transference experiments of McLane, who showed that  $Np(VI)$  forms a negatively charged complex ion even in concentrations of sulfuric acid as low as 0.1M.<sup>17</sup>

Direct observation of the stabilities of the various oxidation states are in agreement with what would be expected on the basis of the oxidation potentials.  $Np(III)$  in 1M HCl is extremely unstable to air oxi-

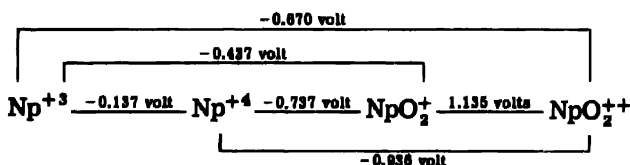
<sup>†</sup>This value is not strictly comparable to the formal potentials in hydrochloric or sulfuric acid, since a more complex system of liquid junctions was present in the cell used for measurement.

dation and can be maintained in solution only by using precautionary measures to exclude oxygen. Both the tetrapositive and pentapositive states have been found to be stable in 1.0M HCl over periods of days. From the potential of the neptunium (IV)/(V) couple of -0.74 volt, air oxidation of Np(IV) to Np(V) can occur, although the reaction is evidently slow. Np(V) would be expected to be very stable in hydrochloric acid on the basis of the potential measurement. This is in agreement with the observed facts. Np(VI) is not stable in hot hydrochloric acid, being slowly reduced to Np(V). Although the reaction with hydrochloric acid is very slow at room temperatures, contact with platinum catalyzes the reduction so that Np(V) is produced at an appreciable rate at the platinum surface. Watters' measurement of the neptunium (III)/(IV) couple indicates that Np(III) will reduce hydrogen ion in sulfuric acid and, therefore, probably could not be maintained long in solution even if air were excluded. Np(IV) and Np(V) appear to be quite stable in 1.0M  $H_2SO_4$ . Np(III) undoubtedly cannot be produced in a nitrate solution, and Np(IV) is slowly oxidized to Np(V) in nitric acid. Np(V) solutions have been prepared in 1M  $HNO_3$  with no spectrophotometric evidence of disproportionation into Np(IV) and Np(VI). It is expected that the Np (IV)/(V) potential in 1M  $HNO_3$  is close to that in hydrochloric acid.

Np(V) disproportionates to a considerable extent in 1.0M  $H_2SO_4$  because of complexing of Np(IV) and Np(VI) by the sulfate ion. In high concentration of sulfuric acid Np(V) would be unstable since, in addition to the sulfate effect, the disproportionation probably has a fourth-power hydrogen-ion dependence.

##### 5. SUMMARY

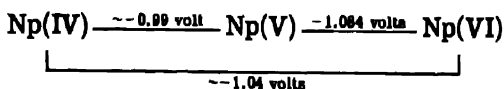
The formal oxidation potentials for the various neptunium couples have been measured in 1.0M HCl. These may be represented schematically as follows:



The neptunium (III)/(IV) and neptunium (V)/(VI) couples have been found to behave reversibly, but the neptunium (IV)/(V) couple is irreversible. In the latter case measurements of the potential in a system in equilibrium with Fe(II) and Fe(III) have been used to obtain the

value of the couple. The neptunium (V)/(VI) couple has been found to be independent of hydrogen-ion concentration in the range 0.1M to 1.0M hydrogen ion at a constant 1.0M nitrate concentration. Partially on the basis of this result it has been concluded that the probable formula of the neptunium(V) ion is  $\text{NpO}_2^+$ .

Because of preferential complexing of neptunium(IV) and neptunium(VI) by sulfate, the potentials of the couples in 1.0M  $\text{H}_2\text{SO}_4$  are altered. The scheme in this acid is



#### REFERENCES

1. L. B. Magnusson, T. J. LaChapelle, and J. C. Hindman, Chemistry of neptunium. Preparation and properties of neptunium(III), Paper 15.3, this volume.
2. H. G. Heal, Canadian Report MC-95 (Oct. 20, 1944).
3. J. C. Hindman, Metallurgical Project Report CK-1587 (May 1944).
4. J. C. Hindman, Metallurgical Project Report CN-3819 (May 19, 1947); also in National Nuclear Energy Series, Division IV, Volume 14 A.
5. W. E. Harris and I. M. Kolthoff, J. Am. Chem. Soc., 67: 1484 (1945).
6. G. E. Moore, Clinton Laboratories Report CL-P-414 (May 16, 1945).
7. K. A. Kraus, J. R. Dam, L. Spector, and J. C. Kroner, Clinton Laboratories Report CL-P-395, (Mar. 14, 1945).
8. L. B. Magnusson, J. C. Hindman and T. J. LaChapelle, Chemistry of neptunium. Kinetics and mechanisms of aqueous oxidation-reduction reactions of neptunium, Paper 15.11, this volume.
9. H. S. Harned and W. J. Hamer, J. Am. Chem. Soc., 57: 27 (1935).
10. W. J. Hamer, J. Am. Chem. Soc., 56: 860 (1934).
11. H. S. Harned and R. S. Ehlers, J. Am. Chem. Soc., 55: 2179 (1933).
12. W. J. Hamer, J. Am. Chem. Soc., 56: 860 (1934).
13. R. E. Connick, Metallurgical Project Report CC-3869 (May 5, 1948); also in National Nuclear Energy Series, Division IV, Volume 14 A.
14. O. von Collenberg, A. Guthe, Z. anorg. Chem., 136: 252 (1924).
15. F. Foerster, E. Fricke, and R. Hausswald, Z. physik. Chem., 146: 81 (1935).
16. O. von Collenberg, Z. physik. Chem., 109: 353 (1934).
17. C. K. McLane, Metallurgical Project Report CN-2495 (January 1945).

## Paper 15.5

# THE BASIC DRY CHEMISTRY OF NEPTUNIUM†

By S. Fried and N. R. Davidson

### 1. INTRODUCTION

Identification of solid reaction products by means of an analysis of their x-ray diffraction patterns can be carried out rapidly and, in favorable cases, with less than 10  $\mu\text{g}$  of material. This is particularly true when the compound produced is isomorphous with known compounds of other elements. Accordingly, the compounds of neptunium were in most cases identified by the x-ray method in the laboratory of Dr. W. H. Zachariasen, and the composition was inferred from a consideration of the crystal form and lattice dimensions.

By use of x-ray methods, together with the development of techniques for handling microgram quantities of solids and a consideration of the methods of preparation, it has been possible to elucidate the structure and/or composition of the several neptunium compounds known in the dry state.

### 2. TECHNIQUES

It is appropriate at this point to describe some of the more common techniques used in the handling of solids on the ultramicro scale. Some of the techniques described were developed by P. L. Kirk and coworkers early in the work on this project, while others were developed by various members in the course of their own work.

A great deal of effort was expended in developing methods for the preparation of samples for x-ray diffraction analysis since, as mentioned above, most of the analyses were done by this method. This

†Contribution from the Chemistry Division of the Metallurgical Laboratory, University of Chicago, now the Argonne National Laboratory.

Based largely on work reported in Metallurgical Project Report CN-3381 (December 1945).

involved the preparation of samples of the order of 5  $\mu\text{g}$  in a suitable form and mounted in very thin-walled glass capillaries.

A brief discussion of the basic experimental techniques is presented in the following paragraphs.

**2.1 Preparation of Capillaries for X-ray Samples.** In order to obtain satisfactory x-ray diffraction patterns of microgram quantities of a solid in a glass capillary, the wall thickness must not be greater than 0.030 mm. One of the most satisfactory methods of obtaining capillaries with this specification is as follows: a 4-in. length of well-cleaned 10 to 12 mm diameter pyrex tubing is drawn down by means of a sharp oxygen-gas flame as shown in Fig. 1. The constricted tube is then heated with an air-gas flame at point A until it

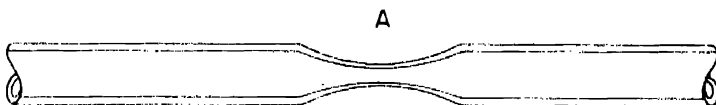


Fig. 1—Constricted 12-mm pyrex tubing for use in preparing x-ray capillaries.

is sufficiently soft and is then rapidly drawn out to a thin capillary. Capillaries of 0.100 mm inside diameter and a wall thickness as low as 0.010 mm may be readily produced by this technique. Capillaries of these dimensions may be cut by gently scratching the capillary at the desired point with a small fragment of porous clay chip. It will be found that light pressure will cause the capillary to break cleanly at the scratched point. The end of the capillary may be satisfactorily sealed by a very small flame. Care should be taken to prevent over-thickening of the glass at the bottom of the capillary since an increase in wall thickness enhances the diffuse scattering of the x-ray beam and thus intensifies background darkening on the film.

Quartz capillaries are much more difficult to make. Ten millimeter quartz tubing with a 1-mm wall may be drawn into satisfactory x-ray capillaries by means of a sharp oxyhydrogen flame in the same manner as described above except that a soft oxyhydrogen flame is used for the final drawing instead of an air-gas flame as in the case of pyrex. These quartz capillaries are generally not circular in cross section, nor are they of uniform wall thickness.

**2.2 Filling X-ray Capillaries.** Since these tubes are of small diameter and very fragile, it is generally preferable to leave the large-diameter stem attached rather than try to fill the fine tube directly. The latter may be done under low magnification, however. The x-ray capillary with attached stem is illustrated in Fig. 2. These tubes may

be held for observation on the stage of a dissecting microscope by means of a lump of modeling clay placed at C. Particles of the solid may be introduced into the larger tube in any convenient way, but care should be taken not to put in too much material at one time or to add particles too large to fall to the bottom of the capillary. In general,

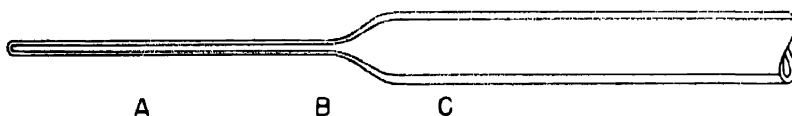


Fig. 2—X-ray capillary with attached stem.

powders may be persuaded to fall to the bottom of a fine capillary by holding it in a vertical position and tapping sharply at C. Sometimes light rubbing at B with a knurled edge or a file will shake the powder loose from the walls into the capillary. Vibration should not be attempted at points lower than B because of the danger of breaking the capillary.

After the particles have been satisfactorily packed into the end of the capillary, it may be sealed off at A. If desirable, the stem of the capillary may end in a ground joint so that the entire system may be evacuated before sealing.

**2.3 Emptying Capillaries.** It is frequently necessary to reuse material submitted for x-ray analysis. In such case, the capillary (usually  $\frac{1}{2}$  to  $\frac{3}{4}$  in. long) is held lightly in the fingers and opened by scratching with a porous clay chip. The opened capillary is then attached to a stout wire with a bit of clay as shown in Fig. 3. The wire is then tapped sharply at A, causing the contents of the capillary to fall out into the container.

### 3. PREPARATION OF SOLIDS FROM SOLUTION

The preparation of solids from solutions involves either evaporation of the solvent or precipitation from solution by a chemical reagent. Evaporation may be carried out from small platinum boats. These boats are usually rectangular in shape, 6 by 3 mm by about 3 mm deep. A solution of a heavy-metal nitrate can be placed in a boat such as this, the solution evaporated to dryness, and if necessary, the nitrate ignited to an oxide. Samples of the oxide or nitrate can be removed from the boat by means of a needle and introduced into an x-ray capillary for examination. As an alternate procedure, the oxide can be treated with other reagents to produce new com-

pounds. These operations can very easily be carried out on the 50- $\mu$ g scale.

In precipitation of solids from solution, the following technique was found very satisfactory in the case of substances precipitating in a

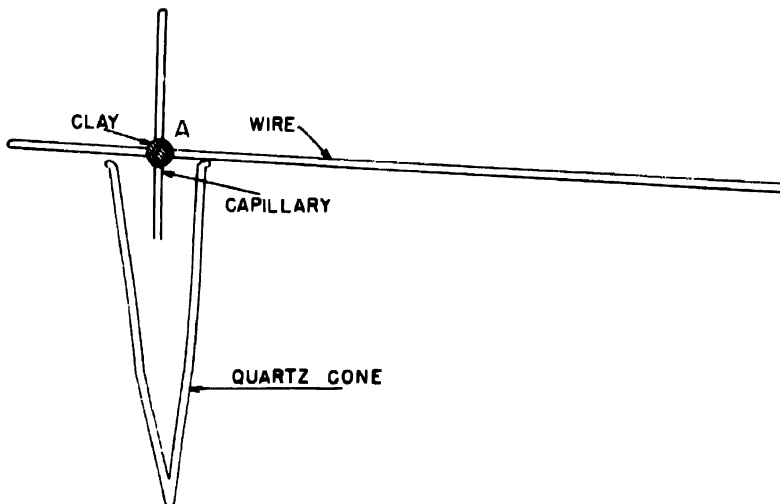


Fig. 3—Method of removing material from x-ray capillaries.

bulky gelatinous form (such as certain hydroxides). These hydroxides can be precipitated, washed, and centrifuged in a microcone. This leaves the desired product tightly packed at the bottom of the cone. The supernatant liquid is removed by a micropipet, and the cone and contents are then dried slowly at about 70°C. It is found that the precipitate has a tendency to shrink away from the walls of the cone under most conditions so that it forms a single loose piece, or at most, several pieces. Various reactions can now be performed on these small amounts of material *in situ*, or the material may be transferred to an x-ray capillary made with a ground joint. When such a system is connected to a vacuum line, various chemical reactions of the hydroxides, such as their reaction with gaseous reagents, may be studied.

This type of manipulation, for example, lends itself to the preparation of halides. These may later be sublimed onto the walls of the capillary, after which the capillary may be sealed off to the proper length and the contents (both the sublimate and residue) studied by x-ray diffraction.

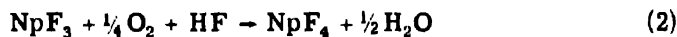
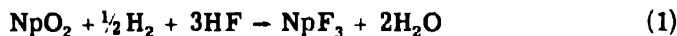
**3.1 Neptunium Dioxide and Sodium Neptunyl Acetate.** These two compounds were the first definitely identified neptunium compounds

prepared. They were both prepared by Magnusson and LaChapelle,<sup>1</sup> the oxide by ignition of a hydroxide precipitate, and the neptunyl acetate by a method similar to that used for the preparation of the analogous uranium and plutonium salts, i.e., precipitation from a Np(VI) solution with sodium acetate.

Neptunium dioxide is a brownish material that has a cubic structure and is isomorphous with UO<sub>2</sub> and PuO<sub>2</sub>.<sup>2</sup> Sodium neptunyl acetate, NaNpO<sub>2</sub>(C<sub>2</sub>H<sub>5</sub>O<sub>2</sub>)<sub>3</sub>, is pink under 30× magnification by transmitted light and pale green by reflected light; it is isomorphous with the corresponding plutonium and uranium compounds.<sup>3</sup>

**3.2 NH<sub>4</sub>Np<sub>2</sub>F<sub>9</sub>.** This compound was also prepared by LaChapelle and Magnusson by adding hydrofluoric acid to a Np(IV) solution containing ammonium ion. NH<sub>4</sub>Np<sub>2</sub>F<sub>9</sub> is isomorphous with KTh<sub>2</sub>F<sub>9</sub> and Ku<sub>2</sub>F<sub>9</sub>.

**3.3 Preparation and Properties of NpF<sub>3</sub> and NpF<sub>4</sub>.**<sup>†</sup> Neptunium trifluoride and neptunium tetrafluoride were prepared by the following reactions:<sup>4</sup>



For the preparation of NpF<sub>3</sub>, Np(IV) hydroxide was precipitated in a microcone by treating a solution containing 50 µg of Np(IV) (at a concentration of 1 g per liter in dilute sulfuric acid) with gaseous ammonia. The gelatinous precipitate was washed and dried in an oven at 70°C to a dry pellet; this was transferred to a platinum vessel (made from the cover of a 1-ml J. Lawrence Smith crucible with a platinum holder spot-welded to it). The platinum vessel was placed in an all-platinum hydrofluorination apparatus and treated with a hydrogen-hydrogen fluoride (approximately 1 to 1) mixture for 1½ hr at 500°C. The system was cooled in the hydrogen-hydrogen fluoride mixture, which was then pumped out and replaced with nitrogen. The reaction product was crushed and transferred to an x-ray capillary for examination by Dr. W. H. Zachariasen. He reported that the sample contained approximately 25 per cent Pt and 75 per cent NpF<sub>3</sub>, which is isomorphous with PuF<sub>3</sub>, UF<sub>3</sub>, and LaF<sub>3</sub>.<sup>5</sup>

After a metallic-looking flake of platinum was removed from the sample of NpF<sub>3</sub>, the remainder was transferred back to the platinum crucible and treated in the hydrofluorination apparatus with an

<sup>†</sup>The authors wish to acknowledge the valuable assistance of A. E. Florin in this stage of the preparation.

oxygen-hydrogen fluoride mixture for 1 hr at 500°C. The light-green reaction product proved to be  $\text{NpF}_4$ .<sup>6</sup>

The  $\text{NpF}_3$ , as observed with about 25  $\mu\text{g}$  of material, was black in appearance, reminiscent of the "black fluoride,"  $\text{PuF}_3$ , which was encountered so frequently when the plutonium fluorides were first being prepared on the microgram scale. Preparations on the 250- $\mu\text{g}$  scale, which were free of platinum, appeared dark purple, darker than  $\text{PuF}_3$ . The  $\text{NpF}_4$  was a light-green material.

These reactions for the preparation of the neptunium fluorides are analogous to reactions for the preparation of  $\text{PuF}_3$  and  $\text{PuF}_4$  from  $\text{PuO}_2$  and  $\text{PuF}_3$ , respectively. It may be inferred that the direct synthesis of  $\text{NpF}_4$  from  $\text{NpO}_2$



will take place with hydrogen fluoride free of hydrogen. Reaction 1 does not take place with  $\text{UO}_2$ ; at 500°C the action of a hydrogen-hydrogen fluoride mixture gives  $\text{UF}_4$ . Neptunium tetrafluoride has also been synthesized directly from the oxide by the action of an oxygen-hydrogen fluoride mixture at 500°C.<sup>7</sup>

One incidental observation on the properties of  $\text{NpF}_4$  has been made. It was desired to convert the sample to  $\text{NpO}_2$  for further experiments; the  $\text{NpF}_4$  was placed in a microcone with 50 microliters of concentrated nitric acid and evaporated to dryness at 70°C. The sample retained its color and shape and had evidently not been attacked.

**3.4 Neptunium Hexafluoride.** This compound was prepared by A. E. Florin according to the following reaction:<sup>8</sup>



The reaction was carried out by heating a sample of  $\text{NpF}_3$  on a nickel filament in a stream of fluorine and condensing the volatile  $\text{NpF}_6$  in a thin-walled capillary U tube. The walls of the U tube were thin enough so that when it was sealed off both below and above the mass of collected material, it could be submitted directly for x-ray examination.

The  $\text{NpF}_6$  as prepared by this method from 0.5 mg of  $\text{NpF}_3$  consisted of a mass of brownish-white crystals, which were shown to be isomorphous with  $\text{UF}_6$ .<sup>9</sup> The melting point was determined as 53°C under its own pressure at that temperature. This substance seemed to be quite volatile and could be sublimed from one end of the capillary to the other by slight warming. Even cooling one end of the capillary while the other remained at room temperature was sufficient to cause sublimation.

The ingenious apparatus used in this preparation is shown in Fig. 4.

**3.5 Preparation and Properties of  $\text{NpCl}_3$  and  $\text{NpCl}_4$ .** It was of interest to investigate the reaction of a neptunium compound with car-

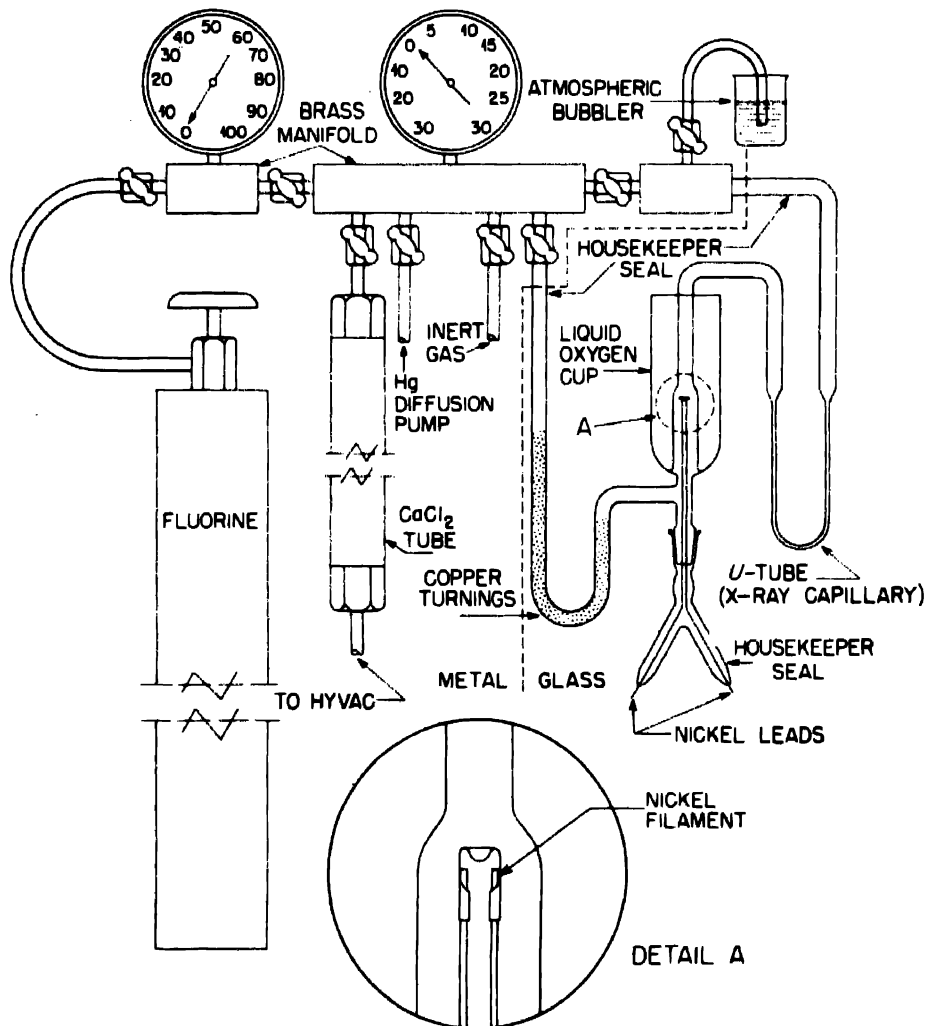


Fig. 4.—Apparatus for the preparation of neptunium hexafluoride.

bon tetrachloride. Uranium dioxide or oxalate reacts with carbon tetrachloride vapor at 450 to 500°C according to the reaction



The  $\text{UCl}_4$  slowly sublimes out of the reactor. Plutonium dioxide, on the other hand, does not react completely with carbon tetrachloride below 750 to 800°C. At this temperature, the reaction is



The  $\text{PuCl}_3$  is obtained as a green sublimate.

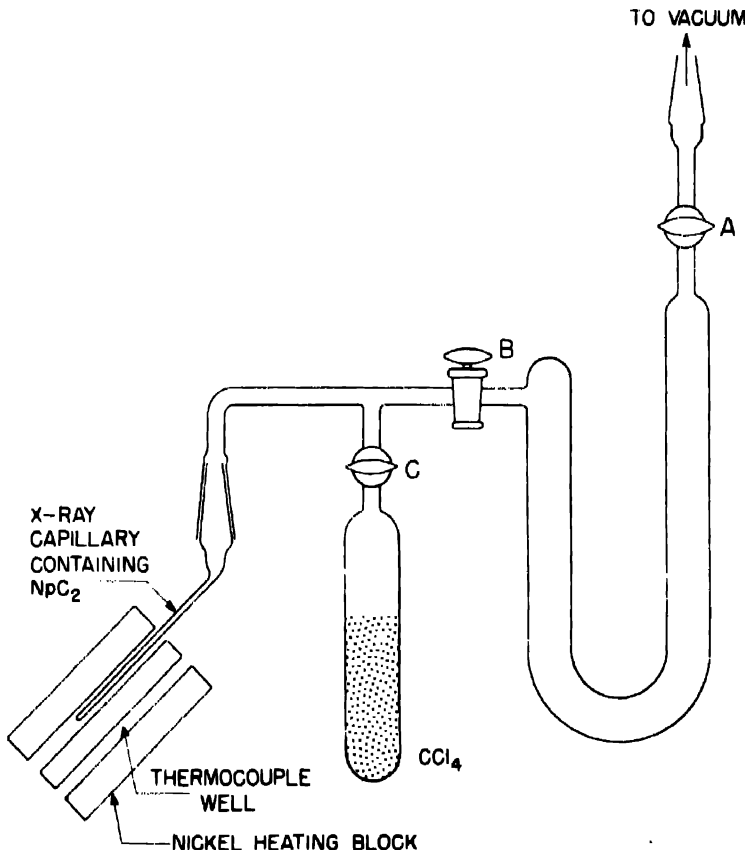


Fig. 5—Apparatus for the preparation of chlorides.

It has been found that  $\text{Np}(\text{IV})$  oxalate (or the dioxide) reacts with carbon tetrachloride vapor at 500°C to give a yellow sublimate of  $\text{NpCl}_4$ .<sup>4</sup> In this respect, therefore, neptunium is more like uranium than plutonium in its chemical behavior. Just as  $\text{UCl}_4$  may be reduced with hydrogen to form  $\text{UCl}_3$ , so  $\text{NpCl}_4$  may be reduced to  $\text{NpCl}_3$ .

Many anhydrous chlorides are extremely hygroscopic, and it was believed that transferring 50-μg samples of neptunium chlorides even

in the relatively anhydrous atmosphere of a dry box would result in hydration. Therefore, the preparations were carried out directly in an x-ray capillary. The apparatus used is shown diagrammatically in Fig. 5. By manipulation of stopcocks B and C it is possible alternately to admit carbon tetrachloride vapor onto the neptunium compound at the bottom of the capillary, and then to pump it out along with the volatile reaction products. During the time when the capillary is evacuated, any volatile neptunium chloride formed has an opportunity to sublime up to the cold portion of the capillary. The heating block was wound with resistance wire, and the temperature determined by means of a thermocouple.

The reaction and apparatus were tested with a sample of about 50  $\mu\text{g}$  of  $\text{UO}_2$ . The temperature of reaction was 530°C, and the carbon tetrachloride was alternately admitted and pumped off every few minutes. This was continued for about a half hour. Some dark material was observed to collect in the capillary just outside the hot nickel block. The capillary was sealed off in two parts, one containing the residue and the other containing the sublimate. Dr. Zachariasen reported that the sublimate was  $\text{UCl}_4$  and the residue primarily  $\text{UO}_2$ . The reaction system is evidently rather inefficient, since only a small portion of the  $\text{UO}_2$  was converted to sublimed  $\text{UCl}_4$  (perhaps 1 to 2  $\mu\text{g}$ ). Fortunately, the small amount of material synthesized was disposed as a thin layer on the walls of the x-ray capillary, in such a position as to be maximally effective in producing diffraction. Hence, an interpretable, although weak, pattern was produced by these few micrograms.

In the experiment with neptunium about 20  $\mu\text{g}$  of oven-dried (70°C)  $\text{Np}(\text{IV})$  oxalate† was treated in the same manner described above. After a short time a yellowish sublimate formed in the capillary just above the hot nickel block. The sublimate was only a small portion of the total amount of neptunium, perhaps 1 to 2  $\mu\text{g}$ . The capillary was sealed off in two portions, and Dr. Zachariasen reported that the residue was  $\text{NpO}_2$  and the sublimate  $\text{NpCl}_4$ , isomorphous with  $\text{UCl}_4$  and  $\text{ThCl}_4$ .<sup>10</sup> In later syntheses, on about the same scale, a larger fraction of the  $\text{NpO}_2$  was converted to sublimed  $\text{NpCl}_4$  by prolonged treatment with carbon tetrachloride vapor at 530°C.

†The oxalate was precipitated from a solution that was 0.8M in  $\text{HNO}_3$  and 0.1M in  $\text{H}_2\text{C}_2\text{O}_4$ , and contained approximately 1 g of Np per liter. The neptunium was believed to be in the tetrapositive state because it was obtained from a neptunium sulfate solution that had been saturated with sulfur dioxide for 12 hr. The neptunium was precipitated with gaseous ammonia and redissolved in nitric acid for the oxalate precipitation. The oxalate precipitated slowly as a crystalline material when an ammonium oxalate solution was added. The observed solubility of the oxalate (assay by Dr. J. C. Hindman) was 200 mg per liter.

The mode of synthesis and the volatilization of  $\text{NpCl}_4$  also indicate its close similarity to  $\text{UCl}_4$  and suggest similar volatility, melting point characteristics, etc. A comparison of some of the physical properties of the isomorphous tetrachlorides is shown in Table 1.

On the basis of the data in Table 1 it seems reasonable to predict that  $\text{NpCl}_4$  will prove to be somewhat more volatile and lower melting than is  $\text{UCl}_4$ .

Table 1—Comparison of the Isomorphous Tetrachlorides of Thorium, Uranium, and Neptunium

	Lattice constants (tetragonal), Å		Refer- ence	M.p., °C	Refer- ence	$\Delta H$ (subl)	Refer- ence	Temp. at which v.p. is $10^{-3}$ mm., °C	Refer- ence
	$a_1$	$a_3$							
$\text{ThCl}_4$	$8.473 \pm 0.003$	$7.488 \pm 0.003$	11	770	12	59,000	12	473	12
$\text{UCl}_4$	$8.296 \pm 0.009$	$7.487 \pm 0.009$	11	590	13	38,600	14	360	14
$\text{NpCl}_4$	$8.25 \pm 0.01$	$7.46 \pm 0.01$	10	?		47,000	15	373	15

The reduction of  $\text{NpCl}_4$  to  $\text{NpCl}_3$  was carried out directly in the x-ray capillary in which the  $\text{NpCl}_4$  had been formed. Several micrograms of yellow-sublimed  $\text{NpCl}_4$  were obtained as previously described. The nickel furnace was moved up to surround the  $\text{NpCl}_4$  and maintained at 450°C. Hydrogen, purified by passing through hot copper and a liquid air-cooled charcoal trap, was admitted to 1 atm pressure into the reaction system through the stopcock B (Fig. 5). The hydrogen was allowed to react for 10 min and was then pumped out to remove the hydrogen chloride formed as a reaction product. Hydrogen was admitted twice more with subsequent pumping. Calculations indicated that these three treatments should provide a more than adequate supply of hydrogen to reduce several micrograms of  $\text{NpCl}_4$  to  $\text{NpCl}_3$ , provided the  $\text{NpCl}_4$  is no more difficult to reduce to  $\text{NpCl}_3$  than is  $\text{UCl}_4$  to  $\text{UCl}_3$ .<sup>16</sup> The material in the capillary had diminished in quantity, suggesting that some sublimation of  $\text{NpCl}_4$  had occurred. Zachariasen<sup>17</sup> identified the residue as  $\text{NpCl}_3$  isomorphous with  $\text{UCl}_3$  and  $\text{PuCl}_3$ . The yellow color of the material had disappeared and the solid appeared white but somewhat iridescent. It is possible that  $\text{NpCl}_3$  may actually be more highly colored, and that the observations merely indicate the unreliability of color observations on such minute quantities.

In later preparations of this compound the difficulty arising from volatilization of the  $\text{NpCl}_4$  during the treatment with hydrogen was circumvented by treating the oxide with a mixture of hydrogen and carbon tetrachloride at relatively low temperatures (350 to 400°C). When the reaction was completed, the  $\text{NpCl}_3$  was sublimed out at 750

to 800°C. For this reaction it is of course necessary to use quartz capillaries.

Table 2 gives the lattice dimensions of the isomorphous hexagonal trichlorides of uranium, neptunium, and plutonium.

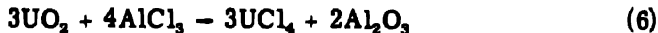
**3.6  $\text{NpCl}_3$ .** This compound formed when a sample of  $\text{NpCl}_4$  was heated to 450°C in vacuum in a sealed capillary. Apparently residual oxygen (or water) adsorbed on the walls was present in sufficient

Table 2—Lattice Dimensions of  $\text{UCl}_3$ ,  $\text{NpCl}_3$ , and  $\text{PuCl}_3$   
(Hexagonal Symmetry)

	Reference	$a_1, \text{ Å}$	$a_2, \text{ Å}$
$\text{UCl}_3$	11	$7.428 \pm 0.003$	$4.312 \pm 0.003$
$\text{NpCl}_3$	17	$7.405 \pm 0.010$	$4.273 \pm 0.005$
$\text{PuCl}_3$	18	$7.384 \pm 0.004$	$4.234 \pm 0.004$

quantity to oxidize (or hydrolyze) the  $\text{NpCl}_4$  to  $\text{NpOCl}_2$ . This compound appeared as clusters of light-yellow needles which could be sublimed at 550°C. An x-ray diffraction pattern of this material showed it to be isomorphous with  $\text{UOCl}_2$ . Attempts to reduce this compound to  $\text{NpOCl}$  with hydrogen at 450°C failed probably because of impurities, such as water, in the hydrogen, and the product was  $\text{NpO}_2$ .

**3.7 Neptunium Tribromide and Neptunium Triiodide.** It has been reported<sup>18</sup> that  $\text{UO}_2$  reacts with aluminum chloride at 250 to 500°C to form  $\text{UCl}_4$  according to the equation



A modification of this method in which neptunium oxide was treated with aluminum metal and the appropriate halogen resulted in the formation of the corresponding trihalides.<sup>20</sup> The reaction probably may be represented by the equation given below, with the qualification that any excess aluminum aids in reduction to the tripositive state.



Ninety micrograms of neptunium oxide, prepared by the precipitation of the hydroxide with gaseous ammonia from an acid sulfate solution, was dried at 70°C for 12 hr so that it formed a small pellet at the bottom of a microcone. A quartz 19/32 joint was drawn into a capillary approximately 0.1 mm in diameter with a wall thickness of 0.015 mm. The capillary was sealed at the end, and the pellet of  $\text{NpO}_2$

was introduced. A small amount of aluminum metal (approximately 50  $\mu\text{g}$ ) was placed on top of the oxide, and the system was connected to a vacuum line. The contents were then dried by heating the tip of the capillary to 400°C for 15 min in vacuum.

At this point bromine vapor that was free of chlorine and iodine was admitted to the mixture of the oxide and aluminum metal. The aluminum slowly reacted with the bromine at slightly elevated temperatures to form aluminum bromide, which condensed as a crystal-

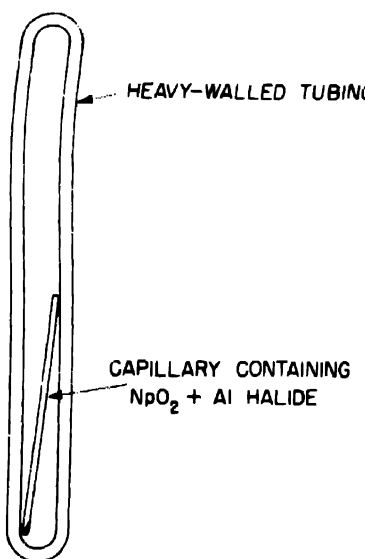


Fig. 6—Micro bomb tube for preparation of neptunium trihalides.

line solid just beyond the warm zone of the tube. When the lumen of the capillary was almost closed by the slug of aluminum bromide, the excess bromine was pumped out and the capillary was sealed off so that its length was about 4 in.

The capillary was then placed inside a heavy-walled glass tube, which contained air at atmospheric pressure and was sealed at both ends. This system was inserted into a steel jacket and heated in a tube furnace to 350 to 400°C for 12 hr. The air inside the heavy-walled tube tended to equalize the strain on the thin-walled quartz capillary as the pressure of the aluminum bromide developed. A sketch of this micro bomb tube is shown in Fig. 6.

At the end of the heating period the heavy glass tube was opened. The capillary was found to contain a greenish melt. Excess aluminum bromide was removed by heating to 250°C and driving it to the cool

end of the capillary where it condensed. The portion of the capillary containing the aluminum bromide was sealed off from the end containing the relatively nonvolatile residue.

On heating the residue to 600°C a silvery material, which was shown by x-ray analysis to be aluminum metal, sublimed out, and on further heating to 800°C a green material distilled, which was shown by the same method to be  $\text{NpBr}_3$ , isomorphous with  $\text{UBr}_3$ . The composition of the nonvolatile residue under these conditions has not yet been determined.

Table 3—Lattice Dimensions of  $\text{UF}_3$ ,  $\text{NpI}_3$ , and  $\text{PuI}_3$   
(Orthorhombic Symmetry)

Reference		$a_1$ , Å	$a_2$ , Å	$a_3$ , Å
$\text{UI}_3$	11	$13.98 \pm 0.02$	$4.33 \pm 0.02$	$9.99 \pm 0.02$
$\text{NpI}_3$	22	$13.93 \pm 0.04$	$4.31 \pm 0.03$	$9.94 \pm 0.05$
$\text{PuI}_3$	23	$13.9 \pm 0.1$	$4.29 \pm 0.04$	$9.90 \pm 0.1$

Neptunium triiodide was prepared in an analogous manner from  $\text{NpO}_2$ , aluminum, and iodine.<sup>20</sup> After removal of the excess aluminum iodide the triiodide was sublimed at 800°C. It proved to be a brownish material (probably slightly contaminated with iodine) and was shown by the x-ray method to be isomorphous with  $\text{PuI}_3$  and  $\text{UI}_3$ .

Table 3 gives the lattice dimensions of the isomorphous orthorhombic triiodides of uranium, neptunium, and plutonium.

3.8 Neptunium Tetrabromide. It was found<sup>21</sup> that  $\text{NpO}_2$  reacts with aluminum bromide in the absence of excess aluminum metal to give  $\text{NpBr}_4$ . Fifty micrograms of neptunium oxide was placed in a thin-walled quartz capillary and dried in vacuum at 400°C for 1 hr. Approximately 250 µg of anhydrous aluminum bromide was added on top of the oxide, this operation being carried out in a dry box, and the system was evacuated and sealed off so that the length of the capillary was about 4 in. The capillary was placed inside a heavy-walled glass tube as described above and heated to 350°C for 12 hr.

At the end of the heating period the capillary was removed from the tube and the excess aluminum bromide was removed by sublimation at 250°C and by sealing off the portion of the capillary containing it. When the residue in the capillary was heated further to 500°C, a reddish-brown substance sublimed out; the x-ray diffraction pattern showed this to be  $\text{NpBr}_4$ , isomorphous with  $\text{UBr}_4$ . On still further heating to 800°C a green material ( $\text{NpBr}_3$ ) distilled out, and at slightly higher temperatures a yellow one. The yellow substance has not been

identified. The amount of  $\text{NpBr}_4$  obtained was approximately 20 to 25 per cent of the total volatile material.

A consideration of the results shows that Eq. 7 does not completely account for the formation of the tripositive neptunium bromide and that the free aluminum metal present in the experiment in which  $\text{NpBr}_3$  was first produced performed a definite, though accessory, function in the reduction of the tetrabromide to the tribromide.

The apparent stability of  $\text{NpBr}_4$  when sublimed in vacuum at 500°C is somewhat surprising in view of the calculations made by Brewer et al.,<sup>24</sup> which indicate that  $\text{NpBr}_4$  should be unstable.

The existence of  $\text{NpBr}_4$  in the solid state furnishes additional evidence that neptunium resembles uranium more than plutonium, and tends to confirm the evidence deduced from a study of neptunium solution chemistry.

**3.9 Preparation and Properties of Neptunium Metal.** Neptunium metal was prepared by the reaction of barium vapor with  $\text{NpF}_3$  at 1200°C in a beryllia double-crucible system.<sup>7</sup> Because only a limited amount of neptunium was available for this purpose (approximately 250 µg), many practice reductions using  $\text{UF}_4$  and  $\text{PuF}_4$  as stand-ins were carried out in an attempt to establish the most favorable conditions for the production of neptunium metal. The reductions were carried out in beryllia double-crucible systems and the conventional tantalum-wound furnaces described for the production of plutonium on the microgram scale.<sup>25</sup> The inner crucibles were vitrified by heating in vacuum at 1500 to 1800°C for 1 hr in order to minimize the soaking of metal into the crucible. Before a run was made, the system was thoroughly outgassed at about 1400°C for 1 hr or until the pressure was reduced to  $10^{-6}$  mm Hg.

Attempts to prepare uranium and plutonium metal on the 50-µg scale by reduction of the tetrafluorides with barium metal at approximately 1200°C were uniformly successful, but two attempts to prepare neptunium metal from  $\text{NpF}_4$  under similar conditions failed completely. When the crucibles were opened they were found to be empty but somewhat α active, suggesting that either the fluoride or metal had soaked into the crucible. These results led to the possibility of two alternative procedures, e.g., the use of a more volatile reductant, such as magnesium, which would minimize the tendency for the metal or fluoride to soak in by permitting the reaction to take place at a lower temperature; or the use of  $\text{NpF}_3$  instead of  $\text{NpF}_4$  as the starting material. Neptunium trifluoride would be expected to have a higher melting point than the tetrafluoride and thus would be less likely to soak into the crucible.

Tests of magnesium as a reducing agent for uranium and plutonium fluorides under the above conditions were not encouraging since the

appearance of the metal produced was not so good as that obtained ordinarily in barium reductions. Therefore it was decided to use  $\text{NpF}_3$  as the starting material.

Accordingly, the remainder of the  $\text{NpF}_4$  (approximately 150  $\mu\text{g}$ ) was converted to the trifluoride by the action of hydrogen fluoride and hydrogen at 500°C, and this material was used in the preparation of neptunium metal after x-ray analysis showed it to be essentially pure  $\text{NpF}_3$ .

Three runs of approximately 50  $\mu\text{g}$  each were made using barium as a reductant at a maximum temperature of about 1200°C for 1.5 to 2 min. Each of these reductions was successful in yielding several pieces of metal weighing from 10 to 40  $\mu\text{g}$ . The neptunium metal is silvery in color and about as malleable as uranium metal prepared under the same conditions. The metal is not particularly affected by air during the time intervals necessary for manipulations ( $\frac{1}{2}$  hr).

The method used for the determination of the density of neptunium metal was the same as that used earlier on plutonium.<sup>26</sup> The displacement of a piece of metal weighing 40.32  $\mu\text{g}$  was measured in two different capillary pycnometers with diameters of 0.231 and 0.333 mm, respectively. The measured densities of the metal were 17.8 and 17.6 g/cc, respectively.

The x-ray diffraction pattern obtained from some flattened pieces of metal by Dr. W. H. Zachariasen was complex and has not yet been interpreted.

The observation that the neptunium apparently soaked into the crucible during the attempted reduction of  $\text{NpF}_4$ , whereas the reductions of  $\text{UF}_4$  were successful, suggests that the melting point of  $\text{NpF}_4$  is less than the melting point of  $\text{UF}_4$  (960°C), and that the  $\text{NpF}_4$  melted and soaked into the crucible before the reductant vapor attacked it. By extrapolation the melting point of  $\text{PuF}_4$  is expected to be still less. Since, however,  $\text{PuF}_4$  readily decomposes in vacuum to  $\text{PuF}_3$ ,<sup>27</sup> the melting and soaking into the crucible of the  $\text{PuF}_4$  during a vapor-phase reduction may be prevented by the formation of a trifluoride skin around the tetrafluoride.

**3.10 The Preparation of Neptunium Hydride.** Neptunium hydride was prepared<sup>28</sup> by the action of hydrogen on the metal. The apparatus used was that developed by Baumbach<sup>28</sup> for the preparation of plutonium hydride on the microgram scale. The metal weighed 20.88  $\mu\text{g}$ ; it did not react with hydrogen when this gas was admitted at a pressure of 1 atm, but after a few minutes' heating to 50°C it rapidly absorbed gas. Examination of the hydride under the microscope showed that the metal had broken up into a black flaky material very similar

in appearance to uranium or plutonium hydride. The volume of hydrogen absorbed corresponded to the formula  $\text{NpH}_{3.5-3.8}$ . No great accuracy is claimed for this formula however.

X-ray diffraction patterns of this compound exhibited lines which could not be assigned to neptunium hydride, but according to Zachariasen they are very probably due to the lower oxide  $\text{NpO}$ . A small amount of oxygen adsorbed on the walls of the capillary could easily account for the presence of this compound.

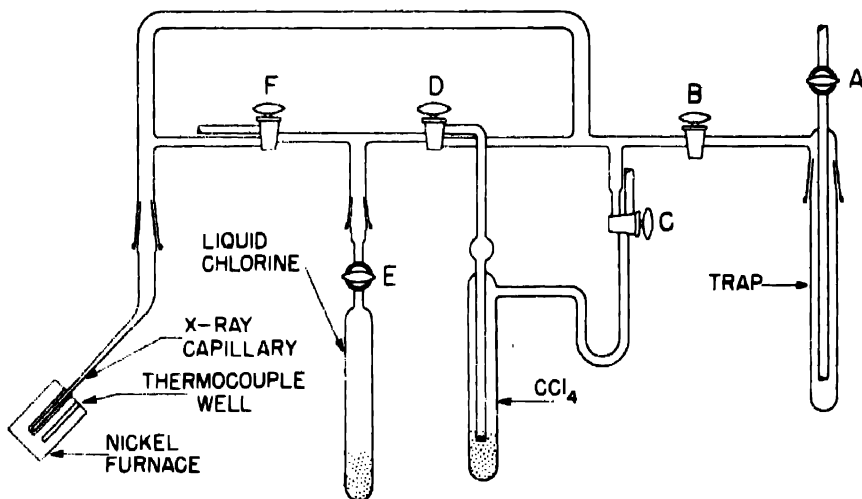


Fig. 7.—Apparatus for the preparation of higher chlorides.

**3.11 Attempted Preparation of a Higher Chloride of Neptunium.** Since neptunium forms ions of oxidation number +5 and +6 as well as +3 and +4 in aqueous solution, it was of interest to attempt the preparation of the higher chloride in the solid state. The experiment described here was an unsuccessful attempt to prepare higher chlorides of neptunium by the action of chlorine gas on  $\text{NpCl}_4$  at elevated temperatures. A sketch of the apparatus used is given in Fig. 7.

The chlorine used in this and the following experiments was tank chlorine that was passed through a sulfuric acid-bead tower, condensed in liquid nitrogen, distilled into a  $-120^\circ\text{C}$  bath (solid ethyl bromide) with pumping to remove oxygen, and finally distilled into the receiver.

It was decided to test this apparatus by using  $\text{UO}_2$  as a stand-in. Accordingly a small quantity of  $\text{UO}_2$  was placed in the x-ray capillary,

and the system was evacuated. Carbon tetrachloride vapor was admitted to the heated  $\text{UO}_2$  and then pumped off. It was found that the optimum temperature range for the formation of  $\text{UCl}_4$  in this apparatus was 510 to 530°C. After sufficient  $\text{UCl}_4$  was formed the furnace was moved up so that the  $\text{UCl}_4$  could be heated. The stopcocks were manipulated so that the carbon tetrachloride was saturated with chlorine gas, and this mixture was passed over the  $\text{UCl}_4$  at 390 to 400°C.

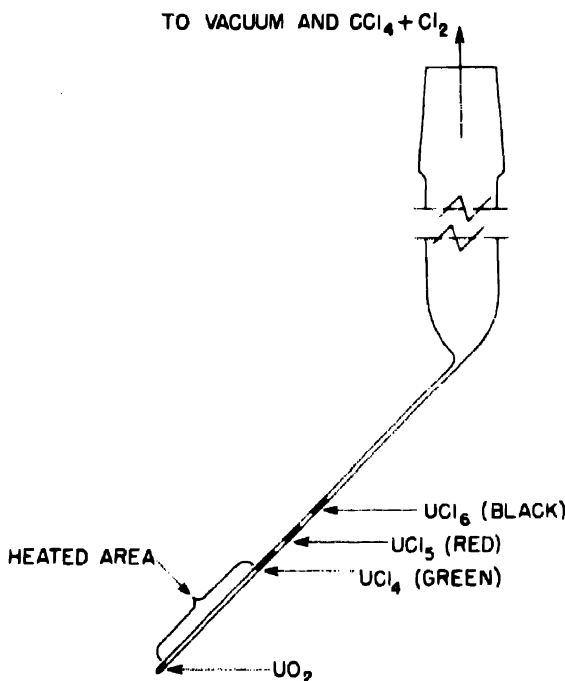


Fig. 8—Capillary containing chlorides.

It was observed that a red zone formed in the cool portion of the capillary and beyond that a black zone. When sufficient material had been collected, the reaction was stopped and the capillary sealed off. Figure 8 shows the appearance of the capillary.

The zones of condensation were about 1 mm wide and were separated from each other by about 0.5 mm. The boundaries were quite sharp, and it was possible to obtain x-ray diffraction patterns of the individual zones. The zone nearest the hot portion of the tube consisted of  $\text{UCl}_4$ . The red zone was  $\text{UCl}_5$ , and the black zone, which had condensed in the coolest portion of the tube, was  $\text{UCl}_6$ .<sup>29</sup>

When this experiment was repeated with  $\text{NpCl}_4$ , the vaporized material failed to condense in distinct zones. Examination of the condensed material under the microscope showed it to consist of transparent yellow bipyramids. In thicker layers or in reflected light the crystals appeared reddish. A study of the x-ray diffraction pattern showed that this substance was  $\text{NpCl}_4$ .

**3.12 Preparation and Properties of  $\text{NpOS}$  and  $\text{Np}_2\text{S}_3$ .**<sup>30</sup> The reaction of hydrogen sulfide on  $\text{ThO}_2$  or  $\text{UO}_2$  at 1000°C gives rise to  $\text{ThOS}$  or  $\text{UOS}$ , according to results obtained at the University of California (Berkeley) project,<sup>31</sup> and it was of interest to attempt a similar reaction with  $\text{NpO}_2$ . The results obtained at Berkeley indicate that a hydrogen sulfide-carbon disulfide mixture is a more potent sulfiding agent at high temperatures than is hydrogen sulfide by itself, and accordingly our experiments were carried out with the gas mixture obtained by bubbling hydrogen sulfide through carbon disulfide at 30°C. The hydrogen sulfide was dried by passage over  $\text{P}_2\text{O}_5$  before it entered the carbon disulfide bubbler.

A quartz microcone containing approximately 50 µg of neptunium as neptunium(IV) hydroxide was placed in a quartz tube and treated with the hydrogen sulfide-carbon disulfide stream for 2 hr at 1000°C. The black brittle reaction product was crushed and submitted for x-ray analysis. Zachariasen<sup>32</sup> identified it as  $\text{NpOS}$ .

The  $\text{NpOS}$  was combined with some  $\text{NpO}_2$  obtained by the ignition of a  $\text{NpF}_4$  sample in air. The mixture was maintained in the hydrogen sulfide-carbon disulfide stream at 1000°C for approximately 12 hr. The product was still a black brittle material. Zachariasen reported that this substance gave only a weak x-ray diffraction pattern, but he finally succeeded in showing<sup>33</sup> that it was  $\text{Np}_2\text{S}_3$ , isomorphous with  $\text{U}_2\text{S}_3$  and  $\text{Th}_2\text{S}_3$ .

The chemistry of the neptunium-sulfur system seems to be intermediate, in a rather interesting way, between that of the uranium sulfides and that of the plutonium sulfides.<sup>34</sup> The oxysulfide of neptunium is  $\text{NpOS}$ , like  $\text{UOS}$  and different from  $\text{Pu}_2\text{O}_2\text{S}$ . In the fully sulfided product, however, the oxidation number of the neptunium is reduced to +3. When  $\text{U}_3\text{O}_8$  is converted to a sulfide by hydrogen sulfide at 1300 to 1400°C in a graphite system, the product is  $\text{US}_2$ , with some decomposition to  $\text{U}_2\text{S}_3$ . The  $\text{U}_2\text{S}_3$  reverts to  $\text{US}_2$  as the reaction product is cooled in hyurogen sulfide.<sup>35</sup> In such a reaction  $\text{PuO}_2$  is converted to  $\text{Pu}_2\text{S}_3$ .<sup>36</sup> While  $\text{Pu}_2\text{S}_3$  is presumably like  $\text{Ce}_2\text{S}_3$ , which is a "normal-valent" sulfide that does not show metallic conductivity,  $\text{U}_2\text{S}_3$  is a "reduced" sulfide showing semimetallic conductivity, and  $\text{US}_2$  is a "normal-valent" sulfide. Since  $\text{Np}_2\text{S}_3$  was prepared under conditions such that in general normal rather than reduced sulfides

are obtained, it is presumably a normal-valent sulfide. However, its crystal structure is isomorphous with that of the reduced sulfide  $\text{U}_2\text{S}_3$ , rather than that of the normal sulfide,  $\text{Pu}_2\text{S}_3$ .

It would be of great interest to synthesize a neptunium sulfide at 1400°C in a graphite system and determine if  $\text{Np}_2\text{S}_3$  with the  $\text{Pu}_2\text{S}_3$  structure were obtained. It would also be of interest to treat  $\text{Np}_2\text{S}_3$  with sulfur at a relatively low temperature in an attempt to prepare  $\text{NpS}_2$ .

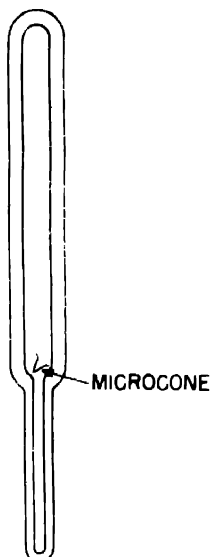


Fig. 9—Oxygen-bomb tube.

**3.13 Attempted Preparation of a Higher Oxide of Neptunium.** On the basis of the similarity of neptunium to uranium it was decided to attempt the preparation of a crystalline higher oxide (higher than  $\text{NpO}_3$ ) of this element by ignition of a neptunium salt in a high pressure of oxygen. The apparatus used in this experiment is diagrammed in Fig. 9. The inside diameter of the heavy-walled bomb tubing was 4 mm, and the inside diameter of the capillary was 1mm. The neptunium salt was contained in the cone. The tube was connected by means of a stopcock to a vacuum line filled with tank oxygen, and oxygen was condensed in the small capillary by means of a liquid-nitrogen bath. The amount condensed was measured as a length in the capillary and was chosen to give a pressure of 28 atm at 400°C after the capillary was sealed off at the proper point. These capillary

bombs were annealed in an oven before use, and if carefully sealed off were found capable of withstanding approximately 30 atm pressure. The bomb tubes were enclosed in steel jackets when heated in a tube furnace. The application of this apparatus to the synthesis of  $\text{UO}_3$  from  $\text{U}_3\text{O}_8$  is described in another report.<sup>34</sup>

The neptunium, as  $\text{Np(VI)}$  in hydrochloric acid, was evaporated to dryness at 70°C, taken up in 6M  $\text{HNO}_3$ , and evaporated to dryness again. From previous observations by L. B. Magnusson it was probably neptunium(IV) nitrate at this stage. The cone was placed in the bomb, which was filled with oxygen to give a pressure of 28 atm at 400°C, and the system was sealed off. When heated to 400°C, the bomb burst at the top seal-off. The sample was intact and was placed in another bomb where it was maintained at 350°C for 5 hr, 250°C for 12 hr, and 125°C for 4 hr. Dr. Zachariasen showed that the sample gave the diffraction pattern of  $\text{NpO}_2$  and a few other weak, unidentifiable lines.

The conditions used in the attempted formation of a crystalline neptunium higher oxide were unfavorable in that (a) it would have been better to start with a neptunium(VI) nitrate and (b) at 400°C any higher oxide of neptunium may have irreversibly decomposed to  $\text{NpO}_2$ , especially when the tube burst and the pressure was released, even though at a lower temperature at the high pressure the higher oxide was stable.

#### 4. SURVEY OF THE DRY CHEMISTRY OF URANIUM, NEPTUNIUM, AND PLUTONIUM

The elements uranium, neptunium, and plutonium exhibit the oxidation numbers +3, +4, +5, and +6 in both aqueous solution and in the anhydrous compounds. They therefore form an interesting series in which to observe the relation between the stability of the different oxidation states in solution and in dry compounds.

The higher oxidation states in aqueous solution are stabilized by solvation and complex formation. In the pure compounds (solid or gaseous) the small positively charged ions of the various oxidation states must be stabilized by coordination with the anions of electro-negative atoms ( $\text{F}^-$ ,  $\text{O}^{--}$ ,  $\text{Cl}^-$ ,  $\text{Br}^-$ ,  $\text{I}^-$ ,  $\text{S}^{--}$ , etc.). The small and difficultly polarizable anions  $\text{O}^{--}$  and  $\text{F}^-$  in general form compounds of higher oxidation number than do the more readily polarizable anions  $\text{Cl}^-$ ,  $\text{Br}^-$ ,  $\text{S}^{--}$ , and  $\text{I}^-$ . It is interesting to observe that in general it is easier to obtain the higher oxidation states of the elements under discussion in solution than among dry compounds. Thus the free energies of solution of  $\text{UO}_3$ ,  $\text{UF}_6$ , and  $\text{UCl}_6$  are more negative than the

free energies of solution of  $\text{UO}_2$ ,  $\text{UF}_4$ , and  $\text{UCl}_4$ . Similarly, plutonium(III) may be oxidized to plutonium(IV) in aqueous solutions by chlorine or bromine, but evidently anhydrous  $\text{PuCl}_4$  or  $\text{PuBr}_4$  do not exist.

Table 4 lists the potentials between the various oxidation states of the ions in hydrochloric acid solution. In Table 5 an attempt has been made to summarize the available information as to the existence and

Table 4—Formal Potentials of Couples in Aqueous Solution of Uranium, Neptunium, and Plutonium

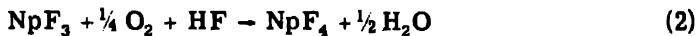
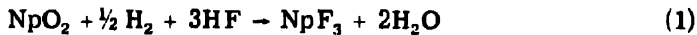
Couple	Uranium	Reference	Neptunium	Reference	Plutonium	Reference
(III)/(IV)	0.63	37	-0.14	38	-0.95	39
(IV)/(V)	-0.6?		-0.7	40	-1.10	41
(IV)/(VI)	-0.54	42	-0.9	38	-1.05	39

stability of compounds of uranium, neptunium, and plutonium of various oxidation states. Deductions as to the existence of certain compounds of neptunium and plutonium are indicated by enclosing the compound in brackets. The reasoning underlying these guesses is generally rather obvious when account is taken of the principles stated above and of the trends apparent in the two tables.

## 5. SUMMARY

A description of the micro techniques used in the preparation of neptunium compounds has been given. Neptunium dioxide and sodium neptunyl acetate have been prepared and identified.

Neptunium trifluoride and tetrafluoride have been prepared by the reactions



The  $\text{NpF}_3$  as observed with about 250  $\mu\text{g}$  of material was dark purple. The  $\text{NpF}_4$  was a light-green material.

Neptunium tetrachloride was prepared by the reaction of carbon tetrachloride vapor on Np(IV) oxalate or  $\text{NpO}_2$  at 500°C in a pyrex x-ray capillary. The  $\text{NpCl}_4$  is formed as a yellow sublimate.

Hydrogen reduction of  $\text{NpCl}_4$  at 450°C yielded  $\text{NpCl}_3$ .

The action of chlorine gas on  $\text{NpCl}_4$  at elevated temperatures failed to yield any higher chlorides of neptunium.

Table 5—Survey of the Dry Chemistry of Uranium, Neptunium, and Plutonium<sup>†</sup>

Coordinating anion	Uranium	Neptunium	Plutonium
	$\text{UO}_3$ : decomposes to $\text{U}_3\text{O}_8$ on ignition above 700°C		
	Uranyl salts, uranates	Neptunyl salts, $\text{NaNpO}_2(\text{C}_2\text{H}_5\text{O}_2)_3$ [ $\text{CaNpO}_4?$ ]	Plutonyl salts, $\text{NaPuO}_2(\text{C}_2\text{H}_5\text{O}_2)_3$ [ $\text{CaPuO}_4?$ ]
	$\text{U}_3\text{O}_8$ : a mixture of U(IV) and U(VI) <sup>43</sup>		
	$\text{UO}_2$ : obtained by action of $\text{H}_2$ on $\text{U}_3\text{O}_8$ , not by thermal decomposition	Only $\text{NpO}_2$ obtained <sup>44</sup> by ignition of Np salts in high-pressure $\text{O}_2$ †	Only $\text{PuO}_2$ obtained <sup>44</sup> by ignition of Pu salts in high-pressure air
	No $\text{U}_2\text{O}_3$	[ $\text{Np}_2\text{O}_3?$ probably not, in view of the difficulty in reducing $\text{PuO}_2$ to $\text{Pu}_2\text{O}_3$ ]	$\text{Pu}_2\text{O}_3$ : obtained by C or Ba reduction of $\text{PuO}_2$ , not by $\text{H}_2$ at 1000°C <sup>45</sup>
$\text{F}^-$	$\text{UF}_4$ : very stable relative to decomposition into $\text{UF}_4$ or $\text{UF}_5$	$\text{NpF}_6$	[ $\text{PuF}_6$ : experiments indicate that it probably exists but is quite unstable] <sup>46</sup>
	$\text{UF}_5$ : U(IV) U(VI)? exists only in solid state	[ $\text{NpF}_5$ very probable]	$\text{PuF}_5?$
	$\text{UF}_4$ : reduced by $\text{H}_2$ (1000°C) to $\text{UF}_3$	$\text{NpF}_4$ : reduced by $\text{H}_2$ in presence of HF to $\text{NpF}_3$	$\text{PuF}_4$ : very readily reduced by $\text{H}_2$ or apparently thermally decomposes to $\text{PuF}_3$
	$\text{UF}_3$ (reference 47)	$\text{NpF}_3$	$\text{PuF}_3$ (reference 27)
$\text{Cl}^-$	$\text{UCl}_6$ , $\text{UCl}_5$ : readily thermally decomposed to $\text{UCl}_4$	[ $\text{NpCl}_5$ ] not formed when $\text{NpCl}_4$ sublimes in $\text{Cl}_2$	Evidently <sup>48</sup> no solid $\text{PuCl}_4$ may exist in gas phase in presence of $\text{Cl}_2$
	$\text{UCl}_4$ : reduced by $\text{H}_2$ to $\text{UCl}_3$	$\text{NpCl}_4$ : reduced by $\text{H}_2$ to $\text{NpCl}_3$	
	$\text{UCl}_3$	$\text{NpCl}_3$	$\text{PuCl}_3$

<sup>†</sup>The authors have attempted to judge which of the facts in Table 5 are sufficiently well known and described in summary references as not to require detailed documentation.

<sup>‡</sup>See Sec. 3.12.

Table 5—(Continued)

Coordinating anion	Uranium	Neptunium	Plutonium
$\text{Br}^-$	No $\text{UBr}_5$  $\text{UBr}_4$ : reduced by $\text{H}_2$ to $\text{UBr}_3$	$\text{NpBr}_4$ : yields $\text{NpBr}_3$ on reduction with Al and also probably on thermal decomposition	
	$\text{UBr}_3$	$\text{NpBr}_3$ (reference 21)	$\text{PuBr}_3$
$\text{I}^-$	$\text{UI}_4$ : marked tendency to decompose thermally to $\text{UI}_3$	[ $\text{NpI}_4$ ? probably not]	
	$\text{UI}_3$ (reference 16)	$\text{NpI}_3$	$\text{PuI}_3$
Oxyhalides	$\text{UO}_2\text{Cl}_2$ , $\text{UOCl}_2$ , etc.; attempts to make $\text{UOCl}$ in this laboratory unsuccessful <sup>49</sup>	[ $\text{NpOCl}$ , $\text{NpOBr}$ , $\text{NpOI}$ ]	[ $\text{PuOCl}_2$ ?], $\text{PuOCl}$ , $\text{PuOBr}$ , $\text{PuOI}$
$\text{S}^{--}$	$\text{US}_2$ : $\text{U}_2\text{S}_3$ is conducting and may contain U(IV) and free electrons; $\text{US}_2$ is said <sup>50</sup> to be unstable in presence of $\text{H}_2 + \text{CS}$ at $1400^\circ\text{C}$ , decomposing to $\text{U}_2\text{S}_3$	$\text{NpS}_2$ ?  $\text{Np}_2\text{S}_3$  $\text{Np}_2\text{O}_2\text{S}$ ?	$\text{Pu}_2\text{S}_3$
	$\text{UOS}$	$\text{NpOS}$	$\text{Pu}_2\text{O}_2\text{S}$

Neptunium tetrabromide was prepared by the action of  $\text{AlBr}_3$  on  $\text{NpO}_2$ , and the tribromide by the same reaction in the presence of excess aluminum.

Neptunium triiodide was prepared by the action of  $\text{AlI}_3$  on  $\text{NpO}_2$ .

The reaction of hydrogen sulfide-carbon disulfide mixture on  $\text{NpO}_2$  at  $1000^\circ\text{C}$  for 2 hr gave  $\text{NpOS}$ . Prolonged treatment under the same conditions yielded  $\text{Np}_2\text{S}_3$ .

Ignition of Np(IV) nitrate under 28 atm pressure of oxygen at  $400^\circ\text{C}$  gave rise to  $\text{NpO}_2$ , not a higher oxide. Under the same conditions  $\text{U}_3\text{O}_8$  is converted to  $\text{UO}_3$ .

A tabular survey of the dry chemistry of uranium, neptunium, and plutonium is given and the relation between the stability of the different oxidation states in solution and in dry compounds is discussed. In general, it is easier to obtain the higher oxidation states of the

elements under discussion in solution than in anhydrous compounds. Among the pure compounds (solid or gaseous) the small positively charged ions of the various oxidation states must be stabilized by co-ordination to the anions of electronegative atoms. The small and less readily polarized anions, O<sup>2-</sup> and F<sup>-</sup>, in general form compounds of higher oxidation number than do the more readily polarized anions, Cl<sup>-</sup>, Br<sup>-</sup>, S<sup>2-</sup>, and I<sup>-</sup>.

## REFERENCES

1. L. B. Magnusson and T. J. LaChapelle, Metallurgical Project Reports CN-2159 (September 1944), p. 16, and CN-1764 (July 1944), p. 9.
2. W. H. Zachariasen, Metallurgical Laboratory Memorandum MUC-FWHZ-31 (June 22, 1944), p. 1.
3. W. H. Zachariasen, Metallurgical Laboratory Memorandum MUC-FWHZ-54 (Aug. 29, 1944), p. 1.
4. S. Fried and N. R. Davidson, Metallurgical Project Report CN-2689 (February 1945), pp. 1-2.
5. W. H. Zachariasen, Metallurgical Laboratory Memorandum MUC-FWHZ-94 (Dec. 29, 1944), p. 1, and Metallurgical Project Report CN-2610 (December 1944), p. 4.
6. W. H. Zachariasen, Metallurgical Laboratory Memorandum MUC-FWHZ-95 (Jan. 2, 1945), p. 1, and Metallurgical Project Report CN-2610 (December 1944), p. 5.
7. S. Fried, Metallurgical Project Report CN-3053 (July 1945), pp. 6-7.
8. A. E. Florin, Metallurgical Laboratory Memorandum MUC-GTS-2165 (Jan. 23, 1946), p. 1.
9. W. H. Zachariasen, Metallurgical Laboratory Memorandum MUC-FWHZ-166 (Jan. 22, 1946), p. 1.
10. W. H. Zachariasen, Metallurgical Laboratory Memorandum MUC-FWHZ-101 (Jan. 18, 1945), p. 1.
11. W. H. Zachariasen, Metallurgical Project Report CC-2768 (March 1945), pp. 6-7.
12. W. Fischer, R. Gewehr, and H. Wingchen, Z. anorg. Chem., 242: 161 (1939).
13. T. Butler and A. Newton, Metallurgical Project Report CC-1500 (May 1944), p. 7.
14. A. Schelberg and R. W. Thompson, Report A-809 (Oct. 10, 1942), p. 5.
15. M. Mueller, University of California Radiation Laboratory Report RL-4.6.257 (May 1944), p. 24.
16. G. E. MacWood and D. Altman, University of California Radiation Laboratory Report RL-4.7.600, p. A-4
17. W. H. Zachariasen, Metallurgical Laboratory Memorandum MUC-FWHZ-102 (Jan. 25, 1945), p. 1.
18. W. H. Zachariasen, Metallurgical Project Report CK-1367 (February 1944), p. 12.
19. S. Fried, Metallurgical Laboratory Memorandum MUC-FWHZ-152 (Oct. 12, 1945), p. 1.
20. S. Fried, Metallurgical Laboratory Memorandum MUC-FWHZ-162 (Dec. 7, 1945), p. 1.
21. S. Fried, Metallurgical Project Report CN-3381 (December 1945), p. 21.
22. W. H. Zachariasen, Metallurgical Laboratory Memorandum MUC-FWHZ-163 (Dec. 10, 1945), p. 1.
23. W. H. Zachariasen, Metallurgical Laboratory Memorandum MUC-FWHZ-39 (July 1944), p. 2.
24. L. Brewer, L. Bromley, P. Gilles, and N. Lofgren, Metallurgical Project Report CN-3306 (October 1945), p. 3.

25. E. F. Westrum, Jr., Metallurgical Project Reports CK-1586 (May 1944), p. 20, and CN-2495 (January 1945), p. 12.
26. P. L. Kirk, R. S. Rosenfels, S. Fried, and H. L. Baumbach, Metallurgical Project Report CK-1145 (December 1943), p. 15.
27. S. Fried and N. R. Davidson, Metallurgical Project Reports CN-2159 (October 1944), p. 5, and CN-2495 (January 1945), p. 1.
28. H. L. Baumbach and S. Fried, Metallurgical Project Report CK-1945 (December 1943), p. 17.
29. W. H. Zachariasen, Metallurgical Laboratory Memorandum MUC-FWHZ-113 (Feb. 28, 1945), p. 1.
30. S. Fried and N. R. Davidson, Metallurgical Project Reports CN-2689 (February 1945), p. 6, and CN-3053 (July 1945), p. 8.
31. N. Lofgren, Metallurgical Project Report CK-941, p. 7.
32. W. H. Zachariasen, Metallurgical Laboratory Memorandum MUC-FWHZ-98 (Jan. 5, 1945), p. 1, and Metallurgical Project Report CN-2610 (December 1944), p. 1.
33. W. H. Zachariasen, Metallurgical Laboratory Memorandum MUC-FWHZ-129 (Apr. 14, 1945), p. 1.
34. S. Fried and N. R. Davidson, Metallurgical Project Report CN-3053 (July 1945), pp. 8-9.
35. L. Brewer, L. A. Bromley, P. W. Gilles, and N. Lofgren, Metallurgical Project Report CT-2290 (November 1944), p. 3.
36. N. R. Davidson, Metallurgical Project Report CN-2431 (December 1944), p. 2.
37. J. J. Howland and L. B. Magnusson, Metallurgical Project Report CN-2888 (April 1945), p. 21.
38. L. B. Magnusson, T. J. LaChapelle, and J. C. Hindman, Metallurgical Project Report CN-3053 (July 1945), p. 27.
39. J. C. Hindman, Metallurgical Project Report CN-2289 (November 1944), pp. 1, 6.
40. L. B. Magnusson, J. C. Hindman, and T. J. LaChapelle, Metallurgical Project Report CN-2767 (March 1945), pp. 22, 27.
41. R. E. Connick, W. H. McVey, and G. E. Sheline, Metallurgical Project Report CN-1912 (July 1944), p. 12.
42. J. J. Howland, Metallurgical Project Report CN-2495 (January 1945), p. 31.
43. W. H. Zachariasen, Metallurgical Project Report CK-2267 (Jan. 1, 1945), p. 11.
44. G. H. Moulton, Los Alamos Report LA-172 (November 1944), p. 2.
45. E. F. Westrum, Jr., Metallurgical Project Report CN-2159 (October 1944), p. 2.
46. A. E. Florin, Metallurgical Project Report CN-2159 (October 1944), p. 5.
47. J. H. Spencer-Palmer, British Report BR-422, p. 10.
48. N. R. Davidson, Metallurgical Project Report CN-3001 (May 1945), p. 4.
49. B. M. Abraham, private communication.

## Paper 15.6

# CHEMISTRY OF NEPTUNIUM. FIRST PREPARATION AND SOLUBILITIES OF SOME NEPTUNIUM COMPOUNDS IN AQUEOUS SOLUTIONS<sup>†</sup>

By T. J. LaChapelle, L. B. Magnusson, and J. C. Hindman

### 1. INTRODUCTION

In the course of investigation of neptunium chemistry several dozen compounds were prepared. In only a few cases were the preparation of the salt and investigation of its properties the primary objectives. Most of the data were collected during the determination of the oxidation states of neptunium and observations on their behavior in aqueous solutions. For this reason the information given on the properties does not represent an exhaustive study. In each case the original method is given. If the compound has been prepared in more than one way, the best method is indicated. All the compounds listed were prepared from aqueous solutions. Compounds formed as a result of gaseous reactions and other dry chemistry methods are recorded elsewhere.<sup>1</sup>

The only known isotope of neptunium having a half life long enough to be useful for determining its chemistry is that of mass 237. Early attempts to prepare neptunium compounds were unsuccessful because only an ultramicro amount of impure neptunium was then available.<sup>2,3</sup> The Np<sup>237</sup> isotope was used in all experiments, in amounts ranging from a few micrograms to several hundred milligrams. This material was purified<sup>4</sup> by separating from all other elements.

Solubilities were measured by transferring an aliquot of the supernatant solution after centrifugation to a thin platinum disk, and deter-

<sup>†</sup>Contribution from the Chemistry Division of the Metallurgical Laboratory, University of Chicago, now the Argonne National Laboratory.

mining the  $\alpha$  activity of the dried material. Most plates prepared in this manner were sufficiently weightless so that self-absorption of the radiation could be neglected. In those cases where the sample was thick enough to introduce an error due to partial absorption of the radiation, approximate corrections were made. The specific-activity value used was 790 counts per minute per microgram of Np<sup>237</sup> (plated as a thin film, in which the absorption of  $\alpha$  particles is negligible, on a smooth platinum disk, the activity being measured in a  $2\pi$ -geometry  $\alpha$  counter).<sup>5</sup> Solubilities are given in terms of grams of neptunium per liter of supernatant solution at 25°C unless otherwise indicated. The usual value of grams of salt per liter is not used since in most cases the exact formula of the solid phase is not known. The values given are actual working solubilities and do not necessarily represent the values that would be obtained under equilibrium conditions.

The preparation of a compound is often best achieved by the initial preparation of the hydroxide of the desired oxidation state, followed by dissolution in the desired acid medium and precipitation of the compound by addition of the proper reagents. In dissolving the neptunium(V) hydroxide, it must be remembered that neptunium(V) disproportionates to neptunium(IV) and (VI) with a hydrogen-ion dependence of about the fourth power.<sup>6</sup> The rate constant is small at room temperature.<sup>7</sup> Occasionally a shorter method not involving the hydroxide intermediary can be used with equal or more success.

Uranium is not known to form any solid compounds of the pentapositive oxidation state from aqueous solution.<sup>8</sup> Only one type compound of pentapositive plutonium<sup>9</sup> has been prepared from solution, and this synthesis requires special conditions. However, since the pentapositive neptunium ion is stable, compounds of this state should be more easily prepared.

The arrangement used for presentation of compounds is practically the same as that given in Gmelins Handbuch ("Gmelins Handbuch der anorganischen Chemie," Uran und Isotope, Verlag Chemie, Berlin, 1936) as well as in the chapter on plutonium compounds in the National Nuclear Energy Series, Volume 14 A.<sup>10</sup> The name given to each compound tells all that is definitely known about it at the time of this writing (1946) including the valence state of the neptunium and the number of other atoms present. When the structure of each compound is better known, the name can be modified to show the additional information. For example, if the formula of potassium neptunium(IV) fluoride is proved to be KNp<sub>2</sub>F<sub>6</sub>, the name would become potassium dineptunium(IV) nonafluoride. Each compound is listed under that element with which its chemistry is most closely associated; thus a nitrate is under nitrogen and not oxygen.

According to a brief survey, solutions and compounds of neptuni-um(IV), (V), and (VI) show no evidence of fluorescence that can be attributed to the neptunium.<sup>11</sup>

## 2. COMPOUNDS OF NEPTUNIUM WITH OXYGEN

**2.1 Neptunium(IV) Dioxide,  $\text{NpO}_2$ .** (a) Properties. The dioxide is a brown solid, the crystalline structure and formula of which were determined by x-ray diffraction studies.<sup>12,13,14</sup> The crystal is face-centered cubic with four metal atoms per unit cell and lattice constant  $a = 5.425 \pm 0.001 \text{ \AA}$ . The Np-O distance is  $2.347 \text{ \AA}$ , and the calculated density is  $11.11 \pm 0.03 \text{ g/cc}$ . The compound shows no signs of decomposition in air at  $800^\circ\text{C}$ . After ignition at an elevated temperature the material is insoluble in dilute or concentrated nitric acid, even when heated; it is only slowly soluble in fuming sulfuric acid and more rapidly soluble in 3M to 10M  $\text{H}_2\text{SO}_4 - 0.1\text{M KBrO}_3$  solution.

(b) Preparation from Neptunium(IV). From a 0.001M Np(IV) solution about  $40 \mu\text{g}$  of neptunium was precipitated as the tan hydroxide by means of a stream of ammonia gas blown at the solution surface. After twice centrifuging and washing with 150-microliter portions of 0.3M  $\text{SO}_2 - 6\text{M NH}_3$  solution, the hydroxide was dried in a platinum crucible at  $105^\circ\text{C}$  and ignited in air at  $700$  to  $800^\circ\text{C}$  for 15 min to produce the anhydrous dioxide.<sup>5,15</sup>

(c) Preparation from Neptunium(V). Ammonia gas was used to precipitate about  $10 \mu\text{g}$  of neptunium as the hydroxide from a 0.04M Np(V) - 0.5M  $\text{HNO}_3$  solution. The precipitate was washed once with strong ammonia water and then redissolved in the same volume of 1M  $\text{HNO}_3$  solution. Reprecipitation with ammonia gas gave a precipitate much more free of adsorbed ions than the first hydroxide. An aliquot of this hydroxide dissolved in 2M  $\text{HNO}_3$  was plated on a platinum disk and carefully evaporated to dryness. Ignition in air at  $800^\circ\text{C}$  for 30 hr produced the dioxide.<sup>5,16</sup>

Presumably, the oxide may be produced by ignition in air at  $700^\circ\text{C}$  of the hydroxide or nitrate of either the neptunium(IV) or (V) state.

**2.2 Neptunium(IV) Peroxide.** (a) Properties. The peroxide is a colorless to white flocculent precipitate. The solubility of the compound in 0.8M  $\text{HNO}_3 - 3\text{M H}_2\text{O}_2$  solution is 0.10 g per liter.<sup>17</sup>

(b) Preparation. A solution containing a few micrograms of neptunium was fumed with sulfuric acid. The dry crystals were dissolved in 50 microliters of water, and neptunium(IV) hydroxide was precipitated by means of ammonia. After centrifugation and washing, the precipitate was dissolved in 50 microliters of 0.5M  $\text{HNO}_3$  solution and reprecipitated with ammonia. After a water wash the hydroxide was carefully dried under an infrared lamp and dissolved in 1.5 micro-

liters of approximately 0.5M HNO<sub>3</sub> solution. The solution was made 1.7M in H<sub>2</sub>O<sub>2</sub> by the addition of 0.3 microliter of 30 per cent peroxide solution. No precipitation occurred within 2 hr. The peroxide concentration was increased to 3M H<sub>2</sub>O<sub>2</sub>. Precipitation of neptunium peroxide gradually occurred. After 1 hr the solution was centrifuged and the solubility as measured on the entire supernatant solution was 0.14 g per liter<sup>17</sup> in 0.4M HNO<sub>3</sub>-3M H<sub>2</sub>O<sub>2</sub> solution.

The peroxide was dissolved in 0.04 microliter of 15M HNO<sub>3</sub> solution, the volume was increased to 0.50 microliter, and 0.25 microliter of 10M H<sub>2</sub>O<sub>2</sub> was added to reprecipitate the peroxide. After 16 hr the precipitate was centrifuged, and the solubility, measured on the entire supernatant solution, was 0.10 g per liter. The peroxide preparation has been repeated on a larger sample.<sup>18</sup>

To determine whether neptunium(V) or neptunium(VI) forms insoluble peroxides, the absorption spectrum of 1.4 ml of 0.0045M Np(VI) in 0.5M HNO<sub>3</sub> solution was observed<sup>19</sup> before and after the addition of the peroxide necessary to make the solution 1.5M in H<sub>2</sub>O<sub>2</sub>. The neptunium(VI) was rapidly reduced to neptunium(V), but no further reduction was observed over a period of 24 hr. No precipitation occurred. Heating produced only decomposition of the hydrogen peroxide. It may be concluded that neptunium(V) and neptunium(VI) probably do not form insoluble peroxides under these conditions.

**2.3 Neptunium(IV) Hydroxide.** (a) Properties. The formula probably is Np(OH)<sub>4</sub>·xH<sub>2</sub>O, but this has not been verified. X-ray diffraction examination of the material gives a pattern which has not been identified. The solid varies in color from tan<sup>20</sup> to an olive-gray.<sup>21,22</sup> The former color especially appears in microgram amounts and the latter in milligram quantities (see below for solubility).

(b) Preparation. The first preparation of this hydroxide occurred during the original preparation of neptunium(IV) dioxide.<sup>5,15</sup> A 150-microliter volume of solution of 1M H<sub>2</sub>SO<sub>4</sub>-0.3M SO<sub>2</sub> containing about 45 µg of neptunium as the sulfate was made 6M in ammonia, precipitating a voluminous tan solid.

If any neptunium compound is dissolved in a dilute (0.5M to 2M) sulfuric acid solution containing 0.3M to 1.3M SO<sub>2</sub>, taken to near dryness by fuming, diluted to approximately 0.5M H<sub>2</sub>SO<sub>4</sub>, and precipitated with hydroxide solution (dilute or concentrated), the product will be neptunium(IV) hydroxide.

From a neptunium(V) or neptunium(VI) solution that is greater than 3M in HCl, excess iodide will cause rapid reduction at 95°C to neptunium(IV). Heating is continued until the disappearance of the iodine color shows that most of the iodine has been removed. Dilution to 0.5M HCl solution and addition of a small amount of hydrazine dihy-

drochloride will convert any remaining iodine to iodide, thus preventing later oxidation of the neptunium(IV) by iodine in basic solution. From this solution containing neptunium(IV), ammonia gas or sodium hydroxide will precipitate neptunium(IV) hydroxide.

The solubility of the hydroxide in a 0.5M  $(\text{NH}_4)_2\text{SO}_4$  solution saturated with ammonia appeared to be 0.0029 g per liter,<sup>18</sup> after 30 min in a 1M  $(\text{NH}_4)_2\text{SO}_4$  solution at 0°C containing a slight excess of ammonia, 0.0022 g per liter,<sup>22</sup> in a 0.8M  $\text{Na}_2\text{SO}_4$ –0.8M NaOH solution, 0.0020 g per liter;<sup>18</sup> in water (no other ions) after 5 min of shaking, 0.00011 g per liter.<sup>18</sup>

**2.4 Neptunium(V) Hydroxide.** (a) Properties. This hydroxide appears to exist in at least three forms: (1) an amorphous-looking green solid, which may be pure hydroxide with the formula  $\text{NpO}_2(\text{OH}) \cdot x\text{H}_2\text{O}$ ; (2) bright-green crystals, which may be a salt-like  $\text{NH}_4\text{NpO}_3 \cdot x\text{H}_2\text{O}$ ; (3) a blue-gray flocculent solid, which may be a salt of the type  $\text{NaNpO}_3 \cdot x\text{H}_2\text{O}$ . X-ray diffraction analysis of the bright-green crystals gave a pattern that is unlike the tetrapositive hydroxide, but it has not yet been interpreted. The hydroxide precipitate of pentapositive neptunium showed no color change after standing 48 hr in contact with the supernatant solution, thus indicating good stability.

(b) Preparation. The original preparation<sup>5,18</sup> occurred during the measurement of the specific activity of  $\text{Np}^{237}$ , although at that time the compound was not recognized as pentapositive. About 15 µg of neptunium as sodium neptunium(VI) dioxytriacetate (commonly called sodium neptunyl acetate) was dissolved in 1.2 microliters of 0.5M  $\text{HNO}_3$ –0.5M  $\text{NaNO}_2$  solution, and ammonia gas was used to precipitate the hydroxide. The precipitate, after being washed with ammonia water, was dissolved in 1.2 microliters of 1M  $\text{HNO}_3$  solution, and green hydroxide was again precipitated with ammonia.

The hydroxide may best be prepared by the addition of either ammonia or an alkali hydroxide solution to a neptunium(V) solution. A sodium neptunium(VI) dioxytriacetate precipitate was dissolved in 0.5M  $\text{H}_2\text{SO}_4$  solution. The 0.080M  $\text{NpO}_2^{++}$  was reduced to a characteristic blue-green  $\text{NpO}_2^+$  solution by directing a stream of sulfur dioxide gas at the surface for 15 min. Treating the solution with ammonia gas produced an amorphous-looking green precipitate [see (1) above]. After standing for 24 hr the precipitate appeared definitely crystalline [see (2) above]. With sodium hydroxide a blue-gray precipitate [see (3) above] is formed from a neptunium(V) solution. This precipitate, upon dissolution in 1M  $\text{H}_2\text{SO}_4$  solution, exhibits the characteristic absorption spectrum of the neptunium(V) ion. The solubility in a 0.5M  $\text{H}_2\text{SO}_4$ –1.0M  $\text{SO}_2$  solution that had been saturated with ammonia was 0.18 g per liter.<sup>18</sup> The solubility of the precipitate in 1M  $\text{NaOH}$ –

1M  $\text{Na}_2\text{SO}_4$  solution is 0.017 g per liter;<sup>22</sup> in 2.2M  $\text{NaOH}$ –1M  $\text{Na}_2\text{SO}_4$  solution, 0.014 g per liter.<sup>22</sup>

By warming a neptunium(IV) solution in 1M  $\text{HNO}_3$  at 80°C for 15 min a pure neptunium(V) solution is produced as ascertained by spectrophotometric observation of the solution. Adding a base to this solution precipitates the neptunium(V) hydroxide. This hydroxide can be dissolved in acid to form a neptunium(V) solution. From a neptunium(VI) solution, in addition to sodium nitrite and sulfur dioxide, the following reducing agents can be used to produce neptunium(V): hydrogen peroxide in dilute nitric acid, stannous chloride in chloride solutions, hydrazine in 1M acid solutions, hydroxylamine in 2M acid solutions, and electrolytic reduction.<sup>7</sup>

**2.5 Neptunium(VI) Hydroxide.** (a) Properties. Both ammonia and sodium hydroxide precipitate a dark brown amorphous-looking solid, which may be  $\text{NpO}_2(\text{OH})_2 \cdot x\text{H}_2\text{O}$  or, more likely,  $(\text{NH}_4)_2\text{NpO}_4 \cdot x\text{H}_2\text{O}$ . Since the solubility is greater in a higher concentration of base, a hydroxy complex presumably exists in these solutions. This action might be indicated by the following type reactions:



The size of the neptunium(VI) ion should allow six oxygen groups around it, and, therefore, the neptunium(VI) dioxytetrahydroxy ion might be postulated as the complex.

(b) Preparation. Five micrograms of neptunium in 10 microliters of 0.75M  $\text{H}_2\text{SO}_4$  solution was oxidized to neptunium(VI) by making the solution 0.2M in  $\text{KBrO}_3$  and heating at 90°C for 30 min. After cooling, the solution was saturated with ammonia by directing a stream of gas at the surface. A very dark brown amorphous-looking precipitate formed. After 1 hr the solution was centrifuged and the supernatant liquid showed a solubility of 0.25 g per liter. After 40 hr equilibrium with no stirring the solubility was 0.10 g per liter.<sup>18</sup>

The hydroxide has also been precipitated from 1M  $\text{HClO}_4$  solution with ammonia and hydroxide.<sup>21</sup> In 0.5M  $(\text{NH}_4)_2\text{SO}_4$  solutions to which ammonia is added the solubility varies thus:<sup>23</sup> in approximately 6M  $\text{NH}_3$ , 0.270 g per liter; in approximately 1M  $\text{NH}_3$ , 0.025 g per liter.

### 3. COMPOUNDS OF NEPTUNIUM WITH NITROGEN

**3.1 Neptunium(IV) Nitrate.** (a) Properties. The solid nitrate has not been prepared, but its formula probably will be  $\text{Np}(\text{NO}_3)_4 \cdot x\text{H}_2\text{O}$ . The nitric acid solution is yellow-green. The solubility of the nitrate

in approximately 5M HNO<sub>3</sub> solution is at least 300 g per liter.<sup>18</sup> A solid phase does not precipitate from a 4M HNO<sub>3</sub> solution containing 80 g per liter.<sup>22</sup>

(b) Preparation. Neptunium(IV) hydroxide will dissolve in nitric acid to give a neptunium(IV) nitrate solution if the temperature is kept below 30°C.

**3.2 Neptunium(V) Nitrate.** (a) Properties. The solid has not been prepared, but its probable formula is NpO<sub>2</sub>NO<sub>3</sub>·xH<sub>2</sub>O. The nitric acid solution is green-blue. In 0.5M HNO<sub>3</sub> solution the solubility exceeds 2.5 g per liter;<sup>23</sup> in 1M HNO<sub>3</sub> it is greater than 8 g per liter;<sup>23</sup> in 5M HNO<sub>3</sub>, it is greater than 50 g per liter.<sup>22</sup>

(b) Preparation. Heating a neptunium(IV) solution in nitric acid at 90°C for several minutes or dissolution of neptunium(V) hydroxide in nitric acid yields a pure neptunium(V) solution. The pentapositive state is obtained as the reduction product of neptunium(VI) in dilute nitric acid when sulfur dioxide, hydrogen peroxide, or sodium nitrite is used as the reductant. Dilute solutions of neptunium(VI) can be reduced to neptunium(V) in 15 min at room temperature<sup>18</sup> in 0.5M HNO<sub>3</sub> by the addition of 0.2M NH<sub>2</sub>OH·H<sub>2</sub>SO<sub>4</sub>.

**3.3 Neptunium(VI) Nitrate.** (a) Properties. The solid has not been prepared; the probable formula is NpO<sub>2</sub>(NO<sub>3</sub>)<sub>2</sub>·xH<sub>2</sub>O. Nitric acid solutions are green, the color being more intense than corresponding neptunium(IV) solutions. In 2.0M HNO<sub>3</sub> the solubility is greater than 38 g per liter.<sup>22</sup>

(b) Preparation. Neptunium(VI) hydroxide dissolves in nitric acid to give a neptunium(VI) nitrate solution. Oxidation of neptunium(IV) to neptunium(VI) in nitric acid<sup>7</sup> occurs with any strong oxidizing agent such as bromate, bismuthate, or cerium(IV).

#### 4. COMPOUNDS OF NEPTUNIUM WITH FLUORINE

**4.1 Ammonium Neptunium(IV) Fluoride.** (a) Properties. A bright green, granular-looking precipitate forms from solutions containing ammonium ion to which hydrofluoric acid is added. The formula is probably similar to NH<sub>4</sub>NpF<sub>3</sub>, analogous to the proposed double potassium fluoride. The solubility in 1M HF - 0.01M NH<sub>4</sub><sup>+</sup> after 2 hr settling was 0.0011 g per liter.<sup>18</sup>

(b) Preparation. The addition of hydrofluoric acid to a solution of neptunium(IV) in the presence of ammonium ion produces the double fluoride. If hydrofluoric acid is added to a solution of neptunium(V) containing ammonium ion and a reducing agent (such as sulfur dioxide), the same product is obtained. The neptunium(V) probably disproportionates into neptunium(IV) and neptunium(VI), the fluoride providing a fast mechanism for the subsequent reduction of neptu-

nium(VI) to neptunium(IV), probably by complex formation.<sup>7</sup> If a reducing agent is not present in the neptunium(V) solution, hydrofluoric acid will precipitate neptunium(IV), leaving neptunium(VI) in solution.

**4.2 Potassium Neptunium(IV) Fluoride.** (a) Properties. The solid is a bright green precipitate whose formula may be  $\text{KNp}_2\text{F}_9$  or  $\text{KNp}_3\text{F}_{13}$  according to x-ray diffraction data.<sup>14</sup>

(b) Preparation. Adding hydrofluoric acid to a solution of neptunium(IV) in the presence of potassium ion precipitates what is probably a complex double fluoride.

A neptunium(IV) solution in  $0.5\text{M H}_2\text{SO}_4 - 0.05\text{M K}_2\text{SO}_4$  was made 2M in hydrofluoric acid. Sixteen hours after mixing, the solubility was found to be 0.0017 g per liter.<sup>18</sup> In  $1.0\text{M H}_2\text{SO}_4 - 1\text{M HF} - 1\text{M KF}$  the supernatant solution contains 0.050 g per liter.<sup>22</sup>

A neptunium(V) solution in 1M HCl was saturated with sulfur dioxide and made 1M in KF and 4M in HF, precipitating the green compound. The concentration of neptunium in the supernatant solution was 0.011 g per liter.<sup>21</sup>

**4.3 Lanthanum Neptunium(IV) Fluoride.** (a) Properties. Since plutonium is believed to form a mixed fluoride with lanthanum,<sup>24</sup> the existence of a neptunium compound appears probable from the color and solubility data. Tracer amounts of neptunium can be carried out of solution by precipitation of lanthanum fluoride from such solutions.<sup>4,25</sup> The solubility of neptunium is also very low if milligram amounts are precipitated from solutions containing equal or greater amounts of lanthanum. One such precipitation of a light-green compound from a solution containing 0.011M Np(IV) - 0.014M La(III) in 3.0 ml gave a neptunium solubility of 0.004 g per liter.<sup>18</sup>

(b) Preparation. From acid solutions containing approximately equal concentrations of lanthanum(III) and neptunium(IV) the addition of hydrofluoric acid precipitates what is probably a mixed fluoride.

## 5. COMPOUNDS OF NEPTUNIUM WITH CHLORINE

**5.1 Neptunium(III) Chloride.** (a) Properties. Only the solution in 1M HCl has been prepared. A 0.005M Np(III) solution is pale purple, with a neptunium solubility greater than 2 g per liter.<sup>26</sup>

(b) Preparation. One and a half milliliters of 0.0075M Np(IV) in 1.63M HCl solution was reduced electrolytically at a mercury pool cathode in a cell with a nitrogen atmosphere. An applied potential of 45 volts was used to maintain a current density of approximately 8 ma/sq cm. The reduction produced a mixture of 86 per cent Np(III) + 14 per cent Np(IV). The reduced solution was stable over a period of 2 hr. Controlled reoxidation by air was slow (several hours) but complete.<sup>27</sup>

**5.2 Neptunium(IV) Chloride.** (a) Properties. The solid prepared from hydrochloric acid solution is yellow, crystalline, and highly deliquescent.<sup>20</sup> The formula is probably  $\text{NpCl}_4 \cdot x\text{H}_2\text{O}$ . Solutions of the chloride vary in color from green in 1M HCl to yellow in 5M HCl. In 0.5M HCl solution the solubility is greater than 24 g per liter; in 2M HCl, greater than 96 g per liter.<sup>18</sup>

(b) Preparation. Ten micrograms of neptunium(IV) hydroxide was precipitated by ammonia from a 1M  $\text{H}_2\text{SO}_4$  solution. The precipitate was partially dried under an infrared lamp. The product was exposed to gaseous hydrogen chloride, yielding a yellow-green solution. Evaporation of the solution at a pressure of approximately  $10^{-2}$  mm Hg gave a yellow crystalline material that was strongly deliquescent.<sup>20</sup>

Neptunium(IV) chloride solutions can be prepared by dissolving neptunium(IV) hydroxide in strong hydrochloric acid. If a higher chloride solution in 3M HCl is treated with Fe(II) at 25°C, the tetrapositive oxidation state is formed. An alternative method is to reduce a higher chloride in 5M HCl solution with excess potassium iodide at 95°C. Free iodine may be reduced by diluting to 0.5M HCl solution, adding hydrazine dihydrochloride, and reheating for 2 min.

**5.3 Neptunium(V) Chloride.** (a) Properties. The solid has not been prepared. In 1M HCl solution the chloride is green-blue in color, having a solubility greater than 70 g per liter.<sup>22</sup> The formula of the hydrated salt will probably be  $\text{NpO}_2\text{Cl} \cdot x\text{H}_2\text{O}$ .

(b) Preparation. Neptunium(VI) chloride can be reduced to neptunium(V) chloride in cold dilute hydrochloric acid by stannous chloride, sulfur dioxide, hydroxylamine hydrochloride, or hydrazine dihydrochloride. A low concentration of chlorine at 75°C will rapidly produce a quite pure neptunium(V) from a neptunium(IV) solution.

**5.4 Neptunium(VI) Chloride.** (a) Properties. The solid has not been separated from an aqueous solution, but if formed its formula probably would be  $\text{NpO}_2\text{Cl}_2 \cdot x\text{H}_2\text{O}$ . Solutions in 1M HCl are dark yellow-green. A solid phase does not separate from 2.5M HCl containing 5 g per liter.<sup>22</sup> In 1.0M HCl solution the solubility is greater than 2 g per liter.<sup>18</sup>

(b) Preparation. Neptunium(VI) hydroxide can be dissolved in hydrochloric acid to form a neptunium(VI) solution. Solutions of neptunium(IV) can be slowly oxidized to neptunium(VI) by the action of chlorine. Cerium(IV) in 1M HCl produces a rapid oxidation.

**5.5 Neptunium(IV) Perchlorate.** (a) Properties. The solid has not been prepared. The salt separating from an aqueous solution will probably have a formula of  $\text{Np}(\text{ClO}_4)_4 \cdot x\text{H}_2\text{O}$ . The solution in 1M  $\text{HClO}_4$  is green, having a solubility exceeding 1 g per liter.<sup>23</sup>

(b) Preparation. Dissolution of neptunium(IV) hydroxide in perchloric acid takes place at a very slow rate because of the lack of

complex formation by the perchlorate ion. The rate of solution is increased by warming, although in this case a large percentage of the neptunium is oxidized to the pentapositive oxidation state.

5.6 Neptunium(V) Perchlorate. (a) Properties. Only solutions have been prepared; that in 1M  $\text{HClO}_4$  is green-blue in color and has a solubility greater than 2 g per liter.<sup>23</sup>

(b) Preparation. The solution can be made by dissolving neptunium(V) hydroxide in perchloric acid, by heating neptunium(IV) in perchloric acid solution, by oxidizing neptunium(IV) with the exact amount of cerium(IV), or by reducing neptunium(VI) with hydrazine or hydroxylamine salts.

5.7 Neptunium(VI) Perchlorate. (a) Properties. The solid has not been made. The color of 0.1M Np(VI) in 1M  $\text{HClO}_4$  is pink. The solubility in 1M  $\text{HClO}_4$  is greater than 2 g per liter.<sup>23</sup>

(b) Preparation. Dissolving neptunium(VI) hydroxide in perchloric acid or the oxidation of a lower state of neptunium in perchloric acid by cerium(IV) or silver(II) will produce neptunium(VI) perchlorate solutions.

## 6. COMPOUNDS OF NEPTUNIUM WITH SULFATE RADICAL

6.1 Neptunium(IV) Sulfate. (a) Properties. Bright green crystals separate from fuming sulfuric acid solutions. The compound appears to be stable in 1M  $\text{H}_2\text{SO}_4$  solution for at least several days. The solubility in 1.0M  $\text{H}_2\text{SO}_4$  solution is about 16 g per liter;<sup>18</sup> in 1M  $\text{H}_2\text{SO}_4$ –0.1M  $\text{K}_2\text{SO}_4$  it is greater than 5 g per liter.<sup>22</sup> The sulfates are much less soluble in concentrated sulfuric acid than they are in dilute acid; in 18M  $\text{H}_2\text{SO}_4$  the solubility is about 3 g per liter.<sup>18</sup> From solutions containing no appreciable concentration of cations other than  $\text{Np}^{+4}$ , the compound  $\text{Np}(\text{SO}_4)_2 \cdot x\text{H}_2\text{O}$  might be formed. Double salts with  $\text{H}^+$ ,  $\text{K}^+$ ,  $\text{NH}_4^+$ , and other ions are possibly formed in solutions containing these ions.

(b) Preparation. A mixed hydroxide of neptunium(IV) and neptunium(V) was dissolved in 0.5M  $\text{H}_2\text{SO}_4$  and fumed to dryness, producing crystals of the sulfate. Dissolution of the crystals in 0.5M  $\text{H}_2\text{SO}_4$  gave a solution that showed pure neptunium(IV) upon spectrophotometric observation.

When the fluoride of neptunium(IV) that precipitates from solutions containing potassium ion is fumed with sulfuric acid, a double sulfate of  $\text{K}^+$  and  $\text{Np}^{+4}$  is probably formed. Dissolution of that compound in 1M  $\text{H}_2\text{SO}_4$  solution showed all the neptunium to be present in the tetrapositive state upon spectrophotometric examination.<sup>21</sup>

Evaporation of a sulfuric acid solution of neptunium(IV) containing ammonium ion produces a compound<sup>20</sup> similar to the above prepara-

tions. The evaporation of 100 microliters of 0.001M Np(IV) in 0.75M H<sub>2</sub>SO<sub>4</sub> solution containing NH<sub>4</sub><sup>+</sup> to a volume of 10 microliters caused the precipitation of a bright-green crystalline compound. X-ray diffraction analysis<sup>20,28</sup> of the material failed to identify the compound by comparison with known thorium, uranium, plutonium, or rare-earth salts.

Reduction of a sulfate of a higher state can be effected at 25°C with excess iron(II) in 1M H<sub>2</sub>SO<sub>4</sub> solution within a few minutes. Oxalic acid will reduce<sup>29</sup> neptunium(V) or neptunium(VI) in about 1 hr at 75°C in 0.6M H<sub>2</sub>SO<sub>4</sub> solution in the presence of Mn<sup>++</sup>, SiF<sub>6</sub><sup>2-</sup>, and PO<sub>4</sub><sup>3-</sup>.

**6.2 Neptunium(V) Sulfate.** (a) Properties. The solid has not been prepared, but its probable formula is (NpO<sub>2</sub>)<sub>2</sub>SO<sub>4</sub>·xH<sub>2</sub>O. The color in 1M H<sub>2</sub>SO<sub>4</sub> solution is green-blue. The solubility in 1M H<sub>2</sub>SO<sub>4</sub> solutions exceeds 2 g per liter.<sup>23</sup>

(b) Preparation. Sodium neptunium(VI) dioxytriacetate was dissolved in 0.5M H<sub>2</sub>SO<sub>4</sub> solution and treated with sulfur dioxide gas to give an immediate change from a green to a green-blue color. The solution proved to be pure neptunium(V) when examined spectrophotometrically.<sup>23</sup> A solution of the sulfate can also be prepared by dissolving neptunium(V) hydroxide in sulfuric acid. Reduction of neptunium(VI) sulfate with hydroxylamine sulfate or hydrazine sulfate in the cold will produce neptunium(V).

**6.3 Neptunium(VI) Sulfate.** (a) Properties. Only solutions have been prepared. These are dark yellow-green in 1M H<sub>2</sub>SO<sub>4</sub>, being more intense than neptunium(IV) solutions. The solubility is greater than 5 g per liter in 1M H<sub>2</sub>SO<sub>4</sub> solution.<sup>22</sup>

(b) Preparation. Neptunium(V) in 1M HNO<sub>3</sub> solution was fumed down with sulfuric acid, dissolved in 0.5M H<sub>2</sub>SO<sub>4</sub> solution, and 0.05M KBrO<sub>3</sub> was added at 25°C to produce very rapid oxidation.<sup>23</sup> Starting with pure neptunium(IV), quantitative oxidation by bromate is very slow at 25°C.<sup>7</sup> Instantaneous oxidation from neptunium(IV) to neptunium(VI) can be effected by cerium(IV) or AgO in 1M H<sub>2</sub>SO<sub>4</sub> solution.<sup>7</sup> Dissolution of neptunium(VI) hydroxide in sulfuric acid will produce pure neptunium(VI) sulfate.

## 7. COMPOUNDS OF NEPTUNIUM WITH ORGANIC RADICALS

**7.1 Sodium Neptunium(VI) Dioxytriacetate, NaNpO<sub>2</sub>(C<sub>2</sub>H<sub>5</sub>O<sub>2</sub>)<sub>3</sub> [or Sodium Neptynyl(VI) Acetate].** (a) Properties. Under daylight or white fluorescent light the crystals are green, and purple-gray under incandescent light. The crystal structure is cubic with four molecules per unit cell, and the lattice constant  $a = 10.659 \pm 0.002$  Å (references 14 and 30 to 33). The density is 2.556 g/cc as calculated from x-ray data. The solubility of the salt in the precipitating medium is about

0.1 g per liter.<sup>18</sup> In 0.5M H<sub>2</sub>SO<sub>4</sub> solution, the acetate dissolves to give a neptunium concentration of about 23 g per liter.<sup>18</sup> (Note: The solubilities given below may be slightly low due to self-absorption of the Np<sup>97</sup> α particles in the high-salt-content plates used for activity measurements.)

(b) Preparation. The original preparation of sodium neptunyl acetate<sup>6,30</sup> involved oxidation of 10 microliters of 0.02M Np<sup>+4</sup> to NpO<sub>2</sub><sup>++</sup> in approximately 0.15M H<sub>2</sub>SO<sub>4</sub>–0.15M KBrO<sub>3</sub> solution by heating at 90°C for 2 hr, cooling to room temperature, and then adding a 4.0M NaNO<sub>3</sub>–4.0M Na(C<sub>2</sub>H<sub>3</sub>O<sub>2</sub>)<sub>3</sub>–0.01M KBrO<sub>3</sub> solution to precipitate the fairly soluble double salt. The solubility was approximately 0.10 g per liter.

The oxidation of 2 ml of 0.013M Np(V) in 0.5M H<sub>2</sub>SO<sub>4</sub> with 0.05M KBrO<sub>3</sub> at room temperature immediately gave NpO<sub>2</sub><sup>++</sup>. Before oxidation the absorption spectrum showed that only neptunium(V) was present. Solid potassium bromate was added, the solution mixed, and the absorption spectrum quickly examined (time interval less than 2 min). The spectrum indicated complete oxidation. Solid reagents were added to make the solution 2.0M in NaNO<sub>3</sub> and 1.6M in NaC<sub>2</sub>H<sub>3</sub>O<sub>2</sub>. The solubility under these conditions was about 0.13 g per liter.<sup>23</sup>

In a 4.0M NaNO<sub>3</sub>–2.0M NaC<sub>2</sub>H<sub>3</sub>O<sub>2</sub> solution the solubility of the double acetate appeared to be about 0.4 g per liter.<sup>23</sup>

7.2 Neptunium(IV) Oxalate. (a) Properties. The solid is green and probably has a formula like Np[(OOC)<sub>2</sub>]<sub>2</sub>·xH<sub>2</sub>O.

(b) Preparation. The oxalate can be precipitated by adding oxalic acid to a neptunium(IV) solution. In 0.87M HCl–0.09M (COOH)<sub>2</sub> solution the solubility was found to be 0.89 g per liter<sup>22</sup> after 60 min.

Adding a soluble oxalate salt to a neptunium(IV) solution will also precipitate the oxalate. Ammonium oxalate solution was added to 0.004M Np(IV) solution in 0.8M HNO<sub>3</sub>–0.1M (COOH)<sub>2</sub>, precipitating a green solid. The concentration of neptunium(IV) remaining in the supernatant solution containing about 0.1M (NH<sub>4</sub>)<sub>2</sub>(OOC)<sub>2</sub> was found to be 0.20 g per liter<sup>24</sup> 12 hr after mixing. The concentration of neptunium in the supernatant solution 90 min after precipitation from 1M HCl–0.014M (NH<sub>4</sub>)<sub>2</sub>(OOC)<sub>2</sub> solution was 0.22 g per liter.<sup>22</sup>

In the presence of 1M H<sub>2</sub>SO<sub>4</sub> solution, the neptunium(IV) oxalate solubility exceeds 5 g per liter.<sup>22</sup>

7.3 Neptunium(IV) Thenoyl Trifluoroacetone. (a) Properties and Preparation.<sup>4</sup> This compound is a green somewhat gelatinous-appearing organic chelate of neptunium(IV) with thenoyl trifluoroacetone (1,1,1-trifluoro, 4-α thenoyl, 2,4-butanedione). Its formula is probably (SC<sub>4</sub>H<sub>7</sub>COCHCOCF<sub>3</sub>)<sub>4</sub>Np.

The green neptunium compound precipitated out<sup>18</sup> at the benzene-water interface when the neptunium concentration in the original

aqueous solution was 0.1M Np(IV), the concentration of the thenoyl trifluoroacetone in benzene was 0.1M, and the volume ratio of water to benzene was unity. With an aqueous solution having a neptunium concentration of 0.008M Np(IV), a 0.06M thenoyl trifluoroacetone solution in benzene, and a volume ratio of 1 no precipitation<sup>22</sup> occurred.

## 8. COMPOUNDS OF NEPTUNIUM WITH PHOSPHORUS

**8.1 Neptunium(IV) Phosphate.** (a) Properties. The solid formed from aqueous solution is a white gelatinous or crystalline compound whose formula may be  $\text{Np}_3(\text{PO}_4)_4 \cdot x\text{H}_2\text{O}$ . Two forms of the compound apparently exist; the crystalline form slowly appears when the gelatinous precipitate is allowed to stand in contact with the supernatant solution.

(b) Preparation. Solutions of neptunium(IV) are precipitated by phosphoric acid. Much of the neptunium left in the supernatant liquid is in a colloidal form, as shown by spectrophotometric examination.

A solution of neptunium(V) in 0.9M  $\text{HNO}_3$ —0.1M  $\text{H}_3\text{PO}_4$  was reduced with 0.004M Fe(II) at 75°C in the presence of 0.2M  $\text{N}_2\text{H}_4 \cdot \text{H}_2\text{SO}_4$ —0.007M Cr(III). After the solution had stood for 17 hr, the concentration of neptunium in the supernatant solution was 0.091 g per liter.<sup>22</sup> All the iron was present as Fe(III).

In another solution containing 0.9M  $\text{HNO}_3$ , 0.06M  $\text{Fe}(\text{NH}_4)_2(\text{SO}_4)_2$ , 0.2M  $(\text{NH}_4)_2\text{SiF}_6$ , 0.1M  $\text{H}_3\text{PO}_4$ , 0.2M  $\text{N}_2\text{H}_4 \cdot \text{H}_2\text{SO}_4$ , and 0.07M Cr(III) the neptunium concentration in the supernatant solution after 19 hr of equilibration was 0.22 g per liter.<sup>22</sup> The increase in solubility was probably due to increased colloid formation caused by the higher iron concentration.

## 9. SUMMARY

Properties and preparations are given for some twenty-four neptunium compounds both in the solid state or as solutions. Where known, properties included are formula, color, crystal structure, density, solubility, and stability. Aqueous solutions of neptunium(III), (IV), (V), and (VI) have been made. From these solutions solid neptunium compounds of the tetrapositive, pentapositive, and hexapositive oxidation states have been prepared which are similar to analogous compounds of uranium and plutonium.

## REFERENCES

1. S. Fried and N. R. Davidson, The basic dry chemistry of neptunium, Paper 15.5, this volume.
2. B. B. Cunningham and L. B. Werner, Metallurgical Project Report CN-556 (Mar. 31, 1943), p. 2.

3. B. B. Cunningham, Metallurgical Project Report CN-991 (Oct. 9, 1943), p. 19.
4. L. B. Magnusson, J. C. Hindman, and T. J. LaChapelle, unpublished work.
5. L. B. Magnusson and T. J. LaChapelle, The first isolation of element 93 in pure compounds and a determination of the half life of  $\text{m-Np}^{157}$ , Paper 1.7, this volume.
6. L. B. Magnusson, J. C. Hindman, and T. J. LaChapelle, Chemistry of neptunium. Formal oxidation potentials of neptunium couples, Paper 15.4, this volume.
7. L. B. Magnusson, J. C. Hindman, and T. J. LaChapelle, Chemistry of neptunium. Kinetics and mechanisms of aqueous oxidation-reduction reactions of neptunium, Paper 15.11, this volume.
8. Metallurgical Project Handbook, Metallurgical Project Report CL-697, Chapter II A (Nov. 24, 1944), p. 1.
9. B. B. Cunningham, Metallurgical Project Report CN-3551 (July 11, 1946), p. 90.
10. B. B. Cunningham, The compounds of plutonium, in National Nuclear Energy Series, Division IV, Volume 14 A.
11. G. R. Price, Metallurgical Project Report CN-3545 (Aug. 13, 1946), p. 11.
12. W. H. Zachariasen, Metallurgical Laboratory Memorandum MUC-WHZ-31 (June 22, 1944).
13. W. H. Zachariasen, Metallurgical Project Report CN-1807 (June 26, 1944).
14. W. H. Zachariasen, Metallurgical Project Report CN-3382 (Jan. 5, 1946).
15. T. J. LaChapelle and L. B. Magnusson, Metallurgical Project Report CN-1764 (July 13, 1944), p. 9.
16. T. J. LaChapelle and L. B. Magnusson, Metallurgical Project Report CN-2159 (Oct. 19, 1944), p. 15.
17. T. J. LaChapelle, Metallurgical Project Report CN-2431 (Dec. 1, 1944), p. 5.
18. L. B. Magnusson and T. J. LaChapelle, unreported results.
19. L. B. Magnusson and J. C. Hindman, Metallurgical Laboratory Memorandum MUC-GTS-2238 (Mar. 14, 1946).
20. L. B. Magnusson and T. J. LaChapelle, Metallurgical Project Report CN-1948 (Aug. 28, 1944), p. 12.
21. L. B. Magnusson, J. C. Hindman, and T. J. LaChapelle, Metallurgical Project Report CN-2767 (March 1945), p. 1.
22. L. B. Magnusson and J. C. Hindman, unreported results.
23. L. B. Magnusson, J. C. Hindman, and T. J. LaChapelle, unreported results.
24. B. B. Cunningham, Metallurgical Project Report CN-3551 (July 11, 1946), p. 108.
25. G. T. Seaborg and A. C. Wahl, Report A-135 (Mar. 19, 1942).
26. L. B. Magnusson, T. J. LaChapelle, and J. C. Hindman, Metallurgical Project Report CN-3053 (July 11, 1945), p. 24.
27. L. B. Magnusson, T. J. LaChapelle, and J. C. Hindman, Chemistry of neptunium. Preparation and properties of neptunium(III), Paper 15.3, this volume.
28. W. H. Zachariasen, private communication (1945).
29. L. B. Magnusson and J. C. Hindman, Metallurgical Laboratory Memorandum MUC-GTS-2157 (Jan. 15, 1946).
30. T. J. LaChapelle and L. B. Magnusson, Metallurgical Project Report CN-2088 (September 1944).
31. W. H. Zachariasen, Metallurgical Laboratory Memorandum MUC-WHZ-54 (Aug. 29, 1944).
32. W. H. Zachariasen, Metallurgical Laboratory Memorandum MUC-WHZ-97 (Jan. 4, 1945).
33. W. H. Zachariasen, Metallurgical Project Report CN-2091 (Sept. 4, 1944), p. 2.

## Paper 15.7

### THE HALIDES OF NEPTUNIUM†

By L. Brewer, L. Bromley, P. W. Gilles, and N. L. Lofgren

#### 1. INTRODUCTION

Because of the close similarity of uranium and neptunium it is possible to estimate many of the thermodynamic properties of neptunium compounds by comparison with uranium. Thus the experimental data for the oxidation-reduction potentials of the neptunium ions and the heat of solution of neptunium metal can be used to estimate the heats of formation of the neptunium halides, by assuming the same heats of solution for the corresponding neptunium and uranium halides. Thermodynamic data for the uranium ions and halides were obtained from the survey report by Brewer, Bromley, Gilles, and Lofgren.<sup>3</sup> Summaries of the constants for neptunium are given in Table 1 and 2.

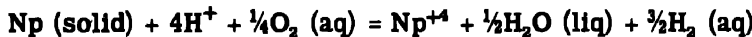
To calculate the equilibrium concentrations of the various neptunium species at elevated temperatures, the methods described in the above-mentioned uranium report and also in a report on the properties of molybdenum and tungsten halides, by Brewer, Bromley, Gilles, and Lofgren,<sup>5</sup> were employed. Values of the free-energy functions  $(\Delta F - \Delta H_{298})/T$  were taken to be the same as for the corresponding uranium compounds. Where volatility data were necessary, the vapor-pressure equations derived for the corresponding uranium compounds were assumed applicable.

The summary report on the chemistry of neptunium by Cunningham and Hindman<sup>7</sup> was the source of most of the information on the methods of preparation and physical properties of the compounds.

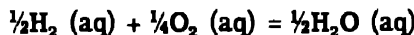
†Contribution from the Department of Chemistry, University of California, Berkeley.

## 2. NEPTUNIUM AQUEOUS IONS

Westrum and Eyring<sup>6</sup> have found the partial molal heat of solution of neptunium metal in 1.55M HCl containing a low concentration of fluosilicate ion to be  $\Delta H_{298} = -165.3$  kcal for the reaction



Taking  $\Delta H_{298} = -32.5$  kcal for



all in 1.55M HCl, and using the partial molal heats of dilution for hydrochloric acid given by Sturtevant<sup>6</sup> and the data on heats of dilution of ThCl<sub>4</sub> and UCl<sub>4</sub> reviewed by the authors in the uranium report,<sup>3</sup> we can calculate  $\Delta H_{298} = -133.2$  kcal for the formation of Np<sup>+4</sup> in 1M HCl. The effect of fluosilicate ion is neglected.

The heat of formation of Np<sup>+3</sup> in 1M HCl was obtained from the Np<sup>+4</sup> heat and the Np<sup>+3</sup>-Np<sup>+4</sup> potential in the following manner. Cunningham and Hindman<sup>7</sup> report  $\Delta F_{298} = 3.2 \pm 0.5$  kcal for



in 1M HCl. The  $\Delta S$  values given by Brewer, Bromley, Gilles, and Lofgren<sup>8</sup> from the corresponding uranium and plutonium couples averaged and combined with the neptunium  $\Delta F$  value to obtain  $\Delta H_{298} = -5.9 \pm 2$  kcal for the Np<sup>+3</sup>-Np<sup>+4</sup> potential. This gave  $\Delta H_{298} = -127.8 \pm 2$  kcal as the partial molal heat of formation of Np<sup>+3</sup> in 1M HCl.

The partial molal free energy of formation of Np<sup>+3</sup> in 1M HCl was obtained by assuming the same  $\Delta S$  of formation as that of uranium. This is not unreasonable since the decrease in entropy due to the decrease in size from U<sup>+3</sup> to Np<sup>+3</sup> is undoubtedly overcome by the addition of magnetic entropy. An abnormal increase in entropy in going from uranium metal to neptunium metal might make the Np<sup>+3</sup>  $\Delta S$  a unit or so more negative than for U<sup>+3</sup>. The difference is undoubtedly less than the 2 kcal uncertainty in the Np<sup>+3</sup> heat. Thus we obtain  $\Delta F_{298} = -128.4$  kcal for Np<sup>+3</sup> in 1M HCl.

The partial molal free energies of Np<sup>+4</sup>, NpO<sub>2</sub><sup>+</sup>, and NpO<sub>2</sub><sup>++</sup> were calculated from the Np<sup>+3</sup> value and the potentials summarized by Cunningham and Hindman.<sup>7</sup> They give  $\Delta F_{298} = 3.2 \pm 0.5$  kcal for the Np<sup>+3</sup>-Np<sup>+4</sup> couple,  $\Delta F_{298} = 20.2 \pm 2$  kcal for the Np<sup>+3</sup>-NpO<sub>2</sub><sup>+</sup> couple, and  $\Delta F_{298} = 46.4 \pm 2$  kcal for the Np<sup>+3</sup>-NpO<sub>2</sub><sup>++</sup> couple. Thus the fol-

lowing values are obtained for  $\text{Np}^{+4}$ ,  $\Delta F_{298} = -125.2$  kcal; for  $\text{NpO}_2^+$ ,  $\Delta F_{298} = -108.2$  kcal; and for  $\text{NpO}_2^{++}$ ,  $\Delta F_{298} = -82.0$  kcal.

To obtain the heats of formation of  $\text{NpO}_2^+$  and  $\text{NpO}_2^{++}$  in 1M HCl from the above  $\Delta F$  values, the average is taken of the  $\Delta S$  values for the corresponding uranium and plutonium species, which yields for  $\text{NpO}_2^+$ ,  $\Delta H_{298} = -94.2$  kcal, and for  $\text{NpO}_2^{++}$ ,  $\Delta H_{298} = -71.9$  kcal.

No results of determinations in perchloric acid solutions are available, but values may be estimated by comparison with uranium and plutonium. By using the same change in  $\Delta H$  in going from 1M HCl to 0.5M  $\text{HClO}_4$  as occurs in the case of  $\text{U}^{+3}$ ,  $\Delta H_{298} = -126.9$  kcal is obtained for  $\text{Np}^{+3}$  in 0.5M  $\text{HClO}_4$ . By using the same  $\Delta S$  as for  $\text{U}^{+3}$ ,  $\Delta F_{298} = -128.4$  kcal is obtained for  $\text{Np}^{+3}$ . The  $\Delta H$  and  $\Delta F$  values for the other ions were obtained by averaging the change on going from hydrochloric to perchloric acid solution for the corresponding uranium and plutonium species. All the results for both solutions are given in Table 1. These values may be used as approximations for other solutions as long as the ions are not hydrolyzed and complexed. Kraus and Nelson<sup>15</sup> report that  $\text{Np}^{+4}$  is unhydrolyzed for pH values below 1.5, that  $\text{NpO}_2^+$  hydrolyzes to a polymer in the pH range 7.5 to 9, and that  $\text{NpO}_2^{++}$  hydrolyzes to a polymer around pH 5 or higher.

Knowing the values for the ions, the heats of formation for the solid halides can now be estimated. The heats of solution were obtained by averaging the uranium and plutonium values and then using this average with the neptunium ion values to obtain the heats given in Table 2.

To illustrate the procedure, the calculation of the heat of formation for  $\text{NpBr}_3$  will be carried out. The  $\Delta H_{298}$  of formation of  $\text{UBr}_3$  is  $-181.1$  kcal, and the  $\Delta H_{298}$  for  $\text{U}^{+3}$  in 0.5M  $\text{HClO}_4$  is  $-123.2$  kcal. The difference,  $\text{UBr}_3 - \text{U}^{+3}$ , is  $-57.9$  kcal. The corresponding difference for  $\text{PuBr}_3 - \text{Pu}^{+3}$  with the ion value for 0.5M  $\text{HClO}_4$  is  $-57.6$  kcal. Applying the average  $-57.75$  to  $-126.9$ , the  $\Delta H_{298}$  for  $\text{Np}^{+3}$  in 0.5M  $\text{HClO}_4$ , we obtain  $-184.7$  for  $\Delta H_{298}$  of  $\text{NpBr}_3$ , which value may be rounded off to  $-185$  kcal.

This may also be done using free energies of formation of the ions. Thus  $\Delta F_{298}$  for  $\text{U}^{+3}$  in 1M HCl is  $-124.7$  kcal and  $\Delta H_{\text{UBr}_3} - \Delta F_{\text{U}^{+3}} = -56.5$ . In the plutonium system,  $\Delta H_{\text{PuBr}_3} - \Delta F_{\text{Pu}^{+3}} = -56.1$ . Applying the average  $-56.3$  to  $-128.4$ , the  $\Delta F_{298}$  value for  $\text{Np}^{+3}$  in 1M HCl, gives  $-184.7$  for  $\Delta H_{298}$  of  $\text{NpBr}_3$ , in agreement with the previous value.

$\Delta H$  and  $\Delta F$  values from both 0.5M  $\text{HClO}_4$  and 1M HCl solutions were used for these calculations. The choice depended on which values were most closely derived from direct experimental determinations. The  $\Delta H$  values of Table 1 are partial molal heat-content changes. The  $\Delta F$  values for 1M acid solutions are the actual partial molal free-

energy changes with all ions in the 1M acid solution with no corrections for activity coefficients. The values given for 0.5M acid solutions are corrected to unit concentration but are not corrected for activity coefficients.

Table 1—Partial Molal Heats and Free Energies of Formation  
for Neptunium Aqueous Ions at 298°K

Reaction	1M HCl	0.5M HClO <sub>4</sub>
$\text{Np} + 3\text{H}^+ = \text{Np}^{+3} + \frac{3}{2}\text{H}_2$ (gas)	$\Delta H_{298} = -127.3$ $\Delta F_{298} = -128.4$	$\Delta H_{298} = -126.9$ $\Delta F_{298} = -133.2$
$\text{Np} + 4\text{H}^+ = \text{Np}^{+4} + 2\text{H}_2$ (gas)	$\Delta H_{298} = -125.2$ $\Delta F_{298} = -124.9$	$\Delta H_{298} = -133.1$ $\Delta F_{298} = -124.9$
$\text{Np} + 2\text{H}_2\text{O}$ (liq) + $\text{H}^+ = \text{NpO}_2^+ + \frac{3}{2}\text{H}_2$ (gas)	$\Delta H_{298} = -94.2$ $\Delta F_{298} = -108.2$	$\Delta H_{298} = -94$ $\Delta F_{298} = -108$
$\text{Np} + 2\text{H}_2\text{O}$ (liq) + $2\text{H}^+ = \text{NpO}_3^{++} + 3\text{H}_2$ (gas)	$\Delta H_{298} = -71.9$ $\Delta F_{298} = -82.0$	$\Delta H_{298} = -72$ $\Delta F_{298} = -82$

Table 2—Estimated Thermodynamic Constants for Neptunium Halides

Compound	$\Delta H_{298^\circ\text{K}}$ , kcal/mole	Compound	$\Delta H_{298^\circ\text{K}}$ , kcal/mole
$\text{NpF}_3$	$-360 \pm 2$	$\text{NpCl}_3$	$-246 \pm 2$
$\text{NpF}_4$	$-428 \pm 3$	$\text{NpCl}_4$	$-230 \pm 2$
$\alpha\text{-NpF}_5$	$-467 \pm 3$	$\text{NpBr}_3$	$-185 \pm 1$
$\text{NpF}_5$ (gas)	$-463 \pm 3$	$\text{NpBr}_4$	$-197.5 \pm 1$
$\text{NpCl}_3$	$-216 \pm 2$	$\text{NpI}_3$	$-141 \pm 1$
$\text{NpCl}_4$	$-237 \pm 1$	$\text{NpI}_4$	$-143$

All values in Table 1 are given in kilocalories per mole. Concentrations are in moles per 1,000 g  $\text{H}_2\text{O}$ . It is not possible to give a very definite uncertainty for these absolute values. They are all based on one determination of the heat of solution of neptunium, for which an uncertainty cannot be given at this time. However, the uncertainties in the differences between values can be given fairly closely and will be found in the text where data for the various couples are given. If the heat of solution of neptunium is revised, all the values given here will be changed by the same amount.

$(\Delta F - \Delta H_{298})/T$  values may be obtained from the uranium survey report by Brewer, Bromley, Gilles, and Lofgren<sup>3</sup> for calculations of  $\Delta F$  values. The remarks on the uncertainties of the  $\Delta H$  values made in connection with Table 1 apply equally well to Table 2. If the heat

of solution of neptunium metal is revised, all the values given here will be changed by the same amount. The uncertainties limit accurate calculations, but much useful qualitative information may be obtained from thermodynamic calculations.

### 3. HIGH-TEMPERATURE CHEMISTRY OF THE NEPTUNIUM HALIDES

**3.1 Neptunium Fluorides.**  $\text{NpF}_3$  is calculated to be quite stable toward decomposition even much above its boiling point of  $2500^\circ\text{K}$ , and it is undoubtedly the major gaseous species at the very highest temperatures. According to the summary by Cunningham and Hindman,<sup>7</sup>  $\text{NpF}_3$  was prepared by the action of hydrogen and hydrogen fluoride on  $\text{NpO}_2$  at  $800^\circ\text{K}$  to form a black-purple hexagonal lanthanum fluoride type of crystal structure with a density of 9.12. The observation that it can be reduced to the metal by barium is in agreement with the heat of formation given in Table 2.

$\text{NpF}_4$  is calculated to be stable toward decomposition even at temperatures well above its boiling point of about  $1700$  to  $1800^\circ\text{K}$ . The action of oxygen and hydrogen fluoride on  $\text{NpO}_2$  at  $800^\circ\text{K}$  produced a light-green monoclinic zirconium fluoride type of crystal structure with a density of 6.84. Fried, Florin, and Davidson<sup>4</sup> found that hydrogen fluoride free of hydrogen is necessary to prevent reduction of  $\text{NpF}_4$  to  $\text{NpF}_3$  at  $800^\circ\text{K}$ , although Florin<sup>10</sup> claims  $\text{NpF}_4$  to be stable in 0.1 atm of  $\text{H}_2$  (gas) and 0.9 atm of HF (gas) on the basis of one observation. We calculate that  $2 \times 10^{-4}$  atm of  $\text{H}_2$  (gas) in 1 atm of HF (gas) would cause reduction at  $800^\circ\text{K}$ .

Solid and liquid  $\text{NpF}_5$  are calculated to be quite stable toward decomposition. At  $1000^\circ\text{K}$ , which is estimated to be the boiling point of  $\text{NpF}_5$ , 1 atm of  $\text{NpF}_5$  is calculated to contain only  $10^{-11}$  atm of  $\text{F}_2$  (gas) and  $10^{-3}$  atm of  $\text{NpF}_6$  (gas) owing to decomposition and disproportionation.  $\text{NpF}_5$  has not been prepared yet because it is difficult to find an oxidizing agent that will oxidize  $\text{NpF}_4$  to  $\text{NpF}_5$  without oxidizing it further to the volatile  $\text{NpF}_6$ . It could best be prepared by passing  $\text{NpF}_5$  (gas) over  $\text{NpF}_4$  (solid) at about  $600$  to  $650^\circ\text{K}$ .

Solid  $\text{NpF}_6$  is calculated to be just barely stable with respect to  $\text{NpF}_5$ , with the fluorine partial pressure reaching about 1 atm just above room temperature, i.e., at about  $300^\circ\text{K}$ . At the sublimation point in the neighborhood of  $330^\circ\text{K}$ , 1 atm of  $\text{NpF}_6$  (gas) is calculated to be in equilibrium with  $\text{NpF}_5$  (solid) and about 1 atm of  $\text{F}_2$  (gas). However, as the temperature is increased,  $\text{NpF}_6$  gas becomes more stable, and at  $500^\circ\text{K}$  1 atm of  $\text{NpF}_6$  (gas) is calculated to be in equilibrium with solid  $\text{NpF}_5$  and about  $10^{-3}$  atm of  $\text{F}_2$  (gas). At  $1000^\circ\text{K}$  a

mixture of  $\text{NpF}_3$  and  $\text{NpF}_6$ , each at 1 atm partial pressure, is calculated to contain about  $5 \times 10^{-8}$  atm  $\text{F}_2$ . According to the summary by Cunningham and Hindman,<sup>7</sup> the  $\text{NpF}_6$ , prepared by passing fluorine over  $\text{NpF}_3$  at a bright-red heat and condensing the volatile product in a liquid-air trap, is white and has the  $\text{UF}_6$  crystal structure. Florin<sup>11</sup> reports a melting point of 326°K and some indication of decomposition of the solid crystals, although the rate at room temperature was too slow to be observed. The observations are in very good agreement with the calculations. Thermodynamically,  $\text{NpF}_6$  is unstable around 330°K with fluorine pressures of less than 1 atm, but it is stable at higher and lower temperatures. The rate of decomposition is undoubtedly slow in the unstable range, and rapid cooling allows the  $\text{NpF}_6$  to be preserved.

**3.2 Neptunium Chlorides.** At room temperature  $\text{NpCl}_3$ ,  $\text{NpCl}_4$ , and  $\text{NpCl}_5$  are all stable toward decomposition.  $\text{NpCl}_3$  is calculated to be stable from its boiling point of about 1800°K to temperatures in the vicinity of the neptunium-metal boiling point, at which temperatures gaseous neptunium and monatomic chlorine are formed with possibly also  $\text{NpCl}_2$  and  $\text{NpCl}$ .  $\text{NpCl}_3$  is reported to be prepared by the action of hydrogen on  $\text{NpCl}_4$  at about 600°K to form a white hexagonal lanthanum chloride type of crystal structure with a density of 5.58.  $\text{NpCl}_3$  is reported to melt around 1073°K, but the presence of impurities was indicated by the fact that the melting point was not sharp.

$\text{NpCl}_4$  is calculated to be stable to temperatures somewhat above 2500°K at atmospheric pressure. Above this temperature it would dissociate appreciably to  $\text{NpCl}_3$  and chlorine. Treatment of  $\text{NpO}_2$  with carbon tetrachloride at about 750°K produces  $\text{NpCl}_4$  in a yellow tetragonal thorium chloride type of crystal form with a density of 4.92. Fried<sup>12</sup> reports a sharp melting point of 811°K. The ready reduction by hydrogen to  $\text{NpCl}_3$  observed by Fried, Florin, and Davidson<sup>4</sup> is in agreement with the thermodynamic data given here.

Although  $\text{NpCl}_6$  is calculated to be unstable in any state,  $\text{NpCl}_5$  is calculated to have a decomposition chlorine pressure of less than  $10^{-3}$  atm at 500°K, and the chlorine pressure does not reach 1 atm until about 800 to 900°K, or close to the boiling point of  $\text{NpCl}_5$ . An equimolar mixture of  $\text{NpCl}_5$  and  $\text{NpCl}_4$  gases at 1000°K will be in equilibrium with very much less than 1 atm of  $\text{Cl}_2$  (gas).  $\text{NpCl}_5$  has not been prepared yet, but a possible method is by passing  $\text{Cl}_2$  (gas) free of oxygen compounds over  $\text{NpCl}_4$  at 500 to 750°K, depending on the rate of reaction.

**3.3 Neptunium Bromides.**  $\text{NpBr}_3$  and  $\text{NpBr}_4$  are both calculated to be stable at room temperature.  $\text{NpBr}_3$  has been found to have a green

hexagonal lanthanum chloride type of crystal structure with a density of 7.11.  $\text{NpBr}_3$  is stable at temperatures much above its boiling point of about  $1800^\circ\text{K}$ , and probably to above  $3000^\circ\text{K}$ , where it would be dissociated to gaseous neptunium and monatomic bromine or lower neptunium bromides.

Solid  $\text{NpBr}_4$  is stable, but liquid  $\text{NpBr}_4$  is calculated to decompose to  $\text{NpBr}_3$  (solid) in an atmosphere of bromine at about  $700$  to  $800^\circ\text{K}$ . As a gaseous species  $\text{NpBr}_4$  is not very important. A bromine atmosphere over  $\text{NpBr}_3$  (liq) at  $1100^\circ\text{K}$  would contain only about 0.1 atm  $\text{NpBr}_4$  (gas). The partial pressure of  $\text{NpBr}_4$  (gas) in  $\text{Br}_2$  (gas) over  $\text{NpBr}_3$  (liq) increases as the temperature is increased until the boiling point of  $\text{NpBr}_3$  is reached.  $\text{NpBr}_4$  was found to have a reddish-brown  $\text{UBr}_4$  type of crystal form. Fried<sup>13</sup> reports a melting point of  $737$  to  $741^\circ\text{K}$ . Fried<sup>14</sup> also observed volatilization with partial decomposition at  $1073^\circ\text{K}$ , which is in partial agreement with the instability calculated from the thermodynamic data, although the observation tends to indicate a slow rate or a greater stability than calculated.

$\text{NpBr}_5$  does not appear to occur appreciably. Its maximum concentration would be found in a bromine atmosphere over  $\text{NpBr}_4$  (liq) at about  $700^\circ\text{K}$ , but its concentration would be very small.

**3.4 Neptunium Iodides.** No iodides above  $\text{NpI}_4$  exist. Solid  $\text{NpI}_4$  is unstable with respect to  $\text{NpI}_3$  and solid iodine. However, some  $\text{NpI}_3$  may be obtained in the gaseous state. At  $1000^\circ\text{K}$  the partial pressure of  $\text{NpI}_4$  (gas) in equilibrium with  $\text{NpI}_3$  and an atmosphere of  $\text{I}_2$  (gas) was calculated to be less than  $10^{-3}$  atm.

$\text{NpI}_3$  is calculated to be stable up to temperatures around  $2500^\circ\text{K}$ , at which temperature it would dissociate to the gaseous elements. The action of aluminum iodide on  $\text{NpO}_2$  yielded  $\text{NpI}_3$  in an orthorhomic lanthanum iodide type of crystal form with a density of 6.82. Fried<sup>13</sup> reports a melting point of  $1033$  to  $1045^\circ\text{K}$ .

**3.5 Neptunium Oxyhalides.** None of the tripositive oxyhalides have been reported, but they all should be stable.  $\text{NpOF}$  probably has the cubic calcium fluoride type of structure and  $\text{NpOCl}$ ,  $\text{NpOBr}$ , and  $\text{NpOI}$  probably have the tetragonal  $\text{PbFCl}$  type of structure, by analogy to uranium and plutonium. In view of the uncertainty of the uranium oxyhalide heats as discussed by Brewer, Bromley, Lofgren, and Gilles,<sup>3</sup> it does not seem profitable to give any estimates of the heats of formation of the neptunium oxyhalides. However, if values are desired, they may be obtained readily in the cases of the tripositive compounds by using the heats of solution of the plutonium compounds. In the cases of the tetrapositive compounds, the heats may be estimated by comparison with the uranium compounds.

Of the tetrapositive compounds,  $\text{NpOCl}_2$  is reported to form yellow crystals with the  $\text{UOCl}_4$  structure.  $\text{NpOBr}_2$  is reported to be a yellow material with the  $\text{UOBr}_4$  structure.

#### 4. SUMMARY

The thermodynamic data for the ions of neptunium, from which the heats of formation of the neptunium halides are obtained, have been given. Using these, the regions of stability of the halides can be calculated. The calculations indicate that  $\text{NpF}_6$  and  $\text{NpCl}_5$  are the stable halides of highest oxidation number.  $\text{NpBr}_4$  is the highest bromide that is stable. In the iodide system only  $\text{NpI}_3$  is stable.

Calculations based on the thermodynamic data of this report were checked against the observed chemical behavior and the excellent checks lend confidence in the use of these data for calculations on unexplored regions.

#### REFERENCES

1. L. B. Magnusson, T. J. LaChapelle, and J. C. Hindman, Metallurgical Project Report CN-3053 (June 28, 1945).
2. L. B. Magnusson, T. J. LaChapelle, and J. C. Hindman, Metallurgical Project Report CN-2767 (March 1945).
3. L. Brewer, L. A. Bromley, P. W. Gilles, and N. L. Lofgren, Manhattan District Declassified Document MDDC-1543 (BC-82) (Apr. 1, 1947).
4. S. Fried, A. E. Florin, and N. R. Davidson, Metallurgical Project Report CN-2689 (Feb. 15, 1945).
5. L. Brewer, L. A. Bromley, P. W. Gilles, and N. L. Lofgren, The thermodynamic properties of molybdenum and tungsten halides and the use of these metals as refractories, National Nuclear Energy Series, Division IV, Volume 19 B, Paper 8, McGraw-Hill Book Company, Inc., New York, in press (Metallurgical Project Report CT-3232, Sept. 1, 1945).
6. L. Brewer, L. A. Bromley, P. W. Gilles, and N. L. Lofgren, The thermodynamic properties and equilibria at high temperatures of the compounds of plutonium, Paper 8.40, this volume; Metallurgical Project Report CN-3378 (Dec. 1, 1945).
7. B. B. Cunningham and J. C. Hindman, Metallurgical Project Report CC-3865 (October 1946).
8. E. F. Westrum, Jr., and L. Eyring, private communication, Radiation Laboratory, Berkeley, September 1947.
9. J. M. Sturtevant, J. Am. Chem. Soc., 62: 3265 (1940); 64: 762 (1942).
10. A. E. Florin, unpublished work mentioned in Metallurgical Project Report CC-3865 (October 1946).
11. A. E. Florin, Metallurgical Laboratory Memorandum MUC-GTS-2163 (Jan. 23, 1946).
12. S. Fried, Metallurgical Project Report CP-3497 (April 1946).
13. S. Fried, Metallurgical Project Report CP-3521 (May 1946).
14. S. Fried, Metallurgical Project Report CP-3381 (Dec. 27, 1945).
15. K. A. Kraus and F. Nelson, Abstracts of the American Chemical Society Meeting, Chicago, Apr. 21, 1948.

## Paper 15.9

# A TRACER STUDY OF THE VALENCE STATES OF NEPTUNIUM<sup>†</sup>

By A. F. Voigt, N. R. Sleight, R. E. Hein, and J. M. Wright

### 1. INTRODUCTION

At the time the studies reported here were being made it was known that neptunium existed in at least two different oxidation states in solution—a higher, fluoride-soluble, and a lower, fluoride-insoluble, state; this is exactly the same information as was known for plutonium when its chemistry was known from tracer studies only. In addition, some work had been done with microgram quantities of neptunium compounds in the solid state. It had been shown by x-ray crystallography<sup>1</sup> that the sodium double-acetate precipitate with the higher valent (fluoride-soluble) neptunium was isomorphous with the compounds  $\text{NaUO}_2(\text{C}_2\text{H}_3\text{O}_2)_3$  and  $\text{NaPuO}_2(\text{C}_2\text{H}_3\text{O}_2)_3$ , which proved that the higher valence was +6. Similarly it had been shown<sup>2</sup> that the oxide obtained on igniting lower valent hydroxides was  $\text{NpO}_2$ , isomorphous with  $\text{PuO}_2$  and  $\text{UO}_2$ . This proved that +4 is one of the valences of neptunium in the solid state, but it did not prove that it is the most stable or even that it exists in dissolved, lower valent neptunium salts.

In a number of tracer studies, differences between the behavior of the reduced states of plutonium and neptunium were demonstrated. These differences were interpreted as showing that the valence states of the two reduced ions differed. It was thought possible, for example, that the common ions in solution were  $\text{Np(III)}$  and  $\text{Pu(IV)}$ , but this belief was later shown to have no basis.

Work done by the Berkeley group<sup>3</sup> was interpreted as demonstrating the existence of a fluoride-soluble sodium acetate-soluble state, intermediate between the two normal states and thus, most probably,

<sup>†</sup>Contribution from the Department of Chemistry and the Institute for Atomic Research of the Iowa State College.

Based on Metallurgical Project Report CN-1979 (Oct. 10, 1944).

Np(V). The basis of this postulate was the observation that, shortly after dichromate was added to reduced neptunium tracer, little carrying (2 to 10 per cent) was obtained with either  $\text{NaUO}_2(\text{C}_2\text{H}_3\text{O}_2)_3$ , or  $\text{LaF}_3$ , when precipitated from aliquots of the same original solution. The conclusion that a valence state existed intermediate between those characterized by insoluble fluoride and insoluble double acetate was apparent.

Later work in Chicago<sup>2</sup> showed that another interpretation was possible without postulating the existence of a third oxidation state. In this work, the solution containing tracer neptunium and oxidizing agent was treated with hydrofluoric acid and excess La(III). The neptunium content was determined by assaying the supernatant solution. A sodium uranyl acetate precipitation was then made, and the precipitate and solution were analyzed. It was found that practically none of the neptunium tracer escaped both precipitations and that no fluoride-soluble, double acetate-soluble state was produced. The explanation offered for the previous results was that there was a greatly increased rate of oxidation in the presence of hydrofluoric acid. Thus when hydrofluoric acid was added to precipitate lanthanum fluoride, the neptunium was rapidly oxidized to the hexapositive state, but it remained in the tetrapositive state during the precipitation of  $\text{NaUO}_2(\text{C}_2\text{H}_3\text{O}_2)_3$ , which precipitation must be carried out in the absence of hydrofluoric acid. The excess La(III) was used in the latter experiment to remove all hydrofluoric acid and to permit the precipitation of the double acetate from the same solution.

A different approach was employed in the work described here, namely, reagents supposedly specific for one valence or for odd or even valences were used. The idea originated in studies on plutonium decontaminated from rare earths, in which a single precipitation of zirconium phenylarsonate was effective in carrying 99 per cent of the Pu(IV) and less than 0.5 per cent of the tripositive rare-earth activities. In applying this to straight plutonium chemistry, it was found that an effective separation of Pu(III) and Pu(IV) could be made by the same method.<sup>4,5</sup> In conversation with R. E. Connick it was learned that the Berkeley group also was successful in applying the phenylarsonate method to valence state distinctions in plutonium. It was decided to try this method in the neptunium case.

As it turned out, the results using phenylarsonate precipitation were reliable.

## 2. EXPERIMENTS WITH ZIRCONIUM PHENYLARSONATE<sup>6</sup>

These studies were made using  $\text{Np}^{230}$  obtained from cyclotron-bombarded uranyl nitrate and separated from fission-product activity

by three lanthanum fluoride oxidation-reduction cycles. A final lanthanum hydroxide precipitate was divided into two portions, one of which was dissolved in hydrochloric acid and the other in nitric acid.

The zirconium phenylarsonate precipitations were made in a uniform manner, from 10 ml of final solution, with 1 mg of Zr carrier, 0.5 mg of La as "holdback" agent and a tenfold excess of phenylarsonic acid. The neptunium left in solution by any procedure was analyzed by sulfur dioxide reduction followed by lanthanum fluoride precipitation. Precipitates of lanthanum fluoride made under various conditions were counted directly; those of zirconium phenylarsonate were dissolved in dilute hydrofluoric acid; and the neptunium was recovered for measurement by lanthanum fluoride precipitation. Final lanthanum fluoride precipitations were made in flattened lusteroid tubes which were dried and mounted before measuring the activity on Lauritsen electroscopes.

It was known that more than 95 per cent of the Pu(IV) was carried by zirconium phenylarsonate under these conditions, but the amount of Np(IV) carried was not known. To obtain data on this, repeated precipitations of the salt were made from several solutions containing neptunium tracer. The results, shown in Table 1, indicate that three precipitations removed only 62 per cent from nitric acid solutions and 93 per cent from hydrochloric acid solutions. The falling off of the carrying from the first to the third precipitation indicates that little more would be carried by further precipitations and, therefore, that 62 per cent and 93 per cent represent all that is in a carryable valence state in these solutions. Actually a small amount of some other state may have been carried, but the separation appears to be quite clear-cut.

The second column under each solution in Table 1 gives the percentage of the total in each precipitate, and the third column gives the percentage of the sum of the three phenylarsonate precipitates found in each. Thus 80 to 89 per cent of that in a state carryable by zirconium phenylarsonate [presumably Np(IV)] was carried in one precipitation under these conditions.

The results of many experiments under varied nonoxidizing conditions are given in Table 2. In all cases duplicate runs were made. Reasonably good agreement was obtained as shown by the  $\pm$  errors, which are mean deviations; the number of runs was usually too small for more rigorous statistical methods to be applied. The results are given on the basis of the activity recovered, and the extent of that recovery is given in the last column.

Examination of the table shows that from 27 to 91 per cent of the neptunium has been carried in the various precipitations. Although

## THE TRANSURANIUM ELEMENTS

Table 1—Carrying of Neptunium by Repeated Precipitations of Zirconium Phenylarsonate

Precipitation	HNO <sub>3</sub> solution			HNO <sub>3</sub> solution			HCl solution		
	d/m	Total, %	PhAsA, <sup>†</sup> %	d/m	Total, %	PhAsA, <sup>†</sup> %	d/m	Total, %	PhAsA, <sup>†</sup> %
1st PhAsA	26.9	50.4	80	24.8	50.3	82	14.8	82	89
2d PhAsA	5.6	10.5	17	4.2	8.5	14	1.5	8.3	9
3d PhAsA	1.0	1.9	3	1.2	2.4	4	0.4	2.0	2.2
LaF <sub>3</sub>	19.0	37		19.1	39		1.3	7.2	

<sup>†</sup>Zirconium phenylarsonate

Table 2—Neptunium Carried by Zirconium Phenylarsonate under Reducing Conditions

Expt. No.	Conditions	No. of runs	PhAsA <sup>†</sup> insoluble, %	PhAsA <sup>†</sup> soluble, %	Recovered, %
1	Original 1N HCl solution	10	88 ± 4	12	94
2	Original 1N HNO <sub>3</sub> solution	8	46 ± 4	54	94
3	HCl solution, precipitated as hydrox- ide, dissolved in hot 1N HNO <sub>3</sub> ,	4	27 ± 4	73	105
4	HCl solution, precipitated as hydrox- ide, dissolved in cold 1N HNO <sub>3</sub> , allowed to stand up to 7 hr	12	61.2 ± 1.3	38.8	104
5	HNO <sub>3</sub> solution, precipitated as hy- droxide, dissolved in HCl	6	39 ± 5	61	98
6	1N H <sub>2</sub> SO <sub>4</sub> , 0.1N HNO <sub>3</sub>	2	38.2 ± 1.3	63.8	100
7	1N HCl, Na <sub>2</sub> S <sub>2</sub> O <sub>3</sub>	2	78 ± 2	22	100
8	1N HNO <sub>3</sub> , Na <sub>2</sub> S <sub>2</sub> O <sub>3</sub> , HNO <sub>3</sub> added to reacidify	2	71 ± 3	29	85
9	1N HNO <sub>3</sub> , Na <sub>2</sub> S <sub>2</sub> O <sub>3</sub> , not reacidified after reduction	2	39 ± 2	61	95
10	1N HCl, saturated SO <sub>2</sub>	4	74 ± 2	26	97
11	HNO <sub>3</sub> solution, precipitated as hy- droxide, dissolved HCl, SO <sub>2</sub> added	2	40 ± 4	60	62
12	1N HNO <sub>3</sub> —saturated SO <sub>2</sub>	2	50 ± 5	50	101
13	HCl solution, precipitated as hydrox- ide, dissolved in HNO <sub>3</sub> , SO <sub>2</sub> added	3	32 ± 3	68	89
14	1N H <sub>2</sub> SO <sub>4</sub> , 0.1N HNO <sub>3</sub> , saturated SO <sub>2</sub>	2	35 ± 3	65	100
15	1N HCl, NH <sub>4</sub> OH	2	88.4 ± 0.2	11.6	84
16	1N HCl, 4% HI	2	90.2 ± 0.1	9.8	
17	1N HCl, Jones reductor	2	91 ± 3	9	104
18	HNO <sub>3</sub> solution, precipitated as hy- droxide, dissolved in HCl, Jones reductor	3	89 ± 2	11	85

<sup>†</sup>Zirconium phenylarsonate

there are some inconsistencies, the highest carrying (90 per cent) was obtained in the presence or after the use of strong reducing agents, hydriodic acid, hydroxylamine, and the Jones reductor. Nearly as much (88 per cent) was obtained from simple hydrochloric acid solutions, but much less (50 per cent) was obtained from nitric acid or from samples allowed to stand in nitric acid but metathesized to hydrochloric acid solutions just before precipitation. Poorest carrying (27 per cent) was under the best oxidizing conditions used in these experiments, a short heating in nitric acid solution.

The chief inconsistencies were observed in the presence of sulfur dioxide. If these precipitations are considered by themselves, it can be seen that the carrying is better in hydrochloric acid than in nitric acid solutions, which fact is consistent with the observations made in the previous paragraph. Interference by sulfate in the carrying would serve as an explanation of the inconsistencies since sulfate would be formed from sulfur dioxide.

Although they are far from quantitative, the results of this series of experiments indicate that better carrying by phenylarsonate is obtained from reducing than from oxidizing conditions. This point was made clearer by experiments under oxidizing conditions listed in Table 3. In order to distinguish three valence states, the phenylarsonate precipitation was followed by one of lanthanum fluoride from the same solution. The remaining neptunium was reduced with sulfur dioxide and carried by a second lanthanum fluoride precipitation. The neptunium content of these precipitates is recorded in the last three columns of Table 3. In the experiments numbered 6, 7, 9, and 11, check runs were made to determine the fraction of the total amount in the lower, fluoride-insoluble valence states. The percentage left in solution by the precipitation of both zirconium phenylarsonate and lanthanum fluoride was as large as that remaining after just lanthanum fluoride precipitation; this proves that the fluoride-soluble state is not carried with zirconium phenylarsonate.

Examination of Table 3 shows that only a small amount of the neptunium is carried by the phenylarsonate under oxidizing conditions. This amount ranges from 0 with potassium dichromate (No. 7) to approximately 28 per cent with nitric acid and hydrochloric acid (No. 1). Much larger amounts were, in general, found in the phenylarsonate-soluble fluoride-insoluble state, particularly with mild oxidizing agents such as hot nitric acid (No. 2) and manganese dioxide (No. 11). The stronger oxidizing agents, potassium bromate (Nos. 5 and 6), potassium dichromate (No. 7), and potassium persulfate (No. 9) produced large amounts of the fluoride-soluble state; but the remainder was mostly, if not all, in the phenylarsonate-soluble state. Sulfur

dioxide reduction of the oxidized neptunium was slow; reduction occurred to the phenylarsonate-soluble state except in experiment No. 4 in which nitric acid was replaced by hydrochloric.

Comparison of the percentages carried by zirconium phenylarsonate in experiments in Table 2 with those in Table 3 shows that the carrying in the presence of oxidizing agents was much less than that

Table 3—Neptunium Carried by Zirconium Phenylarsonate under Oxidizing Conditions

Expt. No.	Conditions	No. of runs	F insoluble, %	F soluble, %	PhAsA† insoluble, %	F insoluble, PhAsA† soluble, %	F soluble, PhAsA† soluble, %
1	1N HNO <sub>3</sub> , 0.1N HCl, 90°C, 1 hr	4			28 ± 12	55 ± 17	17 ± 17
2	1N HNO <sub>3</sub> , 90°C, 1 hr	6			13 ± 10	83 ± 8	2 ± 2
3	SO <sub>2</sub> bubbled into above	2			17	83 ± 2	0
4	Hydroxide precipitation of above, dissolved in HCl, saturated with SO <sub>2</sub>	1			66	34	
5	KBrO <sub>3</sub> , 1N HCl	2			0.7 ± 2.1	23.6 ± 1	69 ± 3
6	KBrO <sub>3</sub> , 1N HNO <sub>3</sub>	2	19 ± 2	81	0.8 ± 0.1	13.5 ± 0.6	85.6 ± 0.6
7	K <sub>2</sub> Cr <sub>2</sub> O <sub>7</sub> , 1N HNO <sub>3</sub>	3	27 ± 2	73	0	8.5 ± 5	91
8	SO <sub>2</sub> reduction of above	2			4	96	0
9	K <sub>2</sub> S <sub>2</sub> O <sub>8</sub> , 1N HNO <sub>3</sub>	2	3	97	2	6	92
10	SO <sub>2</sub> reduction of above	1			0	100	0
11	MnO <sub>2</sub> , 1N HNO <sub>3</sub> , 90°C, 2 hr, filtered	4	100		2 ± 1	82 ± 4	16 ± 4

† Zirconium phenylarsonate

found with reducing agents. Such a comparison, including only the neptunium that is fluoride-precipitable, shows that of this an average of 85 per cent was phenylarsonate-soluble in the presence of oxidizing agents and an average of 33 per cent was phenylarsonate-soluble in the presence of reducing agents. If the results with reducing agents, which are doubtful because of the presence of nitric acid or sulfuric acid along with the reducing agent, are eliminated, the largest amount that is phenylarsonate-soluble is less than 12 per cent.

The conclusion to be drawn from these observations is obvious; the oxidation state characterized by being carried by zirconium phenylarsonate is lower than the state that is not carried. Since those observations have been made in connection with a variety of oxidizing and reducing agents, they would not be easy to explain on other bases such as effect of reagents on the phenylarsonate or on its carrying, or on rates of reaction.

### 3. COMPARISON WITH PLUTONIUM BEHAVIOR

Further evidence that this conclusion is valid can be gained by comparing the behavior of neptunium with that of plutonium under similar conditions. This also serves to make it clear that the phenylarsonate is behaving properly since its carrying of plutonium under various conditions is the same as would be predicted for plutonium, knowing its valence states.

Table 4—Plutonium Carried by Zirconium Phenylarsonate

Expt. No.	Conditions	F insoluble, %	F soluble, %	PhAsA† insoluble, %	F insoluble, PhAsA† soluble, %	F soluble, PhAsA† soluble, %
1	1N HCl, SO <sub>2</sub> , 20 hr			0.5	99.5	
2	1N HCl, NH <sub>4</sub> OH			0.5	99.5	
3	1N HCl, 8 per cent HI, 15 hr			2	98	
4	MnO <sub>2</sub> , 1.5N HNO <sub>3</sub> , 90°C, 2 hr filtered	17	83	13.3	13.4	73
5	PbO <sub>2</sub> , 1.5N HNO <sub>3</sub> , 80°C, 1 hr, filtered	29	71	0.9	3.5	96
6	Same as 5			16.6	10.9	72
7	NaBiO <sub>3</sub> , 5N HNO <sub>3</sub> , 90°C, 1 hr	1	99	1.4	3.2	95
8	K <sub>2</sub> S <sub>2</sub> O <sub>8</sub> , Ag <sup>++</sup> , HNO <sub>3</sub>	0.5	99.5	0.5	3.2	96
9	KBrO <sub>3</sub> , HNO <sub>3</sub>	95.5	4.5	92.9	0.6	6.5
10	K <sub>2</sub> Cr <sub>2</sub> O <sub>7</sub> , HNO <sub>3</sub>	1.8	98.2	0.7	0	99.3

† Zirconium phenylarsonate

The results of Table 4 show that in the presence of the reagents known to produce Pu<sup>+3</sup>, less than 2 per cent of the plutonium is carried by zirconium phenylarsonate. By contrast, in the experiments recorded in Table 2 the same treatment increased the carrying of neptunium. With oxidizing agents a large portion of the plutonium was converted to the fluoride-soluble state. That portion which is fluoride-insoluble is divided with respect to phenylarsonate-carrying, with well over 50 per cent being carried except in those experiments in which more than 95 per cent of the total plutonium was as Pu(VI). These variations in the carrying of plutonium by phenylarsonate under oxidizing conditions may be due to some Pu(V) being produced, but this is merely conjecture.

Considering just the amounts of the two elements in their fluoride-insoluble states, a considerably smaller portion of neptunium is carried by zirconium phenylarsonate under oxidizing conditions than under reducing conditions; with plutonium the situation is reversed. This corroborates the idea that in neptunium the phenylarsonate-

precipitable valence state is the lowest state producible by ordinary reducing agents.

Since zirconium phenylarsonate is not a good carrier for dipositive tracers, it is most probable that this carryable, lowest common state in neptunium is +4 and that the non-carryable, fluoride-insoluble state is +5. The other possibility, that the two states are +2 and +3, is not compatible with the known existence of Np(IV) in  $\text{NpO}_2$ .

#### 4. CONCLUSIONS

The original assumption with which this study was begun was that the lower valence states of neptunium in solution, if more than one existed, would be +3 and +4. These are the only ones below +6 for uranium, and they are the two more stable ones for plutonium. As the results were obtained, however, it appeared that such an assumption could not be justified and that the behavior of neptunium was different from that of plutonium. Experiments run on plutonium for the purpose of checking this point made these differences more apparent.

It was decided that the results were not at all consistent with the hypothesis that +3 and +4 were the principal lower valences of neptunium. The experiments certainly showed that two such valences exist. If results with tracer quantities are at all reliable, and it is the authors' belief that they are, these valence states should be +2 and +3, or +4 and +5, with considerable preference for the latter pair. The fact that +4 was known to be one of the valences of neptunium, at least in the solid state, led the authors to the decision that, on the basis of the evidence at hand, +4 and +5 were the most probable values for the lower valences of neptunium.

That this decision was correct has been shown by work done since the completion of this study by Magnusson and LaChapelle.<sup>7</sup> With the first milligram of neptunium available they produced the tetrapositive and pentapositive states in neptunium salts in solution, measured their absorption spectra, and determined some chemical properties of these ions. A tripositive neptunium ion can also be produced but only under very rigorous reducing conditions. It was first identified by polarographic studies<sup>8</sup> and has been produced by reduction with a mercury cathode.<sup>9</sup>

#### 5. SUMMARY

Studies have been made on the carrying of neptunium tracer on zirconium phenylarsonate in the presence of various oxidizing and

reducing agents. The precipitate, which is quite specific for even-valent ions, particularly tetrapositive ones, carries neptunium better from reducing solutions than from oxidizing solutions. The evidence can best be met by a proposal that the two lower valences stable in solution are +4 and +5. Duplicate experiments with plutonium tracer bear this out since the behavior of plutonium is quite different from that of neptunium.

#### REFERENCES

1. L. B. Magnusson and T. J. LaChapelle, Metallurgical Project Report CN-2088 (Sept. 1, 1944), p. 18.
2. T. J. LaChapelle and L. B. Magnusson, Metallurgical Project Report CN-1764 (July 1, 1944), pp. 7-10.
3. R. B. Duffield and J. W. Gofman, Metallurgical Project Report CN-522, Sec. A (Mar. 15, 1943), pp. 8-11.
4. A. F. Voigt, A. Kant, N. R. Sleight, R. E. Hein, J. M. Wright, F. J. Wolter, and H. D. Brown, The separation of plutonium(IV) and plutonium(III), Paper 3.8, this volume (Argonne National Laboratory Report ANL-4050).
5. A. Kant, Metallurgical Project Report CK-1503 (June 10, 1944), pp. 29-30.
6. N. R. Sleight, R. E. Hein, J. M. Wright, and A. F. Voigt, Metallurgical Project Report CN-1979 (Oct. 10, 1944), pp. 7-18.
7. L. B. Magnusson, J. C. Hindman, and T. J. LaChapelle, Metallurgical Project Report CN-2767 (Mar. 31, 1945).
8. J. I. Watters, Metallurgical Project Report CN-2767 (Mar. 31, 1945), pp. 34-35.
9. L. B. Magnusson, T. J. LaChapelle, and J. C. Hindman, Metallurgical Project Report CN-3053 (June 30, 1945), pp. 24-30.

## Paper 15.10

# THE PREPARATION AND DECONTAMINATION OF $_{93}\text{Np}^{239}$ IN TRACE CONCENTRATIONS†

By Paul Fields

### 1. INTRODUCTION

An isotope of neptunium,  $_{93}\text{Np}^{239}$ , which emits  $\beta$  particles with a 2.3-day half life, is formed by the reactions  $_{92}\text{U}^{238}(\text{n},\gamma) \rightarrow _{93}\text{Np}^{239}$   $\frac{\beta^-}{23 \text{ min}}$ . McMillan and Abelson<sup>1</sup> investigated the radiation characteristics and chemistry of the 2.3-day activity; they were the first to show that this activity was due to an isotope of element 93.

Growth curves obtained by McMillan and Abelson showed that the 2.3-day activity arose from the 23-min uranium. Preliminary studies of the radiation showed it to consist of  $\beta^-$  particles of upper limit 0.47 mev, and a weak complex spectrum of low-energy  $\gamma$  rays (less than 0.3 mev) and probably  $x$  rays. It was found that the chemistry of this active material was not that of a rare earth. It did not precipitate with hydrofluoric acid in the presence of an oxidizing agent (bromate in strong acid); but in the presence of a reducing agent, such as sulfur dioxide, it was found to precipitate quantitatively with hydrofluoric acid. In these experiments cerium was used as the carrier.

Other chemical properties reported by McMillan and Abelson were:

1. In the reduced state, with thorium as a carrier, neptunium precipitated with iodate.
2. In the oxidized state, neptunium is carried with sodium uranyl acetate.
3. Neptunium precipitates in basic solution if carbonate is carefully excluded.

†Contribution from the Chemistry Division of the Metallurgical Laboratory, University of Chicago, now the Argonne National Laboratory.

Based on Metallurgical Project Report CN-2689 (Feb. 27, 1945).

4. Neptunium precipitates with thorium when hydrogen peroxide is added.

This new element had little resemblance to its homologue, rhenium; however, its close resemblance to uranium led them to suggest a new rare-earth series beginning with uranium.

This early work, which was carried out using the cyclotron as a neutron generator, laid the foundation for the larger scale preparation of  $_{93}\text{Np}^{239}$ , in which the reactor was used as a neutron source.

## 2. PREPARATION AND DECONTAMINATION OF $_{93}\text{Np}^{239}$

2.1 Bombardment of Uranium. Both the graphite reactor and the heavy-water reactor at the Argonne Laboratories have been used as sources of neutrons for the production of  $_{93}\text{Np}^{239}$ . In view of the fact that there is no cooling system for the graphite reactor, sustained bombardment at a high power level is impossible. Also, since the neutron flux is not very high, it is necessary to use a fairly large sample of uranium. The uranium salt used in bombardment is usually uranyl nitrate hexahydrate, primarily because it is water soluble and readily available. The sample is enclosed in a thin-walled lead box and placed in the center of the reactor for neutron irradiation.

A much better source of neutrons for  $_{93}\text{Np}^{239}$  production is the heavy-water reactor. For bombardments in this reactor, the hexahydrate has been found unsatisfactory since enough heat is generated to melt the salt;  $\text{U}_3\text{O}_8$  is a much better target material. At the time of this writing, the best material found is  $\text{U}_3\text{O}_8$  that has been depleted of its fissionable  $_{92}\text{U}^{238}$  isotope.<sup>†</sup>

Depleted  $\text{U}_3\text{O}_8$  offers many advantages as a source of  $_{93}\text{Np}^{239}$ , the most obvious of which is the smaller amount of fission products produced along with the neptunium owing to the previous removal of  $_{92}\text{U}^{238}$ . The reduction in fission products means a simplified procedure for isolating and decontaminating the neptunium; it also means a reduction in health hazard. Companion runs have been made to compare a depleted uranium bombardment with natural uranium. The results are shown in Table 1.

2.2 Separation and Decontamination by Coprecipitation. The basic chemistry involved in the coprecipitation method is as follows: As pointed out in the introduction, lanthanum fluoride will carry reduced neptunium, but it will not carry oxidized neptunium. Therefore, as a preliminary step in the separation of uranium from neptunium, sulfur

<sup>†</sup>The use of depleted  $\text{U}_3\text{O}_8$  for the production of  $_{93}\text{Np}^{239}$  was suggested by W. M. Manning.

dioxide is bubbled through the solution to ensure complete reduction of the neptunium. The solution is then made 3N to 4N in HF to ensure complete carrying of neptunium by the lanthanum fluoride from uranium solutions.

The effectiveness of lanthanum fluoride cycles depends on the fact that the lanthanum fluoride will carry reduced neptunium and most of the carryable fission species, in the first precipitation; but since the

Table 1—Comparison of Natural Uranium with U<sup>238</sup> Following Irradiation with Neutrons

Depleted uranium	Natural uranium ( $U^{238}/U^{235} = 140$ )
One lanthanum fluoride cycle sufficient to decontaminate the neptunium	Two lanthanum fluoride cycles necessary to decontaminate the neptunium
Could be worked behind 1 in. of lead without remote control	Had to be worked behind 4 in. of lead with remote control

neptunium is oxidized prior to the second precipitation, it remains in solution. Usually two such cycles are necessary to decontaminate the neptunium.

The following precipitation procedure is recommended for a uranyl nitrate hexahydrate sample that has been bombarded in a graphite reactor.

One pound of neutron-irradiated uranyl nitrate hexahydrate is dissolved in 2 liters of water, the solution is made 2N in HNO<sub>3</sub>, and sulfur dioxide is bubbled through it. Lanthanum ammonium nitrate is added to give a concentration of 0.15 to 0.20 mg of lanthanum ion per milliliter; the solution is made 3N in HF; and the resulting lanthanum fluoride precipitate is allowed to settle. The supernatant liquid is siphoned off or decanted, and the slurried precipitate is centrifuged, washed with water, and transferred to a platinum dish. Enough dilute sulfuric acid is added to cover the precipitate, and the solution is heated to dryness with a heat lamp to avoid spattering. The residue is dissolved in 80 to 100 ml of 2N HNO<sub>3</sub>. In order to oxidize the solution, silver nitrate is added to give a concentration of 2 mg of silver ion per milliliter, and solid ammonium persulfate is introduced until a dark brown color develops. After it has stood 3 hr, the solution is made 2N in HF. The resulting lanthanum fluoride precipitate is centrifuged and washed with water, and the two supernatant liquids are combined. The oxidized solution is reduced by bubbling sulfur dioxide

through it for 30 sec after the brown color has disappeared (too much sulfur dioxide will precipitate silver sulfite). To the vigorously stirred solution is added 25 mg of lanthanum, as a solution of the nitrate, in four portions at 10-min intervals, and the resulting precipitate is centrifuged. After it has been washed with water the lanthanum fluoride is transferred to a platinum dish. Sulfuric acid is again added, and the mixture is fumed to dryness. The residue is dissolved in 10 ml of 2N  $\text{HNO}_3$ ; then it is carried through another oxidation-reduction cycle, in which the amount of lanthanum is reduced, so that the final precipitate contains about 2.5 mg of  $\text{LaF}_3$ .

In the heavy-water reactor smaller samples can be bombarded to give as much neptunium as the larger samples previously bombarded in the graphite reactor. The reduction in the size of the sample makes possible certain modifications in the coprecipitation procedure. Since there is less uranium per sample, smaller volumes may be used, and, more important, only 40 mg of lanthanum is needed in the first precipitation. This reduction in the amount of lanthanum fluoride removes the necessity for fuming with sulfuric acid, the most time-consuming operation in the procedure; in place of this step the lanthanum fluoride may be dissolved in a small volume of zirconyl nitrate solution. Also, bromate may be substituted for the argentic ion in the oxidation. Bromate oxidation is carried out by making the solution 3N in  $\text{H}_2\text{SO}_4$  and 0.15M in  $\text{KBrO}_3$ , and allowing it to stand for 1 hr. The final  $\text{^{238}Np}$  solution should be examined for other fission-product activity by observing decay and absorption curves.

**2.3 Separation and Decontamination by Solvent Extraction from a Zirconyl Solution of Lanthanum Fluoride.** The second method used for separation and decontamination is a solvent-extraction method. Methyl isobutyl ketone, ether, and other solvents have been used for decontamination of neptunium after an initial separation from the bulk of uranium by coprecipitation and lanthanum fluoride.

The solvent-extraction procedure is based on the following facts: lanthanum fluoride dissolves in zirconyl nitrate, aluminum nitrate, or similar solutions; the resulting solutions after addition of ammonium nitrate give a favorable distribution coefficient for neptunium, but they will give unfavorable distribution coefficients for fission products when extracted with ether. When the extracting solvent is washed with distilled water, the distribution coefficient largely favors the water layer, thus providing a method of recovering the neptunium from the organic solvent. Nitric acid is also extracted to some extent, and it goes into the water layer; hence, after a few cycles, enough nitric acid accumulates in the water layer to shift the

distribution coefficient in favor of the solvent again. At this stage a fresh batch of wash water is used.

One pound of uranyl nitrate hexahydrate is dissolved in 2 liters of water. About 200 ml of concentrated nitric acid is added, sulfur dioxide is bubbled through the solution to make certain all the product is in the reduced state, and then a lanthanum fluoride precipitate is thrown down as described in Sec. 2.2 of this paper. The precipitate is allowed to settle overnight, and the supernatant solution is siphoned off. The precipitate is slurried into centrifuge tubes and centrifuged for 10 min. The precipitate is washed and recentrifuged; then the lanthanum fluoride is dissolved in the smallest possible quantity of zirconyl nitrate solution. Hydrogen peroxide is added, the solution is allowed to stand for 10 min, then it is diluted with water, and hydrofluoric acid is added to form another lanthanum fluoride precipitate. This lanthanum fluoride precipitate should now carry down the neptunium free from uranium. The lanthanum fluoride is redissolved in a minimum volume of zirconyl solution.

The zirconyl solution is made 2N in  $\text{HNO}_3$ , and it is then oxidized by adding ammonium hexanitratocerate. To the oxidized solution 1.6 g of  $\text{NH}_4\text{NO}_3$  is added for each milliliter of solution, giving a 10M  $\text{NH}_4\text{NO}_3$  solution, the volume of which is twice that of the original. Two to three volumes of solvent is added for each volume of solution. The mixture is poured into a 100-ml Kjeldahl flask, and it is shaken vigorously for 10 min. The two layers are separated by permitting the flask to stand at rest for 5 min. The flask is then immersed in a freezing mixture of dry ice and acetone to freeze the aqueous layer thoroughly. The solvent layer containing the extracted neptunium is then poured into a second Kjeldahl flask containing 25 ml of distilled water. This flask is then shaken for 10 min (during which time the neptunium passes into the water layer), the mixture is allowed to settle for 5 min, and then it is frozen. In the meantime, the contents of the original flask are thawed out in warm water, and more ammonium hexanitratocerate is added. The solvent is now poured from the second flask back into the original flask; and another two cycles, as just described, are carried out. After the third cycle is completed, the solvent is washed with a fresh batch of water; and another cycle is completed with fresh water used for the final wash. The two water layers are combined, and they are evaporated with nitric acid. Enough nitric acid is added to give a 2N solution when a 10-ml volume is attained. If too much cerium has been introduced as an oxidant and its presence is undesirable in subsequent operations, a lanthanum fluoride cycle will remove it.

Instead of ammonium hexanitratocerate, potassium permanganate or dichromate may be used. However, permanganate is extracted by methyl isobutyl ketone, for example, to give an opaque solution caused by production of manganese dioxide; the manganese dioxide so formed does not carry neptunium, however.

Frequently a gelatinous precipitate forms in the ammonium nitrate layer after two or three extractions with methyl isobutyl ketone. This precipitate can be dissolved by adding dilute nitric acid and heating for a short time. The formation of the gel appears to be due to the extraction of nitric acid by methyl isobutyl ketone and is apparently connected with the presence of some methyl isobutyl ketone in the aqueous layer. There is no gel formation when ether is used although this solvent extracts the acid also.

### 3. SUMMARY

Methods are described for the preparation of pure  $\text{_{93}Np}^{230}$  activity from neutron-irradiated uranium compounds. The methods described fall essentially into two classes: (1) coprecipitation methods, and (2) solvent-extraction methods.

### REFERENCE

1. E. McMillan and P. Abelson, *Phys. Rev.*, 57: 1185 (1940).

## Paper 15.11

# CHEMISTRY OF NEPTUNIUM. KINETICS AND MECHANISMS OF AQUEOUS OXIDATION-REDUCTION REACTIONS OF NEPTUNIUM<sup>†</sup>

By L. B. Magnusson, J. C. Hindman, and T. J. LaChappelle

### 1. INTRODUCTION

Four oxidation states of neptunium, +3, +4, +5, and +6, have been produced in aqueous solution.<sup>1,2</sup> The stabilities of these states are discussed elsewhere.<sup>3</sup> Since neptunium has four stable oxidation states, knowledge of the rates and mechanisms of the reactions involved in changes to the most stable states under any given conditions is of general importance. Extensive quantitative data on rates and mechanisms are yet to be obtained, but a review of the observations to date provides a beginning for an understanding of the reactions as well as some information upon which to base predictions of behavior.

Early experiments with trace concentrations of neptunium were of little or no value in determining rates and mechanisms, since the oxidation states and their stabilities were not known. The information presented here is based principally on direct visual and spectrophotometric observation of the behavior of milligram amounts of neptunium.

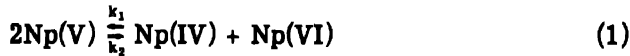
The conditions of reaction in many cases were not designed to yield precise kinetic data since the reactions were observed during the course of preparations for purposes other than kinetic studies, and therefore only qualitative deductions are permissible.

<sup>†</sup>Contribution from the Chemistry Division of the Metallurgical Laboratory, University of Chicago, now the Argonne National Laboratory.

Based in part on Metallurgical Project Reports CN-1764 (July 1944), CN-2767 (March 1945), and CN-2088 (September 1944).

## 2. REACTIONS BETWEEN NEPTUNIUM IONS

Neptunium(V) is appreciably unstable in 1M H<sub>2</sub>SO<sub>4</sub> at 25°C, disproportionating to Np(IV) and Np(VI).



The instability may be attributed to the formation of complex sulfate ions<sup>3,4</sup> with Np(IV) and Np(VI). A determination of the rate of disproportionation may be made most conveniently by measuring the rate, k<sub>1</sub>, of the reverse reaction between Np(IV) and Np(VI).

A solution of Np(IV) of known concentration in 1M H<sub>2</sub>SO<sub>4</sub> was added to a solution of Np(VI) of known concentration in 1M H<sub>2</sub>SO<sub>4</sub> and sealed in a 1-cm absorption cell. The temperature of both solutions was adjusted to 25°C in a water bath before mixing. The initial concentrations after mixing were 0.00466M Np(IV) and 0.00422M Np(VI). The concentration change of Np(IV) with time was followed spectrophotometrically for about 4 hr by measuring the density of the 727-m $\mu$  absorption band. The absorption cell was held in a constant-temperature jacket at 25 ± 0.5°C. An equilibrium measurement of the Np(IV) density was taken after 48 hr.

A graph of the density readings versus time yielded a smooth curve. Column 2 of Table 1 gives the concentration of Np(IV) at 10-min intervals calculated from the optical density corrected for cell, Np(V), and Np(VI) backgrounds.

The equilibrium density measurement after 48 hr permitted calculation of the constant for the disproportionation

$$K = \frac{[\text{Np(IV)}][\text{Np(VI)}]}{[\text{Np(V)}]^2} = \frac{k_2}{k_1} \quad (2)$$

$$K = 2.4 \times 10^{-2}$$

If Eq. 1 is taken as a mechanism for the reaction, the rate of change in concentration of Np(IV) should be

$$-\frac{d(c_0 - c)}{dt} = k_1(c_0 - c)(c'_0 - c) - k_2(2c)^2 \quad (3)$$

where c<sub>0</sub> = initial concentration of Np(IV)

c' = initial concentration of Np(VI)

c = one half the concentration of Np(V) at time t

Substituting for  $k_1$  gives

$$-\frac{d(c_0 - c)}{dt} = k_1(c_0 - c)(c'_0 - c) - k_1 K(2c)^2 \quad (4)$$

Integrating and substituting constants gives

$$(8.28) (10^3) \log \frac{1.808c - (1.166) (10^{-2})}{[1.808c - (6.10) (10^{-3})] (1.91)} = k_1 t \quad (5)$$

The values of  $c$  are given in column 3 of Table 1. The values of  $k_1$ , calculated at each 10-min interval, are given in column 4.

Table 1—Reaction  $\text{Np(IV)} + \text{Np(VI)} \rightarrow 2 \text{Np(V)}$  at  $25^\circ\text{C}$

$t$ , min	$\text{Np(IV)},$ molarity $\times 10^3$	$c,$ molarity $\times 10^3$	$k_1,$ liters/mole/min
10	4.22	0.44	2.53
20	3.89	0.77	2.39
30	3.62	1.04	2.32
40	3.41	1.25	2.23
50	3.21	1.45	2.21
60	3.02	1.64	2.24
70	2.86	1.80	2.24
80	2.72	1.94	2.24
90	2.61	2.05	2.22
100	2.51	2.15	2.19
110	2.42	2.24	2.17
120	2.34	2.32	2.15
130	2.28	2.38	2.10
140	2.22	2.44	2.08
150	2.17	2.49	2.04
160	2.11	2.55	2.04
170	2.05	2.61	2.05
180	1.99	2.67	2.07
190	1.95	2.71	2.05
200	1.91	2.75	2.03
2,800	1.28		

It will be noted that a drift with time to smaller values of  $k_1$  was obtained. The first two values are appreciably higher than the average. A number of known factors could account for drift. Although the temperature of the solutions was adjusted to  $25^\circ\text{C}$  before mixing, the solutions were out of the bath during the brief mixing period. Room temperature was a few degrees higher than  $25^\circ\text{C}$  so that the solution temperature may have risen a half degree or so during the first few minutes of reaction. A half degree lowering of the temperature in the

temperature-controlled absorption-cell compartment over the 4-hr period of observation could likewise account for much of the drift. Other factors that should affect the rate to a small extent would be the change in solution composition caused by decomposition of the Np(IV) and Np(VI) sulfate complexes and the slight increase in hydrogen-ion concentration caused by the transition<sup>3</sup> of  $\text{Np}^{+4}$  to  $\text{NpO}_2^+$ . The average value of  $k_1$  is 2.2 liters/mole/min at 25°C. In 1.86M  $\text{H}_2\text{SO}_4$  at 25°C,  $k_1$  has been measured as approximately 1 liter/mole/min.

The disproportionation rate of Np(V),  $k_2$  in the reaction represented in Eq. 1, in 1.0M  $\text{H}_2\text{SO}_4$  is calculated from the equilibrium constant to be  $5.3 \times 10^{-2}$  liter/mole/min.

The rate of the reaction between Np(IV) and Np(VI) has not been measured in acids other than sulfuric, but presumably the rate would be much larger in noncomplexing media. Np(V) shows no spectrophotometric evidence for disproportionation in 1M solutions of nitric or hydrochloric acid. Since in all probability Np(V) and Np(VI) are oxygenated ions and Np(IV) is not oxygenated, the forward and reverse reactions represented by Eq. 1 should be dependent in some manner on the hydrogen-ion concentration. This dependence has not yet been studied, so that complete mechanisms for the reactions cannot be formulated.

The reactions of Np(III) with neptunium ions of other oxidation states have not been investigated because the tripositive state is so unstable in air that it is of little immediate interest.

### 3. KINETICS OF REACTIONS WITH OXIDIZING AND REDUCING AGENTS

**3.1 Bromate.** The reactions of neptunium with bromate have been studied in some detail since it was found very early<sup>5</sup> that neptunium and plutonium in trace concentrations could be separated by a method involving bromate oxidation. The two elements in "reduced" states, now known to be the tetrapositive oxidation state, in sulfuric acid solution were treated with bromate for about 30 min. Addition of lanthanum(III) and hydrofluoric acid precipitated lanthanum fluoride, which carried the plutonium but left the neptunium in solution. The neptunium presumably was oxidized to a "lanthanum fluoride soluble" state whereas the plutonium was not oxidized. Since the oxidation potential in this type of solution is sufficient to oxidize the plutonium, it is obvious that the success of the method is dependent upon the relative rates of oxidation of the two elements.

Spectrophotometric observation shows that the oxidation of pure Np(IV) in solutions containing bromate and sulfuric acid is slow at room temperature. A complex mechanism is indicated by the fact

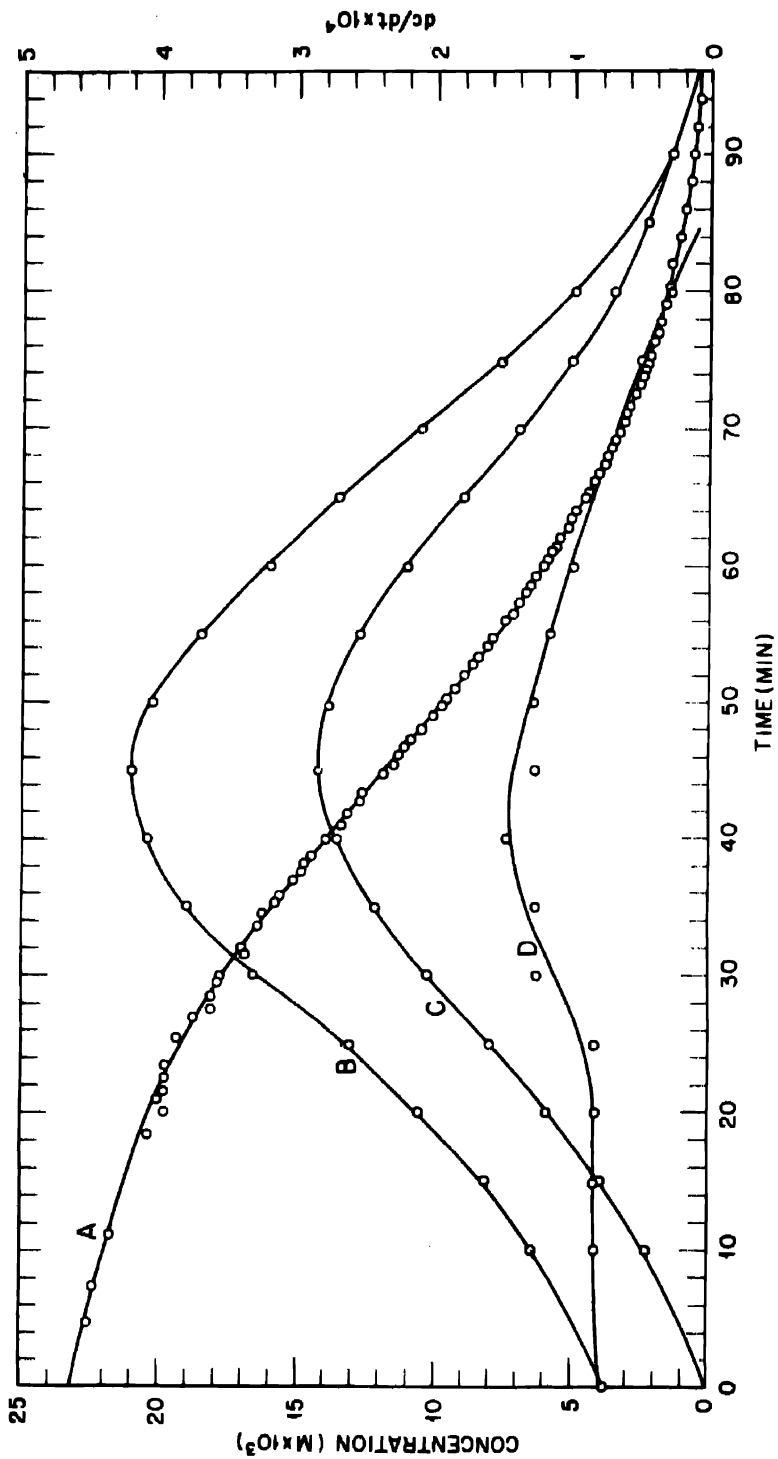


Fig. 1.—Bromate oxidation of neptunium(IV) in 1.0M  $\text{H}_2\text{SO}_4$  at 25°C.

that the rate of oxidation is very slow initially but accelerates after an induction period. It was first believed<sup>8</sup> that the induction period was attributable to the necessity of partially reducing the bromate ion to bromite and hypobromite since it is generally true that fast reducing agents such as bromide ion catalyze bromate oxidations. An induction period, however, was still observable in solutions of neptunium containing bromide or sulfur dioxide. Solutions containing some Np(V) along with the Np(IV) show little or no induction when oxidized with bromate. The following partial step reactions could satisfactorily account for an induction period:



A slower rate for reaction 6 relative to the rate for reaction 7 would result in an induction period. Reaction 8 must occur to a considerable extent since the rate for this reaction is well within the qualitatively observed range of bromate oxidation rates. The Np(V) formed is oxidized to Np(VI) at an extremely rapid rate by reaction 7 since no Np(V) can be detected spectrophotometrically during an oxidation.

The actual mechanism of the bromate oxidation appears to be more complicated than that represented by reactions 6, 7, and 8. All three reactions undoubtedly occur, but Eq. 6 is not an inclusive representation of the inductive mechanism. A graphical test of the observed data will illustrate the complexity of the induction period. A number of bromate oxidations of initially pure Np(IV) in 1.0M H<sub>2</sub>SO<sub>4</sub> at 25°C have been observed spectrophotometrically. Curve A of Fig. 1 is a representative graph of calculated concentrations of Np(IV) against time. A small amount of Fe(II) was added to this solution before the addition of bromate to ensure that the neptunium was pure Np(IV). At zero time the composition was 1.0M H<sub>2</sub>SO<sub>4</sub>, 0.023M Np(IV), 0.01M Fe(II), and 0.094M KBrO<sub>3</sub>. Curve B is a graph of the total reaction rate against time, determined graphically by drawing tangents to the concentration curve. Curve C is a calculated graph of the rates of the reaction between Np(IV) and Np(VI), the rate of which would be given by an equation similar to Eq. 2 except that no reverse reaction occurs and the concentration of Np(VI) increases by the oxidation of Np(IV) through Np(V) to Np(VI). The rate equation in this case is

$$-\frac{d(c_0 - c)}{dt} = k(c_0 - c)c \quad (9)$$

where  $k = 2.15$  liters/mole/min. The points of curve C are the products of the observed concentrations of Np(IV) and Np(VI) and the specific rate constant,  $k_1$ .

The total rate of oxidation clearly is greater than the rate of reaction between Np(IV) and Np(VI), therefore other reactions must contribute significantly to the rate. The difference between the total rate and the rate of the Np(IV)-Np(VI) reaction is given by curve D, which should then represent the rates of the other reactions. If reaction 6 were the only other reaction contributing to the decrease in concentration of Np(IV), curve D would be expected to show a decreasing rate with time. Since curve D goes through a maximum, it appears that reaction 6 is not an inclusive representation of all the side reactions contributing to the oxidation of Np(IV). The complex induction period may involve reduction products of bromate.

Figure 2 is the graph of a bromate oxidation of Np(IV) at 35°C. The concentrations were the same as in the reaction at 25°C with the exception of the Np(IV) concentration. Curve A is the Np(IV) concentration-time graph and curve B gives the graphically determined rates. The rate constant for the Np(IV)-Np(VI) reaction has not been determined at 35°C so graphical analysis of the total rate cannot be made as was done with the reaction at 25°C. It was found, however, that Eq. 10 could be applied to the data to calculate a rate constant on the assumption that the Np(IV)-Np(VI) reaction was the principal rate-determining step near the end of the reaction.

$$k = \frac{-\frac{d(c_0 - c)}{dt}}{(c_0 - c)c} \quad (10)$$

" $k$ " was calculated from the graphically measured rates and the known concentrations of Np(IV) and Np(VI). Table 2 summarizes the data and the calculated values of  $k$ . The value of  $k$  is essentially constant after 30 min. The oxidation rate, therefore, may be dependent only on the concentrations of Np(IV) and Np(VI) after the oxidation has proceeded about 35 min. It may be emphasized, however, that the apparent constancy of  $k$  is not good evidence that the Np(IV)-Np(VI) reaction is the principal rate-determining step since the concentration of Np(VI) near the end of the reaction is not changing much and the evidence may indicate only first order dependence on the Np(IV) concentration. Constancy near the end of the reaction was not attained from similar calculations using the data obtained at 25°C. The 10° temperature rise may accelerate the Np(IV)-Np(VI) reaction considerably more than the others. Curve C is a graph of the rates of the Np(IV)-Np(VI) reaction with  $k$  equal to 9.5 liters/mole/min calculated in an analogous manner to curve C of Fig. 1. It is again apparent that

other reactions contribute markedly to the observed rate, especially during the induction period. The differences between curves B and C are plotted as curve D, which suggests the rate contributions of reactions other than the Np(IV)-Np(VI) reaction.

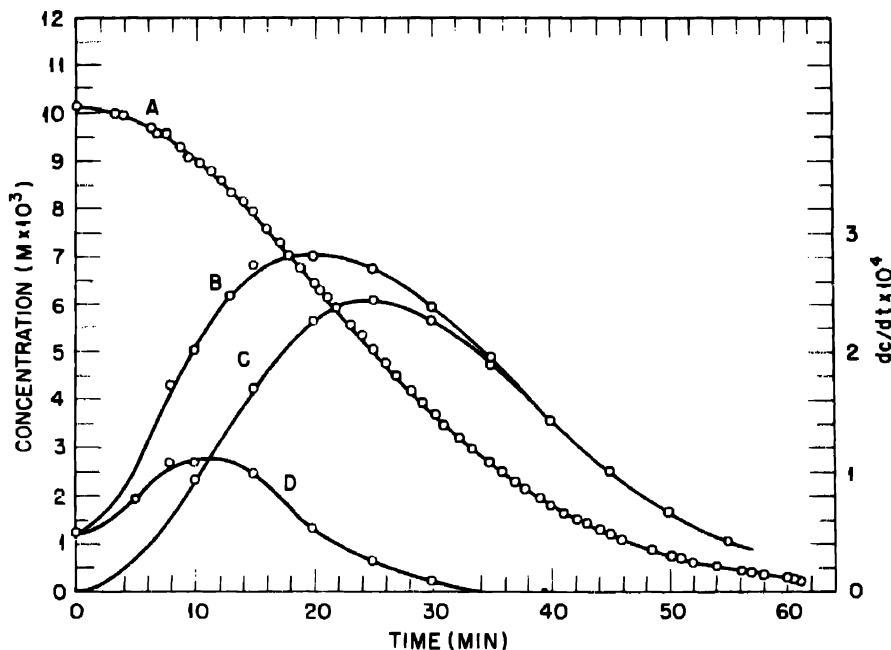


Fig. 2—Bromate oxidation of neptunium(IV) in 1.0M  $\text{H}_2\text{SO}_4$  at 35°C.

In the range of trace concentrations of neptunium the Np(IV)-Np(VI) reaction would be immeasurably slow, and therefore the oxidation of Np(IV) by bromate or its reduction products would become the dominant reaction. Several hours would be required for essential completion. In the early trace-concentration work it was customary to allow about 30 min oxidation time before adding hydrofluoric acid in the bromate-lanthanum fluoride procedure. It is now apparent that very little oxidation of Np(IV) at trace concentration could occur in 30 min. Since neptunium is in the hexapositive oxidation state after precipitation of lanthanum fluoride, the evidence is definite that hydrofluoric acid exerts a powerful accelerating effect on the oxidation. A similar effect was proved in the oxidation of Np(IV) by dichromate in the presence of hydrofluoric acid.<sup>7</sup> It is quite improbable that hydrogen fluoride acts as a catalyst in the usual sense involving an intermediate oxidation-reduction couple, so a reasonable mechanism should be

sought in a complexing effect. It may be that the oxidation of Np(IV) to Np(V) will take place in fluoride solution without the necessity of adding two oxygen atoms per neptunium atom. A half reaction such as the following might be involved:



Table 2—Rate Constant for  $\text{Np(IV)} + \text{Np(VI)} \rightarrow 2\text{Np(V)}$  at  $35^\circ\text{C}$

$t, \text{ min}$	$c_0 - c,$ molarity $\times 10^3$	$c,$ molarity $\times 10^3$	$dc/dt \times 10^4$	$k,$ liters/mole/min
10	9.06	1.10	0.942	
15	7.86	2.30	1.71	15.15
20	6.43	3.73	2.27	11.71
25	5.02	5.14	2.44	10.50
30	3.73	6.43	2.27	9.88
35	2.64	7.52	1.90	9.87
40	1.79	8.37	1.43	9.54
45	1.19	8.97	1.01	9.46
50	0.76	9.40	0.67	9.37
55	0.47	9.69	0.43	9.44

Since this oxidation requires only the removal of an electron, the rate might be expected to be fast. The  $\text{NpF}^{+3}$  ion is very probable since plutonium forms this type of ion predominantly in hydrofluoric-nitric acid solutions.<sup>8</sup> If the hypothetical ion  $\text{NpF}^{+4}$  or something similar has any degree of stability, it may be possible to measure a reversible  $\text{Np(IV)}-\text{Np(V)}$  couple in fluoride solution.

3.2 Cerium(IV). The oxidation of Np(IV) by Ce(IV) in both nitric and sulfuric acids is too rapid to be followed spectrophotometrically at room temperature. The oxidation of Np(V) is much more rapid than that of Np(IV), since a titration of a mixture of Np(IV) and Np(V) in 1M  $\text{H}_2\text{SO}_4$  showed that Ce(IV) preferentially oxidized Np(V) in agreement with the behavior in the bromate oxidation. The over-all rate would depend only on the Ce(IV) and Np(IV) concentrations since the reaction between Np(IV) and Np(VI) is too slow to contribute to any measurable extent.

Bromate oxidation of Np(IV) is catalyzed by cerium ions; the addition of a trace of Ce(III) to a solution containing bromate and Np(IV) in sulfuric acid gives instant oxidation to Np(VI). This effect was first detected on trace concentrations of neptunium.<sup>9</sup> The oxidation potentials of bromate solutions are sufficient to oxidize a fraction of the Ce(III) to Ce(IV), which then reacts with the Np(IV) very rapidly.

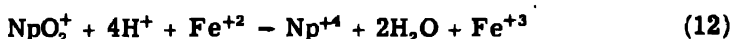
**3.3 Chlorine.** Chlorine is a useful oxidant for the preparation of Np(V) in chloride solutions. The potential of the Np(V)-Np(VI) couple is sufficiently negative in 1M HCl to oxidize a small fraction of chloride to chlorine. Slow escape of chlorine from the solution allows further reduction of Np(VI). The reaction of chlorine with Np(IV) in 1M HCl is very slow at 25°C but is quite rapid at 75°C, producing principally Np(V). A small amount of Np(VI) also forms. If the concentration of chlorine is kept low, very little Np(VI) is formed.

**3.4 Chloride.** Neptunium(VI) is measurably unstable in chloride solutions, as noted above, although the reduction to Np(V) is very slow at room temperature. Platinum and gold metals increase the rate of reduction markedly. It was found that potentials in chloride solutions of Np(VI) are not stable if a gold or platinum electrode is used. Reduction of Np(VI) by chloride or the metal at the electrode causes a continual decrease of the measured emf.

**3.5 Electrolysis.** The cathodic-reduction behavior of neptunium ions is similar to the behavior with chemical reducing agents. Reduction of Np(VI) to Np(V) is rapid and reversible, whereas the reduction of Np(V) to Np(IV) is slow and irreversible. Electrolytic reduction of Np(IV) is probably the best practical method<sup>2,8</sup> of producing Np(III). Measurements<sup>2</sup> of the potential of the Np(III)-Np(IV) couple show it to be reversible, and therefore electrolytic reduction should be rapid. The polarographic results,<sup>9</sup> however, indicated an irreversible reaction. The anomaly has not been removed as yet by experiment, but the possibility exists that hydrolysis at the electrode might account for the polarographic results.

**3.6 Ferrous Iron.** Np(VI) and Np(V) react very rapidly at 25°C with excess of Fe(II) to give Np(IV) in sulfuric acid solutions.

The rate of reduction of Np(V) by Fe(II) is conveniently measurable in hydrochloric acid solutions. The hydrogen-ion dependence of this reduction is of interest since it is believed that the transition from Np(V) to Np(IV) involves a change from the ion  $\text{NpO}_2^+$  to  $\text{Np}^{+4}$ .



A rate equation for the reduction of Np(V) by Fe(II) may be postulated as

$$\frac{dc}{dt} = k (c_0 - c) (c'_0 - c) (\text{H}^+)^x \quad (13)$$

where  $c_0$  = initial concentration Np(V)

$c'_0$  = initial concentration Fe(II)

$c$  = concentration of Np(IV) at time  $t$

$$\frac{1}{t(c'_0 - c_0)} \ln \frac{c_0(c'_0 - c)}{c'_0(c_0 - c)} = (H^+)^x k = k' \quad (14)$$

During the course of preparations for the study of the hydrogen-ion concentration dependence of the potential of the Np(IV)-Np(V) couple some rough measurements of the rate of reduction of Np(V) by Fe(II) were obtained.<sup>10</sup>

Table 3—Hydrogen-Ion Dependence of the Reduction of Np(V) by Fe(II)

t, min	H <sup>+</sup> , moles/liter	d <sub>727</sub>	c	c'_0 - c	k', liters/mole, min
10	0.30	0.017	0.00013	0.00181	2.5
	0.51	0.027	0.00021	0.00173	3.7
	1.0	0.045	0.00036	0.00159	7.7
20	0.30	0.032	0.00025	0.00169	2.5
	0.51	0.055	0.00042	0.00152	4.8
	1.0	0.095	0.00073	0.00121	10.3
30	0.30	0.040	0.00031	0.00163	2.2
	0.51	0.074	0.00057	0.00137	4.8
	1.0	0.126	0.00097	0.00097	10.8
40	0.30	0.045	0.00036	0.00159	1.9
	0.51	0.088	0.00068	0.00126	4.6
	1.0	0.146	0.00112	0.00082	10.7
50	0.30	0.049	0.00038	0.00156	1.7
	0.51	0.100	0.00077	0.00117	4.4
	1.0	0.168	0.00129	0.00065	11.7

Three chloride solutions of different hydrogen-ion concentration, 0.30M, 0.51M, and 1.0M, each 0.00269M in Np(V), were prepared. The ionic strengths of the solutions were equalized at approximately 1.0 with lithium chloride. Each solution was made 0.00194M in Fe(II), and the reductions were followed spectrophotometrically in 1-cm cells at 25°C by measuring the increase in optical density of the Np(IV) 727-m $\mu$  absorption band.

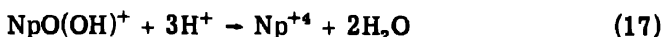
Column 3 of Table 3 gives the observed densities for the three solutions at 10-min intervals. The calculated concentrations of Np(IV) and Fe(II) are given in columns 4 and 5. The values of k' calculated from Eq. 14 are given in the last column of the table.

Although the precision of these measurements is quite low, it is sufficiently good to yield interesting information on the mechanism of the reduction. The reaction obviously does not proceed through a disproportionation of Np(V) since the rate is dependent on the first power of the Np(V) concentration. It may be seen immediately that

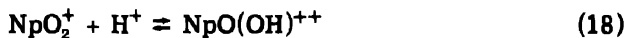
the reaction rate constant  $k'$  does not have a fourth-power dependence on hydrogen-ion concentration which it would have if the over-all reaction 12 were also the rate-determining reaction. The average rate constants for the 0.30M, 0.51M, and 1.0M hydrogen-ion solutions are 2.2, 4.5, and 10.2 liters/mole/min, respectively. If  $k$  is taken to be 10.2 the hydrogen-ion dependences of the rate constants at 0.51M and 0.30M hydrogen-ion concentration may be calculated from the equation

$$\begin{aligned} (\text{H}^+)^x k &= k^1 \\ (\text{H}^+) = 0.51\text{M} &\quad (0.51)^x (10.2) = 4.5 \\ &\quad x = 1.2 \quad (15) \\ (\text{H}^+) = 0.30\text{M} &\quad (0.30)^x (10.2) = 2.2 \\ &\quad x = 1.3 \end{aligned}$$

The rate of reduction, therefore, is dependent on slightly greater than the first power of the hydrogen-ion concentration in the range 0.3M to 1M  $\text{H}^+$  at 25°C. This fact can be utilized as the basis for a reasonable hypothesis for ionic changes occurring in the transition from  $\text{Np(V)}$  to  $\text{Np(IV)}$ . The principal ionic form of  $\text{Np(V)}$  probably contains two oxygen atoms in the range 0.1M to 1.0M hydrogen-ion concentration.<sup>3</sup> Neglecting hydration and complexing anions, the ion may be formulated as  $\text{NpO}_2^+$ . If it is assumed that ion  $\text{Np(IV)}$  may be formulated as  $\text{Np}^{+4}$ , the first-power hydrogen dependence of the reduction of  $\text{Np(V)}$  would lead to the conclusion that the following reactions occur:



Alternatively, it may be postulated that an ion such as  $\text{NpO(OH)}^{++}$  could exist at a low concentration in equilibrium with  $\text{NpO}_2^+$ .



$$k = \frac{[\text{NpO(OH)}^{++}]}{[\text{NpO}_2^+] [\text{H}^+]} \quad (19)$$

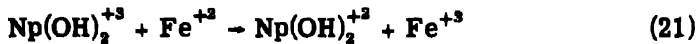
The principal reduction reaction might then be



which would proceed at the rate given by Eq. 13, where  $x = 1$  since the concentration of  $\text{NpO(OH)}^{++}$  is directly proportional to the first power of the hydrogen-ion concentration.

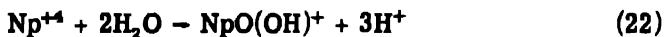
Potential measurements of the  $\text{Np(IV)}-\text{Np(V)}$  couple at various hydrogen-ion concentrations<sup>10</sup> indicate the possible existence of meas-

urable concentrations of ions other than  $\text{NpO}_2^+$  in Np(V) solutions. From the determined value of 3.8 for the hydrogen-ion power dependence of the Np(IV)-Np(V) couple it may be calculated that k, the equilibrium constant of Eq. 19, could be as large as 0.4. Since the power of the hydrogen-ion dependence was found to be approximately 1.2, i.e., higher than 1, there may be some deduction through the reaction



or other similar reactions involving Np(V) ions of varying degrees of hydrolysis.

The rate of the reverse reaction, oxidation of Np(IV) to Np(V), must be inversely proportional to approximately the third power of the hydrogen-ion concentration, so that it is necessary to assume that hydrolyzed Np(IV) ions react with ferric ion, such as the reverse of reaction 20. The concentration of  $\text{NpO(OH)}^+$  in this reaction is dependent on the third power of the concentration of hydrogen ion in the hydrolysis of  $\text{Np}^{+4}$ ,



The formula of the hydrolyzed ion could, of course, just as well be  $\text{Np(OH)}_3^+$ , since it is not possible from the above evidence to differentiate between degrees of hydration or oxygenation.

Although it is true that the concentrations of hydrolyzed ions of Np(IV) in acid solutions may be vanishingly small, it is also true that the rates of change between  $\text{Np}^{+4}$  and  $\text{NpO}_2^+$  are extremely slow relative to the rates of simple electron-transfer reactions. The slow rates would be at least partially explained if the rate-determining steps in the transition between Np(IV) and Np(V) involved hydrolyzed ions of Np(IV) present in very low concentrations.

**3.7 Hydrazine, Hydroxylamine.** Hydrazine and hydroxylamine both reduce Np(VI) to Np(V) instantly in 1M acid solutions, but further reduction is extremely slow. The slow rates of reduction with these agents indicate that the reaction could proceed mainly through disproportionation of Np(V) to Np(IV) and Np(VI).

**3.8 Iodide.** Iodide ion in hydrochloric acid solutions reduces Np(V) much more slowly than does Fe(II) under similar conditions, but the reaction may be made far more complete since a larger reducing potential may be attained in iodide solutions. The rate of reduction in 5M HCl has been found to be dependent on the first power of the Np(V) concentration, essentially complete reduction requiring about 40 min at room temperature. The rate is qualitatively observed to be directly proportional to acid concentration. In 0.3M HCl the rate is extremely slow, and the reaction is incomplete. The rate is somewhat more

rapid at 0.5M HCl and is essentially complete in the absence of iodine. Greatly increased rates are obtained at higher temperatures; complete reduction requires less than 1 or 2 min in 5M HCl at 100°C.

3.9 Nitrate. The stability of Np(IV) in nitric acid solutions is similar to that in perchlorate solutions. Pure Np(V) may be produced by careful heating of Np(IV) nitrate solutions.

3.10 Nitrite. Np(VI) is reduced instantly to Np(V) by nitrite in 1M HNO<sub>3</sub> solution but no further reduction can be detected. This result is entirely consistent with the measured potentials of the neptunium couples.

3.11 Oxygen. The effect of atmospheric oxygen has been detected in solutions of Np(IV) in 1M H<sub>2</sub>SO<sub>4</sub>. Np(V) is formed very slowly, amounting to a few per cent per week.

3.12 Oxalic Acid. Observations of the reducing action of oxalic acid are limited to some very complex solutions containing principally nitrate, sulfate, and phosphate.<sup>11</sup>

The reduction of Np(VI) and Np(V) was in general extremely slow at room temperature. Appreciable rates are obtainable at higher temperatures, but pure Np(IV) was stable in these solutions only with excess oxalate. Prolonged heating destroys the oxalate, and the neptunium partially reoxidizes to Np(V), apparently establishing an equilibrium with nitrate and nitrate-reduction products.

3.13 Perchlorate. Np(IV) oxidizes to Np(V) in hot perchloric acid solutions rapidly. The oxidation is very slow at room temperature; therefore Np(IV) may be maintained in perchloric acid for at least several days.

3.14 Permanganate. Np(IV) reacts with permanganate ion too rapidly to be measured in nitric or sulfuric acid solutions. The relative ease with which oxidation of Np(V) occurs compared to that of Np(IV) is again observed with permanganate in that Np(V) is preferentially oxidized on titration of solutions containing both Np(IV) and Np(V).

3.15 Peroxide. Hydrogen peroxide reduces Np(VI) to Np(V) instantly in 0.5M HNO<sub>3</sub> solutions. Further reduction could not be detected after a period of 24 hr at room temperature.

3.16 Silver. Argentic-ion oxidation of Np(IV) is extremely fast. In 1.0M HClO<sub>4</sub> solution an excess of Ag(II), added as AgO, instantly oxidized Np(IV) to Np(VI).

3.17 Stannous. Np(VI) reduces immediately to Np(V) in the presence of Sn(II) in chloride solutions. Further reduction is extremely slow.

3.18 Sulfite. Sulfur dioxide in sulfuric acid solutions rapidly reduces Np(VI) to Np(V), but further reduction is quite slow. A very fast

reduction to Np(IV) is apparently obtained in solutions containing hydrofluoric acid. It has been observed that sulfur dioxide added to solutions containing Np(VI), hydrofluoric acid, and alkali or ammonium ions causes an almost immediate precipitation of a fluoride of Np(IV). The mechanism for this reduction may be the reverse of that discussed in the section on bromate oxidation.

#### 4. SUMMARY

All available data on the rates of reaction of neptunium ions in acid solutions with various oxidants and reductants is summarized. In general the transitions between Np(III) and Np(IV) and between Np(V) and Np(VI) are rapid whereas the transition between Np(IV) and Np(V) is slow. The rate constant for the reaction  $\text{Np(IV)} + \text{Np(VI)} \rightarrow 2\text{Np(V)}$  in 1.0M  $\text{H}_2\text{SO}_4$  at 25°C is 2.2 liters/mole/min. The rate constant for the reverse reaction is  $5.3 \times 10^{-2}$  liters/mole/min. The oxidation of Np(IV) in bromate solutions is slow and complex. A remarkable acceleration of the bromate oxidation is observed in solutions containing hydrofluoric acid. The hydrogen-ion dependence of the reduction of Np(V) by Fe(II) indicates that the mechanism involves ions of Np(V) and Np(IV) of varying degrees of hydrolysis.

#### REFERENCES

1. J. C. Hindman, L. B. Magnusson, and T. J. LaChapelle, Chemistry of neptunium. The oxidation states of neptunium in aqueous solution, Paper 15.1, this volume.
2. L. B. Magnusson, T. J. LaChapelle, and J. C. Hindman, Chemistry of neptunium. Preparation and properties of neptunium(III), Paper 15.3, this volume.
3. L. B. Magnusson, J. C. Hindman, and T. J. LaChapelle, Chemistry of neptunium. Formal oxidation potentials of neptunium couples, Paper 15.4, this volume.
4. C. K. McLane, J. S. Dixon, and J. C. Hindman, Complex ions of plutonium. Transference measurements, Paper 4.3, this volume.
5. G. T. Seaborg and A. C. Wahl, Report A-135 (Mar. 19, 1942).
6. L. B. Magnusson, T. J. LaChapelle, and J. C. Hindman, Metallurgical Project Report CN-2767 (March 1945).
7. L. B. Magnusson, Metallurgical Project Report CN-1764 (July 1944).
8. C. K. McLane, Complex ions of plutonium. The fluoride complex ions of plutonium(IV), Paper 4.8, this volume.
9. J. I. Watters, Metallurgical Laboratory Memorandum MUC-JTW-53 (Feb. 8, 1945).
10. J. C. Hindman, unpublished results.
11. L. B. Magnusson and J. C. Hindman, Metallurgical Laboratory Memorandum MUC-GTS-2157 (Jan. 15, 1946).

## Paper 16.1

### TECHNIQUES FOR THE PREPARATION OF THIN FILMS OF RADIOACTIVE MATERIAL†

By D. L. Hufford and B. F. Scott

#### 1. INTRODUCTION

Along with the improvement of ionization chambers and the development of range chambers and fission counters has appeared an increased demand for thinner and more uniformly spread radioactive films. Films of active material that are too thick absorb many of the heavy fission particles and, to a lesser extent,  $\alpha$  particles before they can reach the ionizable atmosphere between the two electrodes. Films that are uneven and clumped may cause absorption of emitted particles by as much as 80 to 90 per cent, depending upon the nature and energy of the particle and the degree of nonuniformity of the film. This phenomena of self-absorption by radioactive samples is discussed to a limited extent in the manual by Jaffey, Kohman, and Crawford.<sup>1</sup> The accuracy of range-chamber and fission-chamber measurements is critically dependent upon the thinness and uniformity of the radioactive film.

Certain special problems concerning the preparation of radioactive film deposits have also arisen. For example, one experiment required 1  $\mu\text{g}$  of uranium to be spread on aluminum of 0.1- to 0.2-mil thickness over a 3 sq cm area. Another experiment required 150 mg of uranium to be spread over 250 sq cm of aluminum. Still another required 5 mg of plutonium to be spread over 3 sq cm of platinum.

†Contribution from the Chemistry Division of the Metallurgical Laboratory, University of Chicago, now the Argonne National Laboratory.

Based on Metallurgical Laboratory Memorandums MUC-GTS-557 and MUC-GTS-558 (January 1944), Report A-1235, and Supplement to Los Alamos Report LAMS-100 (July 11, 1944).

It is the purpose of this paper to summarize and discuss in some detail the various techniques that have been used in this laboratory for the preparation of these films. Normal evaporation, tetraethylene glycol spreading, slurry spreading, electrodeposition, and sublimation techniques have all been used here with some success. These various methods will be discussed separately.

## 2. THE NORMAL EVAPORATION TECHNIQUE

**2.1 Principle.** The process of evaporating samples to dryness without the use of spreading agents will be designated as "normal evaporation." If the amount of solid in solution is small, the normal-evaporation technique is feasible and rapid. The required volume of solution is transferred by pipet as a large drop, or as many small drops in a stippled pattern, onto a suitable backing, and the solvent is evaporated to dryness by a 250-watt Mazda heat-reflector bulb, which has been placed from 4 to 6 in. above the sample.

**2.2 Application.** The normal-evaporation method has been used for: (1) the preparation of films containing weightless, trace amounts of  $\alpha$ ,  $\beta$ , or  $\gamma$  activity from aqueous solutions on quartz, glass, platinum, or aluminum mounting plates; (2) the preparation of films of active material containing an average weight density of 1 to 2 mg/sq cm on platinum or quartz mounting plates for  $\beta$  or  $\gamma$  analysis; (3) the preparation of films of active material from sulfuric acid solutions; (4) the preparation of films of active material from organic solvents such as diisopropyl ketone and methyl isobutyl ketone on platinum and quartz mounting plates; (5) the preparation of a point source of radioactivity on the end of a platinum wire.

**2.3 Procedure.** (a) Preparation of Mounting Plates. Circular mounting plates, usually  $\frac{1}{2}$  to 2 in. in diameter, are cut or punched from new, bright platinum sheet of 2 mils thickness or greater. Since smoothness and flatness of the backing plate are essential qualities for good film formation, a platinum punch is used whenever possible in preparing the mounting plates. Scissors tend to crumple and warp platinum when used to cut platinum disks. A satisfactory punch for making flat platinum disks from metal foil is illustrated in Fig. 1.

Three of these platinum punches,  $\frac{1}{2}$ -, 1-, and 2-in. sizes, have been used in this laboratory. If for some reason a platinum mounting plate of a different size must be prepared, sharpened scissors may be used to cut a disk of the desired size, which may then be flattened conveniently by placing the disk in the proper-size punch, e.g., a  $\frac{3}{4}$ -in. disk can be flattened in the 1-in. punch and a  $1\frac{1}{2}$ -in. disk can be flattened in the 2-in. punch. If the diameter of the platinum mounting plate is

larger than 2 in., the disk can be placed between two hard, heavy, flat surfaces and rendered flat by pounding the back of the top surface with a hammer. Grease and dirt may be removed from the platinum disks by boiling them in concentrated nitric acid. A rinse of distilled water and a rinse of acetone complete the cleaning operation.

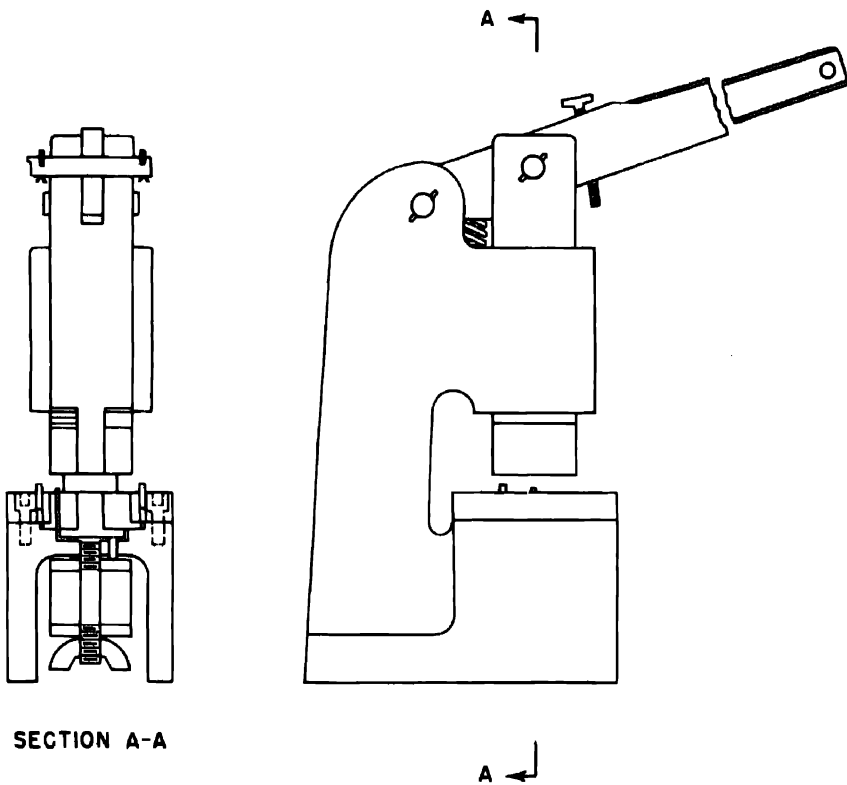


Fig. 1 — Twelve-millimeter platinum punch.

The platinum plates are ignited to dull redness over a bunsen flame prior to preparation of the radioactive film. Often the ignition of the platinum plate in a bunsen flame is the only cleaning treatment required. In order to confine the active solution to the plate it is necessary to paint a ring of zapon lacquer around the periphery. (Grade 1233 clear lacquer from the Atlas Powder Company was used.) A ring 1 to 2 mm wide is sufficient for this purpose. When the zapon is dry the backing plate is ready for the addition of active material.

Quartz or glass mounting plates are made conveniently from polished quartz or glass microscope slides, which can be obtained from

**Thermal Syndicate.** Three 1 sq in. plates may be obtained from a single slide. These mounting plates are cleaned in the same way as the platinum plates.

Aluminum mounting plates are cut or punched from new, bright aluminum sheet of 2 mils thickness or greater. These mounting plates may be cleaned by scrubbing the plates with soap and distilled water. The plates are rinsed with distilled water and subsequently with acetone. After the plates have been cleaned, each plate is placed in a standard ionization chamber and tested for radioactive contamination. Zapon rings are used on the quartz, glass, and aluminum mounting plates for confining the area to be covered. Sometimes a pencil mark or a scratch mark will serve the same purpose when aqueous solutions are being evaporated.

(b) Preparation of Standard Active Solutions. If the specific activity and purity of a given active material are accurately known, the preparation of a standard solution is an easy procedure. A weighed portion of the material is dissolved in an appropriate solvent, and the resulting solution is diluted to a convenient volume in a volumetric flask or a graduated mixing cylinder.

If the specific activity of a given active material is not known, then the specific activity must be determined prior to the preparation of a standard solution. Such a determination has been described as follows by Scott and Cunningham<sup>2</sup> in their discussion of the preparation of a standard uranium solution: "The uranium source may be either  $\text{UO}_2(\text{NO}_3)_2 \cdot 6\text{H}_2\text{O}$  or uranium metal and must be of known purity. If the salt is used, the solution is made up approximately at the concentration desired and standardized by determining the  $\text{U}_3\text{O}_8$  content of a known aliquot. A calibrated pipet should be used for measuring the aliquot, and the temperature of the liquid at the time of withdrawing the aliquot should be noted. The aliquot should be delivered into a clean, weighed platinum dish, evaporated to dryness under a heat lamp, and then placed in a cold muffle furnace. The temperature should then be brought to 800°C over a period of about 20 min and held at this temperature for 15 min. The sample is then allowed to cool and is weighed. The oxide obtained under these circumstances is  $\text{U}_3\text{O}_8$ ." A convenient aliquot is taken from the same solution for the preparation of an assay sample, as described under the TEG (tetraethylene glycol) technique, and the activity of the sample is counted in a standard  $\alpha$ -ionization chamber.

(c) Measurement of Fractional-milliliter Quantities of Active Solution. Scott and Cunningham have described the measurement of fractional-milliliter quantities of uranium solution.<sup>2</sup> This method has also been used for measuring micro quantities of other active solutions.

For most purposes it is not convenient to transfer more than a fraction of a milliliter of solution onto a backing plate, and for that reason the measurement of the aliquot of the standard active solution is done with a syringe-controlled micropipet. (Pipets of this type, in the volume range of 5 to 500 microliters, can be obtained from Microchemical Specialties Company.)

A diagram of the pipet and control is given in Fig. 2.

The pipets are calibrated for content and as supplied by the manufacturer are accurate to about 1 to 2 per cent. For accurate work they should be carefully calibrated. This is done by filling the pipet to the calibration mark with mercury and weighing the mercury. With even the smallest pipets a calibration carried out in this way can be accurate to 0.2 per cent. It should be noted that a pipet calibrated in this way is calibrated for content and must therefore be rinsed to achieve quantitative delivery of an aqueous solution.

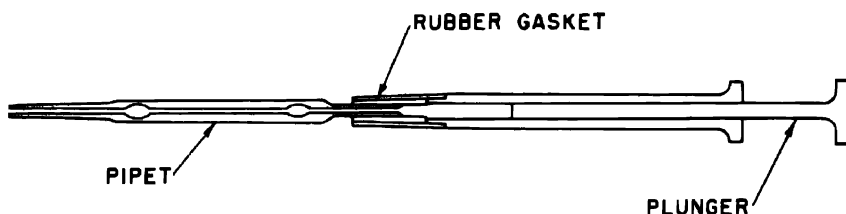


Fig. 2 -- Micropipet and control.

The accurately standardized active solution is drawn into the pipet by means of the syringe control. Care must be taken not to draw the liquid much above the calibration mark. After the pipet is withdrawn from the liquid, the tip should be wiped with Kleenex or similar material. For very accurate work, i.e., work requiring an accuracy greater than 0.5 per cent, if active solution is drawn above the calibration mark, the pipet should be rinsed and dried and the pipetting operation repeated. If the work does not require such accuracy, care should still be taken to avoid drawing the active solution much above the calibration mark. If the active solution is drawn slightly above the calibration mark, the position of the meniscus is adjusted accurately to the mark by repeatedly touching the tip of the pipet to a smooth glass surface such as that provided by a microscope slide.

The measured sample is delivered slowly onto the prepared mounting plate, and the pipet is rinsed with at least one complete filling of water or dilute acid, depending upon the nature of the activity. For

example, in the case of plutonium solutions, 1M HNO<sub>3</sub> must be used. If water is used the plutonium ion will hydrolyze to the insoluble hydroxide, which adheres stubbornly to the inside walls of the pipet, and an incomplete rinsing will result. The rinsing should be carried out with a droplet of liquid on a paraffined slide so that the entire rinse solution may be transferred to the plate. In this way any material on the outside tip that originated from the initial delivery will be transferred to the plate.

The plate usually rests on a stiff asbestos-board backing, and the heat lamp is placed about 4 in. above the sample. If a heat lamp is not available, quick evaporation may be performed by placing an electric hot plate under the asbestos board containing the sample. However, the heat lamp is preferable since it can be adjusted at various distances from the sample. In this way, the rate of evaporation can be carefully controlled, and the chance of activity splattering from the plate is greatly reduced. After the solution has evaporated to dryness, the sample is ignited to dull redness over a small bunsen flame. If mounted on aluminum, the sample cannot be ignited above 600°C since the melting point of aluminum is about 660°C. However, the zapon ring can still be removed by ignition by placing the sample in a cold muffle furnace and bringing the temperature to 500 to 600°C slowly over a ½-hr period. The zapon can also be burned off by placing the sample on a stiff piece of asbestos and holding the asbestos over a small bunsen flame. The time required for ignition by this method is usually between 5 and 10 min.

For work requiring an accuracy of 0.5 per cent or better, there are several precautions to be observed in the preparation of active samples. The pipets used should be rigorously cleaned and tested for activity. Treatment with a hot chromium trioxide-sulfuric acid bath followed by rinses of distilled water and acetone usually results in successful cleaning. The cleaning and rinsing solution should be drawn up into the pipet by the pipet control several times for each pipet and each bath. The pipet may then be tested for activity. A portion of 1N HNO<sub>3</sub> is drawn to the calibration mark, transferred to a clean mounting plate, and evaporated to dryness. The plate is then ignited. The plate is placed in an ionization chamber and tested for activity. If the activity on the plate is well within experimental error, the pipet may be assumed to be sufficiently clean for the proposed work. If the activity is not within experimental accuracy, the pipet should be cleaned again.

If the pipet is to be used several times during the experiment, a more rapid cleaning procedure may be helpful after the pipet has once been used. A simple trap useful in this procedure is illustrated in Fig. 3.

The pipet must fit snugly against the inside walls of the glass tubing. When the aspirator pump is turned on, rinses of concentrated sulfuric acid, concentrated nitric acid, dilute acids, distilled water, and acetone may be drawn through the pipet. This method of cleaning

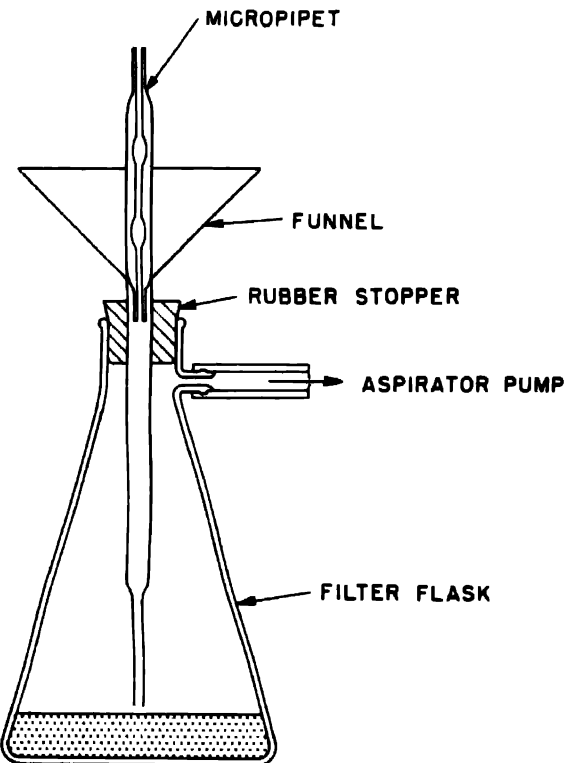


Fig. 3—Pipet-cleaning trap.

a pipet after the first use may be utilized only if in the subsequent use of the pipet the aliquot to be taken is from a solution of the same isotope and is of the same or greater concentration than the previous one. If an aliquot containing another isotope or a smaller concentration of activity is to be measured, either the former method of cleaning and testing pipets should be used or a new pipet should be used.

The pipets should be calibrated by the person who is to use them in order to use the same fiducial mark for the calibrating mercury and the solutions used. The measurement of aliquots of active solutions and of subsequent rinses should consist of drawing the liquid to the calibration mark but not beyond. Care should be taken during the delivery of the sample onto the mounting plate not to push air from the

pipet into the drop of liquid on the plate. Such an air bubble, on breaking, throws some portion of the active material off the mounting plate. Therefore, most, but not quite all, of the aliquot should be delivered onto the plate in one drop. The last fraction of a microliter should be delivered onto a separate portion of the plate. The rinse solution should be delivered onto a separate portion of the mounting plate so that the pipet tip will not become recontaminated and require another rinse.

Another possibility of sputtering and loss of activity arises during evaporation of the sample. Sputtering will be caused by too rapid evaporation; therefore, it is best to adjust the heat lamp to a height that will not cause too rapid evaporation, i.e., a height 4 in. or more above the sample.

Another precaution to be observed is that the solution of active material should not at any time during the preparation of the sample run onto the zapon, since during ignition the zapon tends to flake and blow off the plate before complete burning of the organic layer has occurred. These flakes would carry any activity that was on or in them.

(d) Evaporation of Samples from Solutions Containing Sulfuric Acid. Sometimes it is necessary to evaporate a sample containing sulfuric acid. The standard method described above is not applicable in these instances, since once the water has been driven from the sample, the sulfuric acid tends to creep through the zapon and over the edges of the plate with a resulting loss of activity. A method described by L. Magnusson<sup>3</sup> has proved to be satisfactory. The plate is mounted on a flat metal ring (brass or aluminum) or on a flat aluminum card having a hole in the center of the card. The diameter of the hole in the card or the inside diameter of the ring should be 2 to 4 mm less than the diameter of the platinum mounting plate. The platinum should be absolutely flat and should be flush with the mounting at all points of contact. The plate and mounting are then placed on top of a hot plate. By this method the outside edges of the plate are kept at a slightly higher temperature than the inside portion. The sulfuric acid will thus be confined to the inside area of the plate, and evaporation to dryness is easily performed without any loss of activity.

(e) Evaporation of Samples from Volatile Organic Solutions. Sometimes during the course of extraction work it is desirable to assay an organic solution. Q. Van Winkle<sup>4</sup> describes the preparation of protactinium samples from solutions of diisopropyl ketone. The technique used is the same as that used with aqueous solutions, since diisopropyl ketone has an appreciable surface tension. An aliquot of the activity-containing diisopropyl ketone is delivered onto the plat-

inum mounting plate and evaporated to dryness. As much as 30  $\mu\text{g}$  of protactinium has been spread over a 3 sq cm surface in this manner. The films were described as being very smooth.

Another extraction solvent is methyl isobutyl ketone. This liquid has a very low surface tension, and upon delivery onto a mounting plate it immediately spreads over the whole surface of the plate, dissolving the zapon and spreading over the edges of the plate. Two remedies have been found for this situation. If it is not inconvenient, a liquid having a high surface tension, such as ethyl alcohol, may be added to the methyl isobutyl ketone. The other technique consists of stippling the solvent onto the plate a few microliters at a time, waiting each time for the preceding droplet to evaporate to dryness.

(f) Evaporation of Sample on the End of a Platinum Wire. Some experiments require a point source of activity concentrated on the end of a platinum wire to be used for calibration purposes. In this case the active material can be evaporated at the end of the wire. The concentration of the activity in the solution should be as high as is feasible, i.e., the total amount of activity desired on the end of the wire should be contained in a volume equivalent to the volume of the smallest calibrated pipet available, i.e., a 5-microliter pipet. The aliquot is delivered onto the end of the wire in one or two portions. The wire is heated in a small bunsen flame at a point 2 cm from the end of the wire holding the activity. The solvent evaporates at the end of the wire leaving the active material concentrated at the tip.

2.4 Advantages of Normal Evaporation Technique. The normal evaporation technique is probably the most generally and widely used method of sample preparation since it is simple and requires little time. For quick, weightless assay work there is no better way of preparing samples. An accuracy of 0.5 per cent can easily be obtained. Almost any kind of backing plate that is not seriously attacked by the solution can be used. Platinum, quartz, aluminum, glass, and zapon mounting plates have been used. Point sources as required by back-scattering experiments are easily prepared by this method.

2.5 Disadvantages of Normal Evaporation Technique. When the amount of salt in the aliquot exceeds 25  $\mu\text{g}$ , difficulty in obtaining uniform samples becomes appreciable. The salts, e.g.,  $\text{Pu}(\text{NO}_3)_4$ , often remain in solution until only a few microliters of solvent are left, and then they deposit in thick clumps or ridges. Self-absorption in these thick samples often increases the error as much as 10 to 30 per cent in  $\alpha$  assays. In  $\beta$  and  $\gamma$  assays, of course, the self-absorption factor is not so appreciable, and thicker nonuniform samples can be tolerated. Another difficulty is that when evaporating large amounts over large areas from an aqueous solution, it is almost impossible

to predict what portion or area of the mounting plate is going to be covered. A sample cannot be uniformly spread over more than 1 sq cm, for example, by the normal evaporation technique.

### 3. THE TEG-SPREADING TECHNIQUE

**3.1 Principle.** This technique is described by Scott and Cunningham.<sup>2</sup> The radioactive material is dissolved in TEG (tetraethylene glycol) and the solution is spread as a thin film over a suitable mounting plate. Polymerization of the organic compound is brought about by heating. The polymerized compound is then removed by further heating, and the radioactive material is left as a uniform adherent film on the mounting plate.

**3.2 Application.** The method has been used for (1) the preparation of films of  $\text{U}_3\text{O}_8$  on platinum and quartz plates in the range from trace quantities to 2 mg of oxide per square centimeter of mounting plate; (2) the preparation of films of  $\text{PuO}_2$  and of  $\text{NpO}_2$  on platinum and quartz plates in the range from trace quantities to 100  $\mu\text{g}/\text{sq cm}$ ; and (3) the preparation of films of radioactive gold on platinum disks in the range from trace quantities to 100  $\mu\text{g}/\text{sq cm}$ .

**3.3 Procedure.** (a) Preparation of Mounting Plate and Standard Active Solutions. These preparations are adequately discussed above under the normal evaporation technique. However, the type of mounting plate used in the TEG technique usually is limited to high-melting material such as platinum and quartz, since high ignition temperatures are needed to dispose of all organic matter.

A flat surface is essential in the successful employment of this technique. Mounting plates of platinum are cut or punched from new, bright platinum sheet of 2 mils thickness or greater. The platinum disk can be fastened snugly to the surface of a thick ( $\frac{1}{8}$  in.) flat aluminum or nickel mounting-plate holder by using scotch-tape adhesion around the edge of the platinum disk. A zapon ring painted around the edge of the disk will serve as further binding. The zapon ring should extend 1 to 2 mm onto the platinum, as shown in Fig. 4, and about the same distance onto the mounting-plate holder. When the zapon is dry the mounting plate is ready for the addition of the active material.

(b) Technique of Spreading the Film. Two methods of applying the TEG to the mounting plate have proved successful. Perhaps the most generally used method consists of adding 1 or 2 drops of TEG from a dropper to the plate after the sample and rinse have been delivered. If the weight of material on the plate lies between tracer quantities and 0.5 mg/sq cm from 5 to 10 microliters of TEG is sufficient for each square centimeter of backing to be covered. Thus, if a circular

area having a diameter of 1 in. is to be covered, 1 drop of TEG from a dropper is appropriate. If a circular area having a diameter of 2 in. is to be covered, about 3 drops of TEG from a dropper is adequate. If the weight of material on the plate is greater than 0.5 mg/sq cm,

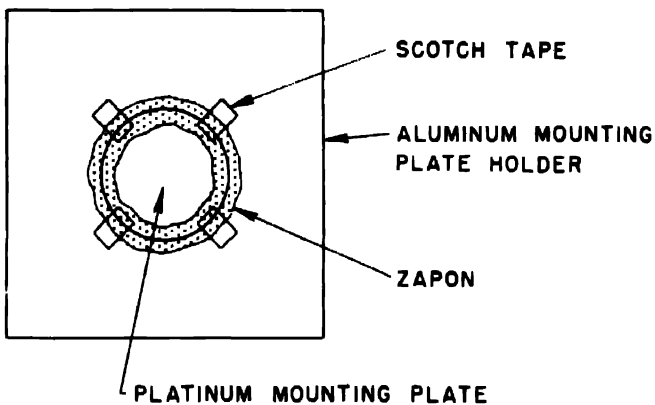


Fig. 4—Method of mounting plates for spreading with tetraethylene glycol.

more TEG per unit area should be used. For example, for thick deposits of about 2 mg/sq cm as much as 1 drop of TEG per square centimeter has been used. As the TEG polymerizes, it serves as a binder for the active material, and more seems to be necessary for thick deposits. Premature flaking and cracking of the heavier films take place if too little TEG is used.

Magnusson has described an alternate procedure, which has proved successful. A dilute solution is prepared containing 10 drops of TEG in 50 ml of water. After the active solution has been delivered onto the sample plate, a drop of this dilute TEG solution is used as rinse solution for the pipet and subsequently transferred onto the sample plate.

The TEG solution and the active solution are thoroughly mixed by rotating and tilting the plate. (The plate and mounting may be placed on a stiff asbestos board that can be rotated and tilted.) The mixture is then placed about 4 in. below a 250-watt heat-reflector bulb and left there until most of the water has evaporated. The heat lamp is then lowered to within about 2 in. of the sample. In the course of from 15 to 20 min partial polymerization of the glycol will occur together with precipitation of a finely divided amorphous film throughout the glycol. At this point it is important to note whether a uniform distri-

bution of material over the plate exists. If not, it may be possible to achieve better spreading by tilting the plate. Heating is continued until the plate appears to be dry. Finally, the organic matter is completely removed by heating the platinum or quartz to redness over a small bunsen flame. In the case of thick deposits the ignition step should be performed in a muffle furnace. The temperatures should be raised to 750°C over a period of 1 hr. In this way the cracking and flaking effect in the film due to temperature gradients between film and mounting plate during the ignition and cooling steps is minimized.

There are a few precautions not taken up in the normal-evaporation technique which apply specifically to the TEG technique. A concentration of nitric acid up to 3M may be tolerated in the active solution. However, care should be taken to evaporate the water and nitric acid from the TEG slowly, i.e., the heat lamp should be maintained about 6 to 10 in. above the sample during the initial stages of the evaporation. If the sample plate becomes too hot, the nitric acid will attack the TEG, forming bubbles of nitrogen dioxide, which, on breaking, splatter active material off the sample plate. The presence of sulfuric acid in the active solution minimizes the chances for an even, uniform spread since the sulfuric acid will attack both the TEG and the zapon. The films tend to clump, flake, and crack more easily, and activity may be lost over the edges of the sample plate. Although no splattering occurs when hydrochloric acid solutions are evaporated to dryness, loss of activity has been observed during the ignition of the samples. Hydrofluoric acid can be tolerated.

The use of very flat and smooth backing plates has already been stressed as highly essential.

If the TEG contains any nonvolatile residues it should be redistilled.

Another precaution to be observed is that the TEG should not at any time run onto the zapon. At the high temperatures employed for evaporation, the zapon is slightly soluble in the TEG. Activity may be lost by the spreading of the TEG over the edges of the plate or by the flaking of the zapon ring during ignition. The ring is adequate as a boundary, however, if the quantities of solution are kept as small as possible.

**3.4 Advantages of the TEG Technique.** The TEG technique is unique inasmuch as uniform, thick films containing no extraneous material can be reproduced within an accuracy of 0.5 per cent. For this reason the TEG technique is often used for specific-activity determinations.

**3.5 Disadvantages of the TEG Technique.** Perhaps the most important objection to the use of TEG is that the time required for a single sample preparation is usually at least 2 hr. Approximate a

assays should be obtained by the normal evaporation technique, and as a rule the TEG technique is employed only when an accurate assay, specific-activity determination, range determination, fission determination, or half-life determination is needed for relatively thick films of material.

Other disadvantages of this technique are the difficulties encountered in obtaining adherent films of deposits that weigh 1 to 2 mg/sq cm, or deposits over areas greater than 20 sq cm.

#### 4. THE SLURRY-SPREADING TECHNIQUE

4.1 Principle. The radioactive material is precipitated as an insoluble compound or is carried in an insoluble compound and slurried onto a suitable mounting plate. A uniform spread is obtained by slurring the radioactive material into a uniform suspension over the area to be covered and allowing the liquid to evaporate. The precipitate deposits evenly over the area to be covered.

4.2 Application. The slurry-spreading technique has been used in this laboratory for: (1) the preparation of films of uranium as  $\text{NH}_4\text{UF}_6$ , on aluminum in the range of 0.6 to 2 mg of uranium per square centimeter, (2) the preparation of films of plutonium as  $\text{NH}_4\text{PuF}_6$ , on aluminum, quartz, or platinum plates in the range 1 to 2 mg of plutonium per square centimeter, and (3) the preparation of films containing tracer amounts of active material but having a carrier density range of 25  $\mu\text{g}$  to 3 mg per square centimeter on platinum, aluminum, glass, or lusteroid backings.

4.3 Procedure. (a) Preparation of Backing Plates. The procedure for cutting and punching plates as described under the normal evaporation method is used for this technique. Since flat, smooth mounting plates are required during the slurry and evaporation steps, platinum and aluminum foils are bound to a flat, stiff mounting by scotch tape as described under the TEG technique. A scratch mark provided by a sharp compass point, or a zapon ring serves to confine the activity to the area to be covered.

(b) Preparation of Uranium and Plutonium Films by the Slurry-spreading Technique. The plutonium or uranium stock solution used must first be converted to the tetrapositive oxidation state before the precipitation of ammonium uranium(IV) fluoride or ammonium plutonium(IV) fluoride can be performed. Usually the plutonium is available in laboratory solutions as the tetrapositive nitrate. However, either tripositive or hexapositive plutonium may be converted to the tetrapositive nitrate by heating a concentrated solution in 10N  $\text{HNO}_3$ . The plutonium is reduced by the traces of  $\text{NO}_3^-$  ion present in concen-

trated solutions of nitric acid, and the tripositive state is oxidized by the  $\text{NO}_3^-$  ion to the tetrapositive valence state.

Uranium is usually available as  $\text{U}_3\text{O}_8$ ,  $\text{UO}_3$ , or  $\text{UO}_2(\text{NO}_3)_2 \cdot 6\text{H}_2\text{O}$ . If the nitrate is the only available form of uranium, it is convenient to convert the salt to  $\text{U}_3\text{O}_8$  before reducing the solution completely to the tetrapositive state. This operation is easily performed by placing the required amount of salt in a platinum crucible and transferring the crucible to a cold muffle furnace. The temperature of the furnace is brought to 800°C during a 20-min period and is held at this temperature for 15 min. Either of the oxides,  $\text{U}_3\text{O}_8$  or  $\text{UO}_3$ , can be dissolved by heating in concentrated hydrochloric acid. Once the uranium is completely dissolved, the solution is diluted to a convenient volume prior to reduction. Electrolytic reduction in a dilute hydrochloric acid electrolyte has proved to be a clean-cut quantitative method for reducing hexapositive uranium to the tetrapositive valence state. This method of reduction was used twice at two different uranium concentrations, 300 mg/ml and 15 mg/ml. In both cases the reduction seemed to be quantitative as shown by spectrophotometric analysis. A hydrogen-platinum cathode and a platinum anode were used. A platinum wire screen was platinized by using the screen as a cathode in a concentrated chloroplatinic acid bath. The platinization was achieved by passing a current of 0.5 amp through the electrolyte for 10 min at a potential difference of 10 volts. The cathode was sealed in a glass tube having an opening that would permit hydrogen to enter the cathode compartment, as pictured in Fig. 5. A glass tube with a disk of coarse sintered glass sealed into one end served as the anode compartment. A platinum wire rested upright on top of the sintered-glass disk. The chlorine gas formed at the anode from the oxidation of the  $\text{Cl}^-$  ion in the hydrochloric acid tended to escape through the top of the anode compartment without reentering the main portion of the electrolyte. Highly purified hydrogen, 99.9 per cent pure, was used for the reduction described here. However, Howland<sup>6</sup> reports that tank hydrogen can be used. The electrolyte, the two electrode compartments, and a glass stirrer were placed in a 150-ml beaker. Hydrogen was passed through the electrolyte for 15 min to remove any oxygen that might have been present in the solution. The reduction was performed over a 3-hr period, using a current of 0.2 amp and a potential of 25 volts. During the 3-hr period hydrogen was continuously bubbled through the cell. After the electrolysis had been discontinued, hydrogen was bubbled through the solution for 15 min in order to remove any chlorine that may have remained behind. The resulting tetrapositive uranium stock solution was then stored under 1 atm of hydrogen in a graduated mixing cylinder having a lubricated glass stopper.

The conditions for the preparation of both the  $\text{NH}_4\text{PuF}_6$  slurry and the  $\text{NH}_4\text{UF}_6$  slurry are essentially the same. A concentration of 10 mg of U(IV) or Pu(IV) per milliliter of solution has been found to be convenient. The precipitation is performed in a paraffined 5- or 15-ml cone. The required amount of plutonium or uranium stock is transferred to the cone. A five- to tenfold excess of  $\text{NH}_4^+$  as ammonium

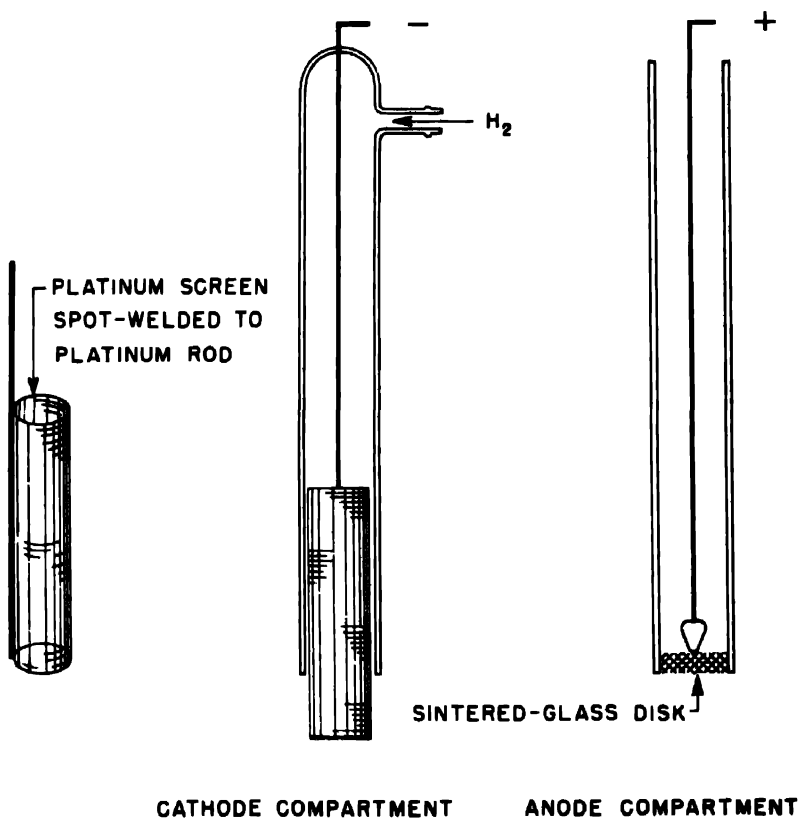


Fig. 5—Electrode compartments for uranium reduction.

chloride (a 1N or 2N solution) is added to the stock solution. The use of ammonium nitrate is inadvisable for the precipitation of  $\text{NH}_4\text{UF}_6$ , since the  $\text{NO}_3^-$  will oxidize tetrapositive uranium ion. Enough distilled water is added to the solution to bring the final  $\text{H}^+$  concentration to 2N. The solution is stirred with a looped platinum wire until completely uniform. A twofold excess of  $\text{F}^-$  as hydrofluoric acid is finally used to precipitate the uranium or plutonium. The slurry is stirred with the platinum wire until the precipitate is uniformly dis-

tributed throughout the aqueous phase. The magnitude of solubility of the compounds used in the presence of an excess of  $\text{NH}_4^+$  ion is about 10 mg per liter. However, too great an excess of  $\text{F}^-$  ion tends to complex the plutonium and uranium and therefore increases solubility losses.

The slurry can be centrifuged in a clinical centrifuge. Since the precipitate is quite crystalline, although very finely divided, 5 to 10 min centrifugation is usually quite sufficient. After centrifugation, the supernatant liquid is drawn off with a 500-microliter micropipet (described under the normal evaporation procedure) and transferred to another paraffined container. The precipitate is then slurried into 1 to 2 ml of distilled water and centrifuged, and the supernatant liquid is again drawn off. This operation is repeated three times in order to free the precipitate completely from free acid or excess salts. It is especially important to rid the precipitate of acid if the mounting plate to be used is aluminum. Aluminum ion tends to dissolve in fluoride solutions with the formation of the  $\text{AlF}_6^{-3}$  complex.

Two methods of slurring the uranium or plutonium onto the plate have been used. If the mounting material is platinum, quartz, or glass, or if the mounting material is aluminum and the area to be covered is less than 20 sq cm, the washed precipitate is slurried with a platinum wire into about 0.5 ml of distilled water and transferred by micropipet directly to the sample plate. As insurance against loss of any part of the precipitate that may have remained behind, another portion of distilled water is added to the cone, and a second transfer to the sample plate is made. This procedure is repeated until all the activity has been transferred. Enough distilled water is added to the plate to cover the required area. A glass micro stirring rod is then used to slurry the entire precipitate into a uniform suspension. The uniformity of the final film depends upon how thoroughly and uniformly the precipitate is slurried into suspension. The slurring operation may sometimes require 10 to 15 min of vigorous agitation before a satisfactory spread is obtained. The active material on the end of the stirring rod is rinsed onto the plate with a drop of distilled water.

Polished aluminum surfaces often present the problem of obtaining adequate wetting by aqueous solutions. If the area of aluminum to be covered is less than 20 sq cm, the vigorous agitation of the slurry with the stirring rod will serve to wet the required surface. If the area to be covered is greater than 20 sq cm, it is often advisable to ensure proper wetting of the required surface area by first placing the right amount of distilled water on the plate. The surface can be wet by repeatedly drawing a film of water over the obstinate area with a micro stirring rod. Finally, after a film of water has been

spread over the selected area, the plutonium or uranium slurry is transferred to the plate, as in the preceding paragraph, and is thoroughly slurried into suspension. Films of uranium have been spread over 250 sq cm in this manner.

The water is evaporated from the sample at room temperature with a minimum of air currents blowing over the surface. In some instances where heat or a current of air has been applied to speed the evaporation, flaking and cracking of the film has resulted, especially when the film deposits have had surface densities greater than 1 mg/sq cm. Slow evaporation seems to minimize the chances of flaking the film.

If the mounting plate is too large to permit assay by placing it in an ordinary  $\alpha$ -counting ionization chamber, the amount of material on the plate must be calculated by subtracting the amount of activity in the supernatant liquid from the total amount of activity added to the paraffined zone. Another alternative is possible if the mounting plate is platinum or quartz. The mounting plate can be weighed before the film is spread. After the water has evaporated from the plate, the sample is placed in a muffle furnace and ignited to 750°C in the case of uranium and to 1000°C in the case of plutonium. The sample plate is again weighed. The difference in weight may be assumed to be  $U_3O_8$  for uranium or  $PuO_2$  for plutonium.

In many instances the film prepared is in the form of the precipitate. If the self-absorption of radiation by the sample is too great, some of the weight may be removed by igniting the sample to the oxide. Samples mounted on aluminum plates may be ignited to 500°C. If the samples are mounted on platinum or quartz plates, the samples can be ignited to 1000°C leaving the composition of the film as  $U_3O_8$  or  $PuO_2$ . Again, care must be taken to raise and lower the temperature of the furnace slowly when thick samples are being ignited in order to minimize the chances of flaking.

Another slurry technique has been used in this laboratory for the preparation of thick films of uranium. A chimney mounted on a sample holder, as pictured in Fig. 6, was the apparatus used for this technique. A quartz disk is placed in the sample holder. A rubber gasket serves as a seal between the sample disk and the chimney. The chimney is held securely in place by four strong rubber bands stretched between the four glass ears on the chimney and the four steel hooks on the steel holder.

Powdered  $U_3O_8$ , which has been either crushed by a ball mill or ground by a mortar and pestle, is suspended in methyl alcohol in a test tube. Heavy particles of the oxide immediately settle to the bottom, but the lighter particles remain in suspension and settle gradu-

ally. This slurry is then poured into the cell pictured in Fig. 6. The methyl alcohol is evaporated by a heat lamp placed about 10 in. above the cell. Uniform deposits of  $\text{U}_3\text{O}_8$  as thick as 10 mg./sq cm have been obtained by this method. This deposit adheres well, but a binder such as zapon or collodion is usually applied to the film to ensure adherence for samples that are to be kept for long periods of time.

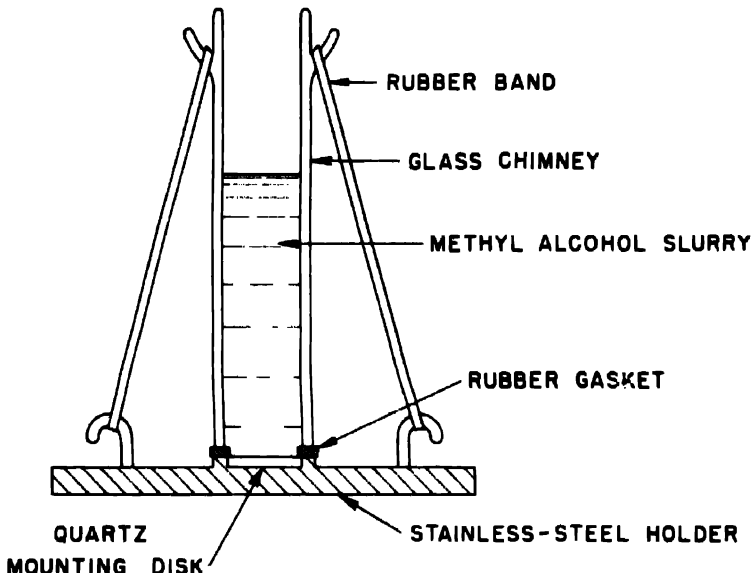


Fig. 6.— $\text{U}_3\text{O}_8$  slurry deposition.

(c) Preparation of Films Containing Tracer Amounts of Activity in Appreciable Amounts of Carrier. Jaffey, Kohman, and Crawford<sup>1</sup> have described the preparation of samples containing tracer amounts of activity in sizeable amounts of carrier.

When the amount of salt in a solution containing tracer amounts of activity is too great for the normal evaporation technique, the active material can be separated by precipitation with a suitable carrier. For example, lanthanum fluoride carries tetrapositive plutonium, barium sulfate carries hexapositive sulfur activity, manganese dioxide carries protactinium, and columbium pentoxide carries columbium activity. The precipitate is centrifuged, washed, centrifuged again, and stirred into a slurry by use of a loop of fine platinum wire. The rotation of the loop in the precipitate is achieved by rolling between the fingers the wire leading from the loop. The slurry is pipetted to

the platinum disk, evaporated to a thick paste, spread smoothly over the disk with a micro stirring rod, and evaporated to dryness.

4.4 Advantages of the Slurry-spreading Technique. If the precipitate is finely divided, the slurry-spreading technique possesses several distinct advantages over other techniques. Thicker, uniform films can be obtained which can be spread over greater areas on almost any type of mounting material. Also, tracer amounts of activity can be separated from concentrated salt solutions if an appropriate carrier is used.

4.5 Disadvantages. The greatest disadvantage of the slurry-spreading technique is the fact that it is not analytically quantitative as are both the common evaporation technique and the TEG-spreading technique. Also, as much as 8 to 10 hr is sometimes required for the preparation of large films of  $\text{NH}_4\text{PuF}_5$  or  $\text{NH}_4\text{UF}_5$ .

## 5. THE ELECTRODEPOSITION TECHNIQUE

5.1 Uranium Electrodeposition. (a) Principle. The uranium is electrolytically reduced from the hexapositive uranyl ion to the tetrapositive state and deposited as a hydrous oxide onto a suitable mounting plate used as the cathode.

(b) Application. This method has been successfully used in this laboratory for the preparation of very uniform films of uranium on platinum plate within the range of 0.05 to 0.75 mg of  $\text{U}_3\text{O}_8$  per square centimeter of platinum. This same technique has been used elsewhere for the preparation of films as thick as 2 mg/sq cm deposited on platinum, aluminum, or lead mounting plates.<sup>7</sup>

(c) Apparatus and Procedure. The electrolytic technique used in this laboratory was designed and is described by Cohen and Hull.<sup>8</sup> A stainless-steel holder serves as the cathode for the electrolysis. A diagram of the holder is given in Fig. 7. The top of the upraised circular center portion of the holder is flat and has approximately the same diameter as the platinum mounting plate upon which the uranium is deposited. A different holder is made for each size of sample disk. The sample disk, cut or punched from sheet platinum having a thickness of 2 mils or greater, is placed on top of the upraised portion of the holder. A gasket made of vinylite, bleached rubber, or neoprene and having a width of  $\frac{1}{8}$  in. and a thickness of  $\frac{1}{32}$  to  $\frac{1}{16}$  in. is fitted on top of the platinum disk and is held in place by fastening the cell chimney to the holder with four strong rubber bands. A thin coating of rubber cement has also been found to serve well as a gasket. The outside diameter of the gasket should be about the same as the diameter of the platinum disk. The chimney is conveniently made from

pyrex tubing having an inside diameter approximately the same as the inside diameter of the gasket. To prevent any leakage from occurring between the gasket and the chimney, the bottom rim of the chimney is ground flat. Strong rubber bands can be easily prepared from Gooch-crucible rubber tubing.

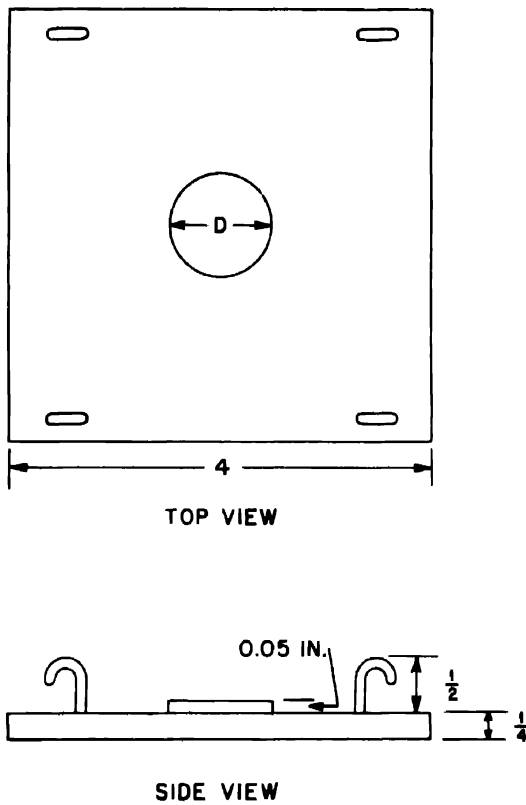


Fig. 7—Stainless-steel cathode holder.

The anode consists of a 10-mil platinum disk that can rotate freely within the glass chimney. This disk is spot-welded onto the end of a stainless-steel rod. The other end of the rod should fit snugly into the chuck of a stirring motor. The rate of stirring is controlled by a Variac interposed between the motor and the line voltage.

A 6-volt storage battery is the source of current and a 10-ohm slide-wire rheostat is used to regulate the current passing through the cell. A cross-sectional diagram of the assembled cell is shown in Fig. 8. The individual parts are scrubbed with soap and water before

the cell is assembled prior to electrolysis. In this laboratory 0.4M ammonium oxalate has been used as the electrolyte. (Kahn<sup>9</sup> has reported another successful electrolyte to be 0.015M NaF.) Approximately 1.3 to 1.5 ml of 0.4M ammonium oxalate is used for each

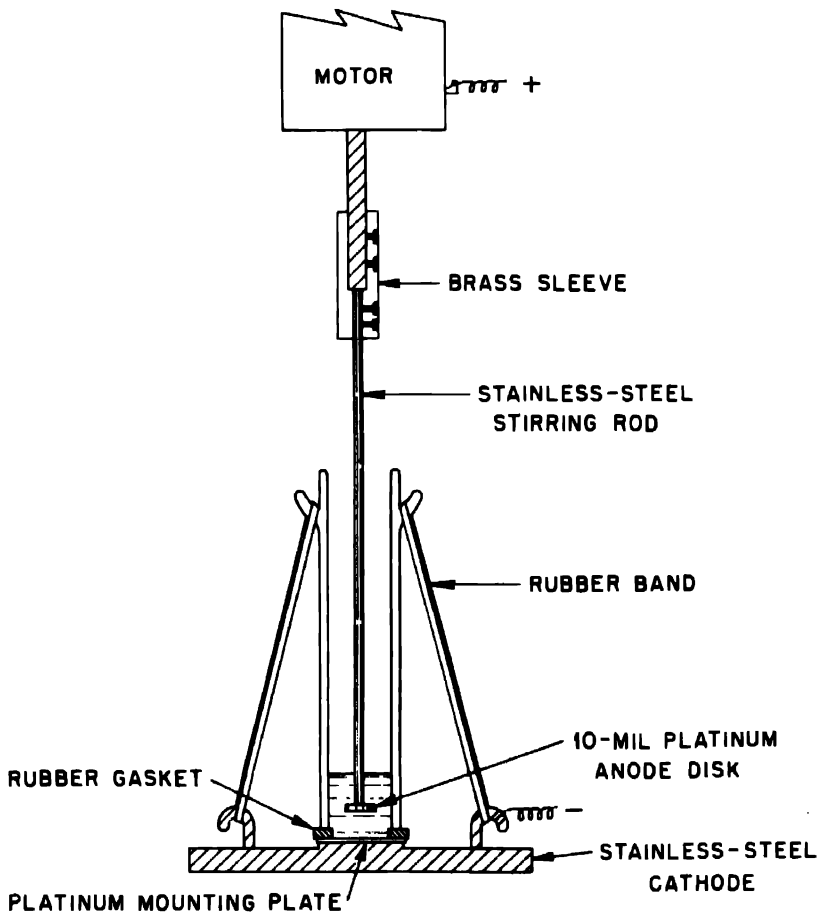


Fig. 8—Electrodeposition cell.

square centimeter of platinum surface to be covered. During the course of their experimentation, Cohen and Hull<sup>8</sup> found this amount of electrolyte to be best for optimum deposition. The appropriate amount of electrolyte is added to the cell, followed by a known weight of uranium in the form of a uranyl salt in aqueous solution. The solution of the uranyl salt may contain any anion that does not attack

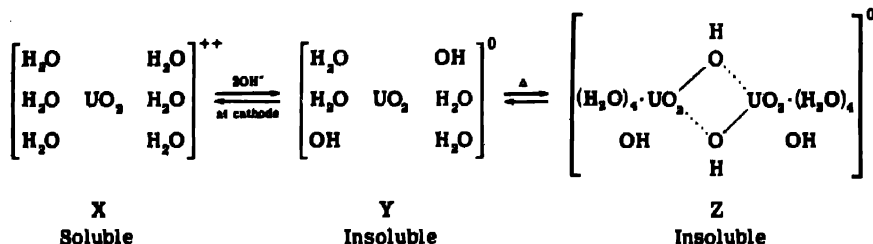
platinum during the electrolytic process (nitrate, acetate, sulfate, and fluoride have all been used successfully), but it should not contain large amounts of free acid. Acid in molar concentration equivalent to the uranyl salt may be tolerated, but not in much greater amount. In cases where appreciable amounts of acid are left behind in the method of preparing the uranyl salt, sufficient ammonium hydroxide must be added to the cell solution to neutralize the free acid.

The cell is placed in a water bath heated by a hot plate. (A 6-in. crystallization dish has been found to be an appropriate container for the water bath.) The bath is heated to about 80°C, and the electrolysis is started. A set of split watch glasses or four glass microscope slides are placed on top of the chimney to catch any spray from the electrolyte. The platinum anode is dipped a few millimeters below the surface of the solution and rotated at about 500 rpm. A current density of 0.13 to 0.15 amp/sq cm is used throughout the electrolysis. If the amperage begins to drop, a few crystals of ammonium oxalate are added to the cell, and the current then rises to its former value. The electrolysis is carried out for 20 to 50 min; about halfway through this period, the watch glass and sides of the cell are washed once with a few milliliters of water. A few crystals of ammonium oxalate are added to readjust the current density.

At the end of the electrolysis 30 to 60 ml of methyl alcohol is added to the plating bath before the current is broken. This acts as a rinse and also helps to leave the cell dry when it is drained. The cell is taken apart, and the platinum disk is ignited for about 5 min at 75°C.

The conditions for the electrolysis as described above are somewhat critical, as reported by Cohen and Hull, and different conditions either change the rate of plating or alter the composition of the electrodeposit. A high current density favors rapid plating, as does the temperature of the electrolyte, which is usually about 10° higher than the water bath. Films prepared at a water-bath temperature of 70 to 80°C have the best appearance. A water-soluble deposit was found to be formed at room temperature.

Cohen and Hull postulate a mechanism of deposition as follows:



They found that the electrodeposit prepared in a hot water bath slowly dissolved when placed in contact with water. Also, the plating of uranium oxide at room temperature took place only over long periods of time. These facts can be explained by assuming that the hydrated uranyl cation, represented by "X," undergoes the schematic changes indicated above when electrolyzed at elevated temperature. Poly-nuclear complex Z can lose additional water on further heating and thus cause films that are made at about 80°C to be more compact and undergo less of a volume change when ignited.

The rate of stirring is an important variable in determining the character of the deposit. Higher rates of stirring are advantageous for rapid plating. However, higher speeds of stirring result in a radical nonuniformity of the film. This can be counteracted to some extent by increasing the concentration of electrolyte but only at the expense of seriously reducing the rate of plating.

Ammonium salts of various organic acids were tested in the electrolyte bath by Cohen and Hull, and ammonium oxalate was found to be the most satisfactory in producing hardness and adherence of film. Films produced with salts such as ammonium nitrate or sulfate were uneven, powdery, and not very adherent. However, nitrate and sulfate ions may be tolerated in the ammonium oxalate electrolyte, since oxalate anions are very effective in displacing other sorbed ions.<sup>10</sup>

These workers also investigated the effect of different types of platinum surfaces and different kinds of metal upon the rate of plating. The following is quoted from Cohen and Hull:<sup>8</sup>

"For a series of different types of surfaces, i.e., etched, cold-rolled, and polished platinum, the rate of plating as well as the upper limit of amount of  $U_3O_8$  per square centimeter of surface increases in the order given, the greatest difference being between the etched platinum and the other two types. This effect is so marked that if any corroded spots develop on a bright platinum disk, the probability is large that peeling of  $U_3O_8$  will take place at those spots. If one considers with Adam [‘Physics and Chemistry of Surfaces,’ Oxford University Press, New York, 1941] that a polished metal surface is an amorphous layer having powers of dissolving other metals not possessed by a crystalline surface, an explanation is then given for the tenacity of adhesion of uranium oxide films to polished platinum."

Jones, Goldstein, and Knesel<sup>11</sup> have reported further evidence that electrodeposits formed on tarnished unpolished surfaces of monel metal tend to have dull finish, amorphous character, and pinwheel effects and that these deposits frequently peeled. After the same monel metal disks have been polished with crocus cloth, smooth metallic

electrodeposits containing up to 1 mg of uranium oxide per square centimeter are easily prepared.

Cohen and Hull<sup>8</sup> also found the rate of plating to be affected by the kind of metal base. They state: "There seems to be a decrease of about 10 per cent in the plating rate in the order of silver, platinum, copper, and tin."

(d) Advantages of the Electrodeposition Technique for Uranium.

The electrodeposition technique described above has been found to be a quantitative method for preparing very uniform, adherent films on the mounting materials, aluminum, lead, and platinum. It is conceivable that quartz could be used if a thin coating of aluminum metal were sublimed over the outside surface.

(e) Disadvantages of the Electrodeposition Technique for Uranium.

Cohen and Hull have found that for an electrolysis lasting 50 min under the conditions described above, 94  $\mu\text{g}$  of platinum deposits with the uranium. Usually this amount of extraneous matter is negligible. However, if a graphite anode could be employed, this deposition of platinum could be eliminated. Kahn<sup>9</sup> reported that the graphite anode was unsuccessful if used with the sodium fluoride electrolyte. A second disadvantage of the electrodeposition technique is that many impurities present in the reagents readily deposit at the high current density that is used.

5.2 Plutonium Electrodeposition. (a) Principle. The plutonium is electrolytically reduced from the hexapositive plutonyl ion to the tetrapositive state and is deposited as the hydroxide onto a suitable backing plate used as the cathode.

(b) Application. This method has been used successfully in this laboratory for the preparation of very uniform films of plutonium on platinum backing at plutonium oxide densities of 10 to 100  $\mu\text{g}/\text{sq cm}$ .

(c) Apparatus and Procedure. The apparatus described in the section on uranium electrodeposition is also used for the plutonium electrodeposition. However, the electrolysis is carried out at room temperature, and no water bath is needed. A 6-in. crystallization dish is used as a container to hold the cell. If any leakage occurs the recovery problem is simplified, since the active solution is prevented from spreading over the hood floor.

The method described by Miller<sup>12</sup> has been found to be useful. She states: "An electrolyte, consisting of 0.125N KOH (Baker's analyzed), has been found more satisfactory than the alkali-carbonate solution heretofore described. Approximately 1.3 to 1.5 ml of solution is used for each square centimeter of area to be covered. The plutonium, which must be in the hexapositive state, is added as the nitrate in a volume of 0.25 ml or less of approximately 0.08M HNO<sub>3</sub>. The addition

is best made very slowly and with stirring. A current density of 10 ma/sq cm is used."

It is convenient to remove an aliquot for counting at the beginning and after 2 to 2½ hr. By this time the count should have fallen to one-tenth of its initial value. The yield is usually from 85 to 90 per cent.

At the end of this plating the electrolyte is poured off, and the plate is washed several times with water while in place. The cell is then taken apart. The plate is rinsed again and ignited 1 to 2 min at red heat over a bunsen flame. The amount of metal on the plate must be determined by counting, since extraneous material is simultaneously deposited making the weight gain of no significance. Plates can be prepared having 0.1 mg of plutonium deposited as oxide per square centimeter.<sup>11</sup>

Hexapositive plutonium nitrate is usually available in laboratory stock solutions. However, tetrapositive plutonium stock can be converted readily to the hexapositive state by oxidation with potassium permanganate. Plutonium is then separated from the permanganate by ether extraction from a saturated ammonium nitrate solution.<sup>12</sup>

A few observations relative to the potassium hydroxide electrolytic procedure have been made in this laboratory. For cells of the 1-in. diameter size the electrodeposition is sometimes successful. Adherent, uniform films having a density of 0.1 mg/sq cm have been attained. However, some difficulty has been experienced in attaining the same density for films prepared from cells of 2-in. size. The upper limit for the density of the deposits obtained from this size cell has been found to be 0.075 mg/sq cm. The force of stirring causes any further deposits of the poorly adherent  $\text{Pu}(\text{OH})_4$  to be swept from the plate. In the absence of stirring, spotted nonuniform films are produced. Both these difficulties can be circumvented by carrying out two successive electrodepositions on the same backing plate. After a film having a density of 0.05 mg/sq cm has been electrodeposited, the cell is dismantled, the plate is washed and ignited, and the same cell containing the same plate with the ignited film of  $\text{PuO}_2$  is reassembled. New electrolyte and hexapositive plutonium stock are added to the cell, and another electrolysis is performed. At the end of the plating the film should contain about 0.1 mg of  $\text{PuO}_2$  per square centimeter of backing plate.

At the time of the writing of this report the method of electrodeposition of plutonium from a potassium hydroxide electrolyte had been found to be undependable in certain experiments. Two months after a hexapositive stock solution had been prepared by permanganate oxidation and subsequent ether extraction from an ammonium

nitrate solution, the yields of the electroplating were observed to have diminished with time. Finally, yields as low as 30 per cent were obtained. It was thought that the hexapositive plutonium had been reduced over a long period of time to the tetrapositive state by traces of  $\text{NH}_4^+$  or ether peroxides carried over by the extraction. Attempts to increase the yields of the electrodeposition by reoxidizing the stock solution with dichromate and argentic ions proved unsuccessful. In some instances yields as low as 2 per cent were obtained when electrolysis was carried out in the presence of the oxidizing agent. It is possible that electrodeposition may not work well in the presence of the chromate or argentic ions. However, it became apparent that the potassium hydroxide electrodeposition of plutonium is sometimes troublesome and is not thoroughly understood at this laboratory.

Therefore a sodium bicarbonate-carbonic acid electrolyte was investigated. The electrolyte consists of a 0.1M  $\text{NaHCO}_3$  solution saturated with carbonic acid by a constant stream of carbon dioxide bubbling through the cell during the electrolysis. A carbon dioxide generator is conveniently prepared by placing dry ice in a stoppered flask having a side arm. A potential difference of 12 to 15 volts and a current density of 40 to 80 ma/sq cm are used. The stock solution of hexapositive plutonium is prepared in the same way as mentioned previously. The yields obtained by this method of electrodeposition for a 2-hr electrolysis have varied from 50 to 70 per cent. The films are thin, uniform, and adherent. Some impurities, either from the anode or the reagents, have been found to deposit with the film.

An attempt to electrodeposit plutonium by using the same electrolyte and conditions for electrolysis as described for the electrodeposition of uranium has proved unsuccessful.

(d) Advantages of Electrodeposition Technique for Plutonium. The films attainable by electrodeposition of plutonium are adherent, very uniform, and very thin. Although the time required to make one sample by this method is relatively long, the amount of time demanded of the operator is comparatively small.

(e) Disadvantages of the Electrodeposition of Plutonium. An upper limit of 0.1 mg/sq cm to the thickness of the plate has not been surmounted. Extraneous material is deposited with the active material, and the technique as described is not analytically quantitative.

5.3 Polonium Electrodeposition. (a) Principle. Tracer amounts of polonium metal are deposited on a platinum cathode by electrolysis.

(b) Application. This method has been used for obtaining samples of pure  $\alpha$  radiation of uniform intensity over a definite area for use as standards in range measurement.

(c) Apparatus and Procedure. The electrolysis vessel used is a cylinder of pyrex glass, a pyrex-glass spacer, and an optically flat platinum cathode  $\frac{1}{8}$  in. thick, made leakproof by compression on polished surfaces by a brass jig, as indicated in Fig. 9. A 40-mil platinum wire is used as an anode.

The cell is cleaned very thoroughly by heating in concentrated  $\text{HNO}_3$ , for a  $\frac{1}{2}$ -hr period and rinsing well with distilled water. If the cathodes are kept grease-free after polishing, they need only to be rinsed before use. The cell solution used is approximately 10 ml of 0.5M  $\text{HNO}_3$ . It has been found that in order to get yields of 50 per cent or more, it is necessary to have an initial polonium concentration of at least 10,000 disintegrations per minute in each milliliter of cell solution.

The polonium is purified from isotopes of bismuth and lead by pre-electrolysis in a beaker using gold-foil electrodes. The current density of the preelectrolysis should be approximately  $3 \mu\text{a}/\text{sq cm}$ . Redissolving the deposit in concentrated nitric acid gives a solution of quite pure polonium. By using such polonium solutions, runs yielding clean plates are made at a current density of  $30 \mu\text{a}/\text{sq cm}$ .

The time required for yields of 80 to 90 per cent for concentrated polonium solutions (greater than 100,000 disintegrations per minute per milliliter) depends to a great extent on the efficiency of agitation. With efficient stirring a good yield is obtained in 5 or 6 hr. Highest yields are obtained with low acidity, but deposits from solutions of higher acidity have been found to be more adherent.

(d) Advantages. Electrolytic deposits of polonium on platinum are very adherent and have little tendency to "creep about" by aggregate recoil. Being a "wet" method in all its phases, electrolytic preparation involves less health hazard than sublimation and evaporation. Furthermore, the yields from concentrated solutions can be made quite high.

(e) Disadvantages. It is a rather long method, but no careful supervision of the operation is necessary. The concentration of polonium deposited by this method is limited to 76 microcuries per square millimeter.<sup>13</sup>

## 6. THE SUBLIMATION TECHNIQUE

6.1 The Acetylacetone-sublimation Technique. Dixon, Smith, and Cunningham<sup>14</sup> have described this sublimation technique as a method for the preparation of uniform films of plutonium and uranium.

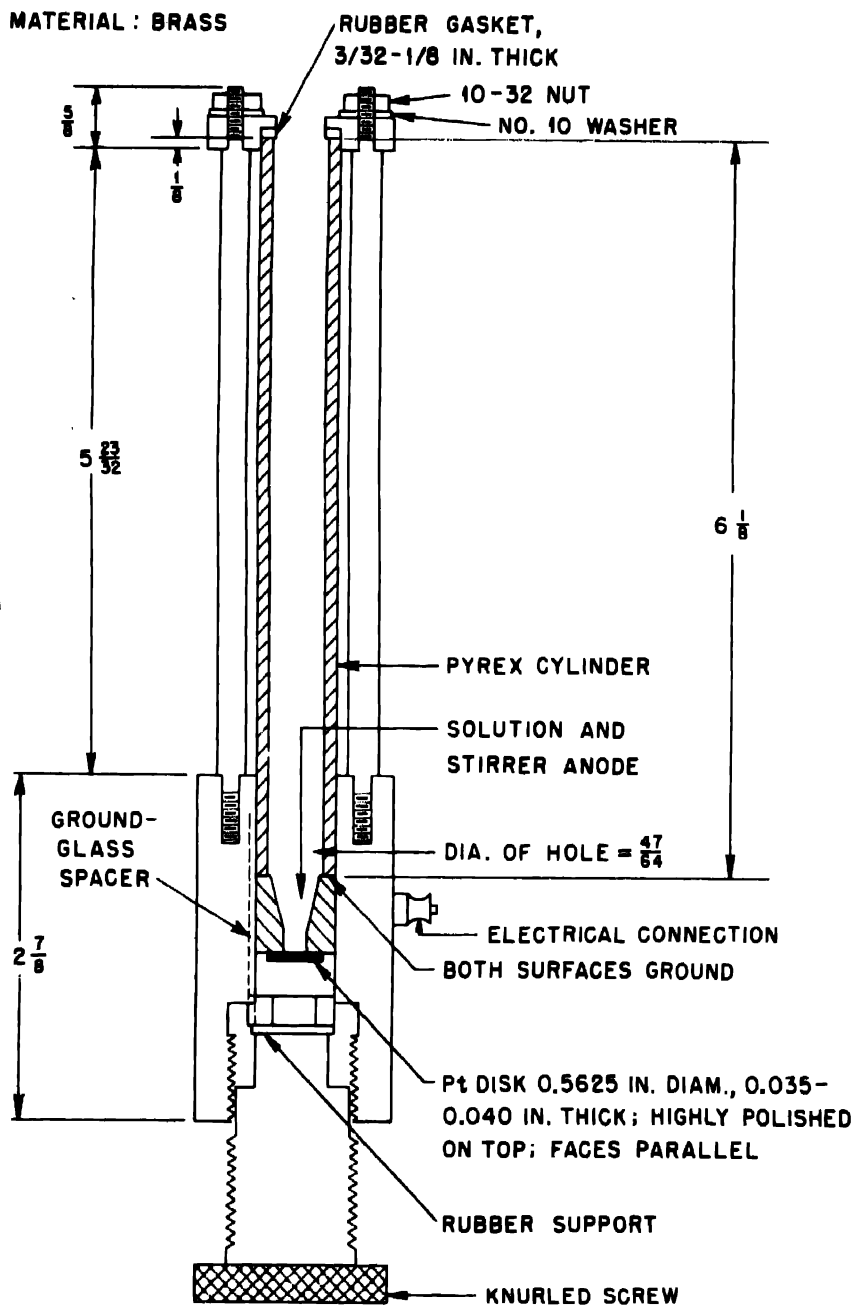


Fig. 9—Polonium electrodeposition cell.

(a) Principle. The radioactive element, in the form of a volatile acetylacetone compound, is sublimed in a vacuum onto a suitable mounting.

(b) Application. This method has been applied to the preparation of thin, uniform deposits of plutonium on aluminum, platinum, and quartz mounting plates at deposit densities of from 0.01 to 100  $\mu\text{g}/\text{sq cm}$ .

(c) Procedure in the Preparation of Plutonium(IV) and Uranium(IV)

Acetylacetone. Dixon and Smith<sup>18</sup> have described the preparation of the plutonium(IV) and uranium(IV) acetylacetones. For the preparation of the plutonium acetylacetone an excess of acetylacetone is added to a concentrated solution of plutonium(IV) contained in a test tube or centrifuge cone. The acidity should be about 0.5M in HCl. Enough sodium or ammonium hydroxide is added with the acetylacetone to bring the pH to about 4 or 5. The resulting reaction mixture is vigorously stirred and is immediately extracted with benzene.

For the preparation of uranium(IV) acetylacetone the same procedure is used. However, uranium(IV) chloride is dissolved in water for the preparation of the stock solution. The refractive index of the acetylacetone used in the preparation should be taken at frequent intervals, i.e., once every month or two to determine the extent of decomposition. Light and moisture catalyze the decomposition of acetylacetone, resulting in the formation of acetic acid and acetone. Both uranium and plutonium acetylacetone, and especially the plutonium acetylacetone, are readily hydrolyzed by water and free acids. If the refractive index of the acetylacetone is low, it is recommended that it be redistilled through an efficient column, i.e., one having an efficiency of 15 to 20 theoretical plates.

The plutonium and uranium acetylacetones can be preserved for a limited time, i.e., 1 to 2 months, in the benzene that is used for extraction. However, if it is desirable to store the compounds in solution over a long period of time, it is advisable to evaporate the benzene solution, dry the acetonate over phosphorus pentoxide, purify by sublimation, and redissolve in benzene that has been dried over metallic sodium.

(d) Operation of the Sublimation Unit. A drawing of the sublimation unit is given in Fig. 10. The operation of the unit is evident from the figure. The radioactive material is confined as a dry powder in an effusion capsule. If the acetylacetone is contained in a benzene stock solution, an appropriate volume of solution is dropped into the capsule with a micropipet by alternately pipetting and evaporating a few microliters of solution at a time. The main portion of the activity can be kept in the center of the effusion capsule by pressing the delivery

tip of the pipet against the center of the platinum dish throughout the evaporation of the benzene. The surface tension of the benzene against the glass pipet tip prevents the solution from creeping over the edges of the capsule. The benzene must be removed completely by evaporation in vacuum at room temperature before sublimation of the acetylacetone is started. The sublimation is carried out at a pressure

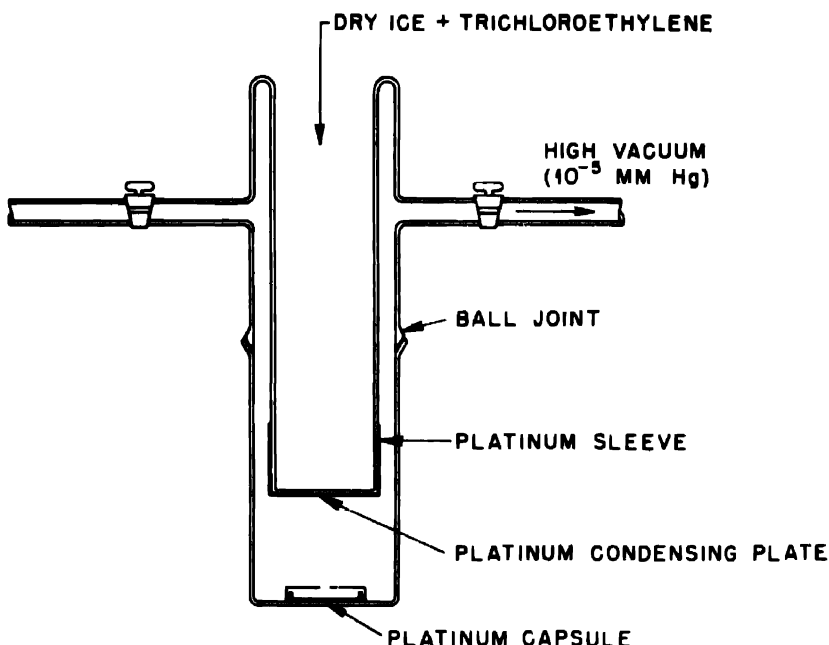


Fig. 10.—Acetylacetone sublimation unit.

sufficiently low for the mean free path to be of the order of several centimeters. In this way the path of the subliming molecules may be defined sufficiently well so that almost all sublimed material will collect on the backing. The density of the deposit formed in this way will not be entirely uniform but will vary inversely as the square of the distance from the effusion hole.

The foil or other backing on which the sublimate is to be collected is affixed to the bottom of the cold finger by means of a platinum sleeve, as shown in the drawing. Very thin foils such as 0.1 mg/sq cm of aluminum should not contact the cold finger directly but only through a peripheral mounting ring. If desirable, a collimating shield may be placed directly beneath the foil in order to limit further the area of deposition.

After the foil is in place, the effusion capsule containing the acetylacetone is placed in the bottom section of the apparatus. A Dewar flask containing liquid air is placed around the trap. The apparatus is then assembled as shown in the drawing and evacuated to  $10^{-4}$  or  $10^{-5}$  mm Hg pressure. Enough time is allowed for any moisture or benzene remaining in the effusion dish to evaporate completely. (If this precaution is not followed, some benzene or water vapor may condense and be frozen on the sublimate plate. A spotted, irregular film will then result. Finally, a dry ice-trichloroethylene mixture is placed in the cold finger, and the bottom of the effusion vessel is heated to the desired temperature by means of a Wood's metal bath. Since a flame is used to heat the Wood's metal bath, a noninflammable liquid is used in the cold finger. The temperature of the bath must be closely watched and maintained between 140 and 165°C. Both of the acetylacetones decompose above 173°C, but below 140°C the rate of sublimation is very slow. At present the data on the vapor pressures of the acetylacetones are limited to measurements at 140°C. At this temperature the vapor pressure of plutonium(IV) acetylacetone is approximately  $4.0 \times 10^{-4}$  mm Hg, and that of uranium(IV) is approximately  $1.6 \times 10^{-2}$  mm Hg.

If the area of the orifice of the effusion capsule is known, the rate of sublimation may be roughly calculated from the effusion formula

$$P = \frac{M}{2\mu RT}$$

where  $\mu$  is number of grams subliming per second per square centimeter, P is vapor pressure in dynes per square centimeter, and M is molecular weight of compound.

When it is judged that a sample of proper density has been collected, the heating bath is removed, the trichloroethylene-carbon dioxide mixture is removed from the cold finger, and the apparatus is allowed to warm to room temperature. The vacuum is then released. If the apparatus is dismantled while the cold finger is cooler than room temperature moisture condenses on the sample. Since the acetylacetones are slightly soluble in water, a spotted irregular film is produced. If the operation has been properly carried out, the deposit appears perfectly smooth.

The total weight of the deposit can be determined accurately by counting in a standard  $\alpha$  chamber. It should be pointed out that the deposits consist of materials that have an appreciable vapor pressure at room temperature and that a slow volatilization of the prepared sample is to be expected. In the case of 0.1 to 1  $\mu\text{g}/\text{sq cm}$  deposits of plutonium on aluminum, the thin film of acetylacetone is not stable,

and the compound converts to a nonvolatile compound. Thicker deposits of plutonium or uranium acetylacetone on platinum or quartz have been stabilized by exposing the film to bromine vapor and then igniting the film to  $\text{PuO}_2$  or  $\text{U}_3\text{O}_8$  in a muffle furnace.

The bromine fixation can easily be accomplished by placing about 100 microliters of bromine in the bottom of an open beaker and inverting the beaker over the sample. Five to ten minutes is usually sufficient time for this fixation. As a health precaution, because of the volatility of the compounds, the ignition step should be performed in a muffle furnace located inside a hood. An efficient gas mask should be worn by the operator at all times when working with appreciable quantities of the plutonium acetylacetone.

(e) Advantages of the Acetylacetone-sublimation Technique. Excellent films of uranium and plutonium are prepared by this technique, and no extraneous material is deposited with the sample. Also, almost any type of sample backing can be used in this method.

(f) Disadvantages of the Acetylacetone-sublimation Technique. Volatile active compounds such as the acetylacetones constitute a health hazard. The over-all yield of this technique is small compared to the other techniques in use, and the amount of time required to prepare a thick sample is sometimes 24 hr.

6.2 Sublimation of  $\text{PuF}_3$ . (a) Principle. Plutonium fluoride sublimes in a vacuum at about  $1200^\circ\text{C}$  and may be collected on a surface chilled by liquid nitrogen.

(b) Application. Flat, uniform samples of plutonium fluoride in the weight density range from trace quantities to 1 mg/sq cm have been obtained for use in range measurements, as fission-rate standards, and for measurement of the absorption spectrum of solid  $\text{PuF}_3$ .

(c) Apparatus. This technique, which requires rather elaborate apparatus, has been described by Phipps, Sears, Seifert, and Simpson.<sup>15</sup>

(d) Advantages and Disadvantages. At present this technique provides more uniform films than any other known method. The purity of the deposit is another great advantage. Its chief disadvantage, aside from the difficult procedure, is the large excess of activity required which prohibits its use in many cases.

## 7. PREPARATION OF PROTECTIVE FILMS OF ZAPON

As a health protection and as precaution against loss of activity from the sample which would affect research results, a binder is sometimes required for thick samples of activity to eliminate the possibility that particles of active material would become dislodged from the plates.

Various methods of estimating the weight of these protective films have been used by this laboratory. If the amount of self-absorption of  $\alpha$  or  $\beta$  particles caused by the zapon binder does not have to be accurately known, a dilute solution of zapon lacquer in ethyl, butyl, or amyl acetate can be pipetted onto the sample or sprayed onto the sample by means of an atomizer. A dilution ratio of 30 parts by volume of solvent to 1 part of zapon lacquer has been found to be convenient. If the sample is weighed before and after the application of the zapon, the density of the binder can be determined.

If a known aliquot of zapon solution is pipetted onto the sample and spread over the sample by rotating and tilting the sample on a suitable backing, the density of the zapon film can be predetermined by a weight assay. A given aliquot of zapon solution is pipetted into a weighing bottle, and the solution is evaporated to dryness at room temperature. The weighing bottle is weighed before the aliquoting and after the evaporation.

Films of zapon spread in the manner described above tend to be heavier at the spots where the last bit of solvent is evaporated since the solubility of the zapon in the acetate esters is large. If the zapon solution is sprayed in fine droplets over the sample, a more uniform protective film is obtained, but the amount of spraying required to give a particular density of binder can only be estimated.

A method has been developed for the preparation of uniform zapon-films with predetermined, accurately known densities.<sup>16</sup> A film of dilute zapon is spread over an appropriate surface area of water contained in a circular vessel such as a crystallizing dish. The solvent evaporates leaving a solid film of zapon covering the surface of the water. A circular copper frame is used to remove the film of zapon from the water. A diagram of the frame is given in Fig. 11.

For this procedure a 2 to 1 ratio of amyl acetate to the "5580" zapon cement is used. A 6-in. crystallizing dish is completely filled with distilled water. The copper frame is made out of  $\frac{1}{16}$ -in. copper wire. It is essential that the ring describe a perfect circle, and that the top of the circular ring be flattened. The ring is placed at the bottom of the dish with the top of the handle hooked over the edge. A selected number of drops of dilute zapon is transferred to the surface of the water. The film of zapon is spread by repeatedly drawing a pencil point through the surface of the solution starting in the center and ending at evenly spaced points around the edge of the dish. At the points where the pencil point is drawn over the edge of the dish, zapon "anchors" are formed, which, when the solvent has evaporated, hold the zapon film taut. As soon as all the solvent has evaporated, the frame is raised until it is in contact with the film. The zapon anchors are then dissolved by the use of a dropper filled with amyl acetate. A

droplet of amyl acetate is forced onto the outside of the tip of the dropper, and the dropper is drawn through the zapon anchor. The frame is slowly lifted from the water, and the zapon film, if the operation is performed correctly, remains stretched across the wire circle. About 2 hr are allowed for the film to dry at room temperature or 15 min in an oven at about 70°C.

After the film has become completely dry its density is determined. A square of cardboard having an accurately known area is used as a pattern. The film is placed between two sheets of tracing paper, and a razor blade is used to cut around the pattern and through the paper

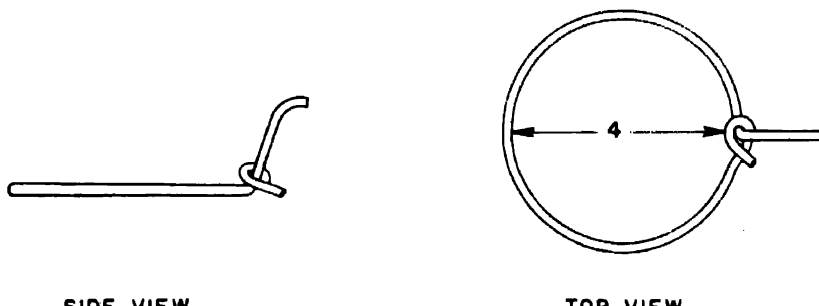


Fig. 11—Copper frame for zapon films.

and film. The two squares of paper are weighed first with and then without the square of film between them, and the difference is the weight of the square of film. Films having surface densities ranging between 40 and 1,000  $\mu\text{g}/\text{sq cm}$  have been prepared in this laboratory using this method.<sup>17</sup> By using the same frame, the same size dish, and the same number of drops of zapon solution, it is possible to reproduce the thickness of film within 5 per cent. Also, with care the density of the film can be made to vary directly with the number of drops of zapon dilution within 5 per cent.

After the zapon dilution has been determined, a film of the desired density is prepared. A ring of aquadag is painted around the periphery of the sample plate, and the film is lowered into contact with the sample plate. After the aquadag cement has dried, the rest of the film is cut away from the sample with a razor blade.

#### 8. METHODS OF CLEANING ACTIVITY FROM PLATES

Three solvents for cleaning ignited plutonium and uranium plates have been used successfully in this laboratory, namely, sulfuric acid, potassium bisulfate, and hydrobromic acid. In the case of each sol-

vent, heating has been required, and the cleaning procedure is repeated until the background of the plate is low enough for the plate to be used as a sample backing again.

Plates containing enough activity to warrant recovery are usually cooked in either hot concentrated sulfuric acid above 200°C or 48 per cent hydrobromic acid at 110°C. Either a hot plate or a heat lamp can be used as a source of heat. It is preferable to use hydrobromic acid to recover activity from plates because any  $\text{SO}_4^{2-}$  ion must be disposed of before methyl isobutyl ketone or ether extraction can be performed with good yields. The hydrobromic acid is evaporated to dryness at about 110°C, and the plates and container are rinsed with concentrated nitric acid. This procedure of evaporating and rinsing is repeated three or four times, and the activity is usually almost quantitatively removed from the plates. For example, O'Connor<sup>5</sup> reports that a 99.7 per cent recovery from a platinum plate containing 1.35 mg of  $\text{PuO}_2$  that had been ignited to 1000°C was accomplished by hydrobromic acid solvation.

Recently a preliminary experiment using very concentrated nitric acid and rather dilute hydrofluoric acid as a hot cleaning solution reduced the activity of  $\text{PuO}_2$  on a platinum disk from 240  $\mu\text{g}$  to 1  $\mu\text{g}$ .<sup>6</sup> Similarly, a concentrated nitric acid-concentrated hydrobromous acid mixture reduces and dissolves  $\text{PuO}_2$  from platinum disks upon heating strongly. In general, contact with strongly reducing concentrated acid solutions has been successful in recovering  $\text{PuO}_2$  deposits from platinum in this laboratory.

The last traces of activity are often readily cleaned from platinum and quartz plates by the potassium bisulfate fusion method. Approximately  $\frac{1}{2}$  lb of potassium bisulfate is placed in a large porcelain or platinum crucible and heated with a Méker burner to a temperature above 210°C, the fusion temperature of potassium bisulfate. Each plate is separately transferred to the bath to ensure good contact with the solvent. After all the plates have been placed in the bath, the bath is heated to a higher temperature. The plates are cooked in this bath for 1 or 2 hr, then the bath is allowed to cool to room temperature, and the crucible and plates are transferred to a concentrated nitric acid bath. This bath is heated until the potassium bisulfate has dissolved, and the plates are rinsed with distilled water followed by an acetone rinse. Two or three potassium bisulfate fusions are usually sufficient to reduce the background of the plates to less than 10 disintegrations per minute. However, if the background cannot be reduced to such a level, it is usually necessary to use a fine emery paper to eliminate the activity that has become dissolved or fused into the platinum surface.

### 9. SUMMARY

Many fundamental measurements on radioactive material require a thin, uniform, smoothly spread source of activity. This requirement has instigated research involving varied principles and techniques whereby smooth films of radioactive deposits may be prepared. This report is concerned chiefly with the preparation of films of uranium and plutonium. However, the principles and techniques described can be applied to other radioactive elements in many instances.

Five general methods, the normal evaporation technique, the tetra-ethylene glycol spreading technique, the slurry-spreading technique, the electrodeposition technique, and the sublimation technique, have been employed successfully in this laboratory, and each of these methods is described in a separate section of this report.

### REFERENCES

1. A. H. Jaffey, T. P. Kohman, and J. A. Crawford, Metallurgical Laboratory Memorandum MUC-GTS-407, (January 1944).
2. B. F. Scott and B. B. Cunningham, Metallurgical Laboratory Memorandum MUC-GTS-557 (Mar. 27, 1944).
3. L. Magnusson, private communication.
4. Q. Van Winkle, private communication.
5. P. O'Connor, private communication.
6. J. J. Howland, private communication.
7. R. Nobles, private communication.
8. B. Cohen and D. E. Hull, Report A-1235 (Aug. 28, 1944).
9. M. Kahn, University of California Radiation Laboratory Report R.L. 16.6.24 (Apr. 22, 1943).
10. A. W. Thomas and B. Cohen, J. Am. Chem. Soc., 59: 268 (1937).
11. W. H. Jones, J. H. Goldstein, and C. F. Knesel, (A) M-2350 (Mar. 28, 1945).
12. M. L. Miller, Supplement to Los Alamos Report LAMS-100 (July 11, 1944).
13. E. Rona and E. A. W. Schmidt, Z. Physik., 43: 784 (1928).
14. J. C. Dixon, C. Smith, and B. B. Cunningham, Metallurgical Laboratory Memorandum MUC-GTS-558 (January 1944).
15. T. E. Philpss, G. W. Sears, R. L. Seifert, and O. C. Simpson, The vapor pressure of plutonium halides, Paper 6.1a, this volume; T. E. Philpss, G. W. Sears, and O. C. Simpson, The volatility of plutonium dioxide, Paper 6.1b, this volume; see also N. D. Erway, L. O. Gilpatrick, Z. V. Jasaitis, F. D. Johnson, T. E. Philpss, G. W. Sears, R. L. Seifert, and O. C. Simpson, Metallurgical Project Report CN-3223 (Sept. 26, 1945).
16. R. Goetz, private communication.
17. Hubert B. Billington, private communication.
18. J. S. Dixon and C. Smith, Preparation and composition of plutonium(IV) acetylacetone, Paper 6.39, this volume (Metallurgical Laboratory Memorandum MUC-GTS-2045).

## Paper 16.2

### AN IMPROVED TECHNIQUE FOR PRECISE ALPHA RADIOMETRIC ASSAY†

By E. F. Westrum, Jr.

#### 1. INTRODUCTION

A precise method of assay for radioactive isotopes is needed in the determination of the specific activity of an isotope or mixtures of isotopes, in the determination of the composition of a compound, in the establishment of purity of a given compound, and in the accurate determination of the concentration of plutonium in a solution, e.g., in calorimetry or in solubility determinations on a micro or semimicro scale. The method described here is not, of course, limited to plutonium, but it should prove of worth generally with radioactive preparations of suitable specific activity in operations on the micro and tracer scales.

The general principles of radiometric assay and of the errors inherent in the counting procedure have been discussed<sup>1</sup> and will not, therefore, be considered here.

#### 2. VOLUMETRIC MEASUREMENT OF FRACTIONAL-MILLILITER QUANTITIES OF ACTIVE SOLUTIONS

Micropipets<sup>2,3</sup> equipped with syringe controls are usually employed for the volumetric delivery of solution samples of the order of 5 to 500 microliters.

Although this technique is rapid and convenient for quantitative work where an uncertainty of the order of 0.5 per cent may be tolerated, it is subject to several limitations for work requiring an ultimate standard error of less than 0.2 per cent.

†Contribution from the Chemistry Division of the Metallurgical Laboratory, University of Chicago, now the Argonne National Laboratory.

In accurate work such pipets must be carefully calibrated, usually by weighing the mercury delivered. Because of the relatively large bore of the capillary in the vicinity of the fiducial mark, very accurate adjustment of the meniscus at the calibration must be made during calibration and use. The calibration is tedious, and the errors introduced by neglect of the difference in curvature of the menisci of mercury and aqueous solution may not be negligible. As an alternate procedure, the pipet may be calibrated with aqueous solutions, for example, by titrating aliquots of standardized acid.

Since the pipet is calibrated for content rather than for delivery, at least two rinsings are necessary to ensure quantitative delivery. As might be expected, the precision of the method varies greatly with the skill and experience of the analyst. Frequently one or more dilutions are required before plating; when this is so, the cumulative uncertainty is large.

### 3. ADVANTAGES OF GRAVIMETRIC MEASUREMENT OF FRACTIONAL-MILLILITER QUANTITIES OF ACTIVE SOLUTIONS

In connection with some calorimetric measurements and some precise relative specific-activity determinations, a more accurate assay technique was required; the gravimetric procedure described below was devised. Briefly, it consists of preparing all the solutions by weight and determining the amount of solution plated gravimetrically rather than volumetrically.

For example, consider the determination of specific activity of a piece of plutonium metal. The weight of the metal is determined on an appropriate balance. Then it is placed in a small, weighed, glass-stoppered Erlenmeyer flask, a suitable quantity of solvent (e.g., dilute aqueous sulfuric acid) is added, and the combined weight of flask and solution is determined after the chemical reaction has taken place.

The concentration of the solution may be expressed in terms of weight of plutonium per unit weight of solution. If the concentration thus obtained is too high for plating, a dilution may be performed by delivering a convenient volume (e.g., 500 microliters) of thoroughly mixed initial solution to a weighed glass-stoppered flask of appropriate size, stoppering it, and reweighing. More solvent is then added from a buret to dilute to exactly the desired concentration, and the weight of the final solution is determined.

Although very small volumetric flasks may be obtained, either the area of the neck in the vicinity of the calibration is too large to permit accurate volume determination, or the neck is so small that it causes difficulty in mixing. The use of small tared Erlenmeyer flasks

gravimetrically enables one to use quite light flasks with small glass stoppers and yet have ease of mixing. Dilution to a given concentration is convenient with the gravimetric procedure; consequently corrections for unequal counting rates may be minimized.

The arrangement shown in Fig. 1 was used for plating. A thin optically flat glass disk was placed on each pan of the balance, and a cleaned backing plate of quartz or platinum was centered on the glass of the left pan and covered with a thin lucite cover.

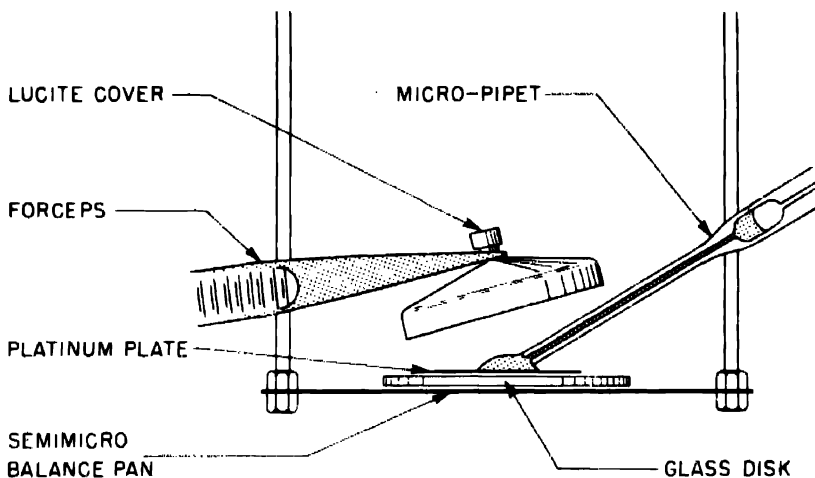


Fig. 1.—Scheme of plating by the gravimetric procedure.

After the apparent weight of the above system had been ascertained, an appropriate quantity of solution was delivered to the center of the backing plate with a micropipet, and the lucite cover was immediately replaced over the sample. A timer started when the sample is delivered makes it possible to record the apparent weight as a function of time and to extrapolate to zero time if the drift is appreciable. The amount of sample delivered is determined by weight; the pipet serves only as a transfer instrument to deliver approximately a prescribed quantity.

Owing to evaporation, the solution will, in general, lose weight. The function of the lucite cover is to retard evaporation and decrease the rate of loss of solvent. A further aid in this direction is the use of sulfuric or perchloric acid solutions to reduce the partial pressure of the water. Although sulfuric acid solutions are considered difficult to plate, the technique described below permits control of the

spreading for all reasonable amounts of acid. It was noted that the use of approximately 3M H<sub>2</sub>SO<sub>4</sub> as solvent gave a drift in the equilibrium position of the balance corresponding to a change of 0.00 to 0.2 per cent per minute for a 100-mg sample, depending on the humidity. Under these conditions the extrapolation over the first 6 to 10 sec while the lucite cover is off can be made with good precision.

Table 1 — Typical Precision of Gravimetric Counting Procedure Applied to the Determination of Specific Activity of Plutonium Metal<sup>a</sup>

Determi-nation No.	Weight of Pu metal, mg	Concentration of solution A, <sup>†</sup> μg Pu/mg solution	Concentration of solution B, <sup>†</sup> μg Pu/mg solution	Amount of solution B plated, mg	Observed relative counting rate, <sup>‡</sup> counts/min./μg
I	5.808	0.08356	0.018913	81.07	70,798 ± 14%
				81.37	70,799 ± 22
II	10.678	0.08650	0.018970	79.54	70,789 ± 20
				80.88	70,805 ± 20
70,798 ± 14 (av.)					

<sup>a</sup> All solutions were 3.0M with respect to H<sub>2</sub>SO<sub>4</sub>. Solution B was prepared by weight from a 550-mg aliquot of solution A.

<sup>†</sup> The observed counting rate has not been corrected for the resolving time of the counter, although the slight correction to an identical average sample size has been made in the observed counting rate. The area over which the active material was distributed varied from 0.3 to 3.0 square centimeters on the various plates.

<sup>‡</sup> The uncertainty attached to these averages of several countings in a parallel-plate argon-carbon dioxide chamber is the standard (statistical) error and agrees with observed variation in the counting rate.

A balance that has proved very convenient for this work is the Christian Becker Semi-Micro Chainomatic Balance No. 360 with a capacity of 100 g and a sensitivity of about 10 divisions per milligram. Buoyancy corrections on the solutions may be neglected since their densities will be nearly identical. Since plating can be done this way with better precision, fewer plates are needed for a given degree of accuracy. Furthermore, corrections for the temperature changes of the solutions are entirely eliminated.

The use of a micro weight-buret for this purpose has been considered, but it was not adopted because small differences between much larger weights would have been required; and the delivery of duplicate samples of very nearly identical size is not feasible. Slight weighing irregularities induced by the handling and manipulation of such a buret and the inconvenience of cleaning and rinsing the buret for use with a different solution suggest that the above gravimetric procedure is more accurate and efficient.

The excellent concordance, indicated in Table 1, of the observed counting rate of four plates prepared from two samples of spectroscopically pure plutonium metal is typical of the precision achieved.

#### 4. A PLATE-HEATING DEVICE FOR CONTROL OF SPREADING SULFURIC ACID SOLUTIONS DURING VAPORIZATION

As has been noted,<sup>2</sup> the normal evaporation technique gives entirely satisfactory plates for  $\alpha$  radiometric assay of material containing on the order of 1  $\mu\text{g}$  of pure plutonium per square centimeter. However, the tendency of the hot concentrated sulfuric acid (produced upon vaporization of most of the water from the relatively dilute solution plated) to spread over the edges of the plates is so pronounced that even with the use of a zapon film special methods are necessary.

Although baked glyptal or bakelite retaining films have been found to be of some value and more uniformly successful with sulfuric acid than zapon, the tendency of the organic film to flake and blow off during flaming before complete combustion has occurred (with a consequent possible loss of active material) has directed interest to a plating process in which organic films could be eliminated completely.

A device that has proved both convenient and satisfactory for this purpose and for controlling the extent of the area over which the active material is distributed is shown in Fig. 2. The nichrome heater maintains the edge of the plate at a slightly higher temperature than the center portion, thus confining the concentrated acid to the inside portion of the plate. The heating unit is wound on a nickel collar that slips over a tube, on top of which rests the quartz or platinum plate. A flange on the collar fits over the edge of the platinum plates and maintains them flat despite the tendency of unannealed platinum to warp and buckle upon heating. The flange thereby assured the absence of cold spots around the edge of the platinum to which the film of acid would flow. Quartz plates are rigid and, consequently, may be placed on the leveled portion of the collar flange. A 250-watt heat lamp is placed about 4 cm above the sample to provide most of the heat for vaporization. Both heater and heat lamp are controlled with Variacs. By maintaining proper balance of the two heat sources the area of the evaporating solution can be controlled at will, and the rate of vaporization can be readily controlled even during the removal of the last trace of solution. Two rapid-acting adjusting screws are provided in the base of the tripod stand to permit leveling of the platinum plate and centering of the solution despite air currents in hoods.

This device has provided a means of preparing uniformly thin films on both quartz and platinum containing as much as several micrograms of plutonium per square centimeter and remarkably even in density when examined microscopically. If the backing plate is properly cleaned and if the redistilled sulfuric acid and source of active material are free of nonvolatile impurities, the presence of films

of density  $1 \mu\text{g}/\text{sq cm}$  frequently cannot be detected with the unaided eye. Table 1 gives a partial indication of the reproducibility of this plating technique for  $\alpha$  counting.

A slight variation in the technique has been used to prepare films containing as much as  $10 \mu\text{g}/\text{sq cm}$  of plutonium on both quartz and

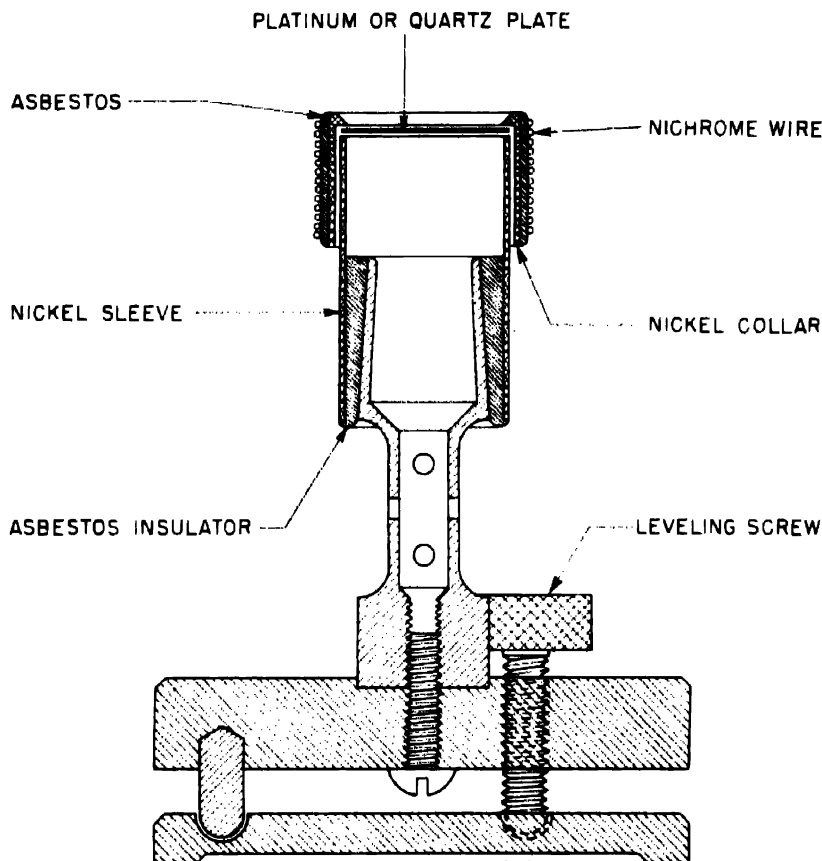


Fig. 2—A convenient device for the controlled spreading and drying of radiometric assay plates.

platinum. The sulfuric acid solution was evaporated to dryness; a drop of 2M  $\text{HNO}_3$  and a drop of redistilled tetraethylene glycol (TEG) were then added to the cool plate, which was reheated with the unit described. No zapon film is required to prevent the solution from spreading over the edge with the use of this heating unit.

Although a slow rate of vaporization and polymerization is desirable in the initial stages of the TEG process,<sup>2</sup> the flexibility of the

heating unit is such that considerably less time is required during the final stages of polymerization and removal of the polymer than is required in the usual method.

With this procedure quite uniform films have been obtained on quartz, pyrex, and platinum. The films have proved satisfactory for  $\alpha$  counting, and they gave counts identical within statistical error to those prepared by direct plating from sulfuric acid solution.<sup>4</sup>

There is some indication that such plates may be suitable for even the more stringent requirements of thermal neutron-induced fission studies.<sup>1</sup>

## 5. SUMMARY

An exclusively gravimetric procedure of high precision for aliquoting and plating samples in the determination of amounts and concentrations of radioactive isotopes has been devised and tested. A convenient heating device for preparing uniformly thin films with microgram amounts of solid is described. This is especially practicable for the controlled evaporation of solutions such as aqueous sulfuric acid and tetraethylene glycol, which tend to spread over the edge of the counting plate.

## REFERENCES

1. A. H. Jaffey, Metallurgical Project Report CC-3771 (Feb. 7, 1947); also in National Nuclear Energy Series, Division IV, Volume 14 A.
2. D. L. Hufford and B. F. Scott, Techniques for the preparation of thin films of radioactive material, Paper 16.1, this volume (Metallurgical Project Report CN-3328).
3. B. F. Scott and B. B. Cunningham, Metallurgical Laboratory Memorandum MUC-GTS-557 (Mar. 27, 1944).
4. E. F. Westrum, Jr., J. C. Hindman, and R. W. Greenlee, The specific alpha radioactivity and half life of plutonium isotope of mass 239, Paper 22.80, this volume.

## Paper 16.3

### BACK-SCATTERING OF Pu<sup>239</sup> ALPHA PARTICLES FROM PLATINUM†

By B. B. Cunningham, A. Ghiorso, and J. C. Hindman

#### 1. INTRODUCTION

At the time when weighable amounts of a pure Pu<sup>239</sup> compound were first isolated,<sup>1</sup> a preliminary estimate of the specific activity and half life was made on the basis of the  $\alpha$ -counting rate of known aliquot portions of a weighed sample. The samples were prepared on platinum plates and placed on an electrode on the inside of an ionization chamber designed to count approximately 50 per cent of the  $\alpha$  particles emitted by the sample. It was found that the counting rate was  $7.5 \times 10^4$   $\alpha$  counts per minute per microgram of plutonium on the assumption that the compound weighed was pure PuO<sub>2</sub>. Some time previously the counting yield of the counters used in this experiment had been evaluated as 45 per cent by the use of a uranium standard. This value for the counting yield was used to calculate the specific disintegration rate of Pu<sup>239</sup> from the observed counting rate. From the specific disintegration rate so obtained the half life was calculated to be 20,000 years.

Later, three additional determinations of the specific disintegration rate were reported.<sup>2</sup> These determinations indicated a counting rate of  $7.3 \times 10^4$ ,  $7.4 \times 10^4$ , and  $7.2 \times 10^4$   $\alpha$  counts per minute per microgram. In the meantime, improvement in counter design had led to a reevaluation of counting yield and a revision to 47 per cent. On this basis the half life was reported to be 21,300 years.

In addition, recent experiments, which are reported in detail in a subsequent report, indicate a counting rate in the 50 per cent geom-

†Contribution from the Chemistry Division of the Metallurgical Laboratory, University of Chicago, now the Argonne National Laboratory.

Based on Metallurgical Project Report CK-888 (Aug. 7, 1943).

etry counters of  $7.1 \times 10^4$   $\alpha$  counts per minute per microgram for thin samples mounted on smooth platinum. However, there is reason to believe that the counting yield is considerably higher than previously estimated, and the half life correspondingly longer. The experimental method used to evaluate the counting yield of the standard 50 per cent high-geometry counters is described below.

## 2. DETERMINATION OF COUNTS PER DISINTEGRATION FOR THE 50 PER CENT HIGH-GEOMETRY COUNTERS

The reevaluation of the counts-to-disintegration ratio in the 50 per cent geometry counters used in determinations of the specific activity of plutonium has been made by calibration against a low-geometry counter of accurately calculable counting geometry. Plutonium samples were counted on the low-geometry counter, dissolved, and counted by the use of accurately measured aliquots on the high-geometry counter. (In the high-geometry, or 50 per cent geometry, counters the sample plate is placed on an electrode, which is placed inside the counting chamber directly below the collecting electrode.)

2.1 Construction and Calibration of Low-geometry Chamber.<sup>3</sup> An accurately known geometry standard was obtained by the method of reducing the solid angle defined between the sample and the aperture of the counting chamber. The sample is mounted in a vacuum at a known distance from a single accurately defined aperture. A thin mica window (about 1.5 mg/sq cm) covered with a film of aquadag separates the evacuated section from the ionization chamber, which is at atmospheric pressure. Alpha particles emitted from the sample in the direction of the aperture travel through the evacuated space, through the window, and then into the ionization chamber; here they produce ions, which are collected and counted in the conventional manner. Negligible absorption of the  $\alpha$  particles by the window and aquadag is indicated by the fact that all the  $\alpha$  "kicks" observed are within 20 per cent of the same height.

The aperture was accurately measured with a short range cathetometer and found to be 1.016 cm in diameter. The distance between sample and aperture was 12.30 cm. If the sample is assumed to be a point source, the solid angle within which  $\alpha$  particles from the sample enter the chamber is easily calculated as being equal to the area of the aperture divided by the area of a sphere of radius equal to the distance of the sample from the aperture.

$$G = \frac{\pi d^2}{4} \times \frac{1}{4\pi r^2} = \frac{1}{16} \frac{d^2}{r^2}$$

Table 1—Evaluation of Counting Yield of 50 Per Cent Geometry Chambers

Sample	Counting rate in $4.26 \times 10^{-4}$ geometry counter	Dis./min not dissolved pre- paratory to aliquotting	Dis./min in sample actually aliquoted	Dis./min in 25-microliter aliquots of sample	Counts/min for aliquots in 50% chambers <sup>t</sup>	Counting yield of 50% chambers
1	98.4 ± 0.5	230,700	600	230,000	575.3	(a) 295.0 ± 3.7 (b) 298.2 ± 3.7 (c) 285.9 ± 2.5
					Av. = 295.7	C.C.I. = 0.7
					Net = 296.4	
2	83.6 ± 0.4	196,200	700	195,599	488.8	(a) 255.5 ± 1.1 (b) 255.7 ± 1.4 (c) 255.2 ± 1.5
					Av. = 255.5	C.C.I. = 0.5
					Net = 256.0	
3	142.7 ± 1.1	334,600	2,800	331,800	829.5	(a) 431.6 ± 1.8 (b) 430.8 ± 2.9 (c) 432.4 ± 3.4
					Av. = 431.9	C.C.I. = 1.5
					Net = 433.4	
4	359.4 ± 1.1	2,046,000	0	2,056,000	2,056	(a) 1,058.7 ± 5.4 (b) 1,062.3 ± 4.9 (c) 1,062.3 ± 4.9
					C.C.I. = 9	C.C.I. = 9
					Net = 1,066	Net = 1,066
					Av. = 1,062.3 ± 4.9	52.1 %
					C.C.I. = 9	51.9 %
					Net = 1,071	
					C.C.I. = 3	51.9 %
					Net = 641	

<sup>t</sup>Corrected for background.  
IC.C. = Coincidence correction (0.8 % per 1,000 counts per minute).

115-microliter aliquot.

Note: The indicated deviations in counts per minute are calculated by the formula  $kN/t = "reliable error"$ , where  $N$  = total number of counts recorded,  $t$  = time in minutes, and  $k = 1.645$ . That is, the chances are 9 out of 10 that if the count in question were repeated, the result would not differ from that given by more than the indicated deviation.

where  $d$  is the diameter of the aperture,  $r$  is the distance between aperture and sample, and  $G$  is the counting yield.

For a point source and the above conditions,  $G = 4.264 \times 10^{-4}$ . Correcting for the fact that the sample was not concentrated at a point but actually occupied a circular area about 5 mm in diameter,  $G$  was calculated to be  $4.26 \times 10^{-4}$ .

**2.2 Comparison of Counting Rates of the Low-geometry and 50 Per Cent High-geometry Counters.** Four Pu<sup>239</sup> samples, (three of approximately 2  $\mu\text{g}$  each and one of 15  $\mu\text{g}$ ) were prepared and spread on platinum over a circular area of approximately 5 mm diameter. Each was counted in the vacuum low-geometry counter. Each sample was then dissolved and made up to 10 ml of solution. Twenty-five-micro-liter aliquots of these solutions were placed on new flat platinum disks, evaporated to dryness, and then ignited, and careful counts were made in the 50 per cent geometry chambers. The calibrations of the volumetric equipment used in this work were checked, and the original plates were examined for undissolved  $\alpha$  activity after the dissolving operation. Corrections were made for the activities left on the plates and in the dissolving dishes. In evaluating the counting yield of the 50 per cent geometry counters by comparison with the vacuum low-geometry counter, it was assumed that back-scattering of  $\alpha$  radiation in the solid angle subtended by the aperture of the low-geometry counter is negligible. These data are given in Table 1.

**2.3 Back-scattering of Alpha Particles.** The results of these experiments indicated that the counting yield of essentially weightless samples of Pu<sup>239</sup>, mounted on platinum, when counted in the 50 per cent geometry counters was actually 52.0 per cent. This result was surprising, since it had always been assumed that the maximum counting yield that could be obtained was 50 per cent. A preliminary calculation by John Crawford<sup>4</sup> indicated that back-scattering of  $\alpha$  particles at small angles could exist to an appreciable extent. To test this possibility some preliminary experiments were made by counting identical weights of U<sub>3</sub>O<sub>8</sub> on platinum and on quartz, on the supposition that back-scattering would decrease with atomic number. A 2.4 per cent (1.2 parts in 50) lower count was observed for two samples on quartz, compared to the identical samples mounted on platinum. Since it was thought that there might still be scattering from the uranium on quartz, the same experiment was repeated using essentially weightless Pu<sup>239</sup> samples. In one experiment two pairs of samples showed a 3.1 per cent (1.55 parts in 50) difference, and in a later experiment three pairs of samples showed a 2.9 per cent (1.45 parts in 50) difference. It seems, therefore, quite possible, though it was not proved, that enough small-angle scattering may occur when

thin  $\alpha$ -active samples are mounted on platinum to increase the counting yield in a 50 per cent geometry counter by as much as 4 per cent (2 parts in 50).

### 3. SPECIFIC ACTIVITY AND HALF LIFE

Using the counting yield (52 per cent) indicated by comparison with the low-absolute-geometry counter, the most recent measurements of the specific counting rate of Pu<sup>239</sup> ( $7.1 \times 10^4$  counts per minute per microgram) indicate a specific disintegration rate of 137,000 disintegrations per minute per microgram and a half life of 24,000 years. At the time of this writing a reliability for this figure of greater than  $\pm 5$  per cent could not be claimed.

### 4. SUMMARY

The apparent specific activity of Pu<sup>239</sup> spread as a thin layer on platinum has been found to be 4 per cent higher in a 50 per cent geometry counter than in a 0.04 per cent geometry counter. The difference is attributed to low-angle back-scattering of  $\alpha$  particles by platinum. Qualitative support for this hypothesis is furnished by the observation that identical weights of Pu<sup>239</sup> show a 3 per cent lower counting rate when mounted on quartz in a 50 per cent geometry counter than similar samples mounted on platinum.

### REFERENCES

1. B. B. Cunningham, M. Cefola, and L. B. Werner, Metallurgical Project Report CN-261 (Sept. 15, 1942), p. 6.
2. B. B. Cunningham and L. B. Werner, Metallurgical Project Report CN-419 (January 1943), p. 15.
3. A. H. Jaffey, Metallurgical Project Report CC-3771 (Feb. 7, 1947), Sec. 5.5; also in National Nuclear Energy Series, Division IV, Volume 14 A.
4. J. A. Crawford, Theoretical calculations concerning back-scattering of alpha particles, Paper 16.55, this volume (Metallurgical Project Report CC-1342).

## Paper 16.4

### NOTE ON BACK-SCATTERING OF Pu<sup>239</sup> ALPHA PARTICLES FROM PLATINUM SAMPLE PLATES†

By J. H. Parsons, O. Flatau, J. K. East, R. Dandl, and C. J. Borkowski

An attempt has been made to evaluate the back-scattering of plutonium  $\alpha$  particles (3.7 cm range in air) from platinum sample plates (see Paper 16.3 of this volume) by first counting the sample in a vacuum low-geometry chamber of calculated geometry, and then counting the same sample in the Simpson proportional counter and correcting for coincidence in both cases. No self-absorption corrections were made inasmuch as the samples were evaporated from tetraethylene glycol and were extremely thin.

The counting yield of the Simpson proportional counter was found to be the same as the standard chambers so that it was assumed that the back-scattering factor obtained for the Simpson proportional counter would also apply to the standard chamber.

The following table gives the data up to the present time:

Sample	Counting rate in vacuum chamber 1 (factor 3654)	Counting rate in vacuum chamber 2 (factor 3872)	Disintegrations per minute in sample	Counts per minute in Simpson proportional counter	Counting yield in Simpson proportional counter, %
1	75.3 $\pm$ 0.4(NTE) <sup>a</sup>		275,200	142,900	51.9
2		73.4 $\pm$ 0.4	277,600	143,000	51.5
3	74.9 $\pm$ 0.4		273,500	142,700	52.1

<sup>a</sup>Nine-tenths error (due to statistics of counting). See National Nuclear Energy Series, Division IV, Volume 8 A.

†Contribution from the Clinton Laboratories, now the Oak Ridge National Laboratory.  
Based on Clinton Laboratories Report CL-P-337 (Oct. 11, 1944).

## Paper 16.6

### APPARENT SPECIFIC ACTIVITY OF URANIUM IN A 2 $\pi$ -GEOMETRY CHAMBER†

By B. B. Cunningham, A. Ghiorso, and A. H. Jaffey

#### 1. INTRODUCTION

Some time ago the specific activity of Pu<sup>239</sup> was reported<sup>1</sup> as 155,000 disintegrations per minute per microgram with a probable error of  $\pm 5$  per cent. The largest single source of error was considered to be in the estimation of counter geometry, which in most of the specific-activity determinations had been taken as 47 or 48 per cent. Recently work has been undertaken to secure a more accurate value for the specific activity and half life of Pu<sup>239</sup>. In this connection the question of counter geometry has received first attention. It was proposed to determine the counter geometry by the simple expedient of determining the counting rate of a known weight of  $\alpha$  emitter of known specific activity. This appeared entirely feasible in view of the very precise values for the specific activity of uranium reported by Kovarik and Adams.<sup>2</sup>

Our efforts to determine counter geometry by this technique have failed in the sense that we have not been able to obtain reasonable figures for counter geometry using uranium and the specific-activity value reported by Kovarik and Adams. The results found by us have, however, been entirely consistent, and we believe that they are of interest as a measurement of the apparent specific  $\alpha$  activity of thinly spread uranium in a 2 $\pi$ -geometry ionization chamber. A detailed description of our technique and results follows.

†Contribution from the Chemistry Division of the Metallurgical Laboratory, University of Chicago, now the Argonne National Laboratory.

Based on Metallurgical Project Report CK-888 (Aug. 7, 1943), p. 8.

## 2. PREPARATION OF STANDARD URANIUM SOURCES

In the work reported here we have used three sources of uranium. The first source was Mallinckrodt  $\text{UO}_2(\text{NO}_3)_2 \cdot 6\text{H}_2\text{O}$ . This material was purified by the manufacturers by ether extraction and was shown by spectrographic analysis to be of excellent purity. The principal impurities were silicon and iron, at levels of 200 and 100 ppm, respectively. All other impurities were at levels below these figures.

The second source was an unopened quarter-pound bottle of Baker and Adamson  $\text{UO}_2(\text{NO}_3)_2 \cdot 6\text{H}_2\text{O}$  (lot 32). The principal impurities listed were alkalies and alkaline-earth sulfates, 0.1 per cent. Other impurities determined totaled 0.013 per cent.

The third source was uranium metal prepared by Westinghouse. No data are available on the purity of this particular sample, but judging from the analysis of other samples of Westinghouse metal, it seems highly unlikely that the impurities could have exceeded 0.5 per cent.

**2.1 Preparation of a Standard Solution of Mallinckrodt Uranyl Nitrate Hexahydrate.** Approximately 40 g of the nitrate was weighed out and dissolved in a liter of water. Clean, but not new, glassware was used in these operations. The solution was thoroughly mixed, its temperature noted, and 5 ml of the solution was pipetted into a clean, weighed platinum evaporating dish. The solution was evaporated to dryness under an infrared lamp, and the residue was ignited to  $\text{U}_3\text{O}_8$  at 800°C. From the weight of the  $\text{U}_3\text{O}_8$  found, the concentration of uranium in the solution was calculated to be 20.09 mg of uranium per milliliter at 29°C.

**2.2 Preparation of a Standard Solution of Baker and Adamson Uranyl Nitrate Hexahydrate.** Approximately 40 g of Baker and Adamson  $\text{UO}_2(\text{NO}_3)_2 \cdot 6\text{H}_2\text{O}$  was taken from a previously unopened quarter-pound bottle of the salt. This was dissolved in about 1 liter of distilled water taken directly from the still tap. In preparing this solution, all apparatus used was taken directly from the original packing of the manufacturer. The solution was thoroughly mixed and then assayed for uranium content as described in Sec. 2.1.

The concentration measured at 33°C was  $19.80 \pm 0.2$  mg of uranium per milliliter.

**2.3 Preparation of a Standard Solution of Uranium from Uranium Metal.** A sample of uranium metal, which had been prepared by Westinghouse, was obtained from Dr. H. S. Brown. After the oxide coating had been removed by treatment with 10N  $\text{HNO}_3$ , the metal was washed in alcohol and dried and weighed as quickly as possible. Some

oxide had re-formed at the time of weighing, as evidenced by the golden appearance of the metal. The weighed metal was dissolved in concentrated nitric acid and diluted to volume in a calibrated volumetric flask. The temperature of the solution was noted. The concentration at 32°C was 26.15 mg of uranium per milliliter.

### 3. PREPARATION OF SAMPLE PLATES

Twenty-five millimeter diameter platinum disks were punched out of a new, bright platinum sheet. The disks were ignited at red heat over a bunsen flame, allowed to cool and a 2-mm-wide ring of zapon was painted around the periphery of each disk. The prepared plates were examined for  $\alpha$  activity. In no case was the  $\alpha$  activity of the plates found to be greater than 0.25 count per minute.

### 4. MEASUREMENT OF SAMPLES FOR ALPHA COUNTING

The samples of the standard uranium solution which were transferred to the counting plates were measured in capillary pipets holding from 5 to 10 microliters. The pipets were calibrated for content by weighing mercury delivered from them. Following the measurement of the standard uranium solution, the pipets were rinsed twice with distilled water. The measurement of liquid volumes of this order of magnitude has been shown to involve an error of not more than a few tenths of 1 per cent.<sup>3</sup>

In measuring the uranium onto the counting plate the practice was to note the temperature of the solution, to fill the capillary pipet and deliver its contents onto the plate, and then to rinse the pipet twice with distilled water by filling the pipet to the mark and delivering its contents onto the plate separately from the initial delivery. Finally, 2 drops of tetraethylene glycol were added to the plate in such a way as to bring about coalescence of all droplets.

The plate was then placed under a heating lamp, and the water and tetraethylene glycol slowly evaporated. During this process the uranium slowly precipitated as a finely divided solid that settled uniformly over the surface of the disk. In some cases, where evaporation was caused to take place at too high a temperature, the uranium separated as fairly large crystals. When this occurred the sample was discarded. The process of evaporation was continued until the uranium appeared to be dry. The plate was then ignited to redness for a few seconds to remove the zapon and any high-boiling residues from the tetraethylene glycol. The weight of uranium present on each plate was calculated from the standardization of the uranium solution,

the temperature of measurement, and the volume of the capillary pipet. The weights of uranium present on each counting plate are given in Table 1.

Table 1.—Weights of Uranium on Standard Counting Plates

Plate No.	Uranium source	Original uranium concentration, mg/ml	Temp. of sample, °C	Uranium concentration of sample, mg/ml	Vol. of sample, ml × 10 <sup>3</sup>	Wt. of uranium, mg
2	UO <sub>2</sub> (NO <sub>3</sub> ) <sub>2</sub> ·6H <sub>2</sub> O§	20.09 at 29°C	31	20.08	10.21	0.2050
3	UO <sub>2</sub> (NO <sub>3</sub> ) <sub>2</sub> ·6H <sub>2</sub> O§	20.09 at 29°C	31	20.08	10.21	0.2050
6	UO <sub>2</sub> (NO <sub>3</sub> ) <sub>2</sub> ·6H <sub>2</sub> O§	20.09 at 29°C	29	20.09	10.10	0.2029
7	UO <sub>2</sub> (NO <sub>3</sub> ) <sub>2</sub> ·6H <sub>2</sub> O§	20.09 at 29°C	30	20.09	10.10	0.2029
8†					10.10	None
9	UO <sub>2</sub> (NO <sub>3</sub> ) <sub>2</sub> ·6H <sub>2</sub> O†	19.80 at 33°C	32.5	19.80	10.10	0.2000
10	UO <sub>2</sub> (NO <sub>3</sub> ) <sub>2</sub> ·6H <sub>2</sub> O†	19.80 at 33°C	32	19.80	10.10	0.2000
11	UO <sub>2</sub> (NO <sub>3</sub> ) <sub>2</sub> ·6H <sub>2</sub> O†	19.80 at 33°C	29	19.82	10.10	0.2002
12	UO <sub>2</sub> (NO <sub>3</sub> ) <sub>2</sub> ·6H <sub>2</sub> O†	19.80 at 33°C	30	19.82	10.10	0.2002
13	Westinghouse metal	26.15 at 32°C	31	26.16	10.10	0.2642
14	Westinghouse metal	26.15 at 32°C	32	26.15	10.10	0.2641
15	Westinghouse metal	26.15 at 32°C	33	26.14	10.10	0.2640
18†					10.10	None
20‡	Westinghouse metal		26.5	26.19	5.08	0.1328

†Blank plates made by substituting distilled water for the uranium solution. All other operations were carried out in exactly the same way as when uranium was present.

‡Sample 20 was mounted on a highly polished gold plate.

§Mallinckrodt.

†Baker and Adamson.

## 5. COUNTING OF URANIUM SAMPLES

The counting of the  $\alpha$  particles from the uranium samples was performed with four different  $\alpha$  counters in regular use in this laboratory. The construction of the ion chambers of these counters is such that it should be possible to obtain a geometry very close to 50 per cent. The two electrodes of the chamber are 5 cm in diameter and are separated by an air gap of 1 cm. The electrical characteristics of the amplifier are such that the signal/noise ratio is more than 6/1 for the smallest pulse height observed on the monitoring oscilloscope.

The samples were counted over a period of 12 days. Most of the counts were of 40 min duration. Checking of each count was done by taking readings every 8 min to be sure that no great number of spurious counts were recorded. A further check on the spurious count level was obtained by taking a liberal number of background counts on each counter throughout the period. The backgrounds varied from

0.7 count per minute to 1.7 counts per minute (the  $\alpha$ -contamination level of the four counters), so it can be seen that any spurious counts had a negligible effect on the data taken.

Table 2—Results of Counting of Uranium Samples

Sample No.	Counter 164-1		Counter 161-2		Counter 163-3		Counter 166-4		Total no. counts	Sample av., c/m	Group av., c/m	Group U wt., mg	Specific activity for 50% geometry
	C/m	Min	C/m	Min	C/m	Min	C/m	Min					
2†			158.3 159.0	40 40	159.9 159.6	40 40	159.1 161.7	20 40	18,160	159.7	159.0	0.2050	1,551
3†			158.7 155.2	40 40	159.7 159.5	40 40	158.2 159.5	40 40	31,860	158.3	157.2	0.2029	1,550
6†			155.8 159.0	40 40	156.3 155.3	40 40	158.0 155.3	56 40	33,870	156.8	155.3	0.2001	1,552
7†	159.2 157.9	40 40	157.2 154.6	40 40	155.5 154.6	40 40	158.2 159.8	40 40	44,100	157.5	155.3	0.2641	1,536
9†			162.1 155.0	48 40	155.0 152.2	40 40	153.0 155.8	16 40	40,600	153.8	155.3	0.2641	1,536
10†	158.8 157.5	40 40	154.0 157.5	40 40	155.9 153.6	40 40	156.0 153.6	24 40	34,940	156.0	155.3	0.2001	1,552
11†	154.8 158.8	40 40	154.5 155.8	40 40	156.2 155.8	40 40	157.6 153.6	40 40	43,950	155.8	155.3	0.2641	1,536
12†	156.0 154.3	40 40	156.1 154.5	40 40	156.8 152.4	96 40	155.3 152.4	40 40	52,210	155.4	155.3	0.2641	1,536
13§	203.8 199.5	40 40	201.9 203.3	40 40	203.6 203.5	40 40	202.5 203.5	40 40	56,730	202.6	155.3	0.2641	1,536
14§	200.5 202.3	40 40	203.3 205.8	40 40	204.4 201.4	40 40	202.8 204.7	40 40	56,810	202.9	155.3	0.2641	1,536
15§			205.8 199.4	40 40	199.2 201.4	40 40	204.8 204.7	40 40	56,810	202.9	155.3	0.2641	1,536
20†			102.5 102.7 102.6	80 48 60	103.1 140		102.4 103.1	80 80	52,220	102.8	102.8	0.1328	1,548

† Mallinckrodt  $\text{UO}_2(\text{NO}_3)_2 \cdot 6\text{H}_2\text{O}$ .‡ Baker and Adamson  $\text{UO}_2(\text{NO}_3)_2 \cdot 6\text{H}_2\text{O}$ .

§ Westinghouse metal.

¶ Gold plate.

The total number of  $\alpha$  particles recorded from each sample varied from 19,000 to 57,000. The results from the four counters indicate that the geometries of each are the same. Therefore, the value of the  $\alpha$ -disintegration rate for each sample can be obtained by averaging the results from all the counters and weighting them only according to the length of count. Blanks (samples 8 and 18) were also counted. There was no evidence of contamination in these samples.

The results of the 56 hr of counting are compiled in Table 2.

### 6. ABSORPTION ERRORS

A rough calculation was made of the loss of  $\alpha$  counts due to self-absorption in the sample. Since the samples were quite thin, losses occurred only at such small angles that the particles had to traverse more than approximately 10 milligrams per square centimeter of  $U_3O_8$ . The assumptions made were that (1) any  $\alpha$  particle emerging from the sample with a residual range of not less than 2 mm of air is counted, all others being considered completely absorbed; (2) the range straggling of  $\alpha$  particles is negligible, i.e., all  $\alpha$  particles have the mean range; and (3) that the Bragg and Kleeman law for variation of stopping power with atomic weight held, so that in  $U_3O_8$   $\alpha$  particles from  $U^{238}$  were effectively absorbed in 8.6 mg per square centimeter while  $U^{234}$   $\alpha$  particles required 10.6 mg per square centimeter. Errors due to deviations from these assumptions are less than the accuracy desired in this calculation.

Calculation shows that  $F$ , the fraction of  $\alpha$  particles lost due to self-absorption, is

$$F = \frac{1}{2} \frac{M}{AS}$$

where  $M$  is the mass of sample in milligrams,  $A$  is the area of sample in square centimeters, and  $S$  is the range of the  $\alpha$  particles in the sample, measured in milligrams per square centimeter.

From this formula it is evident that the self-absorption for even the heaviest samples used is less than 0.5 per cent.

### 7. SUMMARY AND CONCLUSIONS

Using material from three different sources we have consistently obtained values for the specific activity of uranium which are 2 to 3 per cent higher than the value reported by Kovarik and Adams. In calculating specific-activity values we have assumed the counter geometry to be 50 per cent. Calculation of the absorption error, and a consideration of counter characteristics would indicate, however, that none of the values obtained by us should be lower than the true value by more than about 1 per cent.

Excellent agreement ( $\pm 0.1$  per cent) was obtained in the case of uranyl nitrate from two different sources. Uranium from uranium metal gave a somewhat (1 per cent) lower value at 30 per cent greater sample thickness. When the thickness of sample from this source was reduced one-half, a good agreement ( $\pm 0.2$  per cent) was obtained for all sources.

The average value for all sources and all samples counted was found to be  $1,548 \pm 12$   $\alpha$  particles per minute per milligram ( $U^{238} + U^{234} + U^{235}$ ). This figure is to be compared with that of 1,501 found by Kovarik and Adams, and that of 1,517 found by R. Schiedt.<sup>4</sup>

Three explanations of the discrepancy between our values and those of Kovarik and Adams can be made:

1. The values found by Kovarik and Adams are in error.
2. Our sources were uniformly contaminated with an  $\alpha$  emitter of high specific activity.
3. More than 50 per cent of the uranium  $\alpha$  particles emitted by our samples were counted in the apparatus used by us.

Since the work reported here, further work in this laboratory<sup>5</sup> has shown that the counting efficiency in a  $2\pi$  ionization chamber is greater than 50 per cent. This effect is due to the back-scattering of  $\alpha$  particles from the plate upon which the sample is mounted as well as from the sample material itself.

Theoretical analysis by Crawford<sup>6</sup> shows that the back-scattered  $\alpha$  particles are emitted at small angles relative to the surface of the plate. Thus, it would be expected that Kovarik and Adams, who counted only vertically emitted  $\alpha$  particles, measured none of the back-scattered radiation. Schiedt, on the other hand, used a larger solid angle, and hence would have counted some of the back-scattered  $\alpha$  particles.

Assuming the Kovarik and Adams value of 1,501 disintegrations per minute per milligram of uranium to be correct, the average effective back-scattering observed here was 3.1 per cent ( $1,548/1,501 = 1.031$ ); i.e., the geometry was 51.6 per cent. This value is calculated on the assumption that self-absorption was negligible, which was, of course, not the case. Not only were some of the upward-emitted  $\alpha$  particles absorbed, but also a large fraction of the back-scattered ones, since back-scattered  $\alpha$  particles are degraded in energy and hence more subject to absorption. Thus, with thinner samples, the effective back-scattering should be larger. And, indeed, this was found to be the case by Scott,<sup>7</sup> who found that the apparent specific activity of uranium mounted on platinum increased markedly as the sample thickness was decreased to about 10  $\mu\text{g}$  per square centimeter.

In some recent work by Kienberger,<sup>8</sup> the specific activity of uranium measured on nickel plates and extrapolated to zero sample thickness was found to be 1,521 disintegrations per minute per milligram of uranium assuming 50 per cent geometry. Using a value of 1.26 per cent back-scattering derived from Crawford's<sup>6</sup> work (i.e., 50.63 per cent geometry), he found a value of 1,502 disintegrations per minute per milligram of uranium, which checks with the result

of Kovarik and Adams. The lower back-scattering value is due to the lower atomic number of the sample mount.

Because of the difficulty of correcting for the absorption of back-scattered  $\alpha$  particles in the sample material, it is difficult to make a precise quantitative estimate of the consistency of our data with the other values. However, it is quite evident that there is good qualitative agreement, since the discrepancy is in the right direction and of approximately the correct magnitude.

#### REFERENCES

1. B. B. Cunningham and L. B. Werner, Metallurgical Project Report CN-419 (January 1943), p. 15.
2. A. F. Kovarik and N. I. Adams, Phys. Rev., 40: 718 (1932); Kovarik and Adams, Conference on nuclear physics, Oct. 28, 1940, as reported by L. Curtiss, L. Stockman, and B. Brown in Report A-80. The latest value for the specific activity is 1,501 disintegrations per minute per milligram of uranium; Curtiss, Stockman, and Brown report the same figure.
3. R. Lindner and P. L. Kirk, Mikrochemie, 22: 291 (1937).
4. R. Schiedt, Sitzber. Akad. Wiss. Wien, Abt. II a, 144: 191 (1935).
5. B. B. Cunningham, A. Ghiorso, and J. C. Hindman, Metallurgical Project Report CN-1241 (Jan. 5, 1944); Paper 16.3, this volume (Metallurgical Project Report CK-3861); J. H. Parsons, O. Flatau, J. K. East, R. Dandi, and C. J. Borkowski, Clinton Laboratories Report CL-P-337 (Oct. 11, 1944); Paper 16.4, this volume.
6. J. A. Crawford, Theoretical calculations concerning back-scattering of alpha particles, Paper 16.55, this volume (Metallurgical Project Report CC-1342).
7. B. F. Scott, Metallurgical Project Report CN-1764 (July 1, 1944).
8. C. A. Kienberger, Report K-329 (Jan. 5, 1949).

## Paper 16.7

### AN EMANATION METHOD FOR RADIUM ANALYSIS†

By P. Fineman, B. B. Weissbourd, H. H. Anderson, J. Sedlet,  
D. P. Ames, and T. P. Kohman

#### 1. INTRODUCTION

For many years one of the principal methods for the assay of radium has been the emanation technique, in which the radon generated by the radium is separated, collected, and measured. There are numerous variations of this general method, differing in the ways of collecting and measuring the emanation. This technique is especially useful for small quantities of radium because of its high sensitivity, and for low concentrations because the final measurement is independent of the original bulk of the material containing the radium. The greatest sensitivity in the detection of radon is achieved by counting its  $\alpha$  particles, including those of its short-lived descendants. The use of a proportional counter for this purpose has been described by Brown, Elliott, and Evans,<sup>1</sup> and the use of an ionization chamber and pulse amplifier by Poole<sup>2</sup> and by Curtiss and Davis.<sup>3</sup>

This paper describes an emanation method for the analysis of radium which was developed for use in the uranium ore-processing plant. The apparatus and technique are essentially those of Curtiss and Davis, with modifications to achieve simplicity of construction, utilization of existing standard equipment, and ease of operation.

#### 2. EMANATION APPARATUS AND TECHNIQUE

We have been interested principally in radium samples in solution. Accordingly, we have used a simple emanation apparatus (Fig. 1)

†Contribution from the Chemistry Division of the Metallurgical Laboratory, University of Chicago, now the Argonne National Laboratory.

Based on Metallurgical Laboratory Memorandum MUC-GTS-2320 (May 3, 1946).

consisting of a 250-ml boiling flask, A; water-cooled reflux condenser, B; cold trap, C; mercury manometer, D; spray filter, E; and connections at M, F, and K for vacuum pump, ionization chamber, and argon tank, respectively. An important feature for routine measurements is the interchangeability of boiling flasks and ionization chambers. The ionization chambers are not permanently attached either

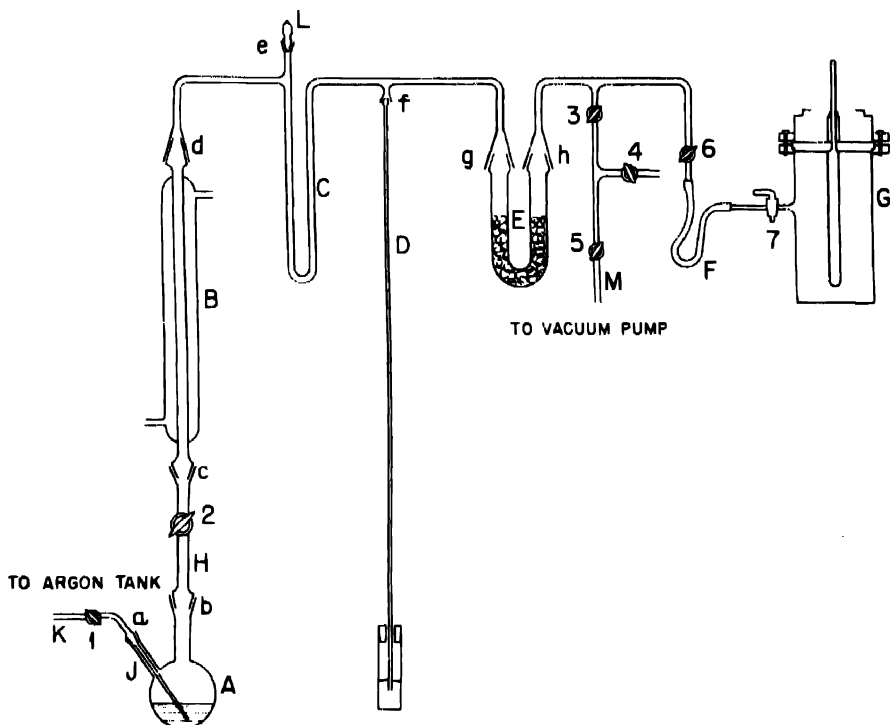


Fig. 1—Emanation apparatus.

to the emanation line or to the electrical circuit but can be connected to either at will. This provides an economy of apparatus, for only one emanation line and one counting circuit are necessary, and neither need be held up by a single sample longer than the time of actual use. It also provides a flexibility of operation, which is convenient when samples cover a wide range of concentrations.

An emanation flask can be sealed when off the line by means of an interchangeable connecting section, H, containing a 6-mm-bore stopcock and standard-taper ground-glass joints fitting the flasks and the condensers. The flask, A, and the connecting sections, H, are held together by means of rubber bands fitting over the female portion of

the stopcock and ears projecting from a metal collar fastened to the flask. Each flask is provided with a side arm, J, into which fits a gas-inlet tube, K, also equipped with a stopcock. The manometer is made of 1-mm-bore capillary tubing to minimize loss of activity. The male joint at f is made by grinding the tube to fit into a standard-taper female joint. Apiezon N grease (Metropolitan-Vickers Electrical Co., Ltd.) is a satisfactory lubricant for stopcocks 3, 4, 5, 6, and 7 and joints d, e, f, g, and h. Cello-Grease (Fisher Scientific Co.) is a good lubricant when high temperatures are involved, as for stopcocks 1 and 2 and joints a, b, and c.

The emanation technique is as follows: The radium-containing sample, in 75 to 125 ml of solution, is placed in a flask and attached to the line. The cooling bath, a mixture of dry ice and *n*-butyl alcohol in a Dewar flask, is placed around the cold trap. The gas-inlet tube is attached to the argon tank with a rubber tube. The system is then opened to the vacuum pump via stopcocks 3 and 5 with stopcocks 1, 2, 4, and 6 closed. After the system has been evacuated, stopcocks 1 and 2 are opened simultaneously, and a slow stream of argon is allowed to enter through stopcock 1 until the mercury column is depressed to 20 to 30 cm. This regulation is achieved readily by integrating the manipulation of stopcocks 1 and 5. The solution is boiled gently for 20 min with a small gas burner. At the end of this time the flame is removed, stopcocks 3 and 5 are closed, and the time at which boiling is discontinued is noted. The argon is allowed to continue to flow until atmospheric pressure is reached. Stopcocks 1 and 2 are closed, and an ice bath is raised around flask A to effect rapid cooling of the solution to room temperature. The system is again brought to atmospheric pressure by opening stopcock 2 and allowing argon to flow through stopcock 1 until this condition is attained. The cooling and the pressure adjustment are accomplished in less than 5 min. Stopcocks 1 and 2 are closed, and the flask is removed from the line. This process flushes the solution and flask of air and radon. It is necessary to adjust the pressure to near atmospheric with the flask at room temperature, otherwise, the pressure differential may cause air to leak in or radon to leak out during the storage period. The flask is stored on a suitable rack until sufficient radon for measurement has accumulated, usually overnight or longer.

In order to measure the radon the aged flask is again attached to the line, and an ionization chamber, G, is attached to outlet F by a short rubber tube, as shown. The chamber and line down to stopcock 2 are pumped out, filled with argon through stopcock 4, and pumped out again. This flushing process is carried out several times. Stopcocks 3, 4, and 5 are closed when the system is left evacuated as

a result of the final flushing. Stopcock 2 is opened, and the emanation is driven off into the chamber with a slow stream of argon through stopcock 1, the flow rate being adjusted to bring the pressure to atmospheric in 20 min and the solution gently boiled with a small burner as before. The time at which boiling is discontinued is noted. The flask may now be stored for another radon-accumulation period. The chamber is removed for counting by the method described in a later section.

From time to time it is necessary to remove the water that has accumulated in the cold trap. This is done with a long, thin-stemmed pipet after removing the ground-glass stopper L.

After the chamber has been counted, it is evacuated and filled several times with argon and allowed to remain evacuated overnight so that the active deposit may decay completely. Before reusing the chamber, it is flushed several times with argon and its background measured. For this flushing process the line is not used; instead, only the chamber is evacuated and filled with argon directly from the tank.

Argon is used as the ionization-chamber gas because of its desirable characteristics for  $\alpha$ -particle counting. It is a free-electron gas, yielding sharp, fast pulses at low collecting potentials. Argon gives a relatively large number of ions per unit of energy expended. Its relatively high atomic weight results in short  $\alpha$  tracks, which reduce the probability of striking a wall before producing sufficient ionization to count. It is readily available in a sufficiently pure state, 99.6 per cent commercial tank argon being highly satisfactory. Sufficiently pure tank nitrogen would be almost as good for this purpose.

For health reasons, i.e., to prevent air contamination by radon, it is advisable to place the vacuum pump in a hood.

The line is checked periodically for contamination by using a flask containing pure water and following the procedure as described above for radium samples.

The spray filter, containing glass wool, was found to be necessary when samples containing extreme amounts of  $\alpha$  activity were tested for radium. For small amounts of radium it may be omitted from the line, but its use is desirable as a precautionary measure.

### 3. IONIZATION CHAMBERS

The ionization-chamber design developed after experimentation with several types is illustrated in Fig. 2; it represents a considerable simplification over that of Curtiss and Davis. By applying the high potential to the center electrode and grounding the outer cyl-

inder, the need for an additional shielding cylinder is eliminated. By supporting the collecting electrode in the middle of the large insulating plate (lucite) that forms the top of the chamber, it becomes unnecessary to use a guard ring, and consequently there is no dead space in the chamber. A further disadvantage of a guard ring is that

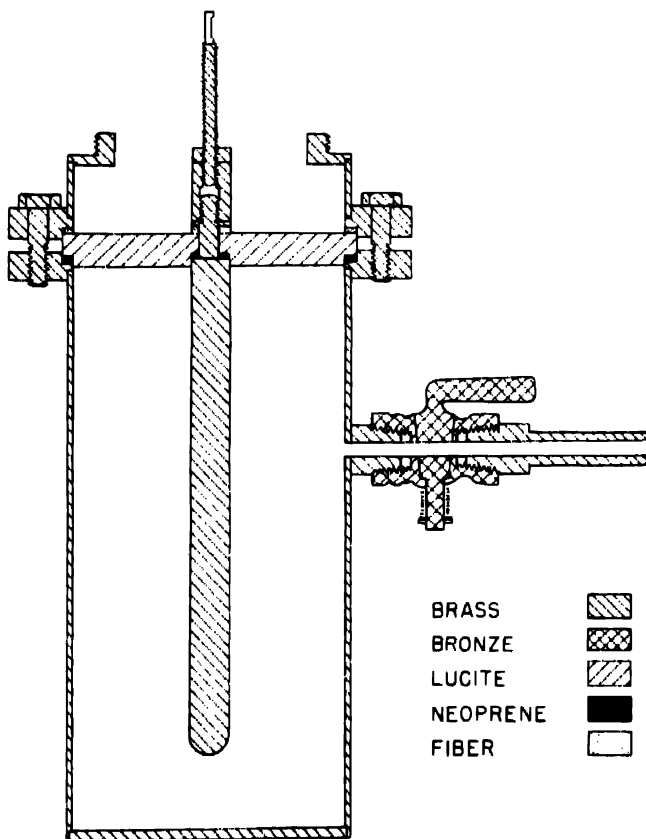


Fig. 2 — Ionization chamber.

it collects electrons produced in the top of the chamber and thus reduces the size of some of the pulses.

The chamber fits into the breech-locking receptacle of the Metallurgical Laboratory Instrument Section standard  $\alpha$  counter<sup>4</sup> by means of the breech thread on the cap. The banana plug on the end of the adjustable extension makes contact with the high-voltage and amplifier circuit as explained below. The valve is a commercial steam cock, No. 1037 bronze-spring key type with double female  $\frac{1}{4}$ -in. I.P.

ends and lever handle, obtained from the Lunkenheimer Co., in which the tightness is maintained by means of a spring. Aplezon N is a satisfactory stopcock lubricant. Neoprene gaskets are used for the gastight seals, and fiber washers are used to protect the outside of the lucite insulator from direct contact with metallic surfaces. Four bolts, evenly spaced around the top, hold the chamber together with sufficient pressure on the gaskets.

The body of the chamber is made of brass, silver-soldered together. Backgrounds, after careful cleaning, are 4 to 10 counts per minute. Painting the inside surface with several coats of silver paint, obtained from the Electrochemicals Dept. of E. I. du Pont de Nemours & Co., reduces the backgrounds to approximately 2 counts per minute. Reducing the background is important because the lower limit of detection of radon varies with the square of the background.

#### 4. CIRCUIT

The circuit used to count the radon  $\alpha$  disintegrations is shown in Fig. 3. It is composed of standard Metallurgical Project units modified for this application.

The chief modifications are in the amplifier, which is basically that used in the standard parallel-plate air chamber for counting flat  $\alpha$  samples.<sup>4</sup> The collecting plate has been replaced by a lucite disk, supporting in its center a banana-plug receptacle for the chamber contact. This contact is connected to the filtered high-voltage supply through a resistance of  $10^{11}$  ohms and to the input grid of the first amplifier tube by a  $50-\mu\text{uf}$  capacitor (Centralab ceramic capacitor No. 850, 5,000 d-c working volts). A ceramic condenser of high leakage resistance is used for this purpose because it must stand the high chamber voltage without introducing spurious pulses or other disturbances. The first three stages of the amplifier, consisting of resistance-capacitance coupled 6AK5 tubes, are mounted in the standard cylindrical casing, which is of the same diameter as the chambers, and which fits the chambers by the breech mechanism on the bottom. The chamber-amplifier assembly is supported from above by rubber tubes to protect it from vibrations. The frequency of maximum response has been raised from that used with air-filled counters by reducing the plate load resistors and coupling capacitances. The response has a maximum at about 25,000 cycles/sec and falls to one-half at about 50,000 cycles/sec.

The scale-of-64, power supply, and high-potential supply are contained in a standard Higinbotham Scaler unit.<sup>4</sup> Because of the wide pulse-size distribution from the emanation counter, a highly stable

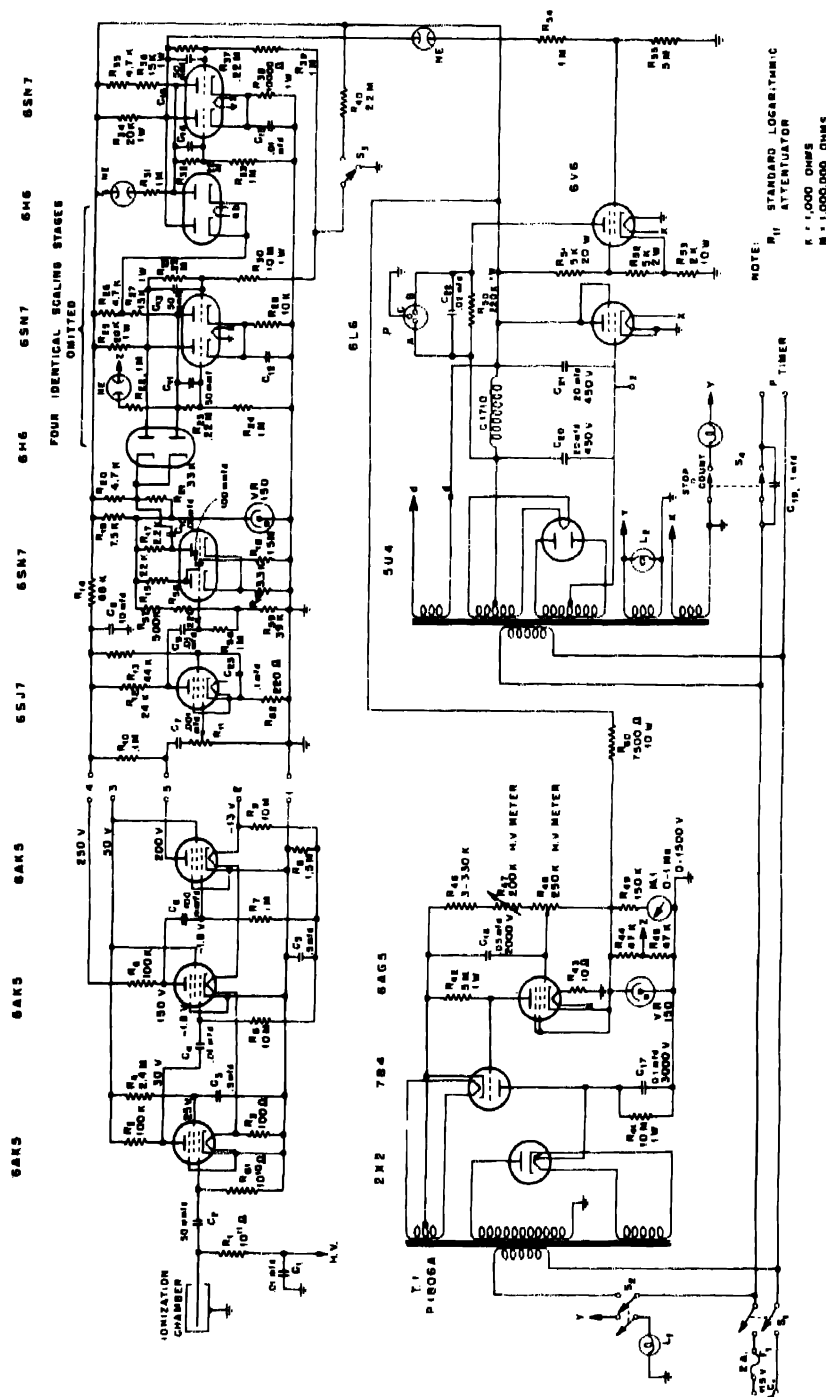


Fig. 3—Circuit.

trigger-pair type pulse selector is used; this is shown in the diagram (Fig. 3). It is sensitive to negative pulses of approximately 0.4 volt in amplitude, and the sensitivity can be varied by the 500K potentiometer in the trigger-pair grid circuit. Stability of gain of the amplifier is achieved by operating the entire circuit from a Sola Transformer a-c voltage stabilizer.

### 5. OPERATING CHARACTERISTICS

Tests of the variation of counting rate as a function of the gain-control setting, with radon and argon in the chamber and with +1,400 volts on the center electrode, were made for center electrodes of  $\frac{1}{8}$ -,  $\frac{1}{4}$ -,  $\frac{1}{2}$ -, and 1-in. diameters. The flattest "plateau" was obtained with the  $\frac{1}{2}$ -in. size; apparently the smaller sizes result in electrical fields in the outer parts of the chamber that are too weak, and the larger size intercepts too large a fraction of the  $\alpha$ -particle tracks. The  $\frac{1}{2}$ -in. size was adopted as standard. Even in this case there is no true plateau where the counting rate is insensitive to gain-setting, since there is a continuous distribution of pulse sizes from the maximum down to the very smallest, coming from  $\alpha$  particles which strike the walls before expending an appreciable fraction of their full energy in ionization. This necessitates the gain stability previously mentioned.

With a  $\frac{1}{2}$ -in. electrode and a gain setting near the center of the plateau of the gain curve, the variation of the counting rate as a function of voltage was studied with a normal chamber filling and with various amounts of air intentionally admitted in addition. With argon alone saturation is achieved at 500 volts, but with air present higher voltages are required. At 1,400 volts, the limit of the voltage supply normally used with the counter, saturation was obtained with amounts of air up to 5 cm Hg in the chamber. These tests were made with an auxiliary voltage unit supplying up to 2,500 volts. A voltage higher than 1,400 volts was not used because of an apparent tendency of the coupling condenser to leak and increase the noise level at 2,500 volts. Fourteen hundred volts is sufficiently high to nullify the effects of small amounts of air or water vapor that may accidentally get into the chambers. It should be noted that although argon, a free-electron gas, is used in the chamber, advantage is not taken of its high-speed counting properties by employing a very-high-frequency amplifier; this would require that oxygen and water vapor be removed to very low levels. By using a free-electron gas with a low-frequency amplifier, it is possible to tolerate small amounts of electron-attaching gases and vapors, thus making elaborate precautions and high-vacuum technique unnecessary.

Because of the slope of the gain curve a check on counter performance is desirable. For this purpose a small parallel-plate air chamber containing a deposit of a long-lived  $\alpha$ -emitting substance is used. This chamber is mounted on a breech mechanism designed to fit in the receptacle of the amplifier unit, and has a contact similar to that of the emanation chambers. Because the geometry of this chamber permits only short  $\alpha$  tracks and because the amplifier frequency is higher than the optimum value for air-ionization pulses, this unit gives many small pulses; consequently its gain curve has a roughly tenfold greater slope than the emanation-chamber curve. If the gain is adjusted so that the test chamber gives a counting rate within 1 per cent of its adopted standard value, the emanation-chamber counting rate should be within 0.1 per cent of its correct value.

In general, the test-chamber counting rate remains essentially constant over long periods of time so that no change of the gain setting is necessary. This indicates that errors due to gain instability are probably negligible.

Deviations from linearity at high counting rates, owing to coincidence losses, were determined by the method of radioactive decay. A chamber is filled with a sample of radon sufficient to give an initial counting rate of about 40,000 counts per minute, and counts are made over a period of several half lives. From the later counts, for which the coincidence losses are small, a provisional value of the initial "corrected" transient equilibrium activity is determined, and provisional values of the corrected activity at the time of each count are calculated. This is feasible in the present case because the half life of radon ( $3.824 \pm 0.002$  days) is known with great accuracy.<sup>5,6</sup> Denoting the provisional corrected rate of sample plus background at a given time by  $N'$  and the recorded rate by  $R$ , the provisional fractional correction,  $f' = (N' - R)/R$ , is calculated for each observation and plotted (Fig. 4). A smooth curve (the broken line in Fig. 4) is drawn through the points. If the provisional initial corrected activity ( $N'_0$ ) is chosen correctly, the fractional-correction curve may be extrapolated back to zero loss at  $R = 0$ . In general, however, this will not be the case, and the extrapolated value ( $f'_0$ ) will not equal zero. In the example shown,  $f'_0 = -2.0$  per cent, indicating that the actual initial corrected activity ( $N_0$ ) is 2.0 per cent lower than the provisional value ( $N'_0$ ). It is now possible to recalculate the results, plotting  $f = (N - R)/R$  instead of  $f'$ , and obtain a curve that can be extrapolated to zero. The same result can be achieved more easily, however, by calculating the value of  $f$  corresponding to a few selected points on the provisional curve from the relation

$$f = f' - \frac{f'_0}{1 + f'_0} (1 + f')$$

The curve joining the calculated points (the solid line in Fig. 4) represents the actual fractional-correction curve.

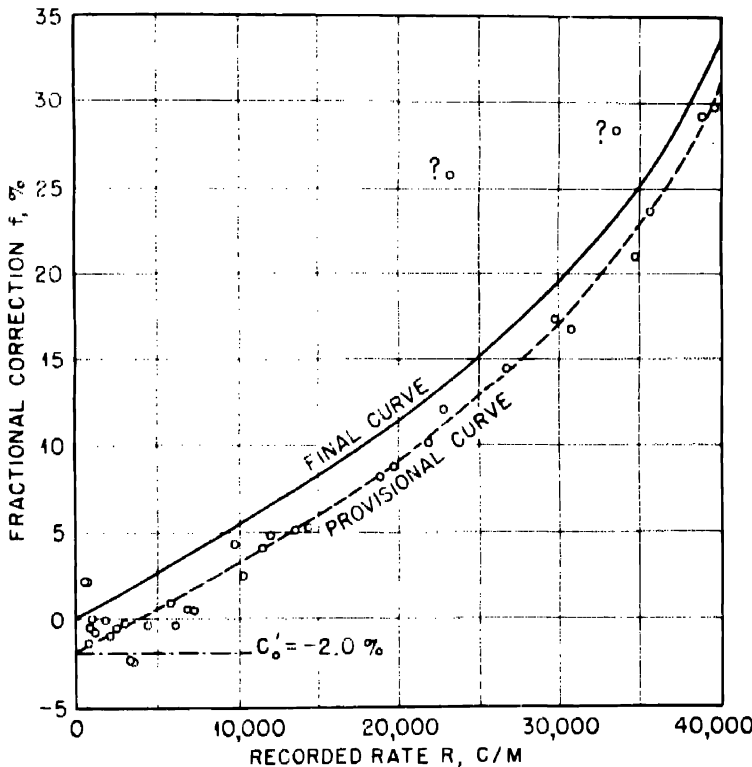


Fig. 4—Nonlinearity correction determination.

The fractional-correction curve obtained (Fig. 4) has an initial slope of 0.5 per cent per 1,000 counts per minute, corresponding to a resolving time of 300  $\mu$ sec. Above several thousand counts per minute the correction becomes greater than is given by this linear relation, and at around 40,000 counts per minute the losses become quite large as the limiting speed of the recorder is approached. Two other coincidence correction measurements gave essentially the same correction curves as the one shown.

All radon measurements are corrected for coincidence loss, before subtraction of the background, by the use of this curve and the relation

$$N = R + Rf$$

#### 6. CALCULATIONS

If a quantity, M, of radium in solution is freed of radon, sealed for a time, t, and then rapidly de-eminated into a chamber, the initial disintegration rate of the radon,  $E_0$ , will be

$$E_0 = MZG(t)$$

where Z = specific activity of radium (approximately  $2.17 \times 10^{12}$  dis-integrations per minute),  $G(t) = 1 - e^{-et}$  (growth factor) and e = decay constant of radon<sup>5,6</sup> ( $2.098 \times 10^{-6} \text{ sec}^{-1}$ ). The  $\alpha$  activity in the chamber, initially due to radon alone, rapidly increases as the short-lived descendants grow in, passes through a broad maximum in several hours, and then slowly decays with the half life of radon. The counting rate varies similarly, but it is not directly proportional to the  $\alpha$  disintegration rate for the reason that the counting yield is not the same for rare-gas atoms ( $Rn = Em^{222}$ ) and for atoms of solid elements ( $RaA = Po^{218}$ ,  $RaC = Bi^{214}$ ,  $RaC' = Po^{214}$ ). For  $Rn$   $\alpha$  particles the counting yield ( $Y_E$ ) should be nearly 1, since virtually all produce ion tracks of sufficient length to produce counts. In the electrostatic field of the chamber the active deposit atoms are probably all collected on the chamber walls, and if the potential has been applied steadily for several hours, the counting yield for the solid elements ( $Y_S$ ) should be approximately  $\frac{1}{2}$ . For accurate measurements it is necessary to maintain a potential across the electrodes continuously for several hours previous to counting; otherwise  $Y_S$  may have some indefinite value greater than  $\frac{1}{2}$ .

The counting rate,  $N(\theta)$  at time  $\theta$  after filling the chamber is given by

$$N(\theta) = Y_E E + Y_S (A + C) = E_0 [Y_E e^{-e\theta} + Y_S F(\theta)]$$

where

$$F(\theta) = \frac{a}{a-e} \left( e^{-e\theta} - e^{-a\theta} \right) + abc \left( \frac{e^{-e\theta}}{(a-e)(b-e)(c-e)} \right. \\ \left. + \frac{e^{-a\theta}}{(e-a)(b-a)(c-a)} + \frac{e^{-b\theta}}{(e-b)(a-b)(c-b)} + \frac{e^{-c\theta}}{(e-c)(a-c)(b-c)} \right)$$

and  $E$  = disintegration rate of Rn at time  $\theta$

$A$  = disintegration rate of RaA at time  $\theta$

$C$  = disintegration rate of RaC at time  $\theta$

$a$  = disintegration constant RaA =  $3.79 \times 10^{-3}$  sec $^{-1}$  (reference 9)

$b$  = disintegration constant RaB =  $4.31 \times 10^{-4}$  sec $^{-1}$  (reference 10)

$c$  = disintegration constant RaC =  $5.86 \times 10^{-4}$  sec $^{-1}$  (reference 11)

Under conditions of transient equilibrium this reduces to

$$\bar{N}(\theta) = Y_E E + Y_S (\bar{A} + \bar{C})$$

where  $\bar{N}(\theta)$  is the counting rate under conditions of transient equilibrium ( $\theta > 5$  hr),  $\bar{A}$  is the disintegration rate of RaA under conditions of transient equilibrium, and  $\bar{C}$  is the disintegration rate of RaC under conditions of transient equilibrium.

But

$$\bar{A} = \frac{a}{a - e} E = 1.00055 E$$

and

$$\bar{C} = \frac{abc}{(a - e)(b - e)(c - e)} E = 1.00902 E$$

Therefore

$$\bar{N}(\theta) = E [ Y_E + Y_S F(\infty) ]$$

where

$$F(\infty) = \frac{a}{a - c} + \frac{abc}{(a - e)(b - e)(c - e)} = 2.00957$$

Although transient equilibrium is not reached until several hours after filling the chamber,  $\bar{N}(\theta)$  has a value, mathematically defined, for all values of  $\theta$ . We define a function

$$D(\theta) = \frac{N(\theta)}{\bar{N}(0)}$$

calling this the "decay factor" because after transient equilibrium is established,

$$D(\theta) = e^{-e\theta} \quad (\theta > 5 \text{ hr})$$

The amount of radium can be related to the counting rate in terms of  $D(\theta)$  as follows:

$$\begin{aligned} \bar{N}(0) &= E_0 [Y_E - Y_S F(\infty)] \\ &= MZ [Y_E + Y_S F(\infty)] G(t) \\ N(\theta) &= \bar{N}(0) D(\theta) \\ &= MZ [Y_E - Y_S F(\infty)] G(t) D(\theta) \\ M &= \frac{K N(\theta)}{G(t) D(\theta)} \end{aligned}$$

where  $K$ , the "chamber constant," is given by the expression

$$K = \frac{1}{Z [Y_E + Y_S F(\infty)]}$$

Since  $Y_E$  and  $Y_S$  cannot be known exactly, and since there is some uncertainty in the value of  $Z$ ,  $K$  must be determined experimentally by using known amounts of radium. This can be done by counting after transient equilibrium prevails; i.e., when  $D(\theta)$  has the known form  $e^{-e\theta}$ , or by determining  $D(\theta)$  for previous instances.  $D(\theta)$  can be calculated if the ratio  $Y_S/Y_E$  is known, as follows:

$$\begin{aligned} D(\theta) &= \frac{N(\theta)}{\bar{N}(0)} \\ &= \frac{E_0 [Y_E e^{-e\theta} + Y_S F(\theta)]}{E_0 [Y_E + Y_S F(\infty)]} \\ &= \frac{e^{-e\theta} + \frac{Y_S}{Y_E} F(\theta)}{1 + \frac{Y_S}{Y_E} F(\infty)} \end{aligned}$$

In Fig. 5,  $D(\theta)$  is plotted as a function of  $\theta$  for several values of  $Y_S/Y_E$ . This ratio is expected a priori to have a value near 0.5. The ratio can be determined experimentally from the shape of the activity curve following the introduction of radon into a counter. Figure 6 is a graph on a semilogarithmic scale of such an experimental curve. The actual situation differs from the hypothetical one considered, in that the radon is not introduced into the chamber instantaneously but over a finite time. However, for all practical purposes the transfer may be considered instantaneous; consequently, after the RaA has essentially reached equilibrium, the curve will follow closely a theoretical

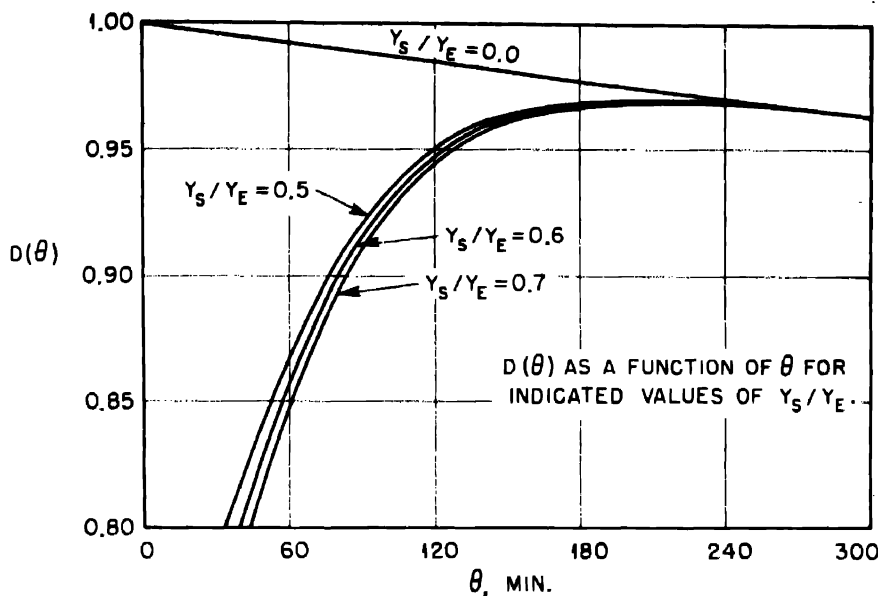
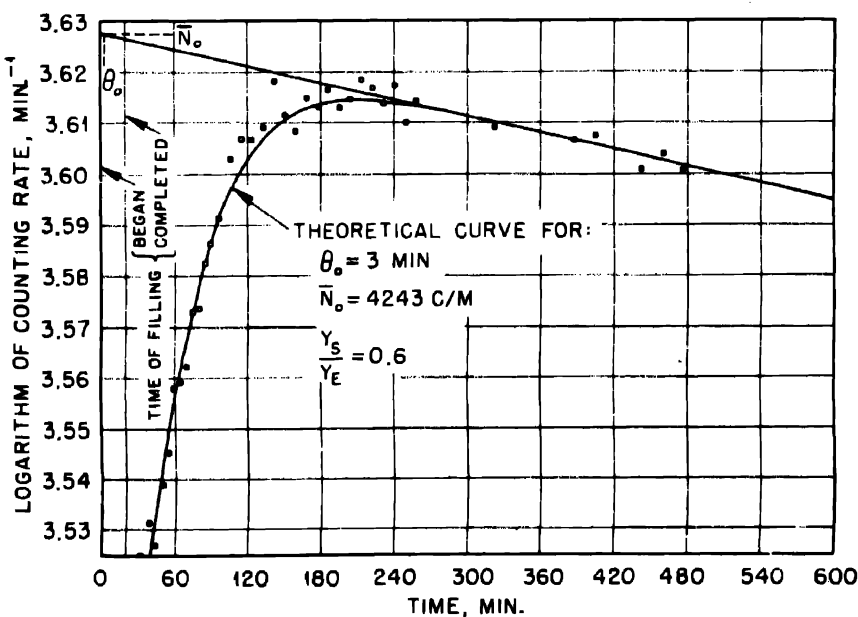
Fig. 5—Calculated growth and decay of radon  $\alpha$  activity.

Fig. 6—Radon activity growth and decay.

FIG. 7.—Radium analysis; emanation and computation data sheet.

one. The theoretical curve that best fits the measurements of Fig. 6, that for  $Y_S/Y_E = 0.6$  and  $\theta = 0$  taken at a time 3 min after the beginning of the de-emanation period, is shown in the figure. This curve is then used to obtain  $D(\theta)$  for the various measurements, the value of  $\theta$  being the interval from 3 min after the beginning of the de-emanation to the mid-point of the counting period. It may be seen from Fig. 5 that the shape of the curve is relatively insensitive to the value of  $Y_S/Y_E$  after 3 hr; thus no appreciable error is introduced by an uncertainty in the ratio. Furthermore, the curve has a broad maximum between the third and fifth hours after filling; therefore the count may be made within this interval and small uncertainties in the times will be unimportant.

For routine use of this method, particularly by a technician, two data sheets have been found useful. One, designated "Radium Assay—Emanation and Computation Data Sheet," contains spaces for entering all the experimental data (except details of counting) and for computing the results. The other, "Emanation Counter Data Sheet," is similar to data sheets used with other types of counters and has provisions for entering the original counting data and for computing the counting rates. Examples of each of these sheets are included in this paper (Figs. 7 and 8).

#### 7. STANDARIZATION AND ACCURACY

The value of the chamber constant, K, was determined by the use of radium standards from the U. S. Bureau of Standards. These consist of sealed glass capsules containing several milliliters of aqueous solution in which is a specified quantity of radium, certified accurate to 0.1 per cent. The standardization of these solutions is based on  $\gamma$  radiation comparisons, which refer back ultimately to actually weighed samples of highly purified radium.

Numerous experiments were carried out to test the effects of several variables which were suspected of giving erroneous results.

It was observed that results obtained when strong nitric acid was used in the radium-containing solution were frequently more divergent than those of other solutions. Consequently, the effects of various acids were tested. The results showed that nitric and hydrochloric acids both give trouble in the form of low results when present in concentrations of 5N or greater, whereas sulfuric acid is tolerable in all concentrations (unless, of course, there is sufficient barium present to cause precipitation of the radium). The effect is probably due to the distillation of vapors that are not held in the cold trap and that have the same effect in the chambers as oxygen. The vapors responsible may be the respective acids themselves, or, in the case of nitric

**Fig. 8**—Emanation-counting data sheet.

acid, oxides of nitrogen resulting from its decomposition. Therefore the concentrations of the interfering acids were kept far below the indicated tolerable limits in all subsequent measurements.

As a result of numerous measurements, the value of the chamber constant for our apparatus was found to be

$$K = 2.44 \times 10^{-13} \text{ gram minute per count}$$

This means that a counting rate of 1 per minute, after application of the growth and decay factors, corresponds to  $2.44 \times 10^{-13}$  g of radium in the sample. No consistent variation of K from chamber to chamber could be detected, and since the chambers are identical it is assumed that the same value of K can be used for all the chambers.

The variations of different measurements made on the same samples corresponded to a probable error of about 2 per cent in the series of runs described. The causes of variations were not studied sufficiently to reduce them to a lower level. Consequently, the above value for K cannot be considered to be accurate, and it should be redetermined for any measurements in which accuracy is desired.

Curtiss and Davis report an observational limit of  $10^{-14}$  curie of radon for their apparatus. The sensitivity and background reported by them is similar to that of our apparatus. This limit corresponds to a counting rate of about 0.04 per minute or about 1 to 2 per cent of the background, an extremely difficult quantity to detect with certainty. We consider the useful lower limit for our apparatus in its present state of development to be about  $10^{-12}$  g of radium, which gives a counting rate of the same order of magnitude as the background after a growth period of several days.

#### 8. PREPARATION OF SAMPLES FOR RADIUM ASSAY

For radium assay by the emanation technique, the radium must be completely and quantitatively dissolved. It is desirable that all the radium of a sample be obtained in a single solution. The volume of solution to be emanated must be not over 125 ml, and it must not contain nitric or hydrochloric acid in concentration greater than 2N when diluted to this volume. If possible, the sample size should be such as to yield, after a convenient growth period, a counting rate between 1,000 and 10,000 per minute, preferably in the range of 3,000 to 5,000 counts per minute. A sample containing  $10^{-8}$  g Ra will give roughly 5,000 counts per minute after an overnight growth period. The approximate counting rate can be adjusted by varying the size of the aliquot and the time of growth.

Procedures for various types of materials follow.

8.1 Radium Standards. U. S. Bureau of Standards radium-solution capsules are opened by filing and breaking the constricted end. The contents are then made up to a known volume in a volumetric flask. Suitable aliquots are taken for measurements and diluted to approximately 100 ml with 1N HCl.

8.2 Process Solutions. These present no difficulty since a measured volume of a solution can be introduced directly into an emanation flask and diluted, if necessary, to about 100 ml. Certain process filtrates contain lead sulfate, which slowly precipitates on cooling and standing. On heating, the precipitates redissolve, so that these samples can be analyzed without additional treatment.

8.3 Pitchblende Ores. A 0.1-g sample is weighed into a 50-ml platinum dish and treated with 15 ml of 2N HNO<sub>3</sub> on a hot plate. When the reaction subsides, 10 to 20 ml of concentrated nitric acid is added, and heating is continued for ½ hr. Ten milliliters of 40 per cent HF and 0.5 ml of 70 per cent HClO<sub>4</sub> are added, and heating is continued until perchloric acid fumes are given off. Additional hydrofluoric acid and nitric acid are added and the dish is again heated until perchloric acid fumes appear. This is repeated once or twice more. Twenty-five milliliters of 6N HNO<sub>3</sub> is added; the solution is heated until clear and is transferred to an emanation flask, using 75 to 100 ml of water to wash the sample quantitatively into the flask.

8.4 Gangue-Lead Sulfate Cakes. The material is dried and ground for analysis. A 0.1- to 0.2-g sample is weighed into a No. 00 porcelain crucible and intimately mixed with ten times its weight of zinc dust. The crucible is covered and heated in a Meker flame for 1 hr. After cooling, the crucible and cover are placed in a 250-ml beaker and covered with 2N HNO<sub>3</sub>. When the reaction subsides, the beaker is heated on a hot plate until the zinc is completely dissolved. The crucible and cover are then removed and washed with water, and the solution is evaporated to about 50 ml and filtered quantitatively. The filter paper with the insoluble residue is transferred to a platinum crucible, and the paper is burned off. The residue is evaporated to dryness twice with 10 ml of hydrofluoric acid. Concentrated nitric acid is added to dissolve the material remaining, and the solution is added to the filtrate obtained previously. The solution is then evaporated to a convenient volume for analysis.

8.5 Barium Sulfate Cakes. The material is dried and ground for analysis. A 0.3- to 0.4-g sample is weighed into a No. 00 porcelain crucible and treated in the manner described for gangue-lead sulfate samples. After treating the filter-paper residue with hydrofluoric acid, some undissolved barium sulfate remains. This is transferred

to a porcelain crucible with water and a rubber policeman, evaporated to dryness, and treated with zinc as before. The sinter dissolves completely in nitric acid. The two solutions are then combined and evaporated to a convenient volume for analysis.

#### 9. SUMMARY

Apparatus and procedure for assay of radium in solution by an emanation method have been described. The radon produced by the radium in a measured time was transferred with a stream of argon into an  $\alpha$ -ionization counting chamber similar to that of Curtiss and Davis but modified to achieve simplicity of construction, utilization of existing standard equipment, and ease of operation. Interchangeability of emanating flasks and ionization chambers provided economy of time and apparatus and flexibility of operation. The use of a free-electron gas with a relatively low-frequency amplifier makes small amounts of electron-attaching gases and vapors in the chamber tolerable. Methods for calibration of the apparatus, determination of operating characteristics and corrections, and interpretation of results have been described. Chemical procedures for obtaining solutions suitable for de-emanation from several types of radium-containing materials were also described.

#### REFERENCES

1. S. C. Brown, L. G. Elliott, and R. D. Evans, *Rev. Sci. Instruments*, 13: 147 (1942).
2. J. H. J. Poole, *Sci. Proc. Roy. Dublin Soc.*, 21: 595, 609 (1938).
3. L. F. Curtiss and F. J. Davis, *J. Research Natl. Bur. Standards*, 31: 181 (1943); Davis, *Ibid.*, 39: 545 (1947); Davis, *J. Assoc. Off. Agr. Chemists*, 28: 682 (1945).
4. A. H. Jaffey, *Metallurgical Project Report CC-3771* (Feb. 7, 1947); also in *National Nuclear Energy Series*, Division IV, Volume 14 A.
5. W. Bothe, *Z. Physik*, 16: 226 (1923).
6. I. Curie and C. Chamié, *J. phys. radium*, (6) 5: 238 (1924).
7. T. P. Kohman, D. P. Ames, and J. Sedlet, *Manhattan District Declassified Document MDDC-852* (1947). See this paper for summary of other determinations.
8. M. Blau, *Sitzber. Akad. Wiss. Wien, Abt. IIa* 133: 17 (1924).
9. M. Curie, "Traité de Radioactivité," Vol. II, p. 322, Gauthier-Villars, Paris, 1910.
10. P. Bracelin, *Proc. Cambridge Phil. Soc.*, 23: 150 (1926).

## Paper 16.8

# A 48-CHANNEL PULSE-HEIGHT ANALYZER FOR ALPHA-ENERGY MEASUREMENTS†

By A. Ghiorso, A. H. Jaffey, H. P. Robinson, and B. B. Weissbourd

### 1. INTRODUCTION

In the program of investigation of new artificial heavy nuclides‡ carried on at the Metallurgical (now Argonne National) Laboratory it was found almost essential to be able to identify and trace specific  $\alpha$  emitters in the presence of other  $\alpha$  emitters. Because many of the nuclides at the upper end of the periodic table are  $\alpha$  emitters, the bombardment of a particular starting material (generally an  $\alpha$  emitter) with neutrons, deuterons, or helium ions usually resulted in the formation of new nuclides which were also  $\alpha$  emitters. The products formed were often present in very low concentrations (with  $\alpha$  activities much lower than that of the starting material), and the chemical properties of the element to be separated were often poorly understood. In either case a good analytical tool was necessary to make possible the tracing of a particular nuclide through a long series of chemical separations. In addition there were a number of cases where the nuclides formed were not chemically separable, being isotopic mixtures (e.g., a mixture of  $\text{Pu}^{238}$ ,  $\text{Pu}^{239}$ , and  $\text{Pu}^{239}$ ), so that chemical identification was impossible. The instrument described here was developed for use in such tracing, and it has also proved useful in following the chemical separation and purification of the natural  $\alpha$  emitters. It has been used for the determination of the  $\alpha$  energies of many of the new isotopes. Although the accuracy of this instrument is less than that of other instruments, the fact that it

†Contribution from the Chemistry Division of the Metallurgical Laboratory, University of Chicago, now the Argonne National Laboratory.

‡Nuclide has been defined<sup>1</sup> as "a species of atom characterized by the constitution of its nucleus, in particular by the numbers of protons and neutrons in its nucleus."

can be used at 50 per cent geometry has often made energy measurements feasible where little activity was available or could be used.

The  $\alpha$ -particle energy of an  $\alpha$ -emitting nuclide is almost specific to that nuclide. In fact, if it were possible to make convenient  $\alpha$ -energy measurements with very high resolution and accuracy, it would probably be possible to make unambiguous determinations of the identity and quantity of any known  $\alpha$  emitter present in sufficient concentration. There are some cases, however, of two or more nuclides that emit  $\alpha$  particles of nearly equal energies,<sup>†</sup> and the limited resolving power and accuracy of the instruments available makes identification very difficult, if not impossible. This ambiguity can often be removed by other methods such as chemical separation or the use of a mass spectrograph or, in some cases, by fission measurements, either spontaneous or neutron induced.

## 2. METHODS OF ALPHA-ENERGY MEASUREMENT

In using the measurement of  $\alpha$  energy as an analytical tool for chemical experiments, a prime consideration is simplicity in the sample preparation, in the operation of the instrument, and in the interpretation of the results. This factor made the use of the magnetic  $\alpha$ -energy analyzer<sup>‡</sup> undesirable because of the necessity of using carefully prepared line sources, because of the bulky and elaborate equipment required, and because of the low geometry involved (less than  $10^{-3}$ ). Good geometry, preferably 50 per cent, was highly desirable because of the low total amounts of  $\alpha$  activity available in some measurements, or because of low specific activities in the sample. It was also desirable that the resolving power and accuracy of energy measurement be as good as was consistent with the requirements of relative simplicity and high geometry.

The measurement of ranges was tried, using uniform foil (mica) absorbers with surface densities from 1 to 8 mg./sq. cm at 50 per cent geometry (parallel-plate ionization chamber).<sup>2</sup> The method is described elsewhere.<sup>2</sup> Although the mica-absorber method has high geometry, it has relatively poor resolving power, and it was decided to use other methods instead. Other methods of range measurement were considered undesirable since the best high-geometry method<sup>3</sup> has poor resolution, whereas the methods having good resolution have quite low geometry.<sup>2,4,5</sup> It was decided that the best results could be

<sup>†</sup> Examples of such pairs are U<sup>232</sup> and Po<sup>210</sup>, U<sup>234</sup> and Np<sup>237</sup>, and Pu<sup>238</sup> and Am<sup>241</sup> (see Table 4).

<sup>‡</sup> Such as those used by Rosenblum, Rutherford, Briggs, Chang, and others. See Jaffey<sup>4</sup> for references.

obtained from the measurement of the total ionization due to an  $\alpha$  particle in a suitable ionization chamber. This method has at least one advantage in that the ionization charge collected is very closely proportional to the  $\alpha$ -particle energy, at least† within the energy region covered by the natural  $\alpha$  emitters (4 to 10 mev).

The method involves (1) an ionization chamber in which the  $\alpha$  particle expends all its energy and in which the charge is rapidly collected, generating across the chamber capacity a voltage pulse of the order of a millivolt, the magnitude of which is at least approximately proportional to the particle energy, (2) a linear pulse amplifier which amplifies this pulse up to a voltage suitable for detection, and (3) a device, electronic or otherwise, for determining the relative number of pulses of various sizes. Plotting relative number vs. pulse size essentially gives a graph of relative number vs.  $\alpha$  energy, assuming a correct calibration of the pulse height-energy relation.

This method has been extensively used,<sup>6-28</sup> for measuring the energies of  $\alpha$  particles, protons, and fission fragments.

### 3. TOTAL-IONIZATION METHOD FOR ALPHA-ENERGY MEASUREMENT

**3.1 Chambers.** Two types of chambers have been in most general use. Air has been used as a chamber gas, usually with parallel-plate electrodes, or free-electron gases‡ (such as H<sub>2</sub>, N<sub>2</sub>, rare gases) have been used either with parallel electrodes or with electrodes with cylindrical symmetry (thin rod as electrode). More recently chambers with grids have been used with free-electron gases.

The optimum amplifier design for a particular type of chamber involves a reconciliation between the following requirements: (1) preservation of pulse height and (2) ability to use high counting rates. If, as is often the case, the charge collection time varies from one  $\alpha$  particle to another because of the angular distribution of the  $\alpha$ -particle paths, the pulse size may also vary if the amplifier is incorrectly designed.

**3.2 Amplifiers.** In all practical circuits the charge collected in the ionization chamber is passed on to the sensitive element of the detector, usually the grid of the first amplifier tube. The capacity of the chamber and tube and the grid input resistance form a parallel RC system which determines the shape of the pulse passing into the amplifier. The electric charge collected in the chamber charges up

†There is fairly good evidence that this holds even below 4 mev.<sup>4</sup>

‡See Sec. 4.2.

the capacity relatively rapidly, and then it discharges slowly through the resistance. The characteristic pulse shape (voltage vs. time) passing out of most pulse ionization chambers consists, therefore, of a rapidly rising part followed by a slow exponential decay, with the pulse height (for sufficiently large input resistance) proportional to the charge collected. One method of preserving the relative pulse sizes arising from various  $\alpha$  particles, independently of collection time, is to reproduce carefully the original pulse shapes in the recording apparatus. In the first use of this method very sensitive electrometers<sup>29,30</sup> with very high input resistance were utilized. For this purpose, however, such electrometers have been largely displaced by d-c amplifiers using electrometer tubes (see references 6, 7, 8, 12, 13, and 15). Recently there has been developed<sup>31</sup> a highly sensitive dynamic condenser electrometer† with great stability, which stability has made it a useful substitute for electrometer-tube circuits. It has been utilized for  $\alpha$ -energy measurements by Jesse.<sup>32</sup>

Because of the very slow decay caused by the large input RC value (more than 1 sec) of such electrometer circuits, the useful counting rates must be low (less than 1 per sec). If the counting rate is too high, excessive superposition of pulses results.

For energy measurement the relation of the frequency response to the collection time is subject to more stringent requirements than is the case when only counting of particles is to be done. It can be shown<sup>33</sup> that for circuits whose frequency response is determined only by RC elements, the pulse height is essentially preserved if the decay time is at least 100 times the collection time. Because of its very long input-time constant, the electrometer circuit (either d-c or vibrating condenser) may be used with chambers having relatively long (more than 1 millisecond) collection times. It may thus be used with air-filled chambers (where charge mobility is relatively low) with electric fields no larger than are necessary to prevent recombination of positive and negative ions (i.e., the saturation field). Of course free-electron gases may also be used, since faster collection times do not affect the preservation of pulse heights.

To use higher counting rates than are possible with electrometer circuits, it is necessary to reduce the decay time by raising the low-frequency cutoff of the amplifier. To preserve the relative pulse heights, the collection times must then be decreased. This can be achieved by the use of higher electric fields in air-filled chambers

†A very-high-resistance vibrating condenser changes a small d-c voltage signal to an a-c voltage, which is amplified through a tuned, high-gain, feed-back-stabilized a-c amplifier and recorded on a pen-writing recorder, such as the Brown recorder.

or through the use of free-electron gases. Corresponding to the increase in the low-frequency cutoff, the high-frequency cutoff is also increased in order to preserve the rise time of the pulse.

Amplifiers in the audio-frequency range with chambers containing either air or free-electron gases have been utilized in a number of applications of the total-ionization method, although with air the electric fields must be high (to decrease collection time) and the low-frequency cutoff must be moderately low. In general, chamber fillings of free-electron gases are the most useful, even with slow amplifiers, since the field strengths required, either for saturation or for short collection times, are considerably smaller than for air.

In addition to allowing higher counting rates, the faster decay time allows greater tolerance for the presence of  $\beta$  and  $\gamma$  rays. With an electrometer circuit, the superposition of the small pulses caused by  $\beta$  particles may seriously interfere by increasing the "background noise" and therefore the "line width" of the pulse distribution. With faster-decaying pulses, the superposition is less likely, so that a given amount of  $\beta$  activity affects the noise level much less.

In recent years full advantage has been taken of the fast collection possible in free-electron gases by using amplifiers with quite high frequency response (approximately 1-megacycle band width) and correspondingly higher low-frequency cutoff. These systems can use much higher counting rates and can tolerate much greater backgrounds of  $\beta$  and  $\gamma$  rays.

**3.3 Pulse-height Recording and Measurement.** In the detection process the pulses are sorted on the basis of magnitude and recorded in some suitable fashion. The most widely used methods have involved one of two procedures: (1) recording (on film or paper) a pulse voltage-vs.-time trace whose vertical displacement is proportional to the pulse height, and subsequently measuring the trace size (the pulse-height sorting is usually done manually) or (2) sorting the pulse sizes electronically and recording them with registers, with or without scalers.

Trace recording has generally been carried out by photographing the movement of a fast string galvanometer, the mirror of a loop oscillograph, or the trace of a cathode-ray oscillograph, with photographic film running past the instrument. This method has been extensively used in the Austrian, German, and Swiss laboratories, while the electronic method has been more widely used in England, Canada, and the United States. Recently Jesse<sup>32</sup> has used the Brown strip recorder as a precise recording device working out of the "vibrating-reed" or dynamic-condenser electrometer. In most cases the trace sizes are measured with a rule and then sorted into groups according

to size. In a recent publication from Switzerland,<sup>34</sup> an ingenious photographic recording method has been described in which a fixed photographic plate is used throughout an experiment and the number of pulses of a given size are measured by determining plate blackening as a function of height on the plate.

For electronic detection, sensitive "relay" circuits have been used, such that a pulse exceeding a critical voltage by a small amount (less than 0.1 volt) causes the recording of that pulse, whereas one smaller than the critical voltage is not recorded. Among the most commonly used of such relay circuits are thyratrons and vacuum-tube trigger pairs. Variation of the d-c bias on the detector grid serves to vary the cutoff point; and since d-c voltages are easily measured, the cutoff point can be precisely determined and reproduced.

With a single variable bias detector of this type, an integral curve may be measured, i.e., the number of pulses above a certain voltage may be measured as a function of that voltage. Thus for  $\alpha$  particles of a single energy in a total-ionization chamber, varying the bias voltage would give a number-vs.-voltage curve with a flat plateau that would drop off suddenly at the pulse height corresponding to the  $\alpha$  energy. The derivative of this integral curve is the pulse-height distribution curve. In determining the differential curve, the number of counts at one point is subtracted from the number at the neighboring point. Since each point is independently measured, the statistical fluctuations of both points enter into the error in the difference. This statistical fluctuation may be greatly reduced by using two detector circuits whose grid biases are kept a fixed voltage apart.<sup>11</sup> The difference between the counts recorded through the two detectors determines directly the number of pulses at the given pulse height, and the counting error in the difference is due solely to the statistical fluctuation of the difference.<sup>†</sup> The pulse distribution (or differential curve) may be determined directly by sweeping the biases of the two detectors over the desired range. Instead of subtracting the total counts passing through one detector from the total of the other, the differences may be determined directly by the use of a cancellation circuit which allows the recording of only those pulses which exceed one bias but not the other.<sup>35,36</sup>

<sup>†</sup>E.g., in an integral curve determined with a single biased detector, the number of counts at one voltage might be  $1,089 \pm 33$  (statistical fluctuation error), whereas the number of counts at the next voltage step might be  $900 \pm 30$ . The number of pulses within this voltage interval would then be  $189 \pm 45$ . If two biased detectors had been used, the number of counts on one might be 1,100 and 904 on the other. The number of pulses in this voltage interval would be  $196 \pm 14$ , or one-third the statistical error.

The photographic method has the serious disadvantage of requiring the tedious measurement of the pulse traces on the film. In the form in which it was often used (with a mechanical oscilloscope) it had the further limitation of requiring low counting rates. This limitation is not inherent in the method since a cathode-ray oscilloscope may be used. It is relatively easy to collect a moderately large number of pulses in a reasonable time since pulses of all sizes are recorded as they come through. Nevertheless, the tedium of measurement makes the collection of a large number of pulses impractical. With only a small number of measured traces, the statistical fluctuations make accurate measurements rather difficult. In addition, the problems involved in making accurate measurements of the film traces also make good accuracy difficult to attain. The precision of Jesse's method, which uses the vibrating reed and the Brown recorder, is better than has been achieved thus far by any photographic method.

The electronic method makes it possible to avoid making visual measurements of a trace by referring measurements to a precisely determined d-c voltage (pulse-height selector bias). It has the disadvantage that only one pulse height is measured at a time. With the differential pulse selector, for example, the pulses measured at any time lie within the narrow band determined by the difference between the two pulse selectors. Thus, in order that each point shall be measured with adequate statistical accuracy, it is necessary to spend considerable time in the complete sweeping of the energy region to be measured. At any one time a large fraction of the pulses formed in the ion chamber are not recorded,<sup>†</sup> resulting in a corresponding increase in the counting time. This carries with it the added disadvantage of possible difficulties if the chamber or amplifier characteristics drift with time.

**3.4 Multichannel Systems.** It would obviously be desirable to combine the advantages of both methods—recording all the  $\alpha$  pulses formed in the ionization chamber and at the same time utilizing the precision and measuring ease of the pulse-height selector method. To achieve this combination a multichannel system, characterized by a series of pulse-height selectors with biases differing by fixed voltage increments, was constructed. In this instrument all the pulses from the ion chamber are recorded, each pulse being applied to every channel, but recording only in the channel whose bias corresponds to

<sup>†</sup>This comment applies also to the case in which all pulses above a certain size are recorded since only those pulses just getting through the pulse-height selector are significant in the numerical differentiation process carried out later to get a curve of number vs. pulse height.

its pulse height. Of course, because of the finite widths of the channels, it is not possible to attain a continuous description of the pulse distribution. This, however, is rarely a limitation since if the channel width is somewhat smaller than the natural width of the pulse-distribution curve, no significant loss in resolution or accuracy occurs (Sec. 9.10, Fig. 22).

After this instrument was built, it came to our attention that a number of such multichannel instruments with quite different designs but with an over-all similarity had been built elsewhere. Owing to the compartmentalization of the various projects during wartime, it was only after our analyzer had been in operation for some time that we found that the British<sup>37</sup> as well as the Canadians,<sup>38</sup> had constructed several such instruments. Still another one had been built at Los Alamos.<sup>39</sup> A description of one of the Canadian analyzers has recently been published,<sup>40</sup> and in it there is also a discussion of some of the problems involved in designing and using a multichannel selector.

Although the instrument described here is hardly equipped with optimum characteristics, it has been used for analyzing thousands of samples; and it was felt, therefore, that a description of its construction and operation was worth while. Work is now going on to improve its stability and resolution.

#### 4. APPARATUS

**4.1 General.** Figure 1 illustrates a block diagram. The pulse from the chamber is amplified in the preamplifier and then in the first amplifier. It is then passed through a prediscriminator stage, which subtracts the same voltage from each pulse. The remaining portion of each pulse is amplified in the second amplifier, the output of which is a cathode follower (Fig. 4). The output stage then feeds into the 48 channels through a subsidiary set of cathode followers. The region of general interest can be spread over all the 48 channels by varying the bias in the prediscriminator and by varying the gain of each amplifier separately. The ability to concentrate all the detectors on a small energy region (thus accentuating energy differences) is important since most of the  $\alpha$  emitters of interest have energies between 4 and 6 mev. Every detector whose bias is less than the pulse size is fired by a pulse, but by means of the cancellation circuit described below the resulting signal is not transmitted to the recorder unless the pulse has not tripped the detector with next higher bias. The counts in each channel are registered by fast mechanical recorders. A photograph of the entire unit is shown in Fig. 2.

**4.2 Chamber.** The design of the chamber is greatly simplified by the use of "free-electron" gases,<sup>41,42,43</sup> instead of air, because of the

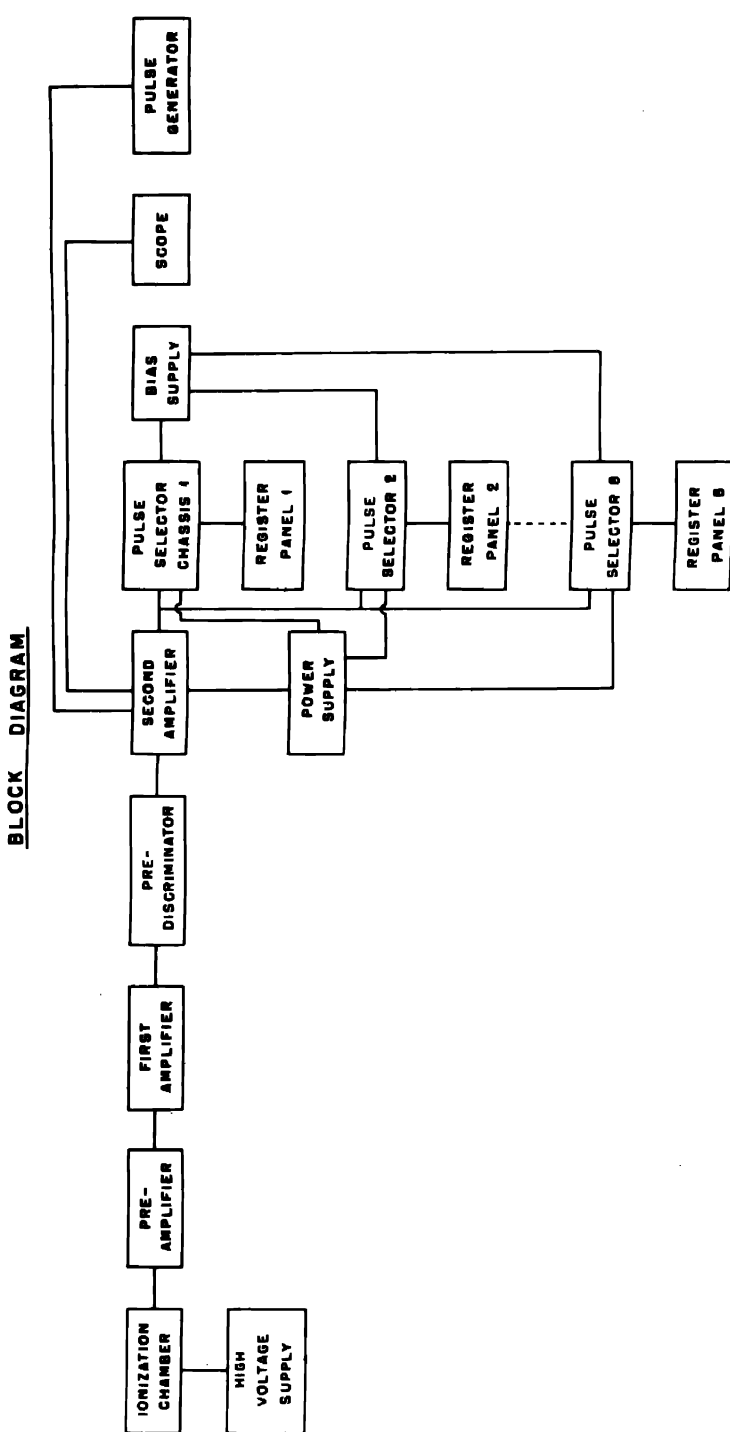
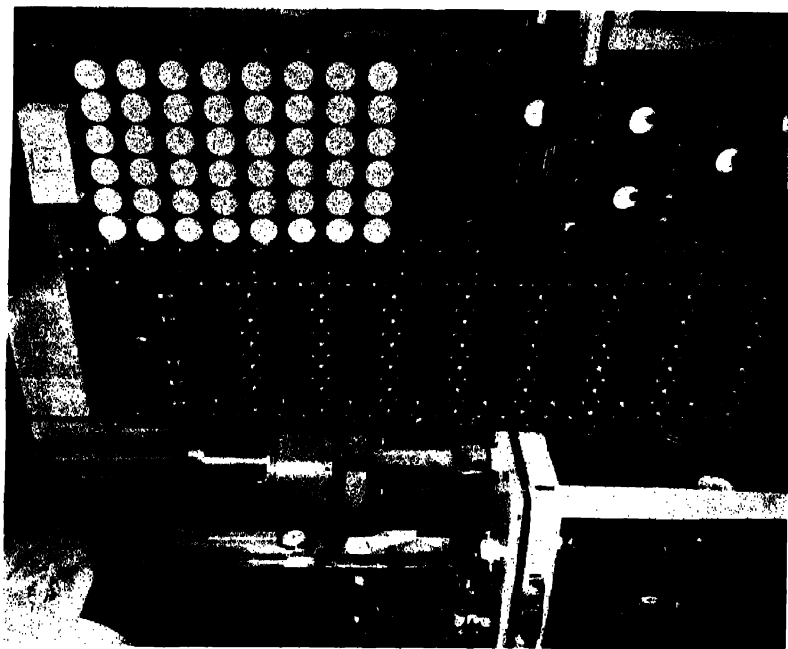


Fig. 1—Block diagram of a 48-channel pulse analyzer for  $\alpha$ -energy measurements.



Back



Front

Fig. 2 — Photographs of front and back of a 48-channel pulse analyzer for  $\alpha$ -energy measurements.

low electric fields necessary in such gases.<sup>†</sup> Low fields suffice because (1) the great mobility of electrons in free-electron gases enables rapid collection of charge even in small electric fields and (2) the field necessary to prevent recombination of positive and negative charges (i.e., the saturation field) is much smaller than in air.

In comparable electric fields, the electron velocities are of the order of a thousand times larger than those of the positive ions, so that during the time in which the electrons are collected, the positive ions hardly move at all. Because of the electrostatic induction effect, the charges affect the electrode<sup>‡</sup> before they actually strike it (see references 44 and 46 to 48). At the instant of charge creation by the  $\alpha$  particle, the net induction effect is zero since both charges of each ion pair are essentially at the same point. As the field moves the charges apart and the electrons approach the electrode, the induction effect due to the electrons increases. The induction effect of the positive ions on the electrode is opposite in sign to that of the electrons, and it therefore tends to partially cancel the electronic effect. Since the positive ions remain practically stationary during the period of electron collection, their cancellation effect remains essentially constant. Thus if only the electronic part of the pulse is used, the total charge collected in the ordinary ionization chamber is smaller than would be the case if both positive and negative charges were completely collected.

The magnitude of such cancellation can be easily calculated if the electrodes have suitable symmetry,<sup>47</sup> such as infinite plane electrodes, infinite coaxial cylinders, or concentric spheres. Each charge is considered separately by treating it as though it were uniformly spread out on a surface lying symmetrically between the two electrodes, the position of the actual charge determining the position of the surface. For example, a charge  $Q$  lying between two concentric-sphere electrodes at a distance  $R$  from the center would be considered spread uniformly over a concentric sphere of radius  $R$ . The magnitude of the total charge induced on both electrodes by the charge  $Q$  is equal to  $Q$ . The partition of the total induction between the two electrodes is determined by the ratio of the electrostatic capacities of the artificial surface to each of the electrodes. The closer the charge  $Q$  is to one electrode, the larger the capacity of the artificial

<sup>†</sup>Such gases are nitrogen, hydrogen, or the noble gases, in which the capture of electrons to form negative ions has very low probability, and hence electrons carry the negative current in an electric field. Oxygen, on the other hand, is highly electronegative, having a high probability of capturing electrons.

<sup>‡</sup>Collecting electrode.

surface to this electrode, and hence the larger the induced charge.<sup>†</sup> For plane parallel electrodes, the effect is linear since the capacity varies directly as the distance between the plates. For the spherical and cylindrical case, the linear relation does not hold.

If the ionization chamber is being used for energy determinations, the "positive-ion effect" is annoying since the magnitude of the cancellation depends upon the geometrical position of the positive ion in the chamber. For  $\alpha$  particles emitted in various directions, the variation in the cancellation effect can cause quite serious differences in pulse heights.<sup>45</sup> This difficulty may be minimized by several methods: (1) The collectrode may be placed at some distance from the ionization path, which decreases the induction effect; (2) advantage<sup>9,11,49</sup> may be taken of the fact that the capacity between concentric-spherical and cylindrical surfaces does not vary linearly with distance from the central surface. The collectrode may be made with so small a radius of curvature that its capacity to any surface even a little distance away is small, and hence practically no induction can take place unless the charges are very close to it. This method has an added advantage in that the small size of the collectrode serves to decrease its capacity to the high-voltage electrode and to the rest of the chamber, thus tending to increase the pulse height. It has the disadvantage that the electric field drops off with distance from the collectrode even more rapidly than does the capacity of the artificial surface. Thus the field is quite nonuniform, and it is relatively weak at the high-voltage electrode, on which the sample is often placed. Fortunately, electron mobilities in free-electron gases are so high that even in weak fields the velocities are high, and saturation is easy to attain.

A third method of reducing the positive-ion effect involves the use of a grid (see references 18, 19, 21, 23, 50, 51, and 52) in front of the collectrode in a parallel-plate ionization chamber. The grid serves to shield the collectrode from induction effects resulting from charges between grid and high-voltage electrode. It has no shielding effect, however, on induction from charges that have passed through the grid into the region between grid and collectrode. Since the positive ions never enter this region, the positive-ion effect is removed. Collection

<sup>†</sup>In the case of two concentric-sphere electrodes, where the inner one is the collectrode, the magnitude of the charge induced on the collectrode is  $Qa(b - R)/R(b - a)$ , where  $a$  = radius of collectrode,  $b$  = radius of outer electrode, and  $R$  is the distance of  $Q$  from the center. Note that the charge is  $Q$  when  $R = a$ , and is zero when  $R = b$ . For the case where  $b \gg a$ , the induced charge is  $Qa(1 - R/b)/R$ , i.e., it drops off hyperbolically with  $R$  (for  $b \gg R$ ).

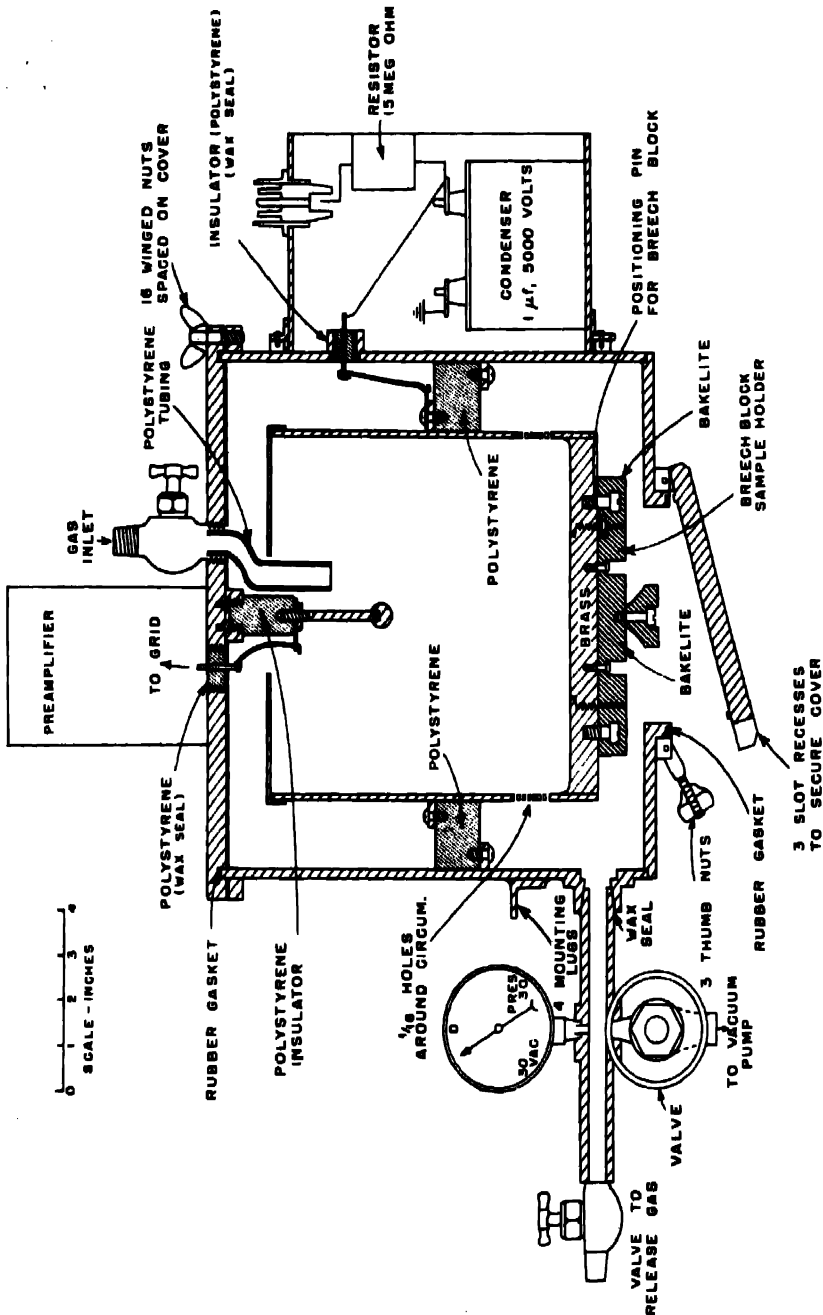


Fig. 3.—Ionization chamber for the 48-channel pulse-height analyzer.

of electrons on the grid is prevented by the use of a high negative potential, but one not as high as that on the high-voltage electrode. From experiments in this and other laboratories it seems that the grid-type chamber is the best kind to use if great uniformity of pulse size is desired under a variety of conditions. The analyzer we are using, however, has been built about a chamber designed to reduce the positive-ion effect by the first two methods.

The ionization chamber (Fig. 3) is mounted in a large steel vacuum-tight enclosure. The high-voltage electrode consists of a covered bucket supported on insulators large enough to allow the use of up to 5,000 volts (negative). Into the bottom of this electrode the sample support is fitted by means of a breech thread, a projecting pin being used to simplify the alignment of the thread as the support is pushed upward. The sample support may be removed through the bottom door which pivots on a single loose hinge and is clamped against the rubber gasket by three thumbscrews. To facilitate rapid clamping, these screws are hinged and slide into slots in the door. The bottoms of the sample support and high-voltage electrode are insulated to protect the instrument operator.

The collectrode consists of a  $\frac{1}{2}$ -in. brass sphere at the end of a narrow rod. To reduce the capacity to ground, the rod is supported by a long insulator; and a fine wire leading from the rod through the insulator in the top of the can is used to carry the signal. The wire and the polystyrene insulator through which it passes are vacuum-sealed with Apiezon W wax, and the insulator is also mechanically supported by screw threads. The high-voltage lead comes through a similar insulator, with a  $1-\mu\text{f}$  (5,000 volts, oil) condenser connected outside the vacuum chamber. The condenser is in a shielding brass box, through the wall of which passes a grounding key for discharging the condenser. The preamplifier is mounted on top of the vacuum can directly above the lead from the collectrode.

After a sample has been introduced, the chamber is evacuated with a high-capacity mechanical pump to a pressure of about 0.07 mm, and then filled with argon. Repetition of this process has been tried, but it seems not to have made any difference in the results, and therefore one pumping is generally considered sufficient. Since the time required for sample changing is short, only a small amount of air is introduced during this operation, and as a result the partial pressure of oxygen after one pumping is tolerably low. Oxygen interferes by combining with the free electrons to form slow-moving negative ions.

The argon used is purchased in large tanks and is said by the manufacturer to be 99.8 per cent pure. It is not prohibitively expensive,

being commercially manufactured for use in welding. For a while, the argon was purified by being passed over hot copper, but it was found that no difference could be noticed when this step was omitted provided the gas was led directly from the tank through copper tubing.

Since no difference has been found in operation characteristics as a result either of purification procedures (for oxygen removal) or of flushing the chamber once with argon, it seems likely that the oxygen content in the chamber is so small as to have little effect. According to the results obtained by Clark, Spencer-Palmer, and Woodward<sup>18</sup> this means that the oxygen content is probably less than 100 parts per million (or less than 0.07 mm at 1 atm). Purified nitrogen has been used, but it is less satisfactory than argon in a number of respects; for example, higher voltage is required for saturation.

After the chamber has been evacuated, it is filled to a pressure of 1 to 2 atm, and it is then used either statically or with gas flowing through at the rate of a few tenths of a milliliter per second. It has been found that the characteristics of the pulses change more rapidly when the gas is merely allowed to stand in the chamber rather than when it is allowed to flow through. Presumably this phenomenon is due to vapors arising from the organic matter in the chamber (insulators and rubber gaskets) or to air entering through very small leaks. The drift with static gas expresses itself as a decrease in pulse size for  $\alpha$  particles of a given energy as well as in a decrease of resolution, i.e., increased spread of pulse heights corresponding to a given energy. When the chamber is adequately vacuumtight, the drifts occurring with flowing gas are smaller than those occurring with static gas, and even these steady down to quite small effects after an initial flowing period. The importance of such drifts as do occur is minimized by the use of  $\alpha$ -emitting standards as described below. The potential on the high voltage is -1,500 to -2,500 volts for 1 atm and -3,000 to -4,000 volts for 2 atm.

Clark, Spencer-Palmer, and Woodward<sup>18</sup> have found that by using a system with practically no rubber and with wax joints, by pumping down to a high vacuum, and by very elaborately purifying the argon with hot copper and drying agents, no drifts due to gas deterioration would occur over some days when the static method was used. At Los Alamos and elsewhere (see references 14, 21, 23, 42, and 53) it has been found that continuous circulation of the argon over hot calcium achieved the same purpose after a preparation period of several hours. However, for large numbers of runs such elaborate preparations are prohibitively time consuming, so that the drifts that may be ascribable to insufficient gas purity have been accepted and their effects minimized, in so far as possible, by the use of standards.

Although the use of a small collectrode located at some distance (12 cm) from the sample tends to minimize the positive-ion effect, it does not eliminate it entirely. The effect may be calculated by using some simplifying assumptions and the mathematical device referred to above.<sup>47</sup> If the electrodes are approximated by two concentric spheres of radii  $\frac{1}{4}$  in. and  $4\frac{1}{4}$  in. and if the  $\alpha$ -particle specific ionization is taken as a constant, then the maximum positive-ion effect (vertically-emitted  $\alpha$  particle) at 1 atm pressure results in a reduction of pulse height of 1.6 per cent for an  $\alpha$  particle of 5.0 cm range, 1.2 per cent for an  $\alpha$  particle of 4.0 cm range, and 0.8 per cent for an  $\alpha$  particle of 3.0 cm range. An  $\alpha$  particle emitted at a small angle to the sample plate undergoes practically no positive-ion effect at all, so that these percentages represent the maximum pulse-height deviation due to the positive-ion effect alone. If the pulse-height distribution without positive-ion effect can be approximately represented by a Gaussian curve, then the reduction in the average pulse height is less than the maximum deviation, being 0.7 per cent for the 5.0-cm  $\alpha$  particle. The effect on the resolution is much less, a straggling parameter<sup>†</sup> of 1.0 per cent increasing only to 1.2 per cent.

The positive-ion effect is evidently nonlinear, being larger for more energetic  $\alpha$  particles. This factor does not introduce any added complications because the slight nonlinearity of the amplifier necessitates the use of  $\alpha$ -energy standards in any case.

The mild reduction of resolution by the positive-ion effect is of importance only when samples are counted at 50 per cent geometry. When, by the use of collimators, only vertically emitted  $\alpha$  particles are counted, all  $\alpha$  particles of a given energy are affected approximately alike. However, the nonlinearity of pulse height variation with energy still remains. The collimation technique is described below.

Besides the positive-ion effect, the angular distribution of the  $\alpha$  particles gives rise to another source of difficulty. The pulse shape and rise time from a vertically emitted  $\alpha$  particle are not the same as those of a horizontally emitted  $\alpha$  particle because of the different induction effects from the various  $\alpha$  tracks. This effect need cause no great difficulty if the amplifier is adequately designed.

**4.3 Amplifier.** The circuits are shown in Fig. 4. The entire amplifier has a moderately low frequency response (Fig. 5). This frequency characteristic was determined empirically to give the best resolution with the chamber of Fig. 3.

<sup>†</sup>If the distribution curve is approximately representable by a Gaussian error curve, the straggling parameter ( $\sigma$ ) is one-half of the width at  $1/e$  of the height (see Sec. 6).

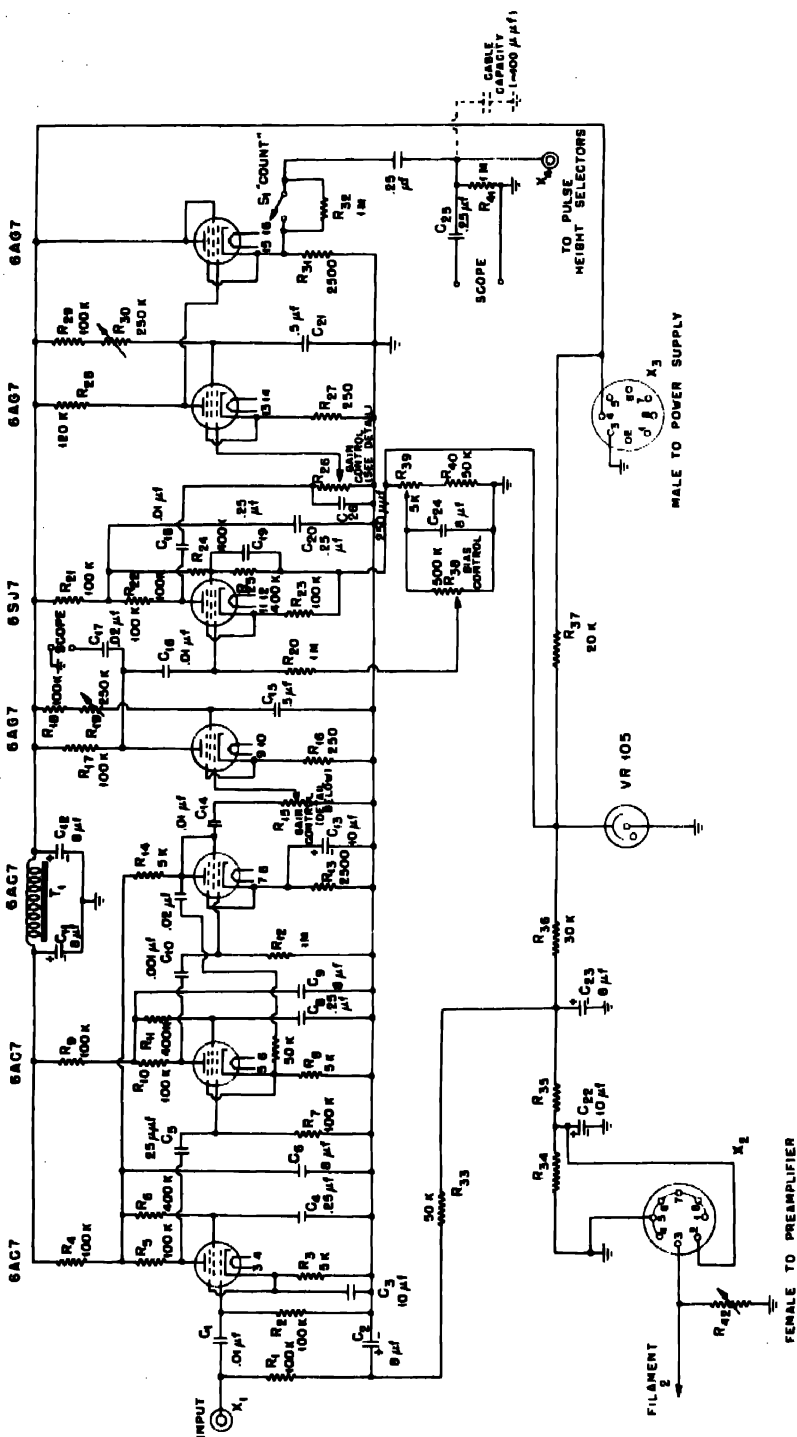


Fig. 4.—Pulse-analyzer amplifier circuit—(continued below).

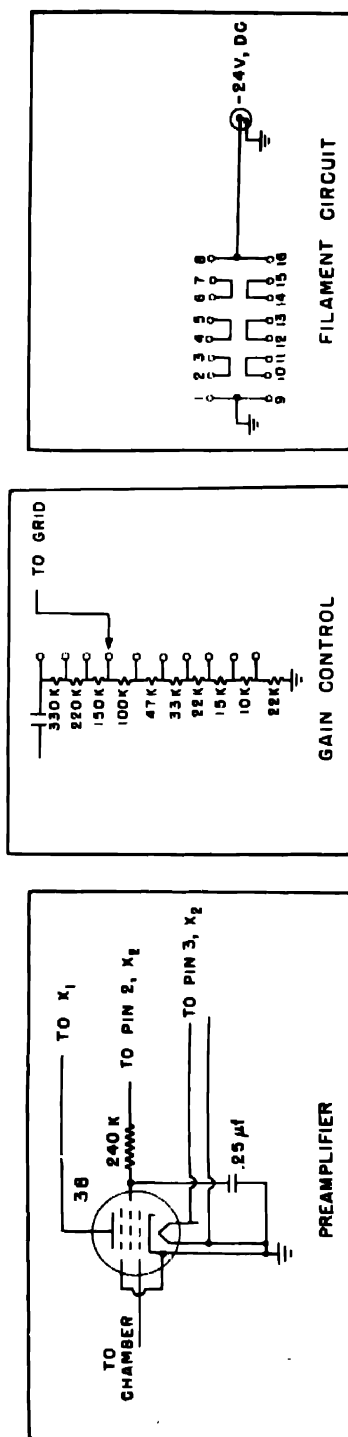


Fig. 4—Pulse-analyzer amplifier circuit.

The preamplifier is mounted directly on the chamber. The filament of the 38 tube is operated in series with the filaments of the first three amplifier tubes from a 24-volt d-c supply† piped into the counting rooms; one side of the 38 filament is grounded. The use of a regulated d-c filament supply prevents hum pickup through the filament and prevents gain variations due to filament voltage changes.

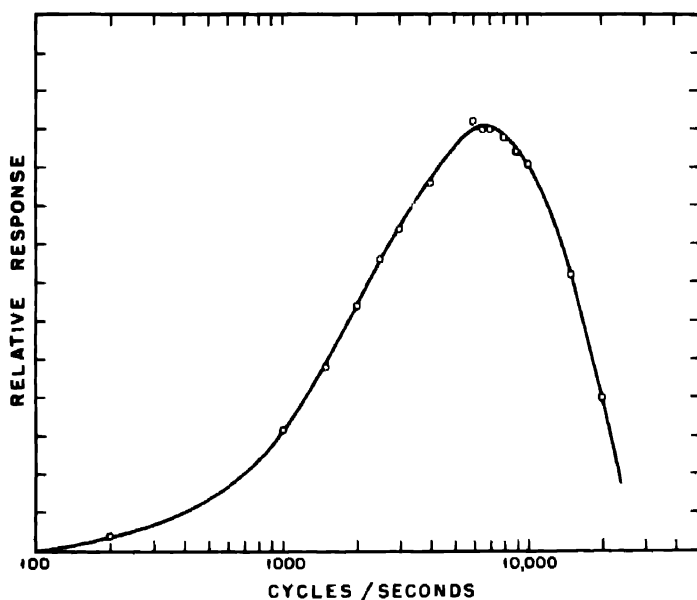


Fig. 5 — Pulse-analyzer amplifier frequency response.

The first amplifier consists of four stages followed by the pre-discriminator. The second amplifier consists of two stages, the last one being a cathode follower. Some of the problems in designing the amplifiers and prediscriminator were (1) to achieve a large signal as close to linear as practicable, (2) to design an output circuit with an output impedance sufficiently low so that the signal would not be attenuated when all the selector units were conducting, (3) to obtain a constant gain and discrimination level, and (4) to use a frequency response that would allow pulses of various rise times to come through with the same output heights.

It is desirable to have a large signal for the prediscriminator input and for the input to the 48 selector units in order to minimize the

†Regulated battery-less supply (Nobatron: Sorenson and Co.)

effect of drifts in the discriminator sensitivities. A linear signal is desirable so that the pulse heights may be linearly related to the  $\alpha$  energies. However, small departures from linearity can be easily allowed for by calibration. There was no difficulty in obtaining linear amplification from the first three stages of the amplifier since the outputs of these tubes are at a low signal level. The fourth stage, however, and the amplifying stage following the prediscriminator are both identical, giving a 160- to 170-volt pulse output. Each has a 250-ohm unby-passed cathode resistor to help increase linearity, and each has a variable screen resistor to adjust for linearity. This adjustment is discussed later in the section on tuning the analyzer.

When the 48 thyratrons in the analyzer strike simultaneously, the grid-to-ground impedance is lowered sufficiently to decrease the signal voltage unless the impedances of the thyratron grid circuits are isolated from the plate circuit of the last amplifying stage. Owing to the finite rise time of the pulse, thyratrons with a larger bias strike later than do those with smaller bias,<sup>10</sup> so that it is important to avoid changing the pulse height by loading the output. To reduce the output impedance, the output amplifier is coupled to a cathode follower on the amplifier chassis which is in turn connected to each of eight cathode followers on each of the eight selector chassis. The low output impedance of the cathode follower also reduces capacitative losses in the cable. Each of the cathode followers uses a 6AG7 tube chosen for its high transconductance, and each of the cathode followers on the selector chassis has a 10,000-ohm stopping resistor in series with the grid in order to prevent oscillations. There is no measurable attenuation of the signal when all the thyratrons are conducting.

The prediscriminator is a 6SJ7 tube operated as a phase inverter. Its cathode is connected through a 0.1-megohm resistor to a 105-volt source stabilized by a VR-105 tube. The grid bias is also derived from the stabilized 105-volt source, and it may be varied with the potentiometer R-38 (bias control). The adjustment of this control in conjunction with the adjustment of the first amplifier gain control (R-15) shifts the position of a particular  $\alpha$  peak among the channels. R-39 is a tapped resistor, which is adjusted so that the zero position of the bias control corresponds to the cutoff voltage of the tube.

Since the pulses entering the prediscriminator are of the order of 100 volts in height, a change of 0.1 volt in the cutoff voltage of the 6SJ7 introduces an error of only 0.1 per cent. The variation in the tube cutoff is ordinarily no greater than 0.1 volt, although fluctuations in the VR tube may result in tripping height variation of as much as 0.3 volt.

The prediscriminator has a gain of 1 since its unby-passed cathode resistor is equal to the plate load resistor. The current feedback resulting from the unby-passed cathode resistor serves to give a linear response for large pulses. The output of the prediscriminator is amplified in a stage identical with the one preceding the 6SJ7 and is fed through the cathode follower output to the 48 channels as described above.

The frequency response shown in Fig. 5 was determined empirically to give the best resolution with the chamber and gas used. The high-frequency response is determined by R-26 and C-26, while the low-frequency response is fixed by R-7 and C-5. Other combinations would undoubtedly work as well; these were left as they were when it was found that they gave good results. The necessity for adjusting the frequency response in this manner occurred primarily when 50 per cent geometry was used. In this case, as discussed above, the pulse rise time depends upon the angle of emission of the  $\alpha$  particle. When the  $\alpha$  particles are collimated, the effect of the frequency response upon pulses of various rise times is relatively unimportant since collimated  $\alpha$  particles give pulses of about the same rise time.

An analysis of the circuit provides an explanation for the existence of an optimum frequency-response band for the chamber and gas used and also for the fact that the pulse height and resolution decrease when a certain optimum high-voltage value is exceeded. The analysis<sup>54</sup> of a circuit whose upper frequency cutoff is determined by one RC constant and whose low frequency cutoff is determined by another RC constant shows that a graph of pulse height vs. pulse rise time goes through a maximum. The breadth of this maximum is determined by the breadth of the frequency-response curve. The moderately narrow band of the present amplifier is adjusted for the rise times occurring with the chamber and gas used. Increase of high voltage beyond a certain point increases the electron velocity, decreasing the rise time of some pulses beyond the maximum. These pulses are diminished in size thus worsening the resolution by broadening the pulse-distribution curve.

At times, when slight leaks or other sources of gas impurities developed, the resolution at 50 per cent geometry was seriously impaired, presumably because the rise times changed sufficiently to move away from the maximum in the curve of pulse height vs. rise time. In these cases operation with collimated sources was feasible. When the leaks became more serious, even collimated sources showed poor resolution, presumably because of negative oxygen ion formation.

The straggling contributed by the amplifier noise and other variations in the electronic circuits was tested by the use of artificial

pulses. The output of a pulse generator, suitably attenuated,<sup>37</sup> was delivered to the collecting electrode by capacitative coupling through the high-voltage electrode. Since the driving frequency was derived from the 60-cycle supply, the output pulses were synchronized with 60 cycles, thus minimizing the variations due to the slight hum in the pulse-generator output. The pulse input was adjusted so that the output corresponded to that caused by a 5-mev  $\alpha$  particle. By roughly approximating the pulse distribution with a Gaussian curve, the straggling parameter was found to be about 12 kev (0.24 per cent). This value gives an upper limit to the straggling due to such electronic factors as amplifier noise. Since, as will be discussed later, this value is less than that found for  $\alpha$  particles, the resolution of the present instrument has not been limited by amplifier noise. The relatively low noise level is at least partially due to the moderately narrow frequency-response band of the amplifier.

**4.4 Multichannel Selector Units.** The multichannel analyzers mentioned above, as well as the one described here, have in common the fact that each channel contains three essential components: (1) a discriminator whose tripping action is set by an externally supplied bias and whose output pulse is independent of the tripping pulse, (2) a cancellation circuit, which cancels the output pulse in all those channels tripped by a pulse except in the channel with highest bias, and (3) a recording circuit. The discriminator outputs should all be the same in order to provide trouble-free cancellation action. The discriminators used have been either thyratrons or trigger pairs, either of which give constant-output pulses. Trigger-pair circuits can be made somewhat more stable in tripping level than thyratrons and can be used at higher counting rates, but they require more circuit components. In order to simplify the circuit construction, thyratrons (type 2050) are used as the discriminators in the analyzer described here. Other factors keep the useful counting rates low enough so that the thyratron is no limitation. The drift of the thyratrons, however, is important and will be discussed below.

The cancellation circuits must allow only the channel whose bias voltage corresponds to the peak voltage of the pulse to record that pulse. For example, if a pulse trips the discriminators of channels 1 to 5, the output pulse from the channel 2 discriminator cancels the output pulse from the channel 1 discriminator, channel 3 cancels channel 2, etc. Only channel 5 remains uncancelled and thus is the only one to record.

Several types of cancellation have been used. In one general type the pulses from the discriminators are used to cancel each other. In one such scheme<sup>38,40</sup> pulses from adjoining channels are fed into a

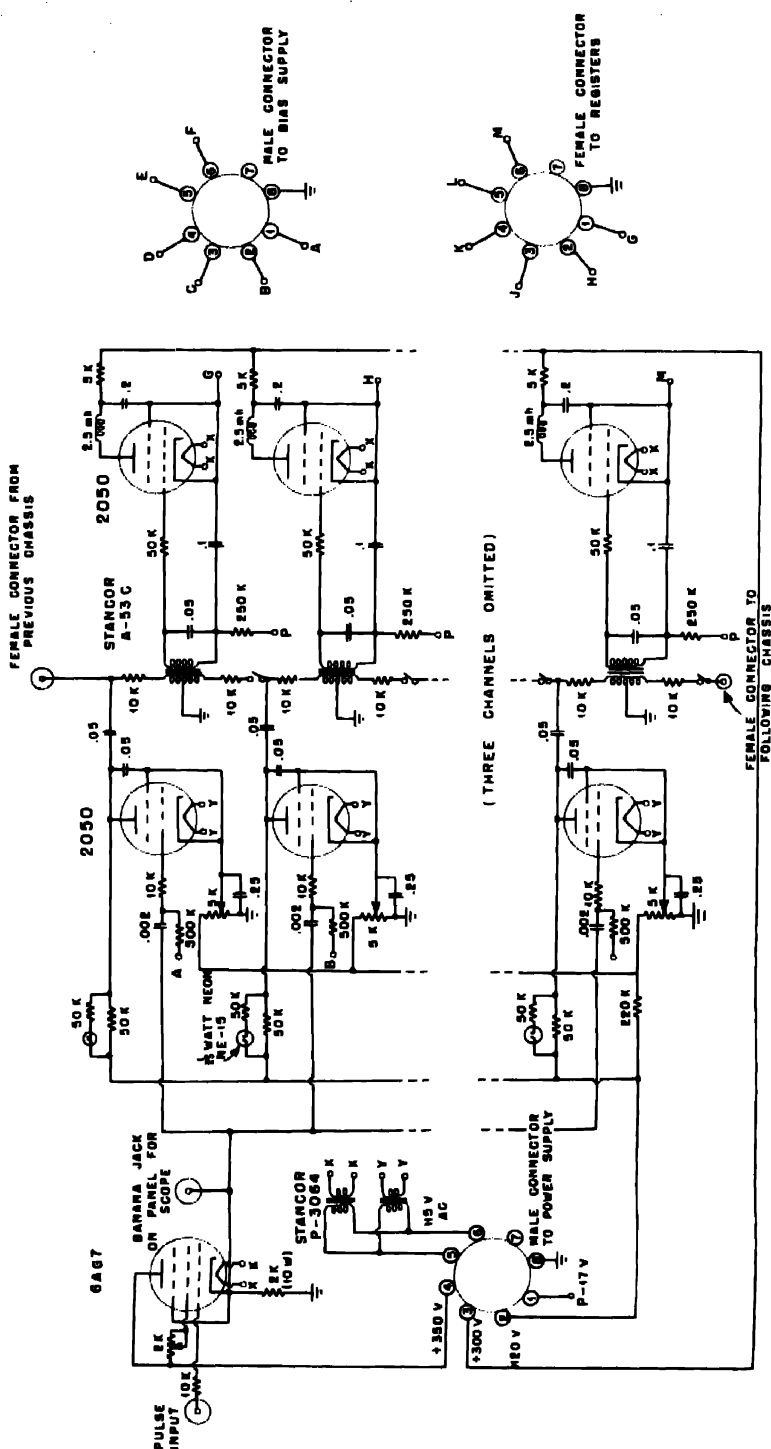


**Fig. 6**—Pulse-analyzer pulse selectors.

multigrid mixer tube in opposite phase; a signal emerges into the recorder only if just one pulse enters the mixer. In another method of this type the pulses from adjacent channels are fed into the opposite ends of an impedance, the total output being the algebraic sum of the two. Cancellation occurs unless only one pulse enters this impedance. One of the British analyzers<sup>18</sup> uses a resistive cancellation circuit of this type, but the analyzer described here uses an interstage transformer. Because of the finite rise time of the pulse emerging from the amplifier, direct cancellation of the discriminator output pulses can be used only with relatively slow pulses.<sup>40</sup>

For cancellation at high counting rates with circuits utilizing fast pulses, gating circuits have been used.<sup>37,38</sup> A pulse from the discriminator activates a gating tube, which may also be deactivated by a pulse from the neighboring channel. A timing circuit, activated by the pulse output of the amplifier, sets off the gating circuits of all the channels at the same time. Only that gating circuit which has been activated by its own channel and has not been deactivated by its neighboring channel allows the count to go through. Since the activating and deactivating pulses can be made to span the rise time, even very fast circuits can be made to cancel correctly with pulses of finite rise time. This type of cancellation circuit is quite complicated, involving many circuit components, so that it would be of little advantage with the analyzer described here, in which the amplifier frequency response and the recorders limit the pulse speed and hence the counting rate.

In this analyzer, the thyratron pulse-height selectors (Fig. 6) consist of eight identical banks. Each bank contains a 6AG7 cathode follower, six selector thyratrons, six cancellation circuits, and six recorder thyratrons. The latter are connected by cable to the recorders, which are mounted in an adjacent relay rack. The eight pulse-selector banks together with the amplifier occupy the other relay rack. Each of the eight banks is connected to the preceding one through a shielded cable to provide cancellation between the first tube of one bank and the last tube of the preceding bank. The last selector on the last bank counts all pulses whose voltages are greater than its bias setting, whereas each of the other selectors counts only those pulses whose voltages are within its 3-volt band.

The cathode follower in each chassis feeds the pulses to six units. Each unit contains a thyratron pulse-height selector, a transformer cancellation circuit connected to the preceding and succeeding units, and a thyratron recording circuit. The bias for each of the 48 selectors comes from an external bias supply. The channel width is variable, but if, as is usual, it is set at 3 volts, then the external bias

supplied to each thyratron is 3 volts more negative than that on the previous tube. Variations in the cutoff characteristic of each thyratron may be corrected for by means of a potentiometer in the thyratron cathode circuit, which can be adjusted from the front panel. A small (approximately  $2\frac{1}{2}$  volts) positive voltage is applied to the potentiometer, and the cathode is tapped off it. The methods of adjusting the 48 potentiometers will be discussed in Sec. 4.7.

In the plate circuit of each 2050 discriminator tube, there is a neon light, mounted on the front panel, which flashes when the tube conducts. This enables visual observation of each pulse height and aids in the tuning process. The thyratron quenching is due to the drop of plate voltage resulting from the discharge of the  $0.05-\mu f$  plate to cathode condenser. Plate voltage is restored by charging through the 50,000-ohm plate load resistor. In each thyratron grid circuit is a 10,000-ohm resistor, which serves to keep the grid impedance during discharge relatively high so that the discharge of the first thyratron does not short-circuit the cathode follower.

The cancellation circuit is a modification of one described by Roberts,<sup>35</sup> and it involves the use of a push-pull transformer for mixing the cancelling pulses. The pulse output of the 6AG7 cathode follower is positive, and if it exceeds the bias on the first selector, the tube trips, giving a negative pulse of about 100 volts, which passes through one side of the transformer. If the cathode follower pulse is too small to trip the second selector, there is no cancelling voltage; and the negative pulse to the input of the transformer appears as a positive pulse of about 100 volts on the secondary output. Since the recording thyratron is biased to only -17 volts, it is tripped by the output pulse, thus activating the register and recording the count. If the cathode follower pulse is large enough to trip the second discriminator, its negative output pulse is applied to the opposite end of the transformer primary in the first channel, and no pulse emerges from the transformer secondary. Since the recording thyratron bias is -17 volts, considerable inequality in the discriminator outputs and the primary windings can be tolerated because incomplete cancellation does not result in recording unless the difference exceeds 17 volts. In practice no difficulty has been encountered even with aging tubes. As may be seen in Fig. 6 the first thyratron selector in each chassis does not have the same plate load as the other thyratrons, except by connection to the previous chassis. To make the plate load for the first thyratron in the first chassis the same as that of the other selectors, a dummy transformer is used. To allow all the chassis to remain interchangeable, this transformer is mounted on

a plug which fits into the female normally used to connect to the previous selector bank.

The recorders are of the Cyclotron Specialties type, which can be made to run at a rate of 60 per second on uniform pulses. To conserve space and for ease of mounting, these were removed from their cases and mounted on panels. It was found that when the recorders were used in the plate circuit of the recording thyratrons, grounding of the recorder shell with the coils at high potential resulted in occasional short-circuiting of the relay coils. Since the d-c voltage on the cathode is zero when the tube is nonconducting, the recorders were placed in the cathode circuits, thus removing the shorting danger.

In each of the cancellation circuits is a switch that is normally closed to allow cancellation. When these switches are open, an integral rather than a differential distribution is measured since each register then records all of the pulses that trip its discriminator. Such integral curves are sometimes used to measure the total counts in a certain number of channels (corresponding perhaps to a particular nuclide) without the bother of adding up the counts in each channel. Usually differential curves are preferred since they not only give the energy distribution directly but also allow higher counting rates. When an integral curve is determined, the first few channels must record all the pulses. Since the recorders limit the useful counting rate per channel, the total counting rate must then be fairly low. When the counts are spread by the differential method over many channels, the counting rates can be considerably higher.

The last register records all the pulses larger than the bias on the last channel.

**4.5 Bias Supply.** The bias supply (Fig. 7) consists of a voltage divider supplying 48 leads which go to the 48 thyratron pulse-height selectors. The first lead can be supplied with any voltage from 0 to 159 volts, and the others can be supplied with voltages increasing by constant steps (called the "channel width"), usually 3 volts, but which may be 2, 1,  $\frac{1}{4}$ ,  $\frac{1}{10}$ , or 0 volts. The channel width is determined by switch S3. The various resistor values were accurately adjusted to give the proper voltages. The parallel and series resistances at the various settings of S3 determine the total voltage across the 48 precision bias resistors, and they thus determine the voltage across each one. They also maintain the total resistance in the voltage-dividing network constant, so that changes in the channel width do not affect the range control.

The voltage on the first thyratron (range) is determined by switches S4 and S5. Since S4 is also arranged so that changes in its setting do

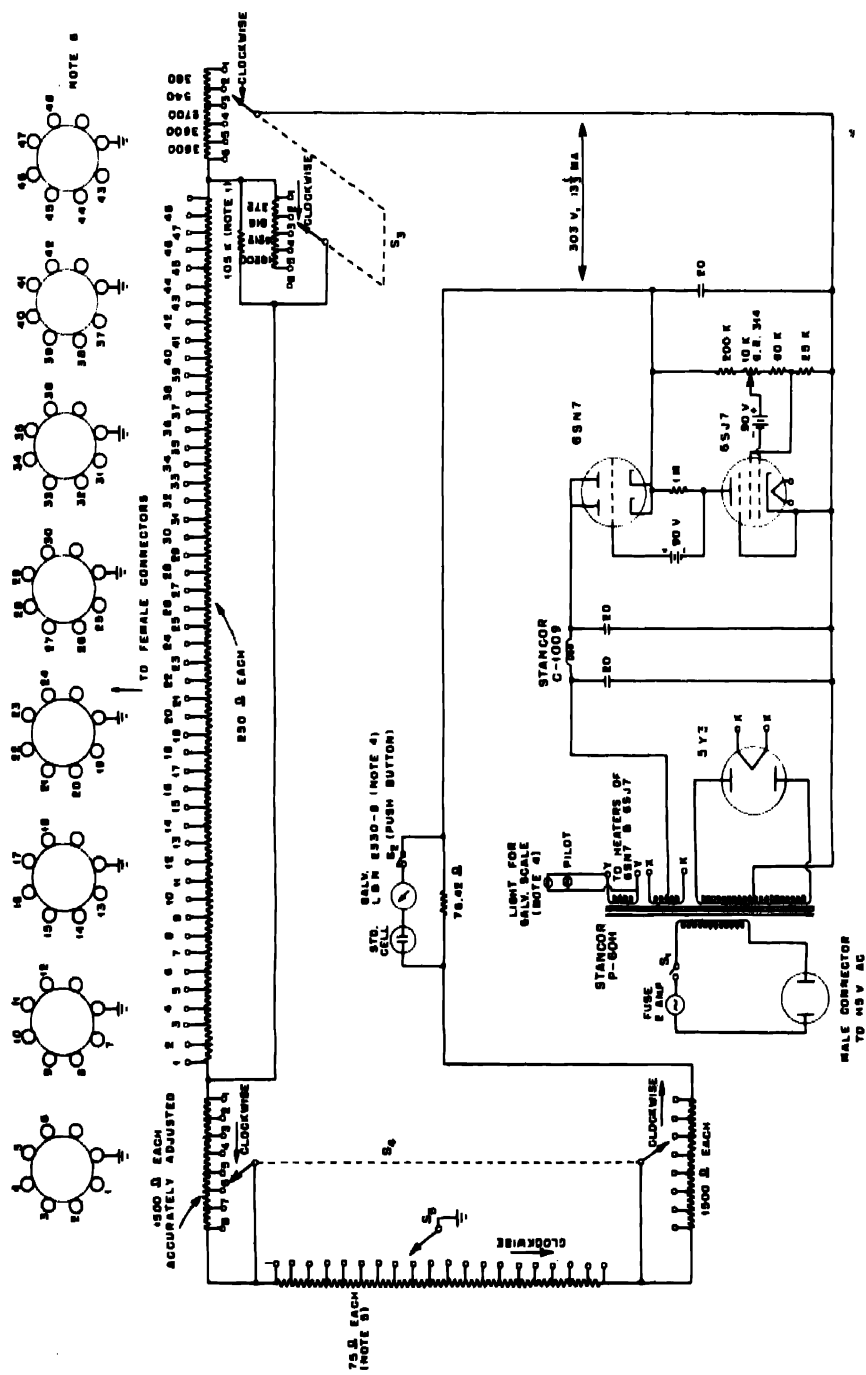


Fig. 7.—See facing page for legend.

not affect the total resistance in the voltage-dividing network, changes in the range control do not affect the band width. S4 provides voltages in 20-volt steps from 0 to 140 volts, and S5 provides voltages in 1-volt steps from 0 to 19 volts. A change in the range control, by changing the bias of the first thyratron selector, changes the bias of each of the selectors by the same amount since the bias difference between successive thyratron selectors is constant.

The original purpose of incorporating variable range and channel-width controls was to allow the pulse distribution from a mixture of  $\alpha$  emitters to be examined in greater or less detail, as desired. Increasing the range-control setting brings the higher-energy  $\alpha$  particles into the recording region of the instrument. Decreasing the channel width increases the sensitivity and detail with which a particular  $\alpha$ -energy region is examined. In actual practice neither control is varied, except during the tuning process. The range control is generally set at 10 volts, and the channel width is set at 3 volts. The maximum channel width is used since using smaller channel widths accentuates the effect of small drifts in the thyratron cutoff characteristics. In practice, changes in the region or detail of examination are made by varying the gain controls in the amplifier and by varying the bias setting of the prediscriminator.

The voltage divider is supplied with 303 volts from a regulated power supply whose reference voltages are taken from dry batteries. The current through the divider is standardized against a standard cell by bucking the cell against the voltage generated across a 76.42-ohm resistor. Divider current changes may be corrected by adjusting the grid bias of the 6SJ7 regulating tube until the galvanometer is balanced at zero. The 48 bias voltages are carried through eight octal cables to each of the eight selector chassis.

Fig. 7.—Pulse-analyzer bias supply.

Note 1. This resistor is adjusted so that the parallel combination has a value of exactly 10,800 ohms.

Note 2. All resistors are wire-wound precision resistors, IRC type WM-4, except for the voltage control to the 6SJ7, which is a General Radio, type 314, potentiometer.

Note 3. The channel widths (voltages obtained across each 250-ohm resistor) are 0, 0.1, 0.25, 1, 2, and 3 volts for positions 1, 2, 3, 4, 5, and 6, respectively on switch S<sub>3</sub>. This is a two-pole six-position switch.

Note 4. The galvanometer is mounted on the chassis behind the panel. The needle is viewed through a 1-in. hole in the panel, and is illuminated with a 6.3-volt pilot lamp placed on one side of the scale.

Note 5. These resistors are adjusted so that the total resistance is 1,425 ohms.

Note 6. These connectors are octal sockets mounted on the back of the chassis.

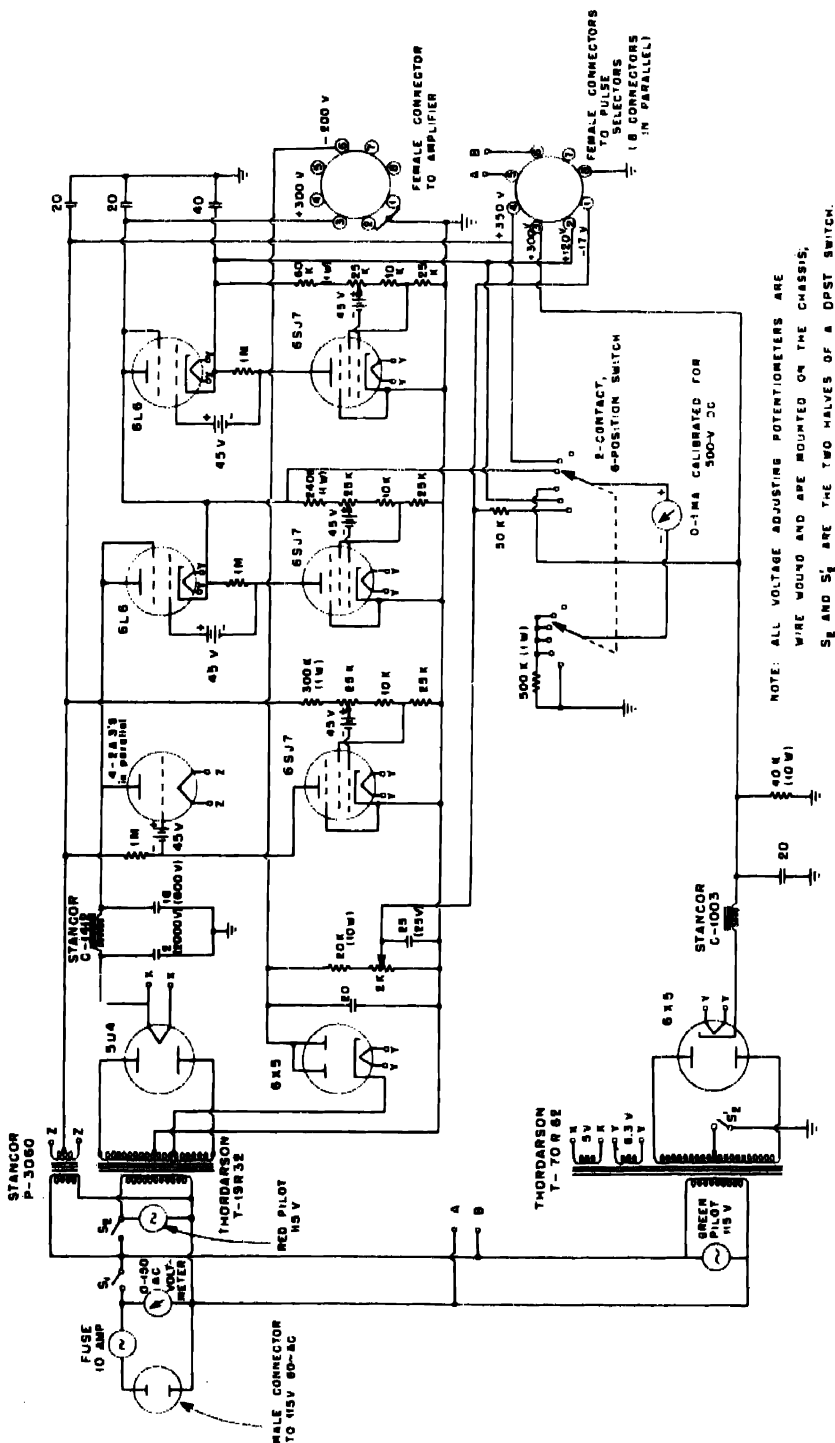


Fig. 8—Pulse-analyzer power supply.

**4.6 Power Supplies.** The low-voltage power supply (Fig. 8) furnishes the following voltages: regulated 350 volts for the 6AG7 cathode followers on the pulse-height selector chassis, regulated 300 volts for the amplifier B+ supply, unregulated 300 volts for the register-driving thyratrons, regulated 120 volts for the selector thyratrons, and unregulated -17 volts for the bias on the register thyratrons. The power supplies are regulated by circuits similar to those used in the bias supply.

The high-voltage supply<sup>55</sup> supplies up to -5,000 volts and is regulated by the use of an a-c saturated transformer. The voltage is adjusted by means of a variable autotransformer in the primary.

The entire 110-volt a-c supply is regulated by means of a Sola transformer.

**4.7 Tuning the Analyzer.** The high-level stages in the amplifier are adjusted for approximate linearity by varying the screen resistors. This adjustment is only approximate, but it serves to avoid gross nonlinearity. After the first lining up, the drift of the circuits is seldom large enough to be detectable by the test used. A signal from a stabilized pulse generator is introduced into the grid of the fourth amplifying stage (6AG7). The output of this stage is connected to the horizontal amplifier of an oscilloscope while the pulse generator is connected to the vertical amplifier. The screen resistor is varied until the scope pattern is a straight line. A similar adjustment is made on the other high-level amplifying stage. Using the pulse generator, the output cathode follower is checked by observing the pulse output with all the thyratrons firing (range control at zero) and with none firing (range control set high). There should be no observable change in the oscilloscope.

Because the analyzer is in constant operation, the components age and drift sufficiently in about a month to require tuning of the selector circuits, although precise work may require more frequent tuning. At times the analyzer has been in operation for two to three months without retuning. The major portion of the drift is probably due to changes in the triggering points of the thyratrons and in the transconductances of the cathode followers. The process of tuning involves adjusting the potentiometers in the cathode-follower screen circuits and in the thyratron-selector cathode circuits until the selectors trip on pulses of the correct voltage.

The method for lining up the selector units involves the use of a pulse generator and the range and bias controls. The pulse generator is connected at some convenient point in the amplifier (generally the second gain control), the channel width is set at zero, and the coarse range control is set at about 130 volts. The pulse generator is then

set so that the selectors are just firing. The triggering of a channel can be easily observed by the flashing of its neon light on the front panel. With slow variation of either the pulse generator or range control the thyratrons which trip at voltages either above or below the norm are located. If they are not too far off, the tripping points may be adjusted with the cathode potentiometers; otherwise the tubes are replaced. For fine control, the pulse is fed in before the prediscriminator, and its bias voltage is varied.

If an entire bank of six selectors is off (either low or high), all (or most) of the channels in that bank will trip before or after the others. The banks may be adjusted relative to each other by adjusting the resistors in the cathode-follower screen circuits while slightly varying the output of the signal generator (or prediscriminator bias) so that the selectors are alternately tripped and are not conducting. Variation between banks can be minimized by using matched 6AG7 cathode-follower tubes. By proper selection of tubes, transconductances can be matched to about 5 per cent.

The entire operation is repeated at several settings of the range control and pulse generator, with adjustments of thyratron and 6AG7 circuits. A method suggested by Kohman<sup>56</sup> for systematically repeating this operation enables the adjustment to be made fairly rapidly. Zero channel width and a large pulse (and correspondingly high voltage on the range control) are used, and the cathode-follower screen resistors are adjusted until all or almost all the channels fire simultaneously. With a small pulse (and low range voltage), the thyratron potentiometers are adjusted until all fire simultaneously. However, the adjustment of the thyratrons at small pulse levels disturbs the alignment at high pulse height, so that the entire alignment procedure is repeated until no discrepancies occur at both pulse heights. Only a few repetitions are necessary since the discrepancies disappear rapidly.

The particular sequence used results from the fact that variations in the cathode-follower gains are of little importance for small pulses, but they are of considerable importance for large pulses. Thus, if  $e_i$  = pulse voltage from pulse generator,  $g_k$  = gain (less than 1) of one cathode follower, and  $e_r$  = range control voltage, then, with zero channel width, the voltage put on the thyratron grids of one selector bank is  $e_i g_k - e_r$ . Suppose  $e_i = 150$  volts, and that  $e_r$  is selected so that the net output voltage is zero for one selector bank. If the gain  $g'_k$  of another cathode follower differs by 5 per cent from  $g_k$ , then the output voltage will differ from zero by 7 volts. If  $e_i = 5$  volts, then the output voltages differ only by  $\frac{1}{4}$  volt. Thus the cathode followers are adjusted with large pulses, where differences in their out-

puts are more important than differences due to misalignment of the thyratron selectors. Correspondingly, the selectors are adjusted with small pulses, where differences between the thyratron selectors are more important than differences due to cathode-follower variation.

As a final test, the tripping of the channels is checked with the range control. First the channel width is set at 1 volt, the pulse generator is set so the last register trips, and the range control is increased in 1-volt steps, so that each register trips in turn. Then the channel width is set at 0.1 volt, and the pulse generator output is varied slowly, so that each succeeding register trips in turn. Since the channel-width bias used regularly is 3 volts, this ensures that the error in the effective channel width is no greater than 3 per cent. A single  $\alpha$  peak is usually covered by at least four or five registers, so that errors tend to cancel when the total count in one peak is determined, unless there is a consistent error in the selector settings. To check the possibility of such cumulative errors, the range control is advanced in 1-volt steps with the channel width set at 0.1 volt. The channels tripped at each range-control setting should change in groups of ten. With a few different pulse-height settings, the possibility of cumulative errors is eliminated.

Despite the tuning, some of the selector banks seem to get out of line more rapidly than would be expected. It is felt that these drifts are due to the thyratrons and to the use of eight cathode followers. Future circuits will utilize more stable selector circuits and will avoid the use of multiple cathode followers.<sup>†</sup>

The registers used have a number of adjustments that can slip or wear over a period of time. Part of the tuning process therefore involves checking and adjusting the registers. The method of adjusting Cyclotron Specialties registers is described elsewhere.<sup>57</sup> Several methods can be used to check them. One is to determine the counting rate of a pulse generator whose repetition frequency has been calibrated. The range control is used to bring in one register at a time, and its ability to follow the pulse generator is determined. Another method, although much noisier, is faster. The switches in the primary circuits of the cancellation transformers are opened. A pulse large enough to trip the last channel is used. All the registers fire away

<sup>†</sup>The circuit has been modified,<sup>58</sup> so that the output of the last amplifier tube drives a single cathode follower composed of eight 6AC7 tubes in parallel. This cathode follower, which has about 100 ohms output impedance, drives the selector thyratrons directly. To decrease the short-circuiting effect of conducting thyratrons, the series grid resistor of the selector tubes has been increased to  $\frac{1}{2}$  megohm, by-passed by a  $25-\mu\mu f$  capacitor.

simultaneously as pulses come through, and it can soon be seen if any are counting ahead or behind the others.

After being tuned, the instrument is usually recalibrated with a standard containing an artificial mixture of several  $\alpha$  emitters of known energy. This is a final check on the tuning process since the counts should fall on smooth distribution curves.

##### 5. SAMPLE PREPARATION AND EFFECT OF SELF-ABSORPTION

To get good results in an  $\alpha$ -energy analysis, self-absorption in the sample must be quite small. For vertically emitted  $\alpha$  particles, the effect of sample thickness is not very serious, within limits, since a vertical  $\alpha$  particle from a sample of surface density 40  $\mu\text{g}/\text{sq cm}$  loses an average of about 0.01 mev. However, the  $\alpha$  particles emitted at an angle to the perpendicular lose considerably more energy, the amount lost increasing with angle. Self-absorption not only reduces the apparent energy, but it also decreases the resolution by spreading the peak. A "thick" sample measured at 50 per cent geometry has a very marked low-energy tail extending down toward zero energy; the greater the thickness, the larger the fraction of  $\alpha$  particles appearing in this tail.

The best kind of sample for use in the analyzer consists of a thin uniform film spread on a smooth surface. A simple method for making samples of this type involves electroplating on polished metal surfaces. (The details of technique in this and other methods have been discussed elsewhere.<sup>2,58,59</sup>) Another method which gives very good samples involves the evaporation of the active material onto a cooled plate in high vacuum. Although the samples prepared in this fashion are more uniform than those made by any other technique, the labor and apparatus involved make the method impractical for most samples. The electroplating method, where applicable, has proven to be the best method. For the best samples, polished stainless steel or Stellite have been used, although disks punched from bright surfaced platinum sheet have given fairly good results. In any of the methods of preparation the sample plate is heated to a high temperature after preliminary drying, in order to remove acids, volatile salts, and traces of moisture. If the platinum sheet is thin (less than 0.005 in.) and if it is strained, it may warp on heating; an  $\alpha$  particle colliding with the warped part of the plate would then give rise to short pulses. The plate may be taped to a thick aluminum disk to flatten it out.

If the radioactivity to be investigated is in solution with a quantity of nonvolatile salt, the activity must be chemically concentrated be-

fore it is practical to prepare samples. Such separation may be performed by solvent extraction, by resin column adsorption, by electrolysis, or by precipitation with specific carriers. The solutions resulting from solvent extraction or resin column absorption may be essentially free of nonvolatile salts, and they can therefore be directly evaporated to give a thin film.

It is often not feasible to use samples prepared with carriers at 50 per cent geometry because of the difficulty in making a solid spread uniformly. Even if the carrier is redissolved and spread, it often tends to clump after evaporation of the solvent. The use of relatively nonvolatile spreading agents (e.g., tetraethylene glycol, TEG) serves to make the deposition more uniform by causing evaporation from a film rather than from a droplet.

In cases where it is necessary to avoid separation of different chemical elements (e.g., uranium and plutonium), chemical concentration from nonvolatile salts may not be feasible and the original material must be spread. The thickness may then be so great that the energy straggling may be excessive, even with the use of TEG. In this case and when there are large amounts of carriers, samples cannot be used at 50 per cent geometry. The collimation methods used are described below.

## 6. RESOLUTION

The ability to detect the presence of one peak when it lies very close to another is determined by the natural width of the peak. Under good conditions, the peak shape may be represented by a Gaussian curve of the form

$$P(E) dE = \frac{1}{\alpha \sqrt{\pi}} e^{-[(E-E_0)^2/\alpha^2]} dE$$

[ $E$  = the energy corresponding to particular pulse height,  $P(E)dE$  = the probability that a particular  $\alpha$  particle gives rise to a pulse corresponding to energy between  $E$  and  $E + dE$ ,  $E_0$  = energy corresponding to maximum of peak,  $\alpha$  = straggling parameter = one-half the peak width at  $1/e$  of the peak height.] When the Gaussian shape applies, the peak width may be described by the straggling parameter, although some authors have used the "half width" (total peak width at one-half the peak height). For a Gaussian curve, the half width is 1.67 times the straggling parameter. Even though the peak shape deviates somewhat from a Gaussian shape, it is still useful to use the straggling parameter measure of peak width. The use of the straggling param-

eter rather than the half width as a measure of resolution is arbitrary since one can be calculated from the other if the pulse shapes are actually Gaussian. Because of asymmetric straggling, however, it is preferable to use a measure of peak width which is determined lower down on the peak. Such a practice gives greater weight to the low-energy tail. Although the choice of  $1/e$  the peak height is certainly arbitrary, the authors believe it to be preferable to the use of the half width.

The width of the approximate Gaussian curve gives a measure of the ease or the possibility of distinguishing another peak close in energy. From the Gaussian measure, however, the ability to find a second peak should be a function only of the straggling parameter and the energy difference ( $\Delta E$ ) of the two peaks, and should not depend upon whether the energy of the second peak is greater or less than that of the first. Actually some of the straggling factors are asymmetric in their effect, which results in greater straggling on the low-energy side. They have the effect not only of widening the peak but also of shifting the peak toward lower energy and, in some cases, of creating a low-energy tail which stretches toward zero energy. If the energy of the first peak is  $E$ , and that of the second peak is  $E - \Delta E$ , it will then be harder to find the second peak than if its energy were  $E + \Delta E$ . In fact, if the second peak is lower in energy and if it is present in very low concentration, it may be impossible to locate it. Despite the fact that the straggling parameter is not an unambiguous measure of the resolution, it is very useful for those cases in which the second peak is present in a concentration sufficient to keep it from being lost in the low-energy tail. This is true only when most of the  $\alpha$  particles (of the more energetic group) are in the main part of the peak. However, when the asymmetric effect is large (e.g., with thick samples), the straggling parameter has little significance because a large fraction of the  $\alpha$  particles is then in the low-energy tail.

Since the natural spread (as emitted) of the  $\alpha$  energies is much less than 1 ev, the observed straggling is an instrumental effect. From the emission of the  $\alpha$  particles to the recording of the resulting pulse height, a number of steps are involved, each step independently introducing its own statistical variations. The most important sources of straggling are (1) source straggling, due largely to variations in self-absorption (energy loss of the  $\alpha$  particle in solids on sample plate) and to  $\alpha$  back-scattering; (2) ionization straggling or variation in number of ion pairs formed by  $\alpha$  particles of identical energy; (3) chamber straggling, due to such things as the positive-ion effect or grid capture of electrons; and (4) amplifier noise. Because the straggling effects are independent of each other, the total straggling pa-

rameter is taken as the square root of the sum of the squares of the individual parameters:

$$\alpha^2 = \alpha_s^2 + \alpha_i^2 + \alpha_c^2 + \alpha_n^2$$

where  $\alpha$  = total straggling parameter, and s = source, i = ionization, c = chamber, and n = amplifier noise.

As mentioned above (Sec. 5), a thick sample results in energy degradation of many of the  $\alpha$  particles, the energy losses being greatest for  $\alpha$  particles emitted at small angles to the sample plate. At 50 per cent geometry this results in a long low-energy tail, but the tail may be decreased in magnitude by collimation (Sec. 7.4).  $\alpha_s$  is of the order of magnitude (1.5 to 2 times) of the energy lost by an  $\alpha$  particle emitted vertically through the entire sample thickness. Thus for a heavy metal oxide (e.g.,  $U_3O_8$ ) uniformly spread on a smooth plate,  $\alpha_s$  is very roughly 15 kev for a  $20 \mu\text{g}/\text{sq cm}$  sample.

Chamber straggling for the type of chamber used in the present instrument is of several types. If a small amount of oxygen is present, there is a statistical variation in the number of electrons captured. At 50 per cent geometry there is a variation in the positive-ion effect. As mentioned above (Sec. 4.2), if the straggling of a 5.0-cm (6.3 mev)  $\alpha$  particle were 1.0 per cent (63 kev), then the total straggling is increased by the positive-ion effect to 1.2 per cent, that is  $\alpha_{\text{positive ion}} = 41 \text{ kev}$ . If the rise times of the pulses corresponding to a particular  $\alpha$  peak are not all the same (e.g., at 50 per cent geometry), the amplifier frequency response may be such as to cause slight variations in the amplification of the pulses. The last two effects are decreased by collimation since they arise from differences between pulses from vertically and horizontally emitted  $\alpha$  particles.

It was pointed out (Sec. 4.3) that the amplifier noise was not a serious source of straggling since pulse-generator tests show  $\alpha_n$  to be about 12 kev.

Ionization straggling has not been investigated to any great extent. It is quite different from range straggling, which results from variations in the number of collisions per unit path length as well as in the energy lost by the  $\alpha$  per collision. Ionization straggling arises from variations in the energy required to form an ion pair. Because a majority of the ion pairs are actually formed by  $\delta$  rays (fast secondary electrons knocked out by the  $\alpha$  particle), there are more actual ionizing events than  $\alpha$  collisions. The statistical variation in the number of ion pairs formed would then be expected to be smaller

than the statistical variations in range straggling. In the simplest type of calculation, assuming a Gaussian distribution, the standard deviation ( $\sigma = \alpha/\sqrt{2}$ ) would be equal to the square root of the number of total events (i.e., number of ion pairs formed). For polonium  $\alpha$

Table 1—Alpha Particle Straggling Parameters<sup>†</sup> Achieved in a Number of Total Ionization Systems

Authors	Average straggling parameters, kev			Type of chamber	Type of charge collection
	50% geometry	Collimated	Gas		
Bunemann, Cranshaw, and Harvey <sup>81</sup>		30 to 35	Argon	Grid	Electron
Schintlmeister <sup>12c</sup> and Schintlmeister and Rona <sup>81</sup>	250 to 280		Air		Ion
Jentschke <sup>10</sup> Stetter <sup>15</sup>		137 27 78 86	Air H <sub>2</sub> Air Argon	Parallel plate	Ion Ion
Maeder <sup>84</sup> Brown and Curtiss <sup>27</sup>	78		Air N <sub>2</sub>	Thin rod collector	Ion
Deutsch and Ramsey <sup>21</sup>	75		2% CO <sub>2</sub> in argon	Grid	Electron
Frisch <sup>19</sup> Clark, Spencer-Palmer, and Woodward <sup>18</sup>		100 60 to 75	N <sub>2</sub> Argon	Grid Grid	Electron Electron
Fowler and Rosen <sup>23</sup>	96		Argon	Grid	Electron
Parsons <sup>24</sup>	50 to 55		Argon	Grid	Electron
Ghiorso, Jaffey, Robinson, and Weissbourd <sup>25</sup>	55 to 70	45 to 70	Argon	Small ball collector	Electron
Jaffey and Connor <sup>26</sup>	45 to 65	45 to 65	Argon	Grid	Electron

<sup>†</sup>These have been measured from the published curves and apply only to  $\alpha$  particles. When more than one or two curves were published, the values representing the best results from each instrument were chosen.

particles (5.30 mev), since 186,200 ion pairs are formed in argon,<sup>15</sup> the standard deviation is 0.0023 per cent or 12.3 kev, and  $\alpha_i = 17.4$  kev. The problem has been theoretically analyzed by Fano,<sup>60</sup> who showed that the standard deviation was  $\sqrt{FJ_0}$ , where  $J_0$  is the total

number of ion pairs, and  $F$  is a factor between 0 and 1 but lies generally between  $\frac{1}{3}$  and  $\frac{1}{2}$ . For  $F = 1$ ,  $\sqrt{FJ_0}$  is the standard deviation for the Poisson distribution (which for large  $J_0$  is representable by a Gaussian curve). Thus, according to Fano, the ionization straggling for polonium should be less than 17.4 kev; taking  $F = 0.5$ ,  $\alpha_i = 12.3$  kev.

Of all the published papers on total-ionization measurements, the paper by Bunemann, Cranshaw, and Harvey<sup>51</sup> reports the achievement of the lowest total straggling parameter (Table 1). By the use of a pulse generator and by varying the chamber straggling through changing the grid structure and voltage, they were able to evaluate  $\alpha_n$  and  $\alpha_c$ . They found (by difference) that  $\sqrt{\alpha_i^2 + \alpha_s^2}$  was about 20 kev. Since their sources were made by simply evaporating polonium solutions on backing plates and since 50 per cent geometry measurements showed a considerable low-energy tail, it is likely that their samples gave rise to a sizable amount of source straggling. It is quite possible, then, that thinner samples might have given a closer check with Fano's results.

If the lowest values for the various individual straggling parameters are taken ( $\alpha_i = 12$  kev,  $\alpha_n = 12$  kev,  $\alpha_c = 3.1$  kev,<sup>51</sup>  $\alpha_s = 5$  kev), then the best straggling parameter that could be expected with this type of instrument is about 18 kev. Although this is greater than that of the best magnetic spectrographs,<sup>2</sup> it is not much greater. In Chang's<sup>2,64</sup> instrument, for example,  $\alpha = 5.4$  kev. Thus, if the total-ionization method can be pushed to its limit, its resolution can be made comparable to that of the best magnetic spectrographs.

The present pulse analyzer has a larger straggling parameter than that found by Bunemann, Cranshaw, and Harvey (see Table 1). Since  $\alpha_n$  was measured to be only 12 kev, since the total  $\alpha$  has been found to be approximately independent of sample, and since Fano's results indicate that  $\alpha_i$  is quite small, it seems apparent that most of the straggling must be due to  $\alpha_c$ . It is probable that this is also true of many of the other systems listed in Table 1.

## 7. TECHNIQUES OF OPERATION

**7.1 Counting Rates, Tolerable Beta Activity, and Gas Pressure.** Because of the relatively low frequency response of the amplifier and the long time constants of the selector and recording circuits, it is not possible to use high counting rates. At 50 per cent geometry the counting rates are generally held to 500 to 1,000 counts per minute if all the activity is concentrated in one peak. If the activity is spread over three or four peaks, the counting rate can be as high as 2,500 counts per minute. Even for a single peak, the counting rate may be increased if the amplifier gain is high, so that the peak is spread

over many channels. If, for some reason, the sample submitted exceeds these values, the effective counting rate is reduced by masking or collimating. The primary limitation on the counting rate is the slowness of the registers. Since the counts occur at random, the maximum counting rate per register must be kept considerably below the permissible rate for uniformly spaced pulses. However, when the peaks are spread over many channels so that the counting rates per register are reasonably low, the maximum counting rate is then limited by the amplifier frequency response, which determines the pulse shape and, in particular, the pulse width. If a pulse enters the amplifier before the decaying tail of the previous one has died away, the height of the new pulse is changed. If this kind of event occurs frequently enough, the pulse distribution is distorted, the peak widths are increased, and the resolution is thereby decreased. This type of partial coincidence is minimized by limitations on the maximum counting rate.

The resolution is also decreased due to peak widening when large numbers of  $\beta$  particles are emitted from the sample. Owing to the random fluctuation of  $\beta$  emission, the effect of the  $\beta$  pulses is to greatly increase the apparent noise level. Generally, more than a few hundred thousand counts per minute of  $\beta$  particles cause difficulty.

The chamber can be used at 1 atm pressure provided the energy is not much greater than 5 mev. For higher energies greater pressures are often used in order to cut down the range and thereby reduce the positive-ion effect. The voltage is then correspondingly increased.

7.2 Operating Region. Although the gain can be lowered enough so that the 48 channels cover the entire energy range of  $\alpha$  emitters, the resolution becomes poorer because the channel width is then about equal to the peak width. Usually preliminary considerations and tests make it possible to eliminate large portions of the energy range before a complete curve is determined, and the gain is set at the point necessary to apply the 48 channels to the region of interest. The bombardment and chemical histories of the samples very often serve to give a fairly good idea as to what nuclides may be present and in what relative concentration. For most samples the 48 channels are concentrated in the 4.6- to 6.0-mev region. To ensure that no activity is missed in the range 4.0 to 4.6 mev, the prediscriminator bias is lowered for a few minutes and the first few banks of registers checked. If no activity shows up, the bias is returned to its usual position, and the pulse analysis is made. The presence of  $\alpha$  particles with energies greater than 6.0 mev is easily detected since these are registered by the forty-eighth channel. If it is desired to see a particular energy range in greater detail, the energy increment per channel may be

decreased by an increase in amplifier gain while the position is set by the prediscriminator bias control.

**7.3 Abundance Determination.** The relative abundance of  $\alpha$  activity at the various peaks is determined simply by adding up the counts in the channels involved at each peak. The comparison made in this manner of the areas under each peak is more reliable than comparison of peak heights because of the possible variation of straggling parameter from peak to peak. A larger straggling parameter drops the peak height even though the area remains the same. If two peaks overlap, the intermediate region must be appropriately divided by drawing the overlapping high- and low-energy tails to correspond to the shapes of the nonoverlapping high- and low-energy tails. Thus, for example, if the two overlapping peaks occur at 5.14 and 5.30 mev, the high-energy side of the 5.14-mev peak is drawn to be similar to the high-energy side of the 5.30-mev peak since this side is unperturbed. In the same fashion, the low-energy sides are made similar. This procedure is based on the assumption that the effects of self-absorption,  $\alpha$  back-scattering, and positive-ion effect are about the same for both peaks. The assumption is approximately true since the energies of two overlapping peaks are fairly close. However, because of this approximation, it is difficult to estimate areas in closely overlapping peaks very accurately, especially when one nuclide is present in low concentration.

In general the total number of counts found under the peaks is less than the counting rate determined in an  $\alpha$  counter; for some samples it is as much as 10 per cent lower. This phenomenon is caused primarily by sample self-absorption and  $\alpha$  back-scattering,<sup>2</sup> both of which cause a reduction in the  $\alpha$  energy. The effect occurs even in well-prepared thin samples, but it is more severe in thicker samples. The energy distribution of the degraded  $\alpha$  particles stretches from the original energy to zero in a continuous fashion, the actual variation depending upon the atomic weight of the backing material and upon the atomic weight and thickness of the sample material. (The back-scattering effect is greater on high-atomic-weight materials, e.g., Pt, than on light metals.) Thus both the fraction of degraded  $\alpha$  particles and their energy distribution are functions of the backing material and of the sample thickness. Since these effects are approximately the same for various energies, the ratio of counts in the peaks gives a fairly close approximation to the relative concentrations of the  $\alpha$  emitters. This may not be accurate if the energies are quite different since the degrading effects do vary somewhat with energy. Another source of difficulty is that some of the degraded  $\alpha$  particles from the high-energy peak appear under the low-energy

peak and raise its apparent concentration. This may be particularly serious if the low-energy peak is present in low concentration. One way to evaluate this effect is to prepare a pure standard sample of the high-energy nuclide, attempting to duplicate the method of sample preparation, and to measure the number of  $\alpha$  particles at the position of the low-energy nuclide.

Because of the energy degradation, ratios of activity can be more accurately determined at 50 per cent geometry than can absolute activities. For this reason, it is best to evaluate the absolute activity of a particular peak by first measuring the activity of that peak relative to the activity of an internal standard and then counting the standard in an  $\alpha$  counter.

Because of such problems as back-scattering, sample self-absorption, overlapping of peaks, and variation in peak shapes with energy, it has not proved possible to make relative-activity determinations with high precision. The major usefulness of the analyzer has been in the following types of measurements: (1) establishing the presence or absence of a particular nuclide (already known), (2) establishing the existence of a new  $\alpha$ -emitting nuclide, (3) determining the  $\alpha$  energies of newly discovered nuclides, and (4) making abundance measurements when highly precise quantitative values are not required.

**7.4 Collimation.** It is possible to decrease the relative concentration of degraded  $\alpha$  particles by collimating the particles emitted from the sample. The method is effective since most of the back-scattered  $\alpha$  particles emerge at small angles to the sample plate,<sup>2,65</sup> while self-absorption is also important only for  $\alpha$  particles emitted at small angles. To cut out these  $\alpha$  particles, the geometry of the collimator need not be very low since the degrading effects are concentrated in the small-angle region. As mentioned above, collimation also has the effect of decreasing the straggling of the pulse-height distribution by minimizing variations in the positive-ion effect and in the collection time of the electrons. Thus, even with well-prepared samples, the best resolution is not obtainable at 50 per cent geometry; it requires some collimation. When the sample is rather thick, the low-energy tail becomes so large that measurements are very difficult. Although in this case the accuracy and resolution cannot be made as good as that of a thin sample, they are improved by collimation.

As mentioned before, collimation is also used to cut the counting rate of the sample. Several different collimators are available to vary the fraction of  $\alpha$  particles cut out.

The collimators consist of brass disks having  $\frac{1}{16}$ -in. holes in close packed array over the area of a circle about 2 in. in diameter. The area occupied by holes is about 68 per cent of the total area. The

thicknesses of the disks used are  $\frac{1}{32}$ ,  $\frac{1}{16}$ ,  $\frac{1}{8}$ ,  $\frac{3}{16}$ ,  $\frac{1}{4}$ ,  $\frac{3}{8}$ , and  $\frac{1}{2}$  in., and the extent of collimation is described by the collimation ratio: hole depth to hole diameter. Thus, the  $\frac{1}{16}$ -in.-thick disk is called the 3 to 1 collimator. In drilling the collimators, use was made of a hardened-steel jig which had been carefully made with a milling machine. In making the thicker collimators, care had to be taken to keep the drill

Table 2—The Collimators

Collimator	Geometry <sup>†</sup> per hole, %	Over-all geometry, %	Energy lost in collimator hole, <sup>‡</sup> mev
½ to 1	18.6	11.3	0.074
1 to 1	9.35	6.39	0.15
2 to 1	2.87	1.98	0.30
3 to 1	1.33	0.909	0.45
4 to 1	0.779	0.532	0.61
6 to 1	0.344	0.235	0.93
8 to 1	0.194	0.133	1.27

<sup>†</sup>Relative to 50 per cent ( $2\pi$ ) geometry.

<sup>‡</sup>Energy lost by vertically emitted polonium  $\alpha$  particles (assuming no ions generated in hole are collected). For the thin collimators,  $\alpha$  particles emitted at an angle lose more energy.

from wandering and making a nonvertical hole. The collimator disks were made with a supporting ring ( $\frac{1}{16}$  in. thick) around the lower edge, which served to lift them above the samples. Table 2 shows the geometry per hole for the various collimators, as well as the over-all geometry (which includes the transparency). The geometry is given relative to 50 per cent geometry. It is evident from the table that even mild collimation causes a considerable decrease in counting rate. The activities required to give reasonable statistics and counting rates greater than background become correspondingly higher.

If the concentration of one  $\alpha$  emitter is a very small fraction (less than 0.1 per cent) of the total  $\alpha$  activity, it is quite difficult to detect and measure it. At 50 per cent geometry it is possible to detect such activity when it is higher in energy than the other  $\alpha$  particles; if it is lower in energy, detection becomes impossible because of the low-energy tail of the high-concentration peak. Even with collimation, detection of low-energy  $\alpha$  particles present in low concentration is difficult because of the presence of a small but definite tail on the peak. This tail is possibly caused by energy degradation resulting from scattering off the collimator. Improved results may be attained

by determining the low-energy background with a pure sample of the high-energy peak. When the low-concentration activity is of higher energy than the main peak, either the 50 per cent geometry or collimation methods may be used. The sample must be counted for a long time in order to accumulate a statistically significant number of counts. This is feasible only if the counter background is very low, at least as low as the activity to be measured. Long counting times may also give rise to errors if there is any tendency of the chamber and circuit characteristics to drift.

7.5 Mica-low-geometry Method. Because the total counting rate that is used is limited, it is not feasible with either the 50 per cent or ordinary collimation method to increase the absolute counting rate of the low-concentration activity by enlarging the total sample activity. However, if it were possible to prevent the large numbers of  $\alpha$  particles from the low-energy peak from entering the ion chamber, the sample size could be increased. This may be done by collimating the sample and using a mica absorber thick enough to absorb all or almost all the low-energy  $\alpha$  particles, but thin enough to allow the higher-energy  $\alpha$  particles to get through. The residual range may be quite small, however, in which case a high amplifier gain must be used. Because a major portion of the range is absorbed in the mica, care must be taken to avoid excessive angle straggling, i.e., significant deviations in path length through the mica. For example, the ratio of maximum to minimum path lengths in the mica is 1.41 for the 1-to-1 collimator, 1.12 for the 2-to-1 collimator, 1.05 for the 3-to-1 collimator, and 1.03 for the 4-to-1 collimator. The average deviation is, of course, smaller. Excessive angle straggling tends to spread the peaks, in which case the small one may not be observable.

If the high-energy peak is quite close to the main peak, the highest resolution is necessary, requiring at least a 4-to-1 or a 6-to-1 collimator. The actual resolution required depends upon the relative amounts of the main activity and the trace activity as well as upon the energy separation. If the concentration of the high-energy activity is very low, the high-energy straggling of the main peak may tend to hide the small peak unless the resolution is very good. On the other hand, if the concentration of the high-energy peak is not too low, the high-energy straggling of the other peak is of less importance. The effect of the high-energy straggling of the main peak is also decreased if the peaks are fairly well separated. This is illustrated in Fig. 9.

If the resolving power is measured by the peak width, then the resolution of the mica-collimation method is generally somewhat poorer than that of the 50 per cent geometry or ordinary collimation methods. This is due to the increased straggling arising from the

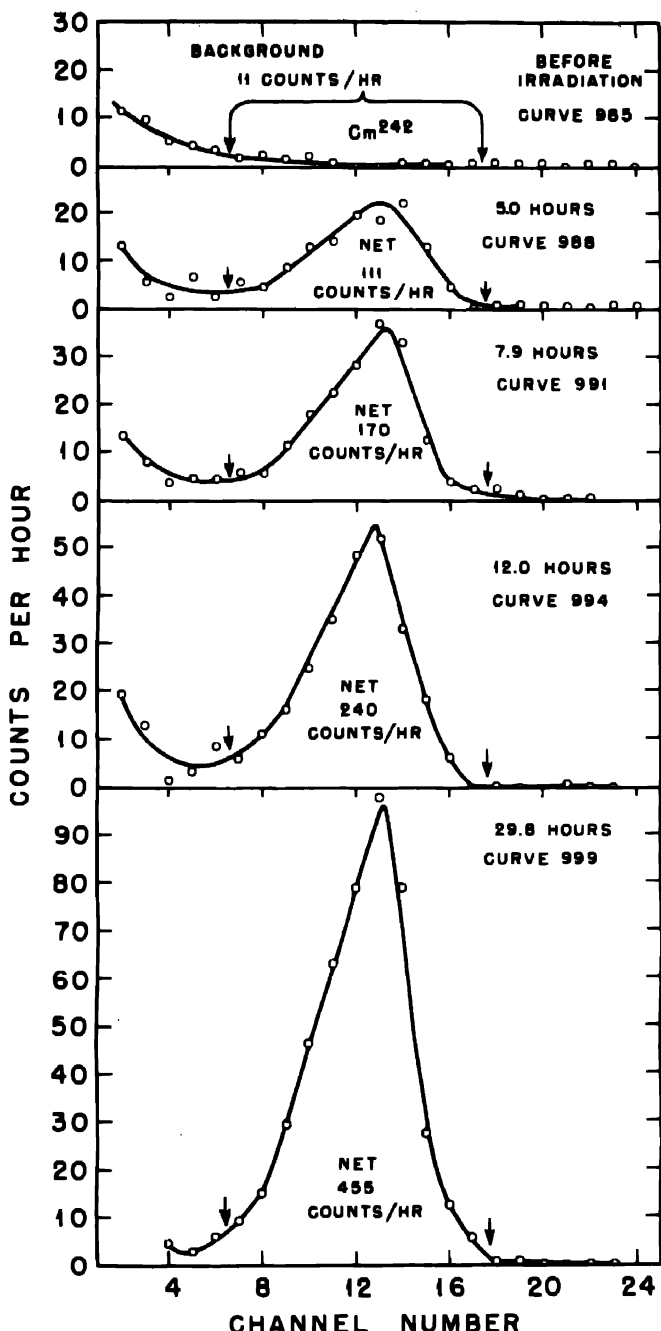


Fig. 9—Growth of Cm<sup>242</sup> from Am<sup>241</sup> sample. Small chamber; 6-to-1 collimator. Mica and air absorption equivalent to 4.31 mg/sq cm of air. Flowing nitrogen. Time since mid-point of neutron bombardment is given.

variation in path length through the mica (angle straggling) and to the fact that straggling in range is greater than straggling in the ionization yield. On the other hand, the mica method increases the stability since most of the  $\alpha$  range is cut off, and variations in the chamber and circuits affect only the small residual ionization. The low counting rates resulting from the high degree of collimation can be partially compensated by long counting times; and because of the increased stability involved in the mica method, instrumental drifts do not cause much difficulty even over quite long counting periods.

However, to get significant results even with long counting times, a very low background is necessary. For the large chamber in Fig. 3, this is difficult to achieve under the best conditions because of the large surface area. Because most of the range is lost in the mica, the resulting pulses are small, and these are about the same size as pulses due to natural  $\alpha$  emitters contained in the chamber walls. A smaller chamber, a modified form of an atmospheric parallel-plate  $\alpha$  counter,<sup>2</sup> serves as a low background chamber. The bottom electrode is lowered to admit the collimator and mica absorber and to allow a few centimeters of argon between the collectrode and mica absorber. The electrode areas are quite small, making a total background of less than 0.5 count per minute possible. Despite the large collectrode, the variation in positive-ion effect is not important, because the range of the  $\alpha$  particles beyond the mica is usually rather small.

The mica absorbers were made by splitting thick mica sheets to approximately the correct thickness and measuring their thickness by weighing and area determination. By selection, it was possible to build up a series of absorbers ranging from about 1.6 to 8.0 mg/sq cm in steps of 0.1 to 0.05 mg/sq cm. These were mounted on thin metal supporting rings about 2 in. in diameter.

**7.6 Energy Calibration of Analyzer.** Calibration of pulse height vs. energy is carried out by the use of standard samples containing  $\alpha$  emitters of known energy. If the output pulse height vs. energy relation could be assumed to be linear and if the amplifier gain and cutoff bias were accurately known, only one  $\alpha$  energy would be necessary to establish the relation. Actually, with our instrument, the curve showing relation between pulse height and energy has a small curvature, which is due to such things as the positive-ion effect and the nonlinearity of the high-level stages in the amplifier. Hence, at least two  $\alpha$  energies in the region of interest are necessary to fix the scale. Because the instrument drifts in calibration, it is checked with standards rather frequently.

The standard samples are mounted on thick Stellite disks, cut into quadrants of a circle, and optically polished to a mirror finish. The activities are electroplated on these quadrants. By combining the quadrants, a number of combinations of  $\alpha$  energies may be made. In

Table 3—Standard Alpha Energy Samples

Standard	Nuclides	Energy, mev	C/m, 50% geometry
4-peak standard	$U^{233}$ , $Pu^{239}$ , $Pu^{238}$ , $Pu^{236}$	4.823, 5.14, 5.50, 5.75	One with 500 c/m per peak; one with 6,000 c/m per peak
MsTh standard (and daughters)	RdTh, ThX, Tn, ThA, ThC, ThC'	5.42, 5.33, 5.68, 6.28, 6.77, 6.05, and 8.78	Total of 1,800 counts (equilibrium concentrations)
	$Io^{230}$	4.68	One with 500 c/m, one with 7,700 c/m
	$U^{234}$ and $U^{235}$	4.76 and 4.40	1,000 c/m
	$Np^{237}$	4.73	5,600 c/m
	$Pa^{231}$	5.01 (87%) 4.74 (13%)	1,960 c/m and 6,500 c/m
	$Pu^{239}$	5.14	One each with 500 c/m, 5,000 c/m, 50,000 c/m, and 300,000 c/m
	$Po^{210}$	5.30	300 c/m, 5,000 c/m, 7,400 c/m
	$U^{232}$	5.31	1,200 c/m and 2,400 c/m
	$Pu^{238}$	5.50	800 c/m and 6,800 c/m
	$Am^{241}$ and $Cm^{242}$	5.46 and 6.10	One each with total counts 11,000 and 670
Radium standard	$Ra^{228}$ , Rn, RaA, RaC'	4.79, 5.49, 6.00, and 7.68	Total of 3,800 c/m (equilibrium concentrations)

Table 3 is a list of the more commonly used standards. Of course for particular experiments special standards of pure nuclides are often prepared.

The four-peak sample is the most popular standard. It serves to provide a rapid energy pulse-height calibration in the region of greatest interest. It also provides a very rapid check on the instrument's resolution because high resolution gives rise to very deep valleys which almost go down to zero, and these can be seen just by watching

the registers. For higher energies the RdTh or the Ra series are usually used.

To make an accurate energy determination, it is necessary to use an internal standard (i.e., a standard sample placed in the chamber with the unknown sample) to avoid the possibility of drift. One method involves the use of one internal energy standard and the energy increment per channel previously evaluated with the four-peak standard. In another method, a high-energy and a low-energy standard are used to bracket the unknown. The  $\alpha$  energies of the new nuclides which have been determined with the pulse analyzer have been measured by these methods. With the instrument we are using, the accuracy has been generally found to be no better than 0.01 to 0.02 mev.

A quick method of identifying an unknown peak that is suspected of being a well-known nuclide is to put in a standard sample containing that nuclide. Perfect superposition serves as identification provided the history of the sample eliminates the possibility of other nuclides with energies very close.

Calibrations made at 50 per cent geometry do not apply when the collimators are used because part of the range is absorbed in the collimator holes. The order of magnitude of this loss is shown in Table 2. Each collimator requires its own calibration, and great care must be taken to make the distances of the sample and standard from the collimator bottom identical.

7.7 Backgrounds. Because of the large surface area of the chamber, the natural  $\alpha$  background (due to the traces of uranium and thorium series normally found in metals) gives rise to a minimum of about 5 counts per minute. These counts are spread over a wide energy range, so that the number of counts per channel is considerably less than 1 count per minute. The background counting rate per channel determines the detectability of low concentrations of activity. To keep the sample support from becoming contaminated, the sample plate is placed on an aluminum disk. This is a thin punched disk, which is discarded after each measurement. Even with this disk, after some use with a number of samples, the chamber inevitably becomes contaminated. When the background becomes too high for use, the chamber is cleaned, first by washing with organic solvents and then by polishing with No. 1 polishing paper. As a final cleanup, the chamber is mounted in a lathe, and strips of polishing paper are used in a manner designed to prevent recontamination of cleaned areas. Each strip is used slightly and then discarded. By this method the background is reduced, although never as low as that of a new chamber. The background is generally less than 0.1 count per minute.

per channel,<sup>†</sup> except in the region 5.1 to 5.5 mev (many of the samples occur in this range) where the background may be 0.2 to 0.3 count per minute. The operating background, after some use, may run as high as 0.5 to 1.0 count per minute per channel; above this level the chamber is cleaned. Contamination of the collimator occurs rather easily because the bottom part of the collimator is brought quite close to the sample in order to minimize the gas absorption. The cleaning process is the same as that used on the chamber, except that greater care must be taken to avoid transferring activity into the collimator holes.

#### 8. USEFUL TABLES

As an aid in interpreting the pulse-analyzer curves, especially in identifying unknown activities, it has proved useful to have several tables readily available. In Table 4 is a list of many of the  $\alpha$  emitters in the heavy region, placed according to energy. This makes possible a ready determination of which nuclides have energies close to the observed one. Table 5, which gives the members of each of the known disintegration chains, makes it easy to see which peaks are likely to occur together due to radioactive equilibrium. Table 6, which gives the  $\alpha$  emitting nuclides of each element, makes it easy to see which peaks will occur together throughout a series of chemical operations. Most of the energies have been taken from Seaborg's table.<sup>66</sup>

#### 9. TYPICAL EXPERIMENTS PERFORMED WITH THE PULSE ANALYZER

**9.1 Detection<sup>67</sup> of Minute Amounts of Cm<sup>242</sup> in the Presence of Large Amounts of Am<sup>241</sup>.** In this experiment an attempt was made, first, to show that Cm<sup>242</sup> could be prepared<sup>67, 68</sup> by  $\text{Am}^{241}(n, \gamma)\text{Am}^{242} \xrightarrow{\beta^-} \text{Cm}^{242}$  and, second, to measure the cross section of the reaction. The method used was to bombard an americium sample in a reactor and then to measure the growth of Cm<sup>242</sup> from the Am<sup>242</sup>  $\beta$  decay. Since the activity of the Cm<sup>242</sup> was far less than that of the Am<sup>241</sup>, this measurement was most conveniently made by cutting out the americium activity by the use of mica. The problem was simplified by the fairly large energy separation (Cm<sup>242</sup>, 6.10 mev, and Am<sup>241</sup>, 5.46 mev). The 6 to 1 collimator was used (0.24 per cent of 50 per cent geometry). With a mica absorber most of the Am<sup>241</sup>  $\alpha$  particles

<sup>†</sup>With the 48 channels spread over the region 4.6 to 6.0 mev.

were cut out, while the  $\text{Cm}^{242}$   $\alpha$  particles came through (tested with a  $\text{Cm}^{242}$  standard). Since the  $\text{Am}^{241}$  activity was  $3.43 \times 10^6$  disintegrations per minute, the americium activity passing through the collimator holes was 4,030 counts per minute. The total background at the  $\text{Cm}^{242}$  position was about 0.18 count per minute, so that concentrations of  $\text{Cm}^{242}$  as low as 25 parts in  $10^6$  (by activity) could be

Table 4—Alpha Emitters Arranged According to Energy

Nuclide	$E(\alpha)$	Nuclide	$E(\alpha)$	Nuclide	$E(\alpha)$
$\text{Th}^{228}$	3.98	$\text{RdTh}^{228}$	5.333 (17%)	$\text{Fr}^{221}$ (?)	6.05 (25%)
$\text{U}^{238}$	4.180	$\text{RdTh}^{228}$	5.418 (83%)	$\text{ThC}^{212}$	6.081 (9%)
$\text{U}^{236}$	4.396	$\text{RaC}^{214}$	5.444 (0.022%)	$\text{Cm}^{242}$	6.10
		$\text{Rn}^{222}$	5.486	$\text{Pu}^{234}$	6.2
$\text{Io}^{230}$	4.66	$\text{Am}^{241}$	5.46	$\text{AcC}^{211}$	6.273 (16%)
$\text{Np}^{237}$	4.73	$\text{Pu}^{238}$	5.50	$\text{Tn}^{230}$	6.282
$\text{Pa}^{231}$	4.736 (13%)	$\text{RaC}^{214}$	5.505 (0.018%)	$\text{Fr}^{221}$	6.30 (75% ?)
$\text{U}^{234}$	4.763	$\text{AcX}^{223}$	5.606 (36%)	$\text{Th}^{226}$	6.30
$\text{Ra}^{228}$	4.791	$\text{Pa}^{230}$	5.66	$\text{Cm}^{240}$	6.3
$\text{U}^{223}$	4.825	$\text{ThX}^{224}$	5.681	$\text{Ra}^{223}$	6.51
$\text{Th}^{228}$	4.85 (~ 70%)	$\text{AcX}$	5.717 (55%)	$\text{AcC}^{211}$	6.619
$\text{Th}^{228}$	4.94 (~ 20%)	$\text{RdAc}^{227}$	5.717 (15%)	$\text{At}^{218}$	6.63
$\text{Ac}^{227}$	4.98 (1%)	$\text{Pu}^{236}$	5.75	$\text{ThA}^{216}$	6.774
$\text{Pa}^{231}$	5.012 (87%)	$\text{RdAc}^{227}$	5.764	$\text{Am}^{219}$	6.824
$\text{Th}^{226}$	5.02 (~ 10%)	$\text{Ac}^{226}$	5.80	$\text{At}^{217}$	7.02
$\text{Po}^{207}$	5.1	$\text{U}^{230}$	5.85	$\text{Em}^{218}$	7.12
$\text{Pu}^{240}$	5.1	$\text{At}^{211}$	5.94	$\text{AcA}^{215}$	7.365
$\text{Pu}^{238}$	5.14	$\text{RdAc}^{227}$	5.988 (25%)	$\text{AcC}^{211}$	7.434
$\text{Po}^{208}$	5.14	$\text{RaA}^{218}$	5.998	$\text{At}^{216}$	7.64
$\text{Po}^{206}$	5.2	$\text{Bi}^{213}$	6.0, 5.86	$\text{RaC}^{214}$	7.68
$\text{Po}^{210}$	5.300	$\text{ThC}^{212}$	6.042 (24%)	$\text{Po}^{213}$	8.336
$\text{U}^{231}$	5.31	$\text{RdAc}^{227}$	6.049 (20%)	$\text{At}^{218}$	8.4
				$\text{ThC}^{211}$	8.776

barely detected. Figure 9 shows the growth of the  $\text{Cm}^{242}$  activity following the neutron bombardment.

**9.2 Detection of Small Concentrations of  $\text{Pu}^{238}$  in the Presence of  $\text{Pu}^{238}$ .** This determination arose in a measurement of the half life of  $\text{Pu}^{238}$  by direct decay measurements.<sup>69</sup> The  $\text{Pu}^{238}$  was formed in the bombardment of normal uranium by the reaction (see references 70 and 71)  $\text{U}^{238}(\text{d},2\text{n})\text{Np}^{238} \xrightarrow{\beta^-} \text{Pu}^{238}$ . Samples containing some solid carrier were counted in a parallel-plate ionization chamber and were followed for almost three years. It was not until near the end of this time that it was found that the  $\text{Pu}^{238}$  sample probably contained  $\text{Pu}^{236}$  as well,<sup>72</sup>

Table 5—Heavy Elements Arranged by Radioactive Series

4n series			E( $\alpha$ ) and branching ratio	(4n+2) series (Cont.)			E( $\alpha$ ) and branching ratio
Z	Nuclide	T <sub>1/2</sub>		Z	Nuclide	T <sub>1/2</sub>	
94	Pu <sup>240</sup>	~ 6,000 yr	5.1	91	U <sup>234</sup>	6.7 hr	$\beta^-$
90	Th <sup>232</sup>	$1.39 \times 10^{10}$ yr	3.98	92	U <sup>234</sup>	$2.35 \times 10^5$ yr	4.763
88	MgTh <sup>232</sup>	6.7 yr	$\beta^-$	90	Io <sup>230</sup>	$8.0 \times 10^4$ yr	4.66
89	MgTh <sup>232</sup>	6.13 hr	4.5 (= 0.01%) <sup>a</sup>	88	Ra <sup>226</sup>	1,822 yr	4.701
			~ 100% $\beta^-$	86	Rn <sup>222</sup>	3.825 days	3.488
90	RdTh <sup>232</sup>	1.90 yr	5.418 (83%)	84	RaA <sup>212</sup>	3.05 min	5.998
			5.333 (17%)	82	RaB <sup>214</sup>	26.8 min	$\beta^-$
88	ThX <sup>234</sup>	3.64 days	5.681	83	RaC <sup>214</sup>	19.7 min	$\beta^-$
86	Th <sup>230</sup>	54.5 sec	6.282	84	RaC <sup>214</sup>	$1.5 \times 10^{-4}$ sec	7.680
84	ThA <sup>210</sup>	0.158 sec <sup>b</sup>	6.774	82	RaD <sup>210</sup>	22 yr	$\beta^-$
82	ThB <sup>210</sup>	10.6 hr	$\beta^-$	83	RaE <sup>210</sup>	5.0 days	$\beta^-$
83	ThC <sup>210</sup>	60.5 min	6.081 (9%)	84	Po <sup>210</sup>	140 days	5.300
			6.042 (24%)	82	Pb <sup>206</sup>	Stable	
			$\beta^-$ (66.3%)				
84	ThC' <sup>210</sup>	$2.6 \times 10^{-4}$ sec	8.776 (86.3%)				
81	ThC' <sup>210</sup>	3.1 min	$\beta^-$ (33.7%)				
82	Pb <sup>208</sup>	Stable <sup>c</sup>					
96	Cm <sup>240</sup>	29 days	6.3				
94	Pu <sup>238</sup>	2.7 yr	5.75				
92	U <sup>232</sup>	70 yr	5.31				
90	RdTh <sup>232</sup>	1.90 yr	5.418 (83%)				
			5.333 (17%)				
etc. as above (descendants of RdTh)							
(4n+1) series			E( $\alpha$ ) and branching ratio	(4n+3) series			E( $\alpha$ ) and branching ratio
Z	Nuclide	T <sub>1/2</sub>		Z	Nuclide	T <sub>1/2</sub>	
95	Am <sup>241</sup>	498 yr	5.46	92	U <sup>230</sup>	20.8 days	5.85
93	Np <sup>237</sup>	$2.20 \times 10^4$ yr	4.73	90	Th <sup>230</sup>	30.9 min	6.30
91	Pa <sup>233</sup>	27.4 days	$\beta^-$	88	Ra <sup>223</sup>	38 sec	6.51
92	U <sup>233</sup>	$1.62 \times 10^4$ yr	4.825	86	Em <sup>210</sup>	0.019 sec	7.12
90	Th <sup>230</sup>	7,000 yr	4.85 (~70%)	84	RaC <sup>214</sup>	$1.5 \times 10^{-4}$ sec	7.680
			4.94 (~20%)				
			5.02 (~10%)				
88	Ra <sup>228</sup>	14.8 days	$\beta^-$				
89	Ac <sup>225</sup>	10.0 days	5.80				
87	Fr <sup>221</sup>	4.8 min	6.30 (75%?)				
			6.05 (?) (25%?)				
85	At <sup>217</sup>	0.018 sec	7.02				
83	Bi <sup>213</sup>	47 min	6.0 (4%), or 5.86 (2%)				
			$\beta^-$ (96%)				
84	Po <sup>211</sup>	$3 \times 10^{-6}$ sec	8.336 (96%) or (98%)				
81	Tl <sup>206</sup>	1 hr	$\beta^-$ (4%) or (2%)				
82	Pb <sup>206</sup>	3.32 hr	$\beta^-$				
83	Bi <sup>206</sup>	Stable					
91	Pa <sup>231</sup>	1.5 days	5.66				
89	Ac <sup>229</sup>	10.0 days	5.80				
etc. as above (descendants of Ac <sup>229</sup> )							
(4n+2) series			E( $\alpha$ ) and branching ratio	(4n+3) series			E( $\alpha$ ) and branching ratio
Z	Nuclide	T <sub>1/2</sub>		Z	Nuclide	T <sub>1/2</sub>	
92	U <sup>238</sup>	$4.498 \times 10^9$ yr	4.180	94	Pu <sup>239</sup>	$2.44 \times 10^4$ yr	5.15
90	UX <sup>234</sup>	24.3 days	$\beta^-$	92	AcU <sup>235</sup>	$8.91 \times 10^5$ yr	4.398
91	UX <sup>234</sup>	1.14 min	99.85% $\beta^-$	90	UY <sup>231</sup>	24.3 hr	$\beta^-$
			0.15% I.T.	91	Pa <sup>231</sup>	$3.45 \times 10^4$ hr	5.012 (87%) 4.736 (13%)
				89	Ac <sup>227</sup>	13.5 hr	4.98 (1%) $\beta^-$ (99%)
				87	AcK <sup>233</sup>	21 min	$\beta^-$ (1%)
				90	RdAc <sup>227</sup>	18.9 days	6.049 (20%) 5.908 (25%) 5.784 (20%) 5.717 (10%)
				88	AcX <sup>233</sup>	11.2 days	5.717 (55%) 5.624 (82%)
				86	An <sup>219</sup>	3.92 sec	6.824 (82%)
				84	AcA <sup>211</sup>	$1.83 \times 10^{-3}$ sec	7.365
				82	AcB <sup>211</sup>	36.1 min	$\beta^-$
				83	AcC <sup>211</sup>	2.16 min	6.619 (84%) 6.273 (18%) 0.32% $\beta^-$
				84	AcC <sup>211</sup>	$5 \times 10^{-3}$ sec	7.434 (0.92%)
				81	AcC <sup>211</sup>	4.76 min	$\beta^-$
				82	Pb <sup>207</sup>	Stable	

probably formed by the reaction  $\text{U}^{235}(\text{d},\text{n})\text{Np}^{236} \xrightarrow{\gamma} \text{Pu}^{236}$ . The relatively short half life (2.7 years<sup>72</sup>) of the  $\alpha$ -emitting  $\text{Pu}^{236}$  caused it to interfere seriously with the decay measurement, although it was present in low concentration. The measurement was salvaged by determining the  $\text{Pu}^{236}$  concentration with the pulse analyzer. Because of the large

Table 6—Alpha Emitters Arranged by Element

Z	Nuclide	T <sub>½</sub>	E( $\alpha$ ) and branching ratio	Z	Nuclide	T <sub>½</sub>	E( $\alpha$ ) and branching ratio
83	RaE <sup>210</sup>	5.0 days	4.8 ( $10^{-4} - 10^{-8}$ %)	89	Ac <sup>228</sup>	10.0 days	5.80
	AcC <sup>211</sup>	2.16 min	6.619 (84%)		Ac <sup>227</sup>	13.5 yr	4.98 (1%)
			6.273 (16%)		MsTh <sup>228</sup>	6.13 hr	4.5 (0.01% ?)
	ThC <sup>212</sup>	60.5 min	6.081 (9%)		Th <sup>226</sup>	30.9 min	6.30
			6.042 (24%)		RdAc <sup>227</sup>	18.9 days	6.049 (20%)
	Bi <sup>212</sup>	47 min	6.05 (4%)				5.988 (25%)
	RaC <sup>214</sup>	19.7 min	5.505 (0.018%)				5.764 (20%)
			5.444 (0.022%)				5.717 (15%)
	Po <sup>208</sup>	9 days	5.2 (10%)		RdTh <sup>226</sup>	1.90 yr	5.418 (83%)
	Po <sup>207</sup>	5.7 hr	5.1 (0.01%)				5.333 (17%)
84	Po <sup>206</sup>	3 yr	5.14	90	Th <sup>228</sup>	7,000 yr	4.85 (~70%)
	Po <sup>210</sup>	140 days	5.300				4.94 (~20%)
	AcC <sup>211</sup>	$5 \times 10^{-3}$ sec	7.434		Io <sup>230</sup>	$8.0 \times 10^4$ yr	4.66
	ThC <sup>212</sup>	$2.6 \times 10^{-6}$ sec	8.776		Th <sup>232</sup>	$1.39 \times 10^6$ yr	3.98
	Po <sup>213</sup>	$3 \times 10^{-6}$ sec	8.336		Pa <sup>229</sup>	1.5 days	5.66
	RaC <sup>214</sup>	$1.5 \times 10^{-4}$ sec	7.680		Pa <sup>231</sup>	$3.45 \times 10^3$ yr	5.012 (87%)
	AcA <sup>210</sup>	$1.83 \times 10^{-1}$ sec	7.365				4.736 (13%)
	ThA <sup>210</sup>	0.158 sec	6.774		U <sup>230</sup>	20.8 days	5.85
	RaA <sup>210</sup>	3.05 min	5.998		U <sup>232</sup>	70 yr	5.31
85	At <sup>211</sup>	7.5 hr	5.94 (40%)		U <sup>233</sup>	$1.62 \times 10^5$ yr	4.825
	At <sup>210</sup>	Short	8.4		U <sub>II</sub> <sup>234</sup>	$2.35 \times 10^6$ yr	4.763
	At <sup>210</sup>	54 sec	7.84		AcU <sup>225</sup>	$8.91 \times 10^6$ yr	4.396
	At <sup>217</sup>	0.018 sec	7.02		U <sub>I</sub> <sup>235</sup>	$4.498 \times 10^9$ yr	4.180
	At <sup>218</sup>	Several sec ?	6.63	93	Np <sup>231</sup>	$2.20 \times 10^6$ yr	4.73
86	Em <sup>210</sup>	0.019 sec	7.12		Pu <sup>234</sup>	8.5 hr	6.2
	An <sup>210</sup>	3.92 sec	6.824 (82%)		Pu <sup>238</sup>	2.7 yr	5.75
	Tn <sup>220</sup>	54.5 sec	6.282		Pu <sup>238</sup>	92 yr	5.50
	Rn <sup>222</sup>	3.825 days	5.486		Pu <sup>239</sup>	$2.44 \times 10^4$ yr	5.14
	Fr <sup>221</sup>	4.8 min	6.30 (75% ?)		Pu <sup>240</sup>	~ 6,000 yr	5.1
88	Ra <sup>222</sup>	38 sec	6.51		Pu <sup>241</sup>	~ 10 yr	(~0.002%)
	AcX <sup>223</sup>	11.2 days	5.717 (55%)		Am <sup>241</sup>	498 yr	5.46
			5.606 (36%)		Cm <sup>240</sup>	29 days	6.3
	ThX <sup>224</sup>	3.64 days	5.681		Cm <sup>242</sup>	150 days	6.10
	Ra <sup>226</sup>	1,622 yr	4.791				

low-energy tail due to sample thickness, this determination was made feasible only because the  $\text{Pu}^{236}$  energy (5.75 mev) was greater than the  $\text{Pu}^{238}$  energy (5.50 mev). Figure 10 shows a typical pulse-analysis curve. The analysis had to be made at 50 per cent geometry, because the total activity of the sample was only 750 counts per minute. Since it was not possible to eliminate the low-energy tails by collimation, the relative concentrations were determined by adding up the counts in the six or seven channels in the neighborhood of each peak, on the

assumption that the low-energy tails of both peaks were similar in shape. The results of a number of runs gave a  $\text{Pu}^{238}$  to  $\text{Pu}^{236}$  activity ratio of  $0.0045 \pm 0.0007$  (probable error), which resulted in a  $\text{Pu}^{238}$  half-life measurement of  $89 \pm 9$  years (most of the error arises from the uncertainty in the  $\text{Pu}^{238}$  concentration). This value agreed with the more accurate value  $92 \pm 2$  years determined by another method.<sup>72</sup>

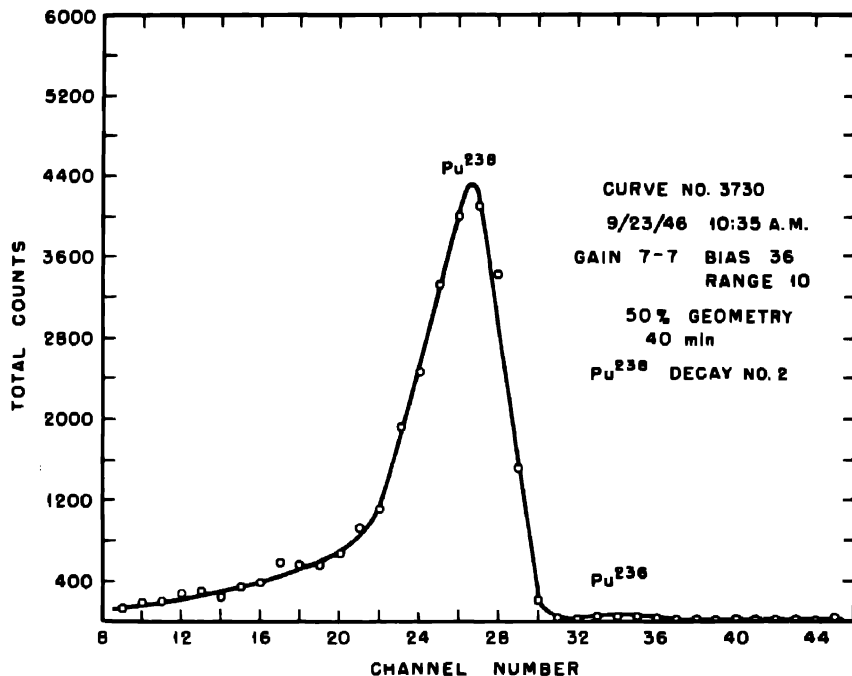


Fig. 10—Pulse analysis of  $\text{Pu}^{238}$  sample.

**9.3 Alpha Energies in the  $(4n+1)$  Series.**<sup>73</sup> These energies are listed in Table 5. They were measured by reference to  $\alpha$  standards of known energy. Figure 11 illustrates a typical pulse analysis in which the energy of the main peak of  $\text{Th}^{229}$  was measured by bracketing it with the standards  $\text{Io}$  ( $\text{Th}^{230}$ ),  $\text{Po}^{210}$ , and  $\text{RdTh}$  ( $\text{Th}^{228}$ ). Although this particular curve resulted in the value 4.86 mev, the average of seven such curves was  $4.85 \pm 0.01^\dagger$  mev.<sup>68</sup> The energies of the other  $\text{Th}^{229}$  peaks were determined (Fig. 12) using as standards the 4.85-mev main peak and the  $\text{RdTh}^{228}$  peaks. The average of twelve curves gave<sup>68</sup>  $4.94 \pm 0.01^\dagger$  mev and  $5.02 \pm 0.01^\dagger$  mev. The sample also showed

<sup>†</sup>Average deviation.

a small peak at 4.66 mev, which was not evident in later samples and may have been due to some  $\text{Io}^{230}$  contamination. Since Io is isotopic with  $\text{Th}^{220}$  and  $\text{RdTh}$ , it would not have separated during the chemical purification. Figure 13 shows some of the other members of the series. The 6.05-mev peak has been assigned to  $\text{Fr}^{221}$  on the basis of

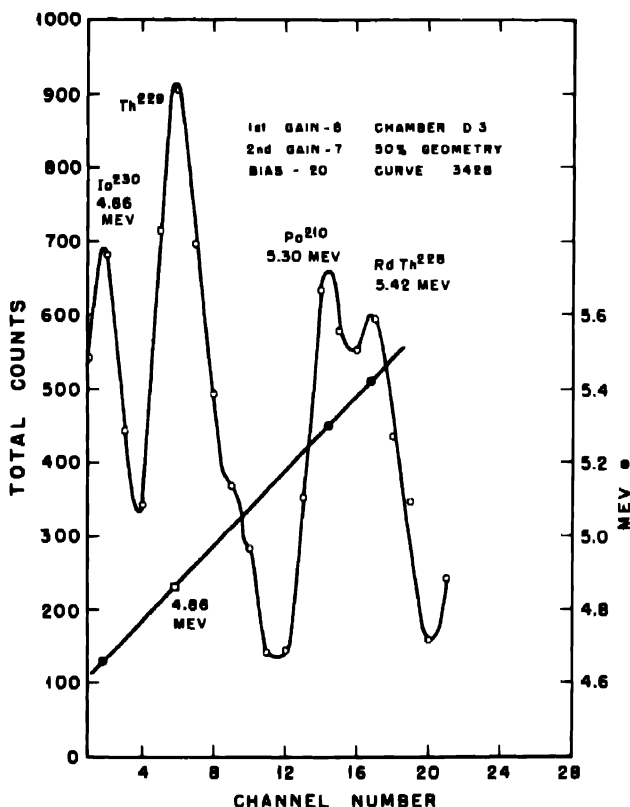


Fig. 11.—Pulse analysis of sample 09-22 ( $\text{RdTh}^{220}$  +  $\text{Th}^{220}$  and descendants) plus  $\text{Io}^{230}$  and  $\text{Po}^{210}$  standards.

abundance considerations. The energies corresponding to the peaks in Fig. 13 were measured relative to a  $\text{MsTh}$  series standard containing  $\text{RdTh}$  and daughters. The energies in Table 5 have been taken from these values and those measured at the Canadian laboratories.<sup>74,75,76</sup>

**9.4 Measurement of Decay.**  $\text{Pa}^{220}$ . The pulse analyzer has proved to be quite useful in the determination of the half life of a particular nuclide when it is present with a number of other growing and decaying  $\alpha$  activities. Although a gross-decay curve would be almost worth-

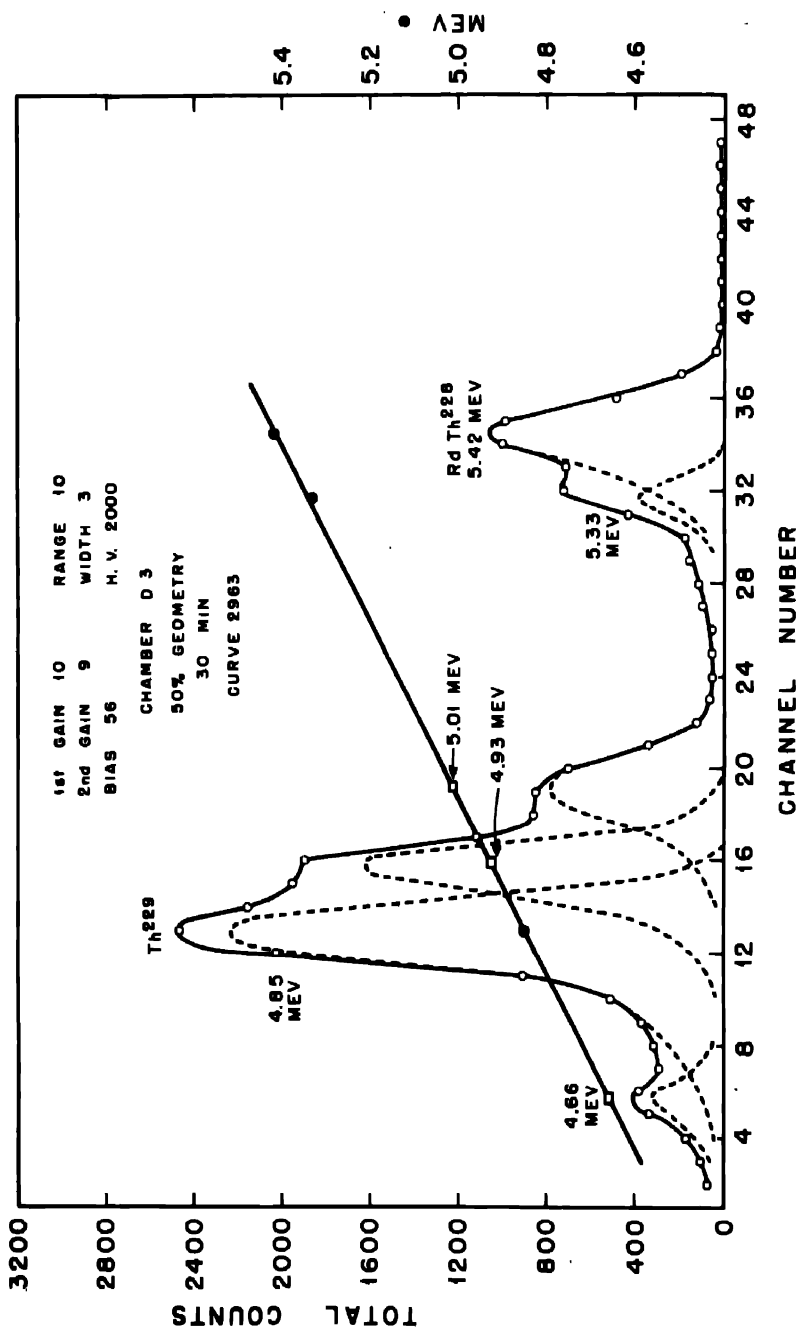


Fig. 12—Pulse analysis of sample 09-20 Th<sup>228</sup> + Th<sup>220</sup> (repurified).

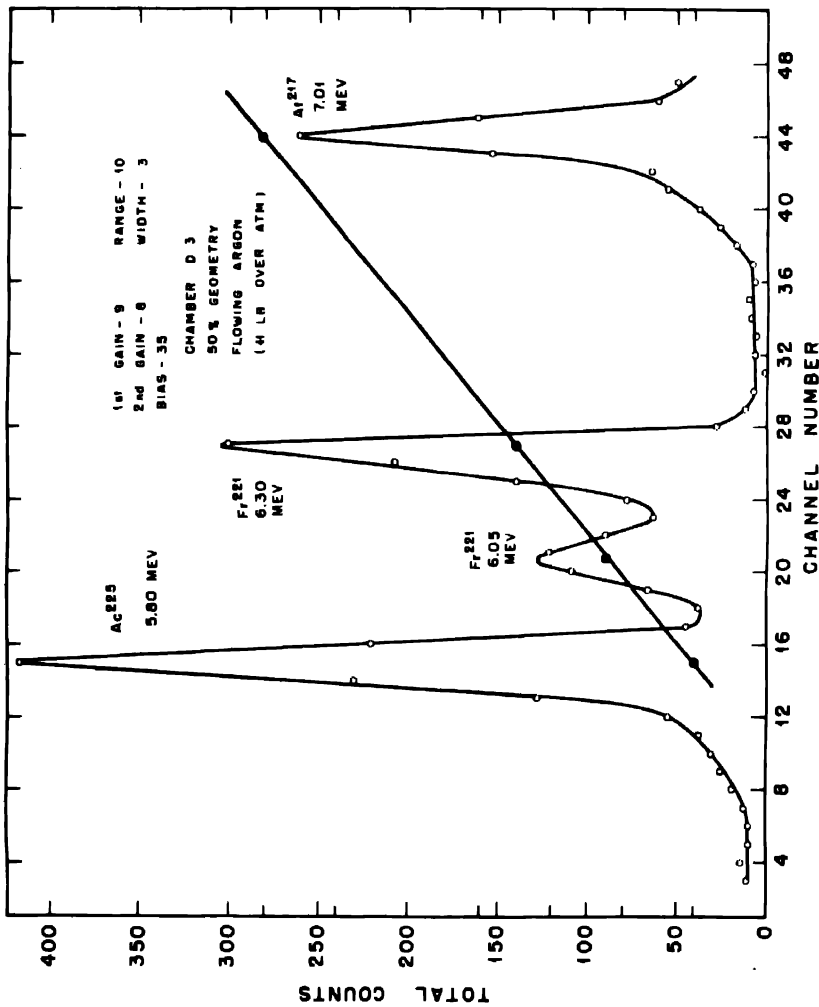


Fig. 13—Pulse analysis of members of (4n+1) series, sample 95-E (thick carrier).

less in such a case, the decay in the activity of a particular peak can be determined with reasonable accuracy. Such a determination was made<sup>77,78</sup> of the half life of Pa<sup>229</sup>. This nuclide was prepared by deuteron bombardment of an Io (Th<sup>230</sup>) sample which contained about five times as much Th<sup>232</sup> as Io. The products of this bombardment included all the protactinium isotopes which could be formed from Th<sup>232</sup> and Io by (d,xn) reactions and by (d,p) reactions followed by  $\beta$  decay. With the 20-mev deuterons used, reactions up to (d,4n) occurred. Thus Pa<sup>233</sup>, Pa<sup>232</sup>, Pa<sup>231</sup>, and Pa<sup>230</sup> were formed<sup>79,80</sup> as well as Pa<sup>229</sup>.

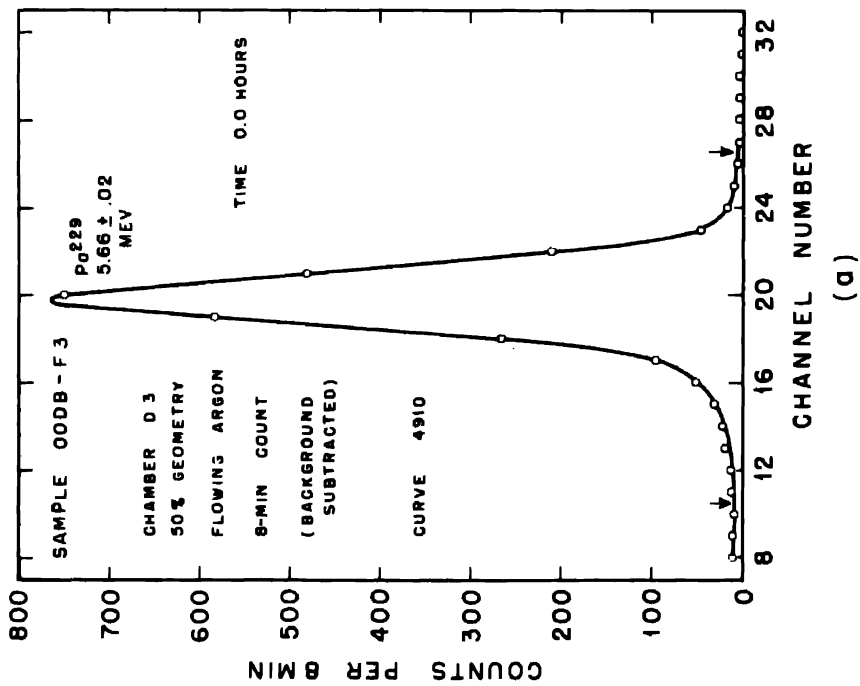
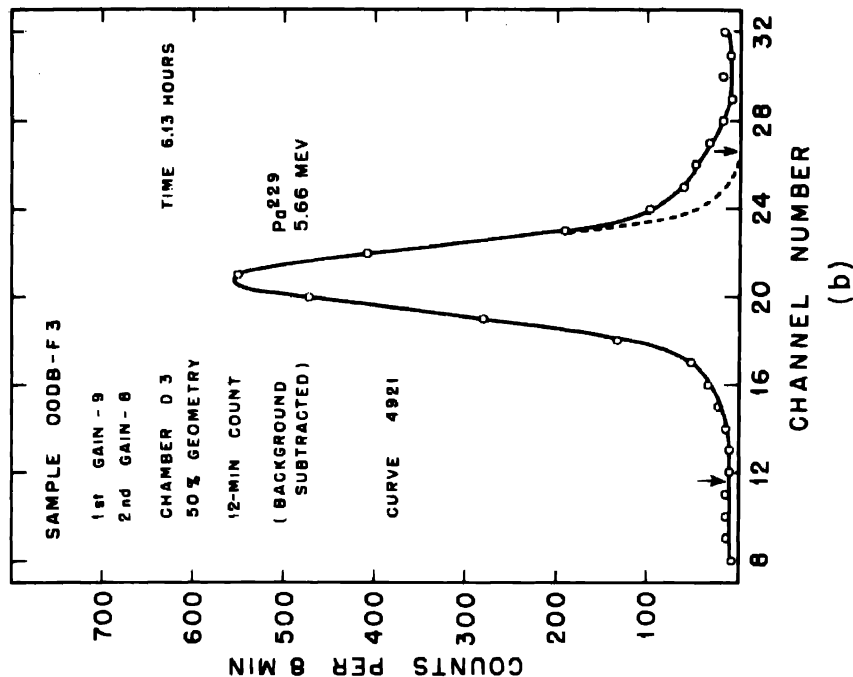
Immediately after the separation of the protactinium fraction from the bombardment mixture, the only significant  $\alpha$  activity in the fraction was caused by Pa<sup>229</sup> since Pa<sup>233</sup> and Pa<sup>232</sup> are  $\beta$  emitters, and the Pa<sup>231</sup> activity was too low for observation owing to its long half life. However, on decaying, the  $\beta$ -active Pa isotopes gave rise to  $\alpha$ -active descendants. The most serious difficulty was due to the formation of U<sup>230</sup>, which immediately gave rise to the entire U<sup>230</sup> series<sup>80,81</sup> (Table 5). In addition, the decay of Pa<sup>229</sup> resulted in the formation of a ten-day member of the (4n+1) series, i.e., Ac<sup>225</sup> (see Table 5), so members of this series soon began to appear as well. Figures 14 a to d show the decay of the Pa<sup>229</sup> peak. Owing to the presence of overlapping peaks, the high-energy side of the Pa<sup>229</sup> peak had to be constructed. This procedure gave rise to an error which became more serious as time passed and the interfering peaks grew relatively larger. The arrows indicate the channels whose counts were added to give the Pa<sup>229</sup> activity. The half life was determined to be 1.50 days.<sup>78</sup> A number of energy measurements gave  $5.66 \pm 0.02$  mev.<sup>78</sup>

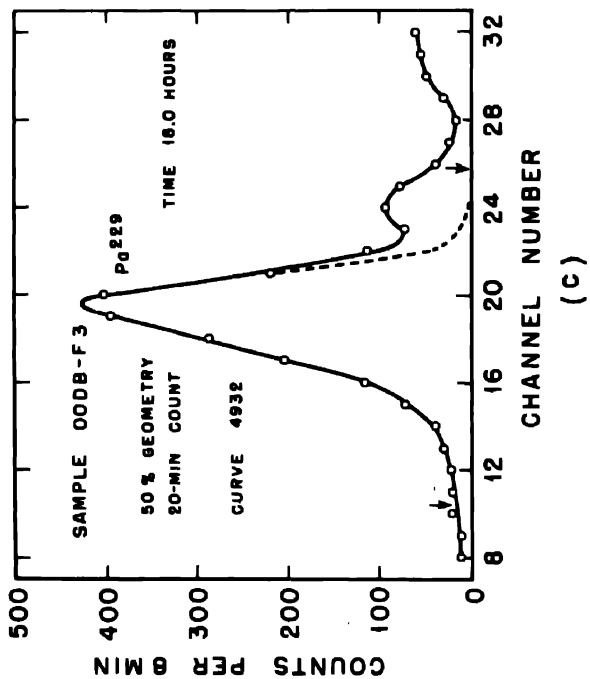
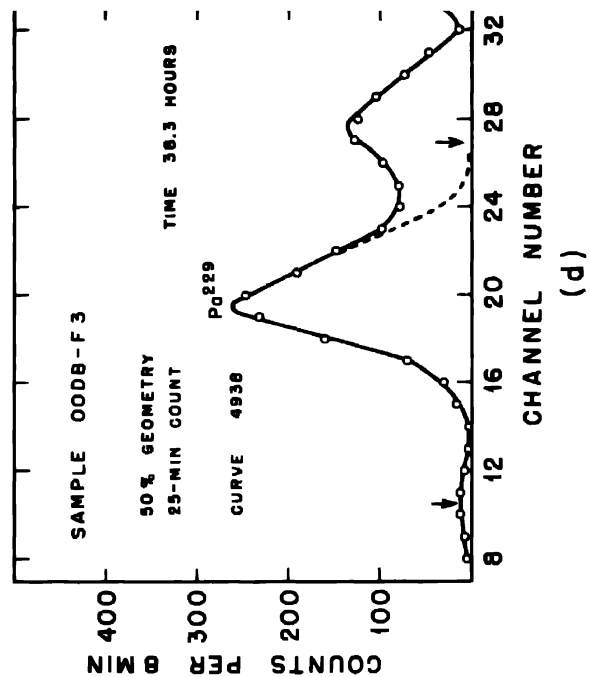
9.5 Determination of Abundances by Means of an Internal Standard. RdAc<sup>227</sup>. In the actinium decay series, the half life of RdAc (Th<sup>227</sup>) is difficult to determine because its descendant AcX (Ra<sup>223</sup>) has a comparable half life (Table 5). Previous half-life measurements had been made by evaluating the constants which would best fit the curves which represented the gross growth and decay of the total  $\alpha$  activity.

The method by which the Pa<sup>229</sup> decay was followed (Sec. 9.4), involving the measurement of the decay of a single peak, could not be easily used here because the daughter activity (AcX) overlaps the RdAc in  $\alpha$  energy.

The method actually used<sup>82</sup> involved the periodic radiochemical isolation of RdAc from a solution containing a decaying sample, and the measurement of this RdAc (Th<sup>227</sup>) activity with the pulse analyzer. To make automatic corrections for chemical losses in separation and purification, an internal standard (Io, i.e., Th<sup>230</sup>) was added to the decaying sample. Thus, to get the RdAc decay curve, it was only nec-

## THE TRANSURANIUM ELEMENTS





Figs. 14a to d—Decay of  $\text{Pa-229}$ .

## THE TRANSURANIUM ELEMENTS

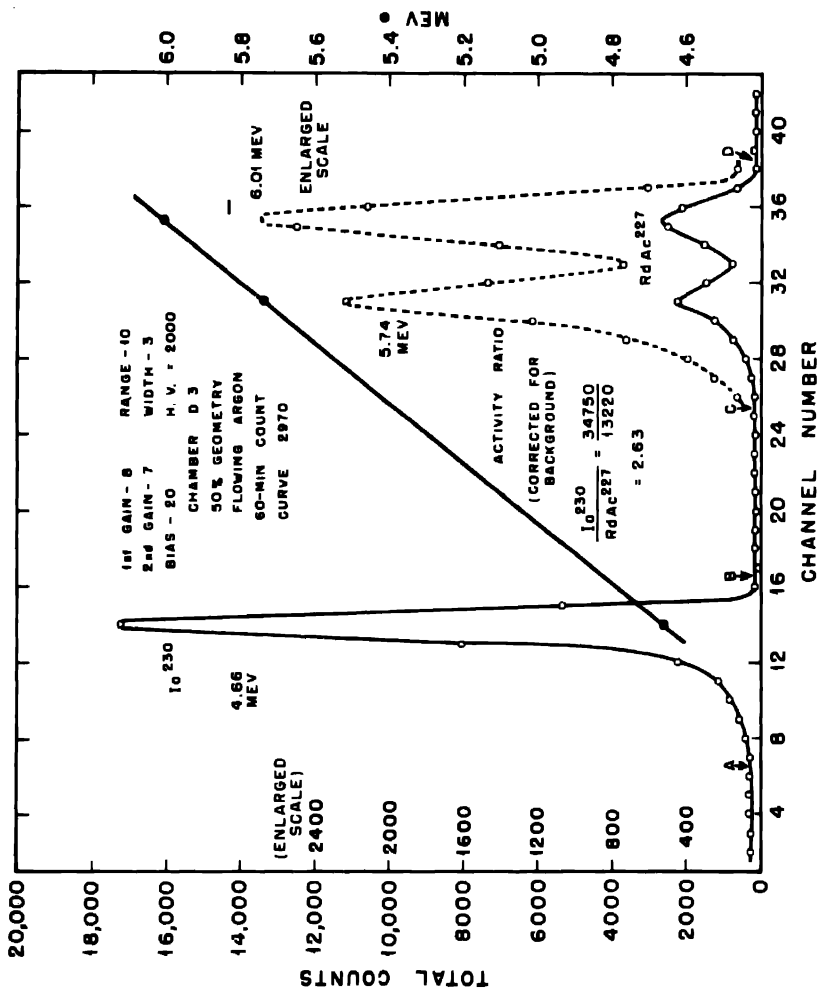


Fig. 15.—Pulse analysis of sample 2201 of  $\text{Io}^{230}$  and  $\text{RdAc}^{227}$  mixture.

essary to measure the ratio of RdAc to Io activity in each isolated thorium sample. Figure 15 shows one of the curves used in this determination.

Although Table 4 lists four energies for RdAc (measured by the magnetic spectrograph), only two peaks are evident in Fig. 15. On the

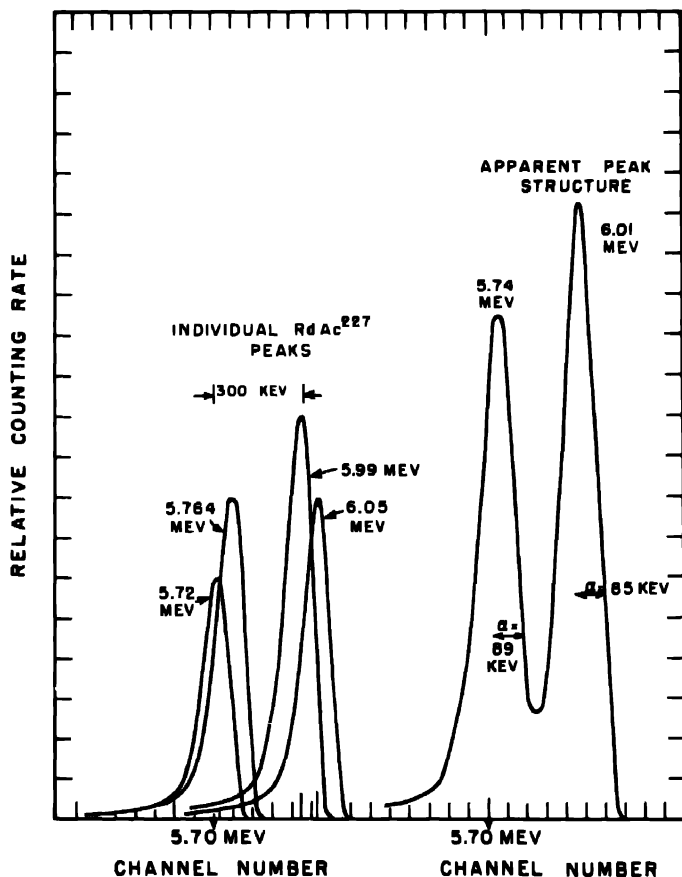


Fig. 16—Construction of  $\text{RdAc}^{227}$  pulse-analyzer peaks using  $\text{Io}^{230}$  peak shape (Fig. 15) as guide.

assumption that the straggling of the RdAc peaks was the same as that of the Io peak, Fig. 16 was constructed. The energies and relative abundances measured with the magnetic spectrograph were used to construct four individual peaks with the same shape as that of the Io peak (Fig. 15). Adding up the points of the four peaks, it can be seen that two peaks result which match quite well with the ones in

## THE TRANSURANIUM ELEMENTS

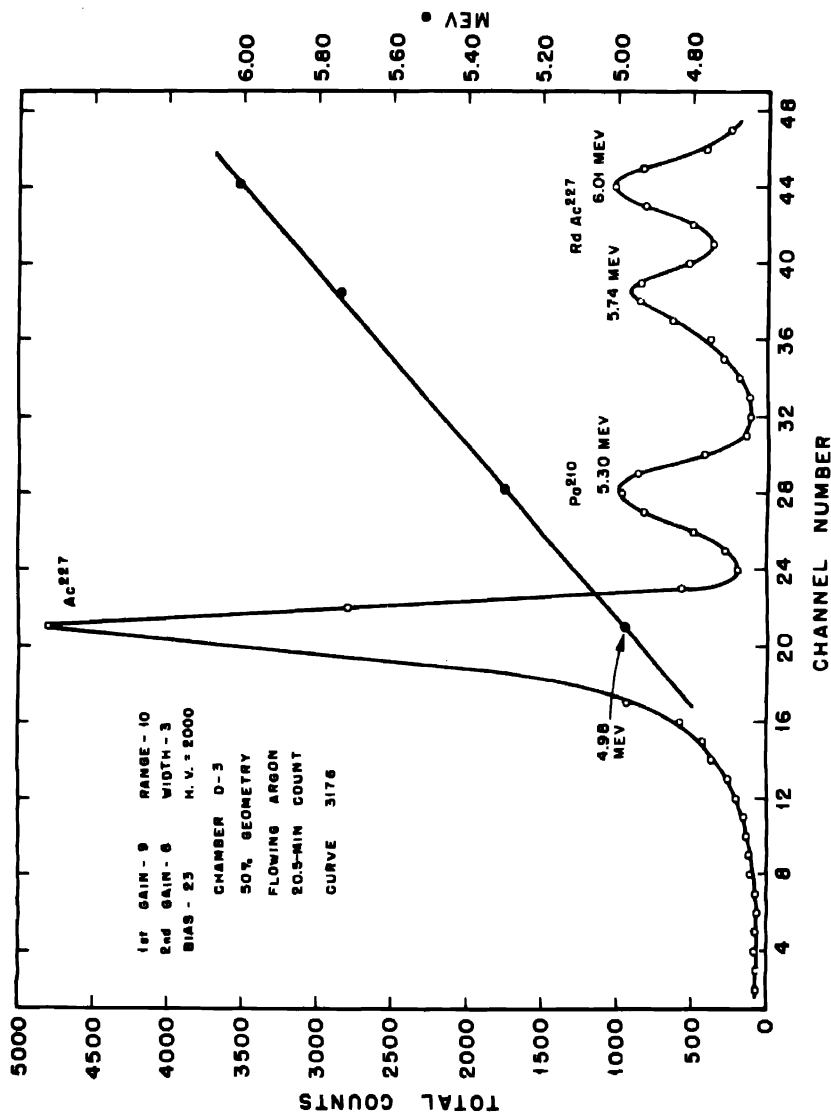


Fig. 17—Pulse analysis of Ac<sup>227</sup> sample (plus descendants) and Po<sup>210</sup> standard.

**Fig. 15.** The RdAc peaks in Fig. 15 are drawn on an enlarged scale to make the likeness more evident. The constructed RdAc peaks (Fig. 16) seem to have better resolution than the actual peaks (Fig. 15) since the valley between the two peaks is deeper in Fig. 16. This discrepancy indicates that the straggling of the RdAc  $\alpha$  particles is not the same as that of the Io  $\alpha$  particles, as was assumed, but that it is actually larger.

**9.6 Energy of Ac<sup>227</sup>.** In an experiment in which the  $\alpha$  branching of Ac<sup>227</sup> was determined,<sup>83</sup> the Ac  $\alpha$  energy was also measured by the use of the standards Po<sup>210</sup> and the daughter of the Ac<sup>227</sup>  $\beta$  decay RdAc (Th<sup>227</sup>). Figure 17 shows the results of the measurement. Extensive sample straggling is quite evident in this figure, and is due to the use of a carrier-containing sample at 50 per cent geometry.

**9.7 Tracing Chemical Separations. Np<sup>237</sup> and Pu<sup>239</sup>.** In working with the  $\alpha$ -emitting heavy nuclides (e.g., Pu<sup>239</sup>), it is convenient to test the efficiency of particular chemical separation procedures by following the gross  $\alpha$  activity. When two or more  $\alpha$  emitters are being separated, measurement of the gross  $\alpha$  activity cannot be used, and the pulse analyzer is used to follow the separation.

Figures 18a to d show the concentration<sup>86,87</sup> of Np<sup>237</sup> from considerably larger amounts (by activity) of Pu<sup>239</sup>. Figure 18a shows the peak separation when a sample of starting material is collimated, while Fig. 18b shows a sample of another batch of starting material measured at 50 per cent geometry. Measurement of the activity of the low concentration Np<sup>237</sup> is evidently easier with a collimated sample than at 50 per cent geometry. Low concentrations of a higher-energy constituent can be measured with or without collimation (Fig. 18d).

**9.8 Products of Alpha Bombardment of Uranium Isotopes.** The nuclides formed by high energy (approximately 40 mev) helium-ion bombardment of a mixture of U<sup>235</sup> and U<sup>238</sup> include<sup>72</sup> the  $\alpha$  emitters Pu<sup>239</sup>, Pu<sup>238</sup>, and Pu<sup>236</sup>. These are formed by ( $\alpha$ ,xn) reactions on both U<sup>235</sup> and U<sup>238</sup> (x varies from 1 to 6). Since these nuclides are isotopic, identification and measurements of concentration could be carried out most conveniently by an instrument like the pulse analyzer. The results of bombarding a sample enriched in U<sup>235</sup>, but containing a considerable amount of U<sup>238</sup>, are shown in Fig. 19.

**9.9 The Protactinium Series.<sup>80</sup>** Pa<sup>230</sup> is formed in the deuteron bombardment of Th<sup>232</sup> by the reaction<sup>80</sup> Th<sup>232</sup>(d,4n), in the bombardment of Io (Th<sup>230</sup>) by the reaction<sup>77</sup> Th<sup>230</sup>(d,2n), and in the bombardment of Pa<sup>231</sup> by the reaction<sup>81</sup> Pa<sup>231</sup>(d,p2n). U<sup>230</sup> is formed by the  $\beta$  decay of Pa<sup>230</sup>, and in a series of  $\alpha$ -decay steps Th<sup>228</sup>, Ra<sup>222</sup>, Em<sup>218</sup>, and RaC' (Po<sup>214</sup>) are formed. Since all the  $\alpha$  emitters but U<sup>230</sup> are short lived, a sample of U<sup>230</sup> soon has all five of the  $\alpha$  particles in

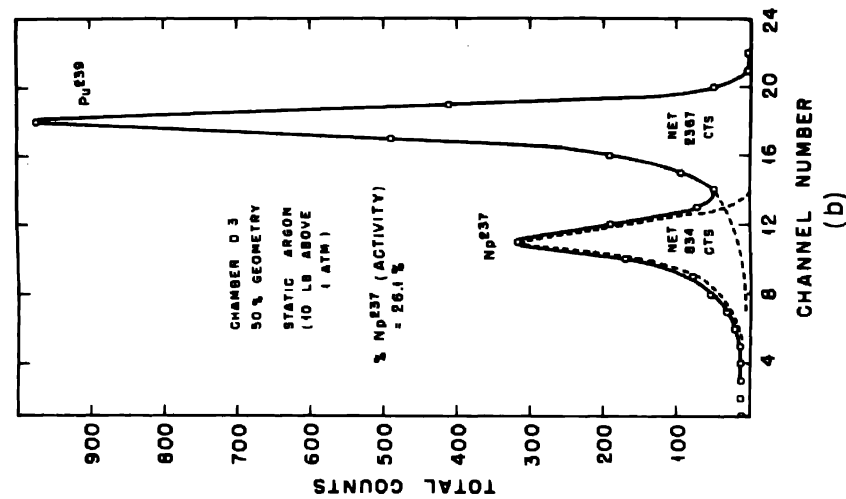


Fig. 18b—Pulse analysis of starting material for Np-Pu separation.

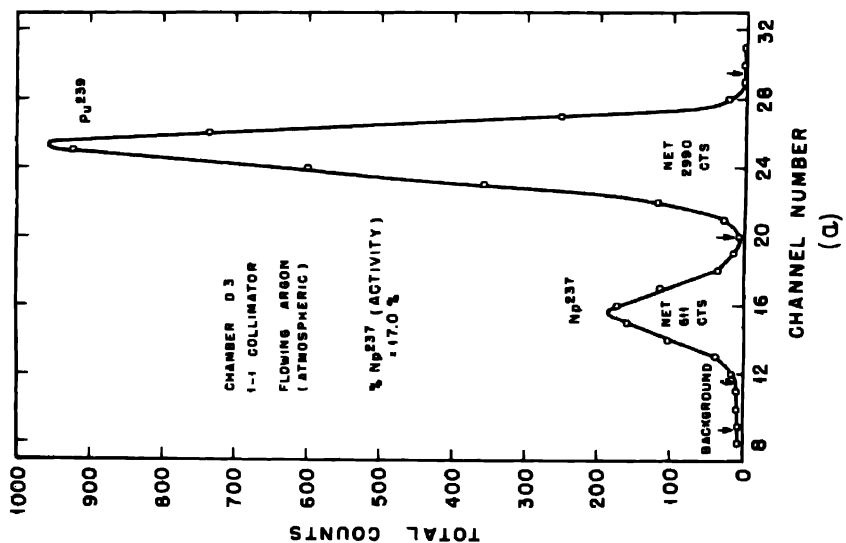


Fig. 18a—Pulse analysis of starting material for Np-Pu separation.

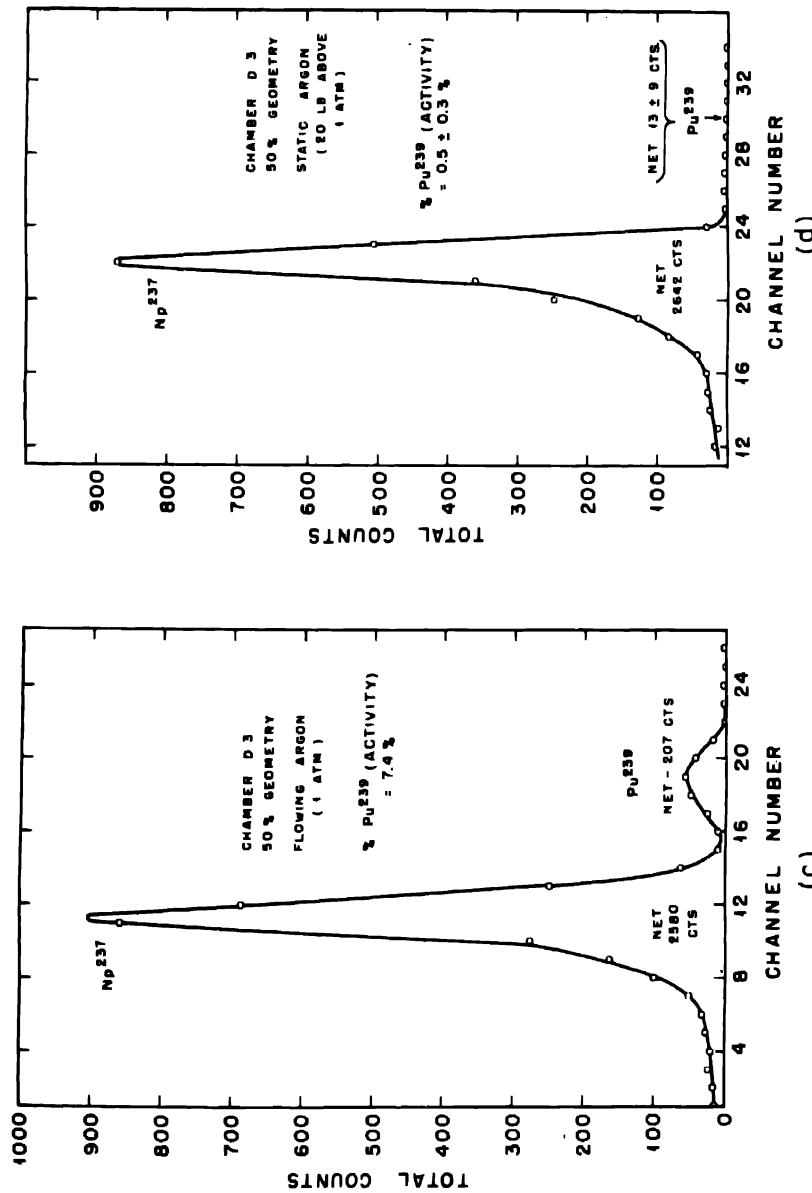


Fig. 18c—Pulse analysis of intermediate-stage material in Np-Pu separation.  
Fig. 18d—Pulse analysis of final stage material in Np-Pu separation.

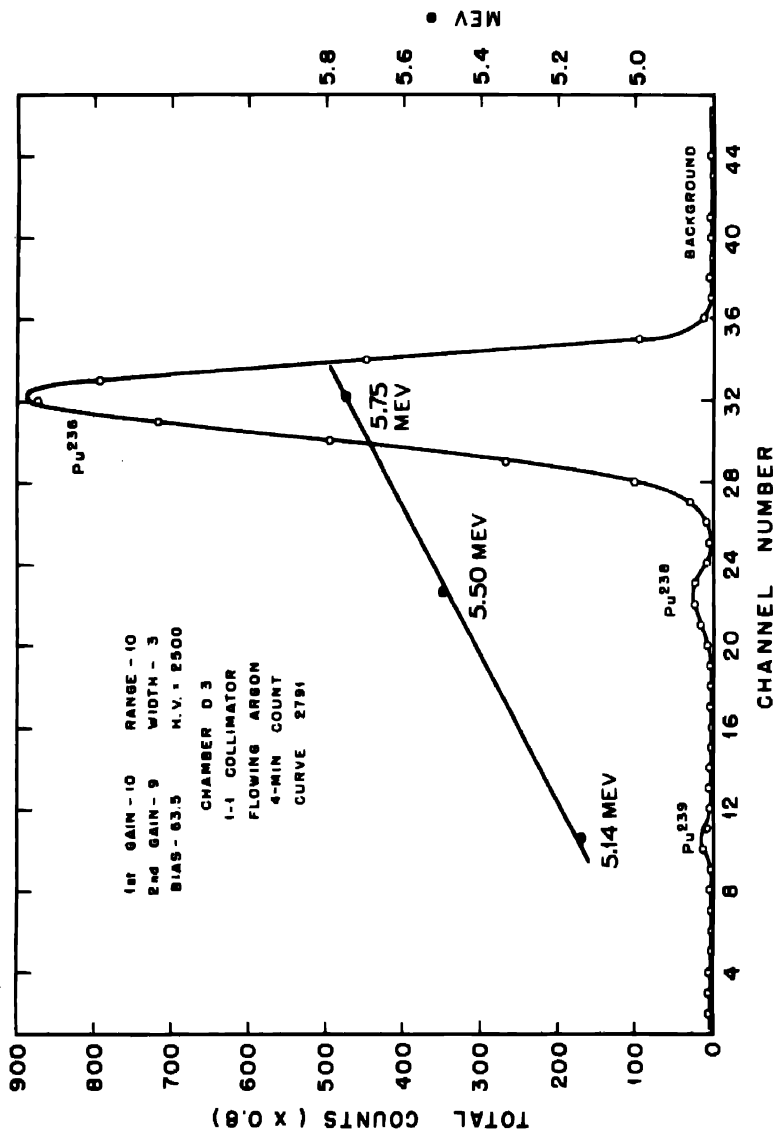


Fig. 19—Pulse analysis of sample 25AB-(4) (Pu fraction from enriched uranium target bombarded with He ions),  $4 \times 10^4$  disintegrations per minute.

PULSE ANALYZER FOR ALPHA-ENERGY MEASUREMENTS

1291

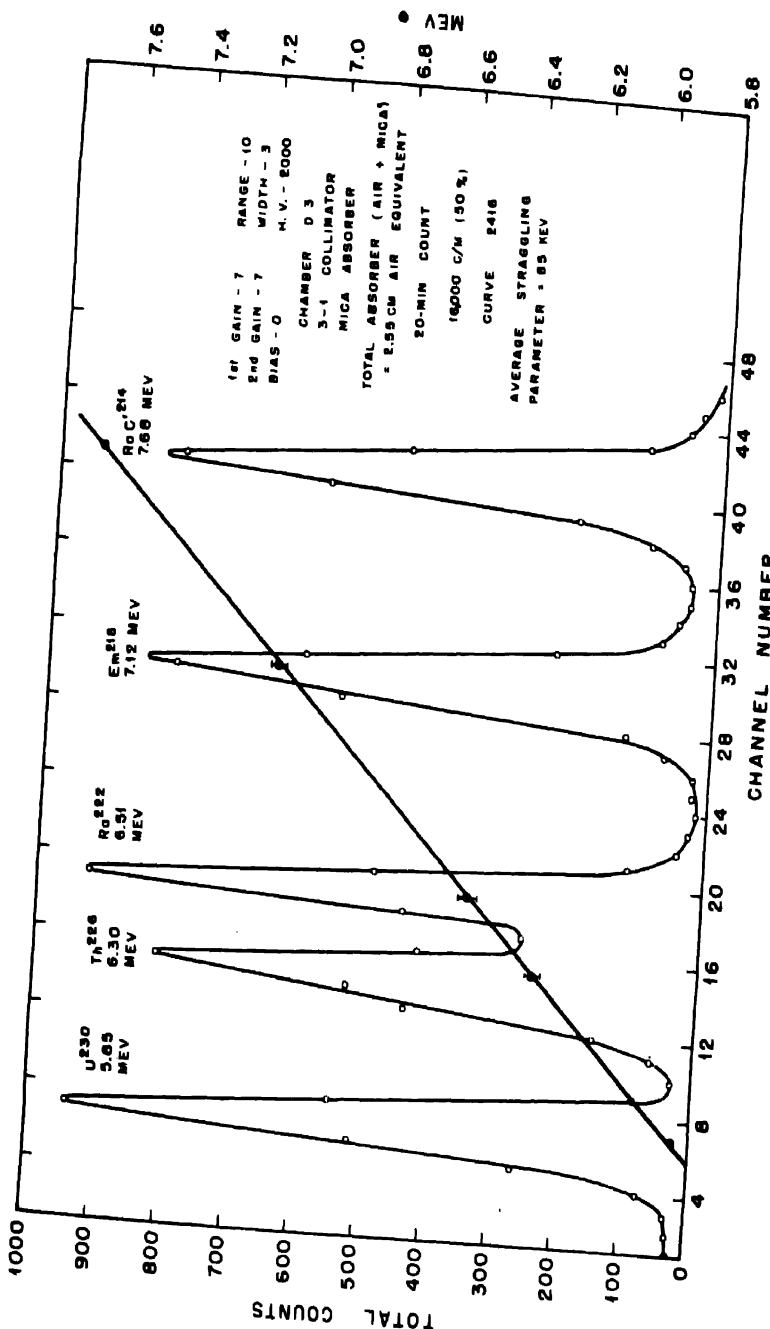


FIG. 20—Pulse analysis of  $\text{Pa}_{226}$  series; sample 11 DA-(I)-1.

equilibrium. The  $\text{U}^{230}$  sample (and daughters in equilibrium) shown in Fig. 20 was separated from  $\text{Pa}^{230}$  formed in the deuteron bombardment of  $\text{Pa}^{231}$ . The energy of  $\text{U}^{230}$  was measured relative to the energies of  $\text{Pa}^{231}$  and  $\text{U}^{232}$  (also formed in the  $\text{Pa}^{231}$  bombardment), and

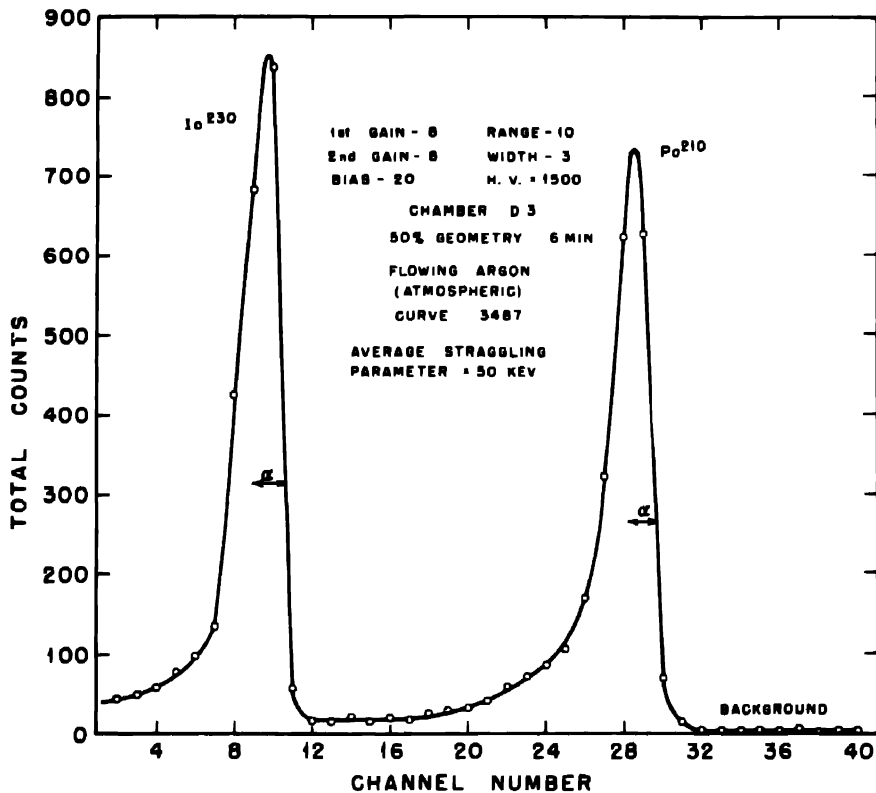


Fig. 21—Pulse analysis of  $\text{Po}^{210}$  standard and  $\text{Io}^{230}$  standard.

also by the use of a RdTh (and daughters) internal standard. It was found<sup>88</sup> to be  $5.85 \pm 0.01$  mev.<sup>†</sup> Since the α particle with highest energy comes from RaC', the energy of which (7.68 mev) has been accurately measured with the magnetic spectrograph, it was used as an internal standard. The energies of  $\text{Th}^{226}$ ,  $\text{Ra}^{222}$ , and  $\text{Em}^{218}$  were determined using  $\text{U}^{230}$  and RaC' as standards; the energies of the  $\text{Ra}^{222}$  and  $\text{Em}^{218}$  α particles were also measured using RdTh (and daughters) as an internal standard. The energies determined<sup>88</sup> were

<sup>†</sup>Average deviation of nine determinations.

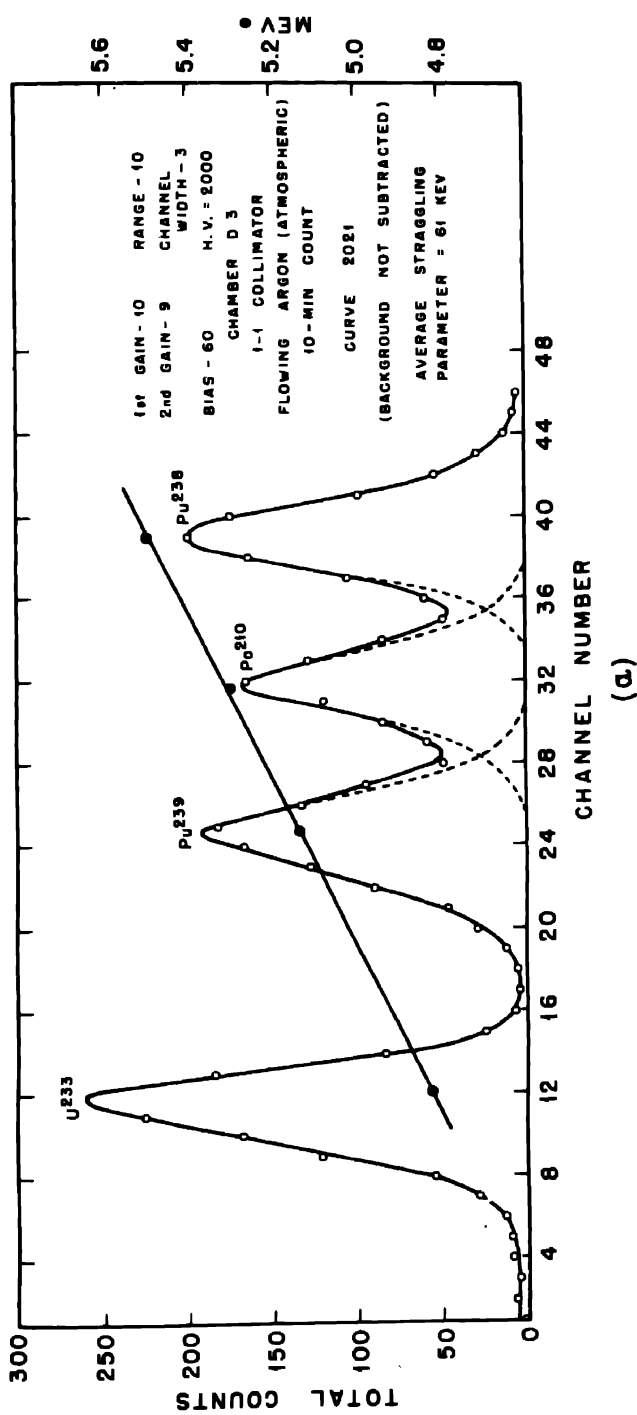


Fig. 22a

## THE TRANSURANIUM ELEMENTS

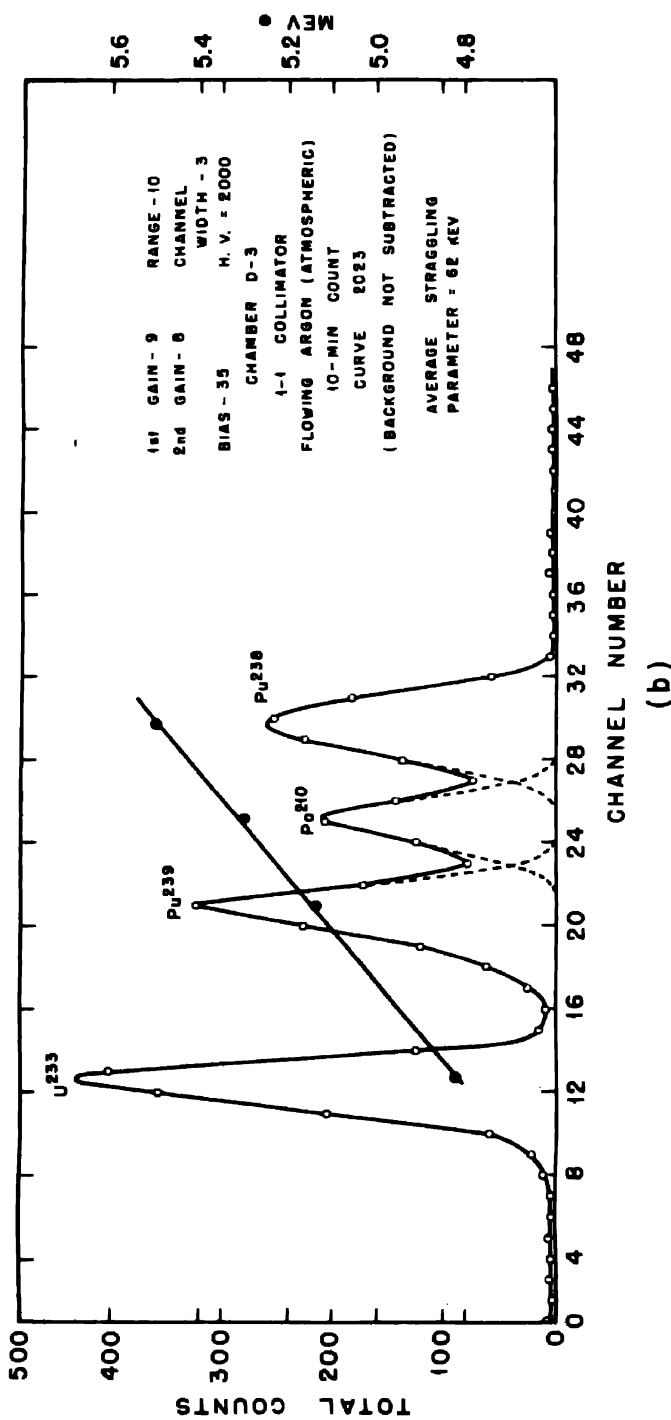
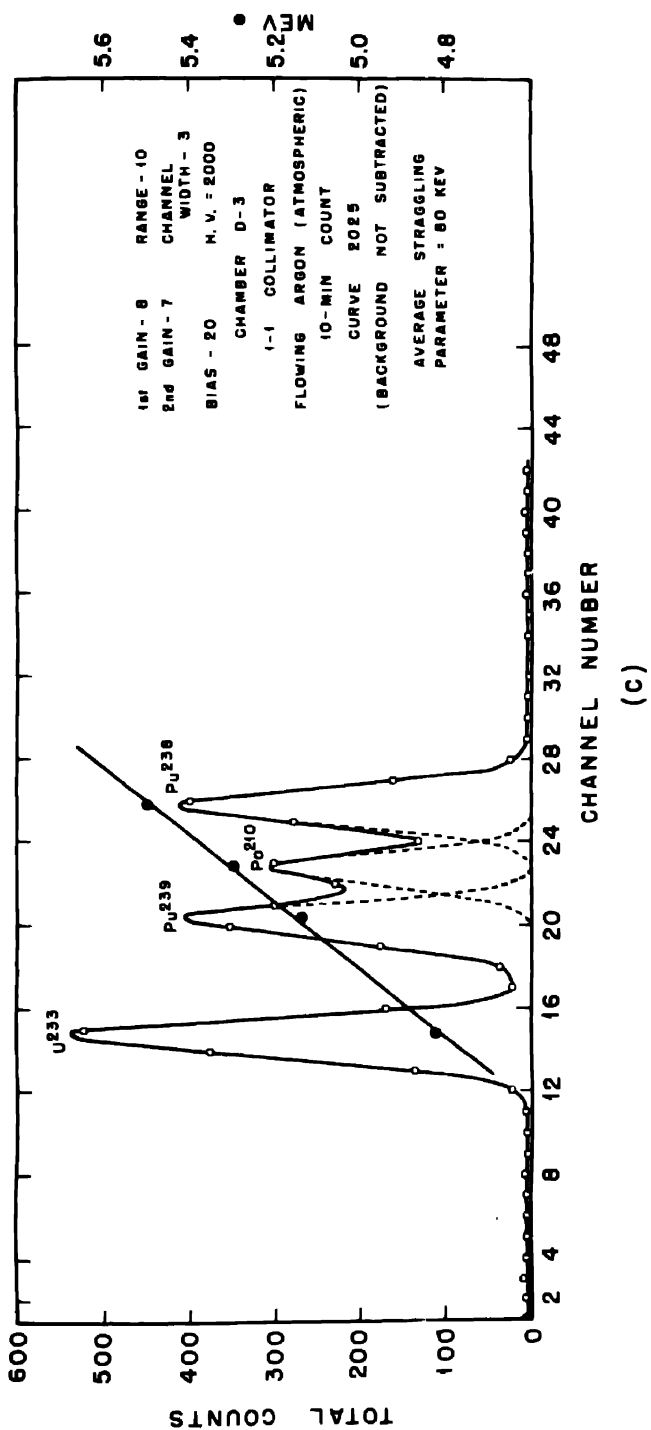


Fig. 22b



Figs. 22a to c—Pulse analysis of U<sup>233</sup>, Pu<sup>239</sup>, Po<sup>210</sup>, Pu<sup>238</sup> standard.

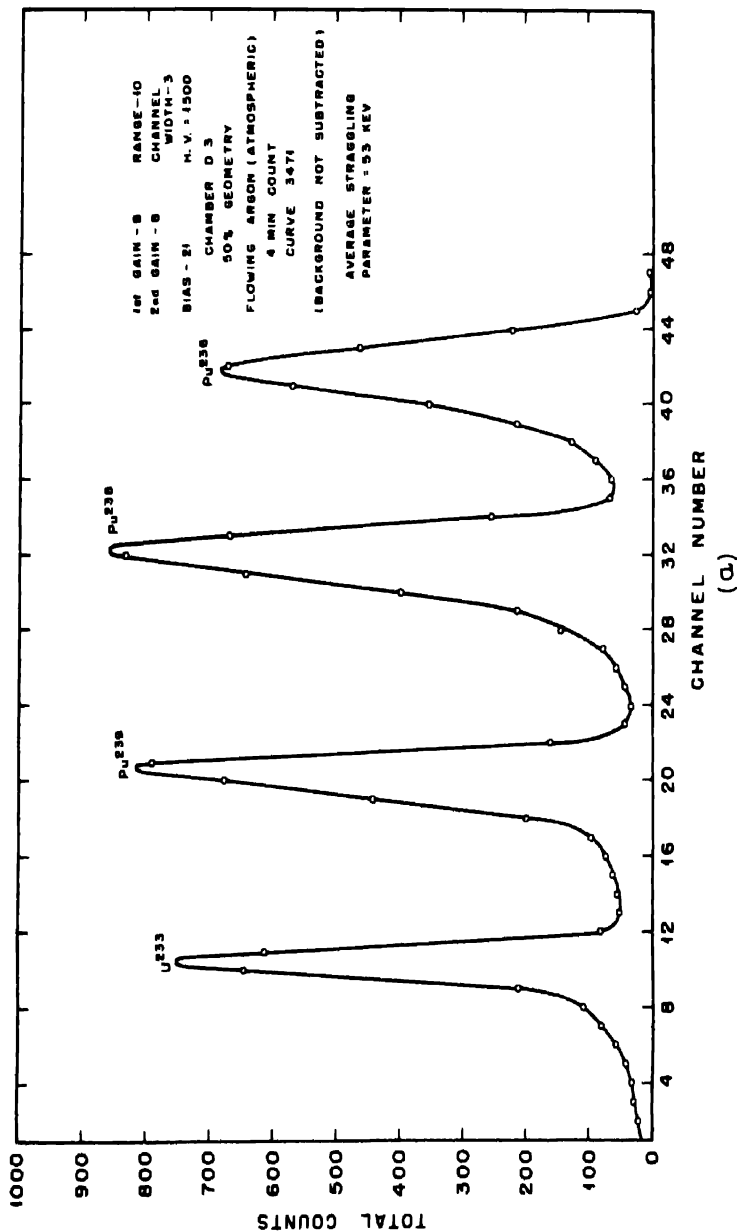


Fig. 23a

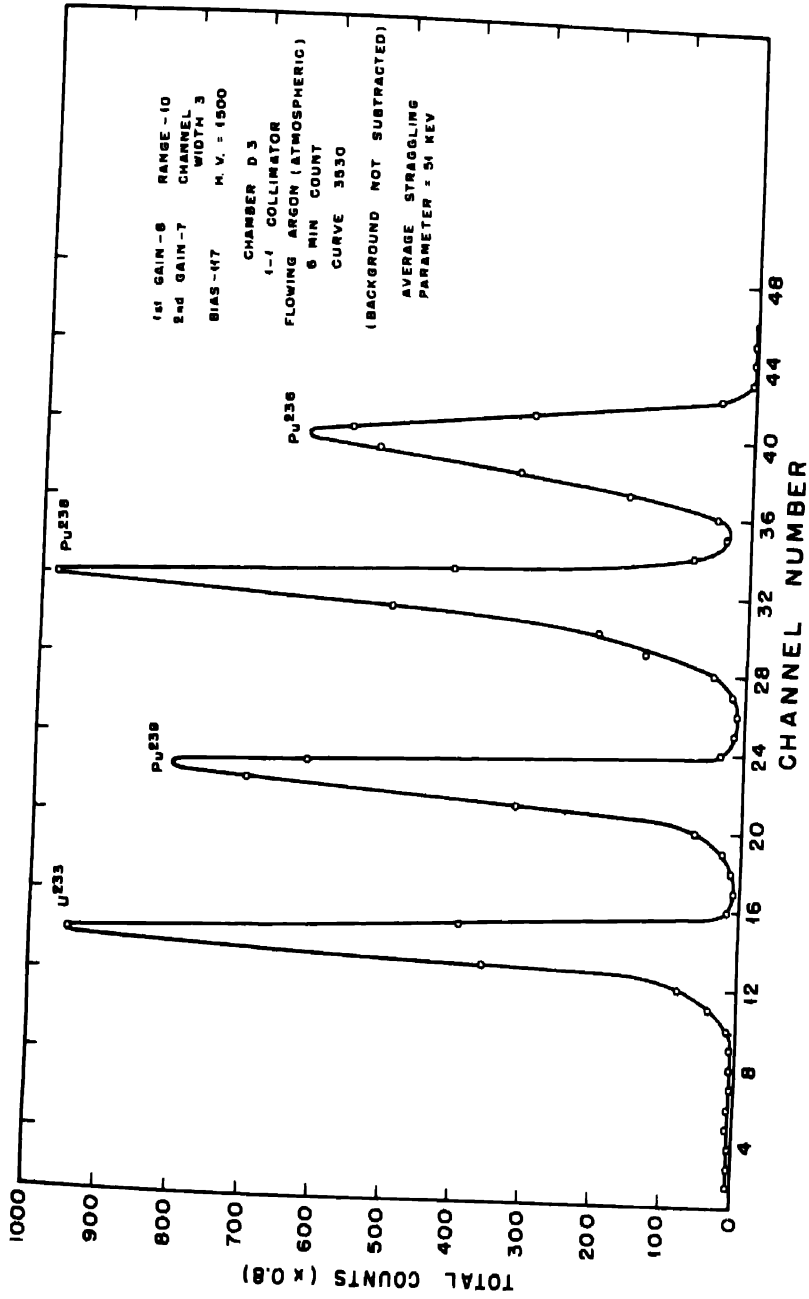
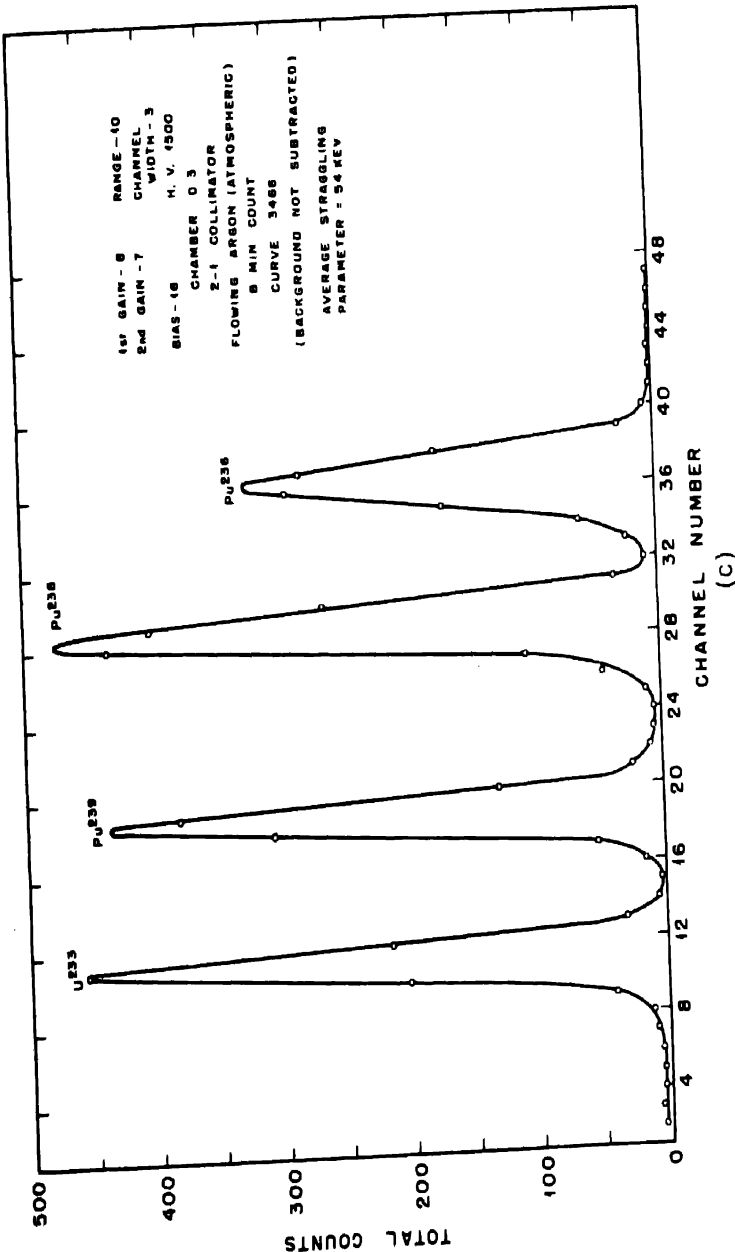


Fig. 23b

## THE TRANSURANIUM ELEMENTS



Figs. 23a to c—Pulse analysis of standard  $\text{U}^{233}$ ,  $\text{Pu}^{239}$ ,  $\text{Pu}^{240}$ ,  $\text{Pu}^{240}$ .

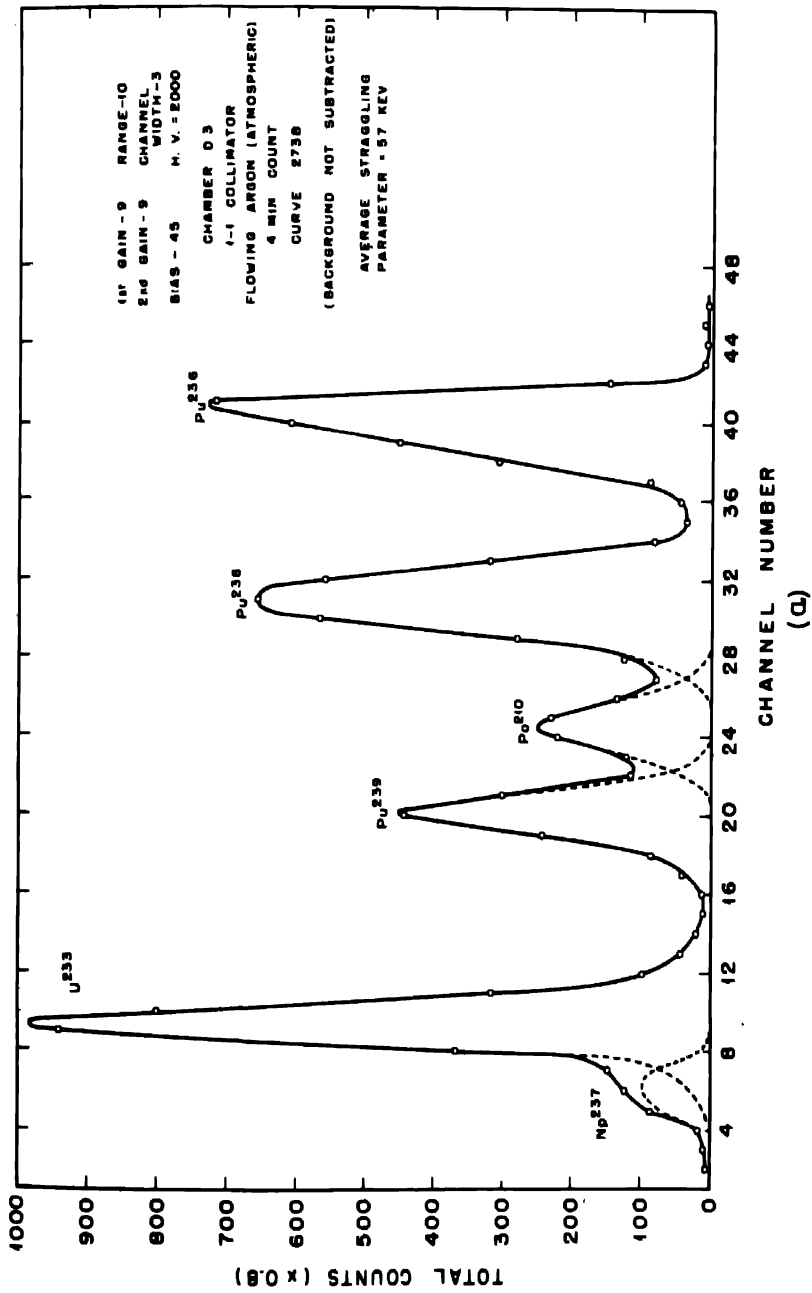
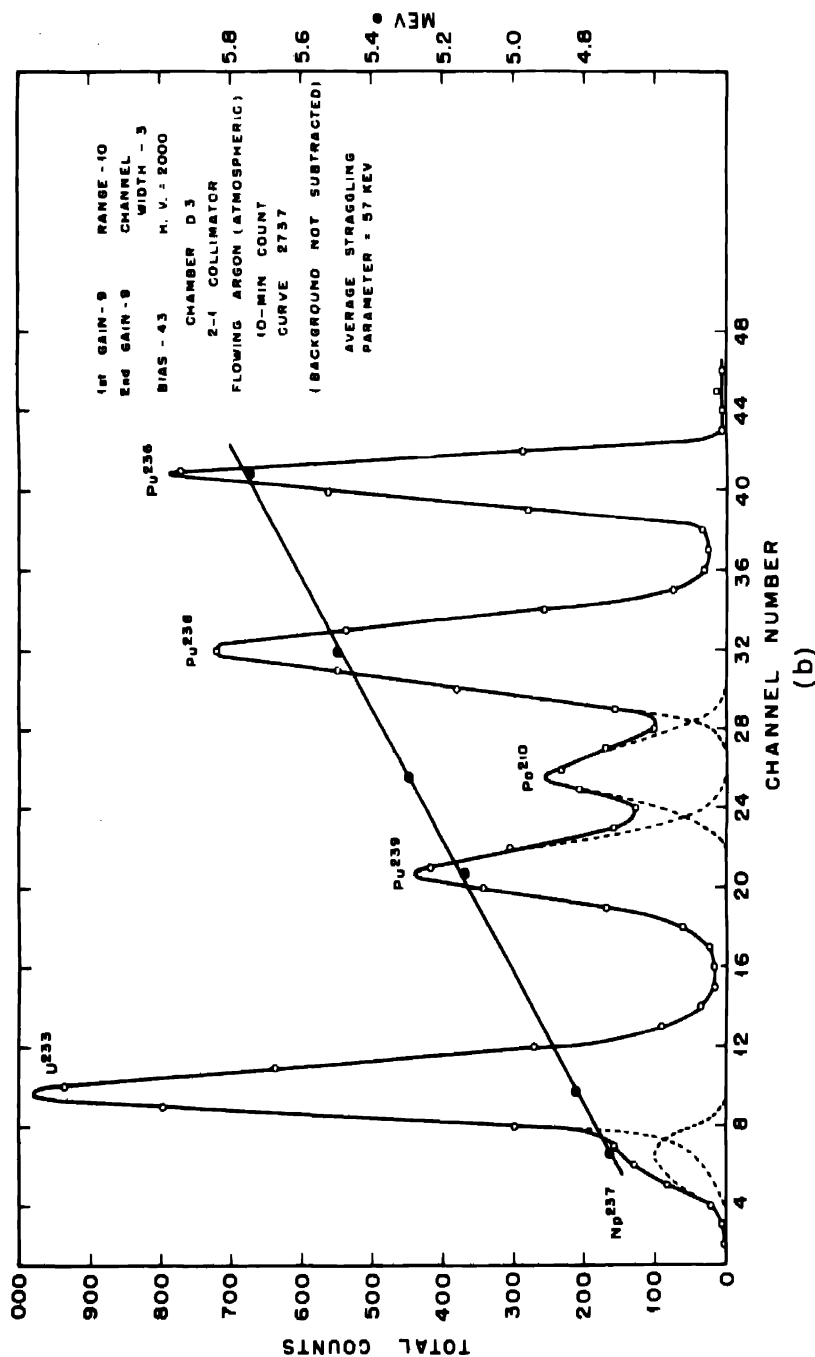


Fig. 24a



Figs. 24a and b—Pulse analysis of sample E-B.  
(b)

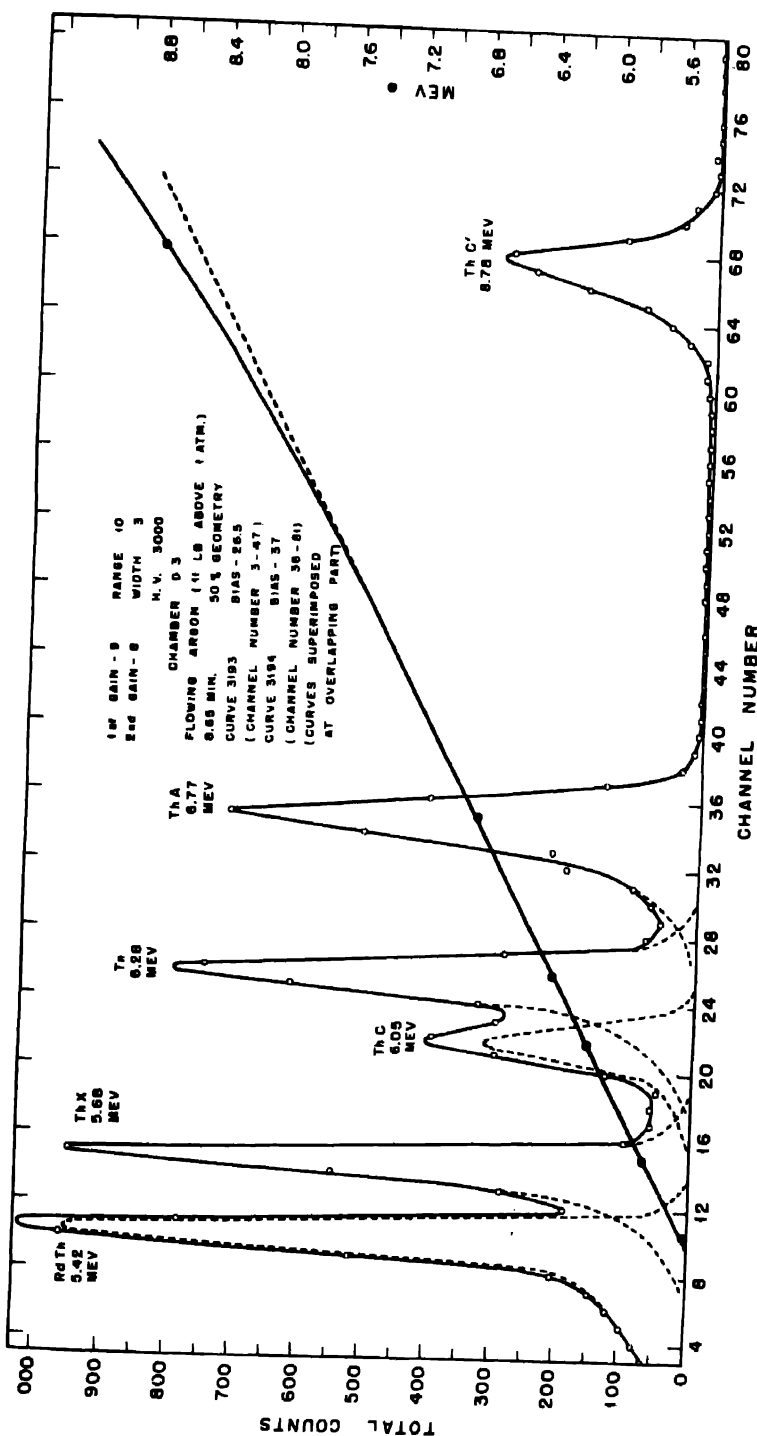


Fig. 25.—Pulse analysis of RdTh and daughters.

$\text{Th}^{230}$ ,  $6.30 \pm 0.02$ , mev; †  $\text{Ra}^{228}$ ,  $6.51 \pm 0.03$  mev; †  $\text{Em}^{218}$ ,  $7.12 \pm 0.02$ , mev. † The assignment of these peaks to the particular nuclides was based upon the Geiger-Nuttall law.

The relatively large average straggling parameter (85 kev) is due partly to the range straggling (and hence straggling in the residual ionization) introduced by the mica and partly to the relatively low collimation (3 to 1) which allows angle straggling (variation in mica absorption with angle of emission) to occur.

**9.10 Some Standard Samples.** An Io ( $\text{Th}^{230}$ ) and a  $\text{Po}^{210}$  standard are shown in Fig. 21. Although the straggling parameters for the two peaks are approximately the same, the low-energy straggling for the Po sample is worse than that of the  $\text{Io}^{230}$  sample. This phenomenon may be due to the same sort of gradual deterioration which has been reported by many other users of Po sources.

Figures 22a to c show the effect of varying the number of channels per peak on the resolution. The straggling parameter is the same for Figs. 22a and b, but it is increased in Fig. 22c, where the peaks are crowded together. The spread of the peaks over the channels was varied by shifting the positions of the gain controls (see Fig. 4).

Figures 23a to c show the effect of collimation. The straggling parameters are about the same for 50 per cent geometry and for 1 to 1 and 2 to 1 collimation. However, the low-energy tails in the 50 per cent geometry measurement decrease the resolution on the low-energy side of each peak, as is evident from the fact that the valleys between the peaks are lower in Figs. 23b and c than in Fig. 23a. No significant difference seems evident between the results obtained with 1 to 1 or 2 to 1 collimation. This fact is also shown in Figs. 24a and b.

The peaks from a RdTh (and daughters) standard are shown in Fig. 25. The nonlinearity of the energy pulse-height relation becomes significant only for the highest energy peak ( $\text{ThC}'$ ). This nonlinearity is probably due both to the positive-ion effect and to amplifier non-linearity at high signal levels.

#### ACKNOWLEDGMENTS

The advice of Drs. W. M. Manning and G. T. Seaborg, under whose general supervision this work was done, is gratefully acknowledged. The authors would also like to thank Donald W. Connor for many helpful discussions.

† Average deviation of twenty determinations.

## REFERENCES

1. T. P. Kohman, Proposed new word: nuclide, Am. J. Phys., 15: 356-357 (1947).
2. A. H. Jaffey, Metallurgical Project Report CC-3771 (Manhattan District Declassified Document MDDC-1336) (Feb. 6, 1947); also in National Nuclear Energy Series, Division IV, Volume 14 A.
3. G. Sizoo and S. Wytzes, Measurement of the range of the alphas of  $U_1$  and  $U_{II}$  with the "sphere method," Physica, 4: 791 (1937).
4. M. G. Holloway and M. S. Livingston, Range and specific ionization of alpha particles, Phys. Rev., 54: 18-37 (1938).
5. E. Rutherford, F. A. B. Ward, and C. E. Wynn-Williams, Differential chamber method for ranges—analysis of groups of alphas. I. Alphas from RaC, ThC, AcC, Proc. Roy. Soc. London, 129: 211 (1930).
6. G. Ortner and G. Stetter, Electronic tube amplifiers for counting particles, Sitz. Akad. Wiss. Wien, Abt. IIa, 137: 667-703 (1938); Z. Physik, 54: 449-476 (1929); Sitz. Akad. Wiss. Wien, Abt. IIa, 142: 471-480, 481-484, 485-491, 492-508 (1933).
7. G. Stetter and J. Schintlmeister, Measurement of beams of particles with a double chamber and the double electrometer tube, Sitz. Akad. Wiss. Wien, Abt. IIa, 142: 427-436 (1933).
8. E. A. W. Schmidt and G. Stetter, Use of the electrometer tube amplifier for researches on protons, Sitz. Akad. Wiss. Wien, Abt. IIa, 138: 271-287 (1929).
9. G. Ortner and J. Schintlmeister, On the radioactivity of samarium, Sitz. Akad. Wiss. Wien, Abt. IIa, 143: 411-416 (1934); Z. Physik, 90: 698-699 (1934).
10. W. Jentschke, Specific ionization of the single alpha particle, Sitz. Akad. Wiss. Wien, Abt. IIa, 144: 151-173 (1935); W. Jentschke and G. Stetter, Z. Physik, 36: 441 (1935).
11. E. Fischer-Colbric, Nuclear disintegration with Ra(B + C) as alpha source, Sitz. Akad. Wiss. Wien, Abt. IIa, 145: 283-300 (1936).
12. J. Schintlmeister, (a) Ionization of the single proton in various gases, Sitz. Akad. Wiss. Wien, Abt. IIa, 141: 539-551 (1932); (b) Search for the source of alphas of 2 cm range, ibid., 145: 450-460 (1936); (c) New determination of the alpha range of thorium, ibid., 146: 371-388 (1937); (d) New determination of ranges of uranium alphas, ibid., 148: 279-295 (1939).
13. J. Schintlmeister, "Use of the Vacuum Tube in Physical Measurements," Verlag Julius Springer, Berlin, 1943.
14. W. Jentschke and F. Prankl, Further measurements on the fission of uranium and thorium under neutron bombardment, Sitz. Akad. Wiss. Wien, Abt. IIa, 148: 237-257 (1939); Energies and masses of uranium fission fragments with thermal neutrons, Z. Physik, 119: 696-712 (1942); Nuclear fragments from neutron-bombarded uranium, Physik. Z., 40: 706-713 (1939).
15. G. Stetter, Ionization (specific and total) of individual alpha particles in various gases, Z. Physik, 120: 639-651 (1943).
16. A. Flammersfeld, P. Jensen, and W. Gentner, Distribution ratio and energy liberation in uranium fission, Z. Physik, 120: 450-467 (1943).
17. W. Jentschke, Energies and masses of uranium fission particles from irradiation with neutrons, Z. Physik, 120: 165-184 (1943).
18. F. L. Clark, H. J. Spencer-Palmer, and R. N. Woodward, British Reports BR-431 (May 4, 1944) (Declassified as BDDA-50), BR-522 (Oct. 10, 1944) and BR-584 (Mar. 5, 1945).
19. O. R. Frisch, British Report BR-49 (June 1942) (Declassified as BDDA-8).
20. A. C. English, Canadian Report MC-145 (May 1945).
21. M. Deutsch and M. Ramsey, Los Alamos Report LA-510 (Jan. 31, 1946).

22. A. Gibert, F. Roggen, and J. Rossel, Nuclear reaction of chlorine with neutrons, *Helv. Phys. Acta*, 17: 97-126 (1944).
23. J. L. Fowler and A. L. Rosen, Los Alamos Report LA-611 (Nov. 18, 1946); *Phys. Rev.*, 72: 926-930 (1947).
24. E. Baldinger and P. Huber, Nuclear transformations of nitrogen with fast neutrons, *Helv. Phys. Acta*, 12: 330-348 (1939); P. Huber, Nuclear reactions of nitrogen and sulfur with neutrons, *ibid.*, 14: 163-188 (1941).
25. M. H. Kanner and H. H. Barschall, Distribution in energy of the fragments from uranium fission, *Phys. Rev.*, 57: 372-378 (1940); On the angular distribution of fast neutrons scattered by hydrogen, deuterium, and helium, *ibid.*, 58: 590-596 (1940).
26. L. Dick, P. Falk-Vairant, and J. Rossel, Energy per ion pair, effects of recombination, and stopping power of various gases for alpha particles, *Helv. Phys. Acta*, 20: 357-372 (1947).
27. B. W. Brown and L. F. Curtiss, Report A-1965.
28. J. H. Parsons, Clinton Laboratories Report Mon-C-416 (Oct. 28, 1947); Atomic Energy Commission Declassified Document AECD-1827.
29. H. Ziegert, Exact measurement of ionization produced by a single alpha particle and the detection of new activities, *Z. Physik*, 46: 668-715 (1928).
30. G. Dieck, Investigation of ion chambers and the definite establishment of radiation of short range, *Z. Physik*, 90: 71-111 (1934).
31. H. Palevsky, R. K. Swank, and R. Grenchik, Design of dynamic condenser electrometers, *Rev. Scientific Instruments*, 18: 298-314 (1947).
32. W. P. Jesse and H. Forstat, *Phys. Rev.*, 73: 928-927 (1948).
33. G. Ortner and G. Stetter, On the choice of the coupling elements for an amplifier with small time constants, *Sitz. Akad. Wiss. Wien, Abt. IIa*, 142: 485-491, (1933).
34. D. Maeder, Vacuum tube spectrograph for measurement of ionization chamber pulses, *Helv. Phys. Acta*, 20: 139-152, 230-234 (1947).
35. A. Roberts, A differential pulse amplitude selector, *Rev. Scientific Instruments*, 11: 44-45 (1940).
36. F. J. Davis and L. F. Curtiss, Report A-1722 (Dec. 22, 1943).
37. M. J. Poole, British Report BR-516 (May 7, 1944) (Declassified as BDDA-17).
38. One of these is reported in an unclassified Canadian report: G. C. Hanna and C. H. Westcott, CRP-291 (PD-200) (Sept. 24, 1946); Pulse amplitude analyzer for nuclear research using pretreated pulses, *Rev. Sci. Instruments*, 20: 181-188 (1949).
39. E. W. Dexter and M. L. Sands, Los Alamos Report LAMS-573 (May 1947).
40. H. F. Freundlich, E. P. Hincks, and W. J. Ozeroff, Canadian Report CRTec-287 (July 1946), *Rev. Scientific Instruments*, 18: 90-100 (1947).
41. G. Ortner and G. Stetter, Pure nitrogen for ionization chambers, *Anz. Akad. Wiss. Wien.*, 70: 241-242 (1933).
42. J. Allen and B. Rossi, Los Alamos Report LA-115 (July 28, 1944) (Declassified as MDDC-448).
43. B. Rossi and H. Staub, Ionization chambers and counters, National Nuclear Energy Series, Division V, Volume 2, Chap. 1.
44. B. Rossi and H. Staub, *ibid.*, Chap. 3.
45. B. Rossi and H. Staub, *ibid.*, Chaps. 3 and 6.
46. G. Stetter, On the collection of charge in an ionization chamber, *Sitz. Akad. Wiss. Wien, Abt. IIa*, 142: 471-480 (1933).
47. T. M. Snyder, Los Alamos Report LA-484 (Dec. 29, 1945) (Declassified as MDDC-475).
48. Ruby Sherr and Rolf Peterson, Los Alamos Report LAMS-436 (Declassified as MDDC-474); *Rev. Scientific Instruments*, 18: 567-575 (1947).
49. G. Ortner and G. Stetter, Nuclear disintegration with Ra(B + C) as source. I. Method, *Sitz. Akad. Wiss. Wien, Abt. IIa*, 142: 492-508 (1933).

50. G. Stetter, A new method of measuring ion mobilities, *Physik. Z.*, 33: 294-296 (1932).
51. O. Bunemann, T. E. Cranshaw, and J. C. Harvey, Canadian Report CRP-247 (Declassified) (May 1, 1946).
52. J. H. Coon and H. H. Barschall, Angular distribution of 2.5-mev neutrons scattered by deuterium, *Phys. Rev.*, 70: 592-596 (1946).
53. E. D. Klema and H. H. Barschall, Saturation characteristics for alpha particles in purified gases, *Phys. Rev.*, 63: 18-23 (1943).
54. D. W. Connor, Quarterly summary report, Chemistry Division, Argonne National Laboratory Report ANL-4143 (Apr. 15, 1948).
55. T. Brill, Metallurgical Project Report CP-3004 (July 1945).
56. T. P. Kohman, private communication.
57. J. K. East, A. A. Jarrett, and J. H. Parsons, Metallurgical Project Report CP-2046 (Mar. 7, 1945).
58. D. L. Hufford and B. F. Scott, Techniques for the preparation of thin films of radioactive material, Paper 16.1, this volume (Metallurgical Project Report CN-3328).
59. J. W. Britain, unpublished work.
60. U. Fano, Ionization yield of radiations. II. The fluctuations of the number of ions, *Phys. Rev.*, 72: 26-29 (1947).
61. E. Rona and J. Schintlmeister, Investigation of the alphas of  $\text{MsThII}$ , *Sitz. Akad. Wiss. Wien, Abt. IIa*, 147: 49-62 (1938).
62. This paper.
63. A. H. Jaffey and D. W. Connor, private communication.
64. W. Y. Chang and S. Rosenblum, A simplified counting system for alpha-ray spectra and the energy distribution of Po alpha particles, *Phys. Rev.*, 67: 222-227 (1945).
65. J. A. Crawford, Theoretical calculations concerning back-scattering of alpha particles, Paper 16.55, this volume (Metallurgical Project Report CC-1342).
66. G. T. Seaborg and I. Perlman, Table of Isotopes, University of California Radiation Laboratory Report BC-59 (May 1947); *Rev. Modern Phys.*, 20: 585-667 (1948).
67. W. M. Manning and L. B. Asprey, Preparation and radioactive properties of  $\text{Am}^{243}$ , Paper 22.7, this volume.
68. G. T. Seaborg, Plutonium and other transuranium elements, Harrison Howe Lecture, *Chem. and Eng. News*, 25: 397 (1947).
69. A. H. Jaffey, Half life of  $\text{Pu}^{238}$  by direct decay measurement, Paper 2.2, this volume (Argonne National Laboratory Report ANL-4020).
70. G. T. Seaborg, A. C. Wahl, and J. W. Kennedy, Report A-136 (Mar. 20, 1942).
71. G. T. Seaborg, E. M. McMillan, J. W. Kennedy, and A. C. Wahl, Radioactive element 94 from deuterons on uranium, *Phys. Rev.*, 69: 366 L (1946).
72. R. A. James, A. E. Florin, H. H. Hopkins, Jr., and A. Ghiorso, Products of helium-ion and deuteron bombardment of  $\text{U}^{235}$  and  $\text{U}^{238}$ , Paper 22.8, this volume.
73. F. Hagemann, L. I. Katzin, M. H. Studier, G. T. Seaborg, and A. Ghiorso, Metallurgical Project Report CB-3692 (Oct. 28, 1946); (Declassified version) *Phys. Rev.*, 72: 252 L (1947).
74. A. C. English, Canadian Report MC-145 (May 1945).
75. A. C. English, T. E. Cranshaw, P. Demers, J. A. Harvey, E. P. Hincks, J. V. Jelley, and A. N. May, The (4n+1) radioactive series, *Phys. Rev.*, 72: 252 L (1947).
76. A. C. English and J. A. Harvey, Canadian Report CRC-269 (May 1946).
77. E. K. Hyde, M. H. Studier, H. H. Hopkins, Jr., and A. Ghiorso, A new isotope of protactinium:  $\text{Pa}^{230}$ , Paper 19.17, this volume (Metallurgical Project Report CC-3648).
78. M. H. Studier, private communication.
79. J. W. Gofman and G. T. Seaborg, Metallurgical Project Report CN-332 (Oct. 20, 1942).

## THE TRANSURANIUM ELEMENTS

80. M. H. Studier and E. K. Hyde, Metallurgical Project Report CC-3662 (October 1946); Phys. Rev., 74: 591-600 (1948); also in National Nuclear Energy Series, Division IV, Volume 17B.
81. D. W. Osborne, R. C. Thompson, and Q. Van Winkle, Products of the deuteron and helium-ion bombardments of  $\text{Pa}^{231}$ , Paper 19.11, this volume.
82. S. Peterson and A. Ghiorso, Half life of  $\text{Th}^{237}$ , Paper 19.12, this volume (Metallurgical Project Report CB-3791).
83. S. Peterson and A. Ghiorso, Alpha branching of  $\text{Ac}^{237}$ , Paper 19.10, this volume (Argonne National Laboratory Report ANL-4043).
84. G. T. Seaborg, R. A. James, and L. O. Morgan, The new element americium (atomic number 95), Paper 22.1, this volume.
85. B. B. Cunningham, The first isolation of americium in the form of pure compounds. Microgram-scale observations on the chemistry of americium, Paper 19.2, this volume.
86. S. Fried, Chemistry Division (Section C-1) summary report for January to March, 1948, Argonne National Laboratory Report ANL-4143 (Apr. 15, 1948).
87. S. Fried, Abstracts of papers at Atomic Energy Commission information meeting at Brookhaven, Paper C4 (April 1948).
88. A. H. Jaffey, Chemistry Division (Section C-1) summary report for April to June, 1948, Argonne National Laboratory Report ANL-4176.

Paper 16.55

THEORETICAL CALCULATIONS CONCERNING  
BACK-SCATTERING OF ALPHA PARTICLES<sup>†</sup>

By J. A. Crawford

If an  $\alpha$ -emitting substance is spread thinly on a platinum plate and counted in a parallel-plate 50 per cent geometry ionization chamber, a certain percentage of the  $\alpha$  particles counted will have been back-scattered from the sample backing. The counting yield (the ratio of counts per minute to disintegrations per minute) should therefore be somewhat more than 50 per cent. The amount of this increase has always been thought to be negligible; a figure of 1/8,000 obtained by Geiger and Marsden<sup>1</sup> from a different type of scattering experiment has often been quoted to prove that this back-scattered fraction is indeed too small to worry about.

However, in August 1943 results were obtained by Cunningham, Ghiorso, and Jaffey<sup>2</sup> which could be interpreted only by assuming an approximately 52 per cent counting yield for samples mounted on platinum or an error in the accepted value for the specific  $\alpha$  activity of normal uranium. At the time, the latter explanation was accepted, but it became important to determine whether it was at all possible that the extra 2 per cent in counting yield could be due to back-scattering. As soon as the matter was examined, it became evident that much more back-scattering might be expected than from the Geiger-Marsden experiment, and so the following calculations<sup>†</sup> were made to estimate a lower limit for this phenomenon.

<sup>†</sup>Contribution from the Chemistry Division of the Metallurgical Laboratory, University of Chicago, now the Argonne National Laboratory.

<sup>1</sup>The author is grateful for helpful discussions and criticism of the manuscript by A. H. Jaffey.

The scattering of  $\alpha$  particles can be divided into three classes: multiple, plural, and single scattering. Multiple scattering is considered the result of a very large number of weak collisions and obeys rather closely a Gaussian distribution. Plural scattering is the result of a smaller number of collisions. Single scattering is the result of only one relatively strong collision produced by a close approach of the  $\alpha$  particle to an atomic nucleus.

Back-scattering in a parallel-plate chamber is most likely due to small-angle scattering, and since that scattering which occurs at small angles is primarily multiple scattering, the calculation has been limited to this effect. Using the data from experiments performed by Geiger in 1910, it was found that on substances of atomic weight as high as that of platinum,  $\alpha$  particles of range 3.68 cm of air were scattered to the extent of 3 to 3½ per cent. On lighter elements the back-scattering was smaller, that on aluminum, for example, being approximately one-fourth that on platinum.

### 1. CALCULATION OF MULTIPLE BACK-SCATTERING OF ALPHA PARTICLES†

We shall first set up Geiger's equations for multiple scattering as they apply to his experiments:

The experimental setup consisted of a narrow parallel pencil of  $\alpha$  particles traversing a thin foil and falling on a screen placed at a distance  $d$  from the foil (see Fig. 1).

The scattering was measured by counting scintillations on the screen.

The probability that a particle hit the element  $dx dy$  of the screen is:

$$P_{x,y} dx dy = \frac{1}{2l^2\pi} e^{-(x^2+y^2/2l^2)} dx dy$$

Introducing polar coordinates and integrating with respect to the angle between 0 and  $2\pi$ , we obtain the probability  $P_\rho$  of any deflection  $\rho$  from the center, namely,

$$P_\rho d\rho = \frac{\rho}{l^2} e^{-\rho^2/2l^2} d\rho$$

†See references 3 to 5.

‡Made thin enough so that the slowing down of the  $\alpha$  particle, as it traverses the foil, is negligible.

The curve  $P_\rho = f(\rho)$  presents a maximum for  $\rho = l$ , so that  $l$  is the most probable deflection in polar coordinates.

These equations can be written in terms of the tangents of the scattering angles as follows:

$$P_{\lambda_x, \lambda_y} d\lambda_x d\lambda_y = \frac{1}{2\pi\Lambda^2} e^{-(\lambda_x^2 + \lambda_y^2/2\Lambda^2)} d\lambda_x d\lambda_y$$

$$P_\lambda d\lambda = \frac{\lambda}{\Lambda^2} e^{-\lambda^2/2\Lambda^2} d\lambda$$

where  $\lambda = \rho/d$ ,  $\lambda_x = x/d$ ,  $\lambda_y = y/d$ , and  $\Lambda = 1/d$ , with  $\Lambda$  being the most probable value of the tangent of the scattering angle in polar coordinates,  $\lambda_x$  and  $\lambda_y$  its x and y components, and  $\lambda$  its actual value.

Now the probability that  $\lambda_y$  lies between  $\lambda_y$  and  $\lambda_y + d\lambda_y$  is

$$P_{\lambda_y} d\lambda_y = \frac{1}{\Lambda\sqrt{2\pi}} e^{-\lambda_y^2/2\Lambda^2} d\lambda_y \quad (1)$$

obtained by integrating over  $\lambda_x$  between the limits  $-\infty$  and  $+\infty$ .

We will henceforth refer to  $\lambda$  as "scattering angle" rather than as "tangent of the scattering angle." This is allowable since  $\lambda \cong \arctan \lambda$  except when the multiple scattering is entirely negligible. Thus we see that the scattering angle in a particular direction, for example, y, obeys a Gaussian distribution law. This fact forms the basis of all our calculations. The parameter  $\Lambda$  is the root-mean-square value of  $\lambda_y$  and in polar coordinates is also the most probable value of  $\lambda$ .†

To apply these considerations to the problem at hand, consider an infinitely thin  $\alpha$ -emitting sample spread over the surface of a flat plate (e.g., gold or platinum).

Consider an  $\alpha$  particle, emitted at the point O (see Fig. 2) in the direction OZ, in the plane of the figure. OZ forms the angle  $\epsilon$  with

† If the probability distribution of two independent variables x,y is Gaussian, then

$$P(x,y) dx dy = \frac{1}{2\pi Z^2} e^{-(x^2+y^2)/2Z^2} dx dy$$

and setting  $\rho = \sqrt{x^2 + y^2}$ , the most probable value of  $\rho$  is  $Z$ . But also, by integrating with respect to x from  $-\infty$  to  $+\infty$ , we get  $\sqrt{y^2} = Z$ . Hence the root-mean-square value of one variable equals the most probable value of the square root of the sum of the squares of the two variables.

the surface of the plate. Because of scattering, the particle will not remain in the plane of the figure. However, the projection of its motion onto that plane will be treated.

Set up a coordinate system with origin O, Z axis along OZ, and X axis perpendicular to the plane of the figure. Let P be the projection of the position of the particle onto this plane. Since multiple scattering is a small-angle phenomenon, the distance traversed by the particle will be nearly equal to its z ordinate and will be treated as

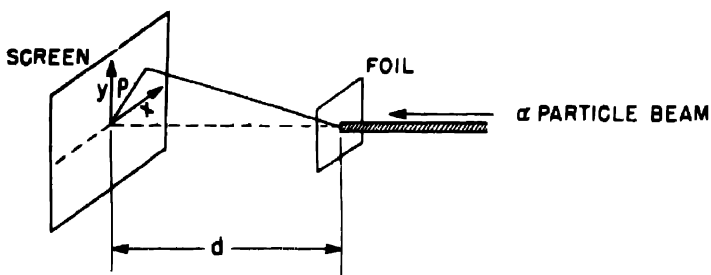


Fig. 1—Experimental setup for calculation of multiple back-scattering of particles.

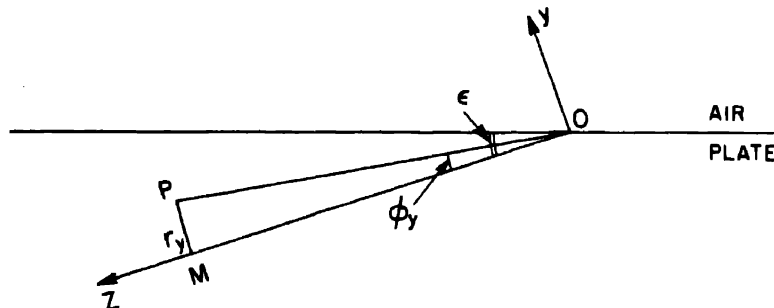


Fig. 2—Diagram showing relation of variables for an infinitely thin  $\alpha$ -emitting sample spread over the surface of a flat plate.

such. The distance of the particle from the line OZ is called the "drift"  $r$  of the particle. We are chiefly interested in the  $y$  component ( $MP = r_y$ ) of this drift. The  $z$  ordinate of the particle is denoted by  $s$ , which is referred to (approximately) as the distance traversed by the particle.

The small angle formed by the position vector of the particle and the  $Z$  axis is known as the "drift angle." The tangent of this angle,

$\phi = r/s$ , is nearly equal to the angle itself and will be identified with it, as was done for the  $\lambda$  factor. We shall be mainly interested in the  $y$  component,  $\phi_y = r_y/s$ , of the drift angle.

Geiger's experiments involved directing a beam of  $\alpha$  particles at a thin foil and measuring the angle through which they were deflected after traversing the foil. His data therefore give the change in direction of motion of particles going through matter. We are interested primarily in the drift. The drift can be computed by integrating in the proper way the change in direction of motion as the particle continues its journey through the scattering material.

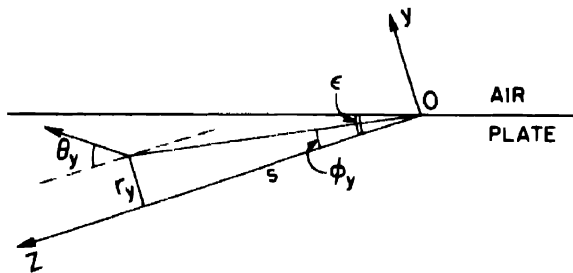


Fig. 3—Relation of variables in the investigation of the scattering and drift of an  $\alpha$  particle.

We shall investigate the scattering (and drift) in the  $y$  direction of an  $\alpha$  particle emitted along the line  $OZ$  (see Fig. 2). Consider the particle as successively traversing thin differential layers of the material, each differential layer being, however, sufficiently thick so that the Gaussian law of multiple scattering in the  $y$  direction holds. If  $\Delta s$  is the thickness of an elementary layer, and  $\Delta\theta_y$  the angle through which a particle is scattered in the  $y$  direction by traversing the layer, then the angle  $\theta_y$  through which it is scattered by traversing a finite thickness, is (see Fig. 3)

$$\theta_y = \lim_{\Delta_i \theta_y \rightarrow 0} \sum_i \Delta_i \theta_y \quad (2)$$

whence†

$$\overline{\theta_y^2} = \lim_{\Delta_i \theta_y \rightarrow 0} \sum_i \overline{(\Delta_i \theta_y)^2} = \lim_{\Delta s_i \rightarrow 0} \sum_i \frac{\overline{(\Delta \theta_y)^2}}{\Delta s_i} \Delta s_i$$

†According to the well-known theorem which states that if  $A = \sum_i a_i$  then  $\overline{A^2} = \sum_i \overline{a_i^2}$  provided the values of  $a_i$  obey a Gaussian distribution law. See Appendix B.

Now we know that

$$\lim_{\Delta s_i \rightarrow 0} \sum_i \frac{(\Delta \theta_y)^2}{\Delta s_i} \Delta s_i$$

is finite.<sup>4</sup> Therefore, differentiating with respect to  $s$ ,

$$\frac{d(\overline{\theta_y^2})}{ds} = \lim_{\Delta s \rightarrow 0} \frac{(\Delta \theta_y)^2}{\Delta s}$$

Denoting  $\sqrt{\overline{\theta_y^2}}$  by  $\Theta$ , we have

$$\frac{d\Theta^2}{ds} = \lim_{\Delta s \rightarrow 0} \frac{(\Delta \theta_y)^2}{\Delta s}$$

Since  $\Delta \theta_y$  obeys a Gaussian law, its distribution is given by Eq. 1, where  $\lambda_y = \Delta \theta_y$  and  $\Lambda = \sqrt{(\Delta \theta_y)^2} =$  the most probable value of  $\Delta \theta_y$  in polar coordinates (see footnote, p. 1309).

With this identification, it is possible to write (see reference 4)†

$$\lim_{\Delta s \rightarrow 0} \left[ \frac{(\Delta \theta_y)^2}{\Delta s} \right]_s = \lim_{\Delta s \rightarrow 0} \left[ \frac{(\Delta \theta_y)^2}{\Delta s} \right]_0 \frac{s^2}{(S - s)^2} \quad (3a)$$

or

$$\left[ \frac{d\Theta^2}{ds} \right]_s = \left[ \frac{d\Theta^2}{ds} \right]_0 \frac{s^2}{(S - s)^2} \quad (3b)$$

where  $S$  is the initial range of the particle,  $s$  the distance already traversed,  $\left[ \frac{d\Theta^2}{ds} \right]_0$  the derivative of  $\overline{\theta_y^2}$ , with respect to  $s$  at  $s = 0$ , before the particle has lost any of its energy. This law states that the root-mean-square value of  $\Delta \theta_y$  is inversely proportional to the remaining range (see Appendix A).

†Our notation differs from that used by Geiger, who takes as his elementary distance  $\Delta s$ , the thickness of a monatomic layer. The two formulations are equivalent.

It seems appropriate at this point to calculate a result that will be applied later, namely, the value of  $\theta$ , the root-mean-square value of  $\theta_y$ , after the particle has traveled a finite distance  $s$ .

This value of  $\theta$  is related to Geiger's L by  $\theta = L/d$  (see reference 4). We have

$$\left[ \frac{d\theta^2}{ds} \right]_t = \left[ \frac{d\theta^2}{ds} \right]_0 \frac{s^2}{(s-t)^2}$$

after the particle has traveled a distance  $t$  (since  $\theta_0^2 = 0$ ).

$$\begin{aligned} \theta_s^2 &= \left[ \frac{d\theta^2}{ds} \right]_0 \int_0^s \frac{s^2 dt}{(s-t)^2} = \left[ \frac{d\theta^2}{ds} \right]_0 s^2 \int_0^s \frac{dt}{(s-t)^2} \\ &= \left[ \frac{d\theta^2}{ds} \right]_0 \frac{Ss}{S-s} \end{aligned} \quad (4)$$

where  $\left[ \frac{d\theta^2}{ds} \right]_0$  is the rate of change of  $\theta^2$  with respect to  $s$  at the beginning of the range.

We shall now proceed to calculate the y component of the drift,  $r_y$ .

$$dr_y = \theta_y ds$$

whence

$$\frac{\partial r(s)}{\partial s} = \theta_y(s) = \lim_{\Delta t_i \rightarrow 0} \sum_{i=0}^{t=s} \Delta_i \theta_y = \lim_{\Delta t_i \rightarrow 0} \sum_{i=0}^{t=s} \frac{\Delta \theta_y}{\Delta t_i} \Delta t_i$$

since  $\theta_y(0) = 0$ .

Now it follows that

$$\lim_{\Delta t_i \rightarrow 0} \sum_{i=0}^{t=s} \frac{\Delta \theta_y}{\Delta t_i} \Delta t_i = \frac{\partial}{\partial s} \lim_{\Delta t_i \rightarrow 0} \sum_{i=0}^{t=s} (s-t) \frac{\Delta \theta_y}{\Delta t_i} \Delta t_i$$

To show this, exactly the same procedure is followed as that used to prove

$$\frac{\partial}{\partial \alpha} \int_a^x f(x, \alpha) dx = \int_a^x \frac{\partial f(x, \alpha)}{\partial \alpha} dx + f(a, \alpha)$$

whence

$$\frac{\partial r_y(s)}{\partial s} = \frac{\partial}{\partial s} \lim_{\Delta t_i \rightarrow 0} \sum_{i=0}^{t=s} (s - t) \frac{\Delta \theta_y}{\Delta t_i} \Delta t_i$$

and

$$r_y(s) = \lim_{\Delta t_i \rightarrow 0} \sum_{i=0}^{t=s} (s - t) \frac{\Delta \theta_y}{\Delta t_i} \Delta t_i + C \quad (5)$$

where  $C$  is independent of  $s$ .

But  $r_y(0) = 0$ ; hence  $C = 0$  and†

$$\begin{aligned} \overline{r_y(s)^2} &= \lim_{\Delta t_i \rightarrow 0} \sum_{i=0}^{t=s} (s - t)^2 \frac{(\Delta \theta_y)^2}{\Delta t_i^2} \Delta t_i^2 \\ &= \lim_{\Delta t_i \rightarrow 0} \sum_{i=0}^{t=s} (s - t)^2 \frac{(\Delta \theta_y)^2}{\Delta t_i} \Delta t_i \end{aligned} \quad (5a)$$

But it was seen that  $\lim_{\Delta t_i \rightarrow 0} \frac{(\Delta \theta_y)^2}{\Delta t_i} = \text{finite} = \frac{d\theta^2}{dt}$  (see Appendix B). Hence  $\overline{r_y(s)^2}$  can be written as an integral

$$\overline{r_y(s)^2} = \int_0^s (s - t)^2 \frac{d\theta^2}{dt} dt = R(s)^2$$

where  $R(s)$  is the root-mean-square value of  $r_y(s)$ .

From Eq. 5 it is found that  $r_y(s)$  is a linear combination of the values of  $\Delta \theta_y$ , which obey a Gaussian law, and hence  $r_y(s)$  obeys a Gaussian law. Now, as before,  $\phi_y$ , the  $y$  component of the drift angle, is defined by  $\phi_y = r_y/s$ . Hence, as  $r_y$  obeys a Gaussian law,  $\phi_y$  obeys a Gaussian law, and  $\Phi$ , the most probable drift angle, is given by

$$\Phi = \frac{R}{s}$$

The above discussion has been based on the tacit assumption that the radioactive atom which emitted the particle was surrounded by an infinite mass of scattering material. In the case at hand, however,

† Refer to footnote, p. 1311.

the Gaussian distribution of  $\phi_y$  at the point s will be modified by the possibility of the  $\alpha$  particle's having escaped from the plate before the point s was reached. It will, however, be possible to apply our treatment to obtain a lower limit for the back-scattering in the following way:

Assume momentarily that the air above the plate actually consists of the same material as the plate. Then the probability that at the point s the particle will lie below the interface is equal to the probability that  $\phi_y < \epsilon$ , which is represented by P. Let p be the probability that, at the point s, the particle lies below the interface and that it has never previously been scattered above the interface. This added restriction means that  $p < P$ .

But p is precisely the probability that in the actual experimental setup the particle has not escaped by the time it has traveled the distance s.

Since  $p < P$  we have  $1 - P < 1 - p$ , i.e.,  $1 - P$  is less than the probability that the particle has escaped before traveling the distance s. Thus,  $1 - P$  furnishes a lower limit for the probability of back-scattering and will be found here, since the difficulty in calculating p exactly is too great to warrant spending time on it for the purpose at hand.

Now P is the probability that  $\phi_y < \epsilon$ . Since  $\phi_y$  obeys a Gaussian law, it is readily seen that†

$$1 - P = \frac{1}{\Phi \sqrt{2\pi}} \int_{-\infty}^{\epsilon} e^{-\phi_y^2/2\Phi^2} d\phi_y$$

giving a lower limit to the probability that if a particle is emitted at an angle  $\epsilon$  from the surface of the plate, it shall be back-scattered before having traveled the distance s. From solid-angle considerations, the probability that, if a particle is emitted downward, it will be

†It is to be remembered that  $\phi_y$  was defined as the tangent of the drift angle; hence the upper limit  $+\infty$ . We are, however, restricted to small angles. But  $1 - P$  can be written

$$1 - P = \frac{1}{\Phi \sqrt{2\pi}} \int_0^l e^{-\phi_y^2/2\Phi^2} d\phi_y + \frac{1}{\Phi \sqrt{2\pi}} \int_l^{\infty} e^{-\phi_y^2/2\Phi^2} d\phi_y$$

where l can be so chosen that, for  $\epsilon < \phi_y < l$ ,  $\phi_y$  is a small angle and, for  $l < \phi_y < \infty$ , the integral has a negligible value.

emitted between  $\epsilon$  and  $\epsilon + d\epsilon$  is  $\cos \epsilon d\epsilon$ . Hence the probability that, if a particle is emitted downward, it will be back-scattered is

$$B = \frac{1}{\Phi \sqrt{2\pi}} \int_0^{\pi/2} \cos \epsilon d\epsilon \int_{\epsilon}^{\infty} e^{-\Phi_y^2/2\Phi^2} d\Phi_y$$

Now determine the value of  $\Phi$ . Choose  $s$  so that the particle has a sufficient range left after escaping to be recorded, and let this value of  $s$  be denoted by  $s_1$ .

Table 1

$S - s_1$ , mm	$\left[ \frac{1}{S} \int_0^{s_1} \left( \frac{s_1 - t}{S - t} \right)^2 dt \right]^{1/2}$	$\frac{S}{s_1} \left[ \frac{1}{S} \int_0^{s_1} \left( \frac{s_1 - t}{S - t} \right)^2 dt \right]^{1/2}$
0	1.000	1.000
1	0.897	0.921
2	0.825	0.872
3	0.765	0.833
4	0.712	0.799
5	0.669	0.774

A safe estimate for  $S - s_1$  seems to be 3 mm. However,  $\Phi$  will be calculated for various residual ranges from 0 to 5 mm.

$$\Phi = \frac{R}{s_1}$$

$$\Phi^2 = \frac{R^2}{s_1^2} = \left[ \left( \frac{d\theta^2}{ds} \right)_0 S \right] \left( \frac{S}{s_1} \right)^2 \frac{\int_0^{s_1} \left( \frac{s_1 - t}{S - t} \right)^2 dt}{S}$$

Now it follows that

$$\frac{1}{S} \int_0^{s_1} \left( \frac{s_1 - t}{S - t} \right)^2 dt = 2 \left( 1 - \frac{s_1}{S} \right) \ln \left( 1 - \frac{s_1}{S} \right) + 2 \frac{s_1}{S} - \left( \frac{s_1}{S} \right)^2 \quad (6)$$

If the  $\alpha$ -particle range in air is 3.68 cm,  $S \approx 3.68$  cm,  $S - s \approx 0, 1, 2, 3, 4, 5$  mm, and the values shown in Table 1 are obtained. (The proportionality constant is the ratio of the range in the material considered to that in air.)

We shall now proceed to calculate the quantity  $\left[ \frac{d\theta^2}{ds} \right]_0 S$ .

Using Geiger's data for gold foils (platinum and gold should behave very nearly alike in back-scattering, since their atomic weights are

so similar), it is seen that, for  $\alpha$  particles of initial range of 5.60 cm in air, a thickness of gold equivalent to 1 cm of air produces a  $\Theta$  of 2.1 deg. Using Eq. 4, we can calculate the value of  $\left[ \frac{d\Theta^2}{ds} \right]_0' S'$  for  $S' < 5.60$  cm.

From Eq. 4,

$$\left[ \frac{d\Theta^2}{ds} \right]_0' S' = (\Theta')^2 \frac{S' - s'}{s'}$$

where

$$\frac{S' - s'}{s'} = \frac{5.60 - 1.00}{1.00} = 4.60$$

Hence

$$\left[ \frac{d\Theta^2}{ds} \right]_0' S' = \left( \frac{2.1 \times \pi}{180} \right)^2 \times 4.60 = 6.19 \times 10^{-3}$$

To calculate  $\left[ \frac{d\Theta^2}{ds} \right]_0' S$  for  $S < 3.68$  cm, write, from Eq. 3,

$$\left[ \frac{d\Theta^2}{ds} \right]_s' = \left[ \frac{d\Theta^2}{ds} \right]_0' \frac{(S')^2}{(S' - s)^2}$$

or

$$\left[ \frac{d\Theta^2}{ds} \right]_s' (S' - s) = \left[ \frac{d\Theta^2}{ds} \right]_0' S' \times \frac{S'}{S' - s}$$

But  $\left[ \frac{d\Theta^2}{ds} \right]_s' (S' - s)$  for  $S' < 5.60$  cm and  $S' - s = 3.68$  cm, is equal to  $\left[ \frac{d\Theta^2}{ds} \right]_0' S$  for  $S < 3.68$  cm.<sup>†</sup>

<sup>†</sup>It should be borne in mind that the scattering in the differential layer  $\Delta s$ , whose mean-square value is  $\overline{\Delta\theta_y^2}$ , depends only on the energy of the  $\alpha$  particles (i.e., on the remaining range) and not on the value of  $\theta_y$  or  $\Theta$  up to that point.

Hence

$$\left[ \frac{d\theta^2}{ds} \right]_0 S = \left[ \frac{d\theta^2}{ds} \right]'_0 S' \times \frac{S'}{S} = 6.19 \times 10^{-3} \times \frac{5.60}{3.68} = 9.40 \times 10^{-3} \quad (7)$$

This gives the values of  $\Phi$  listed in Table 2.

Returning to the calculation of  $B$ ,

$$B = \frac{1}{\Phi \sqrt{2\pi}} \int_0^{\pi/2} \cos \epsilon \, d\epsilon \int_{\epsilon}^{\infty} e^{-\phi_y^2/2\Phi^2} d\phi_y$$

In the above expression  $\cos \epsilon$  can be set equal to 1, for, using  $\Phi = 4.62$  deg ( $S - s = 3$  mm), when  $\epsilon > 18$  deg, the value of

$$\frac{1}{\Phi \sqrt{2\pi}} \int_{\epsilon}^{\infty} e^{-\phi_y^2/2\Phi^2} d\phi_y$$

becomes less than 0.0001, which is negligible. But when  $\epsilon < 18$  deg,  $\cos \epsilon > 0.95$ , and is effectively unity. Hence

$$B = \frac{1}{\Phi \sqrt{2\pi}} \int_0^{\infty} d\epsilon \int_{\epsilon}^{\infty} e^{-\phi_y^2/2\Phi^2} d\phi_y$$

where, for the same reason, we have substituted for convenience the upper limit  $\infty$  for  $\epsilon$  instead of  $\pi/2$ .

We can write  $B$  as

$$\begin{aligned} B &= \frac{\Phi}{\sqrt{2\pi}} \int_0^{\infty} d\sigma \int_{\sigma}^{\infty} e^{-t^2/2} dt \quad \text{where } \sigma = \frac{\epsilon}{\Phi}; t = \frac{\phi_y}{\Phi} \\ B &= \Phi \int_0^{\infty} \left[ \frac{1}{\sqrt{2\pi}} \int_0^{\infty} e^{-t^2/2} dt - \frac{1}{\sqrt{2\pi}} \int_0^{\sigma} e^{-t^2/2} dt \right] d\sigma \\ B &= \Phi \int_0^{\infty} [0.5 - A_0^{\sigma}] d\sigma \end{aligned} \quad (8)$$

where  $A_0^{\sigma}$  is the area from 0 to  $\sigma$  under the normalized Gauss error curve.

The value of this integral was computed by adding together all the values of  $A_0^{\sigma}$  given in the mathematical tables of the "Handbook of Chemistry and Physics," where  $\sigma$  varies from 0 to 3.87 in steps of

0.01; for  $\sigma > 0.387$ , the integrand is less than 0.0001 and was neglected. Effectively, then, we computed

$$\int_0^{3.87} [0.5 - A_0^\sigma] d\sigma$$

This is 0.402, and therefore  $B = 0.402 \Phi$ .

This means that for every 100 particles emitted upward and counted there will be in addition, for example, at least 3.2 particles multiply back-scattered and counted (see Table 3).

Assuming that the correct value for  $S - s_1$  is known, then  $B$  is a lower limit for the back-scattering. It is probably a rather close lower limit. Henceforth we will refer to this lower limit when we speak of the back-scattering. This should not lead to any confusion.

Table 2

$S - s_1$ , mm	$\Phi$ , deg
0	5.55
1	5.11
2	4.84
3	4.62
4	4.44
5	4.30

Table 3 — Multiple Back-scattering for  $\alpha$  Particles of 3.68 Cm Range for Different Values of Residual Range in Air

$S - s_1$ , mm	$B$ , %
0	3.9
1	3.6
2	3.4
3	3.2
4	3.1
5	3.0

## 2. VARIATION OF BACK-SCATTERING WITH THE MATERIAL OF THE SCATTERING PLATE

It has been seen that back-scattering is proportional to  $\Phi$ . Now for particles of a given energy (so that  $s_1/S$  is independent of the material),

$$\Phi^2 \propto \left[ \frac{d\Theta^2}{ds} \right]_0 S$$

Let the differential layer  $ds$  have a thickness equivalent to a specified number,  $\nu$ , of molecules of the substance.

Using the same value  $\nu$  for various substances, Geiger found that

$$\overline{\Delta \theta_y^2} \approx A^2 \quad \text{or} \quad d\theta^2 \approx A^2$$

where  $A$  is the atomic weight of the substance (see reference 4).†

If the substance has a polyatomic molecule, this can be generalized to

$$d\theta^2 \approx \sum_i N_i A_i^2$$

where the summation  $i$  is taken over all the kinds of atoms in the molecule. Hence, if  $\Phi_\sigma^2$  is the value of  $\Phi^2$  for the standard substance,

$$\frac{\Phi^2}{\Phi_\sigma^2} = \frac{\sum N_i A_i^2}{A_\sigma^2} \frac{S/ds}{S_\sigma/ds_\sigma}$$

But since  $ds$  is equivalent to a specified number  $\nu$  of molecules of the substance,

$$\frac{S}{ds} = \frac{n_0}{\nu} \quad \frac{S_\sigma}{ds_\sigma} = \frac{n_{0\sigma}}{\nu} \quad \frac{S/ds}{S_\sigma/ds_\sigma} = \frac{n_0}{n_{0\sigma}}$$

where  $n_0$  is the number of molecules equivalent to the range  $S$ .

Hence

$$\frac{\Phi^2}{\Phi_\sigma^2} = \frac{\sum N_i A_i^2}{A_\sigma^2} \frac{n_0}{n_{0\sigma}}$$

But  $n_0/n_{0\sigma}$  is equal to the reciprocal of the ratio of the atomic stopping powers of the two substances.‡

$$\frac{n_0}{n_{0\sigma}} = \frac{\sqrt{A_\sigma}}{\sum N_i \sqrt{A_i}}$$

† Geiger's notation is somewhat different but can be interpreted in this manner.

‡ See Bragg and Kleeman's law for the stopping of particles.

Hence

$$\frac{\Phi}{\Phi_\sigma} = \left[ \frac{\sum N_i A_i^2}{A_\sigma^{3/2} \sum N_i \sqrt{A_i}} \right]^{1/2}$$

Using the value of the back-scattering for gold as unity, the relative back-scattering coefficients for different substances, for an  $\alpha$  particle of specified energy, are given in Table 4.

### 3. VARIATION OF BACK-SCATTERING WITH THE RANGE OF THE ALPHA PARTICLES

Let  $\Phi_\mu$  now be the  $\Phi$  for the standard range (here 3.68 cm), and let

$$\rho = \left( \frac{S}{s_1} \right)^2 \cdot \frac{\int_0^{s_1} \left( \frac{s_1 - t}{S - t} \right)^2 dt}{S}$$

We have then

$$\frac{\Phi^2}{\Phi_\mu^2} = \frac{d[\Theta^2]_0}{d[\Theta_\mu^2]_0} \cdot \frac{S}{S_\mu} \cdot \frac{\rho}{\rho_\mu}$$

From Eq. 3,<sup>†</sup>

$$\frac{d[\Theta^2]_0}{d[\Theta_\mu^2]_0} = \frac{S_\mu^2}{S^2}$$

Hence

$$\frac{\Phi^2}{\Phi_\mu^2} = \frac{S_\mu}{S} \cdot \frac{\rho}{\rho_\mu}$$

The value of  $\rho$  will depend on the value of  $s_1/S$ , where  $S - s_1$  is the residual range in air necessary to produce a recordable pulse (refer to Eq. 6). Since  $\rho$  does not vary rapidly with respect to  $S$ , we may say that  $B$  is approximately inversely proportional to the square root of the range.

We shall limit ourselves to the case of the  $\alpha$  particles emitted from U(I), whose range is 2.70 cm, and assume  $(S - s_1) = 0.3$  cm.

<sup>†</sup> The use of Eq. 3 to deduce this result is similar to the deduction of Eq. 7.

From Eq. 6,  $\rho = 0.637$  and  $\rho_\mu = 0.694$ . Therefore

$$\frac{\Phi^2}{\Phi_\mu^2} = \frac{3.68}{2.70} \times \frac{0.637}{0.694} = 1.252$$

$$\frac{\Phi}{\Phi_\mu} = 1.12$$

To obtain the scattering of U(I)  $\alpha$  particles in  $U_3O_8$  ( $B_1$ ) relative to that of 3.68-cm  $\alpha$  particles in gold ( $B_0$ ), it is necessary to multiply

Table 4—Back-scattering Coefficients for Different Substances

Substance	Back-scattering
Au	1.00
Pt	0.99
$U_3O_8$	0.894
$SiO_2$ (quartz)	0.19
Al	0.23
Be	0.10

together the two factors obtained for scattering in  $U_3O_8$  relative to gold and for scattering of U(I)  $\alpha$  particles relative to 3.68-cm  $\alpha$  particles. This gives (see Table 4)

$$\frac{B_1}{B_0} = 0.894 \times 1.12 = 1.00$$

Hence, coincidentally, the back-scattering of U(I)  $\alpha$  particles in  $U_3O_8$  is the same as the back-scattering of 3.68-cm  $\alpha$  particles on gold or platinum, for  $(S - s_1) = 3$  mm of air.

#### 4. SPECIAL CASES

4.1 Multiple Back-scattering for an Infinitely Thin Sample Spread on a Foil of Finite Thickness t, Small Compared to  $s_1$ . Here the plate is not infinitely thick and therefore  $\epsilon$  is not integrated from 0 to  $\pi/2$  but from 0 to  $t/s_1$ , where  $t$  is the thickness of the foil and

$$B = \frac{\Phi}{\sqrt{2\pi}} \int_0^{t/s_1\Phi} d\sigma \int_{\sigma}^{\infty} e^{-t^2/2} dt = \Phi \int_0^{t/s_1\Phi} [0.5 - A_0^\sigma] d\sigma$$

**4.2 Multiple Back-scattering for a Case Similar to That of a Finite Thickness of  $U_3O_8$  Evenly Spread on a Thick Platinum Plate. The  $U_3O_8$  has essentially the same value of  $\Phi$  as the platinum:**

$$\frac{\Phi_{U_3O_8}}{\Phi_{Pt}} = 1.12 \quad (\text{see above})$$

We are essentially considering the case of a finite layer of active  $U_3O_8$  spread over a thick plate of imaginary inactive  $U_3O_8$ . Consider

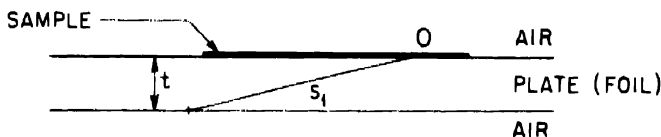


Fig. 4 — Infinitely thin sample spread on a foil of finite thickness  $t$  (see Eq. 8).

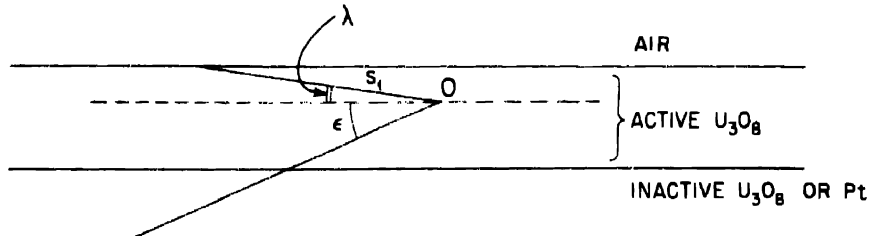


Fig. 5 — Back-scattering of an  $\alpha$  particle, considering a finite layer of active  $U_3O_8$  spread over a thick plate of imaginary inactive  $U_3O_8$ .

an  $\alpha$  particle emitted at O in the direction  $\epsilon$ . The probability that the particle will escape is

$$\frac{1}{\Phi \sqrt{2\pi}} \int_{\epsilon+\lambda}^{\infty} e^{-\phi_y^2/2\Phi^2} d\phi_y$$

The probability that the particle will be emitted between  $\epsilon$  and  $\epsilon + d\epsilon$  is  $\frac{1}{2} \cos \epsilon d\epsilon$  (considering the  $4\pi$  solid angle). Hence the prob-

ability that the particle emitted at O will be back-scattered is obtained by integrating  $\epsilon$  from  $-\lambda$  to  $\pi/2$  or

$$P' = \frac{1}{2} \int_{-\lambda}^{\pi/2} \cos \epsilon d\epsilon \int_{\epsilon+\lambda/\Phi}^{\infty} \frac{1}{\Phi \sqrt{2\pi}} e^{-\phi_y^2/2\Phi^2} d\phi_y$$

$$P' \cong \frac{\Phi}{2} \int_{-\lambda/\Phi}^{\infty} d\sigma \int_{\sigma+\lambda/\Phi}^{\infty} \frac{1}{\sqrt{2\pi}} e^{-t^2/2} dt$$

where  $t = \phi_y/\Phi$  and  $\sigma = \epsilon/\Phi$ . Let  $\sigma + \lambda/\Phi = \omega$  and  $d\sigma = d\omega$ . Then

$$P' = \frac{\Phi}{2} \int_0^{\infty} d\omega \int_{\omega}^{\infty} \frac{1}{\sqrt{2\pi}} e^{-t^2/2} dt = \frac{0.402 \Phi}{2}$$

Integrating over the thickness of active  $U_3O_8$  gives  $P = 0.402 \Phi/2 = P'$ , where  $P$  is the probability that any emitted  $\alpha$  particle will be back-scattered.

The probability that a particle will be counted is  $0.5 - t/4s_1 + 0.402/2$ , where  $-t/4s_1$  is the ordinary self-absorption correction.<sup>†</sup> Thus it is seen that the back-scattering correction  $0.402/2$  is independent of the thickness  $t$  of the sample.

## 5. SUMMARY

Calculations indicate that  $\alpha$  particles with a range of 3.68 cm in air are back-scattered from a platinum sample mounting to the extent of 3 to 3.5 per cent. The calculations were based on Geiger's multiple-scattering data. Variations of back-scattering with range and with substrate were also calculated.

## APPENDIX A

A word should be said about the validity of Eq. 3, on which our calculations are partly based. Equation 3 states that  $\sqrt{d\theta^2}$  is inversely proportional to the remaining range,  $S - s$ , of the  $\alpha$  particle. This law was established experimentally by Geiger for ranges between about 1 and 5.6 cm. However, the assumption has been made that

<sup>†</sup>Since the term  $-t/4s_1$  does not contain the ratio  $s_1/S$ ,  $s_1$  must be expressed in terms of length units in the  $U_3O_8$ .

this law holds to the end of the range, and this assumption must be justified.

If we plot  $1/\sqrt{d\theta^2}$  vs. S from Geiger's data (see Fig. 6), we obtain a fairly good straight line, except for one point that may be in error. It is possible to extrapolate down to 0 range since, from physical

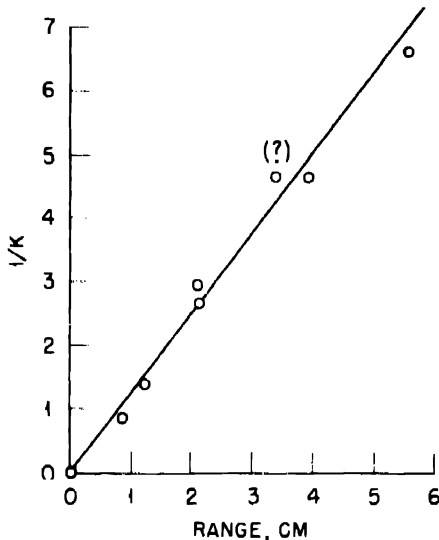


Fig. 6—Graph showing the validity of the law expressed by Eq. 3. K is proportional to  $\sqrt{d\theta^2}$ . (See Geiger and Marsden,<sup>1</sup> Table IV.)

considerations, we see that, as we approach the end of the range,  $\sqrt{d\theta^2}$  becomes infinite. As the particle slows down, its motion approaches complete randomness, and it can be shown that the root mean square of the tangent of the deflection approaches infinity. Hence the curve passes through the origin.

It is seen from this curve that the law expressed by Eq. 3 is approximately valid for ranges from 0 to 5.6 cm.

#### APPENDIX B

The use of the difference notation  $\Delta\theta_y$ , and of the summation sign, rather than the differential notation and the integral sign, is necessitated by the fact that no meaning can be given to the symbol  $d\theta_y$ , since  $\Delta\theta_y/\Delta s$  does not approach a limit as  $\Delta s$  goes to 0. To illustrate this, we can use the root-mean-square value for  $\Delta\theta_y$ :

$$\frac{1}{\Delta s} = \frac{(\Delta\theta_y)^2}{\Delta s} \cdot \frac{1}{\sqrt{(\Delta\theta_y)^2}}$$

As  $\Delta s$  goes to 0,  $(\Delta \theta_y)^2 / \Delta s$  approaches a finite limit (as shown by Geiger's experiments).

The whole expression therefore becomes infinite.

Thus we see that the function  $\theta_y = f(s)$  can be regarded as a kind of continuous function which is not differentiable at any point.

#### REFERENCES

1. H. Geiger and E. Marsden, Proc. Roy. Soc. London, 82: 495 (1909).
2. B. B. Cunningham, A. Ghiorso, and A. H. Jaffey, Metallurgical Project Report CK-888, Aug. 7, 1943.
3. H. Geiger, Proc. Roy. Soc. London, 83: 492 (1910) (exp).
4. H. Geiger, Proc. Roy. Soc. London, 86: 235 (1911) (theory).
5. W. Bothe, Z. Physik, 4: 300 (1921).

Paper 17.1

THE SPECTRUM OF PLUTONIUM†

By H. W. Dodgen, J. Chrisney, and G. K. Rollefson

Two photographs of the spectrum of plutonium have been made with a 3-meter focal-length grating of approximately 60,000 lines. A Paschen mounting was used so that the entire spectrum was taken in a single exposure. The first photograph was obtained in June 1943 with a 20- $\mu\text{g}$  sample supplied by Dr. Cunningham of the Metallurgical Laboratory at Chicago. The second one, taken in June 1944, was made from 0.5 mg of plutonium taken from a supply sent from Clinton to the Chemistry Department at California. The supply from Clinton had been given a preliminary purification by precipitation of sodium plutonyl acetate. The 0.5-mg sample was further purified by precipitation from a 2M  $\text{NH}_4\text{OH}$  solution after it had been reduced by sulfur dioxide. After being washed, the sample was dissolved in concentrated hydrochloric acid; the solution was then diluted, and the sample was precipitated a second time and washed. This second precipitate was dissolved in a small volume of concentrated hydrochloric acid and carefully evaporated on a copper electrode. The samples were excited by a condensed spark produced by a 15,000-volt, 0.9-kva neon sign transformer with a 0.015- $\mu\text{f}$  condenser in the circuit. In order to recover the samples, the electrodes were enclosed in a specially made glass shield, which was fitted onto a quartz lens.

Experiments with uranium samples of various sizes showed that for samples of the order of magnitude of 20  $\mu\text{g}$ , many more lines characteristic of the sample were obtained if the electrodes were of silver rather than of copper. This dependence on the nature of the electrodes was less with larger samples and was not significant for samples as large as 0.5 mg. Hence the first sample was mounted on

†Contribution from the Department of Chemistry, University of California, Berkeley.

silver electrodes, but the second on copper. In the first case, the glass shield was filled with air, but in the second case helium was used, since it was found that this reduced the background without otherwise affecting the spectrum. In both cases the sample was mounted on the electrode by evaporating a solution of the chloride which contained some excess acid.

The slit widths used were 0.10 mm for the first and 0.04 mm for the second. Since the dispersion was approximately 5.5 Å per millimeter, the image of a line covers approximately 0.2 Å, even for the narrowest width used. In order to obtain settings as accurate as possible, the plates were measured with a projection-type comparator, which gave a magnification of a little more than ten diameters. On the basis of a comparison of our measured values for the wavelengths of some of the lines known to be due to impurities with the values listed in the M.I.T. tables, we believe that our wavelengths are good to about  $\pm 0.07$  Å (average).

In some regions of the spectrum the error may run up to 0.2 Å because of the large distance between good reference lines.

Eastman spectrographic plates were used. For wavelengths less than 4590 Å the type III-0 was used, and for longer wavelengths, 103F. The range covered was from 2100 to 7240 Å. In this range five narrow intervals were not covered because they fell at the junctions of the plates or behind supporting strips in the shield, which was placed in front of the plate rack. The intervals thus excluded are 3156 to 3167, 3917 to 3938, 4584 to 4595, 5618 to 5643, and 5985 to 5995 Å.

The wavelengths of the lines measured are given in Tables 1 and 2. Those in Table 1 are the ones that are considered definitely characteristic of the sample. Lines have been eliminated which could be definitely attributed to the presence of impurities, e.g., the persistent lines of calcium and magnesium. All these lines have been checked by at least two observers. The values in Table 2 represent those lines that are considered uncertain because of extreme faintness (0 on the scale to be described) or because of proximity to a strong line in the background spectrum. Although most of these lines probably are characteristic of plutonium it is preferable to list them separately for the present. On the other hand, the only lines in Table 1 to which any uncertainty is attached are those which fall close to a persistent line of some element which might be present as an impurity. Those cases have been indicated by inserting at the right of the wavelength the symbol of the element that has a persistent line close to the listed wavelength. This procedure has been followed even though the presence of such an element was considered improbable.

Table 1—Wavelengths of Plutonium Spectrum

Angstroms	I	Angstroms	I	Angstroms	I
2611.74	1	2805.21	1	2885.40	3vh
2612.80	1	2805.48	1	2886.83	2h
2614.85	1	2806.06	2	2887.79	1h
2631.23p	1	2806.37	1	2890.72	2
2658.47	2	2806.93	1	2891.71	3
2661.10	1	2808.38	4	2892.64	4
2662.58	1h	2810.38	2	2894.54	4h
2664.54	1vh	2811.26	2	2895.67	2
2668.35	1	2815.78	2	2897.90B1?	5
2668.69	1	2816.41	1	2899.62	3
2669.71	1	2818.22	1h	2900.80	2h
2670.87	1	2822.93	5	2903.19	1
2674.74	1	2826.36	1	2904.17	3
2690.75	1	2827.46	1	2904.87†	6
2694.46	1	2833.26	4	2906.88	3
2708.27	1	2834.93	2	2909.47	1
2728.15	1	2835.70Cr?	8	2910.43	8
2729.53	1	2838.73	1	2911.50	1
2730.76	1	2840.57	3	2912.50	2
2744.21	1	2842.72	2	2913.79	1
2746.97p	2	2847.22	1	2914.17	1
2748.51Cd?	1	2849.29	1	2914.82	3
2754.76	2	2850.12	1	2915.69	5
2758.64	1	2851.20	3	2918.10	8
2760.31	1	2852.95	3	2918.84	1
2771.04	1	2856.17	2	2919.97	2
2776.36	2	2857.06	5	2921.83	3
2779.90	1	2859.19	1	2923.02	4
2781.41	3	2860.03p	5	2923.70	1
2784.50	5	2861.16	1h	2925.26†	7
2785.64	2	2862.57	4h	2926.53†	5
2787.31	2	2866.42	3	2928.14†	6
2789.10	3	2866.96	3	2929.37	6
2793.32	1	2867.63	1	2930.82	2
2794.64	1	2869.05	4	2932.17	2
2797.16	1	2870.05	2	2933.22	3bh?
2798.76	1	2872.20	2h	2936.36	4h
2800.40	1	2874.79	2	2937.52	2
2801.61	1	2876.56	2h	2938.90	8
2803.98	2	2879.96	2	2941.27	6

Table 1—(Continued)

Angstroms	I	Angstroms	I	Angstroms	I
2943.04	2	3015.05	3	3109.30p	2
2949.85p	7	3015.97	2	3118.75	2
2951.64p	3h	3018.21	4	3121.18	2
2954.33p	7	3019.50†	4	3137.52	2
2956.30	2h	3021.14p†	8	3165.52	2
2963.40	2	3023.42p†	7	3167.58	1
2964.70p†	8	3025.96p	4	3171.44	1
2966.09p	1	3028.84	6	3173.12	2h
2966.80p	2	3029.89p	7	3174.68	3
2967.58	2	3031.42	8	3176.67	1
2968.98p†	5	3032.47p	8	3179.71	6
2969.91	1	3033.97Sn?p	4	3182.36	4
2970.52p	3	3035.26	1	3183.55	1h
2972.51p†	10	3038.50p	4h	3184.49	1
2973.45	2	3039.23	3h	3185.65	4
2978.03†	7	3041.51	3	3196.34	1h
2978.49p†	9	3042.67†	5	3197.85	2
2980.27p†	10	3043.05p†	5	3198.48†	6
2981.26	3	3046.36	7	3200.39	5
2982.65	1	3047.42	3	3201.59	5h
2984.24	1	3048.25	1	3203.07	6vh
2984.98	1	3049.01	1	3204.75	3h
2987.12p	6	3051.11	5	3206.98	4
2988.21p†	10	3052.16	2	3211.26	1h
2990.09	2	3053.16†	8	3213.73	1h
2991.55p	8h	3053.89	1h	3215.33	1
2992.80	2	3055.24	3vh	3216.21	3
2994.06p	10	3055.86	3vh	3217.21	2
2996.46p	9	3056.81	3	3218.18	1
2998.46p	3	3057.64†	2	3219.10	3
3000.62p†	10	3058.41†	4	3221.01†	7
3002.43	2h	3060.18†	4	3221.73-	8
3004.86p	3	3061.76	4	3222.65	1
3005.46	2	3069.25p†	9	3229.66	2vh
3007.38	5	3074.65†	3	3231.89	9
3009.14Sn?p†	6	3075.47	1	3232.61Sb?	4
3009.83†	6	3076.01	1	3234.74	5
3012.88	1	3079.77	2	3236.82	1
3013.58	2	3084.63	4	3241.37	8
3014.54	3	3105.28	3	3242.04	7

Table 1—(Continued)

Angstroms	I	Angstroms	I	Angstroms	I
3245.23	6	3416.74	2	3479.06	1
3253.75	4	3417.96	1	3479.88	2
3254.58	3	3418.91p	10	3483.18p†	7
3261.20Cd?	3	3421.30Pd?	3	3488.17	2
3263.17	2	3422.67	2	3491.31	1h
3264.21	3	3424.12p	8	3494.45	3
3271.26	4	3424.61	8	3496.35	2
3279.17	1	3425.45p	10	3497.25†	4
3287.83	1	3428.33	6	3504.89	2
3298.42	8	3428.24	1	3506.88	1
3302.52	3	3429.27	1	3515.25	1
3312.61	8	3430.29	1	3516.73Pd?	2
3313.57	2	3431.17	1	3533.33	3
3314.69	1	3432.90	4	3540.76†	7
3315.38	7	3434.28	2	3542.03	2h
3316.27	2h	3435.00Rh?	8	3550.63	1h
3321.76	2	3439.42	1	3578.05	1
3323.83	8	3442.26	4vh	3578.62	4
3324.73	4	3444.04	2	3579.45	2
3327.58	2	3444.77	2	3685.92p†	10
3374.61	1	3445.81	1vh	3588.05	2
3377.34	8	3447.16	1vh	3589.52	1
3379.41	1	3449.10	4	3590.21	3
3383.99	1	3453.02	1	3591.68p	2
3387.08	1h	3453.79Co?	1	3592.53	2
3387.91	2h	3455.26	6	3593.34	4h
3389.30	6	3456.21	2	3594.16	3h
3390.13	4	3457.05	1	3595.19	2
3391.40	8	3458.88	6	3596.01	1
3392.20	3h	3460.33Re?	2h	3596.24	2
3392.92	2h	3460.81	9h	3600.48p	8
3393.97	1	3461.89	2	3602.79p	1h
3394.39	1	3462.67	6	3603.72p	8h
3397.36	9	3463.53	3	3605.02	1
3401.03p	10	3465.02p†	10	3605.98p	8
3407.36	1	3469.22†	10	3607.22	4h
3410.12	4vh	3470.43	1h	3607.80	4h
3412.41	4	3471.00	1h	3608.75p	4
3414.23	5	3473.67p†	10	3609.58Pd?p	4
3415.02	1	3478.24	2h	3612.36	2vh

Table 1—(Continued)

Angstroms	I	Angstroms	I	Angstroms	I
3615.05	1	3678.77	1h	3807.84	3
3615.62	3	3679.65	5	3808.57	2
3616.09	2	3680.52	3	3809.61	3h
3616.90	1	3681.98	2vh	3810.52	9
3617.78	1	3682.92	8	3812.02	5
3619.26p	3	3685.46	3	3812.67	7
3621.50p	8	3688.65	2h	3815.26	8
3623.05	2	3689.82	2	3824.24p	7
3625.49	6h	3690.44p	6	3826.16p	4
3628.70	3	3691.34p	3	3827.66	6
3629.73	2	3693.68p	5	3828.00	1
3630.29	1	3695.21p	5	3829.50Mg?	6
3631.96 to } p	10vh,bh?	3696.77	1	3832.28Mg?	4h
3632.77	3	3699.35p	5	3833.61	3
3634.97Pd?	2	3714.01	2h	3835.52	6
3635.87p	8	3714.78	2	3836.12	6
3636.47p	8	3718.69p	10	3837.00	8
3638.07	3	3720.32p	7	3839.98	1
3638.65	1	3721.50p	8	3840.79	8
3639.90	3h	3724.09	1	3841.45	2
3644.24	1h	3725.99p	10	3842.21	5
3645.77p	8	3726.71p	10	3843.49	1
3647.92p	8	3732.04p	8	3845.80	3h
3649.20p	6	3732.46	4	3846.72	10
3650.43	4	3736.17	2	3848.11	1
3651.40p	8	3737.30p	2h	3849.01	2
3652.23	2	3739.24p	7	3850.18	6
3657.70Rh?	2	3758.19p	2	3851.19p	9
3659.39p	5	3758.64p	4	3851.86	7
3660.62p	2	3761.13	2	3852.70p	8
3661.87	1	3763.05	3	3853.17	2h
3663.82	3	3764.12	3h	3854.08	1
3664.49	1	3765.05	3h	3858.42	2
3667.31	2	3767.34	2	3859.17	3
3667.88	7	3770.21p	7	3861.12	9
3668.83	2	3770.98	1	3862.44	4
3670.07	3	3771.85	7	3864.98	9h
3673.35	1vh	3773.44p	9	3866.75	7
3674.88	7	3776.00p	9h	3871.86	4
3678.41	1h	3806.18	1	3872.35	4

Table 1—(Continued)

Angstroms	I	Angstroms	I	Angstroms	I
3874.23	4	4032.92	1	4175.52	1
3874.92	7	4034.93	4	4178.33p	2
3876.82	1	4035.80	6	4190.02	8
3878.47p	2	4037.20	4	4190.83	5
3906.24	10h	4039.38p	6	4198.21p	9
3945.42	1h	4048.83p	4	4203.19	1vh
3946.93	4	4058.71	6h	4204.79	3
3949.19	10h	4064.70p	9	4205.80	2
3950.31	2	4065.67	2	4206.42	2vh
3951.60	4	4066.80p	9	4208.26p	8
3952.97p	8	4071.30	2	4208.77	7
3956.46	1h	4071.90	2	4212.07	7
3957.56	2h	4074.22	6h	4215.26	5
3958.93p	8	4074.58	8	4216.39	9
3962.68	3	4078.09	8	4219.01	5
3965.44p	3	4084.39	1	4229.79	8
3967.24	2	4088.85	8	4230.78	4h
3970.11	2	4097.76	7	4233.82	6
3971.52p	3	4101.02	5	4237.85	6
3972.18p	9	4102.04	2	4249.84	3
3972.96	1	4103.28	1	4251.38	2
3975.40p	9	4103.86	6	4254.77p	4
3975.82p	6	4106.00	8	4255.93p	6
3979.83	1	4107.34	6	4273.31p	8
3980.34	6	4108.52	3h	4279.67p	1
3984.13	3	4112.54	2	4280.18	8
3985.48	9	4113.20	2	4281.12	2
3989.76p	9	4114.99	1	4282.10	1
3992.24	6	4116.54p	7	4283.80p	7
3996.08	4	4117.33	1	4285.88	1
4000.25	2	4136.76	9	4287.48	1
4001.94	2	4146.39	2h	4289.08p	9
4002.59	4	4146.76	1h	4299.48	6
4004.84	1	4149.16	2h	4307.18?	4h
4006.37	7	4150.00	4	4309.73	1
4007.73	1	4155.98	1	4311.92	1vh
4010.56	2	4159.85	2vh	4313.33?	2h
4014.62	1	4160.68	1	4314.43p	6h
4015.74p	6	4167.76p	10	4316.68	2h
4019.22	1	4169.78	1	4318.76	1

Table 1—(Continued)

Angstroms	I	Angstroms	I	Angstroms	I
4320.29	2h	4619.00	1	4927.44	2
4320.81	2h	4627.43	7	4937.98	1h
4322.04	1	4639.50	4	4945.25	1
4324.35	4	4655.26	1	4957.40	1
4326.36	2h	4656.60	1	4969.83	1vh
4330.65p	10h	4657.42	4	4970.88	1
4336.09	6	4664.23	6	4982.59	1
4337.19	9	4671.00	2h	5023.31	1
4341.48	10	4673.13	3h	5038.04	1
4352.62p	10	4680.23	3	5057.33	1
4357.96p	7	4689.52	6	5078.11	2vh
4371.42	2	4690.72	1vh	5103.13	1h
4379.81p	5	4692.10	3	5169.93	1
4381.02	4	4693.93	1	5194.00	2
4383.46p	7	4698.76	2	5209.80	2
4385.40	9	4701.27	7	5221.41	1
4392.80	2	4711.32	1	5268.05	1
4393.92p	9	4722.81	2	5288.62	1
4396.35	9	4726.41	2	5423.26	4
4404.17	1h	4731.22	3h	5767.96	1
4404.95	7	4748.84	1	5818.46	1
4406.80	7	4767.22	8	5857.02	4
4419.42p	8	4768.62	1vh	5892.94	2
4421.73	2vh	4781.01	2vh	6192.72	1h
4435.53p	1	4794.57C1?	10	6321.87	1h
4437.26	2	4802.09	1	6323.81	1h
4440.24	2	4809.05	1	6324.75	1
4441.63p	6	4810.05C1?	9	6380.89	3h
4448.27	2	4819.27C1?	8	6417.39	1
4456.72	3	4823.00	6		
4459.12	1	4842.40	1vh		
4502.23	1	4847.49	1vh		
4504.90p	7	4850.07	3		
4511.13In?	1h	4884.75	1h		
4533.59	1	4884.30	1		
4536.05p	10	4886.83	1vh		
4554.15Ba?	2h	4887.30	1vh		
4579.58	1	4894.42	1vh		
4610.59	2	4896.73	2		
4615.42	1	4904.71	2		

Table 2—Uncertain Lines in Plutonium Spectrum

Angstroms	Angstroms	Angstroms	Angstroms	Angstroms	Angstroms
2512.02	2742.05	3026.80	3760.67	4325.63	5476.18
2514.26	2749.32	3037.55	3817.06	4329.31	5703.37
2580.98	2750.64	3049.73	3826.97	4345.97	5837.73
2583.78	2757.00	3050.18	3865.98	4348.63	5891.82
2586.46	2761.64	3060.99	3939.51	4347.51	6017.38
2588.77	2768.94	3064.28	3944.86	4362.63	6018.99
2593.18	2771.94	3175.37	3946.37	4386.23	6050.36
2606.57	2774.54	3180.92	3947.68	4395.47	6190.78
2608.20	2778.74	3190.40	3960.25	4405.86	6193.75
2610.46	2798.20	3191.73	3974.29	4438.23	6279.02
2622.65	2821.31	3233.89	4001.22	4451.46	6339.96
2628.30	2822.19	3275.02	4005.23	4452.71	6389.21
2632.49	2829.58	3299.89	4019.88	4454.56	6408.86
2633.28	2830.36	3399.91	4021.30 <sub>p</sub>	4491.73	6445.22
2636.30	2832.45	3400.43	4054.85	4500.93	7221.46
2637.91	2836.89	3403.27	4078.68	4503.40	
2641.59	2839.39	3403.79Cd?	4098.82	4578.27	
2644.63	2843.77	3427.66	4104.55	4617.24	
2650.83	2846.40	3431.83	4105.35	4618.13	
2652.38	2848.01	3438.24	4111.24	4684.31	
2653.29	2849.88Cr?	3451.92	4118.13	4686.07	
2655.95	2865.62	3467.91	4144.62	4686.96	
2660.07	2874.20	3474.89	4145.03	4688.06	
2676.05	2978.81	3480.92	4147.77	4899.48	
2680.39	2881.49	3539.18	4153.21	4747.99	
2681.96	2893.57	3583.14	4154.62	4787.13	
2683.80	2896.74	3583.79	4157.09	4804.89	
2685.02	2901.91	3584.75	4158.42	4808.06	
2687.89	2902.80	3588.67	4213.24	4817.89	
2693.41	2905.98	3599.98	4225.51	4840.63	
2698.14	2916.85	3600.93	4278.70	4845.56	
2711.52	2935.15	3604.49	4282.62	4853.81	
2711.80	2944.10	3633.99	4283.09	4876.36	
2712.39	2974.24	3637.59	4285.43	4880.66	
2718.78	2986.10	3640.83	4286.64	4885.21	
2720.62	2988.00Bi?	3643.07	4304.75	4888.30	
2726.452	2994.90	3647.25	4309.18	4961.72	
2732.08	2995.28	3653.08	4309.99	5082.03	
2733.98	3017.20	3677.74	4310.54	5086.29	
2735.30	3024.89	3718.91	4315.87	5408.59	

The intensities listed in Table 1 represent an attempt to indicate qualitatively the appearance of the line on the plate. No attempt has been made to correct for the variation in sensitivity of the plate with wavelength, or for the two types of plates used. Hence the intensities are of value only in that they indicate the relative intensities of lines in the same region of the spectrum. The scale is made by designating with 0 the faintest lines that could be detected, with 1 those which are just strong enough to be distinguished from the 0 lines, and so on up the scale. Obviously, different observers will vary some in using such a scale, but there can be little doubt that if one line is listed as 6 and another as 2 the former appears much stronger than the latter.

The lines marked "p" in Table 1 are those which were found in both photographs. Some of the lines listed in the previous report on the 20- $\mu\text{g}$  sample<sup>1</sup> were not found in the second photograph. In some cases that difference can be attributed to differences in the background spectrum which interfere with the observations, but some must be classed as accidental fluctuations in the background and these were interpreted as lines. On the other hand, some strong lines in the second photograph were not found with the small sample because of interference from silver lines; for example, the line at 3985.48 Å was not separated from the silver line at 3985.19 Å in the first photograph.

Lines marked with a dagger were also found in the second order.

Other markings are as follows: bh, possible band head; h, a hazy line; and vh, a very hazy line.

#### REFERENCE

1. G. K. Rollefson and H. W. Dodgen, Metallurgical Project Report CK-812 (July 1943).

## Paper 17.4

### THE QUANTITATIVE MICRO DETERMINATION OF PLUTONIUM<sup>†</sup>

By C. W. Koch

It has become desirable for some purposes to have a method for the analysis of plutonium more dependable than counting procedures, and since, in our work, micro quantities could be used, a method was devised using an approximately 2.5-mg sample of plutonium.

Aliquots of a standard plutonium(IV) sulfate solution (4.961 mg of plutonium per milliliter) were reduced with zinc, and plutonium(III) was determined volumetrically by oxidation with ceric sulfate to plutonium(IV). The indicator that was used was the ferrous complex of *o*-phenanthroline.

The plutonium sulfate was standarized by two different methods; first, by evaporating a measured aliquot of the plutonium solution to dryness and then igniting to the oxide, the oxide being weighed to constant weight on a microbalance. The second method used was to count measured aliquots of the solution and compare them with prepared standards of the same magnitude. The average value of these two methods was taken as the true concentration of the solution. The two methods checked to within  $\pm 0.1$  per cent.

Aliquots of the standard plutonium sulfate solution were run through a small Jones reductor of 5 mm inside diameter and 14 cm length. The outlet of the reductor was turned so that it touched the side of the 25-ml Erlenmeyer flask used as a receiver in order that no splashing would occur. The pipet, calibrated for total delivery, was washed out into the reductor four times with 1N H<sub>2</sub>SO<sub>4</sub> to ensure quantitative transfer of the plutonium, and the reductor was then washed with 0.5-ml portions of 1N H<sub>2</sub>SO<sub>4</sub> until the volume in the receiver was approximately 10 ml. The plutonium(III) was titrated to plutonium(IV) with 0.004515M ceric sulfate. Stirring was done with a mechanical

<sup>†</sup>Contribution from the Department of Chemistry, University of California, Berkeley.

stirrer. The buret tip consisted of capillary tubing for approximately 2 in. to prevent any appreciable diffusion of the ceric sulfate from the tip, which was immersed in the solution during the titration to avoid splashing. The results are presented in Table 1.

Two titrations were made by adding a threefold excess of ceric sulfate to the plutonium(III) and allowing this solution to stand for 2 hr before titrating the excess ceric ion with ferrous ammonium sulfate. One solution was 1N in  $H_2SO_4$ , and the other was 5N in  $H_2SO_4$ . These two samples gave results 8 per cent and 7 per cent high, respectively, indicating only slow oxidation past the tetrapositive state.

Table 1—Results of Plutonium Determinations  
Ce(IV), 0.004515M; indicator, 20 microliters of 0.025M Fe(II) orthophenanthroline

Sample	Used in titration, ml	Vol. of blank, ml	True vol., ml	Pu found, mg	Pu present, mg	Error, %
1	2.441	0.118	2.323	2.507	2.507	0
2	2.403	0.118	2.285	2.466	2.507	-1.6
3	2.447	0.118	2.329	2.513	2.507	0.20
4	2.439	0.118	2.321	2.504	2.507	-0.12
5	2.441	0.118	2.323	2.507	2.507	0.0
6	2.446	0.118	2.328	2.512	2.507	0.20
7	2.439	0.118	2.321	2.504	2.507	-0.12
8	2.445	0.118	2.327	2.511	2.507	0.16

The blank of 0.118 ml includes indicator and Jones reductor blanks and appears to be reproducible to  $\pm 0.003$  ml. However, care must be taken to wash the Jones reductor thoroughly before use because much larger blanks are obtained if this precaution is not taken. After the reductor had stood for longer than 30 min it was usually washed with 20 to 25 ml of 1N  $H_2SO_4$  before a sample was introduced.

To determine the end point accurately and consistently, daylight is much better than artificial light. Also, it is much easier to obtain uniform end points if a blank is prepared in which the correct amount of indicator has been added to a small excess of ceric sulfate, so that the color of the indicator is definitely blue. Then titrations on samples are run until the color of the sample just reaches that of the blank.

Summary. A quantitative method for the determination of plutonium using ceric sulfate has been developed. A Jones reductor is used to reduce all the plutonium to plutonium(III), and the plutonium(III) is then titrated to plutonium(IV) with ceric sulfate. The ferrous complex of o-phenanthroline is the indicator used. The reproducibility on 2.5-mg samples of plutonium is  $\pm 0.25$  per cent.

## Paper 19.1

### THE TRACER CHEMISTRY OF AMERICIUM AND CURIUM IN AQUEOUS SOLUTIONS†

By S. G. Thompson, L. O. Morgan, R. A. James, and I. Perlman

#### 1. INTRODUCTION

During the past few years the chemical properties of the transuranium elements have aroused considerable interest and acquired importance in fundamental chemistry and physics as well as in more practical applications. Significant progress toward an understanding of the chemistry of these elements has been made by the use of tracer methods, in which the behavior of an element at extremely low concentrations is followed by means of its radioactivity. Since all known isotopes in this particular region in the periodic table are radioactive, tracer methods may be used effectively, but it is commonly necessary to separate the isotope of the element under investigation from other radioactive elements. Studies on the chemistry of plutonium have served adequately to establish the reliability of the tracer methods, which more recently have been applied in the study of americium and curium.

The discovery of americium (element 95, symbol Am) by Seaborg, James, and Morgan<sup>1</sup> and the discovery of curium (element 96, symbol Cm) by Seaborg, James, and Ghiorso<sup>2</sup> were aided by the hypothesis that these elements are members of an "actinide series" in which the (III) oxidation states are chemically similar to the (III) rare-earth elements. According to this hypothesis<sup>3</sup> the relation of actinium to the actinide series is analogous to that of lanthanum and the succeeding fourteen rare-earth elements. Thus the first 5f electron might appear

†Contribution from the Department of Chemistry and the Radiation Laboratory, University of California, Berkeley, and from the Chemistry Division of the Metallurgical Laboratory, University of Chicago, now the Argonne National Laboratory.

in thorium, just as the first 4f electron appears in cerium. If this hypothesis were correct, it seems likely that both americium and curium would be predominantly (III) in aqueous solutions. This has been found to be true of both elements. Americium was found in the rare-earth fraction separated from plutonium that had been bombarded with deuterons in the 60-in. Berkeley cyclotron. Similar behavior was demonstrated in the case of curium following bombardment of plutonium with  $\alpha$  particles.

Following their discovery, americium and curium were produced in quantities sufficient to permit more extensive investigation of their chemical properties by tracer methods. This program together with that involving the study of the nuclear properties of these elements required the development of methods for the separation of americium and curium from other elements, particularly the rare-earth fission products. These objectives were accomplished but only after the examination of several different methods. The frequently necessary determination of the composition of  $\alpha$ -emitting isotopes of americium and curium was accomplished by means of a sensitive  $\alpha$ -pulse analyzer. In experiments involving only one of the two elements, ordinary  $\alpha$  counters were used.

In the following discussion no attempt is made to present complete experimental details. Rather, attention is focused only on those experiments which are believed to be most significant even though not entirely conclusive. Hitherto unreported work of investigators other than the authors is included.

## 2. EXPERIMENTAL WORK

2.1 Insoluble Compounds of Am(III) and Cm(III). (a) Fluorides. Lanthanum fluoride has been employed as a satisfactory carrier for Am(III) and Cm(III) in both nitric and hydrochloric acid solutions. The conditions are not critical, and those most commonly employed in the absence of interfering ions are: 1N  $\text{HNO}_3$ , 0.2 mg of La per milliliter, 1N HF, a few minutes' digestion at room temperature, and separation of the flocculent  $\text{LaF}_3$  by centrifugation. Ions that inhibit the precipitation of  $\text{LaF}_3$  decrease the completeness of separation of americium and curium; such ions include Al(III), Fe(III), and others that form complex fluorides. There is a difference in the behavior of Am(III) and Cm(III) as compared with the rare-earth elements in the presence of fluosilicic acid. In the presence of fluosilicic acid the rare earths are precipitated more completely than are Am(III) and Cm(III). This provides a useful and comparatively rapid method for the separation of Am(III) and Cm(III) from the rare-earth elements as a group. This method is discussed in more detail in a later section.

Work done thus far suggests that the solubilities of  $\text{AmF}_3$  and  $\text{CmF}_3$  are of the same order of magnitude as that of  $\text{LaF}_3$ . On the basis of the properties of the preceding members of the actinide series (i.e., thorium, protactinium, uranium, neptunium, and plutonium) it seems likely that  $\text{AmF}_3$  and  $\text{CmF}_3$  are isomorphous with  $\text{LaF}_3$ . Obviously  $\text{LaF}_3$  is not the only satisfactory fluoride carrier. The rare-earth and rare-earth-like fluorides in general are good carriers, e.g.,  $\text{CeF}_3$  and  $\text{YF}_3$ , both of which have been used satisfactorily.

(b) Oxalates. Both lanthanum oxalate and bismuth oxalate precipitated from nitric acid solutions have been employed satisfactorily as carriers for Am(III) and Cm(III). From solutions containing high concentrations of oxalate ion (e.g., at high pH in solutions containing ammonium hydroxide), complete precipitation of lanthanum oxalate leaves Y(III) in solution but Am(III) exhibits behavior intermediate between lanthanum and yttrium. Under these conditions the coprecipitation of Am(III) by oxalates appears to be greatly influenced by temperature. At elevated temperatures (e.g., 90°C) almost complete precipitation of bismuth oxalate leaves most of the Am(III) (approximately 75 per cent) and Y(III) (approximately 90 per cent) in solution. If the solutions are first cooled to room temperature, nearly all the Am(III) (approximately 90 per cent) is carried, but most of the Y(III) remains in solution. However, at higher acidities, such as 3N  $\text{HNO}_3$ , the concentration of oxalate ion is less, the complexing action of the oxalate ion is minimized, and Am(III) is carried more nearly completely by bismuth oxalate than is La(III). This suggests that Am(III) oxalate is more insoluble than lanthanum oxalate. Under similar conditions, however, Y(III) is less completely carried, and the decreasing order of solubilities of the oxalates appears to be



In reaching this conclusion it is assumed that the equilibrium effects are not obscured by rate phenomena.

These results indicate that Am(III) exhibits a tendency toward the formation of a soluble complex oxalate. Under conditions favorable to the formation of such a complex, the carrying of americium shows a marked dependence on temperature. At low temperatures and high pH values a fairly good separation of Am(III) from Y(III) may be obtained.

Less extensive studies on the behavior of curium oxalate have provided no evidence of separation of curium from americium over a wide range of experimental conditions. It seems very likely that the two elements are quite similar in their chemical properties.

(c) Phosphates. From information available at this time it appears that the solubilities of  $\text{AmPO}_4$  and  $\text{CmPO}_4$  are comparable to those of  $\text{CePO}_4$  and  $\text{LaPO}_4$ . Zirconium phosphate precipitated from solutions containing nitric acid at concentrations greater than 1N carries only a small proportion of the Am(III) and Cm(III) present. The fraction carried increases with decrease in acidity and is decreased by the presence of certain ions, notably Fe(III).

Lanthanum phosphate precipitated from 0.1M ammonium citrate solutions at pH approximately 2 and phosphate concentrations of 0.5M has been a useful carrier for Am(III). Good yields of Am(III) were obtained when this method was used to separate Am(III) from large amounts of calcium in nitrate solutions.

(d) Iodates. The behavior of the iodates is similar to that of the phosphates although the carrying of Am(III) and Cm(III) by compounds such as Ce(IV), Th(IV), or Zr(IV) iodates is less dependent on hydrogen-ion concentration than it is in the case of the phosphates. Even at high concentrations of nitric acid (e.g., 5N to 6N) in the presence of  $\text{BrO}_3^-$  or  $\text{Ag}^{(II)}$ , more than 50 per cent of the Am(III) or Cm(III) may be carried by  $\text{Ce}(\text{IO}_3)_4$  or  $\text{Zr}(\text{IO}_3)_4$ . However, the carrying is quite erratic and under roughly comparable conditions may vary between 5 and 70 per cent in extreme cases. The reasons for these deviations are not known, but similar behavior has been observed in the case of the carrying of rare-earth elements that do not have oxidation numbers greater than 3. It seems probable that conditions for satisfactory carrying of Am(III) and Cm(III) by iodates are critical, perhaps with respect to variables such as temperature and time of digestion.

(e) Hydroxides. It is evident from a very large number of observations that the hydroxides of americium and curium exhibit solubilities comparable to those of the rare-earth hydroxides. At tracer concentrations, Am(III) and Cm(III) are carried essentially completely by a wide variety of insoluble hydroxides, and precipitations with both ammonium hydroxide and potassium hydroxide fail to provide evidence of either complex cation formation or amphotерism. There is evidence that the hydroxide of americium is somewhat less soluble than that of lanthanum.

Lanthanum hydroxide has been used effectively to separate Am(III) from solutions containing calcium. Precipitation is performed by the addition of a moderate excess of ammonium hydroxide. The percentage of calcium carried by the precipitate appears to be greater than that carried by lanthanum phosphate, as mentioned in Sec. 2.1c.

2.2 Soluble Compounds of Am(III) and Cm(III). The solubilities of the nitrates, halides, and perchlorates of Am(III) and Cm(III) are

probably similar to those of the corresponding compounds of the rare-earth elements. The sulfides and sulfates appear to be moderately soluble.

**2.3 Behavior of Americium and Curium in Conventional Rare-earth-group Separations.** Comparison of the behavior of americium and curium with the rare-earth elements in conventional procedures for their separation has been made. The method used was a modification of a part of a procedure described by Noyes and Bray.<sup>4</sup> Approximately equal quantities of americium and curium  $\alpha$  activities were used as a mixture. Unfortunately it was not possible to determine the percentage of each component in the fractions resulting from the chemical separations since adequate equipment for such determinations was not available at the time the experiment was performed. However, in view of the marked similarity of americium and curium as demonstrated by other experiments, it seems reasonable to assume that the two elements exhibited similar behavior in the experiment described below.

The americium-curium tracer mixture was added to a 3M HCl solution containing the elements indium, cerium, lanthanum, yttrium, samarium, praseodymium, europium, scandium, and gadolinium at equal concentrations. These elements were precipitated as fluorides, separated, and leached with concentrated ammonium fluoride solution. The leachings (scandium fraction) contained less than 1 per cent of the total  $\alpha$  activity. The fluorides were then converted to hydroxides, which were dissolved in 6M acetic acid. Saturation of this solution with hydrogen sulfide produced  $In_2S_3$ , which was separated and found to contain about 10 per cent of the total  $\alpha$  activity. The solution was heated to expel the hydrogen sulfide and then evaporated to dryness. Ce(III) was oxidized to Ce(IV) by heating with nitric acid and potassium perchlorate, after which  $Ce(IO_3)_4$  was precipitated, separated, and found to contain about 20 per cent of the total  $\alpha$  activity. The remaining elements were precipitated as hydroxides and converted to chlorides. The chlorides were dissolved in 45 per cent  $K_2CO_3$ , diluted to a potassium carbonate concentration of 10 per cent, and heated for 2 hr in a nickel crucible. The cerium-group precipitate was separated and found to contain about 30 per cent of the total  $\alpha$  activity; the remaining 40 per cent was retained in the soluble fraction containing the yttrium-group elements.

The results of this experiment show that americium and curium are similar to the rare-earth elements. The new elements exhibit no tendency to follow scandium and are not carried appreciably by indium sulfide. In potassium carbonate solutions americium and curium seem to distribute themselves throughout the rare-earth group as a whole rather than to fall at either end of the series.

In separating small amounts of americium or curium in pure form from other elements some of the steps that have been effective are as follows:

1. Carry with  $\text{LaF}_3$  or  $\text{CeF}_3$ .
2. Ignite to oxide or convert to hydroxide by metathesis with potassium hydroxide.
3. Separate insoluble sulfides from approximately 0.3N HCl, leaving Am(III) in solution.
4. Precipitate  $\text{La}(\text{OH})_3$  or  $\text{Ce}(\text{OH})_3$  and Am(OH)<sub>3</sub> with excess ammonium hydroxide.
5. Separate rare earths from Am(III) or Cm(III) by at least one of the following steps:
  - a. Use adsorption-elution method with Dowex-50 resin as described below (also separate americium from curium).
  - b. Use fluosilicate procedure described below.
  - c. Precipitate americium from potassium carbonate solutions by oxidation with hypochlorite.

**2.4 Use of Fluosilicic Acid in the Separation of Americium and Curium from the Rare-earth Elements.** Lanthanum (or rare-earth) fluoride carriers for Am(III) and Cm(III) tracers have often been employed successfully in glass equipment when the time of contact with hydrofluoric acid solutions was short. However, after overnight contact between glass and 6M HF, it was found that  $\text{CeF}_3$  failed to carry Am(III) and Cm(III) tracers completely. Further study showed similarly poor carrying of Am(III) and Cm(III) when  $\text{H}_2\text{SiF}_6$  was added to precipitate the rare-earth carrier when lusteroid or other plastic containers were used. Other experiments led to the elimination of hydrofluoric acid and an increase in the amount of rare-earth carrier. Under these conditions the carrier precipitate is believed to be a fluoride rather than fluosilicate.

With this procedure americium and curium were separated effectively<sup>5</sup> from yttrium, lanthanum, praseodymium, neodymium, element 61, and europium, as well as from cerium, by a separation factor of 10<sup>8</sup>. The work of S. Peterson<sup>6</sup> has shown that the behavior of Ac(III) toward  $\text{H}_2\text{SiF}_6$  is similar to that of Am(III). Thus the use of  $\text{H}_2\text{SiF}_6$  provides a group separation of the (III) rare-earth elements from Am(III) and Cm(III). Although other methods provide more satisfactory separations from lanthanum or from single rare-earth elements, they do not permit a sharp group separation.

Apparently the optimum procedure for the use of fluosilicate is as follows: To a 5M  $\text{HNO}_3$  solution containing Am(III) and/or Cm(III) tracer is added (in the form of a concentrated solution) 5 to 10 mg of Ce(III) per milliliter of the 5M  $\text{HNO}_3$  solution. This is heated to 35 to

40°C, and 30 per cent  $H_2SiF_6$  solution is added slowly, with stirring, over a period of  $\frac{1}{2}$  to 1 hr until the total volume is  $1\frac{1}{3}$  times the volume of the original 5M  $HNO_3$  solution (i.e., a final  $H_2SiF_6$  concentration of approximately 1M) and is then digested at 35 to 40°C for an additional  $\frac{1}{2}$  to 1 hr.

After application of this procedure followed by separation of the rare-earth precipitate, the solution is usually found to contain about 70 to 85 per cent of the americium and/or curium and about 8 to 10 per cent of the rare earths. Americium and curium may then be removed from solution by making the fluosilicate solution 5M in HF, whereupon residual rare earths in the solution (0.5 to 1 mg per milliliter) precipitate as fluorides and carry approximately 97 per cent of the americium and curium. If necessary, Ce(III) carrier may be added [0.5 mg of Ce(III) per milliliter of fluosilicate solution] if the solution does not contain a sufficient concentration of rare-earth elements to act as the carrier. If further separation of americium and curium from the rare earths is desired, additional fluosilicate cycles may be used. The rare-earth fluoride precipitate (containing the americium and curium) is converted to hydroxide by agitation and digestion with hot concentrated potassium hydroxide solution for several minutes. Following centrifugation, the clear supernatant solution is withdrawn, more potassium hydroxide solution is added, and the above treatment is repeated. Finally, the hydroxide precipitate is separated, washed with water, and dissolved in nitric acid; the resulting solution is used in another fluosilicate cycle.

In a typical fluosilicate cycle the completeness of precipitation of rare-earth elements increases with increase in time of digestion, but it reduces the proportion of americium and curium remaining in the solution. This relation is shown in Fig. 1. After digestion for 2 hr, about 75 per cent of the americium and 4 per cent of the cerium remain in solution. The rate of precipitation of both americium and rare earths increases with increase in temperature or decrease in the concentration of nitric acid. Decrease in the concentration of  $H_2SiF_6$  leads to poorer separation of americium and curium from rare earths, but the separation is not improved by making the  $H_2SiF_6$  concentration greater than 1M, and effective separation is favored by slow rate of addition of  $H_2SiF_6$ . La(III), Y(III), and Ce(III) are equally good carriers, and the rare-earth carrier precipitates serve to separate small amounts of Th(IV) and Pu(IV) rather completely. Precipitation of the rare-earth fraction is inhibited by Zr(IV) but is not significantly influenced by the presence of Fe(III).

Experiments employing fluomolybdate and fluoborate substitutes for fluosilicate have led to less satisfactory separations.

The experiments using fluosilicates to separate actinide and lanthanide elements suggest that rare-earth fluorides may be more insoluble than the fluorides of Am(III) and Cm(III) although the differences may not be very large. It may also be true that complex

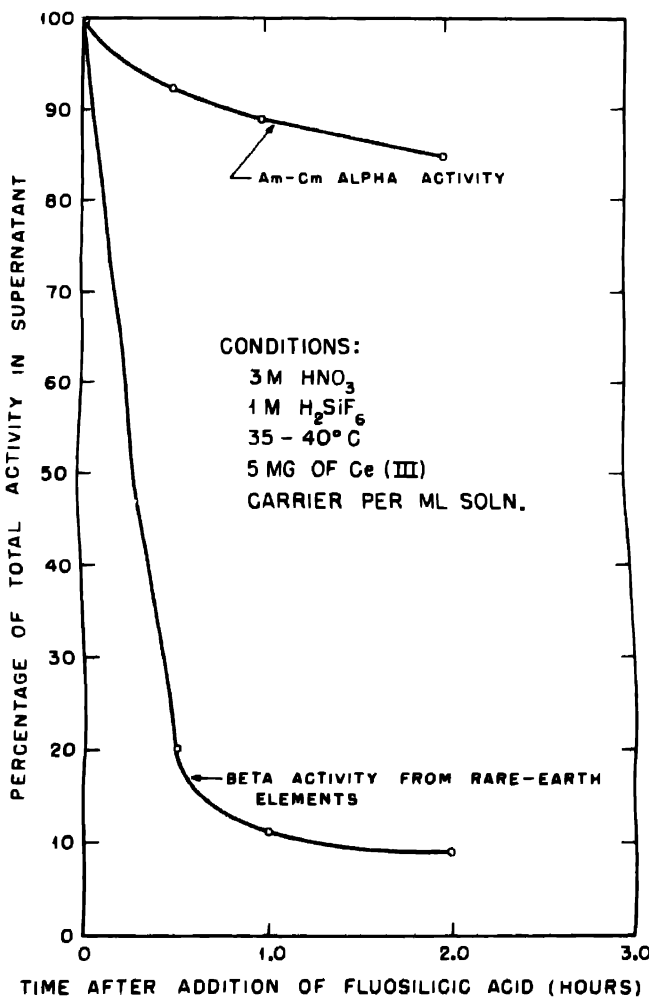


Fig. 1—Comparison of precipitation of Am, Cm, and rare-earth elements as a function of time from fluosilicate solutions using cerium(III) carrier.

fluorides of the type  $\text{AmF}_2^+$ , in which a difference in the stability of actinides and lanthanides exists, are involved. It should be emphasized that it is in this fluoride-fluosilicate system that the greatest differences in properties between Am(III) or Cm(III) and the rare earths have been observed.

**2.5 Attempted Oxidation of Am(III) and Cm(III) in Aqueous Mediums.** Demonstration of the existence of oxidation states other than (III) for americium and curium is of interest not only in relation to possible methods of separation but also because of its importance in connection with the actinide hypothesis. Since americium and curium would be analogous to europium and gadolinium, respectively, americium would be expected to be more readily convertible to other oxidation states than curium. Because americium is preceded by actinide elements that exhibit oxidation states higher than are encountered among the corresponding rare-earth elements, the probability of oxidation states higher than the (III) should be greater for americium than for europium. Such speculations, however, should recognize the possibility of a marked trend toward stabilization of the (III) state.

These expectations are indeed borne out by the results of tracer experiments. There is evidence that Am(III) may be oxidized and reduced in aqueous solutions, but the resulting oxidation states have not been definitely identified; and these changes may be brought about only by the use of the most powerful oxidizing and reducing agents. Similar experiments involving Cm(III) provided no evidence whatever of either oxidation or reduction. These results provide strong evidence in support of the actinide hypothesis.

(a) Basic Mediums. Attempts have been made to oxidize Am(III) and Cm(III) by using the strongest oxidizing agents under a variety of conditions. The best possibility seemed to involve the use of oxidizing agents such as peroxide and hypochlorite in basic solutions, and several experiments employing these reagents have been performed. In basic solutions, however, there are few if any carriers that may be used to distinguish between Am(III) or Cm(III) and their oxidation products. If the hydroxides of higher oxidation states are insoluble (as might be expected by analogy with neptunium and protactinium), these, as well as the (III) state of americium and curium, would most likely be carried by any insoluble hydroxide carrier. Thus the identification of higher oxidation states of americium or curium would probably require the use of a selective complexing agent that would exhibit stability in strongly basic mediums. The latter requirement is unlikely to be satisfied, particularly by organic complexing agents.

Attempts have been made to use potassium carbonate as the complexing agent and peroxide as the oxidizing agent. It was anticipated that an insoluble peroxide of Am(>III) might be produced and might coprecipitate with perceric hydroxide ( $\text{CeO}_3 \cdot 2\text{H}_2\text{O}$ ) or thorium peroxide precipitated from the same medium. At the same time it was expected that Am(III) and the rare-earth elements would remain complexed in the carbonate solution and consequently would not co-

precipitate with the carrier unless oxidation occurred. Treatment with 5 per cent  $H_2O_2$  by weight in 20 per cent  $K_2CO_3$  solution over a period of 15 min at room temperature appeared to cause nearly complete precipitation of cerium as  $CeO_3 \cdot 2H_2O$  or of thorium peroxide, but these precipitates carried less than 2 per cent of the americium-tracer and 3 per cent of the lanthanum-tracer activity. Thus there was no evidence of oxidation of Am(III) over a short period of time. However, it would seem worth while to extend the time for reaction under a variety of experimental conditions.

L. B. Werner and I. Perlman<sup>18</sup> have found that Am(III) in concentrated solutions of potassium carbonate may be converted to a higher oxidation state [probably the (V) state] and carried from the carbonate solution by precipitation of a Pu(V) compound. Conversion of americium to the higher oxidation state occurs in the presence of hypochlorite. Separations of americium from curium and rare earths have been made using this procedure, but plutonium is not an ideal carrier because of the ease with which it is converted to oxidation states other than the (V) state in which it does not precipitate from carbonate solutions. A carrier that would make rapid, efficient separations possible has not been found.

(b) Acidic Mediums. Oxidation of Am(III) and Cm(III) has been attempted by use of  $K_2Cr_2O_7$ ,  $KMnO_4$ ,  $NaBiO_3$ , and  $Ag(II)-K_2S_2O_8$ . Only the experiments involving potassium bromate provided any evidence of oxidation of Am(III), and it is not clear why this reagent alone should lead to such results. Work relating to potassium bromate is described below. In connection with the use of various oxidizing agents, attempts have been made to employ solvents that are immiscible with water and nitric acid. These experiments are discussed in the section on solvent extraction.

1. Potassium Bromate in Nitric Acid Solutions. Early attempts to separate americium from rare-earth elements involved the separation of cerium by reprecipitation of  $Ce(IO_3)_4$  after oxidation of Ce(III) to Ce(IV) by means of  $BrO_3^-$ . This method was used successfully for some time. In most cases 10 to 20 per cent of the americium tracer was carried by  $Ce(IO_3)_4$  when the latter was precipitated at room temperature from 5M to 6M  $HNO_3$  at an iodic acid concentration of approximately 0.4M. In later experiments, however, it was found sometimes that as much as 90 per cent of the americium was carried. This suggested that Am(III) was being oxidized by  $BrO_3^-$ , perhaps to Am(IV), which was carried nearly completely by  $Ce(IO_3)_4$ . Subsequent experiments designed to explore this possibility further led to results that are certainly not conclusive. In some cases treatment with

potassium bromate in concentrated nitric acid led to enhanced carrying of americium by  $\text{Ce}(\text{IO}_3)_4$ . In other experiments there was no detectable difference in the carrying of either americium or curium, and both were carried to the extent of about 50 per cent. Since it was not expected that curium would be carried and since a similar erratic behavior has been demonstrated in the case of coprecipitation of the lanthanum tracer by  $\text{Ce}(\text{IO}_3)_4$ , it seems evident that a more thorough study of variables should precede conclusions regarding the oxidation of either Am(III) or Cm(III).

Attention has been called to the fact that bromate is the only oxidizing agent that has provided evidence for the existence of Am(>III) at tracer concentrations in acidic aqueous solution, and that other oxidizing agents such as argentic ion and sodium bismuthate failed to provide similar evidence. No explanation is available for the erratic behavior of bromate ion.

Attempts to oxidize Am(III) by bromate at high temperatures were unsuccessful, perhaps because the rate of decomposition of bromate and the liberation of bromine increase greatly at high temperatures.

After oxidation by means of bromate in concentrated nitric acid had been tried, attempts were made to use zirconium phosphate as a carrier for Am(>III). This compound may be precipitated rather completely at high concentrations of nitric acid, and the phosphate of Am(IV) would be expected to be sufficiently insoluble to permit coprecipitation at nitric acid concentrations between 5N and 10N. By analogy with the carrying of Pu(IV), that of Am(IV) should certainly be greater than 50 per cent under these conditions. However, oxidation with bromate in concentrated nitric acid followed by precipitation of Zr(IV) phosphate from 8M  $\text{HNO}_3$  - 0.5M  $\text{H}_3\text{PO}_4$  carried only a few per cent of the americium tracer and provided no evidence for a separation of americium and curium. Failure of coprecipitation with zirconium phosphate might be due to the fact that the americium did not exist as Am(>III) at the time of precipitation owing to inadequate initial conditions of oxidation or to reduction that may have occurred on dilution to lower acidity during carrier precipitation. On the other hand, the americium may have been converted to an oxidation state [other than Am(IV)] that is not carried by zirconium phosphate.

**2. Argentic Ion in Nitric Acid Solutions.** One of the first oxidizing agents used in attempts to oxidize Am(III) was argentic ion formed from silver nitrate and potassium or ammonium persulfate in nitric acid solutions. At acidities ranging from 0.5M to 10M  $\text{HNO}_3$ , evidence of oxidation was not obtained using zirconium phosphate as the carrier. Certain experiments involving zirconium phosphate at high

concentrations of nitric acid employed mixtures of americium and curium, and the percentage of each carried was determined. Differences attributable to oxidation of Am(III) were not observed.

In other experiments differences in completeness of coprecipitation as a function of acidity were anticipated and realized. In 3M HNO<sub>3</sub>-0.1M H<sub>3</sub>PO<sub>4</sub>, zirconium phosphate in some cases carried as much as 25 per cent of the americium. The percentage of the americium carried decreased with increase in the concentration of acid. This was probably due to enhanced solubility of americium phosphate.

**3. Other Oxidizing Agents.** Attempts to obtain evidence of oxidation of Am(III) by use of the oxidizing agents listed below were unsuccessful. The conditions and carriers employed are as follows:

K<sub>2</sub>Cr<sub>2</sub>O<sub>7</sub>: 1M to 5M HNO<sub>3</sub>; heating at 50 to 95°C for as long as 2 hr; LaF<sub>3</sub>, Zr<sub>3</sub>(PO<sub>4</sub>)<sub>4</sub>, and Ce(IO<sub>3</sub>)<sub>4</sub> carriers. (The carrying was always comparable to that found using rare-earth tracers.)

NaBiO<sub>3</sub>: 1M to 10M HNO<sub>3</sub>; 25 to 60°C; 5 min to 2 hr; LaF<sub>3</sub> and Zr<sub>3</sub>(PO<sub>4</sub>)<sub>4</sub> carriers. (The carrying was typical of (III) rare-earth elements.)

KMnO<sub>4</sub>: 1M to 10M HNO<sub>3</sub>; 25 to 75°C; approximately 1 hr; MnO<sub>2</sub> carrier. (Carrying was essentially the same for americium and lanthanum.)

**2.6 Oxidation of Am(III) and Cm(III) by Fusion with Sodium Nitrate.** Rare-earth separations that depend on the production of higher oxidation states of certain rare-earth elements other than cerium (e.g., praseodymium and terbium) have been reported in the literature. One such method<sup>7</sup> involves oxidation by fusion with sodium nitrate, followed by dissolution in an acetate-buffered solution, which leaves the higher oxides undissolved. Thus a reasonably good separation of lanthanum from praseodymium may be accomplished. According to the actinide hypothesis it might be expected that americium would follow praseodymium and curium would follow lanthanum in such a separation.

At the time these experiments were performed, evidence for the oxidation of Am(III) was lacking. It was believed, however, that in view of the known behavior of these rare-earth elements, fusion with sodium nitrate offered promise as a means of oxidation of Am(III). A separation of americium from curium was obtained by this method. The undissolved oxide fraction contained a higher proportion of americium than the curium, whereas the aqueous leachings contained a higher proportion of curium than of americium. The change in the

ratio of americium to curium, however, was not great enough to provide a satisfactory separation of the two elements.

In three separate experiments, each using a different rare-earth carrier, the maximum change in the americium/curium ratio was obtained using terbium as carrier. Initially, the americium/curium tracer ratio was 1.14/1. After fusion for 1.5 hr at 460°C followed by leaching, the ratio in the  $TbO_2$  was 2.0/1. With  $PrO_2$  and  $CeO_2$ , the ratios were 1.5/1 and 1.3/1, respectively. In all these experiments lanthanum equivalent to the oxidizable rare-earth carrier was added as a holdback agent.

**2.7 Reduction of Am(III) and Cm(III) in Aqueous Media.** (a) Use of Zinc Amalgam. Early in the search for methods for the separation of americium from curium and other elements, the possibility of reduction to Am(II) was investigated. It was anticipated that the solubility of  $AmSO_4$  would be similar to that of  $EuSO_4$ . Accordingly the reduction of Am(III) by means of zinc amalgam was attempted, and Eu(III) was used for comparison. In this experiment a solution containing Eu(III) and Am(III) tracer was passed through the reduction column and into sulfuric acid solution, whereupon  $EuSO_4$  precipitated. Throughout these operations an inert atmosphere was maintained in the entire system. Since a major fraction of the americium was not carried by the  $EuSO_4$ , it appears that  $AmSO_4$  is not carried well by  $EuSO_4$  or, more probably, that Am(III) is not reduced by zinc amalgam. If the latter conclusion is correct, the potential of the couple  $Am(II) = Am(III) + e^-$  under these conditions must be more positive than that of the couple,  $Zn = Zn(II) + 0.76$ .

(b) Use of Sodium Amalgam. In subsequent attempts to reduce Am(III), sodium amalgam was used as the reducing agent in a method similar to that employed by J. K. Marsh<sup>8</sup> in the separation of certain of the rare-earth elements. A sulfuric acid solution containing La(III), Sm(III), and Eu(III) together with Am(III) and Cm(III) tracers was shaken with sodium amalgam. The resulting precipitate of  $EuSO_4$  and  $SmSO_4$  was separated and leached rapidly with cold dilute nitric acid. (According to Marsh this treatment dissolves  $SmSO_4$  and leaves most of the  $EuSO_4$  undissolved.) About 40 per cent of the americium tracer and 20 per cent of the curium tracer were found in the soluble fraction. The increase in the americium/curium ratio in the Samarium fraction suggests that Am(III) may have been partly reduced to Am(II).

(c) Use of Barium. The results obtained by the use of sodium amalgam suggested other experiments which might not only confirm the existence of Am(II) but also provide a method for the separation

of americium and curium based on differences in oxidation state. In the separation of americium and curium following reduction with sodium amalgam, the carrying of Am(II) by the mixture of EuSO<sub>4</sub> and SmSO<sub>4</sub> might not be particularly selective in comparison with the carrying of Am(III). A better separation might be accomplished by the use of a more selective carrier such as barium chloride. Barium metal and concentrated hydrochloric acid containing americium and curium tracers were employed, and a precipitate of BaCl<sub>2</sub> formed as the barium dissolved slowly over a period of about 5 min. The americium/curium ratio in the original hydrochloric acid solution was 0.9 whereas that found in the BaCl<sub>2</sub> precipitate was 1.4.

2.8 Comparative Behavior of Americium, Curium, and Rare-earth Elements toward Adsorption on Cation-exchange Resins and Elution with Ammonium Citrate. (a) Amberlite IR-1 Resin. A method for the separation of rare-earth elements by adsorption on an Amberlite IR-1 resin followed by selective elution with ammonium citrate has been devised by W. Cohn and his associates.<sup>9</sup> Further development of the method by Cohn, F. H. Spedding,<sup>10</sup> and their coworkers has led to the efficient separation of many of the rare-earth elements by this method. In view of the similarity between americium and the rare-earth elements in other systems, it was obviously worth while to study their behavior in the IR-1 citrate system from the standpoint of possible separations.

Preliminary experiments employed a 12-in. column of 1 cm I.D. packed with 40- to 60-mesh IR-1 resin. The resin was washed with 0.1M HCl, and the excess acid was removed by washing with water. A mixture of Am(III) and, for example, Y(III) tracers was adsorbed on the column from a 0.1M HCl solution. After displacement of the residual acid with water, 5 per cent ammonium citrate solution (pH = 2.75) was passed through the column, and the elutriant was collected in a number of small fractions. These were analyzed separately for both americium and yttrium activities.

From this and similar experiments involving comparison of americium with other elements, the decreasing order of rate of elution was found to be: Y > 61 > Am > Ce > La. Americium falls between element 61 and element 58 (cerium) and was more similar to element 61 in this system.

Other experiments designed to separate americium from several of the rare-earth elements employed a 6-ft column. Some separation was accomplished, and rare-earth elements in the region of element 61 were separated by a factor of approximately 2.

Peterson's work<sup>11</sup> on the adsorption and elution of actinium has shown that it is more slowly eluted from IR-1 with citrate than is lanthanum. Thus the decreasing order of rate of elution of actinium in comparison with members of the actinide- and lanthanide-series elements is as follows: Y > 61 > Am > Ce > La > Ac. Hence it appears that the behavior of the elements of the actinide series (with respect to adsorption and elution) is similar to that of the rare earths. Differences between individual members of each series must be of about the same magnitude and in the same direction with increase in atomic number.

The difference in behavior of actinide and lanthanide elements in fluosilicate solutions suggested an experiment in which a mixture of Am(III) and La(III) were adsorbed on IR-1 resin and were eluted with fluosilicate. In this case the two were removed from the column at approximately the same rate.

(b) Dowex-50 Cation Exchange Resin. The application of Dowex-50 resin to the problems of separating Am(III) and Cm(III) from each other and from other elements was remarkably successful. It was much superior to Amberlite IR-1 resin not only in the rates at which separations could be made but also in the degree of separation as shown by the sharpness of the bands in the elution curves. Other methods such as the fluosilicate procedure had been more successfully used than the IR-1 method in the separations of americium and curium from fission-product elements.

The use of Dowex-50 for the americium-curium separations was initiated at Berkeley by B. B. Cunningham as a result of the successful work of E. R. Tompkins<sup>12</sup> and others at Clinton Laboratories who were using Dowex-50 for rare-earth separations. Tompkins and Cohn supplied some of the new resin, and Tompkins came to Berkeley to participate in some of the experiments. The best results were obtained with Dowex-50 colloidal aggregates, although the characteristics of this resin varied from batch to batch, and variations within each batch were also observed. Cunningham participated in nearly all the experiments reported here.

The normal procedure for the use of the resin was to screen it to obtain the 250- to 300-mesh fraction and to convert it to the ammonium form by digestion with saturated ammonium chloride solution. The excess ammonium chloride was removed by washing with water, and the resin was graded by settling in water to remove "fines." The fraction which settled in 10 min from a water suspension in a 50-ml graduate was used to pack glass columns of various sizes. The mix-

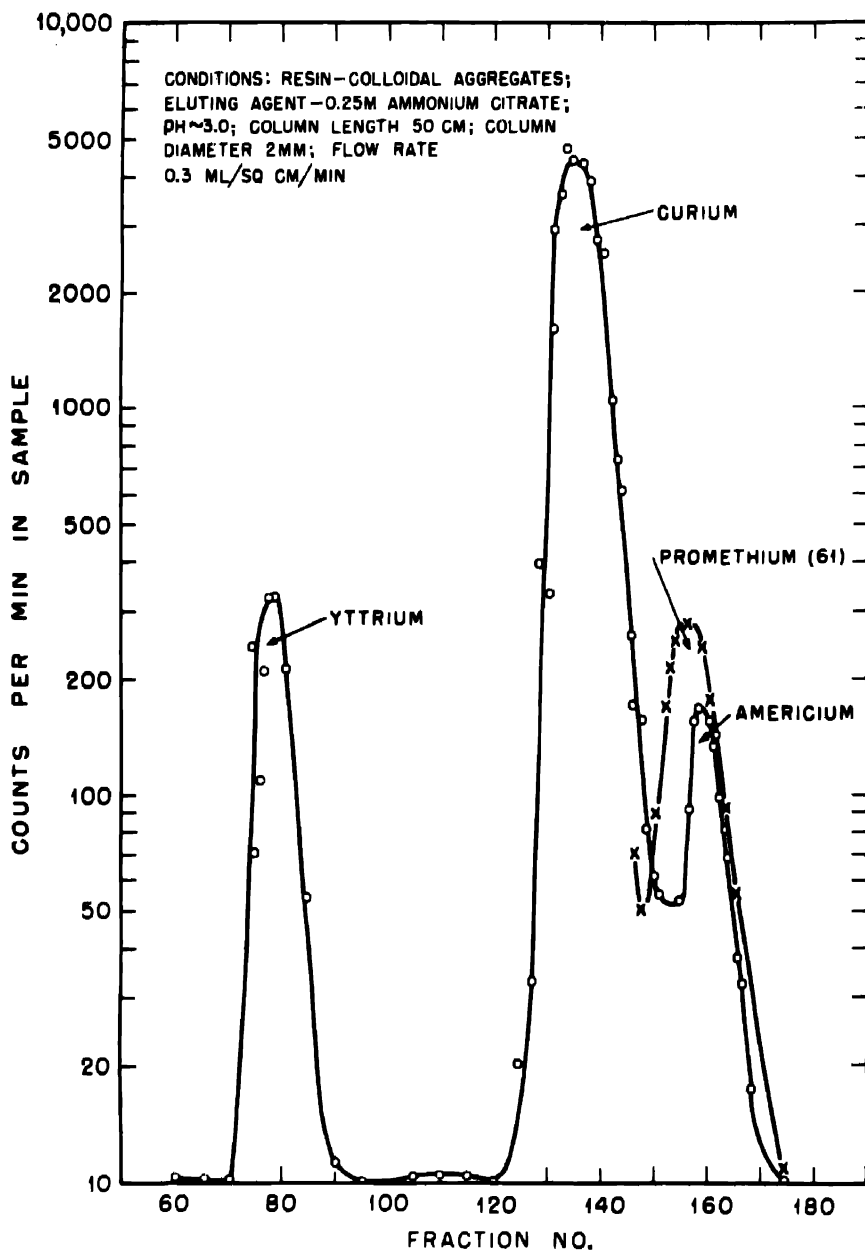


Fig. 2—Separation of Am(III) and Cm(III) using Dowex-50 resin citrate elution.

tures of Am(III), Cm(III), and rare earths in solutions of acidities corresponding to approximately 0.1N HCl or less were adsorbed on some of the same resin. This resin was then transferred to the top of the column, and 0.25M ammonium citrate at a pH of approximately 3 was passed through the column at flow rates varying between 0.15 and 0.30 ml/sq cm/hr. Samples of the elutrient were collected at relatively short intervals and analyzed by counting the  $\alpha$  radiations of americium and curium or by counting the  $\beta$  radiations of the fission products in conventional mica-window Geiger counters. In the americium-curium separations a sensitive pulse analyzer for the particles was used to distinguish between the two. Other data pertinent to the experiments are shown in Fig. 2.

The data show that Am(III) and Cm(III) are eluted in sharply defined bands similar to those of the rare earths and that these bands are sufficiently spread so that very good separations of Am(III) and Cm(III) from each other and from most of the rare earths can be obtained. However, the elution band of Am(III) falls very close to that of element 61, promethium; and the Cm(III) band falls very close to that of element 62, samarium. Therefore the separation of Am(III) and Cm(III) from these particular elements is not very satisfactory. It will be noted here that the relative positions of actinide and lanthanide elements remain about the same with Dowex-50 as in the Amberlite IR-1 system.

James and Street<sup>13</sup> have developed a method for separating americium, curium, and rare earths in which a fluosilicate solution is used as the eluting agent to remove the elements selectively from columns of Dowex-50 resin. In this case the order of elution is changed so that the Cm(III) peak is close to that of Ce(III), and Am(III) appears to elute at a rate between that of La(III) and that of Ce(III). By proper combinations of separations using fluosilicate and citrate separately Am(III) and Cm(III) can be separated very completely from all the rare earths with very good yields. The conditions used in the experiments with fluosilicate were as follows:

The resin is prepared, the column packed, and the sample transferred to the column in the same manner as was described above for the runs involving citrate. The elements are eluted by passing a 0.5M ammonium fluosilicate solution at pH 2.5 through the column at a flow rate of 0.15 to 0.30 ml/sq cm/min. The fractions are collected and analyzed as described above for the case of citrate elution. Some of the results are indicated in Figs. 3 and 4.

D. C. Stewart and Cunningham<sup>14</sup> have performed some experiments to determine the equilibrium of Am(III) and Cm(III) between Dowex-50

resin and citrate solutions of varying pH. They obtained the family of curves shown in Fig. 5 for different weights of resin per milliliter of solution. A comparison between the distribution ratios of element 61, promethium, and americium was obtained using 100 mg of resin per milliliter of solution, and the two curves were practically indistinguishable. The curium curve may be in error owing to the presence of some  $\text{Pu}^{238}$ .

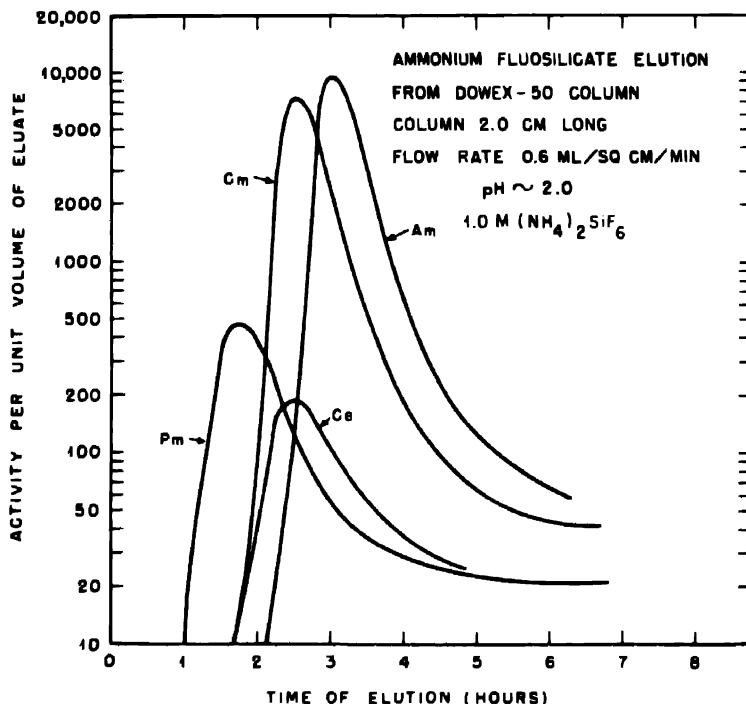


Fig. 3—Elution from Dowex-50 colloidal aggregates with fluosilicate.

Using complexing agents other than citrate and fluosilicate, Street† has undertaken a study of the rates and order of elution of actinide and lanthanide elements from Dowex-50 resin. Although this investigation is as yet incomplete, the results indicate that elution occurs with ammonium nitrate, hydrochloric acid, and hydrobromic acid, but to a much lesser extent with perchloric acid. The results with hydrochloric acid at high concentration (approximately 9M) were most

†Unreported work.

interesting in that the order of elution was shifted so that Am(III) and Cm(III) were removed from the column considerably ahead of element 61, promethium. Therefore, since the yields of fission products above elements 61 and samarium are normally low, this method shows promise of becoming a particularly good method of separating Am(III) and Cm(III) from rare-earth fission products.

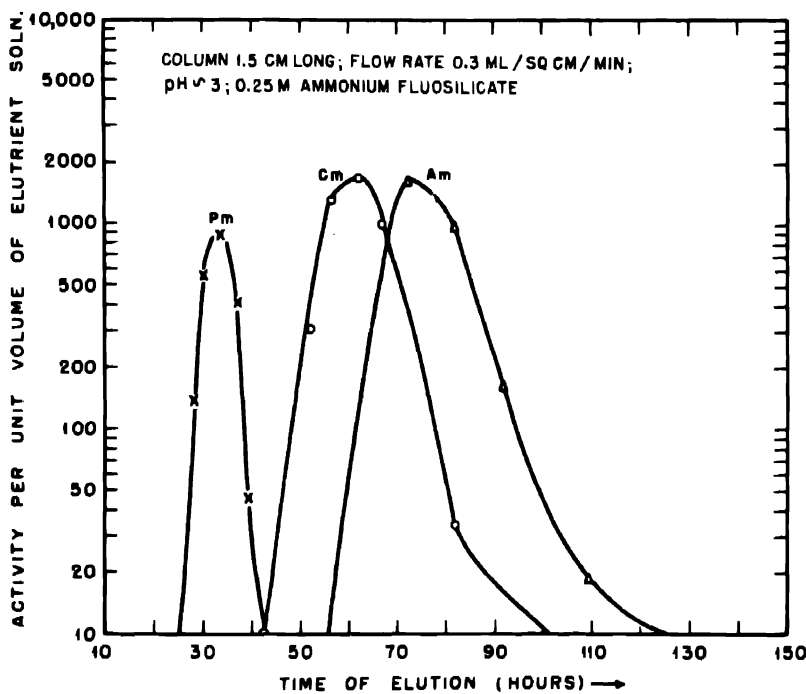


Fig. 4—Elution from Dowex-50 colloidal aggregates with fluosilicate.

**2.9 Solvent-extraction Methods for the Separation of Americium and Curium from Each Other and from Other Elements.** Separations based upon extraction of inorganic compounds from aqueous solutions into organic solvents are known to be advantageous from the standpoint of both rate and efficiency of separation. Such methods may depend upon the formation of a complex between the ion to be extracted and molecules of the organic solvent into which the complexed component of the aqueous solution is extracted. Efficient separations have been made through the use of extraction columns employing counter-current flow.

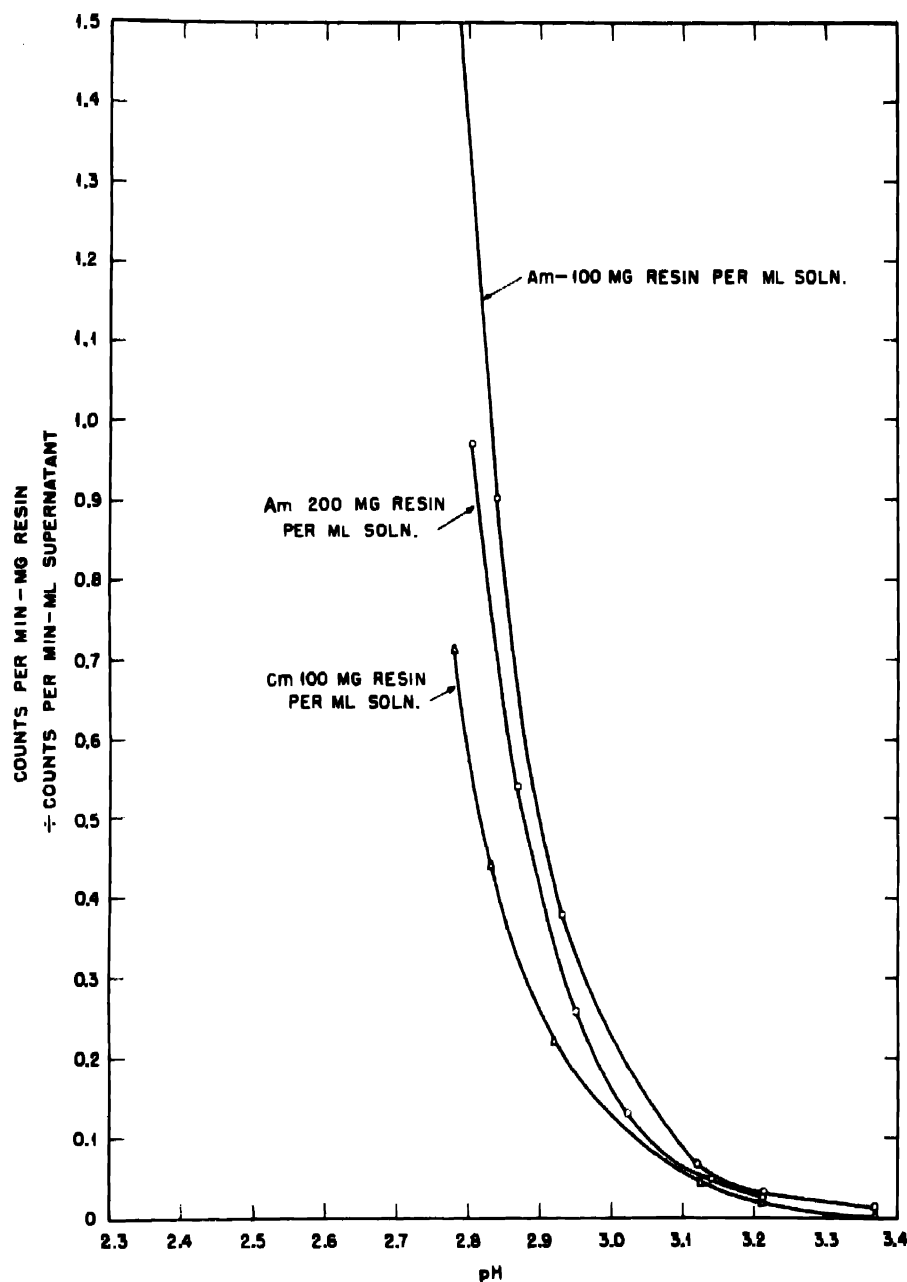


Fig. 5—Equilibrium distribution of Am(III) and Cm(III) between Dowex-50 resin and 0.25M ammonium citrate solution as a function of pH.

In the earliest work on the separation of americium and curium by solvent extraction, aqueous solutions containing hydroxamic acids† were used. At Iowa State College, Wolters and Brown<sup>15</sup> have used these compounds successfully in connection with the extraction of other actinide elements by benzene. On the basis of Brown's work and in view of the actinide hypothesis, it was anticipated that Am(III) and Cm(III) would be extracted similarly. Experimentally such was found to be the case, and a fairly good separation of Am(III) from La(III) was demonstrated. However, rare-earth elements (particularly those in the region of element 61) were not separated to any significant extent; development of the method was temporarily abandoned.

Still another approach to the separation of americium and curium from each other and from other elements by means of solvents has involved the use of powerful oxidizing agents in the attempts to produce higher oxidation states which might be extracted more readily than Am(III) or Cm(III). Thus one might be able to extract Am(IV) or Am(V) into an organic solvent and leave Cm(III) and unoxidized rare earths in the aqueous phase. Because of the known difficulty of oxidation of Am(III), such an approach places upon the organic solvent the requirement of an extreme stability sufficient to resist oxidation by (for example) bromate in concentrated nitric acid. Even limited decomposition of the organic solvent might result in the reduction of any americium which may have been oxidized.

(a) Use of Hydroxamic Acids and Chloroform. The extraction of americium in comparison with actinium and the rare-earth elements has been investigated in experiments in which benzohydroxamic acid was used. The procedure was as follows: To an acid solution containing the tracer activities to be separated, potassium benzohydroxamate (5 mg per milliliter) was added, and the pH was then adjusted to 5 to 6 by addition of sodium acetate. The mixture was shaken and allowed to stand for about 2 hr at room temperature. The aqueous solution was then shaken with an equal volume of chloroform, the two liquid phases were separated, and each was analyzed for the activities in question.

Although most of the Am(III) was extracted into the  $\text{CHCl}_3$ , the results varied considerably. These variations may have been due to failure to duplicate conditions exactly and to establish optimum conditions for this extraction. As judged from separate experiments which were not necessarily conducted under identical conditions, the approximate extent of extraction was found to be as follows: Am (75

†General formula,  $\text{RCONHOH}$ .

per cent), element 61 (65 per cent), Y (50 per cent), La (40 per cent), Ac (8 per cent).<sup>16</sup> The experimental values for element 61, yttrium, lanthanum, and actinium were converted to values corresponding to 75 per cent extraction of americium.

Although less satisfactory than certain other methods, the foregoing experiments show that americium may be separated effectively from some elements. The experiments also serve to demonstrate again the similarity between the lanthanide and actinide elements.

(b) The Possible Use of a Combination of Oxidation and Solvent Extraction. If Am(III) could be oxidized to Am(IV), (V), or (VI), extraction from the oxidation medium into an organic solvent might be possible providing that a solvent sufficiently resistant to oxidation could be found. Thus a separation from (III) curium and rare-earth elements might be accomplished. Despite the probability of oxidation of the solvent and consequent reduction of any oxidized americium, these possibilities of extraction of Am(III) have been explored by Asprey and Stewart.<sup>17</sup> A summary of these results follows:

Solvents investigated were: butyl phosphate, butyl phosphate and pyridine, diethyl ether, diethyl cellosolve, dibutyl cellosolve, nitro-methane, and dibutyl carbitol. Several different combinations of these solvents with acidic mediums together with oxidizing agents such as  $\text{NaBiO}_3$ ,  $\text{NaBrO}_3$ , or  $\text{KBrO}_3$  were investigated. In general, the extraction of americium and lanthanum tracers from 0.5 to 12M  $\text{HNO}_3$  was compared. Some experiments showed an extraction of americium, but in most of these cases there was a similar but lesser extraction of lanthanum. None of these experiments provided evidence of extraction dependent upon oxidation of Am(III). The extraction of Am(IV), if formed, would be predicted, but the possibility of oxidation to an unextractable Am(V) should not be overlooked.

### 3. SUMMARY

1. Both americium and curium are predominantly (III) in aqueous solution and exhibit great similarity to the (III) rare-earth elements, particularly those of atomic numbers 60 to 64.
2. Evidence for the oxidation of Am(III) has been obtained from tracer experiments involving sodium nitrate fusions or the use of powerful oxidizing agents in aqueous mediums. Similar experiments provided no evidence of oxidation of Cm(III).
3. Evidence for the reduction of Am(III) has been obtained by the use of sodium amalgam, but Am(III) is not reduced under conditions adequate for the reduction of Eu(III). All attempts to reduce Cm(III) were unsuccessful.

4. Am(III) and Cm(III) differ from the (III) rare-earth elements in the following respects:

a. From nitric acid solutions containing fluosilicic acid, the rare-earth elements may be precipitated almost completely whereas most of the americium and curium remains in solution. It is in this fluoride-fluosilicate system that the maximum differences in properties between Am(III) or Cm(III) and the rare earths have been observed.

b. Separation from some of the rare earths may be obtained by extraction of americium from aqueous hydroxamic acid solutions into chloroform. This procedure results in better separation of americium from lanthanum than of yttrium and element 61 from lanthanum.

c. Americium(III) in concentrated solutions of potassium carbonate may be converted to a higher oxidation state (probably +5) by treatment with hypochlorite. This higher oxidation is carried from the potassium carbonate solutions by precipitation of a plutonium(V) compound.

d. Americium(III) and curium(III) may be separated from each other and from all rare-earth elements by adsorption on columns of Dowex-50 resin and selective elution of the elements alternately with ammonium citrate and fluosilicate solutions.

5. The results of tracer experiments support the actinide hypothesis on the basis of which americium and curium are analogous to the rare-earth elements, europium and gadolinium, respectively.

#### ACKNOWLEDGMENTS

The authors wish to acknowledge their indebtedness to G. T. Seaborg, George W. Watt, W. M. Manning, and B. B. Cunningham for their assistance in connection with this work. A number of the tracers used were generously supplied by W. Cohn and W. Rubinson.

#### REFERENCES

1. G. T. Seaborg, R. A. James, and L. O. Morgan, The new element americium (atomic number 95), Paper 22.1, this volume.
2. G. T. Seaborg, R. A. James, and A. Ghiorso, The new element curium (atomic number 96), Paper 22.2, this volume.
3. G. T. Seaborg, Metallurgical Laboratory Memorandum MUC-GTS-858 (July 1944).
4. A. A. Noyes and W. C. Bray, "A System of Qualitative Analysis for the Rare Elements," pp. 210, 454-456, The Macmillan Company, New York, 1927.
5. H. H. Hopkins, Jr., and S. G. Thompson, unreported work.
6. S. Peterson, private communication (1945).

7. A. A. Noyes and W. C. Bray, "A System of Qualitative Analysis for the Rare Elements," pp. 215-218, The Macmillan Company, New York, 1927.
8. J. K. Marsh, J. Chem. Soc., 1942: 398; 1943: 531.
9. W. Cohn et al., Metallurgical Project Report CC-2827 (June 1945).
10. F. H. Spedding et al., Metallurgical Project Report CC-2720 (May 1945); J. Am. Chem. Soc., 69: 2800 (1947).
11. S. Peterson, Metallurgical Project Report CC-3248; C. K. McLane and S. Peterson, Tracer chemistry of actinium, Paper 19.3, this volume.
12. D. H. Harris and E. R. Tompkins, J. Am. Chem. Soc., 69: 2777 (1947); E. R. Tompkins, J. X. Khym, and W. E. Cohn, Metallurgical Project Report CC-2827 (June 1945), Metallurgical Project Report CL-WEC-10; E. R. Tompkins et al., Metallurgical Project Reports CH-2189 (October 1944), CH-2202 (December 1944), CN-2563 (February 1945), CN-2675 (January 1945), and CN-2839 (June 1945); Clinton Laboratories Reports Mon-N-2, Mon-N-15, and CL-ERT-3 (May 28, 1947).
13. R. A. James and K. Street, unreported work.
14. D. B. Stewart and B. B. Cunningham, unreported work.
15. F. J. Wolters and H. D. Brown, Metallurgical Project Report CN-2719 (June 1945).
16. S. Peterson and S. G. Thompson, unpublished work.
17. L. B. Asprey and D. C. Stewart, Metallurgical Laboratory Memorandum MUC-WMM-3 (May 1946).
18. L. B. Werner and I. Perlman, The preparation and isolation of curium, Paper 22.5, this volume.

## Paper 19.2

# THE FIRST ISOLATION OF AMERICIUM IN THE FORM OF PURE COMPOUNDS; MICROGRAM-SCALE OBSERVATIONS ON THE CHEMISTRY OF AMERICIUM†

By B. B. Cunningham

Element 95, americium, was discovered in November 1944 by Seaborg, James, and Morgan,<sup>1</sup> who used radiochemical methods to study the chemical properties of the element in highly dilute aqueous solutions. These studies and subsequent investigations by Thompson, Morgan, James, and Perlman<sup>2</sup> demonstrated the pronounced stability of the tripositive oxidation state and the close resemblance of the aqueous tripositive ion of americium to the tripositive ions of the rare earths.

It is the purpose of this paper to describe briefly the first isolation of americium in the form of pure compounds and to summarize the early microgram-scale observations on the chemistry of this element.

The first isolation of americium in the form of pure compounds was carried out at the Metallurgical Laboratory in Chicago during the period July to October, 1945.

The amount of americium available for this work was only a few micrograms; therefore, the final operations designed to isolate the element in the pure state were carried out with the aid of a microscope.

The microchemical apparatus that was used for the isolation and study of americium compounds was essentially the same as that used earlier for the isolation of microgram quantities of plutonium<sup>3</sup> and neptunium.<sup>4</sup> The principal features of chemical work on this scale have been reported by Seaborg.<sup>5</sup>

†Contribution from the Department of Chemistry and the Radiation Laboratory, University of California, Berkeley, and from the Chemistry Division of the Metallurgical Laboratory, University of Chicago, now the Argonne National Laboratory.

The chemical problem of isolating americium differed from the problems that were encountered in the isolation of plutonium and neptunium in the following respects:

1. It was difficult, if not impossible, to obtain the element in any oxidation state other than +3.
2. Methods of separating americium from a group of naturally occurring elements, the rare earths, could not be applied on the microgram scale without prohibitive losses.
3. The half life of the principal isotope was uncertain by at least one order of magnitude; therefore, there was no way of knowing beforehand what quantity of americium to expect in the isolation, and there was no way of judging its probable degree of purity from an amount obtained.

In the method devised for the isolation of americium the problem of separation from the rare earths was solved by subjecting the parent material to exhaustive purification from the rare earths before the americium was formed in it. Rigid precautions were then taken to prevent accidental recontamination with rare earths from the reagents or glassware used.

After the americium had been formed in the parent substance, the bulk of this was separated, and the americium activity was concentrated in a small volume. The method used for the concentration of the americium was relatively nonspecific. A number of common elements, derived mainly from impurities in the reagents used, were concentrated with it. These were separated by standard chemical procedures, and the americium activity was further concentrated so that it was all present in a solution that was only a few microliters in volume. A small fraction of this solution was then submitted for spectrographic analysis. The analysis was carried out by Drs. Mark Fred and Frank Tomkins. The only impurities detected were  $0.2 \mu\text{g}$  of lead and  $0.1 \mu\text{g}$  of iron.

Lead was removed from the americium solution by precipitation as sulfide. The supernatant solution was transferred to a paraffin-coated microcone, and the solution was made 3M in hydrofluoric acid. After 10 min the solution was centrifuged, and the cone was examined carefully under the microscope. It was observed that a small amount of precipitate had collected in the tip of the cone. The color of the precipitate was a faint but definite pink.

On the basis of this observation alone it was possible to eliminate from consideration as principal components of the precipitate all except four previously known elements. These elements are manganese, europium, neodymium, and erbium. These possibilities were examined in turn by the following procedures:

1. Repeated washing of the precipitate with water failed to dissolve an appreciable fraction of it; hence it could not be  $MnF_2$ .

2. On direct comparison of the sample with a similar amount of  $NdF_3$ , the precipitates were found to be distinctly different in color. The precipitate was therefore not  $NdF_3$ .

3. Comparison with  $EuF_3$  showed the europium fluoride to be much less strongly colored; hence the precipitate was not  $EuF_3$ .

4. Comparison with  $ErF_3$  showed a similarity of shade but not of intensity of color.

The fluoride precipitate was washed carefully with water, transferred to a clean, previously weighed platinum boat, ignited to redness in air, and then examined under the microscope. The color of the deposit was observed to be jet black except at the very thin edges, which were brown. The deposit was entirely different in color from  $Er_2O_3$  but strikingly similar to that of the rare-earth oxides,  $Pr_6O_{11}$  and  $Tb_4O_7$ . Since in the case of the rare earths the color of the sesquioxide is usually very similar to that of the trifluoride, it appeared that ignition in air converted the fluoride to an oxide of americium in which at least part of the americium was in a higher oxidation state.

The oxide was weighed to the nearest 0.01  $\mu g$  on the quartz fiber microbalance. The instrument used was that designed by Kirk, Craig, and Gullberg.<sup>6</sup>

The  $\alpha$  activity associated with this known weight of americium oxide was determined in a special low-geometry counter. The counting was done in collaboration with Albert Ghiorso. The half life computed from the measured specific  $\alpha$  activity was 498 years. The computation was made on the assumption that the formula of the compound weighed was  $AmO_2$ . Because the composition of the black oxides of the rare earths does not correspond exactly to  $RO_2$ , it seems likely that a similar situation exists in the case of the black oxide of americium. Because of this uncertainty and other errors connected with the measurement, a probable error of  $\pm 5$  per cent was assigned to the half-life value. Two subsequent determinations yielded figures that gave  $510 \pm 22$  years as the best value from all determinations.

The black oxide of americium was subsequently dissolved in a few microliters of 1M HCl solution, and one-fifth of this was submitted to Fred and Tomkins for spectrographic analysis by the copper spark method. The only known elements detected in the sample were La 2 per cent, Mg 0.1 per cent, and Pt 6 per cent.

Because platinum had not been found in the americium solution before the americium was transferred to the weighing boat, it was concluded that the platinum was dissolved from the boat when the oxide was dissolved.

The spectrographic plate obtained in the analysis showed, in addition to the lines of the elements listed, 51 lines that could not be attributed to any known element. The wavelengths of these lines were measured to the nearest 0.01 Å by Fred and Tomkins. In the region 2700 to 4000 Å the strongest line was found at 2920.61 Å. The wavelengths of a few other strong lines that were found in this region are 3926.27, 3161.98, 2966.71, and 2756.55 Å.

Since platinum had not been found in the americium solution before the solution was transferred to the weighing boat, it was concluded that when the oxide was dissolved, oxidation and solution of the platinum occurred. This was considered further evidence that at least part of the americium in the black oxide was in an oxidation state higher than +3.

It was subsequently shown by W. H. Zachariasen<sup>7</sup> that the black oxide of americium possessed the fluorite structure and was isomorphous with the dioxides of plutonium and neptunium.

The americium that remained after the spectrographic analysis was purified by precipitating the platinum in it with hydrogen sulfide, centrifuging, and separating the supernatant solution. The hydroxide of americium was precipitated with ammonia and examined carefully. This compound was found to be of the same delicate pink color as the fluoride. A photomicrograph of the precipitated hydroxide is shown in Fig. 1. Radiometric assay of the supernatant solution indicated that the solubility of the hydroxide was of the order of 1 mg per liter in dilute ammonia solution.

When the hydroxide was dissolved in a very small volume of dilute nitric acid, the nitrate solution was found to be pink also.

The solution was made 2M in nitric acid, and attempts were made to oxidize the americium to a higher oxidation state. A small amount of argentic oxide was added to the solution, and the sample was observed under the microscope. The color of the sample remained at all times that which was expected for a mixture of the pink americium(III) and brown silver(II). When after about 10 min the color of the argentic ion had faded there appeared to have been no change in the color of the americium.

Because oxidation of americium(III) to americium(IV) by silver(II) requires only simple electron transfer, the reaction would be expected to be rapid. It was concluded that the formal oxidation-reduction potential for the couple  $\text{Am(III)} = \text{Am(IV)} + e$  in acid solution was more negative than about -2 volts.

The experiment did not exclude the possibility that  $\text{Ag}^{++}$  might be capable of oxidizing americium(III) to an ion of the type  $\text{AmO}_2^+$  since this reaction might conceivably be slow.

However, on the assumption that the potential for the reaction  $\text{Am(III)} = \text{Am(IV)} + e$  was more negative than -2 volts, there still remained the possibility of bringing about the oxidation in alkaline solution. On the basis of solubility product values for  $\text{Th(OH)}_4$  and  $\text{La(OH)}_3$ , given by Latimer,<sup>8</sup> it was estimated that on changing from 1M  $\text{H}^+$  to 1M  $\text{OH}^-$  the potential for the couple would become more positive by

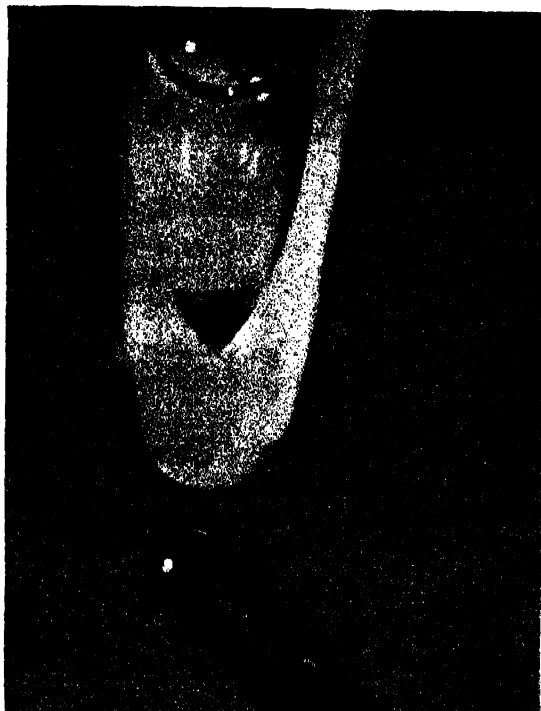


Fig. 1—Photograph of first americium compound, which was isolated January 1946. The eye of the needle shows the degree of magnification.

more than 1 volt. The potential for the couple involving the formation of  $\text{AmO}_2^+$  would also be expected to have a strong hydrogen-ion-concentration dependence and to become much more positive in alkaline solution.

Two oxidizing agents,  $\text{ClO}_4^-$  and  $\text{HO}_2^-$ , were used in attempts to obtain evidence for the oxidation of americium(III) in alkaline solution.

When americium(III) was precipitated as the hydroxide in alkaline solution in the presence of peroxide, the precipitate was colored a bright red-brown. This color faded when the excess peroxide in the solution had decomposed.

When americium(III) was precipitated as the hydroxide by excess base containing  $\text{ClO}_4^-$ , the color of the precipitate was initially light salmon-pink, but changed within 30 min to deep brown.

These experiments were interpreted as evidence for oxidation of americium(III) in alkaline solution, but the evidence was not conclusive. A possible explanation involving the assumption of formation of strongly colored peroxy complexes of americium(III) could not be excluded. (These complexes were produced directly in one case and as a consequence of the  $\alpha$ -particle decomposition of the solution in the other.) Definite evidence for the oxidation of americium(III) to a higher oxidation state by  $\text{ClO}_4^-$  in strong carbonate solution was obtained at a later date by L. B. Werner.<sup>9</sup>

The experiments on the oxidation of americium were followed by experiments in which evidence for a lower-oxidation state was sought. These investigations were carried out by L. B. Asprey, who used a Heyrovsky-type polarograph and special microcells. The apparatus was found to give excellent results on microgram amounts of europium, and well-defined waves showing the reduction of europium(III) to europium(II) were obtained. Americium solutions, however, failed to show any evidence for reduction of the tripositive state at potentials less positive than +0.9 volt (Lewis and Randall convention), the limiting potential imposed by the reduction of the  $\text{H}^+$  in these solutions.

The first conclusive evidence for the existence of americium in an oxidation state lower than +3 was obtained by Sherman Fried<sup>10</sup> at Chicago during an attempt to reduce the higher oxide of americium to the sesquioxide, using hydrogen. The compound  $\text{Am}_2\text{O}_3$ , identified from its x-ray diffraction pattern by W. H. Zachariasen, was obtained.

The polarographic runs on americium were followed by a determination of the absorption spectrum of americium(III) using the Beckman model DU spectrophotometer and special microcells. The spectrum was found to consist of a single sharp absorption band at 5020 Å, a series of incompletely resolved bands in the region 7800 to 8400 Å, and slight absorption with some evidence of structure, which increased generally with decreasing wavelength in the region 3500 to 4500 Å. The spectrum exhibited markedly fewer absorption bands in the region that was examined than did plutonium(III). The striking fact about this is that precisely the same situation is true for the absorption spectrum of europium(III), the rare-earth analogue of americium(III) on the basis of Seaborg's actinide hypothesis, as compared to samarium(III), the rare-earth analogue of plutonium(III). The available data on the absorption spectra of the aqueous tripositive ions of the lanthanides were then examined for further analogies. These data permitted comparison only in the region 3500 to 7000 Å, but within

this region they indicated that the correspondence between analogous members of the two series held true not only with respect to the relative number of bands but also roughly for the distribution of the bands, in the sense that where uranium(III) showed general absorption over the 3500 to 7000 Å region, neodymium(III) also showed general absorption, and where europium(III) showed no absorption in the region 5700 to 7000 Å, americium(III) also showed no absorption. It did appear to be true, however, that the general tendency for all ions to show absorption in the region of shorter wavelengths began at around 2500 Å for the lanthanide elements but at about 3500 Å for the actinide elements, so that certain absorption bands, at least, were shifted to the longer wavelengths in the actinide element. On the basis of these analogies it was predicted that curium(III) would show little or no absorption in the visible region, that absorption would be confined to the shorter wavelengths, and that solutions of curium(III) would be either colorless or faintly yellow. These predictions were confirmed recently by Werner and Perlman,<sup>9</sup> who determined the absorption spectrum of curium(III).

A more detailed comparison of the absorption spectra of the lanthanide and actinide elements is now being made, using solid compounds and instruments designed to give better resolution of the spectra.

#### SUMMARY

The first isolation of americium in the form of pure compounds has been described. Evidence has been presented to show that in the black oxide americium exists at least partially in an oxidation state higher than +3. The black oxide is obtained by igniting americium nitrate in air. Experiments have been described which indicate that the formal oxidation-reduction potential in acid solution for the couple



is more negative than approximately -2 volts, and that the potential in acid solution for the couple



is more positive than approximately +0.9 volt.

The relation of the absorption spectrum of americium(III) to that of europium(III), its rare-earth analogue on the basis of the actinide hypothesis, is indicated.

The determination of the half life of Am<sup>241</sup> from specific-activity measurements is described in outline, and the most probable value from these measurements is given as 510 ± 22 years.

## REFERENCES

1. G. T. Seaborg, R. A. James, and L. O. Morgan, The new element americium (atomic number 95), Paper 22.1, this volume.
2. S. G. Thompson, L. O. Morgan, R. A. James, and I. Perlman, The tracer chemistry of americium and curium in aqueous solutions, Paper 19.1, this volume.
3. B. B. Cunningham and L. B. Werner, The first isolation of a synthetic element:  $_{94}\text{Pu}^{239}$ , Paper 1.8, this volume.
4. L. B. Magnusson and T. J. LaChapelle, The first isolation of element 93 in pure compounds and a determination of the half life of  $_{93}\text{Np}^{237}$ , Paper 1.7, this volume.
5. G. T. Seaborg, Chem. Eng. News, 24: 1193 (1946).
6. P. L. Kirk, R. Craig, J. E. Gullberg, and R. Q. Boyer, Anal. Chem., 19: 427 (1947).
7. W. H. Zachariasen, Metallurgical Laboratory Memorandum MUC-FWHZ-158 (Nov. 3, 1945).
8. W. M. Latimer, "The Oxidation States of the Elements and their Potentials in Aqueous Solution," Prentice-Hall, Inc., New York, 1938.
9. L. B. Werner and I. Perlman, The preparation and isolation of curium, Paper 22.5, this volume.
10. Sherman Fried, private communication (1946).

## Paper 19.3

# TRACER CHEMISTRY OF ACTINIUM<sup>†</sup>

By C. K. McLane and S. Peterson

### 1. INTRODUCTION

Different problems in the chemistry of tracer concentrations of actinium have been investigated for different purposes. Some phases of the work were concerned with possible separations from lanthanum, others with separations from other elements in the radioactive-decay series. Some work was aimed at a better understanding of the tri-positive state of the heavy elements, in particular americium and curium, while other work was undertaken primarily to increase our fundamental knowledge of radiochemistry.

### 2. CARRYING OF ACTINIUM ON ZIRCONIUM IODATE

The effect of several variables on the carrying of actinium by zirconium iodate has been studied. To avoid the possibility of lanthanum iodate precipitation, carrier-free Ac<sup>228</sup> was used.<sup>1</sup> In all experiments the iodate was added last either as 0.35M KIO<sub>3</sub> or as solid KIO<sub>3</sub>. The precipitation was made in 3.5 to 5.0 ml volume at room temperature, and the precipitate collected after brief digestion. Beta activity was counted both in the lanthanum fluoride precipitated from the supernatant solution and in either the iodate precipitate or lanthanum fluoride precipitated from a hydrofluoric acid solution of the iodate.

Figure 1 shows the very great effect of iodate concentration on carrying. Some effect is seen to remain even if the carrying is repressed by 7M NH<sub>4</sub>NO<sub>3</sub>. It may be noted that zirconium failed to precipitate from the 7M NH<sub>4</sub>NO<sub>3</sub> solution when only 0.02M IO<sub>3</sub><sup>-</sup> was used.

<sup>†</sup>Contribution from the Chemistry Division of the Metallurgical Laboratory, University of Chicago, now the Argonne National Laboratory.

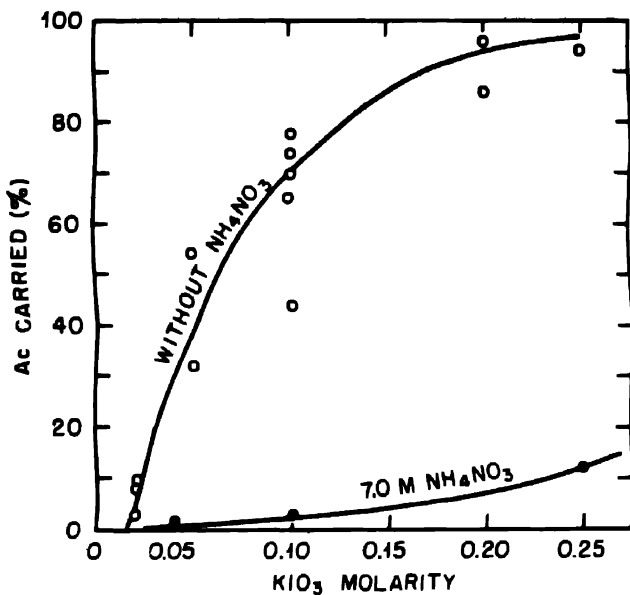


Fig. 1—Effect of  $\text{IO}_3^-$  concentration on carrying of actinium by 0.1 g of Zr per liter from 0.2M  $\text{HNO}_3$ .

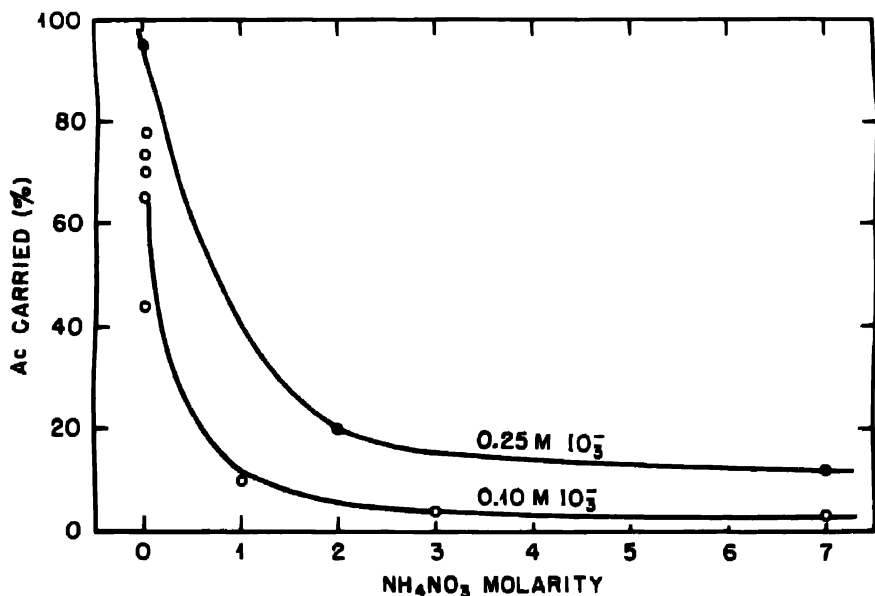


Fig. 2—Effect of ammonium nitrate concentration on carrying of actinium by 0.1 g of Zr per liter from 0.2M  $\text{HNO}_3$ .

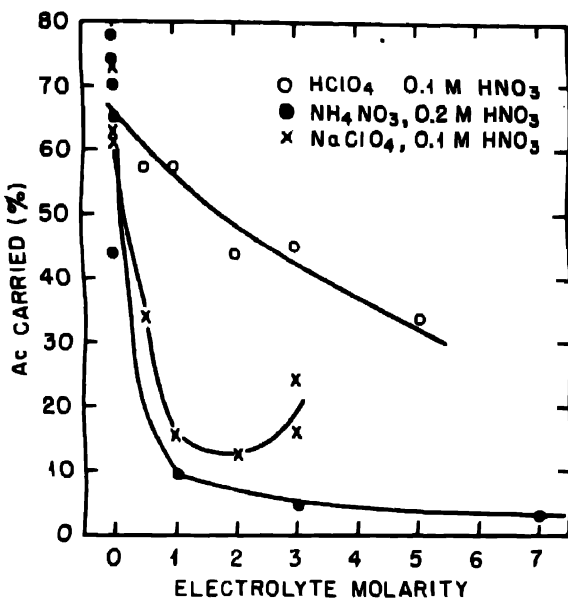


Fig. 3—Effect of electrolyte concentration on carrying of actinium by 0.1 g of Zr per liter from 0.10M  $\text{IO}_4^-$ .

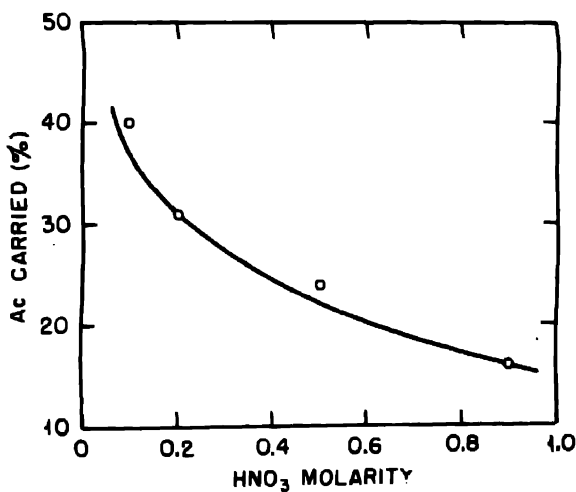


Fig. 4—Effect of nitric acid concentration on the carrying of actinium by 0.1 g of Zr per liter from 0.05M  $\text{IO}_4^-$ .

That the presence of ammonium nitrate greatly decreases the carrying of actinium on zirconium iodate is demonstrated by Fig. 2. Since neutral salts considerably increase the solubility of lanthanum iodate,<sup>2</sup> the effect was believed to be one of ionic strength, and other salts were tested. In Fig. 3 ammonium nitrate is compared with sodium perchlorate, which not only has a smaller effect but appears to have a minimum effect at 2M concentration. In Table 1 several electrolytes are compared.

Table 1 -- Effect of Electrolytes on Carrying of Actinium by Zirconium Iodate  
(0.1 g of Zr per liter, 0.10M  $\text{IO}_3^-$ )

Electrolyte present	Actinium carried, %	
	From 1M electrolyte	From 3M electrolyte
$\text{HNO}_3$	34.5	10.5
$\text{HClO}_4$	57.5	45
$\text{NaNO}_3$	17.5	
$\text{NaClO}_4$	15	16.24
$\text{NH}_4\text{NO}_3$	9	4.5
$\text{NH}_4\text{ClO}_4$	15	

Both Table 1 and Fig. 3 show that perchloric acid decreases carrying much less than do other electrolytes. Apparently  $\text{H}^+$  has less effect than other ions. Since iodic acid is a strong acid,  $\text{H}^+$  would not be expected to have the same effect as in carrying by a phosphate or oxalate. The effect of varying the concentration of nitric acid while keeping other concentrations constant is shown in Fig. 4.

### 3. CARRYING OF ACTINIUM BY BISMUTH PHOSPHATE

The influence of several variables on the carrying of actinium by bismuth phosphate has been studied. Carrier-free  $\text{Ac}^{228}$  was used.<sup>1</sup> In all experiments the bismuth was precipitated by adding phosphoric acid over a 20-min period. During both the precipitation and the subsequent 1-hr digestion the solutions were kept in a 75 to 80°C water bath. Beta activity was counted in lanthanum fluoride precipitated from the supernatant liquid as well as either in the bismuth phosphate precipitate or in lanthanum fluoride precipitated from a hydrochloric acid solution of the bismuth phosphate.

As predicted from the effect of acid on phosphate solubilities, the carrying is very sensitive to nitric acid concentration; this is seen in Fig. 5. Although the  $\text{Bi(III)}$  concentration was shown to have no great

Table 2—Carrying of Actinium by 1.0 g of Bi per Liter from 0.5M  $H_3PO_4$ , 0.1M  $HNO_3$ , and 1.5M Salt

Salt studied	Actinium carried, %
$NaClO_4$	95
$NH_4ClO_4$	94
$NaNO_3$	68
$NH_4NO_3$	35
$NH_4NO_2$	52

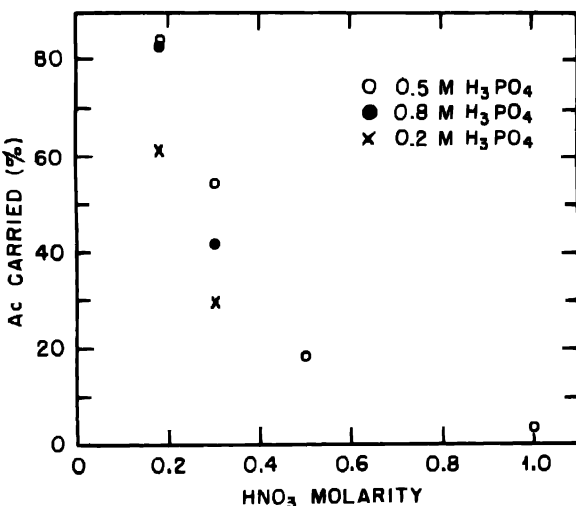


Fig. 5—Effect of nitric acid and phosphoric acid concentrations on the carrying of actinium by 2.0 g of Bi per liter (phosphate).

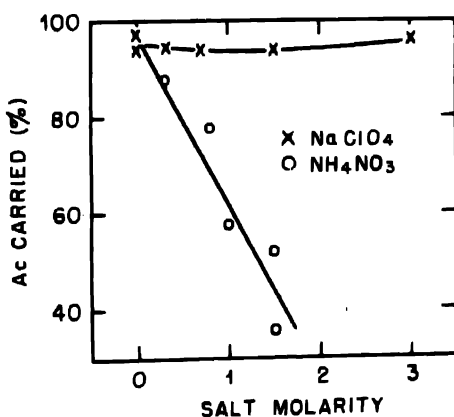


Fig. 6—Effect of salt concentration on the carrying of actinium by 1.0 g of Bi per liter from 0.1M  $HNO_3$  and 0.5M  $H_3PO_4$ .

effect on the carrying, a peculiar effect was observed with variation of the phosphoric acid concentration. Figure 5 shows that at two different acidities the actinium is carried to a greater extent from 0.5M  $H_3PO_4$  than from 0.2M or 0.8M.

The study of salt effect (Fig. 6) shows that sodium perchlorate exerts very little effect on the carrying of actinium by bismuth phosphate, but the effect of ammonium nitrate, although less than that of nitric acid, is pronounced. Comparing the effects of several salts (Table 2) demonstrates a specific effect due to  $NO_3^-$ . It is therefore probable that perchloric acid would have a smaller effect than nitric acid.

#### 4. FRACTIONATION OF ACTINIUM IN LANTHANUM OXALATE AND IN LANTHANUM PHOSPHATE

The distribution of actinium tracer between precipitate and solution in the partial precipitation of lanthanum oxalate and lanthanum phosphate illustrates the smaller affinity of actinium compared with lanthanum toward basic anions.

Table 3—Distribution of Actinium in Partial Precipitation of Lanthanum Phosphate

Approximate $NH_4^+$ concentration, molarity	Activity found, %			
	Actinium		Lanthanum	
	Precipitate	Supernatant	Precipitate	Supernatant
0.12	42	36	90	11
0.25	80	22	94	4
0.37	81	9	98	2

Lanthanum tracer used in the experiments was separated from  $Ba^{140}$  parent by triple hydroxide precipitation. Actinium tracer<sup>3</sup> was  $Ac^{228}$ . In experiments using mixed activities, analysis of the decay served to measure the individual activities.

The carrying of actinium by lanthanum phosphate was investigated by precipitation of various fractions of the lanthanum from a solution containing mixed tracer, approximately 0.7 g of La per liter, and 0.8M  $H_3PO_4$ . This was accomplished by addition of ammonium hydroxide followed by 20 min heating at 75 to 80°C. The results given in Table 3 show that the lanthanum which precipitates is depleted in actinium under these conditions.

The distribution of actinium tracer between precipitate and supernatant was studied in the partial precipitation of 0.1 g of La per liter

with 50 g of  $(\text{NH}_4)_2\text{C}_2\text{O}_4$  per liter in solutions of pH about 4.5, which were heated 20 to 30 min at 75 to 80°C. The results (Table 4) show that carrying of actinium is complete even though only 70 per cent of the lanthanum precipitates. The presence of yttrium, the solubility of which is about 65 mg per liter owing to the presence of an oxalate complex under these conditions,<sup>4</sup> has no apparent effect.

Table 4—Distribution of Actinium in Partial Precipitation of Lanthanum Oxalate

Time of heating, min	Yttrium, g/liter	Activity found, %			
		Actinium		Lanthanum	
		Precipitate	Supernatant	Precipitate	Supernatant
20	0.0	84	<1	63	27
	0.0				
	0.1	87	<2	52	38
	0.1				
30	0.0	98	0	76	22
	0.1	79	0	70	30
	0.1	99	0	77	23
	0.2	99	0	77	23

By precipitating lanthanum oxalate from nitric acid solutions, Mme. Curie<sup>5</sup> was able to deplete the lanthanum in actinium, and, by fractionation, to obtain a 35-fold enrichment. A number of experiments have been carried out in the attempt to improve the fractionation by adding less than equivalent amounts of oxalic acid to a concentrated lanthanum solution in 1M HNO<sub>3</sub>. The thickness and irregularity of the samples prevented accurate measurement of the activity, but precipitation of approximately one-third of the lanthanum carried no more than one-tenth of the actinium.

##### 5. MISCELLANEOUS EXPERIMENTS ON CARRYING

Results of tests of the coprecipitation of actinium tracer<sup>1,3</sup> with several carriers are presented in the following paragraphs.

5.1 Barium Sulfate. That actinium is adsorbed on barium sulfate has long been known.<sup>6</sup> In our work 0.5 g of Ba per liter was precipitated from 0.5M HNO<sub>3</sub> by addition of one drop of concentrated sulfuric acid per milliliter. All precipitates were digested with frequent stirring for 1 hr. The data in Table 5 show that small amounts of lanthanum act to displace actinium from the barium sulfate.

5.2 Lanthanum Fluoride. Carrying of actinium by lanthanum fluoride has been studied as a method of concentrating actinium activity

into a sufficiently small bulk for counting radiations. Under almost all conditions, greater than 98 per cent of the actinium precipitates with 0.3 g of La per liter from 5M HNO<sub>3</sub> solutions when the solutions are made 3M in HF. Substances not interfering were 0.4M H<sub>2</sub>C<sub>2</sub>O<sub>4</sub>, 0.2M citric acid, 1M H<sub>3</sub>PO<sub>4</sub>, and 1 g of Zr per liter. However, from a 2M HNO<sub>3</sub>-5M NH<sub>4</sub>NO<sub>3</sub> solution only 87 per cent was carried.

Fluosilicic acid has been found to interfere with carrying of transplutonium activities by rare-earth fluorides,<sup>7</sup> and a similar, though less pronounced, effect is found with actinium. From solutions from which 90 per cent of the La should precipitate, only 50 to 75 per cent of the Ac precipitates.

Table 5—Adsorption of Actinium on Barium Sulfate

Approximate La concentration, g/liter	Temperature, °C	Precipitate	Activity found, %
0	85	96	4
0	85	95	5
0.3	25	30	69
0.3	80	35	63

**5.3 Rare-earth Hydroxides.** Precipitation of 1 g of La per liter with 4M NH<sub>4</sub>OH was found to carry actinium tracer quantitatively from both aqueous and 70 per cent ethanol solutions.

With 12M NH<sub>4</sub>OH, in seven experiments, cerium (0.5 to 2.0 g per liter) carried only 96 per cent of actinium tracer from 0.00M to 1.7M NH<sub>4</sub>NO<sub>3</sub>. From 0.86M NH<sub>4</sub>NO<sub>3</sub>, 0.5 g of Ce per liter carried 88 per cent when precipitated with 5M NH<sub>4</sub>OH.

**5.4 Lead Sulfate.** Over 98 per cent of Ac tracer (carrier-free) precipitated with 1 g of Pb per liter from 6M H<sub>2</sub>SO<sub>4</sub>. The presence of 1M NH<sub>4</sub>NO<sub>3</sub> did not change the result.

**5.5 Uranyl Peroxide.** In a study of the actinium-thorium-uranium separations, it was noted that uranyl peroxide (20 g of U per liter) when precipitated from 0.33M HNO<sub>3</sub> and 10 per cent H<sub>2</sub>O<sub>2</sub> carried no more than 2 per cent of the actinium. To avoid interference from β-emitting decay products of uranium, Ac<sup>225</sup> α tracer (obtained from U<sup>233</sup> decay products) was used. The uranium precipitate was dissolved in a nitric acid-sulfuric acid solution from which lanthanum fluoride was precipitated. The fluoride precipitate contained α activity corresponding to 2.5 per cent of the actinium or 0.05 per cent of the uranium. Failure of the samples to decay showed uranium to be the principal component.

**5.6 Zirconium Phosphate.** Precipitation of 0.25 g of Zr per liter from 1M HNO<sub>3</sub> made 0.12M in H<sub>3</sub>PO<sub>4</sub> carried only 1 per cent of the  $\beta$  activity from a crude mesothorium mixture. Less than 1.2 per cent of the Ac<sup>228</sup> present must have precipitated to give this result.

## 6. THE ACTINIUM BENZHYDROXAMATE COMPLEX†

Benzhydroxamate ion has been studied as a possible method of separation of element 95 from rare earths. In this work actinium is compared with element 95.

Table 6—Results of Benzhydroxamate Experiments

Experiment	Element	Activity, counts/min		Distribution coefficient, organic/aqueous	Amount extracted by CHCl <sub>3</sub> , %
		In H <sub>2</sub> O phase	In CHCl <sub>3</sub> , phase		
1	Ac	14,590	8,530	0.585	37
	95	790	22,480	28.5	97
2	Ac	4,200	310†	0.07†	7†
	La	13,070	6,850	0.53	34
	95	6,510	10,980	1.69	63

†Counting error may easily make these values in error by 40 per cent.

The slowness and uncertainty in the formation of the complex makes necessary the comparison of different elements by using a mixture of tracers in one experiment. Tracer  $\alpha$ -emitting 95<sup>241</sup> was mixed with Ac<sup>228</sup>  $\beta$  tracer.<sup>3</sup> In the second experiment La<sup>140</sup>, separated from the barium parent by triple hydroxide precipitation, was also present. To the tracer mixture was added 2.5 ml of potassium benzhydroxamate solution (20 g per liter). With sodium acetate and water the solution was adjusted to a pH of 5.0 and a volume of 5.0 ml. Approximately 2 hr was allowed for the complex to form; then the solution was shaken with 5.0 ml of CHCl<sub>3</sub>. Lanthanum fluoride was precipitated from 0.50-ml samples of each phase and transferred to platinum disks for activity measurement. Alpha counting was used to measure element 95,  $\beta$  counting to measure the actinium. In the second experiment analysis of the  $\beta$  decay gave assays for both lanthanum and actinium.

The results of the experiments are given in Table 6. Element 95 is much more easily complexed than actinium; lanthanum behavior is

†This work was done with the cooperation of S. G. Thompson.

intermediate. This parallels the relative affinities of these cations for other basic anions.

### 7. SUMMARY

Carrying of actinium by zirconium iodate is sensitive to the iodate concentration, varying from less than 10 per cent to over 90 per cent with other conditions unchanged. Neutral salts decrease the carrying; acid exerts a similar but smaller effect. Although nitrate ion also decreases carrying, perchlorate does not.

Lanthanum can be depleted in actinium by phosphate precipitation. Lanthanum oxalate precipitated from strong acid is depleted in actinium; when precipitated from a concentrated ammonium oxalate solution, lanthanum is enriched in actinium. Actinium is almost completely carried by barium sulfate; lanthanum interferes. Lanthanum fluoride can be precipitated from most solutions; it carries actinium quantitatively; fluosilicic acid and 5M  $\text{NH}_4\text{NO}_3$  interfere. Lanthanum hydroxide, cerous hydroxide, and lead sulfate carry actinium nearly completely; uranyl peroxide and zirconium phosphate do not carry actinium.

### REFERENCES

1. S. Peterson, Preparation of carrier-free  $\text{Ac}^{228}$  ( $\text{MsTh}_2$ ) tracer, Paper 19.8, this volume (Argonne National Laboratory Report ANL-4041).
2. A. Seidell, "Solubilities," Vol. I, pp. 890-891, D. Van Nostrand Company, Inc., New York, 1940.
3. C. K. McLane and S. Peterson, Preparation of radioactively pure  $\text{Ac}^{228}$  ( $\text{MsTh}_2$ ), Paper 19.7, this volume (Argonne National Laboratory Report ANL-4040).
4. L. O. Morgan, private communication.
5. M. Curie, J. chim. phys. 27: 1-8 (1930).
6. L. Imre, Z. physik. Chem., A153: 262-286 (1931); Z. Elektrochem., 38: 535-543 (1932).
7. S. G. Thompson, L. O. Morgan, R. A. James, and I. Perlman, The tracer chemistry of americium and curium in aqueous solutions, Paper 19.1, this volume.

## Paper 19.4

### THERMAL NEUTRON FISSION PROPERTIES OF Ac<sup>227</sup>, Ra<sup>223</sup>, AND Ra<sup>228</sup> †

By S. Peterson and A. Ghiorso

A preliminary study has been made of the thermal neutron fission properties of several naturally occurring radioactive isotopes. These include the 13.5-year  $\beta$ -emitting Ac<sup>227</sup>; the 11.2-day  $\alpha$ -emitting Ra<sup>223</sup> (actinium X), and the 6.7-year  $\beta$ -emitting Ra<sup>228</sup> (MsTh<sub>1</sub>). The Ra<sup>228</sup> sample was obtained from commercial sources, and it was further purified to separate it from uranium and daughter activities. The other isotopes were obtained from a sample of several milligrams of protactinium that had decayed for a period of nearly 10 years without separation from daughter activities. The exact procedures employed in the separation and purification of Ac<sup>227</sup> and its daughters have been described by McLane and Peterson.<sup>1</sup> Briefly, the Ac<sup>227</sup> was separated from Th<sup>227</sup> by extraction into a benzene solution of  $\alpha$ -thenoyl-trifluoroacetone under controlled pH conditions, and it was separated from Ra<sup>223</sup> by coprecipitation with cerous hydroxide. The Th<sup>227</sup> was separated by coprecipitation with zirconium iodate, then concentrated on cerous fluoride, and finally purified by extraction into a solution of  $\alpha$ -thenoyl-trifluoroacetone in benzene. The Ra<sup>223</sup> was concentrated from hydroxide and fluoride solutions on lead sulfate, dissolved in hydrochloric acid, and separated from lead with hydrogen sulfide. It was separated from Ac<sup>227</sup> and Th<sup>227</sup> by cerous hydroxide precipitation. All samples were evaporated on 2-mil platinum foil for fission measurements.

Fission measurements were made in the thermal column of the Argonne heavy-water pile with the high-sensitivity fission-counting apparatus described by Ghiorso and Bentley.<sup>2</sup> The fission rate of

†Contribution from the Chemistry Division of the Metallurgical Laboratory, University of Chicago, now the Argonne National Laboratory.

each sample was compared to that of a standard thin sample of  $\text{Pu}^{239}$  measured under identical neutron-flux conditions. The thermal nature of the neutrons was confirmed by repeating measurements with the fission chamber enclosed in a cadmium shell of small thickness. Under these conditions fission rates were reduced by a factor of 100 or more.

A single sample containing approximately  $10^{-8}$  g of  $\text{Ac}^{227}$  was tested for fissionability 9 and 19 days after separation from  $\text{Th}^{232}$ . Thermal neutron cross sections were calculated for  $\text{Ac}^{227}$ , and it seems quite certain that the thermal neutron fission cross section of  $\text{Ac}^{227}$  is less than  $2 \times 10^{-24}$  sq cm.

A sample containing approximately  $4 \times 10^{-9}$  g of  $\text{Ra}^{228}$  showed no fission counts above a background for the counting apparatus of 125 fissions per minute. Assuming that 10 fissions per minute could have been detected, an upper limit of  $2 \times 10^{-24}$  sq cm may be set for the thermal neutron fission cross section of  $\text{Ra}^{228}$ .

A sample containing approximately  $5 \times 10^{-11}$  g of  $\text{Ra}^{223}$  likewise showed in two measurements no fission counts above backgrounds of 105 and 103 fissions per minute. Again assuming that 10 fissions per minute could have been detected, an upper limit of  $100 \times 10^{-24}$  sq cm may be set for the thermal neutron fission cross section of  $\text{Ra}^{223}$ .

## SUMMARY

The following limits on thermal neutron fission cross sections have been determined:  $\text{Ac}^{227}$ , less than  $2 \times 10^{-24}$  sq cm;  $\text{Ra}^{223}$ , less than  $100 \times 10^{-24}$  sq cm;  $\text{Ra}^{228}$ , less than  $2 \times 10^{-24}$  sq cm.

## ACKNOWLEDGMENTS

The authors are pleased to acknowledge the cooperation of Dr. W. H. Zinn, who made available the facilities of the Argonne heavy-water pile. They also wish to acknowledge their indebtedness to Drs. G. T. Seaborg and W. M. Manning, under whose general direction the experiments were performed.

## REFERENCES

1. C. K. McLane and S. Peterson, Preparation of radioactively pure  $\text{Ac}^{228}$  ( $\text{MsTh}_2$ ), Paper 19.7, this volume (Argonne National Laboratory Report ANL-4040).
2. A. Ghiorso and W. C. Bentley, High-sensitivity apparatus for fission counting, Paper 22.29, this volume (Argonne National Laboratory Report ANL-4048).

## Paper 19.5

### THERMAL NEUTRON FISSION PROPERTIES OF Ra<sup>226</sup>†

By D. Ames and A. Ghiorso

An upper limit for fissionability with thermal (i.e., cadmium-absorbable) neutrons has been set for the 1,600-year Ra<sup>226</sup> (natural radium). An early measurement using 50 µg of radium in the fission-counting chamber had indicated a limit of 0.003 barn. More recent samples of repurified material show that this limit can be lowered to 10<sup>-4</sup> barn.

The radium used in the early measurement was not purified but was taken directly from a source of radium chloride. Spectrographic analysis showed 0.4 per cent Ba, 0.2 per cent Ca, 0.04 per cent Mg, and 0.02 per cent Si.

The second set of samples was prepared from 20 mg of radium chloride that had been carried through 10 crystallization cycles. One cycle consisted of precipitating the chloride from distilled (20 per cent) hydrochloric acid in an ice bath, digesting for approximately ½ hour, centrifuging, and redissolving in 100 to 200 microliters of Barnstead distilled water. Spectrographic analysis showed no significant impurities.

The sample plates were prepared by adding the chloride to the plate and spreading by dilution so that the solution almost covered the plate. A few drops of approximately 1M H<sub>2</sub>SO<sub>4</sub> were added so that the sulfate was spread evenly on the plates.

Two samples, each weighing 100 µg, were carefully evaporated on platinum plates in the manner described and tested for fission in the thermal column of the Argonne heavy-water pile. One had a fission counting rate of 43 fissions per minute and the other a rate of 18 fis-

†Contribution from the Chemistry Division of the Metallurgical Laboratory, University of Chicago, now the Argonne National Laboratory.

sions per minute over a background of 100 fissions per minute. Comparison with fission standards showed these rates to correspond to cross sections of  $2.6 \times 10^{-4}$  barn and  $1.1 \times 10^{-4}$  barn, respectively. Taking the lowest value we can then say that the thermal neutron fission cross section of Ra<sup>228</sup> is no more than  $1.1 \times 10^{-4}$  barn. The value is only an upper limit, since a fission rate of 18 per minute, if significant at all over a background of 100 per minute, might be due to undetected traces of plutonium or uranium.

Summary. An upper limit for the thermal neutron fission cross section of Ra<sup>228</sup> has been established as  $1.1 \times 10^{-4}$  barn.

## Paper 19.6

### SEPARATION OF ACTINIUM FROM RARE EARTHS USING ION-EXCHANGE RESIN†

By C. K. McLane and S. Peterson

#### 1. INTRODUCTION

Isolation of actinium ( $\text{Ac}^{227}$ ) from natural radioactive ores involves a separation from far larger quantities of the chemically very similar rare earths. Since the use of Amberlite IR-1 cation-exchange resin has been found successful for the separation of rare earths from each other,<sup>1</sup> it was thought that the method might be applicable to the separation of actinium from the rare earths. Lanthanum is the rare earth most closely resembling actinium. Other rare earths need not be studied, since it is known that they can be readily separated from lanthanum.

#### 2. EXPERIMENTAL PROCEDURE

A column was constructed of a 35-cm length of 7-mm I.D. pyrex tubing fitted at the bottom with a capillary stopcock and sealed at the top to a short length of 18-mm tubing. A wad of glass wool kept particles of resin from entering the stopcock. Solutions were added to the column through separatory funnels fitted to the column with rubber stoppers.

The resin used was 20- to 65-mesh Amberlite IR-1, washed with dilute hydrochloric acid to remove metal cations and with distilled water to remove the finer particles of resin. The column was filled by pouring the resin in as an aqueous slurry. It was pretreated by washing with several volumes of the same solution subsequently used for elution.

† Contribution from the Chemistry Division of the Metallurgical Laboratory, University of Chicago, now the Argonne National Laboratory.

Tracer Ac<sup>228</sup> (MsTh<sub>2</sub>) was prepared by the Haissinsky-McLane method.<sup>2</sup> La<sup>140</sup> was isolated from a solution of its barium parent by adding stable lanthanum carrier and introducing ammonia gas to precipitate the hydroxide. The tracer was purified by two reprecipitations. The tracer activity in the column effluent samples was determined by adding 2 mg of inactive lanthanum, acidifying to 1M to 2M in nitric acid and 2M to 3M in hydrofluoric acid, and measuring the  $\beta$  activity

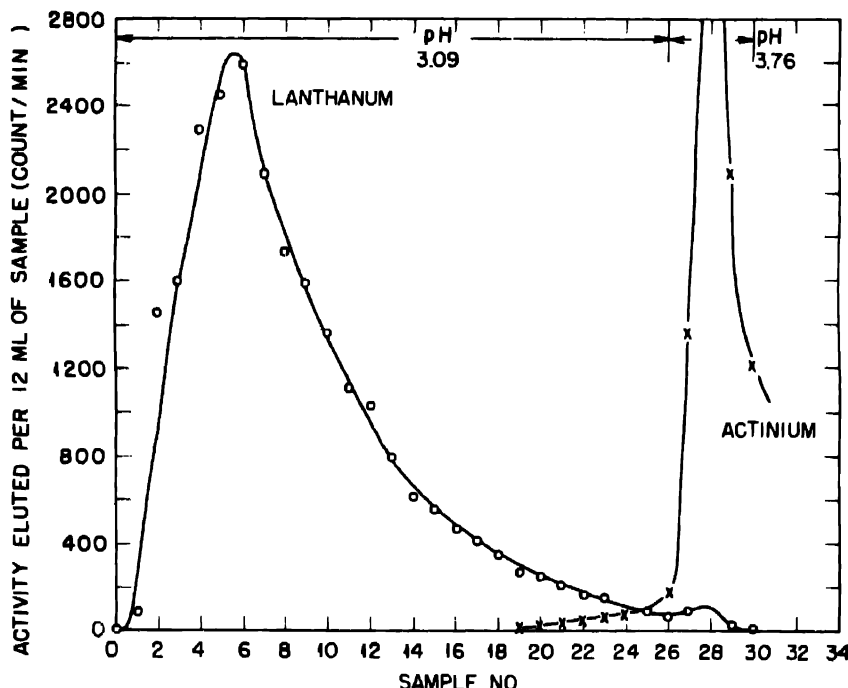


Fig. 1.—Separation of lanthanum and actinium by elution from Amberlite IR-1 with 0.25M citrate solution.

in the precipitated lanthanum fluoride. Actinium is carried quantitatively by lanthanum fluoride precipitated from the citrate solutions used in the columns.<sup>3</sup> The citrate solutions were prepared by mixing proper proportions of reagent-grade citric acid and diammonium citrate and dissolving in sufficient distilled water to make the total citrate 0.25M.

Separation of mixed Ac<sup>228</sup> and La<sup>140</sup> tracers was demonstrated by eluting the 35-cm pretreated column with a 0.25M citrate solution containing 2.4 parts of citric acid to 1 part of diammonium salt (at pH 3.09 as determined by a Coleman glass-electrode apparatus). The

radioactive isotopes with approximately 2 mg of inactive lanthanum carrier were dissolved in 6.6 ml of the citrate-elution solution, added to the column, and immediately eluted at a flow rate of about 1.5 ml per minute. The first 5 ml of effluent was discarded; then twenty-six 12-ml samples were taken. Four additional samples were taken after changing the eluting solution to 0.5M monoammonium citrate (pH 3.76).

The eluted activity was identified by counting at intervals and comparing the decay with that expected for the 40.0-hr half life of pure La<sup>140</sup> and the 6.13-hr decay of Ac<sup>228</sup>. Figure 1 shows the separation that was achieved with the 35-cm column. The slight overlapping of the two peaks indicates that a somewhat longer resin bed would be necessary for complete separation.

### 3. SUMMARY

Almost complete separation of tracer quantities of actinium and lanthanum has been obtained by elution of the adsorbed mixture from Amberlite IR-1 cation-exchange resin with 0.25M citrate solution of pH near 3.

### REFERENCES

1. F. H. Spedding, N. R. Sleight, E. M. Gladrow, and A. F. Volgt, Metallurgical Project Report CC-2720 (May 9, 1945); J. A. Marinsky and L. E. Glendenin, Metallurgical Project Report CC-2829 (June 1, 1945).
2. C. K. McLane and S. Peterson, Preparation of radioactively pure Ac<sup>228</sup> (MsTh<sub>4</sub>), Paper 19.7, this volume.
3. C. K. McLane and S. Peterson, Tracer chemistry of actinium, Paper 19.3, this volume.

## Paper 19.7

### PREPARATION OF RADIOACTIVELY PURE Ac<sup>228</sup>(MsTh<sub>2</sub>)†

By C. K. McLane and S. Peterson

#### 1. INTRODUCTION

For study of the tracer chemistry of actinium, Ac<sup>228</sup>(MsTh<sub>2</sub>) is usually the best isotope to use. The long-lived Ac<sup>227</sup> is not only difficult to get in sufficient quantities, but can be measured with satisfactory accuracy only by following the slow and complicated growth of its daughters. The artificially produced Ac<sup>225</sup> cannot be obtained in quantities sufficient for any extensive work.

Since the immediate decay product of Ac<sup>228</sup>, 1.9-year Th<sup>228</sup>(RdTh), has a relatively long half life, samples of Ac<sup>228</sup> tracer can be corrected for decay by the simple exponential law. The half life of Ac<sup>228</sup>, 6.13 hr, is long enough to be satisfactory for experiments requiring less than 1 day. The activity can be obtained by separation from its parent, 6.7-year Ra<sup>228</sup>(MsTh<sub>1</sub>), immediately before use. For preparation of radioactively pure tracer, separation must also be made from the daughters, Th<sup>228</sup>, Ra<sup>224</sup>(ThX), Pb<sup>212</sup>(ThB), and Bi<sup>212</sup>(ThC). The method described here is a modification of that used by Haissinsky.<sup>1</sup>

#### 2. CHEMICAL PROCEDURE

The chemistry involved in the process is identical with that used by Haissinsky except for the addition of lead and thorium ions to the starting solution. However, by substitution of centrifugation for the filtration used in the original method, the operations can be carried out more quickly and with the use of less inactive carrier for the tracer quantities of the radioactive isotopes. Except for the final

†Contribution from the Chemistry Division of the Metallurgical Laboratory, University of Chicago, now the Argonne National Laboratory.

evaporation and ignition, all operations can be speedily and efficiently carried out in 15-ml centrifuge cones.

Haissinsky added the thorium as the dry nitrate after alcohol extraction. This requires frequent purification of the thorium stock solution to prevent reappearance of Ra<sup>228</sup> (daughter of Th<sup>232</sup>) in the tracer after the extraction. Thorium nitrate dissolves satisfactorily in alcohol without interfering with the lanthanum-actinium extraction, so that old Th(NO<sub>3</sub>)<sub>4</sub> may be used in the modified method.

The separation of actinium from radium isotopes is carried out by evaporating to dryness a mixed nitrate solution containing Ra<sup>228</sup> and its decay products and 1 mg each of Ba(II), Pb(II), Th(IV), and La(III). (The 0.2- to 0.4-ml solution can be evaporated quickly in a 100°C oil bath in a current of air.) The dry nitrate mixture is extracted three times by stirring for several seconds with 1-ml portions of alcohol (isopropyl or absolute ethyl). The radium isotope remains in the lead-barium residue, which may be dissolved in 1N HNO<sub>3</sub> and reused by addition of more lanthanum and thorium after sufficient Ac<sup>228</sup> has grown in. Separation from Th<sup>228</sup> is achieved by adding 2 ml of pyridine to the 3-ml alcohol solution and digesting for 10 min in a hot-water bath (approximately 70°C). The thorium slowly precipitates as a pyridine-complex salt. The separation from lead and bismuth activity is brought about by addition of 1 mg each of Pb(II) and Bi(III) (1 to 2 drops each of nitrate solution in dilute nitric acid) to the alcohol-pyridine solution, and saturation with hydrogen sulfide. The lead sulfide-bismuth sulfide precipitate is discarded. The acid from the reagents is sufficient to prevent precipitation of lanthanum hydroxide. Separation from excess reagents may be accomplished by evaporating the hydrogen sulfide solution to dryness, igniting to remove organic matter, and dissolving the tracer (in lanthanum oxide carrier) in any desired acid solution.

Tracer of 99.95 per cent purity was prepared by the above method. Decay of one sample was followed for 3 days (almost 12 half lives), using a Geiger counter with known increases in geometry as the activity decreased. At the end of the 3 days, 28 counts per minute remained out of the 20,000 counts per minute originally in the sample. The deviation from logarithmic decay with the accepted half life (6.13 hr) was no greater than this remainder, most of which could have been decay products of the tracer (about 10 counts per minute expected) and residual Ac<sup>228</sup> (about 6 counts per minute).

The result of this work may be considered not only the preparation of very pure actinium tracer, but also a verification of the reported<sup>2</sup> half life of the isotope.

### 3. SUMMARY

An improved and rapid method has been found to prepare Ac<sup>228</sup> of higher than 99.95 per cent radioactive purity.

### REFERENCES

1. M. Haissinsky, Compt. rend., 196: 1778-1779 (1933).
2. O. Hahn and O. Erbacher, Physik. Z., 27: 531 (1926).

Paper 19.8

PREPARATION OF CARRIER-FREE Ac<sup>228</sup>(MsTh<sub>2</sub>) TRACER†

By S. Peterson

For experiments in which lanthanum might interfere, it was necessary to prepare "carrier-free" Ac<sup>228</sup>. If lanthanum carrier is omitted from the modified Haissinsky separation,<sup>1</sup> the actinium isotope is not extracted by alcohol. Lanthanum, however, may be satisfactorily replaced by cerium, the higher oxidation state affording ready means of removal.

Method of Tracer Preparation. Separation of actinium from radioactive parent and daughters is achieved by following the procedure of McLane<sup>1</sup> except that cerium is substituted for lanthanum. Instead of lanthanum oxide the ignited final product is cerium(IV) oxide. While the crucible is still hot, the ignited CeO<sub>2</sub> is dissolved in 28 per cent H<sub>2</sub>O<sub>2</sub> which is 1N in HNO<sub>3</sub>. Ignited CeO<sub>2</sub>, which is ordinarily very difficult to dissolve, is reduced by the hydrogen peroxide to Ce(III). Without removal from the crucible, the solution is evaporated under a heat lamp to dryness to remove the excess hydrogen peroxide which otherwise would interfere with the subsequent oxidation.

The cerium(III) nitrate solution containing the tracer is dissolved in 1N HNO<sub>3</sub> and transferred in 0.5 to 1.0 ml of 1N HNO<sub>3</sub> to a centrifuge cone. A very few milligrams of solid silver oxide is added with stirring until an excess persists briefly.

To separate from cerium and silver, the oxidized solution is diluted to 5 to 7 ml with 1N HNO<sub>3</sub>. The minimum excess of 1M HIO<sub>3</sub> is added dropwise to precipitate the cerium and silver. Since the carrying by iodates of tracer actinium is very sensitive to the iodate concentration, use of excess iodic acid results in a decreased yield.

†Contribution from the Chemistry Division of the Metallurgical Laboratory, University of Chicago, now the Argonne National Laboratory.

The supernatant solution from the iodate precipitation is evaporated to dryness and ignited in a platinum crucible. (The very minute amounts of material might be strongly adsorbed by porcelain.) Volatile reagents (hydrogen peroxide, hydrochloric acid, and hydriodic acid) were tried and found unsatisfactory for removing iodic acid. However, gentle ignition easily decomposes the solid to water, iodine, and oxygen.

The tracer may be removed from the crucible by washing with dilute acid (less than 0.1N HNO<sub>3</sub> is inadequate).

Purity of Tracer. Spectrographic analysis<sup>2</sup> of one batch of approximately 10<sup>6</sup> counts per minute of tracer prepared by this process showed the principal impurities to be calcium (more than 5 µg) and aluminum (approximately 1 µg) (probably from the glassware). Rare earths, platinum, barium, thorium, lead, and bismuth were not detected. Silver was the only likely impurity not tested for.

Radioactive purity of the tracer was found satisfactory by observation of decay of numerous samples.

Summary. The McLane-Haissinsky actinium tracer preparation has been modified by substitution of cerium for lanthanum carrier. The cerium is then removed by oxidation with silver peroxide and precipitation with iodic acid. Excess iodate is removed by ignition in platinum.

#### REFERENCES

1. C. K. McLane and S. Peterson, Preparation of radioactively pure Ac<sup>225</sup>(MsTh<sub>2</sub>), Paper 19.7, this volume (Argonne National Laboratory Report ANL-4040).
2. F. Tomkins, Metallurgical Laboratory Memorandum MUC-JIW-688.

## Paper 19.9

### TRANSMUTATION OF RADIUM TO ACTINIUM ( $\text{Ac}^{227}$ )†

By S. Peterson

#### 1. INTRODUCTION

Three possible sources of  $\text{Ac}^{227}$  are occurrence in uranium ores, growth in protactinium ( $\text{Pa}^{231}$ ), and artificial transmutation of some more abundant element. The first method requires a tedious separation of a rare-earth fraction from the uranium ore, followed by a difficult separation of actinium from the much larger mass of rare earths. The second method would require all the protactinium thus far isolated to grow 0.2 mg of actinium in 10 years. The third has been found to be feasible. Neutron capture by  $\text{Ra}^{226}$  yields  $\text{Ra}^{227}$ , which should be a relatively short-lived  $\beta$  emitter, decaying to  $\text{Ac}^{227}$ . The availability of gram quantities of radium and the high neutron flux of plutonium production piles make possible the production of milligram quantities of actinium.

#### 2. EXPERIMENTAL PROCEDURE

Approximately 1 mg of  $\text{Ra}^{226}$  was bombarded 13 days in the Clinton pile. The active material was rinsed with dilute hydrochloric acid from the quartz tube in which it was irradiated and was adsorbed on a column of Amberlite IR-1 cation-exchange resin (7 mm in diameter and 35 cm long). The actinium was eluted with 150 ml of 0.25M monoammonium citrate, which tracer experiments had shown would quantitatively remove actinium but only 1 part in  $10^6$  of radium. The radium was washed from the column with 3M HCl and was found by emanation measurement (analysis by P. Fineman) to contain 0.97 mg of  $\text{Ra}^{228}$ .

†Contribution from the Chemistry Division of the Metallurgical Laboratory, University of Chicago, now the Argonne National Laboratory.

The actinium fraction from the first IR-1 column was acidified with an amount of hydrochloric acid equivalent to the citrate, diluted to 0.10M in citric acid, and adsorbed on a second column similar to the first. Again the actinium was removed in 150 ml of 0.25M  $\text{NH}_4\text{H}_2\text{-C}_6\text{H}_5\text{O}_7$ , acidified, diluted, and readSORBED on a 7 mm by 35 cm column. At this stage the sample was presumably free from  $\text{Ra}^{226}$ . The third column was washed with 0.1M HCl to remove  $\text{NH}_4^+$  and with 3M HCl to remove the actinium. The first 3M HCl fraction contained considerable  $\beta$  activity from the radium series present before the bombardment. Lead and bismuth carriers were precipitated from the solution with hydrogen sulfide to remove these impurities. The supernatant solution was combined with the other parts of the eluted actinium and evaporated down to a few milliliters volume. Another lead-bismuth sulfide separation was made, excess hydrogen sulfide was boiled out, and the sample was rinsed into a 5.0-ml volumetric flask.

Because of the difficulty in measuring the very weak  $\beta$  radiation of  $\text{Ac}^{227}$ , it was not possible to follow the actinium during the separation. The usual method of analysis for actinium is to measure activity of the decay series, which grows into radioactive equilibrium in four months. In the thin actinium samples obtained from this experiment, it was possible to observe the growth of  $\alpha$  activity of  $\text{Th}^{227}(\text{RdAc})$ ,  $\text{Ra}^{223}(\text{AcX})$ , and the short-lived activities in equilibrium with  $\text{Ra}^{223}$ .

The  $\alpha$  activity, growing in 60 days into samples of the actinium from the first column, corresponds to  $2.95 \times 10^6$  disintegrations per minute of  $\text{Ac}^{227}$ . Sufficient  $\text{Ra}^{226}$  to introduce appreciable error in this value should not have been present; correction was made for the 20 per cent  $\text{Po}^{210}$  found by pulse analysis. Calculating from the known half life of  $\text{Ac}^{227}$  and the bombardment data, the cross section for neutron capture by  $\text{Ra}^{226}$  is 20 barns. A similar assay of the actinium fraction after final purification showed  $1.95 \times 10^6$  disintegrations per minute. An 18-barn cross section would be calculated from this value and the expected 75 per cent chemical yield.

### 3. SUMMARY

One milligram of radium has been bombarded with pile neutrons, producing  $\text{Ac}^{227}$  corresponding to a cross section of 18 to 20 barns for neutron capture by  $\text{Ra}^{226}$ . The actinium was separated from the radium by a resin adsorption-elution process.

Paper 19.10

ALPHA BRANCHING OF Ac<sup>227</sup>†

By S. Peterson and A. Ghiorso

Previous study<sup>1</sup> of the  $\alpha$  decay of Ac<sup>227</sup> has made use of measurement of the  $\beta$  activity of the decay product Fr<sup>223</sup>, yielding at best only a rough estimate of the branching ratio. Use of the differential pulse analyzer makes possible a branching measurement not subject to the errors due to the complex growth of daughter activities and the estimation of  $\beta$ -counting efficiencies.

The  $\alpha$  activity of a freshly purified sample of Ac<sup>227</sup> is given by

$$A = A_0 b + A_0(1 - b)\lambda_1 t + 4A_0 b\lambda_2 t \quad (1)$$

where  $A_0$  is the total Ac<sup>227</sup> activity in equivalent  $\alpha$  counts per minute (disintegrations per minute times counting efficiency of  $\alpha$  particles);  $b$  is the fraction of actinium atoms decaying by  $\alpha$  emission;  $\lambda_1$  is the decay constant of Th<sup>227</sup>(RdAc);  $\lambda_2$  is the decay constant of Ra<sup>223</sup>(AcX); and  $t$  is time in hours since purification. The time,  $t$ , must be shorter than 6 hr so there is no appreciable decay of Th<sup>227</sup> and Ra<sup>223</sup>, and yet longer than 1 hr to allow the shorter-lived activities to be essentially in equilibrium with their parents.

The rate of growth of  $\alpha$  activity during the period of validity of Eq. 1 is then

$$\frac{dA}{dt} = A_0(1 - b)\lambda_1 + 4A_0 b\lambda_2 \quad (2)$$

Substituting the values for the decay constants  $\lambda_1 = 2.59 \times 10^{-5} \text{ min}^{-1}$  and  $\lambda_2 = 4.28 \times 10^{-5} \text{ min}^{-1}$  calculated from the half lives 18.6 days<sup>2</sup> and 11.2 days,<sup>3</sup> this becomes

$$\frac{dA}{dt} = A_0(2.59 \times 10^{-5} + 1.46 \times 10^{-4}b) \quad (3)$$

†Contribution from the Chemistry Division of the Metallurgical Laboratory, University of Chicago, now the Argonne National Laboratory.

Combination of a pulse-analyzer measurement of  $A_0 b$ , the  $\alpha$  activity due to  $\text{Ac}^{227}$ , with a measurement of the linear rate of growth of activity in the same sample then yields a value of  $b$ .

A sample of  $\text{Ac}^{227}$  (obtained from an old  $\text{Pa}^{231}$  sample) was purified from daughters by the method of McLane.<sup>5</sup> The final ignited lanthanum oxide containing the activity was dissolved in dilute nitric acid, mixed with barium, lead, and thorium nitrate carriers, and carried through a second separation from radium and thorium isotopes, evaporated, and ignited. A portion of the final purified actinium (with lanthanum carrier) was dried and mixed with hydrofluoric acid to give a thin, even sample on a platinum disk.

The sample was counted twice in the differential pulse analyzer, giving values of 890 and 908 counts per min in the  $\text{Ac}^{227}$  peak. In one count a  $\text{Po}^{210}$  standard was counted simultaneously; comparison showed the actinium particles to have a range of  $3.46 \pm 0.03$  cm, corresponding to an energy of  $4.95 \pm 0.05$  mev. The same sample was counted in a standard parallel-plate air-ionization chamber over a period of 6 hr (starting 1 hr after purification) except for two intervals during which the energy analyses were made.

The growth of activity showed appreciable deviation from linearity only during the last hour of counting. The rate of growth,  $dA/dt$ , during the 5-hr period was found by least-squares analysis of the counting data<sup>2</sup> to be  $1.996 \pm 0.020$  counts per min. Combining this with  $A_0 b = 899 \pm 9$  counts per min and using Eq. 3 gives  $b = 0.0125 \pm 0.0002$ .

### SUMMARY

By measurement of the rate of growth of  $\alpha$  activity in an actinium sample purified from daughters and  $\alpha$ -energy analysis of the same sample,  $\text{Ac}^{227}$  was found to decay  $1.25 \pm 0.02$  per cent by emission of  $\alpha$  particles of  $4.95 \pm 0.05$  mev.

### REFERENCES

1. M. Perey, J. phys. rad., 10: 435 (1939).
2. S. Peterson and A. Ghiorso, unpublished work.
3. S. Meyer and F. Paneth, Sitzber. Akad. Wiss. Wien, Math. naturw. Klasse Abt. IIa, 127: 147 (1918).
4. A. Ghiorso, A. H. Jaffey, H. P. Robinson, and B. Weissbourd, A 48-channel pulse-height analyzer for alpha-energy measurements, Paper 16.8, this volume (Metallurgical Project Report CC-3887).
5. C. K. McLane and S. Peterson, Preparation of radioactively pure  $\text{Ac}^{228}(\text{MsTh}_2)$ , Paper 19.7, this volume (Argonne National Laboratory Report ANL-4040).

## Paper 19.11

### PRODUCTS OF THE DEUTERON AND HELIUM-ION BOMBARDMENTS OF $\text{Pa}^{231}\dagger$

By D. W. Osborne, R. C. Thompson, and Q. Van Winkle

#### 1. INTRODUCTION

During October 1945, there became available in this laboratory sufficient  $\text{Pa}^{231}$  to permit cyclotron bombardments to produce for study a number of isotopes near  $\text{Pa}^{231}$  on the isotope chart. The isotopes in the region of  $\text{Pa}^{231}$  that were known at the start of this work are shown in Fig. 1. It was expected that bombardment with 22-mev deuterons would produce the known protactinium isotopes  $\text{Pa}^{232}$ ,  $\text{Pa}^{230}$ , and  $\text{Pa}^{228}$  by ( $d,pxn$ ) reactions, the known uranium isotopes  $\text{U}^{232}$  and  $\text{U}^{230}$  by decay of  $\text{Pa}^{232}$  and  $\text{Pa}^{230}$  as well as by ( $d,xn$ ) reactions, and perhaps activities that could be assigned to the unknown isotopes  $\text{U}^{231}$  and  $\text{U}^{229}$ . No neptunium isotopes were expected since  $\text{U}^{232}$  and  $\text{U}^{230}$  are  $\alpha$  emitters, and any uranium isotopes with masses of 231 or less would not be expected to decay by  $\beta^-$  emission. Bombardment with 44-mev helium ions was expected to produce the same protactinium isotopes as in deuteron bombardment (except  $\text{Pa}^{232}$ ) by ( $\alpha,\alpha xn$ ) reactions, the same uranium isotopes (plus undetectable amounts of long-lived  $\text{U}^{233}$  and  $\text{U}^{234}$ ) by decay and by ( $\alpha,pxn$ ) reactions, and  $\text{Np}^{234}$  and perhaps unknown neptunium isotopes of mass less than 234 by ( $\alpha,xn$ ) reactions.

#### 2. EXPERIMENTAL WORK

The  $\text{Pa}^{231}$  used in these experiments was concentrated from uranium ores and residues by members of this laboratory<sup>1-3</sup> and by A. V.

<sup>†</sup>Contribution from the Chemistry Division of the Metallurgical Laboratory, University of Chicago, now the Argonne National Laboratory.

Grosse and M. S. Agruss,<sup>1</sup> All the Pa<sup>231</sup> was highly purified in this laboratory by procedures that included repeated ether extractions of dilute nitric acid solutions salted with ammonium nitrate to remove traces of uranium and extractions of protactinium from 6N to 8N HNO<sub>3</sub> solution with diisopropyl ketone, followed by several washes of the ketone with 1N HNO<sub>3</sub>, and then precipitation of the protactinium with hydrogen peroxide solution.

					Np <sup>234</sup> K 4.40 days	Np <sup>235</sup> K 400 days
		U <sup>230</sup> $\alpha$ 20.8 days		U <sup>232</sup> $\alpha$ 70 years	U <sup>233</sup> $\alpha$ $1.62 \times 10^5$ years	U <sup>234</sup> $\alpha$ $2.35 \times 10^5$ years
		Pa <sup>230</sup> K $\alpha(0.1\%)$ 1.4 days	Pa <sup>230</sup> $\beta^-$ 17 days	Pa <sup>231</sup> $\alpha$ $3.43 \times 10^4$ years	Pa <sup>232</sup> $\beta^-$ 1.4 days	Pa <sup>233</sup> $\beta^-$ 27.4 days
Th <sup>230</sup> $\alpha$ 30.9 min	Th <sup>231</sup> $\alpha$ 18.9 days	Th <sup>232</sup> $\alpha$ 1.90 years	Th <sup>230</sup> $\alpha$ 7000 years	Th <sup>230</sup> $\alpha$ $8.3 \times 10^4$ years	Th <sup>231</sup> $\beta^-$ 24.6 hr	Th <sup>232</sup> $\alpha$ $1.39 \times 10^{10}$ years
Ac <sup>233</sup> $\alpha$ 10.0 days		Ac <sup>234</sup> $\beta^- (99\%)$ $\alpha(1.2\%)$ 13.5 years	Ac <sup>233</sup> $\beta^-$ $\alpha(\text{small \%})$ 6.13 hr			

Fig. 1—Isotopes in the region of Pa<sup>231</sup> that were known at the beginning of these bombardments.

The precipitated protactinium was dissolved in hydrofluoric acid, placed on a small platinum interceptor target (0.85 sq cm area) by evaporation of the solution to dryness in small portions, ignited to the oxide, and covered with approximately 4 mg/sq cm of aluminum foil. The bombardments were carried out by Dr. J. G. Hamilton and co-workers with the Berkeley 60-in. cyclotron. In the first bombardment, 2 mg of Pa<sup>231</sup> was bombarded with 452  $\mu$ a-hr of deuterons over a period of 8 days, then 4 mg of Pa<sup>231</sup> was bombarded with 179  $\mu$ a-hr of helium ions over a period of 15 days, and finally 8 mg of Pa<sup>231</sup> was bombarded with 239  $\mu$ a-hr of deuterons over a period of 4 days. At a later date two short bombardments with helium ions were made, and the material was worked up by two of the authors (Osborne and

Thompson) at the Radiation Laboratory in Berkeley, to look for  $\text{U}^{239}$ .

For all the bombardments the maximum energies of the helium ions and of the deuterons were slightly less than the 44-mev and 22-mev values originally expected. The maximum energies were 42 and 21 mev for helium ions and deuterons, respectively, as determined by the range of the  $\alpha$  particles in air, and the energies of the maximum number of helium ions and deuterons as determined by absorption in aluminum were 38 and 19 mev, respectively.<sup>5</sup>

Each of the first three targets was returned to this laboratory as quickly as possible. Uranium and protactinium fractions were isolated chemically from the deuteron-irradiated material, and neptunium, uranium, and protactinium fractions were isolated chemically from the material that had been irradiated with helium ions. The first fraction was isolated 1 to 1½ days after the end of the bombardment. Aliquots of the fractions were evaporated on platinum foils 0.005 cm thick for studying (1) the  $\alpha$  activities by decay measurements and by means of the differential  $\alpha$ -pulse analyzer,<sup>6</sup> and (2) the Geiger-Mueller activities by decay and absorption measurements.

Decay and absorption measurements were also made on samples of unbombarded  $\text{Pa}^{231}$  under the identical conditions used for measurements on the protactinium fractions from the bombardments. The purpose of this was to enable corrections to be made for the appreciable Geiger-Mueller activity of the  $\text{Pa}^{231}$  in these fractions. The amounts of  $\text{Pa}^{231}$  in the smaller protactinium samples were determined by  $\alpha$  counting. The decay and absorption curves were usually made with two or three samples, varying in activity by steps approximately tenfold, and the curves were normalized to one sample by means of ratios of the activity taken at suitable times or with suitable absorbers. Beta and x-ray standards were counted in each series of measurements, and corrections were made for variations in the counting rate of the standards. Corrections were also made for coincidence losses. Absorbers were placed as near as possible to the counter window to minimize the counting of scattered components.

The instruments used for  $\alpha$  counting were: an atmospheric  $\alpha$  counter in conjunction with a linear amplifier and scaler manufactured by the Cyclotron Specialties Co.; an argon-carbon dioxide fast counter;<sup>7</sup> and a methane proportional counter.<sup>8</sup> Geiger-Mueller activities were determined with end-window brass-wall counters with mica windows of 3.3 to 3.8 mg/sq cm thickness and usually a filling of 1 cm Hg pressure of ethyl alcohol and 9 cm Hg pressure of argon.<sup>9</sup> Xenon-filled counters were used in determining decay and some absorption curves of the neptunium fraction in the first helium-ion bombardment. Each counter was provided with a shelf arrangement for holding

samples and absorbers at standard distances from the window. The body of the counter was surrounded by a close-fitting cylindrical sheath of lead 1.2 cm thick, and the counter assembly was enclosed in an aluminum-lined housing with lead walls 5 cm thick. A Neher-Harper quenching circuit and a Cyclotron Specialties Co. scaler were used with the Geiger-Mueller counters.

### 3. CHEMICAL PROCEDURES

The procedure used to isolate the uranium and protactinium fractions in the deuteron bombardments will now be described briefly. It was necessary to destroy carbonaceous material which accumulated on the target, probably from the oil diffusion pumps of the cyclotron, by fuming with nitric and perchloric acids, or better by ignition in a muffle furnace at 750°C for about 40 min. The material was removed from the target by a combination of scraping and dissolving in concentrated hydrofluoric and nitric acids. The solution was evaporated to dryness, a little concentrated hydrofluoric acid was added, and the solution was evaporated nearly to dryness, so that a trace of fluoride remained to aid in holding the protactinium in solution. The residue was then dissolved in a few milliliters of 2N HNO<sub>3</sub>. A portion of this solution was saved, and the remainder was transferred to a small Kjeldahl flask, to which solid ammonium nitrate was added to make a solution approximately 1N in HNO<sub>3</sub> and 9N to 10N in NH<sub>4</sub>NO<sub>3</sub>. Uranium was extracted from this solution by a technique that is standard in this laboratory. Four to six double-volume portions of diethyl ether were used, and sufficient nitric acid was added before each extraction to keep the acid concentration 0.1N or higher. The layers were separated by freezing the aqueous layer with solid carbon dioxide and acetone and pouring off the ether layer. Each portion of ether was shaken with two or three wash solutions containing 0.1N HNO<sub>3</sub> and 9N to 10N NH<sub>4</sub>NO<sub>3</sub>, and finally the washed ether was stripped of uranium by means of water. A fresh portion of water was used for each portion of ether. The water extracts, combined and evaporated to a small volume, constituted the uranium fraction. The protactinium was separated from fluoride and the large concentration of ammonium nitrate by twice precipitating it with sodium hydroxide or ammonia and washing several times with water. The protactinium hydroxide was dissolved in 10 ml of 6N HNO<sub>3</sub> per milligram of protactinium, and the protactinium was extracted with two or three approximately equal-volume portions of diisopropyl ketone that had previously been shaken with an equal volume of 6N HNO<sub>3</sub>. The diisopropyl ketone layers were shaken first with two washes of water or 1N HNO<sub>3</sub>, and then with 3 per

cent  $\text{H}_2\text{O}_2$  solution to precipitate the protactinium. The solution of this protactinium peroxide in concentrated nitric acid constituted the protactinium fraction.

Several times it was desired to isolate protactinium and thorium daughters from the uranium fraction, and the following procedure was generally used. The solution was made 1N in  $\text{HNO}_3$  and 9N to 10N in  $\text{NH}_4\text{NO}_3$ . Uranium was extracted by several portions of diethyl ether and set aside for repetition of the isolation of daughters at a later time. Then protactinium was extracted by means of diisopropyl ketone. After removal of uranium and protactinium from the aqueous layer, thorium was coprecipitated on zirconium iodate. The bulk of the carrier was reduced by dissolving the iodate precipitate and precipitating a small amount of lanthanum fluoride, which carried the thorium.

The chemical procedure for the material bombarded with helium ions included separation of a neptunium fraction. After ignition to destroy carbonaceous matter and removal of the material from the target by scraping and dissolving in hydrofluoric and nitric acids, the solution was evaporated just to dryness, and the residue was taken up in dilute nitric acid. Sodium bromate was added, and the solution was heated at 100°C for 10 min to oxidize neptunium to  $\text{Np(VI)}$ . A combined neptunium and uranium fraction was then separated by ether extraction, following the same procedure used to isolate the uranium fraction in the deuteron bombardments. The uranium-neptunium fraction was evaporated to dryness with concentrated hydrochloric acid to convert the nitrates to chlorides and was then dissolved in dilute hydrochloric acid. Ammonium iodide and hydrazine hydrochloride were added to reduce the neptunium to  $\text{Np(IV)}$ , and the solution was then diluted. Neptunium was extracted from this solution with thenoyl-trifluoroacetone in benzene and then reextracted into hydrochloric acid. The uranium remained in the hydrochloric acid solution and was purified further from neptunium by another extraction. A protactinium fraction was separated by the method used for the deuteron bombardments.

#### 4. RESULTS OF DEUTERON BOMBARDMENTS

4.1  $\text{Pa}^{232}$ . Decay of the protactinium fractions was followed with a mica end-window Geiger-Mueller counter through the following combinations of absorbers: no absorber, 2.0 g/sq cm of beryllium (to absorb the  $\beta$  radiations), 2.0 g/sq cm of beryllium plus 60 mg/sq cm of lead (to absorb the  $\beta$  rays and L x rays), and 2.0 g/sq cm of beryllium plus 5.1 g/sq cm of lead (to absorb all but the hard  $\gamma$  radiation).

After correction for the Geiger-Mueller activity of  $\text{Pa}^{231}$  and its daughters, as determined by measurements on unbombarded  $\text{Pa}^{231}$  under the same conditions, the decay curves could be resolved into two half lives, 31 to 36 hr (average, 33 hr) and 17.7 days, which are attributed to  $\text{Pa}^{232}$  and to  $\text{Pa}^{230}$ , respectively. Figure 2 shows one of these decay curves. The value of 33 hr for the half life of  $\text{Pa}^{232}$  is in satisfactory agreement with the more accurate value of 31.7 hr reported by Jaffey and Hyde.<sup>10</sup>

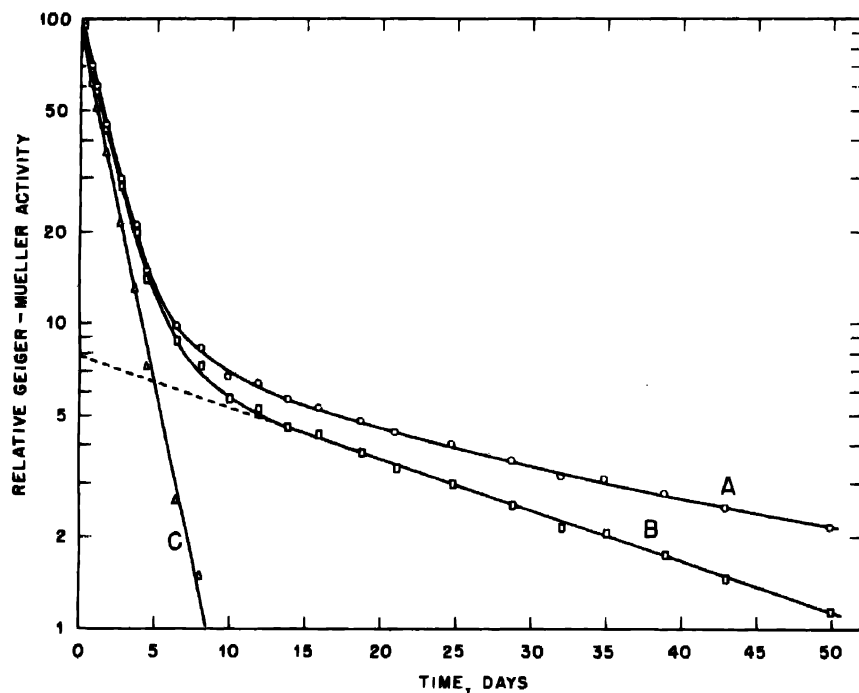


Fig. 2—Decay of protactinium fraction from deuteron bombardment, through 2.0 g/sq cm of beryllium plus 5.1 g/sq cm of lead. A, gross decay curve. B, decay curve corrected for  $\text{Pa}^{231}$  Geiger-Mueller activity. Resolution is shown into a 17.7-day period ( $\text{Pa}^{230}$ , curve B) and a 32-hr period ( $\text{Pa}^{232}$ , curve C).

The radiations of the 33-hr activity were characterized by absorption curves in lead, with 2.0 g/sq cm of beryllium covering the sample, and by absorption curves in aluminum. These curves were determined as soon as possible after separation of the protactinium fraction, and corrections were made for  $\text{Pa}^{230}$  by comparison with curves taken on the same samples 9 days later (Figs. 7 to 10), when the 33-hr activity was much smaller than the 17.7-day  $\text{Pa}^{230}$  activity. Corrections for  $\text{Pa}^{231}$  were determined by means of absorption curves

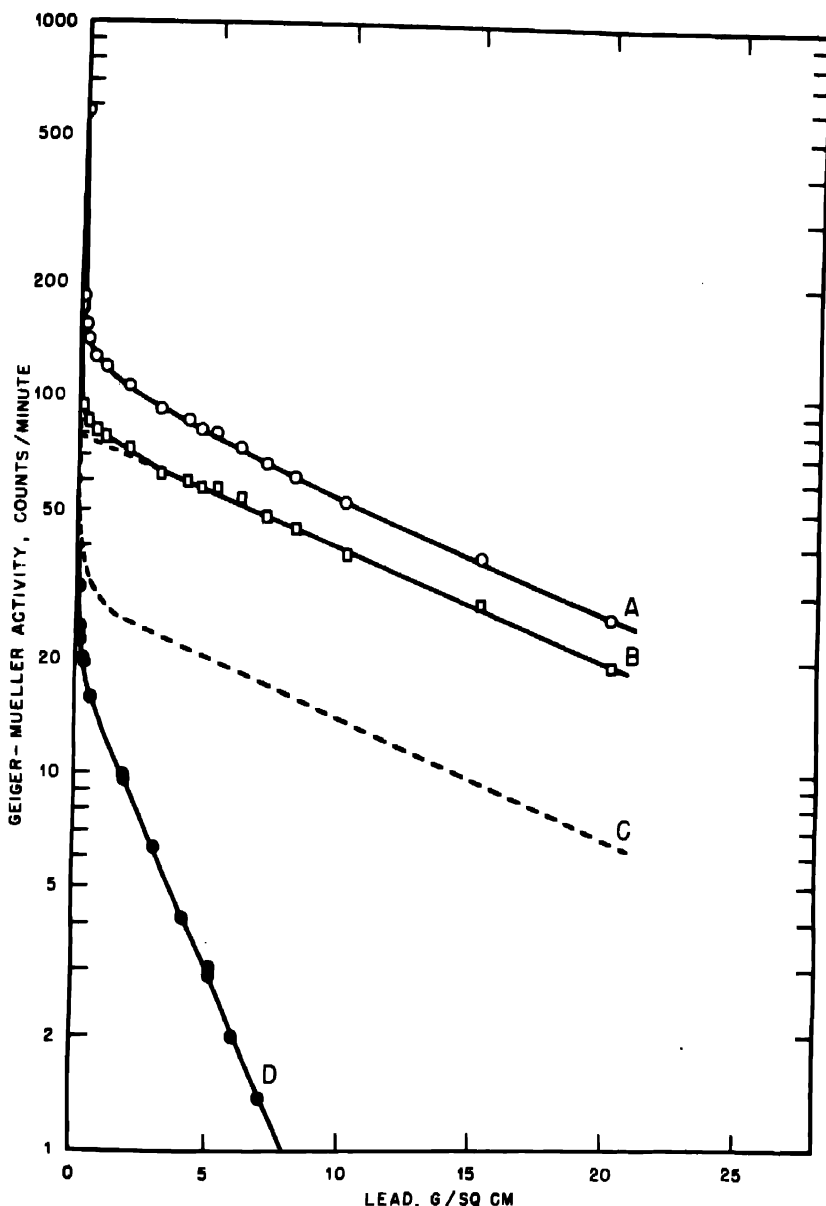


Fig. 3—Absorption of  $\text{Pa}^{232}$  electromagnetic radiations in lead. Sample covered with 2.0 g/sq cm of beryllium. A, total activity. B, absorption curve of  $\text{Pa}^{232}$ , obtained by correcting curve A for  $\text{Pa}^{230}$  (curve C) and for  $\text{Pa}^{231}$  (curve D). The half thickness of the  $\text{Pa}^{232}$  hard  $\gamma$  ray is 10.1 g/sq cm of lead (1.02 mev).

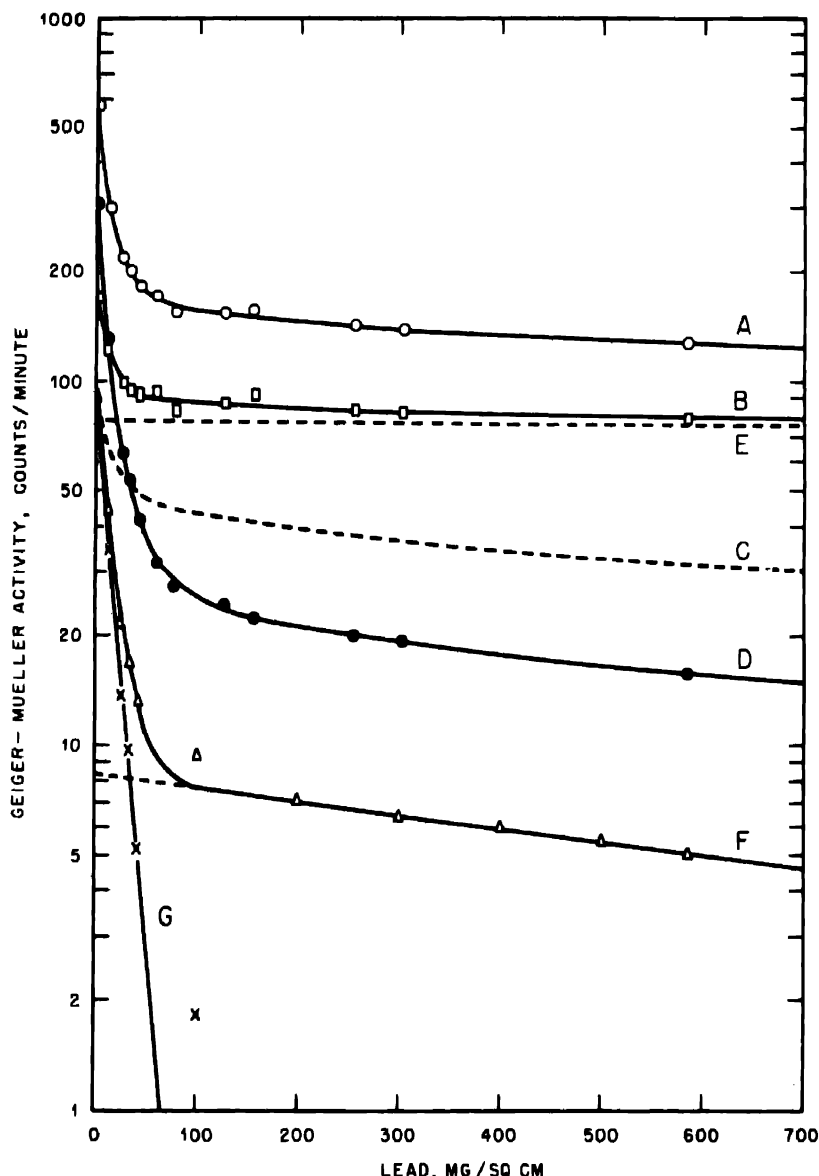


Fig. 4—Absorption of  $\text{Pa}^{232}$  electromagnetic radiations in lead. Sample covered with 2.0 g/sq cm of beryllium. A, total activity. B, absorption curve of  $\text{Pa}^{232}$ , obtained by correcting curve A for activity due to  $\text{Pa}^{230}$  (curve C) and  $\text{Pa}^{231}$  (curve D). After subtraction of the  $\text{Pa}^{232}$  hard  $\gamma$  ray (curve E), curve B can be resolved into a  $\gamma$  ray (curve F) of 800 mg/sq cm half thickness (0.21 mev) and a component (curve G) with 11 mg/sq cm half thickness (23 kev), probably L x rays.

on samples of unbombarded  $\text{Pa}^{231}$  made at the same time under exactly the same conditions.

The absorption curve in lead, with 2.0 g/sq cm of beryllium covering the sample, is given in Figs. 3 and 4. After correction for  $\text{Pa}^{230}$

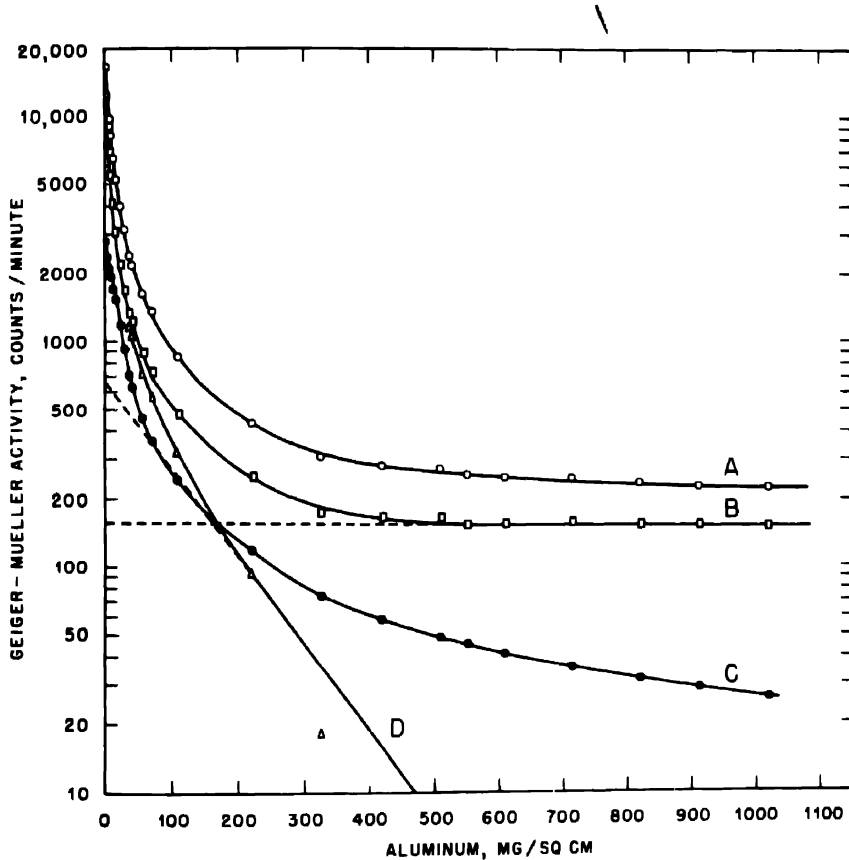


Fig. 5—Absorption of  $\text{Pa}^{231}$  radiations in aluminum. A, total activity. B,  $\text{Pa}^{232}$  aluminum absorption curve, obtained by correcting curve A for  $\text{Pa}^{230}$  (Figs. 9 and 10, corrected for decay) and for  $\text{Pa}^{231}$  (curve C). Resolution of a hard  $\gamma$  component and of L x rays (curve D), with half thickness of 78 mg/sq cm (14.6 kev), is shown.

and  $\text{Pa}^{231}$  the curve can be resolved into a hard  $\gamma$ -ray component of half thickness 10.1 g/sq cm (1.02 mev), a softer  $\gamma$  ray of half thickness 0.80 g/sq cm (0.21 mev), and a component with a half thickness of 11 mg/sq cm (23 kev). The last component is probably a mixture of L x rays, which have energies of 13.5 to 20.2 kev for uranium. No K x rays, which would be expected from decay of 1.4-day  $\text{Pa}^{230}$  by K electron capture, were found although 5 counts per minute might not

have been resolved. The abundances and energies of the radiations are in satisfactory agreement with those observed by Jaffey and Van Winkle<sup>11</sup> from a sample of  $\text{Pa}^{232}$  that was not accompanied by any other activity in an appreciable amount.

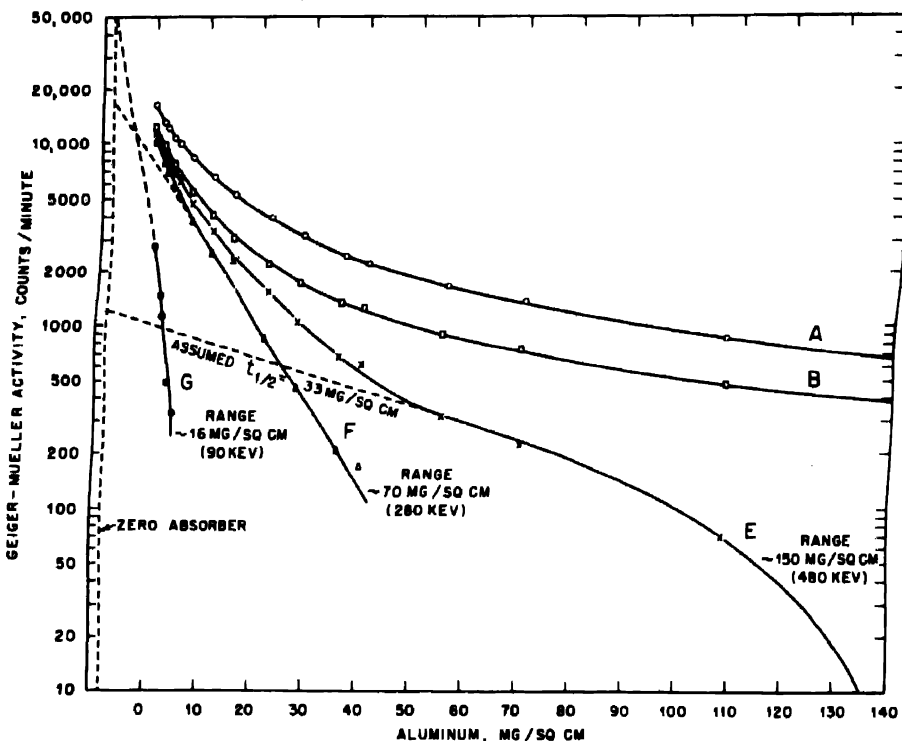


Fig. 6—Absorption of  $\text{Pa}^{232}$  radiations in aluminum. A, total activity. B,  $\text{Pa}^{232}$  aluminum absorption curve, obtained by correcting curve A for  $\text{Pa}^{232}$  (Figs. 9 and 10, corrected for decay) and for  $\text{Pa}^{231}$  (Fig. 5, curve C). E, curve B corrected for hard  $\gamma$  and L x rays (Fig. 5, curve D), showing  $\beta$  component with range of about 150 mg/sq cm (480 kev) and initial half thickness 33 mg/sq cm, assumed from Jaffey and Van Winkle's results.<sup>11</sup> F, curve E corrected for  $\beta$  component with 6.9 mg/sq cm initial half thickness, showing  $\beta$  component with 6.9 mg/sq cm initial half thickness and range of about 70 mg/sq cm (about 280 kev). G, soft  $\beta$  component, initial half thickness 1.9 mg/sq cm and range about 16 mg/sq cm (about 90 kev). The softest component was not observed in  $\text{Pa}^{232}$  by Jaffey and Van Winkle and may be spurious or due to  $\text{Pa}^{231}$ .

The absorption curve in aluminum is given in Figs. 5 and 6. This curve was made 25 hr before the beryllium-plus-lead curve shown in Figs. 3 and 4, on the same samples and under the same conditions. The tube had a 3.76 mg/sq cm window, and the samples were at a distance of 3.69 cm below the window. The curve can be resolved into a hard component; L x rays; a soft  $\beta$  particle or conversion electron

(assuming an initial half thickness of 33 mg/sq cm and a range of about 150 mg/sq cm, corresponding to a maximum energy of about 480 kev, in agreement with values given by Jaffey and Van Winkle<sup>11</sup>); a soft  $\beta$  particle with an initial half thickness of 6.9 mg/sq cm, a range of about 70 mg/sq cm, and an energy of about 280 kev; and a very soft  $\beta$  particle or conversion electron with an initial half thickness of about 1.9 mg/sq cm, a range of about 16 mg/sq cm, and an energy of about 90 kev. These results are in reasonable agreement with those of Jaffey and Van Winkle,<sup>11</sup> except that they did not observe the 90-kev  $\beta$  particle. It is not known at present whether this component is a spurious scattered component arising from the geometry or whether it is a  $\beta$  or conversion electron from some other isotope such as Pa<sup>230</sup>. Data were not available from the other deuteron bombardment to check this curve.

The yield of Pa<sup>232</sup> was estimated from the counts per minute of the 330-kev  $\beta$  particle obtained from resolution of the Pa<sup>232</sup> aluminum absorption curve, assuming one 330-kev  $\beta$  particle per disintegration and using a back-scattering factor<sup>12</sup> of 1.60. From the yield estimated in this manner the cross section for the formation of Pa<sup>232</sup> by the reaction Pa<sup>231</sup>(d,p)Pa<sup>232</sup> was calculated to be  $40 \times 10^{-27}$  sq cm in the first deuteron bombardment and  $60 \times 10^{-27}$  sq cm in the second.

**4.2 Pa<sup>230</sup>.** Alpha-pulse analyses soon after separation of the protactinium fraction showed Pa<sup>231</sup> and a small amount of  $\alpha$  activity due to the U<sup>230</sup> decay series<sup>13</sup> but no other  $\alpha$  activity. Repetition of the pulse analyses at later dates showed that the U<sup>230</sup> series had grown into the protactinium fraction, establishing the presence of  $\beta$ -emitting Pa<sup>230</sup>.

The half life of Pa<sup>230</sup> was determined by following through various absorbers the decay of the Geiger-Mueller activity in the protactinium fraction and in samples of unbombarded Pa<sup>231</sup>. The best value is  $17.7 \pm 0.5$  days from the decay through 2.0 g/sq cm of beryllium plus 5.1 g/sq cm of lead (Fig. 2), the combination of absorbers through which the fraction of the activity caused by Pa<sup>231</sup> was least. A concordant value has been obtained by Studier and Hyde,<sup>13</sup> who followed the growth and decay of the  $\alpha$  activity in samples of Pa<sup>230</sup> from deuteron bombardment of Th<sup>232</sup> and from these measurements calculated a half life of  $17.0 \pm 0.5$  days for Pa<sup>230</sup>. Because of the abundant presence of Pa<sup>231</sup> they were unable to obtain the half life by direct decay or to study the radiations of Pa<sup>230</sup>.

The radiations of Pa<sup>230</sup> were characterized by absorption curves after the Pa<sup>231</sup> had decayed until it was nearly negligible. The absorption of the Pa<sup>230</sup> radiations in lead with 2.0 g/sq cm of beryllium covering the sample is shown in Figs. 7 and 8. After correction for

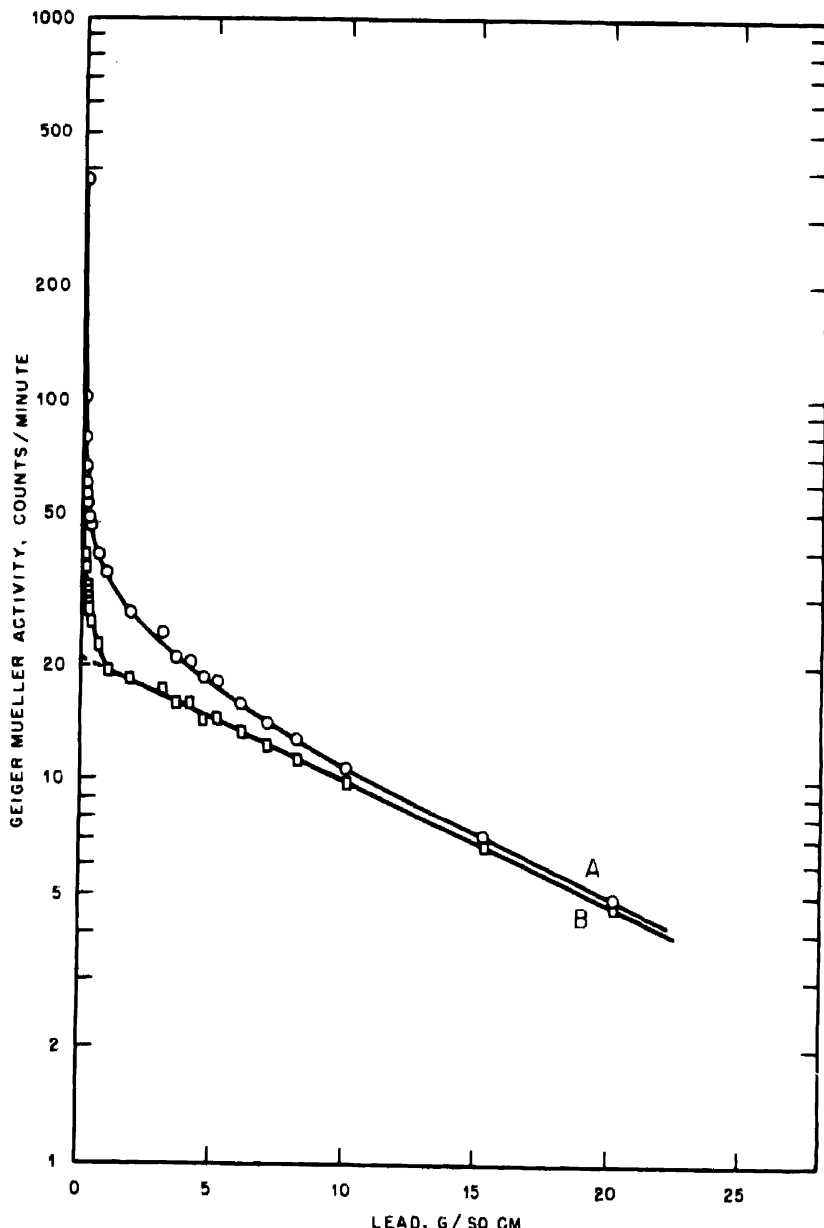


Fig. 7—Absorption of  $\text{Pa}^{230}$  electromagnetic radiations in lead. Sample covered with 2.0 g/sq cm of beryllium. A, total activity. B, absorption curve of  $\text{Pa}^{230}$ , obtained by correcting curve A for  $\text{Pa}^{231}$  and  $\text{Pa}^{232}$  (Figs. 3 and 4, corrected for  $\text{Pa}^{232}$  decay). The  $\gamma$  component with half thickness 9.4 g/sq cm (0.94 mev) is shown.

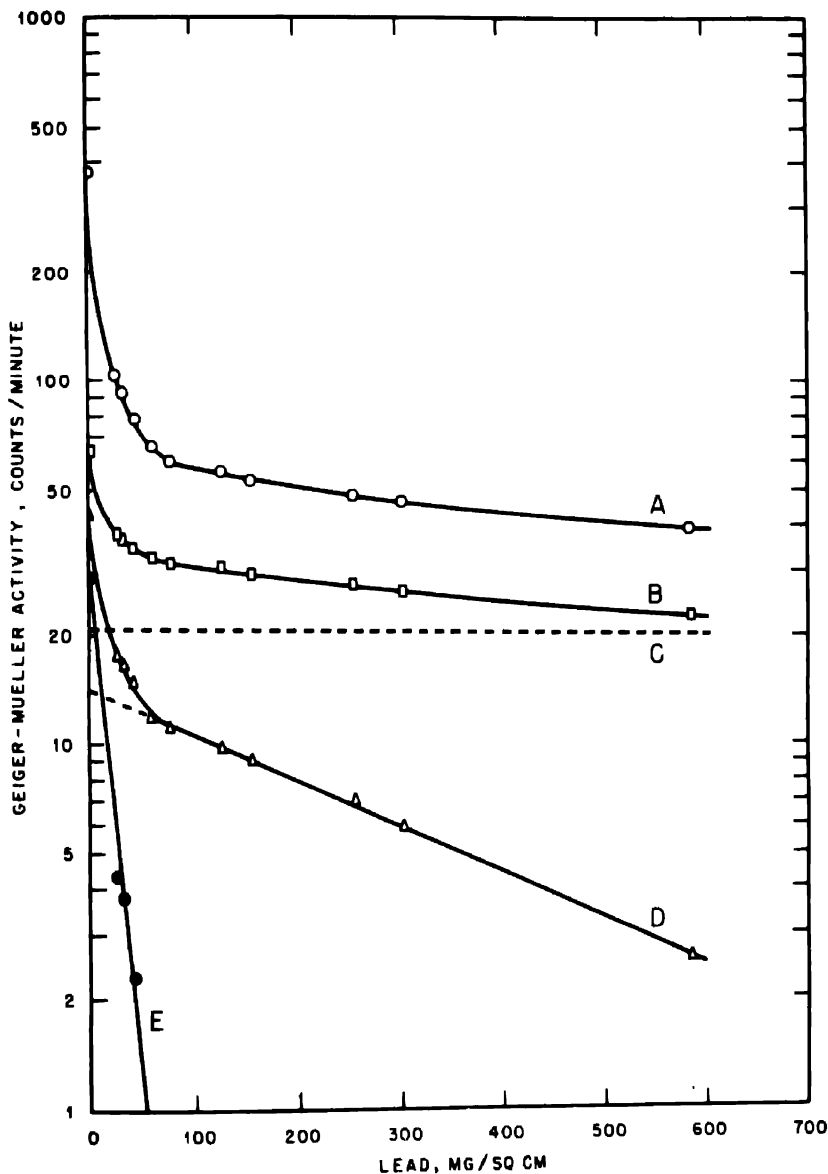


Fig. 8.—Absorption of  $\text{Pa}^{230}$  electromagnetic radiations in lead. Sample covered with 2.0 g/sq cm of beryllium. A, total activity. B, absorption curve of  $\text{Pa}^{230}$ , obtained by correcting curve A for  $\text{Pa}^{231}$  and  $\text{Pa}^{232}$  (Fig. 4, corrected for  $\text{Pa}^{232}$  decay). C, 0.94-mev  $\gamma$  ray. D, curve B minus curve C, showing component with half thickness 245 mg/sq cm (74 or 131 kev), probably K x rays. E, curve D minus 245 mg/sq cm component, showing component with half thickness 10.8 mg/sq cm (23 kev), probably L x rays.

$\text{Pa}^{231}$  and for  $\text{Pa}^{232}$  (from Figs. 3 and 4, allowing for 9 days decay), the curve can be resolved into a  $\gamma$ -ray component with a half thickness of 9.4 g/sq cm (0.94 mev), a  $\gamma$  ray with a half thickness of 245 mg/sq cm (74 or 131 kev, probably 100 kev K x rays), and a softer com-

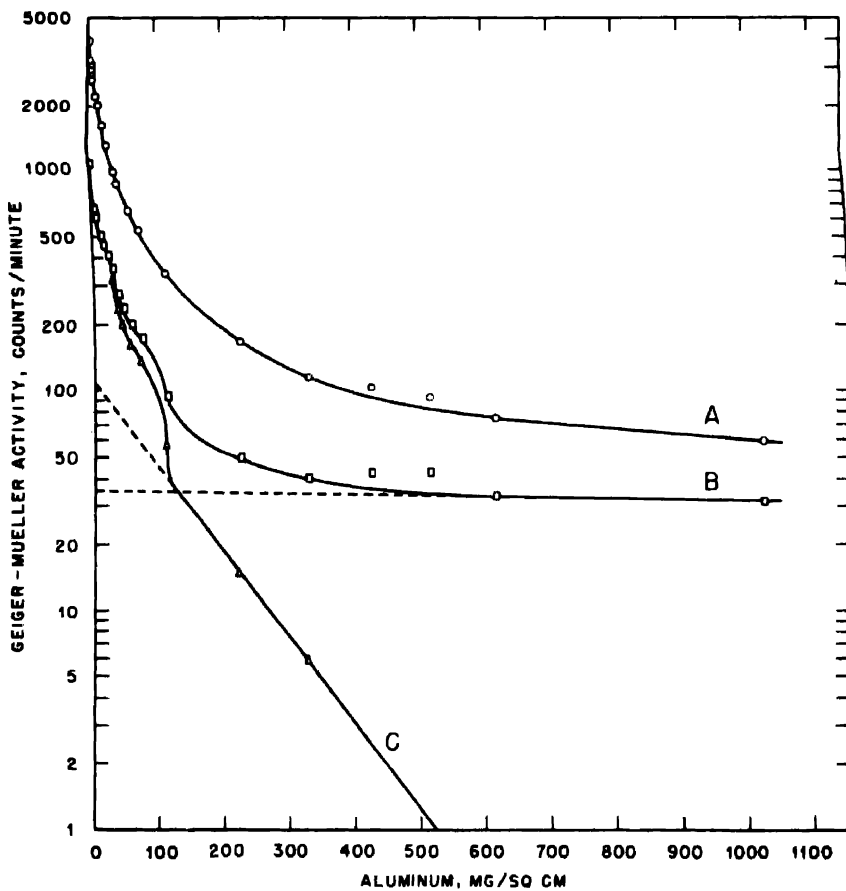


Fig. 9—Absorption of  $\text{Pa}^{232}$  radiations in aluminum. A, total activity. B, aluminum absorption curve of  $\text{Pa}^{232}$ , obtained from curve A by correcting for  $\text{Pa}^{231}$  and  $\text{Pa}^{233}$  (Figs. 5 and 6, corrected for  $\text{Pa}^{232}$  decay), showing hard component. C, curve B corrected for hard component, showing L x-ray component with a half thickness of 79 mg/sq cm (14.6 kev).

ponent with a half thickness of 10.8 mg/sq cm (23 kev, probably L x rays). This curve agrees within experimental error with a beryllium-plus-lead absorption curve made on a protactinium sample from the first deuteron bombardment which was repurified chemically after decay of the  $\text{Pa}^{232}$ .

In Figs. 9 and 10 is shown the aluminum absorption curve of  $\text{Pa}^{230}$ . After correction for  $\text{Pa}^{231}$  and for  $\text{Pa}^{232}$  (from Figs. 5 and 6, allowing for 9 days decay) the curve can be resolved into a hard  $\gamma$  component (a mixture of the 0.94-mev  $\gamma$  and the K x rays found in the beryllium-plus-lead curve), L x rays (79 mg/sq cm half thickness, 14.6 kev), a  $\beta$  component with a range of roughly 130 mg/sq cm (430 kev), a  $\beta$  component with an initial half thickness of 14 mg/sq cm and a range of roughly 50 mg/sq cm (220 kev), and a softer  $\beta$  component, possibly

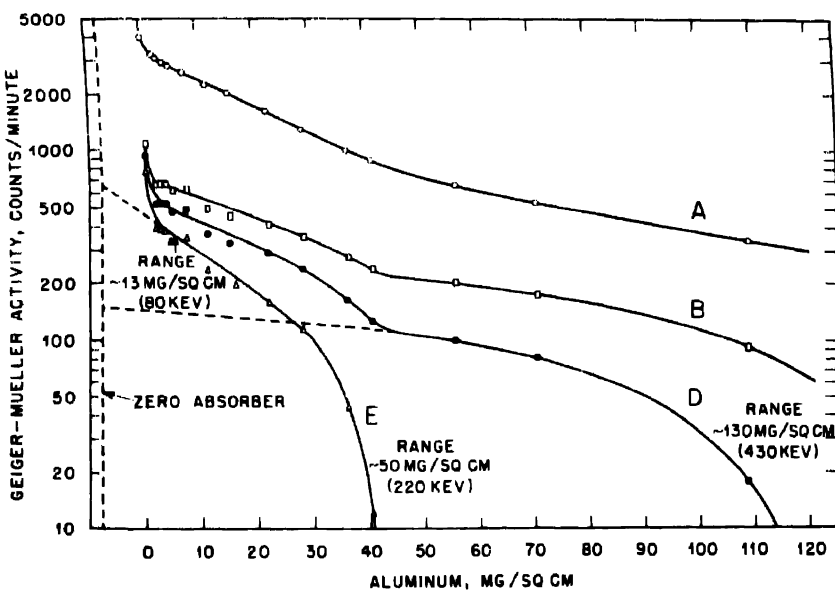


Fig. 10—Absorption of  $\text{Pa}^{230}$  radiations in aluminum. A, total activity. B, aluminum absorption curve of  $\text{Pa}^{230}$ , obtained from curve A by correcting for  $\text{Pa}^{231}$  and  $\text{Pa}^{232}$  (Figs. 5 and 6, corrected for  $\text{Pa}^{232}$  decay). D, curve B corrected for hard  $\gamma$  and L x rays (Fig. 9). This is resolved into  $\beta$  components with ranges of about 130 mg/sq cm (430 kev), 50 mg/sq cm (220 kev) (curve E), and 13 mg/sq cm (80 kev).

spurious, with a range of about 13 mg/sq cm (about 80 kev). An aluminum absorption curve made on a sample of protactinium from the other bombardment which was repurified after decay of the  $\text{Pa}^{232}$  did not show the softest  $\beta$  component but otherwise agreed within experimental error.

The abundances of the various components found in the beryllium-plus-lead and aluminum absorption curves may be compared with the number of  $\text{Pa}^{230} \beta^-$  disintegrations per minute determined from the growth of  $\text{U}^{230}$ . The curves shown in Figs. 7 to 10 have been normalized to a sample in which there were  $1.01 \times 10^4 \text{ Pa}^{230} \beta^-$  disintegra-

tions per minute at the time the curves were determined. The geometry was 4.2 per cent. The results are shown in Table 1, together with the back-scattering factors and counting efficiencies used in calculating the abundances. The K x rays have been corrected to zero absorber assuming a half thickness of 5.0 g/sq cm in beryllium. The softest component has not been included in the table. It appears from these data that there are 9 K-x-ray quanta emitted per  $\beta^-$  disintegration, indicating that decay of  $\text{Pa}^{230}$  by capture of a K electron is 9 times as frequent as decay by  $\beta^-$  emission. A more reliable value of

Table 1 — Radiations of  $\text{Pa}^{230}$  from a Sample with  $1.01 \times 10^4 \text{ Pa}^{230}$   
 $\beta^-$  Disintegrations per Minute

Radiation	Counts/min at no ab- sorber (4.2 % geom.)	Back-scattering factor	Counting efficiency	Events/min
220-kev $\beta^-$	660	1.60	100	$0.98 \times 10^4$
430-kev $\beta^-$	150	1.60	100	$0.22 \times 10^4$
L x rays	114	1.00	2.0	$14 \times 10^4$
K x rays	19	1.00	0.5	$9.0 \times 10^4$
0.94-mev $\gamma$	21	1.00	1.0	$5.0 \times 10^4$

10 for the  $K/\beta^-$  branching ratio of  $\text{Pa}^{230}$  has been determined by M. H. Studier and R. J. Bruehlman<sup>14</sup> by comparing the yields of  $\text{Th}^{230}$  and of the  $\text{U}^{230}$  series growing into a large sample of  $\text{Pa}^{230}$  from deuteron bombardment of  $\text{Th}^{232}$ . The present data indicate that the 0.94-mev  $\gamma$  ray is associated with the decay by K capture and that there is one 220-kev  $\beta^-$  per disintegration to  $\text{U}^{230}$ .

In order to calculate the cross section for the  $\text{Pa}^{231}(\text{d},\text{p}2\text{n})\text{Pa}^{230}$  reaction, the value of 10 for the  $K/\beta^-$  branching ratio of  $\text{Pa}^{230}$  was used with observations of the growth of the  $\text{U}^{230}$  series into the protactinium fraction. A cross section of  $23 \times 10^{-27}$  sq cm was obtained in the first deuteron bombardment and  $37 \times 10^{-27}$  sq cm in the second.

**4.3  $\text{Pa}^{229}$ .** Other observers<sup>15,16</sup> have produced this isotope by the reaction  $\text{Th}^{230}(\text{d},3\text{n})\text{Pa}^{229}$  and have observed a peak due to it in  $\alpha$ -pulse analyses. This peak decays with a half life of  $1.4 \pm 0.4$  days according to the first observations<sup>15</sup> and  $1.5 \pm 0.1$  days according to later work.<sup>16</sup> It has been estimated, mainly from consideration of yields, that  $\text{Pa}^{229}$  decays approximately 1 per cent by  $\alpha$  emission and 99 per cent by orbital-electron capture.<sup>17</sup>

In this work qualitative evidence for the presence of  $\text{Pa}^{229}$ , which was probably formed by the reaction  $\text{Pa}^{231}(\text{d},\text{p}3\text{n})\text{Pa}^{229}$  and by decay of

a short-lived K-capturing  $\text{U}^{229}$  formed by a ( $d, 4n$ ) reaction, was obtained in the following manner: Approximately 20 per cent of the original solution from the first deuteron bombardment was evaporated to dryness and heated under a heat lamp to remove traces of fluoride, the residue was taken up in 6N  $\text{HNO}_3$ , and all but 1 per cent of the protactinium and uranium was extracted with diisopropyl ketone. The aqueous layer was made 3N in HF, and 0.3 mg of lanthanum fluoride was precipitated by addition of lanthanum nitrate solution. It was expected that lanthanum fluoride precipitated in this manner would carry actinium but not protactinium. The lanthanum fluoride was washed with a mixture of hydrofluoric and nitric acids, slurried on to large platinum plates, flamed to drive off  $\text{Fr}^{221}$ , and rapidly placed in an  $\alpha$  counter to watch for the 5-min growth characteristic of  $\text{Ac}^{225}$ . However, about  $5 \times 10^4$  counts per minute of  $\alpha$  activity (0.3 per cent of the initial  $\alpha$  activity) was carried on the lanthanum fluoride, and the 5-min growth could not be observed above this background. Then a sample of the lanthanum fluoride precipitate was left for 40 min in an atmospheric  $\alpha$  counter, and after removal of the sample the background built up in the counter by recoil atoms was followed and was found to decay with a half life of 47 min. This is believed to indicate  $\text{Bi}^{213}$  and  $\text{Po}^{213}$ , daughters of  $\text{Ac}^{225}$  and  $\text{Pa}^{229}$ .

No evidence for  $\text{Pa}^{229}$  could be found in  $\alpha$ -pulse analyses of the protactinium fractions. The limit of detection by this method, assuming 1 per cent  $\alpha$  branching, gives a cross section of less than  $1 \times 10^{-27}$  sq cm for formation of  $\text{Pa}^{229}$ . If there were 5 counts per minute of K x rays from  $\text{Pa}^{229}$  which were unresolved in the beryllium-plus-lead absorption curve of Fig. 3, the cross section for formation of  $\text{Pa}^{229}$  (assuming 99 per cent decay by K-electron capture, one K x ray per disintegration, and 0.5 per cent counting efficiency) would be  $9 \times 10^{-27}$  sq cm.

An attempt was also made to find  $\text{Pa}^{229}$  by isolating a protactinium fraction from a portion of the uranium fraction of the first deuteron bombardment 42 hr after the initial separation. The fraction was examined by pulse analysis, and no  $\text{Pa}^{229}$  was found. This observation is to be expected in view of later work, which has shown  $\text{U}^{229}$  to have a half life of only 58 min.<sup>17</sup>

**4.4  $\text{U}^{230}$ .** Alpha-pulse analyses of the uranium fraction soon after separation showed the five peaks characteristic of the  $\text{U}^{230}$  series,<sup>13</sup> and the total  $\alpha$  activity of the uranium fraction decayed with a half life close to the known value for  $\text{U}^{230}$ , 20.8 days.<sup>13</sup> The relative amounts of  $\text{U}^{230}$  and  $\text{Pa}^{231}$  were determined by  $\alpha$  counting of the separated uranium and protactinium fractions and also by  $\alpha$ -pulse analysis of the original solution of the target material. The yield of  $\text{U}^{230}$  was

greater than could be accounted for by  $\beta^-$  decay of  $\text{Pa}^{230}$ , and the excess corresponded to a cross section for the reaction  $\text{Pa}^{231}(\text{d},\text{3n})\text{U}^{230}$  of  $5 \times 10^{-27}$  sq cm in the first deuteron bombardment and  $17 \times 10^{-27}$  in the second.

**4.5  $\text{U}^{232}$ .** This isotope was determined quantitatively in two ways: by  $\alpha$ -pulse analyses of the uranium fraction after the  $\text{U}^{230}$  series had decayed, and by isolating its daughter,  $\text{Th}^{228}$ , from the uranium fraction. In the pulse analyses  $\text{U}^{232}$  was not resolved from  $\text{Po}^{210}$  and  $\text{Th}^{228}$ , but the  $\text{Po}^{210}$  activity could be calculated from the amount of  $\text{U}^{230}$  originally present in the sample, and the ratio of  $\text{Th}^{228}$  to  $\text{U}^{232}$  activities could be calculated from the known half lives of  $\text{Th}^{228}$  (1.90 years<sup>18</sup>) and of  $\text{U}^{232}$  (70 years<sup>19</sup>). The  $\text{Th}^{228}$  content of the thorium isolated from the uranium fraction was determined both by following the growth of  $\alpha$  activity and by pulse analyses. The chemical yield was measured by means of UX, ( $\text{Th}^{234}$ ) tracer.

The yields of  $\text{U}^{232}$  seemed to be in excess of the amounts arising from the decay of  $\text{Pa}^{232}$ . From the difference the cross section for the formation of  $\text{U}^{232}$  by the reaction  $\text{Pa}^{231}(\text{d},\text{n})$  was calculated to be  $5 \times 10^{-27}$  sq cm in the first deuteron bombardment and  $23 \times 10^{-27}$  sq cm in the second. This cross section is very inaccurate because most of the  $\text{U}^{232}$  came from decay of  $\text{Pa}^{232}$ , and the determination of the  $\text{Pa}^{232}$  was subject to the usual errors of absolute  $\beta^-$  counting.

**4.6  $\text{U}^{231}$ .** A new 4.2-day x-ray activity, found in the uranium fraction, has been tentatively assigned to K-electron capture by  $\text{U}^{231}$ . The assignment has the following basis. From energy considerations the only uranium isotopes that could be produced by bombardment of  $\text{Pa}^{231}$  with 21-mev deuterons are  $\text{U}^{232}$ ,  $\text{U}^{231}$ ,  $\text{U}^{230}$ , and  $\text{U}^{229}$ . These could be produced either directly by (d,xn) reactions or by  $\beta^-$  decay of protactinium isotopes formed by (d,pxn) reactions.  $\text{U}^{232}$  and  $\text{U}^{230}$  had previously been definitely assigned to other activities by identification of daughter activities known in the natural radioactive series.<sup>13,20</sup> Orbital-electron capture by  $\text{U}^{229}$  was ruled out by the failure to find  $\text{Pa}^{229}$  by  $\alpha$ -pulse analysis of a protactinium fraction isolated from the uranium fraction 42 hr after the initial separation, as mentioned under  $\text{Pa}^{230}$ . Furthermore, subsequent work by Meinke, Ghiorso, and Seaborg<sup>17</sup> has shown that  $\text{U}^{229}$  is a 1-hr K-capturing isotope. The possibility that the activity is an isomeric transition seems to be eliminated by the high yield, which is comparable with the yield of  $\text{U}^{230}$  by the (d,3n) reaction. The remaining possibility is  $\text{U}^{231}$ .

The half life was determined by observation of the decay of the activity, as shown in Fig. 11. The half life of the long-lived tail due to  $\text{U}^{230}$  was taken as 20.8 days,<sup>13</sup> and a calculated correction for the growth of daughters of  $\text{U}^{230}$  and  $\text{U}^{232}$  was applied to the decay curve

obtained through thin cellophane.<sup>†</sup> The average value of the half life from all the curves is  $4.2 \pm 0.1$  days.

Lead and aluminum absorption curves of the uranium fraction a few days after separation are given in Figs. 12 and 13. The lead curve

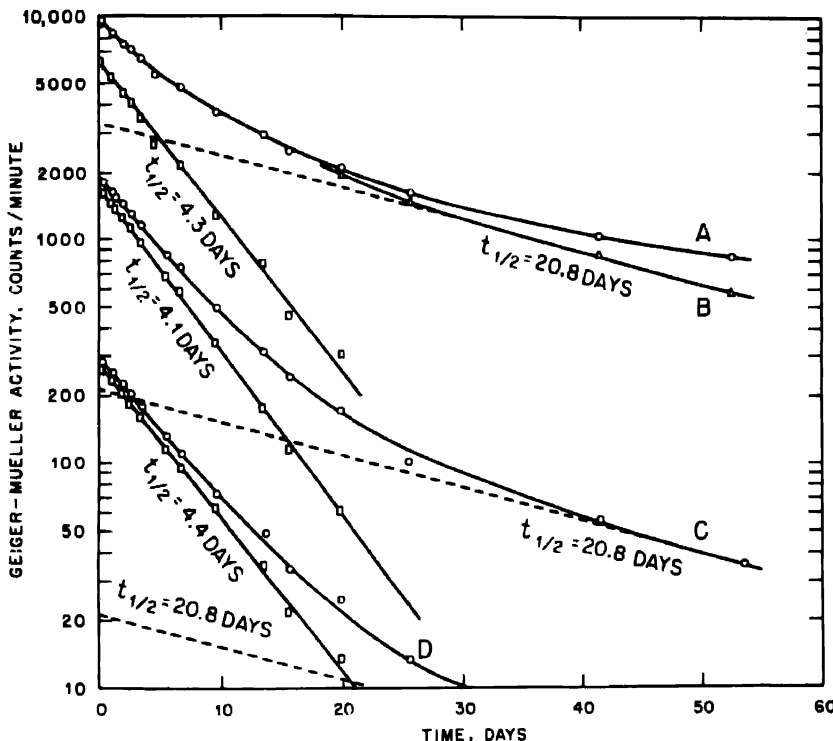


Fig. 11—Decay of Geiger-Mueller activity in uranium fraction from first deuteron bombardment. A, through cellophane (12.1 mg/sq cm total absorber). B, curve A minus calculated correction for growth of daughters of  $\text{U}^{230}$  and  $\text{U}^{232}$ . C, through 2.0 g/sq cm of beryllium. D, through 2.0 g/sq cm of beryllium plus 77 mg/sq cm of lead. The curves are resolved into 20.8 day and 4.1- to 4.4-day half lives.

has a small component with 3.0 to 3.5 g/sq cm half thickness (0.40 to 0.43 mev), one with about 210 mg/sq cm half thickness (70 or 123 kev), believed to be mainly K x rays, which have an energy of about 100 kev, and softer components. The aluminum curves show a component with 5.2 g/sq cm half thickness (170 kev), believed to be mainly K x rays, and softer components with half thicknesses of 192 mg/sq

<sup>†</sup>Cellophane was used to cover the samples of the uranium fraction to avoid contamination of the counter with recoil atoms from the  $\text{U}^{230}$  series.

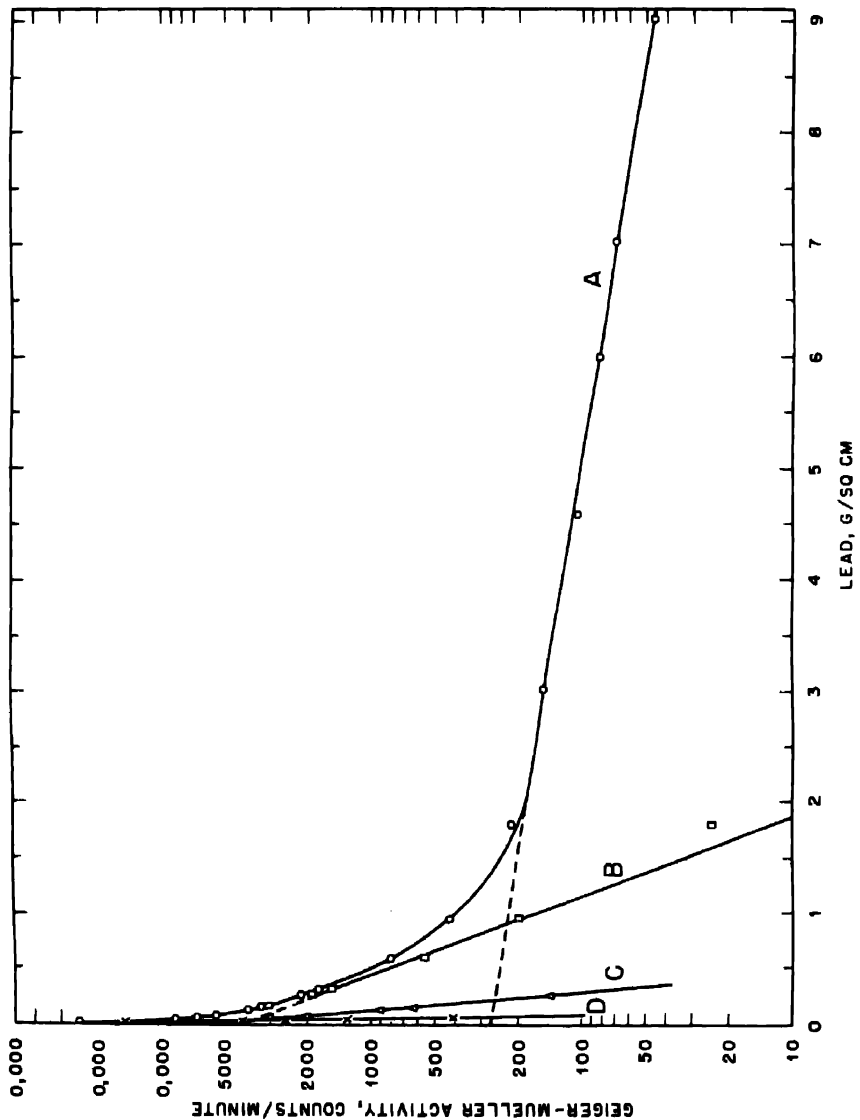


Fig. 12—Lead absorption curves of uranium fraction, resolved into curve A, 3.5 g/sq cm half thickness (0.43 mev); curve B, 210 mg/sq cm half thickness (70 or 123 kev); curve C, 46 mg/sq cm half thickness (40 kev); and curve D, 10 mg/sq cm half thickness (13 or 22 kev).

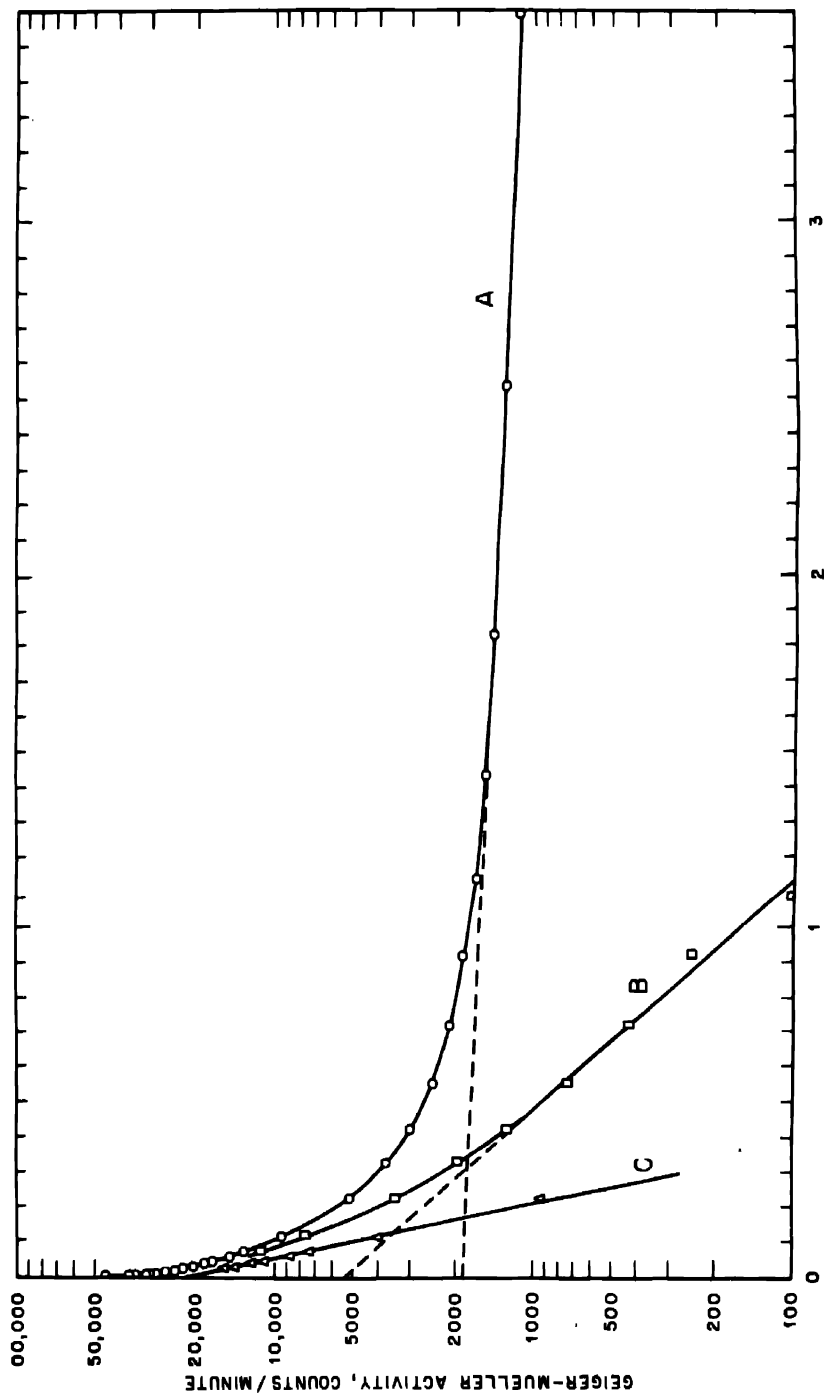


Fig. 13—Aluminum absorption curves of uranium fraction, resolved into curve A, 5.2 g/sq cm alf thickness (170 kev); curve B, 192 mg/sq cm half thickness (20 kev); and curve C, 45 mg/sq cm thickness (13.5 kev).

cm (20 kev) or less. A lead absorption curve with 2.0 g/sq cm of beryllium covering the sample was also taken, and a component with a half thickness of 202 mg/sq cm of lead (69 or 121 kev) and softer components were found. The softer components may not be significant because the decay curves show that approximately 25 per cent of the activity through cellophane was due to the 20.8-day tail at the time the aluminum absorption curve was determined. Because of the growth of daughters of  $U^{230}$  and  $U^{232}$  it was not possible to determine the correction by remeasuring the absorption curves after the  $U^{231}$

Table 2 — Reactions and Cross Sections Observed in Bombardment of  $Pa^{231}$  with 21-mev Deuterons

Reaction	Cross section, sq cm $\times 10^{-27}$	
	Bombardment 1	Bombardment 2
$Pa^{231}(d,p)Pa^{232}$	40	60
$Pa^{231}(d,p2n)Pa^{230}$	23	27
$Pa^{231}(d,p3n)Pa^{229}$		
$+ Pa^{231}(d,4n)U^{229} \xrightarrow{K\gamma} Pa^{229}$	<1	
$Pa^{231}(d,n)U^{232}$	5	23
$Pa^{231}(d,2n)U^{231}$	3	7
$Pa^{231}(d,3n)U^{230}$	5	17

had decayed. The contribution of the 20.8-day tail was not so important for the harder components, but it may account for finding somewhat high values for the K x-ray energy.

The yield of  $U^{231}$  was calculated from the average abundance of the K x rays in the absorption curves, assuming a counting efficiency of 0.5 per cent and one K x ray per disintegration. The cross section for the reaction  $Pa^{231}(d,2n)U^{231}$  was  $3 \times 10^{-27}$  sq cm in the first bombardment and  $7 \times 10^{-27}$  sq cm in the second.

In order to determine the  $U^{231}$   $\alpha$  branching and half life for  $\alpha$  emission, thorium daughters were isolated four times from a portion of the uranium fraction at intervals from 42 to 475 hr after the initial uranium separation. The thorium daughters,  $Th^{227}$  and  $Th^{228}$ , were determined by following the growth and decay of  $\alpha$  activity in the thorium fraction.  $Th^{228}$  was found in all the extractions.  $Th^{227}$  was found in the first isolation, but none was found in subsequent thorium extractions. The  $Th^{227}$  found in the first thorium extraction probably was a daughter of  $Pa^{231}$ , and a small amount was extracted with the uranium fraction. From the limit of detection of  $Th^{227}$  in these experiments the  $U^{231}$   $\alpha$  branching is less than 0.05 per cent and the  $U^{231}$  half life is greater than 20 years.

4.7 Summary of Reactions and Cross Sections. A summary of the reactions and cross sections observed in the deuteron bombardments is given in Table 2.

### 5. RESULTS OF HELIUM-ION BOMBARDMENTS

5.1  $\text{Pa}^{230}$ . The only activity found in the protactinium fraction other than  $\text{Pa}^{231}$  was  $\text{Pa}^{230}$ . However, the proportion of the Geiger-Mueller activity due to the  $\text{Pa}^{230}$  was too small for absorption curves of this fraction to be useful for characterization of the radiations of  $\text{Pa}^{230}$ . The yield of  $\text{Pa}^{230}$  was obtained by chemical isolation of uranium from the protactinium fraction 21 days after the original separation from uranium. A value of 10 was used for the  $K/\beta^-$  branching ratio<sup>14</sup> in the calculations. Pulse analyses showed only  $\text{U}^{230}$  series in this uranium fraction. From the yield of  $\text{Pa}^{230}$  a cross section of  $6 \times 10^{-27}$  sq cm was calculated for the reaction  $\text{Pa}^{231}(\alpha, \alpha n)\text{Pa}^{230}$ . Some  $\text{Pa}^{230}$  could conceivably arise from  $\alpha$  branching of  $\text{Np}^{234}$ , but, since the upper limit of the  $\alpha$  branching of  $\text{Np}^{234}$  is less than 0.1 per cent<sup>21</sup> (correcting<sup>14</sup> for the  $K$  branching of  $\text{Pa}^{230}$ ) and the observed yield of  $\text{Np}^{234}$  was smaller than the  $\text{Pa}^{230}$  yield, it follows that the quantity of  $\text{Pa}^{230}$  that could have been formed by  $\alpha$  decay of  $\text{Np}^{234}$  was entirely negligible.

5.2  $\text{U}^{230}$ . The most abundant  $\alpha$  activity in the uranium fraction, as shown by pulse analyses and also by  $\alpha$  decay, was the  $\text{U}^{230}$  series. The yield from all reactions corresponded to a cross section of  $0.16 \times 10^{-27}$  sq cm. All this could be accounted for by  $\beta^-$  decay of  $\text{Pa}^{230}$ , but because of experimental uncertainties the cross section for the formation by the reactions  $\text{Pa}^{231}(\alpha, p4n)\text{U}^{230}$  and  $\text{Pa}^{231}(\alpha, \alpha n)\text{Np}^{230} \xrightarrow{K?} \text{U}^{230}$  might possibly be as large as  $0.01 \times 10^{-27}$  sq cm.

5.3  $\text{U}^{232}$ . After decay of the  $\text{U}^{230}$  series, pulse analyses showed that there was  $\text{U}^{232}$  in the uranium fraction, and the amount gave a cross section of approximately  $9 \times 10^{-27}$  sq cm for the reaction  $\text{Pa}^{231}(\alpha, p2n)\text{U}^{232}$  plus possibly  $\text{Pa}^{231}(\alpha, 3n)\text{Np}^{232} \xrightarrow{K?} \text{U}^{232}$ .

5.4  $\text{U}^{229}$ . About 3 per cent of the initial  $\alpha$  activity of the uranium fraction seemed to decay with a half life of the order of 1.5 days, which corresponds to a cross section of  $7 \times 10^{-30}$  sq cm. In order to determine whether this activity was a real one that could be assigned to  $\text{U}^{229}$  or merely a spurious instrumental effect, two short helium-ion bombardments were later carried out at the Radiation Laboratory, University of California. A combined uranium-neptunium fraction was separated quickly and examined with the pulse analyzer. No  $\alpha$  activities other than the  $\text{U}^{230}$  series were found, and hence it is believed that the effect was merely instrumental error. Other observers

have subsequently produced  $U^{220}$  by bombardment of thorium with higher energy helium ions and have shown that it is a 58-min isotope, which decays approximately 20 per cent by  $\alpha$  emission and 80 per cent by capture of an orbital electron.<sup>17</sup>

5.5  $U^{231}$ . The 4.2-day x-ray activity found in the uranium fractions of the deuteron bombardments was also found in the uranium

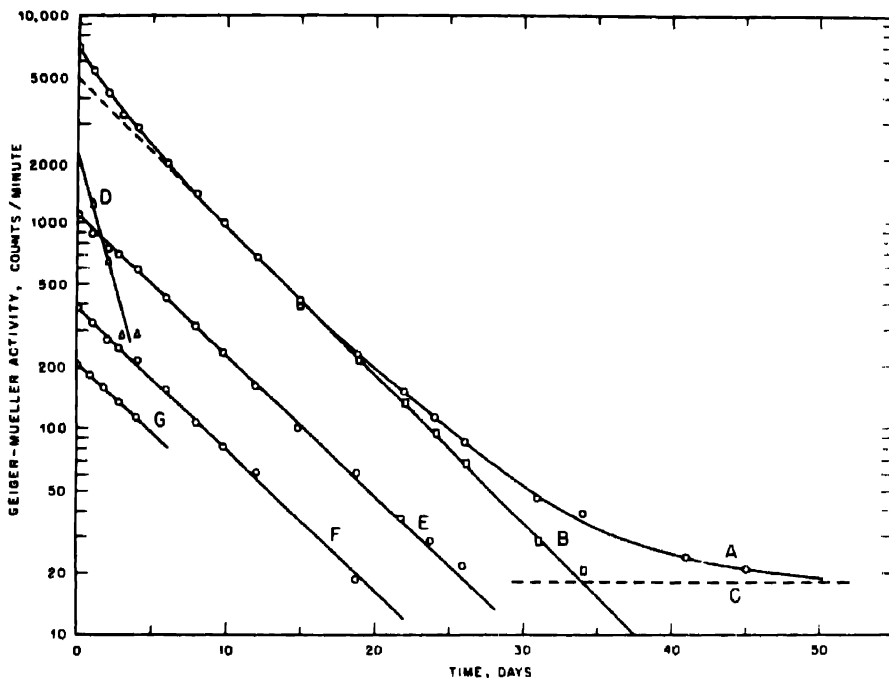


Fig. 14—Decay of Geiger-Mueller activity in neptunium fraction from helium-ion bombardment. A, decay through cellophane. B (half life, 4.2 days), curve A less long-lived tail, curve C, due to  $Pa^{231}$  contaminant. D, approximately 1.2-day component of decay through cellophane. E (half life, 4.4 days), decay through 2.0 g/sq cm of beryllium. F (half life, 4.4 days), decay through 2.0 g/sq cm of beryllium plus 59 mg/sq cm of lead. G (half life, 4.4 days), decay through 5.0 g/sq cm of lead. Determined on xenon-filled counter.

fraction from the first helium-ion bombardment. Geiger-Mueller decay curves and absorption curves were essentially the same for the uranium fractions from all the bombardments. The total cross section for the formation of  $U^{231}$  by the reaction  $Pa^{231}(\alpha, p3n)U^{231}$  plus possibly the reaction  $Pa^{231}(\alpha, 4n)Np^{231}$ .  $U^{231}$  was calculated to be  $0.4 \times 10^{-27}$  sq cm from the abundance of K x rays found in the absorption curves.

**5.6 Np<sup>234</sup>.** An activity with a hard  $\gamma$  ray (about 1.9 mev) and K and L x rays, which decayed with a half life of 4.4 days, was found in the neptunium fraction. The radiations and half life agree with those found by Hyde, Studier, and Ghiorso<sup>21</sup> in the neptunium fractions from deuteron and helium-ion bombardments of U<sup>233</sup>, which have been assigned<sup>21</sup> to Np<sup>234</sup>.

Figure 14 shows the decay of the Geiger-Mueller activity in the neptunium fraction through various absorbers, as measured on a xenon-filled counter. A 4.2- to 4.4-day component was found in all the decay curves. The best value for the half life was 4.4 days, obtained from the decay through 2.0 g/sq cm of beryllium and through this amount of beryllium plus 59 mg/sq cm of lead.

Table 3—Reactions and Cross Sections Observed in Bombardment of Pa<sup>231</sup> with 42-mev Helium Ions

Reaction	Cross section, sq cm $\times 10^{-27}$
Pa <sup>231</sup> ( $\alpha$ , $\alpha$ n)Pa <sup>230</sup>	6
Pa <sup>231</sup> ( $\alpha$ ,p2n)U <sup>232</sup>	
+ Pa <sup>231</sup> ( $\alpha$ ,3n)Np <sup>232</sup> $\xrightarrow{K\gamma}$ U <sup>232</sup>	9
Pa <sup>231</sup> ( $\alpha$ ,p3n)U <sup>231</sup>	
+ Pa <sup>231</sup> ( $\alpha$ ,4n)Np <sup>231</sup> $\xrightarrow{K\gamma}$ U <sup>231</sup>	0.4
Pa <sup>231</sup> ( $\alpha$ ,p4n) U <sup>230</sup>	
+ Pa <sup>231</sup> ( $\alpha$ ,5n)Np <sup>230</sup> $\xrightarrow{K\gamma}$ U <sup>230</sup>	<0.01
Pa <sup>231</sup> ( $\alpha$ ,n)Np <sup>234</sup>	1.5
Pa <sup>231</sup> ( $\alpha$ , fission)	300

The yield was determined from the K x-ray component of the absorption curves, assuming a counting efficiency of 0.5 per cent and one K x ray per disintegration. The cross section for the reaction Pa<sup>231</sup>( $\alpha$ ,n)Np<sup>234</sup> was calculated to be  $1.5 \times 10^{-27}$  sq cm.

**5.7 1.2-day Neptunium.** A neptunium  $\beta$  activity with a half life of approximately 1.2 days was also found in the decay of Geiger-Mueller activity through cellophane (Fig. 14). The sample was examined for positrons by means of a crude magnet counter, and none were detected. The cross section for the formation of the 1.2-day activity, assuming that it was formed from Pa<sup>231</sup>, was only  $9 \times 10^{-29}$  sq cm. The activity is believed to be due to 2.33-day Np<sup>230</sup> or 2.10-day Np<sup>238</sup> from a small uranium impurity in the sample of Pa<sup>231</sup> that was bombarded.

**5.8 Alpha-fission Cross Section.** A rough value for the cross section for fission of Pa<sup>231</sup> by 38-mev helium ions was determined by

measuring the yield of  $\text{Ba}^{140}$ . Assuming the same yield curve as for fission of  $\text{U}^{238}$  by thermal neutrons, a value of  $0.3 \times 10^{-24}$  sq cm was obtained.

**6.9 Summary of Reactions and Cross Sections.** A summary of the reactions and cross sections observed in the first helium-ion bombardment is given in Table 3.

## 6. SUMMARY

Bombardments of  $\text{Pa}^{231}$  have been carried out with 21-mev deuterons and 42-mev helium ions. The isotopes produced and identified were  $\text{Pa}^{232}$ ,  $\text{Pa}^{230}$ ,  $\text{Pa}^{229}(?)$ ,  $\text{U}^{232}$ ,  $\text{U}^{231}$ , and  $\text{U}^{230}$  in the deuteron bombardments, and  $\text{Pa}^{230}$ ,  $\text{U}^{232}$ ,  $\text{U}^{231}$ ,  $\text{U}^{230}$ , and  $\text{Np}^{234}$  in the helium-ion bombardments. Cross sections for the various reactions have been determined.

A new uranium isotope with a half life of  $4.2 \pm 0.1$  days, which emits K and L x rays and a few 0.4-mev  $\gamma$  rays, has been found and tentatively assigned to  $\text{U}^{231}$ . The  $\alpha$  branching of  $\text{U}^{231}$  has been found to be less than 0.05 per cent, and the  $\alpha$  half life is greater than twenty years.

The radiations of  $\text{Pa}^{232}$  and  $\text{Np}^{234}$  have been characterized by absorption measurements, and the results are in essential agreement with previous work.

$\text{Pa}^{230}$  was found to have a half life of  $17.7 \pm 0.5$  days by observation of the decay of Geiger-Mueller activity through beryllium and lead absorbers, and it was found to have a 0.94-mev  $\gamma$  ray, K x rays, L x rays, a  $\beta$  particle with a maximum energy of approximately 430 kev, and a  $\beta$  particle with a maximum energy of about 220 kev. The abundances per  $\beta^-$  disintegration into  $\text{U}^{230}$ , corrected for counting efficiencies and back-scattering, were approximately 5, 9, 14, 0.22, and 1, respectively. These results indicate a  $K/\beta^-$  branching ratio of 9.

## ACKNOWLEDGMENTS

The advice and encouragement of Drs. G. T. Seaborg and W. M. Manning, who suggested the problem and under whose direction the work was performed, is gratefully acknowledged. The authors wish also to thank Dr. J. G. Hamilton and his associates, who carried out the bombardments with the Berkeley 60-in. cyclotron, and A. Ghiorso, B. Weissbourd, H. Robinson, and D. Connor, who made most of the pulse analyses.

## REFERENCES

1. K. A. Kraus and Q. Van Winkle, Metallurgical Project Report CC-3365 (1945); National Nuclear Energy Series, Division IV, Volume 17B.
2. R. G. Larson, L. I. Katzin, and E. Hausman, Argonne National Laboratory Report ANL-4091 (1947); National Nuclear Energy Series, Division IV, Volume 17B.
3. R. C. Thompson, Q. Van Winkle, and J. G. Malm, Metallurgical Project Report CC-3789 (1947); National Nuclear Energy Series, Division IV, Volume 17B.
4. A. V. Grosse and M. S. Agruss, *J. Am. Chem. Soc.*, 56: 2200 (1934).
5. J. G. Hamilton, private communication.
6. A. Ghiorso, A. H. Jaffey, H. P. Robinson, and B. Weissbourd, A 48-channel pulse-height analyzer for alpha-energy measurements, Paper 16.8, this volume (Metallurgical Project Report CC-3887).
7. A. H. Jaffey, Radiochemical assay by alpha and fission measurements, Metallurgical Project Report CC-3771 (1947); also in National Nuclear Energy Series, Division IV, Volume 14A.
8. J. A. Simpson, Metallurgical Project Reports CP-1527 (1944) and CP-1817 (1945).
9. A. H. Jaffey, T. P. Kohman, and J. A. Crawford, Metallurgical Project Report CC-1602 (1944); Manhattan District Declassified Document MDDC-388.
10. A. H. Jaffey and E. K. Hyde, Argonne National Laboratory Report ANL-4102 (1948); National Nuclear Energy Series, Division IV, Volume 17B; cited by G. T. Seaborg and I. Perlman, *Revs. Modern Phys.*, 20: 585 (1948).
11. A. H. Jaffey and Q. Van Winkle, Argonne National Laboratory Report ANL-4193 (1948); National Nuclear Energy Series, Division IV, Volume 17B; cited by G. T. Seaborg and I. Perlman, *Revs. Modern Phys.*, 20: 585 (1948).
12. D. W. Engelkemeir, J. A. Seiler, E. P. Steinberg, L. Winsberg, and T. B. Novey, National Nuclear Energy Series, Division IV, Volume 9, Paper 5.
13. M. H. Studier and E. K. Hyde, Metallurgical Project Report CC-3662 (1946); National Nuclear Energy Series, Division IV, Volume 17B; *Phys. Rev.*, 74: 591 (1948).
14. M. H. Studier and R. J. Bruehlman, private communication.
15. E. K. Hyde, M. H. Studier, H. H. Hopkins, Jr., and A. Ghiorso, A new isotope of protactinium:  $\text{Pa}^{233}$ , Paper 19.17, this volume (Metallurgical Project Report CC-3648); cited by G. T. Seaborg and I. Perlman, *Revs. Modern Phys.*, 20: 585 (1948).
16. E. K. Hyde, M. H. Studier, and R. J. Bruehlman, Argonne National Laboratory Report ANL-4112 (1948); cited by G. T. Seaborg and I. Perlman, *Revs. Modern Phys.*, 20: 585 (1948).
17. W. W. Melinke, A. Ghiorso, and G. T. Seaborg, unpublished data (1948); cited by G. T. Seaborg and I. Perlman, *Revs. Modern Phys.*, 20: 585 (1948).
18. M. Curie, A. Debierre, A. S. Eve, H. Geiger, O. Hahn, S. C. Lind, S. Meyer, E. Rutherford, and E. Schmidler, *Revs. Modern Phys.*, 3: 427 (1931).
19. R. A. James, A. E. Florin, H. H. Hopkins, Jr., and A. Ghiorso, Products of helium-ion and deuteron bombardment of  $\text{U}^{235}$  and  $\text{U}^{238}$ , Paper 22.8, this volume (Metallurgical Project Report CC-3860); cited by G. T. Seaborg and I. Perlman, *Revs. Modern Phys.*, 20: 585 (1948).
20. J. W. Gofman and G. T. Seaborg, Metallurgical Project Report CN-332 (1942); cited by G. T. Seaborg and I. Perlman, *Revs. Modern Phys.*, 20: 585 (1948).
21. E. K. Hyde, M. H. Studier, and A. Ghiorso, Products of the deuteron and helium-ion bombardments of  $\text{U}^{233}$ , Paper 22.15, this volume (Metallurgical Project Report CB-3736); cited by G. T. Seaborg and I. Perlman, *Revs. Modern Phys.*, 20: 585 (1948).

Paper 19.12

HALF LIFE OF Th<sup>227</sup> (RADIOACTINIUM)†

By S. Peterson and A. Ghiorso

Because of the complicated growth and decay of activity in samples of Th<sup>227</sup>(RdAc), previous measurement of the half life<sup>1</sup> has depended on an involved mathematical analysis of carefully determined activity-time curves. Use of the multichannel differential pulse analyzer,<sup>2</sup> which can measure individual  $\alpha$  activities in a mixture, is a method with fewer inherent errors.

Since the  $\alpha$ -particle energies of Th<sup>227</sup> overlap those of its daughter Ra<sup>223</sup>(AcX), simply following decay of Th<sup>227</sup> with the pulse analyzer is unsatisfactory. However, samples of the activity mixed with isotopic standards can be purified from daughter activities with measurable yields and thus afford a good measure of the rate of decay.

Thorium iodate was precipitated from an approximately 3M HNO<sub>3</sub> solution containing tracer activity of Th<sup>227</sup> and long-lived Th<sup>230</sup> (ionium). The precipitate was dissolved in nitric acid by use of sulfur dioxide and reprecipitated with iodic acid to separate it from isotopes of radium and actinium. The second precipitate was dissolved and diluted to a thorium concentration of 0.5 g per liter in 3M HNO<sub>3</sub>. On 11 occasions, spread over a period of 76 days, the thorium was precipitated from successive 50-microliter portions of the solution and reprecipitated a sufficient number of times to ensure complete separation from isotopes of radium.

Each final iodate precipitate was mounted on a platinum disk, and the  $\alpha$  particles from Th<sup>227</sup> and Th<sup>230</sup> were counted simultaneously in the pulse analyzer. The ratio of the two activities was found both graphically and by least-squares analysis to decay exponentially with a half life of  $18.6 \pm 0.1$  days.

†Contribution from the Chemistry Division of the Metallurgical Laboratory, University of Chicago, now the Argonne National Laboratory.

Table 1—Decay of Th<sup>227</sup>

Time, days	Ratio of $\alpha$ activities, Th <sup>227</sup> /Th <sup>230</sup>	Time, days	Ratio of $\alpha$ activities, Th <sup>227</sup> /Th <sup>230</sup>
1.01	1.654	31.1	0.5327
4.17	1.420	40.0	0.3859
7.15	1.309	50.0	0.2663
11.13	1.121	62.2	0.1676
15.04	0.9835	76.1	0.0979
19.10	0.8464		

Summary. Direct decay of Th<sup>227</sup> has been measured by periodical purification from daughters of portions of a solution containing Th<sup>230</sup> and measurement of the ratio of the two activities with the pulse analyzer. The half life is  $18.6 \pm 0.1$  days.

## REFERENCES

1. H. N. McCoy and E. D. Leman, Phys. Rev., 4: 409-419 (1914).
2. A. Chiarso, A. H. Jaffey, H. P. Robinson, and B. Weissbourd, A 48-channel pulse-height analyzer for alpha-energy measurements, Paper 16.8, this volume (Metallurgical Project Report CC-3887).

## Paper 19.13

### NUCLEAR PROPERTIES OF U<sup>233</sup>: A NEW FISSIONABLE ISOTOPE OF URANIUM†

By G. T. Seaborg, J. W. Gofman, and R. W. Stoughton

The bombardment of thorium with slow neutrons produces Th<sup>233</sup> [by the reaction Th<sup>232</sup>(n, $\gamma$ )Th<sup>233</sup>], which emits  $\beta$  particles and has a half life of 23.5 min. The daughter of Th<sup>233</sup> is the 27.4-day  $\beta$ -emitting Pa<sup>233</sup>, which in turn decays to U<sup>233</sup>. We have measured the radioactive and fission properties of U<sup>233</sup>. This isotope has a half life of about  $1.2 \times 10^5$  years and emits  $\alpha$  particles having a range of  $3.1 \pm 0.2$  cm. Our measurements on a sample of U<sup>233</sup> weighing 3.8  $\mu$ g show that this isotope undergoes fission with slow neutrons with a cross section of the same order as that of U<sup>235</sup>. The same result was obtained in a check experiment with another sample of U<sup>233</sup> weighing 0.8  $\mu$ g.

†Contribution from the Department of Chemistry and the Radiation Laboratory, University of California, Berkeley.

This paper was mailed from Berkeley, California, to the Uranium Committee in Washington, D. C., on April 14, 1942. The experimental work was done during 1941 and the early part of 1942.

Paper 19.14

PRODUCTION AND PROPERTIES OF U<sup>232</sup> AND Pa<sup>232</sup>†

By J. W. Gofman and G. T. Seaborg

It might be expected that the bombardment of thorium (single isotope,  $_{90}\text{Th}^{232}$ ) with deuterons (about 14 mev energy) in the 60-in. Berkeley cyclotron would result in the production of the isotope  $_{91}\text{Pa}^{232}$  by the (d,2n) reaction, in addition to the production of  $_{90}\text{Th}^{233}$  by the (d,p) reaction and the production of  $_{91}\text{Pa}^{233}$  by the (d,n) reaction. Since the  $_{91}\text{Pa}^{232}$  might decay to  $_{92}\text{U}^{232}$ , which could be very useful as a tracer isotope for uranium, this experiment was undertaken. It was found that the deuteron bombardment of thorium produces a 1.6-day  $\beta$ - and  $\gamma$ -emitting  $_{91}\text{Pa}^{232}$ , which decays to a 30-year  $\alpha$ -emitting  $_{92}\text{U}^{232}$ .

A target of metallic thorium was bombarded with 500  $\mu\text{a}\cdot\text{hr}$  of deuterons. After the bombardment the protactinium was isolated chemically with the help of zirconium as a carrier. The thorium was digested for several hours with aqua regia, after which a fairly large fraction still remained undissolved. The solid residue was taken up in 18N  $\text{H}_2\text{SO}_4$  and fumed for several hours to convert into the sulfate, which then dissolved completely upon dilution of the acid to 3N concentration. Zirconium nitrate was then added to both the aqua regia and sulfuric acid fractions, and the protactinium was separated by two successive zirconium phosphate precipitations from each fraction. The zirconium phosphate precipitates, containing the protactinium, were washed with 6N HCl and then dissolved in 6N HF. A small amount of thorium fluoride, which had coprecipitated with the zirconium phosphate, precipitated at this point and was centrifuged out. The hydrofluoric acid solution, which contained the protactinium, was

†Contribution from the Department of Chemistry and the Radiation Laboratory, University of California, Berkeley.

This paper was submitted as a report to the Metallurgical Laboratory of the Plutonium Project on Oct. 20, 1942.

Paper 19.13

NUCLEAR PROPERTIES OF U<sup>233</sup>: A NEW FISSIONABLE ISOTOPE  
OF URANIUM†

By G. T. Seaborg, J. W. Gofman, and R. W. Stoughton

The bombardment of thorium with slow neutrons produces Th<sup>233</sup> [by the reaction Th<sup>232</sup>(n,γ)Th<sup>233</sup>], which emits β particles and has a half life of 23.5 min. The daughter of Th<sup>233</sup> is the 27.4-day β-emitting Pa<sup>233</sup>, which in turn decays to U<sup>233</sup>. We have measured the radioactive and fission properties of U<sup>233</sup>. This isotope has a half life of about  $1.2 \times 10^5$  years and emits α particles having a range of  $3.1 \pm 0.2$  cm. Our measurements on a sample of U<sup>233</sup> weighing 3.8 μg show that this isotope undergoes fission with slow neutrons with a cross section of the same order as that of U<sup>235</sup>. The same result was obtained in a check experiment with another sample of U<sup>233</sup> weighing 0.8 μg.

†Contribution from the Department of Chemistry and the Radiation Laboratory, University of California, Berkeley.

This paper was mailed from Berkeley, California, to the Uranium Committee in Washington, D. C., on April 14, 1942. The experimental work was done during 1941 and the early part of 1942.

Paper 19.14

PRODUCTION AND PROPERTIES OF U<sup>232</sup> AND Pa<sup>232</sup>†

By J. W. Gofman and G. T. Seaborg

It might be expected that the bombardment of thorium (single isotope,  $_{90}\text{Th}^{232}$ ) with deuterons (about 14 mev energy) in the 60-in. Berkeley cyclotron would result in the production of the isotope  $_{91}\text{Pa}^{232}$  by the (d,2n) reaction, in addition to the production of  $_{90}\text{Th}^{233}$  by the (d,p) reaction and the production of  $_{91}\text{Pa}^{233}$  by the (d,n) reaction. Since the  $_{91}\text{Pa}^{232}$  might decay to  $_{92}\text{U}^{232}$ , which could be very useful as a tracer isotope for uranium, this experiment was undertaken. It was found that the deuteron bombardment of thorium produces a 1.6-day  $\beta$ - and  $\gamma$ -emitting  $_{91}\text{Pa}^{232}$ , which decays to a 30-year  $\alpha$ -emitting  $_{92}\text{U}^{232}$ .

A target of metallic thorium was bombarded with 500  $\mu\text{a}\cdot\text{hr}$  of deuterons. After the bombardment the protactinium was isolated chemically with the help of zirconium as a carrier. The thorium was digested for several hours with aqua regia, after which a fairly large fraction still remained undissolved. The solid residue was taken up in 18N  $\text{H}_2\text{SO}_4$  and fumed for several hours to convert into the sulfate, which then dissolved completely upon dilution of the acid to 3N concentration. Zirconium nitrate was then added to both the aqua regia and sulfuric acid fractions, and the protactinium was separated by two successive zirconium phosphate precipitations from each fraction. The zirconium phosphate precipitates, containing the protactinium, were washed with 6N HCl and then dissolved in 6N HF. A small amount of thorium fluoride, which had coprecipitated with the zirconium phosphate, precipitated at this point and was centrifuged out. The hydrofluoric acid solution, which contained the protactinium, was

†Contribution from the Department of Chemistry and the Radiation Laboratory, University of California, Berkeley.

This paper was submitted as a report to the Metallurgical Laboratory of the Plutonium Project on Oct. 20, 1942.

cooled to 0°C and poured into an excess of ice-cold 4N NaOH. The resulting zirconium hydroxide precipitate, containing protactinium hydroxide, was centrifuged out and dissolved in 4N HNO<sub>3</sub>.

At this stage in the chemical procedure the amount of zirconium carrier was reduced by carrying out a fractional precipitation of zirconium iodate. More than 96 per cent of the protactinium radioactivity was concentrated in the first 10 per cent of the zirconium precipitated as the iodate.

The zirconium iodate was dissolved in 9N HCl and a second phosphate-hydrofluoric acid-sodium hydroxide cycle was carried out. The final zirconium hydroxide precipitate, containing the protactinium hydroxide, was dissolved in a mixture of hydrochloric, nitric, and sulfuric acids and evaporated to dryness to convert it to the sulfate. The dried zirconium sulfate, 36 mg in weight, was dissolved in 30 ml of 0.3M NH<sub>4</sub>F solution; the pH was adjusted to the methyl red end point; and the solution was electrolyzed for about 10 hr, a copper cathode being used. In this procedure, with about 16 volts across the electrodes and about 110 ma of current, the protactinium is deposited quantitatively, leaving the zirconium in solution.

The decay of this sample was followed with a Lauritsen quartz-fiber electroscope, with and without lead absorbers. An analysis of the decay curve showed, in addition to the 27.4-day Pa<sup>233</sup>, a  $\beta$ - and  $\gamma$ -emitting activity of 1.6 days half life, presumably due to Pa<sup>232</sup> formed in the reaction Th<sup>232</sup>(d,2n)Pa<sup>232</sup>. Since the 1.6-day Pa<sup>232</sup> emits  $\beta$  particles, the daughter must be U<sup>232</sup>. The growth of  $\alpha$  particles due to U<sup>232</sup> was observed in the sample by using an  $\alpha$ -counting ionization chamber and linear pulse amplifier together with a magnetic field to bend out the very strong  $\beta$ -particle background radiation. The growth curve indicated a half life of 1.6 days for the parent activity, which was to be expected.

The possibility existed that the  $\alpha$ -particle emitter was actually 93<sup>232</sup> or 94<sup>232</sup> formed by short-lived successive  $\beta$  decays from Pa<sup>232</sup>. This possibility was disproved by showing that the activity did not behave chemically like elements 93 or 94, but rather like uranium. Therefore the  $\alpha$  emission is certainly due to the isotope U<sup>232</sup>.

It is interesting to note that <sub>92</sub>U<sup>232</sup> must be the parent of <sub>90</sub>RdTh<sup>228</sup> (radiothorium). Radiothorium emits  $\alpha$  particles with a half life of 1.90 years, and there are four other relatively short-lived  $\alpha$ -particle emitters among the short-lived active substances that follow in the decay chain to stable <sub>82</sub>Pb<sup>208</sup>. This means that after the complete decay of Pa<sup>232</sup> into U<sup>232</sup>,  $\alpha$ -particle activity must continue to grow at a relatively slow rate (corresponding to a 1.9-year daughter) in the

U<sup>232</sup> sample. Observation over a period of 75 days showed that the  $\alpha$ -particle activity in the U<sup>232</sup> sample continued to grow at just the rate calculated for the growth of radiothorium (together with its decay products).

Since U<sup>232</sup> is too long-lived to permit following its decay readily, its half life can best be evaluated by using the measured value of the intensity of the  $\beta$  particles of the 1.6-day Pa<sup>232</sup>, together with the corresponding measured value of the intensity of  $\alpha$  particles from the daughter U<sup>232</sup>. For this purpose the Lauritsen electroscope should be calibrated in an absolute manner for the Pa<sup>232</sup>  $\beta$  radiation, so that the electroscope reading can be converted into radioactivity intensity units (e.g., microcuries). Since the electroscope was not calibrated for Pa<sup>232</sup> radiation, a rough answer could be obtained by assuming that the efficiency of the electroscope is the same for Pa<sup>232</sup> radiation as it is for Pa<sup>233</sup> radiation, for which the electroscope had been calibrated in previous work. In this manner it was found that 0.12 millicurie of Pa<sup>232</sup>  $\beta$  radioactivity decayed to 0.016 microcurie of U<sup>232</sup>  $\alpha$  activity. These data lead to a value of about thirty years for the half life of U<sup>232</sup>.

Our thick-target yield data are probably worth discussing even though they are rather rough. The relative yield of Pa<sup>232</sup> to that of Pa<sup>233</sup> gives the yield of the (d,2n) reaction relative to the sum of the (d,n) and (d,p) reactions. [The (d,p) reaction gives the 23.5-min Th<sup>233</sup>, which decays to Pa<sup>233</sup>.] In the thorium-plus-deuterons bombardment, the value of about 0.4 was obtained for the ratio of the yield of Pa<sup>232</sup> to that of Pa<sup>233</sup>. It is interesting to note that the corresponding ratio of yields in the bombardment of uranium (thick target) with 60-in. cyclotron deuterons,<sup>1</sup> that is the ratio of the yield of 2.0-day 93<sup>238</sup> to that of 2.3-day 93<sup>239</sup>, is about 0.1. The errors in these values for the ratio of the yield of Pa<sup>232</sup> to that of Pa<sup>233</sup> and the ratio of the yield of 93<sup>238</sup> to that of 93<sup>239</sup> are such that these ratios might well be about equal.

Following are the approximate yields per 1,000  $\mu$ a-hr of deuterons in the 60-in. cyclotron on a pure, thick thorium target: about 10 millicuries of 1.6-day Pa<sup>232</sup> and, from the decay of this, about 1 microcurie of 30-year U<sup>232</sup>; about 2 millicuries of 27.4-day Pa<sup>233</sup>, and, from the decay of this, about 0.001 microcurie of 120,000-year U<sup>233</sup>. For purposes of comparison it may be stated that the bombardment of 5 kg of thorium nitrate with the neutrons from 1,000  $\mu$ a-hr of deuterons on beryllium in the 60-in. cyclotron produces about 10 millicuries of 27.4-day Pa<sup>233</sup> and, from the decay of this, about 0.01 microcurie (0.5  $\mu$ g) of 120,000-year U<sup>233</sup>.

Summary. The bombardment of thorium with deuterons in the 60-in. Berkeley cyclotron produces, in addition to the 27.4-day  $\text{Pa}^{233}$ , the new isotope  $\text{Pa}^{232}$ , which emits  $\beta$  particles and  $\gamma$  rays with a half life of 1.6 days. The 1.6-day  $\text{Pa}^{232}$  decays to  $\text{U}^{232}$ , which emits  $\alpha$  particles with a half life of about thirty years. The isotope  $\text{U}^{232}$ , which is formed in rather good yield (about 1 microcurie per 1,000  $\mu\text{a}\cdot\text{hr}$  of deuterons) will be useful as a tracer isotope for uranium and especially useful for tracing microgram and less than microgram amounts of uranium.

#### REFERENCE

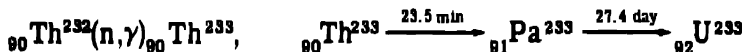
1. G. T. Seaborg, A. C. Wahl, and J. W. Kennedy, Nuclear properties of  $94^{233}$  and  $93^{233}$ , Paper 1.4, this volume.

## Paper 19.15

### DETERMINATION OF THE HALF LIFE OF U<sup>233</sup>†

By E. K. Hyde

The half life of the  $\alpha$ -emitting radioactive isotope, U<sup>233</sup>, was originally determined by Seaborg, Gofman, and Stoughton<sup>1</sup> as  $1.2 \times 10^5$  years. The amounts of U<sup>233</sup> available to them were so minute that an indirect method had to be employed. This method consisted of measuring the rate at which  $\alpha$  particles were emitted following the complete decay of a strong sample of Pa<sup>233</sup>, which had been isolated chemically from a strongly neutron-irradiated sample of thorium nitrate. The nuclear transformations involved may be represented as



From the total  $\alpha$  activity resulting from the complete decay of 16 millicuries of Pa<sup>233</sup> activity, the half life of U<sup>233</sup> was calculated.

In this method the experimentally measured activities were subject to a number of large corrections owing to the following factors:

1. The observed Geiger-Mueller activity included a high percentage of conversion electrons (1.3 conversion electrons per Pa<sup>233</sup>  $\beta$  particle).
2. The back-scattering of the Pa<sup>233</sup>  $\beta$  particles from the copper disks on which the samples were mounted was high (49 per cent).
3. Ten per cent of the observed  $\alpha$  activity represented Pa<sup>231</sup> activity resulting from an (n,2n) reaction in the original bombardment.
4. The counting-yield factor of the  $\alpha$  counter used was 45 per cent. Since the figure<sup>2</sup> accepted at time of this writing for the counting-yield factor of the same type of  $\alpha$  counter is 52 per cent, this may have introduced an error of several per cent.

†Contribution from the Chemistry Division of the Metallurgical Laboratory, University of Chicago, now the Argonne National Laboratory.

Uncertainties in the corrections necessitated by these factors reduced the accuracy of the determination and made it desirable to repeat the determination by a direct method when more material was available. This has now been done with samples of several milligrams of chemically pure U<sup>233</sup>. The new value obtained for the half life is  $1.62 (\pm 0.01) \times 10^8$  years.

Preparation and Purification of U<sup>233</sup>. The uranium used in the determination was produced by irradiation for several months of thorium with the neutrons of the uranium-graphite chain-reacting pile at the Clinton Laboratories. An ether extraction of the solution formed by the dissolution of the irradiated thorium in nitric acid was employed to extract the uranium from the large quantities of thorium and from smaller amounts of protactinium, fission products, and other impurities. One sample of U<sup>233</sup> was isolated in this way by Hagemann, Katzin, and Studier;<sup>3</sup> a second sample was later isolated from a separate batch of irradiated thorium by Hagemann.<sup>4</sup>

For further assurance of chemical and radiochemical purity these samples were subjected to several precipitations including those of ammonium diuranate by ammonia, of sodium uranyl acetate from dilute acetic acid solution, and of uranyl peroxide by 10 per cent hydrogen peroxide. The final treatment was an ether extraction from a solution 0.2N in HNO<sub>3</sub> and saturated with ammonium nitrate.

Determination of Isotopic Purity. It was necessary to measure the specific  $\alpha$  disintegration rate and the isotopic purity of the uranium samples in order to calculate the half life of pure U<sup>233</sup>. The isotopic purity was determined through the kind cooperation of Dr. A. J. Dempster and members of his section by mass-spectrographic analysis.

Using uranium tetrafluoride samples prepared by Hagemann<sup>3</sup> and employing a direct electrometer comparison of the ions collected, including a correction for the scattering of the U<sup>233</sup> atoms to the U<sup>238</sup> position, these investigators found the U<sup>233</sup> content to be  $96.4 \pm 0.4$  per cent in these samples.<sup>5</sup> It was fortuitous that these two U<sup>233</sup> preparations had identical isotopic purities.

The source of the U<sup>238</sup> isotope found as an impurity was a small concentration of natural uranium in the thorium used in the production of the U<sup>233</sup>.

Determination of the Specific Activity. A sample of the purified U<sup>233</sup> was ignited to U<sub>3</sub>O<sub>8</sub> in a weighed platinum crucible at 750°C. This oxide was dissolved in nitric acid, quantitatively transferred to a calibrated volumetric flask, and diluted to volume. Aliquots, ranging in size from 50 to 250 microliters, were removed by means of calibrated micropipets, transferred to separate volumetric flasks,

and diluted to volume. Aliquot samples of the resulting solutions were mounted on platinum disks and counted in a standard pulse ionization chamber.<sup>2</sup> A resolution-loss correction of 0.8 per cent per 1,000 counts per minute was applied. In one case, instead of making a dilution, aliquot samples of the first solution were mounted on counting disks and counted in a nitrogen-filled  $\alpha$  counter equipped with a scale-of-64 scaling circuit.<sup>2</sup> With this counter the coincidence correction was negligible. The samples were counted for a length of time sufficient to reduce the probable fractional error to less than 0.3 per cent.

The contribution of the U<sup>238</sup> impurity to the measured  $\alpha$  activity is entirely negligible, since it is approximately a one-millionth part of the total activity.

Results. Summarized in Table 1 are the details of the individual determinations.

Table 1—Half Life of U<sup>233</sup>

	Determination		
	1†	2	3
Weight oxide, mg	5.273	8.15	1.49
Mass-spectrographic analysis: <sup>5</sup>			
U <sup>233</sup> , %	96.4 ± 0.4	96.35 ± 0.4	96.35 ± 0.4
U <sup>238</sup> , %	3.6 ± 0.4	3.65 ± 0.4	3.65 ± 0.4
Volume of first solution, ml	25.0	50.0	10.00
No. of dilutions	4	1	0
No. of aliquots counted	10	2	2
Mean corrected aliquot count	1,895	723	13,200
Dilution factor†	2.49 × 10 <sup>4</sup>	1.000 × 10 <sup>5</sup>	1.000 × 10 <sup>5</sup>
Counting yield, %	52	52	52
Calculated specific activity, disintegrations per min per $\mu$ g pure U <sup>233</sup>	2.11 × 10 <sup>4</sup>	2.09 × 10 <sup>4</sup>	2.09 × 10 <sup>4</sup>
Calculated half life, years	1.61 × 10 <sup>5</sup>	1.63 × 10 <sup>5</sup>	1.63 × 10 <sup>5</sup>

†The U<sup>233</sup> isolated by Hagemann, Katzin, and Studier<sup>3</sup> was used in determination 1. The U<sup>233</sup> used in determinations 2 and 3 was isolated in a later preparation by Hagemann.<sup>4</sup>

†The dilution factor is the number by which the aliquot count must be multiplied to give the  $\alpha$  count of the entire sample.

The best value of the half life is 1.62 ( $\pm 0.01$ ) × 10<sup>5</sup> years. Possible error in the 52 per cent counting-yield factor<sup>2</sup> used in the calculations is not included in the limits of error. When this factor is determined directly for samples mounted on platinum and emitting particles of the energy of the U<sup>233</sup>  $\alpha$  particle, a recalculation of the half-life value may be necessary.

**SUMMARY**

The half life of the  $\alpha$ -emitting isotope U<sup>233</sup> has been redetermined to be  $1.62 (\pm 0.01) \times 10^5$  years.

**ACKNOWLEDGMENTS**

The author wishes to thank Dr. L. I. Katzin for suggesting the problem and for many helpful suggestions. The assistance of M. S. Studier in carrying out one of the specific-activity determinations is gratefully acknowledged.

**REFERENCES**

1. G. T. Seaborg, J. W. Gofman, and R. W. Stoughton, Nuclear properties of U<sup>233</sup>: A new fissionable isotope of uranium, Paper 19.13, this volume; Phys. Rev., 71: 378 (1947).
2. A. H. Jaffey, Metallurgical Project Report CC-3771 (Feb. 7, 1947); also in National Nuclear Energy Series, Division IV, Volume 14 A.
3. F. Hagemann, L. I. Katzin, and M. H. Studier, in National Nuclear Energy Series, Division IV, Volume 17 B.
4. F. Hagemann, in National Nuclear Energy Series, Division IV, Volume 17 B.
5. W. Rall and A. J. Dempster, in National Nuclear Energy Series, Division IV, Volume 17 B; Metallurgical Project Report CP-3530 (June 6, 1946).

**Paper 19.16**

**DETERMINATION OF THE HALF LIFE OF IONIUM†**

By E. K. Hyde

The thorium isotope of mass 230, called "ionium," is present in all uranium ores because it is a member of the uranium decay chain. Ionium isolated from these ores is always contaminated with thorium 232. Hence the determination of the half life of pure ionium by measurements of naturally occurring ionium involves a determination of the isotopic composition as well as the determination of the specific disintegration rate of the sample.

The presently accepted value of the ionium half life was determined by Curie and Cottelle,<sup>1</sup> who measured the rate of growth of radium into a mixed sample of ionium and thorium, the isotopic composition of which had been determined gravimetrically by Hoenigschmid and Horovitz.<sup>2</sup> The radium was measured indirectly by measuring the radon in equilibrium with it. The value so determined was  $8.23 \times 10^4$  years, the limit of error being set at 3 per cent.

This paper reports a redetermination of the ionium half life, effected by measuring directly the specific  $\alpha$  disintegration rate of an ionium-thorium mixture, the isotopic composition of which had been determined by mass-spectrographic analysis. The value obtained in these experiments was  $(8.0 \pm 0.3) \times 10^4$  years.

This determination would not have been possible without the mass spectrographic measurements of Wilfred Rall and A. J. Dempster.

**EXPERIMENTAL WORK**

The ionium sample was purified by a number of precipitations including a hydroxide precipitation with ammonia and an oxalate precipitation from 1N HNO<sub>3</sub>. The final purification<sup>3</sup> was carried out by repeated extraction with diethyl cellosolve from an aqueous solution

†Contribution from the Chemistry Division of the Metallurgical Laboratory, University of Chicago, now the Argonne National Laboratory.

10N in  $\text{NH}_4\text{NO}_3$  and 1N in  $\text{HNO}_3$ . The ionium was removed from the diethyl cellosolve with distilled water. This extraction effects excellent purification of thorium from traces of all impurities<sup>4</sup> except one or two of the heavier element nitrates, which are removed by the previous precipitations.

A portion of the purified ionium was given to Wilfred Rall and A. J. Dempster, who kindly determined the isotopic composition in the mass spectrograph. In nine separate trials, using a direct electrometer comparison of the ions collected, they obtained a best value of  $26.4 \pm 1.1$  per cent for the atomic percentage of ionium in the sample. Their determination is described in detail elsewhere.<sup>5</sup>

The main portion of the purified sample was transferred to a small platinum crucible, precipitated as oxalate, and ignited at  $700^\circ\text{C}$  to convert the oxalate to the dioxide. The crucible was weighed, and the oxide was dissolved in concentrated nitric acid containing<sup>6</sup> 0.01N HF and transferred to a weighed 10-ml mixing cylinder. The crucible was reignited and reweighed. The solution was diluted to 10 ml with water and perchloric acid to make a solution 5N in perchloric acid. After the mixing cylinder had been reweighed, weighed aliquots of this solution were removed and diluted to 10 ml with 5N  $\text{HClO}_4$ . Weighed aliquots of the diluted solutions were then mounted on 1-in. quartz disks by means of the gravimetric aliquoting method described by Westrum.<sup>7</sup> These samples were counted in several pulse ionization  $\alpha$ -counting chambers, and a counting yield factor of 52 per cent was applied.<sup>8</sup> The contribution of the  $\text{Th}^{232}\alpha$  particles to the total  $\alpha$  count was entirely negligible.

The specific activity determination was checked in the following manner. The ionium was precipitated from the perchloric acid solution as the oxalate, redissolved by passing  $\text{SO}_2$  into an aqueous suspension of the oxalate, reprecipitated as the hydroxide, and dissolved in nitric acid. Ammonium nitrate was added to this acid solution, and the ionium was extracted with redistilled diethyl cellosolve. The specific activity of this repurified ionium was redetermined in exactly the same manner as described above.

The data and calculations are summarized in Tables 1 and 2.

The average value of the half life derived from the two specific activity determinations is  $8.05 \times 10^4$  years. The accuracy of this value is limited principally by the error associated with the mass-spectrographic analysis. The specific disintegration rate determination is accurate to within 0.5 per cent, whereas the standard error associated with the isotopic composition is 4 per cent. In addition, some uncertainty is attached to the use of a counting yield factor of 52 per cent for the ionium samples mounted on quartz since this factor has not been directly determined for this combination.<sup>8</sup>

Table 1—Data for First Specific Activity Determination

Wt. of dioxide, mg		6.91		
Wt. of solution, g		13.311		
Wt. of aliquot, g	0.1336		0.1337	
Wt. of diluted solution, g	12.991		12.665	
Wt. of aliquot of diluted solution, g	0.0647	0.0641	0.0632	0.0633
Disintegrations per minute in aliquot	3,417	3,388	3,442	3,446
Calculated specific activity, disintegrations per minute per microgram	11,270	11,290	11,310	11,300
Average value of specific activity		11,290		
Percentage of ionium in sample		26.4		
Calculated specific activity of pure ionium, disintegrations per minute per microgram of metal		42,770		
Half life of ionium, years		$8.07 \times 10^4$		

Table 2—Data for Second Specific Activity Determination

Wt. dioxide, mg		5.45		
Wt. of solution, g		13.681		
Wt. of aliquot, g	0.1346		0.1357	
Wt. of diluted solution, g	12.905		12.834	
Wt. of aliquot of diluted solution, g	0.0635	0.0637	0.0623	0.0632
Disintegrations per minute in aliquot	1,368	1,390	1,344	1,374
Calculated specific activity, disintegrations per minute per microgram	11,370	11,510	11,220	11,320
Average value of specific activity, disintegrations per minute per microgram of metal		11,360		
Percentage of ionium in sample		26.4		
Calculated specific activity of pure ionium, disintegrations per minute per microgram of metal		43,000		
Half life of ionium, years		$8.03 \times 10^4$		

This redetermination of the ionium half life agrees, within experimental error, with the value reported by Curie and Cottelle.<sup>1</sup> The fact that these two completely independent methods yield the same value increases the confidence with which the value may be accepted.

#### REFERENCES

1. M. Curie and S. Cottelle, Compt. rend., 190: 1289 (1930).
2. O. Hoenigschmid and S. Horovitz, Sitzb. kais. Akad. Wiss., Wien, Abt. IIa, 125: 179-189 (1916).
3. E. K. Hyde and M. J. Wolf, in National Nuclear Energy Series, Division IV, Volume 17B.
4. E. F. Orleman, Metallurgical Laboratory Memorandum MUC-GTS-858 (July 17, 1944).
5. W. Rall and A. J. Dempster, Metallurgical Project Report CP-3398 (Jan. 8, 1946).
6. F. W. Schuler, F. L. Steahly, and R. W. Stoughton, Metallurgical Project Report CC-3576; also in National Nuclear Energy Series, Division IV, Volume 17B.
7. E. F. Westrum, Jr., An improved technique for precise alpha radiometric assay, Paper 16.2, this volume (Metallurgical Project Report CN-3433).
8. A. H. Jaffey, Metallurgical Project Report CC-3771 (Feb. 7, 1947); also in National Nuclear Energy Series, Division IV, Volume 14A.

Paper 19.17

A NEW ISOTOPE OF PROTACTINIUM:  $\text{Pa}^{229}\dagger$

By E. K. Hyde, M. H. Studier, H. H. Hopkins, Jr., and A. Ghiorso

The known isotopes of protactinium include  $\text{Pa}^{234}$  ( $\text{UX}_2$ ),  $\text{Pa}^{233}\text{ }^{1,2}$ ,  $\text{Pa}^{232}\text{ }^3$ , and the recently discovered  $\text{Pa}^{230}\text{ }^4$ . Evidence has been found for a new isotope of protactinium,  $\text{Pa}^{229}$ , produced by the reaction  $\text{Io}^{230}(\text{d},3\text{n})\text{Pa}^{229}$ .

A 35-mg sample of the dioxide of an ionium-thorium mixture (26.4 per cent  $\text{Io}^{230}$ , 73.6 per cent  $\text{Th}^{232}$ ) was bombarded with 70  $\mu\text{a}\cdot\text{hr}$  of 22-mev deuterons in the Berkeley 60-in. cyclotron by Dr. Hamilton and his colleagues.

The dissolution of the target and the separation of a protactinium fraction by diisopropyl ketone extraction were done in a manner very similar to that described elsewhere.<sup>4</sup>

A search in the protactinium fraction for unidentified activities that might be due to  $\text{Pa}^{229}$  and  $\text{Pa}^{228}$  revealed the presence of a previously unknown  $\alpha$  emitter. The decay of this activity could not be followed directly because  $\text{U}^{230}$  and its daughters were growing into the protactinium fraction.<sup>‡</sup>

However, it was possible to follow the decay of the unknown activity by making frequent measurements of the  $\alpha$ -ray spectrum of the protactinium fraction with a pulse analyzer<sup>5</sup> and by following the decay of the unknown peak. From such measurements a half life of  $1.4 \pm 0.4$  days was determined. The energy of the  $\alpha$  particle, determined by the relation of its peak in the  $\alpha$  spectrum to the peaks of the protactinium series, was estimated to be 5.4 mev.

<sup>†</sup>Contribution from the Department of Chemistry and the Radiation Laboratory, University of California, Berkeley, and from the Chemistry Division of the Metallurgical Laboratory, University of Chicago, now the Argonne National Laboratory.

<sup>‡</sup>The  $\text{U}^{230}$  resulted from the  $\beta$  decay of the  $\text{Pa}^{230}$  formed during the bombardment by the reaction  $\text{Io}^{230}(\text{d},2\text{n})\text{Pa}^{230}$ , as well as by the reaction  $\text{Th}^{232}(\text{d},4\text{n})\text{Pa}^{230}$ .

The mass assignment was made by isolating and identifying isotopes of the neptunium ( $4n+1$ ) series<sup>6</sup> from an initially pure protactinium fraction 1 or 2 days after the protactinium fraction had been isolated. Alpha emission of  $\text{Pa}^{229}$  produces  $\text{Ac}^{225}$  and thus gives rise to the whole neptunium series below  $\text{Ra}^{225}$ . Hence the identification of those products is proof for the mass assignment. The amount of  $\text{Ac}^{225}$  that would have grown into the protactinium fraction from the  $\text{Pa}^{233}$  [present owing to the nuclear reaction  $\text{Th}^{232}(\text{d},\text{n})\text{Pa}^{233}$ ] was calculated and found to be entirely negligible.

The experimental evidence for the isotopes of the neptunium series was obtained as follows: An aliquot of the protactinium fraction was made 1N in HF, and lanthanum fluoride was precipitated by the addition of 1 mg of lanthanum nitrate. This precipitation is known to carry actinium in good yield but not protactinium. When this fluoride precipitate was slurried onto a platinum plate, it showed the behavior, characteristic of  $\text{Ac}^{225}$ , of growing in  $\alpha$  activity with a half-life period of 5 min immediately after flaming the plate to red heat to drive off the volatile  $87^{221}$ . The  $\alpha$  count grew from 2,200 counts per minute to 2,900 counts per minute with a 5-min period changing over into an approximately 45-min period as  $\text{Bi}^{213}$  grew in. A recoil-atom activity amounting to 56 counts per minute, which was left in the  $\alpha$  counting chamber after the sample was removed, decayed with the 5-min half life of  $87^{221}$ .

The lanthanum fluoride precipitate was dissolved in concentrated nitric acid, evaporated to dryness, and taken up in dilute nitric acid. From this solution  $\text{Bi}^{213}$  was separated by coprecipitation of lead sulfide when 0.5 mg of lead nitrate and hydrogen sulfide were added. The  $\alpha$  count of the sulfide sample decayed from an initial 280 counts per minute to 3 counts per minute with a half life of  $45 \pm 3$  minutes. These  $\alpha$  particles resulted from  $\text{Po}^{213}$ , disintegrating at a rate determined by the rate of formation from its 47-min  $\beta$ -emitting parent,  $\text{Bi}^{213}$ .

From theoretical considerations it is expected that the  $\alpha$  decay of  $\text{Pa}^{229}$  is paralleled by an electron-capture decay. The low energy of the  $\text{Pa}^{229}$   $\alpha$  particle was unexpected because of its 1.4-day half life, and this may indicate that the true  $\alpha$  half life is considerably longer. It was not possible to prove this by observing a 1.4-day x-ray decay in samples of the protactinium fraction because the  $\text{Pa}^{229}$  activity was masked by a high background from the  $\text{Pa}^{232}$ ,  $\text{Pa}^{233}$ , and  $\text{Pa}^{230}$  radiations. The  $\text{Pa}^{232}$ , in particular, made the measurements almost impossible because of the near identity of the  $\text{Pa}^{232}$  and  $\text{Pa}^{229}$  half lives.

The nuclear reaction  $\text{Th}^{232}(\text{d},2\text{n})\text{Pa}^{232}$  occurred with a cross section of  $4 \times 10^{-27}$  sq cm in this bombardment; the reaction  $\text{Io}^{230}(\text{d},3\text{n})\text{Pa}^{229}$

occurred with a cross section of only  $0.24 \times 10^{-27}$  sq cm, assuming that  $\text{Pa}^{229}$  decays solely by  $\alpha$  emission. Since the cross-section data now available for bombardments of heavy nuclei with 22-mev deuterons indicate that (d,2n) and (d,3n) reactions should occur with approximately equal cross sections, the low value of this second figure may be taken as evidence for branching decay of  $\text{Pa}^{229}$  by orbital-electron capture.

No evidence was found for the unknown isotope  $\text{Pa}^{228}$ , which is undoubtedly formed in the bombardment by the nuclear reaction  $\text{Io}^{230}(\text{d},4\text{n})\text{Pa}^{228}$ .

#### SUMMARY

A new isotope of element 91,  $\text{Pa}^{229}$ , has been produced by the nuclear reaction,  $\text{Io}^{230}(\text{d},3\text{n})\text{Pa}^{229}$ . This isotope emits  $\alpha$  particles of 5.4-mev energy with an apparent half life of  $1.4 \pm 0.4$  days. It is believed that  $\text{Pa}^{229}$  decays principally by orbital-electron capture, but the x rays were not detected because of conflicting activities.

#### REFERENCES

1. G. T. Seaborg, J. W. Gofman, and J. W. Kennedy, Radioactive isotope of protactinium, *Phys. Rev.*, 59: 321 (1941).
2. A. V. Grosse, E. T. Booth, and J. R. Dunning, The fourth (4n+1) radioactive series, *Phys. Rev.*, 59: 322 (1941).
3. J. W. Gofman and G. T. Seaborg, Production and properties of  $\text{U}^{232}$  and  $\text{Pa}^{232}$ , Paper 19.14, this volume.
4. M. H. Studier and E. K. Hyde, National Nuclear Energy Series, Division IV, Volume 17 B; *Phys. Rev.*, 74: 591 (1948).
5. A. Ghiorso, A. H. Jaffey, H. P. Robinson, and B. Weissbourd, A 48-channel pulse-height analyzer for alpha-energy measurements, Paper 16.8, this volume (Metallurgical Project Report CC-3887); A. H. Jaffey, Metallurgical Project Report CC-3771 (Feb. 7, 1947); also in National Nuclear Energy Series, Division IV, Volume 14 A.
6. F. Hagemann, L. I. Katzin, M. H. Studier, G. T. Seaborg, and A. Ghiorso, National Nuclear Energy Series, Division IV, Volume 17 B; The (4n+1) radioactive series: the decay products of  $\text{U}^{233}$ , *Phys. Rev.*, 72: 252 (1947).

## Paper 20.1

### CRYSTAL STRUCTURE STUDIES OF OXIDES OF PLUTONIUM†

By R. C. L. Mooney and W. H. Zachariasen

#### 1. $\text{PuO}_2$ ‡

In November 1943 Dr. P. Kirk submitted a sample of plutonium oxide for x-ray diffraction study. The sample consisted of about  $10 \mu\text{g}$  of yellow powder imbedded in a small piece of lucite.

The specimen gave a satisfactory x-ray diffraction pattern using CuK radiation filtered through nickel foil. The observed diffraction lines corresponded to a face-centered cubic structure with  $a = 5.37 \text{ \AA}$ . The sample probably contained impurities in solid solution because later samples of high purity gave  $a = 5.386 \pm 0.001 \text{ \AA}$ . The diffraction data as obtained with a later sample are shown in Table 1.

When the sample was submitted the yellow plutonium oxide was generally believed to be  $\text{PuO}_2$ . However, no chemical analysis had been made because of the small amounts of plutonium available at the time. Hence there was some uncertainty as to the formula  $\text{PuO}_2$  being correct.

It had been shown that an oxygen atom in uranium compounds required a volume of  $19 \text{ \AA}^3$ , this value being accurate to 10 per cent.<sup>2</sup> The observed intensities require four metal atoms per unit cell and since the volume of the unit cell is  $155 \text{ \AA}^3$ , it contains  $155 / 19$  or eight oxygen atoms. The formula  $\text{PuO}_2$  was thus confirmed by the crystal structure data.

Using the later value of  $a = 5.386 \pm 0.001 \text{ \AA}$  the calculated density becomes  $\rho = 11.44 \pm 0.01$ .

†Contribution from the Physics Division of the Metallurgical Laboratory, University of Chicago, now the Argonne National Laboratory.

‡See bibliographic reference 1.

Compared to plutonium the effect of oxygen on the intensity of x-ray scattering is small. It is observable, however, and shows that  $\text{PuO}_2$  has the fluorite type of structure. The last column of Table 1 shows the intensities as calculated from the expression

$$I(\text{calc.}) \propto |F|^2 p \frac{1 + \cos^2 2\theta}{\sin^2 \theta \cos \theta} \quad (1)$$

where F is the structure factor and p the multiplicity factor. Since the effects of heat motion and of absorption are not taken into account in Eq. 1, calculated and observed intensities should be compared only for neighboring reflections.

Table 1—X-ray Diffraction Data for  $\text{PuO}_2$  ( $\text{CuK}\alpha$ )

$\sin^2 \theta$	$H_1 H_2 H_3$	I (obs.)	I (calc.)
0.0628	111	VS	14.8
0.0834	200	W+	5.7
0.1658	220	S	7.2
0.2272	311	S+	7.0
0.2480	222	W	1.6
0.3903	331 $\alpha_1$	M	2.8
0.4108	420 $\alpha_1$	M-	2.1
0.4918	422 $\alpha_1$	M	2.5
0.5526	511 $\alpha_1$ , 333 $\alpha_1$	M	2.5
0.6547	440 $\alpha_1$	W-	1.0
0.7154	531 $\alpha_1$	S	3.7
0.7357	600 $\alpha_1$ , 442 $\alpha_1$	M	2.0
0.8162	620 $\alpha_1$	M+	2.6
0.8770	533 $\alpha_1$	M+	2.8
0.8973	622 $\alpha_1$	M+	2.7
0.9785	444 $\alpha_1$	W+	

In the  $\text{PuO}_2$  structure each plutonium atom is bonded to eight oxygen atoms with  $\text{Pu}-\text{O} = 2.322 \text{ \AA}$ . The relation of  $\text{PuO}_2$  to other dioxides is discussed in National Nuclear Energy Series, Division IV, Volume 14 A.

## 2. $\text{Pu}_2\text{O}_3-\text{Pu}_4\text{O}_7$

In January 1944 Dr. J. Karle submitted a sample that he had prepared in an attempt to reduce  $\text{PuF}_3$  with atomic hydrogen.

The x-ray diffraction pattern showed the sample to contain 50 per cent  $\text{PuO}_2$ , 15 per cent of a phase that was identified as  $\text{PuN}$ , and 35 per cent of a third phase.<sup>3</sup> The third phase was found to be body-

centered cubic with a lattice constant  $a = 11.01 \pm 0.01$  Å. The observed intensities and sine squares for the diffraction lines of this phase up to  $\sin^2 \theta = 0.5$  are shown in Table 2.

It is seen from Table 2 that there is a face-centered pseudo lattice with half the lattice constant of the true cell.

Table 2 — X-ray Diffraction Data for  $\text{Pu}_2\text{O}_3\text{-Pu}_4\text{O}_7$  ( $\text{CuK}\alpha$ )

I (obs.)	$\sin^2 \theta = (H_1^2 + H_2^2 + H_3^2)$	$\times$	$\lambda^2/4a^2$
VW	0.0292 =	6	× 0.00487
VS	0.0589 =	12	× 0.00491
M	0.0788 =	16	× 0.00493
VW	0.0879 =	18	× 0.00488
VVV	0.1076 =	22	× 0.00489
W-	0.1273 =	26	× 0.00490
trace	0.1462 =	30	× 0.00487
S	0.1572 =	32	× 0.00491
S†	0.1641 =	34	× 0.00488
VW-	0.1867 =	38	× 0.00491
trace	0.2081 =	42	× 0.00491
MS	0.2157 =	44	× 0.00490
S-	0.2252 =	46	× 0.00490
VW	0.2355 =	48	× 0.00491
W	0.2459 =	50	× 0.00492
trace	0.2642 =	54	× 0.00489
W-	0.2730 =	56	× 0.00488
VW	0.3138 =	64	× 0.00490
W†	0.3267 =	68	× 0.00495
trace	0.3428 =	70	× 0.00490
VVV	0.3624 =	74	× 0.00490
W+	0.3714 =	78	× 0.00489
M†	0.3897 =	80	× 0.00487
trace	0.4223 =	86	× 0.00491
VVV	0.4938 =	90	× 0.00489
W†	0.4695 =	96	× 0.00489
W+†	0.4904 =	100	× 0.00490

†Coincidence with diffraction lines of  $\text{PuO}_2$  or  $\text{PuN}$ .

Because of the similarity of the x-ray diffraction of this phase to that of the modification C of the rare-earth sesquioxides, it was concluded that the phase was  $\text{Pu}_2\text{O}_3$  with 16 molecules per unit cell.

The phase was next observed in September 1944 in the x-ray diffraction pattern of a sample that Dr. E. F. Westrum had prepared by heating  $\text{PuO}_2$  to  $1700^\circ\text{C}$ . No other phases were found in this sample. The lattice constant was found to be  $a = 10.945 \pm 0.003$  Å.

Because of the variation of the lattice constant and because the hexagonal  $\text{La}_2\text{O}_3$  structure was to be expected for  $\text{Pu}_2\text{O}_3$ , from the ionic radius of  $\text{Pu}^{+3}$  it was concluded that the phase under discussion contained excess oxygen with the composition lying in the range  $\text{Pu}_2\text{O}_3$ - $\text{Pu}_4\text{O}_7$  (reference 4).

### 3. $\text{PuO}^\dagger$

In December 1943 Dr. Sherman Fried<sup>7</sup> treated plutonium fluoride with barium and submitted the resulting sample for x-ray analysis.

Table 3—X-ray Diffraction Data for  $\text{PuO}$  ( $\text{CuK}\alpha$ )

$\sin^2 \theta$	$H_1H_2H_3$	I (obs.)	I (calc.)
0.0730	111	M+	10.8
0.0974	200	M	6.5
0.1937	220	M	5.0
0.2667	311	S	4.8
0.2906	222	W	1.4
0.3890	400	VW	0.8
0.4606	331	M	2.1
0.4843	420	M+	2.4
0.5799	422	M+	2.0
0.6532	511, 333	S-	2.2
0.7728	440	W	1.1
0.8448	531 $\alpha_1$	S+	4.6
0.8689	442 $\alpha_1$ , 600 $\alpha_1$	S	3.5
0.9655	620 $\alpha_1$	S+	3.5

The data as taken from the original x-ray diffraction pattern are shown in Table 3. The observations correspond to a cubic face-centered structure with  $a = 4.948 \pm 0.002$  Å. Dr. Fried made chemical tests which indicated that the material was some suboxide of plutonium rather than plutonium metal.

The small effect of the oxygen atoms on the intensity of x-ray scattering indicates the sodium chloride type of structure and the phase was accordingly tentatively identified as  $\text{PuO}$  (reference 6).

The calculated density of  $\text{PuO}$  is  $\rho = 13.89$ . Column 4 of Table 3 gives the intensities calculated from Eq. 1.

Each plutonium atom is bonded to six oxygen atoms at a distance  $\text{Pu}-\text{O} = 2.474$  Å.

<sup>†</sup>See bibliographic references 5 and 6.

PuO and other interstitial compounds of plutonium are discussed in National Nuclear Energy Series, Division IV, Volume 14 A.

#### 4. PLUTONIUM(IV) PEROXIDES †

Samples of peroxides of tetravalent plutonium have been examined by the x-ray diffraction method. Two different phases have been observed, but the authors do not know the exact chemical formula of either phase. One of these phases was first observed in a sample submitted by Dr. S. G. English of the Clinton Laboratories. This phase is probably cubic face-centered with  $a = 16.5 \pm 0.1$  Å (reference 9). The second phase was first observed in a sample submitted by Dr. J. W. Hamaker of the University of California in Berkeley. This phase gave an x-ray diffraction pattern corresponding to a two-dimensional hexagonal lattice with  $a_1 = 4.00 \pm 0.02$  Å (reference 10). The analogous thorium phase (with  $a_1 = 4.15 \pm 0.02$  Å) has been observed.

#### 5. SUMMARY

This paper contains a brief account of the crystal structure studies of oxides of plutonium.

PuO<sub>2</sub> has been found to have the fluorite type of structure with  $a = 5.386 \pm 0.001$  Å and a calculated density of  $\rho = 11.44 \pm 0.01$ .

Another plutonium oxide phase was identified as Pu<sub>2</sub>O<sub>3</sub> with some excess oxygen corresponding to a composition in the range Pu<sub>2</sub>O<sub>3</sub>-Pu<sub>4</sub>O<sub>7</sub>. This phase is cubic body-centered with  $a = 11.01 \pm 0.01$  Å and 32 plutonium atoms per unit cell. The structure is similar to that of the C modification of the rare earth sesquioxides.

A suboxide of plutonium was identified as PuO. It has the sodium chloride type of structure with  $a = 4.948 \pm 0.002$  Å and a calculated density of  $\rho = 13.89 \pm 0.02$ .

Some x-ray data for two plutonium peroxides have been given. One of these peroxides gives an x-ray diffraction pattern corresponding to a two-dimensional hexagonal lattice with  $a_1 = 4.00 \pm 0.02$  Å. The other peroxide is cubic face-centered with  $a = 16.5 \pm 0.1$  Å.

#### REFERENCES

1. R. C. L. Mooney and W. H. Zachariasen, Metallurgical Laboratory Memorandum MUC-SKA-303 (November 1943) and Metallurgical Project Report CK-1119 (Dec. 8, 1943).
2. W. H. Zachariasen, Metallurgical Project Report CK-1259 (Jan. 25, 1944).
3. W. H. Zachariasen, Metallurgical Project Report CK-1530 (Mar. 30, 1944).
4. W. H. Zachariasen, Metallurgical Project Report CN-2069 (August 1944), p. 35.

†See bibliographic reference 8.

5. R. C. L. Mooney and W. H. Zachariasen, Metallurgical Project Report CK-1250 (Jan. 22, 1944), p. 2.
6. W. H. Zachariasen, Metallurgical Project Report CK-1367 (Feb. 25, 1944), p. 10.
7. S. Fried, Metallurgical Project Report CK-1221 (Jan. 5, 1944), p. 12.
8. J. C. Kroner and L. Spector, Metallurgical Project Report CN-2213 (June 30, 1945).
9. W. H. Zachariasen, Metallurgical Project Report CF-3070 (June 1945), p. 3.
10. W. H. Zachariasen, Metallurgical Project Report CN-2797 (Mar. 15, 1945), p. 6.
11. R. C. L. Mooney and W. H. Zachariasen, Metallurgical Project Report CK-1377 (Feb. 26, 1944), p. 2.

## Paper 20.2

# THE CRYSTAL STRUCTURE OF PLUTONIUM NITRIDE AND PLUTONIUM CARBIDE†

By W. H. Zachariasen

## 1. ORIGIN OF THE PLUTONIUM NITRIDE SAMPLES

J. Karle attempted a reduction of  $\text{PuF}_3$  with atomic hydrogen and submitted the resulting preparation for x-ray diffraction study.

The diffraction pattern showed the sample to contain about 50 per cent  $\text{PuO}_2$ , 35 per cent of a phase identified as  $\text{Pu}_2\text{O}_3$ , with some excess oxygen, and 15 per cent of a third phase tentatively identified as plutonium nitride.<sup>1</sup> Subsequent samples, described below, confirm the identification of the third phase as plutonium nitride.

The plutonium nitride phase was next observed in x-ray diffraction patterns of samples prepared by E. F. Westrum and B. M. Abraham.<sup>2</sup> Westrum's sample was made by treating plutonium metal with ammonia on a platinum support at 1000°C. The x-ray examination showed it to contain 40 per cent  $\text{PuO}_2$ , 35 per cent  $\text{PuN}$ , and 25 per cent unidentifiable constituents. Abraham made his sample by heating  $\text{PuCl}_3$  in ammonia. According to the x-ray data it contained 50 per cent  $\text{PuO}_2$ , 35 per cent  $\text{PuN}$ , and 15 per cent  $\text{PuOCl}$ .

The x-ray diffraction pattern of plutonium nitride, without the superposition of patterns due to other phases, was obtained in October 1944 with a preparation that Westrum made by firing plutonium metal in a hydrogen-ammonia mixture at 600°C.

†Contribution from the Physics Division of the Metallurgical Laboratory, University of Chicago, now the Argonne National Laboratory.

## 2. CRYSTAL STRUCTURE OF PLUTONIUM CARBIDE AND PLUTONIUM NITRIDE

X-ray diffraction examination of a sample of plutonium carbide showed that it contained 30 per cent PuO, 45 per cent of a phase identified as PuC, and 25 per cent of a third phase.<sup>3</sup> The third phase is cubic body-centered with lattice constant  $a = 8.11 \pm 0.01$  Å, and could conceivably be  $\text{Pu}_2\text{C}_3$ , with eight molecules per unit cell.

The observed values of sine squares and intensities for the x-ray diffraction lines of plutonium nitride and plutonium carbide are given

Table 1—X-ray Diffraction Data for Plutonium Nitride and Plutonium Carbide (CuK $\alpha$ )

$H_1H_2H_3$	PuN		PuC		
	I (obs.)	$\sin^2 \theta$	I (obs.)	$\sin^2 \theta$	I (calc.)
111	M	0.0749	S	0.0746	4.6
200	W+	0.0998	M	0.0997	3.8
220	M	0.1994	S-	0.1985	6.2
311	M	0.2738	S	0.2719	9.0
222	W	0.2988	W+	0.2963	3.3
400	VW	0.3976	VW	0.3959	2.3
331	M-	0.4704	W	0.4688	7.0
420	M	0.495	W	0.4935	7.8
422	M	0.5935	W+	0.5915	7.0
511, 333	M	0.6671	M	0.6656	7.7
440	W-	0.7902	W	0.7882	3.0
531 $\alpha_1$	S	0.8638	S	0.8581	10.6
600 $\alpha_1$ , 442 $\alpha_1$	M	0.8882	S	0.8829	7.1
620 $\alpha_1$	S	0.9866	M	0.9804	5.4

in Table 1. The observations correspond to a cubic face-centered structure of the rock-salt type. The lattice constants and the calculated densities are

$$\begin{array}{lll} \text{PuN:} & a = 4.895 \pm 0.001 \text{ \AA} & \rho = 14.23 \\ \text{PuC:} & a = 4.910 \pm 0.005 \text{ \AA} & \rho = 13.99 \end{array}$$

The last column of Table 1 gives the calculated values  $|F|^2 p$  for plutonium carbide, where  $F$  is the structure factor, and  $p$  the permutation factor.

It is shown in another paper of this volume that PuO has the sodium chloride type of structure with lattice constant  $a = 4.948 \pm 0.002$  Å.

The three compounds PuO, PuN, and PuC are typical examples of "interstitial compounds." The interstitial compounds of plutonium and neptunium are briefly discussed in the chapter on the crystal chemistry of plutonium and neptunium, National Nuclear Energy Series, Division IV, Volume 14 A.

### 3. SUMMARY

Plutonium nitride and plutonium carbide have the sodium chloride type of structure. The lattice constants and calculated densities are

$$\begin{array}{lll} \text{PuN: } & a = 4.895 \pm 0.001 \text{ \AA}, & \rho = 14.23 \pm 0.01 \\ \text{PuC: } & a = 4.910 \pm 0.005 \text{ \AA}, & \rho = 13.99 \pm 0.05 \end{array}$$

This paper describes the determination of the crystal structure of plutonium nitride and plutonium carbide. The work was carried out using plutonium preparations of unknown composition. Therefore the presence of the compounds PuN and PuC in the preparations was deduced from the x-ray diffraction examination.

### ACKNOWLEDGMENT

The x-ray diffraction patterns were determined by Anne Plettinger.

### REFERENCES

1. W. H. Zachariasen, Metallurgical Project Report CK-1530 (Mar. 30, 1944).
2. E. F. Westrum, Jr., and B. M. Abraham, Metallurgical Project Report CN-2159 (Sept. 1, 1944), p. 3.
3. W. H. Zachariasen, Metallurgical Project Report CN-1957 (July 29, 1944), p. 5.

## Paper 20.3

### THE CRYSTAL STRUCTURE OF PuSi<sub>2</sub>†

By W. H. Zachariasen

Westrum<sup>1</sup> submitted for x-ray diffraction study a sample that he had prepared in an attempt to reduce PuF<sub>3</sub> with CaSi<sub>2</sub>.

A satisfactory x-ray diffraction pattern was obtained using CuK radiation filtered through nickel foil. Table 1 shows the observed intensities and sine squares.

The observations correspond to a single phase, which is tetragonal body-centered with lattice dimensions

$$a_1 = 3.97 \pm 0.01 \text{ \AA} \text{ and } a_3 = 13.55 \pm 0.05 \text{ \AA}$$

It is seen from Table 1 that there are many absent reflections in addition to those required by a body-centered translation lattice. These additional absences are: H<sub>1</sub>H<sub>2</sub>H<sub>3</sub> absent if (a) H<sub>1</sub> and H<sub>2</sub> are both even and H<sub>3</sub> = 4n + 2, (b) H<sub>1</sub> and H<sub>2</sub> are both odd and H<sub>3</sub> = 4n.

The absences lead to the space group I4/amd (D<sub>4h</sub><sup>19</sup>) or to one of its subgroups.

In order to explain the main features of the intensity distribution, it becomes necessary to place four plutonium atoms in the unit cell and at positions (0 0 0) ( $\frac{1}{2}$   $\frac{1}{2}$   $\frac{1}{2}$ ) (0  $\frac{1}{2}$   $\frac{1}{2}$ ) ( $\frac{1}{2}$  0  $\frac{1}{2}$ ).

Certain details in the intensity distributions remain unaccounted for, and it is therefore evident that the phase must contain lighter atoms as well as plutonium. Assuming the phase to be a silicide and making use of volume considerations (based on results for known silicides), it is found that PuSi<sub>2</sub> is the only formula compatible with

†Contribution from the Physics Division of the Metallurgical Laboratory, University of Chicago, now the Argonne National Laboratory.

Based on work reported in Metallurgical Project Reports CN-1957 (July 29, 1944) and CN-2275 (Oct. 25, 1944).

the observed unit cell volume.<sup>2</sup> The identification of the phase as  $\text{PuSi}_3$  became certain when isomorphism with  $\text{ThSi}_3$  (see reference 3) and  $\text{USi}_3$  (see reference 4) was established.

The eight silicon atoms per unit cell are at position:  $(0\ 0\ 0)$  ( $\frac{1}{2}\ \frac{1}{2}\ \frac{1}{2}$ ) +

$$(0\ 0\ u)\ (0\ 0\ \bar{u})\ (0,\ \frac{1}{2},\ \frac{1}{4}+u)\ (0,\ \frac{1}{2},\ \frac{1}{4}-u)$$

and agreement with the observed intensities is obtained for  $u = 0.417$ .

Table 1—X-ray Diffraction Data for  $\text{PuSi}_3$  (CuK $\alpha$ )

$\sin^2\theta$	$H_1H_2H_3$	I (obs.)	$ F ^2 p$
0.0415	101	S	16.4
0.0518	004	W	10.1
0.0671	103	M	25.6
0.0892	112	S	61.8
0.1192	105	WM	33.2
0.1528	200	W+	32.4
0.1929	211 + 116	M	24.2 + 22.6
0.1945	107	W	27.6
0.2043	204 + 008	W	29.8 + 7.4
0.2187	213	W+	37.0
0.2708	215	M-	50.0
0.3022	220 + 109	W-	24.3 + 15.9
0.3462	217	W+	42.5
	301	Nil	10.0
0.3557	224 + 208	W+	23.4 + 23.4
0.3699	303	VW	14.4
0.3913	312	W+	34.8
0.3983	1.1.10	W-	34.8
0.4211	305	VW	
0.4289	1.0.11	VW	
0.4507	219	W	
0.4948	321 + 316 + 307	M	

The last column of Table 1 gives the calculated values of  $|F|^2 p$  where F is the structure factor and p the multiplicity factor.

The calculated density for  $\text{PuSi}_3$  is  $\rho = 9.12$ .

Each plutonium atom is bonded to twelve silicon atoms with  $\text{Pu-Si} = 3.01$  Å, and each silicon atom is bonded to six plutonium atoms and to three other silicon atoms with  $\text{Si-Si} = 2.27$  Å. The Si-Si distance in metallic silicon is, for comparison, 2.34 Å.

Summary.  $\text{PuSi}_3$  is tetragonal. The unit cell contains four molecules and has dimensions  $a_1 = 3.97 \pm 0.01$  Å and  $a_2 = 13.55 \pm 0.05$  Å. The calculated density is  $\rho = 9.12$ .

The space group is I4/amd and the atomic positions are: (0 0 0)  
 $(\frac{1}{2} \frac{1}{2} \frac{1}{2})+$

4Pu in (0 0 0) (0  $\frac{1}{2}$   $\frac{1}{4}$ )

8Si in (0 0 u) (0 0  $\bar{u}$ ) (0,  $\frac{1}{2}$ ,  $\frac{1}{4}$  + u) (0,  $\frac{1}{2}$ ,  $\frac{1}{4}$  - u)

The parameter value is u = 0.417.

Each plutonium atom is bonded to twelve silicon atoms, and each silicon atom is bonded to six plutonium atoms and three silicon atoms. The interatomic distances are Pu-Si = 3.01 Å and Si-Si = 2.27 Å.

The compounds ThSi<sub>2</sub>, USi<sub>2</sub>, and CeSi<sub>2</sub> are isomorphous.

#### REFERENCES

1. E. F. Westrum, Jr., Metallurgical Project Report CN-2159 (Sept. 1, 1944), p. 1.
2. W. H. Zachariasen, Metallurgical Project Report CN-1957 (July 29, 1944), p. 4.
3. G. Brauer and A. Mitius, Z. anorg. Chem., 249: 325 (1942).
4. W. H. Zachariasen, Metallurgical Project Report CP-2298 (Oct. 28, 1944), p. 17.

## Paper 20.4

### CRYSTAL STRUCTURE STUDIES OF SULFIDES OF PLUTONIUM AND NEPTUNIUM†

By W. H. Zachariasen

#### 1. PuS

Westrum<sup>1</sup> carried out a calcium reduction of  $\text{PuF}_3$  in a barium sulfide crucible. On the basis of a microscopic examination Dr. Westrum suspected that a plutonium sulfide had been formed by reaction with the crucible, and he submitted the sample for x-ray diffraction examination.

The diffraction pattern showed that 85 per cent of the sample consisted of a cubic face-centered phase with the sodium chloride type of structure and with a lattice constant<sup>2</sup>  $a = 5.525 \pm 0.001 \text{ \AA}$ . It was suggested that the phase was PuS, although the possibility of its being barium oxide could not be excluded by the x-ray data alone.

The formula PuS was checked as follows: Dr. Westrum ignited the sample, and an x-ray diffraction pattern of the ignition product was taken. The diffraction pattern showed the bulk of the sample to be  $\text{PuO}_2$ .

Table 1 shows the observed intensities and sine squares as obtained from the diffraction pattern. The intensities clearly show that the structure type is that of sodium chloride. The calculated density is  $\rho = 10.60$ .

The compounds ThS, US, and CeS are isomorphous. The lattice constants are shown in Table 2.

†Contribution from the Physics Division of the Metallurgical Laboratory, University of Chicago, now the Argonne National Laboratory.

Table 1—X-ray Diffraction Data for PuS (CuK $\alpha$ )

I (obs.)	$\sin^2 \theta$	$H_1^2 + H_2^2 + H_3^2$
M+	0.0603	3
M+	0.0797	4
S	0.1581	8
S	0.2167	11
W	0.2361	12
W-	0.3140	16
WM	0.3716	19
M+	0.3909	20
M	0.4676	24
M-	0.5262	$27\alpha_1$
W	0.6216	$32\alpha_1$
S	0.6797	$35\alpha_1$
S	0.6994	$36\alpha_1$
S	0.7760	$40\alpha_1$
WM	0.8335	$43\alpha_1$
S	0.8525	$44\alpha_1$
W	0.9291	$48\alpha_1$
S	0.9871	$51\alpha_1$

Table 2—Lattice Constants for Compound XS

XS	a, Å
ThS	$5.671 \pm 0.002$
US	$5.473 \pm 0.002$
PuS	$5.525 \pm 0.001$
CeS	$5.766 \pm 0.002$

2.  $\text{Pu}_{3-x}\text{S}_4$ 

Dr. N. R. Davidson investigated the reaction of hydrogen sulfide gas on  $\text{PuO}_2$  at high temperatures and submitted his preparations for x-ray diffraction examination.

One of Dr. Davidson's preparations gave a diffraction pattern corresponding to a single phase that was found<sup>4</sup> to be cubic body-centered with  $a = 8.4373 \pm 0.0005$  Å.

The x-ray diffraction data are given in Table 3.

It was further found that the observed intensities proved the phase to be isomorphous with the cerium sulfide  $\text{Ce}_{3-x}\text{S}_4$ , the detailed structure of which had been determined.<sup>5</sup> It could thus be stated that Dr.

Davidson's plutonium sulfide preparation was  $\text{Pu}_{3-x}\text{S}_4$ . For cerium sulfide the composition varies from  $\text{Ce}_2\text{S}_3$  ( $x = 0.33$ ) to  $\text{Ce}_3\text{S}_4$ . The exact composition of the plutonium sulfide could not be determined from the x-ray diffraction data, i.e., if it was  $\text{Pu}_2\text{S}_3$ ,  $\text{Pu}_3\text{S}_4$ , or intermediate between these extremes.

Table 3—X-ray Diffraction Data for  $\text{Pu}_{3-x}\text{S}_4$  (CuK $\alpha$ )

$\text{H}_1^2 + \text{H}_2^2 + \text{H}_3^2$	$\sin^2 \theta$	$\text{Pu}_{3-x}\text{S}_4$	$\text{Ce}_3\text{S}_4$	
2		Nil	Nil	0
4		Nil	Nil	0
6	0.0510	M	M	80
8		Nil	Trace	7.8
10	0.0843	M	S	81
12		Nil	Nil	0
14	0.1178	W+	M+	45
16		Nil	Nil	0.5
18		Nil	Nil	0
20	0.1678	W+	M	28
22	0.1847	W	W+	19
24	0.2012	Trace	VW	6.1
26	0.2182	M	M	19
30	0.2509	VW-	VW	7.3
32		Nil	Trace	1.0
34		Nil	Nil	0.5
36		Nil	Nil	0
38	0.3181	S-	S	24
40	0.3336	VW-	VW+	4.6
42	0.3513	W-	W+	11
44		Nil	Nil	0
46	0.3838	Trace	VW	4.1
48	0.4010	VW	VW+	5.6
50		Nil	Trace	0.7
52	0.4337	VW+	W-	6.0
54	0.4502	M+	S	18
56	0.4667	VVV	VW-	4.0
58	0.4853	Trace	Trace	1.3
62	0.5168	VVV	VW-	3.4
64		Nil	VVV	1.9

The structure type of  $\text{Ce}_3\text{S}_4$  will be discussed in detail in another paper; accordingly, the structure of  $\text{Pu}_{3-x}\text{S}_4$  is only briefly described here.

The space group is  $\bar{I}43d$  ( $T_d^6$ ). In the unit cell there are four molecules  $\text{Pu}_{3-x}\text{S}_4$ . Thus the calculated density must lie in the range 8.41 (for composition  $\text{Pu}_2\text{S}_3$ ) to 9.28 (for composition  $\text{Pu}_3\text{S}_4$ ).

The atomic positions are as follows: (0 0 0) ( $\frac{1}{2} \frac{1}{2} \frac{1}{2}$ ) + 10.67 - 12 Pu atoms in ( $\frac{1}{4} \frac{3}{4} 0$ ) ; ( $\frac{3}{4} \frac{1}{4} 0$ ) ; 16 S atoms in (x x x); ( $\frac{1}{2} + x, \frac{1}{2} - x, \bar{x}$ ) ; ( $\frac{1}{4} + x, \frac{1}{4} + x, \frac{1}{4} + x$ ); ( $\frac{3}{4} + x, \frac{1}{4} - x, \frac{3}{4} - x$ ). Thus, some of the metal sites may be vacant, and the phase has a wide homogeneity range.

The intensity considerations show the parameter x for the sulfur positions to be x = 0.083.

Table 3 gives the intensities observed for  $\text{Ce}_3\text{S}_4$  and  $\text{Pu}_{3-x}\text{S}_4$  and calculated for  $\text{Ce}_3\text{S}_4$  with the aid of the formula

$$I(\text{calc.}) \propto |F|^2 p \frac{1 + \cos^2 2\theta}{\sin^2 \theta \cos \theta}$$

where F is the structure factor and p the multiplicity factor.

In the structure each plutonium atom is bonded to six sulfur atoms with Pu-S = 2.92 Å.

$\text{Ce}_2\text{S}_3$ - $\text{Ce}_3\text{S}_4$  and  $\text{La}_2\text{S}_3$  are isomorphous compounds.

### 3. $\text{Pu}_2\text{O}_2\text{S}$

Davidson<sup>3</sup> submitted another sample resulting from his studies of the reaction of hydrogen sulfide gas on  $\text{PuO}_2$ .

The x-ray diffraction pattern showed Davidson's sample to contain  $\text{PuO}_2$  to the extent of 30 per cent, the remainder of the sample being a hexagonal phase with lattice dimensions

$$a_1 = 3.919 \pm 0.003 \text{ \AA} \quad a_3 = 6.755 \pm 0.010 \text{ \AA}$$

This phase was observed to be isomorphous with  $\text{Ce}_2\text{O}_2\text{S}$ , the crystal structure of which had been previously examined,<sup>6</sup> and hence it could be concluded that the plutonium compound<sup>7</sup> was  $\text{Pu}_2\text{O}_2\text{S}$ .

There is one molecule of  $\text{Pu}_2\text{O}_2\text{S}$  per unit cell, giving a calculated density of  $\rho = 9.95$ .

The x-ray diffraction observations are given in Table 4.

The atomic positions are

2 Pu in  $\pm (\frac{1}{3} \frac{2}{3} u_1)$  with  $u_1 = 0.22$

2 O in  $\pm (\frac{1}{3} \frac{2}{3} u_2)$  with  $u_2 = -0.125$

1 S in (0 0  $\frac{1}{2}$ )

The values  $|F|^2 p$  calculated with this structure are shown in the last column of Table 4.

Each plutonium atom is bonded to three sulfur atoms with Pu-S = 2.94 Å, to three oxygen atoms with Pu-O = 2.35 Å, and to a fourth oxygen atom with Pu-O = 2.33 Å.

The Ce<sub>2</sub>O<sub>2</sub>S and Pu<sub>2</sub>O<sub>2</sub>S structure type can be regarded as obtained from the structure type of the A modification of rare-earth sesquioxides by substituting sulfur atoms for one-third of the oxygen atoms.

Table 4—X-ray Diffraction Data for Pu<sub>2</sub>O<sub>2</sub>S (CuK $\alpha$ )

H <sub>1</sub> H <sub>2</sub> H <sub>3</sub>	$\sin^2 \theta$	I (obs.)	F  <sup>2</sup> p
001		Nil	0.2
100, 002	0.0526	WM	5.8 + 6.7
101	0.0653	S	35.5
102	0.1046	S	15.6
003		Nil	2.8
110	0.1562	M	26.5
111, 103	0.1705	M	0.9 + 25.9
200, 112, 004	0.2077	M	4.1 + 29.2 + 3.8
201	0.2204	WM	26.2
202, 104	0.2596	W	11.9 + 13.5
113	0.2729	VW	11.8
005, 203	0.3249	W	2.1 + 19.8
210, 114	0.3634	W-	6.1 + 18.4
211, 105	0.3745	M	40.0 + 15.3
212, 204	0.4134	M	
300	0.4639	W-	
301, 203	0.4782	M	

#### 4. NpOS

Fried and Davidson<sup>8</sup> made a neptunium preparation by reacting NpO<sub>2</sub> with hydrogen sulfide and carbon disulfide.

The x-ray diffraction pattern showed the sample to contain a single phase. This phase was found to be tetragonal and to have the PbFCl type of structure with lattice dimensions 0.5 per cent smaller than for the isomorphous compound<sup>9</sup> UOS. Thus the neptunium preparation could be identified as NpOS, and the detailed crystal structure was obtained.<sup>10</sup>

The lattice dimensions and calculated density of NpOS are

$$a_1 = 3.817 \pm 0.002 \text{ \AA} \quad a_3 = 6.641 \pm 0.010 \text{ \AA} \quad \rho = 9.71$$

The x-ray diffraction data are shown in Table 5.

The space group is P4/nmm and the atomic positions are

2 Np in ( $\frac{1}{2} 0 u_1$ ) ( $0 \frac{1}{2} \bar{u}_1$ )

2 O in (0 0 0) ( $\frac{1}{2} \frac{1}{2} 0$ )

2 S in ( $\frac{1}{2} 0 u_2$ ) ( $0 \frac{1}{2} \bar{u}_2$ )

with  $u_1 = 0.200 \pm 0.006$  and  $u_2 = 0.638$ .

Table 5—X-ray Diffraction Data for NpOS (CuK $\alpha$ )

I (obs.)	$\sin^2 \theta$	H <sub>1</sub> H <sub>2</sub> H <sub>3</sub>
S	0.0543	101, 002
M-	0.0818	110
M-	0.0951	102
M-	0.1360	112
M-	0.1630	200, 103
W-	0.2037	113
M+	0.2177	211, 202
M-	0.2573	212, 104
VW	0.2835	203
W+	0.3254	220, 213
W	0.3804	301, 222
W	0.4070	310
M	0.4190	302, 214, 115
W-	0.4615	312
VW-	0.4874	303
VW+	0.4991	205
W-	0.5274	313, 106
W-	0.5424	321, 215
W	0.5820	322, 304
VW	0.6499	400, 323
VW	0.6610	225
VW	0.6860	216

Table 6—Calculated and Observed Intensities for NpOS

H <sub>1</sub> H <sub>2</sub> H <sub>3</sub>	F  <sup>2</sup> p	I (obs.)
101, 002	35 + 7.7	S
110	28	M-
111	1.1	Nil
102	24	M-
003	4.0	Nil
112	35	M-
200, 103	29 + 16.2	M-
201	3.4	Nil
113	20	W-
211, 202	49 + 22	M-
004	0.6	Nil
212, 104	35 + 34	M-
203	12.4	VW
114	0.6	Nil
220, 213	21 + 24	W+
221, 005	2.2 + 8.0	Nil
204	1.6	Nil
301, 222	20 + 18.0	W
105	0.5	Nil
310	32	W

Table 6 shows the comparison between observed intensities and calculated values  $|F|^2 p$ .

In the structure each neptunium atom is bonded to four oxygen atoms at  $Np-O = 2.32 \text{ \AA}$  and to five sulfur atoms at  $Np-S = 2.91 \text{ \AA}$ .

The lattice dimensions of the isomorphous compounds ThOS, UOS, and NpOS are shown below.

	$a_1, \text{ \AA}$	$a_3, \text{ \AA}$
ThOS	$3.955 \pm 0.002$	$6.733 \pm 0.004$
UO	$3.835 \pm 0.001$	$6.681 \pm 0.001$
NpOS	$3.817 \pm 0.002$	$6.641 \pm 0.010$

### 5. $Np_2S_3$

Fried and Davidson<sup>11</sup> made another neptunium sulfide preparation. This sample gave an x-ray diffraction pattern too poor to permit accurate measurements. It showed, however, that the substance was isomorphous with  $Th_2S_3$  (reference 12) and  $U_2S_3$  (reference 13), and hence the preparation was identified<sup>13</sup> as  $Np_2S_3$ .

The compounds  $Th_2S_3$ ,  $U_2S_3$ , and  $Np_2S_3$  are orthorhombic with four molecules per unit cell. The lattice dimensions and the calculated densities are

	$a_1, \text{ \AA}$	$a_2, \text{ \AA}$	$a_3, \text{ \AA}$	$\rho$
$Th_2S_3$	$10.83 \pm 0.05$	$10.97 \pm 0.05$	$3.95 \pm 0.03$	7.87
$U_2S_3$	$10.6 \pm 0.02$	$10.39 \pm 0.02$	$3.88 \pm 0.01$	8.78
$Np_2S_3$	$10.6 \pm 0.1$	$10.3 \pm 0.1$	$3.85 \pm 0.05$	8.9

The space group is Pnam. The complete structure of  $Th_2S_3$  and  $U_2S_3$  will be discussed elsewhere. The structure type is essentially that of  $Bi_2S_3$  and  $Sb_2S_3$ .

### 6. DISCUSSION

A complete study of the systems Pu-O-S and Np-O-S has not been made. The scattered observations described in the preceding sections and the compilation given below show, however, that plutonium behaves like cerium, but neptunium behaves like uranium.

In the sulfide series plutonium is considerably smaller than cerium, but there is very little difference in size among tetrapositive or tri-

positive oxygen and fluorine compounds. It must accordingly be concluded that the chemical bonds in the sulfides, to a considerable extent, have metallic character.

### Isomorphous Sulfides

PuS	ThS, US, CeS
$\text{Pu}_2\text{S}_3$	$\text{Ce}_2\text{S}_3$ , $\text{La}_2\text{S}_3$
$\text{Pu}_2\text{O}_2\text{S}$	$\text{Ce}_2\text{O}_2\text{S}$
NpOS	ThOS, UOS
$\text{Np}_2\text{S}_3$	$\text{Th}_2\text{S}_3$ , $\text{U}_2\text{S}_3$

### 7. SUMMARY

The determination of the chemical identity and crystal structure of several sulfides and oxysulfides of plutonium and neptunium has been discussed. The discussion includes PuS,  $\text{Pu}_{3-\delta}\text{S}_4$ ,  $\text{Pu}_2\text{O}_2\text{S}$ , NpOS, and  $\text{Np}_2\text{S}_3$ . Lattice dimensions and atomic positions are given.

This paper gives a brief account of crystal structure investigations that have been carried out on the sulfides of plutonium and neptunium: PuS,  $\text{Pu}_2\text{S}_3$ - $\text{Pu}_3\text{S}_4$ ,  $\text{Pu}_2\text{O}_2\text{S}$ ,  $\text{Np}_2\text{S}_3$ , and NpOS.

### ACKNOWLEDGMENT

The author is grateful for the assistance given by Anne Plettinger who took the x-ray diffraction patterns.

### REFERENCES

1. E. F. Westrum, Jr., Metallurgical Project Report CN-2159 (Sept. 1, 1944), p. 3.
2. W. H. Zachariasen, Metallurgical Project Report CN-1957 (July 29, 1944), p. 6.
3. N. R. Davidson, Metallurgical Project Report CN-2431 (Dec. 1, 1944), p. 2.
4. W. H. Zachariasen, Metallurgical Project Report CN-2382 (Nov. 17, 1944).
5. W. H. Zachariasen, Metallurgical Project Report CP-1576 (Apr. 24, 1944), p. 23.
6. W. H. Zachariasen, Metallurgical Project Report CP-1728 (May 25, 1944), p. 20.
7. W. H. Zachariasen, Metallurgical Project Report CN-2381 (Nov. 15, 1944).
8. S. Fried and N. R. Davidson, Metallurgical Project Report CN-2689 (Feb. 15, 1945), p. 6.
9. W. H. Zachariasen, Metallurgical Project Report CP-2090 (Aug. 28, 1944), p. 24.
10. W. H. Zachariasen, Metallurgical Project Report CN-2615 (Jan. 9, 1945).
11. S. Fried and N. R. Davidson, Metallurgical Project Report CN-3053 (June 1945), p. 8.
12. W. H. Zachariasen, Metallurgical Project Report CP-1811 (June 23, 1944), p. 23.
13. W. H. Zachariasen, Metallurgical Project Report CF-2926 (Apr. 15, 1945), p. 12.

## Paper 20.5

# X-RAY DIFFRACTION STUDIES OF FLUORIDES OF PLUTONIUM AND NEPTUNIUM; CHEMICAL IDENTITY AND CRYSTAL STRUCTURE<sup>†</sup>

By W. H. Zachariasen

### 1. INTRODUCTION

This paper describes a series of x-ray diffraction studies on fluorides of plutonium and of neptunium. The list of compounds to be discussed includes  $\text{PuF}_3$ ,  $\text{NpF}_3$ ,  $\text{PuOF}$ ,  $\text{NaPuF}_4$ ,  $\text{PuF}_4$ ,  $\text{NpF}_4$ ,  $\text{PuF}_4 \cdot 2.5\text{H}_2\text{O}$ ,  $\text{NaPuF}_5$ ,  $\text{KPuF}_5$ ,  $\text{RbPuF}_5$ ,  $\text{KPu}_2\text{F}_9$ ,  $\text{KNp}_2\text{F}_9$ , and  $\text{NpF}_6$ . None of these compounds had been chemically identified when its x-ray diffraction pattern was obtained; consequently the determination of the chemical identity of the various compounds became an important part of the investigations.

The first part of this paper gives the origin of the preparations that were examined and describes how the various compounds were identified. The crystal structure results are presented in the second part.

### 2. IDENTIFICATION OF THE COMPOUNDS

It would be entirely misleading to give the impression that the chemical identity of the various fluorides was determined from the x-ray diffraction patterns with no information from other sources. In the first place, it was known that the submitted samples were plutonium or neptunium preparations, respectively. Second, there was information as to how the samples had been prepared. Thus the presence of fluorides in the samples was either to be expected or to be suspected.

<sup>†</sup>Contribution from the Physics Division of the Metallurgical Laboratory, University of Chicago, now the Argonne National Laboratory.

In some instances ( $\text{PuF}_3$  or  $\text{PuOF}$ ) the x-ray diffraction study did not lead to a unique determination of the chemical formula of the fluoride; it was possible to state only that the formula was one or the other of two alternatives.

2.1  $\text{NaPuF}_4$ . In November 1943 a sample, hoped to be plutonium metal in powder form, was submitted for x-ray diffraction study. At the time it was of importance to know the density of plutonium metal, and Dr. K. T. Bainbridge had suggested that an attempt ought to be made to determine the density by means of the crystal structure method. Baumbach<sup>1</sup> had prepared the sample by sodium-vapor reduction of plutonium fluoride.

The x-ray diffraction pattern could be interpreted as due to a single phase, which was hexagonal with lattice dimensions  $a_1 = 6.12 \pm 0.02$  Å and  $a_3 = 3.75 \pm 0.01$  Å.<sup>2</sup> The crystal structure results showed that the phase could not possibly be plutonium metal. On the assumption that the phase contained only the elements plutonium, fluorine, and oxygen, it was shown that the chemical formula would have to be either  $\text{PuOF}_2$  or  $\text{PuF}_3$ .<sup>3</sup> Both of these suggested formulas had to be rejected later, and the identity of the phase was to remain unknown for a great many months.

In the course of extensive studies of the fluoride system the author prepared a compound of lanthanum, first thought<sup>4</sup> possibly to be  $\text{NaLa}_2\text{OF}_5$ , but later shown<sup>5</sup> to be  $\text{NaLaF}_4$ .

This lanthanum compound is hexagonal with  $a_1 = 6.167$  Å and  $a_3 = 3.819$  Å, and the x-ray diffraction pattern as regards intensity distribution was so nearly identical with that of the plutonium phase referred to above that there could be no doubt about the isomorphism of the two compounds.<sup>6</sup> Thus the unknown plutonium phase was at last identified as  $\text{NaPuF}_4$ .

2.2  $\text{PuF}_3$ . In December 1943 Florin and Heath<sup>7</sup> prepared a sample of plutonium fluoride and submitted it for x-ray study. At the time, the plutonium fluoride preparations were believed to be  $\text{PuF}_4$ , but great color variations from one preparation to the next had been noted. This particular sample was black.

The x-ray diffraction pattern corresponded to a single hexagonal phase with  $a_1 = 4.085$  Å and  $a_3 = 7.236$  Å and two metal atoms per unit cell.<sup>8</sup> It was shown that the assumed formula  $\text{PuF}_4$  could not be correct. The unit cell has a volume of 105 Å<sup>3</sup>, and each fluorine or oxygen atom requires a space of about 19 Å<sup>3</sup>. Hence it could be stated<sup>9</sup> that the phase was either  $\text{PuF}_3$  or  $\text{PuOF}_2$ . A direct chemical analysis<sup>9</sup> gave a ratio of F to Pu varying from 2.8/1 to 3.7/1 and thus decided in favor of the first of the alternative formulas deduced from crystal structure considerations.

2.3 PuF<sub>4</sub>. PuO<sub>2</sub> had been shown<sup>2</sup> to be isomorphous with ThO<sub>2</sub>, UO<sub>2</sub>, and ZrO<sub>2</sub> and to have lattice dimensions intermediate between UO<sub>2</sub> and ZrO<sub>2</sub>. It had also been shown<sup>10</sup> that ThF<sub>4</sub>, UF<sub>4</sub>, and ZrF<sub>4</sub> were isomorphous. Accordingly, it was to be expected that PuF<sub>4</sub> would also be isomorphous.

In January 1944 Florin and Heath<sup>7</sup> prepared a light-brown plutonium fluoride. The x-ray diffraction pattern of this sample showed isomorphism with UF<sub>4</sub>, and it could thus be stated<sup>9,11</sup> that the sample contained PuF<sub>4</sub>.

2.4 PuOF. In January 1944 Karle<sup>12</sup> attempted an atomic hydrogen reduction of plutonium fluoride and submitted the resulting sample for x-ray diffraction study.

The diffraction pattern showed the sample to be a mixture of PuF<sub>3</sub> and a second phase that was cubic face-centered<sup>13</sup> with  $a = 5.70 \pm 0.01$  Å.

The author first suggested that this phase might be PuF<sub>2-3</sub> and later showed<sup>14</sup> that the formula would have to be either PuOF or PuF<sub>2.3</sub>. A subsequent direct fluorine analysis<sup>12</sup> furnished evidence in favor of the formula PuOF.

2.5 PuF<sub>4</sub>·2.5H<sub>2</sub>O. Meyer<sup>15</sup> prepared a sample that he believed to be PuF<sub>4</sub>·xH<sub>2</sub>O.

The x-ray diffraction study<sup>16</sup> proved the exact formula of the substance to be PuF<sub>4</sub>·2.5H<sub>2</sub>O as shown by isomorphism with UF<sub>4</sub>·2.5H<sub>2</sub>O.

2.6 KPuF<sub>5</sub>, NaPuF<sub>5</sub>, RbPuF<sub>5</sub>. Smith<sup>17</sup> prepared a sample that he suggested might be K<sub>2</sub>PuF<sub>6</sub>·xH<sub>2</sub>O.

The author<sup>18</sup> erroneously attributed a series of weak lines in the x-ray diffraction pattern to impurities, and hence arrived at the incorrect formula K<sub>2</sub>PuF<sub>6</sub>.

Later Anderson<sup>18</sup> prepared the isomorphous sodium and rubidium compounds, and these were accordingly assigned the incorrect formulas Na<sub>2</sub>PuF<sub>6</sub> and Rb<sub>2</sub>PuF<sub>6</sub>.

Subsequently the author prepared the isomorphous compounds of thorium and uranium and showed them to be KThF<sub>6</sub> and KUF<sub>6</sub>; hence, the earlier formula for the plutonium compounds was corrected<sup>19</sup> to RPuF<sub>6</sub>.

The composition RPuF<sub>6</sub> was later confirmed by Anderson<sup>20</sup> by direct analysis.

2.7 KNp<sub>2</sub>F<sub>6</sub> and KPu<sub>2</sub>F<sub>6</sub>. LaChapelle and Magnusson<sup>21</sup> submitted for x-ray study two fluoride samples that they had isolated from neptunium solutions, one from a pentapositive and the other from a tetrapositive solution.

The latter sample had reacted with the glass of the x-ray capillary and contained K<sub>2</sub>SiF<sub>6</sub> as the major phase. The minor phase (or phases)

was the same phase (or phases) that made up all the sample isolated from the pentapositive solution.<sup>22</sup> The author<sup>8</sup> next succeeded in preparing the analogous and isomorphous fluorides using thorium or tetrapositive uranium as stand-ins for neptunium and suggested the tentative formula  $\text{KNp}_2\text{F}_9$ . The correctness of the formula  $\text{KX}_2\text{F}_9$  for the isomorphous compounds was later proved beyond reasonable doubt.<sup>23</sup>

The compound  $\text{KPu}_2\text{F}_9$  was first prepared by Anderson<sup>18</sup> and described as "H<sup>+</sup>-Pu<sup>+4</sup>-fluoride." It was identified as  $\text{KPu}_2\text{F}_9$  from the x-ray diffraction pattern<sup>8</sup> by its isomorphism with  $\text{KNp}_2\text{F}_9$ .

**2.8 NpF<sub>3</sub> and NpF<sub>4</sub>.** The compounds NpF<sub>3</sub> and NpF<sub>4</sub> were first prepared by Fried, Florin, and Davidson.<sup>24</sup> Only about 25 µg was involved in these preparations, and the chemical identity of these fluorides was therefore determined from x-ray diffraction studies.

The first neptunium fluoride sample submitted by Fried, Florin, and Davidson was found to be hexagonal with  $a_1 = 4.108 \text{ \AA}$  and  $a_3 = 7.273 \text{ \AA}$ . These lattice dimensions are intermediate between those of UF<sub>3</sub> and PuF<sub>3</sub>. Furthermore, the relative intensities of the various lines in the diffraction pattern of the neptunium compound were the same as those observed for UF<sub>3</sub> and PuF<sub>3</sub>. Hence, the neptunium fluoride was identified as NpF<sub>3</sub>, and the hitherto unknown tripositive state of neptunium was definitely established.<sup>25-27</sup>

The second neptunium fluoride preparation of Fried, Florin, and Davidson gave an x-ray diffraction pattern that proved isomorphism with UF<sub>4</sub> and PuF<sub>4</sub>, and the lattice dimensions of the neptunium compound were found to be intermediate between those of UF<sub>4</sub> and those of PuF<sub>4</sub>. On the basis of these observations and the knowledge that the substance was a neptunium compound, it could be stated<sup>28,28</sup> that the phase was NpF<sub>4</sub>.

**2.9 NpF<sub>6</sub>.** The hexafluoride of neptunium was prepared by Florin. Florin<sup>29</sup> was fairly certain that his preparation was NpF<sub>6</sub>.

The x-ray diffraction pattern showed the sample to contain a single phase, which was orthorhombic with  $a_1 = 9.91 \pm 0.02 \text{ \AA}$ ,  $a_2 = 8.97 \pm 0.02 \text{ \AA}$ , and  $a_3 = 5.21 \pm 0.02 \text{ \AA}$ . The x-ray diffraction pattern was indistinguishable<sup>30</sup> from that of UF<sub>6</sub>. Assuming that there was no uranium in the sample, the compound would have to be NpF<sub>6</sub>.

### 3. THE CRYSTAL STRUCTURES OF FLUORIDES OF PLUTONIUM AND NEPTUNIUM

In this part of the present paper the crystal structures of the individual fluorides of plutonium and neptunium are discussed briefly.

**3.1  $\text{PuF}_3$  and  $\text{NpF}_3$ .** Table 1 gives the observed intensities and sine squares as obtained from x-ray diffraction patterns of  $\text{PuF}_3$  (see references 8 and 27) and  $\text{NpF}_3$ , (see references 25 to 27).

Table 1—X-ray Diffraction Data for  $\text{PuF}_3$  and  $\text{NpF}_3$  ( $\text{CuK}\alpha$ )

$\text{PuF}_3$		$\text{NpF}_3$		
I (obs.)	$\sin^2\theta$	I (obs.)	$\sin^2\theta$	$H_1H_2H_3$
M	0.0454	WM	0.0450	002
W	0.0470	W	0.0474	100
S	0.0586	S	0.0585	101
W-	0.0925	W-	0.0922	102
M	0.1420	M	0.1409	110
M+	0.1494	M+	0.1481	103
VVW	0.1818	VVW	0.1792	004
M	0.1880	M	0.1859	112, 200
W+	0.2013	W+	0.1991	201
VW-	0.2290	VVW	0.2267	104
VW-	0.2350	VVW	0.2318	202
W+	0.2914	W	0.2885	203
W+	0.3236	W	0.3202	114
W	0.3313	W	0.3278	105, 210
M-	0.3433	W+	0.3399	211
Trace	0.3714			204
VVW	0.3767	VVW	0.3723	212
VVV	0.4075			006
VW-	0.4271			300
W+	0.4342	W	0.4259	213
VW-	0.4540	VW	0.4500	106
W+	0.4731	W	0.4660	302, 205

The diffraction patterns show that  $\text{PuF}_3$  and  $\text{NpF}_3$  have the tysonite type structure.<sup>31</sup> The compounds  $\text{LaF}_3$ ,  $\text{CeF}_3$ ,  $\text{PrF}_3$ ,  $\text{NdF}_3$ ,  $\text{SmF}_3$ ,  $\text{UF}_3$ ,<sup>32</sup>  $\text{ThOF}_2$ ,<sup>33</sup>  $\text{BaThF}_6$ ,<sup>4</sup>  $\text{PbThF}_6$ ,<sup>34</sup>  $\text{SrThF}_6$ ,<sup>4</sup>  $\text{CaThF}_6$ ,<sup>34</sup>  $\text{BaUF}_6$ ,<sup>4</sup>  $\text{PbUF}_6$ ,<sup>4</sup> and  $\text{SrUF}_6$ ,<sup>4</sup> are isomorphous.

In Table 1 the diffraction patterns are indexed in accordance with a hexagonal cell containing two molecules of  $\text{XF}_3$ . This is probably a pseudocell.<sup>31</sup>

Referred to this cell the lattice dimensions of  $\text{PuF}_3$  and  $\text{NpF}_3$  become

	$a_1, \text{\AA}$	$a_3, \text{\AA}$	$\rho$
$\text{PuF}$	$4.087 \pm 0.001$	$7.240 \pm 0.001$	9.32
$\text{NpF}$	$4.108 \pm 0.001$	$7.273 \pm 0.004$	9.12

and the atomic positions are

$$2X \text{ in } \pm (\frac{1}{3} \frac{2}{3} \frac{1}{4})$$

$$2F \text{ in } \pm (0 0 \frac{1}{4})$$

$$4F \text{ in } \pm (\frac{1}{3} \frac{2}{3} u) (\frac{1}{3}, \frac{2}{3}, \frac{1}{2}-u) \text{ with } u = -0.075$$

The interatomic distances are

	Pu, Å	Np, Å
3F at	2.36	2.37
2F at	2.35	2.36
6F at	2.68	2.69
Mean	2.53	2.54

$\text{LaF}_3$  and  $\text{PuF}_3$  have been shown to form an unbroken series of solid solutions.

The lattice dimensions of isomorphous trifluorides are given in the chapter on the crystal chemistry of plutonium and neptunium in National Nuclear Energy Series, Division IV, Volume 14 Å.

3.2  $\text{PuOF}$ .<sup>14</sup> The x-ray diffraction observations for  $\text{PuOF}$  are shown in Table 2.

$\text{PuOF}$  has the fluorite type of structure with  $a = 5.70 \pm 0.01$  Å. The calculated density is  $\rho = 9.76$ .

The lattice constant<sup>35</sup> of the isomorphous  $\text{LaOF}$  is, for comparison,  $a = 5.76$  Å.

3.3  $\text{NaPuF}_4$ .<sup>8,36</sup> Table 3 gives some of the x-ray diffraction data for  $\text{NaPuF}_4$ .

The hexagonal unit cell, which contains 1.5 molecules, has dimensions  $a_1 = 6.12 \pm 0.02$  Å and  $a_3 = 3.75 \pm 0.01$  Å corresponding to a density of  $\rho = 6.87$ .

The lattice dimensions<sup>37</sup> of the isomorphous compound  $\text{NaLaF}_4$  are, for comparison,  $a_1 = 6.167 \pm 0.001$  Å and  $a_3 = 3.819 \pm 0.002$  Å.

3.4  $\text{PuF}_4$  and  $\text{NpF}_4$ .  $\text{PuF}_4$  (see reference 38) and  $\text{NpF}_4$  (see reference 26) are monoclinic with twelve molecules per unit cell. The lattice dimensions and calculated densities are

	$a_1$ , Å	$a_2$ , Å	$\alpha'$	$a_3$ , Å	$\rho$
$\text{PuF}_4$	$12.59 \pm 0.06$	$10.55 \pm 0.05$	$126^\circ 10' \pm 40'$	$8.26 \pm 0.05$	7.0
$\text{NpF}_4$	$12.67 \pm 0.06$	$10.62 \pm 0.05$	$126^\circ 10' \pm 40'$	$8.31 \pm 0.05$	6.8

## THE TRANSURANIUM ELEMENTS

Table 2—X-ray Diffraction Data for PuOF (CuK $\alpha$ )

I (obs.)	$\sin^2\theta$	=	$(H_1^2 + H_2^2 + H_3^2) (\lambda^2 / 4a^2)$
S	0.0553	=	$3 \times 0.01843$
W	0.0741	=	$4 \times 0.01853$
M†	0.1476	=	$8 \times 0.01845$
M†	0.2029	=	$11 \times 0.01845$
VW	0.2206	=	$12 \times 0.01838$
VW†	0.2942	=	$16 \times 0.01839$
W+†	0.3463	=	$19 \times 0.01823$
VW	0.3664	=	$20 \times 0.01832$
W†	0.4379	=	$24 \times 0.01825$
VW	0.4946	=	$27 \times 0.01832$
VVV	0.5808	=	$32 \times 0.01815$
VW+	0.6390	=	$35 \times 0.01826$
VVV	0.6575	=	$36 \times 0.01827$
VVV	0.7298	=	$40 \times 0.01825$

†Coincidence with diffraction lines of PuF<sub>3</sub>.

Table 3—X-ray Diffraction Data for NaPuF<sub>4</sub> (CuK $\alpha$ )

I (obs.)	$\sin^2\theta$	H <sub>1</sub> H <sub>2</sub> H <sub>3</sub>
S	0.0636	110, 101
M	0.1268	201
W	0.1478	210
W-	0.1682	002
M	0.1889	300, 211, 102
W	0.2311	301, 112
W-	0.2514	202, 220
Trace	0.2727	310
W+	0.3145	311, 212
VW	0.3360	400
W-	0.3582	302
VW	0.4009	320, 103
VVV	0.4183	222
W+	0.4413	410, 321, 312
VVV	0.4646	203

The space group is C2/c. The positions of the metal atoms are (0 0 0) ( $\frac{1}{2} \frac{1}{2} 0$ ) +

4X in  $\pm(0 u \frac{1}{4})$

8X in  $\pm(x y z) (x, y, \frac{1}{4} - z)$

with u = 0.20, x = 0.21, y = 0.44, and z = -0.17.

The fluorine positions are not known.

Isomorphous compounds are ZrF<sub>4</sub>, HfF<sub>4</sub>, CeF<sub>4</sub>, ThF<sub>4</sub>, and UF<sub>4</sub>.

**3.5  $\text{PuF}_4 \cdot 2.5\text{H}_2\text{O}$ .**<sup>39</sup> The compound  $\text{PuF}_4 \cdot 2.5\text{H}_2\text{O}$  is orthorhombic with eight molecules per unit cell.

The lattice dimensions and calculated density are

$$a_1 = 12.63 \pm 0.05 \text{ \AA}, a_2 = 11.01 \pm 0.05 \text{ \AA}, a_3 = 6.98 \pm 0.05 \text{ \AA}, \rho = 4.89$$

The space group is Pnam. The eight plutonium atoms per unit cell fall into two sets of four having positions  $\pm(x \ y \ z)$   $(x + \frac{1}{2}, \frac{1}{2} - y, \frac{1}{2})$  with parameter values

	x	y
Pu(I)	0.055	0.014
Pu(II)	-0.250	-0.139

The fluorine and oxygen positions are not known.

The compound  $\text{UF}_4 \cdot 2.5\text{H}_2\text{O}$  is isomorphous.

**3.6  $\text{NaPuF}_5$ ,  $\text{KPuF}_5$ ,<sup>18</sup>  $\text{RbPuF}_5$ .** The compounds  $\text{RPuF}_5$  are rhombohedral with six molecules per unit cell. The lattice dimensions and calculated densities are

	a, \text{\AA}	$\alpha$	$\rho$
$\text{NaPuF}_5$	$8.93 \pm 0.03$	$107^\circ 28' \pm 10'$	6.03
$\text{KPuF}_5$	$9.27 \pm 0.03$	$107^\circ 2' \pm 10'$	5.66
$\text{RbPuF}_5$	$9.46 \pm 0.03$	$106^\circ 56' \pm 10'$	5.88

The space group is  $R\bar{3}(C_{3i}^2)$ . The six plutonium atoms and the six alkali atoms per unit cell are in positions  $\pm(x \ y \ z)$   $(y \ z \ x)$   $(z \ x \ y)$  with the following parameter values:

	x	y	z
Pu	$\frac{3}{13}$	$\frac{1}{13}$	$\frac{9}{13}$
R	$\frac{6}{13}$	$\frac{2}{13}$	$\frac{5}{13}$

There is a pseudocubic pseudocell that contains 3.7 metal atoms and 9.2 fluorine atoms whose structure closely resembles that of fluorite. The dimensions of this rhombohedral pseudocell are

	a, \text{\AA}	$\alpha$
$\text{NaPuF}_5$	$5.650 \pm 0.005$	$90^\circ$
$\text{KPuF}$	$5.86 \pm 0.01$	$89^\circ 20'$
$\text{RbPuF}_5$	$6.00 \pm 0.02$	$89^\circ 10'$

Isomorphous compounds are  $\text{KCeF}_5$ ,  $\text{KThF}_5$ ,  $\text{KUF}_5$ , and  $\text{NaUF}_5$ .

**3.7  $KPu_2F_9$  and  $KNp_2F_9$ .** The compounds  $KPu_2F_9$  and  $KNp_2F_9$  are orthorhombic with four molecules per unit cell. Lattice dimensions and calculated densities are

	$a_1, \text{ Å}$	$a_2, \text{ Å}$	$a_3, \text{ Å}$	$\rho$
$KPu_2F_9$	$8.56 \pm 0.04$	$6.95 \pm 0.04$	$11.33 \pm 0.06$	6.73
$KNp_2F_9$	$8.63 \pm 0.05$	$7.01 \pm 0.05$	$11.43 \pm 0.07$	6.54

The space group is Pnam. The eight plutonium or neptunium atoms per unit cell are at positions

$$\pm(x\ y\ z) (x, y, \frac{1}{2}-z) (x + \frac{1}{2}, \frac{1}{2}-y, z) (x + \frac{1}{2}, \frac{1}{2}-y, \frac{1}{2}-z)$$

with  $x = 0.17$ ,  $y = 0.15$ , and  $z = 0.055$ .

The fluorine positions are not known.

Isomorphous compounds are  $KTh_2F_9$  and  $KU_2F_9$ .

**3.8  $NpF_6$ .**  $NpF_6$  is orthorhombic with four molecules per unit cell. The lattice dimensions and calculated density are

$$a_1 = 9.91 \pm 0.02 \text{ Å}, \quad a_2 = 8.97 \pm 0.02 \text{ Å}, \quad a_3 = 5.21 \pm 0.02 \text{ Å}, \quad \rho = 5.00$$

The space group is Pnma.

$NpF_6$  is isomorphous with  $UF_6$ , the complete structure of which has been found.<sup>40</sup>

#### 4. SUMMARY

The determination of the chemical identity and of the crystal structure of a number of plutonium and neptunium fluorides is discussed. The list of fluorides includes  $PuF_3$ ,  $NpF_3$ ,  $PuOF$ ,  $NaPuF_4$ ,  $PuF_4$ ,  $NpF_4$ ,  $PuF_4 \cdot 2.5H_2O$ ,  $NpF_6$ ,  $KPu_2F_9$ ,  $KNp_2F_9$ ,  $NaPuF_5$ ,  $KPuF_5$ , and  $RbPuF_5$ .

Lattice dimensions and partial or complete structures are given for all the compounds.

#### ACKNOWLEDGMENT

Dr. R. C. L. Mooney gave valuable aid in the work on  $NaPuF_4$  and  $PuF_3$ . All the x-ray diffraction patterns were taken by Anne Plettinger. B. Rosenbaum and W. C. Koehler helped in measuring some of the diffraction patterns.

## REFERENCES

1. H. L. Baumbach, Metallurgical Project Report CK-1145 (Dec. 11, 1943), p. 12.
2. R. C. L. Mooney and W. H. Zachariasen, Metallurgical Project Report CK-1096 (Nov. 27, 1943), p. 12.
3. W. H. Zachariasen, Metallurgical Project Report CK-1259 (Jan. 25, 1944).
4. W. H. Zachariasen, Metallurgical Project Report CF-2796 (Mar. 15, 1945), p. 17.
5. W. H. Zachariasen, Metallurgical Project Reports CF-2926 (Apr. 15, 1945), p. 11, and CC-3401 (Jan. 10, 1946).
6. W. H. Zachariasen, Metallurgical Project Report CN-2797 (Mar. 15, 1945), pp. 4-6.
7. A. E. Florin and R. E. Heath, Metallurgical Project Report CK-1372 (Mar. 1, 1944), p. 7.
8. W. H. Zachariasen, Metallurgical Laboratory Memorandum MUC-FWHZ-3 (N-1287a) (Dec. 8, 1943); Metallurgical Project Report CK-1250 (Jan. 22, 1944), p. 2.
9. R. W. Spence and R. P. Straitz, Metallurgical Project Report CK-1326 (Feb. 1, 1944).
10. W. H. Zachariasen, Metallurgical Project Report CP-1168 (Dec. 25, 1943), p. 12.
11. W. H. Zachariasen, Metallurgical Project Report CK-1250 (Jan. 22, 1944), p. 3.
12. I. Karle, Metallurgical Project Report CK-1701 (June 1, 1944), p. 21.
13. W. H. Zachariasen, Metallurgical Project Report CK-1377 (Feb. 26, 1944), p. 3.
14. W. H. Zachariasen, Metallurgical Project Report CK-1530 (Mar. 30, 1944), p. 10.
15. F. Meyer, Metallurgical Project Report CN-1586 (May 1, 1944), p. 10.
16. W. H. Zachariasen, Metallurgical Project Report CN-1813 (June 23, 1944), pp. 3-4.
17. C. Smith, Metallurgical Project Report CN-1764 (July 1, 1944), p. 3.
18. H. H. Anderson, Metallurgical Project Report CN-2767 (March 1945), p. 39; W. H. Zachariasen, Metallurgical Project Report CN-2797 (Mar. 15, 1945), p. 2.
19. W. H. Zachariasen, Metallurgical Project Report CP-3028 (May 1945), p. 3.
20. H. H. Anderson, Alkali plutonium(IV) fluorides, Paper 6.9, this volume (Argonne National Laboratory Report ANL-4054).
21. T. J. LaChapelle and L. B. Magnusson, Metallurgical Project Report CS-1951 (January 1945), p. 3.
22. W. H. Zachariasen, Metallurgical Project Report CN-2742 (Feb. 15, 1945), p. 3.
23. W. H. Zachariasen, Metallurgical Project Report CC-3426 (Feb. 9, 1946).
24. S. Fried, A. E. Florin, and N. R. Davidson, Metallurgical Project Report CN-2689 (Feb. 15, 1945), p. 1.
25. W. H. Zachariasen, Metallurgical Laboratory Memorandum MUC-FWHZ-94 (December 1944).
26. W. H. Zachariasen, Metallurgical Project Report CN-2610 (Dec. 3, 1945), pp. 4-5.
27. W. H. Zachariasen, Metallurgical Project Report CN-2526 (Jan. 2, 1945).
28. W. H. Zachariasen, Metallurgical Laboratory Memorandum MUC-FWHZ-95 (Jan. 2, 1945).
29. A. E. Florin, Metallurgical Laboratory Memorandum MUC-GTS-2165 (N-2210) (Jan. 23, 1946).
30. W. H. Zachariasen, Metallurgical Laboratory Memorandum MUC-FWHZ-166 (Jan. 22, 1946).
31. I. Oftedal, *Z. physik. Chem.*, 5: 272 (1929); 13: 190 (1931).
32. W. H. Zachariasen, Metallurgical Project Report CP-1376 (Feb. 26, 1944), p. 17.
33. W. H. Zachariasen, Metallurgical Laboratory Memorandum MUC-FWHZ-168 (N-2218) (Feb. 11, 1946).
34. W. H. Zachariasen, Metallurgical Project Report CP-2090 (Aug. 28, 1944), p. 22.
35. W. Klemm and H. A. Klein, *Z. anorg. Chem.*, 248: 167 (1941).
36. W. H. Zachariasen, Metallurgical Project Report CK-1096 (Nov. 27, 1943), p. 12.

37. W. H. Zachariasen, Metallurgical Project Reports CF-2796 (Mar. 15, 1945), p. 17, and CC-3401 (Jan. 10, 1946), p. 9.
38. W. H. Zachariasen, Metallurgical Project Report CN-2069 (August 1944), p. 7.
39. W. H. Zachariasen, Metallurgical Project Report CN-1957 (July 29, 1944), p. 2.
40. J. L. Hoard and J. D. Stroupe, Report A-1296 (June 30, 1944).

## Paper 20.6

# CRYSTAL STRUCTURE STUDIES OF CHLORIDES, BROMIDES, AND IODIDES OF PLUTONIUM AND NEPTUNIUM<sup>†</sup>

By W. H. Zachariasen

### 1. INTRODUCTION

Crystal structure studies of chlorides, bromides, and iodides of plutonium and of neptunium are discussed in this paper. Complete crystal structures have been found for the compounds  $\text{PuCl}_3$ ,  $\text{NpCl}_3$ ,  $\text{NpBr}_3$ ,  $\text{PuBr}_3$ ,  $\text{PuI}_3$ ,  $\text{NpI}_3$ ,  $\text{PuOCl}$ ,  $\text{PuOBr}$ ,  $\text{PuOI}$ , and  $\text{NpCl}_4$ . Only lattice dimensions are known for the compound  $\text{Cs}_2\text{PuCl}_6$ . X-ray diffraction patterns have been obtained for  $\text{PuCl}_3 \cdot \text{H}_2\text{O}$ ,  $\text{PuCl}_3 \cdot 6\text{H}_2\text{O}$ ,  $\text{PuBr}_3 \cdot 6\text{H}_2\text{O}$ ,  $\text{NpBr}_4$ ,  $\text{NpOCl}_2$ , and  $\text{NpOBr}_2$ , but the author has not succeeded in analyzing these patterns.

The crystal structure determinations were carried out with the aid of powder-diffraction patterns obtained with samples ranging in weight from a few micrograms in some instances ( $\text{NpCl}_3$ ,  $\text{NpCl}_4$ ) to a hundred micrograms in others. All the x-ray diffraction patterns were taken with CuK radiation filtered through nickel foil. Because of the health hazard, all plutonium and neptunium preparations were in sealed glass capillaries. These were of pyrex or quartz glass with a wall thickness of about 20  $\mu$ .

When a plutonium or neptunium preparation was submitted for x-ray study, the chemical identity was as a rule unknown. Indeed, one of the important purposes of the x-ray diffraction examination was the identification of the phase or phases in the sample. Thus, of the compounds specifically mentioned above, all but  $\text{PuBr}_3$ ,  $\text{Cs}_2\text{PuCl}_6$ , and  $\text{PuCl}_3 \cdot \text{H}_2\text{O}$  were first identified by the x-ray diffraction method and a knowledge of how the samples had been prepared. The chemical

<sup>†</sup>Contribution from the Physics Division of the Metallurgical Laboratory, University of Chicago, now the Argonne National Laboratory.

formulas of  $\text{PuBr}_3$ ,  $\text{Cs}_2\text{PuCl}_6$ , and  $\text{PuCl}_3 \cdot \text{H}_2\text{O}$  were first deduced from direct chemical analysis.

## 2. THE COMPOUNDS $\text{PuCl}_3$ , $\text{NpCl}_3$ , AND $\text{NpBr}_3$

2.1 Origin and Identification of the Samples. (a)  $\text{PuCl}_3$ . The first successful preparation of a chloride of plutonium was carried out by Hagemann,<sup>1</sup> who submitted his sample for x-ray diffraction study.

The interpretation of the x-ray diffraction pattern showed the preparation to contain a single phase, which was hexagonal and isomorphous with  $\text{UCl}_3$ , the structure of which had previously been investigated.<sup>2</sup> It could thus be concluded from the x-ray study that the plutonium chloride preparation was  $\text{PuCl}_3$  (see reference 3). The identification was subsequently confirmed by direct analysis<sup>1</sup> which gave a Cl to Pu ratio varying from 2.8 to 3.28.

(b)  $\text{Pu}(\text{Br},\text{Cl})_3$ . Hagemann<sup>4</sup> later attempted a preparation of plutonium bromide by reaction of bromine gas on plutonium metal.

The x-ray diffraction study showed that the preparation was isomorphous with  $\text{UCl}_3$ . However, the observed lattice constants were too small for the sample to be pure  $\text{PuBr}_3$ . It was accordingly suggested that the bromine gas used in the preparation contained chlorine as an impurity, and that consequently a trihalide estimated to be  $\text{Pu}(\text{Br}_{0.8},\text{Cl}_{0.2})_3$  had been formed.<sup>5</sup> The suggested explanation was found to be correct. However,  $\text{PuBr}_3$  prepared from pure bromine gas and metal is not isomorphous with  $\text{UCl}_3$ .

(c)  $\text{NpCl}_3$ . The first preparation of  $\text{NpCl}_3$  was made by Fried and Davidson.<sup>6</sup> The identification of the preparation as  $\text{NpCl}_3$  (with 10 to 15 per cent  $\text{NpO}_2$ ) was made from the x-ray diffraction pattern, which showed isomorphism of  $\text{NpCl}_3$  with  $\text{UCl}_3$  and  $\text{PuCl}_3$  (see reference 7).

(d)  $\text{NpBr}_3$ . Fried<sup>8</sup> was the first to prepare  $\text{NpBr}_3$ . Again the x-ray diffraction study provided the identification.<sup>9</sup>

2.2 The Crystal Structure of  $\text{PuCl}_3$ ,<sup>3,10</sup>  $\text{Pu}(\text{Br}_{0.8},\text{Cl}_{0.2})_3$ ,<sup>5</sup>  $\text{NpCl}_3$ ,<sup>7</sup> and  $\text{NpBr}_3$ .<sup>9</sup> As stated above the compounds  $\text{PuCl}_3$ ,  $\text{NpCl}_3$ , and  $\text{NpBr}_3$ , and the solid solution  $\text{Pu}(\text{Br}_{0.8},\text{Cl}_{0.2})_3$  all have the  $\text{UCl}_3$  type of structure.

A detailed account of the crystal structure determination of  $\text{UCl}_3$  and isomorphous compounds has been given elsewhere.<sup>10</sup>

Some of the x-ray diffraction data for  $\text{PuCl}_3$ ,  $\text{NpCl}_3$ ,  $\text{Pu}(\text{Br}_{0.8},\text{Cl}_{0.2})_3$ , and  $\text{NpBr}_3$ , are shown in Tables 1 and 2.

The compounds are hexagonal with two molecules per unit cell. The lattice dimensions and calculated densities are given in Table 3 together with those of isomorphous substances.

Table 1—X-ray Diffraction Data for  $\text{PuCl}_3$  and  $\text{NpCl}_3$ 

$H_1H_2H_3$	$\text{PuCl}_3$ I (obs.)	$\sin^2 \theta$	$\text{NpCl}_3$ I (obs.)	$\sin^2 \theta$	$\text{UCl}_3$ $ F ^2 p$
100	M	0.0148	M	0.0145	4.1
110	M	0.0437	M	0.0435	8.9
101q	S	0.0480	S	0.0472	14.9
200	W	0.0582	W	0.0583	4.1
111	W	0.0767	VW	0.0761	2.5
201	S	0.0918	M	0.0907	27.0
210	W-	0.1019	VW	0.1015	5.4
300, 002	W	0.1314	W	0.1298	15.9 + 7.4
211	S	0.1359	M	0.1340	36.3
102	VW	0.1478	VW	0.1439	5.6
301	Nil		Nil		0
220, 112	WM	0.1763	W+	0.1734	22.7
310, 202	W	0.1904	VW+	0.1883	11.8
221	Nil		Nil		0.3
311	W+	0.2223	W+	0.2206	19.1
400, 212	W-	0.2339	VW+	0.2308	12.2
401, 302	M	0.2640	W+	0.2604	31.9
320	VW	0.2758	VVW	0.2730	5.8
410, 321, 222, 103	M+, broad	0.3080	M, broad	0.3058	
312	VW+	0.3113	VVW	0.3166	
203	W-	0.3558	VW	0.3495	
500, 402	VW	0.3644	VVW	0.3617	
330, 501, 213	M+, broad	0.3988	W	0.3928	
420, 322	VVV	0.4080	VVW	0.4053	
421, 412	M	0.4375	W	0.4342	

The space group is  $C6_3/m$  ( $C_{6h}^2$ ) and the atomic positions are:

2 metal atoms in  $\pm (\frac{1}{3} \frac{2}{3} \frac{1}{4})$

6 halogen atoms in  $\pm (x \ y \ \frac{1}{4})(y - x, \bar{x}, \frac{1}{4})(\bar{y}, x - y, \frac{1}{4})$   
with  $x = 0.375$  and  $y = 0.292$

The agreement between observed intensities and calculated values  $|F|^2 p$  (where  $F$  is the structure factor and  $p$  the multiplicity of the reflecting plane) is shown in Tables 1 and 2.

Each metal atom is bonded to nine halogen atoms, three of which are at a slightly different distance than are the other six. The interatomic distances are

	$\text{PuCl}_3$	$\text{NpCl}_3$	$\text{NpBr}_3$
3 halogens at	2.93 Å	2.94 Å	3.14 Å
6 halogens at	2.92 Å	2.94 Å	3.08 Å

Table 2—X-ray Diffraction Data for  $\text{Pu}(\text{Br},\text{Cl})_3$  and  $\text{NpBr}_3$ 

$H_1H_2H_3$		$\text{Pu}(\text{Br},\text{Cl})_3$	$\text{NpBr}_3$	$\text{UBr}_3$
	I (obs.)	$\sin^2 \theta$	$\sin^2 \theta$	$ \mathbf{F} ^2 p$
100	S	0.0135	0.0131	
110	M	0.0392	0.0377	4.2
101	M+	0.0457	0.0437	9.2
200	W	0.0524	0.0507	5.3
111	M	0.0718	0.0687	13.7
201	S	0.0852	0.0810	44.1
210	W	0.0914	0.0883	9.4
300	M-	0.1178	0.1136	24.0
211	S	0.1239	0.1192	41.4
002	W	0.1298	0.1232	14.8
102	W-	0.1423	0.1366	6.1
301	Nil			0.4
220	W-	0.1568	0.1529	7.0
310, 112	M-	0.1692	0.1638	16.2
202	VW+	0.1818	0.1746	7.9
221	Nil			1.5
311	W	0.2018	0.1942	12.1
400	VW	0.2085	0.2023	6.4
212	W	0.2203	0.2126	13.7
401	Nil			1.6
302, 320	S-	0.2474	0.2376	46.6
410	W-	0.2732	0.2636	58.5
222	VW	0.2860		
312	VW+	0.2976	0.2898	
500, 113	VW+	0.3283	0.3151	
203	W	0.3420	0.3280	
501	W-	0.3573	0.3453	

Table 3—Lattice Dimensions and Calculated Densities for Isomorphous Trichlorides and Tribromides

$\text{KCl}_3$ or $\text{XBr}_3$	$a_1, \text{ Å}$	$a_2, \text{ Å}$	$\rho$
$\text{LaCl}_3$	$7.468 \pm 0.003$	$4.366 \pm 0.003$	<b>3.84</b>
$\text{CeCl}_3$	$7.436 \pm 0.004$	$4.304 \pm 0.004$	<b>3.95</b>
$\text{UCl}_3$	$7.428 \pm 0.003$	$4.312 \pm 0.003$	<b>5.51</b>
$\text{NpCl}_3$	$7.405 \pm 0.010$	$4.273 \pm 0.005$	<b>5.58</b>
$\text{PrCl}_3$	$7.41 \pm 0.01$	$4.25 \pm 0.01$	<b>4.02</b>
$\text{PuCl}_3$	$7.380 \pm 0.001$	$4.238 \pm 0.001$	<b>5.70</b>
$\text{NdCl}_3$	$7.381 \pm 0.004$	$4.231 \pm 0.003$	<b>4.14</b>
$\text{LaBr}_3$	$7.951 \pm 0.003$	$4.501 \pm 0.003$	<b>4.07</b>
$\text{CeBr}_3$	$7.936 \pm 0.003$	$4.435 \pm 0.003$	<b>5.18</b>
$\text{UBr}_3$	$7.926 \pm 0.002$	$4.432 \pm 0.002$	<b>6.53</b>
$\text{NpBr}_3$	$7.917 \pm 0.005$	$4.382 \pm 0.005$	<b>6.61</b>
$\text{PrBr}_3$	$7.92 \pm 0.01$	$4.38 \pm 0.01$	<b>5.26</b>
$\text{Pu}(\text{Br}_{0.8},\text{Cl}_{0.2})_3$	$7.806 \pm 0.018$	$4.302 \pm 0.004$	

3. THE COMPOUNDS  $\text{PuBr}_3$ ,  $\text{PuI}_3$ , AND  $\text{NpI}_3$ 

3.1 Origin and Identification of the Preparation.  $\text{PuBr}_3$  was first prepared by Hyde,<sup>11</sup> and the identity of the preparation was established by direct chemical analysis.

Table 4—X-ray Diffraction Data for  $\text{PuBr}_3$ 

$H_1H_2H_3$	$\sin^2 \theta$	I (obs.)	$ F ^2 p$
200	0.0153	S	6.1
201		Nil	0.1
002	0.0289	M	4.4
110		Nil	0.2
202	0.0437	M-	5.6
111	0.0463	M-	11.6
400	0.0605	Trace	0.5
401			2.2
112	0.0673	W	12.0
310	0.0692	W	4.4
311	0.0762	S+	52.0
203	0.0790	W+	8.2
402	0.0881	M	26.0
312		Trace	3.6
113	0.1029	S-	38.4
004	0.1137	W-	13.7
403		Nil	0.2
204			7.2
510	0.1288	VW	0
313	0.1329	W	24.4
600			5.0
511	0.1355	W	18.4
020			21.0
601	0.1417	W	1.4
114		Nil	0.4
220			8.4
512	0.1567	VW	2.8

Hagemann<sup>12</sup> was the first to prepare  $\text{PuI}_3$ . The identification was made from the x-ray diffraction pattern, which showed that it was isomorphous with  $\text{PuBr}_3$  and  $\text{UI}_3$ .<sup>13</sup>

$\text{NpI}_3$  was made by Fried.<sup>14</sup> The identity of the preparation was deduced from the x-ray diffraction pattern.<sup>15</sup>

3.2 Crystal Structure of  $\text{PuBr}_3$ ,<sup>13,16</sup>  $\text{PuI}_3$ ,<sup>13,16</sup> and  $\text{NpI}_3$ .<sup>15</sup>  $\text{PuBr}_3$ ,  $\text{PuI}_3$ , and  $\text{NpI}_3$  and also  $\text{NdBr}_3$ ,  $\text{SmBr}_3$ , and  $\text{LaI}_3$  are examples of a new structure type. This should be called the  $\text{PuBr}_3$  type of structure since this compound was the first of the isomorphous series to be investigated.

Some of the x-ray diffraction observations for  $\text{PuBr}_3$  are shown in Table 4. Because of the low symmetry the interpretations of the diffraction pattern succeeded only after considerable expenditure of time and effort.

Attempts to interpret the observed sine squares in accordance with cubic, hexagonal, or tetragonal symmetry failed. However, the observations did fit an orthorhombic quadratic form. The deduced lattice dimensions are:

	$a_1, \text{ Å}$	$a_2, \text{ Å}$	$a_3, \text{ Å}$
$\text{PuBr}_3$	$12.57 \pm 0.05$	$4.11 \pm 0.03$	$9.13 \pm 0.04$
$\text{PuI}_3$	$13.9 \pm 0.1$	$4.29 \pm 0.04$	$9.90 \pm 0.10$
$\text{NpI}_3$	$13.93 \pm 0.04$	$4.31 \pm 0.03$	$9.94 \pm 0.05$

Since the volume of the unit cell for  $\text{PuBr}_3$  is  $471 \text{ Å}^3$  and since each bromine atom requires a space of about  $40 \text{ Å}^3$ , there must be four molecules per unit cell. The calculated densities are:  $\rho = 6.69$  for  $\text{PuBr}_3$ , 6.9 for  $\text{PuI}_3$ , and 6.82 for  $\text{NpI}_3$ .

The observations show that reflections  $H_1H_2H_3$  are absent if  $H_1 + H_2$  is odd. In addition the reflections  $0H_2H_3$  are absent unless  $H_3$  is even. Accordingly, one is led to the space group Ccmm ( $D_{2h}^{17}$ ) or one of its subgroups. The holohedral space group Ccmm was assumed to be the correct one.

It was found that agreement between observed and calculated intensities could be attained if the atoms were distributed over the available positions of the space group Ccmm as follows:

$$(0\ 0\ 0)(\frac{1}{2}\ \frac{1}{2}\ 0)+$$

4 metal atoms in  $\pm(x_1, 0, \frac{1}{2})$

4 halogen atoms in  $\pm(x_2, 0, \frac{1}{2})$

8 halogen atoms in  $\pm(x_3, 0, z)(x_3, 0, \frac{1}{2} - z)$

For  $\text{PuBr}_3$ , the best agreement between observed and calculated intensities was obtained for the following parameter values:

$$x_1 = 0.25, \quad x_2 = -0.07, \quad x_3 = 0.36, \quad z = -0.05$$

The same parameter values also give satisfactory agreement for the other members of the isomorphous series. The last column of Table 4 gives the calculated values of  $|F|^2 p$  for  $\text{PuBr}_3$ .

In the structure each metal atom is bonded to eight halogen atoms. The interatomic distances are:

	PuBr <sub>3</sub>	PuI <sub>3</sub>	NpI <sub>3</sub>
2 halogen atoms at	3.06 Å	3.31 Å	3.32 Å
2 halogen atoms at	3.08 Å	3.36 Å	3.37 Å
4 halogen atoms at	3.08 Å	3.32 Å	3.33 Å

The structure is of layer-structure type. Across the planes  $X = 0$  and  $X = \frac{1}{2}$  the structure is held together only by van der Waals binding between bromine or iodine atoms. Thus the crystals should exhibit excellent cleavage parallel to (1 0 0).

#### 4. THE COMPOUNDS PuOCl, PuOBr, AND PuOI

4.1 Origin and Identification of the Preparation. The compound PuOI was first observed and identified from the x-ray diffraction pattern<sup>17</sup> in preparations which Hagemann<sup>4</sup> had made in attempts to prepare PuI<sub>3</sub>.

The oxybromide PuOBr was first prepared by Hyde and Hagemann,<sup>18</sup> and PuOCl by Brody.<sup>19</sup>

The oxybromide as well as the oxychloride was identified by interpretation of the x-ray diffraction patterns.<sup>17</sup>

4.2 The Crystal Structure of PuOCl,<sup>17</sup> PuOBr,<sup>17</sup> and PuOI.<sup>17</sup> PuOCl, PuOBr, and PuOI all have the PbFCl type of structure. They are thus isomorphous with the corresponding compounds of bismuth<sup>20</sup> and of lanthanum.<sup>21</sup>

The author has prepared additional isomorphous oxyhalides, namely PrOCl,<sup>22</sup> NdOCl,<sup>23</sup> YOCl,<sup>24</sup> and NdOBr.<sup>24</sup> These compounds were made by heating the trihalides in air.

The lattice dimensions of the tetragonal unit cell which contains two molecules are shown in Table 5. The calculated densities are  $\rho = 8.81$  for PuOCl, 9.07 for PuOBr, and 8.46 for PuOI.

The x-ray diffraction observations up to  $\sin^2 \theta = 0.500$  are given in Tables 6 and 7.

The structure of the oxyhalides is as follows. The space group is P4/nmm ( $D_{4h}^7$ ) and the atomic positions are:

- 2 metal atoms in (0 0 u<sub>1</sub>) ( $\frac{1}{2} \frac{1}{2} \bar{u}_1$ )
- 2 oxygen atoms in ( $\frac{1}{2} 0 0$ ) (0  $\frac{1}{2} 0$ )
- 2 halogen atoms in (0 0 u<sub>2</sub>) ( $\frac{1}{2} \frac{1}{2} \bar{u}_2$ )

## THE TRANSURANIUM ELEMENTS

Table 5 - Lattice Dimensions for Oxyhalides

	$a_1, \text{ Å}$	$a_3, \text{ Å}$	$a_3/a_1$
BiOCl	3.883	7.348	1.892
LaOCl	4.113 $\pm$ 0.003	6.871 $\pm$ 0.009	1.671
PrOCl	4.045 $\pm$ 0.003	6.786 $\pm$ 0.009	1.678
PuOCl	4.004 $\pm$ 0.002	6.779 $\pm$ 0.010	1.693
NdOCl	4.03 $\pm$ 0.03	6.73 $\pm$ 0.04	1.677
YOCl	3.892 $\pm$ 0.002	6.591 $\pm$ 0.004	1.693
BiOB <sub>r</sub>	3.916	8.077	2.063
LaOB <sub>r</sub>	4.147 $\pm$ 0.003	7.376 $\pm$ 0.012	1.779
PuOB <sub>r</sub>	4.014 $\pm$ 0.004	7.556 $\pm$ 0.011	1.882
NdOB <sub>r</sub>	4.009 $\pm$ 0.006	7.604 $\pm$ 0.020	1.897
BiOI	3.985	9.129	2.291
LaOI	4.144	9.126	2.202
PuOI	4.034 $\pm$ 0.002	9.151 $\pm$ 0.015	2.268

Table 6 — X-ray Diffraction Data for PuOCl

I (obs.)	$\sin^2 \theta$	H <sub>1</sub> H <sub>2</sub> H <sub>3</sub>
M+	0.0498	101, 002
M	0.0737	110
M	0.0887	102
VW-	0.1161	003
W+	0.1259	112
M	0.1478	200
VVV	0.1537	103
VW	0.1607	201
M-	0.1900	113
M	0.1978	211
Trace	0.2067	202
M	0.2356	212
W+	0.2440	104
W	0.2637	203
VW	0.2800	114
W	0.2944	220
Trace	0.3005	213
VVV	0.3071	221
VW-	0.3220	005
W	0.3448	301, 222
VVV	0.3543	204
VW-	0.3597	105
W	0.3682	310
W	0.3821	311, 302
W+	0.3901	214
VW	0.3960	115
W	0.4096	223
W	0.4199	312
VW	0.4693	205
W	0.4836	313
W	0.4915	321

Table 7—X-ray Diffraction Data for PuOBr and PuOI

PuOBr			PuOI		
I (obs.)	$\sin^2 \theta$	$H_1H_2H_3$	I (obs.)	$\sin^2 \theta$	$H_1H_2H_3$
W	0.0422	002	S	0.0658	102
M	0.0474	101	S	0.0737	110
M	0.0738	110	VW-	0.0816	111
S	0.0791	102	W+	0.1020	112, 103
VW	0.0949	003	VW+	0.1129	004
VW-	0.1162	112	M+	0.1469	200
M	0.1478	200	VW+	0.1529	201
VW	0.1589	201	M	0.1867	114
M	0.1679	113, 004	S+	0.2119	212
W+	0.1945	211	W	0.2473	213
W+	0.2043	104	W	0.2602	204
S	0.2265	212	M	0.2928	220, 106
M-	0.2413	203, 114	VW	0.3223	220, 205
W+	0.2965	220, 105	M	0.3573	302
W	0.3138	204	M	0.3654	310
W+	0.3512	214	VW	0.3835	107
M	0.3686	310	VW	0.3937	312
M	0.3740	302, 006	VW+	0.4061	224
VW+	0.3889	223	VW+	0.4377	216
W+	0.4094	106	W-	0.4768	314
W+	0.4470	215, 116			
W+	0.4608	313, 224			
VW	0.4904	321			
VW	0.4976	304			

The parameters  $u_1$  and  $u_2$  were determined using the intensities of reflections with high values of the index  $H_3$ . The results are:

	$u_1$	$u_2$
PuOC1	0.181	0.640
PuOBr	0.161	0.640
PuOI	0.125	0.667

The interatomic distances are:

	Pu-O	Pu-X
PuOC1	2.35 Å	3.08 Å and 3.11 Å
PuOBr	2.34 Å	3.21 Å
PuOI	2.32 Å	3.44 Å

In all three compounds each plutonium atom is linked to four oxygen atoms. In PuOBr and PuOI, plutonium is bonded to four halogen atoms, whereas in PuOC1 five Pu-Cl bonds are present.

The plutonium to oxygen distances are smaller, and the plutonium to halogen distances are larger than the sum of the ionic radii.

### 5. THE COMPOUND $\text{NpCl}_4$

The compound  $\text{NpCl}_4$  was first prepared by Fried and Davidson.<sup>6</sup> The substance was identified by its x-ray diffraction pattern, which was isomorphous with  $\text{UCl}_4$  and  $\text{ThCl}_4$ .<sup>7</sup>

Table 1 shows the x-ray diffraction data up to  $\sin^2 \theta = 0.350$ .

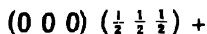
The complete structure of  $\text{UCl}_4$  has been found by Mooney.<sup>25</sup> The structure is tetragonal with four molecules per unit cell.

The lattice dimensions and calculated densities are:

	$a_1, \text{ Å}$	$a_3, \text{ Å}$	$\rho$
$\text{ThCl}_4$	$8.473 \pm 0.003$	$7.468 \pm 0.003$	4.60
$\text{UCl}_4$	$8.296 \pm 0.009$	$7.487 \pm 0.009$	4.87
$\text{NpCl}_4$	$8.25 \pm 0.01$	$7.46 \pm 0.01$	4.92

These values are taken from references 26, 25, and 7, respectively.

According to Mooney<sup>25</sup> the space group for the  $\text{UCl}_4$  type of structure is I4/amd ( $D_{4h}^{10}$ ). The atomic positions are:



4 metal atoms in  $(0\ 0\ \frac{1}{2})\ (0\ \frac{1}{2}\ \frac{1}{4})$

16 chlorine atoms in  $(0\ x\ z)\ (0\ \bar{x}\ z)\ (0,\ x + \frac{1}{2}, \frac{1}{4} - z)$

$(0, \frac{1}{2} - x, \frac{1}{4} - z)\ (x\ 0\ z)\ (\bar{x}\ 0\ \bar{z})\ (x + \frac{1}{2}, 0, z - \frac{1}{4})\ (\frac{1}{2} - x, 0, z - \frac{1}{4})$

For  $\text{UCl}_4$  Mooney found  $x = 0.28$  Å and  $z = 0.40$ , so that each uranium atom is linked to four chlorine atoms at 2.44 Å and to four additional chlorine atoms at 3.20 Å. The difference between the two sets of U-Cl distances is unreasonably large.

By minor adjustments of the parameter values it is possible to make the two sets of distances more nearly equal. The parameter values for  $\text{NpCl}_4$  are therefore chosen as

$$x = 0.310 \text{ Å} \quad \text{and} \quad z = 0.430$$

With these values each neptunium atom is bonded to four chlorine atoms at a distance of 2.61 Å and to four additional chlorine atoms at 2.86 Å. These interatomic distances cannot be made exactly equal because of chlorine-chlorine repulsion.

The last two columns of Table 8 give the observed intensities and the calculated values  $|F|^2 p$  as reported by Mooney for  $\text{UCl}_4$ .

Table 8—X-ray Diffraction Data for  $\text{NpCl}_4$ 

$\text{NpCl}_4$			$\text{UCl}_4$	
I (obs.)	$\sin^2 \theta$	$H_1 H_2 H_3$	I (obs.)	$ F ^2 p$
S	0.194	101	S	25
S	0.0347	200	S	31
W+	0.0542	211	M-	31
M-	0.0601	112	M	45
VW-	0.0703	220	Trace	3
VW-	0.0777	202	VW	14
M	0.0894	301	M+	32
W+	0.1051	103	M	28
W+	0.1243	321	M+	48
M	0.1302	312	S	75
W+	0.1400	400, 213	M-	66
W-	0.1589	411	W+	52
W	0.1746	420, 303	W	43
W	0.1997	332	W+	35
VW	0.2054	204	W	30
W	0.2293	431, 501	W+	53
VW	0.2410	224	W	57
VW	0.2438	413	W-	40
VW	0.2699	512	W-	45
Trace	0.2799	440	N11	14
W-	0.3112	404, 215		
W-	0.3138	600, 433, 503		
Trace	0.3339	611		
VVW	0.3392	532		
VW-	0.3460	424, 305		
VW	0.3491	620, 523		

6. THE COMPOUND  $\text{Cs}_2\text{PuCl}_6$ 

Anderson<sup>27</sup> prepared the compound and determined the composition by direct chemical analysis.

The x-ray diffraction pattern of Anderson's sample corresponds to a hexagonal structure. The lattice dimensions are<sup>28</sup>

$$a_1 = 7.45 \pm 0.02 \text{ \AA}, \quad a_3 = 6.05 \pm 0.02 \text{ \AA}$$

The unit cell can accommodate but one molecule. Thus the calculated density is  $\rho = 4.05$ .

The plutonium atom is at the position (0 0 0) and the two cesium atoms are at  $\pm(\frac{1}{2} \frac{1}{2} \frac{1}{2})$ . The positions of the chlorine atoms have not been determined.

### 7. OTHER CHLORIDES, BROMIDES, AND IODIDES

The compounds  $\text{PuCl}_3 \cdot 6\text{H}_2\text{O}$  and  $\text{PuBr}_3 \cdot 6\text{H}_2\text{O}$  are isomorphous with  $\text{NdCl}_3 \cdot 6\text{H}_2\text{O}$ .  $\text{NpBr}_4$  is isomorphous with  $\text{UBr}_4$ ;  $\text{NpOCl}_2$  and  $\text{NpOBr}_2$  are isomorphous with  $\text{UOCl}_2$  and  $\text{UOBr}_2$ .

The identity of these plutonium and neptunium compounds was determined from the x-ray diffraction patterns, but the author did not succeed in deducing the lattice dimensions.

### 8. SUMMARY

Complete crystal structures have been found for the compounds  $\text{PuCl}_3$ ,  $\text{NpCl}_3$ ,  $\text{PuBr}_3$ ,  $\text{NpBr}_3$ ,  $\text{PuI}_3$ ,  $\text{NpI}_3$ ,  $\text{PuOCl}$ ,  $\text{PuOBr}$ ,  $\text{PuOI}$ , and  $\text{NpCl}_4$ .

$\text{PuCl}_3$ ,  $\text{NpCl}_3$ , and  $\text{NpBr}_3$  are hexagonal with the  $\text{UCl}_3$  type of structure in which each metal atom is bonded to nine halogen atoms.

$\text{PuBr}_3$ ,  $\text{PuI}_3$ , and  $\text{NpI}_3$  are orthorhombic and isomorphous. The structure is of layer-lattice type with each metal atom bonded to eight halogen atoms.

$\text{PuOCl}$ ,  $\text{PuOBr}$ , and  $\text{PuOI}$  all have the  $\text{PbFCl}$  type of structure.  $\text{NpCl}_4$  is isomorphous with  $\text{UCl}_4$ .

Only the lattice dimensions and the positions of the metal atoms have been found for the compound  $\text{Cs}_2\text{PuCl}_6$ .

### ACKNOWLEDGMENT

Miss Anne Plettlinger gave valuable assistance by taking all the x-ray diffraction patterns.

### REFERENCES

1. F. Hagemann, Metallurgical Project Report CK-1372 (Mar. 1, 1944), pp. 11-12.
2. W. H. Zachariasen, Metallurgical Project Report CP-1249 (Jan. 22, 1944), p. 14.
3. W. H. Zachariasen, Metallurgical Project Report CK-1377 (Feb. 26, 1944), p. 3.
4. F. Hagemann, Metallurgical Project Report CK-1701 (June 1, 1944), p. 6.
5. W. H. Zachariasen, Metallurgical Project Reports CK-1566 (Apr. 13, 1944) and CK-1597 (Apr. 24, 1944), p. 2.
6. S. Fried and N. R. Davidson, Metallurgical Project Report CN-2689 (Feb. 15, 1945), p. 2.
7. W. H. Zachariasen, Metallurgical Project Report CN-2686 (Jan. 15, 1945), pp. 2-3.
8. S. Fried, Metallurgical Project Report CP-3383 (December 1945), p. 2.

9. W. H. Zachariasen, Metallurgical Project Report CP-3383 (December 1945), p. 2.
10. W. H. Zachariasen, Metallurgical Project Report CK-1487 (Mar. 21, 1944).
11. E. K. Hyde, Metallurgical Project Report CK-1586 (May 1, 1944), p. 7.
12. F. Hagemann, Metallurgical Project Report CK-1783 (July 1, 1944), p. 9.
13. W. H. Zachariasen, Metallurgical Project Report CN-1813 (June 23, 1944), p. 4.
14. S. Fried, Metallurgical Project Report CP-3383 (December 1945), p. 2.
15. W. H. Zachariasen, Metallurgical Project Report CP-3383 (December 1945), p. 3.
16. W. H. Zachariasen, Metallurgical Project Report CN-1957 (July 27, 1944), p. 2.
17. W. H. Zachariasen, Metallurgical Project Report CN-1733 (May 25, 1944).
18. E. K. Hyde and F. Hagemann, Metallurgical Project Report CK-1701 (June 1, 1944), p. 7.
19. B. Brody, Metallurgical Project Report CK-1701 (June 1, 1944), p. 4.
20. A. Bannister and M. H. Hey, Mineralog. Mag., 24: 49 (1935).
21. L. G. Sillén and A. L. Nylander, Svensk. Kem. Tid., 53: 367-72 (1941).
22. W. H. Zachariasen, Metallurgical Project Report CP-1954 (July 29, 1944), p. 24.
23. W. H. Zachariasen, Metallurgical Project Report CP-1576 (Apr. 24, 1944), p. 22.
24. W. H. Zachariasen, Metallurgical Project Report CP-2160 (Sept. 23, 1944), p. 17.
25. R. C. L. Mooney, Metallurgical Project Report CP-1533 (Mar. 31, 1944).
26. W. H. Zachariasen, Metallurgical Project Report CN-3382 (Dec. 28, 1945), p. 4.
27. H. H. Anderson, Dicesium plutonium(IV) hexachloride and related compounds, Paper 6.13, this volume (Argonne National Laboratory Report ANL-4056).
28. W. H. Zachariasen, Metallurgical Project Report CP-3445 (February 1946), p. 3.

## Paper 20.7

### THE CRYSTAL STRUCTURE OF SODIUM PLUTONYL AND SODIUM NEPTUNYL ACETATES†

By W. H. Zachariasen

The compound  $\text{NaPuO}_2(\text{C}_2\text{H}_3\text{O}_2)_3$  was prepared and identified by R. Craig, J. W. Hamaker, and G. E. Sheline,<sup>1</sup> who also showed that there was isomorphism with the corresponding uranyl compound. The sample used in the present investigation was prepared by Clifford Smith.

L. B. Magnusson and T. J. LaChapelle<sup>2</sup> prepared the compound  $\text{NaNpO}_2(\text{C}_2\text{H}_3\text{O}_2)_3$ . The x-ray diffraction pattern proved this to be the composition of their sample,<sup>3</sup> thus for the first time demonstrating the existence of the hexapositive state for neptunium.

X-ray diffraction data (for low-angle reflections) are given in Table 1 for  $\text{NaPuO}_2(\text{C}_2\text{H}_3\text{O}_2)_3$ . Except for a slight shift in the positions of the diffraction lines the patterns of the plutonium and neptunium compounds are practically indistinguishable. A few observations for both compounds taken from the back-reflection region are shown in Table 2.

The corresponding uranium compound had been studied by I. Fan-kuchen,<sup>4</sup> who suggested a complete structure.

The dimensions of the unit cube and the calculated densities for the three substances are:

	a, Å	ρ
U compound	$10.671 \pm 0.001$	2.554
Np compound <sup>5</sup>	$10.659 \pm 0.002$	2.556
Pu compound <sup>6</sup>	$10.643 \pm 0.002$	2.578

†Contribution from the Physics Division of the Metallurgical Laboratory, University of Chicago, now the Argonne National Laboratory.

Table 1—X-ray Diffraction Data for  $\text{NaPuO}_2(\text{C}_2\text{H}_5\text{O}_2)_3$  ( $\text{CuK}\alpha$ )

I (obs.)	$\sin^2 \theta$	$H_1^2 + H_2^2 + H_3^2$
S	0.0162	3
W+	0.0213	4
S	0.0267	5
S-	0.0323	6
VWV	0.0426	8
S-	0.0481	9
W+	0.0532	10
VW-	0.0584	11
VW-	0.0636	12
VW+	0.0689	13
S	0.0749	14
MS	0.0904	17
VW-	0.0953	18
W-	0.1006	19
W	0.1114	21
VW+	0.1269	24
W	0.1322	25
S	0.1378	26
W+	0.1433	27
M+	0.1534	29
W+	0.1591	30

Table 2—Back-reflection Data ( $\text{CuK}\alpha$ )

$H_1^2 + H_2^2 + H_3^2$	Pu compound		Np compound	
	$\sin^2 \theta$	a, Å	$\sin^2 \theta$	a, Å
185 $\alpha_1$	0.9647	10.644	0.9624	10.658
186 $\alpha_1$	0.9698	10.645	0.9671	10.661
187 $\alpha_1$	0.9750	10.642	0.9726	10.659
189 $\alpha_1$	0.9859	10.643	0.9832	10.658

As shown by I. Fankuchen the space group is  $P2_13$  ( $T^4$ ), and the four heavy-metal atoms per unit cell are at positions

$$(u \ u \ u) (u + \frac{1}{2}, \frac{1}{2} - u, \bar{u}) (\bar{u}, u + \frac{1}{2}, \frac{1}{2} - u) (\frac{1}{2} - u, \bar{u}, u + \frac{1}{2})$$

with  $u = 0.428 \pm 0.002$ . The same value for  $u$  is valid for all three compounds.

The positions of the light atoms are uncertain.

The x-ray diffraction patterns were taken by Anne Plettinger.

Summary.  $\text{NaPuO}_2(\text{C}_2\text{H}_3\text{O}_2)_3$  and  $\text{NaNpO}_2(\text{C}_2\text{H}_3\text{O}_2)_3$  are isomorphous with the corresponding uranyl compound. The unit cube containing four molecules has an edge  $a = 10.659 \pm 0.002$  Å for the neptunium compound and  $a = 10.643 \pm 0.002$  Å for the plutonium compound. The calculated densities are  $\rho = 2.556$  for the neptunium compound and  $\rho = 2.578$  for the plutonium compound.

The space group is  $P2_13$ . Only the positions of the heavy-metal atoms are known.

#### REFERENCES

1. R. Craig, J. W. Hamaker, and G. E. Sheline, Metallurgical Project Report CN-723 (June 20, 1943), p. 10.
2. L. B. Magnusson and T. J. LaChapelle, Metallurgical Project Report CN-2088 (Sept. 1, 1944), p. 18.
3. W. H. Zachariasen, Metallurgical Project Report CN-2091 (Aug. 28, 1944), p. 2.
4. I. Fankuchen, Z. Krist., 91: 473 (1935).
5. W. H. Zachariasen, Metallurgical Project Report CK-1518 (Mar. 27, 1944), p. 4.

Paper 20.8

THE CRYSTAL STRUCTURE OF  $\text{NpO}_2$  AND  $\text{NpO}^\dagger$

By W. H. Zachariasen

$\text{NpO}_2$  and  $\text{NpO}$  are the only two oxides of neptunium for which crystal structure data are available. Fried<sup>1</sup> made an unsuccessful attempt to prepare a higher oxide of neptunium, and  $\text{NpO}_2$  and  $\text{NpO}$  appear to be the only neptunium oxides that are known.

Identification and Crystal Structure of  $\text{NpO}_2$ . In June 1944, T. J. LaChapelle and L. B. Magnusson submitted a neptunium preparation for x-ray study. They had prepared the sample by ignition of a hydroxide precipitate.<sup>2</sup>

This was the first neptunium preparation to be examined by the x-ray diffraction method. At the time, some observations on the oxidation states in solutions had been made,<sup>2</sup> but not a single valence state had been identified. Hence the only statement that could be made about the submitted sample was that the preparation was some oxide of neptunium.

A fair x-ray diffraction pattern of the sample was obtained using CuK radiation filtered through nickel foil. The weight of the sample was estimated to be about 10  $\mu\text{g}$ , and the exposure time was 4 hr.

The observed intensities and sine squares as obtained from the original diffraction pattern are shown in Table 1.

As indicated in Table 1 the observed values could be interpreted as being due to two cubic face-centered phases, one with a lattice constant of  $a = 3.910 \text{ \AA}$  present to a small extent, and the other with  $a = 5.42 \pm 0.01 \text{ \AA}$ , this latter making up the bulk of the sample.

<sup>†</sup>Contribution from the Physics Division of the Metallurgical Laboratory, University of Chicago, now the Argonne National Laboratory.

The first phase is clearly metallic platinum. Its presence in the sample was understandable since the neptunium oxide had been gently scraped from a platinum crucible.

The diffraction intensities show that the second phase contains four metal atoms per unit cube. The volume of the unit cell is 159 Å<sup>3</sup>, and

Table 1—X-ray Diffraction Data for NpO<sub>2</sub>

I (obs.)	$\sin^2 \theta =$	$(H_1^2 + H_2^2 + H_3^2)(\lambda^2/4a^2)$
MS	0.0611	= 3 × 0.02037
W	0.0812	= 4 × 0.02041
W-	0.1163	= 3 × 0.03876
M-	0.1623	= 8 × 0.02029
M-	0.2230	= 11 × 0.02027
VW	0.2422	= 12 × 0.02018
VW-	0.3099	= 8 × 0.03874
VVW	0.3234	= 16 × 0.02021
W-	0.3840	= 19 × 0.02021
VW+	0.4039	= 20 × 0.02020
VW	0.4261	= 11 × 0.03874
VW+	0.4848	= 24 × 0.02020
VW+	0.5450	= 27 × 0.02018
VW+	0.7046	= 35 × 0.02013
VVW	0.8066	= 40 × 0.02017

Table 2—X-ray Diffraction Data for NpO (CuKα)

I (obs.)	$\sin^2 \theta$	H <sub>1</sub> H <sub>2</sub> H <sub>3</sub>
W	0.0715	111
W-	0.0956	200
VW	0.1902	220
VW+	0.2617	311
VW-	0.2879	222
VW	0.4491	331
VW+	0.4766	420

the space requirement of an oxygen atom is 19 Å<sup>3</sup> as shown by earlier work.<sup>3</sup> Hence there are eight oxygen atoms per unit cell, and the identity<sup>4</sup> of the phase is NpO<sub>2</sub>. Thus a compound and a valence state of neptunium had been identified for the first time.

Later samples of NpO<sub>2</sub> permitted a more accurate determination of the lattice constant. The best value<sup>5</sup> is  $a = 5.425 \pm 0.001$  Å, giving a calculated density  $\rho = 11.11$ .

The oxygen atoms have a small effect on the intensity of scattering, but the effect is sufficient to show that the structure of  $\text{NpO}_2$  is of the fluorite type. Thus each neptunium atom is bonded to eight oxygen atoms with a Np-O distance 2.349 Å.

The lattice constants and interatomic distances for the isomorphous series of dioxides are given in the chapter on the crystal chemistry of plutonium and neptunium, National Nuclear Energy Series, Division IV, Volume 14 A.

Identification and Crystal Structure of  $\text{NpO}$ . Fried<sup>6</sup> prepared neptunium metal and neptunium hydride. The x-ray diffraction pattern<sup>†</sup> of the hydride sample showed the diffraction lines of  $\text{NpO}_2$  and of a second phase. The second phase is cubic face-centered with  $a = 5.00 \pm 0.01$  Å. The data for the diffraction lines are shown in Table 2. The relative intensities of the pairs of reflections 1 1 1, 2 0 0; 3 1 1, 2 2 2; 3 3 1, 4 2 0 indicate the sodium chloride type of structure.

It could thus be stated<sup>5</sup> that the phase probably was  $\text{NpO}$ . The calculated density is  $\rho = 13.35$ .

The lattice constant of  $\text{PuO}$  is, for comparison,  $a = 4.948 \pm 0.002$  Å.

Summary. A preparation of neptunium oxide has been shown to be  $\text{NpO}_2$ . This compound has the fluorite type of structure with  $a = 5.425 \pm 0.001$  Å and a calculated density of  $\rho = 11.11$ .

A preparation of neptunium hydride is shown to contain  $\text{NpO}_2$  and a phase that probably is  $\text{NpO}$ . The monoxide has the sodium chloride type of structure with the value of  $a = 5.00 \pm 0.01$  Å and a calculated density of  $\rho = 13.34$ .

#### REFERENCES

1. S. Fried, Metallurgical Project Report CN-3381 (Dec. 27, 1945), p. 30.
2. T. J. LaChapelle and L. B. Magnusson, Metallurgical Project Report CN-1784 (July 1, 1944), p. 9.
3. W. H. Zachariasen, Metallurgical Project Report CK-1259 (Jan. 25, 1944).
4. W. H. Zachariasen, Metallurgical Project Report CN-1807 (June 22, 1944).
5. W. H. Zachariasen, Metallurgical Project Report CN-3382 (Dec. 28, 1945), pp. 3-9.
6. S. Fried, Metallurgical Project Report CN-3053 (June 1945).

<sup>†</sup>The x-ray diffraction patterns were taken by Anne Plettinger.

## Paper 21.1

### ELECTRONIC STRUCTURE OF THE HEAVIEST ELEMENTS†

By G. T. Seaborg

#### 1. HISTORICAL BACKGROUND

1.1 Before the Discovery of the Transuranium Elements. The intensive study of the heaviest elements during the last few years has given information and data that now enable us to make some definite statements as to their electronic structure and their place in the periodic table. These are to an appreciable extent two different questions. Such elements (compare, for example, the rare-earth elements) will probably find their place in the periodic system on the basis of their chemical properties as a group rather than on the basis of the individual electronic structures of their gaseous atoms. The information obtained about the recently discovered synthetic transuranium elements has been particularly useful in this connection, and it is largely on the basis of these new elements that this question is now well understood.

The heaviest natural elements, thorium, protactinium, and uranium, of atomic numbers 90, 91, and 92, respectively, have been placed in corresponding positions just below the sixth period "transition" elements—hafnium, tantalum, and tungsten—in which the 5d electron shell is being filled. Hafnium, tantalum, and tungsten are similar in their chemical properties to the corresponding transition elements in the fifth period—zirconium, columbium, and molybdenum—in which the 4d shell is being filled.

It has long been known that the chemical properties of thorium, protactinium, and uranium resemble those of the 4d and 5d elements. For this reason most of the textbooks and standard works on chemis-

†Contribution from the Department of Chemistry and the Radiation Laboratory, University of California, Berkeley.

try and physics in which the electronic structure is discussed have accepted the view that it is the 6d shell that is being filled. Thus the structures of the elements above radon (element 86) through uranium have been written to show the addition of the next two electrons in the 7s shell for element 87 (francium) and element 88 (radium) and addition in the 6d shell for actinium, thorium, protactinium, and uranium.<sup>1</sup>

Many of the early papers that appeared after N. Bohr's classical work<sup>2</sup> on the quantized nuclear atom discuss the electronic structure of the heaviest elements. It has been recognized by many that the next hypothetical rare gas should have the atomic number 118 in a place 32 elements beyond radon ( $Z = 86$ ), thus implying transition groups similar to those between xenon ( $Z = 54$ ) and radon ( $Z = 86$ ). Rydberg<sup>3</sup> as early as 1913 implied that this was to be expected. There has been general agreement that some type of transition group should begin in the neighborhood of uranium, although there have been differences of opinion as to where it begins and as to which electron shell is involved. A number of the earliest publications have suggested that this transition series involves the filling of the 5f shell, thus possibly giving rise to a "rare-earth" group in a manner analogous to that resulting from the filling of the 4f shell. The filling of the 4f shell results in the well-known group of fourteen rare-earth elements of atomic numbers 58 to 71, inclusive; these elements follow lanthanum. It is of interest here to note a few of the early and also the later suggestions in order to review the general previous status of this question. Most of these early investigators thought that the filling of the 5f shell should begin at some point beyond uranium, that is, beyond the elements that were known to them.

In early papers Bohr<sup>4</sup> suggested that the addition of the 5f electrons might begin in this region, and in a Bohr-Thomsen type of periodic table he pictured the first entry at the element with atomic number 94. Goldschmidt<sup>5</sup> thought the transuranium elements up to atomic number 96 should be homologues of the platinum group, and Hahn<sup>6</sup> thought this view was worthy of serious consideration. Sugira and Urey,<sup>7</sup> using the old quantum theory, published the results of their calculations, which indicated that the first entry of an electron into the 5f shell should occur at element 95, whereas Wu and Goudsmit,<sup>8</sup> on the basis of a more refined calculation, showed that their solution of the Schrodinger equation indicated such entry at uranium or element 93. McLennan, McLay, and Smith<sup>9</sup> suggested as an alternative to the filling of the 6d shell the possibility that the 5f shell begins to be occupied in thorium. In a review article Dushman<sup>10</sup> stated that it is doubtful that the added electrons enter the 6d level (thus implying an analogy with cerium, etc.). Swinne<sup>11</sup> pointed out that the available

evidence on thorium and uranium was consistent with the first entry of 5f electrons at protactinium or uranium, but he also thought that it might occur beyond uranium. Saha and Saha<sup>12</sup> suggested as an alternate possibility to the filling of the 6d shell the entry of the first 5f electron at thorium. Karapetoff<sup>13</sup> suggested that the element with atomic number 93 might be the first in which the 5f shell begins to be filled, and Von Grosse<sup>14</sup> suggested as a possible alternative to filling of the 6d shell the entry of the first electron in the 5f shell at uranium. Quill,<sup>15</sup> largely for the purpose of illustration, presented periodic table arrangements in which the first 5f electron appears in element number 95 in one case and in element number 99 in another. Perrin,<sup>16</sup> Rudy,<sup>17</sup> and Carranza<sup>18</sup> on general considerations proposed as a possibility the theory that the first 5f electron appears in thorium, and Villar<sup>19</sup> more recently suggested that some of the chemical evidence supports this viewpoint of an "actinide" transition group. Somewhat earlier, on the basis of his crystallographic work, Goldschmidt<sup>20</sup> had changed his original point of view and had come to the view that the first 5f electron enters at protactinium, which is the first element beyond thorium, although he pointed out the possibility that this might occur earlier, in thorium, or later, in uranium, or in the (at the time unknown) transuranium elements. By analogy with the name "lanthanide" series, which he had already proposed<sup>21</sup> for the rare-earth elements because these fourteen elements following lanthanum have lanthanum as their prototype, he proposed the name "thoride" series for the fourteen elements following thorium. At the same time he was the first to suggest that terms such as "actinide," "protactinide," and "uranide" might describe the group if it should eventually be found to begin earlier or later than this.

It can be seen that although many interesting and perspicacious proposals had been made up to this time, the electronic structure and place in the periodic table of these elements could not be regarded as established.

**1.2 After the Discovery of the Transuranium Elements.** The recent discovery of the transuranium elements and the study of their properties, especially the chemical properties, have furnished a tremendous amount of additional evidence of just the type needed to clarify this problem. It is in the transuranium elements that the really definitive chemical properties, from the standpoint of placing the heaviest elements in the periodic table, first appear. The first conclusive evidence that the 5f shell undergoes filling in this heavy region came from the tracer chemical observations of McMillan and Abelson<sup>22</sup> on element 93, neptunium. Upon their discovery of neptunium, the first transuranium element, McMillan and Abelson were

able to show definitely that it resembles uranium in its chemical properties and bears no resemblance to rhenium, which is the element immediately above it in the periodic table. This excellent experimental evidence was interpreted by them to indicate that this new "rare-earth" group of similar elements starts with uranium. The later calculations of Mayer<sup>23</sup> indicated that the energy and spatial extension of the 5f eigenfunctions drop sharply at about element 91 and therefore that the filling of the 5f shell might begin at protactinium or uranium. Daudel<sup>24</sup> in commenting on Mayer's paper made some remarks concerning the special nature of the f electrons at the beginning of the rare-earth and the heavy-transition groups. Starke<sup>25</sup> and Bedreag<sup>26</sup> also interpreted the tracer experiments with element 93 as indicating that the first 5f electron comes at element 93, but Strassmann and Hahn<sup>27</sup> thought, on the basis of their tracer experiments with this element, that it was difficult to make any deduction. As a result of their first tracer experiments with element 94 together with their consideration of the tracer investigations with element 93, Seaborg and Wahl<sup>28</sup> in 1942 made the suggestion that this transition group might begin earlier and that thorium or actinium might be the zero element in the series. On the basis of his complete crystallographic evidence, including especially observations on the transuranium elements, Zachariasen<sup>29</sup> agreed with Goldschmidt that a thoride series is involved. Some spatial classifications<sup>30,31</sup> of the elements have appeared recently in which the heaviest elements, starting with thorium as the homologue of cerium, are listed as the chemical homologues of the rare-earth elements, but the reason in these cases appears to be mainly connected with the symmetry of and the ease of making such an arrangement.

Following the first tracer work on the transuranium elements, the elements neptunium (atomic number 93) and plutonium (atomic number 94) have been extensively investigated with substantial weighable quantities. Americium (atomic number 95) and curium (atomic number 96) also have been available for investigation, on a more limited scale, in weighable quantities. The recent extensive investigations on thorium, protactinium, and uranium also have contributed to the evidence that is now useful in interpreting this question. All this information, especially the chemical evidence concerning americium and curium, seems to lead to a self-consistent and unambiguous picture concerning the nature of this transition series.

## 2. ACTINIDE CONCEPT

**2.1 General.** The evidence now available leads to the definite view that it is the 5f electron shell that is being filled in these heaviest

elements. The evidence seems sufficient to go further than this, and to suggest<sup>32,33</sup> that this rare-earth-like series begins with actinium in the same sense that the rare-earth or "lanthanide" series<sup>21</sup> begins with lanthanum. On this basis it might be termed the "actinide" series,<sup>32,33</sup> and the first 5f electron might, although would not necessarily, appear in thorium. The salient point is that the characteristic oxidation state is the III state. (The characteristic oxidation state is exhibited by the member containing seven 5f electrons and presumably also by the member containing fourteen 5f electrons, namely, curium and element 103.)

There is much evidence pointing toward this view. The following evidence will be discussed: (1) chemical properties, (2) absorption spectra in aqueous solution and crystals, (3) crystallographic structure data, (4) magnetic susceptibility data, and (5) spectroscopic data.

It should be emphasized that the discussion so far has been carried on in a somewhat oversimplified manner. This was done because the details concerning the possible physical or chemical forms in which these elements might exist have a bearing on the electronic structures, as is the case for all the other transition groups, including the rare-earth elements. Differences of this sort should be much more pronounced for the 5f transition group than for the 4f transition group owing to the lower binding and shielding of the 5f electrons. The effect that this should have on making the heavy rare-earth-like series different from the light rare-earth group has not been generally well recognized, even though Bohr<sup>34</sup> pointed out clearly more than twenty-five years ago that this looser binding would obscure the place of beginning for the heavy series. Thus the number of 5f electrons in the atom in the gaseous state might differ from that in the metallic state (which in turn can differ from one phase to another), and in turn neither of these structures might correspond directly to the chemical properties, in which hydration and lattice energies play an important role. It is the chemical properties (including absorption spectra, crystallographic data, etc., on the compounds) that should be determinative in placing these elements in the periodic table, just as was the case for the rare-earth elements. The rare-earth elements would be placed differently if their electronic structures alone were considered.

**2.2 Chemical Evidence.** On the basis of an actinide series the characteristic oxidation number for the series is III, and this shows up strikingly in the stabilization of the lower oxidation states with increasing atomic number. In going from uranium to plutonium it becomes increasingly difficult to effect the oxidation from the IV to

the VI state, and with americium it is impossible in aqueous solution to effect an oxidation to the VI state. Similarly, it becomes increasingly difficult to effect oxidation from the III to the IV state in going from uranium to plutonium. With americium the evidence indicates that it probably is not possible to effect this oxidation in acid solution. If this oxidation should be proved possible, the indications are that

Table 1—Some Oxidation Potentials of the Actinides  
(Aqueous Solution, 1 molar)

Atomic no.	Element	Potential, volts	
		III to IV	IV to VI
92	U	+0.63	-0.60
93	Np	-0.14	-0.94
94	Pu	-0.95	-1.11
95	Am	~-2.6	

the potential is so great that the higher oxidation state of americium is reduced rapidly by water and cannot be maintained in aqueous solution for any great length of time. These considerations are illustrated in Table 1. In Table 1 the standard oxidation-reduction potentials, referred to the hydrogen-hydrogen ion couple as zero,<sup>35</sup> are listed for the III-IV and IV-VI oxidations for these elements.<sup>36</sup>

Much of the work done with curium has necessarily been limited to the tracer scale, and therefore it has been impossible to make corresponding quantitative deductions. This work, however, has led to the definite qualitative conclusion that it is impossible in aqueous acid solution to oxidize curium to the VI state, and that it is also impossible to oxidize it from the III to the IV state. In fact, the experiments of Thompson, Morgan, James, and Perlman,<sup>37</sup> in which tracer amounts of curium and americium were subjected to strong oxidation under alkaline fusion, indicate that it is more difficult to oxidize curium from the III to a higher state than is the case for americium, and it may be actually impossible to effect this oxidation. These experiments indicate that americium may be oxidized in alkaline mediums and can in this manner be separated from curium. In fact, Werner and Perlman<sup>38</sup> were able to oxidize americium(III), in 40 per cent potassium carbonate solution by the use of the strong oxidizing agent hypochlorite, to an insoluble compound, probably a compound of americium(V). The result was an almost complete separation from curium(III), which apparently is not oxidized under these severe con-

ditions. The microchemical experiments of Werner and Perlman<sup>39</sup> with macroscopic concentrations of curium also point toward the existence of curium solely in the III oxidation state.

This tendency toward increasing stabilization of the lower oxidation states, especially the III state, with increasing atomic number also manifests itself notably in the stability of the solid compounds of the various oxidation states of these elements. The best illustration arises from a consideration of the solid nonoxyxygenated halides of these elements. The first possibility of the production of a trifluoride appears with uranium trifluoride, which can be prepared only under drastic reducing conditions. The stability and ease of reduction to the trifluoride increase in going to neptunium and then to plutonium. In the case of americium it has not been possible to produce any higher fluoride than the trifluoride.

With respect to the other halides it has been impossible to prepare any plutonium or americium chloride, bromide, or iodide of oxidation state higher than III. It has been possible to prepare only the chloride and bromide of neptunium of oxidation state IV, in addition to the chloride, bromide, and iodide of oxidation state III. In the case of uranium it has been known for some time that there are chlorides of oxidation state higher than IV and a chloride, bromide, and iodide of oxidation state IV. These considerations are well illustrated in Table 2, which lists all the halides of uranium, neptunium, plutonium, and americium that have been prepared and maintained as stable in the solid state. So far the chemical evidence indicates that it will be difficult, probably impossible, to prepare any of the nonoxyxygenated halides of americium and curium of oxidation state higher than III. In fact, Fried and Florin<sup>40</sup> have treated  $\text{AmF}_3$ , with fluorine at elevated temperatures and have obtained no evidence for the formation of a higher fluoride.

This chemical evidence indicates that the 5f electrons are more easily removed by oxidation than the 4f electrons, as would be expected on the basis of the predicted lower ionization potentials of 5f as compared to 4f electrons, provided the hydration and lattice free energies were not such as to reverse the effect, which might conceivably have been the case. Thus the III state of thorium cannot exist in aqueous solution, and the IV and III states of protactinium are presumably unstable in aqueous solution, although evidence for a valence state lower than V has been reported.<sup>41</sup> In the case of solid compounds it has been possible to prepare thorium triiodide<sup>42-44</sup> and sesquisulfide,<sup>45</sup> as well as compounds of lower oxidation states,<sup>43,45</sup> under rather severe reducing conditions. It seems likely that tetrapositive and tripositive compounds of protactinium will be prepared as soon

as efforts in this direction are made. In fact, Zachariasen<sup>46</sup> and McCullough<sup>47</sup> already have some crystallographic evidence for a dioxide of protactinium with the fluorite structure, although this may be a case of solid solution of two oxidation states similar to the solutions studied by Marsh<sup>48</sup> and Prandtl and Rieder<sup>49</sup> in the  $\text{PrO}_2\text{-Gd}_2\text{O}_3$ ,  $\text{TbO}_2\text{-Nd}_2\text{O}_3$ , and  $\text{Pr}_2\text{O}_3\text{-PrO}_2$  systems and similar to the well-known solid

Table 2 — Halides of Some of the Heaviest Elements

Atomic no.	Element	Fluorides				Chlorides				Bromides		Iodides
92	U	$\text{UF}_6$	$\text{UF}_5$	$\text{UF}_4$	$\text{UF}_3$	$\text{UCl}_6$	$\text{UCl}_5$	$\text{UCl}_4$	$\text{UCl}_3$	$\text{UBr}_4$	$\text{UBr}_3$	$\text{UI}_4$
93	Np	$\text{NpF}_6$	$\text{NpF}_5$	$\text{NpF}_4$	$\text{NpF}_3$		$\text{NpCl}_4$		$\text{NpCl}_3$	$\text{NpBr}_4$	$\text{NpBr}_3$	$\text{NpI}_3$
94	Pu			$\text{PuF}_4$	$\text{PuF}_3$			$\text{PuCl}_3$		$\text{PuBr}_3$		$\text{PuI}_3$
95	Am				$\text{AmF}_3$			$\text{AmCl}_3$		$\text{AmBr}_3$		$\text{AmI}_3$

solutions in the iron oxide systems. It is not known whether the utilized electrons in these lower oxidation states are in the 5f or the 6d configuration or in some combination of these, because this is the precise area where the binding energies for the two types of electrons come closest to equality. From the behavior of uranium, neptunium, and plutonium it must be deduced that as many as three of the 5f electrons are given up quite readily but with increasing difficulty as the atomic number increases. In this connection it is interesting to note that for lanthanide elements not only are there several instances of dipositive oxidation states, from which 4f electrons are lost upon oxidation to the corresponding tripositive states, but also in the gaseous atoms there are, generally, only two electrons (beyond the xenon structure) outside the 4f shell (see Table 5), although the persistent oxidation state is certainly the III state. Another noteworthy example of a compound of this type is cerium sesquioxide, which is so unstable toward oxidation to the dioxide that the former is extremely difficult to prepare and maintain. As Connick<sup>49a</sup> has pointed out, the stability of the III oxidation state in the rare-earth elements is as much a consequence of the hydration and lattice free energies as of the ionization potentials.

Americium might possess an oxidation state of II. It would attain the II oxidation state through the presence of seven electrons in the 5f shell in a manner analogous to the II state of europium, the element immediately preceding gadolinium, with its seven 4f electrons. Because of the greater ease in the removal of the 5f electrons, it might require a considerably stronger reducing agent to reduce americium from the III to the II state than would be required for

europerium. It is not impossible that it will be found that americium can be reduced to the II state in aqueous solution, although it is more likely that dipositive solid compounds will be prepared. Thompson and coworkers<sup>37</sup> in some rough preliminary experiments have made partial separations of americium, presumably as americium(II), from curium in tracer amounts in aqueous solution. This was done by using sodium amalgam as the reducing agent and carrying americium selectively with samarium(II) sulfate and, in addition, by using barium as the reducing agent and carrying americium selectively with

Table 3—Oxidation States of Lanthanide and Actinide Elements

Atomic no. Element Oxidation states	57 La	58 Ce	59 Pr	60 Nd	61 Pm	62 Sm	63 Eu	64 Gd	65 Tb
	3	3	3	3	3	3	3	3	3
		4	4	(4) <sup>†</sup>					4
					(5)				
Atomic no. Element Oxidation states	89 Ac	90 Th	91 Pa	92 U	93 Np	94 Pu	95 Am	96 (2) Cm	
	3	(3)	(3)	3	3	3	3	3	
		4	(4)	4	4	4	(4)		
			5	5	5	5	(5)		
				6	6	6			

<sup>†</sup>Explanation of parentheses is in text.

barium chloride from concentrated hydrochloric acid solution. Curium, with its seven 5f electrons, should exhibit the III state almost exclusively, and all evidence obtained from both tracer and macroscopic quantities indicates that this is the case. However, it would not be surprising if it should prove possible to prepare  $\text{CmO}_2$  owing to the great stability of this dioxide structure (see Sec. 2.4).

Table 3 summarizes the known oxidation states of the lanthanide and actinide elements in such a way as to bring out the analogy between the two groups and to show the greater ease of oxidation for the members of the latter group. The uncertain or unusual states are designated by parentheses, and those states with metallic or possibly metallic character in their bonding that have an oxidation number less than III are omitted. Such a table has only limited meaning because oxidation states of solid compounds formed under drastic conditions, which vary in their severity, are included. But the method of listing only those states that are stable in aqueous solution also has shortcomings, because the existence of an aqueous ion, besides being

limited by the ionization potentials of its electrons, is affected by specific chemical processes of hydration and complex formation and is arbitrarily confined within the limits of its oxidation or reduction by water.

The metals of the elements thorium to americium, inclusive, have been prepared and their properties studied; these bear a striking resemblance to the metals of the rare-earth elements. All are highly electropositive and to about the same degree. In this property they are similar to the rare-earth metals and different from the corresponding 5d elements, hafnium (element 72) to iridium (element 77), inclusive. In the 5d elements the electropositive character of hafnium is lost as 5d electrons are added in going toward iridium. Another remarkable resemblance to the rare-earth elements lies in the densities of the metals. Both americium<sup>50</sup> and the analogous 4f element europium<sup>51</sup> have densities much lower than their neighboring elements. Thus, these metals seem to have radium-like or barium-like structures with abnormally high radii and analogous electronic structures. A comparison with tungsten, rhenium, osmium, and iridium shows no such analogy.

**2.3 Absorption Spectra in Aqueous Solution and Crystals.** One of the characteristic properties of the elements of the lanthanide series, a property which depends upon the 4f electrons, is their sharp absorption bands, which are to a large extent in the visible spectrum. The absorption is due to transitions involving the 4f electrons, and the sharpness results from the shielding of these electrons, in both the ground and excited states, by electrons in the outer shells. The investigations of this type with the elements uranium, neptunium, plutonium, americium, and curium have shown a striking similarity in this property to the rare earths. This similarity is further evidence that we are dealing with 5f electrons. The analogy between the rare earths and uranium(IV) in this property was noticed by Goldschmidt,<sup>52</sup> and the analogy between the rare earths and uranium(III) and uranium(IV) was noticed by Ephraim and Mezener<sup>53</sup> many years ago. This similarity between the actinide and the lanthanide elements is more than qualitative, because the general complexity of the absorption picture undergoes analogous simplification as we approach the middle of the two series — that is, as we approach the elements gadolinium and curium, with their seven 4f or 5f electrons. Unfortunately, up to the present the most extensive work on the absorption of uranium and the transuranium elements has been done in solution, where much of the sharpness is lost, and with instruments of not very high resolving power. The aqueous-solution absorption spectra of the tripositive actinides taken from various sources on the Plutonium

Project<sup>54</sup> are shown in Fig. 1, and the corresponding spectra of the rare-earth elements also are shown for purposes of comparison. Although the absorption curves of Prandtl and Scheiner<sup>55</sup> are available for comparison, this work was not done under conditions comparable to those under which the work on the actinides was done. Stewart<sup>56</sup> has measured the absorption spectra of the rare-earth elements under comparable conditions, his results also being given in Fig. 1. The preliminary results of Lantz and Parker<sup>57</sup> on the absorption spectrum of prometheum (element 61) are also included. It appears that as we approach the middle of the two series, that is, as we approach the elements gadolinium and curium, the ground states involving the 5f electrons uniformly fall increasingly below the next higher states. This leads to energy differences for curium of such a magnitude that the absorption falls outside the visible and in the ultraviolet region as in the case of gadolinium. The analogous peaks of europium and americium at 4000 and 5000 Å, respectively, have been studied in detail by Jones and Cunningham,<sup>58</sup> who have shown that in aqueous solution these elements display striking similarity even in their "fine structure."

The best method for the comparison of the absorption spectra of the two groups of elements is to compare the spectra obtained with crystals, in which the absorption lines are known to be very sharp for the rare-earth elements on the basis of a large number of measurements with many of these elements. Some such measurements have been made for a number of the transuranium elements, and the results so far indicate striking analogies. Freed and Leitz<sup>59, 60</sup> have measured the absorption spectrum of solid americium trichloride, finding sharp lines of the order of 1 to 5 Å wide. This width is comparable with that of lines in the sharpest rare-earth spectra. In fact the sharpness in the spectra<sup>60</sup> of americium chloride and americium bromide is so extreme at room temperature and at 77°K that only the tripositive europium ion is comparable; since the absorption spectrum of the latter originates from a ground state involving six 4f electrons, it seems very likely that the basic state of tripositive americium contains six 5f electrons. Freed and Leitz<sup>60</sup> also measured the absorption spectra of uranium tetrachloride, neptunium tetrachloride, and plutonium trichloride at room temperature and at 77°K; the sharpness of the lines indicates that the least stable electrons of these ions are in the inner 5f shell in the activated as well as in the basic electronic states.

**2.4 Crystallographic Data.** As mentioned above, crystallographic evidence points, in addition, to the filling of the 5f shell in this neighborhood of heavy elements. Some years ago Goldschmidt<sup>20, 61, 62</sup> had

already noticed the isomorphism of  $\text{ThO}_2$  and  $\text{UO}_2$  and the decrease in size in going from  $\text{ThO}_2$  to  $\text{UO}_2$ , and he had interpreted this to indicate the presence of 5f electrons in uranium. The observation by Zachariassen<sup>46</sup> of the isomorphism of the compounds  $\text{ThO}_2$ ,  $\text{PaO}_2$ ,  $\text{UO}_2$ ,  $\text{NpO}_2$ ,  $\text{PuO}_2$ , and  $\text{AmO}_2$ ,<sup>63</sup> together with his observation of the regular decrease in radius of the metallic ion in these oxides, has been interpreted by him to be excellent evidence that the electrons are going into the 5f shell. [In this series, however, the lattice constants of the  $\text{PaO}_2$  (see references 46 and 47), possibly also  $\text{AmO}_2$  (see reference 64), do not fit perfectly into the regular pattern for decrease in atomic radius of the metallic ions. This failure to fit may be due to mixed oxidation states similar to the situation found for the higher praseodymium oxides by Marsh.<sup>48</sup>] The relative ease with which  $\text{PaO}_2$  and  $\text{AmO}_2$  may be formed by heating in air is in sharp contrast to the instability of the tetrapositive states of these elements in aqueous solution and illustrates the great stabilizing influence of the dioxide crystal lattice. Both of these investigators have advanced the hypothesis that it is a thoride series, i.e., that the first 5f electron appears in the first element beyond thorium, namely, protactinium.

Zachariassen has used the x-ray diffraction method to determine the molecular structures of a great number of compounds of thorium, uranium, and the transuranium elements. All these measurements point toward the filling of the 5f shell, since analogous compounds are found to be isomorphous. This indicates that the successive electrons are added in such a way (i.e., to an inner shell) as to allow the analogous compounds of successive elements to have identical molecular structures. Zachariassen<sup>65</sup> has found that practically all the various halide types shown in Table 2 have isomorphous structures; for example, all members of the group  $\text{ThF}_4$ - $\text{UF}_4$ - $\text{NpF}_4$ - $\text{PuF}_4$  are of identical structure types, all members of the group  $\text{UF}_3$ - $\text{NpF}_3$ - $\text{PuF}_3$ - $\text{AmF}_3$  are isomorphous, and for the group  $\text{UCl}_3$ - $\text{NpCl}_3$ - $\text{PuCl}_3$ - $\text{AmCl}_3$  the same is true. In some instances there is a change in structure type in proceeding through the group, as occurs in the group  $\text{UBr}_3$ - $\text{NpBr}_3$ - $\text{PuBr}_3$ - $\text{AmBr}_3$ . However, this is to be expected on the basis of the contraction that takes place, and it is entirely consistent with the addition of the successive electrons to the 5f shell. Zachariassen<sup>65</sup> has used these structure data to calculate ionic radii, and these radii show a progressive decrease in size with increasing atomic number in a manner quite analogous to the well-known "lanthanide contraction" observed with the rare-earth elements. The compounds of the rare-earth elements are in turn isomorphous with the corresponding compounds of the actinide elements. In order to illustrate further these considerations Table 4 gives the ionic radii of a number of

ELEMENT AND  
ATOMIC NO.

LANTHANIDES

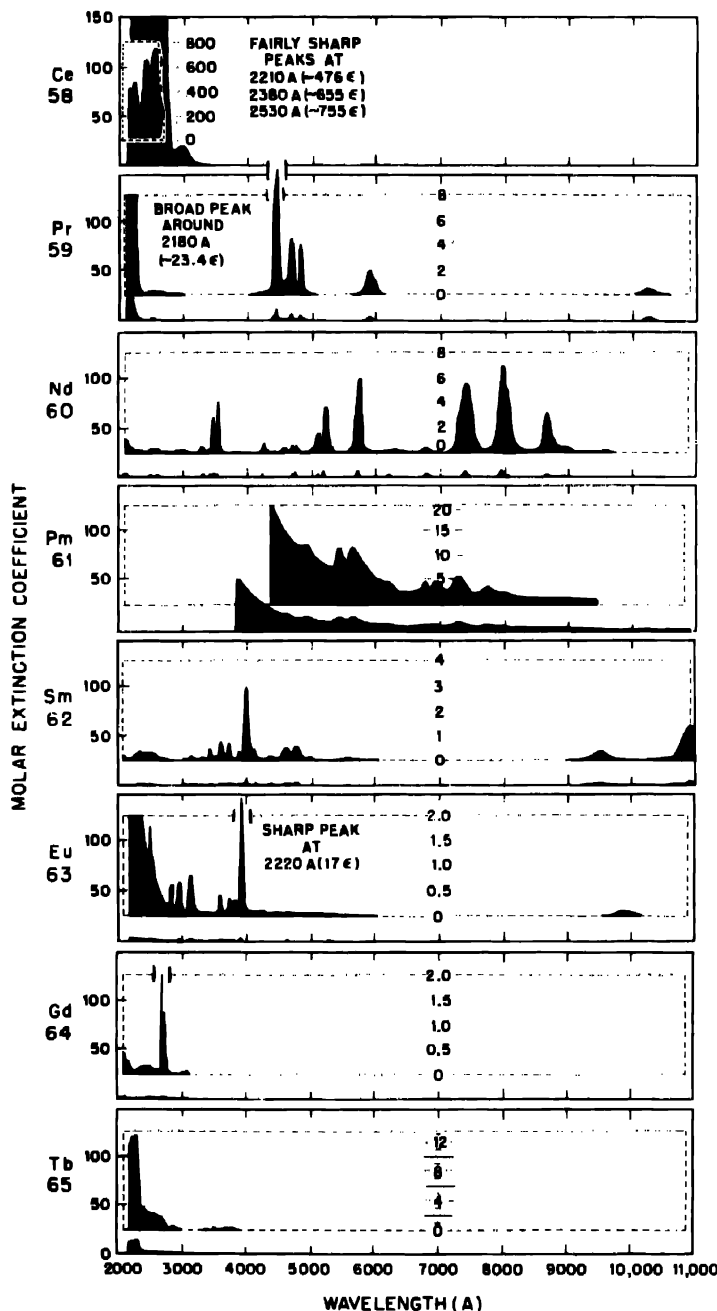


Fig. 1—Absorption spectra of aqueous tripositive lanthanides and actinides.

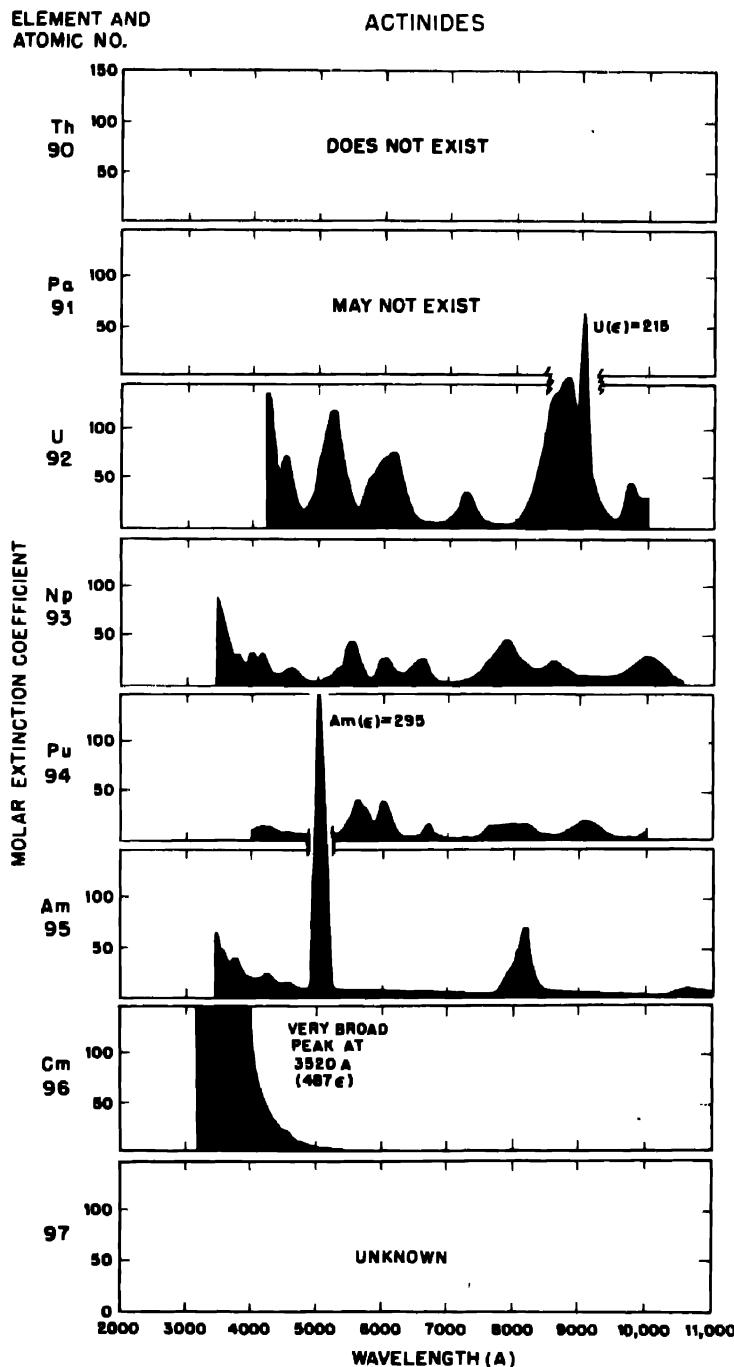


Fig. 1—(cont.)

the actinide and lanthanide elements<sup>65</sup> with interpolated values in parentheses.

2.5 Magnetic Susceptibility Data. Magnetic susceptibility measurements on compounds of the heaviest elements ideally should lead to the resultant magnetic moments in fundamental units and in this way give information as to the quantum states of the responsible electrons. As evidenced by the rare-earth elements, the situation is

Table 4 -- Ionic Radii of Actinide and Lanthanide Elements

No. of 4f or 5f electrons	Actinide series				Lanthanide series	
	III state		IV state		Element	Radius, Å
	Element	Radius, Å	Element	Radius, Å	Element	Radius, Å
0	Ac <sup>+3</sup>	1.11	Th <sup>+4</sup>	0.95	La <sup>+3</sup>	1.04
1	(Th <sup>+3</sup> )	(1.08)	Pa <sup>+4</sup>	0.91	Ce <sup>+3</sup>	1.02
2	(Pa <sup>+3</sup> )	(1.06)	U <sup>+4</sup>	0.89	Pr <sup>+3</sup>	1.00
3	U <sup>+3</sup>	1.04	Np <sup>+4</sup>	0.88	Nd <sup>+3</sup>	0.99
4	Np <sup>+3</sup>	1.02	Pu <sup>+4</sup>	0.86	Pm <sup>+3</sup>	(0.98)
5	Pu <sup>+3</sup>	1.01	Am <sup>+4</sup>	0.85	Sm <sup>+3</sup>	0.97
6	Am <sup>+3</sup>	1.00			Eu <sup>+3</sup>	0.97

rather complex, and the exact behavior expected for the heaviest elements on the basis of the presence of either 5f or 6d electrons cannot be, or at least has not been, predicted. Nevertheless, such measurements should give, and indeed have given, information on this point.

The earliest magnetic susceptibility measurements that were made on the compounds of uranium<sup>66-69</sup> and plutonium<sup>70</sup> showed that these are paramagnetic, yet the results are difficult to interpret quantitatively. A simple qualitative explanation of the magnetic susceptibilities of plutonium(III), plutonium(IV), and plutonium(VI) lies in the assumption that there are five 5f electrons in plutonium(III) which are successively removed as the higher oxidation states are reached. These measurements, however, do not lead to this interpretation as the sole and unambiguous one, and as a result they must be regarded only as being consistent with and lending weight to this view but not as proving it.

Hutchison and Elliott<sup>72</sup> later made magnetic susceptibility measurements over a wide range of temperatures on a number of solid compounds of the heaviest elements. In the case of uranium(IV) compounds<sup>71,72</sup> they discovered that a number of them behave in a manner similar to praseodymium(III) compounds; this indicates that these two groups of compounds have isoelectronic structures with respect to f electrons and thus have two such electrons. They found, in addition,

that the temperature dependence of the magnetic susceptibility of these uranium(IV) compounds obeys the Curie-Weiss law over a range of temperatures, and through extrapolation with the use of this law they deduced a resultant magnetic moment very close to that expected for two f electrons. They also concluded that the crystal fields produce more pronounced perturbing effects in this case than in the corresponding case involving 4f electrons. Their measurements on neptunium(V), which is isoelectronic with uranium(IV), also indicated the presence of two f electrons here.

Howland and Calvin<sup>73</sup> have measured the magnetic susceptibilities of the cations of uranium, neptunium, plutonium, and americium in most of their stable oxidation states in aqueous solution. In order to account consistently for the observed values of the magnetic susceptibilities, the heavy atoms must be assumed to have electronic configurations, beyond the radon structure, of the type  $(5f)^{1-6}$ ; for example, neptunium(VI) corresponds to the structure 5f, uranium(IV), neptunium(V), and plutonium(VI) to 5f<sup>2</sup>, neptunium(IV) to 5f<sup>3</sup>, plutonium(IV) to 5f<sup>4</sup>, plutonium(III) to 5f<sup>5</sup>, and americium(III) to 5f<sup>6</sup>. The experimental effective magnetic moments are generally lower than the theoretical values and lower than experimental values for corresponding lanthanide 4f<sup>n</sup> cations; this would be expected on the basis of the Stark effect produced by electric fields of anions and of water dipoles. Failure of the Russell-Saunders approximation to the coupling between electrons may account for some of the error in the theoretical calculations. That the susceptibilities of plutonium(III) and americium(III) are many times lower than those of samarium(III) and europium(III), respectively, is attributed to wider multiplet splitting in the actinide atoms. Figure 2 is a graph comparing the experimental magnetic susceptibilities of the lanthanide and actinide cations in such a way as to show their remarkable analogy in this property.

2.6 Spectroscopic Data. Spectroscopic evidence also lends support to the actinide interpretation. Kiess, Humphreys, and Laun<sup>74,75</sup> investigated the spectrum of uranium atoms. They gave the interpretation that the electron configuration of the lowest state of neutral uranium is 5f<sup>3</sup>6d7s<sup>2</sup> (beyond radon), a configuration that fits in well, since uranium is the third element in the series. Other work by Schuurmans and coworkers<sup>76,77</sup> on the spectrum of gaseous uranium(II) and uranium(I) and by McNally and Harrison<sup>78</sup> on uranium(II) has given results that are consistent with this as the ground term for the neutral uranium atom. Other observations<sup>79-82</sup> made on the gaseous thorium(II) spectrum indicate that the 5f electron is very close to the 6d electron in binding energy in the neutral free thorium atom. Russell<sup>83</sup> has made a complete analysis of the x-ray data for radium,

thorium, and uranium and has concluded that the 5f lies lower than the 6d level and that the 5f shell begins to fill at thorium.

Tomkins and Fred<sup>34</sup> have made a qualitative comparison of the emission spectra of the actinide and the lanthanide elements. They found such a strong analogy between the average intensity of the lines in the case of americium and europium that it seems safe to conclude

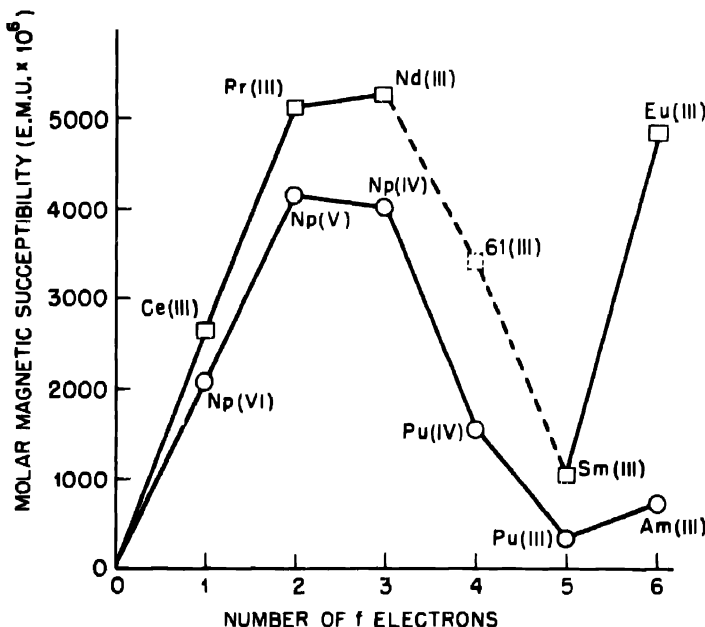


Fig. 2.—Graph of molar magnetic susceptibilities of some aqueous actinide and lanthanide ions.

that these have similar electronic structures in their ground states. This indicates that the configuration of the gaseous atom of americium is  $5f^77s^2$ .

### 3. CORRELATIONS AND DEDUCTIONS

**3.1 Electronic Configurations.** Table 5 gives what appears to be the configuration or the best prediction for the configuration, beyond the radon structure, of the ground state of the neutral gaseous atom for each of the elements actinium to curium, inclusive. The trend in the chemical properties, with its implication that the 5f becomes progressively of lower energy, compared to the 6d level, as the atomic number increases, has been used as an aid in making the predictions.

The configurations,<sup>85-87</sup> beyond xenon, of the corresponding neutral rare-earth elements are given for comparison. The ground states given for cerium and praseodymium are those predicted<sup>88,87</sup> on the basis of the recently determined ground states of the singly ionized atoms,<sup>89</sup> and that of element 61 is obtained by interpolation; consequently, these are subject to some doubt. The ground states given for neodymium,<sup>70</sup> samarium, europium, and gadolinium are those spectroscopically determined<sup>88</sup> for the neutral atoms and should be considered as well established.

Table 5.—Suggested Electron Configurations (beyond Radon and Xenon) for Gaseous Atoms of Actinide and Lanthanide Elements

Atomic no.	Element	Configuration	Atomic no.	Element	Configuration
89	Ac	6d7s <sup>2</sup>	57	La	5d6s <sup>2</sup>
90	Th	6d <sup>2</sup> 7s <sup>2</sup> (or 5f6d7s <sup>2</sup> )	58	Ce	4f <sup>2</sup> 6s <sup>2</sup>
91	Pa	5f <sup>2</sup> 6d7s <sup>2</sup> (or 5f6d <sup>2</sup> 7s <sup>2</sup> )	59	Pr	4f <sup>3</sup> 6s <sup>2</sup>
92	U	5f <sup>3</sup> 6d7s <sup>2</sup>	60	Nd	4f <sup>4</sup> 6s <sup>2</sup>
93	Np	5f <sup>4</sup> 7s <sup>2</sup> (or 5f <sup>4</sup> 6d7s <sup>2</sup> )	61	Pm	4f <sup>5</sup> 6s <sup>2</sup>
94	Pu	5f <sup>5</sup> 7s <sup>2</sup> (or 5f <sup>5</sup> 6d7s <sup>2</sup> )	62	Sm	4f <sup>6</sup> 6s <sup>2</sup>
95	Am	5f <sup>6</sup> 7s <sup>2</sup>	63	Eu	4f <sup>7</sup> 6s <sup>2</sup>
96	Cm	5f <sup>7</sup> 6d7s <sup>2</sup>	64	Gd	4f <sup>7</sup> 5d6s <sup>2</sup>

It should be emphasized that it would be entirely consistent from the point of view that we are dealing here with a series of actinide elements if it should eventually be found that there are no 5f electrons present in thorium (or protactinium). It is quite possible, on the basis of present evidence, that protactinium, or even uranium, may be the first to have 5f electrons. It seems very likely, however, that electrons will be placed in the 5f shell earlier in the series than uranium and that protactinium will have at least one such electron. An essential point is that curium definitely seems to have seven 5f electrons, and element 103 probably would have fourteen 5f electrons.

In the case of some of the elements in the series it may be difficult to assign electrons to the 5f or 6d shells, because the energy necessary for the shift from one shell to the other may be within the range of chemical binding energies. Many of the experimental facts already described, such as the ease of oxidation to higher states and the more complicated situation for the magnetic susceptibilities as compared to the rare-earth elements, point to lower binding and less electrostatic shielding by outer electrons of 5f than of 4f electrons. This was to be expected, and the magnitude of these effects seems reason-

able. The electronic configuration may differ from compound to compound or even with the physical state of a given compound. Moreover, one certainly can not be sure that the configuration of the gaseous atom, for example, will correspond to that of the compounds or of the hydrated ions in solution. In the case of the lanthanides, in fact, the configuration of the gaseous atom has in general only two electrons (beyond the xenon structure) outside the 4f shell, although the predominant oxidation state is certainly the III state. Since the energy difference between such far-outlying levels as the 5f and 6d shells is rather small, and since resonance effects should be rather large, these may predominate in determining that a composite energy level lies lowest. Thus some of these elements may possibly constitute what might more properly be called a 5f-6d range in this series rather than being considered as part of a totally 5f transition group.

The evidence that has accumulated so far seems, nevertheless, to point to lower energies for the 5f levels, as compared to the 6d levels, for the compounds of the element, as early as uranium in this series. It is in the case of the elements thorium and protactinium that the relative energy positions of these levels are as yet most uncertain. As in the other transition series, the relative energy level of the shell that is undergoing the filling process becomes lower as the successive electrons are added, and by the time americium and curium, and presumably the subsequent members of the series, are reached, the 5f shell seems clearly to be of lower energy than the 6d shell. Also, it is not yet possible to place the electrons in neptunium and plutonium with confidence, and hence in Table 5 alternative structures for gaseous neptunium and plutonium are suggested. It seems quite possible, for those elements in which the energies are so nearly equal, that the 5f as well as the 6d and outer orbits may be involved in the chemical binding in some compounds and complex ions, an interesting possibility for a new type of bonding.

Figure 3 is an extremely rough and qualitative pictorial representation of the binding energy of the most easily removable 5f and 6d electron (of those present) for each of the heaviest elements. A rough representation such as this can be justified only if it helps somewhat in the understanding of the situation. It is hoped that such is the case.

**3.2 Possible Deductions without Data on Transuranium Elements.** Although it is the information on the transuranium elements that has been decisive in enabling us to come to the present view concerning the electronic structure of, or, more properly speaking, the best position in the periodic table for, the heaviest elements, it is interesting to conjecture, in retrospect, whether it would have been possible to arrive at a similar conclusion without this information. Actually

there has been much information about actinium, thorium, protactinium, and uranium, especially about the latter, which pointed in this direction. As mentioned above, there is the similarity among the metals of these elements with respect to electropositive character. In addition the melting point of uranium metal seems to relate it more closely to the immediately preceding elements than to tungsten and molybdenum. The analogy of uranium to neodymium with respect to

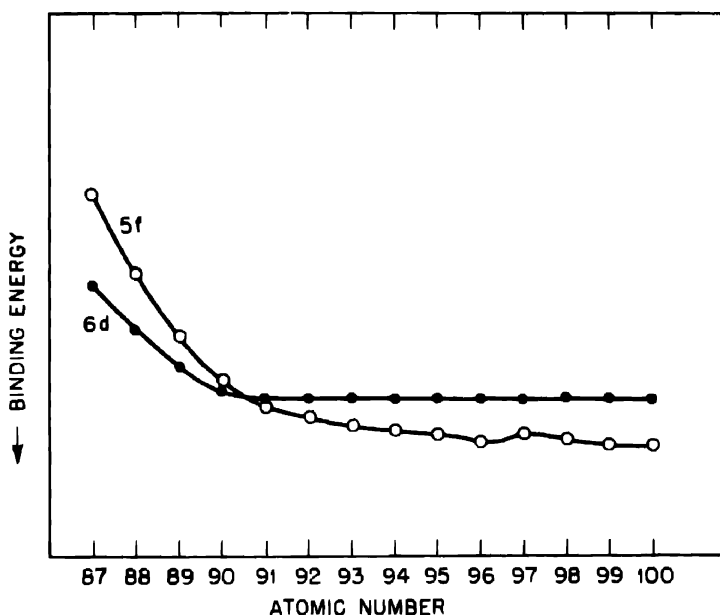


Fig. 3—Qualitative representation of electronic binding energies in the heaviest elements.

light absorption by the tripositive ions and the spectroscopic evidence for a ground state of the gaseous uranium atom involving three 5f electrons has already been mentioned.

Uranium differs considerably from tungsten and molybdenum in the chemistry of the lower oxidation states. Uranium(III) has great similarity to the tripositive rare-earth elements and actinium, and uranium(IV) resembles thorium and cerium(IV). Thus uranium(III) and uranium(IV) are not acidic in character; they do not tend, like tungsten and molybdenum, to form such exceedingly strong complex ions in solution; they have fluorides that are insoluble and isomorphous with the fluorides of the rare-earth elements; and they have other halides with crystal structures that are in general isomorphous

with the corresponding rare-earth halides. On the other hand, tungsten(III) and tungsten(IV) exist in aqueous solution predominantly as strong complex ions; for example, tungsten(III) has a strong chloride complex ion, and tungsten(IV) forms strong fluoride and cyanide complex ions. In this connection Thompson<sup>89</sup> has pointed out that tungsten(IV) forms the very stable complex ion  $\text{W}(\text{CN})_6^{4-}$  with the stable configuration of eighteen outer electrons, but uranium(IV) possesses no significant tendency to form an analogous complex cyanide ion, as would probably be expected if uranium possessed the same outer electronic structure as tungsten.

Although molybdenum dioxide and tungsten dioxide have isomorphous crystal structures, tungsten dioxide and uranium dioxide do not, but uranium dioxide, thorium dioxide, and cerium dioxide do have isomorphous structures. It is interesting to note that although uranium is not associated with tungsten in minerals, uranium and thorium minerals practically always have the rare-earth elements associated with them, and the rare-earth minerals practically always contain uranium or thorium.

Arguments on the basis of the scanty evidence from the chemical properties of thorium and uranium alone have been given by others, including Villar<sup>19</sup> and, more recently, Stedman,<sup>90</sup> for a 5f-type transition series in the heaviest elements, beginning with thorium.

**3.3 Position in Periodic Table and Nomenclature.** Soon after the establishment of the concept of atomic number, the rare-earth elements could be properly fitted into the classification of the elements, and the periodic table took its present form. There is general agreement as to the various groups and subgroups, with differences only in regard to the best geometrical arrangements for presenting the information. Thus even the undiscovered elements with atomic numbers within the confines of this classification had their places fixed, and, when they were discovered, no reasons were found to change their positions. However, this is not the situation with respect to the transuranium elements, whose positions could only be fixed after experimental determination of their properties. Their positions, in turn, apparently influence the positions of elements that had been given places previously.

Since this seems to present a new problem, it is necessary to consider carefully the facts that have given rise to the present classification in order to try to find the traditional criteria for placement in the periodic table to apply to the elements now under consideration. The chemical properties, especially in aqueous solution, have been important criteria. Thus, the rare-earth elements assumed a position by virtue of their predominant trivalence in aqueous solution, a

property that is not deducible from the electronic structure of their atomic ground states. However, the spectroscopic data have determined the general regions of the transition series, where the 3d, 4d, 5d, and 4f shells undergo filling, and seem to have influenced the practice of uninterrupted placing of the transition elements in subgroups. (That is, all ten 3d transition elements from  $_{21}^{Sc}$  to  $_{30}^{Zn}$  are usually in uninterrupted subgroups, and the same holds true for the 4d, 5d, and 4f transition series.)

With such criteria the best method of presenting the actinide elements in the periodic table seems to be that shown in Fig. 4. Here are shown the fourteen elements of atomic numbers 90 to 103, inclusive, with actinium, element 89, as the prototype. These fourteen elements are listed as a series below, and in a manner similar to, the common listing of the fourteen rare-earth elements of atomic numbers 58 to 71, inclusive, for which lanthanum, element 57, is the prototype. It is not suggested that this particular form of the periodic table has any more merit than any of a number of others that place these elements in positions homologous to the rare-earth elements, because it is obvious that they can be analogously placed in a number of other types of tables or charts. The elements 90 to 96, inclusive, or the first few of them, could in addition be listed separately below the 5d elements in recognition of the resemblance of the first few of these to 5d elements. This appears to be undesirable, however, because the last members of this group bear no such resemblance, and it is probably impossible to draw a line as to just where the resemblance ends.

Since the suggestion<sup>93</sup> that the information on the transuranium elements appeared to have reached such a state as to make it possible to place the heaviest elements in definite positions in the periodic table (as an actinide transition series), a number of publications<sup>91-97</sup> commenting on this proposal have appeared. These in general agree with the suggestion, although in some cases the reasons therefor differ and in others there is an understandable expression of desire to see more of the evidence in detail. A number of different periodic tables in which these elements have been placed as actinides homologous to the lanthanides have been published recently.<sup>98-102</sup>

As mentioned above, a very important point is the presence of seven 5f electrons in stable tripositive curium (element 96), making this element very actinium-like. A series of thoride elements, for example, would imply stable IV oxidation states in elements 95 and 96 and the presence of seven 5f electrons and the IV state almost exclusively in element 97. A series of this type seems to be ruled out by the now-known instability of americium in solution in the IV state

## THE TRANSURANIUM ELEMENTS

<b>1</b>	<b>H</b>	<b>2</b>	<b>He</b>
<b>1.008</b>		<b>4.003</b>	
<b>3</b>	<b>4</b>		
<b>Li</b>	<b>B<sub>e</sub></b>		
<b>6.940</b>	<b>9.072</b>		
<b>11</b>	<b>12</b>		
<b>Na</b>	<b>Mg</b>		
<b>22.997</b>	<b>24.312</b>		
<b>19</b>	<b>20</b>	<b>21</b>	<b>T<sub>1</sub></b>
<b>K</b>	<b>Ca</b>	<b>Sc</b>	<b>V</b>
<b>39.966</b>	<b>40.08</b>	<b>45.10</b>	<b>47.90</b>
<b>37</b>	<b>38</b>	<b>39</b>	<b>40</b>
<b>Rb</b>	<b>Sr</b>	<b>V</b>	<b>Cr</b>
<b>85.48</b>	<b>87.63</b>	<b>88.92</b>	<b>91.22</b>
<b>55</b>	<b>56</b>	<b>57</b>	<b>58-71</b>
<b>C<sub>s</sub></b>	<b>Ba</b>	<b>L<sub>a</sub></b>	<b>Hf</b>
<b>132.91</b>	<b>137.36</b>	<b>134.92</b>	<b>178.6</b>
<b>87</b>	<b>88</b>	<b>89</b>	<b>Se</b>
<b>Fr</b>	<b>Ra</b>	<b>Ac</b>	<b>Series</b>
<b>5</b>	<b>6</b>	<b>7</b>	<b>8</b>
<b>B</b>	<b>C</b>	<b>N</b>	<b>O</b>
<b>10.82</b>	<b>12.010</b>	<b>14.088</b>	<b>16.000</b>
<b>13</b>	<b>14</b>	<b>15</b>	<b>16</b>
<b>Al</b>	<b>Si</b>	<b>P</b>	<b>S</b>
<b>26.97</b>	<b>28.06</b>	<b>30.98</b>	<b>32.06</b>
<b>5</b>	<b>6</b>	<b>7</b>	<b>8</b>
<b>B</b>	<b>C</b>	<b>N</b>	<b>O</b>
<b>10.82</b>	<b>12.010</b>	<b>14.088</b>	<b>16.000</b>
<b>13</b>	<b>14</b>	<b>15</b>	<b>16</b>
<b>Al</b>	<b>Si</b>	<b>P</b>	<b>S</b>
<b>26.97</b>	<b>28.06</b>	<b>30.98</b>	<b>32.06</b>
<b>5</b>	<b>6</b>	<b>7</b>	<b>8</b>
<b>Cu</b>	<b>Ni</b>	<b>Co</b>	<b>F</b>
<b>58.69</b>	<b>61.57</b>	<b>58.94</b>	<b>65.36</b>
<b>13</b>	<b>14</b>	<b>15</b>	<b>16</b>
<b>Al</b>	<b>Si</b>	<b>P</b>	<b>S</b>
<b>26.97</b>	<b>28.06</b>	<b>30.98</b>	<b>32.06</b>
<b>5</b>	<b>6</b>	<b>7</b>	<b>8</b>
<b>Ge</b>	<b>In</b>	<b>Ga</b>	<b>Br</b>
<b>69.72</b>	<b>72.60</b>	<b>74.81</b>	<b>78.96</b>
<b>13</b>	<b>14</b>	<b>15</b>	<b>16</b>
<b>Al</b>	<b>Si</b>	<b>P</b>	<b>S</b>
<b>26.97</b>	<b>28.06</b>	<b>30.98</b>	<b>32.06</b>
<b>5</b>	<b>6</b>	<b>7</b>	<b>8</b>
<b>Ge</b>	<b>In</b>	<b>Ga</b>	<b>Br</b>
<b>69.72</b>	<b>72.60</b>	<b>74.81</b>	<b>78.96</b>
<b>13</b>	<b>14</b>	<b>15</b>	<b>16</b>
<b>Al</b>	<b>Si</b>	<b>P</b>	<b>S</b>
<b>26.97</b>	<b>28.06</b>	<b>30.98</b>	<b>32.06</b>
<b>5</b>	<b>6</b>	<b>7</b>	<b>8</b>
<b>Pd</b>	<b>Ag</b>	<b>Rh</b>	<b>Cd</b>
<b>46</b>	<b>47</b>	<b>48</b>	<b>49</b>
<b>107.860</b>	<b>108.7</b>	<b>102.91</b>	<b>112.41</b>
<b>13</b>	<b>14</b>	<b>15</b>	<b>16</b>
<b>Sn</b>	<b>In</b>	<b>Rh</b>	<b>Pd</b>
<b>114.76</b>	<b>118.70</b>	<b>101.7</b>	<b>107.860</b>
<b>13</b>	<b>14</b>	<b>15</b>	<b>16</b>
<b>Sn</b>	<b>In</b>	<b>Rh</b>	<b>Pd</b>
<b>114.76</b>	<b>118.70</b>	<b>101.7</b>	<b>107.860</b>
<b>5</b>	<b>6</b>	<b>7</b>	<b>8</b>
<b>Pt</b>	<b>Au</b>	<b>Os</b>	<b>Hg</b>
<b>195.23</b>	<b>190.2</b>	<b>186.31</b>	<b>187.2</b>
<b>13</b>	<b>14</b>	<b>15</b>	<b>16</b>
<b>Pt</b>	<b>Au</b>	<b>Os</b>	<b>Hg</b>
<b>195.23</b>	<b>190.2</b>	<b>186.31</b>	<b>187.2</b>
<b>5</b>	<b>6</b>	<b>7</b>	<b>8</b>
<b>Pb</b>	<b>Bi</b>	<b>T<sub>1</sub></b>	<b>T<sub>2</sub></b>
<b>204.39</b>	<b>209.00</b>	<b>209.00</b>	<b>207.21</b>
<b>13</b>	<b>14</b>	<b>15</b>	<b>16</b>
<b>Pb</b>	<b>Bi</b>	<b>T<sub>1</sub></b>	<b>T<sub>2</sub></b>
<b>204.39</b>	<b>209.00</b>	<b>209.00</b>	<b>207.21</b>
<b>5</b>	<b>6</b>	<b>7</b>	<b>8</b>
<b>Eu</b>	<b>Tb</b>	<b>Dy</b>	<b>Er</b>
<b>156.9</b>	<b>159.2</b>	<b>162.46</b>	<b>163.5</b>
<b>13</b>	<b>14</b>	<b>15</b>	<b>16</b>
<b>Eu</b>	<b>Tb</b>	<b>Dy</b>	<b>Er</b>
<b>156.9</b>	<b>159.2</b>	<b>162.46</b>	<b>163.5</b>
<b>5</b>	<b>6</b>	<b>7</b>	<b>8</b>
<b>Gd</b>	<b>Tb</b>	<b>Dy</b>	<b>Er</b>
<b>156.9</b>	<b>159.2</b>	<b>162.46</b>	<b>163.5</b>
<b>13</b>	<b>14</b>	<b>15</b>	<b>16</b>
<b>Gd</b>	<b>Tb</b>	<b>Dy</b>	<b>Er</b>
<b>156.9</b>	<b>159.2</b>	<b>162.46</b>	<b>163.5</b>
<b>5</b>	<b>6</b>	<b>7</b>	<b>8</b>
<b>Tm</b>	<b>Yb</b>	<b>Lu</b>	<b>Lu</b>
<b>163.5</b>	<b>167.2</b>	<b>159.4</b>	<b>174.94</b>
<b>13</b>	<b>14</b>	<b>15</b>	<b>16</b>
<b>Tm</b>	<b>Yb</b>	<b>Lu</b>	<b>Lu</b>
<b>163.5</b>	<b>167.2</b>	<b>159.4</b>	<b>174.94</b>
<b>5</b>	<b>6</b>	<b>7</b>	<b>8</b>
<b>Lu</b>	<b>Lu</b>	<b>Lu</b>	<b>Lu</b>
<b>163.5</b>	<b>167.2</b>	<b>159.4</b>	<b>174.94</b>
<b>13</b>	<b>14</b>	<b>15</b>	<b>16</b>
<b>Lu</b>	<b>Lu</b>	<b>Lu</b>	<b>Lu</b>
<b>163.5</b>	<b>167.2</b>	<b>159.4</b>	<b>174.94</b>
<b>5</b>	<b>6</b>	<b>7</b>	<b>8</b>
<b>Lu</b>	<b>Lu</b>	<b>Lu</b>	<b>Lu</b>
<b>163.5</b>	<b>167.2</b>	<b>159.4</b>	<b>174.94</b>
<b>13</b>	<b>14</b>	<b>15</b>	<b>16</b>
<b>Lu</b>	<b>Lu</b>	<b>Lu</b>	<b>Lu</b>
<b>163.5</b>	<b>167.2</b>	<b>159.4</b>	<b>174.94</b>
<b>5</b>	<b>6</b>	<b>7</b>	<b>8</b>
<b>Lu</b>	<b>Lu</b>	<b>Lu</b>	<b>Lu</b>
<b>163.5</b>	<b>167.2</b>	<b>159.4</b>	<b>174.94</b>
<b>13</b>	<b>14</b>	<b>15</b>	<b>16</b>
<b>Lu</b>	<b>Lu</b>	<b>Lu</b>	<b>Lu</b>
<b>163.5</b>	<b>167.2</b>	<b>159.4</b>	<b>174.94</b>
<b>5</b>	<b>6</b>	<b>7</b>	<b>8</b>
<b>Lu</b>	<b>Lu</b>	<b>Lu</b>	<b>Lu</b>
<b>163.5</b>	<b>167.2</b>	<b>159.4</b>	<b>174.94</b>
<b>13</b>	<b>14</b>	<b>15</b>	<b>16</b>
<b>Lu</b>	<b>Lu</b>	<b>Lu</b>	<b>Lu</b>
<b>163.5</b>	<b>167.2</b>	<b>159.4</b>	<b>174.94</b>
<b>5</b>	<b>6</b>	<b>7</b>	<b>8</b>
<b>Lu</b>	<b>Lu</b>	<b>Lu</b>	<b>Lu</b>
<b>163.5</b>	<b>167.2</b>	<b>159.4</b>	<b>174.94</b>
<b>13</b>	<b>14</b>	<b>15</b>	<b>16</b>
<b>Lu</b>	<b>Lu</b>	<b>Lu</b>	<b>Lu</b>
<b>163.5</b>	<b>167.2</b>	<b>159.4</b>	<b>174.94</b>
<b>5</b>	<b>6</b>	<b>7</b>	<b>8</b>
<b>Lu</b>	<b>Lu</b>	<b>Lu</b>	<b>Lu</b>
<b>163.5</b>	<b>167.2</b>	<b>159.4</b>	<b>174.94</b>
<b>13</b>	<b>14</b>	<b>15</b>	<b>16</b>
<b>Lu</b>	<b>Lu</b>	<b>Lu</b>	<b>Lu</b>
<b>163.5</b>	<b>167.2</b>	<b>159.4</b>	<b>174.94</b>
<b>5</b>	<b>6</b>	<b>7</b>	<b>8</b>
<b>Lu</b>	<b>Lu</b>	<b>Lu</b>	<b>Lu</b>
<b>163.5</b>	<b>167.2</b>	<b>159.4</b>	<b>174.94</b>
<b>13</b>	<b>14</b>	<b>15</b>	<b>16</b>
<b>Lu</b>	<b>Lu</b>	<b>Lu</b>	<b>Lu</b>
<b>163.5</b>	<b>167.2</b>	<b>159.4</b>	<b>174.94</b>
<b>5</b>	<b>6</b>	<b>7</b>	<b>8</b>
<b>Lu</b>	<b>Lu</b>	<b>Lu</b>	<b>Lu</b>
<b>163.5</b>	<b>167.2</b>	<b>159.4</b>	<b>174.94</b>
<b>13</b>	<b>14</b>	<b>15</b>	<b>16</b>
<b>Lu</b>	<b>Lu</b>	<b>Lu</b>	<b>Lu</b>
<b>163.5</b>	<b>167.2</b>	<b>159.4</b>	<b>174.94</b>
<b>5</b>	<b>6</b>	<b>7</b>	<b>8</b>
<b>Lu</b>	<b>Lu</b>	<b>Lu</b>	<b>Lu</b>
<b>163.5</b>	<b>167.2</b>	<b>159.4</b>	<b>174.94</b>
<b>13</b>	<b>14</b>	<b>15</b>	<b>16</b>
<b>Lu</b>	<b>Lu</b>	<b>Lu</b>	<b>Lu</b>
<b>163.5</b>	<b>167.2</b>	<b>159.4</b>	<b>174.94</b>
<b>5</b>	<b>6</b>	<b>7</b>	<b>8</b>
<b>Lu</b>	<b>Lu</b>	<b>Lu</b>	<b>Lu</b>
<b>163.5</b>	<b>167.2</b>	<b>159.4</b>	<b>174.94</b>
<b>13</b>	<b>14</b>	<b>15</b>	<b>16</b>
<b>Lu</b>	<b>Lu</b>	<b>Lu</b>	<b>Lu</b>
<b>163.5</b>	<b>167.2</b>	<b>159.4</b>	<b>174.94</b>
<b>5</b>	<b>6</b>	<b>7</b>	<b>8</b>
<b>Lu</b>	<b>Lu</b>	<b>Lu</b>	<b>Lu</b>
<b>163.5</b>	<b>167.2</b>	<b>159.4</b>	<b>174.94</b>
<b>13</b>	<b>14</b>	<b>15</b>	<b>16</b>
<b>Lu</b>	<b>Lu</b>	<b>Lu</b>	<b>Lu</b>
<b>163.5</b>	<b>167.2</b>	<b>159.4</b>	<b>174.94</b>
<b>5</b>	<b>6</b>	<b>7</b>	<b>8</b>
<b>Lu</b>	<b>Lu</b>	<b>Lu</b>	<b>Lu</b>
<b>163.5</b>	<b>167.2</b>	<b>159.4</b>	<b>174.94</b>
<b>13</b>	<b>14</b>	<b>15</b>	<b>16</b>
<b>Lu</b>	<b>Lu</b>	<b>Lu</b>	<b>Lu</b>
<b>163.5</b>	<b>167.2</b>	<b>159.4</b>	<b>174.94</b>
<b>5</b>	<b>6</b>	<b>7</b>	<b>8</b>
<b>Lu</b>	<b>Lu</b>	<b>Lu</b>	<b>Lu</b>
<b>163.5</b>	<b>167.2</b>	<b>159.4</b>	<b>174.94</b>
<b>13</b>	<b>14</b>	<b>15</b>	<b>16</b>
<b>Lu</b>	<b>Lu</b>	<b>Lu</b>	<b>Lu</b>
<b>163.5</b>	<b>167.2</b>	<b>159.4</b>	<b>174.94</b>
<b>5</b>	<b>6</b>	<b>7</b>	<b>8</b>
<b>Lu</b>	<b>Lu</b>	<b>Lu</b>	<b>Lu</b>
<b>163.5</b>	<b>167.2</b>	<b>159.4</b>	<b>174.94</b>
<b>13</b>	<b>14</b>	<b>15</b>	<b>16</b>
<b>Lu</b>	<b>Lu</b>	<b>Lu</b>	<b>Lu</b>
<b>163.5</b>	<b>167.2</b>	<b>159.4</b>	<b>174.94</b>
<b>5</b>	<b>6</b>	<b>7</b>	<b>8</b>
<b>Lu</b>	<b>Lu</b>	<b>Lu</b>	<b>Lu</b>
<b>163.5</b>	<b>167.2</b>	<b>159.4</b>	<b>174.94</b>
<b>13</b>	<b>14</b>	<b>15</b>	<b>16</b>
<b>Lu</b>	<b>Lu</b>	<b>Lu</b>	<b>Lu</b>
<b>163.5</b>	<b>167.2</b>	<b>159.4</b>	<b>174.94</b>
<b>5</b>	<b>6</b>	<b>7</b>	<b>8</b>
<b>Lu</b>	<b>Lu</b>	<b>Lu</b>	<b>Lu</b>
<b>163.5</b>	<b>167.2</b>	<b>159.4</b>	<b>174.94</b>
<b>13</b>	<b>14</b>	<b>15</b>	<b>16</b>
<b>Lu</b>	<b>Lu</b>	<b>Lu</b>	<b>Lu</b>
<b>163.5</b>	<b>167.2</b>	<b>159.4</b>	<b>174.94</b>
<b>5</b>	<b>6</b>	<b>7</b>	<b>8</b>
<b>Lu</b>	<b>Lu</b>	<b>Lu</b>	<b>Lu</b>
<b>163.5</b>	<b>167.2</b>	<b>159.4</b>	<b>174.94</b>
<b>13</b>	<b>14</b>	<b>15</b>	<b>16</b>
<b>Lu</b>	<b>Lu</b>	<b>Lu</b>	<b>Lu</b>
<b>163.5</b>	<b>167.2</b>	<b>159.4</b>	<b>174.94</b>
<b>5</b>	<b>6</b>	<b>7</b>	<b>8</b>
<b>Lu</b>	<b>Lu</b>	<b>Lu</b>	<b>Lu</b>
<b>163.5</b>	<b>167.2</b>	<b>159.4</b>	<b>174.94</b>
<b>13</b>	<b>14</b>	<b>15</b>	<b>16</b>
<b>Lu</b>	<b>Lu</b>	<b>Lu</b>	<b>Lu</b>
<b>163.5</b>	<b>167.2</b>	<b>159.4</b>	<b>174.94</b>
<b>5</b>	<b>6</b>	<b>7</b>	<b>8</b>
<b>Lu</b>	<b>Lu</b>	<b>Lu</b>	<b>Lu</b>
<b>163.5</b>	<b>167.2</b>	<b>159.4</b>	<b>174.94</b>
<b>13</b>	<b>14</b>	<b>15</b>	<b>16</b>
<b>Lu</b>	<b>Lu</b>	<b>Lu</b>	<b>Lu</b>
<b>163.5</b>	<b>167.2</b>	<b>159.4</b>	<b>174.94</b>
<b>5</b>	<b>6</b>	<b>7</b>	<b>8</b>
<b>Lu</b>	<b>Lu</b>	<b>Lu</b>	<b>Lu</b>
<b>163.5</b>	<b>167.2</b>	<b>159.4</b>	<b>174.94</b>
<b>13</b>	<b>14</b>	<b>15</b>	<b>16</b>
<b>Lu</b>	<b>Lu</b>	<b>Lu</b>	<b>Lu</b>
<b>163.5</b>	<b>167.2</b>	<b>159.4</b>	<b>174.94</b>
<b>5</b>	<b>6</b>	<b>7</b>	<b>8</b>
<b>Lu</b>	<b>Lu</b>	<b>Lu</b>	<b>Lu</b>
<b>163.5</b>	<b>167.2</b>	<b>159.4</b>	<b>174.94</b>
<b>13</b>	<b>14</b>	<b>15</b>	<b>16</b>
<b>Lu</b>	<b>Lu</b>	<b>Lu</b>	<b>Lu</b>
<b>163.5</b>	<b>167.2</b>	<b>159.4</b>	<b>174.94</b>
<b>5</b>	<b>6</b>	<b>7</b>	<b>8</b>
<b>Lu</b>	<b>Lu</b>	<b>Lu</b>	<b>Lu</b>
<b>163.5</b>	<b>167.2</b>	<b>159.4</b>	<b>174.94</b>
<b>13</b>	<b>14</b>	<b>15</b>	<b>16</b>
<b>Lu</b>	<b>Lu</b>	<b>Lu</b>	<b>Lu</b>
<b>163.5</b>	<b>167.2</b>	<b>159.4</b>	<b>174.94</b>
<b>5</b>	<b>6</b>	<b>7</b>	<b>8</b>
<b>Lu</b>	<b>Lu</b>	<b>Lu</b>	<b>Lu</b>
<b>163.5</b>	<b>167.2</b>	<b>159.4</b>	<b>174.94</b>
<b>13</b>	<b>14</b>	<b>15</b>	<b>16</b>
<b>Lu</b>	<b>Lu</b>	<b>Lu</b>	<b>Lu</b>
<b>163.5</b>	<b>167.2</b>	<b>159.4</b>	<b>174.94</b>
<b>5</b>	<b>6</b>	<b>7</b>	<b>8</b>
<b>Lu</b>	<b>Lu</b>	<b>Lu</b>	<b>Lu</b>
<b>163.5</b>	<b>167.2</b>	<b>159.4</b>	<b>174.94</b>
<b>13</b>	<b>14</b>	<b>15</b>	<b>16</b>
<b>Lu</b>	<b>Lu</b>	<b>Lu</b>	<b>Lu</b>
<b>163.5</b>	<b>167.2</b>	<b>159.4</b>	<b>174.94</b>
<b>5</b>	<b>6</b>	<b>7</b>	<b>8</b>
<b>Lu</b>	<b>Lu</b>	<b>Lu</b>	<b>Lu</b>
<b>163.5</b>	<b>167.2</b>	<b>159.4</b>	<b>174.94</b>
<b>13</b>	<b>14</b>	<b>15</b>	<b>16</b>
<b>Lu</b>	<b>Lu</b>	<b>Lu</b>	<b>Lu</b>
<b>163.5</b>	<b>167.2</b>	<b>159.4</b>	<b>174.94</b>
<b>5</b>	<b>6</b>	<b>7</b>	<b>8</b>
<b>Lu</b>	<b>Lu</b>	<b>Lu</b>	<b>Lu</b>
<b>163.5</b>	<b>167</b>		

and by the apparent nonexistence in aqueous solution of any oxidation state other than III in curium. Moreover, the III state of uranium would be surprising on this basis, because this element would be the second member of a thoride, or "IV oxidation state," series. The fact that nearly a year was spent in an unsuccessful effort to separate tracer amounts of americium and curium from the rare earths, immediately following the discovery of these two elements, illustrates how unnatural it would be to regard them as members of a thoride, or IV oxidation state, group.

The group probably could have been described just as well by some other term, such as "curide series," rather than "actinide," which is derived by analogy with the term "lanthanide." Another possibility would be to use a term such as "type 5f rare earths" or another name analogous to rare earths. A possibility here might be "synthetic earths" in view of the synthetic source of all except the first three members. [The best source of actinium is synthetic; actinium comes from pile neutrons by the reactions  $\text{Ra}^{226}(\text{n},\gamma)\text{Ra}^{227} \xrightarrow{\beta^-} \text{Ac}^{227}$ .] Irrespective of the name that usage will finally assign to this group of elements, however, it seems that the outstanding characteristics of the group, namely, the ekagadolinium character of curium (and the presumed ekalutecium character of element 103), together with the regularly increasing trend toward actinium-like character in going from thorium to curium, are best represented by listing these elements in corresponding positions under the rare-earth elements if it is desirable to give each element only one place in the periodic table.

**3.4 Predicted Properties of Transcurium Elements.** There has been a great deal of speculation concerning the upper limit of atomic number for the existence of elements, consideration being given to the fact that such a limit might arise from either atomic or nuclear (radioactivity or spontaneous fission) instability. If the former is not the limiting factor, it appears likely, on the basis of extrapolation from the nuclear properties of the heaviest elements, that the first few elements above element 96 will have isotopes of sufficiently long life to make possible their investigation at least on the tracer scale, if the problem of their production in detectable amount should be solved.

It is interesting to speculate about the chemical properties of these undiscovered elements beyond curium. The seven elements immediately following, that is, elements 97 to 103, inclusive, should constitute the second half of this rare-earth-like transition group. It appears likely that the electrons added in proceeding up this series

will be placed in a 5f shell of definitely lower energy than the 6d shell. Element 97 will probably have a IV as well as a III oxidation state, and in view of the lower binding energy of the 5f as compared to the 4f electrons it might be easier to oxidize element 97 (eka-terbium) to this IV state than is the case for terbium since the hydration and lattice energies do not appear to reverse the simple prediction for oxidation potentials from ionization potentials in these elements. Correspondingly, it should be easier to oxidize element 98 (ekadysprosium) to the IV and V oxidation states than is the case for dysprosium, for which oxidation above the III state is practically impossible. Toward the end of the series, elements 102 and 101 should be capable of being reduced to the II oxidation state, which would be analogous to the reduction of ytterbium and thulium, and element 103 should be similar to lutecium with respect to the complete stability of the III state.

Element 104 should continue with the filling of the 6d shell and be a true ekahafnium. After the filling of the 6d shell in the following elements there would be addition to the 7p shell, with the attainment of the rare-gas structure at hypothetical element 118 (on the logical assumption that the 5g shell does not start to fill before this point).

#### 4. SUMMARY

All available evidence leads to the view that the 5f-electron shell is being filled in the heaviest elements, giving rise to a transition series. This transition series begins formally with actinium in the same sense that the rare-earth or "lanthanide" series begins with lanthanum. Such an "actinide" series is suggested on the basis of the following evidence: (1) chemical properties, (2) absorption spectra in aqueous solution and crystals, (3) crystallographic structure data, (4) magnetic susceptibility data, and (5) spectroscopic data. This series differs from the rare-earth series in having more oxidation states above the III state, and it differs in other ways that are connected with the lower binding of 5f compared to 4f electrons. The salient point is that the characteristic oxidation state is the III state, and the group is placed in the periodic table on this basis. (The characteristic oxidation state is exhibited by the member containing seven 5f electrons and presumably also by the member containing fourteen 5f electrons, curium and element 103.) The data also make it possible to give a suggested table of electronic configurations of the ground state of the gaseous atom for each of the elements from actinium to curium, inclusive.

## APPENDIX†

Plutonium is the eighth element in the seventh period of the periodic table. The correlation of its chemical properties with its atomic structure can best be accomplished by considering it together with a number of the other elements in the seventh period (elements 89 to 94) in a discussion involving the chemical and physical properties of these elements.

It seems very probable that some kind of a transition group should begin in the neighborhood of these elements. The elements 90 to 94 lie in corresponding positions just below the sixth-period transition elements hafnium to osmium (atomic numbers 72 to 76), in which the 5d shell is being filled. The transition elements hafnium to osmium are very similar in their chemical properties to the corresponding 4d transition elements of the fifth period (zirconium to ruthenium, atomic numbers 40 to 44). Although the first members (<sub>90</sub>Th, <sub>91</sub>Pa) of the group 90 to 94 show a great deal of resemblance in chemical properties to the first members (<sub>72</sub>Hf, <sub>73</sub>Ta) in the 5d transition series and to the first members (<sub>40</sub>Zr, <sub>41</sub>Cb) in the 4d transition series, the later members (<sub>93</sub>Np, <sub>94</sub>Pu) show practically no resemblance to <sub>76</sub>Re and <sub>78</sub>Os or to element 43 and <sub>44</sub>Ru. Neptunium and plutonium are much more electropositive in character than the noble elements rhenium, element 43, osmium, and ruthenium. There is no evidence for a volatile plutonium tetroxide in contrast with the volatile osmium and ruthenium tetroxides, and there is no evidence for an oxidation number of VIII in plutonium. Thus it seems certain that the transition in the elements 89 to 94 does not involve the simple filling in of the 6d shell.

On the other hand, the chemical properties of neptunium and plutonium are very similar to those of uranium and thorium and are such as to suggest that the 5f shell is being filled and that we are dealing with another rare-earth series similar to the well-known lanthanide series, <sub>58</sub>Ce-<sub>71</sub>Lu, in which the 4f shell becomes filled. Many people had suggested, on the basis of considerations of electronic structure, that a rare-earth-like series should begin in this region. There has been a large degree of uncertainty in these predictions with regard to the starting point of this series. The two principal choices have been

†This appendix is reproduced from Metallurgical Laboratory Memorandum MUC-GTS-858 (July 17, 1944) and Metallurgical Project Report CK-1968, pp. 55-57 (July 17, 1944).

between a thoride and a uranide series. From the standpoint of the chemical properties of  $_{90}\text{Th}$ ,  $_{91}\text{Pa}$ , and  $_{92}\text{U}$  considered alone, the evidence for such a series was not strong. However, with the discovery of neptunium and plutonium and the observation of the marked similarity of these elements to uranium and thorium in chemical properties, the chemical evidence for a rare-earth-like series has become very strong.

The persistence of the IV oxidation state through the elements thorium, uranium, neptunium, and plutonium is certainly good evidence that electrons are going into the 5f shell. The observation by Zachariasen of the isomorphism of the compounds  $\text{ThO}_2$ ,  $\text{UO}_2$ ,  $\text{NpO}_2$ , and  $\text{PuO}_2$  and his observation of the regular decrease in radius of the metallic ion in these oxides in the anticipated manner are also very good evidence that the electrons are going into the 5f shell. A number of other crystallographic observations by Zachariasen lend support to this view. There are other points of evidence, for example (1) magnetic susceptibility measurements on uranium and plutonium, (2) the sharpness of the optical absorption in aqueous solutions of uranium and plutonium, and (3) evidence for organic complexes of  $\text{U}^{+4}$  and  $\text{Pu}^{+4}$  in which these elements have a coordination number of 8 (indicating that the 6d, 7s, and 7p orbitals are available), which facts also give strong support to this conclusion. It seems very probable from these lines of evidence that uranium and plutonium (and neptunium) have electrons in the 5f shell; however, it is not possible to deduce whether or not uranium is the first element in the series for which this is the case. It would be consistent with this evidence for thorium and protactinium to have no electrons in the 5f shell and for uranium to have two electrons in this shell.

An attractive hypothesis is that this rare-earth-like series begins with actinium in the same sense that the lanthanide series begins with lanthanum. On this basis it may be termed the "actinide series," and the first 5f electron may appear in thorium. Thus, the ground state of thorium may have the structure  $5\text{f}^16\text{d}7\text{s}^2$  beyond the radon core. With an actinide series, uranium may have the electron configuration  $5\text{f}^36\text{d}7\text{s}^2$ , neptunium the configuration  $5\text{f}^46\text{d}7\text{s}^2$ , and plutonium the configuration  $5\text{f}^56\text{d}7\text{s}^2$ . It is very interesting to note that Kiess, Humphreys, and Laun<sup>74</sup> give a preliminary description of the analysis of the spectrum of neutral uranium atoms and come to the conclusion that the electron configuration of the lowest state of uranium is  $5\text{f}^36\text{d}7\text{s}^2$  (with the term symbol  $^3\text{L}_6$ ), which supports the above view.

It may be that, as in the lanthanide series, electrons do not tend to occupy the 6d orbital; rather, an additional electron goes into a 5f orbital and gives, for example, the configuration  $5\text{f}^27\text{s}^2$  for thorium

and the configuration  $5f^17s^2$  for uranium. There is evidence that thorium emits a complex spectrum corresponding to a rare earth with an electron structure like that of  $_{59}\text{Ce}$ , whose ground state is known to have the configuration  $4f^26s^2$ , and that uranium has a spectrum similar to that of the rare-earth element  $_{80}\text{Nd}$ , whose ground state is known to have the configuration  $4f^46s^2$ .

It may be, of course, that there are no 5f electrons in thorium and protactinium and that the entry into a rare-earth-like series begins at uranium, with three electrons in the 5f shell. It would still seem logical to refer to this as an actinide series.

In an actinide series it may seem rather peculiar at first sight that the persistent oxidation number of IV should be in this region. The IV oxidation state seems to be most prevalent and generally most stable among these elements. However, as referred to above, in the lanthanide series there are usually only two electrons present in the 5d and 6s shells, whereas the persistent oxidation state is certainly III. This generally involves the removal of a 4f electron. There are also a number of cases in the lanthanide series where the oxidation number IV is found. In the "actinide" series, although the oxidation number IV is perhaps prevalent, the oxidation number III seems also to be found in most of the members of the series. Zachariasen has recently reported crystallographic evidence for tripositive thorium compounds ( $\text{ThF}_3$  and  $\text{ThOF}$ ), although magnetochemical experiments by Selwood have failed to confirm this report.

There is one way in which the actinide series definitely differs from the lanthanide series. This is in the existence of oxidation states higher than IV [protactinium(V), uranium(VI), neptunium(VI), plutonium(VI)] in the series. It must be concluded that the 5f electrons are not so tightly bound as the 4f electrons. This is certainly reasonable. However, the evidence so far is in favor of a maximum oxidation number of VI in this series, so that the removal of three electrons, or four if there are no electrons in the 6d orbitals, from the 5f orbitals is the maximum that occurs in ordinary chemical reactions.

It is interesting to speculate a little about the chemical properties of the series members which we have not yet had an opportunity to study. The element  $_{91}\text{Pa}$  is obviously interesting to study from a chemical and crystallographic point of view in order to throw further light on the situation. It seems very likely that this element will have oxidation states of IV and III in addition to the V state, and probably at least the IV state will have a reasonable amount of stability. It seems almost certain, also, that neptunium will have an oxidation state of III, intermediate in stability between  $\text{U}^{+3}$  and  $\text{Pu}^{+3}$ . If the picture of the actinide series is correct, the configuration  $5f^76d^17s^2$

may be reached with element 96 (similar to the configuration of  $_{64}\text{Gd}$ ); this configuration should be especially stable. The prediction may be made that with element 96 it will be very difficult, if not impossible, to reach any oxidation states above III or IV. In the case of element 95 the configuration  $5f^77s^2$ , similar to  $_{63}\text{Eu}$ , may be possible, and it may be expected that the oxidation state II will exist. Oxidation states higher than IV may also be difficult or impossible to reach in the case of element 95. There already seems to be some evidence for a trend toward greater stability for the lower oxidation states in the members of the series that have been studied so far. Thus, in going from uranium to plutonium, there seems to be a trend toward greater stability of the III oxidation state and greater difficulty in reaching the VI state. If the series is truly a thoride or a uranide series, the most stable lower oxidation states will occur at elements beyond 95 and 96; however, even in this event some tendency may be expected in this direction at elements 95 and 96. It would obviously be of great interest and value in elucidating the nature of this series to study the chemical properties of elements such as 95 and 96.

## REFERENCES

1. W. M. Latimer and J. H. Hildebrand, "Reference Book of Inorganic Chemistry," p. 519, The MacMillan Company, New York, 1940; H. S. Taylor and S. Glasstone, "Treatise on Physical Chemistry," Vol. 1, p. 298, D. Van Nostrand Company, Inc., New York, 1942; "Handbook of Chemistry and Physics," Chemical Rubber Publishing Company, Cleveland, Ohio; F. K. Richtmeyer and E. H. Kennard "Introduction to Modern Physics," p. 707, McGraw-Hill Book Company, Inc., New York, 1942.
2. N. Bohr, Phil. Mag., 26: 1. 476 (1913).
3. J. R. Rydberg, Lunds Univ. Årsskr., 2: (No. 18) 9 (1913).
4. N. Bohr, Nature, 112: 30 (1923).
5. V. M. Goldschmidt, Norske Videnskaps-Acad. Skrifter, Geochemiske Verteilungsgesetze der Elemente, 2: 23 (1924).
6. O. Hahn, Angew. Chem., 42: 924 (1929).
7. Y. Sugaira and H. C. Urey, Kgl. Danske Videnskab. Selskab, Math. fys. Medd., 7: (No. 13) 3 (1926).
8. T. Y. Wu and S. Goudsmit, Phys. Rev., 43: 496 (1933); T. Y. Wu, Phys. Rev., 44: 727 (1933).
9. J. C. McLennan, A. B. McLay, and H. G. Smith, Proc. Roy. Soc. London, A112: 76 (1926).
10. S. Dushman, Chem. Revs., 5: 137 (1926).
11. R. Swinne, Z. tech. Physik, 7: 205 (1926).
12. M. N. Saha and N. K. Saha, "Treatise on Modern Physics," pp. 583 and 588, The Indian Press, Ltd., Allahabad and Calcutta, 1934.
13. V. Karapetoff, J. Franklin Inst., 210: 609 (1930).
14. A. Von Grosse, J. Am. Chem. Soc., 57: 440 (1935); Chem. Ber., 61: 233 (1928); J. Am. Chem. Soc., 52: 1742 (1930).

15. L. L. Quill, *Chem. Revs.*, 23: 87 (1938).
16. J. Perrin, "Grains de matière et de lumière," Vol. II, p. 30, Hermann & Cie, Paris, 1935.
17. R. Rudy, *Rev. gen. sci.*, 38: 671 (1927).
18. M. Carranza, *Bol. soc. quim. Peru*, (I) 6: 41 (1935).
19. G. E. Villar, *J. Chem. Education*, 19: 329 (1942); *Anais acad. brasil. cienc.*, 12: 51 (1940).
20. V. M. Goldschmidt, "Travaux du Congrès Jubilaire Mendeleev," II, 387, 1937.
21. V. M. Goldschmidt, T. Barth, and G. Lunde, *Norske Videnskaps-Acad. Skrifter 1, Geochemische Verteilungsgesetze der Elemente*, V: 10 (1925).
22. E. M. McMillan and P. H. Abelson, *Phys. Rev.*, 57: 1185 (1940).
23. M. Goeppert Mayer, *Phys. Rev.*, 60: 184 (1941).
24. R. Daudel, *Compt. rend.*, 217: 396 (1943).
25. K. Starke, *Z. anorg. Chem.*, 251: 251 (1943).
26. C. G. Bedreag, *Naturwissenschaften*, 31: 490 (1943).
27. F. Strassmann and O. Hahn, *Naturwissenschaften*, 30: 256 (1942).
28. G. T. Seaborg and A. C. Wahl, Report A-135; The chemical properties of elements 94 and 93, Paper 1.6, this volume; *J. Am. Chem. Soc.*, 70: 1128 (1948) (paper written Mar. 19, 1942).
29. W. H. Zachariasen, Metallurgical Project Reports CK-1518 (March 1944), p. 3, and CN-1807 (June 1944).
30. G. E. Djounkovsky and S. Kavos, *J. phys. radium*, (8) 5: 53 (1944).
31. L. Talpain, *J. phys. radium*, (8) 6: 176 (1945).
32. G. T. Seaborg, Metallurgical Laboratory Memorandum MUC-GTS-858; Metallurgical Project Report CK-1968 (A-2845) (July 17, 1944), p. 55 (see Appendix of this paper).
33. G. T. Seaborg, *Chem. Eng. News*, 23: 2190 (1945); *Science*, 104: 379 (1946).
34. N. Bohr, "Theory of Spectra and Atomic Constitution," 2d ed., p. 112, Cambridge University Press, London, 1924.
35. W. M. Latimer, "The Oxidation States of the Elements and Their Potentials in Aqueous Solutions," Prentice-Hall, Inc., New York, 1938.
36. See for uranium: E. Rabinowitch and J. J. Katz, National Nuclear Energy Series, Division VIII, Volume 5; for neptunium: B. B. Cunningham and J. C. Hindman, Metallurgical Project Report CC-3685 (October 1946); also in National Nuclear Energy Series, Division IV, Volume 14A; for plutonium: R. E. Connick, Metallurgical Project Report CC-3869 (May 5, 1948); also in National Nuclear Energy Series, Division IV, Volume 14A; for americium: B. B. Cunningham, The first isolation of americium in the form of pure compounds; microgram-scale observations on the chemistry of americium, Paper 19.2, this volume; L. B. Asprey and B. B. Cunningham, University of California Radiation Laboratory Report UCRL-329 (April 1949).
37. S. G. Thompson, L. O. Morgan, R. A. James, and I. Perlman, The tracer chemistry of americium and curium in aqueous solutions, Paper 19.1, this volume.
38. L. B. Werner and I. Perlman, Reported in University of California Radiation Laboratory (Chemistry Group) Progress Report RL-4.5.46 (June 1946).
39. L. B. Werner and I. Perlman, Reported in University of California Radiation Laboratory (Chemistry Group) Progress Report BC-80 (August 1947).
40. S. Fried and A. E. Florin, private communication (October 1947); S. Fried, Atomic Energy Commission Declassified Document AECD-1930.
41. M. Haissinsky, Reported at symposium on the chemistry of the heavy elements sponsored by British Atomic Energy Research Establishment, Oxford, England (Mar. 28, 1949); *Compt. rend.*, 226: 573 (1948).
42. E. Hayek and T. Rehner, *Experientia*, 5: 114 (1949).

43. J. S. Anderson and R. W. M. D'Eye, Reported at symposium on the chemistry of the heavy elements sponsored by British Atomic Energy Research Establishment, Oxford, England (Mar. 28, 1949).
44. E. F. Westrum, Jr., private communication (April 1949).
45. E. D. Eastman, L. Brewer, L. A. Bromley, P. W. Gilles, and N. L. Lofgren, Reported at spring meeting American Chemical Society, San Francisco, California (Mar. 27, 1949). (Published in abstracts of Division of Physical and Inorganic Chemistry.)
46. W. H. Zachariasen, Metallurgical Laboratory Memorandum MUC-FWHZ-175 (1946); also in National Nuclear Energy Series, Division IV, Volume 14A.
47. J. D. McCullough, Reported in University of California Radiation Laboratory (Chemistry Group) Progress Report RL-4.5.56 (April 1947).
48. J. K. Marsh, J. Chem. Soc., 1946: 15.
49. W. Prandtl and G. Rieder, Z. anorg. Chem., 238: 225 (1938).
- 49a. R. E. Connick, Reported at symposium on the chemistry of the heavy elements sponsored by British Atomic Energy Research Establishment, Oxford, England (Mar. 28, 1949); J. Chem. Soc., in press.
50. E. F. Westrum, Reported in University of California Radiation Laboratory (Chemistry Group) Progress Report RL-4.5.49 (September 1946) and Report UCRL-46 (January 1948).
51. For the rare-earth metal densities, see D. M. Yost, H. Russell, Jr., and C. S. Garner, "The Rare-earth Elements and Their Compounds," p. 2, John Wiley & Sons, Inc., New York, 1947.
52. V. M. Goldschmidt, Fortschr. Mineral., Krist. Petrog., 15: 93 (1931).
53. F. Ephraim and M. Mezener, Helv. Chim. Acta, 16: 1257 (1933); J. Indian Chem. Soc., Ray memorial volume, p. 243, 1933.
54. For uranium: J. J. Howland, Jr., in National Nuclear Energy Series, Division VIII, Volume 6; for neptunium: J. C. Hindman, L. B. Magnusson, and T. J. LaChapelle, Metallurgical Project Report CN-3053 (June 1945) and J. Am. Chem. Soc., 71: 687 (1949); for plutonium: J. C. Hindman and D. P. Ames, Metallurgical Project Report CN-3053 (June 1945) and J. C. Hindman, Metallurgical Project Report CN-3819 (May 19, 1947); also in National Nuclear Energy Series, Division IV, Volume 14A; for americium: B. B. Cunningham, The first isolation of americium in the form of pure compounds; microgram-scale observations on the chemistry of americium, Paper 19.2, this volume; for curium: L. B. Werner and I. Perlman, The preparation and isolation of curium, Paper 22.5, this volume (Atomic Energy Commission Declassified Document AECD-1898).
55. W. Prandtl and K. Scheiner, Z. anorg. Chem., 220: 107 (1934).
56. D. C. Stewart, private communication (January 1948).
57. P. M. Lantz and G. W. Parker, Clinton Laboratories Report CNL-37 (Apr. 16, 1948), p. 114.
58. B. M. Jones and B. B. Cunningham, Reported in University of California (Chemistry Division) Quarterly Progress Report UCRL-172 (June-August 1948).
59. S. Freed and F. J. Leitz, Clinton Laboratories Report CNL-6 (September to November 1947), p. 48.
60. S. Freed and F. J. Leitz, Jr., Reported at symposium on chemistry of transuranium elements, 1948 Spring Meeting American Chemical Society, Chicago; Atomic Energy Commission Declassified Document AECD-1890 (March 1948).
61. V. M. Goldschmidt, Norske Videnskaps-Acad. Skrifter 1, Geochemische Verteilungsgesetze der Elemente VII, 56 (1926).
62. V. M. Goldschmidt, Fra Fysikkens Verden (Norsk Fysisk Tidsskrift) 3: 179 (1941-1942).

63. W. H. Zachariasen, Metallurgical Laboratory Memorandum MUC-FWHZ-156 (Nov. 3, 1945).
64. D. H. Templeton, Reported in University of California Radiation Laboratory (Chemistry Group) Progress Report UCRL-15 (November 1947).
65. W. H. Zachariasen, The crystal chemistry of plutonium and neptunium, in National Nuclear Energy Series, Division IV, Volume 14A; *Phys. Rev.*, 73: 1104 (1948); *Acta Crystallographica*, 1: 265 (1948); *J. Chem. Phys.*, 16: 254 (1948).
66. R. W. Lawrence, *J. Am. Chem. Soc.*, 56: 776 (1934).
67. H. Haraldsen and R. Bakken, *Naturwissenschaften*, 28: 127 (1940).
68. H. Bommer, *Z. anorg. Chem.*, 247: 249 (1941).
69. W. Sucksmith, *Phil. Mag.*, 14: 1115 (1932).
70. M. Calvin, Metallurgical Project Report CK-2411 (Oct. 1, 1944); M. Calvin, M. Kasha, and G. Sheline, Magnetic susceptibilities of plutonium in its various oxidation states in aqueous solution, Paper 4.23, this volume (Atomic Energy Commission Declassified Document AECD-2002).
71. C. A. Hutchison, Jr., and N. Elliott, *Phys. Rev.*, 73: 1229 (1948); *J. Chem. Phys.*, 16: 920 (1948).
72. C. A. Hutchison, Jr., and N. Elliott, Reported at symposium on chemistry of transuranium elements, 1948 Spring Meeting American Chemical Society, Chicago.
73. J. J. Howland and M. Calvin, Reported at symposium on chemistry of transuranium elements, 1948 Spring Meeting American Chemical Society, Chicago; *J. Chem. Phys.*, to be published.
74. C. C. Kiess, C. J. Humphreys, and D. D. Laun, Report A-1747, Natl. Bur. Standards U. S. (Feb. 7, 1944).
75. C. C. Kiess, C. J. Humphreys, and D. D. Laun, *J. Research Natl. Bur. Standards*, 37: 57 (1946); *J. Optical Soc. Am.*, 36: 357 (1946).
76. P. Schuurmans, *Physica*, 11: 419 (1946).
77. P. Schuurmans, J. C. Van Den Bosch, and N. Dijkwel, *Physica*, 13: 117 (1947).
78. J. R. McNally, Jr., and G. R. Harrison, Carbide and Carbon Chemicals Corporation (Y-12 plant), Unclassified Report Y-340 (Feb. 11, 1949).
79. J. R. McNally, Jr., *J. Optical Soc. Am.*, 35: 390 (1945).
80. J. R. McNally, Jr., G. R. Harrison, and H. B. Park, *J. Optical Soc. Am.*, 32: 334 (1942).
81. T. L. deBruin, P. Schuurmans, and P. F. A. Klinkenberg, *Z. Physik*, 121: 667 (1943).
82. T. L. deBruin, P. F. A. Klinkenberg, and P. Schuurmans, *Z. Physik*, 122: 23 (1944).
83. H. Russell, Jr., Los Alamos Report LA-145 (Sept. 24, 1944); Manhattan District Declassified Document MDDC-406 (Oct. 22, 1946).
84. F. S. Tomkins and M. Fred, private communication (Mar. 3, 1948); *J. Optical Soc. Am.*, 39: 357 (1949).
85. D. M. Yost, H. Russell, Jr., and C. S. Garner, "The Rare-earth Elements and Their Compounds," pp. 3-4, John Wiley & Sons, Inc., New York, 1947.
86. W. F. Meggers, *Science*, 105: 514 (1947).
87. P. F. A. Klinkenberg, *Physica*, 13: 1 (1947).
88. W. F. Meggers, *Rev. Mod. Physics*, 14: 96 (1942).
89. S. G. Thompson, private communication, October 1947.
90. D. F. Stedman, *Can. J. Research*, 25B: 199 (1947).
91. K. E. Zimen, *Festskrift Tillagnad J. Arvid. Hedvall*, 1948: 635.
92. B. G. Harvey, *Nucleonics*, 2: (No. 4) 30 (1948).
93. W. F. Meggers, *Science*, 105: 514 (1947).
94. R. Spence, *Research*, 2: 115 (1949).

95. A. G. Maddock, Research, 1: 690 (1948).
96. B. C. Purkayastka, Nucleonics, 3: (No. 5) 2 (1948).
97. T. J. Hardwick, Proceedings of Conference in Nuclear Chemistry, Part 1, p. 44, McMaster University, Canada, 1947.
98. T. S. Wheeler, Chemistry & Industry, 639-642 (1947).
99. B. M. Summons, J. Chem. Education, 24: 588 (1947).
100. G. E. Villar, Bol. soc. quím. Peru, 13: 73 (1947).
101. A. G. Oppegaard, J. Chem. Soc., 318-321 (1948).
102. A. I. Akhumov, J. Gen. Chem. U.S.S.R., 17: 1241 (1947).

## Paper 22.1

### THE NEW ELEMENT AMERICIUM (ATOMIC NUMBER 95)†

By G. T. Seaborg, R. A. James, and L. O. Morgan

#### 1. INTRODUCTION

Isotopes of the element with atomic number 95 have been produced and identified in experiments carried out with material activated in the 60-in. cyclotron of the University of California. The target materials that have been successfully used in the production of these isotopes are  $U^{238}$ ,  $Np^{237}$ , and  $Pu^{239}$ . The helium-ion bombardment of  $U^{238}$  leads to the formation of plutonium isotopes of mass numbers 236 to 241, of which  $Pu^{238}$ ,  $Pu^{239}$ , and  $Pu^{240}$  are known to be  $\beta$  stable.  $Pu^{241}$  is shown in this work to be unstable toward the emission of  $\beta$  particles, leading to the production of  $95^{241}$ . The helium-ion bombardment of  $Np^{237}$  and the deuteron bombardment of  $Pu^{239}$  are capable of forming isotopes of element 95 directly, the expected mass numbers being 235 to 240.

At the beginning, in the search for activities due to isotopes of element 95 it was assumed that the chemical properties would be similar to those of the lanthanide elements in the tripositive oxidation state. It has been pointed out<sup>1</sup> that the chemical properties of the elements following actinium (element 89) in the periodic system may be explained on the assumption that they constitute a rare-earth-like series (actinide series) in which the 5f shell of electrons is in the process of completion. On this basis it was predicted that the increasing stability of the tripositive state of the actinide elements should culminate in very stable tripositive states in elements 95 and 96.

†Contribution from the Department of Chemistry and the Radiation Laboratory, University of California, Berkeley, and from the Chemistry Division of the Metallurgical Laboratory, University of Chicago, now the Argonne National Laboratory.

The first positive evidence for the existence of element 95 was found in the late fall of 1944 in the form of nuclear and chemical data pertaining to the isotope  $^{95}\text{Am}^{241}$ . It is suggested that the new element be named "americium," in honor of the Americas, and have the symbol "Am." This name is based on the strong analogy between element 95 and europium, Eu, named after Europe, of the lanthanide-rare-earth series.

## 2. $\text{Am}^{241}$ AND RELATED ISOTOPES

**2.1 Helium-ion Bombardment of  $\text{U}^{238}$ .** Uranium, in which the isotopic content of  $\text{U}^{235}$  was reduced by the electromagnetic process,<sup>2</sup> was bombarded in the 60-in. cyclotron at Berkeley with helium ions of approximately 38 mev energy. Such bombardments are discussed in more detail in another paper.<sup>3</sup> The activated metallic uranium was milled from the target plates in layers that are about 100 mg/sq cm. Each of the layers was processed separately to yield radiochemically pure plutonium fractions. Standard  $\alpha$ - and  $\beta$ -particle measurements with the purified plutonium samples revealed the presence of no radiations except those which could be accounted for on the basis of the radiations from previously known plutonium isotopes. Investigation of the very low-energy  $\beta$  spectrum, however, indicated the presence of  $\beta$  particles with approximately 20 kev maximum energy. The measurements were made in an apparatus designed by Raynor,<sup>4</sup> in which window and gas absorption of the particles to be counted is reduced to approximately 300  $\mu\text{g}/\text{sq cm}$ . In this case provision was made for absorption measurements using a limited number of absorbers made from thin calibrated films of cellulose nitrate. The  $\beta$ -particle range was estimated visually on a semilogarithmic plot of the counting data to be 600 to 800  $\mu\text{g}/\text{sq cm}$ , which corresponds to 20 kev maximum energy as obtained from the range-energy data of Schonland<sup>5</sup> for low-energy electrons. Absorption curves for the 20-kev  $\beta$ -particle component of the plutonium activities from the first and third layers of the activated uranium target are given in Fig. 1, in which  $\beta$ -particle intensities are normalized to the  $\text{Pu}^{239}$   $\alpha$ -particle activities in each sample. Thus, the lower intensities shown for the first layer indicate that the yield of the isotope responsible for the  $\beta$ -particle activity increases relative to the yield of  $\text{Pu}^{239}$  as the depth of penetration of the helium ion increases. From the data compiled by Livingston and Bethe<sup>6</sup> on the relative stopping power of various elements for helium ions, the maximum energy of the ions in the first and third uranium layers was calculated to be 38 mev and 28 mev, respectively. At the lower energy, the ratio of yields, ( $\alpha, < 3n$ ) to ( $\alpha, 3n$ ), should be greater

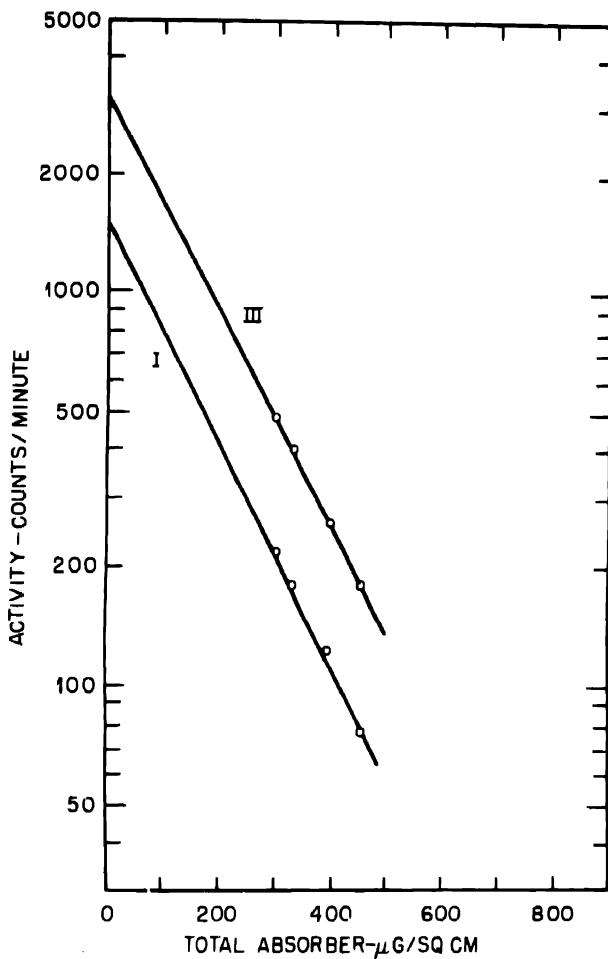
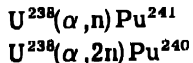


Fig. 1—Cellulose nitrate absorption curves for  $\beta$ -particle activity due to  $\text{Pu}^{241}$  in the first (I) and third (III) 100 mg./sq. cm layers of a helium-ion-bombarded uranium target.

than at a higher energy. On this basis, the decrease in 20-kev  $\beta$ -particle activity relative to  $\text{Pu}^{239}$   $\alpha$ -particle activity is an indication that it is due to an isotope resulting from the  $(\alpha,n)$  or  $(\alpha,2n)$  reaction



Of these,  $\text{Pu}^{241}$ , with an odd number of neutrons, is the most probable source of  $\beta$ -particle activity.

An estimate of the half life for  $\text{Pu}^{241}$   $\beta$ -particle emission may be made with the following observations:

1. The  $\beta$  activity of curve I, Fig. 1, extrapolated to zero absorption as shown, is 1,550 counts per minute.
2. In the same sample and at the same counting geometry there are 54 counts per minute of  $\alpha$  particles due to  $\text{Pu}^{239}$ .
3. The half life for  $\alpha$ -particle emission of  $\text{Pu}^{239}$  is 24,300 years.
4. The yield from the  $(\alpha, n)$  reaction relative to that from the  $(\alpha, 3n)$  reaction is usually approximately 0.01 in the 38-mev helium-ion bombardment of heavy isotopes.

From these considerations the half life of  $\text{Pu}^{241}$  for  $\beta$ -particle emission is approximately 10 years.

The rare-earth fraction from a similarly activated uranium sample contained an  $\alpha$ -particle activity (energy of 5.45 mev) of long half life. Numerous tracer chemical experiments that were carried out with such activity are reported in another paper.<sup>7</sup> The evidence obtained shows conclusively that the activity is due to a previously unknown element. The occurrence of relatively energetic  $\alpha$ -particle emission in a rare-earth fraction (lanthanum fluoride carryable) may be considered sufficient evidence, of itself, for the presence of an isotope of a rare-earth-like heavy element, since  $\alpha$ -particle radioactivity is an extremely rare property in isotopes of atomic number less than 82. The direct formation of americium isotopes by the helium-ion bombardment of  $\text{U}^{238}$  is not possible; therefore, the presence of the  $\alpha$ -particle activity must be considered evidence for the formation of  $\text{Am}^{241}$  as the product of  $\beta$ -particle emission by  $\text{Pu}^{241}$ .

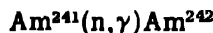
Several samples known to contain appreciable amounts of  $\text{Pu}^{241}$  were carefully purified to remove all traces of rare-earth and rare-earth-like radioactive substances, then were allowed to stand for long periods of time. When rare-earth fractions were again removed from the samples, the  $\alpha$  activity previously observed was again found, having grown into the samples from the plutonium source. Standard samples of the previously known plutonium isotopes were treated in a similar manner, but failed to yield a comparable  $\alpha$  activity. Samples of the  $\alpha$  activity were removed again and again from the plutonium samples, resulting in the following observations:

1. The rate of formation of the  $\alpha$ -particle activity was constant over a period of several years, owing to the long half life of the parent isotope.
2. The yield from a given sample was a linear function of the time allowed for growth.

3. The amount of growth in similar periods of time was directly dependent upon the intensity of 20-kev  $\beta$  particles, i.e., the amount of  $\text{Pu}^{241}$ , in the plutonium samples.

This evidence proves that the  $\alpha$  activity is due to  $\text{Am}^{241}$  arising from the  $\beta$ -particle emission of  $\text{Pu}^{241}$ .

Several samples of  $\text{Am}^{241}$  were irradiated with thermal neutrons over a long period of time. The principal product observed was an isotope of curium<sup>9</sup> (element 96),  $\text{Cm}^{242}$ , as determined by the half life (approximately five months) and the  $\alpha$ -particle energy (6.1 mev). Separation of the curium and americium activities was later achieved by the use of a Nalcite (Dowex-50) resin column with selective elution in ammonium citrate solution.<sup>9</sup> The  $\text{Cm}^{242}$  was formed by the reaction



followed by rapid negative  $\beta$ -particle decay of  $\text{Am}^{242}$ . In a later irradiation carried out in the Argonne heavy-water pile, Manning and Asprey<sup>10</sup> detected the  $\beta$  particles from  $\text{Am}^{242}$  and found the half life to be approximately 16 hr. They also demonstrated the growth of  $\text{Cm}^{242}$   $\alpha$  activity corresponding to the same 16-hr half life. A further discussion of  $\text{Am}^{242}$  is given in the next section.

All the experiments with the 5.45-mev  $\alpha$  activity are consistent with its assignment to  $\text{Am}^{241}$ . The isotope results from the  $\beta$  decay of  $\text{Pu}^{241}$ ; thermal-neutron irradiation of the material results in the formation of a  $\beta$ -active isotope, which decays to  $\text{Cm}^{242}$ , which in turn decays to  $\text{Pu}^{238}$ , a well-known isotope of plutonium.

Samples of plutonium analogous to those in which  $\text{Am}^{241}$  growth was observed were processed to yield radiochemically pure uranium fractions by an oxidation-reduction method employing nitric acid oxidation of uranium in sulfuric acid solution, precipitation of  $\text{PuF}_4$  and carrier  $\text{LaF}_3$ , then titanous chloride reduction and  $\text{LaF}_3$  precipitation to remove uranium as uranium(IV) from the solution. The uranium fractions were found to contain a  $\beta$  activity of 6.8-day half life, corresponding to  $\text{U}^{237}$ , which could be formed as a result of  $\alpha$  decay of  $\text{Pu}^{241}$ . The yield of the activity that was present in the plutonium at its equilibrium value was compared with the yield of  $\text{Am}^{241}$  from the same plutonium sample to give a value for the branching ratio of  $\text{Pu}^{241}$  (number of  $\alpha$  disintegrations per  $\beta$  disintegration) of approximately  $2 \times 10^{-5}$ .

2.2 Chemical Properties of Americium. A large number of tracer chemical experiments were carried out with the 5.45-mev  $\alpha$  activity and are described in detail in another paper.<sup>7</sup> It is of considerable

interest, however, that the unique chemical nature of americium may be shown by consideration of a relatively few experiments.

1. The activity coprecipitates with the rare-earth fluorides from strongly oxidizing solutions, such as 0.1M  $K_2Cr_2O_7$  in 1M  $HNO_3$  solution, and  $Ag^{++}$  with  $(NH_4)_2S_2O_8$  in 2M  $HNO_3$  solution. Those elements, without regard to the plausibility of their formation in the nuclear processes described, which are not eliminated from consideration on the basis of this, are scandium, yttrium, indium, lanthanum, the rare-earth elements, actinium, thorium, and possibly protactinium and thallium.

2. Among the more logical possible  $\alpha$ -particle emitters to be considered, we may eliminate thallium, lead, bismuth, and polonium because of the fact that the activity does not coprecipitate with bismuth sulfide from 0.25N HCl solution.

3. Thorium peroxide does not carry the activity under conditions in which thorium precipitates quantitatively. This fact eliminates thorium.

4. Actinium tracer activity and the activity in question may be fractionated by coprecipitation with zirconium or ceric iodate from 0.035M potassium iodate-1N  $HNO_3$  solution. The actinium tracer is carried to a greater extent.

5. The activity may be separated from tracer or macro amounts of the rare-earth elements by the precipitation of a lanthanum compound of undetermined composition from 1M ammonium fluosilicate-5M  $HNO_3$  solution. The  $\alpha$  activity remains largely in solution, but the rare-earth elements are almost completely precipitated under these conditions.

6. The activity may be separated from curium activity by selective elution with ammonium citrate solution from columns of resin, such as Amberlite IR-1, or Nalcite (Dowex-50). Curium is removed more easily.

This chemical evidence, together with the nuclear evidence previously given, establishes beyond any reasonable doubt that the activity is due to an actinium-like transplutonium element, i.e., to americium.

2.3 Nuclear Radiations of Am<sup>241</sup>. The disintegration of Am<sup>241</sup> is accompanied by the emission of  $\alpha$  particles and some associated electromagnetic radiation. The energy of the  $\alpha$  particles has been measured by two methods: (1) absorption in thin mica sheets of known thickness and (2) differential analysis, by electronic means, of the pulses produced by the  $\alpha$  particles in an ionization chamber<sup>11</sup> (Fig. 2). In both methods the energy was obtained from direct comparison with standard samples of other  $\alpha$  activities of known energies. The values

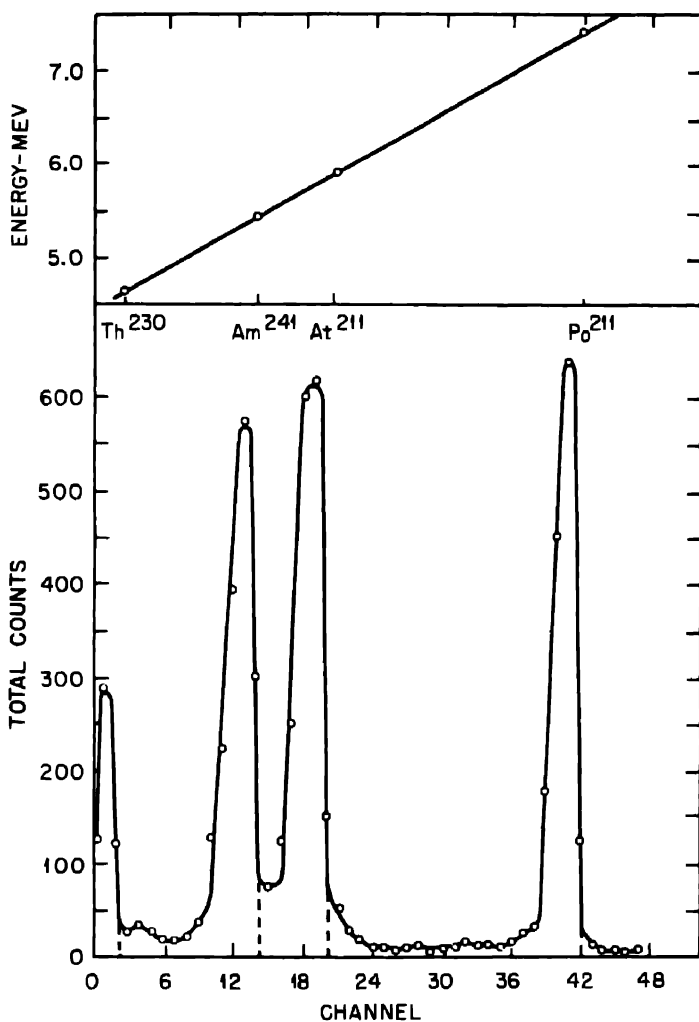


Fig. 2—Alpha-particle pulse-analysis curve for Am<sup>24¹</sup> and  $\alpha$ -particle-energy determination with Th<sup>23⁹</sup> (Io), At<sup>2¹¹</sup>, and Po<sup>2¹¹</sup>  $\alpha$ -particle standards.

from the two methods check closely at  $5.45 \pm 0.05$  mev. In the mica-absorption method the observed value is in terms of the range in air, which is converted to energy in million electron volts by use of the range-energy relation given by Holloway and Livingston.<sup>12</sup>

Absorption measurements on the electromagnetic radiations are shown graphically in Figs. 3 to 5. The intensities shown are for a sample containing  $10^6$  disintegrations per minute of  $\alpha$ -particle activity. The apparatus used to detect the radiations was a bell-jar-type

## THE TRANSURANIUM ELEMENTS

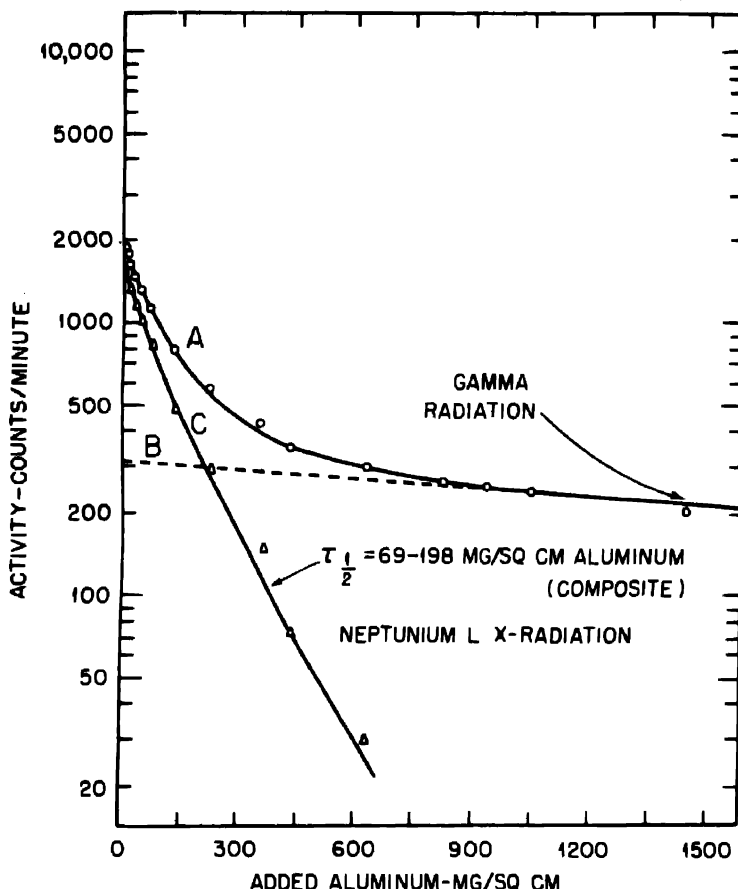


Fig. 3—Aluminum absorption curve for  $\text{Am}^{241}$  electromagnetic radiation. A: observed absorption curve; B:  $\gamma$  radiation; C: L x radiation (neptunium), half thickness = 69 to 198 mg/sq cm aluminum (composite).

Geiger counting tube,  $1\frac{1}{8}$  in. in diameter and  $2\frac{5}{8}$  in. in length. The window was of mica, approximately 3 mg/sq cm thick, and the body of the tube was copper. The tube was filled with a 90 per cent argon-10 per cent ethanol mixture to 10 cm Hg pressure. The anode was a 5-mil tungsten wire terminating in a small glass bead  $\frac{3}{16}$  in. from the mica window. Samples were counted in such a position as to have a 10 per cent geometry factor.

The electromagnetic radiations observed are seen to be of two classes: (1) a 62-kev component, the counting efficiency for which is about 0.5 per cent under the above conditions, and (2) a complex mixture of radiations apparently covering the range 10 to 20 kev, which

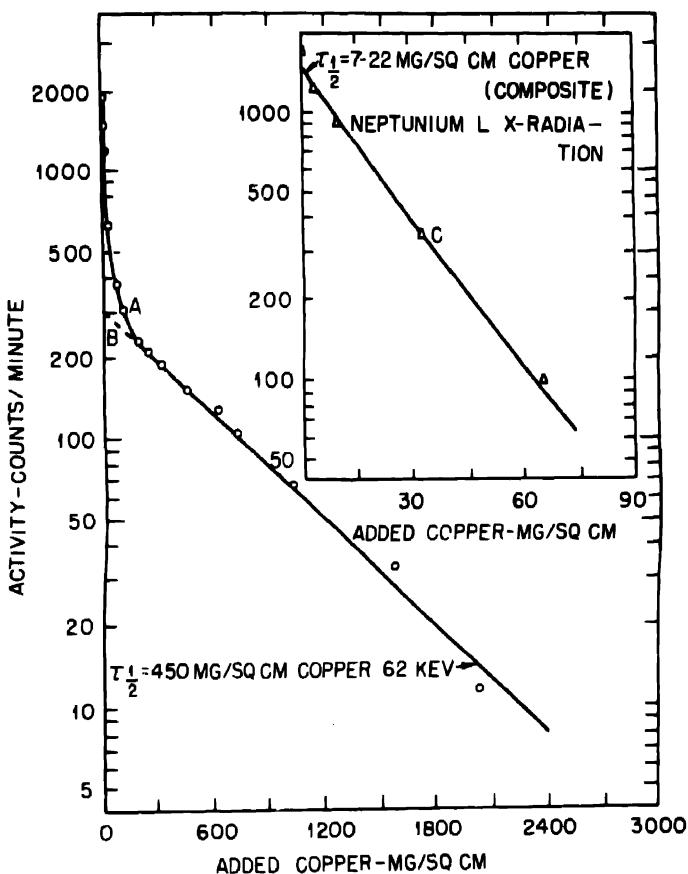


Fig. 4—Copper absorption curve for  $\text{Am}^{241}$  electromagnetic radiations. A: observed absorption curve; B:  $\gamma$  radiation (62 kev), half thickness = 450 mg/sq cm copper; C: L x radiation (neptunium), half thickness = 7 to 22 mg/sq cm copper (composite).

have approximately the absorption characteristics of neptunium L x radiation. The counting efficiency for the latter is not readily calculated, but is probably approximately 1.5 per cent under the above conditions. The aluminum absorption curve expected for the mixture of neptunium L x rays was constructed from an extrapolation of known L x-ray energies tabulated by Compton and Allison<sup>13</sup> and the relative intensities given for uranium by Allison.<sup>14</sup>

Using the counting efficiencies assumed in the above discussion, the neptunium L x rays are emitted in approximately 100 per cent of the  $\alpha$  disintegrations, and the 62-kev  $\gamma$  rays are emitted in approximately 80 per cent.

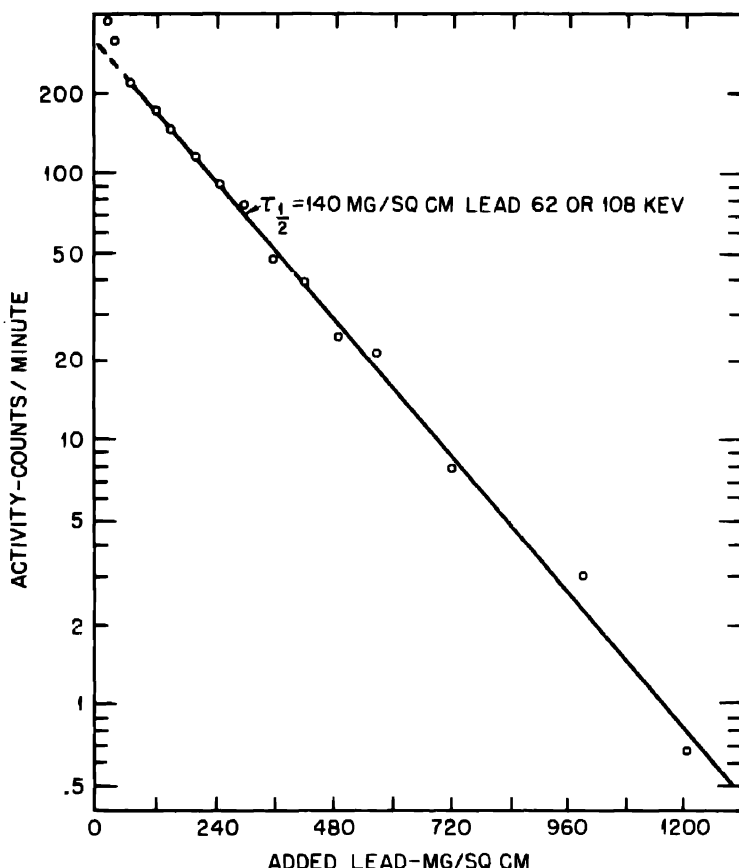


Fig. 5—Lead absorption curve for  $\text{Am}^{241}$  showing the 62-kev  $\gamma$  radiation; half thickness = 140 mg/sq cm lead; 62 or 108 kev.

Internal conversion of a  $\gamma$  ray whose energy is insufficient to excite the K electrons (binding energy approximately 120 kev) may take place in the L shell where the binding energy is much less (approximately 24 kev) if enough energy is available. The subsequent occupation of the vacant L electron state by another electron is accompanied by the characteristic L x radiation of the product element. The energy of the electrons in the case of the conversion of 62-kev  $\gamma$  rays is about 35 kev. Such electrons are not energetic enough to pass through the 3 mg/sq cm mica window of the Geiger tube described above and would not have been detected.

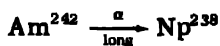
The half life of  $\text{Am}^{241}$  has been determined by Cunningham<sup>15</sup> to be  $510 \pm 20$  years. The value is based on specific-activity measurements carried out on the ultramicrochemical scale.

### 3. NUCLEAR PROPERTIES OF Am<sup>242</sup>

The production of Am<sup>242</sup> by the thermal-neutron irradiation of Am<sup>241</sup> has been mentioned in Sec. 2. The existence of the isotope was first indicated by the formation of an isotope of curium (atomic number 96), Cm<sup>242</sup>, under conditions expected to result in the formation of Am<sup>242</sup>, i.e., the radiative capture of thermal neutrons in Am<sup>241</sup>. The emission from Am<sup>242</sup> of negative  $\beta$  particles with a half life short compared to the total time of irradiation results in the observation given above. The first detection and half-life measurement of the actual process of  $\beta$ -particle decay of Am<sup>242</sup> was achieved by Manning and Asprey in samples investigated soon after termination of irradiation in the Argonne pile.<sup>10</sup> A decay curve obtained in recent experiments at this laboratory is given in Fig. 6 for the Am<sup>242</sup>  $\beta$  particles. A long-lived background activity is present owing to the electromagnetic radiations from Am<sup>241</sup> and the radiations arising in a long-lived isomer of Am<sup>242</sup> to be described later. The predominant activity due to 17-hr Am<sup>242</sup> consists of the  $\beta$  particles whose aluminum absorption characteristics are shown graphically in Fig. 7.

A sample of thermal-neutron-activated Am<sup>241</sup> was carefully purified and allowed to stand for several months. At the time of purification the 17-hr Am<sup>242</sup> should have disappeared completely from the sample. A combined plutonium and neptunium fraction was then removed from the sample and purified by oxidation-reduction cycles. Samples of the neptunium-plutonium fraction were observed to contain  $\beta$ -particle active material that decayed with a 2.0-day half life. The aluminum absorption characteristics of the  $\beta$  particles were entirely consistent with those of Np<sup>238</sup> (see reference 16) whose half life is 2.0 days (Fig. 8).

Np<sup>238</sup> is a "shielded" isotope in the sense that it is not produced by either negative  $\beta$ -particle emission or by orbital-electron capture, the hypothetical parents of Np<sup>238</sup> by these processes being Pu<sup>238</sup> and U<sup>238</sup>, respectively. Each of these is stable with reference to the process by which it would produce Np<sup>238</sup>. Since the Np<sup>238</sup> was observed to grow in the irradiated americium sample, a long-lived Am<sup>242</sup> that decays by the emission of  $\alpha$  particles must be responsible



After allowing time for restoration of the Am<sup>242</sup>-Np<sup>238</sup> equilibrium, a second separation was made in which the results were the same as in the first. The 2.0-day half life of Np<sup>238</sup> is evidently short compared to that of the long-lived Am<sup>242</sup>, and the equilibrium value of the Np<sup>238</sup>

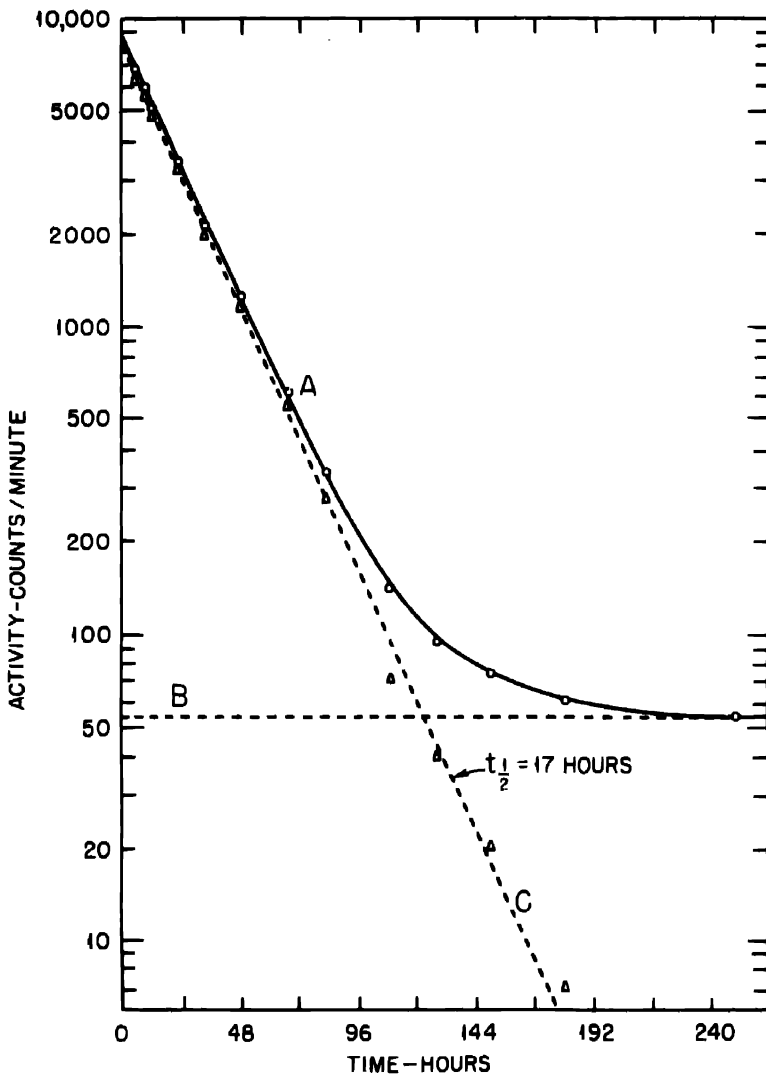


Fig. 6—Decay curve obtained for the americium fraction from neutron-irradiated Am<sup>241</sup>. A: decay of activity measured through a 7 mg/sq cm aluminum filter; B: long-lived activity; C: decay of  $\beta$  particles of Am<sup>242</sup> ( $t_{1/2} = 17$  hr).

activity is a measure of the  $\alpha$  activity in Am<sup>242</sup>. If it is assumed, entirely for the sake of discussion with no thought that this need be true, that the cross section for the formation of the long-lived Am<sup>242</sup> is the same as that for the 17-hr isomer, the half life for  $\alpha$ -particle emission is calculated to be approximately  $3 \times 10^5$  years on the basis of the observed Np<sup>238</sup> activity.

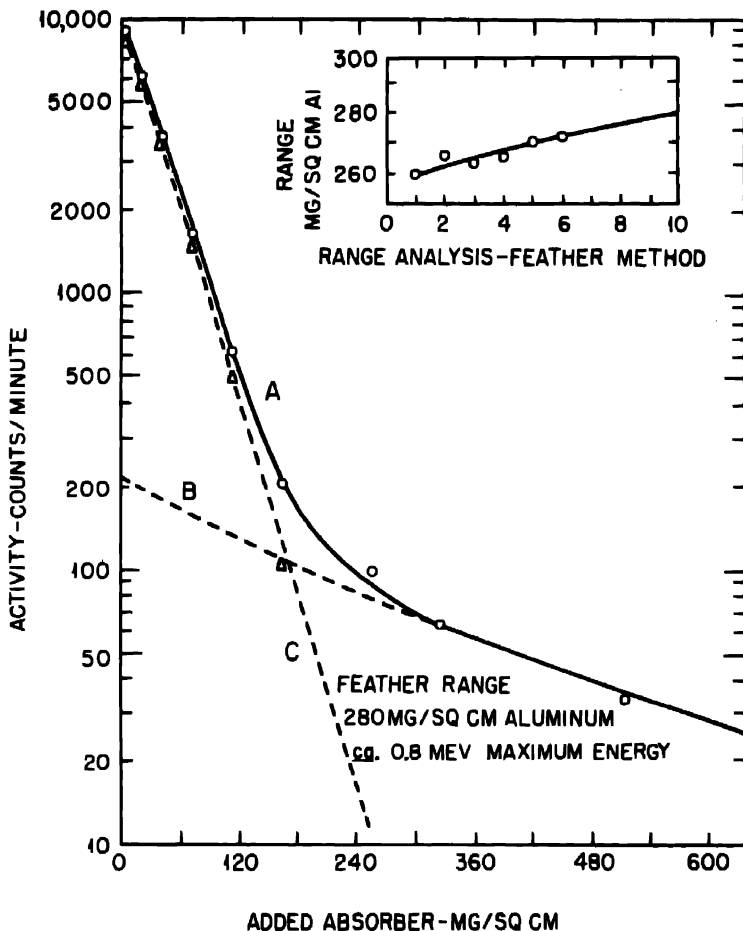


Fig. 7.—Aluminum absorption curve for the americium fraction from neutron-irradiated  $\text{Am}^{241}$ . A: observed absorption curve; B: components due to long-lived activity; C:  $\beta$  particles of  $\text{Am}^{242}$ . Feather range, 280 mg/sq cm aluminum; about 0.8 mev maximum energy.

An aluminum absorption curve of the radiations from the old activated americium sample reveals the presence of  $\beta$  particles of approximately 0.5-mev maximum energy (Fig. 9). The other radiations in the sample are essentially those due to  $\text{Am}^{241}$ . In view of the  $\beta$  instability of the 17-hr isomer of  $\text{Am}^{242}$ ,  $\beta$ -particle emission in the long-lived isomer is not surprising. Again arbitrarily assuming equal cross sections for the formation of both isomers, the half life of the long-lived  $\text{Am}^{242}$  for the emission of  $\beta$  particles is approximately 600 years. This half life and that calculated for the emission of

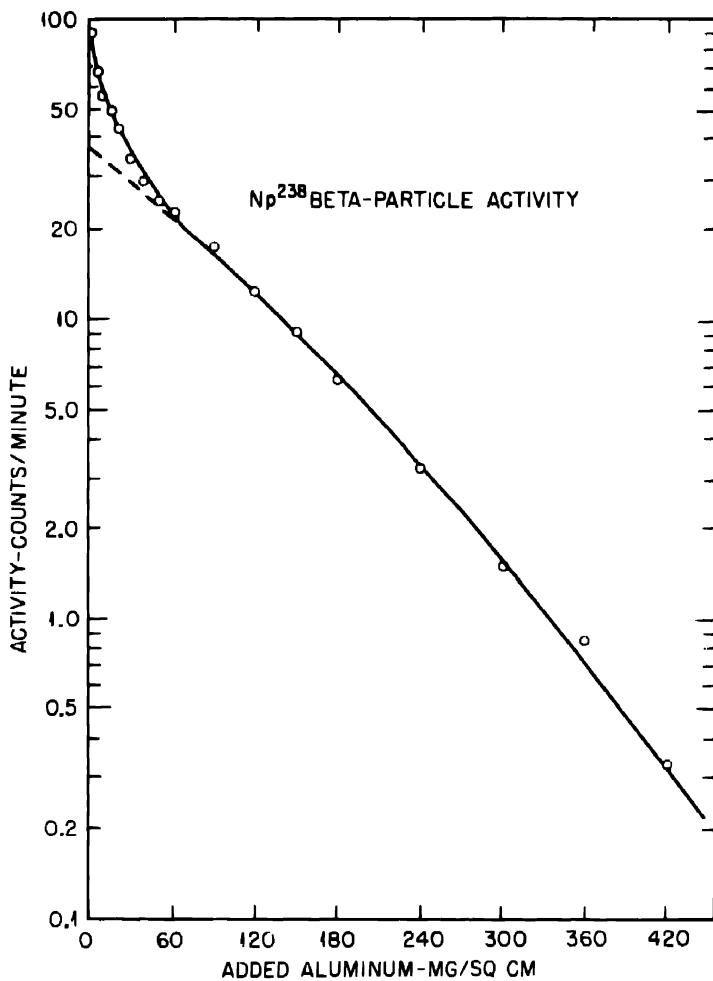


Fig. 8.—Aluminum absorption curve obtained for  $\beta$  activity in the neptunium fraction removed from neutron-irradiated Am<sup>241</sup> after six months. The solid line is the absorption curve for known Np<sup>238</sup>.

$\alpha$  particles are directly proportional to the assumed cross section, and a reduction of the latter would decrease the calculated half lives.

#### 4. OTHER ISOTOPES OF AMERICIUM

Americium isotopes of mass number equal to or less than 239 are expected to decay by the capture of orbital electrons since their nuclei are deficient in neutrons. Am<sup>240</sup>, by virtue of its position close to the region of maximum stability, might decay either by the emis-

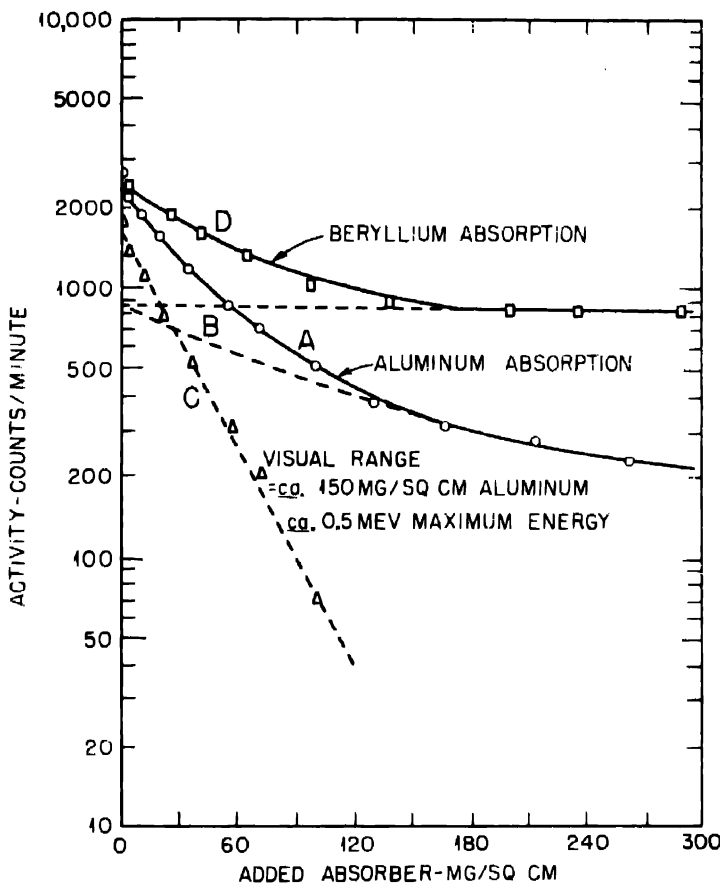


Fig. 9.—Absorption curves for the long-lived  $\beta$  activity of Am<sup>242</sup>. Counting geometry, 10 per cent. A: aluminum absorption curve for  $\beta$  and electromagnetic radiations in the americium fraction of neutron-irradiated Am<sup>241</sup> (after several months). Visual range, about 150 mg/sq cm aluminum, about 0.5 mev maximum energy. B: electromagnetic components, due largely to Am<sup>241</sup>; C:  $\beta^+$  activity of Am<sup>242</sup> (long-lived); D: beryllium absorption curve for  $\beta$  and electromagnetic radiations in the americium fraction.

sion of negative  $\beta$  particles or by orbital-electron capture, or by both processes. Branching decay with  $\alpha$ -particle emission is possible in any of the isotopes and may be found if the half lives of the competing processes are appropriate.

4.1 Deuteron Bombardment of Pu<sup>239</sup>. Several targets of Pu<sup>239</sup> were bombarded with 19-mev deuterons in the 60-in. cyclotron in order to produce americium isotopes of mass numbers 237 to 240. The targets were prepared by the evaporation of slurries of plutonium(IV)

fluoride on rectangular platinum plates of 1 sq cm area (interceptor targets). After ignition in air, the samples were placed in the target chamber of the cyclotron in such a way as to intercept the most intense portion of the ion beam. As soon as possible after the end of the bombardment, the samples were dissolved and processed chemically to yield rare-earth fractions by the successive precipitation of lanthanum(III) fluoride carrier from strongly oxidizing solutions. The actinide elements were separated from lanthanide elements by the precipitation of lanthanum(III) from 3M HNO<sub>3</sub>-1M H<sub>2</sub>SiF<sub>6</sub> solution.<sup>7</sup> Such precipitates are known to carry 90 per cent of rare-earth active substances and only 10 to 30 per cent of actinide active substances. Recovery of the actinides (in this case americium) was effected by the addition of sufficient concentrated hydrofluoric acid to precipitate the remaining lanthanum, which under these conditions carried the transplutonium activities. Cycles such as this were repeated until the activity had a constant composition with respect to all types of radiation and until the chemical yield per cycle was that expected of americium isotopes.

Decay measurements were made under four sets of counting conditions, using a thin-window (approximately 3 mg/sq cm mica) Geiger tube detector:

1. 7 mg/sq cm aluminum filter, to prevent the detection of  $\alpha$  particles.
2. 1,500 mg/sq cm beryllium filter, to allow passage of most electromagnetic radiation, but stop all except the most energetic  $\beta$  particles.
3. 1,500 mg/sq cm beryllium + 150 mg/sq cm lead combined filter, to detect electromagnetic radiation of greater than about 200 kev energy, but not that of less than about 200 kev energy.
4. 5 g/sq cm lead filter, to prevent detection of all but energetic  $\gamma$  radiation.

The difference in intensity observed under conditions 2 and 3 above, the differential count, was a measure of the low-energy electromagnetic radiation (probably x rays).

In rare-earth activities obtained in the thermal-neutron irradiation of uranium or plutonium, the activity measured by a differential count is only a few tenths per cent of the activity measured through 7 mg/sq cm aluminum. The activity observed in the rare-earth fractions of deuteron-bombarded Pu<sup>239</sup> often gave a differential count as high as 1 per cent of the total. In general, this increased to 5 to 10 per cent in the americium fractions resulting from the fluosilicate cycles.

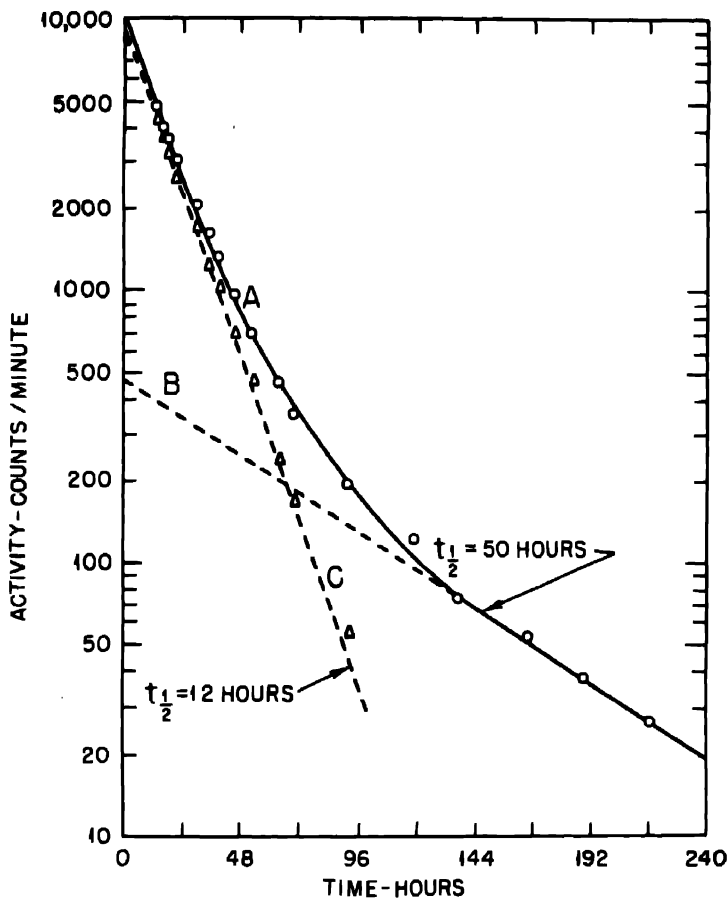


Fig. 10—Decay of  $\beta$  and electromagnetic radiations in the americium fraction from deuteron-bombarded  $\text{Pu}^{239}$ , measured through a 7 mg/sq cm aluminum filter. Counting geometry, 10 per cent. A: observed decay; B: 50-hr component; C: 12-hr component.

Two half-life periods, 12 hr and 50 hr, respectively, were observed in the decay of the total activity and the activity measured by the differential count (Figs. 10 and 11). Only the 50-hr period was found in the decay measured with a 5 g/sq cm lead filter (Fig. 12). At several times during the decay of the observed activities, absorption data were taken in order to identify and characterize the radiations due to each activity. Measurements of the electromagnetic radiations were made with a 1,500 mg/sq cm beryllium filter to eliminate the  $\beta$  or electron activity. Examples of the data for the 50-hr activity, taken after complete decay of the 12-hr activity, are shown in Figs. 13

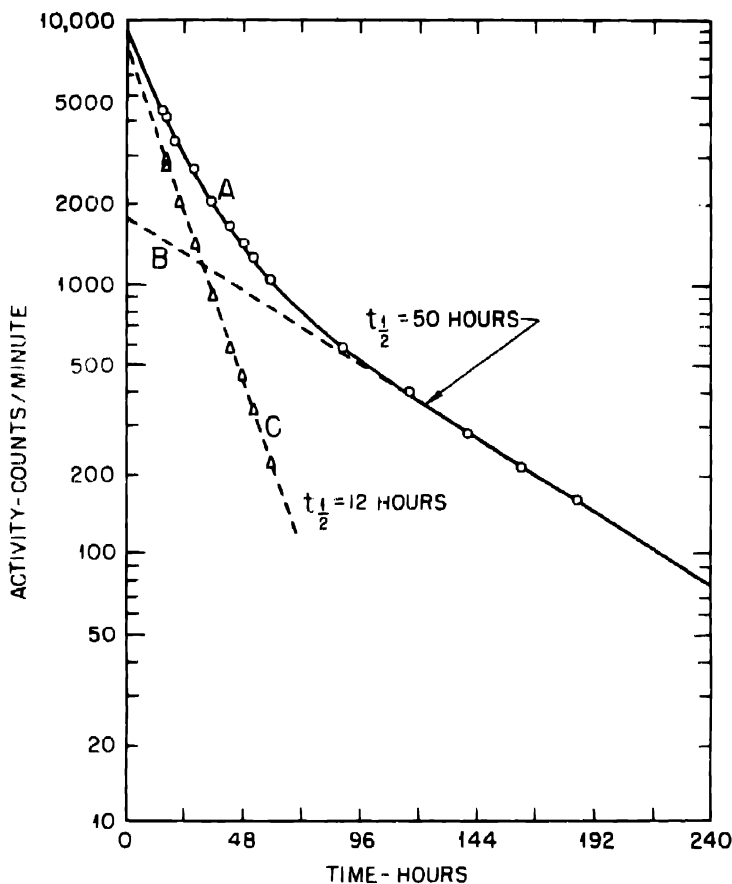


Fig. 11—Decay of low-energy electromagnetic radiations in the americium fraction from deuteron-bombarded  $\text{Pu}^{239}$ . Data were obtained as the difference between the amount of activity passing through a 1,500 mg/sq cm beryllium filter and that passing through a combination of 1,500 mg/sq cm beryllium and 160 mg/sq cm lead filters. Counting geometry, 10 per cent. A: observed decay; B: 50-hr component; C: 12-hr component.

to 15, and examples of data for the 12-hr activity, taken after subtraction of the radiations due to the 50-hr activity, are shown in Figs. 16 to 18. The curves were quite complex and the resolutions can only be approximate, especially in the case of the 12-hr activity. However, the electromagnetic radiations of each of the activities correspond rather closely to the expected L and K  $\times$  radiation of plutonium, with some additional  $\gamma$  radiation. The electron activities in each of the isotopes are best explained as being due to internal conversion of the  $\gamma$  rays, and the respective energies are consistent with

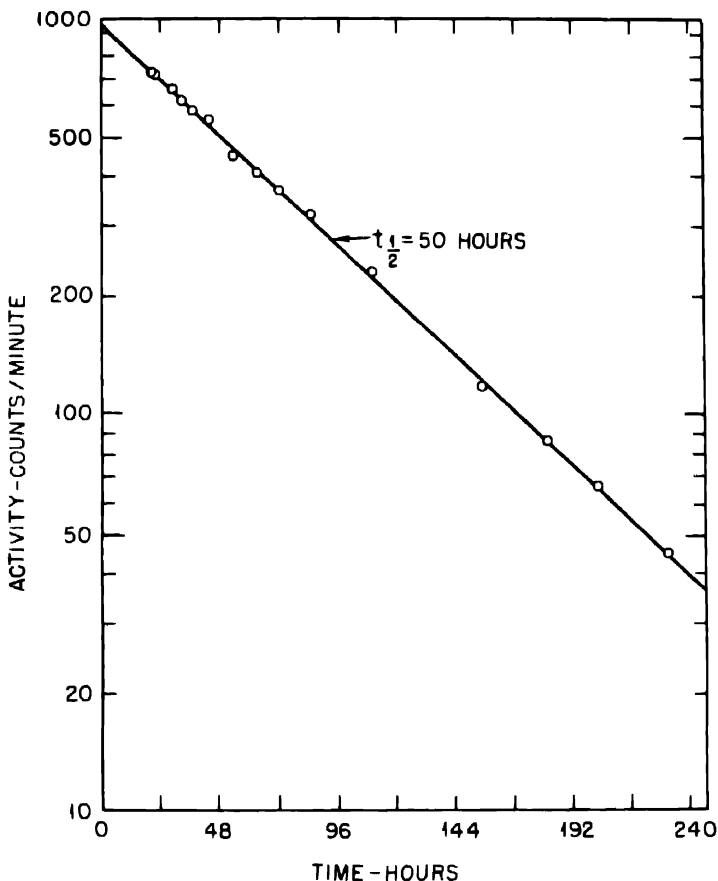


Fig. 12—Decay of hard  $\gamma$  radiation (5 g/sq cm lead filter) in the americium fraction from deuteron-bombarded  $\text{Pu}^{238}$ . Counting geometry, 10 per cent;  $t_{1/2} = 50$  hr.

this interpretation. Relative intensities are limited in their accuracy to that of the values of the counting efficiency for each of the components. These values are not too well known for low-energy electromagnetic radiation. The results obtained from several bombardments are given in Table 1.

Measurements of the electron components were made using a strong, variable magnetic field to enable determination of values of  $H\rho$ . The device used was designed for high geometry, and consequently the resolution was poor. However, the distribution observed for the low-energy electrons of the 12-hr isotope was that characteristic of monoenergetic electrons of approximately 200 kev average

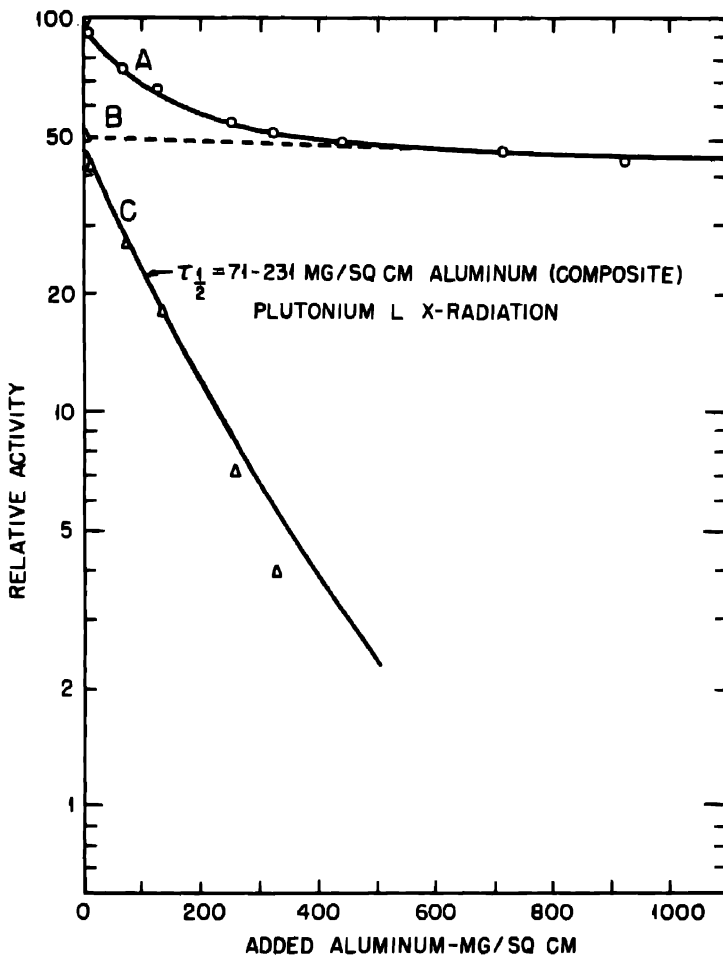


Fig. 13.—Aluminum absorption curve for electromagnetic radiations due to the 50-hr activity in the americium fraction of deuteron-bombarded  $\text{Pu}^{239}$  (1,500 mg/sq cm beryllium filter to remove electrons). Counting geometry, 10 per cent. A: observed absorption curve; B:  $\gamma$  and K x radiations; C: L x radiation (curve drawn for plutonium L x rays), half thickness = 71 to 231 mg/sq cm aluminum (composite).

energy. In all the samples measured, the 1.2- to 1.3-mev electrons were just detectable over the counter background and therefore could not be studied with any degree of accuracy with the magnetic device.

Alpha-particle decay measurements showed the presence of an  $\alpha$  activity of 12-hr half life. The branching ratio ( $\alpha$  disintegrations per orbital-electron capture) was found to be approximately 0.1 per cent, corresponding to a partial  $\alpha$  half life of approximately 500 days.

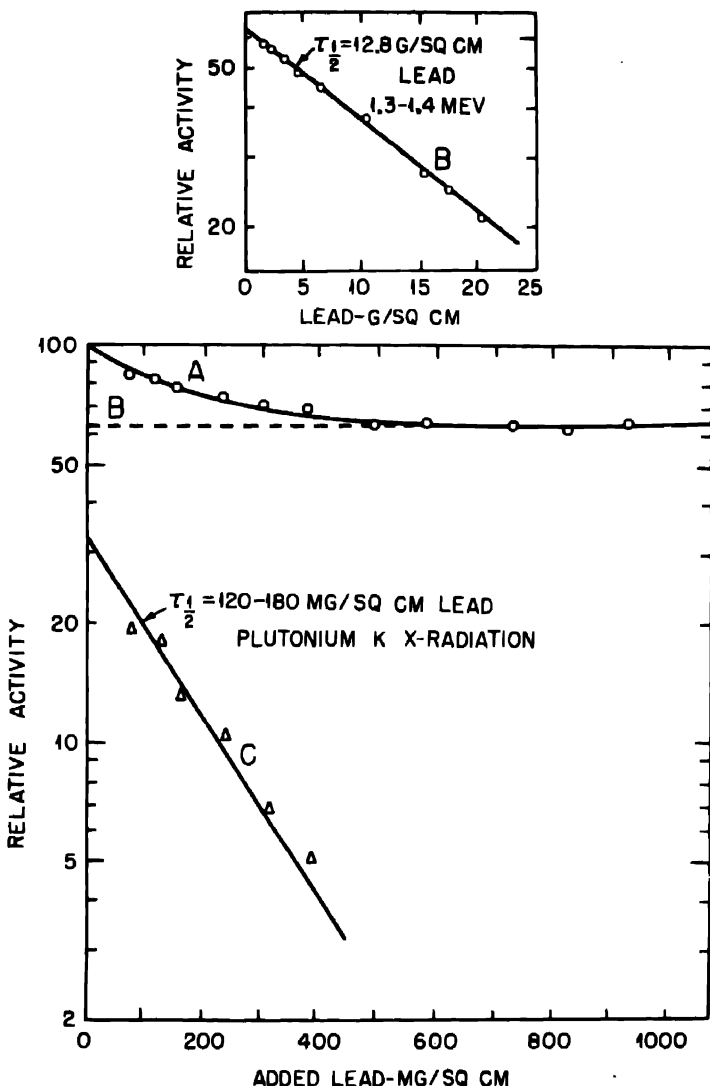


Fig. 14—Lead absorption curve for electromagnetic radiations due to 50-hr activity in the americium fraction from deuteron-bombarded  $\text{Pu}^{239}$  (1,500 mg/sq cm beryllium filter). Counting geometry, 10 per cent. A: observed absorption curve; B:  $\gamma$  radiation, half thickness = 12.8 g/sq cm lead, 1.3 to 1.4 mev; C: K x radiation (curve drawn for plutonium K x rays), half thickness = 120 to 180 mg/sq cm lead.

The  $\alpha$  activity was always present in low intensity in the observed samples and no energy determinations were made.

Samples of the americium-curium fraction were carefully examined for the presence of  $\text{Cm}^{240}$ , which might have grown from  $\text{Am}^{240}$  by the

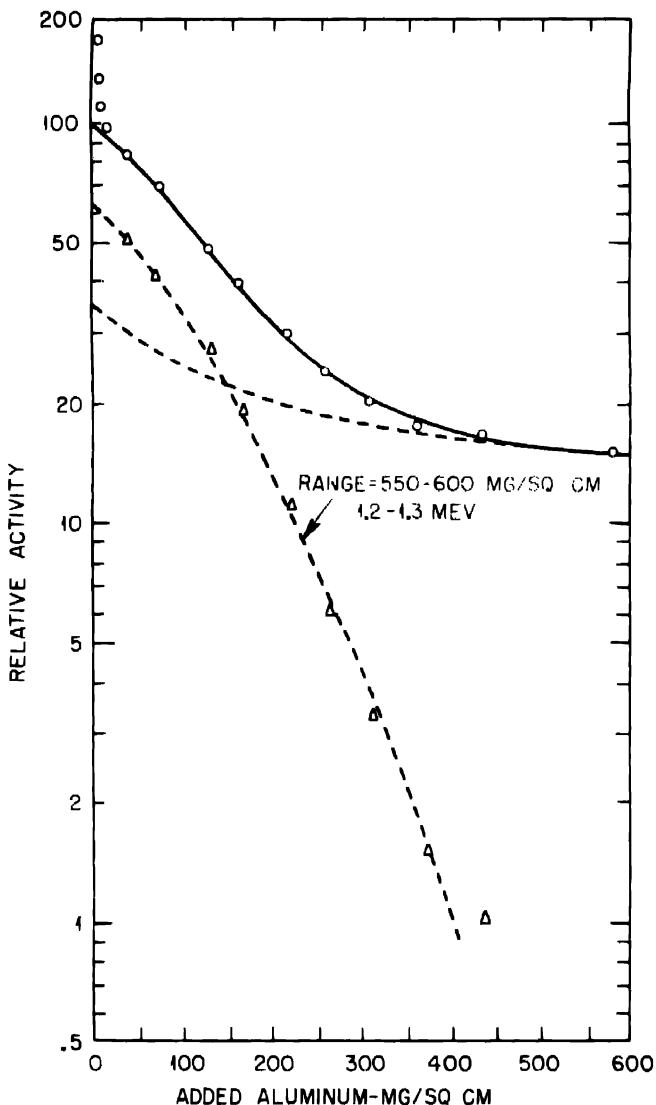


Fig. 15—Aluminum absorption curve for electron activity associated with the 50-hr activity in the americium fraction of deuteron-bombarded  $\text{Pu}^{239}$ . Electromagnetic radiations have been subtracted. Counting geometry, 10 per cent.

emission of negative  $\beta$  particles. Since no  $\text{Cm}^{240}$  was observed either immediately after bombardment or growing in over a period of a year,  $\text{Am}^{240}$  does not decay by emission of negative  $\beta$  particles.

4.2 Helium-ion Bombardment of  $\text{Np}^{237}$ . Samples of  $\text{Np}^{237}$  were prepared, and bombardments were carried out in a manner analogous

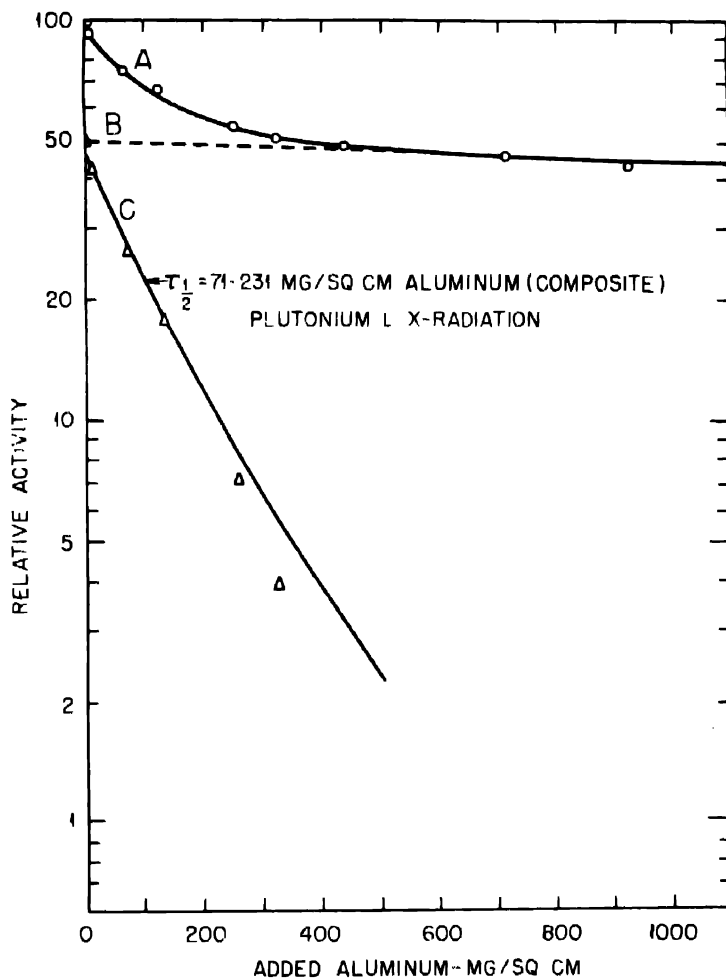


Fig. 16—Aluminum absorption curve for electromagnetic radiations due to 12-hr activity in the americium fraction from deuteron-bombarded Pu<sup>239</sup> (1,500 mg/sq cm beryllium filter). Counting geometry, 10 per cent. A: absorption curve obtained by subtraction of 50-hr components; B:  $\gamma$  and K x radiations; C: L x radiation (curve drawn for plutonium L x rays), half thickness = 71 to 231 mg/sq cm aluminum (composite).

to the methods of Sec. 4.1 for deuteron bombardments of Pu<sup>239</sup>. The activated samples were chemically processed in the same way, and fractions similar to those in the previous part were obtained. Analysis of the radiations from americium samples resulted in decay and absorption data that provided ample evidence for the presence of 12-hr and 50-hr activities with the same nuclear properties as de-

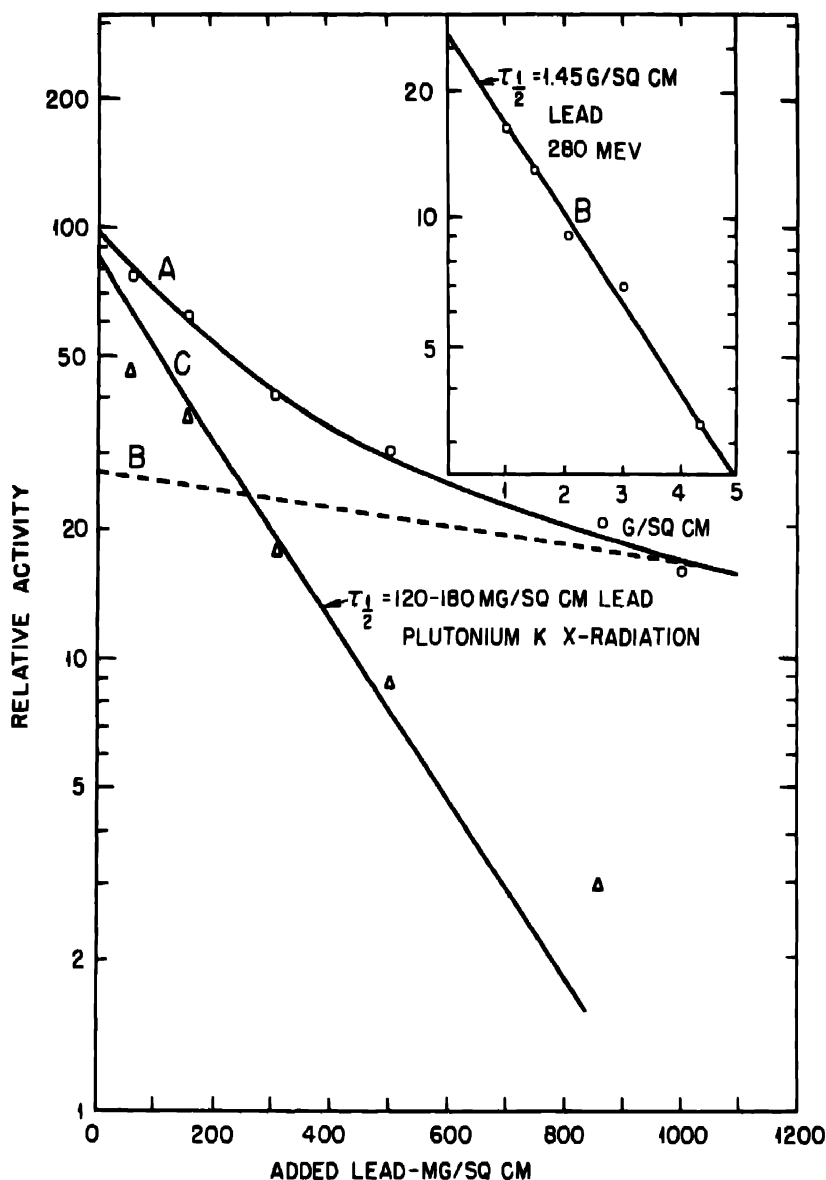


Fig. 17—Lead absorption curve for electromagnetic radiations due to 12-hr activity in the americium fraction from deuteron-bombarded  $\text{Pu}^{239}$  (1,500 mg/sq cm beryllium filter). Counting geometry, 10 per cent. A: absorption curve obtained by subtraction of 50-hr components; B:  $\gamma$  radiation, half thickness = 1.45 g/sq cm lead, 0.280 mev; C: K x radiation (curve drawn for plutonium K x rays), half thickness = 120 to 180 mg/sq cm lead.

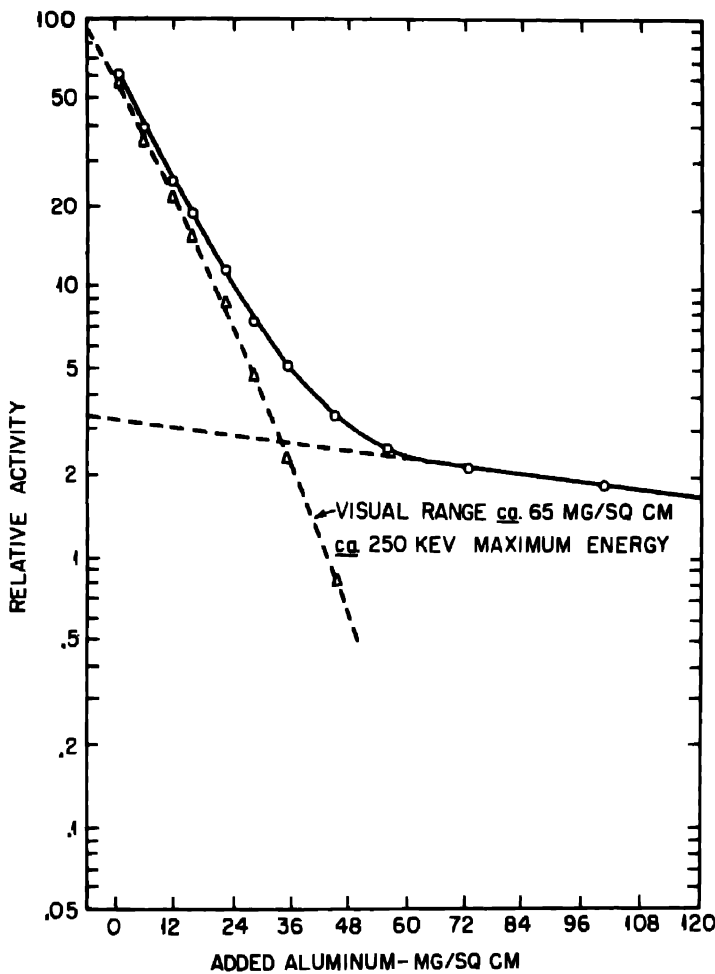


Fig. 18.—Aluminum absorption curve for electron activity associated with 12-hr activity in the americium fraction of deuteron-bombarded  $\text{Pu}^{239}$ . Fifty-hour electron activity and all electromagnetic radiations have been subtracted. Counting geometry, 10 per cent. Visual range of  $\Delta$  curve, about 65 mg/sq cm, about 250 kev maximum energy.

scribed in Sec. 4.1. The possible products of the helium-ion bombardment of  $\text{Np}^{237}$  are just those expected in the deuteron bombardment of  $\text{Pu}^{239}$ , since the same compound nucleus is formed in each case.

In comparable bombardments, the relative yield of the 12-hr isotope compared to the 50-hr isotope was somewhat higher for the case of helium ions on  $\text{Np}^{237}$ . The kinetic energy of the helium ions was

reduced from 38 to 32 mev in one case with a consequent change in relative yield. These results and the corresponding results from the  $\text{Pu}^{239}$ -deuteron experiments are discussed in Sec. 4.4.

**4.3 Helium-ion Bombardment of  $\text{Pu}^{239}$ .** In the helium-ion bombardment of  $\text{Pu}^{239}$ , the particle and electromagnetic radiations of the 50-hr activity could be observed in the combined americium-curium fraction and in the americium fraction after separation of the americium and curium by means of their selective elution from a resin

Table 1—Observed Radiations in Americium Fractions

Component	12-hr activity			50-hr activity		
	Observed relative activity	Assumed		Observed relative activity	Assumed	
		counting efficiency, %	Relative no. of events		counting efficiency, %	Relative no. of events
L x radiation	2.7	1.5	0.9	2.8	1.5	0.9
K x radiation	1.0	0.5	1.0	1.0	0.5	1.0
285-kev $\gamma$ radiation	0.4	0.5	0.4			
1.3- to 1.4-mev $\gamma$ radiation				2.3	1.2	0.95
200- to 240-kev electrons	38.3	100	0.2			
1.2- to 1.3-mev electrons				11.5	100	0.06

(Dowex-50) adsorption column with ammonium citrate solution. The 12-hr activity may well have been present initially but the time involved in this separation was so long that none remained after the separation. The formation of the 50-hr activity may have been due to deuteron contamination of the ion beam or to reactions of the ( $\alpha, pxn$ ) type.

**4.4 Mass Assignments.** The isotopes of americium discussed in the previous parts of this section should, on the basis of their method of formation, have mass numbers in the range from 237 to 240. There is no genetic relation between the two, as might have been possible, since the 12-hr activity could decay by isomeric transition. If the 50-hr activity were produced by decay of the 12-hr isotope, the logarithmic decay of the  $\gamma$  activity shown in Fig. 12 would not be observed, but rather the curve would be convex due to the superposition of a 12-hr growth component for the 50-hr activity upon the decay of the initial independently formed 50-hr activity.

Neptunium and plutonium fractions were removed from portions of the americium fractions from the deuteron bombardment of  $\text{Pu}^{239}$  after allowing time for the growth of daughter activities. The methods were sensitive enough to have detected  $\text{Np}^{236}$  (17 hr,  $\beta$ -particle emission) as the daughter of the 12-hr  $\alpha$  activity if the latter were due to  $\text{Am}^{240}$ , but it has not been observed. The only other daughter isotope capable of being formed with sufficient yield to be detected as a result of growth from the americium activities is  $\text{Pu}^{238}$  (approximately 90 years,  $\alpha$ -particle emission). If formed from  $\text{Am}^{238}$  by electron capture. Unfortunately, the amounts of this isotope expected from the most radioactive samples of americium obtained were just on the limit of detection, so the fact that no  $\text{Pu}^{238}$  was found does not eliminate the possibility that one of these activities is due to  $\text{Am}^{238}$ .

A quantitative evaluation of relative yields of different isotopes as a function of bombardment energy may often give an idea of their mass assignments, especially if the mass number of one of the isotopes is known. In this case both are unknown. Since the half lives of the isotopes are different, the calculation must be based upon an accurate knowledge of the cyclotron beam intensity at each time in the bombardment, if the latter is longer than, or comparable to, the half lives of the isotopes. The beam intensity may, in some cases, vary widely from time to time, making summation methods necessary.

Using such methods it was found that no very large variation occurs in the ratio of the cross sections for formation of these two isotopes when the kinetic energy of the bombarding particles is changed from 38 to 32 mev for helium ions and from 13 to 19 mev for deuterons. This would seem to indicate that reactions with a large number of emitted particles, such as the  $(d,3n)$  and  $(d,4n)$  reactions, are not involved since their cross sections would be expected to vary much more rapidly with these variations in energy than would the cross sections of the  $(d,n)$  and  $(d,2n)$  reactions.

This evidence leads, then, to the assumption that the two activities are due to  $\text{Am}^{239}$  and  $\text{Am}^{240}$ . If the 12-hr activity were  $\text{Am}^{240}$ , the growth of  $\text{Np}^{236}$  should have been observed. However, as was mentioned earlier in this section,  $\text{Np}^{236}$  definitely did not grow from the 12-hr  $\alpha$  activity. Alpha decay of  $\text{Am}^{239}$ , on the other hand, would produce  $\text{Np}^{235}$  which decays by orbital-electron capture with a half life of 400 days so that its growth could not have been observed in the small samples available. Mass assignments, which are consistent with these observations, are (a)  $\text{Am}^{240}$  for the 50-hr isotope and (b)  $\text{Am}^{239}$  for the 12-hr isotope.

### 5. SUMMARY

Several isotopes of the new element 95 have been produced and their radiations characterized. The chemical properties of this tripositive element are similar to those of the typical tripositive lanthanide rare-earth elements. Element 95 is different from the latter in the degree and rate of formation of certain compounds of the complex ion type, which makes possible the separation of element 95 from the lanthanide rare earths.

The name americium, after the Americas, and the symbol Am are suggested for the element on the basis of its position as the sixth member of an actinide rare-earth series, analogous to europium, Eu, of the lanthanide series.

The isotopes found and studied in this work are:

1. Am<sup>241</sup>, which decays by the emission of  $\alpha$  particles (energy of 5.45 mev) with a  $510 \pm 20$  year half life and which is produced by the  $\beta$  decay of Pu<sup>241</sup>, which, in turn, is produced by the ( $\alpha, n$ ) reaction on U<sup>238</sup>.

2. Am<sup>242</sup>, which decays by the emission of  $\beta$  particles (approximately 0.8 mev maximum energy) with a 17-hr half life or, in another isomeric form, by branching decay with the emission of  $\alpha$  particles (energy unknown) and  $\beta$  particles (approximately 0.5 mev maximum energy) in the proportion of approximately 0.002  $\alpha$  particle per  $\beta$  particle; both isomers are produced by neutron capture in Am<sup>241</sup>.

3. Am<sup>239</sup>, which undergoes branching decay, decaying (a) by orbital-electron capture with a 12-hr half life and emitting 0.285-mev  $\gamma$  rays and conversion electrons in addition to the characteristic x rays, and (b) by  $\alpha$ -particle emission (energy unknown) in the proportion of approximately 0.001  $\alpha$  particle per electron capture. This isotope is produced by the (d,2n) reaction on Pu<sup>239</sup> and by the ( $\alpha, 2n$ ) reaction on Np<sup>237</sup>.

4. Am<sup>240</sup>, which decays by orbital-electron capture with a 50-hr half life, emitting 1.3- to 1.4-mev  $\gamma$  rays and conversion electrons in addition to the characteristic x rays. Am<sup>240</sup> is produced by the (d,n) reaction on Pu<sup>239</sup> and by the ( $\alpha, n$ ) reaction on Np<sup>237</sup>.

### ACKNOWLEDGMENTS

We wish to thank Prof. J. G. Hamilton, Mr. T. M. Putnam, and their associates in the Crocker Radiation Laboratory for their cooperation in providing bombardments with the 60-in. cyclotron. Mr. Albert Ghiorso and Dr. S. G. Thompson participated in many of the experi-

ments. The cooperation of the groups at the Clinton Laboratories and the Hanford Engineer Works in making the neutron irradiations is also gratefully acknowledged.

## REFERENCES

1. G. T. Seaborg, Chem. Eng. News, 23: 2192 (1945).
2. H. D. Smythe, "Atomic Energy for Military Purposes," pp. 188-205, Princeton University Press, Princeton, N. J., 1945.
3. R. A. James, A. E. Florin, H. H. Hopkins, and A. Ghiorso, Products of helium-ion and deuteron bombardment of  $U^{235}$  and  $U^{238}$ , Paper 22.8, this volume.
4. S. Raynor, unpublished work (1943).
5. B. F. J. Schonland, Proc. Roy. Soc. London, A108: 187 (1925).
6. M. S. Livingston and H. A. Bethe, Revs. Modern Phys., 9: 271 (1937).
7. S. G. Thompson, L. O. Morgan, R. A. James, and I. Perlman, The tracer chemistry of americium and curium in aqueous solutions, Paper 19.1, this volume.
8. G. T. Seaborg, R. A. James, and A. Ghiorso, The new element curium (atomic number 96), Paper 22.2, this volume.
9. B. B. Cunningham, L. B. Werner, L. B. Asprey, and D. C. Stewart, private communication, 1946.
10. W. M. Manning and L. B. Asprey, Preparation and radioactive properties of  $Am^{243}$ , Paper 22.7, this volume.
11. A. Ghiorso, A. H. Jaffey, H. P. Robinson, and B. Weissbourd, A 48-channel pulse-height analyzer for alpha-energy measurements, Paper 16.8, this volume (Metallurgical Project Report CC-3887).
12. M. G. Holloway and M. S. Livingston, Phys. Rev., 54: 18 (1938).
13. A. H. Compton and S. K. Allison, "X-Rays in Theory and Experiment," p. 791, D. Van Nostrand Company, Inc., New York, 1935.
14. S. K. Allison, Phys. Rev., 30: 245 (1927); 32: 1 (1928).
15. B. B. Cunningham, The first isolation of americium in the form of pure compounds; microgram-scale observations on the chemistry of americium, Paper 19.2, this volume.
16. A. H. Jaffey and L. B. Magnusson, The radiations of  $Np^{238}$  and the half life of  $Pu^{238}$ , Paper 14.2, this volume.

## Paper 22.2

### THE NEW ELEMENT CURIUM (ATOMIC NUMBER 96)†

By G. T. Seaborg, R. A. James, and A. Ghiorso

#### 1. INTRODUCTION

A series of experiments has been carried out which has resulted in the first production and identification of isotopes of the element with atomic number 96. A brief description of these experiments and the radioactive and chemical properties of this element, which have been deduced therefrom, is given here.

A consideration of the methods by which isotopes of element 96 might be produced led to the use of two methods. The bombardment of plutonium with high-energy helium ions should produce isotopes of this element. The neutron irradiation<sup>1</sup> of Am<sup>241</sup> should lead to capture of neutrons and formation of Am<sup>242</sup>, which would decay by negative  $\beta$ -particle emission to 96<sup>242</sup>. Both of these methods were used in the present investigation, and both led to the production of element 96.

It was, of course, expected that only minute (tracer) amounts of the new element would be formed and that identification would be possible only if the radioactive characteristics were favorable. Complete identification would depend upon showing by radiochemical techniques that the radioactivity resided in an element with unique chemical properties, different from all other known elements. It was necessary, in order to plan the chemical identification experiments, to have some idea as to the chemical properties of element 96, and for this purpose advantage was taken of some predictions of its chemical properties. The chemical investigation of the heaviest known elements (atomic numbers 89 to 92 inclusive) and the more recently

†Contribution from the Department of Chemistry and the Radiation Laboratory, University of California, Berkeley, and from the Chemistry Division of the Metallurgical Laboratory, University of Chicago, now the Argonne National Laboratory.

discovered neptunium and plutonium has led to the view that the heavy elements constitute a new "rare-earth" series in which the 5f electron shell is being filled and which formally begins with thorium. On this basis it was expected that element 96 would have a very stable tripositive oxidation state with higher states being formed with great difficulty, if at all. Thus the anticipated chemical properties to be utilized for the isolation of detectable amounts of this element were to be those of elements with the typical tripositive oxidation state such as the rare earths. It was essential to have at hand from the beginning a means for the complete chemical separation of the new element from plutonium, since the  $\alpha$  activity due to this element would be less than 1 ppm of that due to plutonium.

## 2. EXPERIMENTAL WORK

The plutonium targets for cyclotron bombardment were prepared by the evaporation of plutonium nitrate solutions on grooved platinum plates, followed by mild ignition to form plutonium oxide. These targets were then bombarded directly in the target chamber of the cyclotron. There were two such bombardments in the 60-in. cyclotron of the University of California at Berkeley, the first one employing helium ions of 32 mev energy, and the second, helium ions of 40 mev.

Following the bombardments, the plutonium oxide was dissolved by the use of sulfuric acid, heating the mixture until copious fumes of sulfur trioxide appeared, and then taking to dryness. This was followed by the dissolution of the plutonium sulfate in dilute nitric acid, and the remaining undissolved oxide was dissolved by heating with nitric acid and a small amount of added hydrofluoric acid.

On the assumption that the III oxidation state of element 96 would be present and would have an insoluble fluoride, lanthanum fluoride was precipitated from the solution after oxidizing the plutonium to the soluble hexapositive oxidation state with 0.7N nitric acid (in some experiments 0.1N potassium dichromate was used with equally satisfactory results). The precipitate contained the  $\beta$ -active rare-earth fission-product elements and presumably also any element 96 that was present in the III oxidation state. The precipitate was dissolved and the operation was repeated until all the plutonium was eliminated. Although this procedure necessarily led to a concentration of a large amount of  $\beta$  activity because of fission-product concentration with the element 96, it was still possible to examine the  $\alpha$  activity remaining in this fraction.

At the beginning of the investigation the  $\alpha$  particles were identified as to range by means of absorption in very thin mica sheets placed

immediately over the sample in an ordinary parallel-plate ionization chamber. Later a multichannel pulse analyzer was constructed, and all subsequent energy measurements were made with it. With this instrument a thin sample is placed in an ionization chamber in which the total ionization of an  $\alpha$  particle can be measured as a voltage pulse. Individual pulses are sorted electronically and recorded on a number of fast mechanical registers in such a way as to separate the individual  $\alpha$ -particle energies in a mixture of  $\alpha$  emitters.

The neutron irradiation of the americium samples was made in the uranium-graphite chain-reacting piles at the Clinton Laboratories and the Hanford Engineer Works. The samples irradiated in the Clinton pile were placed in the removable graphite stringer at the approximate center of the pile. In the Hanford pile the samples were inserted in the regular channels with graphite spacers between the sample cans and the uranium slugs.

In the experiments in which the plutonium daughters were chemically separated after their growth as decay products from the isotopes of element 96, essentially the same method of chemical separation of plutonium from element 96 was used. In this case, of course, it was the oxidized plutonium that was recovered following the successive separation of lanthanum fluoride precipitates, which removed the element 96.

### 3. RESULTS

3.1 The Isotope  $96^{242}$ . The helium-ion bombardment of plutonium led to the first definite identification (in July and August of 1944) of an isotope of element 96. In the first helium-ion bombardment about 10 mg of  $Pu^{239}$  was bombarded with helium ions of 32 mev energy for a total of about 37  $\mu$ a-hr in the Berkeley 60-in. cyclotron. After the chemical separations described above, the rare-earth fraction was found to contain about 500 disintegrations per minute of  $\alpha$  activity with a range of about  $4.75 \pm 0.1$  cm in air at  $15^\circ C$  and 760 mm Hg pressure. This activity decayed with a half life of five months ( $5.0 \pm 0.1$  months). The first isotopic assignment of this activity was to the isotope  $96^{242}$ , formed in the reaction  $Pu^{239}(\alpha, n)96^{242}$ . That this has now been confirmed to be the correct isotopic assignment will be made clear from the discussion of the remainder of the results of this investigation.

This same radioactivity was produced later (November and December of 1944) in a series of neutron bombardments of americium in which both bombardment time and total neutron exposure varied widely as a result of using the chain-reacting piles at both Clinton and Hanford. In all these neutron irradiations it was found that the ratio of the total intensity of the 4.75-cm  $\alpha$  particles to that of the

4.05-cm  $\alpha$  particles of  $\text{Am}^{241}$  varied approximately as the first power of the total neutron irradiation. The following sequence of nuclear reactions accounts for these observations:



The 4.75-cm  $\alpha$  particles are due to the isotope  $96^{242}$ . The decay rate here again corresponds to a half life of five months so that this radioactivity agrees both in half life and  $\alpha$ -particle range with the  $96^{242}$  formed from the helium-ion bombardment of  $\text{Pu}^{239}$ .

The chemical evidence that allowed all previously known elements to be eliminated is as follows:

1. The activity is carried quantitatively by lanthanum fluoride from solutions previously treated with various reducing and oxidizing agents, ranging from zinc amalgam to argentic ion. The carrying is not influenced by the use of ammonium fluoride instead of hydrofluoric acid. This evidence alone eliminates all previously known elements except indium, lanthanum and all the rare earths, yttrium, actinium, thorium, and possibly protactinium.

2. The activity is not precipitated with indium sulfide from acetic acid solution, thus eliminating indium.

3. Under the same conditions of acidity and concentration of reagents the activity is not coprecipitated with ceric or zirconium iodates to as great an extent as are actinium, protactinium, and thorium, thus eliminating these last three elements and cerium.

4. The activity can be partially separated from the rare-earth-yttrium subgroup by any one of three standard procedures, i.e., precipitation of the activity with lanthanum or praseodymium carrier as (a) carbonate, (b) oxalate, or (c) formate in neutral or alkaline solution with yttrium, gadolinium, or lutecium as holdback agents.

5. Europium can be separated by reduction to the dipositive oxidation state with zinc amalgam and precipitation of  $\text{EuSO}_4$ . The activity is not coprecipitated with europium under these conditions.

6. Fractional separation from the remaining elements (lanthanum, praseodymium, neodymium, element 61, and samarium) can be achieved by the use of fluosilicate ion in solution during a partial precipitation of rare earth fluoride as carrier.

Confirmation of the isotopic assignment of the five months  $\alpha$ -activity of 4.75-cm range came from a study of its decay product. A sample containing about  $2 \times 10^6$  disintegrations per minute of  $96^{242}$  (produced by neutron irradiation of  $\text{Am}^{241}$ ) was allowed to decay for about a month and at the end of this time the plutonium fraction was

isolated and was found to consist of an  $\alpha$  activity with range of 4.05 cm which can be ascribed<sup>2</sup> to  $\text{Pu}^{238}$ . The amount of  $\text{Pu}^{238}$  that grew was quantitatively determined in another experiment by addition of  $\text{Pu}^{239}$  tracer to establish the chemical loss during separation of the plutonium. The details of this experiment were as follows: A sample containing  $1.29 \times 10^8$  counts per minute of  $96^{242}$  was very carefully purified of all plutonium; 1,102 counts per minute of  $\text{Pu}^{239}$  was then

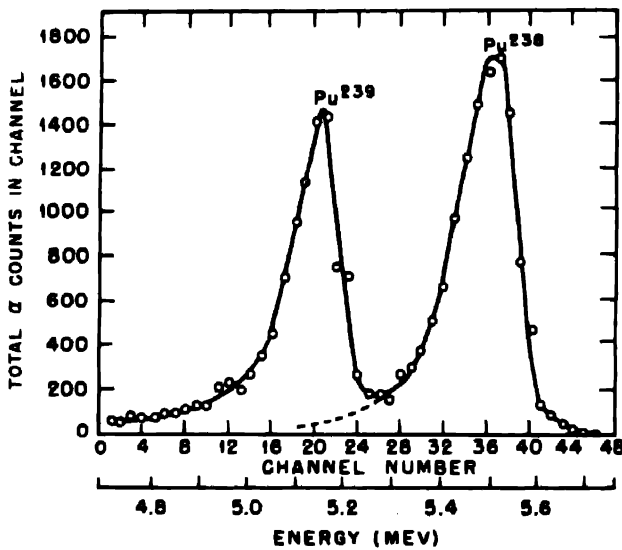


Fig. 1—Alpha-particle pulse-analysis curve of plutonium that grew from  $96^{242}$  (with added  $\text{Pu}^{239}$ ).

added, and the sample allowed to stand for 70 days. At the end of that time the plutonium was separated from the element 96, and the ratio of  $\text{Pu}^{238}$  to  $\text{Pu}^{239}$  determined by pulse analysis (Fig. 1). The average of several such pulse analyses gave the value 1.45 for the ratio of  $\text{Pu}^{238}$  to  $\text{Pu}^{239}$ . From these data and taking the half life of  $96^{242}$  as 150 days, the half life of  $\text{Pu}^{238}$  is calculated to be  $92 \pm 2$  years, within the limit of error of the value obtained by Jaffey<sup>3</sup> in direct decay measurements.

In addition to its  $\alpha$  particles,  $96^{242}$  also emits a small amount of soft electromagnetic radiation and some electrons. Absorption curves of the radiations emitted by samples of  $96^{242}$  produced by neutron irradiation of  $\text{Am}^{241}$  are shown in Figs. 2 to 5. The  $96^{242}$  in these samples was decontaminated from rare-earth fission products by means of the fluosilicate procedure mentioned above and separated

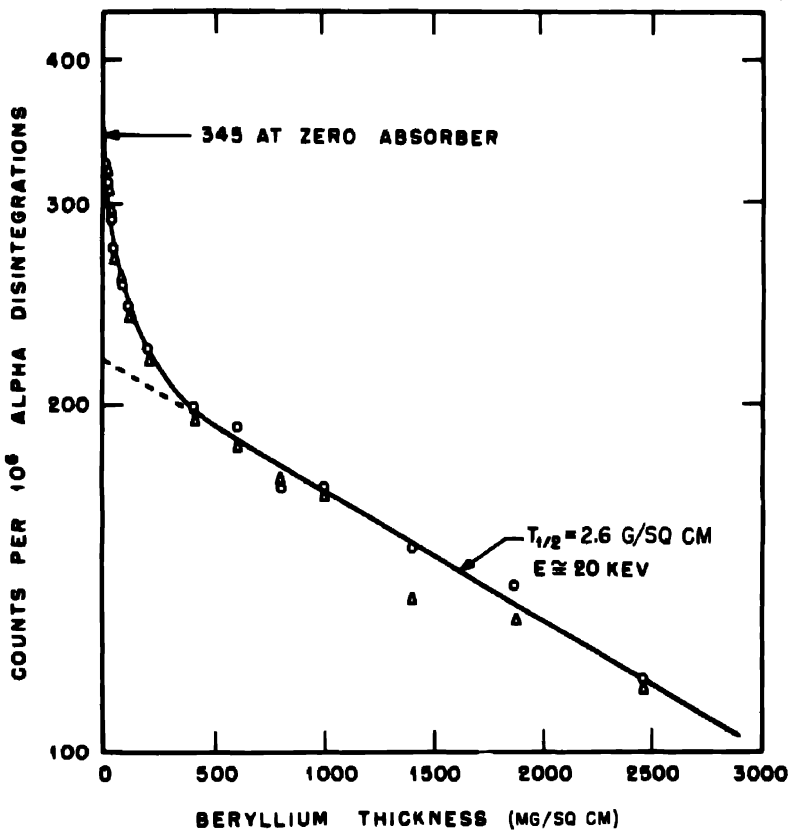


Fig. 2—Geiger-counter beryllium absorption curve of  $96^{242}$  radiations. The geometrical efficiency was about 10 per cent, and the curve has been normalized to  $10^6$  disintegrations per minute. ○, points for  $96^{242}$  produced by neutron irradiation of  $\text{Am}^{241}$  of  $8.6 \times 10^{10}$  neutrons per square centimeter. △, points for  $96^{242}$  produced by neutron irradiation of  $\text{Am}^{241}$  of  $2.0 \times 10^{20}$  neutrons per square centimeter.

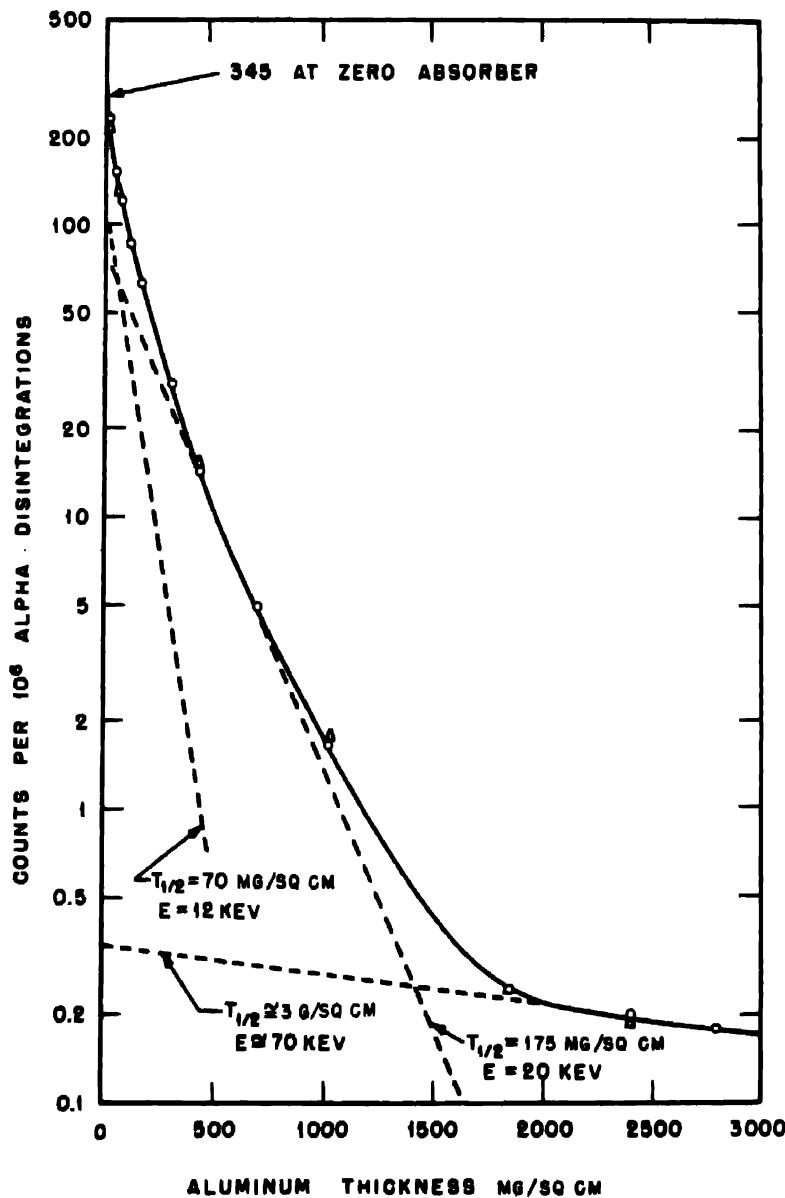


Fig. 3—Geiger-counter aluminum absorption curve of  $96^{m42}$  radiations. Geometrical efficiency was about 10 per cent, and the curve has been normalized to  $10^6$   $\alpha$  disintegrations per minute.  $\circ$ , points for  $96^{m42}$  produced by neutron irradiation of  $\text{Am}^{241}$  of  $6.6 \times 10^{20}$  neutrons per square centimeter.  $\triangle$ , points for  $96^{m42}$  produced by neutron irradiation of  $\text{Am}^{241}$  of  $2.0 \times 10^{20}$  neutrons per square centimeter.

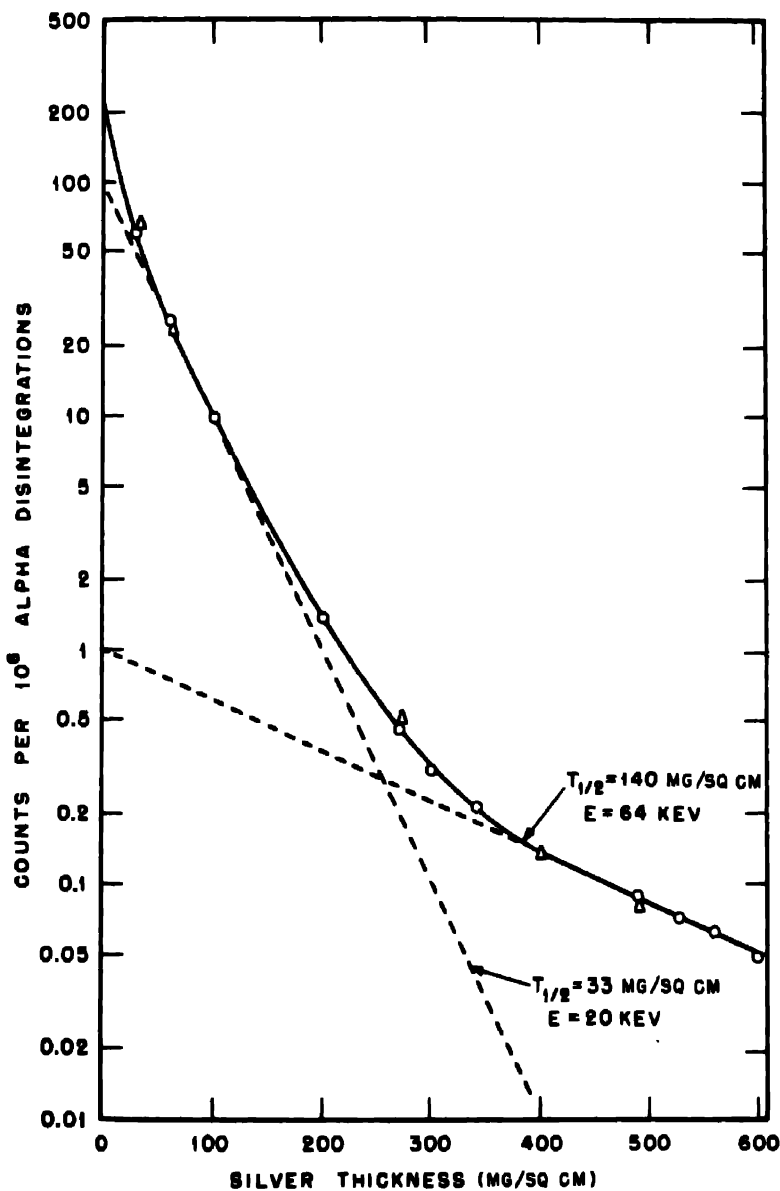


Fig. 4—Geiger-counter silver absorption curve of  $96^{242}$  radiations. A 400 mg/sq cm beryllium absorber was between silver and counter at all points.  $\circ$ , points for  $96^{242}$  produced by neutron irradiation of  $\text{Am}^{241}$  of  $6.6 \times 10^{18}$  neutrons per square centimeter.  $\Delta$ , points for  $96^{242}$  produced by neutron irradiation of  $\text{Am}^{241}$  of  $2.0 \times 10^{20}$  neutrons per square centimeter.

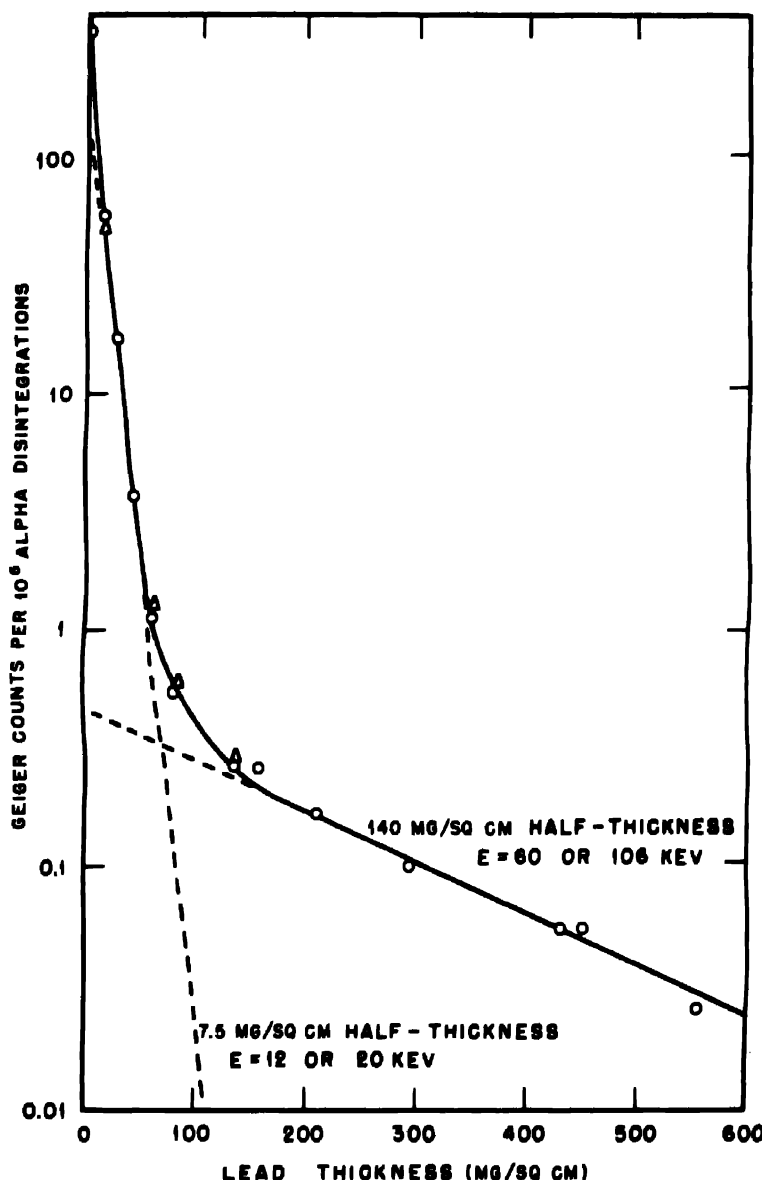


Fig. 5—Geiger-counter lead absorption curve of radiations of  $^{96}\text{Ru}$ . A beryllium absorber was between lead and counter at all points. ○, points for  $^{96}\text{Ru}$  produced by neutron irradiation of  $\text{Am}^{241}$  of  $6.6 \times 10^{19}$  neutrons per square centimeter. △, points for  $^{96}\text{Ru}$  produced by neutron irradiation of  $\text{Am}^{241}$  of  $2.0 \times 10^{20}$  neutrons per square centimeter.

from americium by selective elution from a resin (Dowex 50) adsorption column.<sup>4</sup> Samples from two different neutron irradiations of Am<sup>241</sup>, differing by a factor of approximately 3 in total number of neutrons, were measured, and the absorption curves were found to be identical in all respects showing that (1) the radiations are not due to fission-product contamination since the two samples had radically

Table 1—Electromagnetic and Electron Radiations of 96<sup>242</sup>

	Counts per 10 <sup>6</sup> $\alpha$ disintegrations at 10% geometrical efficiency	Assumed counting efficiency, %	Number of events per disintegration
65-kev gamma ray	0.5	1	$1.8 \times 10^{-3}$
L x rays	200	1.5	0.13
Softer x rays	100		
Electrons	40	100	$4 \times 10^{-4}$

different chemical histories and times of decay between removal from the pile and measurement of the radiations; and (2) that the radiations are actually due to 96<sup>242</sup> and not to 96<sup>243</sup> or a higher-mass isotope, since, if they were due to 96<sup>243</sup>, the level of activity would have been much higher in the sample that received longer irradiation. In addition to these curves it was found by means of bending the particles in a magnetic field that approximately 12 per cent of the counts at zero absorber are due to low-energy negative electrons. These radiations and their approximate abundances are summarized in Table 1.

3.2 The Isotope 96<sup>240</sup>. In a second bombardment of Pu<sup>239</sup> (March 1945) helium ions of 40 mev energy were used to bombard 100 mg of Pu<sup>239</sup> for 63.1  $\mu$ a-hr. A sample was treated by the same chemical procedure as already described, and the final element 96 fraction contained about  $2 \times 10^6$   $\alpha$ -particle disintegrations per minute.

It was found that 20 per cent of this activity was the 96<sup>242</sup> activity described above, and the remaining 80 per cent was due to another  $\alpha$  emitter that emits  $\alpha$  particles with a range of  $4.95 \pm 0.1$  cm in air at 15°C and 760 mm Hg pressure. The over-all decay rate of this sample gave a half life of about one month, indicating that the half life of the 4.95-cm-range activity was somewhat less than one month and later resolution (Fig. 6) gave a value of 26.8 days. This activity was thought to be due to either 96<sup>241</sup> or 96<sup>240</sup> produced by the reaction Pu<sup>239</sup>( $\alpha$ ,2n)96<sup>241</sup> or Pu<sup>239</sup>( $\alpha$ ,3n)96<sup>240</sup>.

A sample with this activity was set aside and allowed to decay from the second to the fourth day after shutdown of the cyclotron. The plutonium fraction was then isolated, and the pulse-analysis curve (Fig. 7a) as well as the  $\alpha$ -decay curve (Fig. 7b) of this plutonium sample gave definite evidence of  $\text{Pu}^{238}$  whose radioactive properties had been definitely established.<sup>5</sup> The element 96 fraction was

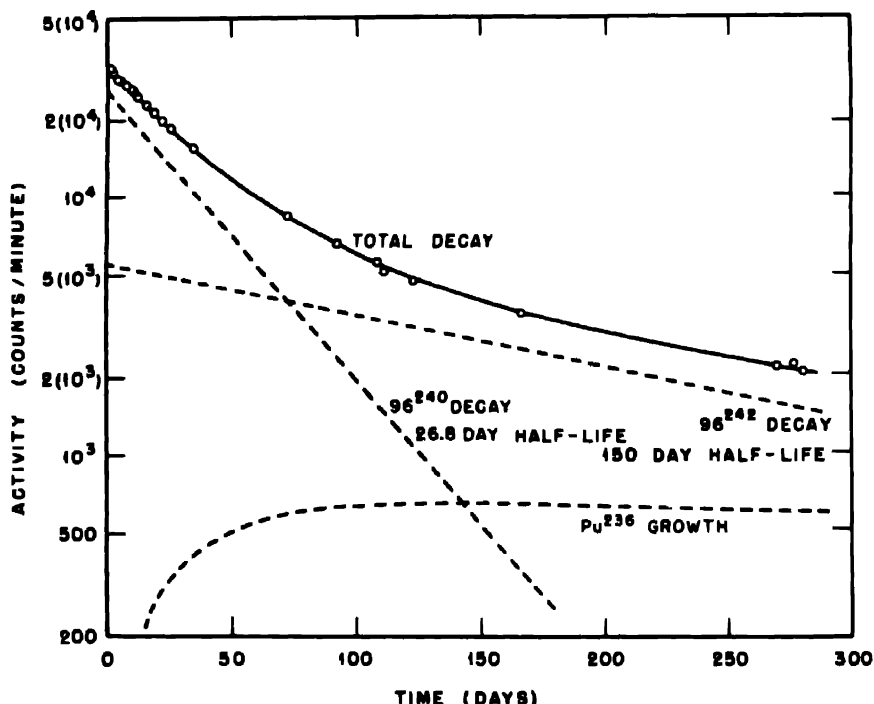


Fig. 6—Alpha decay curve of element 96 fraction from bombardment of  $\text{Pu}^{239}$  with helium ions.

then allowed to grow plutonium again (77 days of growth) and the amount of  $\text{Pu}^{238}$  that had grown was quantitatively determined by the addition of  $\text{Pu}^{239}$  tracer to establish the chemical loss in the process of separation of the plutonium from the element 96. The additional details of this experiment, which allowed a calculation of the half life of the element 96 parent, were as follows: A sample of the  $96^{242} - 96^{240}$  mixture with activity of  $1.38 \times 10^5$   $\alpha$  counts per minute, of which initially 70.2 per cent was due to  $96^{240}$ , was allowed to decay for 77 days. At the end of that time the plutonium fraction was isolated after addition of 1,935 counts per minute of  $\text{Pu}^{239}$ , and the resulting plutonium

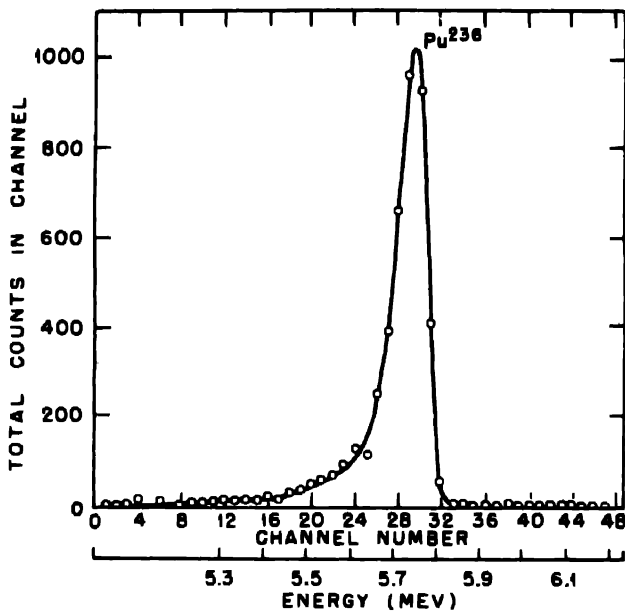


Fig. 7a—Alpha-particle pulse-analysis curve of activity in plutonium fraction removed from element 96 fraction of a  $\text{Pu}^{239}$  target bombarded with helium ions. Growth period, second to fourth day after end of bombardment.

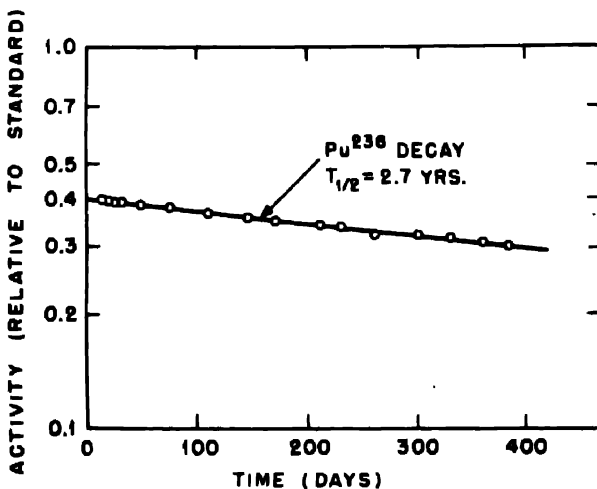


Fig. 7b—Decay of  $\alpha$  activity in plutonium fraction removed from element 96 produced by bombarding  $\text{Pu}^{239}$  with helium ions. Growth period, second to fourth day after end of bombardment.

sample was pulse-analyzed. The average of several such pulse analyses (see Fig. 8) gave 1.14 as the value of the ratio of  $\text{Pu}^{238}$  to  $\text{Pu}^{239}$ . Using the value 983 days (obtained from Fig. 7b) for the half life of  $\text{Pu}^{238}$ , 26.7 days is calculated as the half life of  $96^{240}$ , which is in excellent agreement with the value of 26.8 days obtained by resolution of the  $\alpha$ -decay curve (Fig. 6).

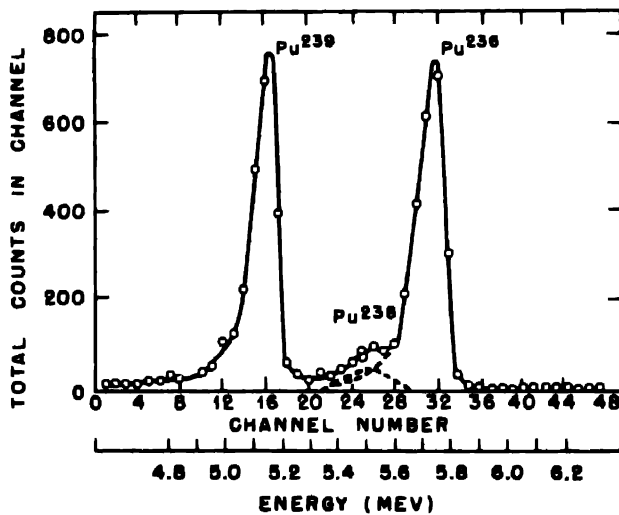


Fig. 8—Alpha-particle pulse-analysis curve of plutonium that grew in element 96 produced by helium-ion bombardment of  $\text{Pu}^{239}$ . Growth period, fifth to eighty-second day after end of bombardment. ( $\text{Pu}^{239}$  tracer added to determine yield.)

**3.3 Other Isotopes of Element 96.** In addition to the isotopes  $96^{240}$  and  $96^{242}$  one other activity has been observed which may be due to either an isotope of element 96 or to an americium (element 95) isotope.

When the Geiger-counter activity of the combined americium-element 96 fraction of plutonium targets bombarded with helium ions is followed with various absorbers, the decay curves shown in Figs. 9 to 11 are obtained. From the percentage of the  $\alpha$  activity in the sample which is due to  $96^{242}$ , the Geiger-counter activity due to this isotope can be obtained from Figs. 2 to 5. If this is done it is found that there remains, in addition to an activity corresponding to the  $96^{240}$  half life, an activity of about 55 days half life and one of about 2 days half life. The approximately 2-day activity is very probably the same activity as the one found in deuteron bombardments<sup>1</sup> of  $\text{Pu}^{239}$ , i.e. the 50-hr  $\text{Am}^{240}$ . The 55-day activity has a large amount of soft

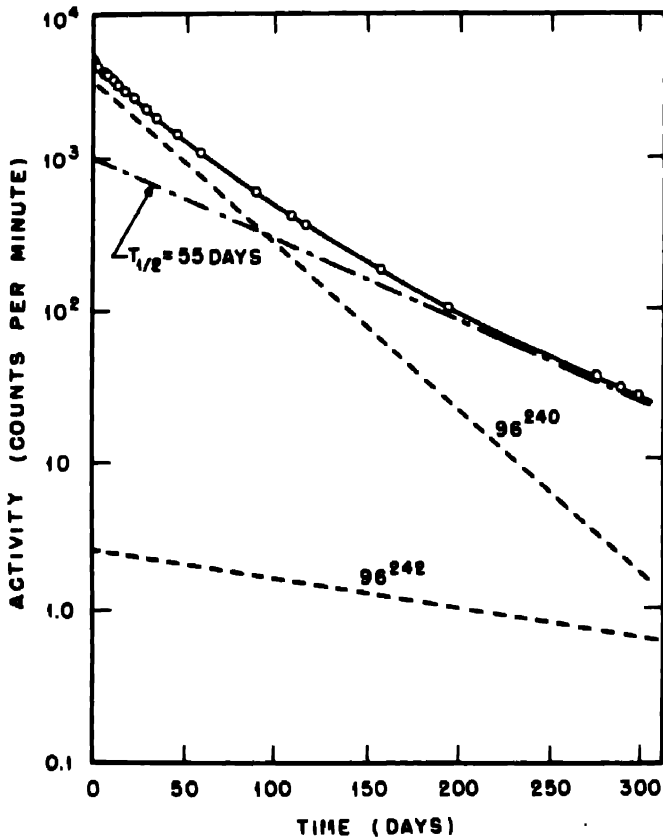


Fig. 9—Geiger-counter decay of americium-element 96 fraction of  $\text{Pu}^{239}$  target bombarded with helium ions. Decay measured through 7 mg/sq cm aluminum. The  $96^{240}$  curve was constructed from a knowledge of the number of  $96^{240}$   $\alpha$  particles in the sample together with the corresponding number of counts through 7 mg/sq cm aluminum per  $10^6 \alpha$  particles obtained from Fig. 3.

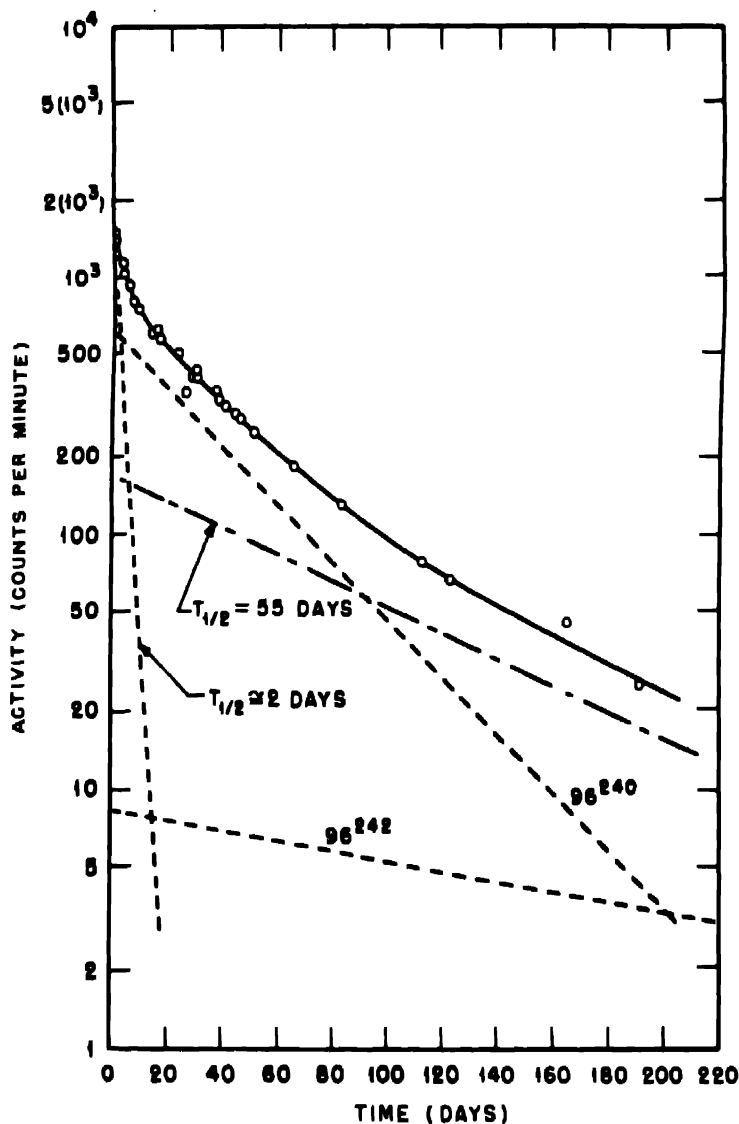


Fig. 10—Geiger-counter decay of americium-element 96 fraction of  $\text{Pu}^{239}$  target bombarded with helium ions (1.85 g/sq cm beryllium filter).

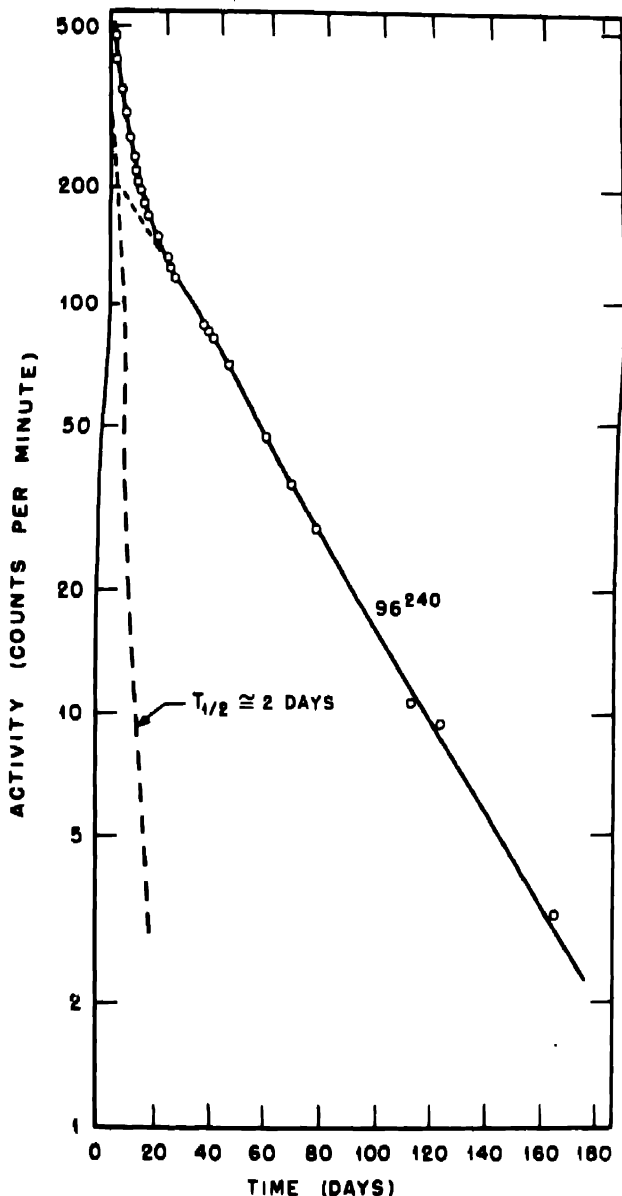


Fig. 11—Geiger-counter decay of americium-element 96 fraction of  $\text{Pu}^{239}$  target bombarded with helium ions (5 g/sq cm lead filter).

electromagnetic radiation, perhaps some electrons, but no hard  $\gamma$  rays. It is probable that the activity is due to  $^{96}_{\text{Zr}}^{241}$  or  $^{96}_{\text{Zr}}^{243}$  decaying by orbital-electron capture.

#### 4. NAME FOR ELEMENT 96

As the name for the element of atomic number 96 we should like to propose "curium," with symbol Cm. The evidence indicates that element 96 contains seven 5f electrons and is thus analogous to the element gadolinium, with its seven 4f electrons in the regular rare-earth series. On this basis, element 96 is named after the Curies in a manner analogous to the naming of gadolinium, in which the chemist Gadolin was honored.

#### 5. SUMMARY

Two isotopes of the element with atomic number 96 have been produced by the helium-ion bombardment of plutonium. These isotopes are: (1)  $^{96}_{\text{Zr}}^{242}$ , which emits  $\alpha$  particles with a range  $4.75 \pm 0.1$  cm in air (energy 6.1 mev) and decays with a half life of  $5.0 \pm 0.1$  months; and (2)  $^{96}_{\text{Zr}}^{240}$ , which emits  $\alpha$  particles with a range of  $4.95 \pm 0.1$  cm in air (energy 6.3 mev) and decays with a half life of  $26.8 \pm 0.3$  days.  $^{96}_{\text{Zr}}^{242}$  has also been produced by neutron irradiation of  $^{95}_{\text{Zr}}^{241}$ . The mass assignments of these isotopes have been verified by isolation of their daughters,  $\text{Pu}^{238}$  and  $\text{Pu}^{236}$ . Some evidence for the isotope  $^{96}_{\text{Zr}}^{241}$  or  $^{96}_{\text{Zr}}^{243}$ , decaying by orbital-electron capture, has been presented. The name curium, symbol Cm, has been proposed for element 96. The chemical experiments have indicated that the most stable oxidation state of curium is the tripositive state.

#### ACKNOWLEDGMENTS

It is a pleasure to acknowledge the help and cooperation of Dr. J. G. Hamilton and his group who rebuilt the Berkeley 60-in. cyclotron in order to make much of this work possible and who performed the bombardments. The cooperation of the groups at the Clinton Laboratories and the Hanford Engineer Works in making the neutron irradiations is also gratefully acknowledged.

#### REFERENCES

1. G. T. Seaborg, R. A. James, and L. O. Morgan, The new element americium (atomic number 95), Paper 22.1, this volume.

2. G. T. Seaborg, A. C. Wahl, and J. W. Kennedy, Nuclear properties of  $^{94}\text{Cm}$  and  $^{93}\text{Cm}$ , Paper 1.4, this volume; G. T. Seaborg, E. M. McMillan, J. W. Kennedy, and A. C. Wahl, Phys. Rev., 69: 366 (1946) (Submitted Jan. 28, 1941); G. T. Seaborg, A. C. Wahl, and J. W. Kennedy, Phys. Rev., 69: 367 (1946) (Submitted Mar. 7, 1941).
3. A. H. Jaffey, Half life of  $\text{Pu}^{244}$  by direct decay measurement, Paper 2.2, this volume (Argonne National Laboratory Report ANL-4020).
4. B. B. Cunningham, L. B. Asprey, D. C. Stewart, and L. B. Werner, private communication, 1946.
5. R. A. James, A. E. Florin, H. H. Hopkins, Jr., and A. Ghiorso, Products of helium-ion and deuteron bombardment of  $\text{U}^{235}$  and  $\text{U}^{238}$ , Paper 22.8, this volume.
6. A. Ghiorso, A. H. Jaffey, H. P. Robinson, and B. Weissbourd, A 48-channel Pulse-height analyzer for alpha-energy measurements, Paper 16.8, this volume. (Metallurgical Laboratory Report CC-3887).

Paper 22.3

THE NEPTUNIUM ( $4n + 1$ ) RADIOACTIVE FAMILY†

By G. T. Seaborg

One of the interesting results of the research program connected with the Plutonium Project is the production by synthetic means and the detailed study of a new heavy radioactive family, which is analogous in extent and complexity to the three heavy natural radioactive families. This entire series of radioactive isotopes, which is completely missing from nature, has been synthesized and traced from the transuranium region down to the stable end product  $\text{Bi}^{209}$ , and the radioactive properties of all the individual isotopes have been studied in a research program extending over the last seven or eight years. The present discussion is concerned with a description of this interesting research development.

Such a discussion of this new, fourth radioactive family would not be complete without some description of the interesting background of research work that led to the unraveling and understanding of the three natural radioactive families.

The discovery of radioactivity and the discovery of the electron and the x ray, all of which took place in the last decade of the past century, must be ranked as three major experimental advances that marked a turning point in physics and chemistry and in the understanding of matter. Because the discovery of the other two items is so intimately connected with the discovery of radioactivity, it is hardly possible to describe the latter without some mention of the former. The discovery of the electron is not so clear-cut as the other two, extending as it did over a period of some fifty years, but it may be said that besides the work of P. Lenard<sup>1</sup> the culminating ex-

†Contribution from the Department of Chemistry and the Radiation Laboratory, University of California, Berkeley, and from the Chemistry Division of the Metallurgical Laboratory, University of Chicago, now the Argonne National Laboratory.

periments were those of J. J. Thomson<sup>1</sup> and his coworkers, who definitely established the existence of widely prevalent small particles with mass about  $\frac{1}{2000}$  of that of the hydrogen atom and carrying identical negative electrical charges.

As is so often the case with important experimental discoveries, the other two were essentially accidental in nature. The German physicist W. K. Roentgen in the year 1895 was studying the passage of cathode rays, that is, the electrons, through matter when he was surprised to notice that a fluorescent screen, which happened to be lying near by, became luminous when the discharge tube was running. He was amazed to find that this was the case even when black paper was interposed between the fluorescent screen and the discharge tube. Roentgen had the perspicacity to follow up on this observation, and within a few weeks he presented his classical paper on the discovery of x rays.<sup>2</sup>

Following up on this discovery, the French scientist H. Becquerel began to study the relationship between fluorescence and phosphorescence and the emission of x rays. While investigating uranium compounds as fluorescent material he found that uranium that had been exposed to sunlight could affect a photographic plate although the latter was covered with black paper. Upon continuing these investigations he noticed that uranium salts could cause blackening of photographic plates even when they were not exposed to sunlight, thus showing that this was an intrinsic property of uranium itself, and his classic papers<sup>3</sup> describing this phenomenon and published in 1896 present his description of the discovery of radioactivity.

The discovery of radioactivity in uranium was closely followed by a number of observations showing that this property is also exhibited by other heavy elements. In 1898 Marie Curie<sup>4</sup> and G. C. Schmidt<sup>5</sup> independently found that thorium also exhibits this property. The Curies, continuing the investigation of the activity of various compounds of uranium and thorium and of ores containing these elements, found that the activity of certain uranium ores such as pitchblende was many times stronger than that of the element uranium itself. This led them to the natural conclusion that the activity might be due to a more highly radioactive substance present in small quantities, and a systematic analysis of uranium ores was made which led to the discovery of the two new radioactive elements, polonium<sup>6</sup> and radium.<sup>7</sup> Soon after this the radioactive actinium was discovered by Debierne<sup>8</sup> and independently by Giesel.<sup>9</sup>

The nature of the radiations immediately became the subject for investigations, and it was soon concluded that they are of three general types: the  $\alpha$  rays, which are positively charged particles, not

very penetrating but very ionizing; the  $\beta$  rays, which are negatively charged particles more penetrating and less ionizing; and the  $\gamma$  rays, which cannot be deflected by a magnetic field and are the most penetrating type. A further number of radioactive species were found, some of which were chemically inseparable from each other; it was noticed that some of these seemed to show a constant radioactivity, but others seemed to lose this property within a few hours or days. The Curies, very early in their study, explained this gradual disappearance of radioactivity in some elements by postulating that perhaps the energy of these rays comes from the atom itself. These facts and many others were put into good order when Rutherford and Soddy in 1903 advanced their disintegration theory.<sup>10</sup> According to this theory, radioactive atoms are unstable, undergoing spontaneous disintegration in such a manner that each individual transformation is accompanied by the expulsion of an  $\alpha$  or a  $\beta$  particle. The chemical and physical properties of the remaining atom are different from the original one, and this new atom may also be unstable as a member of a succession of radioactive transformations or of a disintegration series.

For the next decade after Rutherford and Soddy advanced their disintegration theory there was a great deal of study of the radioactive substances then known and of their relationship to the various disintegration series. During this interval the study of radioactivity assumed a stature comparable with a great many of the older sciences, and it is interesting to note that Debierne<sup>11</sup> in a review of radioactivity published in 1908 pointed out that this was such a large subject that a whole-year course was taught at the Sorbonne by Mme. Curie.

The intensity of investigation was such that by 1913 some thirty to thirty-five radioactive substances were known, and at about this time it was becoming clear how these might fit into the ten available places in the periodic table. (It should be mentioned that it had been noticed by Ramsay and Soddy<sup>12</sup> as early as 1903 that helium is constantly produced by such radioelements as radium and actinium, and in a series of beautiful experiments, Rutherford and Royds<sup>13</sup> positively identified in 1909 the  $\alpha$  particles as positively charged helium ions; the identification of the  $\beta$  particles as electrons had already been made earlier.<sup>13a</sup>) Soddy,<sup>13b</sup> together with Fleck,<sup>13c</sup> working in his laboratory, had established the chemical inseparability of a number of radioactive substances from other substances, radioactive or inactive. After the recognition by Soddy of the displacement caused by the emission of  $\alpha$  particles and the considerations of Russell<sup>14</sup> concerning possible connections between the shift of an element one way or another in the periodic table upon the emission of an  $\alpha$  particle or a

$\beta$  particle, Fajans<sup>15</sup> presented these connections clearly as the "displacement law." This displacement law connects the emission of an  $\alpha$  particle with a shift of the element two places down in atomic number in the periodic table, leaving the remaining element four units less in atomic weight, and the emission of a  $\beta$  particle with a shift of the element one place up in the periodic table, leaving the atomic weight essentially unchanged. The further chemical investigations of Fajans as well as of Hevesy and Paneth<sup>16</sup> and also of McCoy<sup>17</sup> and others made it possible to place a number of these radioactive species in the periodic table, and it was noticed, because of the large number of species and the small number of places available, that it was necessary in many cases to place more than one species in the same place in the periodic table.<sup>17a</sup> While the significance of this was recognized by some of these investigators, Soddy<sup>13b</sup> emphasized that the radioactive species in such cases are chemically identical and inseparable, and he gave to the species that occupy the same place in the periodic table the name "isotopes," from the Greek meaning "same place."

One of the aims, of course, was to correctly assign the various radioactive substances to, and place them within, the different radioactive families. It was thought for a while that there might be four distinct disintegration series, each named for the most prominent element in the series: uranium, radium, thorium, and actinium. However, the considerations of Rutherford<sup>18,19</sup> and Soddy and the experimental work of Boltwood<sup>20</sup> made it clear that uranium and radium are genetically related through a long-lived intermediate isotope ionium, and thus are both members of the one family, the uranium family or the "uranium-radium" family as it is sometimes called. The origin of the actinium series was doubtful for a time, although Rutherford<sup>20a</sup> had discussed a possible connection with uranium as early as 1906. The isotope Pa<sup>231</sup>, the parent of actinium, Ac<sup>227</sup>, was discovered some years later independently by Hahn and Meitner<sup>21</sup> and by Soddy and Cranston.<sup>22</sup> Because of the fact that the ratio of actinium to uranium in uranium minerals from all over the world was shown to be constant, Russell<sup>23</sup> and others postulated that perhaps the actinium series came from a rare isotope of uranium, and in 1935 Dempster<sup>24</sup> discovered the rare isotope U<sup>235</sup>, which is now known to constitute the natural beginning of the actinium series—or the "actino-uranium" family as it is sometimes called.

Thus it was suspected at a rather early date and finally became completely clear that there exist in nature three parallel and similar lines of radioactive decay, now known as the uranium (or uranium-radium) series, the thorium, and the actinium (or actino-uranium)

series, which families were found to account for all the heavy natural radioactive isotopes. (It should be recalled here that for historical reasons many of the intermediate products in these disintegration series have names indicating their genetic relationships and not their chemical nature. For example, UX<sub>1</sub> and UX<sub>2</sub> are not isotopes of uranium but of thorium; UX<sub>2</sub> is an isotope of protactinium; RaC and RaE are isotopes of bismuth, etc.) Because of the nature of radioactive

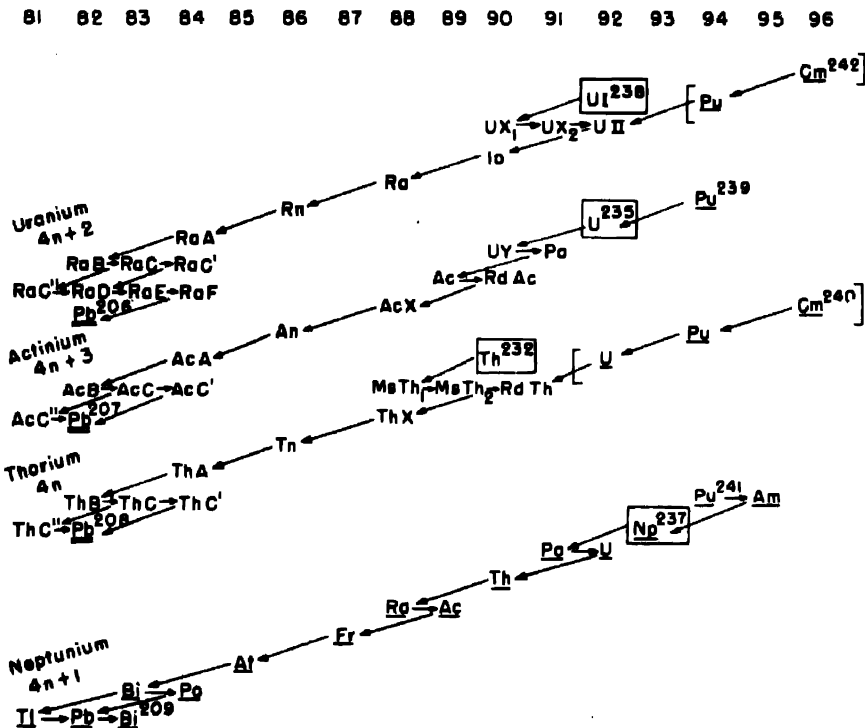


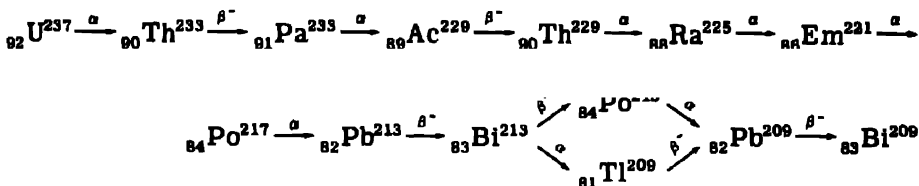
Fig. 1 — The four radioactive families.

disintegration within each of these three families, that is, the emission of  $\beta$  particles (of mass nearly zero) or  $\alpha$  particles (of mass four), the masses of all the members of the thorium series, which begins with  $\text{Th}^{232}$ , can be designated by the formula  $4n$ , where  $n$  is an integer. Similarly, the uranium and the actinium families, starting with  $\text{U}^{238}$  and  $\text{U}^{235}$ , respectively, can be described by the formulas  $(4n + 2)$  and  $(4n + 3)$ , respectively. The courses of decay within the three families bear striking resemblances to each other, and each of the families ends with a stable isotope of lead, namely,  $\text{Pb}^{206}$ ,  $\text{Pb}^{207}$ , and  $\text{Pb}^{208}$ .

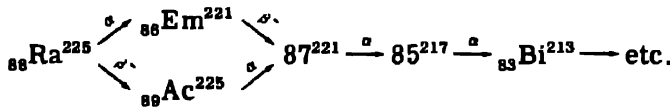
Figure 1 shows diagrammatically the main lines of decay of the three natural radioactive families as they are now known, excluding for purposes of simplicity of illustration the recently found branching decays of small relative percentage (for example, the 1 per cent  $\alpha$  branching of  $\text{Ac}^{227}$  to form the isotope  $\text{Fr}^{223}$  of the new element francium<sup>25</sup>).

However, although careful searches have been made, no radioactive chain corresponding to the formula  $(4n + 1)$ , nor any of the individual members, have been found in nature. Also, there are no stable isotopes of lead of this type, but the one known stable isotope of bismuth,  $\text{Bi}^{209}$ , is of the  $(4n + 1)$  mass type.

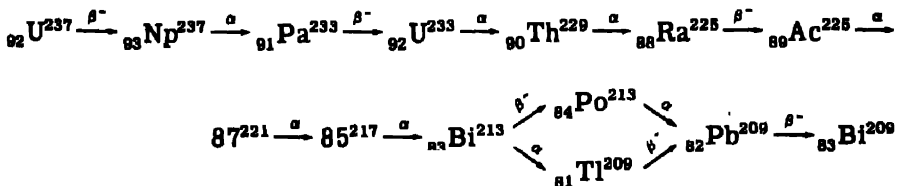
As early as 1923 Russell<sup>23</sup> deduced that there should be four independent disintegration series, rather than only the three then known, and he predicted for the fourth, the  $(4n + 1)$  series, the following decay scheme:



The following year Widdowson and Russell<sup>24</sup> revised this prediction and said that beginning with  $\text{Ra}^{225}$  the decay chain should proceed as follows:



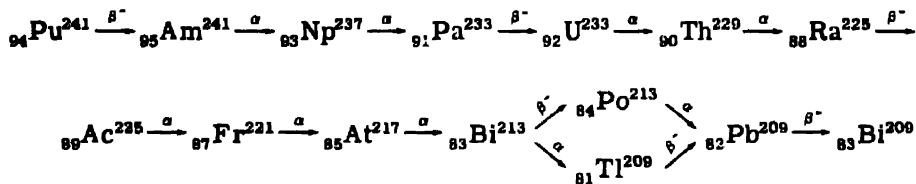
A good many years later, in 1940, Turner<sup>27</sup> predicted a somewhat different beginning for the series but otherwise agreed in general with the second suggestion above. He proposed the following decay scheme:



Ponisovsky<sup>28</sup> also was led from his considerations to predict a decay scheme which is very similar to this, with the difference that  $\text{Th}^{229}$

is predicted to emit  $\beta$  particles leading to an  $\alpha$ -active  $\text{Pa}^{229}$ , which decays to  $\text{Ac}^{225}$ .

Experimental work during the last seven or eight years, much of which was performed in connection with the Plutonium Project, has led to the observation of all the members of this  $(4n + 1)$  radioactive series and to a complete elucidation of the course which this series takes in its decay. It should be noted that the longest-lived member is now known to be an isotope of a transuranium element. This longest-lived isotope is  $\text{Np}^{237}$ , and this may justify the suggestion that the series be known as the "neptunium family" by analogy with the uranium, thorium, and actino-uranium families whose parents,  $\text{U}^{238}$ ,  $\text{Th}^{232}$ , and  $\text{U}^{235}$ , which occur in nature, are their longest-lived members. Including a couple of pre-neptunium members, the established experimental line of decay is as follows:



This is shown diagrammatically in Fig. 1. In addition, there are now known a number of nuclei of the  $(4n + 1)$  mass type, which may be referred to as "collateral" members, that is, branch members outside the main line of decay. There are the negative  $\beta$ -particle-emitting  $\text{Th}^{233}$  and  $\text{U}^{237}$ , the orbital-electron-capturing  $\text{Cm}^{241}$  and  $\text{Pu}^{237}$ , and the orbital-electron-capturing and  $\alpha$ -particle-emitting  $\text{U}^{229}$  and daughters.

The isotope that may be considered to be the parent of this series,  $\text{Np}^{237}$ , was first separated and measured by Wahl and Seaborg<sup>29</sup> in 1942. It was observed to be a long-lived  $\alpha$  emitter with a half life of about  $3 \times 10^6$  years, formed as a result of the  $\beta$  decay of the previously discovered isotope  $\text{U}^{237}$ . The isotope  $\text{U}^{237}$  was first reported by Nishina and coworkers<sup>30</sup> and by McMillan,<sup>31</sup> who found that it is a  $\beta$  emitter with a half life of about 7 days, produced from an  $(n,2n)$  reaction by the bombardment of  $\text{U}^{238}$  with fast neutrons. This half life for  $\text{Np}^{237}$  was determined<sup>29</sup> by measuring the growth of  $\alpha$  particles from known amounts of the parent  $\text{U}^{237}$ . Fortunately, this isotope is also produced as a by-product during the production of  $\text{Pu}^{239}$  in the uranium-graphite chain-reacting piles at a rate amounting to the order of 0.1 per cent of the rate at which the  $\text{Pu}^{239}$  itself is produced. In fact it has already been possible, as the result of special chemical separation procedures at the Hanford, Washington, plutonium-production plant, to isolate several hundred milligrams of this material.

The careful specific-activity measurements performed in 1945 by Magnusson and LaChapelle,<sup>32</sup> working at the wartime Metallurgical Laboratory (now the Argonne National Laboratory) of the Plutonium Project, have led to a value for the half life of  $2.20 \times 10^6$  years, which must be considered as the best value. LaChapelle<sup>33</sup> has measured the mean range of the  $\alpha$  particles and has found the value  $3.23 \pm 0.02$  cm under standard conditions, corresponding to an energy of  $4.73 \pm 0.02$  mev according to the range-energy relationship of Holloway and Livingston.<sup>34</sup> Carefully purified samples have been found by Magnusson and Ghiorso to emit soft electromagnetic radiation, similar to the characteristic x rays of a heavy element, and low-energy conversion electrons, indicating that the  $\alpha$  spectrum of this isotope would probably show fine structure under sufficiently high resolution.

Before proceeding to a discussion of the decay products of Np<sup>237</sup>, it is worth while to say a few words about the two pre-neptunium members of this family which are now known, namely the Pu<sup>241</sup> and Am<sup>241</sup>. These two isotopes were first observed during late 1944 and early 1945 by Seaborg, James, and Morgan,<sup>35</sup> working at the Metallurgical Laboratory. These investigators have found that Pu<sup>241</sup> has a half life of about ten years for the emission of  $\beta$  particles with an upper energy limit of about 10 to 20 kev. This isotope is produced by the bombardment of uranium with high-energy helium ions (30 to 40 mev) according to the reaction U<sup>238</sup>( $\alpha$ ,n)Pu<sup>241</sup>. The isotope Am<sup>241</sup> is an  $\alpha$  emitter of long half life, and according to the same investigators the  $\alpha$  particles have a range of  $4.05 \pm 0.1$  cm, corresponding to an energy of 5.5 mev. The best value for the half life is about 500 years, as determined by Cunningham<sup>36</sup> through his careful specific-activity measurements.

The first daughter of the parent isotope Np<sup>237</sup> is the isotope Pa<sup>233</sup>. This isotope was first observed as a result of the neutron bombardment of thorium. Fermi and coworkers<sup>37</sup> first showed that such neutron bombardment leads to the 23-min  $\beta$ -emitting Th<sup>233</sup> formed in the reaction Th<sup>232</sup>(n, $\gamma$ )Th<sup>233</sup>. The  $\beta$ -emitting daughter of this isotope, Pa<sup>233</sup>, was first reported by Meitner, Strassmann, and Hahn<sup>38</sup> and the doubts as to this isotopic assignment, which later arose as a result of the discovery of fission, were cleared up by the work of Grosse, Booth, and Dunning<sup>39</sup> and of Seaborg, Gofman, and Kennedy.<sup>40</sup> The best value<sup>39</sup> for the half life is 27.4 days. The maximum energy<sup>41</sup> for the  $\beta$  particles is 230 kev. There are a number of lines of conversion electrons, corresponding to  $\gamma$  rays of about 310 and 83 kev.<sup>41,42</sup> The isotope Pa<sup>233</sup> must, of course, grow from the isotope Np<sup>237</sup>, and that this is the case has been actually demonstrated in an experiment performed at the Metallurgical Laboratory by LaChapelle.

The isotope  $U^{233}$ , which is the daughter of the  $Pa^{233}$ , was first separated and examined by Seaborg, Gofman, and Stoughton<sup>43</sup> at the University of California in 1941-1942. These investigators produced this isotope as the result of the irradiation of thorium with cyclotron neutrons and observed that it decays by the emission of  $\alpha$  particles; from measurements on its rate of growth from known amounts of the parent isotope  $Pa^{233}$  they determined a value for the half life of about  $1.2 \times 10^8$  years. Since this first work this isotope has been isolated nearly pure in weighable amounts, and the best value for its half life has been determined by Hyde<sup>44</sup> at the Argonne National Laboratory, from specific-activity measurements, to be  $1.62 \times 10^8$  years. The best value for the energy of the  $\alpha$  particles is 4.80 mev.<sup>45</sup>

The isotope  $U^{233}$  is a very important one in the series because it is through the use of this isotope to study its decay products that the major number of members of the series have been investigated. This isotope has been available for this purpose in milligram amounts formed as a result of the intense neutron bombardment of thorium in the uranium-graphite chain-reacting piles. It is very fortunate that this isotope has been available in such amounts because its immediate daughter,  $Th^{229}$ , is quite long-lived (about 7,000 years), and since the entire series following  $Th^{229}$  depends on the growth of this long-lived member, it is necessary to have at least milligram amounts of  $U^{233}$  in order to make feasible a study of all its decay products. The decay products of  $U^{233}$  have been thoroughly studied and completely identified by two research teams, who have been working independently: A. C. English, T. E. Cranshaw, P. Demers, J. A. Harvey, E. P. Hincks, J. V. Jelley, and A. N. May<sup>46</sup> working on the Canadian atomic-energy project, and F. Hagemann, L. I. Katzin, M. H. Studier, A. Ghiorso, and G. T. Seaborg<sup>47,48</sup> working on the American project.

The chemical procedures and radiochemical techniques brought to bear on this problem were quite ingenious, representing in many respects advances in the methods used for this type of work. For example, the unraveling of the decay chain was tremendously aided through the use of a pulse-analyzer apparatus consisting of an ionization chamber for the measurement of  $\alpha$  pulses, which is connected to a circuit that sorts out the different pulse heights electronically. However, a description of these chemical separations, radiochemical techniques, and new counting methods is beyond the scope of the present discussion, and they are certain to be treated more fully in forthcoming publications describing these investigations.

The results are listed in Table 1.

The isotope  $Pb^{209}$  has been previously reported as a result of its production by the  $(d,p)^{51}$   $(n,\gamma)^{49}$  and  $(n,p)^{48}$  reactions. Hagemann<sup>51a</sup>

has found that  $Tl^{209}$  decays with a half life of 2.2 min by the emission of  $\beta$  particles of 1.8 mev energy.

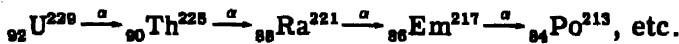
The collateral member of the series,  $Pa^{229}$ , was first produced at the Metallurgical Laboratory by Hyde, Studier, Hopkins, and Ghiorso,<sup>52</sup> who found that this isotope is produced as the result of the bombardment of ionium with 20-mev deuterons in the Berkeley 60-in. cyclotron according to the reaction  $Th^{230}(d,3n)Pa^{229}$ . This isotope has a half life of 1.4 days and decays by the emission of  $\alpha$  particles, as was

Table 1—Decay Products of  $U^{233}$

Isotope	Type of radiation	American group		Canadian group	
		Half life	Energy of radiation, mev	Half life	Energy of radiation, mev
$Th^{229}$	$\alpha$	$7,000 \pm 2,000$ years	4.85	$\sim 10^4$ years	$\sim 5$
$Ra^{228}$	$\beta^-$	$14.8 \pm 0.2$ days	$\sim 0.2$	$\sim 14$ days	$< 0.05$
$Ac^{225}$	$\alpha$	$10.0 \pm 0.1$ days	5.80	10 days	5.81
$Fr^{221}$	$\alpha$	$4.8 \pm 0.1$ min	6.30	5 min	6.33
$At^{217}$	$\alpha$	$0.018 \pm 0.002$ sec	7.00	0.021 sec	6.97
$Bi^{213}$	$\beta^-$	$47 \pm 1$ min	$\sim 1.2(\beta^-)$	46 min	$\sim 1.3(\beta^-)$
$Po^{213}$	$\alpha$ (4%)	Very short	6.0( $\alpha$ )	$(10^{-8} ?$ sec)	3.28
$Tl^{209}$	$\beta^-$	2.2 min	1.8	?	?
$Pb^{209}$	$\beta^-$	$3.3 \text{ hr}^{49,50}$	$0.7^{50,50a}$		
$Bi^{209}$	Stable				

deduced by observation of the  $\alpha$  particles and also indirectly from the observation of the growth of  $Ac^{225}$  and its decay products. There is also some evidence that it decays by the orbital-electron-capture mechanism, in which case its daughter would be  $Th^{229}$ . The collateral member  $Pu^{237}$  was first found at the Metallurgical Laboratory by James, Florin, Hopkins, and Ghiorso.<sup>53</sup> They produced this isotope in the bombardment of natural uranium with 40-mev helium ions in the Berkeley cyclotron [the reaction  $U^{238}(\alpha,5n)Pu^{237}$ ] and found that it decays by the orbital-electron-capture mechanism with a half life of about 40 days. The isotope  $Cm^{241}$  was first identified at the University of California by James and Seaborg, who produced it by the reaction  $Pu^{239}(\alpha,2n)Cm^{241}$  and who established that it decays by orbital-electron capture with a half life of about two months. Meinke, Ghiorso, and

Seaborg<sup>53a</sup> have produced U<sup>229</sup> with 100-mev helium ions according to the reaction Th<sup>232</sup>( $\alpha$ , 7n)U<sup>229</sup>, and this gives rise to the following collateral chain:



The half lives and  $\alpha$  energies (in mega electron volts) are as follows: U<sup>229</sup>, 58 min (6.42); Th<sup>228</sup>, 7.8 min (6.57); Ra<sup>221</sup>, 31 sec (6.71); Em<sup>217</sup>,  $\sim 10^{-5}$  sec (7.74). The U<sup>229</sup> and Th<sup>228</sup> also decay by electron capture.

Table 2—Radioactive Properties of the Neptunium Family

Isotope	Type of radiation	Half life	Energy of radiation, mev
<sup>94</sup> Pu <sup>241</sup>	$\beta^-$	~10 years	0.01 - 0.02
<sup>95</sup> Am <sup>241</sup>	$\alpha$	500 years	5.5
<sup>93</sup> Np <sup>237</sup>	$\alpha$	$2.20 \times 10^6$ years	4.73
<sup>91</sup> Pa <sup>233</sup>	$\beta^-$ , $\gamma$ , $e^-$	27.4 days	0.230 ( $\beta^-$ ) 0.310, 0.083 ( $\gamma$ )
<sup>92</sup> U <sup>233</sup>	$\alpha$	$1.62 \times 10^5$ years	4.80
<sup>90</sup> Th <sup>229</sup>	$\alpha$	7,000 years	4.85
<sup>88</sup> Ra <sup>228</sup>	$\beta^-$	14.8 days	~0.2
<sup>89</sup> Ac <sup>228</sup>	$\alpha$	10.0 days	5.80
<sup>87</sup> Fr <sup>221</sup>	$\alpha$	4.8 min	6.30
<sup>85</sup> At <sup>217</sup>	$\alpha$	0.018 sec	7.00
<sup>83</sup> Bi <sup>213</sup>	$\beta^-$ (96%) $\alpha$ (4%)	47 min	1.2 ( $\beta^-$ ) 6.0 ( $\alpha$ )
<sup>84</sup> Po <sup>213</sup>	$\alpha$	$\sim 10^{-5}$ sec?	8.30
<sup>81</sup> Tl <sup>209</sup>	$\beta^-$	2.2 min	1.8
<sup>82</sup> Pb <sup>209</sup>	$\beta^-$	3.3 hr	0.7
<sup>83</sup> Bi <sup>209</sup>	Stable		

Table 2 summarizes what probably are the best values for the radioactive constants of all the members of the main line of decay of the neptunium family.

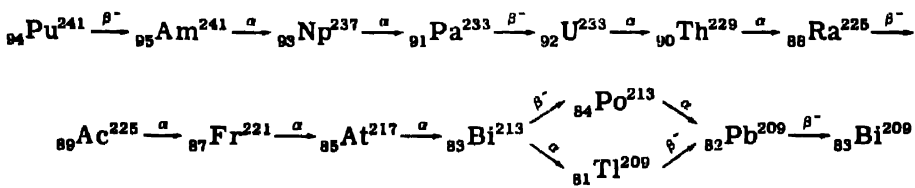
There are a number of particularly interesting aspects to this radioactive family, and it is worth while to summarize these briefly. As already stated, none of the members is found in nature. The key member of the series, Np<sup>237</sup>, is an isotope of a transuranium element, neptunium; and, in addition, two other transuranium elements, plutonium and americium are represented in the direct line of decay. There is no emanation isotope, of atomic number 86, as is the case for each of the other families; but instead there are main-line representatives of the newly discovered elements astatine<sup>54</sup> and francium<sup>55</sup> (atomic numbers 85 and 87, respectively), which are not in the main

line of decay of the other families and hence are missing from or very rare in nature. Still another interesting feature of this family is the presence of the important isotope  $U^{233}$ , which undergoes fission with thermal neutrons and is therefore a possible "nuclear-fuel" material. Since  $U^{233}$  is formed as a result of the absorption of neutrons by thorium it is possible to use nonfissionable thorium as a nuclear-fuel source indirectly through the fissionable isotope  $U^{233}$ .

Thus it can be seen that these researches have led to the elucidation of an entire new radioactive family, comparable in complexity to the three natural radioactive series, and, as a result of the new-found methods of transmutation on the macroscopic scale together with intense investigation and the availability of new techniques and instruments, it has been possible to compress this investigation into a period of about half a dozen years as compared to the 30 or 40 years spent in unraveling the natural radioactive families.

#### SUMMARY

The experimental work of the last seven or eight years had led to the production and the measurement of the radioactive properties of all the members of the missing,  $(4n + 1)$  mass type, radioactive family. The main line of decay for this series, for which the name "neptunium family" is suggested by analogy with the names for the other natural radioactive families, is as follows:



The radioactive properties of  $\text{Th}^{233}$ ,  $\text{U}^{237}$ ,  $\text{Cm}^{241}$ ,  $\text{Pu}^{237}$ , and  $\text{Pa}^{229}$ , as well as  $\text{U}^{229}$  and daughters, nuclei of the  $(4n + 1)$  mass type but known as "collateral" members because they are not in the direct line of decay of this family, are now also known.

#### ACKNOWLEDGMENTS

Professors K. Fajans and F. A. Paneth have kindly read this manuscript, and their assistance, especially in connection with the historical survey of the early work on natural radioactivity, is gratefully acknowledged. The assistance of Mrs. Carol H. Dauben was also of great value in the development of this historical-background material.

## REFERENCES

1. P. Lenard, Nobel Prize Address, 1905.
- 1a. J. J. Thomson, Proc. Roy. Inst. G. Brit., 15: 419 (1897); Phil. Mag., 44: 293 (1897); 46: 528 (1898); 48: 547 (1899); also, J. J. Thomson and G. P. Thomson, "Conduction of Electricity through Gases," Cambridge University Press, London, any edition.
2. W. K. Roentgen, Sitzber Wuerzburger Phys. Med. Ges., December 1895, p. 132, and March 1896, p. 11.
3. H. Becquerel, Compt. rend., 122: 420, 501, 559 (1896).
4. M. Curie, Compt. rend., 126: 1101 (1898).
5. G. C. Schmidt, Ann. Phys. Chem., 65: 141 (1898).
6. P. Curie and M. Curie, Compt. rend., 127: 175 (1898).
7. P. Curie, M. Curie, and G. Bernont, Compt. rend., 127: 1215 (1898).
8. A. Debierne, Compt. rend., 129: 593 (1899); 130: 906 (1900).
9. F. O. Giesel, Chem., Ber., 35: 3608 (1902); 36: 342 (1903); 37: 1896, 3963 (1904).
10. E. Rutherford and F. Soddy, Phil. Mag., 4: 370, 579 (1902); 5: 441, 445, 561, 576 (1903).
11. A. Debierne, Chem. News, 99: 235 (1908).
12. W. Ramsay and F. Soddy, Proc. Roy. Soc. London, 72A: 204 (1903); 73A: 346 (1904).
13. E. Rutherford and T. Royds, Chem. News, 99: 49 (1908).
- 13a. F. Giesel, Ann. Physik, 69: 834 (1899); S. Meyer and E. R. v. Schweidler, Physik. Z., 1: 90, 113 (1899); H. Becquerel, Compt. rend., 129: 996, 1205 (1899); 130: 809 (1900); P. Curie, Compt. rend., 130: 73 (1900).
- 13b. F. Soddy, Chem. News, 107: 97 (1913).
- 13c. A. Fleck, J. Chem. Soc., 103: 381, 1052 (1913).
14. A. S. Russell, Chem. News, 107: 49 (1913).
15. K. Fajans, Physik. Z., 14: 131, 136 (1913).
16. G. v. Hevesy and F. A. Paneth, Physik. Z., 16: 45 (1915); and earlier papers.
17. H. N. McCoy and C. H. Viol, Phil. Mag., 25: 333 (1913).
- 17a. K. Fajans, Physik. Z., 16: 456 (1915).
18. E. Rutherford, "Radioactivity," p. 459, Cambridge University Press, London, 1905.
19. E. Rutherford, Chem. News, 99: 171, 181 (1908).
20. B. B. Boltwood, Am. J. Sci., 25: 365 (1908).
- 20a. K. Fajans, "Radioelements and Isotopes," pp. 23-46, McGraw-Hill Book Company, Inc., New York, 1931.
21. O. Hahn and L. Meitner, Physik. Z., 19: 208 (1918).
22. F. Soddy and J. A. Cranston, Proc. Roy. Soc. London, 94: 384 (1918).
23. A. S. Russell, Phil. Mag., 46: 842 (1923).
24. A. J. Dempster, Nature, 136: 180 (1935).
25. M. Perey, Compt. rend., 208: 97 (1939); J. phys. radium, 10: 435 (1939); J. chim. phys., 43: 262, 289 (1946).
26. W. P. Widdowson and A. S. Russell, Phil. Mag., 48: 293 (1924).
27. L. A. Turner, Phys. Rev., 57: 950 (1940).
28. L. Ponisovsky, Nature, 152: 187 (1943).
29. A. C. Wahl and G. T. Seaborg, Nuclear properties of  $93^{237}$ , Paper 1.5, this volume; Phys. Rev., 73: 940 (1948).
30. Y. Nishina, T. Yasaki, H. Ezoe, K. Kimura, and M. Ikawa, Phys. Rev., 57: 1182 (1940).
31. E. M. McMillan, Phys. Rev., 58: 178 (1940).
32. L. B. Magnusson and T. J. LaChapelle, The first isolation of element 93 in pure compounds and a determination of the half life of  $_{93}\text{Np}^{237}$ , Paper 1.7, this volume.

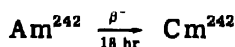
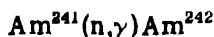
33. T. J. LaChapelle, Range of  $\text{Np}^{237}$  alpha particles in air, Paper 14.1, this volume (Argonne National Laboratory Report ANL-4037).
34. M. G. Holloway and M. S. Livingston, Phys. Rev., 54: 18 (1938).
35. G. T. Seaborg, R. A. James, and L. O. Morgan, The new element americium (atomic number 95), Paper 22.1, this volume.
36. B. B. Cunningham, The first isolation of americium in the form of pure compounds; microgram-scale observations on the chemistry of americium, Paper 19.2, this volume.
37. E. Fermi, E. Amaldi, O. D'Agostino, F. Rasetti, and E. Segre, Proc. Roy. Soc. London, A146: 483 (1934).
38. L. Meitner, F. Strassmann, and O. Hahn, Z. Physik, 109: 538 (1938).
39. A. V. Grosse, E. T. Booth, and J. R. Dunning, Phys. Rev., 59: 322 (1941).
40. G. T. Seaborg, J. W. Gofman, and J. W. Kennedy, Phys. Rev., 59: 321 (1941).
41. E. Haggstrom, Phys. Rev., 59: 322 (1941).
42. E. Haggstrom, Phys. Rev., 62: 144 (1942).
43. G. T. Seaborg, J. W. Gofman, and R. W. Stoughton, Nuclear properties of  $\text{U}^{233}$ : A new fissionable isotope of uranium, Paper 19.13, this volume; Phys. Rev., 71: 378 (1947).
44. E. K. Hyde, Determination of the half life of  $\text{U}^{233}$ , Paper 19.15, this volume (Metallurgical Project Report CB-3634).
45. A. H. Jaffey, private communication.
46. A. C. English, T. E. Cranshaw, P. Demers, J. A. Harvey, E. P. Hincks, J. V. Jelley, and A. N. May, Phys. Rev., 72: 253 (1947).
47. F. Hagemann, L. I. Katzin, M. H. Studier, G. T. Seaborg, and A. Ghiorso, The  $(4n + 1)$  radioactive series: The decay products of  $\text{U}^{233}$ , Phys. Rev., in press.
48. F. Hagemann, L. I. Katzin, M. H. Studier, A. Ghiorso, and G. T. Seaborg, Phys. Rev., 72: 252 (1947).
49. W. Maurer, and W. Ramm, Z. Physik, 119: 602 (1942).
50. K. Fajans and A. F. Voigt, Phys. Rev., 60: 619, 626 (1941).
- 50a. R. S. Krishnan and E. A. Nahum, Proc. Cambridge Phil. Soc., 36: 490 (1940).
51. R. L. Thornton and J. M. Cork, Phys. Rev., 51: 383 (1937).
- 51a. F. Hagemann, Argonne National Laboratory Report ANL-4143 (May 1948), p. 7.
52. E. K. Hyde, M. H. Studier, H. H. Hopkins, Jr., and A. Ghiorso, A new isotope of protactinium:  $\text{Pa}^{239}$ , Paper 19.17, this volume (Metallurgical Project Report CC-3648).
53. R. A. James, A. E. Florin, H. H. Hopkins, and A. Ghiorso, Products of helium-ion and deuteron bombardment of  $\text{U}^{235}$  and  $\text{U}^{238}$ , Paper 22.8, this volume.
- 53a. W. W. Meinke, A. Ghiorso, and G. T. Seaborg, Phys. Rev., 75: 314 (1949).
54. E. Perrier and E. Segre, J. Chem. Phys., 5: 712 (1937).

## Paper 22.5

### THE PREPARATION AND ISOLATION OF CURIUM†

By L. B. Werner and I. Perlman

The preparation and identification of  $\text{Cm}^{242}$  by Seaborg, James, and Ghiorso<sup>1</sup> by the cyclotron bombardment of  $\text{Pu}^{239}$  with helium ions, constituted the discovery of curium, element 96. This isotope is an  $\alpha$  emitter with a 5-month half life. It can also be prepared by the irradiation of  $\text{Am}^{241}$  with neutrons in the nuclear reaction<sup>1,2</sup>



With the huge neutron fluxes available from the chain-reacting piles it becomes possible to transmute appreciable percentages of substances provided the transmutation can be effected by slow neutrons. The 500-year isotope of americium,  $\text{Am}^{241}$ , has been isolated by Cunningham<sup>3</sup> so that it seemed possible to prepare microgram quantities of  $\text{Cm}^{242}$  by a prolonged neutron irradiation.

The problem of isolating curium was largely that of separating it from many times its weight of americium. The chief radiation hazard was that of the curium  $\alpha$  particles, the activity of which amounts to about 7 billion disintegrations per minute per microgram of  $\text{Cm}^{242}$ . The chemistry of curium, as determined on the tracer scale, has indicated that only the tripositive oxidation state exists in aqueous solution.<sup>4</sup> It shows very much the same precipitation properties as the tripositive rare earths, and attempts to oxidize or reduce it to other oxidation states proved unsuccessful. Since the most stable

†Contribution from the Department of Chemistry and the Radiation Laboratory, University of California, Berkeley.

state of americium is also tripositive, the problem of separating curium from americium may be compared to that of separating adjacent rare-earth elements.

One method of separation, by which it was possible to effect a partial removal of americium, did involve a change in oxidation state of americium under special conditions. It was found that in slightly alkaline solution americium could be oxidized by NaOCl to a higher state, which has a low solubility in the presence of carbonate. The method is limited by the solubility of the americium and does not allow its removal to the point where its concentration in solution is small compared to the curium. In practice the oxidation of Am(III) was carried out in 20 per cent  $K_2CO_3$  solution, making it 0.1M in NaOCl. A precipitate of americium formed slowly, and a minimum solubility of 5 mg of americium per liter was encountered after about 24 hr. The oxidation state of the americium is assumed to be pentapositive, since tripositive and hexapositive oxidation states of other actinide elements do not exhibit these solubility properties, whereas Pu(V) does show this behavior.<sup>5</sup> [Partial success in further removing americium from the solution was attained by using insoluble Pu(V) as a carrier, but the method was not developed.] The precipitate of Am(V) once formed could be dissolved in 0.1M  $H_2SO_4$ , in which solution the Am(V) is slowly reduced to Am(III) at room temperature. The absorption spectrum of Am(V) was taken in a Beckman spectrophotometer and showed absorption bands at 5070 and 7100 Å. In Fig. 1 the spectrum of Am(V) in 0.1M  $H_2SO_4$  is shown, along with that for Am(III) in 1M HCl.

A much better method of separating americium and curium was suggested by the successful use of ion-exchange resins for separating rare-earth elements without change of oxidation state. The development of these methods has been reviewed by Johnson, Quill, and Daniels.<sup>6</sup> The cation-exchange resin used, Dowex-50,<sup>7</sup> is a development of the Dow Chemical Company and has been used for rare-earth separations by Harris and Tompkins<sup>8</sup> at Clinton Laboratories in Oak Ridge.

The separation of the irradiated americium was made with a glass column 50 cm in length and 8 mm in diameter, packed with the ammonium form of the resin. The mixture of americium and curium was adsorbed from pH 1.5 citrate solution onto a top layer of the column, after which a 0.25M citrate solution at pH 3.05 was passed through slowly. Owing to difference in the ion-exchange equilibrium and the strengths of the citrate complexes, the americium and curium separate into bands, with the curium coming off the column first. The eluate was collected in many small samples of about 2 ml each. These

were analyzed first for the total  $\alpha$  activity in order to localize, in as small a volume as possible, the americium and curium. These solutions, which contained appreciable quantities of  $\alpha$  activity, were fur-

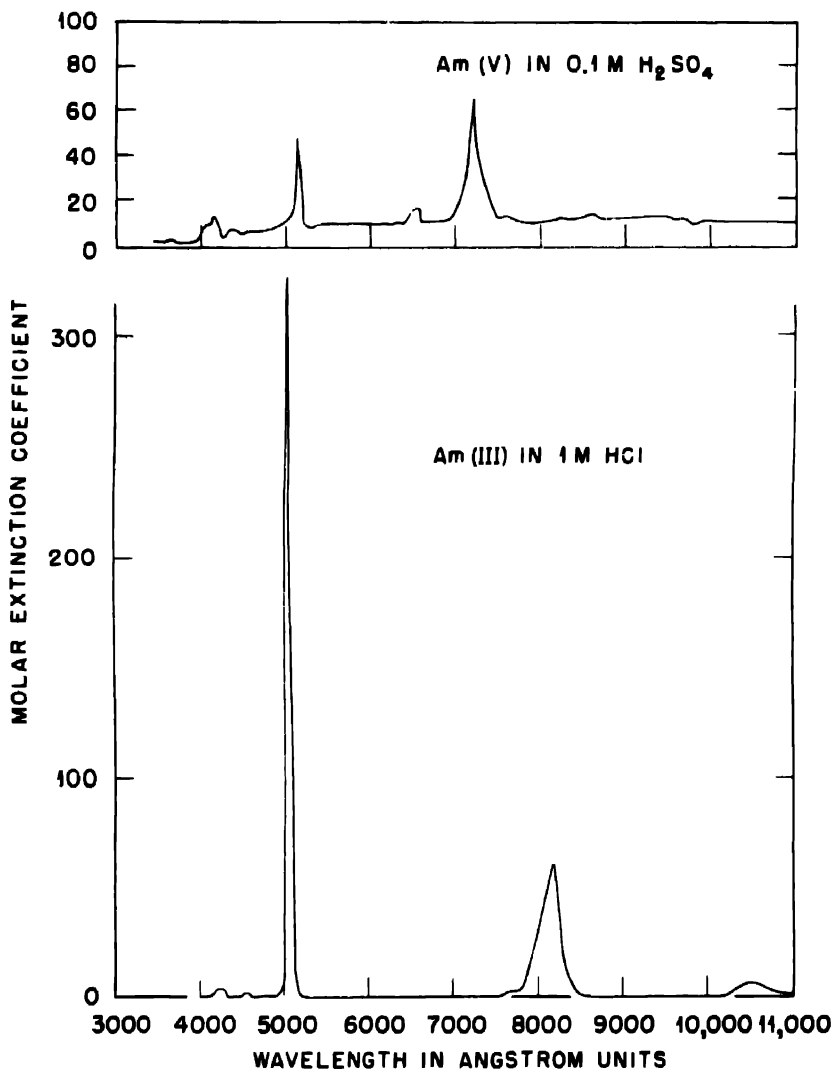


Fig. 1 — Absorption spectrum of americium(V) and americium(III).

ther subjected to americium and curium analysis by determining the numbers of  $\alpha$  particles with ranges of the respective isotopes, using an  $\alpha$ -particle pulse analyzer designed by Ghiorso, Jaffey, Robinson, and Weissbourd.<sup>9</sup>

An elution curve, so obtained, is shown in Fig. 2. The americium curve is lower than that for curium owing to the 1,000-fold difference in specific activities. One cut was taken out which was essentially

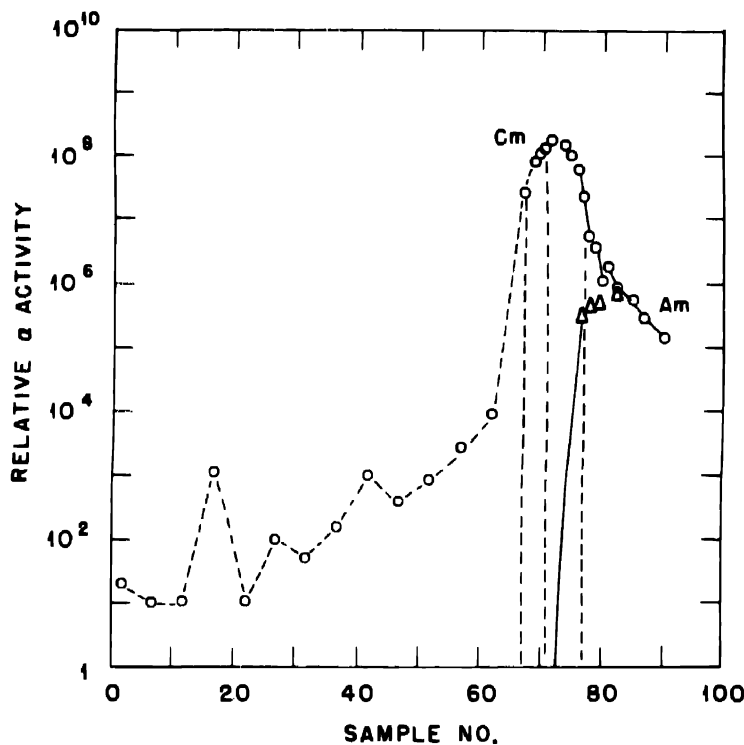


Fig. 2 — Elution curve of americium and curium.

pure curium, and another which was almost pure americium; the intermediate fraction was reprocessed for further separation. In this manner over 90 per cent of the curium was recovered essentially free of americium.

The curium in citrate solution was concentrated and purified by means of the following steps:

1. The citrate was decomposed by heating with concentrated sulfuric and nitric acids.
2. The resulting solution was heated to dryness, and the residue was dissolved in a minimum amount of 0.1N acid solution.
3.  $\text{Cm}(\text{OH})_3$  was precipitated by adding ammonium hydroxide. The precipitate was slightly yellow and had a measured solubility of the order of 20 mg of curium per liter.

4.  $\text{CmF}_3$  was precipitated from a solution containing argentic ion. The solubility of the  $\text{CmF}_3$  was found to be of the order of 20 mg of curium per liter. The precipitate appeared to be nearly colorless.

5. Sulfide-insoluble impurities were removed from a solution of the curium in 0.1N HCl.

The fluoride precipitation was carried out in the presence of argentic ion, which oxidizes the accumulated daughter element  $\text{Pu}^{238}$  to a fluoride-soluble state and achieves thereby a separation from it. Plutonium is always present as an impurity except immediately after separation, owing to the fact that  $\text{Cm}^{242}$  decays at a rate of nearly 0.5 per cent per day. The high  $\alpha$ -decay rate has other interesting consequences in that the aqueous solutions of the salts are decomposed and evolve hydrogen and oxygen continuously, as well as build up an appreciable concentration of hydrogen peroxide in the solution. The gas evolution interfered seriously with the separation of solutions from centrifuged precipitates and posed a special problem with respect to operation of the resin column. Spongy palladium was mixed with the resin in order to minimize bubble formation in the column.

In Fig. 3 is shown a preparation of the hydroxide, which was originally compacted in the bottom of the tube but was soon stirred up by gas evolution. The second picture in Fig. 3 is that of a solution of curium taken by its own light.

The purity of the isolated curium was checked in several ways. First an examination of the absorption spectrum of the solution was taken, and, from a measurement of the characteristic absorption band of Am(III), a maximum limit was placed of approximately 5 per cent americium by weight of curium present.

A considerable fraction of the sample was sacrificed for a complete spectrographic analysis, which was performed by John Conway of this laboratory.<sup>†</sup> The only detectable impurity was about 1 per cent lead, which had not been entirely removed by the sulfide precipitation. Although no other elements were detected, it should be pointed out that because of the small quantity of sample analyzed and the limits of detection of many of the elements, the presence of a considerable total impurity was not precluded. This was considered unlikely, however, in most cases in view of the highly specific nature of the separations with the resin column.

One further determination of the purity of the sample was carried out. Since the half life of  $\text{Cm}^{242}$  is known from the direct observation

<sup>†</sup>In addition to the analysis for impurities, Mr. Conway recorded 45 spectral lines attributable to curium, the most prominent of which fell at 3220.5, 3426.5, 3472.8, 3546.3, 3905.2, 3909.4, and 4207.5 Å.

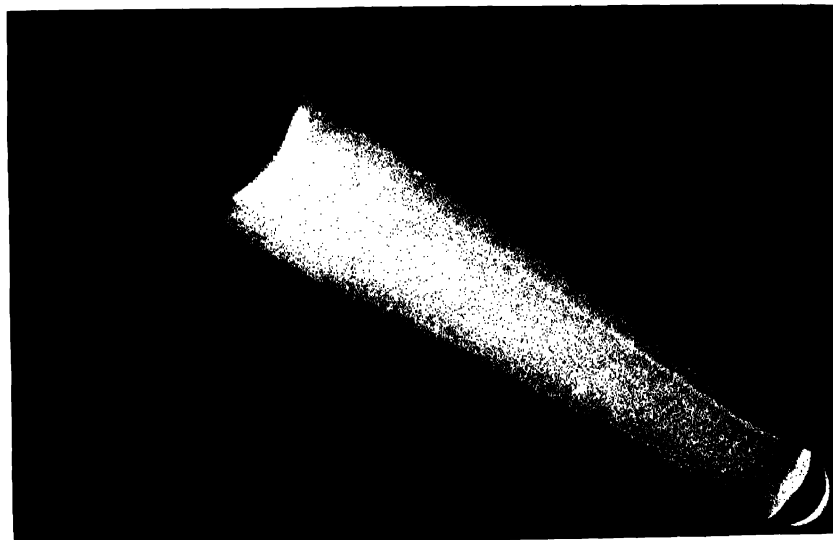


Fig. 3 — Top, early preparation of curium hydroxide in bottom of microcentrifuge cone. Bottom, solution of curium photographed by its own light.

of the radioactive decay, the specific activity becomes an index of the purity of the preparation. By preparing and subsequently weighing a sample of curium oxide on a quartz microbalance,<sup>10</sup> the amount of total impurities could be directly calculated. Taking into account the known impurities consisting of lead, Am<sup>241</sup>, and Pu<sup>238</sup>, a maximum limit of unknown impurities was set at approximately 10 per cent.

Some difficulty was experienced in weighing the sample of curium oxide on the ultramicrobalance because the apparent weight of the sample continued to increase over a period of days. This increase seemed to be some indirect effect of the intense radioactivity of the

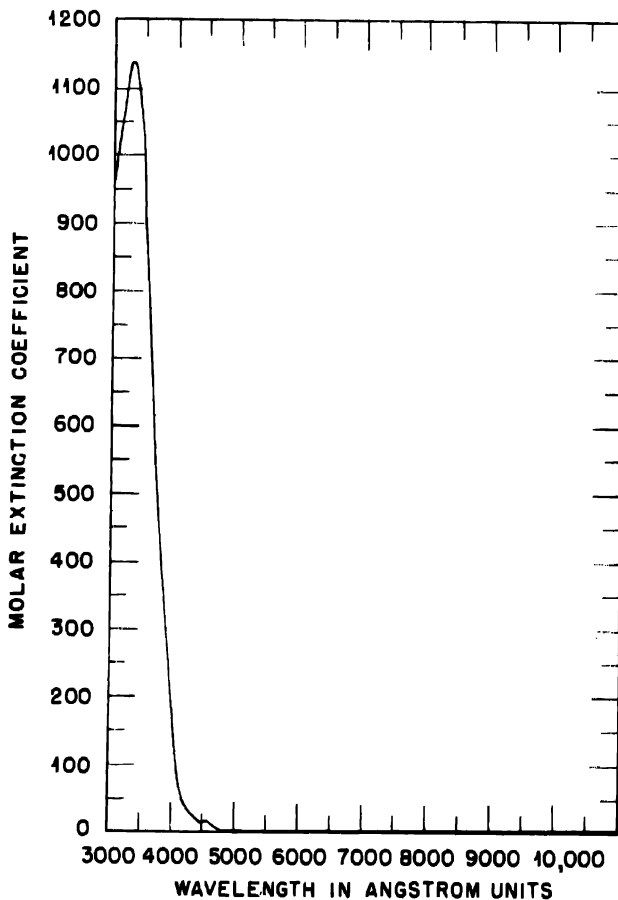


Fig. 4 — Absorption spectrum of curium(III) in 0.5M HCl.

sample and could not be attributed to operation of the balance or the chemical composition of the sample.

Some interesting information on the electronic structure of curium can be inferred from the absorption spectrum in aqueous solution, which was taken with microadapters in the spectrophotometer. As seen in Fig. 4, curium shows virtually no absorption in the visible

range but absorbs heavily below 4500 Å. It is known that the absorption of gadolinium, whose electronic structure is the stable  $4f^7$  configuration, is limited to the ultraviolet region of the spectrum, whereas rare earths on both sides of gadolinium have absorption bands extending into the visible region. A similar trend is noted between

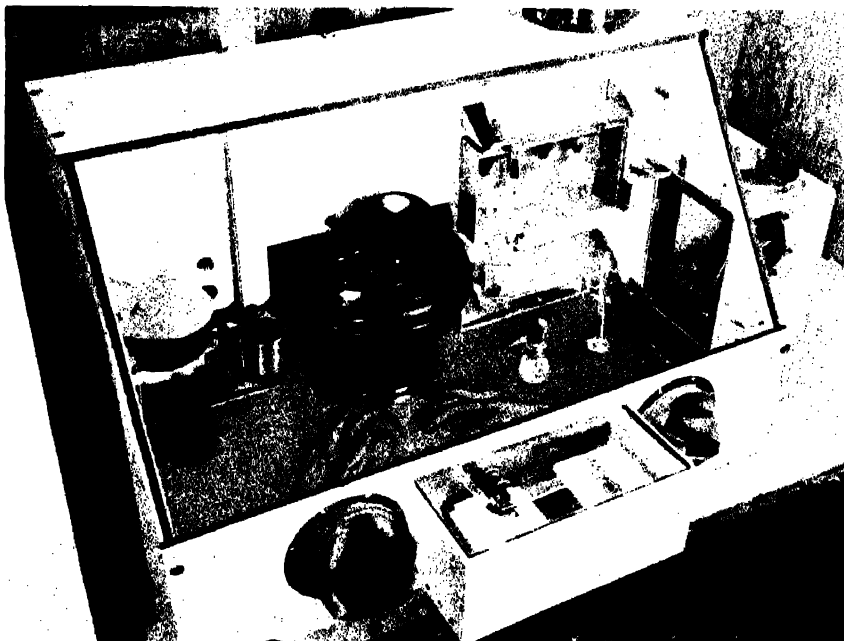


Fig. 5 — Glove box.

Cm(III) and the preceding heavy elements in their tripositive states. The observation that the curium absorption lies principally in the ultraviolet is, therefore, in agreement with the hypothesis<sup>11</sup> that curium occupies a position analogous to that of gadolinium with respect to its electronic configuration, namely, that of a stable half-completed f shell, in this case  $5f^7$ .

Because of the hazards involved in handling the large amounts of  $\alpha$  activity which accompany visible amounts of Cm<sup>242</sup>, all the work was carried out in "glove boxes" of the type shown in Fig. 5. We are indebted to Nelson Garden and his radiation-protection group for the design of the equipment used in these studies.

Summary. Curium, in the form of the isotope Cm<sup>242</sup>, has been isolated in relatively pure form. Microgram quantities were made

by transmutation of  $\text{Am}^{241}$  in a high flux of neutrons. The emission spectrum and the absorption spectrum in solution have been measured, and certain other chemical properties, which can only be determined at macro concentrations, have also been measured. The absorption spectrum, when compared to other heavy elements, is analogous to that of gadolinium in the rare-earth series. This finding, along with the apparent predominance of the tripositive state for curium, gives added evidence for placing curium as the seventh element of a heavy-element transition series.

## REFERENCES

1. G. T. Seaborg, R. A. James, and A. Ghiorso, The new element curium (atomic number 96), Paper 22.2, this volume.
2. W. M. Manning and L. B. Asprey, Preparation and radioactive properties of  $\text{Am}^{241}$ , Paper 22.7, this volume.
3. B. B. Cunningham, First isolation of americium in the form of pure compounds; microgram-scale observations on the chemistry of americium, Paper 19.2, this volume.
4. S. G. Thompson, L. O. Morgan, R. A. James, and I. Perlman, The tracer chemistry of americium and curium in aqueous solutions, Paper 19.1, this volume.
5. K. A. Kraus, G. E. Moore, D. E. Kosland, and J. R. Dam, unpublished work.
6. W. C. Johnson, L. L. Quill, and F. Daniels, Chem. Eng. News, 25: 2494 (1947).
7. W. C. Bauman and J. Erickhorn, J. Am. Chem. Soc., 69: 2830 (1947).
8. D. H. Harris and E. R. Tompkins, J. Am. Chem. Soc., 69: 2792 (1947).
9. A. Ghiorso, A. H. Jaffey, H. P. Robinson, and B. Weissbourd, A 48-channel pulse-height analyzer for alpha-energy measurements, Paper 18.8, this volume (Metallurgical Project Report CC-3887).
10. P. L. Kirk, R. Craig, J. E. Gullberg, and R. Q. Boyer, Anal. Chem., 19: 427 (1947).
11. G. T. Seaborg, Science, 104: 379 (1946); Electronic structure of the heaviest elements, Paper 21.1, this volume.

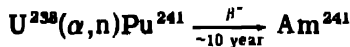
## Paper 22.7

### PREPARATION AND RADIOACTIVE PROPERTIES OF Am<sup>242</sup>†

By W. M. Manning and L. B. Asprey

#### 1. INTRODUCTION

Seaborg, James, and Morgan<sup>1</sup> showed that bombardment of U<sup>238</sup> with 38- to 40-mev helium ions yields an isotope of americium, <sub>95</sub>Am<sup>241</sup> (a 5.46-mev  $\alpha$  emitter), by the series of reactions



They also observed that bombardment of Am<sup>241</sup> with thermal neutrons produced a 6.10-mev  $\alpha$  activity. Seaborg, James, and Ghiorso<sup>2</sup> found that the 6.10-mev activity is also formed by helium-ion bombardment of Pu<sup>239</sup>, and they showed that it is due to <sub>96</sub>Cm<sup>242</sup>, produced by the reaction Am<sup>241</sup>(n, $\gamma$ )Am<sup>242</sup> $\xrightarrow{\beta^-}$ Cm<sup>242</sup>, by Pu<sup>239</sup>( $\alpha$ ,n)Cm<sup>242</sup>, and perhaps by Pu<sup>239</sup>( $\alpha$ ,p)Am<sup>242</sup> $\xrightarrow{\beta^-}$ Cm<sup>242</sup>.

The 6.10-mev activity assigned to Cm<sup>242</sup> decayed with a half life of approximately 150 days. The 5.46-mev Am<sup>241</sup> activity did not decay appreciably (the half life is now known to be about 510 years).<sup>3</sup> No activity attributable to Am<sup>242</sup> was observed in these experiments. In the absence of additional evidence, it was not possible to decide whether Am<sup>242</sup> was a short-lived  $\beta$  emitter decaying to a 150-day  $\alpha$ -emitting Cm<sup>242</sup>, or whether it was a 150-day  $\beta$  emitter decaying to a short-lived  $\alpha$ -emitting Cm<sup>242</sup>. If it were the latter, the Am<sup>242</sup>  $\beta$  radiation might be too soft to detect with an ordinary mica-window counter. In the earliest tracer studies on mixtures of the 5.46- and

†Contribution from the Chemistry Division of the Metallurgical Laboratory, University of Chicago, now the Argonne National Laboratory.

Preliminary reports were made in Metallurgical Project Reports CS-3237 (September 1945) and CS-3471 (March 1946).

6.10-mev  $\alpha$  activities<sup>1,2</sup> no chemical separation was observed. It was not clear whether the failure to separate the two activities was due to almost identical chemical properties of elements 95 and 96, or to the possibility that Cm<sup>242</sup> was a short-lived  $\alpha$  emitter quickly growing into equilibrium with a long-lived Am<sup>242</sup> parent.<sup>†</sup>

The purpose of the present investigation was (1) to attempt to fix the half life of the shorter-lived nucleus, either Am<sup>242</sup> or Cm<sup>242</sup>, by bombarding Am<sup>241</sup> with thermal neutrons for a short period and then quickly observing the growth of the Cm<sup>242</sup>  $\alpha$  activity in the sample; (2) having found the approximate half life of the short-lived activity, to look for a decay of  $\beta$  activity with a corresponding half life. The experiments described below show that Am<sup>242</sup> is in fact the shorter lived (half life about 16 hr). Consequently the 150-day half life can definitely be assigned to Cm<sup>242</sup>.

## 2. EXPERIMENTAL WORK

2.1 Source of Am<sup>241</sup>. Am<sup>241</sup> formed by  $\beta$  decay of Pu<sup>241</sup> was partially separated from plutonium by the usual procedures for separating plutonium and rare earths.<sup>3,7</sup> Iron, which tended to concentrate as an impurity with the americium, was removed by ether extraction from concentrated hydrochloric acid. Finally, the remaining plutonium was reduced to a low level by three successive extractions with methyl isobutyl ketone from concentrated nitric acid solution.

2.2 Growth of Cm<sup>242</sup>  $\alpha$  Activity. An aliquot from the Am<sup>241</sup> solution was plated and examined in a 24-channel pulse analyzer<sup>8</sup> to determine the residual plutonium content. The Am<sup>241</sup> purity thus determined was adequate for following the growth of Cm<sup>242</sup> activity. A larger sample of Am<sup>241</sup> was spread with tetraethylene glycol<sup>9</sup> on a 1-in. quartz disk. Quartz rather than platinum was chosen as the backing material because neutron-irradiated quartz was found to show less  $\beta$  activity a few hours after bombardment. Preliminary tests showed that the activity induced in the irradiated quartz would not interfere with the use of the  $\alpha$ -pulse analyzer. Before neutron irradiation the Am<sup>241</sup> sample was examined in the pulse analyzer with collimation giving a counting geometry of 0.12 per cent and a mica absorber that absorbed nearly all the 5.46-mev  $\alpha$  activity while transmitting any 6.10-mev activity. The background counts corresponding to the Cm<sup>242</sup> energy were found to be extremely low (see top curve in Fig. 1).

The Am<sup>241</sup> sample was irradiated in the thimble of the Argonne heavy-water pile for 90 min, and it was then transported to the pulse

<sup>†</sup>Clear-cut separations of curium from americium have subsequently been effected despite their similarity in chemical properties.<sup>4-6</sup>

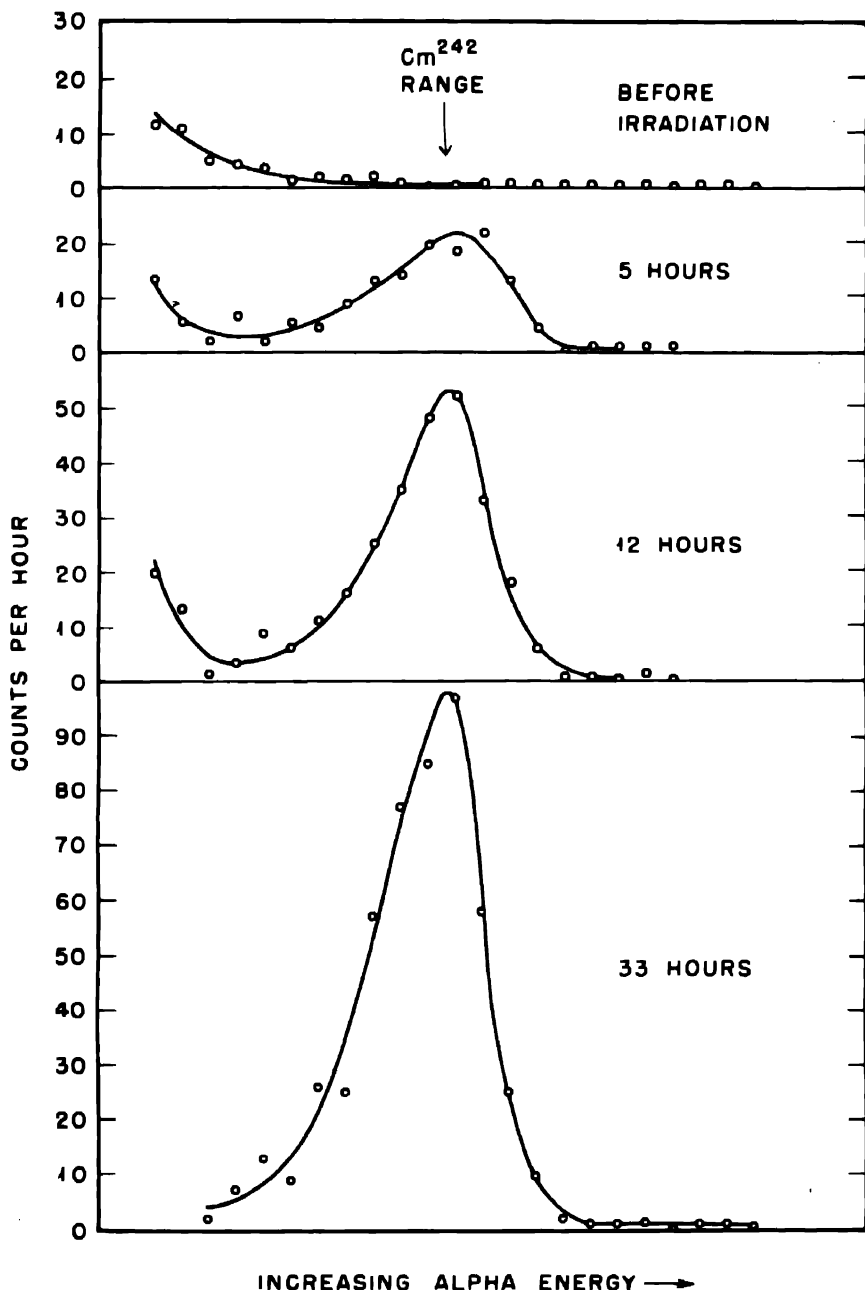


Fig. 1.—Pulse-analysis curves showing growth of Cm<sup>242</sup> 6.10-mev  $\alpha$  activity after a 90-min irradiation of Am<sup>241</sup> in the Argonne heavy-water pile. Times shown are from mid-point of bombardment to mid-point of count. Counting geometry, 0.12 per cent. Duration of counts, reading from top down, 83, 55, 92, and 276 min, respectively. Points at extreme left of curves show the long-range "tail" of the 5.46-mev Am<sup>241</sup>.

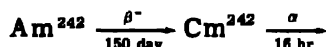
analyzer. The growth of 6.10-mev  $\alpha$  activity was followed for 60 hr. Figure 1 shows the growth for three intermediate times. A growth curve is shown in Fig. 2 in which the difference between the estimated final maximum activity and the observed activity at a given time is plotted as a function of time from the mid-point of the bombardment to the mid-point of each count. The slope for the best straight line through the experimental points depends somewhat on the particular maximum value which is assumed for the 6.10-mev activity. Apparatus difficulties made it impossible to follow the growth experimentally beyond the 64-hr point. The assumed maximum of 8,730 disintegrations per minute and the slope corresponding to the 16-hr half life shown in Fig. 2 represent approximately the best fit for the experimental data, but reasonably good fits (except for the last three points, whose positions would be very sensitive to small variations in counter sensitivity) are obtained for assumed maximum activities ranging from 8,200 to 9,400 disintegrations per minute, with corresponding half lives ranging from 14 to 18 hr.

The maximum growth of  $Cm^{242}$  activity in this experiment corresponded to an increase of much less than 1 per cent in total  $\alpha$  activity on the plate. A selective method of recording the long-range activity was therefore essential to the success of the experiment.

**2.3 Decay of  $Am^{242}\beta^-$  Activity.** The experiment just described did not serve to distinguish between the alternative modes of decay



and



The combination of fission activity and activity induced in the quartz backing plate would have obscured any  $\beta$  activity of  $Am^{242}$ .

To remove further the fissionable  $Pu^{239}$  before another neutron bombardment, the remainder of the  $Am^{241}$  solution previously prepared was extracted three additional times with methyl isobutyl ketone. A quartz disk was thoroughly cleaned with concentrated nitric acid; then it was plated with  $2.50 \times 10^6$   $\alpha$  disintegrations per minute of  $Am^{241}$ . The sample was checked for initial Geiger activity penetrating 4 mg/sq cm of air and 3.4 mg/sq cm of mica. Attributing all the observed counts to electrons, the " $\beta$ "/ $\alpha$  ratio was estimated at approximately 0.015.

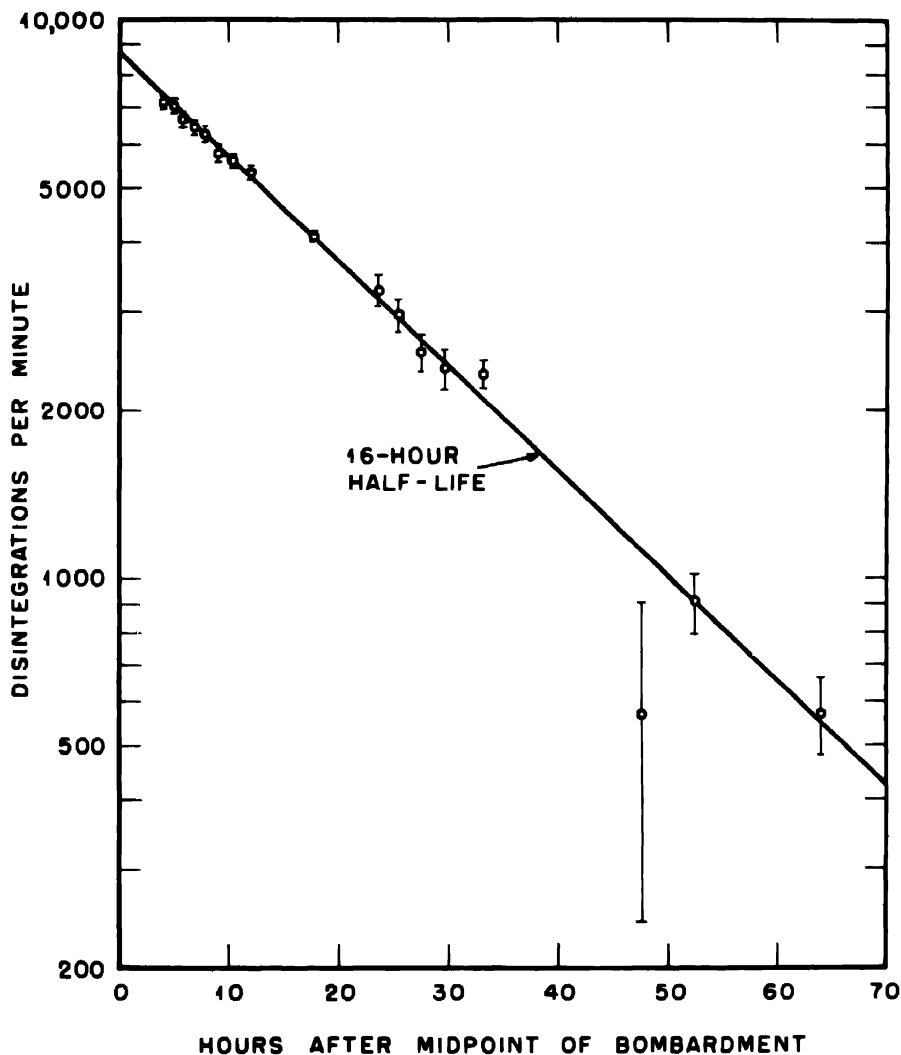


Fig. 2—Growth of Cm<sup>243</sup>  $\alpha$  activity, plotted as difference between estimated final maximum activity and observed activity at a given time. Vertical lines through points indicate standard errors of counting.

The sample was then bombarded in the thimble of the Argonne heavy-water pile, returned to the laboratory, and dissolved from the quartz with nitric acid. Analysis of an aliquot of this solution 4 hr after the mid-point of bombardment showed a total  $\beta$  activity of  $1.73 \times 10^6$  disintegrations per minute, again through 4 mg/sq cm of air and 3.4 mg/sq cm of mica. This corresponds to a  $\beta/\alpha$  ratio of

0.69, or 46 times the ratio before irradiation. A portion of the solution was then carried through two lanthanum fluoride - fluosilicic acid cycles<sup>1</sup> to obtain some decontamination from fission products formed during bombardment. The  $\beta/\alpha$  ratio of the decontaminated sample

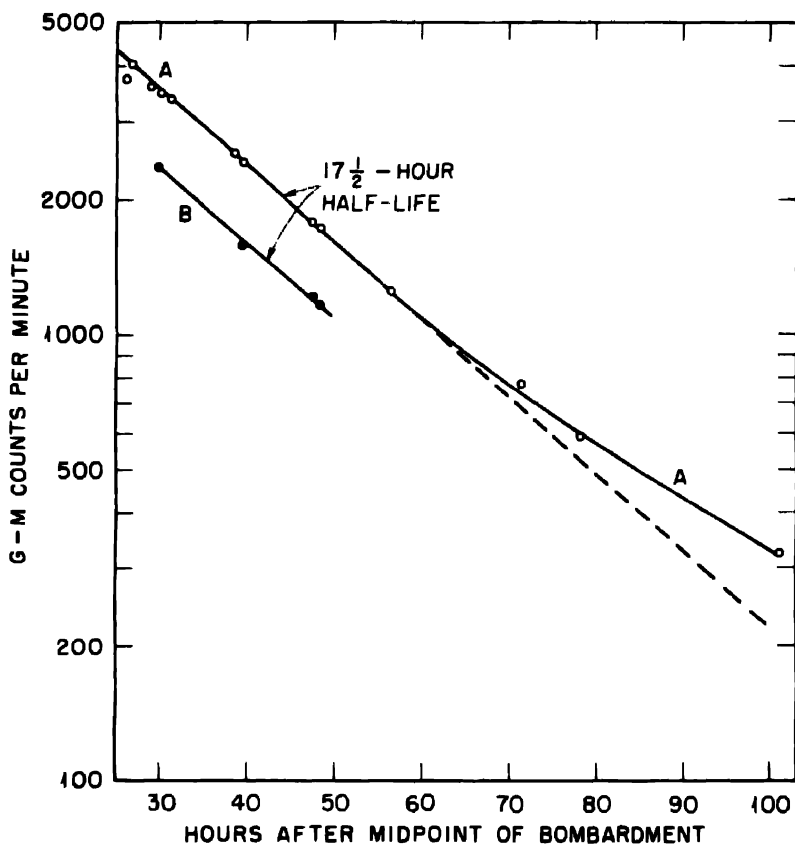


Fig. 3—Decay of Am<sup>242</sup>  $\beta$  activity. Curve A, through 3.4 mg/sq cm of mica and 4.0 mg/sq cm of air. Curve B, through 11.0 mg/sq cm of aluminum in addition to 7.4 mg/sq cm of mica and air.

was only 7 per cent lower than that of the undecontaminated solution, indicating that nearly all the activity in the bombarded material was due to Am<sup>242</sup> rather than to fission products or other impurities.  $\beta$ -decay curves for a sample prepared from the decontaminated solution are shown in Fig. 3. Both curves are corrected for a small amount of hard residual activity, presumably due to Am<sup>241</sup>, which was unabsorbed by 223 mg/sq cm of aluminum and showed practically no decay. Both curves show a slope corresponding to a 17.5-hr half life

up to 50 or 60 hr after the mid-point of bombardment. The diminished slope of the more complete decay curve after 60 hr indicates the presence of long-lived impurities, perhaps fission products not completely removed during the decontamination procedure. The curve

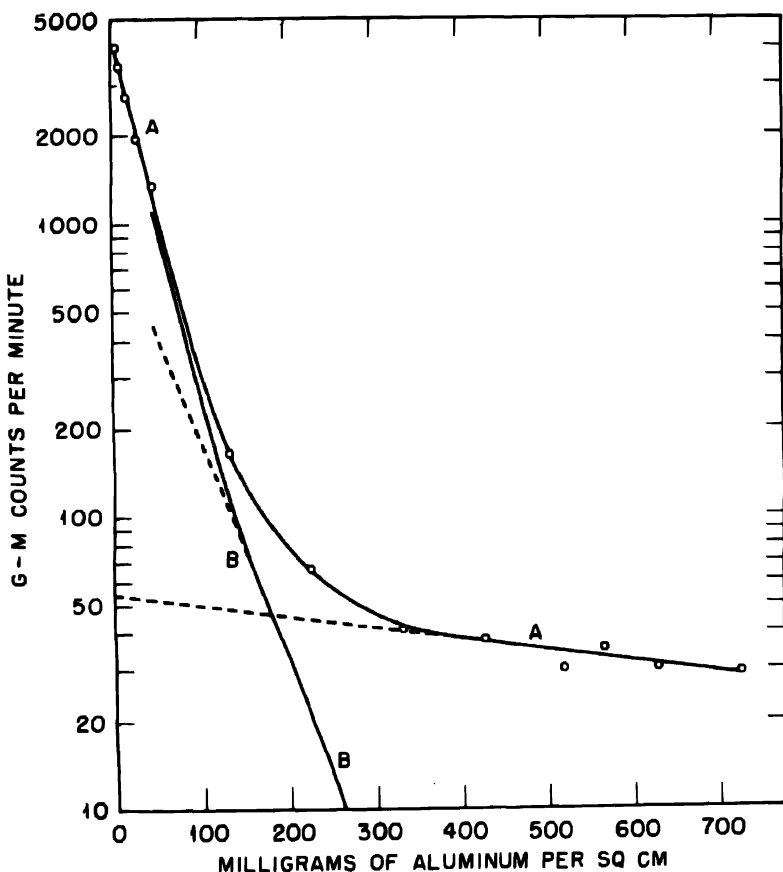


Fig. 4—Aluminum absorption curve of Am<sup>242</sup> radiation. Curve A, uncorrected. Curve B, corrected  $\beta$ -absorption curve (hard component subtracted from curve A).

was not followed long enough to permit a quantitative correction for the long-lived activity or activities. However, a properly corrected curve would presumably show a slope corresponding to a half life somewhat shorter than 17.5 hr.

Figure 4 shows an aluminum absorption curve for a sample prepared from the decontaminated americium after bombardment. A sample of the undecontaminated material yielded an almost identical

curve. The slope of the hard component in Fig. 4, presumably electromagnetic radiation, represents a half thickness of about 620 mg/sq cm, corresponding to an energy of about 0.03 mev. At least part of this radiation is due to Am<sup>241</sup>. The slope of the corrected  $\beta$ -absorption curve suggests the possible presence of more than a single  $\beta$  component. Analysis of the curve by the Feather<sup>10</sup> method does not give very satisfactory results, but it indicates a maximum  $\beta$  range in the neighborhood of 400 mg/sq cm. This corresponds to a maximum  $\beta$ -ray energy of about  $1.0 \pm 0.3$  mev.<sup>11</sup> The activities available were not intense enough to make it feasible to search for more energetic  $\gamma$  radiation.

The ratio of  $\beta$  activity formed in this bombardment to the Cm<sup>242</sup>  $\alpha$  activity formed in the bombardment described in the preceding section is in good agreement with the value calculated for a 16-hr activity decaying to a 150-day activity. The observed ratio after correction for decay and for differences in sample size and bombardment but not for absorption by 7 mg/sq cm of mica and air is 220, in good agreement with the 150-day/16-hr ratio of 225.

The observed half life for  $\beta$  decay of Am<sup>242</sup>, 17.5 hr, agrees with the 16-hr value calculated from the growth of Cm<sup>242</sup>  $\alpha$  activity. Since the apparent  $\beta$  half life was presumably influenced by the presence of a long-lived contaminant, a value of 16 hr ( $\pm 3$  hr maximum error) for the Am<sup>242</sup> half life is the best estimate from these experiments.

Since the completion of the experimental work described here, a very long-lived isomer of Am<sup>242</sup> has been found by Seaborg, James, and Morgan<sup>1</sup> to be produced, in addition to the 16-hr isomer, as a result of neutron capture by Am<sup>241</sup>.

### 3. SUMMARY

$_{95}\text{Am}^{241}$  captures neutrons to yield Am<sup>242</sup>, a  $\beta$  emitter with a half life of  $16 \pm 3$  hr. The maximum  $\beta$  energy for Am<sup>242</sup> is approximately  $1.0 \pm 0.3$  mev.

### ACKNOWLEDGMENT

The authors wish to acknowledge the advice and assistance of A. H. Jaffey, S. G. Thompson, B. B. Weissbourd, and J. W. Britain.

### REFERENCES

1. G. T. Seaborg, R. A. James, and L. O. Morgan, The new element americium (atomic number 95), Paper 22.1, this volume.

2. G. T. Seaborg, R. A. James, and A. Ghiorso, The new element curium (atomic number 96), Paper 22.2, this volume.
3. B. B. Cunningham, The first isolation of americium in the form of pure compounds; microgram-scale observations on the chemistry of americium, Paper 19.2, this volume.
4. S. G. Thompson, L. O. Morgan, R. A. James, and I. Perlman, The tracer chemistry of americium and curium in aqueous solutions, Paper 19.1, this volume.
5. N. D. Erway and O. C. Simpson, unpublished work.
6. B. B. Cunningham, E. R. Tompkins, and S. G. Thompson, private communication.
7. L. B. Werner and D. R. Miller, private communication.
8. A. Ghiorso, A. H. Jaffey, H. P. Robinson, and B. B. Weissbourd, A 48-channel pulse-height analyzer for alpha-energy measurement, Paper 16.8, this volume (Metallurgical Project Report CC-3887).
9. D. L. Hufford and B. F. Scott, Techniques for the preparation of thin films of radioactive material, Paper 18.1, this volume (Metallurgical Project Report CN-3328).
10. N. Feather, Further possibilities for the absorption method of investigating the primary beta particles from radioactive substances, Proc. Cambridge Phil. Soc., 34: 599 (1938).
11. L. E. Glendenin and C. D. Coryell, National Nuclear Energy Series, Division IV, Volume 9, Paper 11.

## Paper 22.8

# PRODUCTS OF HELIUM-ION AND DEUTERON BOMBARDMENT OF U<sup>235</sup> AND U<sup>238</sup>†

By R. A. James, A. E. Florin, H. H. Hopkins, Jr., and A. Ghiorso

### 1. INTRODUCTION

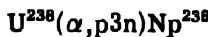
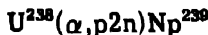
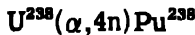
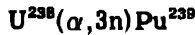
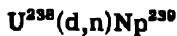
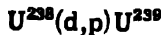
The first bombardments of uranium with deuterons<sup>1</sup> and helium ions<sup>2</sup> showed that fission is produced with both kinds of particles. Later work<sup>3</sup> demonstrated that U<sup>239</sup> and Np<sup>239</sup>, which had also been produced by bombardment of uranium with neutrons,<sup>4</sup> and a 2.0-day  $\beta$  particle-emitting neptunium are produced by the bombardment of uranium‡ with 16-mev deuterons. The same workers<sup>3</sup> showed that this 2.0-day neptunium decays to an  $\alpha$ -emitting isotope of plutonium with a half life of approximately 50 years. It was also shown<sup>5</sup> by bombardment of uranium enriched relative to U<sup>238</sup> that each of these products was largely the result of nuclear reactions of deuterons with U<sup>238</sup>. The yield of the 2.0-day neptunium with deuterons of various energies was measured,<sup>6</sup> and it was concluded that this activity is Np<sup>238</sup> resulting from a (d,2n) reaction on U<sup>238</sup>. A bombardment of uranium with 32-mev helium ions<sup>7</sup> resulted in the formation of Pu<sup>239</sup>, Pu<sup>238</sup>, Np<sup>239</sup>, and Np<sup>238</sup>.

Thus the information available at the time the work reported here was begun can be summarized by the following nuclear reactions

†Contribution from the Department of Chemistry and the Radiation Laboratory, University of California, Berkeley, and from the Chemistry Division of the Metallurgical Laboratory, University of Chicago, now the Argonne National Laboratory.

‡The word "uranium" when referring to target material is to be taken to mean the natural mixture of isotopes.

which had been observed to occur with 16-mev deuterons and 32-mev helium ions.



When sizable quantities of fairly pure U<sup>238</sup> and greatly enriched U<sup>235</sup> became available, it was possible to bombard these isotopes separately. Fortunately, at about this same time J. G. Hamilton and his group at Berkeley modified the 60-in. cyclotron to produce 22-mev deuterons; they were also able to get a rather high current of 44-mev helium ions. Such an increase in energy was expected to cause many other types of reactions; for example, the (d,3n) and (d,4n) reactions might be expected as well as reactions of the type (d,p2n), (d,p3n), etc. With helium ions of 44 mev energy even more excitation energy is available so that a larger number of particles than had previously been observed might be emitted from the compound nucleus before a stable state is reached. The following is a list of the reactions that might be expected in the bombardment of U<sup>238</sup> and U<sup>235</sup> with 22-mev deuterons and 44-mev helium ions.

U <sup>238</sup> (d,n)Np <sup>239</sup> †	U <sup>235</sup> (d,n)Np <sup>236</sup> †
U <sup>238</sup> (d,2n)Np <sup>238</sup> †	U <sup>235</sup> (d,2n)Np <sup>235</sup> †
U <sup>238</sup> (d,3n)Np <sup>237</sup>	U <sup>235</sup> (d,3n)Np <sup>234</sup> †
U <sup>238</sup> (d,4n)Np <sup>236</sup> †	U <sup>235</sup> (d,4n)Np <sup>233</sup>
U <sup>238</sup> (d,p)U <sup>239</sup> †	U <sup>235</sup> (d,p)U <sup>236</sup>
U <sup>238</sup> (d,pn)U <sup>238</sup>	U <sup>235</sup> (d,pn)U <sup>235</sup>
U <sup>238</sup> (d,p2n)U <sup>237</sup> †	U <sup>235</sup> (d,p2n)U <sup>234</sup>

†Reaction has been observed and is reported in this paper.

$U^{238}(d,p3n)U^{235}$	$U^{238}(d,p3n)U^{233}$
$U^{238}(d,\alpha)Pa^{236}$	$U^{238}(d,\alpha)Pa^{233}$
$U^{238}(d,\alpha n)Pa^{235}$	$U^{238}(d,\alpha n)Pa^{232}$
$U^{238}(d,\alpha 2n)Pa^{234}$	$U^{238}(d,\alpha 2n)Pa^{231}$
$U^{238}(\alpha,n)Pu^{241}\dagger$	$U^{238}(\alpha,n)Pu^{235}\dagger$
$U^{238}(\alpha,2n)Pu^{240}\dagger$	$U^{238}(\alpha,2n)Pu^{237}\dagger$
$U^{238}(\alpha,3n)Pu^{239}\dagger$	$U^{238}(\alpha,3n)Pu^{236}\dagger$
$U^{238}(\alpha,4n)Pu^{238}\dagger$	$U^{238}(\alpha,4n)Pu^{235}$
$U^{238}(\alpha,5n)Pu^{237}$	$U^{238}(\alpha,5n)Pu^{234}$
$U^{238}(\alpha,6n)Pu^{236}$	$U^{238}(\alpha,6n)Pu^{233}$
$U^{238}(\alpha,p)Np^{241}$	$U^{238}(\alpha,p)Np^{238}\dagger$
$U^{238}(\alpha,pn)Np^{240}$	$U^{238}(\alpha,pn)Np^{237}$
$U^{238}(\alpha,p2n)Np^{239}\dagger$	$U^{238}(\alpha,p2n)Np^{236}$
$U^{238}(\alpha,p3n)Np^{238}\dagger$	$U^{238}(\alpha,p3n)Np^{235}$
$U^{238}(\alpha,p4n)Np^{237}$	$U^{238}(\alpha,p4n)Np^{234}$
$U^{238}(\alpha,\alpha n)U^{237}\dagger$	$U^{238}(\alpha,\alpha n)U^{234}$
$U^{238}(\alpha,\alpha 2n)U^{236}$	$U^{238}(\alpha,\alpha 2n)U^{233}$

## 2. EXPERIMENTAL WORK

**2.1 Targets.** The targets for bombardment were of several types: (1) metal disks of uranium which fit on the regular target holder inside the chamber of the cyclotron at Berkeley, (2) uranium oxide in a grooved copper or platinum backing that fits into the regular target holder, (3) special small interceptor targets of uranium oxide on platinum in the beam in front of the regular target.

The metal disks are preferred to oxide targets and were used wherever possible. They have the advantages of eliminating losses of target material into the cyclotron chamber and of presenting a pure smooth target for the beam. Also, successive thin layers, constituting

<sup>†</sup>Reaction has been observed and is reported in this paper.

regions where the bombarding particles have progressively decreasing energy, can be milled off and worked up separately to give fractions with varying proportions of individual reaction products. In many respects this procedure is more convenient and flexible than the foil method<sup>4</sup> for determination of excitation curves.

A special holder was constructed for these targets to facilitate the operation of milling off thin layers of the target area. It consisted of a steel block, which could be bolted to the table of a vertical milling machine, for a base. The target was clamped to the base and adjusted so that the surface was as level as possible. The sides and top of the holder were made of lucite to avoid loss of shavings from the milling operation and at the same time allow the operator to see the milling operation. An autoradiograph of the target was made, and the most active area was outlined before the milling operation was begun. After a thin layer, usually 0.001 or 0.002 in., had been milled off the shavings were washed out of the holder into a beaker through a spout provided in the bottom of the holder. After all shavings had been thoroughly washed out another cut was made, care being taken not to include any of the top surface or the burrs pushed up around the edge in the first milling operation. The procedure was repeated until as many layers as were desired had been cut. These layers were then worked up separately as described in the next section.

When oxide targets were used, the material was either scraped off the target with a sharp steel tool and dissolved or dissolved directly off the target plate. This latter method has the disadvantage of sometimes introducing foreign material, such as solder, from the target backing into the solution.

**2.2 Chemical Processing.** The method of chemical separation chosen depends to a large extent upon the element first wanted in pure form. This is usually the element with the shorter-lived isotopes, and in these targets it was generally neptunium. The uranium or uranium oxide is dissolved in nitric acid, and the plutonium and neptunium are reduced to the tripositive and tetrapositive states with sulfur dioxide and precipitated with lanthanum fluoride. This precipitate is then stirred with potassium hydroxide, which converts the lanthanum fluoride to lanthanum hydroxide. After this lanthanum hydroxide has been washed thoroughly, it is dissolved in nitric acid. The neptunium and plutonium are oxidized to the hexapositive state by heating at 80°C for 15 min in 0.2M KBrO<sub>3</sub> solution. Calcium nitrate is then added to make the solution 5M, and the neptunium and plutonium are extracted into a volume of ether approximately equal to the volume of the salt

solution. This ether extract is washed with two successive portions of a 10M  $\text{NH}_4\text{NO}_3$  solution to remove any fission-product activity that was mechanically transferred with the ether from the original salt solution. After the washes, the ether is equilibrated with water, which washes out the neptunium and plutonium. The ether is then put back with the original salt solution, and the process is repeated several times to increase the yield of neptunium and plutonium. After this ether extraction the neptunium and plutonium are contained in the water fraction with only a very small amount of activity from fission products.

Small Kjeldahl flasks are much more convenient than separatory funnels for ether extraction of these small quantities of relatively inactive materials since the ether layer is the one of interest. The aqueous layer is frozen in an acetone-dry ice bath, and the ether is decanted into the next flask.

After the neptunium and plutonium are completely in the water wash, this solution is evaporated down to a small volume, and after reduction of the neptunium and plutonium with sulfur dioxide, lanthanum hydroxide is precipitated. This precipitate is washed to remove all traces of the nitrate ion, and it is then dissolved in a solution of hydrochloric acid.

The plutonium and neptunium are separated from each other by reducing the neptunium to its tetrapositive state, reducing the plutonium to its tripositive state with iodide ion, and extracting the neptunium, after a ten-fold dilution, into a 0.2M solution of thenoyl trifluoroacetone in benzene.

**2.3 Preparation of Plates for Counting.** In preparing plates, hydrochloric acid solution can be evaporated directly onto platinum or glass disks. When extremely thin and uniform plates are desired, as for the pulse analyzer, it is better to electroplate the samples. In these cases the hydrochloric acid solution is evaporated to dryness and dissolved in nitric acid to eliminate the chloride ion. The plutonium is then oxidized to its hexapositive state with potassium persulfate, and it is added to an electrolysis cell containing a bicarbonate-carbonate buffer.<sup>9</sup>

**2.4 Counting Instruments.** For the actual counting of samples a number of different instruments have been used. The  $\alpha$ -particle ranges were determined by means of the pulse analyzer,<sup>10</sup> an instrument which gives pulses of a size proportional to the energy of the particles producing them. These pulses are then sorted electronically according to size into a number of different channels and finally recorded separately on mechanical registers. X-ray and  $\gamma$ -ray energies

were determined by means of absorption curves using various absorber materials. The combination of a 2 g/sq cm beryllium absorber with thin aluminum and lead absorbers has been particularly useful for x rays. Aluminum and lead curves were determined as a matter of general practice, and beryllium, copper, silver, and gold curves have been used when ambiguity existed in interpretation of the results. The x-ray decay curves were generally obtained from the difference in the activity with (1) only a 2 g/sq cm beryllium absorber which allows K and L x rays and  $\gamma$  rays to pass through and (2) a 2 g/sq cm beryllium absorber plus a 100 to 150 mg/sq cm lead absorber, which absorb most of the x rays but only a very small fraction of the moderately hard  $\gamma$  rays.

The  $\alpha$ -particle counters used were the standard 52 per cent geometry type and the argon-CO<sub>2</sub> filled type for fast counting rates. The vacuum low-geometry type was also used occasionally for very active samples.<sup>11</sup>

### 3. RESULTS

3.1 Np<sup>236</sup> and Pu<sup>236</sup>. In the bombardment of uranium with helium ions, a plutonium isotope was observed which emits  $\alpha$ -particles with a range of 4.3 cm of air and decays with a half life of 2.7 years. A helium-ion bombardment of enriched U<sup>235</sup> showed that the isotope is primarily the result of a reaction between the helium ions and U<sup>235</sup>. It was also observed that if the neptunium fraction is isolated fairly soon after bombardment, the 4.3-cm plutonium  $\alpha$  activity grows into it. The amount of this activity produced is quite large as is shown by the following example. Bombardment of 200 mg of U<sup>235</sup> with 540  $\mu$ a-hr of 44-mev helium ions produced  $2.4 \times 10^6$  disintegrations per minute of the 4.3-cm  $\alpha$  activity.

This same activity and its growth was observed when U<sup>235</sup> was bombarded with deuterons. Bombardment of 200 mg of U<sup>235</sup> with 71  $\mu$ a-hr of 22-mev deuterons produced  $3 \times 10^5$  disintegrations per minute of the 4.3-cm  $\alpha$  activity.

A bombardment of U<sup>238</sup> with 22-mev deuterons using the metal disk type of target and the milling technique described above showed that the activity is also produced in small amount in the upper layers by a reaction with U<sup>238</sup>. Figure 1 gives the cross section calculated for the reaction producing this isotope as a function of energy of deuterons. The energy was calculated by using approximations to the stopping power of uranium, and the graphs of energy vs. range given by Holloway and Livingston.<sup>12</sup> The relative values of these cross sections may be considered quite accurate, but the absolute value should be

taken only as an order of magnitude. It may be noted that there is a rapid decrease in the cross section with decrease in energy of the deuterons. The cross section for formation of  $\text{Pu}^{238}$  by the reaction



is plotted in the same figure, and it is observed to be comparatively constant. This rapid decrease in the relative amounts of 4.3-cm

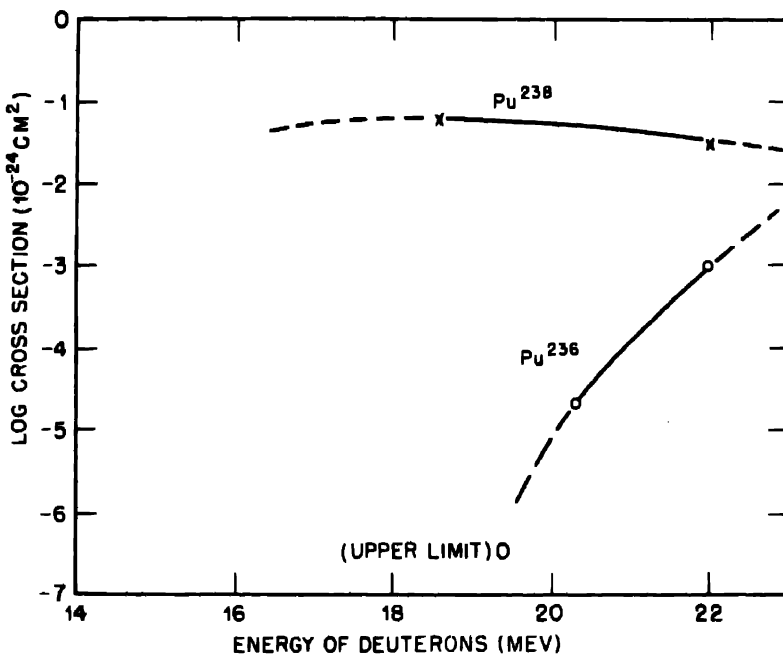


Fig. 1—Cross section for formation of  $\text{Pu}^{238}$  and  $\text{Pu}^{236}$  by deuteron bombardment of  $\text{U}^{238}$  as a function of deuteron energy (log scale used to expand scale).

activity formed indicates that more energy is required for the reaction than for the  $(\text{d},2\text{n})$  reaction and hence that more than two neutrons are emitted from the compound nucleus. The  $(\text{d},3\text{n})$  reaction would give rise to  $\text{Np}^{237}$ , which is known to be a long-lived  $\alpha$  emitter. This then means that the neptunium isotope must have a mass number less than 237.

A fairly large sample ( $8.6 \times 10^5$  disintegrations per minute) of the 4.3-cm  $\alpha$ -emitting plutonium obtained from  $\text{U}^{238}$  bombarded with helium ions was set aside and allowed to decay for 49 days. At the end of that time the sample was divided into two equal parts, and a known

amount of U<sup>233</sup>, to be used as tracer, was added to one part. The uranium was then isolated from each of the two halves, and pulse-analyzer curves were made from the final uranium plates (Fig. 2). These two curves considered together with the amount of U<sup>233</sup> added

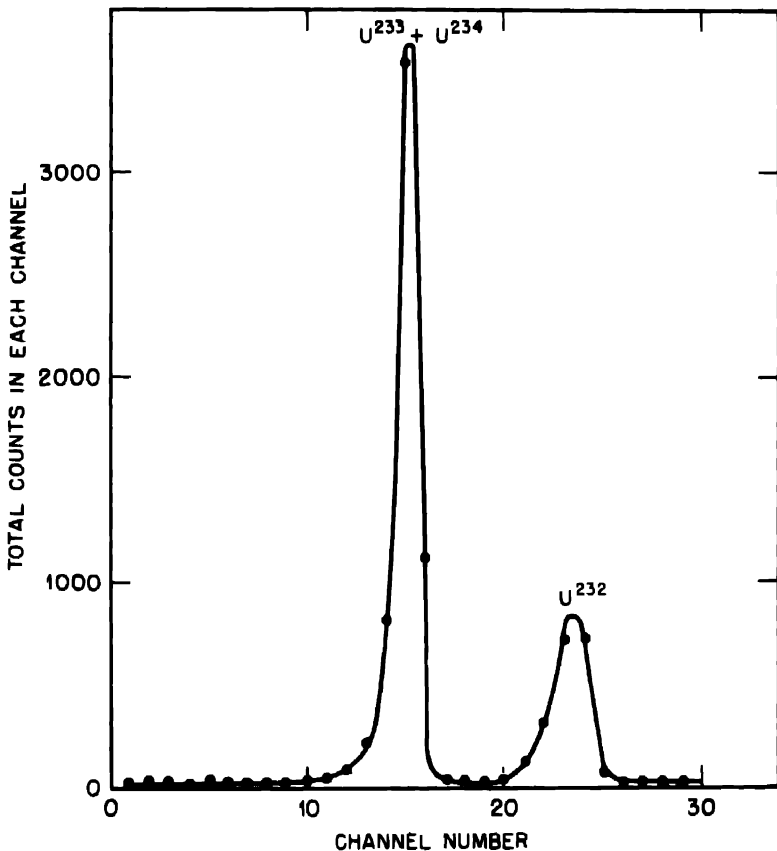


Fig. 2a—Pulse-analysis curve of U<sup>232</sup> isolated from Pu<sup>238</sup> with U<sup>233</sup> tracer; counting time 10 min. From curve, ratio (U<sup>233</sup> + U<sup>234</sup>)/U<sup>232</sup> = 3.46

gave the amount of U<sup>232</sup> that had grown into the plutonium sample and allowed a correction to be made for the amount of U<sup>234</sup> originally present in the plutonium and for the losses in chemical separations. The data were as follows: 278 counts per minute of U<sup>232</sup> grew from  $2.15 \times 10^8$  counts per minute of Pu<sup>238</sup> in 49 days. The half-life of U<sup>232</sup> was calculated from these facts to be 70 years. This value is believed to be more accurate than the value of 30 years obtained previously.<sup>13</sup>

The isolation of  $U^{232}$  as the daughter then definitely establishes these isotopes as  $Np^{238}$  and  $Pu^{238}$ .

The half life of  $Np^{238}$  has been measured in two ways:

1. The neptunium fraction from a bombardment of  $U^{235}$  with helium ions was isolated free of plutonium, and the growth of  $\alpha$  particles into

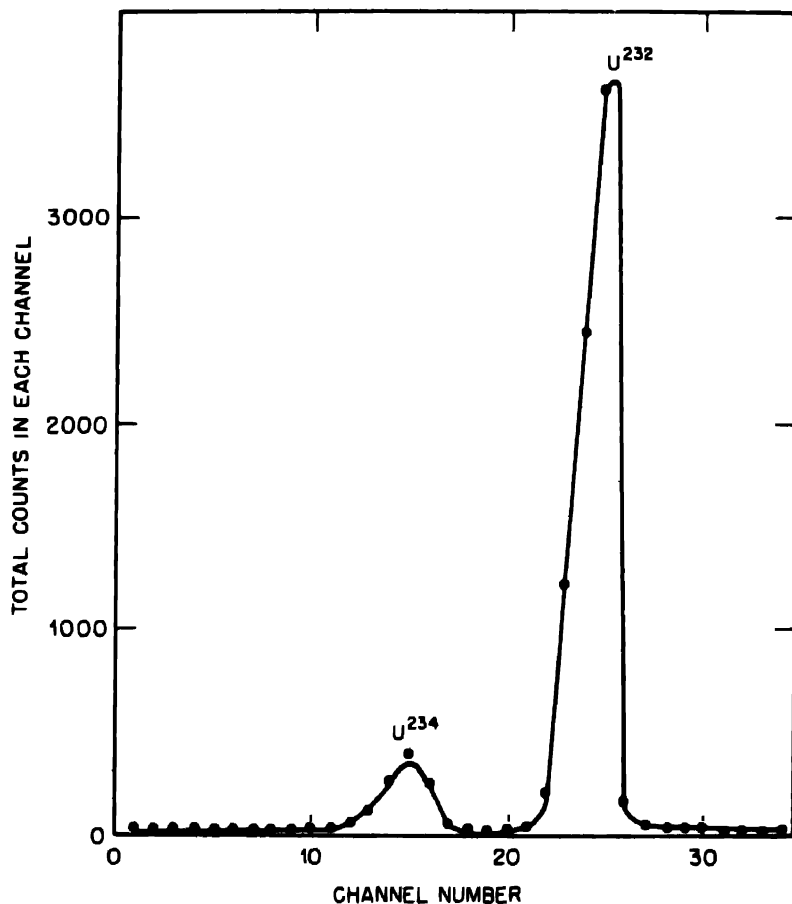


Fig. 2b—Pulse-analysis curve of  $U^{232}$  isolated from  $Pu^{238}$ , no  $U^{233}$  tracer added; counting time 40 min. From curve, ratio  $U^{232}/U^{234} = 7.30$

this fraction was observed (see Fig. 3). The sample also contained  $Np^{238}$  and  $Np^{239}$ ; therefore  $Pu^{238}$  and  $Pu^{239}$  were also growing into the sample. After the growth was essentially completed, a pulse-analyzer curve was taken to establish how much  $Pu^{238}$ ,  $Pu^{239}$ , and  $Pu^{236}$  had grown. It was found that 88 per cent of the growth was due to  $Pu^{238}$ .

and 12 per cent was due to Pu<sup>238</sup>, the amount of Pu<sup>239</sup> being negligible. The half life of Np<sup>238</sup> calculated from these data is 22 hr (Fig. 4).

2. A sample of the same neptunium fraction was followed on a

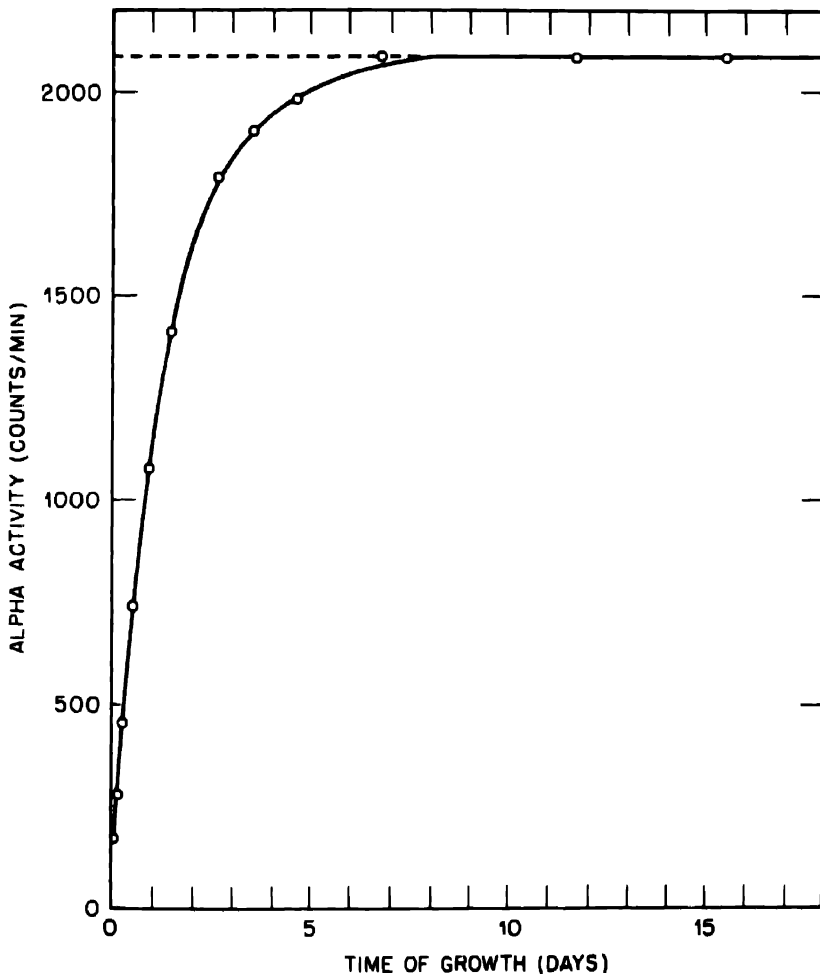


Fig. 3—Growth of Pu<sup>238</sup> from Np<sup>238</sup> (pulse analysis at 20 days; 12 per cent Pu<sup>238</sup>, 88 per cent Pu<sup>239</sup>).

Geiger-Mueller counter through several half lives and then resolved into the various components. After subtraction of the Np<sup>238</sup> and Np<sup>239</sup> a component remained with a half life of 21 hr, in reasonable agreement with the 22-hr value obtained from the growth curve.

Unfortunately, all samples of Np<sup>238</sup> obtained so far contained preponderantly the isotopes Np<sup>238</sup> and Np<sup>239</sup>, so it has not been possible

to determine the characteristics of the radiations from  $\text{Np}^{238}$  with any certainty. Qualitatively it can be said that the maximum energy of the  $\beta$  particles is between 0.1 and 1.2 mev. There seems to be a fair number of soft  $\gamma$  rays in the range 0.1 to 0.5 mev, but there appears

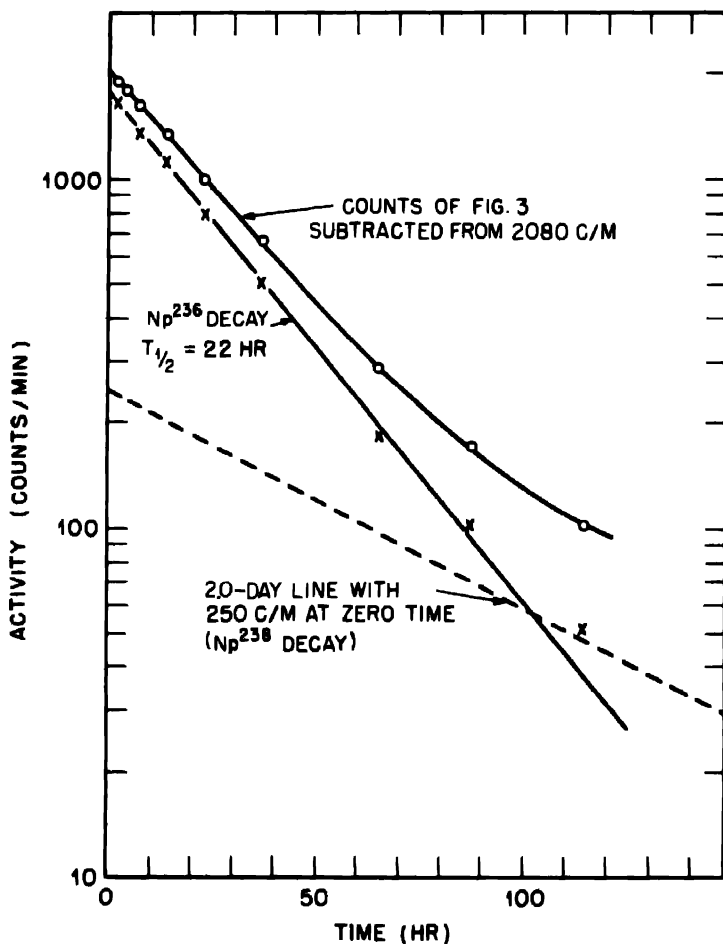


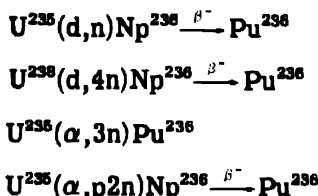
Fig. 4—Resolution of Fig. 3 into components.

to be none or at most a small number with an energy greater than 1 mev.

Several samples of  $\text{Pu}^{238}$  have been followed for  $\alpha$  decay to determine its half life. Two kinds of samples are available for such measurements, and both have disadvantages: (1) samples of the original plutonium fraction from  $\text{U}^{238}$  targets bombarded with helium ions, and

(2) samples which are known to have grown from neptunium. The first kind consist almost entirely of 4.3-cm range  $\alpha$  activity, but they may be complicated by  $\alpha$  particles from Pu<sup>237</sup> (see section on Pu<sup>237</sup>). The second kind could not have Pu<sup>237</sup>, but they do contain a considerable percentage of Pu<sup>238</sup> so that the accuracy of the half life determined depends on the accuracy with which this percentage is known. From measurements on both types of samples, the best value for this half life is considered to be  $2.7 \pm 0.3$  years.

The reactions by which these isotopes are produced with 22-mev deuterons and 44-mev helium ions are



and probably



and



They have also been produced by<sup>14</sup>



and<sup>15</sup>



**3.2 Np<sup>235</sup>.** Even with the lower-energy deuterons (16 mev) before the cyclotron had been improved, small amounts of a new neptunium activity were observed in uranium targets bombarded with deuterons. This activity decays by the emission of characteristic K and L x rays with a half life of approximately  $400 \pm 20$  days.

Deuteron bombardments of U<sup>235</sup> produced much more of this activity (71  $\mu$ a-hr of 22-mev deuterons produced 1,200 counts per minute through 10 mg of absorber at 28 per cent geometry). The activity is not produced by the bombardment of U<sup>238</sup> with deuterons,<sup>16</sup> but it is produced in helium-ion bombardments of U<sup>238</sup>.<sup>15</sup> It seems quite cer-

tain that  $\text{Np}^{238}$  is the correct isotopic assignment and that the following reactions are responsible for its production:



and probably



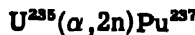
No positron emission or annihilation radiation accompanies the characteristic x rays, so it is probable that the mode of decay is electron capture.

**3.3  $\text{Pu}^{237}$ .** By the bombardment of uranium with helium ions, a plutonium isotope was formed that emits x rays with energies characteristic of an element in this region and that decays with a half life of about 40 days. The same activity was also found to be produced by the bombardment of  $\text{U}^{238}$  with helium ions, and the relative amount was such as to show that this activity was primarily the result of a nuclear reaction involving the  $\text{U}^{238}$ . A bombardment of 200 mg of  $\text{U}^{238}$  with 541  $\mu\text{a}\cdot\text{hr}$  of 44-mev helium ions produced  $1.2 \times 10^4$  K x-ray counts per minute at 10 per cent geometry. The counting efficiency is believed to be about 0.5 per cent, which would give a cross section of 0.003 barn for the formation of this isotope.

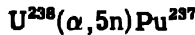
A sample of this 40-day activity was allowed to decay for about one half life, and then the neptunium fraction was isolated from the sample. If the x rays were due to  $\text{Pu}^{238}$ , then the decay of the sample would have been expected to produce several thousand x-ray counts per minute of  $\text{Np}^{238}$ ; but if the 40-day x rays were due to  $\text{Pu}^{237}$ , only about 0.05  $\alpha$  counts per minute of  $\text{Np}^{237}$  would have grown. No activity of any kind was found, indicating that the 40-day x rays are probably due to  $\text{Pu}^{237}$ . Another piece of evidence that also points to  $\text{Pu}^{237}$  being the correct assignment is the fact that none of this activity is observed when  $\text{U}^{238}$  is bombarded with helium ions.<sup>16</sup>

No  $\gamma$  rays nor positrons were found with this 40-day x-ray activity, so it is probable that  $\text{Pu}^{237}$  decays by orbital electron capture. Since all samples in which  $\text{Pu}^{237}$  has been found also contain a large amount of  $\alpha$  activity from  $\text{Pu}^{238}$  and a small amount from  $\text{Pu}^{239}$ , the  $\alpha$  branching of  $\text{Pu}^{237}$  has not been established. This is especially true if the range of  $\text{Pu}^{237}$   $\alpha$  particles happens to be quite close to the range of either  $\text{Pu}^{238}$  or  $\text{Pu}^{239}$ .

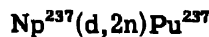
The nuclear reactions responsible for the production of Pu<sup>237</sup> in these bombardments are



and probably



Pu<sup>237</sup> is also formed<sup>14</sup> in the deuteron bombardment of Np<sup>237</sup> by the reaction

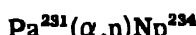
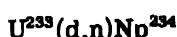


**3.4 Np<sup>234</sup>.** In the bombardment of U<sup>235</sup><sup>†</sup> with deuterons, an examination of the neptunium fraction revealed that there was a large excess of hard  $\gamma$  rays. That is, the ratio of  $\gamma$  rays to  $\beta$  particles was several times as high as is found in pure Np<sup>238</sup>, and it was higher still when consideration was given to the fact that the sample contained some Np<sup>239</sup>, which does not have a hard  $\gamma$  ray. The decay curve of the hard  $\gamma$  rays showed that they were a mixture of the 2.0-day Np<sup>238</sup>  $\gamma$  and a new activity with a half life of approximately 4.5 days.

The same activity has been produced in a purer form by the bombardment of U<sup>238</sup> with deuterons<sup>15</sup> and the bombardment of Pa<sup>231</sup> with helium ions.<sup>17</sup> It has been given the assignment Np<sup>234</sup> although it may possibly be Np<sup>233</sup>. With purer samples investigators<sup>15, 17</sup> were able to show that characteristic x rays accompany the  $\gamma$  ray, that the energy of the  $\gamma$  ray is 1.85 mev, and that a more accurate value of the half life is 4.44 days.

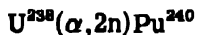
It has been assumed that the mode of decay is electron capture since no positron emission or annihilation radiation was detected. The experimental methods of looking for these types of radiation were, however, very insensitive; and it is possible that at least a small percentage of the decay is by positron emission.

This isotope is produced by the reactions



<sup>†</sup>The "U<sup>235</sup>" contained approximately 13 per cent of U<sup>238</sup>, which was the source of the Np<sup>238</sup> and Np<sup>239</sup>.

**3.5  $\text{Pu}^{240}$ .** The first evidence for the isotope  $\text{Pu}^{240}$  was that reported by Chamberlain, Farwell, and Segré.<sup>18</sup> It was possible to predict on the basis of known nuclear-reaction yields that  $\text{Pu}^{240}$  should be produced by the bombardment of  $\text{U}^{238}$  with high-energy helium ions by the reaction



with a yield comparable to the yield of  $\text{Pu}^{239}$  which is produced by the reaction



However, in targets bombarded with 36-mev helium ions no plutonium  $\alpha$  activity with a range different from those of the known isotopes was found. It was observed that the amount of activity at the  $\text{Pu}^{239}$  range was several times that expected from the known yields of the  $(\alpha, 3n)$  reaction and that this peak was noticeably broadened on the low-energy side. It was therefore concluded that this excess of  $\alpha$  particles was due to  $\text{Pu}^{240}$ , which emits  $\alpha$  particles with an energy very close to but slightly less than those of  $\text{Pu}^{239}$ . On the basis of this broadening, the range was taken as 3.60 cm of air; and from the yield of these  $\alpha$  particles the half life of  $\text{Pu}^{240}$  was estimated to be approximately 6,000 years.

**3.6  $\text{Pu}^{241}$ .** The plutonium fraction of uranium targets bombarded with helium ions shows a soft  $\beta$ -particle activity corresponding to the  $\text{Pu}^{241}$  decay. This is discussed in another paper in this volume.<sup>18</sup> The reaction responsible for the production of this isotope by helium ion bombardment is



**3.7  $\text{U}^{237}$ .** It has been observed that  $\text{U}^{237}$  is produced by the bombardments of  $\text{U}^{238}$  with both deuterons and helium ions. The yields are too high to be accounted for by an  $(n, 2n)$  reaction produced by the fast neutrons present in such bombardments, so it is believed that the reactions responsible are  $\text{U}^{238}(\alpha, \alpha n)\text{U}^{237}$  and  $\text{U}^{238}(d, p2n)\text{U}^{237}$ . In the upper layer of a target bombarded with 22-mev deuterons or 44-mev helium ions these reactions have yields comparable to the other prolific reactions such as  $(d, 2n)$  and  $(\alpha, 3n)$ .

**3.8 Other Isotopes and Reactions.** Again referring to the list of reactions given in the introduction, there are some reactions which have not been observed and some unknown isotopes which should have

been produced but have, so far, escaped detection. These reactions and products fall into two main classes.

1. Those in which the product is known or believed to be long lived so that not enough activity was produced to be observed easily. These include Np<sup>237</sup>, U<sup>236</sup>, and U<sup>233</sup> as well as those identical with the target material, i.e., U<sup>238</sup>, U<sup>235</sup>, and U<sup>234</sup>.

Table 1—Summary of the Isotopes of Neptunium and Plutonium

Z	Isotope	Type of radiation	Half life	Energy of radiation particles	$\gamma$ , mev
93	Np <sup>234</sup> or Np <sup>233</sup>	E.C., $\gamma$	4.5 days	Soft e <sup>-</sup>	1.8
	Np <sup>235</sup>	E.C.	~400 days	Soft e <sup>-</sup>	None
	Np <sup>236</sup>	$\beta^-$	22 hr	>0.1 and < 1.2	?
					(<1 mev if present)
	Np <sup>237</sup>	$\alpha$	$2.20 \times 10^6$ years	4.73	?
	Np <sup>238</sup>	$\beta^-$	2.0 days	1.0	1.1
					1.3
94	Np <sup>239</sup>	$\beta^-$	2.33 days	0.70	0.22, 0.27
	Pu <sup>236</sup>	$\alpha$	2.7 years	5.7	?
	Pu <sup>237</sup>	E.C.	40 days	Soft e <sup>-</sup>	None
	Pu <sup>238</sup>	$\alpha$	90 years	5.57	?
	Pu <sup>239</sup>	$\alpha$	$2.44 \times 10^4$ years	5.15	0.05
					0.03
	Pu <sup>240</sup>	$\alpha$	~6,000 years	5.1	?
	Pu <sup>241</sup>	$\beta^-$ ( $\alpha$ 0.002 %)	~10 years	<0.1 mev ( $\alpha$ ?)	?

2. The time that elapsed between the shutdown of the cyclotron and the separation and examination of the separate chemical fractions was usually about 36 hr. This means that any activities with half lives shorter than 12 or 15 hr would probably not have been detected. It is quite probable that most of the remaining isotopes, Np<sup>233</sup>, Np<sup>240</sup>, Np<sup>241</sup>, Pu<sup>235</sup>, Pu<sup>234</sup>,† Pu<sup>233</sup>, and Np<sup>232</sup> fall within this class.

The following table gives the isotopes of neptunium and plutonium produced by these bombardments and their radioactive properties.

#### ACKNOWLEDGMENTS

We wish to acknowledge the assistance of Dr. G. T. Seaborg, who suggested the problem and aided in the interpretation of many of the

† Since this paper was written radiations ascribed to Pu<sup>234</sup> have been found.<sup>18,19</sup>

results. We also wish to thank Dr. J. G. Hamilton and his associates, who performed the bombardments in the Berkeley 60-in. cyclotron.

#### 4. SUMMARY

In addition to the well-known isotopes of neptunium and plutonium— $\text{Pu}^{238}$ ,  $\text{Pu}^{239}$ ,  $\text{Np}^{237}$ ,  $\text{Np}^{238}$ , and  $\text{Np}^{239}$ —several more isotopes of these elements have been produced.

$\text{Np}^{236}$  is a  $\beta$ -particle emitter with a half life of 22 hr. Its daughter,  $\text{Pu}^{236}$ , emits  $\alpha$  particles with a range of 4.3 cm (energy 5.7 mev); it decays with a half life of 2.7 years.  $\text{Np}^{235}$  decays by orbital-electron capture with a half life of approximately  $400 \pm 20$  days. A plutonium isotope that decays by orbital-electron capture with a half life of 40 days has been assigned the mass number 237. A neptunium isotope ( $\text{Np}^{234}$  or  $\text{Np}^{233}$ ) has been found which decays by orbital-electron capture with a half life of about 4.5 days; its characteristic x rays are accompanied by a  $\gamma$  ray with an energy of 1.8 mev.

$\text{U}^{237}$ ,  $\text{Pu}^{240}$ , and  $\text{Pu}^{241}$  are also produced in these bombardments.

#### REFERENCES

1. D. H. T. Gant, *Nature*, 144: 707 (1939).
2. E. Fermi and E. Segrè, *Phys. Rev.*, 56: 680 (1941).
3. G. T. Seaborg, E. M. McMillan, A. C. Wahl, and J. W. Kennedy, A new element: Radioactive element 94 from deuterons on uranium, Papers 1.1a and 1.1b, this volume; *Phys. Rev.*, 69: 366-367 (1946) (submitted Jan. 28, 1941); G. T. Seaborg, A. C. Wahl, and J. W. Kennedy, Nuclear properties of  $94^{238}$  and  $93^{238}$ , Paper 1.4, this volume; *Phys. Rev.*, 69: 367 (1946) (submitted Mar. 7, 1941).
4. E. M. McMillan and P. H. Abelson, *Phys. Rev.*, 57: 1185 (1940).
5. J. W. Kennedy, M. L. Perlman, E. Segrè, and A. C. Wahl, Formation of the 50-year element 94 from deuteron bombardment of  $\text{U}^{238}$ , Paper 1.9, this volume.
6. S. G. English and R. A. James, private communication (1942).
7. L. B. Magnusson and A. Ghiorso, private communication (1944).
8. L. B. Magnusson, J. C. Hindman, and T. J. LaChapelle, unpublished work.
9. J. W. Britain, unpublished work.
10. A. Ghiorso, A. H. Jaffey, H. P. Robinson, and B. Weissbourd, A 48-channel pulse-height analyzer for alpha-energy measurements, Paper 16.8, this volume (Metallurgical Project Report CC-3887).
11. A. H. Jaffey, T. P. Kohman, and J. A. Crawford, Metallurgical Project Report CC-1802 (March 1944).
12. M. G. Holloway and M. S. Livingston, *Phys. Rev.*, 54: 18 (1938).
13. J. W. Gofman and G. T. Seaborg, Production and properties of  $\text{U}^{233}$  and  $\text{Pa}^{232}$ , Paper 19.14, this volume.
14. R. A. James, S. G. Thompson, and H. H. Hopkins, Jr., Bombardment of  $\text{Np}^{237}$  with deuterons and helium ions, Paper 22.16, this volume.
15. E. K. Hyde, M. H. Studier, and A. Ghiorso, Products of the deuteron and helium-ion bombardments of  $\text{U}^{238}$ , Paper 22.15, this volume (Metallurgical Project Report CB-3736).

16. O. Chamberlain, G. W. Farwell, E. Segrè, private communication (September 1944).
17. D. Osborne, R. C. Thompson, and Q. Van Winkle, Products of the deuteron and helium-ion bombardments of Pa<sup>231</sup>, Paper 19.11, this volume.
18. G. T. Seaborg, R. A. James, and L. O. Morgan, The new element americium (atomic number 95), Paper 22.1, this volume.
19. I. Perlman, P. R. O'Connor, and L. O. Morgan, The bombardment of U<sup>233</sup> with 44-mev helium ions and the formation of Pu<sup>234</sup>, Paper 22.30, this volume (Argonne National Laboratory Report ANL-4049).

Paper 22.15

PRODUCTS OF THE DEUTERON AND HELIUM-ION  
BOMBARDMENTS OF U<sup>233</sup>†

By E. K. Hyde, M. H. Studier, and A. Ghiorso

1. INTRODUCTION

The bombardment of U<sup>238</sup> with energetic deuterons and helium ions has been extensively used for the preparation and study of the heavier isotopes of neptunium and plutonium. Plutonium was, in fact, discovered<sup>2</sup> in the products of a deuteron bombardment of U<sup>238</sup>. The bombardment of lighter isotopes of uranium with such ions is an excellent way to produce the lighter isotopes of neptunium and plutonium, which have received no study until recently. The availability of samples of uranium highly enriched in U<sup>235</sup> and of nearly pure U<sup>233</sup> has made it possible to carry out such studies. The results of the bombardment of U<sup>233</sup> with deuterons and helium ions are described elsewhere.<sup>1</sup> In this report the neptunium and plutonium isotopes produced by cyclotron bombardments of U<sup>233</sup> are discussed. It was possible to draw several conclusions from a correlation of the results of the two sets of bombardments.

Three 10-mg samples of U<sup>233</sup> in the form U<sub>3</sub>O<sub>8</sub> were bombarded in the 60-in. cyclotron at Berkeley.‡ Two of the samples, one of which contained 4 per cent and the other of which contained 2 per cent of natural uranium impurity, were bombarded with 44-mev helium ions for 30 and 93  $\mu$ a-hr, respectively. The third sample, containing 4 per cent natural-uranium impurity, was bombarded with 22-mev deuterons

† Contribution from the Department of Chemistry and the Radiation Laboratory, University of California, Berkeley, and from the Chemistry Division of the Metallurgical Laboratory, University of Chicago, now the Argonne National Laboratory.

‡ This was carried out with the kind cooperation of Dr. J. G. Hamilton's cyclotron group.

for 322  $\mu$ a-hr. The target material in all cases was mounted on a small water-cooled platinum "interceptor" target inserted in the center of the cyclotron beam.

After bombardment the irradiated material was put through an extensive series of chemical operations to isolate in a pure state the various fractions of major interest.

Previous experience on bombardments with 44-mev helium ions and 22-mev deuterons had indicated what types of nuclear transformations would occur. Figure 1 indicates what neptunium, plutonium, and uranium isotopes were expected to be produced in the bombardment of U<sup>233</sup> (and of its main impurity, U<sup>238</sup>). The primary nuclear reaction producing an isotope is indicated in the lower right-hand corner of each isotope square. Broken lines around a square indicate that the isotope was unknown at the time these studies were begun. In addition to the known isotopes listed in Fig. 1 three other isotopes of unknown mass assignment had been observed in U<sup>238</sup> bombardments. These included two orbital-electron-capturing neptunium isotopes with half lives of 8.3 months and of approximately 5 days whose mass assignment could be limited to 233, 234, and 235 and a 40-day orbital-electron-capturing plutonium isotope that was either Pu<sup>237</sup> or Pu<sup>238</sup>.

The facts that were discovered about the nature of these unknown and uncertain isotopes by a study of the U<sup>233</sup> bombardments will now be presented.

## 2. DEUTERON BOMBARDMENT OF U<sup>233</sup>

The purified neptunium fraction from the deuteron bombardment had considerable  $\beta$  activity representing a mixture of Np<sup>238</sup>, Np<sup>239</sup>, and Np<sup>236</sup>. No new  $\beta$  activity could be resolved out of this mixture, nor could any  $\alpha$  activity be detected other than that of the Pu<sup>238</sup> and Pu<sup>236</sup> growing in from their neptunium parents.

A very considerable amount of x-ray activity was found. This x-ray activity consisted principally of a  $4.40 \pm 0.05$  day activity with no evidence even in very active samples for any longer-lived x-ray activity (see Fig. 2). There were some x rays of half life less than 4.4 days, but these may well have resulted from Np<sup>238</sup>, Np<sup>239</sup>, and Np<sup>236</sup>; whether they indicated an unknown neptunium isotope could not be determined. As mentioned above an x-ray activity of approximately 4 to 5 days half life was also observed in bombardments of U<sup>238</sup> with 22-mev deuterons.<sup>1</sup> The only neptunium isotopes that would be produced in both bombardments are Np<sup>234</sup> and Np<sup>233</sup>, but no direct evidence was immediately available for choosing between them. Orbital-electron capture by Np<sup>234</sup> or Np<sup>233</sup> would lead to the  $2.69 \times 10^5$  year  $\alpha$ -emitting U<sup>234</sup>

Np <sup>231</sup>	Np <sup>232</sup>	Np <sup>233</sup>	Np <sup>234</sup>
(d, 4n)	(d, 3n)	(d, 2n)	(d, n)
U <sup>231</sup> 4.1 days K capture (d,p3n)	U <sup>232</sup> 70 years α (d,p2n)	U <sup>233</sup> $1.62 \times 10^4$ years α (d,pn)	U <sup>234</sup> $2.69 \times 10^8$ years α (d,p)

(a)

Np <sup>230</sup> 22 hr β <sup>-</sup> (d, 4n)	Np <sup>231</sup> $2.25 \times 10^6$ years α (d, 3n)	Np <sup>232</sup> 2.0 days β <sup>-</sup> (d, 2n)	Np <sup>233</sup> 2.33 days β <sup>-</sup> (d, n)
U <sup>230</sup> α (d,p3n)	U <sup>231</sup> 6.8 days β <sup>-</sup> (d,p2n)	U <sup>232</sup> $4.51 \times 10^8$ years α (d,pn)	U <sup>233</sup> 23.5 min β <sup>-</sup> (d,p)

(b)

Products Expected from the Bombardment of (a) U<sup>233</sup> and (b) the U<sup>233</sup> Impurity with 22-mev Deuterons

Pu <sup>231</sup> (α, 6n)	Pu <sup>232</sup> (α, 5n)	Pu <sup>233</sup> (α, 4n)	Pu <sup>234</sup> (α, 3n)	Pu <sup>235</sup> (α, 2n)	Pu <sup>236</sup> 2.7 years α (α, n)
Np <sup>231</sup> (α, p5n)	Np <sup>232</sup> (α, p4n)	Np <sup>233</sup> (α, p3n)	Np <sup>234</sup> (α, p2n)	Np <sup>235</sup> (α, pn)	Np <sup>236</sup> 22 hr β <sup>-</sup> (α, p)

(a)

Pu <sup>230</sup> 2.7 years α (α, 6n)	Pu <sup>231</sup> (α, 5n)	Pu <sup>232</sup> 110 years α (α, 4n)	Pu <sup>233</sup> $2.43 \times 10^4$ years α (α, 3n)	Pu <sup>234</sup> ~6000 years α (α, 2n)	Pu <sup>235</sup> ~10 years β <sup>-</sup> (α, n)
Np <sup>230</sup> 22 hr β <sup>-</sup> (α, p6n)	Np <sup>231</sup> $2.25 \times 10^6$ years α (α, p5n)	Np <sup>232</sup> 2.0 days β <sup>-</sup> (α, p3n)	Np <sup>233</sup> 2.33 days β <sup>-</sup> (α, p2n)	Np <sup>234</sup> (α, pn)	Np <sup>235</sup> (α, p)

(b)

Products Expected from the Bombardment of (a) U<sup>233</sup> and (b) the U<sup>233</sup> Impurity with 44-mev Helium Ions

Fig. 1.—Products expected from the bombardment of U<sup>233</sup> (a) and the U<sup>233</sup> impurity (b) with 22-mev deuterons; and products expected from the bombardment of U<sup>233</sup> (a) and the U<sup>233</sup> impurity (b) with 44-mev helium ions.

or the  $1.62 \times 10^5$   $\alpha$ -emitting U<sup>233</sup>, both of which are so long lived that no  $\alpha$  growth would be detected in the decay of the neptunium samples available. A preliminary assignment of the 4.4-day activity to Np<sup>234</sup><sup>†</sup> was made on the basis of theoretical considerations of O. C. Simpson

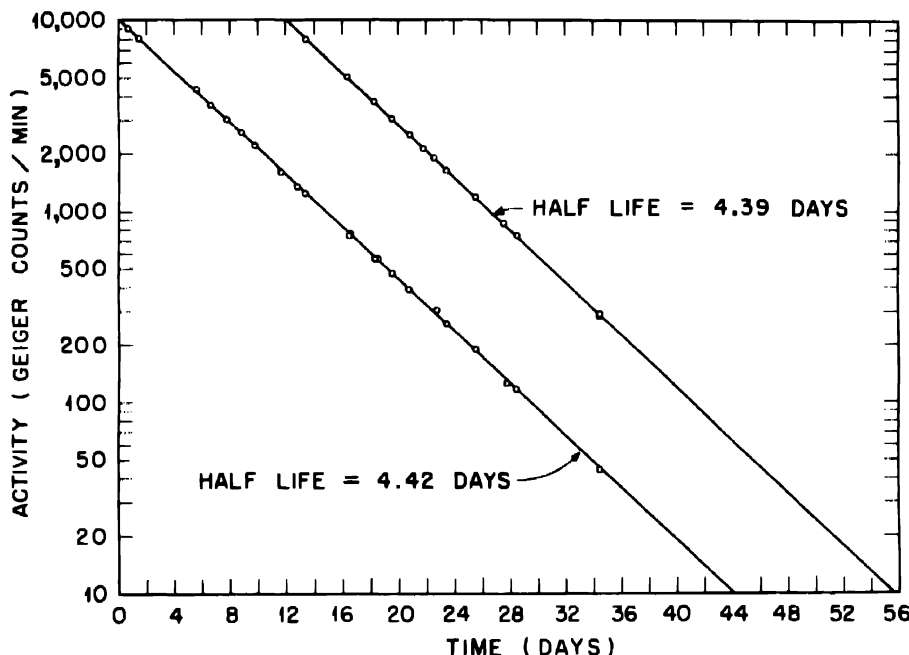


Fig. 2—Decay of x rays and  $\gamma$  radiation in the neptunium fraction from the deuteron bombardment of U<sup>233</sup>. Upper curve represents decay measured through 2 g per square centimeter of beryllium absorber. Lower curve represents decay measured through 1 g per square centimeter of beryllium plus 8 g per square centimeter of lead absorber.

and T. P. Kohman concerning the unlikelihood that Np<sup>233</sup> would have a  $\gamma$  ray as energetic (1.9 mev) as that which accompanied the x rays (see below).

The decay of x ray plus  $\gamma$  activity of the neptunium fraction as measured through 2 g of beryllium absorber (to cut out the  $\beta$  radiation) in a xenon-alcohol filled Geiger-Mueller tube is shown in Fig. 2. Figure 2 also shows the decay through 1 g of beryllium (to cut out  $\beta$  radiation) plus 8 g of lead absorber (to cut out x rays). The identity

<sup>†</sup>Later work by Hyde, Bentley, Hagemann, and Wagner, as yet unpublished, on the fission cross section associated with the 4.4-day activity indicated that it was very probably due to Np<sup>234</sup>. Hence the nuclear reaction involved in its formation is U<sup>233</sup>(d,n)Np<sup>234</sup>.

of the half life for decay in the two cases indicates that the  $\alpha$  radiation and the  $\gamma$  radiation resulted from the same isotope.

The energy of the energetic  $\gamma$  ray was determined from a lead absorption curve (Fig. 3) made on a sample after the  $\beta$  activity had

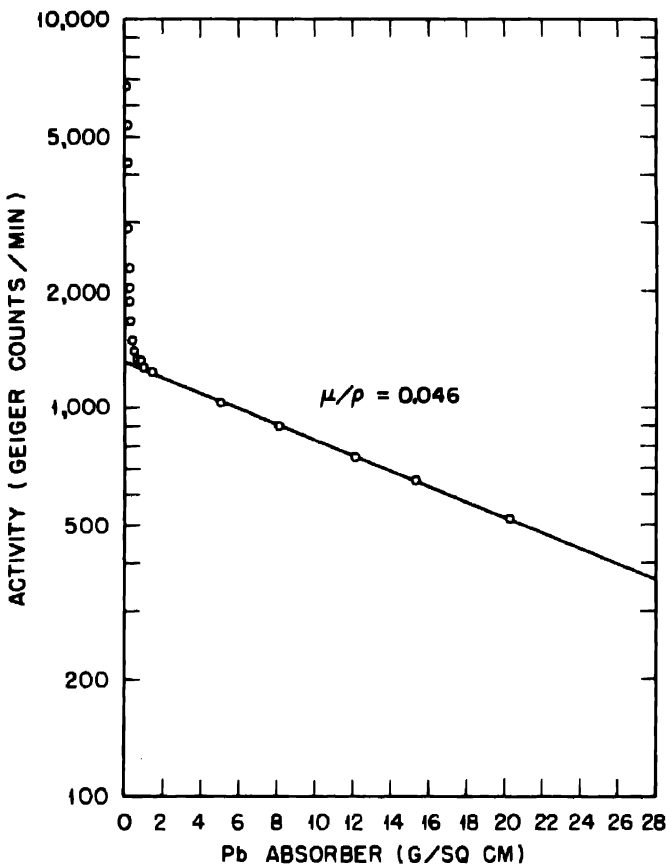


Fig. 3—Lead-absorption curve for  $\gamma$  radiation (hard region) accompanying the 4.40-day neptunium isotope.

almost completely decayed. The Geiger-Mueller tube was an argon-alcohol filled end-window tube,<sup>3</sup> wrapped in lead, except for the window, in order to cut out scattered radiations. The sample was placed on the second shelf; the absorbers were placed immediately below the window. A mass absorption coefficient of 0.0458 corresponding to an energy of 1.9 mev<sup>4</sup> was obtained for the most energetic radiation.

The resolution of the lead absorption curve in the low-energy region by subtracting out the 1.9-mev component (Fig. 4) revealed a

second component with a mass absorption coefficient of 6.3 corresponding to an energy of 96 kev, which is about the correct energy for a K  $\alpha$  ray of uranium.

With somewhat less certainty a third component could be resolved.

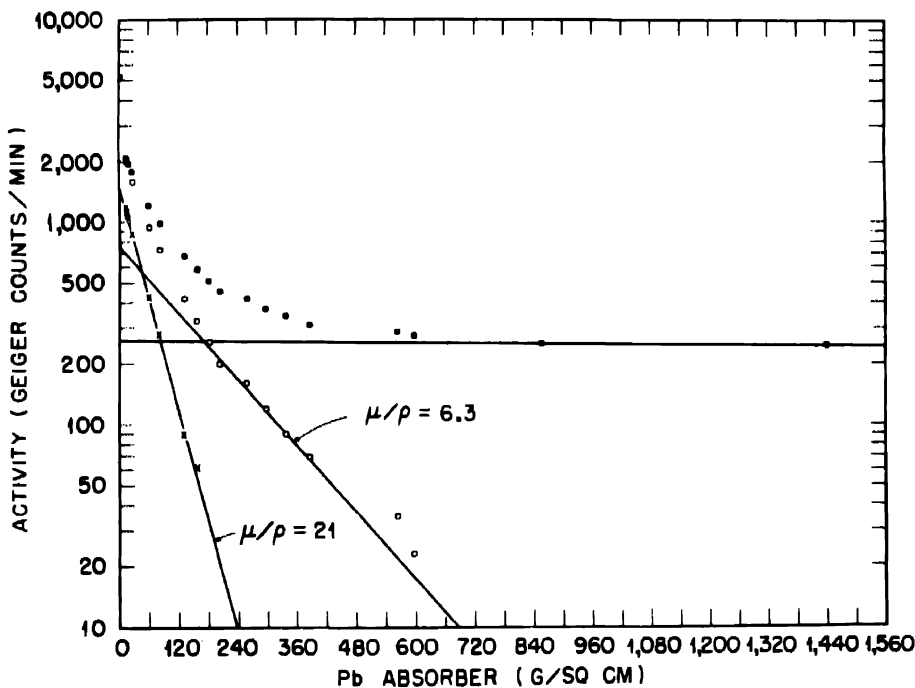


Fig. 4—Lead-absorption curve (soft region) for the 4.40-day neptunium isotope.

The mass absorption coefficient of this radiation was 21. The nature and origin of this radiation has not been completely determined as yet.

The ratio of experimentally observed counts of electromagnetic radiation of 96 kev energy to the counts of the 1.9-mev  $\gamma$  ray varied from 2.9 to 1 in a xenon-alcohol filled tube to 2.4 to 1 as measured in an argon-alcohol filled tube. Considering that  $\alpha$  rays count less efficiently than  $\gamma$  rays (about 0.5 per cent as compared to about 3 per cent in this case), it is evident that there cannot be 1  $\gamma$  ray emitted per K  $\alpha$  ray.

The cross section of the nuclear reaction producing Np<sup>234</sup> was calculated to be approximately  $2 \times 10^{-26}$  sq cm = 0.02 barn.

An 8.3-month  $\alpha$ -ray emitter had been found<sup>1</sup> in the neptunium fraction from deuteron-bombarded U<sup>235</sup>. The possible mass assignments

for this isotope would be 235, 234, or 233. Since this x-ray activity was absent in the neptunium fraction of the U<sup>233</sup> bombardment (see Fig. 2) in which no Np<sup>235</sup> could be present, it may be definitely assigned to Np<sup>235</sup>.

A search with a crude magnetic setup failed to reveal any evidence for positrons.

No evidence was found for Np<sup>231</sup>, Np<sup>232</sup>, and Np<sup>233</sup>. It is possible that short-lived radiations from these isotopes were obscured by the  $\beta$  background from Np<sup>238</sup>, Np<sup>239</sup>, and Np<sup>236</sup> and the x-ray background from Np<sup>234</sup>. Or, more likely, these isotopes were so short lived that they had completely decayed before the chemical separations could be performed. A third possibility, namely, that they are too long lived to observe, seems unlikely. A search in the uranium fraction for possible daughters of neptunium isotopes was futile because of the 10 mg of highly radioactive U<sup>233</sup> in this fraction. No activity was found in the plutonium fraction of the deuteron bombardment, other than a few  $\alpha$  counts per minute of Pu<sup>238</sup> and Pu<sup>239</sup>.

A small amount of Pa<sup>230</sup> was found in the protactinium fraction of the deuteron bombardment. This was identified by observing the growth and decay of U<sup>230</sup>  $\alpha$  activity in this fraction (see Studier and Hyde<sup>5</sup> for theoretical curve) and by specifically isolating the first daughter of U<sup>230</sup>, Th<sup>228</sup>, and identifying it by its 30.9-min half life.<sup>6</sup> Pa<sup>230</sup> could arise only from  $\alpha$  decay of Np<sup>234</sup> or directly in the bombardment by the reaction U<sup>233</sup>(d, $\alpha$ n)Pa<sup>230</sup>. If Pa<sup>230</sup> arose by  $\alpha$  branching of the 4.4-day Np<sup>234</sup>, then a 4.4-day  $\alpha$  decay should have been observed, and Pa<sup>230</sup> should have grown into the neptunium fraction. No such behavior was noted in any of the neptunium fractions. The best data set an upper limit of  $\alpha$  branching of Np<sup>234</sup> as 0.01 per cent. By using this figure the amount of Pa<sup>230</sup> that could have grown into the target material before the extraction of the neptunium fraction was calculated, and it was found to be much less than the amount of Pa<sup>230</sup> actually isolated. Furthermore, although the 4.4-day Np<sup>234</sup> was observed in the helium-ion bombardments (see Sec. 3), no Pa<sup>230</sup> was isolated.

Hence it seems evident that Pa<sup>230</sup> is formed by the hitherto unobserved type of nuclear transformation, (d, $\alpha$ n). The product was observed in spite of the low cross section for the reaction, approximately  $10^{-8}$  barn =  $10^{-32}$  sq cm, because of its short half life and its short-lived  $\alpha$  daughters.

### 3. HELIUM-ION BOMBARDMENTS OF U<sup>233</sup>

The neptunium fraction of the helium-ion bombardment contained a considerable amount of  $\beta$  activity, representing a mixture of Np<sup>239</sup>,

Np<sup>238</sup>, and Np<sup>236</sup>. No new  $\beta$  activities were detected. A considerable amount of the 4.4-day activity produced by the reaction U<sup>233</sup>( $\alpha$ ,p2n)Np<sup>234</sup> was observed. The x-ray decay showed a long-lived component, indicating the presence of the 8.3-month Np<sup>235</sup> produced by the reaction U<sup>233</sup>( $\alpha$ ,pn)Np<sup>235</sup>, but this decay was not carefully followed in order to complete the identification of the half period.

The fraction of greatest interest in the  $\alpha$  bombardments was the plutonium fraction, in which in addition to a small amount of Pu<sup>238</sup> and Pu<sup>236</sup> with  $\alpha$  ranges of 4.35 cm and 4.10 cm, respectively, a small amount of an unknown  $\alpha$  activity of about 4.7 cm range (6.0 mev energy) was observed. Only a few hundred  $\alpha$  counts per minute of this activity were isolated in either of the helium-ion bombardments because low beam intensity during the final period of the cyclotron bombardments allowed nearly complete decay of this isotope before the plutonium fractions were isolated. Hence measurements of half life and  $\alpha$  range were only approximate. Resolution of the  $\alpha$  decay of the plutonium fraction yielded a half life of 10 hr in one case and of 6 hr in another. By measuring the  $\alpha$  spectrum of the plutonium fraction in a multichannel differential pulse analyzer<sup>6</sup> at frequent intervals and plotting the specific decay of the 6.0-mev peak, values of 12.5 and 5.1 hr were obtained for the half life. The  $\alpha$  half life may be taken as roughly 8  $\pm$  4 hr.

This previously unknown plutonium isotope was tentatively identified as Pu<sup>234</sup> by establishing the presence of its U<sup>230</sup> daughter in the uranium fraction.

To accomplish this, Th<sup>228</sup>, the daughter of U<sup>230</sup>, was isolated from one-fifth of the uranium fraction of the second helium-ion bombardment by coprecipitating it on 1 mg of zirconium phosphate carrier. It was found that 2,200  $\alpha$  counts per minute over and above a background of 1,000 counts per minute of U<sup>233</sup> decayed with the 30-min half life of Th<sup>228</sup>.

In addition, samples of the uranium fraction directly plated out showed the property of contaminating the  $\alpha$ -counting chambers with 30-min Th<sup>228</sup> recoil activity, a behavior<sup>8</sup> characteristic of samples of U<sup>230</sup>. Furthermore, analysis of the  $\alpha$  spectrum in the multichannel differential pulse analyzer of samples of the uranium fraction showed peaks at the proper ranges for the protactinium-series  $\alpha$  emitters although the ratio of this activity to the U<sup>233</sup>  $\alpha$  activity was too low to make very good measurements possible.

The evidence for the presence of U<sup>230</sup> may be taken as conclusive, but there is a slight possibility that the U<sup>230</sup> was formed by the nuclear reaction U<sup>233</sup>( $\alpha$ , $\alpha$ 3n)U<sup>230</sup> rather than by  $\alpha$  decay of Pu<sup>234</sup>. Hence before the mass assignment of the 8-hr  $\alpha$  emitter can be taken as cer-

tain, the growth of  $U^{230}$  must be directly observed in a sample of this isotope initially purified from uranium. Such an identification was attempted in the second helium-ion bombardment by isolating a thorium fraction on zirconium iodate carrier from the plutonium fraction after complete decay of the 8-hr  $\alpha$  activity. The amount of the 8-hr activity was so small that the thorium fraction so isolated amounted to only 10 counts per minute, which, within rather large experimental error, decayed with a 30-min half life. This experiment needs to be repeated with a larger sample.

It is possible that the 8-hr  $\alpha$  decay of  $Pu^{234}$  is only an apparent  $\alpha$  half life resulting from a small  $\alpha$  decay branching of a predominantly orbital-electron-capturing isotope. The low mass number and the fact that the 6.0-mev energy is somewhat low for an 8-hr  $\alpha$  emitter suggest this. The small size of the samples coupled with the low counting efficiency of x rays made the observation of the x rays difficult. It was not established whether the few short-lived x rays observed in the plutonium fraction were of the same half life as was the new  $\alpha$  activity.

Studies of helium-ion bombardments of  $U^{235}$  had revealed a 40-day orbital-electron-capturing plutonium isotope that could tentatively be assigned either to  $Pu^{236}$  or to  $Pu^{237}$ . No evidence for such an isotope was found in the helium-ion bombardments of  $U^{233}$ , in which  $Pu^{235}$  should be formed in good yield by the reaction  $U^{233}(\alpha, 2n)Pu^{235}$ . Hence this 40-day activity may be definitely assigned to  $Pu^{237}$ .

The lack of any evidence for the isotopes  $Pu^{238}$ ,  $Pu^{233}$ ,  $Pu^{232}$ , and  $Pu^{231}$ , which were unquestionably formed during the helium-ion bombardments, indicates that their half lives are short, probably of the order of hours or less or, less likely, that they are too long lived to observe.

No evidence for any protactinium isotopes was found after the helium-ion bombardments.

#### 4. EXPERIMENTAL WORK; CHEMICAL SEPARATIONS

The purpose of the chemical procedures applied to the target material after bombardment was to separate the fractions of major radioactive interest, particularly the plutonium and neptunium fractions, from the unchanged  $U^{233}$  (representing  $10^6 \alpha$  disintegrations per minute), from the radioactive daughters of  $U^{233}$ , from the daughters of the primary bombardment products, and from the radioactive fission products formed by the deuteron or helium-ion induced fission of the  $U^{233}$  (representing up to several roentgens of  $\beta$  and  $\gamma$  radiation). It was necessary to carry out these separations rapidly since many of

the isotopes being sought were expected to be short lived. Without chemical separations no significant measurements would have been possible.

4.1 Carrier Method. In the first helium-ion bombardment a carrier method based on the work of Seaborg and Wahl<sup>7</sup> was used. This method consists essentially of lanthanum fluoride precipitations to separate a combined neptunium-plutonium fraction free from uranium, fission products, and other elements. This is followed by bromate cycles in which neptunium is selectively oxidized and in which the plutonium is carried on lanthanum fluoride while the oxidized neptunium remains in solution. For a number of reasons this method did not prove satisfactory and was abandoned in favor of the one described in detail below.

4.2 Ignition and Dissolving Step. The U<sub>3</sub>O<sub>8</sub> together with the thin aluminum foil used to cover it during the bombardment were ignited to 750°C for 20 min in a small crucible in order to remove several milligrams of insoluble carbonaceous material resulting principally from the carbonizing of the organic cement used to hold the aluminum foil in place. The U<sub>3</sub>O<sub>8</sub> was then dissolved in nitric acid, assayed radioactively, and pipetted into a 30-ml Kjeldahl flask. Here the plutonium and neptunium were oxidized by making the solution 0.2M in KBrO<sub>3</sub>, and by heating to 95°C for 20 min. Solid ammonium nitrate was added to make 5 ml of solution 10N in NH<sub>4</sub>NO<sub>3</sub> and 1N in HNO<sub>3</sub>.

4.3 Ether Extraction. This solution was then subjected to an ether extraction. Previous experiments under the conditions of the extraction had shown that of all the elements present, the nitrates of only elements 92, 93, and 94 would be extracted. The extraction was adequate for the separation of pure neptunium and plutonium fractions and served to reduce the physiological hazard from the intense β and γ radiation.

The first solution was shaken with 15 ml of ethyl ether for 1 or 2 min. The aqueous phase was frozen out in a dry ice-acetone bath to permit pouring the ether phase out of this flask into a second 30-ml Kjeldahl flask. In this second flask the ether layer was shaken with 5 ml of a wash solution consisting of 10N NH<sub>4</sub>NO<sub>3</sub>, 1N HNO<sub>3</sub>, and 0.2M KBrO<sub>3</sub>. After these two phases had been equilibrated and the aqueous phase had been frozen in the same manner, the ether was shaken with two more wash solutions in two succeeding Kjeldahl flasks and then equilibrated with 5 ml of pure water in a final flask. This final water solution removed the heavy metal nitrates that had been extracted into the ether. The stripped ether was returned to the original flask and the entire process was repeated. Six such cycles were carried out.

**4.4 Extraction of a Pure Neptunium Fraction.** The water solution in the last Kjeldahl flask was assayed for  $U^{233}$  and then evaporated to dryness in a 5-ml beaker. The nitrate salts were converted to chloride by repeated evaporation to dryness with hydrochloric acid.

The residue was taken up in 1 ml of a solution 5N in hydrochloric acid, 0.1M in potassium iodide, and 0.1M in hydrazine. This solution was heated in boiling water for 2 min. Under these conditions neptunium is rapidly reduced to the tetrapositive state, and plutonium is reduced to the tripositive state. The solution was then diluted to 10 ml and again heated for 1 min. Under these conditions the hydrazine rapidly reduces the free iodine back to iodide and prevents a slow reoxidation of neptunium.<sup>†</sup>

The solution was then shaken for 20 min with 10 ml of a 0.15M solution of thenoyltrifluoroacetone<sup>‡</sup> in benzene. This organic complexing agent under the conditions used extracts neptunium(IV) but fails to extract plutonium(III) and uranium(VI).

**4.5 Extraction of a Protactinium Fraction.** A protactinium fraction was isolated from the first aqueous layer of the original ether extraction by extraction with diisopropyl ketone. The extraction of protactinium with diisopropyl ketone is based on the work of Hyde and Wolf.<sup>8</sup>

First the residual  $U^{233}$   $\alpha$  activity left behind in the solution by the ether extraction (even 0.1 per cent would represent  $10^5$  disintegrations per minute) was reduced by exhaustive ether extraction with six 15-ml portions of fresh ether.

Then the acidity of the solution was adjusted to 1N, and the protactinium was extracted from the solution with 15 ml of diisopropyl ketone. After the aqueous phase had frozen out, the ketone was poured into a second 30-ml Kjeldahl flask in which it was contacted with 5 ml of a wash solution of composition 3N  $NH_4NO_3$  and 1N  $HNO_3$ . The ketone was equilibrated with another of these wash solutions before being placed in a final flask in contact with 7 ml of 0.05M  $HNO_3$ . This last solution reextracted the protactinium (if any) from the ketone. The ketone was then returned to the original flask and was put through the same sequence two more times. The final aqueous solution was changed at the end of each cycle. The combined aqueous solutions from the final flask were combined. Aliquots of this solution were subjected to radioactive analysis.

<sup>†</sup>These conditions are based on the work of L. B. Magnusson.

<sup>‡</sup>This reagent was developed and introduced for the extraction of heavy metals by the organic group at Berkeley under the direction of Dr. Calvin.

### 5. SUMMARY

Information concerning the lighter isotopes of neptunium and plutonium has been obtained by studying the products of the bombardment of U<sup>233</sup> with deuterons and helium ions from the 60-in. cyclotron. Np<sup>234</sup> is shown to be an orbital-electron-capturing isotope of  $4.40 \pm 0.05$  days half life with an associated  $\gamma$  ray of 1.9 mev energy. Evidence is presented that the isotope Pu<sup>234</sup> decays by the emission of  $\alpha$  particles of approximately 6.0 mev energy with an apparent half life of  $8 \pm 4$  hr.

Pa<sup>230</sup> is shown to be produced by a (d, $\alpha$ n) reaction.

By correlation of information from these bombardments with information obtained by others<sup>1</sup> from bombardments of U<sup>233</sup>, Np<sup>235</sup> is identified with an 8.3-month orbital-electron-capturing isotope, and Pu<sup>237</sup> is identified with a 40-day orbital-electron-capture decay.

From the failure to find any evidence for plutonium isotopes of mass 231, 232, 233, and 235, and for neptunium isotopes of mass numbers 231, 232, and 233, some conclusions regarding their half lives are reached.

### ACKNOWLEDGMENT

The authors wish to acknowledge the assistance of Bernard Weissboard in running differential pulse analyses on many of the  $\alpha$ -emitting samples.

### REFERENCES

1. R. A. James, A. E. Florin, H. H. Hopkins, Jr., and A. Ghiorso, Products of helium-ion and deuteron bombardment of U<sup>235</sup> and U<sup>238</sup>, Paper 22.8, this volume.
2. G. T. Seaborg, E. M. McMillan, J. W. Kennedy, and A. C. Wahl, A new element: radioactive element 94 from deuterons on uranium, Paper 1.1a, this volume.
3. D. H. Copp and D. M. Greenberg, Rev. Sci. Instruments, 14: 205 (1943).
4. W. Heitler, "The Quantum Theory of Radiation," pp. 215-216, Oxford University Press, New York, 1936.
5. M. H. Studier and E. K. Hyde, National Nuclear Energy Series, Division IV, Volume 17 B; Phys. Rev., 74: 591 (1948).
6. A. Ghiorso, A. H. Jaffey, H. P. Robinson, and B. Weissboard, A 48-channel pulse-height analyzer for alpha-energy measurements, Paper 16.8, this volume (Metallurgical Project Report CC-3887).
7. G. T. Seaborg and A. C. Wahl, The chemical properties of elements 94 and 93, Paper 1.6, this volume.
8. E. K. Hyde and M. J. Wolf, National Nuclear Energy Series, Division IV, Volume 17 B.

## Paper 22.16

# THE BOMBARDMENT OF Np<sup>237</sup> WITH DEUTERONS AND HELIUM IONS†

By R. A. James, S. G. Thompson, and H. H. Hopkins, Jr.

After bombardments of U<sup>238</sup> and U<sup>235</sup> had produced isotopes of plutonium with masses 236 and 237 (reference 1), it was thought advisable to verify these findings by producing the same isotopes by deuteron bombardment of Np<sup>237</sup>. Helium-ion bombardment of Np<sup>237</sup> should produce some unknown isotopes of americium as well as some of the same plutonium isotopes as are produced by helium-ion bombardment of U<sup>238</sup> and deuteron bombardment of Np<sup>237</sup>. Both kinds of bombardments were made with 22-mev deuterons and 44-mev helium ions produced by the 60-in. Berkeley cyclotron. This paper describes the results of these bombardments.

### 1. EXPERIMENTAL WORK

The targets for bombardment were prepared by mounting 10 to 15 mg of Np<sup>237</sup> as the oxide on small grooved platinum interceptor targets approximately 0.8 sq cm in area. This interceptor was then bombarded in the Berkeley cyclotron directly in front of the regular target disk.

After bombardment, the neptunium was scraped off the platinum backing under water; it was then fumed to dryness in sulfuric acid and the residue was dissolved in 2M HNO<sub>3</sub>.

Lanthanum carrier was then added to this solution; and after the neptunium and plutonium had been oxidized to their hexapositive states with argentic ion, americium was coprecipitated with lanthanum by the addition of hydrofluoric acid. This lanthanum fluoride

†Contribution from the Department of Chemistry and the Radiation Laboratory, University of California, Berkeley, and from the Chemistry Division of the Metallurgical Laboratory, University of Chicago, now the Argonne National Laboratory.

was dissolved and reprecipitated several times, the neptunium and plutonium having been oxidized to the hexapositive state each time before addition of hydrofluoric acid. The activity of the final lanthanum fluoride precipitate after this treatment was due to americium and to rare-earth fission products. Approximately 25 per cent of this fraction was then set aside, and plutonium-neptunium fractions were separated from it periodically by ether extraction for the purpose of locating neptunium and plutonium daughters of americium isotopes. The remaining 75 per cent was fractionated from the rare earths by the use of the fluosilicate-fluoride cycles described in another paper.<sup>2</sup>

The neptunium and plutonium contained in the supernatant liquid after precipitation of americium with lanthanum fluoride were reduced with sulfur dioxide; an insoluble fluoride compound of neptunium that also carried the plutonium was thus precipitated. This fraction was then further purified from the fission products by extraction of plutonium and neptunium(VI) nitrates into ether from a 10M NH<sub>4</sub>NO<sub>3</sub> solution.

Plutonium and neptunium were separated from each other by reducing the neptunium to its tetrapositive state and reducing the plutonium to its tripositive state with potassium iodide in 5M HCl, and by extracting the neptunium, after a tenfold dilution, into a 0.2M solution of  $\alpha$ -thenoyltrifluoroacetone in benzene.<sup>3</sup>

The characteristics of the activities of each of the fractions were then studied to determine their energies and half lives.

## 2. RESULTS

2.1 Deuteron Bombardment. A pulse-analysis curve of the  $\alpha$  activities of the combined neptunium-plutonium fraction before separation of these two elements gave the percentages of the various components as listed in the accompanying table.

Range, cm	Isotope	Percentage
3.25	Np <sup>237</sup>	84.3
3.68	Pu <sup>239</sup>	2.6
4.00	Pu <sup>238</sup>	1.6
4.35	Pu <sup>236</sup>	11.5

The Pu<sup>239</sup> was not produced in the bombardment but was present as an impurity in the Np<sup>237</sup> before bombardment; this was shown by a pulse-analysis curve determined for a sample of the original neptunium.

The bombardment was 483  $\mu\text{a}\cdot\text{hr}$  or  $1.36 \times 10^{18}$  deuterons per square centimeter; if 2.7 years and 90 years are taken as the half lives of  $\text{Pu}^{236}$  and  $\text{Pu}^{238}$ , respectively, then the cross sections for their production (total for all reactions) are

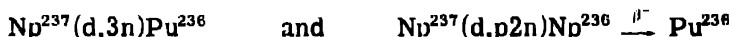
$$\text{Pu}^{236} = 0.0094 \text{ barn}$$

$$\text{Pu}^{238} = 0.071 \text{ barn}$$

A Geiger-Mueller activity that decayed with a half life of 40 days was also found in this plutonium fraction. Absorption curves in aluminum, lead, copper, and beryllium showed that this activity consisted of electromagnetic radiation with 110-kev and 16-kev components and some very soft radiations that appeared to include both particles and electromagnetic radiation. No  $\gamma$  rays with energy greater than the 110-kev component were found. The radiations have been interpreted to be the K and L x rays characteristic of neptunium arising from a plutonium isotope decaying by electron capture. The characteristics observed here agree in all respects with the 40-day plutonium isotope found in helium-ion bombardments of  $\text{U}^{235}$ , and the isotope is believed to be  $\text{Pu}^{237}$ .<sup>1</sup>

If it is assumed that one K x ray is emitted per disintegration and that the counting efficiency for these K x rays in a bell-type Geiger-Mueller tube filled to 10 cm Hg pressure with argon-alcohol mixture is 0.5 per cent, then the cross section for formation of  $\text{Pu}^{237}$  is 0.0024 barn.

That the cross section for formation of  $\text{Pu}^{237}$  is approximately one-fourth that of  $\text{Pu}^{236}$  and one-thirtieth of that of  $\text{Pu}^{238}$  can be at least partially explained by the fact that  $\text{Pu}^{237}$  is produced only by the ( $d,2n$ ) reaction whereas  $\text{Pu}^{236}$  is produced by the two reactions



and  $\text{Pu}^{238}$  is similarly produced by the two reactions



**2.2 Helium-ion Bombardment.** At the time of this bombardment no satisfactory method for complete separation of americium and curium from the fission-product rare-earth elements had been devised. For this reason very little can be said about the radiations of

the expected americium isotopes, Am<sup>238</sup> to Am<sup>240</sup>, inclusive. Some of the daughters of these americium isotopes for various assumed modes of decay are, however, well-characterized isotopes of curium, plutonium, and neptunium; some limitations can therefore be imposed upon the allowable half lives for these possible modes of decay.

Beta particles or electrons having an energy of approximately 1 mev and decaying with an approximately 2-day half life were observed in the radioactivity of the americium-curium fraction; and, from the behavior of this activity in fluosilicate-fluoride cycles, it would appear to be an isotope of americium or curium. Of the americium isotopes expected as products, the ones most likely to decay by negative  $\beta$ -particle emission are Am<sup>240</sup> and perhaps Am<sup>238</sup>. Fairly good evidence was found that Am<sup>238</sup> decays to Pu<sup>238</sup>, as will be discussed later; this eliminated Am<sup>238</sup> as a source of  $\beta$  particles. Since no Cm<sup>240</sup>  $\alpha$  particles<sup>4</sup> were found in this fraction, Am<sup>240</sup> cannot be a  $\beta$ -particle emitter with a half life less than 10 years. The most reasonable explanation for these particles seems to be that they are very energetic conversion electrons coming from a  $\gamma$  ray emitted by one of the americium isotopes either in an isomeric transition or accompanying decay by electron capture. Such energetic conversion electrons are relatively rare, but they have been observed, as, for example, in the RaC line with an energy of 1.4 mev.<sup>†</sup>

The daughter of Am<sup>238</sup> [formed by the ( $\alpha$ ,3n) reaction] would be Pu<sup>238</sup> if it decayed by electron capture or positron emission. The amount of Pu<sup>238</sup> found gives a cross section for its production of 0.12 barn. This relatively large cross section agrees with that expected for the ( $\alpha$ ,3n) reaction, and it is too large to be accounted for by the ( $\alpha$ ,p2n) reaction. It therefore seems reasonably certain that Am<sup>238</sup> decays either by positron emission or electron capture to Pu<sup>238</sup> with a half life of a few days or less.

To summarize, no  $\alpha$  particles were observed from the americium isotopes Am<sup>240</sup>, Am<sup>239</sup>, Am<sup>238</sup>, Am<sup>237</sup>, and Am<sup>236</sup>, and the half life for  $\alpha$  emission of the isotope giving rise to Geiger-Mueller activity in the americium fraction must be less than 1 day or longer than 10 years. The isotope Pu<sup>238</sup> was found in an amount sufficiently large to suggest that Am<sup>238</sup> decays by electron capture or by positron emission with a short half life (a few days or less).

No Cm<sup>240</sup> was found, and this eliminated the possibility that Am<sup>240</sup> was a  $\beta$  emitter with a half life of less than 10 years. It may de-

<sup>†</sup>Since the writing of this paper the 2-day activity has been investigated further<sup>5,6</sup> and assigned to Am<sup>240</sup>.

cay with a short half life by orbital-electron capture with  $\alpha$ -decay branching.

### 3. SUMMARY

The bombardment of Np<sup>237</sup> with deuterons has produced Np<sup>238</sup>, Np<sup>236</sup>, Pu<sup>238</sup>, Pu<sup>236</sup>, and the 40-day electron-capture plutonium, which is probably Pu<sup>237</sup>. Helium-ion bombardment produced some Geiger-Mueller activities that may be due to isotopes of americium, but definite assignments cannot be made at this time.

### ACKNOWLEDGMENTS

The authors wish to acknowledge the cooperation of Dr. J. G. Hamilton and his group at Berkeley, who bombarded the targets, and of J. C. Hindman and L. B. Magnusson who prepared the neptunium for bombardment. The plans for the bombardments of Np<sup>237</sup> were made by Dr. Glenn T. Seaborg, who actively participated in the planning of the experimental operations and interpretation of the data.

### REFERENCES

1. R. A. James, A. E. Florin, H. H. Hopkins, Jr., and A. Ghiorso, Products of helium-ion and deuteron bombardment of U<sup>238</sup> and U<sup>236</sup>, Paper 22.8, this volume.
2. S. G. Thompson, L. O. Morgan, R. A. James, and I. Perlman, The tracer chemistry of americium and curium in aqueous solutions, Paper 19.1, this volume.
3. L. B. Magnusson, J. C. Hindman, and T. J. LaChapelle, unpublished work.
4. G. T. Seaborg, R. A. James, and A. Ghiorso, The new element curium (atomic number 96), Paper 22.2, this volume.
5. G. T. Seaborg, R. A. James, and L. O. Morgan, The new element americium (atomic number 95), Paper 22.1, this volume.
6. K. Street, Jr., and G. T. Seaborg, unpublished work, 1948.

Paper 22.26

THERMAL NEUTRON FISSION PROPERTIES OF Np<sup>237</sup>†

By A. Ghiorso, D. W. Osborne, and L. B. Magnusson

Thermal (i.e., cadmium-absorbable) neutron-fission measurements were first undertaken on Np<sup>237</sup> samples to determine the extent of Pu<sup>239</sup> contamination. The early measurements were handicapped by insufficient sensitivity of the fission pulse-counting apparatus; however, it was determined that a small fission rate observed with Np<sup>237</sup> samples was unaffected by repeated purifications from Pu<sup>239</sup>. It was deduced that the thermal neutron-fission cross section of Np<sup>237</sup> must be approximately  $0.01 \times 10^{-24}$  sq cm.

Since the fission cross section of Np<sup>237</sup> is small compared to that of Pu<sup>239</sup> and since it is formed as a by-product in chain-reacting piles for production of plutonium, careful purification from plutonium is required to reduce the fission rate due to Pu<sup>239</sup> to a few per cent of that due to Np<sup>237</sup>.

Recently it has been possible to follow the course of purification of Np<sup>237</sup> by using Pu<sup>238</sup> as a tracer. The Pu<sup>238</sup> tracer was formed in the Np<sup>237</sup> sample by irradiation with neutrons in the Hanford reactor according to the reaction  $\text{Np}^{237}(n,\gamma)\text{Np}^{238} \xrightarrow[2.0 \text{ day}]{\beta^-} \text{Pu}^{238}$ . The Np<sup>237</sup> used had been highly purified prior to irradiation. After irradiation, plutonium and neptunium fractions were separated and purified, and fission measurements were made on the plutonium fraction which showed Pu<sup>239</sup> to be present to the extent of less than 3.1 per cent of the Pu<sup>238</sup> by weight.<sup>1</sup> The neptunium fraction was further purified by three extractions into a benzene solution of  $\alpha$ -thenoyltrifluoroacetone by the use of a procedure<sup>2</sup> in which ammonium iodide under controlled conditions reduced plutonium to the nonextractable tripositive state. The

†Contribution from the Chemistry Division of the Metallurgical Laboratory, University of Chicago, now the Argonne National Laboratory.

final  $\text{Pu}^{238}$  content of the  $\text{Np}^{237}$  sample, as determined by  $\alpha$ -pulse analysis,<sup>3</sup> was 1.5 per cent by  $\alpha$  activity or  $6 \times 10^{-5}$  per cent by weight, and the  $\text{Pu}^{239}$  content was therefore less than  $0.031 \times 6 \times 10^{-5}$  per cent, or  $2 \times 10^{-6}$  per cent.

A thin sample for fission measurements was prepared by electroplating by use of a method<sup>4</sup> similar to that which has been used for uranium.<sup>5,6</sup> A platinum foil 2.5 cm in diameter was attached with rubber cement to the ground bottom edge of a glass cylinder, and the whole was held firmly with rubber bands against a stainless-steel plate immersed in a water bath at 80°C. The cylinder contained the purified neptunium, previously oxidized to  $\text{Np(VI)}$  by means of potassium bromate, in 0.01M  $\text{HNO}_3$  and 0.03M ammonium oxalate. The anode was a platinum wire wound tightly on a glass stirrer, and the platinum foil was the cathode. After electrolysis with stirring for 1 hr at 0.6 amp, the platinum foil was removed from the cylinder, washed with methanol, air-dried, and flamed. The mass of the  $\text{Np}^{237}$  was determined by  $\alpha$  counting to be  $142 \times 10^{-6}$  g.

The fissionability was measured in a sensitive ionization chamber<sup>7</sup> inserted in the thermal column of the Argonne heavy-water reactor. The fission rate of the  $\text{Np}^{237}$  sample was compared under identical neutron-flux conditions with that of a standard thin sample of  $\text{Pu}^{239}$ . A fission rate of 6,000 fissions per minute was observed for the  $\text{Np}^{237}$  sample. Assuming that all the fissions observed were due to  $\text{Np}^{237}$  and using the known thermal neutron-fission cross section of  $\text{Pu}^{239}$ , the thermal neutron-fission cross section of  $\text{Np}^{237}$  was determined<sup>8</sup> to be  $0.019 \times 10^{-24}$  sq cm. This cross section is for fission by neutrons with a Maxwellian distribution of energy corresponding to a temperature of 293°K.

The thermal nature of the neutrons employed was confirmed by repeating the measurements with the fission chamber surrounded by a cadmium shell 0.027 cm thick. Under these conditions the fission rates were reduced by a factor of 100 or more.

The error due to the plutonium present in the purified neptunium is less than  $0.001 \times 10^{-24}$  sq cm. Errors due to counting statistics and self-absorption of the fission particles are not greater than a few per cent at most. However, in view of the ever-present danger of accidental contamination of the samples with fissionable material, conservative limits of error have been set, rather arbitrarily, as  $\pm 0.003 \times 10^{-24}$  sq cm.

Summary. The thermal neutron-fission cross section of  $\text{Np}^{237}$  has been determined to be  $0.019 \times 10^{-24}$  sq cm.

## ACKNOWLEDGMENTS

The authors are pleased to acknowledge the cooperation of Dr. W. H. Zinn in making available the facilities of the Argonne heavy-water reactor, and their indebtedness to Drs. G. T. Seaborg and W. M. Manning, under whose general direction the experiments were performed. Thanks are also due the staff of the Hanford Engineer Works, Richland, Wash., for their handling of the neutron bombardment of the Np<sup>237</sup> sample. The work described in this paper was completed in March 1946.

## REFERENCES

1. D. W. Osborne and A. Ghiorso, Argonne National Laboratory Report ANL-4046 (1947).
2. L. B. Magnusson, J. C. Hindman, and T. J. LaChapelle, unpublished work.
3. A. Ghiorso, A. H. Jaffey, H. P. Robinson, and B. Weissbourd, A 48-channel pulse-height analyzer for alpha-energy measurements, Paper 18.8, this volume (Metallurgical Project Report CC-3887).
4. J. C. Hindman and J. W. Britain, Metallurgical Laboratory Memorandum MUC-GTS-2105 (Dec. 19, 1945).
5. M. Kahn, University of California Radiation Laboratory Report RL 16.6.24 (Apr. 22, 1943).
6. B. Cohen and D. E. Hull, Report A-1235, Part II (Aug. 28, 1944).
7. A. Ghiorso and W. C. Bentley, High-sensitivity apparatus for fission counting, Paper 22.29, this volume (Argonne National Laboratory Report ANL-4048).
8. Los Alamos handbook of nuclear physics, supplement to second edition, Los Alamos Report LA-140A (Apr. 21, 1945).

**Paper 22.29**

**HIGH-SENSITIVITY APPARATUS FOR FISSION COUNTING<sup>†</sup>**

**By A. Ghiorso and W. C. Bentley**

**1. INTRODUCTION**

In order to make the most of the thermal neutron-fissionability tests that have been performed in this laboratory, it has been found necessary to develop radically new and different techniques for measuring fission recoil fragments. Since the isotopes that must be measured are for the most part obtainable in only very small quantities, i.e., less than 1  $\mu\text{g}$ , it is necessary to use very high neutron fluxes to secure reasonable counting rates. It was found early that a conventional fission chamber would not work properly at a high flux. The cause for failure was found to lie in the secondary radiation effects from the capture of neutrons by the materials that make up the chamber. It is possible that the effect, a tremendous "hash" background, can be attributed to electrons from the conversion of high-energy  $\gamma$  rays from the  $(n,\gamma)$  process. Also, it soon became apparent that the metal walls of the chambers, usually 2S aluminum or stainless steel, contained a large amount of fissionable contaminant. This "natural" contamination corresponded to approximately 1 ppm of uranium. A third major problem that had to be contended with was the very large amount of induced radioactivity ( $\beta$  and  $\gamma$ ) that was obtained with ordinary chambers when placed in a very high neutron flux. The health hazard was serious enough to make impossible any rapid or extensive measurements.

A solution to all three troubles was obtained by constructing the fission chamber and accessories of lucite and bakelite, with a minimum of metal exposed to the neutrons inside the thermal column.

<sup>†</sup>Contribution from the Chemistry Division of the Metallurgical Laboratory, University of Chicago, now the Argonne National Laboratory.

Necessary conducting surfaces were silvered with a quick-drying silver paint, which was found to be comparatively low in fissionable contaminants. A remote-control loading and unloading mechanism for changing samples was developed. For this purpose the sample plates were fastened to silvered lucite disks, which were then inserted into the chamber. Commercial argon was passed at atmospheric pressure through the chamber, the design of which was such that it could be quickly and easily replaced by another in case of accidental contamination. The preamplifier was housed in a cadmium shield placed about 1 ft from the chamber. The rest of the amplifier and scaler circuits were the conventional ones, suited to fast-electron collection. These measures resulted in a fission-counting apparatus with a very high signal-to-noise ratio, a background rate of approximately 35 fissions per minute (due chiefly to residual uranium contamination in the silver paint and the lucite), and ease and safety of handling, which were quite satisfactory.

Since the neutron-flux level may vary as much as 1 per cent over a period of minutes, it is necessary to monitor this intensity. The most accurate method developed was one which required the use of an exactly similar chamber and circuit. The monitor chamber was mounted directly over the sample chamber, and since it was identical with the latter it could be used interchangeably for the sample or the monitor.

## 2. DESCRIPTION OF APPARATUS

Figure 1 is a cross-sectional drawing of the removable fission chamber. The materials of construction for the chamber are lucite and 2S aluminum (cross-hatched). A bakelite tube, O, supports the chamber in position in the neutron flux and carries the electrical leads and the small stainless-steel tube that supplies argon to the chamber. The removable fission chamber is held rigidly to the bakelite support by two stainless-steel springs. The electrode system consists of the lucite plate A, carrying sample C, and the lucite semi-spherical piece B. The lucite is made conductible by painting it with metallic silver paint (DuPont # 4817). The plate A is at ground potential, and the collecting electrode B is maintained at about +250 volts. The insert piece D is removable for easy cleaning of the chamber in case of accidental contamination. The argon gas, which flows through the chamber at atmospheric pressure, is delivered through tube L into annulus M, and feeds through four holes such as J into the sensitive volume of the chamber. The gas escapes through small slots milled in the face of the lucite piece E, which is used to hold in

place the lucite disk on which the sample plate is mounted. Since the collecting electrode is also the high-voltage electrode, any capacitance of the connecting lead to ground acts as an ionization chamber. To reduce collection of electrons arising from ionization in these

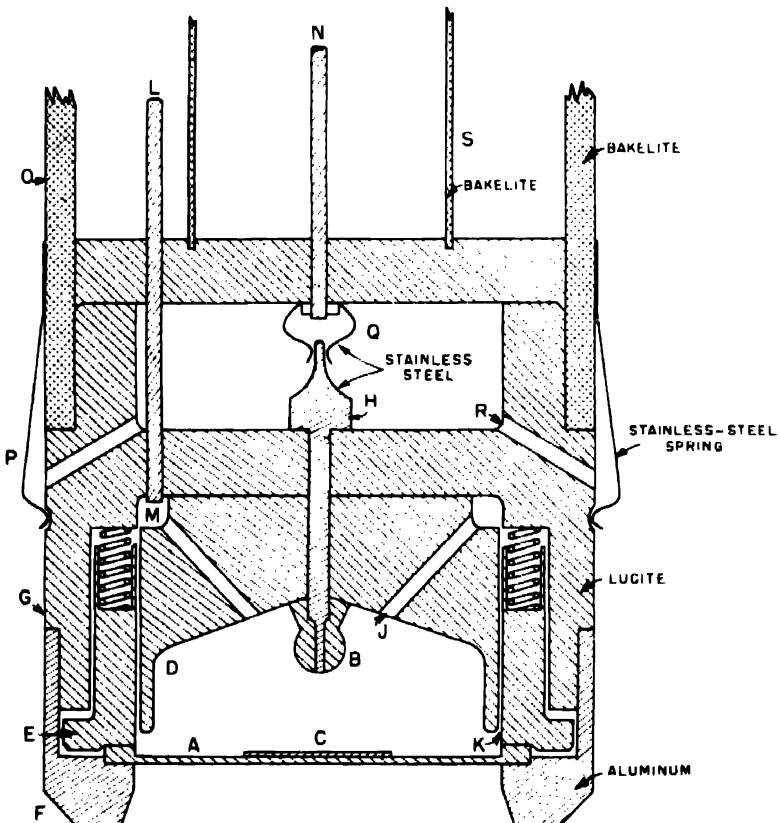


Fig. 1—Cross section of removable fission chamber.

regions, air vents, such as R, are provided so that any argon leaking into such cavities is diluted heavily with air. In addition to this the silver-painted bakelite tube S, which surrounds the lead from chamber to amplifier, is connected to the high-voltage supply, so that it serves as a guard ring and shields this lead from unwanted pickup.

Figure 2 shows one-half of the complete assembly, which is placed in the neutron beam. An identical unit is placed immediately above the one shown and fastened to it. The preamplifier of each unit is housed within a cadmium shield, not only to keep it from becoming too radioactive but also to protect the vacuum tubes from slow-neutron

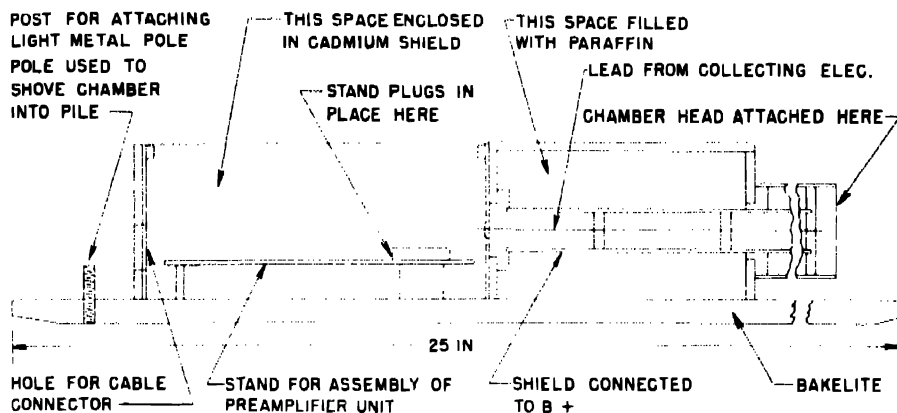


Fig. 2—Cross section of composite fission chamber showing some of construction details.

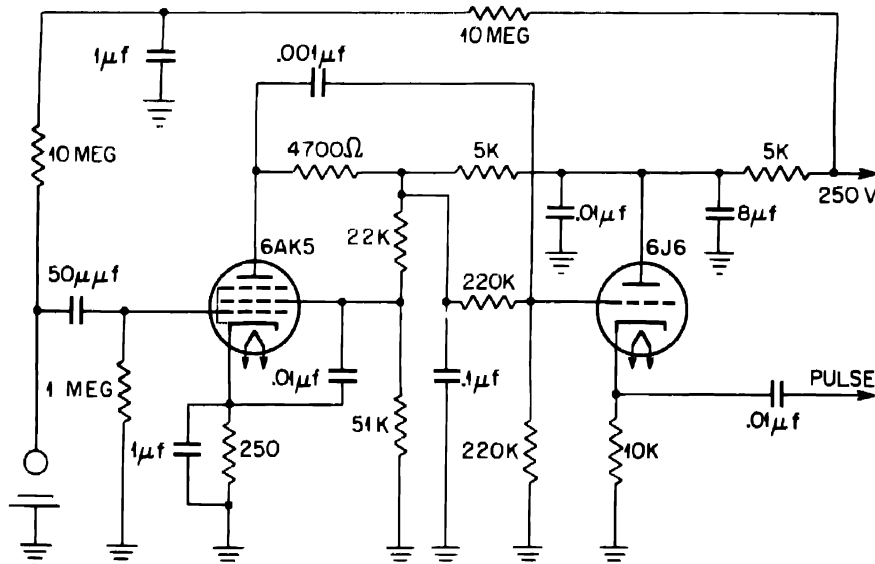


Fig. 3—Preamplifier circuit.

bombardment, which over a period of time would cause them to deteriorate. In order to facilitate servicing, the preamplifier is built on a metal plate, which plugs into place on the assembly.

The amplifiers and scaling circuits used for the two chambers are of the standard fast type, which have been in use at the Argonne Lab-

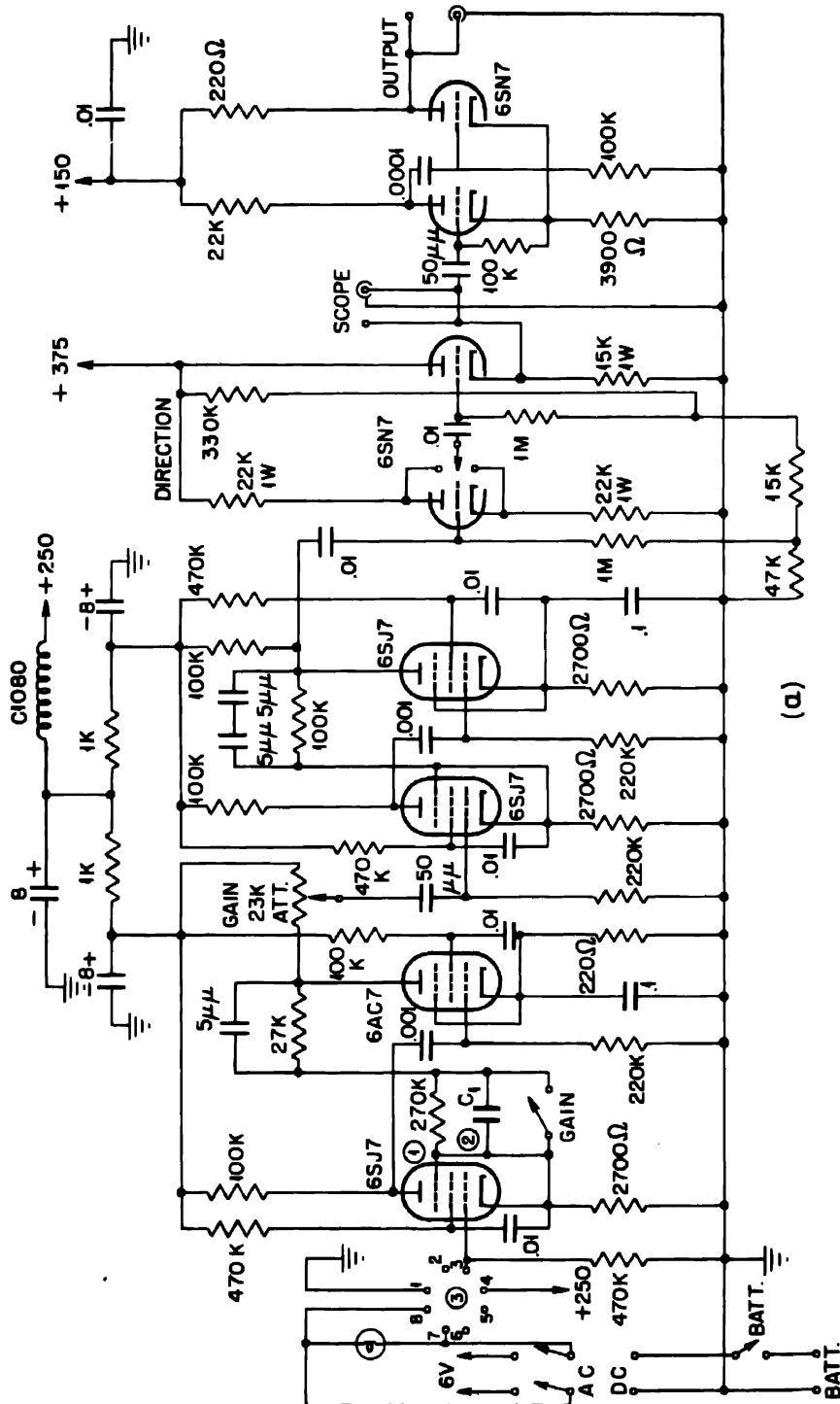


Fig. 42

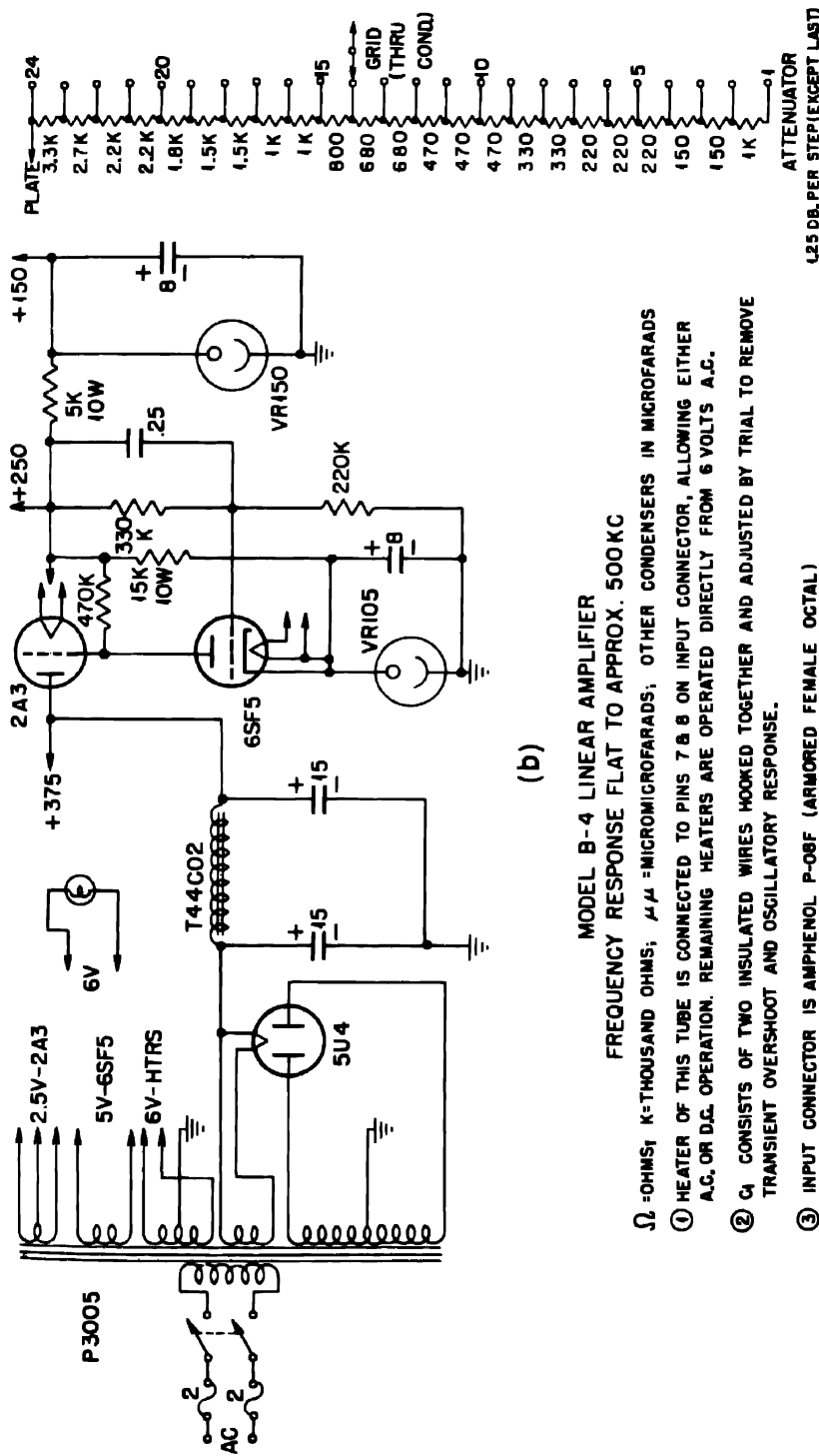


Fig. 4a and b—Amplifier circuit.

oratory for some time. Figures 3 and 4 show the circuits for the pre-amplifier and amplifier. As indicated, the preamplifier consists of a 6AK5 moderate-gain amplifying stage, driving a 6J6 cathode-follower output. The signal from this tube is fed through the 35-ft power and output cable to the main amplifier, and then finally into the scaling

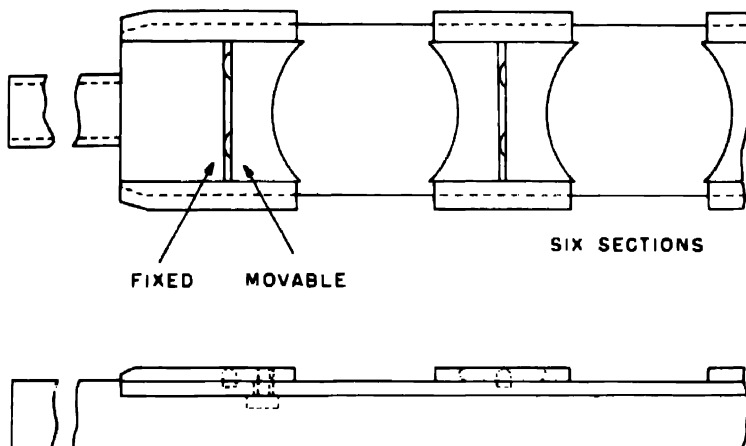


Fig. 5.—Sample changer.

circuit (scale of 512). To obtain the greatest precision, the two scalers are turned on simultaneously by means of relays operated by one switch.

It is necessary to shield the chamber and accessories from the operator when changing samples, since many roentgens of  $\beta$  and  $\gamma$  activity are induced in the counter assembly after only a few minutes of exposure to the neutron beam. For this purpose a lead cave, built on a strong movable wooden stand, is used at the face of the thermal column. The whole double assembly is moved, by means of a long duralumin pole, from the thermal column into the cave. The operator is always at a safe distance during this operation.

Figure 5 is a sketch of the remote sample-changing mechanism. As many as six of the silvered lucite disks, bearing sample plates, are held in this device by springs acting on opposite edges of the disks. The disks held in the sample changer may be slipped into the fission chamber from the side, and, when they are exactly centered in the chamber, the sample changer is pulled loose from the disk. Samples are removed in a similar manner by fitting the changer onto the sample-bearing disk as it is mounted in the fission chamber and then

sliding the disk out. The sample-changing device is mounted at the end of an aluminum pole so that the operator need come no closer than 4 to 6 ft from either the fission chamber or the recently irradiated samples.

### 3. OPERATING CHARACTERISTICS

The resolving-power loss of the fission-counting circuit has been determined experimentally to be 1.5 per cent per  $10^5$  fission counts per minute. For most purposes this is satisfactory, since the counting rates are usually less than 50,000 counts per minute.

The tolerance of the chamber was found to be  $10^7$  to  $10^8$   $\alpha$  particles per minute. This is somewhat below the  $\alpha$ -particle tolerance level usually obtained with a fast fission counter, and is due chiefly to the fact that the  $\alpha$  particles emitted from the sample travel a fairly long distance (1 cm) before they strike the walls of the chamber. Ordinarily a spacing of approximately 2 mm is used in fission chambers, and, since the specific ionization of a fission-fragment recoil is much greater at the beginning of its range, a maximum ratio of fission pulse to  $\alpha$  pulse is obtained in this manner. However, for our purpose it was more important to discriminate between the fission pulses and the high hash level caused by the secondary effects of the capture of neutrons. For this purpose a larger spacing was found to be more satisfactory.

The  $\beta$  tolerance of the chamber has not been measured, but has been estimated to be as high as several curies. Under maximum flux conditions, the fission pulse-to-hash ratio for a thin sample is 20 or more.

Perhaps the greatest error encountered in fission measurements is the uncertain loss of counts due to absorption of the fission fragments by the material of the sample itself. The ranges of the recoils in air are between 1.5 and 2.5 cm and are therefore readily absorbed by even a thin sample. A rough estimate of whether a sample has too much self-absorption is usually obtained by noting the ratio of counting rates between a high- and a low-amplifier gain setting. For a very thin sample, the difference in these two rates is approximately 1 per cent. For a very thick sample this difference may increase to as much as 15 per cent.

At maximum sensitivity the normal background is 15 to 50 fissions per minute, so that much of the time this quantity is the limiting factor in determining the accuracy of a measurement. The exact background level that can be obtained is somewhat variable. It has been found advantageous to purify a platinum solution from uranium and

then to electroplate from this solution a thick coating on the 1-mil thick platinum disks on which the samples are mounted. The surface of the inner lucite cup is usually painted with Amphenol coil dope, which fortuitously had been found to be relatively free of uranium contamination.

#### ACKNOWLEDGMENT

The authors wish to acknowledge the helpful encouragement and assistance of W. H. Zinn and T. W. Brill of the Argonne Laboratory.

Paper 22.30

THE BOMBARDMENT OF  $U^{233}$  WITH 44-MEV HELIUM IONS  
AND THE FORMATION OF  $Pu^{234}$  †

By I. Perlman, P. R. O'Connor, and L. O. Morgan

An isotope of plutonium having an observed half life of  $8.5 \pm 1$  hr has been identified among the transmutation products of the nucleus  $U^{233}$  that had been bombarded with 44-mev helium ions. The activity was first detected by Hyde, Studier, and Ghiorso,<sup>1</sup> who isolated the plutonium fraction from a sample of bombarded  $U^{233}$  and observed the decay of the total  $\alpha$  activity in this fraction.

Our studies have confirmed the formation of this short-lived plutonium isotope by the helium-ion bombardment of  $U^{233}$  and have resulted in the isotopic assignment  $Pu^{234}$ . Although the isotope is most easily identified by the observation of the  $\alpha$  particles associated with its decay, the predominant mode of disintegration may be orbital-electron capture.

A total of three bombardments of  $U^{233}$  with helium ions were carried out. In each bombardment approximately 3 mg of  $U^{233}$ , as  $U_3O_8$ , was spread on small platinum plates having an area of 0.9 sq cm. These plates were placed in the target chamber of the 60-in. cyclotron at Berkeley in such a way as to intercept the most intense portion of the beam of accelerated helium ions (44 mev energy). Each sample received a total bombardment of about  $20 \mu\text{a}\cdot\text{hr}$  over a period of 10 to 20 hr. The samples were then dissolved and subjected to chemical processes that were designed to separate relatively pure neptunium and plutonium fractions from the other elements that might be present. Samples of these fractions were then examined with the use of

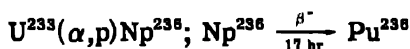
†Contribution from the Department of Chemistry and the Radiation Laboratory, University of California, Berkeley.

thin-wall Geiger-Mueller counters,  $\alpha$ -particle counters, and an  $\alpha$ -particle pulse-analysis apparatus.<sup>3</sup> This pulse-analysis apparatus is an instrument designed to sort, according to their energy, the electrical pulses caused by the passage of  $\alpha$  particles through an ionization chamber. With the use of this instrument approximate energies of groups of  $\alpha$  particles can be obtained by comparison with known standards.

In each plutonium fraction the total  $\alpha$  activity was observed to decay initially with a half life of  $8.5 \pm 1$  hr. In addition, there was present a background activity, which did not decay appreciably over a period of several months. Upon examination of the activities with the  $\alpha$ -pulse-analysis apparatus, there was found a group of  $\alpha$  particles having an energy of  $6.2 \pm 0.1$  mev. This group decayed with a half life of about 9 hr. Another group was observed with 5.75 mev energy. This group did not decay in a period of several months. The characteristics of this group are those of the  $\alpha$  particles from  $\text{Pu}^{238}$ , which could have been formed by the reaction



or

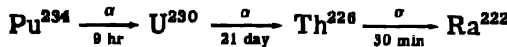


The yield of the latter reaction is probably low since no 17-hr negative  $\beta$ -particle activity was observed in any of the neptunium fractions.

The decay of the 8.5-hr  $\alpha$ -particle activity was accompanied by the growth of long range  $\alpha$  particles. One of the possible assignments for the 8.5-hr activity is  $\text{Pu}^{234}$ , which isotope would be consistent with the growth of  $\alpha$  activity of  $\text{U}^{230}$  and its disintegration products.<sup>3</sup> This process was confirmed by isolation and identification of the 30-min  $\alpha$  activity of  $\text{Th}^{226}$ , the daughter of  $\text{U}^{230}$ .

Another possible mechanism that would fit the same data would consist of the decay of the 8.5-hr  $\text{Pu}^{234}$  by orbital-electron capture to a short-lived  $\text{Np}^{234}$   $\alpha$  emitter, which in turn would give rise successively to  $\text{Pa}^{230}$ ,  $\text{U}^{230}$ , and its decay products. However, it has been found that  $\text{Np}^{234}$  probably decays with 4.4-day half life by orbital-electron capture<sup>4</sup> so that the  $\alpha$  particle undoubtedly belongs to  $\text{Pu}^{234}$ . This mechanism was also ruled out by isolating the protactinium fraction from the initial plutonium fraction and finding no evidence for the growth of  $\text{U}^{230}$  and its products after a one-month period.

On the basis of the above results the following decay sequence may be written:



The original plutonium fractions also contained a considerable amount of Geiger-Mueller counter activity consisting of radiation capable of penetrating 7 mg/sq cm aluminum. This activity could partially penetrate 2 g/sq cm of Be but was stopped with 2 g/sq cm of Be and 100 mg/sq cm of Pb in combination. This is strong evidence that there is soft electromagnetic radiation, which may be either low energy  $\gamma$  rays or x rays. This observed activity decayed initially with a half life of  $8 \pm 1$  hr and gradually underwent transition to a half life of 4.5 days. The data are compatible with the orbital-electron capture of Pu<sup>234</sup> to yield Np<sup>234</sup>, which decays by orbital-electron capture with a half life of 4.4 days although the Np<sup>234</sup> was not isolated for identification. The amount of 4.5-day activity was approximately that expected to be formed by the decay of an  $8 \pm 1$  hr parent. However, later work by Street, James, and Seaborg<sup>5</sup> would indicate that there is less electromagnetic radiation associated with Pu<sup>234</sup> than was found in these experiments. As a result it is not possible to determine the K/ $\alpha$  branching ratio within wide limits.

The neptunium fractions also contained 4.5-day Geiger-Mueller counter activity, probably owing to the decay of Pu<sup>234</sup> to Np<sup>234</sup> previous to the separation of plutonium and neptunium as well as to direct formation by the reaction U<sup>233</sup>( $\alpha$ ,p2n)Np<sup>234</sup>.

**Summary.** The isotope Pu<sup>234</sup> has been identified as a product of the bombardment of U<sup>233</sup> with 44-mev helium ions. Its mass assignment was made by the identification of members of the U<sup>230</sup> series following its decay. The isotope Pu<sup>234</sup> has a half life of 8 to 9 hr and probably decays by orbital-electron capture as well as by  $\alpha$ -particle emission. The  $\alpha$  particles from Pu<sup>234</sup> have an energy of  $6.2 \pm 0.1$  mev.

The isotopes Pu<sup>230</sup> and Np<sup>234</sup> were also observed as products of the 44-mev helium-ion bombardment of U<sup>233</sup>.

#### ACKNOWLEDGMENT

The authors are indebted to Dr. J. G. Hamilton and his group, who carried out the bombardments with the 60-in. Berkeley cyclotron.

## REFERENCES

1. E. K. Hyde, M. H. Studier, and A. Ghiorso, Products of the deuteron and helium-ion bombardments of  $U^{235}$ , Paper 22.15, this volume (Metallurgical Project Report CB-3736).
2. A. Ghiorso, A. H. Jaffey, H. P. Robinson, and B. Weissbourd, A 48-channel pulse-height analyzer for alpha-energy measurements, Paper 16.8, this volume (Metallurgical Project Report CC-3887).
3. M. H. Studier and E. K. Hyde, National Nuclear Energy Series, Division IV, Volume 17 B; Phys. Rev., 74: 591 (1948).
4. R. A. James, A. E. Florin, H. H. Hopkins, Jr., and A. Ghiorso, Products of helium-ion and deuteron bombardment of  $U^{235}$  and  $U^{238}$ , Paper 22.8, this volume.
5. K. Street, R. A. James, and G. T. Seaborg, private communication.

## Paper 22.50

### A GENERAL METHOD FOR DETERMINING COINCIDENCE CORRECTIONS OF COUNTING INSTRUMENTS†

By T. P. Kohman

#### 1. INTRODUCTION

All instruments that count random events, such as those encountered in the measurement of radioactivity, have finite resolving powers and therefore are unable to distinguish and record separately events that occur very close together in time. As a consequence some counts are missed; the fraction lost increases as the counting rate increases. This results in a nonlinear variation of the response of the instrument to the intensity of the source of events. The difference between the recorded rate and the true rate (i.e., the rate that would be observed if the instrument could count all events to which it is normally sensitive) is called the "coincidence loss" or "correction."

In practice coincidence losses are often appreciable. Therefore, in order to obtain accurate measurements in radioactivity with counting instruments, it is necessary to correct the recorded counting rates for this effect. Moreover, the useful upper limit of a counter is greatly extended by a knowledge of its coincidence corrections. Coincidence-loss measurements also supply valuable information about the mode of operation of counters and provide a useful guide in improving instruments in order to decrease their losses.

The problem has received attention for a number of years, and several methods of determining and applying coincidence corrections

†Contribution from the Technical Department, Hanford Engineer Works, E. I. du Pont de Nemours & Co., Richland, Wash.

Original Report No. SE-PC-46, dated June 13, 1945. Reissued by Metallurgical Laboratory as Report No. (H) CP-3275 in November 1945. Reissued by United States Atomic Energy Commission as Manhattan District Declassified Document MDDC-905 in May 1947.

are described in the literature. However, all these methods are either inconvenient, not generally applicable, or not sufficiently accurate. Recent experience at the Hanford Engineer Works and other Metallurgical Project sites has indicated the importance of the problem and the inadequacy of the previously described methods. This paper describes a new method, which is capable of any desired accuracy and which is almost completely general in its applicability.

## 2. THEORY OF THE METHOD

**2.1 Notation.** In order to facilitate the discussion, the notation to be used is presented below.

R = recorded rate

N = true or corrected rate (including background)

b = background rate

$N' = N - b$  = corrected rate due to source alone

t = time of count

Subscripts A and B refer to individual members of a pair of sources

Subscript C refers to the combined sources of the pair

$\tau$  = resolving time of counter

$\nu, \phi, \dots$  = supplementary parameters

**2.2 Methods Involving the Use of Paired Sources.** Reviews of methods of determining coincidence corrections have been given by Beers<sup>1</sup> and by Kohman.<sup>2</sup> The use of paired sources, first proposed by Moon,<sup>3</sup> has been employed frequently (see references 1, 2, and 4 to 7). If each of two radioactive sources of approximately equal strength is measured separately, and the two are then measured together, taking care to keep geometrical factors constant throughout, the combined counting rate (corrected for background) will be less than the sum of the individual rates (corrected for background) since the fractional counting loss is greater at the higher counting rate. If a simple mathematical relation between recorded and true rates involving but a single parameter applies for the instrument, a single set of measurements on one pair of sources can be used to evaluate the parameter (see references 1, 2, 4, and 6 to 8). However, it has been shown that the simple one-parameter relations previously proposed do not adequately express the behavior of real counters.

In order to avoid this difficulty, a completely general method, which involves no assumed mathematical relation between true and recorded rates, was developed.<sup>2</sup> This method uses a number of paired sources of different intensities covering the range of the instrument, and the data are analyzed by a graphical method of successive approximations

which gives a curve of fractional correction vs. recorded rate. Unfortunately, this method is tedious and time-consuming and is possibly subject to personal factors. A completely mathematical analysis of the data would be a considerable improvement. A prerequisite for this analysis is a mathematical relation between true and recorded rates.

Single-parameter relations between  $N$  and  $R$  that have been proposed are the following:

1. Johnson and Street,<sup>9</sup> Ruark and Brammer<sup>10</sup>

$$N = R + \tau NR \quad (1)$$

2. Volz,<sup>11</sup> Schiff<sup>12</sup>

$$N = Re^{\tau N} \quad (2)$$

3. An approximation of Eq. 2, due to Hull<sup>1</sup>

$$N = R + \tau R^2 + \frac{1}{2}\tau^2 R^3 \quad (3)$$

4. An approximation<sup>2,6,7</sup> of Eq. 1

$$N = R + \tau R^2 \quad (4)$$

For each of these relations, methods have been developed for evaluating the parameter  $\tau$  from a set of paired source measurements:<sup>†</sup>

1. Beers<sup>1</sup>

$$\tau = \frac{R_A + R_B - R_C - b}{2(R_A - b)(R_B - b)} - \frac{\left[ \frac{(R_A + R_B - R_C - b)(R_C - b)}{(R_A - b)(R_B - b)} \right]^2}{8(R_C + b)} \quad (5)$$

- Kohman<sup>6</sup>

$$\tau = \frac{1}{R_C} \left( 1 - \sqrt{1 - \frac{R_C}{R_A R_B} (R_A + R_B - R_C - b)} \right) \quad (6)$$

Equation 5 is more exact at low counting rates, and Eq. 6 at high counting rates.

<sup>†</sup>The derivations of Eqs. 5 to 9 proceed from the fact that  $N'_A + N'_B = N'_C$ .

2. Crawford<sup>6</sup>

$$N_C = \frac{(R_A + R_B)^2}{R_C} \quad (7)$$

$\tau$  is then obtained from  $N_C$ ,  $R_C$ , and Eq. 2. In order for Eq. 7 to be applicable the background must be small enough to be neglected, and  $R_A$  and  $R_B$  must be very nearly equal.

3. Hull<sup>4</sup>

$$\frac{1}{2} (R_A^3 + R_B^3 - R_C^3) \tau^2 + (R_A^2 + R_B^2 - R_C^2) \tau + R_A + R_B - R_C - b = 0 \quad (8)$$

$\tau$  is obtained by solution of this equation by the quadratic formula.

4. Jarrett,<sup>6</sup> Kohman,<sup>2,8</sup> and Metcalf and Hennessee<sup>7</sup>

$$\tau = \frac{R_A + R_B - R_C - b}{R_C^2 - R_A^2 - R_B^2} \quad (9)$$

Inspection of Eqs. 1 to 4 reveals that they are all nearly equivalent for low counting rates in which the difference between  $N$  and  $R$  is very small (approximately 1 per cent). Moreover, any one will adequately represent the behavior of actual counters in the region of small losses. Equation 4 means that the fractional correction is proportional to  $R$ ; and because of the simplicity of this equation and its corollary, Eq. 9, these equations have received extensive use in rough evaluations and applications of coincidence corrections.<sup>6,8,13</sup> However, in general no single-parameter equation, theoretical or empirical, can adequately relate  $N$  and  $R$  when the losses are large. As an illustration, a semitheoretical equation that expresses the observed behavior of a Geiger-Mueller counter over a wide range of counting rates contains three parameters;<sup>2</sup> but that equation is not suitable for practical application, nor is it applicable to other types of instruments.

In theory the relation between two dependent variables such as  $N$  and  $R$  can be expressed by an infinite power series:

$$N = c_0 + c_1 R + c_2 R^2 + c_3 R^3 + c_4 R^4 + \dots \quad (10)$$

If we set  $c_0 = 0$ ,  $c_1 = 1$ , and  $c_2 = \tau$ , Eq. 10 becomes the equivalent of Eqs. 1 to 4 for small values of  $R$ . Hence we are justified in rewriting the series as follows:

$$N = R + \tau R^2 + \nu R^3 + \phi R^4 + \dots \quad (11)$$

For practical purposes the number of terms of Eq. 11 to be retained will be determined by the behavior of the instrument and the precision required.

As previously mentioned, when only two terms of Eq. 11 are used, giving Eq. 4, the parameter can be evaluated from measurements on a single pair of sources by means of Eq. 9. It has been pointed out by Jarrett<sup>6</sup> that the first three terms of Eq. 11 might be used similarly to evaluate the two parameters from measurements on two pairs of sources. Two equations analogous to Eq. 9 are obtained, but this involves the two unknown parameters, and their simultaneous solution yields the values of the latter. Similarly, this method can be extended to any number of terms of Eq. 11 by employing as many pairs of sources as there are parameters.

**2.3 The Least-squares Evaluation of Paired Source Data.** The use of equations such as Eq. 9 or its higher analogues, according to the method of Jarrett, has a serious disadvantage in that only a limited number of measurements can be admitted into the evaluation of the parameters. It is generally desirable to employ a greater number of measurements in obtaining the final result so that an error in one measurement will not seriously affect the values of the parameters (as would be the case when the minimum number of measurements is used) and so that the entire counting range of the instrument can be represented in the data. The method of least squares provides a means of doing this.

Consider a pair of sources that have been counted separately and together. Let us define the quantity  $\delta$ , which we will call the "residual," as follows:

$$\delta = N'_A + N'_B - N'_C$$

If the  $N$  values were the true values, as would be the case if the correction of the  $R$  values were perfect, then  $\delta$  would equal zero (except for statistical fluctuations due to the random distribution of counts). Actually, when the  $N$  values are obtained by an equation such as will be used in practice, the corrections will not be perfect, and  $\delta \neq 0$ .  $\delta$  is the algebraic sum of the errors in the corrections to  $R_A$ ,  $R_B$ , and  $R_C$ . It may be considered as a measure of the error in the correction to  $R_C$  since this is the largest correction, and hence it is expected to have the largest error. Similarly the fractional residual may be defined as  $\epsilon = \delta/R_C$ , which may be considered a measure of the fractional error in the correction to  $R_C$ .

If a number of such paired source measurements have been made, the best values of the parameters in Eq. 11 are those which make  $\Sigma\epsilon^2$  a minimum.

$$\frac{\partial}{\partial \tau} \sum \epsilon^2 = 0$$

$$\frac{\partial}{\partial \nu} \sum \epsilon^2 = 0$$

$$\frac{\partial}{\partial \phi} \sum \epsilon^2 = 0, \text{ etc.}$$

**2.4 One-parameter Case.** For the case in which only two terms of Eq. 11 are retained, giving Eq. 4, the evaluation of the parameter  $\tau$  by the least-squares method proceeds as follows:

$$\begin{aligned}\epsilon &= \frac{\delta}{R_C} = \frac{N'_A + N'_B - N'_C}{R_C} \\ &= \frac{N_A + N_B - N_C - b}{R_C} \\ &= \frac{R_A + R_B - R_C - b + \tau(R_A^2 + R_B^2 - R_C^2)}{R_C} \\ &= \frac{D + \tau E}{R_C}\end{aligned}$$

where

$$D = R_A + R_B - R_C - b$$

$$E = R_A^2 + R_B^2 - R_C^2$$

$$\begin{aligned}\sum \epsilon^2 &= \sum \frac{1}{R_C^2} (D + \tau E)^2 \\ &= \sum \frac{1}{R_C^2} (D^2 + 2\tau DE + \tau^2 E^2) \\ &= \sum \frac{D^2}{R_C^2} + 2\tau \sum \frac{DE}{R_C^2} + \tau^2 \sum \frac{E^2}{R_C^2} \\ &= G + 2\tau H + \tau^2 L\end{aligned}$$

where

$$G = \sum \frac{D^2}{R_C^2}$$

$$H = \sum \frac{DE}{R_C^2}$$

$$L = \sum \frac{E^2}{R_C^2}$$

The condition for best fit is:

$$\frac{d}{d\tau} \sum \epsilon^2 = 0 = 2H + 2\tau L$$

whence

$$\tau = -\frac{H}{L} \quad (12)$$

**2.5 Two-parameter Case.** For the case in which three terms of Eq. 11 are used,

$$N = R + \tau R^2 + \nu R^3 \quad (13)$$

the least-squares evaluation of the two parameters follows:

$$\begin{aligned} \epsilon &= \frac{R_A + R_B - R_C - b + \tau(R_A^2 + R_B^2 - R_C^2) + \nu(R_A^3 + R_B^3 - R_C^3)}{R_C} \\ &= \frac{D + \tau E + \nu F}{R_C} \end{aligned}$$

where

$$D = R_A + R_B - R_C - b$$

$$E = R_A^2 + R_B^2 - R_C^2$$

$$F = R_A^3 + R_B^3 - R_C^3$$

$$\begin{aligned} \sum \epsilon^2 &= \sum \frac{1}{R_C^2} (D + \tau E + \nu F)^2 \\ &= \sum \frac{1}{R_C^2} (D^2 + 2\tau DE + 2\nu DF + 2\tau\nu EF + \tau^2 E^2 + \nu^2 F^2) \\ &= \sum \frac{D^2}{R_C^2} + 2\tau \sum \frac{DE}{R_C^2} + 2\nu \sum \frac{DF}{R_C^2} + 2\tau\nu \sum \frac{EF}{R_C^2} + \tau^2 \sum \frac{E^2}{R_C^2} + \nu^2 \sum \frac{F^2}{R_C^2} \\ &= G + 2\tau H + 2\nu J + 2\tau\nu K + \tau^2 L + \nu^2 M \end{aligned}$$

where

$$G = \sum \frac{D^2}{R_C^2}$$

$$H = \sum \frac{DE}{R_C^2}$$

$$J = \sum \frac{DF}{R_C^2}$$

$$K = \sum \frac{EF}{R_C^2}$$

$$L = \sum \frac{E^2}{R_C^2}$$

$$M = \sum \frac{F^2}{R_C^2}$$

The condition for best fit is

$$\frac{\partial}{\partial \tau} \sum \epsilon^2 = 0 = 2H + 2\nu K + 2\tau L$$

$$\frac{\partial}{\partial \nu} \sum \epsilon^2 = 0 = 2J + 2\tau K + 2\nu M$$

Solving these simultaneous equations yields

$$\tau = \frac{JK - HM}{LM - K^2}$$

$$\nu = \frac{HK - JL}{LM - K^2} \quad (14)$$

**2.6 Three-parameter Case.** The derivation of the method for the case in which three parameters are used,

$$N = R + \tau R^2 + \nu R^3 + \phi R^4 \quad (15)$$

proceeds similarly. Three simultaneous equations are obtained in three unknowns, the solution of which yields the desired values. The solution is straightforward, but the computation is somewhat longer than in the two-parameter case, especially since the solution of simultaneous equations containing more than two unknowns is somewhat involved. Consequently, the two-parameter case is probably the most satisfactory for routine practical use. Only if high accuracy is needed and the experimental measurements have been made with a compatible degree of precision, or if the fractional corrections are quite large (approximately 50 per cent) should it be necessary to invoke additional parameters. Obviously the method can be extended to any number of parameters.

**2.7 Significance of the Parameters.** It is customary to consider the coincidence losses of a counter in terms of quantities called the

"resolving time," the "insensitive time," and the "dead time." The resolving time is defined as the minimum interval between two events that can both be registered by the instrument. The insensitive time is the interval following a recorded event during which the instrument is incapable of recording another event. The dead time is a quantity peculiar to Geiger-Mueller counters. It is the interval following a discharge during which the tube is incapable of producing an electron avalanche.

The insensitive time is not a property of the instrument but is a particular event recorded by the instrument. With practically all types of counters this quantity is not a constant but may be different for different events. For example, the insensitive time of a Geiger-Mueller-counter discharge may be shortened by the occurrence of another discharge a short time previously,<sup>2,6,14</sup> or it may be lengthened by the occurrence of an unrecorded discharge near the end of the interval. The insensitive time of a pulse in an  $\alpha$ -particle counter may depend on the length and position of the track of the particle. If the insensitive time had a constant value, the resolving time would have this same value. But, in view of the variability of insensitive times, the simple definition for resolving time given above has no clear meaning. Nevertheless it is desirable to retain the idea of the resolving time as a characteristic of the instrument in the sense that the insensitive time is a characteristic of an individual event.

Equations 1 and 2 are derived theoretically from certain physical assumptions, among which is that of a constant insensitive time or resolving time  $\tau$ . The parameter has the same meaning in other approximate equations, such as Eqs. 3 and 4. Since the empirical Eq. 11 becomes essentially equivalent to these equations at very low counting rates,  $\tau$  may also be called the resolving time in the latter. Physically, it is the limiting average value of the insensitive time as the counting rate approaches zero. With Geiger-Mueller counters, the insensitive time is constant at very low rates, but with proportional counters or counting ionization chambers the insensitive time varies; therefore the average is specified. Mathematically, the resolving time may be defined as follows:

$$\tau = \left[ \frac{d(N/R)}{dR} \right]_{R=0} = - \left[ \frac{d(R/N)}{dN} \right]_{N=0}$$

The parameters  $v, \phi, \dots$  of Eq. 11 have no simple physical significance; they are merely constants employed to correlate the experimental observations.

The parameter  $\tau$ , being the resolving time, has the dimension of time and is always positive. The parameters  $v, \phi, \dots$  have the dimensions time<sup>2</sup>, time<sup>3</sup>, ..., and may have either sign.

The discussion thus far has been confined to counting instruments. The method is equally applicable to some other types of measuring instruments that do not count. All radiation-measuring instruments are expected to deviate increasingly from linear as the radiation intensity increases. Examples to which the method can be applied are Lauritsen quartz-fiber electroscopes, high-pressure  $\gamma$ -ray ionization chambers,  $\beta$ -ray ionization-chamber d-c-amplifier assemblies, photo-cells, etc. In such cases, the notion of a resolving time no longer applies, and it is more logical to rewrite Eq. 11 as

$$I = M + aM^2 + bM^3 + cM^4 + \dots \quad (16)$$

where  $M$  and  $I$  are the measured and true intensities, respectively.

Once the parameters have been evaluated for a particular instrument by the method described, subsequent measurements made with the instrument can be corrected by the use of the corresponding equation, e.g., Eqs. 4, 13, or 15. The coincidence correction should be added before subtracting the background, especially if both are large. To facilitate the application of corrections, a graph or table showing the correction as a function of the recorded rate may be employed.

### 3. APPLICATION OF THE METHOD

**3.1 Procedure for Taking Data.** The experimental part of the determination of coincidence corrections of an instrument consists of taking a series of sets of paired source measurements. Each set is comprised of four measurements involving two approximately equal sources:  $R_A$ ,  $R_B$ ,  $R_C$ , and  $b$ . The series should contain three or more sets with counting rates covering the range of the instrument for which the corrections are desired.

The procedure for taking a set of measurements is as follows. Sources and counting conditions are chosen which will give the desired counting rates. (With many instruments the counting rate can be adjusted by varying the distance between source and detector or by inserting suitable absorbers.) In order to eliminate possible changes due to variations in geometry, a dummy source should occupy the place of each active source when the latter is not in position. The order of measurements follows:

1. Place both dummies in position. Measure  $b$ .
2. Replace dummy A by active source A. Measure  $R_A$ .

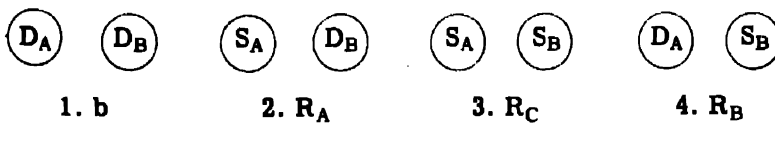
3. Replace dummy B by source B, with care not to disturb the position of source A. Measure  $R_C$ .

4. Replace source A by dummy A, with care not to disturb the position of source B. Measure  $R_B$ .

Table 1—Length of Counting Interval ( $t$ ) in Minutes Required for a Given Fractional Probable Error (P) for Various Combined-source Counting Rates ( $R_C$ ) in Counts per Minute

$R_C$	Fractional probable error, P					
	5%	2%	1%	0.5%	0.2%	0.1%
1,000	1.5	9.1	36	146	910	3640
2,000	0.7	4.6	18	73	455	1820
5,000	0.3	1.8	7.3	29	182	728
10,000	0.15	0.9	3.6	15	91	364
20,000	0.07	0.5	1.8	7.3	46	182
50,000	0.03	0.2	0.7	2.9	18	73
100,000	0.015	0.09	0.4	1.5	9.1	36
200,000	0.007	0.05	0.2	0.7	4.6	18
500,000	0.003	0.02	0.07	0.3	1.8	7.3
1,000,000	0.001	0.01	0.04	0.15	0.9	3.6

The sequence is illustrated in the figure below, where  $S_A$  and  $S_B$  are the active sources and  $D_A$  and  $D_B$  the dummies:



It is generally desirable to count  $R_A$ ,  $R_B$ , and  $R_C$  for equal periods of time. In this manner the greatest statistical accuracy can be obtained for a given total number of counts.<sup>1</sup> This is desirable with instruments such as Geiger-Mueller counters whose lifetime is a function of usage. The greatest statistical accuracy for a given total expenditure of time is obtained when:

$$t_A : t_B : t_C : t_b = \sqrt{R_A} : \sqrt{R_B} : \sqrt{R_C} : \sqrt{b} \approx 1 : 1 : 1 : \sqrt{2} : \sqrt{b/R_A}$$

However, the loss in accuracy by making  $t_A = t_B = t_C$  is slight; therefore, even for instruments that are not damaged by usage the convenience of using equal counting periods is sufficient to justify it. It

is also desirable to make  $t_b$  greater than indicated by the above ratio, since a more exact value of the background is a useful indication of whether the instrument is functioning properly.

The counting time necessary for each set depends on the accuracy required in the corrections, and may be estimated as follows: Consider an instrument for which Eq. 4 holds and  $\tau$  has a value of approximately  $10^{-5}$  min. In order to determine  $\tau$  from a single set of paired-source measurements using Eq. 9, the counting rates being approximately 1,000, 1,000, and 2,000 per minute, an accuracy (fractional probable error) of 0.5 per cent in corrected measurements at 2,000 counts per minute is required. The coincidence correction at this rate is approximately 40 counts per minute and this quantity must be known with an accuracy of 10 counts per minute, or 25 per cent of its value. This means that  $\tau$  must be known with an accuracy of 25 per cent, which in turn means that  $D (= R_A + R_B - R_C - b)$  must also have an accuracy of 25 per cent. Since  $D \approx 20$  counts per minute, its probable error must be 5 counts per minute. The probable error in  $D$  is equal to

$$0.6745 \sqrt{\frac{R_A}{t_A} + \frac{R_B}{t_B} + \frac{R_C}{t_C} + \frac{b}{t_b}} \approx 0.6745 \sqrt{\frac{2R_C}{t}}$$

when the counting times are equal. From this it follows that  $t = 73$  min. The general formula for the counting interval is

$$t \approx \frac{8K^2}{P^2 R_C} = \frac{3.64}{P^2 R_C} \quad (17)$$

where  $t = t_A = t_B = t_C =$  required counting interval

$P$  = fractional probable error required at  $R = R_C$

$K = 0.6745$  = factor used in computing probable errors†

It is to be noted that the time requirement is independent of the resolving time. From Eq. 17, Table 1 has been prepared.

In cases in which Eq. 4 does not hold and the method described herein is to be used instead, each set of paired source measurements may be imagined to establish a point on the correction curve. Hence the same considerations apply, and Eq. 17 and Table 1 can be used as a general guide in paired-source measurements. Thus, when a series of such measurements is made, each set should contain approximately the same total number of counts.

† If it is desired to express  $P$  in terms of some other measure of deviation than the probable error, the corresponding value of  $K$  must be used instead.

The choice of counting rates for the various sets of paired source measurements can be made from the following considerations. The  $R_C$  values should be fairly evenly distributed over the useful range of the instrument. The maximum useful rate of a counter for general purposes may be considered to be that for which the coincidence loss is about 10 or 20 per cent. Some Geiger-Mueller counters, however, have lower useful limits because high rates may permanently alter the tube characteristics. Since sets with low values of  $R_C$  require long counting intervals and enter into the computations with less weight than the higher sets, it is usually not profitable to use  $R_C$  values lower than that counting rate for which the coincidence correction is about 1 or 2 per cent. If more than 3 or 4 sets are taken duplication is permissible, and this has the advantage of indicating the consistency and reproducibility of the data.

**3.2 Sample Data.** To illustrate the application of the method to actual counting instruments, several series of data taken with various types of instruments are presented in Tables 2 to 5 together with the results of the computations. The examples have been chosen to illustrate the one-, two-, and three-parameter cases.

**3.3 Preliminary Examination of Data.** In order to obtain an idea of the consistency of the data and to determine the number of parameters that should be computed, a preliminary examination of the data should be made by applying Eq. 9 to each set of measurements. The value of  $\tau$  so obtained is designated as  $\tau_1$ , since it implies a one-parameter relation, Eq. 4. The values of  $\tau_1$  are included in Tables 2 to 5.

If, as in Table 2, the variations in  $\tau_1$  show no trend with counting rate and are no greater than expected from statistical fluctuations, a one-parameter computation should suffice. The data in Tables 3 and 4 show a progressive increase in  $\tau_1$  (the initial decrease in Table 3 is not significant), indicating that two parameters should be computed. The data in Table 5 show a significant decrease in  $\tau_1$ , followed by a significant increase, which suggests that three parameters are probably required to express the behavior of the counter.

**3.4 Sample Computation.** In order to demonstrate the manner in which the computations are set up and carried out, a typical two-parameter computation is shown in Table 6. The computations involving a different number of parameters follow similar patterns, except that with three or more parameters the solution of the simultaneous equations must be handled differently.

In the computation, sufficient significant figures should be carried to allow for the loss that occurs in solving the simultaneous equations. In the three-parameter computation (Table 5) three significant figures

## THE TRANSURANIUM ELEMENTS

Table 2—Paired-source Measurements on Geiger-Mueller Counter; Argon-alcohol-filled Bell-type Mica-window Tube with Self-quenching Circuit and Offner Scaler†

No.	R <sub>A</sub> , counts per minute	R <sub>B</sub> , counts per minute	R <sub>C</sub> , counts per minute	b	τ <sub>1</sub> , minutes	δ, counts per minute	ε, %
I	2,334	2,485	4,750	30	3.6 × 10 <sup>-6</sup>	-6	-0.13
II	3,077	3,155	6,133	28	3.9 × 10 <sup>-6</sup>	-4	-0.07
III	3,089	3,116	6,134	28	2.3 × 10 <sup>-6</sup>	-33	-0.54
IV	3,727	3,696	7,293	33	3.8 × 10 <sup>-6</sup>	-9	-0.12
V	3,779	3,692	7,324	29	4.6 × 10 <sup>-6</sup>	+12	+0.16
VI	5,452	5,356	10,505	33	5.2 × 10 <sup>-6</sup>	+56	+0.53
VII	5,334	5,411	10,508	34	3.9 × 10 <sup>-6</sup>	-14	-0.13

†Result of computation:

$$\tau = 4.12 \times 10^{-6} \text{ min}$$

$$N = R + \tau R^2$$

Table 3—Paired-source Measurements on α Counter; Air-filled Parallel-plate Ionization Chamber with Linear Pulse Amplifier and Offner Scaler†

No.	R <sub>A</sub> , counts per minute	R <sub>B</sub> , counts per minute	R <sub>C</sub> , counts per minute	b	τ <sub>1</sub> , minutes	δ, counts per minute	ε, %
I	294.4	313.4	603.4	2.0	13 × 10 <sup>-6</sup>	+0.6	+0.10
II	546.5	538.2	1,076.6	2.0	11 × 10 <sup>-6</sup>	+0.4	+0.04
III	736	725	1,450	2	9 × 10 <sup>-6</sup>	-2	-0.14
IV	1,323	1,143	2,436	2	9.7 × 10 <sup>-6</sup>	-18	-0.74
V	2,459	2,514	4,782	2	17.9 × 10 <sup>-6</sup>	+13	+0.27
VI	4,454	4,327	8,131	2	23.5 × 10 <sup>-6</sup>	+1	+0.01
VII	5,924	6,245	10,860	2	29.8 × 10 <sup>-6</sup>	-7	-0.06

†Result of computation:

$$\tau = 8.20 \times 10^{-6} \text{ min}$$

$$\nu = 1.147 \times 10^{-6} \text{ min}^2$$

$$N = R + \tau R^2 + \nu R^3$$

Table 4—Paired-source Measurements on α Counter;† Nitrogen-filled Parallel-plate Ionization Chamber with High-frequency Amplifier and Offner Scaler

No.	R <sub>A</sub> , counts per minute	R <sub>B</sub> , counts per minute	R <sub>C</sub> , counts per minute	b	τ <sub>1</sub> , minutes	δ, counts per minute	ε, %
I	41,287	41,111	81,094	2	4.10 × 10 <sup>-7</sup>	+70	+0.09
II	80,308	70,495	145,492	3	5.44 × 10 <sup>-7</sup>	-135	-0.09
III	108,794	123,160	216,621	2	7.73 × 10 <sup>-7</sup>	+74	+0.03

†Result of computation (see Table 6):

$$\tau = 1.814 \times 10^{-7} \text{ min}$$

$$\nu = 1.662 \times 10^{-12} \text{ min}^2$$

$$N = R + \tau R^2 + \nu R^3$$

were lost in the solution of the equations; therefore eight figures were carried up to this point in order to give satisfactory accuracy in the result. Because of its length, this computation was consequently quite tedious.

**3.5 Checking the Computations.** Computations should be checked against the data by computing the residual ( $\delta$ ) and the fractional residual ( $\epsilon = \delta/R_C$ ) for each set. If the values of  $\epsilon$  are all small (i.e.,

Table 5—Paired-source Measurements on Geiger-Mueller Counter; Hydrogen-filled Thin-walled Glass Tube (Eck and Krebs), with Neher-Harper Quenching Circuit and McKibben Scalert  
(Data from Reference 2)

No.	R <sub>A</sub> , counts per minute	R <sub>B</sub> , counts per minute	R <sub>C</sub> , counts per minute	b	τ <sub>1</sub> , minutes	δ, counts per minute	ε, %
I	579	647	201	16	$13 \times 10^{-6}$	+1	+0.06
II	2,054	2,491	4,386	18	$11.0 \times 10^{-6}$	+39	+0.88
III	5,580	7,090	11,960	20	$10.8 \times 10^{-6}$	+12	+0.10
IV	7,320	9,970	16,120	20	$10.6 \times 10^{-6}$	+66	+0.41
V	17,880	18,460	33,100	20	$7.4 \times 10^{-6}$	-470	-1.42
VI	28,800	32,600	53,700		$6.9 \times 10^{-6}$	+630	+1.18
VII	53,500	58,200	93,200		$7.6 \times 10^{-6}$	-430	-0.47
VIII	65,700	77,400	114,000		$10.8 \times 10^{-6}$	+200	+0.18

†Result of computation:

$$\tau = 1.217 \times 10^{-6} \text{ min}$$

$$\nu = -8.76 \times 10^{-11} \text{ min}^2$$

$$\phi = 5.29 \times 10^{-15} \text{ min}^3$$

$$N = R + \tau R^2 + \nu R^3 + \phi R^4$$

of the order of magnitude of  $P$  in Eq. 17) and are distributed randomly in sign, it is assumed that the equation obtained satisfactorily represents the behavior of the instrument. If, however, the values of  $\epsilon$  are all of the same sign or show a significant trend, an error in the computations is indicated or an additional parameter must be computed.

In Tables 2, 3, 4, and 5 are given, for each set of measurements, the values of  $\delta$  and  $\epsilon$  computed from the result of the least-squares computation. In each case these quantities are small and of random sign, indicating that the equation obtained is adequate for the correction of measurements made with the instrument.

**3.6 Graphical Illustration of Results.** For two of the examples considered the fractional correction has been plotted as a function of the recorded rate. Figure 1 shows the behavior of the  $\alpha$  counter with which the data of Table 3 were taken. For comparison, the dashed line indicates the previously assumed losses of such instruments, 0.8 per cent per 1,000 counts per minute.<sup>13</sup> The difference between

Table 6.—Sample Computation, Illustrating Method of Laying Out Work for Determining Two Parameters with Aid of Calculating Machine.  
(Data from Table 4)

Set No.	I	II	III
R <sub>A</sub>	41,287	80,308	108,794
R <sub>B</sub>	41,111	70,495	123,160
R <sub>C</sub>	81,094	145,492	216,621
b	2	3	2
R <sub>A</sub> + R <sub>B</sub> - R <sub>C</sub> - b = D	1,302	5,308	15,331
R <sub>A</sub> <sup>2</sup>	1.70461 × 10 <sup>9</sup>	6.44937 × 10 <sup>9</sup>	1.18361 × 10 <sup>10</sup>
R <sub>B</sub> <sup>2</sup>	1.69011 × 10 <sup>9</sup>	4.96954 × 10 <sup>9</sup>	1.51684 × 10 <sup>10</sup>
R <sub>C</sub> <sup>2</sup>	6.57623 × 10 <sup>9</sup>	2.11679 × 10 <sup>10</sup>	4.69246 × 10 <sup>10</sup>
R <sub>A</sub> <sup>3</sup> + R <sub>B</sub> <sup>3</sup> - R <sub>C</sub> <sup>3</sup> = E	-3.18151 × 10 <sup>9</sup>	-9.74901 × 10 <sup>9</sup>	-1.99201 × 10 <sup>10</sup>
R <sub>A</sub> <sup>3</sup>	7.03782 × 10 <sup>13</sup>	5.17936 × 10 <sup>14</sup>	1.28770 × 10 <sup>15</sup>
R <sub>B</sub> <sup>3</sup>	6.94821 × 10 <sup>13</sup>	3.50328 × 10 <sup>14</sup>	1.88614 × 10 <sup>15</sup>
R <sub>C</sub> <sup>3</sup>	5.33293 × 10 <sup>14</sup>	3.07976 × 10 <sup>15</sup>	1.01649 × 10 <sup>16</sup>
R <sub>A</sub> <sup>3</sup> + R <sub>B</sub> <sup>3</sup> - R <sub>C</sub> <sup>3</sup> = F	-3.93432 × 10 <sup>14</sup>	-2.21150 × 10 <sup>15</sup>	-7.00903 × 10 <sup>15</sup>
DE/R <sub>C</sub> <sup>2</sup> = V	-6.29960 × 10 <sup>3</sup>	-2.44463 × 10 <sup>3</sup>	-6.50821 × 10 <sup>3</sup>
DF/R <sub>C</sub> <sup>2</sup> = W	-7.78970 × 10 <sup>7</sup>	-5.54549 × 10 <sup>8</sup>	-2.28996 × 10 <sup>8</sup>
EF/R <sub>C</sub> <sup>2</sup> = X	1.90338 × 10 <sup>14</sup>	1.01852 × 10 <sup>15</sup>	2.97542 × 10 <sup>15</sup>
E <sup>2</sup> /R <sub>C</sub> <sup>2</sup> = Y	1.53918 × 10 <sup>9</sup>	4.48998 × 10 <sup>9</sup>	8.45636 × 10 <sup>9</sup>
F <sup>2</sup> /R <sub>C</sub> <sup>2</sup> = Z	2.35376 × 10 <sup>19</sup>	2.31044 × 10 <sup>20</sup>	1.04692 × 10 <sup>21</sup>
ΣV = H	-9.58280 × 10 <sup>3</sup>		
ΣW = J	-2.92240 × 10 <sup>9</sup>		
ΣX = K	4.18428 × 10 <sup>15</sup>		
ΣY = L	1.44855 × 10 <sup>10</sup>		
ΣZ = M	1.30150 × 10 <sup>21</sup>		
JK	-1.22281 × 10 <sup>28</sup>		
HM	-1.24720 × 10 <sup>28</sup>		
JK - HM	2.439 × 10 <sup>23</sup>		
HK	-4.00971 × 10 <sup>19</sup>		
JL	-4.23324 × 10 <sup>19</sup>		
HK - JL	2.2353 × 10 <sup>19</sup>		
LM	1.88529 × 10 <sup>21</sup>		
K <sup>2</sup>	1.75082 × 10 <sup>21</sup>		
LM - K <sup>2</sup>	1.3447 × 10 <sup>20</sup>		
JK - HM LM - K <sup>2</sup> = τ	1.814 × 10 <sup>-7</sup>		
HK - JL LM - K <sup>2</sup> = ν	1.662 × 10 <sup>-12</sup>		

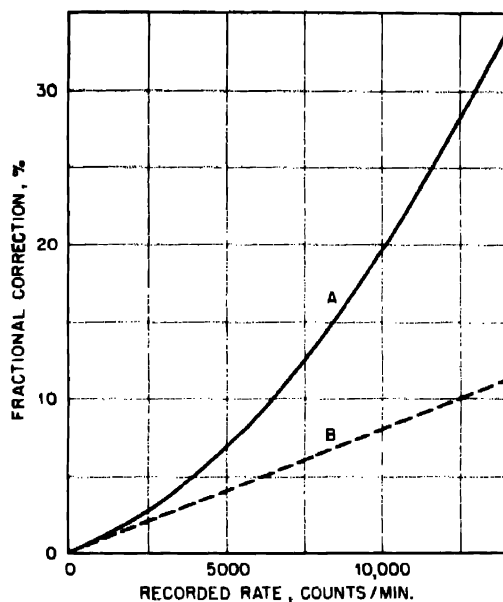


Fig. 1—Coincidence corrections for  $\alpha$  counter, from data of Table 3. A, found by the method described in this paper. B, previously assumed for this type of instrument.

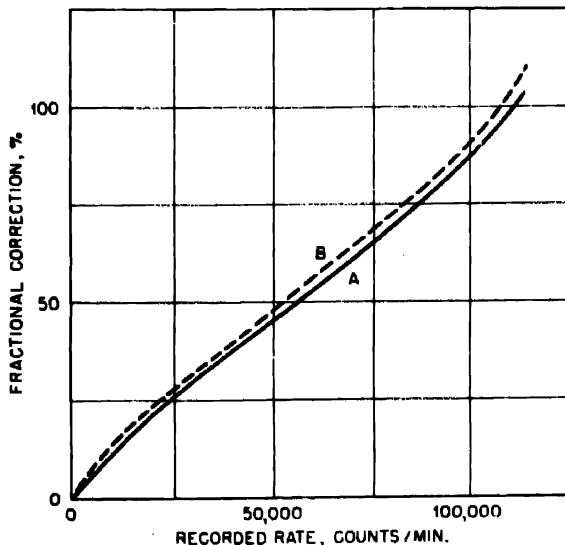


Fig. 2—Coincidence corrections for Geiger-Mueller counter, from data of Table 5. A, found by the method described in this paper. B, previously found by method of successive graphical approximations.

## THE TRANSURANIUM ELEMENTS

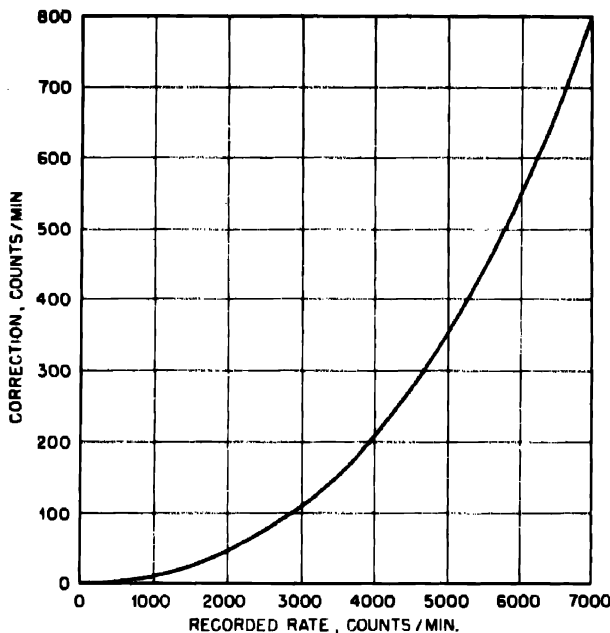


Fig. 3—Coincidence correction chart for  $\alpha$  counter, from data of Table 3. Linear graph.

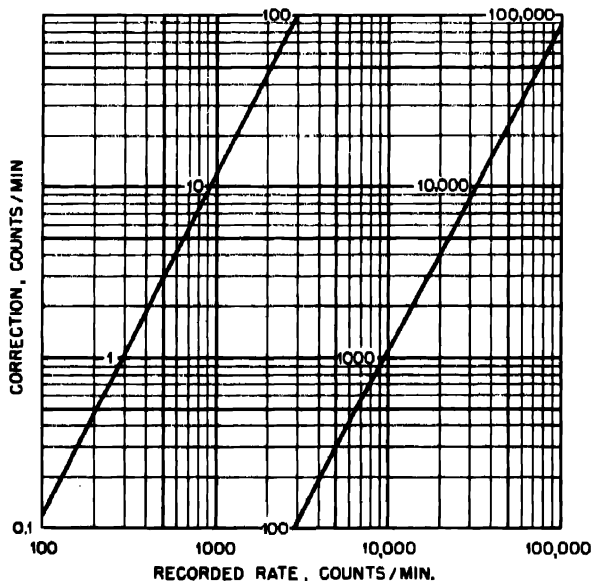


Fig. 4—Coincidence correction chart for Geiger-Mueller counter, from data of Table 5. Logarithmic graph.

the two curves indicates the necessity of determining coincidence corrections separately for every instrument.

In Fig. 2 the continuous line shows the results of the three-parameter computation based on the Geiger-Mueller-counter data of Table 5. The dashed line is the result of the independent analysis of the same data by the method of successive graphical approximations.<sup>2</sup> The two curves coincide within the accuracy of the measurements, indicating the validity of both methods. The dashed curve is perhaps the better of the two since it yields a value for  $\Sigma\epsilon^2$  of 0.00005, whereas that obtained by the present method is 0.00046. A fourth parameter would presumably reduce the difference between the two curves.

To facilitate the correction of counter data it is often convenient to use a graph showing the correction ( $N - R$ ) as a function of the recorded rate  $R$  instead of applying the correction equation to the individual results. The graph may be made on Cartesian or logarithmic coordinate paper, depending on the range of values. Such graphs are shown in Figs. 3 and 4.

#### 4. SUMMARY

The method herein described for determining and applying coincidence corrections in counters is an extension of the general method of paired sources. Several pairs of radioactive sources were used, and for each pair counts were taken with the instrument on the sources separately and together. A general relation between the recorded counting rate  $R$  and the true rate  $N$  was assumed, being the first few terms of an infinite power series:

$$N = R + \tau R^2 + \nu R^3 + \phi R^4 + \dots$$

where  $\tau$  is the resolving time of the counter and  $\nu, \phi, \dots$  are independent parameters. By a least-squares method, the values of the parameters that most adequately correlated the experimental data for the instrument in question were determined. Subsequent measurements made with the instrument could then be corrected by means of this equation.

A few examples of the use of this method have been presented. They indicate that the method is a satisfactory solution of the problem and should be of considerable value.

#### ACKNOWLEDGEMENTS

The data of Tables 2 and 3 were obtained with the cooperation of Robert Jolly. The computations were made by Robert R. Jones, Virginia Webb, and Mrs. Gertrude Paas, with the cooperation of Benjamin Butler.

## REFERENCES

1. Y. Beers, *Rev. Sci. Instruments*, 13: 72 (1942).
2. T. P. Kohman, Ph.D. Thesis, University of Wisconsin, Madison, pp. 50-70, 1943; to be published in *Rev. Sci. Instruments*; abstract in *Phys. Rev.*, 65: 63 (1944).
3. P. B. Moon, *J. Sci. Instruments*, 14: 189 (1937).
4. D. E. Hull, *Rev. Sci. Instruments*, 11: 404 (1940).
5. D. E. Hull and H. Seelig, *Phys. Rev.*, 60: 553 (1941).
6. E. L. Brady, J. A. Crawford, A. Ghiorso, A. H. Jaffey, A. A. Jarrett, T. P. Kohman, and B. F. Scott, unpublished work at Metallurgical Laboratory, University of Chicago, and Clinton Laboratories.
7. R. P. Metcalf and E. Hennessy, Metallurgical Project Report CP-2582 (1945).
8. T. P. Kohman, Metallurgical Laboratory Memorandum N-1487 (1944).
9. T. H. Johnson and J. C. Street, *J. Franklin Inst.*, 215: 239 (1933).
10. A. E. Ruark and F. E. Brammer, *Phys. Rev.*, 52: 322 (1937).
11. H. Volz, *Z. Physik*, 93: 539 (1935).
12. L. I. Schiff, *Phys. Rev.*, 50: 88 (1936).
13. A. H. Jaffey, T. P. Kohman, and J. A. Crawford, Metallurgical Project Report CC-1602 (1944).
14. W. E. Danforth, *Phys. Rev.*, 46: 1026 (1934).

## Paper 22.60

### THE SPECIFIC ACTIVITY OF RADIUM†

By T. P. Kohman, D. P. Ames, and J. Sedlet

#### 1. INTRODUCTION

Radium‡ occupies a special position among radioactive substances, having been used for many years as a reference material for numerous measurements in the field of radioactivity. The practical unit of radioactivity, the curie, was originally based on radium. The results of many of the measurements involving radium as a reference material depend upon the value of its specific  $\alpha$  activity, or the number of  $\alpha$  particles emitted per unit time by unit weight of radium. Unfortunately, the measurement of the specific activity in the case of radium is attended with special difficulties. The half life is too long to permit accurate decay measurements, and the short-lived descendants interfere in measurements of the  $\alpha$  particles. Consequently a variety of methods, mostly indirect, have been employed.

In spite of the importance attributed to a knowledge of this constant and the great number of published determinations, its value is still subject to an uncertainty of several per cent. Table 1 summarizes the more recent determinations, as well as some of the earlier ones, of the specific activity of radium in disintegrations per second per gram. In some cases the specific activity was not given directly in the publication but has been calculated from the data given. In others the reported value has been recalculated from the data, with the now more accurately known values of various physical constants entering into the calculation.

†Contribution from the Chemistry Division of the Argonne National Laboratory.

‡In this paper the term "radium" refers to the nuclide Ra<sup>226</sup>.

The general importance of knowing radioactive disintegration constants, as well as the special interest in radium mentioned above, led to the attempt to make a more accurate determination with improved radiometric techniques and instruments now available. The counting of  $\alpha$  particles from weighed quantities was successfully applied to a number of long-lived  $\alpha$  emitters in the Argonne National Laboratory. This direct method has rarely been applied to radium because of the difficulties mentioned. An application of this method to radium is described in this paper.

Table 1—Experimental Determinations of the Specific Alpha Activity of Radium

Method	Experimenters and reference	Value <sup>a</sup>
Visual counting of galvanometer deflections from RaC $\alpha$ particles in proportional counter	E. Rutherford and H. Geiger, Proc. Roy. Soc. London, A81: 141 (1908)	3.4 3.57 <sup>b</sup>
Growth rate of Ra in Io	B. B. Boltwood, Am. J. Sci., (4) 25: 493 (1908)	2.98 <sup>c</sup>
Rate of He evolution by Ra	J. Dewar, Proc. Roy. Soc. London, A81: 280 (1908)	2.9 <sup>d</sup> 3.88 <sup>d,e</sup>
Rate of He evolution by Ra	J. Dewar, Proc. Roy. Soc. London, A83: 404 (1910)	3.70 <sup>d</sup>
Rate of He evolution by Ra	B. B. Boltwood and E. Rutherford, Phil. Mag., (6) 22: 586 (1911)	3.33
Heat generation by Ra $\alpha$ particles	V. F. Hess, Wien. Ber., (IIa) 121: 1419 (1912)	3.75
Electric charge of $\alpha$ particles from Rn and descendants	J. Danysz and W. Duane, Am. J. Sci., (4) 35: 295 (1913)	3.22 3.15 <sup>f</sup>
Growth rate of Ra in Io	E. Gleditsch, Am. J. Sci., (4) 41: 112 (1916)	3.53 <sup>c</sup>
Growth rate of Ra in Io	S. Meyer and R. W. Lawson, Wien. Ber., (IIa) 125: 723 (1916)	3.4
Visual counting of galvanometer deflections from RaC $\alpha$ particles in proportional counter	V. F. Hess and R. W. Lawson, Wien. Ber., (IIa) 127: 405 (1918)	3.72
Photographic oscillographic counting of RaC $\alpha$ particles proportional counter	R. W. Lawson and V. F. Hess, Wien. Ber., (IIa) 127: 461 (1918)	3.7
Visual counting of scintillations from Rn and descendants by two observers	H. Geiger and A. Werner, Z. Physik, 21: 187 (1924)	3.40
Pressure and volume measurements of Rn	L. Wertenstein, Phil. Mag., (7) 6: 17 (1928)	3.62 3.60 <sup>h</sup>
Electric charge of $\alpha$ particles from RaB + C deposit	H. Jadrzejowski, Compt. rend., 184: 1551 (1927); Ann. phys., (10) 9: 128 (1928)	3.50 3.48 <sup>k</sup>
Heat generation by $\alpha$ particles from Rn + RaA + B + C, RaB + C, and RaC	S. W. Watson and M. C. Henderson, Proc. Roy. Soc. London, A118: 318 (1928)	3.72 3.63 <sup>i</sup>

Table 1 — (Continued)

Method	Experimenters and reference	Value <sup>a</sup>
Comparison of ionization of single RaC $\alpha$ particles with gross ionization from RaC deposit	H. Ziegert, Z. Physik, 46: 668 (1928)	3.71
Electric charge of $\alpha$ particles from RaB + C deposit	H. J. J. Braddick and H. M. Cave, Proc. Roy. Soc. London, A121: 367 (1928)	3.68 <sup>b</sup> 3.69 <sup>j</sup> 3.67 <sup>k</sup>
Photographic oscillographic counting of RaB + C $\alpha$ particles in ionization chamber	F. A. B. Ward, C. E. Wynn-Williams, and H. M. Cave, Proc. Roy. Soc. London, A125: 713 (1929)	3.66
Heat generation by Po standardized against Ra by ionization measurements	L. Meitner and W. Orthmann, Z. Physik, 60: 143 (1930)	3.68
Growth rate of Ra in Io	E. Gleditsch and E. Foyn, Am. J. Sci., (5) 24: 387 (1932)	3.47 <sup>c</sup>
Electric charge of $\alpha$ particles from Po standardized against Ra by ionization measurements	R. Grégoire, Ann. phys., (11) 2: 161 (1934)	3.68 3.65 <sup>g,l</sup>
Growth rate of Ra in Io	E. Gleditsch and E. Foyn, Am. J. Sci., (5) 29: 253 (1935)	3.47 <sup>c</sup>
Rate of He evolution by Ra	P. Guenther, Z. physik. Chem., A185: 367 (1939)	3.67
Electrical counting of $\alpha$ particles from weighed and purified Ra in ionization chamber	T. P. Kohman, D. P. Ames, and J. Sedlet, this paper (1947)	3.61

<sup>a</sup>In units  $10^{10}$   $\alpha$  particles per second per gram.<sup>b</sup>Corrected to International Radium Standard (E. Rutherford, J. Chadwick, and C. D. Ellis "Radiations from Radioactive Substances," p. 60, Cambridge University Press, London, 1930).<sup>c</sup>Calculated from disintegration constant given using currently accepted value of Avogadro number.<sup>d</sup>Calculated from rate of helium evolution given using currently accepted value of Loschmidt number.<sup>e</sup>Corrected according to following paper.<sup>f</sup>Calculated from heat generation rate given using currently accepted value of  $\alpha$  disintegration energy.<sup>g</sup>Recalculated using currently accepted value of electronic charge.<sup>h</sup>Recalculated using currently accepted value of Loschmidt number.<sup>i</sup>Recalculated using currently accepted values of  $\alpha$  disintegration energies.<sup>j</sup>Corrected by authors elsewhere.

## 2. METHOD

**2.1 General Description.** Radium was carefully purified and weighed as  $\text{RaCl}_2$ . Aliquots in solution were spread in thin layers on platinum plates and treated in such a manner as to remove radon completely and to remove the A, B, and C products to a large extent.

The samples were counted over a period of about 8 hr in a parallel-plate  $\alpha$  counter; and from the curve of counting rate vs. time, the rate due to the radium alone was determined in a manner to be described. From the known counting yield of the instrument the specific activity was calculated, and from this the disintegration constant and half life were determined.

The rapid growth of  $\alpha$ -active disintegration products in radium, coupled with the volatility of radon and the recoil of disintegrating atoms from thin samples, makes the interpretation of the counting rates the most critical part of the experiment. The  $\alpha$  activity of a sealed sample of purified radium will increase to a value four times that of the radium alone as the  $\alpha$ -active Rn, RaA, and RaC + C' grow in to their equilibrium values. For the situation reported in this paper the equations of Bateman,<sup>1</sup> describing this growth, must be modified to account for loss by emanation of radon and by recoil of product atoms. If the sample originally contains short-lived descendants of radon, but no radon, the decay of the original short-lived complex will be superposed upon the growth of the radon and its newly formed daughters. The activity curve will approach that of purified radium; and if the original activity of the short-lived components is only a few per cent of that of the radium, the two curves will become practically identical within a few hours. If the shape of the theoretical radium curve is known or can be determined, it can be used to extrapolate the last part of the experimental curve back to zero time, giving the activity of radium alone. It was found possible to determine the theoretical curve for each sample from the last part of its experimental curve.

**2.2 Calculations.** In the absence of losses by recoil or emanation, the  $\alpha$  activity of a sample of radium purified at time  $t = 0$  is given by

$$N = R + M + A + C$$

$$M = R(1 - e^{-mt})$$

$$A = R \left( 1 - \frac{a}{a-m} e^{-mt} - \frac{m}{m-a} e^{-at} \right)$$

$$C = R \left( 1 - \frac{abc}{(a-m)(b-m)(c-m)} e^{-mt} - \frac{mbc}{(m-a)(b-a)(c-a)} e^{-bt} \right)$$

$$- \frac{mac}{(m-b)(a-b)(c-b)} e^{-at} - \frac{mab}{(m-c)(a-c)(b-c)}$$

where  $N$  = total  $\alpha$  activity

$R$  =  $\alpha$  activity of radium

$M$  =  $\alpha$  activity of radon

$A$  =  $\alpha$  activity of RaA

$C$  =  $\alpha$  activity of RaC + C'

$t$  = time

$m$  = disintegration constant of radon

$a$  = disintegration constant of RaA

$b$  = disintegration constant of RaB

$c$  = disintegration constant of RaC

In the counter used, a stream of gas passes continuously over the sample, and any radon that escapes from the sample is immediately swept out and lost (those atoms disintegrating before being swept out may be regarded as not having escaped the sample). If the recoil atom from a disintegrating radium atom escapes from the sample, it immediately becomes a neutral radon atom in the gas phase<sup>2</sup> and is swept away. Nearly all the recoils from the other  $\alpha$  emitters, however, remain positively charged<sup>3</sup> and are re-collected on the sample plate since in the counter used this plate is at a negative potential.<sup>†</sup> Consequently it is necessary to consider the loss by recoil of radon only. The  $\alpha$  activity of radon, RaA, and RaC + C' will be reduced by the amount so lost. Let  $G$  be defined as the recoil retention factor, it being the fraction of the radon atoms remaining in the sample at their birth. In order to correct for the recoil loss the equation for  $N$  must be modified as follows:

$$N = R + G(M + A + C)$$

In addition, some radon will diffuse out of the sample and escape. It is assumed as an approximation that every radon atom in the sample has the same probability,  $d$ , of escaping by diffusion in unit time. The total decay constant,  $w$ , of the radon is then given by the sum of the constants for the two separate modes of disappearance.

$$w = m + d$$

Let  $F$  be defined as the diffusion retention factor, it being the fraction of the radon atoms originally retained in the sample which decay radioactively in the sample.

<sup>†</sup>The collection of recoil atoms of solid elements by the negative electrode in a gas-filled chamber has been observed repeatedly by others at the Argonne National Laboratory.

$$F = m/(m + d) = m/w$$

The diffusion loss requires that the equation for N be modified further as follows:

$$N = R + GF(M' + A' + C')$$

where  $M'$ ,  $A'$ , and  $C'$  are given by the expressions for  $M$ ,  $A$ , and  $C$ , respectively, but where  $w$  is substituted for  $m$  throughout.

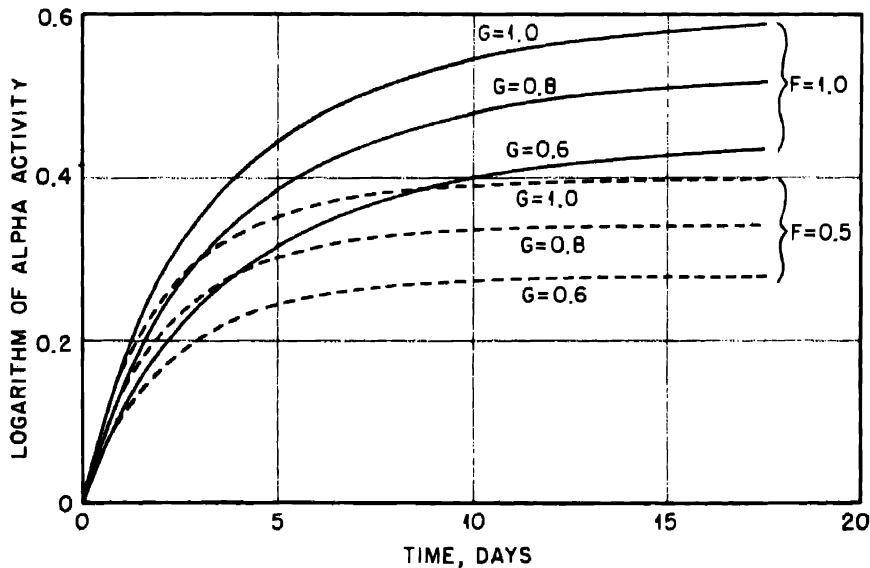


Fig. 1 — Theoretical growth curves of purified radium.

Typical long-time theoretical curves corresponding to various values of  $F$  and  $G$  are shown in Figs. 1 and 2.

By counting radium samples over periods of several radon half lives, it was determined that diffusion losses were small ( $F \approx 0.95$ ), in agreement with the known poor emanating characteristics of inorganic solids.<sup>4</sup> This fortunate circumstance permits the assumption that  $F = 0.98$  for all samples. The shape of the growth curve is relatively insensitive to the value of  $F$  during the first 8 hr when  $F$  is near unity; and when  $d$  is small, the error in assuming its constancy throughout the sample is trivial. The experiments indicated that  $G$

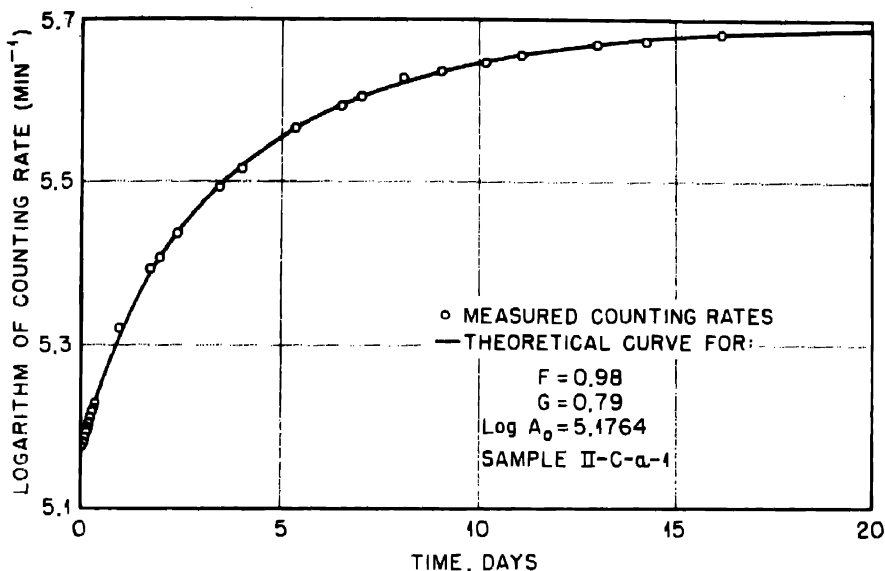


Fig. 2—Experimental growth curve of purified radium.

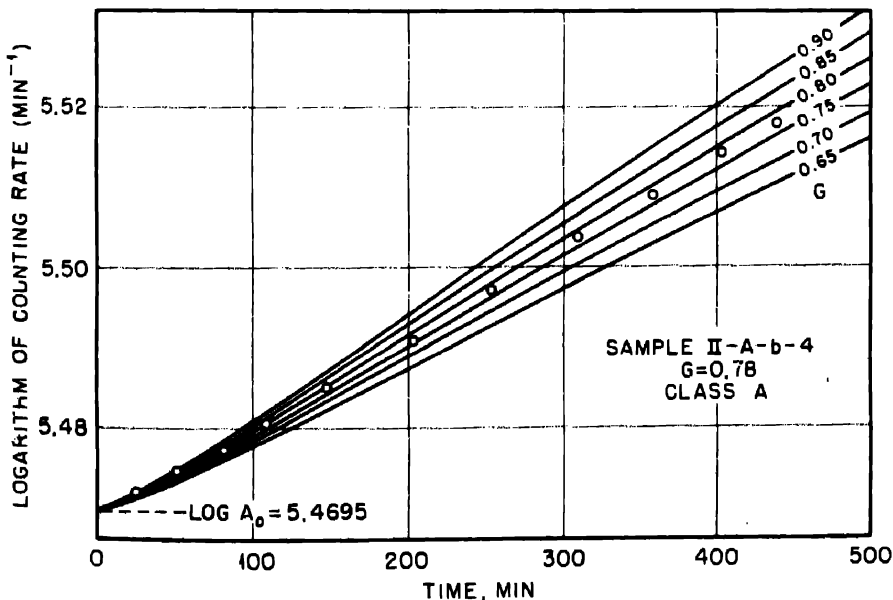


Fig. 3—Method of extrapolation of counting rate to zero time. Class A fit (good).

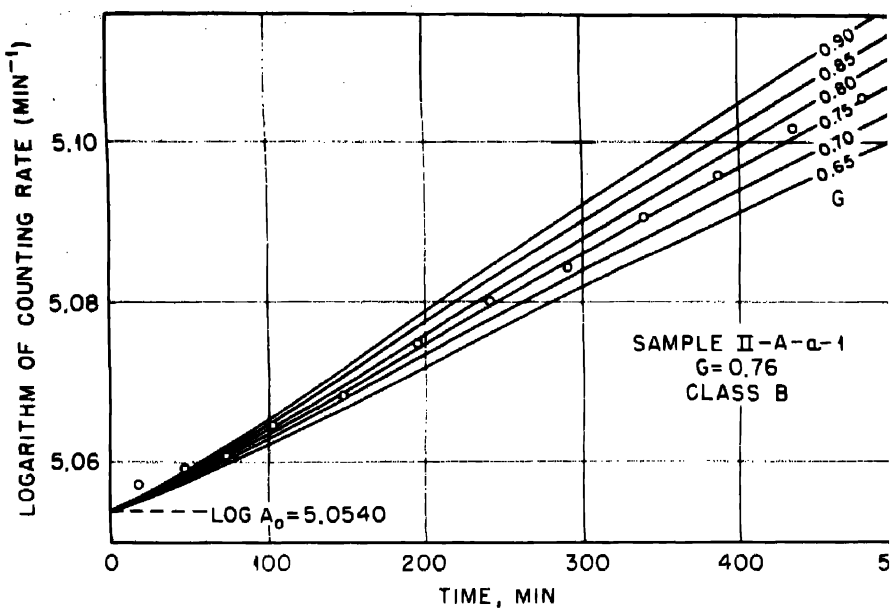


Fig. 4—Method of extrapolation of counting rate to zero time. Class B fit (fair)

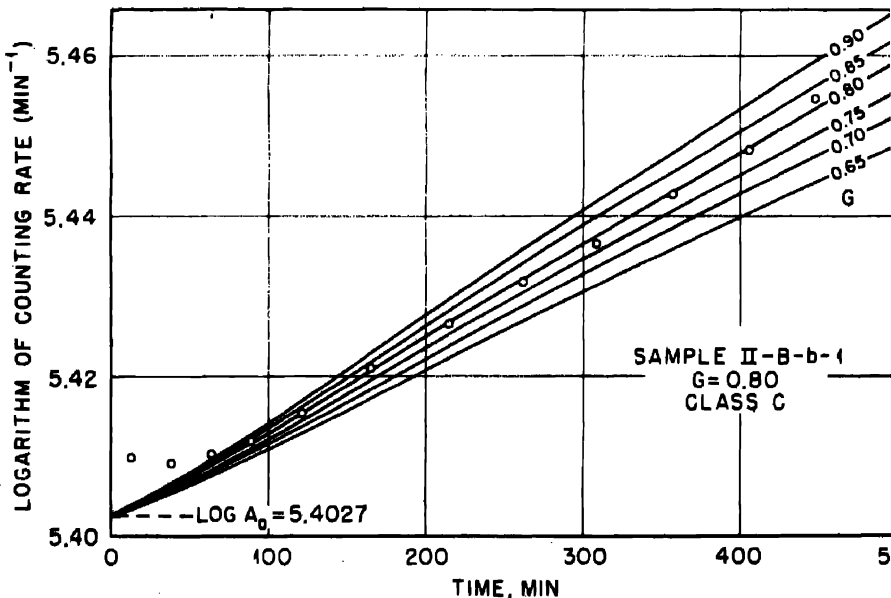


Fig. 5—Method of extrapolation of counting rate to zero time. Class C fit (poor)

varies appreciably from sample to sample, and hence it must be determined separately for each sample.

Typical short-time theoretical curves corresponding to  $F = 0.98$  and to various values of  $G$  are shown in Figs. 3 to 5.

### 3. MATERIALS, APPARATUS, AND TECHNIQUES

**3.1 Reagents.** The water used in these experiments was ordinary distilled water redistilled in a Barnstead still and kept in quartz bottles. Approximately 6N HCl was prepared by distilling a mixture of equal parts of reagent concentrated acid and Barnstead water in a pyrex still with a fractionating column. It was spectrographically pure. From this, concentrated hydrochloric acid was prepared by saturation with gaseous hydrogen chloride (Harshaw) that had been purified by passage through pyrex wool, concentrated sulfuric acid, and spray traps. Reagent-grade perchloric acid was redistilled at low pressure in pyrex apparatus.

**3.2 Radium and Its Purification.** Commercial radium bromide obtained from pitchblende (Canadian or African) was used. Since these ores normally contain less than 1 per cent as much thorium as uranium, the amount of mesothorium ( $\text{Ra}^{228}$ ) present was negligible. The radium as supplied was said to contain less than 1 per cent barium. One sample showed by spectrographic analysis 0.4 per cent barium.

In order to free the radium of the remaining barium, fractional crystallization of the chloride from hydrochloric acid solution<sup>5</sup> was employed. Because of the small scale of the work described in this paper, adopted in order to reduce the hazards of handling radium, the usual techniques involving shallow evaporating and crystallizing vessels could not be used, so the precipitations were made in quartz test tubes. All apparatus coming into contact with the radium solutions or reagents to be added to radium solutions was made of quartz. For transfer of reagents and radium solutions, micropipets<sup>6</sup> constructed of quartz and attached to a hypodermic syringe control were used. A clinical centrifuge (International) was used to separate crystals from solutions, and mother liquors were withdrawn with uncalibrated quartz micropipets.

A series of total precipitations of radium from concentrated hydrochloric acid was performed. Five mg of radium was dissolved in 150 microliters of water to which was then added 2 ml of concentrated hydrochloric acid with stirring. After cooling approximately  $\frac{1}{2}$  hr at  $0^\circ\text{C}$  in an ice bath, the white crystals were centrifuged down; the supernatant solution was then withdrawn, and the chloride was redissolved in 150 microliters of water. This cycle was repeated for a

total of 10 crystallizations. In this as well as in the other series of crystallizations, after every fifth crystallization the radium solution was centrifuged and transferred to a clean tube in order to remove any insoluble matter present. The yield of radium through this series of crystallizations was approximately 90 per cent. Spectrographic analysis showed that the barium content had not been appreciably altered. Presumably the solubility of radium and barium chlorides in concentrated hydrochloric acid is so low that both are essentially completely precipitated, or else the rate of precipitation is too rapid to permit a discrimination against barium ions during crystal formation. Hence this procedure was unsatisfactory for removal of barium, but it proved useful for preliminary or final purification of the radium from common impurities or from its decay products.

A series of crystallizations from approximately 6N (20 per cent) HCl, in which the solubility of radium and barium chlorides is somewhat greater, was then performed. Fifteen milligrams of radium was dissolved in 200 microliters of water, and 3 ml of 6N HCl was added, the remainder of the cycle being the same as above. Eighteen such crystallizations were performed. The yield of radium through this series was approximately 60 per cent, and spectrographic analysis showed less than 0.02 per cent barium (the limit of detection). Apparently the greater solubility and slower rate of crystallization from 6N HCl allow the radium chloride to separate in purer form than when precipitated by concentrated acid. This is in agreement with the experience of Hoenigschmid and Sachtleben.<sup>7</sup> Other elements looked for were also below the spectrographic limit of detection. Portions of this solution (I) were used in the first series of experiments.

Another sample of radium, 50 mg, was purified by a series of 10 crystallizations from 6N HCl in the manner just described, with the same volumes as for the 15-mg sample being used. The yield was approximately 70 per cent, and the radium was spectroscopically pure, with barium less than 0.02 per cent. This material was combined with that remaining from the first set of experiments, and the combined material (II) was used for the second set.

**3.3 Weighing of Radium Chloride.** Two sets of experiments were performed, with different stock solutions of purified radium (I and II) being used, as already mentioned.

(a) Series I, Micro Scale. Quartz dishes weighing approximately 15 to 20 mg were made by rounding the ends of 2-mm O.D. quartz tubing, sawing off a few millimeters from the ends, grinding down with emery paper to a height of about 2 mm, and grinding flat on the bottom.

Weighings were made on a Kirk-Craig quartz-fiber ultramicro balance,<sup>8</sup> calibrated with a 1-mg weight certified by the National Bureau of Standards to be accurate within 0.5 per cent. The sensitivity was 1.664  $\mu\text{g}$  per division of the torsion wheel. Weighings were reproducible to about 0.01  $\mu\text{g}$ .

Heating at 300°C in a current of hydrogen chloride gas was employed to obtain anhydrous radium chloride for weighing. An electric sleeve furnace surrounding a quartz tube 1 in. in diameter was used. A quartz boat attached to a long quartz fiber for insertion and removal supported the sample dishes. A tank of hydrogen chloride (Harshaw) was attached through a pyrex-wool filter, and a cold trap (dry ice - *n*-butyl alcohol) was attached to the quartz tube.

The dishes were heated for an hour at a time in hydrogen chloride until constant weight was achieved. While being cooled or while not in use, the dishes were kept in a desiccator containing ascarite, which was changed frequently. The disks were handled with platinum-tipped forceps or a fork made of platinum wire. A dummy dish similarly heated to constant weight was used as a counterpoise in weighing.

Shortly before use, the radium was reprecipitated from concentrated hydrochloric acid and redissolved. This reduced the  $\gamma$  activity to a level safe for handling without shielding and removed radium D and polonium, whose  $\alpha$  activity might appear later as radium. A portion containing approximately 30  $\mu\text{g}$  of radium chloride was introduced to a dish by means of a quartz capillary pipet, the dish being held in a clamp to prevent adherence to the pipet by surface tension. The filling was observed under a low-power microscope. The water was evaporated under an infrared heat lamp, and the sample was re-examined under the microscope to make sure all the crystals were in the bottom of the dish. The dish was placed in the furnace, and, with hydrogen chloride flowing, the temperature was slowly raised to 300°C and maintained for several hours. Heating for approximately an hour at 300° was repeated until a constant weight was reached. If microscopic examination revealed dust particles or evidence of spattering of crystals, the sample was rejected.

(b) Series II, Semimicro Scale. The procedure was the same as for series I except that larger dishes weighing approximately 300 mg were made from 8-mm O. D. quartz tubing, the height being about 5 mm. Weighings were made on an Ainsworth keyboard-type assay balance, with a dummy dish heated to constant weight being used as a counterpoise. The weights were calibrated against a set calibrated by the National Bureau of Standards. The accuracy of weighing was approximately 0.005 mg. The radium chloride samples weighed ap-

proximately 3 mg. These larger dishes did not need to be clamped during filling.

**3.4 Aliquoting.** After weighing, each radium chloride sample and its dish were placed in a small quartz or Vycor test tube with a few drops of water. The dissolved radium was transferred to a weighed pyrex flask, and the tube and dish were rinsed with numerous small portions of 7M  $\text{HClO}_4$ , each being added to the flask. An appreciable residue of undissolved radium could be detected in the boats at this stage, the  $\alpha$  activity being of the order of a few tenths of 1 per cent for the small samples. Hence each dish was boiled several hours in 2M HCl in a pyrex flask to which was sealed a tube to act as a reflux condenser. The solution was concentrated to a small volume and added to the flask. The residual activity of the dish corresponded to less than 0.01 per cent of the radium in series I and to much less in series II.

For series I, 5- or 10-ml volumetric flasks were used to receive the solution. They did not need to be calibrated since the aliquoting procedure was gravimetric. After bringing to volume, but before mixing, the stopper was inserted, and the flask was again weighed. The stopper was then sealed in with paraffin, and the contents were shaken. The weighings were performed on a Christian Becker semi-micro chainomatic balance capable of weighing to 0.01 mg, using calibrated weights.

For series II, an intermediate dilution stage was required. The original solution of radium was made up in a 50-ml glass-stoppered Erlenmeyer flask, the weighings being made on an Ainsworth chainomatic analytical balance with calibrated weights. Samples of approximately 0.5 ml were weighed into 10-ml glass-stoppered mixing cylinders and made up to volume. These weighings were made on the Becker balance.

All ground-glass stoppers were reground before use. While containing radium solutions not in use, they were sealed with paraffin.

The final solutions in all cases contained 1.5 to 4.0  $\mu\text{g}$  of radium per gram of solution of density about 1.4, so that 20- to 80-microliter portions, weighing 30 to 100 mg, contained 0.1 to 0.3  $\mu\text{g}$  of radium, an amount suitable for counting. For mounting the radium, platinum disks 1 in. in diameter were punched from new sheet stock 0.005 in. thick, carefully flattened, and ignited by the technique described below. Each was weighed on the Becker balance before and after a portion of the radium solution was placed on it. The 7M  $\text{HClO}_4$  was used as the solvent because it was found to change weight only very slowly in air under the prevailing room conditions of temperature and

humidity. To further reduce the weight change, a small box that was equipped with a removable but snugly fitting cover and into which the disks just fitted was carried by the balance pan.<sup>†</sup>

**3.5 Preparation of Samples for Counting.** The platinum plate containing the radium in perchloric acid solution was centered on an upright brass cylinder 1.5 in. in diameter and 2 in. high containing an axially centered well 0.5 in. in diameter extending from the top to within 0.5 in. of the bottom. The cylinder rested on a hot plate; and since the platinum plate received heat from the edges and lost it to the evaporating solution in the center, a temperature gradient was maintained. This kept the solution from running to the edges of the disk while evaporating. Evaporation to dryness took approximately 15 min, and the bulk of the radon, if not all of it, was removed. After an hour or two, during which the A, B, and C bodies largely decayed out, a few drops of 7M HClO<sub>4</sub> were added to the plate to dissolve the deposit, and the evaporation was repeated. This removed the bulk, if not all, of any radon remaining from the first evaporation and that growing in since. A third evaporation was sometimes performed. The plate was then heated to a red heat with a Meker burner, while being supported by a platinum sheet containing a 0.75-in. diameter hole so that it would not sag or bend when heated, as would be the case if it were held at one point by forceps. The flaming removed residual water and acid so that a thin deposit remained. It also served to expel any remaining traces of radon, and the instant of flaming was taken as zero time for each plate.

It was found that a sample plate could never again be freed of radon after it had been flamed once. When the deposits on plates treated as described above and then counted were redissolved in acid and re-treated, a higher counting rate always resulted, probably because of fusion of some of the deposit with the platinum to form a substance from which radon could not be released by the dissolving procedure, or because recoil radon nuclei penetrated too far into the metal surface. However, when the flaming (and counting) was omitted and the sample was allowed to stand several days, repetition of the evaporation treatment followed by flaming gave results indistinguishable from those obtained with freshly prepared samples from the same solution. If the recoil explanation is correct, the water and acid remaining in the deposit before flaming must prevent appreciable numbers of recoil nuclei from entering the platinum. Since each plate could only be

<sup>†</sup>This gravimetric aliquoting technique was adapted from one devised by Edgar F. Westrum, Jr.<sup>8</sup>

flamed once, it could only be counted once, and duplicate checks on individual samples could not be made.

In spite of the peripheral heating, the evaporating solutions sometimes tended to spread to the edge of the plate. Since the punching process sometimes left irregularities at the edge of the plates,  $\alpha$  particles emitted from the edge might have a different probability of being counted than those emitted from the center. Furthermore, the solution might run or creep over, losing radium. In the latter case the deposit often became heavier instead of lighter, presumably because dissolved brass from the support worked its way through the solution onto the plate. Consequently the evaporation was carefully watched, and any tendency to run was countered by slightly tipping the assembly.

Each sample plate was examined, after counting, with a stereoscopic microscope at 24 $\times$  to 36 $\times$ . Although only 0.1 to 0.5  $\mu\text{g}$  of radium was present, the deposit appeared to contain several micrograms of solid of a brownish tinge. The bulk of the deposit was presumably platinum dissolved from the surface, since similar deposits were obtained in the absence of radium. Much of the solid matter seemed to be present in irregular rings and lines, which under the microscope resembled thin shoals of sand possibly 10 to 20  $\mu$  thick at the thickest points, with occasional peaks or groups of grains possibly 25 to 50  $\mu$  high. Although the range of  $\alpha$  particles in solid matter is about 25  $\mu$ , self-absorption did not seem to be serious in deposits of the type described. This is probably due to the small size of the individual crystals, their loose packing, and physical separation of the radium and inert solids. Samples examined in an  $\alpha$ -particle pulse analyzer<sup>10</sup> showed the two main  $\alpha$  groups of radium<sup>11</sup> resolved to within the capacity of the instrument. This is further evidence that self-absorption effects were small. In some samples, however, the deposits were thicker, and some deposits extended to the edge of the plates. Plates were therefore classified according to the following schemes:

- a. Deposit thin at all points with no material extending to the edge of the plate.
- b. Deposit thin at all points but extending to edge of plate; no evidence for running off, and no deposit in irregularities of platinum.
- c. Deposit somewhat thicker in places than a, but not extending to edge.
- d. Same as c, but deposit extending to edge.
- e. Deposit fairly thick or bunched in places, but not extending to edge.
- f. Sample obviously faulty because of great thickness, bunching, running off edge, inclusion in irregular regions of plate, etc.

**3.6 Alpha-particle Counting.** The counter was a parallel-plate ionization chamber through which flowed a mixture of 95 per cent argon (tank 99.6 per cent purity) and 5 per cent carbon dioxide at atmospheric pressure. The plates were horizontal and 2.5 cm apart, the lower plate serving as the sample support and the upper serving as the collector. The sample was 1,500 volts negative with respect to the collecting electrode, which was near ground potential. Pulses were amplified by a high-frequency amplifier, selected from amplifier noise,  $\beta$ -ray pulses, etc., by a biased discriminator, and counted by means of a scale-of-512 and electromagnetic recorder.<sup>†</sup>

The coincidence correction as a function of counting rate was determined by the method of least-square analysis of multiple paired-source data.<sup>13</sup> It was found that up to 1,200,000 counts per minute the recorded rate ( $R$ ) was related to the true rate ( $N$ ) as follows:

$$N = R + (5.52 \times 10^{-8} \text{ min}) R^2 + (6.97 \times 10^{-14} \text{ min}^2) R^3$$

The correction was thus 1.4 per cent at 200,000 counts per minute, 4.5 per cent at 500,000 counts per minute, and 12.5 per cent at 1,000,000 counts per minute. Sufficient counts were taken to give a probable error in the correction of approximately 0.1 per cent of the rate. For convenience, a graph of the additive correction vs. the observed rate was constructed and used.

The background of the counter was around 50 counts per minute. The high value was due to previous contamination of the counter by extensive use in the laboratory, but because of the high counting rates its uncertainty introduced no appreciable error. No contamination of the counter by the radium samples was observed. This is further evidence that active atoms leaving the plate are either swept out of the counter or re-collected on the sample plate.

The counting yield of a thin  $\alpha$ -emitting sample spread on a flat surface exceeds the geometry factor, 0.5, by a small amount as a result of back-scattering of particles entering the support at glancing angles.<sup>14,15</sup> Values reported for thin  $\text{Pu}^{239}$  samples on platinum mounts in various types of  $\alpha$  counters are as follows:

Air parallel-plate chamber <sup>14</sup>	0.520
Argon-carbon dioxide parallel-plate chamber <sup>16</sup>	$0.519 \pm 0.002$
Methane proportional counter <sup>17</sup>	0.518

<sup>†</sup>This counter was built by A. Ghiorso and A. C. Krueger, who used designs and circuits developed at the Argonne National Laboratory and at Los Alamos. The high mobility of electrons in argon-carbon dioxide mixtures was reported by J. Allen and B. Rossi.<sup>13</sup>

Since the energy of the main Ra<sup>228</sup>  $\alpha$  group, 4.79 mev,<sup>18</sup> does not differ greatly from that of Pu<sup>239</sup>, 5.15 mev,<sup>19</sup> it is probable that the counting yields for the two nuclides are similar. Plutonium samples of approximately 10  $\mu$ g mounted on platinum were used for a direct comparison of the radium counter with a low-geometry  $\alpha$  counter.<sup>†</sup> The latter had a vacuum collimator whose dimensions were accurately measured and whose counting yield, assumed equal to the geometry factor, approximately  $10^{-4}$ , could be accurately calculated by the method of Kovarik and Adams.<sup>20</sup> ‡ Two different plutonium samples gave 0.515 and 0.519 for the counting yield of the parallel-plate counter. The average, 0.517, is somewhat lower than the values previously reported, presumably because of the finite thickness of the plutonium samples in the present measurements. Our radium samples resembled our plutonium samples under the microscope and appeared to be slightly thicker on the average. Consequently a somewhat lower value,  $0.515 \pm 0.003$ , was adopted for the average counting yield and estimated probable error in these experiments.

The determinations of the coincidence corrections and of the counting yield were done at approximately the same time. At this time also a series of Pu<sup>239</sup> samples was accurately counted to serve as standards. Subsequently the standards were checked frequently; and if the rates deviated from the original values, the discriminator was adjusted to bring them back into correspondence. This was necessitated by occasional breakdown and repair and drifts in the characteristics of the counter.

Generally two radium samples were prepared early in the same day and counted alternately throughout the day, at first for 10-min intervals and, after about 2 hr, for 20-min intervals. About 5 min was required for changing samples. The counting rates were in the range 100,000 to 300,000 per minute.

**3.7 Interpretation of Counting Data.** For each sample the logarithm of the counting rate, corrected for coincidence loss and background, was plotted on transparent graph paper as a function of the mid-time of the counting interval.

It has been mentioned that the diffusion retention factor, F, can be assumed equal to 0.98 for all samples but that the recoil retention factor, G, must be determined for each. To do this, a family of

<sup>†</sup>The counter was made by A. Ghiorso, and the geometrical measurements were carried out by Patricia Walsh.

<sup>‡</sup>The implicit assumption that the large-angle back-scattering of  $\alpha$  particles by thick mounts contributes negligibly to the counting yield of low-geometry counters appears reasonable but is being investigated theoretically.

theoretical curves representing the growth of  $\alpha$  activity of pure radium samples corresponding to  $F = 0.98$  and to various values of  $G[0.65(0.05)0.90]$  was constructed on a separate transparent sheet on the same scale as the experimental plots. The curves had a common origin at  $t = 0$  but rose at different rates. This sheet was secured to a ground-glass pane illuminated from behind.

Each experimental plot was superposed on the theoretical curves and, with the vertical axes kept together, was slid up or down until the best fit of the observed points, in the later hours, with a theoretical curve was obtained. The position of the origin of the latter then gave the logarithm of the counting rate of the radium alone. Because of the presence of some short-lived  $\alpha$  emitters at  $t = 0$ , the experimental points always started somewhat higher (0.1 to 2.0 per cent) than the theoretical curve selected, but approached the latter in from 1 to 4 hr. A knowledge of the history of the sample previous to  $t = 0$  was an aid in fitting the curves because it gave an indication of the excess activity to be expected at the start. For example, if the interval between the two evaporation was shorter than 1 hr, the excess was greater, and sometimes the gross activity showed an initial net decay; whereas if the interval was greater than 2 hr or if three evaporation were performed, the points could be fitted to a curve almost from the beginning.

The ease with which a given set of points could be fitted with a curve and the uncertainty of the fit varied with individual samples. Consequently each sample was judged to fall into one of the following four classes:

- A. Unique fit, fairly certain extrapolation
- B. Moderately good fit, reasonably certain extrapolation
- C. Poor fit, uncertain extrapolation
- D. Impossible to fit because of scattering of points, obvious error in data, instrumental difficulties, etc.

Figures 3, 4, and 5 illustrate the method of curve fitting and extrapolation to  $t = 0$  for samples of each of the first three classes.

#### 4. RESULTS

**4.1 Experimental Data.** The gravimetric data for the radium chloride samples and solutions made therefrom are given in Table 2.

To determine the magnitude of the radon diffusion and recoil losses, several radium samples were counted over periods of 15 to 20 days. By plotting the data on transparent semilogarithmic paper and comparing with similarly plotted theoretical curves, the values of  $F$  and  $G$  corresponding to each experimental curve were determined. Figure 2

shows one set of measurements and its best-fitting theoretical curve; the results of all the long-time experiments are given in Table 3. The fact that recoil loss is considerable—roughly half the radon atoms recoil in an upward direction and escape from the sample—is indicative of the small self-absorption of these samples for the much more penetrating  $\alpha$  particles.

Table 2—Gravimetric Data on Radium Chloride and Solutions

Stock solution No.	Primary samples			Secondary samples		
	No.	Wt. of $\text{RaCl}_2$	Wt. of solution, g	No.	Wt. of aliquot, g	Final wt., g
I	B	33.332 $\mu\text{g}$	6.3751			
	C	30.487 $\mu\text{g}$	12.8950			
II	A	4.2816 mg	64.3371	a	0.71972	14.1841
				b	0.73184	14.0838
	B	3.1647 mg	59.7122	a	0.69154	14.1482
	C	2.3218 mg	49.6751	b	0.69957	14.1756
				a	0.68912	14.0907
				b	0.68687	14.4319

Table 3—Experimental F and G Factors

Plate No.	F	G
I-A-8	0.96	0.75
I-A-9	0.98	0.68
I-A-10	0.98	0.75
II-B-a-1	0.99	0.77
II-B-a-2	0.98	0.75
II-C-a-1	0.98	0.79
II-C-a-2	1.00	0.76

Table 4 contains the data for the individual samples that were counted for 8-hr periods. Column 2 gives the weight of solution taken, and from this and the data of Table 2 is calculated the weight of radium on each plate, column 3. Columns 4 and 5 give the classification according to the codes described for the sample spread and the curve extrapolation, respectively. In column 6 the recoil retention factors are recorded. Column 7 contains the counting rates extrapolated to zero time. The specific counting rate, obtained by dividing column 7 by column 3, appears in column 8. The last column contains the weighting factor for each value, derived from columns 4 and 5, as described below.

## SPECIFIC ACTIVITY OF RADIUM

1893

Table 4—Data for Individual Counting Samples

Plate No.	Weight of solution, mg	Weight of Ra, $\mu\text{g}$	Class†			Counting rate at $t = 0$ , c/m	Specific counting rate, c/m/ $\mu\text{g}$	Weighting factor
			Pl.	Cu.	G			
I-B-12	53.80	0.21412	b	A	0.71	239,010	1.1162	3
	13	54.13	0.21543	a	B	0.77	241,330	1.1202
	14	61.87	0.24624	b	B	0.80	273,910	1.1124
	15	72.10	0.28695	a	B	0.78	317,770	1.1074
	16	41.37	0.16465	f	D			
	17	55.10	0.21929	b	C	0.68	242,780	1.1071
	18	46.31	0.18431	a	A	0.83	206,070	1.1181
	19	38.55	0.15343	a	A	0.70	171,010	1.1146
	20	66.82	0.26594	f	A	0.83	290,540	(1.0925)
	21	40.33	0.16051	a	A	0.84	179,300	1.1171
	22	44.17	0.17579	a	A	0.80	197,470	1.1233
	23	53.50	0.21292	f	A	0.71	220,300	(1.0347)
I-C-1	89.80	0.16161	b	A	0.77	180,140	1.1146	3
	2	68.25	0.12283	a	A	0.75	136,530	1.1115
	3	82.37	0.14824		D			
	4	74.63	0.13431	a	A	0.80	147,980	1.1018
	5	31.34	0.05640	b	C	0.72	62,880	1.1149
	6	48.64	0.08754	f	B	0.78	94,710	(1.0819)
	7	66.91	0.12042	a	B	0.65	133,730	1.1105
	8	100.83	0.18164	a	C	0.68	202,490	1.1148
	9	77.77	0.13896	a	C	0.82	153,710	1.0982
	10	53.83	0.09688	f	B	0.82	104,480	(1.0784)
	11	98.46	0.17720	a	D			
	12	73.31	0.13194	a	C	0.73	147,100	1.1149
	13	99.16	0.17846	b	A	0.74	197,610	1.1073
	14	39.31	0.07075	a	B	0.65	78,400	1.1081
	15	81.57	0.14680	e	C	0.72	158,860	(1.0822)
II-A-a-1	68.48	0.12324	a	B	0.72	135,860	1.1032	2
	39.17	0.10068	a	B	0.76	113,240	1.1248	2
	2	37.54	0.09649	a	C	0.77	108,800	1.1276
	3	89.47	0.22997	f	A	0.82	235,240	(1.0229)
	4	104.04	0.28742	f	B	0.85	290,810	(1.0875)
	5	66.53	0.17101	a	B	0.77	190,990	1.1168
	7	59.30	0.15242	c	A	0.77	170,770	1.1204
	8	80.61	0.20720	e	A	0.78	226,890	(1.0955)
II-A-b-1	9	82.70	0.21257	c	A	0.79	239,340	1.1259
	89.38	0.23527	a	C	0.77	264,310	1.1234	
	2	60.21	0.15848	a	C	0.80	177,020	1.1169
	3	104.39	0.27479	a	A	0.79	308,600	1.1267
	4	101.14	0.26623	b	A	0.78	294,780	1.1073
II-B-a-1	63.23	0.12468	a	A	0.85	138,530	1.1111	3
	2	78.51	0.15481	a	A	0.81	171,840	1.1100
II-B-b-1	113.40	0.22577	c	C	0.80	252,740	1.1195	1
	2	81.85	0.16256	a	C	0.73	182,940	1.1254
	3	54.34	0.10819	a	A	0.79	120,120	1.1103
	4	76.25	0.15181	a	A	0.73	170,140	1.1207
II-C-a-1	77.73	0.13525	a	C	0.84	150,110	1.1099	1
	2	101.87	0.17725	d	B	0.88	164,410	(1.0968)
	3	75.26	0.13095	a	A	0.80	145,420	1.1105
	4	97.93	0.17040	a	B	0.77	189,980	1.1149
II-C-b-1	73.62	0.12466	d	B	0.78	137,710	(1.1047)	2
	2	111.02	0.18799	a	B	0.81	208,980	1.1116
	3	76.24	0.12910	d	B	0.85	141,910	(1.0992)
	4	100.03	0.16938	a	A	0.80	188,330	1.1119

†Pl. = plate; Cu. = curve.

The reason for the difference in G obtained for a given sample in the short-time (Table 4) and long-time (Table 3) experiments is not understood. The fact that the values for the long-time experiments are always lower may mean that diffusion losses may be larger than deduced from the long-time experiments alone, although still not sufficiently large to appreciably change the shape of the growth curves in the first 8 hr. Alternatively, the samples may change their characteristics after standing several days exposed to the atmosphere. In

Table 5—Average Values of Specific Counting Rate for Each Weighed Radium Chloride Sample

RaCl <sub>2</sub> sample No.	Average specific counting rate, c/m/ $\mu\mu$ g	P. E. of average, <sup>†</sup> c/m/ $\mu\mu$ g	Weight for final average
I-B	1.1161	0.0011	1
I-C	1.1087	0.0012	1
II-A	1.1206	0.0016	2
II-B	1.1144	0.0016	2
II-C	1.1118	0.0005	2

<sup>†</sup>Calculated from the individual values (x), their weights (w), the average ( $\bar{x}$ ), and the number of values (n) according to

$$\text{P. E. of average} = 0.6745 \sqrt{\frac{\sum w(x - \bar{x})^2}{(n - 1)\sum w^2}}$$

any event, the correct G factor for extrapolation of the short-time data is that deduced from the same data; the points could not be fitted to curves having the lower G values derived from the long-time experiments.

**4.2 Weighting and Averaging.** The data were examined from the statistical point of view and the following conclusions were reached.

The plates made from each final solution gave values whose distribution was not inconsistent with the normal law, if plates of classes d, e, and f are rejected. This is not true if these classes are included, for they all give lower values than the others, and a highly unsymmetrical distribution results. These samples are a priori likely or certain to be low, and are therefore rejected in the final calculations. Class b and c samples show no tendency to give lower values than class a samples and hence are retained. The mere fact that a deposit extends to the edge of its plate, or is slightly thicker than the best spreads, apparently does not appreciably affect the counting rate. A

combination of these two circumstances, however, is possible evidence for running off of the solution, with acquisition of dissolved brass on the plate; hence the rejection of class d samples with the retention of classes b and c is not an inconsistency.

In averaging the samples that were retained because of the nature of the deposit, weighting factors of 3, 2, and 1 were assigned to samples whose curves fell in classes A, B, and C, respectively; class D samples were rejected.

The averages for the two groups of plates from each pair of corresponding A and B solutions in series II do not differ significantly from each other. This is the result that would be expected if both groups were drawn from the same parent population. This indicates that any error introduced by the gravimetric dilution process is negligible compared to other errors. Consequently all samples derived from a given weighed radium chloride sample were averaged together; the averages are given with their calculated probable errors in Table 5. It is evident that the spread of the averages is considerably greater than would be expected from their probable errors. This indicates that the greatest source of error probably occurs in the weighing of the radium chloride samples.

A final average value was obtained from the averages for the separate radium chloride samples. The averages in the I and II series were weighted in the ratio 1:2, respectively, since the latter radium chloride weighings were done on a larger scale using weights whose absolute calibration was known to a higher degree of accuracy. The final average specific counting rate and its probable error are

$$1.1148 \pm 0.0013 \times 10^{12} \text{ counts per minute per gram}$$

The indicated probable error is merely a precision index, representing random errors in weighing, aliquoting, counting, and curve fitting. It does not include possible systematic errors such as those in the absolute weight calibrations and in the method of interpreting the counting data. To allow for the possibility of such errors a generous estimate of 0.5 per cent probable error is made, yielding for the specific counting rate and over-all probable error

$$1.1148 \pm 0.0059 \times 10^{12} \text{ counts per minute per gram}$$

#### 4.3 Specific Alpha Activity, Disintegration Constant, and Half Life. The counting yield has been given above as $0.515 \pm 0.003$ . On dividing

the specific counting rate by the counting yield, the specific  $\alpha$  activity is obtained

$$2.165 \pm 0.017 \times 10^{12} \text{ } \alpha \text{ counts per minute per gram}$$

$$3.608 \pm 0.028 \times 10^{10} \text{ } \alpha \text{ counts per second per gram}$$

From this the disintegration constant is calculated to be

$$1.354 \pm 0.011 \times 10^{-11} \text{ sec}^{-1}$$

$$4.274 \pm 0.034 \times 10^{-4} \text{ year}^{-1}$$

and the half life is calculated as

$$1622 \pm 13 \text{ years}$$

## 5. DISCUSSION

**5.1 Comparison with Other Determinations.** The result obtained by the method described in this paper has been included in Table 1, where it may be compared with earlier values obtained by different methods. It occurs approximately in the middle of the range of the more recent values. The spread of the values is considerably greater than would be expected from the precision or probable accuracy claimed for the various methods.

Most of the other determinations are not as direct as the one given in this paper. For example, in many the radium used was "weighed" by comparison of its  $\gamma$  activity with that of a standard radium source, and the amount of radium present was subject to errors in the standard source and in the  $\gamma$ -radiation measurement. The material used in many of the experiments was radon or an active deposit instead of radium itself, and the corrections necessitated by the decay of the source and by the  $\gamma$  radiation of the other chain members introduce additional uncertainties. The indirect methods of determining the  $\alpha$  activity, such as measuring heat evolution, electric charge carried by the particles, or ionization currents, all involve corrections or uncertain conversion factors. The large discrepancies of the values depending on geological methods, such as the comparison of the growth rate of radium from ionium with the radium-ionium ratio in minerals, can be explained by assuming that the minerals used were not sufficiently ancient or intact for exact equilibrium to prevail. Thus it is perhaps understandable that large errors may exist in previously

reported measurements. This is suggested strongly by the different results obtained by the same method in separate laboratories.

The method described in this paper is also subject to uncertainties and errors. It is believed that the precision index given (0.8 per cent probable error) is a reasonable estimate of the uncertainty of the final result due to all likely sources of error.

Rutherford, Chadwick, and Ellis<sup>21</sup> concluded in 1930 that the specific activity probably is between  $3.65 \times 10^{10}$  and  $3.70 \times 10^{10}$   $\alpha$  particles per second per gram, and they adopted the latter value. This value was also recommended by the International Radium Standards Commission report of the same year.<sup>22</sup> In view of the result recorded in this paper, these values seem to be too high.

**5.2 Suggested Method for More Accurate Determination.** The measurement of the  $\alpha$  activity of radium might be improved by counting the  $\alpha$  particles from larger radium samples directly with a vacuum low-geometry collimator and an ionization chamber of sufficient size to completely stop in its gas all the particles. With a differential pulse amplitude selector, the radium  $\alpha$  particles could be counted separately in the presence of the more energetic particles from its descendants and the less energetic back-scattered particles. With this method the counting yield could be known more accurately and the interference of the daughters and of back-scattering would be less important than in the experiments described in this paper. Such a method, coupled with weighings of somewhat larger samples, could be expected to give a value for the specific  $\alpha$  activity accurate to 0.1 or 0.2 per cent.

## 6. SUMMARY

The specific activity of radium has been determined by counting the  $\alpha$  particles emitted by aliquots of weighed samples of highly purified radium chloride in a high-speed parallel-plate ionization counting chamber. Comparison of the observed curves of counting rate as a function of time after sample preparation with theoretical curves permitted an evaluation of the amount of radon lost by recoil and diffusion and a correction for the  $\alpha$  activity of radon and its descendants, the unavoidable presence of which is the chief difficulty in this direct method. The measurements yielded a specific counting rate of  $1.1148 \pm 0.0059 \times 10^{12}$  counts per minute per gram of radium. The counting yield of the counter used was estimated as  $0.515 \pm 0.003$  from a comparison of the counter with a low-geometry counter by means of  $\text{Pu}^{239}$  samples and a consideration of previous determinations for similar

counters. The specific activity is calculated to be  $3.608 \pm 0.028 \times 10^{10}$   $\alpha$  disintegrations per second per gram, the disintegration constant to be  $4.274 \pm 0.034 \times 10^{-4}$  year $^{-1}$  or  $1.354 \pm 0.11 \times 10^{-11}$  sec $^{-1}$  and the half life to be  $1622 \pm 13$  years.

#### ACKNOWLEDGMENTS

We wish to thank the following: Dr. Glenn T. Seaborg, who suggested this problem and under whose supervision the work was initiated; Dr. Winston M. Manning, under whose supervision it was concluded; Dr. Frank S. Tomkins, who performed the spectrographic analyses; Miss Patricia Walsh, who made the measurements of the low-geometry  $\alpha$  collimator; Mr. Albert Ghiorso, who made the pulse analyses; persons in the Argonne National Laboratory too numerous to mention who contributed by making available to us their unpublished techniques or by maintenance of counters and balances.

#### REFERENCES

1. H. Bateman, Proc. Cambridge Phil. Soc., 15: 423 (1910).
2. G. H. Briggs, Phil. Mag., (6) 50: 600 (1925).
3. O. Hahn, Physik. Z., 10: 81 (1909); O. Hahn and L. Meitner, Verhandl. deut. physik. Ges., 11: 55 (1909); E. M. Weilisch, Phil. Mag., (6) 26: 623 (1913); 28: 417 (1914); G. H. Briggs, Phil. Mag., (6) 41: 357 (1921).
4. O. Hahn, "Applied Radiochemistry," Chap. 11, Cornell University Press, Ithaca, N. Y., 1936.
5. M. Curie, Thesis, Paris, 1903; Chem. News, 88: 85 (1903).
6. R. C. Sisco, B. Cunningham, and P. L. Kirk, J. Biol. Chem., 139: 1 (1941).
7. O. Hoenigschmid and R. Sachtleben, Z. anorg. Chem., 221: 65 (1934).
8. P. L. Kirk, R. Craig, J. E. Gullberg, and R. Q. Boyer, Anal. Chem., 19: 427 (1947).
9. E. F. Westrum, Jr., An improved technique for precise alpha radiometric assay, Paper 16.2, this volume (Metallurgical Project Report CN-3433).
10. A. Ghiorso, A. H. Jaffey, H. P. Robinson, and B. B. Weissbourd, A 48-channel pulse-height analyzer for alpha-energy measurements, Paper 16.8, this volume (Metallurgical Project Report CC-3887).
11. S. Rosenblum, Compt. rend., 195: 317 (1932).
12. J. Allen and B. Rossi, Los Alamos Report LADC-177 (1944).
13. T. P. Kohman, A general method for determining coincidence corrections of counting instruments, Paper 22.50, this volume; see Phys. Rev., 72: 181 (1947); Anal. Chem., 21: 352 (1949).
14. B. B. Cunningham, A. Ghiorso, and J. C. Hindman, Back-scattering of Pu<sup>239</sup> alpha particles from platinum, Paper 16.3, this volume (Metallurgical Project Report CK-3861).
15. J. A. Crawford, Theoretical calculations concerning back-scattering of alpha particles, Paper 16.55, this volume (Metallurgical Project Report CC-1342).
16. E. F. Westrum, Jr., J. C. Hindman, and R. Greenlee, The specific alpha radioactivity and half life of plutonium isotope of mass 239, Paper 22.80, this volume.
17. J. H. Parsons, O. Flatau, J. K. East, R. D. Dandl, and C. J. Borkowski, Note on the back-scattering of Pu<sup>239</sup> alpha particles from platinum sample plates, Paper 16.4, this volume.

18. W. B. Lewis and B. V. Bowden, Proc. Roy. Soc. London, A145: 235 (1934); calculated from measurements of Rosenblum, reference 11.
19. O. Chamberlain, J. W. Gofman, E. Segrè, and A. C. Wahl, Los Alamos Report LA-9 (1943).
20. A. F. Kovarik and N. I. Adams, Phys. Rev., 40: 718 (1932).
21. E. Rutherford, J. Chadwick, and C. D. Ellis, "Radiations from Radioactive Substances," p. 63, Cambridge University Press, London, 1930.
22. M. Curie, A. Debierne, A. S. Eve, H. Geiger, O. Hahn, S. C. Lind, S. Meyer, E. Rutherford, and E. Schweidler, Revs. Modern Phys., 3: 427 (1931).

## Paper 22.70

### RAPID RADIOMETRIC ASSAY FOR RADIUM AND APPLICATION TO URANIUM ORE PROCESS SOLUTIONS<sup>†</sup>

By D. P. Ames, J. Sedlet, H. H. Anderson, and T. P. Kohman

#### 1. INTRODUCTION

The needs of the Manhattan Project for large quantities of uranium for military and nuclear-power purposes required not only an increase in production facilities but also improvements in processing techniques. Although radium is now regarded as a secondary rather than, as formerly, the primary constituent of uranium ores, its economic importance is still such that it must be completely accounted for and largely recovered in the processing of high-grade uranium ores. This in turn requires adequate analytical methods for radium at various points in the uranium-processing procedure. It is necessary in particular to be able to determine the radium content of certain of the process solutions rapidly so that further processing of these solutions may proceed without delay. The time available was given as 30 to 60 min. On the other hand, the accuracy needed in such a rapid assay is not great, particularly in the low-radium solutions. For some of these it is necessary only to state whether or not the radium concentration is below a designated value. This permissible upper limit was specified as  $10^{-9}$  g/ml.

Assays for small quantities of radium are conventionally made by the emanation method, of which there are numerous variations. In general, to achieve the required sensitivity, these methods require more time than is here available. Consequently, we have investigated the feasibility of direct counting of the  $\alpha$  particles of radium itself as

<sup>†</sup>Contribution from the Chemistry Division of the Metallurgical Laboratory, University of Chicago, now the Argonne National Laboratory.

Based on Metallurgical Laboratory Memorandum MUC-GTS-2251 (Apr. 13, 1946).

an alternate method. This is simply a modification of an old method in which the ionization current produced by a thinly spread layer of radium in an ionization chamber was measured with an electrometer.<sup>1</sup>

Alpha-particle counting requires that the active substance be separated in a small bulk of material and in most cases spread as a thin

Table 1.—Alpha Activities (Disintegrations per Minute) Associated with 1 g of Uranium in Pitchblende<sup>†</sup>

Element	Radium series		Actinium series		Thorium series	
	Isotope	Activity	Isotope	Activity	Isotope	Activity
92 U	U I	733,000	Ac U	34,000	Th	< 2,400
	U II	733,000	Pa	34,000		
91 Pa			Rd Ac	33,600	Rd Th	< 2,400
90 Th	Io	733,000	Ac	400		
89 Ac			Ac X	34,000	Th X	< 2,400
88 Ra	Ra	733,000	An	34,000	Tn	< 2,400
87 Fr			At <sup>215</sup>	~ 0.2		
86 Em	Rn	733,000	Ac A	34,000	Th A	< 2,400
85 At <sup>218</sup>	At <sup>218</sup>	~ 300				
84 Po	Ra A	733,000	Ac(C+C')	34,000	Th(C+C')	< 2,400
	Ra F	733,000				
83 Bi	Ra(C+C')	733,000				
	Ra E	~ 1				

<sup>†</sup>The values for the thorium series are upper limits, corresponding to thorium-uranium ratio of 1 per cent by weight, greater than that generally found.

layer of solid on a flat surface. Besides separating radium from the bulk of inert material with which it is associated, the procedure must also effect a separation from other  $\alpha$ -active substances in the ore. In ores not subject to excessive weathering or leaching, such as most pitchblendes, radioactive equilibrium prevails, and the members of the actinium and radium series are present with activities in the ratio 0.046/1, respectively. In pitchblendes the thorium content is generally so low that the thorium-series activities always are overshadowed greatly by those of the two uranium series.<sup>†</sup> Table 1 summarizes the  $\alpha$  activities associated with 1 g of uranium, assuming a thorium/uranium ratio of 1 per cent by weight. The elements of im-

<sup>†</sup>According to analyses,<sup>2</sup> the thorium content of pitchblende is less than about 0.01 per cent. A single gravimetric analysis was made which indicated approximately 1 per cent thorium; this, however, would not invalidate the above generalization.

portance because of their  $\alpha$ -active isotopes are U, Pa, Th, Em, Po, Bi, and Pb, the latter because of daughter Po and Bi activities.

Precipitation is the most convenient means of accomplishing the isolation of radium for counting. Because of the insolubility of radium sulfate, the presence or absence of sulfate in the solution to be assayed is an important consideration. Methods for both sulfate-free and sulfate-containing solutions are needed.

## 2. APPARATUS

Most of the precipitations are carried out in 5- or 15-ml centrifuge cones. Platinum wire, 10 gauge, is used for stirring. Sedimentation is accomplished with an International Clinical Centrifuge at 2,000 to 5,000 rpm. For aliquoting small quantities of reagents and standard solutions micropipets purchased from Microchemical Specialties Co. (usually of 50 microliters capacity) are used. For quantitative transfers of small amounts of solutions, such as in the spreading of dissolved precipitates on counting plates, uncalibrated capillary pipets are employed.

Platinum foil, which is generally used in this laboratory for mounting samples for  $\alpha$ -particle analysis, was found unsatisfactory because of the difficulty of cleaning and testing for reuse. Pyrex disks 2 to 3 mm thick and 4 cm in diameter† (purchased from Scientific Glass Apparatus Co.) were found suitable; they can be discarded after one use. Before a plate is used a 2- to 4-mm margin of Zapon lacquer is painted around the upper surface and allowed to dry to keep the solution from running off. The solution is evaporated by placing the disk on a thin asbestos sheet on a hot plate under an infrared lamp (General Electric Co. 250-watt reflector heat lamp).

For the measurement of  $\alpha$  activities a parallel-plate ionization chamber is used in conjunction with a pulse amplifier, scaler, and recorder. For most of this work, in which precision was of no importance and in which high counting rates were not encountered, the standard type of air-chamber  $\alpha$  counter used on the Metallurgical Project<sup>a</sup> was satisfactory.

## 3. PREPARATION AND COUNTING OF RADIUM SAMPLES

Radium compounds sufficiently insoluble in acid solution for precipitation separations are the sulfate, chloride, bromate, and nitrate. In general, the sulfate is unsatisfactory because of the well-known

†Preliminary experiments were done with 4-cm squares cut from 2-mm pyrex sheets, but these are not so convenient for counting.

tendency of  $\text{BaSO}_4$  to carry down impurities from solution. Chloride precipitation of barium has found extensive use on the Metallurgical Project in fission-product studies<sup>4</sup> and consequently was adopted for this work. The solubilities of radium and barium chlorides depend markedly on the HCl concentration, being moderately high in water or dilute acid and very low in concentrated solutions (6N or greater). Precipitates are thus conveniently dissolved in a small amount of water, and the compound is reprecipitated by adding a large excess of concentrated HCl. Nitrate and bromide precipitations were not tried because the chloride method was so successful.

Because of the small amounts of radium to be precipitated, a carrier is always necessary. Barium is very similar to radium in its chemical properties<sup>5</sup> and can be used in all cases except those in which a large amount of carrier is required and a separation from the carrier must be made later, or when sulfate is present, causing  $\text{BaSO}_4$  to form. In such cases lead sulfate was found useful as an alternate carrier.

The final step in the radiometric analysis consists in spreading the separated radium with its barium carrier on a flat plate and counting in a parallel-plate ionization chamber before the radon and other active descendants grow in to an appreciable extent. When a solution containing a few milligrams of  $\text{BaCl}_2$  is simply evaporated to dryness on a flat surface an irregular deposit is obtained, resulting in large and variable self-absorption of  $\alpha$  particles. If, however, sulfuric acid is added to the solution during evaporation, there results a uniform deposit of  $\text{BaSO}_4$ , suitable for  $\alpha$  counting. A satisfactory technique is to evaporate the solution 2 to 3 min so that any radon can escape, add 5 drops of 1N  $\text{H}_2\text{SO}_4$ , and continue the evaporation to dryness. The plate is then flamed to a red heat in a Meker burner to drive off residual sulfuric acid and to burn off the lacquer border.

When radium is precipitated with a few milligrams of  $\text{BaCl}_2$ , dissolved in water, and mounted on a plate as just described, the counting rate starts at a minimum and grows steadily as radon and its daughters accumulate, as shown in Fig. 1, curve A. This is evidence that the  $\text{BaCl}_2$  precipitation effects a separation from the active deposit activities. In such cases it is desirable to count the sample immediately, say within 20 min. If, however, radium that has not been freshly prepared is transferred directly to a plate and mounted, the counting rate decreases at first because of the decay of the RaA-B-C complex; reaches a minimum in 1 to 3 hr, depending on the amount of these activities present; and then increases slowly, as shown in Fig. 1, curve B. In general, 2 hr is sufficient time to wait before counting in such cases, and the activity counted will be 3 to 8 per cent high as a result of the daughter activities present.

The effect of self-absorption (i.e., absorption of the radium  $\alpha$  particles in the deposit with a resultant decrease in the counting rate) was studied by adding to counting plates a constant amount of radium and variable amounts of barium, preparing the deposits as usual, and

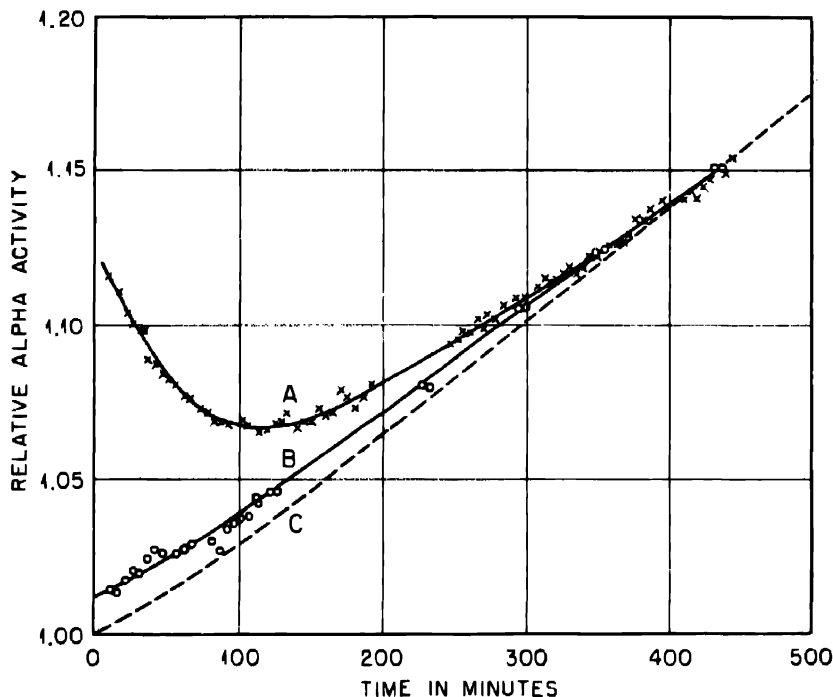


Fig. 1—Variation of  $\alpha$  activity of radium deposits with time. A, old radium sample. B, freshly precipitated radium. C, theoretical for initially pure radium, assuming no loss of radon by recoil or diffusion. Curves arbitrarily normalized at 7 hr. On scale Ra = 1.00, curves A and B would be lower because of recoil and diffusion losses.

counting after 2 hr. The results are shown in Fig. 2. Although the decrease in counting rate is theoretically nearly a linear function of the sample thickness for thin uniform deposits, the curve obtained in this experiment drops rapidly at first and then more slowly. This is probably because the deposits are not truly uniform but form fairly large particles of  $\text{BaSO}_4$ , even when only small amounts are present. Knowing the weight of carrier used, it is possible to correct the result for self-absorption by use of the curve of Fig. 2 or a curve similarly obtained for the particular technique employed.

The conditions for the chloride precipitation are essentially those used for barium.<sup>4</sup> To 1 volume of the solution is added 7 volumes of

ice-cold HCl-ether solution consisting of 6 parts of concentrated HCl and 1 part of ethyl ether. The ether is effective in reducing the solubility of the BaCl<sub>2</sub>-RaCl<sub>2</sub>. The precipitation is complete almost immediately if the solution is stirred vigorously. Following centrifuga-

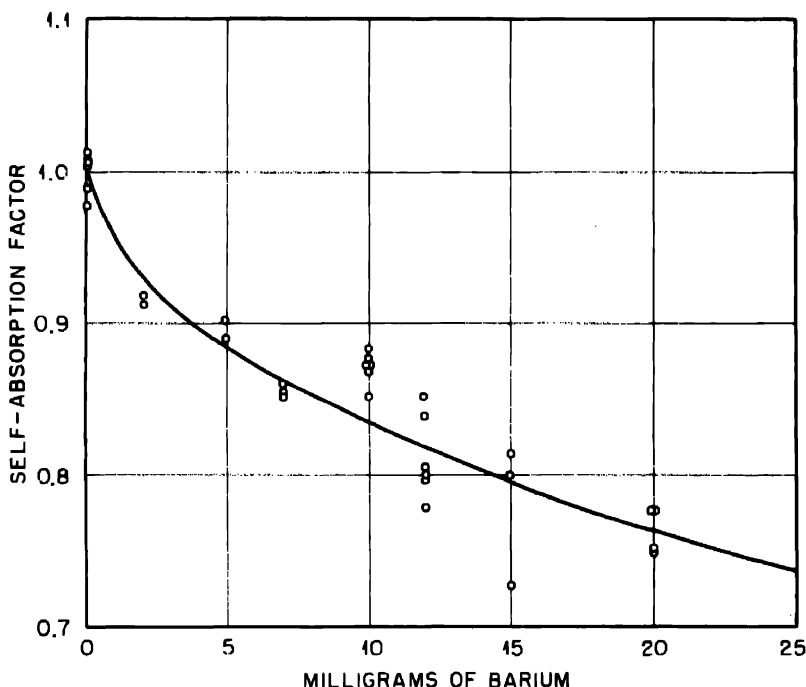


Fig. 2.—Self-absorption of radium  $\alpha$  particles in barium sulfate deposits.

tion and decantation of the supernatant liquid, the precipitate is washed twice by suspension in 1 volume of cold HCl-ether and centrifugation. It can be dissolved in a small amount of water or dilute acid and reprecipitated with 1 to 2 volumes of cold HCl-ether reagent to effect a purification.

In order to determine the amount of barium needed to carry radium quantitatively in this procedure, tests were made using a constant amount of radium and varying amounts of barium in 1 ml of uranyl nitrate solution (200 mg of uranium per milliliter). Following addition of 7 ml of HCl-ether, the solution was stirred for 1 to 2 min in an ice bath and centrifuged for 5 min. The precipitate was washed twice with 1 ml of HCl-ether, dissolved in a few drops of 1N HNO<sub>3</sub>, and transferred to a counting plate with a capillary pipet. The centrifuge

cone and pipet were rinsed onto the plate with several portions of 1N HNO<sub>3</sub>. The amount of radium present at the beginning was determined by transferring equal aliquots directly to plates and counting. (In experiments of this type it is necessary to use radium that has been recently purified by BaCl<sub>2</sub> precipitation to free it of polonium, which

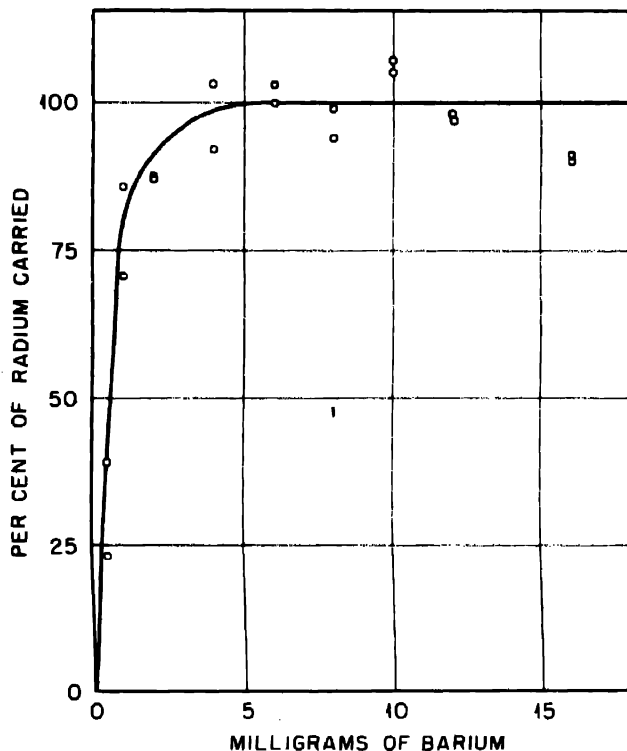


Fig. 3.—Carrying of radium by barium chloride from uranyl nitrate solutions; 7 ml of HCl-ether reagent added to 1 ml of solution containing radium, protactinium, and 200 mg of uranium.

is found in aged radium solutions.) The results of the carrying tests, corrected for self-absorption by means of Fig. 2, are plotted in Fig. 3. It is seen that 5 mg of barium per milliliter of solution is necessary for complete carrying, and 10 mg per milliliter was adopted for standard procedure.

When the barium is added to the solution after the addition of the HCl-ether, complete carrying occurs if stirring is rapid and complete. However, in many instances incomplete carrying was observed, particularly with smaller amounts of carrier. Therefore barium should be added before the HCl-ether whenever this is possible.

#### 4. CONVERSION FACTORS, SENSITIVITY, AND ACCURACY

The half life and specific activity of radium are known only to an accuracy of several per cent. The most probable half life is 1,620 years, corresponding to a specific  $\alpha$  activity of  $2.17 \times 10^{12}$  disintegrations per minute per gram.<sup>6</sup> For thin deposits on glass the counting yield in parallel-plate ionization chambers is approximately 0.51 (slightly greater than  $\frac{1}{2}$  because of back-scattering), leading to a specific counting rate of  $1.10 \times 10^{12}$  counts per minute per gram under ideal conditions.

Because of the possibility of small chemical losses due to solubilities and mechanical losses in centrifugal separations, because of irregularities in the distribution of samples on counting plates, and because of the difficulty of completely eliminating interference by the daughters of radium, results are not reproducible to better than several per cent by this method. Since chemical losses and self-absorption both lead to low results, a net specific counting rate of  $1.00 \times 10^{12}$  counts per minute per gram is assumed for approximate purposes. Thus 1 count per minute conveniently corresponds to  $1\mu\mu\text{g}$  ( $10^{-12}$  g) of radium. Where greater accuracy is required, the factor can be determined empirically for the particular technique used, and the effect of self-absorption can be considered for each measurement.

The background counting rate of ordinary  $\alpha$  counters is usually about 0.5 to 2 counts per minute. The sensitivity of the method for pure radium samples, using counting periods of 10 to 20 min, is thus about 1 count per minute or  $10^{-12}$  g of radium.

From the spread of the individual values in Figs. 2 and 3 and from other experience with this method, it is estimated that the accuracy of the method at high radium levels corresponds to a probable error of 3 to 10 per cent, depending on the particular application. Apparently the greatest cause of variation is the irreproducibility of the deposits on the counting plates.

#### 5. ASSAY OF SULFATE-FREE SOLUTIONS

Tests of the separation of each of the important  $\alpha$ -emitting elements by  $\text{BaCl}_2$  precipitation from sulfate-free solutions were made by precipitating  $\text{BaCl}_2$  in the absence of radium from solutions containing suitable radioactive isotopes of those elements to serve as indicators. The results, summarized in Table 2, indicate that a single precipitation followed by two washes adequately eliminates interference from all other  $\alpha$  emitters. Separation from bismuth appears to be not quite so good as from U, Pa, Th, Po, and Em, but only small

amounts of bismuth  $\alpha$  activities can be present. Later data (Table 4) and the experience of others in this laboratory indicate that actinium is carried to a considerable extent by  $\text{BaCl}_2$ ; however, negligible actinium  $\alpha$  activity is encountered in uranium ores (Table 1).

Table 2—Separation of  $\alpha$ -active Contaminants by  $\text{BaCl}_2$  Precipitation from Sulfate-free Solutions

Element	Indicator	Procedure	Per cent carried
U	Natural U ( $\alpha$ )	1 ml of 20% uranyl nitrate hexahydrate 7 ml of HCl-ether, 2 mg of Ba 2 washes with 1 ml of HCl-ether	$\leq 0.001^\dagger$
		1 ml of 40% uranyl nitrate hexahydrate 7 ml of HCl-ether, 11.5 mg of Ba 2 washes with 1 ml of HCl-ether	$\leq 0.003^\dagger$
Pa	$\text{Pa}^{233}$ ( $\beta$ )	1 ml of 1N $\text{HNO}_3$ 7 ml of HCl-ether, 11 mg of Ba 2 washes with 1 ml of HCl-ether	0.051 0.035
		1 ml of 1N $\text{HNO}_3$ , 7 ml of HCl-ether, 11 mg of Ba 2 washes with 1 ml of HCl-ether	0.01 0.01
Th	Io ( $\alpha$ )	1 ml of 1N $\text{HNO}_3$ , 7 ml of HCl-ether, 11 mg of Ba 2 washes with 1 ml of HCl-ether	0.01 0.01
Em	Rn ( $\alpha$ )	Evaporation of Ra samples $\text{BaCl}_2$ precipitation of Ra $\text{RaCl}_2$ precipitation (pure Ra)	< 0.1 $^\dagger$
Po	RaF ( $\alpha$ )	1 ml of 1N $\text{HNO}_3$ , 7 ml of HCl-ether, 10 mg of Ba 2 washes with 1 ml of HCl-ether Plates flamed in Meker burner	0.04 0.05
Bi	RaE ( $\beta$ )	1 ml of 1N $\text{HNO}_3$ , 7 ml of HCl-ether, 10 mg of Ba 2 washes with 1 ml of HCl-ether	0.5 0.3
Pb	$\text{Ra(B+C+C''})$ ( $\gamma$ )	$\text{RaCl}_2$ precipitation (pure Ra)	< 1 $^\dagger$

$^\dagger$ Numerous experiments.

The presence of uranium in concentrations up to 300 mg per milliliter was found not to interfere with the quantitative carrying of radium by  $\text{BaCl}_2$ .

As a result of these tests it is evident that the procedure described is satisfactory for sulfate-free solutions that do not contain excessive amounts of barium.

## 6. ASSAY OF SULFATE-CONTAINING SOLUTIONS

Since significant amounts of radium may remain in sulfate solutions in spite of the low solubility of  $\text{RaSO}_4$ , an assay procedure applicable to sulfate-containing solutions is necessary.  $\text{BaSO}_4$  precipitated from a solution containing uranyl nitrate and sulfuric acid carries appreciable amounts of uranium  $\alpha$  activity that cannot be removed by numerous washings;  $\text{BaSO}_4$  is known to carry other impurities as well. Since no simple method of dissolution and reprecipitation is available, this procedure is obviously unsuited to radium assay.

Attempts were made to precipitate  $\text{BaCl}_2$  preferentially from solutions containing sulfate by first adding a large excess (7 volumes) of HCl-ether mixture and then introducing the barium. When the  $\text{H}_2\text{SO}_4$  concentration of the original solution was 0.5N or greater, the precipitate obtained was in part the sulfate, as indicated by its failure to dissolve completely in water. Since solutions having appreciable sulfate concentrations may be encountered, this procedure is not satisfactory.

A means of separating the radium from the sulfate-containing solution preliminary to its precipitation with  $\text{BaCl}_2$  was then sought. Of the methods tried, preliminary precipitation of  $\text{PbSO}_4$ , which is known to be a good carrier for  $\text{Ra}^{6,7}$  was found to be satisfactory.  $\text{PbSO}_4$  is readily soluble in the HCl-ether solution, and the amount of sulfate now present is so small that the precipitate formed on addition of barium is exclusively the chloride, as indicated by its complete solubility in water.

Suspension of the  $\text{PbSO}_4$  precipitate in water for washing, which is necessary to remove  $\text{H}_2\text{SO}_4$ , results in a layer of the precipitate that clings to the surface of the solution and creeps up the walls of the tube so that it cannot be centrifuged down. This can be prevented by the addition of a drop of 5 per cent aerosol solution (5 per cent aqueous solution of Aerosol-OT, dioctyl sodium sulfosuccinate, manufactured by American Cyanamid Company) to 1 ml of wash water. Aerosol results in a water-insoluble residue in the subsequent  $\text{BaCl}_2$  precipitation, and it must be removed by a final wash with water in which care is taken not to disturb the packed precipitate.

Experiments were performed to determine the conditions necessary for complete carrying of radium by  $\text{PbSO}_4$ . In some experiments the  $\text{PbSO}_4$  precipitates were spread on plates and counted, and in others the precipitates were dissolved in HCl-ether and assayed by  $\text{BaCl}_2$  precipitation. In 6N  $\text{H}_2\text{SO}_4$ , in which the solubility of  $\text{PbSO}_4$  is a

minimum, a lead concentration of 2 mg per milliliter was found necessary for complete carrying; 5 mg per milliliter was adopted for the standard procedure. With this lead concentration 2N H<sub>2</sub>SO<sub>4</sub>, was found to be sufficient in the absence of uranium, but, to compensate

Table 3—Separation of  $\alpha$ -active Contaminants by PbSO<sub>4</sub> Precipitation from Sulfate-containing Solutions

Element	Indicator	Procedure	Per cent carried
U	Natural U ( $\alpha$ )	1 ml of 40% uranyl nitrate hexahydrate	2.0
		5 mg of Pb, 6N H <sub>2</sub> SO <sub>4</sub>	1.5
		No washing	1.7
		Same, but 3 washes with 1 ml of H <sub>2</sub> O	$\leq 0.01^\dagger$
Pa	Pa <sup>231</sup> ( $\beta$ )	1 ml 1N HNO <sub>3</sub>	3.5
		5 mg of Pb, 6N H <sub>2</sub> SO <sub>4</sub>	3.7
		3 washes with 1 ml of H <sub>2</sub> O	
Th	Io ( $\alpha$ )	1 ml of 40% uranyl nitrate hexahydrate	7.7
		5 mg of Pb, 6N H <sub>2</sub> SO <sub>4</sub>	7.2
		3 washes with 1 ml of H <sub>2</sub> O	7.5
Ac	MsTh <sub>2</sub> ( $\beta$ )	1 ml of 1N HNO <sub>3</sub>	90
		5 mg of Pb, 6N H <sub>2</sub> SO <sub>4</sub>	
		No washing	
		Same, but 3 washes with 1 ml of H <sub>2</sub> O	36
Po	RaF ( $\alpha$ )	1 ml of 1N HNO <sub>3</sub>	90
		5 mg of Pb, 6N H <sub>2</sub> SO <sub>4</sub>	
		3 washes with 1 ml of H <sub>2</sub> O	
		Plate not flamed	
		Same, but plates flamed in Meker burner	2.5
			2.1
			0.9
Bi	RaE ( $\beta$ )	1 ml of 1N HNO <sub>3</sub>	47
		5 mg of Pb, 6N H <sub>2</sub> SO <sub>4</sub>	44
		3 washes with 1 ml of H <sub>2</sub> O	

<sup>†</sup>Numerous experiments.

for possible complexing of sulfate by uranium, 6N H<sub>2</sub>SO<sub>4</sub> was retained. Addition of extra H<sub>2</sub>SO<sub>4</sub> may be necessary.

The behavior of contaminating elements in the PbSO<sub>4</sub> precipitation and in the over-all two-step procedure is shown by the results of tests tabulated in Tables 3 and 4, respectively. Although the first step does

**Table 4—Separation of  $\alpha$ -active Contaminants by  $PbSO_4$ - $BaCl_2$  Precipitation Procedure from Sulfate-containing Solutions**

Element	Indicator	Procedure	Per cent carried
Natural U ( $\alpha$ )		1 ml 40% uranyl nitrate hexahydrate 5 mg of Pb, 6N $H_2SO_4$ 3 washes with 1 ml of $H_2O$ 2 ml of HCl-ether, 2 mg of Ba 2 washes with 1 ml of HCl-ether	$\leq 0.003^\dagger$
Pa	$Pa^{231}$ ( $\alpha$ )	1 ml of 1N $HNO_3$ 5 mg of Pb, 6N $H_2SO_4$ 4 washes with 1 ml of $H_2O$ 2 ml of HCl-ether, 2 mg of Ba 2 washes with 1 ml of HCl-ether	0.48 0.25
Th	Io ( $\alpha$ )	1 ml of 1N $HNO_3$ , 5 mg of Pb, 6N $H_2SO_4$ 3 washes with 1 ml of $H_2O$ 2 ml of HCl-ether, 2 mg of Ba 2 washes with 1 ml of HCl-ether  Same, but no washing	0.02 0.02 0.03  0.23
Ac	$MsTh_2$ ( $\beta$ )	1 ml of 1N $HNO_3$ , 5 mg of Pb, 6N $H_2SO_4$ 3 washes with 1 ml of $H_2O$ 2 ml of HCl-ether, 2.3 mg of Ba 2 washes with 1 ml of HCl-ether	9.5 7.4
Po	RaF ( $\alpha$ )	1 ml of 1N $HNO_3$ , 5 mg of Pb, 6N $H_2SO_4$ 4 washes with 1 ml of $H_2O$ 2 ml of HCl-ether, 2 mg of Ba 2 washes with 1 ml of HCl-ether  Plates not flamed  Same, but plates flamed in Meker burner	0.5 0.5  0.03 0.01
Bi	RaE ( $\beta$ )	1 ml of 40% uranyl nitrate hexahydrate 5 mg of Pb, 6N $H_2SO_4$ 4 washes with 1 ml of $H_2O$ 2 ml of HCl-ether, 2 mg of Ba 2 washes with 1 ml of HCl-ether	1.2 1.4 1.3 2.0

$^\dagger$  Numerous experiments.

not give clean precipitation, both steps together give satisfactory separation from all important contaminants. Protactinium and bismuth are not so cleanly separated as uranium, thorium, and polonium, but the small  $\alpha$  levels of these elements make the observed separation adequate. These experiments indicate that it is important to flame the plates so that polonium will be volatilized off.

It is to be noted that this two-step procedure can, if desired, be used as a means of concentrating radium from a considerable volume of solution for counting, provided the amount of barium present is negligible. For example, precipitation of radium from 100 ml of solution by the HCl-ether method would require several hundred milligrams of barium carrier. If, however, it were first carried with 200 mg of lead as the sulfate and dissolved in 10 ml of HCl-ether, it could be precipitated for counting with only 10 mg of barium.

#### 7. APPLICATION TO URANIUM ORE PROCESS SOLUTIONS

While developing the assay procedures, numerous tests were made on actual process solutions. The true radium contents of these solutions were determined by an emanation procedure.<sup>8</sup>

In the early comparisons with aged solutions, there were observed systematic discrepancies between the precipitation and emanation results. The former were always appreciably higher than the latter and presumably correct values. This was attributed to the presence of  $\alpha$ -emitting AcX( $Ra^{223}$ ) in the solutions. Since this is isotopic with  $Ra^{228}$ , it is removed to the same extent as the latter. However, if its parent,  $RdAc(Th^{227})$ , is not removed, AcX will grow from it at an initial rate corresponding to 0.28 per cent of the original radium  $\alpha$  activity per day. This interpretation was checked by precipitation assays made at various time intervals after removal of radium from the solutions; the  $\alpha$  activity increased with time and corresponded approximately to the amount expected from the ages of the solutions. Moreover, when the process solutions were freed of radium by  $BaCl_2$  precipitation, radium  $\alpha$  activity again grew into the solutions.

It is evident that this assay method is not specific for  $Ra^{228}$  but is a general one for radium  $\alpha$  activity. In uranium processing it can be applied only on fresh solutions. The results of tests on fresh process solutions are shown in Table 5. From these results it appears that the two-step method for sulfate-containing solutions gives values for fresh solutions that are consistently about  $10^{-10}$  g per milliliter higher than does the emanation method. This difference is probably due to slight contamination by the various  $\alpha$ -active materials present. Since this is only about a tenth of the permissible radium concentra-

tion, approximately  $10^{-9}$  g per milliliter, the error in assuming a constant correction of  $10^{-10}$  g per milliliter will be negligible. The sensitivity of the method for fresh process solutions is thus about  $10^{-10}$  g per milliliter.

The results on sulfate-free solutions by  $\text{BaCl}_2$  precipitation were not conclusive. On the basis of early experiments, 2 mg of barium

Table 5—Assay of Pilot-plant Process Solutions for Radium

Sample		Ra concentration by precipitation assay, (g/ml) $\times 10^{-10}$			Ra concentration by emanation assay, (g/ml) $\times 10^{-10}$
Type	Age	Method†	Amount	Ave.	
Sulfate-containing	Fresh	A	1.5	1.4	0.5
		A	1.3		
		A	1.5		
	2 days	A	10		
Sulfate-containing	Fresh	A	4.7	4.8	4.5
		A	5.0		
Sulfate-containing	Fresh	A	3.4	3.3	2.2
		A	3.2		
Sulfate-free	6 days	B‡	4.7	5.2	0.75
		B‡	5.8		
Sulfate-free	6 days	B‡	6.3	7.1	
		B‡	7.8		
Sulfate-free	Fresh	B‡	14	17	32
		B‡	16		
		C‡	26		
		C‡	12		

†Methods: A,  $\text{PbSO}_4$  precipitation followed by  $\text{BaCl}_2$  precipitation. B, single  $\text{BaCl}_2$  precipitation. C, double  $\text{BaCl}_2$  precipitation.

‡Precipitation results low because of inadequate carrier (see Sec. 7).

per milliliter was used as carrier in these tests. The low and erratic results on the fresh solution as well as the data of Fig. 3 indicate that carrying was incomplete because of insufficient barium. Similarly, the results on 6-day-old solutions were considerably below the values expected from  $\text{AcK}$  growth (approximately  $10 \times 10^{-10}$  g per milliliter Ra equivalent). It is noteworthy that on the fresh sulfate-free solution the precipitation assay was lower than the emanation

result; the high radium level of this solution concealed any possible contamination effect. There was no opportunity to continue these tests, but, as a result of subsequent experiments with synthetic solutions, it appears certain that the  $\text{BaCl}_2$  precipitation method should be satisfactory for sulfate-free solutions if an original barium concentration of 10 mg per milliliter is used.

#### 8. DETAILS OF PROCEDURES FOR URANIUM ORE PROCESS SOLUTIONS

The details of technique and interpretation of the assay method for a particular routine application should be determined by further experiments on actual samples. For sulfate-free solutions it will be necessary to determine whether a single  $\text{BaCl}_2$  precipitation is sufficient, or whether a double precipitation is required. The correction for contaminating  $\alpha$  activity should be determined for each type of solution by a number of parallel precipitation and emanation analyses. It may be desirable to determine more accurately the factor for converting counting rates to radium concentrations, by adding known amounts of radium to process solutions. If the techniques are standardized, the empirical determination of this factor will make a knowledge of chemical losses, self-absorption, etc., unnecessary. The rate of growth of  $\text{AcX}$  activity in the particular type of solutions to be assayed should be determined. Finally, it may be possible to simplify the assay techniques by eliminating washes, etc.

Tentative procedures for the assay of process solutions are given in detail below.

##### 8.1 Sulfate-free Solutions. Total time required: 25 min.

1. Measure 1 ml of the fresh solution into a 15-ml centrifuge cone.
2. Add 0.05 ml of 1.5M  $\text{BaCl}_2$  solution (10 mg of Ba).
3. Add 7 ml of a cold ( $0^\circ\text{C}$ ) mixture of 6-to-1 concentrated HCl-ether mixture, stir with a platinum wire (20 gauge), keeping tube in ice bath.
4. Centrifuge 3 min at 3,000 rpm, withdraw supernatant liquid with transfer pipet, discard supernatant liquid.
5. Wash precipitate with 1 ml of ice-cold HCl-ether, centrifuge, discard supernatant liquid.
6. Repeat step 5.
7. Add 0.5 ml of 1N  $\text{HNO}_3$  to dissolve precipitate. Using a transfer pipet, transfer the solution to a clean pyrex counting plate (2 mm thick, 4 cm in diameter) ringed with Zapon lacquer (applied with a brush in a margin 2 to 4 mm wide around the edge and allowed to dry).

Rinse the centrifuge tube and pipet several times with 1N HNO<sub>3</sub> to obtain a complete transfer.

8. Place the counting plate on a thin asbestos sheet on a small hot plate and heat from above with an infrared heat lamp (250 watt) until bubbles begin to form and rise (2 to 3 min, to drive off radon).

9. Add 5 drops of 1N H<sub>2</sub>SO<sub>4</sub> and evaporate to dryness.

10. Flame the plate with a Meker burner to burn off the Zapon ring and to drive off all H<sub>2</sub>SO<sub>4</sub>.

11. Count the deposit immediately (within 20 min) in a standard parallel-plate  $\alpha$  counter.

12. Calculate the radium content of the process solution as follows:

$$\text{Radium concentration (g/ml)} = \text{counting rate (c/m)} \times 10^{-12}$$

8.2 Sulfate-containing Solutions. Total time required: 45 min.

1. Measure 1 ml of the fresh solution into a 15-ml centrifuge cone.

2. Add 0.05 ml of 0.3M Pb(NO<sub>3</sub>)<sub>2</sub> solution (3 mg of lead). Stir well with a platinum wire (20 gauge).

3. Add 0.2 ml of concentrated H<sub>2</sub>SO<sub>4</sub>, stir vigorously (final H<sub>2</sub>SO<sub>4</sub> concentration 6N). Cool 2 to 3 min in ice bath.

4. Centrifuge 3 min at 3,000 rpm, withdraw supernatant liquid with transfer pipet and discard.

5. Add 1 ml of distilled water and 1 drop of 5 per cent aerosol, suspend precipitate by stirring with platinum wire, centrifuge, and remove supernatant liquid as before.

6. Repeat step 5.

7. Repeat step 5 again.

8. Carefully add 1 ml of water without stirring, centrifuge, and remove supernatant liquid (to remove aerosol).

9. Add 1.5 ml of a cold (0°C) mixture of 6-to-1 concentrated HCl-ether mixture; stir to dissolve precipitate, keeping tube in ice bath.

10. Add 0.05 ml of 0.3M BaCl<sub>2</sub> solution (2 mg of Ba); stir well.

11. Centrifuge; discard supernatant liquid.

12. Suspend precipitate in 1 ml of ice-cold HCl-ether mixture, centrifuge, and discard supernatant liquid.

13. Repeat step 12.

14. Add 0.5 ml of 1N HNO<sub>3</sub> to dissolve precipitate. Using a transfer pipet, transfer the solution to a clean pyrex counting plate (2 mm thick, 4 cm in diameter) ringed with Zapon lacquer (applied with a brush in a margin 2 to 4 mm wide around the edge and allowed to dry). Rinse the centrifuge tube and pipet several times with 1N HNO<sub>3</sub> to obtain a complete transfer.

15. Place the counting plate on a thin asbestos sheet on a small hot plate and heat from above with an infrared heat lamp (250 watts) until bubbles begin to form and rise (2 to 3 min, to drive off radon).

16. Add 5 drops of 1N  $H_2SO_4$  and evaporate to dryness.
17. Flame the plate with a Meker burner to burn off the Zapon ring and to drive off all  $H_2SO_4$ .
18. Count the deposit immediately (within 20 min) in a standard parallel-plate  $\alpha$  counter.
19. Calculate the radium content of the process solution as follows:  
Radium concentration (g/ml) = counting rate (c/m)  $\times 10^{-12}$

#### 9. SUMMARY

A rapid method of assay for radium in solution, based on the precipitation of radium with barium as carrier and counting of its  $\alpha$  particles, has been described. In sulfate-free solutions  $(Ba,Ra)Cl_2$  is precipitated with concentrated HCl and ether. In sulfate-containing solutions  $(Pb,Ra)SO_4$  is first precipitated, followed by a  $(Ba,Ra)Cl_2$  precipitation. The chloride is converted to the sulfate on a pyrex disk for  $\alpha$ -particle counting in a parallel-plate ionization chamber. The method is general for all  $\alpha$ -emitting radium isotopes, is sensitive to  $10^{-12}$  g of  $Ra^{226}$ , and is accurate to 3 to 10 per cent. It separates radium from all other  $\alpha$ -emitting substances accompanying it in nature. Applications of this method to uranium ore process solutions have also been described. The method is suitable for certain control problems in which knowledge of approximate radium concentrations is required in 30 to 60 min. In this application the sensitivity is limited by interfering activities to  $10^{-10}$  g of radium per milliliter.

#### REFERENCES

1. H. Geiger, Proc. Roy. Soc. London, A82: 486 (1909).
2. Reports A-1023 (Jan. 31, 1944) and A-1028 (Mar. 15, 1944).
3. A. H. Jaffey, Metallurgical Project Report CC-3771; also in National Nuclear Energy Series, Division IV, Volume 14 A.
4. D. N. Hume, N. E. Ballou, and L. E. Glendenin, Metallurgical Project Report CN-2815 (1945).
5. O. Hahn, "Applied Radiochemistry," Chap. 4, Cornell University Press, Ithaca, N.Y., 1936.
6. T. P. Kohman, D. P. Ames, and J. Sedlet, The specific activity of radium, Paper 22.60, this volume (Manhattan District Declassified Report MDDC-852, 1947).
7. J. F. Flagg, E. Alling, and C. Hallett, University of Rochester Project Report 13 (November 1944).
8. P. Fineman, B. B. Weissbourd, H. H. Anderson, J. Sedlet, D. P. Ames, and T. P. Kohman, An emanation method for radium analysis, Paper 16.7, this volume.

# THE SPECIFIC ALPHA RADIOACTIVITY AND HALF LIFE OF PLUTONIUM ISOTOPE OF MASS 239†

By E. F. Westrum, Jr., J. C. Hindman, and R. Greenlee

In addition to interest in the specific activity of a long-lived isotope in the calculation of its radioactive disintegration constants and nuclear energetics, accurate determinations of the specific activity are of value in the analysis of compounds of the radioactive element. The establishment of the composition, the purity, or the concentration in solution of plutonium compounds can often be made with convenience and precision for physicochemical measurements if a reliable value of the specific activity is available.

## 1. EARLY MEASUREMENTS OF THE HALF LIFE OF Pu<sup>239</sup>

Wahl and Seaborg<sup>1</sup> measured the ratio of 23.2-min U<sup>239</sup> β particles to daughter Pu<sup>239</sup> α particles in the chain



They assumed that U<sup>239</sup> emitted no conversion electrons detectable in their experiments and obtained a value of  $2.3 \times 10^4$  years for the half life of Pu<sup>239</sup>.

A preliminary determination, primarily of historical interest, of the specific activity of Pu<sup>239</sup> was made by weighing only 4.45 μg of the first preparation of plutonium dioxide on a Salvioni microbalance at a time when the chemical formula of the compound had not been definitely established.<sup>2</sup>

<sup>†</sup>Contribution from the Chemistry Division of the Metallurgical Laboratory, University of Chicago, now the Argonne National Laboratory.

Based on work reported in Metallurgical Laboratory Memorandums MUC-GTS-2042 (Oct. 25, 1945), MUC-GTS-2075 (Nov. 11, 1945), and MUC-GTS-2032 (Nov. 13, 1945).

Additional results were presented later.<sup>3</sup> Three more determinations<sup>4</sup> of the specific activity of plutonium and a revision of the counting yield to 47 per cent were reported by weighing about 7.5 µg of PuO<sub>2</sub> on a platinum disk on a Salvioni microbalance, another by weighing about 3 µg of Pu(IO<sub>3</sub>)<sub>4</sub>, and the third by weighing about 50 µg of

Table 1—Summary of Early Specific Activity Values<sup>2-4</sup> for Pu<sup>239</sup>

Compound weighed	Microbalance used	Amount weighed, µg	Reported	Specific activity, dis/min/µg Corrected to 52% geometry
PuO <sub>2</sub>	Salvioni	4.5	167,000	145,000
PuO <sub>2</sub>	Salvioni	(?)	163,000	141,000
PuO <sub>2</sub>	Salvioni	~ 7.5	157,000	142,000
Pu(IO <sub>3</sub> ) <sub>4</sub>	Salvioni	~ 3	155,000	140,000
Pu(IO <sub>3</sub> ) <sub>4</sub>	Ainsworth	~ 50	154,000	139,000
				141,000† (av.)

†The authors estimated a probable error of 5%.

Pu(IO<sub>3</sub>)<sub>4</sub> on an Ainsworth microbalance. A summary of the early values is presented in Table 1. Despite the limited microquantities of plutonium available, these values are certainly within the experimental uncertainty of the latest values of specific activity.

## 2. COUNTING INSTRUMENTS AND PRELIMINARY MEASUREMENTS

**2.1 Instruments and Procedure.** Most of the measurements described in this paper were made on a single parallel-plate nitrogen-filled counter (Metallurgical Laboratory counter N-4) with three scalar circuits cumulating a count of 512. This instrument is characterized by a counting yield of almost 52 per cent and a relatively short resolving time. The coincidence correction is about 1.1 per cent at 100,000 counts per minute. Commercially available nitrogen was suspected as the cause of fluctuations in the counting efficiency observed in early measurements, and a mixture of 96 per cent argon and 4 per cent CO<sub>2</sub> by volume was employed with very reproducible results in most of the later measurements. Since 99.9 per cent argon and various argon-CO<sub>2</sub> mixtures were employed at various times and since electronic and inexplicable variations in the counting efficiency were occasionally observed, several "standard" control plates were counted to at least equivalent statistical certainty at the beginning and end of the day that other plates were counted. In this way it was possible for convenience of presentation and comparison to report most

of the data obtained on this counter over a period of months on the basis of the standard behavior of the N-4 counter at the time when its counting efficiency was compared to a special low-geometry counter. In this way the fluctuations in the observed counts due to changes in the gas mixture, pulse-height selector setting, plateau, electronics, and unknown effects are largely eliminated.

Since the original purpose of the measurements was to produce relative values of the amounts of plutonium dissolved rather than absolute specific activities, this presentation occasions no uncertainty. The plates of interest in such a comparison were repeatedly counted in rotation in such an order as to minimize the drift in the counter efficiency. A sufficient number of counts were made to ensure a statistical uncertainty not larger than several hundredths of a per cent. The duration of the counting period was determined with a stop watch calibrated against the time signals broadcast by the National Bureau of Standards.

**2.2 Conventions Regarding Estimation of Reliability of the Data.** The procedures recommended by Rossini and Deming<sup>5</sup> for the statistical treatment of data were applied to all measurements here reported. The estimated standard deviation  $S'$  of the mean value  $\bar{x}$  of a set of  $N$  individual determinations  $x_i$  is defined as

$$S' = \frac{\sum(x_i - \bar{x})^2}{N(N - 1)}^{1/2}$$

in their notation and is a measure of the spread or deviations actually observed in the set. It is not to be confused with the statistical reliability ("standard error") based on the number of observed disintegrations. Unless otherwise noted, this statistical variation in the disintegration rate on the basis of the total observed counts is smaller than the observed deviation counts on the same or similar samples. Combination and cumulation of errors are computed by application of the usual rules.

The values of standard deviations appended to the mean values in the data are indeed measures of the precision of the measurements, but are not to be construed as intended specifications of probable errors for the absolute value of the measurement.

By virtue of the nature of the original problems of which much of these data are a by-product, no initial attempts were made by the authors to purify the extremely pure and well-decontaminated stock solutions prepared by other individuals. Also additional purifications and decontaminations were not followed by repeated  $\alpha$  radiometric assays to establish the absolute specific activity of the sample.

**2.3 Counter Geometry and Preliminary Measurements.** Cunningham, Ghiorso, and Hindman<sup>6</sup> constructed and calibrated a low-geometry counter of accurately calculable geometry and compared the counting rates of the low-geometry counter and that of the standard parallel-plate air-filled counter.

For this comparison three Pu<sup>239</sup> samples (approximately 2  $\mu\text{g}$  each) were prepared and spread over an area of about 20 sq mm of platinum and counted in the vacuum low-geometry counter. Each sample was then dissolved completely and diluted to 10 ml. Twenty-five-microliter aliquots of the resultant solution were placed on new flat platinum disks, evaporated to dryness, ignited, and counted in the "50 per cent" standard chamber. These data are presented in Table 2.

Table 2—Evaluation of the Counting Yield of the Standard Parallel-plate Chamber<sup>a</sup>

Sample and plates	Counting rate in $4.26 \times 10^{-4}$ geometry counter	Dis/min calculated from column 2	Dis/min not dissolved preparatory to aliquoting	Counting rate in parallel-plate chambers†	Counting yield of parallel-plate chamber, %
1 a, b, c	98.4 $\pm$ 0.5	230,700	600	296.4 3.2	51.5
2 a, b, c	83.6 $\pm$ 0.4	196,200	700	256.0 1.2	52.4
3 a, b, c	142.7 $\pm$ 1.1	334,600	2,800	433.4 2.7	52.2
4 a	359.4 $\pm$ 1.1	2,056,000	0	1066 5.4	51.8
b				1071 4.9	52.1
c				841 1.3‡	51.9

<sup>a</sup> Of a  $2.5 \times 10^{-3}$  aliquot of the samples corrected for background and coincidence (0.8 per cent per 1,000 counts per minute).

† $1.5 \times 10^{-3}$  aliquot.

The calibrations of the volumetric equipment used in this work were checked, and the plates were examined for undissolved  $\alpha$  activity after the dissolving operation. Corrections were made for the activities left on the plates and in the dissolving dishes. In evaluating the counting yield of the 50 per cent geometry counters by comparison with the vacuum low-geometry counter, it was assumed that back-scattering of  $\alpha$  radiation in the solid angle subtended by the aperture of the low-geometry counter was negligible. (Run 4 is a last-minute run using 15  $\mu\text{g}$ .)

**2.4 Back-scattering of  $\alpha$  Particles.** The resulting 52.0 per cent counting yield (cf. Table 2) was quite surprising since it had been assumed that the maximum counting yield obtainable was 50 per cent. A preliminary calculation by Crawford<sup>7</sup> indicated that back-scattering of  $\alpha$  particles at small angles could exist to an appreciable extent. To test this possibility some preliminary experiments were made by counting weights of U<sub>3</sub>O<sub>8</sub> on platinum and on quartz on the supposition

that back-scattering would decrease with atomic number. A 2.4 per cent (1.2 parts in 50) lower count was observed for two samples on quartz compared to the identical samples mounted on platinum. Since it was thought that there might still be scattering from the uranium on quartz, the same experiment was repeated using essentially weightless Pu<sup>239</sup> samples. In one experiment two pairs of samples showed a 3.1 per cent (1.55 parts in 50) difference and in a later experiment three pairs of samples showed a 2.9 per cent (1.45 parts in 50) difference.

### 3. MICROCHEMICAL DETERMINATION OF THE SPECIFIC ACTIVITY<sup>a</sup>

Samples of PuO<sub>2</sub> of 50 to 200 µg, prepared by igniting the nitrate for several hours at 700°C, were weighed on the quartz torsion microbalance, dissolved in concentrated H<sub>2</sub>SO<sub>4</sub>-HNO<sub>3</sub> mixture by fuming,

Table 3—Specific Activity of Pu<sup>239</sup> by Microchemical Weighing† of Oxide<sup>b</sup>

Sample	Weight of oxide, µg	Corresponding specific activity, counts/min./µg	Mean, counts/min./µg
H-1	124.47	70,562 ± 71	
H-2	127.61	70,380 ± 38	
E-1	194.26	70,038 ± 71	
A-1	98.81	71,131 ± 125	70,530 ± 520
L-1	76.496	70,376 ± 86	
L-2	64.859	70,665 ± 123	

†Plates: platinum, containing 1 to 2 µg per plate.

Counters: parallel-plate nitrogen counters (Metallurgical Laboratory designations N-3 and N-4).

Corrections applied: background, coincidence.

diluted in calibrated glassware, and assayed for plutonium by counting plates prepared from aliquots.

Spectrochemical analyses of the carefully purified stock solutions from which the oxide was prepared indicated only insignificant traces of metallic impurities.

The precision of the weighing, aliquoting, and counting is of the order of several tenths of a per cent, but the accuracy which can be claimed for determination is limited in that the microbalance was calibrated with a 1-mg aluminum weight certified by the National Bureau of Standards (Class S) only to the nearest 0.01 mg. Counting was done in the parallel-plate nitrogen counters (N-3, N-4) for sufficiently long periods to make the statistical uncertainty in the count-

ing less than 0.1 per cent. The results of these specific-activity determinations are shown in Table 3; they indicate a specific  $\alpha$  activity of 70,530 counts per minute per microgram. Using a 52 per cent "geometry factor," this corresponds to a value of  $(135.6 \pm 1) \times 10^3$  disintegrations per minute per microgram, and to a half life of  $24,490 \pm 180$  years.

#### 4. SPECIFIC ACTIVITY OF PLUTONIUM FROM MEASUREMENTS SUPPLEMENTARY TO CALORIMETRIC WORK<sup>9</sup>

In the course of some precise thermochemical measurements on plutonium compounds<sup>10,11</sup> it was desirable to confirm the amounts

Table 4.—Specific Activity of Pu<sup>239</sup> from Supplementary Measurements on Calorimetric Samples<sup>10,11</sup>

Substance weighed	No. of samples	Purity of sample	Specific activity, counts/min/ $\mu$ g	
			Observed counts/min/ $\mu$ g	Average counts/min/ $\mu$ g
Pu metal	3	No evidence of oxide	70,670 $\pm$ 70	
PuCl <sub>3</sub>	2	Gravimetric analysis indicates 99.8 $\pm$ 0.2% PuCl <sub>3</sub>	70,730 $\pm$ 60	70,700 $\pm$ 60
PuBr <sub>3</sub>	1	Gravimetric analysis indicates 99.9 $\pm$ 0.2% PuBr <sub>3</sub>	70,690 $\pm$ 150	
PuBr <sub>3</sub>	1	Gravimetric analysis indicates 99.9 $\pm$ 0.2% PuBr <sub>3</sub>	70,710 $\pm$ 110	

<sup>†</sup>Plates: platinum, 0.4 to 2.2  $\mu$ g of plutonium deposited from excess nitric acid. At least two plates of each sample were counted.

Counter: parallel-plate nitrogen counter. (Metallurgical Laboratory designation N-4.)

Corrections applied: background, coincidence (determination of Greenlee, Dixon, et al., private communication), standard counting efficiency.

and/or composition of plutonium metal and compounds, and, with certain substances, the completeness of solution. Independent microchemical analysis of the purity of the compounds and the consistent excellent agreement of amounts of plutonium by weight and by radio-

metric assay suggested the use of the intended supplementary analytical data as a source of precise specific-activity values free of some of the uncertainties<sup>12</sup> of other determinations.

The plutonium used in the preparation of the metal and the compounds was specially purified by the Recovery Group from the regular Section C-1 Metallurgical Laboratory stock. Spectrochemical analysis revealed only traces of metallic impurities. Although no uranium was detected, the limit of detection of the method was 0.2 per cent.

As indicated in Table 4, three independent micro-scale vacuum reduction preparations of plutonium metal, two weighed samples of a single preparation of  $\text{PuCl}_3$ , and two  $\text{PuBr}_3$  preparations were used. The weights of these samples were of the order of 20 to 100 mg and were measured against weights calibrated and certified by the National Bureau of Standards. They were dissolved in an accurately known weight (about 200 g) of 6M hydrochloric acid in the process of calorimetric measurement. Dilution and plating of these solutions were accomplished by the usual volumetric micropipet procedure, and the volumetric compositions of the original solutions were computed from their densities. Several platinum plates, each containing from 0.4 to 2.2  $\mu\text{g}$  of plutonium were repeatedly counted in the parallel-plate nitrogen counter for sufficiently long periods to make the statistical uncertainty small compared to the standard deviations shown in Table 4.

These data indicate the specific  $\alpha$  activity to be 70,700 counts per minute per microgram on counter N-4 with considerable precision.

##### 5. DISINTEGRATION RATE AND HALF LIFE OF $\text{Pu}^{239}$

In order to translate the observed counting rate from counts to disintegrations the parallel-plate nitrogen counter (N-4) was compared with a vacuum-type low-geometry counter of which the effective geometry was accurately known.<sup>13,14</sup>

Thin plates containing appropriate amounts of plutonium for each counter were prepared by microvolumetric aliquoting of a nitric acid solution of plutonium made up of weighed amounts of plutonium metal produced by thermal reduction in vacuum on the milligram scale.<sup>15</sup>

Five platinum plates, containing 12.61  $\mu\text{g}$  of  $\text{Pu}^{239}$  per plate, gave corrected observed counts of  $1188 \pm 6$ ,  $1183 \pm 7$ ,  $1197 \pm 5$ ,  $1194 \pm 2$ ,  $1171 \pm 2$ ; mean  $1183 \pm 4$  in a vacuum-type low-geometry counter (Metallurgical Laboratory designation V-2; medium position; factor=1505). Corrections for background and for coincidence were made.

Microgram plates made from the same solution showed counting rates of  $70,480 \pm 20$ ,  $70,520 \pm 25$ ,  $70,660 \pm 15$ ; mean  $70,540 \pm 70$  in the

parallel-plate nitrogen counter (N-4) when corrected for background and coincidence and to standard counting efficiency.

The most precise specific activities of this work were obtained on two high purity samples of micro-scale-produced plutonium metal.<sup>16</sup> The metal samples were massed against National Bureau of Standards calibrated weights, were dissolved in a slight excess of dilute HCl, and were diluted to the desired concentration with 4M H<sub>2</sub>SO<sub>4</sub>. The solutions were prepared, subsequently diluted, and aliquoted for plating by a gravimetric technique of high precision.<sup>17</sup> Spectrochemical analyses of aliquots of the solution revealed the presence of no metallic impurities aggregating 0.01 per cent above that of the redistilled acid used for the blanks. No uranium was detected but a sensitivity of only 0.2 per cent was claimed. The precision of the plating technique eliminated the need of many duplicate plates.

The chief potential source of error of the method is probably the possibility of undetected impurities in the metal. The spectrochemical analysis in general established the absence of significant amounts of metal impurities with the possible exception of uranium. The excellent agreement between different samples of metal tends to confirm the lack of impurities in the metal.

Platinum plates containing 1.5 µg of Pu<sup>239</sup> were counted in the parallel-plate counter (N-4) using an argon-carbon dioxide gas mixture. The details and results of the counting have been presented in detail.<sup>18</sup> Corrected to standard counting efficiency the mean specific activity is  $70,660 \pm 20$  counts per minute per microgram.

In recapitulation, the values of the specific-activity determinations based on weighing plutonium metal and converting observed  $\alpha$  counts to standard counting efficiency in the parallel-plate counter (N-4) are presented in Table 5. Excellent confirmation of these values has, as indicated, been obtained by  $\alpha$  radiometric assay of weighted plutonium oxide and halide preparations.

Although none of the specific-activity measurements by Westrum were meant to yield absolute values such as disintegration constants, it is possible to compute a rather accurate value from the data presented. An "effective counting yield" for the parallel-plate counter N-4 which will enable one to evaluate the best value of the specific activity in terms of the counting rate on the low-geometry vacuum counter and to compute the specific disintegration rate without the determination or estimation of back-scattering corrections, which are involved in the higher geometry counters, may be made from the relative observed counting data presented here.

The best value of the specific activity of  $70,650 \pm 50$  corresponds to a specific disintegration rate of  $136,060 \pm 400$  disintegrations per

minute per microgram corresponding to a half life of  $24,400 \pm 70$  years. This value is in good agreement with that obtained with the microchemical method of the preceding section, and within the experimental uncertainty of a value obtained in a fairly extensive study at Hanford;<sup>19</sup> 16 disks were prepared and counted for long periods to minimize counting errors, and 10 chemical titration analyses were made to establish a valid chemical value for the amount of plutonium per plate. The specific activity of pure plutonium at  $137,000 \pm 1,041$  disintegrations per minute per microgram was established.<sup>19</sup>

Table 5—Summary of Specific Activity of Pu<sup>239</sup>

Source of data	No. of metal samples	Specific activity, counts/min./μg
Reference 10, 11; Table 4	3	$70,670 \pm 60$
Reference 14	1	$70,540 \pm 70$
Reference 18	2	$70,660 \pm 70$
Mean value (weighed)		$70,650 \pm 50$

The rate of energy production of a 120-g sphere of relatively pure Pu<sup>239</sup> measured calorimetrically<sup>20</sup> by the comparison of the rate of evaporation of liquid nitrogen by the sphere and by the input of electrical energy was  $1.923 (\pm 1$  per cent) absolute watts per gram. Combining this value with the energy of  $\alpha$  particles from range and range energy measurements,  $2.41 \times 10^4$  years as the half life of Pu<sup>239</sup> with respect to  $\alpha$  emission is obtained.

All the reported measurements are therefore in agreement within their respective experimental accuracies.

## 6. SUMMARY

Several series of measurements of the specific  $\alpha$  activity of Pu<sup>239</sup> have been described. Plates for radiometric assay were made by weighing samples of metal and of pure compounds from highly purified plutonium stocks. The specific activity of Pu<sup>239</sup> is  $136,060 \pm 400$  disintegrations per minute per microgram. This corresponds to a half life of  $24,400 \pm 70$  years.

## ACKNOWLEDGMENTS

The authors wish to acknowledge the cooperation of the several other groups, in particular the Analytical Chemistry Group and the Recovery Group, also under the general direction of Dr. G. T. Seaborg, whose support was essential to the completion of these measurements.

## REFERENCES

1. A. C. Wahl and G. T. Seaborg, Metallurgical Project Report CN-266 (Sept. 14, 1942), p. 1.
2. B. B. Cunningham, M. Cefola, and L. B. Werner, Metallurgical Project Report CN-261 (Sept. 15, 1942), p. 6.
3. B. B. Cunningham and L. B. Werner, Metallurgical Project Report CN-299 (1942), p. 1, 2.
4. B. B. Cunningham and L. B. Werner, Metallurgical Project Report CN-419 (January 1943), p. 15.
5. F. D. Rossini and W. E. Deming, J. Wash. Acad. Sci., 29: 418 (1939).
6. B. B. Cunningham, A. Ghiorso, and J. C. Hindman, Metallurgical Project Report CN-1241 (A-1818) (Jan. 5, 1944), pp. 1-3.
7. J. A. Crawford, Theoretical calculations concerning back-scattering of alpha particles, Paper 16.55, this volume (Metallurgical Project Report CC-1342).
8. J. C. Hindman and R. Greenlee, unpublished data.
9. E. F. Westrum, Jr., Metallurgical Laboratory Memorandum MUC-GTS-2042 (Oct. 25, 1945).
10. E. F. Westrum, Jr., and H. P. Robinson, The heat of formation of plutonium trichloride, Paper 6.53, this volume (Metallurgical Project Report CC-3872).
11. E. F. Westrum, Jr., The heat of formation of plutonium tribromide, Paper 6.55, this volume (Metallurgical Project Report CC-3879).
12. J. C. Hindman, Metallurgical Laboratory Memorandum MUC-GTS-1833 (July 6, 1945), p. 6.
13. E. F. Westrum, Jr., and A. Ghiorso, unpublished data.
14. E. F. Westrum, Jr., Metallurgical Laboratory Memorandum MUC-GTS-2075 (Nov. 11, 1945).
15. E. F. Westrum, Jr., Metallurgical Project Reports CK-1586 and CN-2495; J. Am. Chem. Soc., 70: 3543 (1948).
16. E. F. Westrum, Jr., Metallurgical Laboratory Memorandum MUC-GTS-2082 (Nov. 13, 1945).
17. E. F. Westrum, Jr., An improved technique for precise alpha radiometric assay, Paper 16.2, this volume (Metallurgical Project Report CN-3433).
18. Ibid., Table 1.
19. HEW Progress Letter No. 82, HW-3-3987, p. 4.
20. J. W. Stout and W. M. Jones, Phys. Rev., 71: 582 (1947).

## **CONTRIBUTING AUTHORS OF PARTS I AND II**

- B. M. Abraham**, Chemistry Division, Argonne National Laboratory  
**D. P. Ames**, Department of Chemistry, University of Wisconsin  
**H. H. Anderson**, Auburndale, Mass.  
**L. B. Asprey**, Los Alamos Scientific Laboratory  
**W. C. Beard, Jr.**, Litchfield, Conn.  
**W. C. Bentley**, Chemistry Division, Argonne National Laboratory  
**N. A. Bonner**, Department of Chemistry, Washington University, St. Louis, Mo.  
**C. J. Borkowski**, Chemistry Division, Oak Ridge National Laboratory  
**L. Brewer**, Department of Chemistry, University of California, Berkeley  
**B. B. Brody**, University of Rochester Medical School  
**L. Bromley**, Department of Chemistry, University of California, Berkeley  
**H. D. Brown, Ames**, Iowa  
**H. S. Brown**, Institute for Nuclear Studies, University of Chicago  
**M. Calvin**, Department of Chemistry, University of California, Berkeley  
**M. Cefola**, Knolls Laboratory, General Electric Company, Schenectady, N. Y.  
**J. Chrisney**, University of California, Berkeley  
**R. E. Connick**, Department of Chemistry, University of California, Berkeley  
**O. A. Cook**, College of Agriculture, University of California, Davis  
**C. D. Coryell**, Department of Chemistry, Massachusetts Institute of Technology  
**J. A. Crawford**, Department of Physics, University of Chicago  
**B. B. Cunningham**, Department of Chemistry and Radiation Laboratory, University of California, Berkeley  
**J. R. Dam**, Kalamazoo, Mich.  
**R. Dandl**, Chemistry Division, Oak Ridge National Laboratory  
**N. R. Davidson**, Department of Chemistry, California Institute of Technology  
**J. S. Dixon**, Department of Chemistry, Washington University, St. Louis, Mo.  
**H. W. Dodgen**, Department of Chemistry, Washington State College  
**J. K. East**, Chemistry Division, Oak Ridge National Laboratory

- N. Elliott, Brookhaven National Laboratory  
D. W. Engelkemeir, Chemistry Division, Argonne National Laboratory  
M. W. Evans, College of Engineering, Research Division, New York University  
L. Eyring, Department of Chemistry, State University of Iowa  
P. Fields, Chemistry Division, Argonne National Laboratory  
P. Fineman, Chemical Engineering Division, Argonne National Laboratory  
O. Flatau, North Fargo, N. D.  
A. E. Florin, Chemistry Division, Los Alamos Scientific Laboratory  
S. Fried, Chemistry Division, Argonne National Laboratory  
H. W. Fulbright, Department of Physics, Carnegie Institute of Technology  
C. S. Garner, Department of Chemistry, University of California, Los Angeles  
L. H. Gevantman, Department of Chemistry, University of Notre Dame  
A. Ghiorso, Radiation Laboratory, University of California, Berkeley  
P. W. Gilles, Department of Chemistry, University of Kansas  
J. W. Gofman, Division of Medical Physics, Department of Physics, University of California, Berkeley  
R. Greenlee, Battelle Memorial Institute, Columbus, Ohio  
F. Hagemann, Chemistry Division, Argonne National Laboratory  
J. W. Hamaker, Department of Chemistry, Whittier College, Whittier, Calif.  
R. E. Hein, Institute for Atomic Research, Iowa State College  
J. C. Hindman, Chemistry Division, Argonne National Laboratory  
H. H. Hopkins, Jr., Hanford Engineer Works  
J. J. Howland, Jr., Brookhaven National Laboratory  
D. L. Hufford, Los Alamos Scientific Laboratory  
E. K. Hyde, Chemistry Division, Argonne National Laboratory  
A. H. Jaffey, Chemistry Division, Argonne National Laboratory  
R. A. James, Department of Chemistry, University of California, Los Angeles  
A. Kant, Department of Chemistry, Carnegie Institute of Technology  
I. Karle, Naval Research Laboratory, Washington, D. C.  
M. Kasha, Department of Physics, University of Chicago  
J. J. Katz, Chemistry Division, Argonne National Laboratory  
J. W. Kennedy, Department of Chemistry, Washington University, St. Louis, Mo.  
E. L. King, Department of Chemistry, University of Wisconsin  
C. W. Koch, Department of Chemistry, University of California, Berkeley

- T. P. Kohman, Department of Chemistry, Carnegie Institute of Technology
- D. E. Koshland, Jr., Department of Chemistry, Harvard University
- K. A. Kraus, Chemistry Division, Oak Ridge National Laboratory
- J. C. Kroner, Nahomet, Ill.
- T. J. LaChapelle, Department of Chemistry, University of California, Los Angeles
- N. L. Lofgren, Chico State College, Chico, Calif.
- C. K. McLane, Department of Physics, University of Wisconsin
- E. M. McMillan, Department of Physics and Radiation Laboratory, University of California, Berkeley
- W. H. McVey, Hanford Engineer Works
- L. B. Magnusson, Chemistry Division, Argonne National Laboratory
- W. M. Manning, Chemistry Division, Argonne National Laboratory
- R. C. L. Mooney, Newcomb College, Tulane University
- G. E. Moore, Chemistry Division, Oak Ridge National Laboratory
- L. O. Morgan, Department of Chemistry, University of Texas
- T. B. Novey, Chemistry Division, Argonne National Laboratory
- P. R. O'Connor, Department of Chemistry, University of Minnesota
- E. F. Orlemann, Department of Chemistry, University of California, Berkeley
- D. W. Osborne, Chemistry Division, Argonne National Laboratory
- J. H. Parsons, Los Alamos Scientific Laboratory
- R. L. Patton, Department of Entomology, Cornell University
- I. Perlman, Department of Chemistry and Radiation Laboratory, University of California, Berkeley
- M. L. Perlman, Brookhaven National Laboratory
- S. Peterson, Department of Chemistry, University of Louisville, Louisville, Ky.
- T. E. Phipps, Department of Chemistry, University of Illinois
- W. H. Reas, Hanford Engineer Works
- H. P. Robinson, Radiation Laboratory, University of California, Berkeley
- G. K. Rollefson, Department of Chemistry, University of California, Berkeley
- B. F. Scott, Able Scientific Glass Apparatus Co., Chicago, Ill.
- G. T. Seaborg, Department of Chemistry and Radiation Laboratory, University of California, Berkeley
- G. W. Sears, General Electric Company, Schenectady, N. Y.
- J. Sedlet, Department of Chemistry, Purdue University
- E. Segrè, Department of Physics and Radiation Laboratory, University of California, Berkeley
- R. L. Seifert, Department of Chemistry, University of Indiana
- I. Sheft, Chemistry Division, Argonne National Laboratory

- G. E. Sheline, Billings Hospital, University of Chicago  
O. C. Simpson, Chemistry Division, Argonne National Laboratory  
N. R. Sleight, St. Johns, Mich.  
C. Smith, Owens-Illinois Glass Company, San Francisco, Calif.  
L. Spector, Oak Ridge National Laboratory  
R. W. Stoughton, Chemistry Division, Oak Ridge National Laboratory  
M. H. Studier, Chemistry Division, Argonne National Laboratory  
R. C. Thompson, Department of Chemistry, University of Texas  
S. G. Thompson, Radiation Laboratory, University of California,  
Berkeley  
A. Turkevich, Institute for Nuclear Studies, University of Chicago  
Q. Van Winkle, Department of Chemistry, Ohio State University  
A. F. Voigt, Institute for Atomic Research, Iowa State College  
A. C. Wahl, Department of Chemistry, Washington University, St.  
Louis, Mo.  
B. B. Weissbourd, Chicago, Ill.  
L. B. Werner, Hunter's Point Naval Radiation Laboratory, San Fran-  
cisco, Calif.  
E. F. Westrum, Jr., Department of Chemistry, University of Michigan  
M. J. Wolf, Northern Regional Laboratory of the U. S. Department of  
Agriculture, Peoria, Ill.  
F. J. Wolter, Esso Laboratories, Elizabeth, N. J.  
J. M. Wright, Institute for Atomic Research, Iowa State College  
W. H. Zachariasen, Department of Physics, University of Chicago,  
and Argonne National Laboratory

## AUTHOR INDEX FOR PARTS I AND II

### A

Abraham, B. M., 740, 779, 814, 945, 957  
Ames, D. P., 348, 1206, 1383, 1675, 1700  
Anderson, H. H., 724, 775, 793, 796, 801,  
  806, 810, 818, 825, 964, 1206, 1700  
Asprey, L. B., 1595

### B

Beard, W. C., Jr., 637  
Bentley, W. C., 1642  
Bonner, N. A., 84  
Borkowski, C. J., 1197  
Brewer, L., 861, 1111  
Brody, B. B., 118, 740  
Bromley, L., 861, 1111  
Brown, H. D., 162  
Brown, H. S., 100

### C

Calvin, M., 632  
Cefola, M., 822, 848  
Chrisney, J., 1327  
Connick, R. E., 142, 168, 172, 175, 227,  
  268, 335, 336, 345, 445, 559, 830  
Cook, O. A., 147  
Coryell, C. D., 100  
Crawford, J. A., 1307  
Cunningham, B. B., 51, 121, 1192, 1198,  
  1363

### D

Dam, J. R., 468, 478, 528  
Dandl, R., 1197  
Davidson, N. R., 100, 740, 759, 779, 784,  
  814, 831, 841, 945, 957, 1072  
Dixon, J. S., 358, 855  
Dodgen, H. W., 1327

East, J. K., 1197  
Elliott, N., 100  
Engelkemeir, D. W., 100  
Evans, M. W., 282  
Eyring, L., 908

### F

Fields, P., 1128  
Fineman, P., 1206  
Flatau, O., 1197  
Florin, A. E., 1604  
Fried, S., 784, 1072  
Fulbright, H. W., 1011

### G

Garner, C. S., 84  
Gevantman, L. H., 500, 602  
Ghiorso, A., 1192, 1198, 1226, 1381,  
  1383, 1395, 1424, 1439, 1554, 1604,  
  1622, 1639, 1642  
Gilles, P. W., 861, 1111  
Gofman, J. W., 336, 1426, 1427  
Greenlee, R., 1717

### H

Hagemann, F., 740, 759, 957  
Hamaker, J. W., 666  
Hein, R. E., 162, 1119  
Hindman, J. C., 121, 133, 348, 358, 370,  
  388, 405, 1032, 1039, 1050, 1097, 1134,  
  1192  
Hopkins, H. H., Jr., 635, 940, 1430,  
  1604, 1634, 1717  
Howland, J. J., Jr., 121, 133  
Hufford, D. L., 1149  
Hyde, E. K., 759, 1431, 1435, 1439, 1622

## J

Jaffey, A. H., 89, 100, 978, 1198, 1226  
 James, R. A., 1339, 1525, 1554, 1604,  
 1634

Orleman, E. F., 118  
 Osborne, D. W., 1397, 1639

## P

Parsons, J. H., 1197  
 Patton, R. L., 849, 851, 853  
 Perlman, I., 1339, 1586, 1651  
 Perlman, M. L., 8, 79  
 Peterson, S., 1371, 1381, 1385, 1388,  
 1391, 1393, 1395, 1424  
 Phipps, T. E., 682, 704

## R

Reas, W. H., 423  
 Robinson, H. P., 887, 889, 914, 922, 930,  
 952, 1226  
 Rollefson, G. K., 1327

## S

Scott, B. F., 1149  
 Seaborg, G. T., 1, 3, 5, 8, 13, 21, 25, 84,  
 1426, 1427, 1492, 1525, 1554, 1572  
 Sears, G. W., 682, 704  
 Sedlet, J., 1206, 1675, 1700  
 Segré, E., 5, 79  
 Seifert, R. L., 682  
 Sheft, I., 759, 831, 841, 957  
 Sheline, G. E., 175, 180, 227, 335, 336,  
 345, 559, 632  
 Simpson, O. C., 682, 704  
 Sleight, N. R., 162, 1119  
 Smith, C., 822, 850, 855  
 Spector, L., 731  
 Stoughton, R. W., 1426  
 Studier, M. H., 1439, 1622

## T

Thompson, R. C., 1397  
 Thompson, S. G., 1339, 1634  
 Turkevich, A., 100

## N

Novey, T. B., 100

## V

Van Winkle, Q., 1397  
 Voigt, A. F., 162, 1119

## O

O'Connor, P. R., 1651

## W

- Wahl, A. C., 1, 3, 5, 13, 21, 25, 79  
Weissbourd, B. B., 1206, 1226  
Werner, L. B., 51, 1586  
Westrum, E. F., Jr., 729, 814, 887, 889,  
908, 914, 922, 926, 930, 938, 945,  
1185, 1717

Wolf, M. J., 740.

Wolter, F. J., 162

Wright, J. M., 162, 1119

## Z

- Zachariasen, W. H., 1442, 1448, 1451,  
1454, 1462, 1473, 1486, 1489











